Manuscript Report Series No. 5 -10

The Effect of Tidal Barriers upon the M_2 Tide in the Bay of Fundy

Ken B. Yuen

1967-69

CONTENTS

THE EFFECT OF TIDAL BARRIERS UPON THE M_2 TIDE IN THE BAY OF FUNDY

I. INTRODUCTION

The Bay of Fundy has attracted the attention of the mariner, scientist, and the curious on-looker for many years because of its remarkable tides. The possibility of harnessing the tides of the bay for tidal power developments has not been overlooked either in the past 30 years (Hachey, 1934, and Ippen and Harleman, 1958). In recent years attention has been focussed on Passamaquoddy Bay and lately on Chignecto Bay, Shepody Bay and Cumberland Basin by the Atlantic Development Board. The purpose of this study is to examine the effect of tidal barriers upon the M_2 tide in the Bay of Fundy.

The Bay of Fundy is situated on the east coast of Canada, centred at approximately 45°N latitude, 66°W longitude (Fig. I. 1), bounded on the northwest by the coast of New Brunswick and on the southeast by the coast of Nova Scotia. Towards the head, the bay splits into two branches: the Chignecto Bay - Shepody Bay - Cumberland Basin system to the northeast, and the Minas Channel - Minas Basin system to the east.

The depth distribution in the bay (Fig. I. 2) is not an exact duplicate of the depth but a smoothed configuration used in the numerical models presented in this manuscript. The deepest area of the bay is over 600 feet and lies to the east and southeast of Grand Manan Island. Several deep trenches also exist in Minas Channel. The sides of the bay are generally steep-sided but the most irregular feature of the topographyis the existence of Cape Split which acts as an impedance to the tidal streams entering Minas Basin.

The location of past and present tide gauge stations in the Bay of Fundy is shown in Figure I. 1 also. Many were established on a temporary basis for reduction of soundings or for correlation of "head difference" measurements during tidal current surveys but some, such as St. John, N. B. and Digby, N. S. are permanent installations. Prior to 1962, the harmonic analysis of tidal data was carried out by the Tidal Institute and Observatory, Liverpool, England. In subsequent years, the work has been undertaken by the Tides, Currents and Water Levels Section, Canadian Hydrographic Service.

The amplitude, H, and phase lag, g, of the most important harmonic constituents at various tide gauge stations in the Bay of Fundy are listed in Table I. 1. The phase lag here is given with respect to the moon's passage over the Meridian of Greenwich. The subscripts of the constituents refer to the species of tide; 1. diurnal, 2. semi-diurnal, etc.

The amplitude of the M_2 is large, being the dominant constituent in the Bay of Fundy (Table I. 1). An example of the large tidal range in the Bay of Fundy is the tide at Burncoat Head in Minas Basin. Here, the mean tidal range is 38. 4 ft., but even more impressive is the height of over 53 ft. recorded on July 16, 17, of 1916. Another interesting phenomena is the occurrence of the tidal bore in the Petitcodiac River during periods of large tides.

It would be convenient, indeed, if this study could be restricted to the M_2 constituent. To justify such a restriction, let us refer to the accepted tidal theories of Defant (1961). Defant refers to a ratio

$$F = \frac{H(K_1) + H(O_1)}{H(M_2) + H(S_2)}, \qquad \text{I. 1}$$

defined by Courtier (1938) where F is called the "Form-zahl" and is interpreted as follows:

F	Character of Tide	Mean Spring Range
0. - 0. 25	semi-diurnal	$2(M_2 + S_2)$
0. 25 - 1. 5	mixed, mainly semi-diurnal	$2(M_2 + S_2)$
1. 5 - 3. 0	mixed, mainly diurnal	$2(K_1 + O_1)$
3. 0 -	diurnal	$2(K_1 + O_1)$

For St. John, N. B.

$$F(\text{St. John}) = \frac{.51 \text{ ft} + .38 \text{ ft}}{9.95 \text{ ft} + 1.65 \text{ ft}} = 0.08$$

indicating that the Bay of Fundy tide is very strongly semi-diurnal.

The mean range of a spring tide of semi- diurnal type is given as

$$2\left[H(M_2) + H(S_2)\right], \qquad \text{I. 2}$$

and for St. John, the M_2 is

$$\frac{9.95}{9.95 + 1.65} = 0.86$$

or 86% of the mean spring range. Therefore the M_2 constitutes most of the Bay of Fundy tide and the study can now be restricted to the M_2 alone.

The diurnal inequality of the tide is the difference in height between two successive high or low waters. For example, the maximum range at St. John is about 27 ft. The maximum diurnal inequality is roughly 2 ft. or 8% of the maximum range with F equal to .08. In moderate contrast, F is 0.28 for Sept Iles in the St. Lawrence River, where the maximum diurnal inequality is about 3.5 ft. or 35% of the total range. These two examples indicate that for dominantly semi-diurnal tides there exists an almost one-to-one relationship between F and the maximum inequality expressed as a fraction.

The first question that must be answered is why the M_2 tide is so greatly amplified from the mouth to the head of the bay. The Bay of Fundy generally diminishes in width and depth towards the head, and the tide is amplified by this convergence. Another significant factor is near resonance. The average depth of the bay is about 240 ft. and the angular speed of the M_2 is 28.984 degrees per hour, which corresponds to a resonance length or quarter wavelength of 185 miles. In practice, the effective length of the bay is difficult to judge and seems to be about 150-160 miles, but this seems close enough to create partial resonance. From Table I. 1, notice that the amplification of the semi-diurnal constituents is greater than 2 between Lighthouse Cove and Five Islands but the corresponding gain for the diurnal constituent, K_1, is less than 1 1/2. If partial resonance were not present, then amplification of both the diurnal and semi-diurnal tide would be equal. Therefore, partial resonance does occur and is responsible for perhaps 60-70% of the tidal amplification, while convergence of the bay may account for 30-40%.

It is evident that the length of the bay is shorter than the resonance length. Complications arise at the head of the Minas Basin system and the Chignecto Bay branch, since the Minas Basin branch is longer than the Chignecto Bay branch. On this basis Minas Basin contributes more to resonance than Chignecto Bay.

What is the speed of the M_2 tidal wave? The difference in the M_2 phase lag between Grand Manan I. and Cape Chignecto is about 20 degrees or 40 minutes of time which is equivalent to a speed in excess of 200 ft./sec. A gravity wave in a channel 240 ft. deep travels only 88 ft./sec. Thus, the M_2 in the main part of the Bay of Fundy is not only a partially resonant wave but also a near standing wave. In the upper arms of the bay, however, the wave is much slower and can be considered as a progressive wave.

Figures I. 3 and I. 4 show the M_2 corange and cotidal lines for the Bay of Fundy. The corange lines are lines of equal amplitude and the cotidal lines are lines of equal phase lag. The tidal data were obtained from coastal tide gauge stations and as such, they have been perturbed by shallow water effects. Therefore the "observed cotidal and corange lines" are only "intelligent guesses" at whatever values may be found in the centre of the bay. Later on, we shall compare calculated values to these "observed values".

The M_2 cotidal and corange surfaces (it is often more convenient to call them surfaces rather than lines) are fairly smooth and continuous, and contain no nodes in the Bay of Fundy. Normally at a node for the vertical tide, there would be zero amplitude, with the cotidal lines rotating about that point. Gradients in both surfaces bear some relation to the depth distribution. At the head of the bay, where the depth is shallower and the width narrower, the cotidal and corange contours are closer together than they are near the mouth.

The tidal wave from the ocean travels through the Gulf of Maine and enters the Bay of Fundy in the vicinity of Lighthouse Cove. The cotidal surfaces indicate that the wave first enters in a northerly direction. This will also be substantiated later by calculations for the pattern of current ellipses in the bay. The wave takes a finite time interval to travel to the opposite shore and the result is a difference in phase lag of 10-12 degrees between points on opposite shores in the vicinity of the mouth. This sloping of the cotidal lines with respect to the cross channel direction persists, but gradually decreases until the wave reaches Cape Chignecto. As has already been mentioned, this gives the tide the appearance of a standing wave along the length of the bay. However, the standing wave character soon breaks down and in the two branches at the head of the bay progressive wave character is predominant. In Minas Channel, the narrow width and the barrier-like effect of Cape Split produce a large gradient in the cotidal surface. The phase lag in Minas Channel is clearly later than the phase lag in Chignecto Bay. Finally, the cotidal lines are curved near shore reflecting a shallow water effect.

For the M_2 amplitude, which is not nearly as sensitive to depth as is the phase lag, there is only a slight difference of amplitude at the mouth between points on opposite shores. The depth there is over 100 fathoms and thus amplifies the M_2 amplitude only slightly. This inequality is nil in the vicinity of Digby. Over the upper reaches of the bay, the M_2 amplitude on the southeast shore is greater than that on the northwest shore. As in the case of the M_2 phase lag, the physical dimensions of Minas Channel create a large gradient in the M_2 corange surface. The amazing thing here is that the tide manages to survive the constriction at Cape Split and continues to grow in amplitude in Minas Basin.

As a matter of interest, the N_2 and S_2 configurations are shown in Figure I. 5 to I. 8. Since they are also semi-diurnal constituents, the N_2 and S_2 surfaces are very similar to the M_2 surfaces already discussed.

In view of the large tides in the Bay of Fundy, especially in Minas Basin, there is a large potential of energy which man has yet to trap. In spite of the advent of nuclear power as a source of energy, advances have been made and are still being made in the extraction of energy from tidal sources. For example, a tidal power project is nearing completion in the estuary of La Rance River in northwestern France. In the area of Passamaquoddy Bay (near the mouth of the Bay of Fundy on the northwestern shore), engineering

studies have been carried out by the International Passamaquoddy Tidal Power Project (1959). We will see later that Minas Basin has greater potential than Passamaquoddy Bay but the cost of a dam in Minas Channel will likely be greater because of the depth and width. One point in favour of the Minas Channel site is the possibility of a causeway over the dam, saving motorists the distance and time in driving around Minas Basin.

In building a power dam, there is the question of the effect of the dam upon the existing M_2 configuration. If the dam were to decrease the range critically, say 50%, then it may no longer be feasible to extract power from the tide. In this study we shall try to calculate the effects of complete barriers upon the present tidal configuration. This will be done by means of the following models.

1. Numerical Solution - 1 dimensional
2. Analytic Solution - 1 dimensional
3. Numerical Solution - 2 dimensional - coarse grid
   - fine grid

Even without carrying out any calculations, we can estimate qualitatively the effects of a tidal barrier. Since the bay is already shorter than the resonance length, a barrier will make it even shorter and therefore further off from resonance, which in turn would cause a decrease in the tidal amplitude. Furthermore, since the Minas Channel branch contributes more to resonance than does the Chignecto Bay branch, a larger decrease in tidal range would be expected in Minas Channel than in Chignecto Bay for any barrier in the two channels equi-distant from the junction at Cape Chignecto. A decrease in phase lag or an advancement of time of high water would occur with the incoming tide being reflected at the barrier instead of going up to the head of the two channels and being dissipated by bottom friction. Lastly, since the Minas Channel branch is longer, greater advancement of high water for a Minas Channel barrier than for an equivalent Chignecto Bay barrier would result.

II. ONE DIMENSIONAL NUMERICAL MODEL

In 1964, Dr. J. R. Rossiter, Director of the Tidal Institute and Observatory, Liverpool, was asked to make a preliminary investigation into the effects of tidal barriers on tidal propagation in the Bay of Fundy. In particular, he investigated the effects of a barrier at the entrance to Minas Basin, running from Cape Sharp southward to the opposite shore. This was done by using three different approaches.

In his first approach, Rossiter divided the Bay of Fundy system into five frictionless channels, each of constant length, width and depth (Fig. II. 1). The effects of viscous and Coriolis forces were ignored. The tidal regime at the mouth of the bay was assumed to be unaffected by the erection of the barrier in Minas Basin. The horizontal motion was considered as the depth-mean motion of a single harmonic, and the flow at section F was assumed to be zero.

The motion without the barrier was expressed as

$$Z = -H \sin \sigma t, \qquad \text{II. 1}$$

and

$$u = -U \cos \sigma t, \qquad \text{II. 2}$$

where H = amplitude of vertical oscillation
U = amplitude of horizontal oscillation
Z = water level with respect to mean sea level
u = x - component of velocity
σ = angular speed of the single harmonic, in this case the M_2 constituent
t = time

In terms of the velocity at the barrier site, the change in the motion was given by

$$Z = 1.214\, U \sin \sigma t, \qquad \text{II. 3}$$

and

$$u = U \cos \sigma t. \qquad \text{II. 4}$$

Thus the resultant motion at the barrage site is

$$Z = 1.214\, U \sin \sigma t - H \sin \sigma t. \qquad \text{II. 5}$$

Using a value of U = 4 knots and H = 15 feet, the following values were obtained for the percent decrease in M_2 amplitude at various cross sections for a barrier at Cape Sharp.

Table II. 1

Cross-section	A	B	C	D	E	F
% decrease in M_2 amplitude	--	5%	16%	26%	31%	16%

To help examine the validity of these results, an energy budget was then carried out. The expression for the average tidal energy transport is

$$E_t = \frac{1}{2} \rho g A H U \cos(g' - \gamma), \qquad \text{II. 6}$$

where ρ = density of water
g = gravity
A = cross-sectional area
H = depth
U = speed
g' = phase lag of vertical tide (M_2)
γ = phase lag of horizontal tidal stream (M_2)

In a study of energy in the Bay of Fundy by McLellan (1958), a similar expression was derived for the energy. The energy flux at the mouth of the bay was calculated to be 3.09×10^7 kilowatts (kw), which is in good agreement with the Tidal Institute's value of 3.17×10^7 kw. Rossiter's calculations show that 2.60×10^7 kw are dissipated in the bay while McLellan calculated a value 2.71×10^7 kw, again in close agreement. From Figure II. 2, it can be seen that out of the total energy transport across the cross-section at Cape Chignecto, 1.12×10^7 kw enters Minas Channel but only $.42 \times 10^7$ kw into Chignecto Bay. This implies that the effect of tidal propagation in the Bay of Fundy would be greater for a barrier in Minas Basin than for a barrier in Chignecto Bay, since the latter case involved less redistribution of tidal energy.

The third and last approach by the Tidal Institute was to solve the simplified one-dimensional hydrodynamical equations by numerical integration in time using the "Initial Value Method" by Rossiter and Lennon (1965). Their only calculation was for a barrier at Cape Sharp in Minas Basin.

The author's work with numerical tidal models commenced here. This initial work consisted of a model similar to the Tidal Institute's, and, quite naturally, the first calculation was also for the Cape Sharp barrier. A description of the model follows:

In the integration of the one dimensional hydrodynamical equations, quadratic friction is used and coriolis and viscous effects are neglected. The expansion of $\frac{du}{dt}$ gives

$$\frac{du}{dt} = \frac{\partial u}{\partial t} + u u_x + w u_z, \qquad \text{II. 7}$$

where the last two terms on the right are the advection terms. The wu_z term is neglected since w is usually very small. The uu_x term is also left out for this solution but its effect upon the tide will be examined later. The hydrodynamic equations are now given as

$$\frac{\partial u}{\partial t} = -g \frac{\partial Z}{\partial x} - \frac{k|u|u}{H} \qquad \text{II. 8}$$

and

$$\frac{\partial Q}{\partial x} = -b \frac{\partial Z}{\partial t}, \qquad \text{II. 9}$$

where u = velocity in x direction
g = gravity
Z = water level with respect to equilibrium depth
k = friction co-eff = . 0025
H = total depth of water
Q = flow in x direction
b = breadth of the channel

To facilitate a solution, Equations II. 8 and II. 9 were transformed into a finite difference form and integrated in time. The Bay of Fundy was divided into a number of 15. 5 nautical miles sections, each of constant breadth and depth (Fig. II. 3 and Table II. 2). The finite difference forms of II. 8 and II. 9 are

$$u(m+\tfrac{1}{2}, n+\tfrac{1}{2}) = u(m-\tfrac{1}{2}, n+\tfrac{1}{2}) \left[1 - \frac{k\,|u(m-\tfrac{1}{2}, n+\tfrac{1}{2})|}{H}\right] - \frac{g\tau}{\epsilon}\left[Z(m, n+1) - Z(m, n)\right]. \qquad \text{II. 10}$$

and

$$Z(m, n) = Z(m-1, n) - \frac{\tau}{S_n}\left[Q(m-\tfrac{1}{2}, n+\tfrac{1}{2}) - Q(m-\tfrac{1}{2}, n-\tfrac{1}{2})\right] \qquad \text{II. 11}$$

where Z = water level with respect to equilibrium level,
H = total depth,
b = breadth,
A = bH = area of the cross section,
u = velocity in x direction,
k = friction coefficient = . 0025,
S_n = surface area of section n,
τ = time step = 621. 030 sec,
ϵ = grid length = 15. 5 nautical miles,
Q = Au = volume flow.

The double subscripts in II. 10 and II. 11 refer to the time step and space step, respectively.

The grid configuration of II. 10 and II. 11 is shown in Figure II. 4. The Z values are calculated in space at integral grid lengths, n, while u values are calculated at half integral grid lenghts, n + 1/2. Similarly, the Z and u values in time are calculated at integral and half integral time steps, m and m + 1/2, respectively. Thus this system is "staggered" in time and space.

For various grid systems in the finite difference solution of the hydrodynamical equations, there can often be found an explicit relationship given by

$$\begin{pmatrix} U^{m+\frac{1}{2}} \\ Z^{m+1} \end{pmatrix} = \begin{pmatrix} \text{Amplification} \\ \text{Matrix} \end{pmatrix}^{-2-} \times \begin{pmatrix} U^{m-\frac{1}{2}} \\ Z^{m} \end{pmatrix} . \qquad \text{II. 12}$$

The criterion for computational stability is

$$|\lambda_i| \leq 1 , \qquad \text{II. 13}$$

where the λ_i are the eigen values of II. 12. For II. 10 and II. 11, the amplification matrix is a 2 x 2 matrix. Fischer (1965) (in discussing numerical stability) derived the stability criterion used for this one-dimensional "time and space staggered" system. The condition is

$$2\Delta t \leq \frac{2\Delta l}{\sqrt{g H_{max}}} . \qquad \text{II. 14}$$

For this study, the tide at the mouth of the bay is taken to be the observed M_2 tide so that

$$Z(m, 1) = 7.5 \cos(m\tau - 331°) . \qquad \text{II. 15}$$

At the junction of Cape Chignecto, the continuity condition is

$$Q(m - \frac{1}{2}, 5\frac{1}{2}) = Q(m - \frac{1}{2}, 6\frac{1}{2})_{\text{Chignecto}} + Q(m - \frac{1}{2}, 6\frac{1}{2})_{\text{Minas}} . \qquad \text{II. 16}$$

For a further simplification of the boundary conditions, set

$$Q(m, 8\frac{1}{2}) = 0 . \qquad \text{II. 17}$$

First calculation was for a barrier at Cape Sharp and is similar to the calculation by the Tidal Institute. The boundary condition is

$$Q(m, 10) = 0. \qquad \text{II. 18}$$

The water level at the barrier site, Z (m, 10), was calculated by a different scheme. Z (m, 9 3/4) was first calculated and Z (m, 10) taken as

$$Z(m, 10) = \frac{1}{3}\left[-Z(m, 9) + 4\,Z(m, 9\tfrac{3}{4})\right]. \qquad \text{II. 19}$$

In the figures, the subscript n=9 3/4 has been replaced by n=11 to facilitate computer programming.

All calculations were carried out on the CDC 3100 digital computer and were started at time m=0. The initial water levels were calculated from the cosine of the observed phase lag. Initial values for the current were assumed to be zero. Since the total time of calculation is only four or five tidal cycles, the incorrect initial currents are of no concern. This only slightly influences the time it takes for the solution to reach a steady state. In longer calculations, poor initial values may drastically affect the final results.

The calculated M_2 amplitude with the Cape Sharp barrier is compared with the observed or normal M_2 amplitude in Chignecto Bay (Fig. II. 5). The abscissa in Figure II. 5 represents distance from the mouth of the model, with each unit step equal to 15. 5 nautical miles. The decrease in amplitude is less towards the head of Chignecto Bay because greater distance towards the head of Chignecto Bay means greater distance from the barrier. Figure II. 6 shows the same quantities plotted for Minas Channel. As expected, the difference between the observed and calculated M_2 amplitude is greatest at the barrier site.

The perturbed phase lag is compared with the observed phase lag in Minas Channel (Fig. II. 7). When section 10 is closed off, the difference in phase lag between the mouth and Cape Chignecto is only 6 or 7 degrees and the tidal wave has the appearance of a standing wave. Figure II. 8 shows the observed and calculated phase lags for Chignecto Bay. The perturbed tidal wave there displays more progressive wave character than standing wave character.

It is more convenient to express the change in M_2 amplitude as a percentage rather than as an absolute value (Fig. II. 9). The greatest decrease (20%) occurs at the barrier site, as does the largest gradient, apparently caused by the barrier and the narrowness of Minas Channel. The gradient in Chignecto Bay is smaller, but still larger than the gradient in the main part of the bay. Over one-half of the perturbation, the percent decrease in

amplitude caused by the barrier, extends beyond Cape Chignecto.

The largest decrease in phase lag (also found at the barrier site) of 12 degrees is attenuated even more quickly than the percent decrease in amplitude (Fig. II. 10).

Even though we have already calculated the effects of a barrier at Cape Sharp, we have not yet shown that the model is valid. This can be done by reproducing the natural M_2 distribution. Instead of u (m, 10) = 0, Z (m, 10) is now inputted as the observed M_2 tide.

The calculated normal M_2 tide and the observed M_2 tide in Minas Channel are equal by assumption at sections 1 and 10 (Fig. II. 11). They differ most at section 5 but only by . 5 ft. Similar conditions are found in Chignecto Bay (Fig. II. 12), but the agreement is not as good as the case for Minas Channel.

The calculated normal M_2 phase lag and observed phase lag for Chignecto Bay are shown in Figure II. 13. The calculated curve is somewhat irregular, but the maximum difference between the two curves is several degrees. In Minas Channel (Figure II. 14) the correlation is much better.

The perturbed state of the tide has been compared with the observed state, but this is valid only if the model is capable of reproducing the natural configuration very accurately.

It has been found, though, that the model does produce errors; however, if the errors in the model are produced to the same magnitude in all calculations, then it would be much better to measure the effects of the barrier by comparing them with the calculated natural distribution rather than with the observed (Fig. II. 15 and II. 16). The results are similar to the previous comparison except that the perturbation in Chignecto Bay now has a smaller gradient.

Attempts were made to reproduce the N_2 configuration, but the calculations were unstable, even after 10-12 tidal cycles.

The depth was made constant at 200 ft. as a final study with this model to yield the effects of depth on the normal tidal configuration. The calculated normal M_2 distribution with natural depth is compared with the distribution at the constant depth of 200 ft. (Fig. II. 17 to II. 20). It is apparent that towards section 1, where the depth is greater than 200 ft., the amplitude for constant depth is greater than the amplitude for natural depth. Towards section 8 in Chignecto Bay, where the depth is less than 200 ft., the situation is reversed. Similarly, the M_2 phase lag for constant depth is greater at the mouth and less in Chignecto Bay than for the case of natural depth. We can guess that the tide attempts to do the same thing in Minas Channel, but

Z (m, 10) has been fixed and this probably prevents the two curves in Figure II. 18 from crossing each other as they did in Chignecto Bay. It is concluded that decreased depth increases the amplitude and phase lag.

III. ONE DIMENSIONAL ANALYTIC SOLUTION

An analytic solution to the hydrodynamical equations was undertaken to provide a check on the accuracy of the numerical results obtained by the one-dimensional finite difference computations. This solution will be restricted to the one-dimensional case. Solution of the two-dimensional case is lengthy (e. g. Godin, 1965) and of questionable value here.

The bay was divided into a series of channels, each of constant length, width, and depth (Fig. III. 1). Table III. 1 gives the physical dimensions of each section, along with some other useful constants. The schematization for the analytical model is identical to the one used in the one-dimensional numerical model with the exception that section 7 has been increased to 23. 3 nautical miles. This change gives a more realistic approximation to Chignecto Bay.

The method of solution is the harmonic method (Dronkers, 1964). The equations are simplified by neglecting the advective, viscous and Coriolis terms, so that the primitive equations become

$$\frac{\partial Q}{\partial x} = -b \frac{\partial Z}{\partial t} \qquad \text{III. 1}$$

and

$$\frac{\partial Q}{\partial t} + \lambda Q + g A \frac{\partial Z}{\partial x} = 0. \qquad \text{III. 2}$$

where λ is a friction co-efficient.

If we assume that the x and t dependence of the solutions are separable and harmonic, then the solutions of III. 1 and III. 2 can be expressed in complex form as

$$Z_n(x, t) = H_n(x) e^{+i\omega t} + H_{-n}(x) e^{-i\omega t}, \qquad \text{III. 3a}$$

and

$$Q_n(x, t) = Q_n(x) e^{+i\omega t} + Q_{-n}(x) e^{-i\omega t} \qquad \text{III. 3b}$$

where ω = angular speed of the M_2 tide.

Also,

$$H_n = H^*_{-n}, \qquad \text{III. 4a}$$

and

$$Q_n = Q^*_{-n}, \qquad \text{III. 4b}$$

where * denotes the complex conjugate.

For simplicity of calculation, it is assumed that at time zero high water occurs at the mouth of the bay. This leads to the following:

$$Z_1(x, t) = H_1(x)\, e^{iwt} + H_{-1}(x)\, e^{-iwt} \qquad \text{III. 5}$$

so that $Z_1(x, 0) = H_1(x) + H_{-1}(x)$ III. 6

We further assume that

$$|H_1(0)| = |H_{-1}(0)| = \frac{1}{2} Z_1(0, 0) \qquad \text{III. 7}$$

With these assumptions Q can be eliminated from III. 1 and III. 2, giving

$$\frac{\partial^2 Z_n}{\partial t^2} + \frac{\lambda \partial Z_n}{\partial t} = c_n^2 \frac{\partial^2 Z_n}{\partial x^2}, \qquad \text{III. 8}$$

where $c_n = \sqrt{g \dfrac{A_n}{b_n}}$ = speed of gravity wave. III. 9

Then

$$c_n^2 \frac{\partial^2 H_n}{\partial x^2} + (\omega^2 - \lambda i) H_n = 0. \qquad \text{III. 10}$$

Therefore, $H_n(x)$ is of the form

$$H_n(x) = F_1(x)\, e^{k_n x} + F_2(x)\, e^{-k_n x}, \qquad \text{III. 11}$$

where

$$k_n = \pm \frac{\omega}{c_n} \sqrt{-1 + i \frac{\lambda}{\omega}}. \qquad \text{III. 12}$$

However, by the following expression,

$$\lambda = \frac{8 g \quad Q_{max}}{3 \pi \; C^2 a_n A_n}, \qquad \text{III. 13}$$

where C^2= de Chezy coefficient

$$C^2 = \frac{2 g}{f} \qquad \text{III. 14}$$

we find that
$$\frac{\lambda}{\omega} \approx 10\,f. \qquad \text{III. 15}$$

If we set
$$f = .01, \qquad \text{III. 16}$$

then
$$\frac{\lambda}{\omega} \approx .1. \qquad \text{III. 17}$$

The solution will be much simpler if we set λ identical to zero (i. e. no friction), so that

$$k_n = \pm \frac{\omega\, i}{c_n} \qquad \text{III. 18}$$

is pure imaginary.

The positive value of k_n is used and the solution becomes

$$Z_n(x, t) = \left[H_n(0) \cosh k_n x + Q_n(0) \frac{k_n i}{b_n \omega} \sinh k_n x \right] e^{i\omega t} + \text{c. c.} \qquad \text{III. 19}$$

and
$$Q_n(x, t) = \left[Q_n(0) \cosh k_n x - H_{-n}(0) \frac{\omega b_n i}{k_n} \sinh k_n x \right] e^{i\omega t} + \text{c. c.}\,. \qquad \text{III. 20}$$

This gives
$$H_n(x) = H_n(0) \cosh k_n x + Q_n(0) \frac{k_n i}{b_n \omega} \sinh k_n x \qquad \text{III. 21}$$

and
$$Q_n(x) = Q_n(0) \cosh k_n x - H_n(0) \frac{\omega b_n i}{k_n} \sinh k_n x, \qquad \text{III. 22}$$

as defined in equations III. 3 and III. 4.

Equations III. 21 and III. 22 can be reduced by using the relations

$$\sinh i x = i \sin x \qquad \text{III. 23a}$$

and
$$\cosh i x = \cos x, \qquad \text{III. 23b}$$

giving
$$H_n(x) = H_n(0) \cos \frac{\omega x}{c_n} - Q_n(0) \frac{i}{c_n b_n} \sin \frac{\omega x}{c_n} \qquad \text{III. 24}$$

and III. 25

$$Q_n(x) = Q_n(0)\cos\frac{\omega x}{c_n} - H_n(0)\,i\,b_n c_n \sin\frac{\omega x}{c_n}.$$

Thus, for constant width and depth, the solutions for the frictionless case are trigonometric functions. For the case of exponential width and depth, the solutions are Bessel functions, $J_{\pm n}(x)$, where n is a function of the exponents of width and depth.

At the junction of each rectangular channel, the continuity conditions for tidal height and transport are

$$H_n(1_n) = H_{n+1}(0) \qquad \text{III. 26}$$

and III. 27

$$U_n(1_n) = \frac{A_{n+1}}{A_n} \quad U_{n+1}(0),$$

where A_n= cross-sectional area of section n.

At the junction between Chignecto Bay and Minas Channel

$$H_6(1_6) = H_a(0) = H_b(0) \qquad \text{III. 28}$$

and III. 29

$$A_6 U_6(1_6) = A_a U_a(0) + A_b U_b(0).$$

As in Chapter II, there is the condition of no flow at the end of the model in Chignecto Bay, so that

$$U_7(1_7) = 0. \qquad \text{III. 30}$$

It is seen from Equations III. 24 and III. 25 that the tide and current at each section can now be expressed as:

$$H_n = A_n H_1(0) + B_n U_1(0)\,i \qquad \text{III. 31}$$

and

$$U_n = C_n U_1(0) + D_n H_1(0)\,i, \qquad \text{III. 32}$$

where $U_1(0)$ = vel. at section 1 (mouth)

$H_1(0)$ = vertical tide at section 1 (mouth)

$Q_n = A_n U_n$ (here A_n is cross-sectional area)

and A_n, B_n, C_n, D_n, are constants to be determined by the boundary conditions.

It can be shown that

$$A_n = A_{-n}, \qquad \text{III. 33}$$

$$B_n = -B_{-n}, \qquad \text{III. 34}$$

$$C_n = C_{-n}, \qquad \text{III. 35}$$

$$D_n = -D_{-n}. \qquad \text{III. 36}$$

Table III. 2 lists the values of A_n, B_n, C_n and D_n. From section 1 to 6, these constants vary quite smoothly, with A_n positive and decreasing from 1. 0, B_n negative and decreasing from 0. 0, C_n positive and increasing from 1. 0 and D_n negative and decreasing from 0. 0. This smoothness is soon disrupted due to the condition of no flow at section 1_7 which was simply expressed by setting $C(1_7)$ and $D(1_7)$ equal to zero. C_n and D_n for sections a, 7 and 1_7 are no longer smooth; in fact, D_n is now positive. In order to preserve continuity, it is necessary to find a combination of C_n and D_n such that $U(1_7)$ remains zero but with the constants fitting into the regular smooth pattern, a difficult and perhaps impossible task.

This is now a frictionless model, with the current exactly 90 degrees in advance of the vertical tide; in other words, $H_1(0)$ is real and $U_1(0)$ is imaginary. In Equations III. 3 and III. 4, $H_n(x)$ and $U_n(x)$ refer to the progressive wave travelling up the bay, and the complex conjugates, $H_{-n}(x)$ and $U_{-n}(x)$, refer to the retrogressive wave going back down the bay, so that

$$U_1(0) = |U_1(0)|\ i \quad \text{for the progressive wave} \qquad \text{III. 37}$$

and

$$U_{-1}(0) = -|U_1(0)|\ i \quad \text{for the retrogressive wave.} \qquad \text{III. 38}$$

We find that $H_n(x)$ is real and equals $H_{-n}(x)$ while $U_n(x)$ is imaginary and equals $U_{-n}(x)$. In this way, the functions $Z_n(x, t)$ and $U_n(x, t)$ reduce to cosine functions in the variable t (time).

The currents in this area have been measured but only at a finite number of points and for relatively short periods. The most recent surveys were carried out by Forrester (1958) and Langford (1965). Forrester's current studies were displayed graphically in steps of .5 knot intervals and at integral numbers of hours before and after high and low water only, while Langford's current data are still being analyzed. The value of B_n becomes very large so that rough estimates of $|U_1(0)|$ are not sufficient to yield accurate values of $H_n(0)$. However, reasonable values of $H_n(0)$ are available and we can deduce a value of $|U_1(0)|$ by evaluating Equation III. 31 for each of the 10 cross sections of the model. A final single value of $|U_1(0)|$ can be obtained by the least squares method which, for a linear equation, is equivalent to the algebraic average. The average value of $|U_1(0)|$ was 1.70 ft./sec., taking $H_1(0)$ as 7.5 ft. The M_2 amplitude and flow were calculated for each cross section.

To determine the amplitude in the case of a barrier at section l_9, Cape Sharp, $U_9(l_9)$ is set to zero in Equation III. 32, giving

$$U_9(l_9) = C_9 \; |U_1(0)'| \; i + D_9 H_1(0)\, i, \qquad \text{III. 39}$$

so that

$$|U_1(0)'| = \frac{-D_9}{C_9} H_1(0), \qquad \text{III. 40}$$

where $|U_1(0)'|$ is the value of $|U_1(0)|$ for which $U_9(l_9) = 0$. Substitution of $|U_1(0)'|$ instead of $|U_1(0)|$ into equation III. 31 yields the new value of $H(l_9)$ for section l_9 closed. The value of $|U_1(0)'|$ was 1.46 ft./sec.

The M_2 amplitudes in Chignecto Bay and Minas Channel are plotted in Figure III. 2 and III. 3, respectively. A discrepancy of .3 ft. between the observed and the calculated M_2 tide occurs in Chignecto Bay. Although section l_7 lies approximately at Cape Maringouin, the assumption of zero flow is not entirely valid. Furthermore, the river discharge from the Petitcodiac River into Shepody Bay has also been neglected. Nevertheless the agreement between the two curves is good. The M_2 amplitude is also shown for section l_9 closed. By assumption the three curves match at the mouth. When section l_9 is closed, there is a sizeable drop of 3.2 feet at the barrier site, a decrease of 20%, which is in close agreement with the numerical model. In Chignecto Bay, the maximum decrease is about 12%, and does not agree too well with the previous value of 6% or 7% (Fig. II. 16). The percentage decrease throughout the bay (Fig. III. 4) is different from the previous calculation (Fig. II. 16). The first major difference is a smaller slope in Minas Channel. The second is a positive slope in Chignecto Bay (Fig. II. 16). This corroborates the suspicion that setting C_n and D_n to zero at section l_7 was not a good way to set $U_7(l_7) = 0$.

The volume transports both before and after closing section l_9 (Fig. III. 5 and III. 6) show a discontinuity because the Bay of Fundy splits

into two branches. Naturally, the total flow crossing section 1_6 balances. It is necessary to recall that the assumption of no effect upon the height at section 1 is not perfect. The results at the barrier site are valid and become less and less valid towards the mouth. The degree of validity at the mouth also depends on the size of the perturbation.

The analytical model agrees very well with the numerical model in predicting the water level in Minas Channel, but differs in predicting water levels in Chignecto Bay.

IV. TWO DIMENSIONAL NUMERICAL MODEL

The effects of a barrier upon the M_2 tide in the up and down stream directions have been determined in previous models. These results are not entirely satisfactory but are fairly good approximations. As noted, the M_2 distribution varies across the channel, especially the cotidal surface. The two dimensional model can reproduce the cross stream distribution and permit the inclusion of the Coriolis acceleration in the hydrodynamical equations. The grid lengths used in the two dimensional program are smaller than that used in the one-dimensional, thereby allowing for better approximations of the bottom topography.

The finite difference technique has been used successfully by Prof. W. Hansen of the Institüt für Meereskunde, Hamburg, on the study of storm surges. A study of the M_2 tide in the North Sea was carried out by Brettschneider (1963) of that Institüt using this approach. The equations used here are the same as those employed by Brettschneider.

$$U_t + r\,(U^2 + V^2)^{\frac{1}{2}}\,\frac{U}{H} - f\,V + g\,Z_x = 0, \tag{IV. 1}$$

$$V_t + r\,(U^2 + V^2)^{\frac{1}{2}}\,\frac{V}{H} + f\,U + g\,Z_y = 0, \tag{IV. 2}$$

$$(H\,U)_x + (H\,V)_y + Z_t = 0, \tag{IV. 3}$$

where U = x component of depth mean velocity
V = y component of depth mean velocity
Z = vertical tide, with respect to equilibrium depth
V = friction coefficient
f = Coriolis parameter
H = total depth of water
and g = gravity

For our rectilinear co-ordinate system, the x direction is along the length of the bay, positive towards the head or northeast. The y direction is cross-channel, positive in the north west direction. The z co-ordinate is positive in the upward direction. Quadratic friction is used here; surface wind stress and other meteorological variables are neglected.

To facilitate the finite-difference calculations, the Bay of Fundy was divided into a grid, consisting of U, V and Z field. As in the one-dimensional case, the grid is staggered in time and space. Figure IV. 1

shows the grid configuration and notation. This particular notation was devised tocut down memory requirements in the computer program. The original program was run on a CDC 3100 digital computer with only 16 K word memory. Later, the program was switched to an IBM 360 where concern for the storage capacity of the computer was not a problem.

This particular staggered grid system permits easy computation of Z_x at U-points and Z_y at V-points. One could argue that a grid system where the grid points were 2 Δ 1 apart with U, V and Z calculated at all points gave equal resolution. This is true, but in the latter case, derivatives are calculated from the difference of the value between two points which are 4 Δ 1 apart. The derivatives in the staggered system are based on two points only 2 Δ 1 apart, thereby giving a closer approximation of the derivative. Another advantage of the staggered system is that time integration takes place as a central difference whereas in the other system mentioned, forward and backward differences are employed.

The differential equations were transformed into difference equations of the central difference type. All time derivatives are derived from Taylor expansions:

$$F(t+\Delta t) = F(t) + \Delta t \frac{\partial F(t)}{\partial t} + \frac{(\Delta t)^2}{2!} \frac{\partial^2 F(t)}{\partial t^2} + \frac{(\Delta t)^3}{3!} \frac{\partial^3 F(t)}{\partial t^3} + O(\Delta t^4), \qquad \text{IV. 4}$$

$$F(t-\Delta t) = F(t) - \Delta t \frac{\partial F(t)}{\partial t} + \frac{(\Delta t)^2}{2!} \frac{\partial^2 F(t)}{\partial t^2} - \frac{(\Delta t)^3}{3!} \frac{\partial^3 F(t)}{\partial t^3} + O(\Delta t^4). \qquad \text{IV. 5}$$

This gives IV. 6

$$\frac{F(t+\Delta t) - F(t-\Delta t)}{2t\Delta t} \approx \frac{\partial F(t)}{\partial t}.$$

This is the central difference approximation to the time derivative, where the error is given by

IV. 7

$$\text{Error} = \text{Order}\left[\frac{(\Delta t)^2}{3!} \frac{\partial^3 F(t)}{\partial t^3}\right].$$

The values of Z are calculated by the time integration of Equation IV. 3 at odd times t + 1, where t is an even integer.

$$Z_t^{(t+1)} \approx \frac{Z^{(t+2)} - Z^{(t)}}{2 \Delta t}, \qquad \text{IV. 8}$$

where the superscript refers to the time step. Equation IV. 8 indicates that Z will always be known at even time steps.

The variables U and V are calculated by the time integration of Equation IV. 1 and IV. 2, respectively, at even times t + 0, giving

$$U_t^{(t)} \approx \frac{U^{(t+1)} - U^{(t-1)}}{2 \Delta t}, \qquad \text{IV. 9}$$

and

$$V_t^{(t)} \approx \frac{V^{(t+1)} - V^{(t-1)}}{2 \Delta t}. \qquad \text{IV. 10}$$

This implies that U and V will be calculated at odd times only.

The spatial approximations for Z point calculations are:-

Z (m, n) = water level with respect to equilibrium level at the point Z (m, n)
DEEPU (m, n) = equilibrium depth at the point U (m, n)
ZATU (m, n) = value of Z at the point U (m, n)

$$\text{ZATU}(m, n) = \frac{1}{2}\left[Z(m, n) + Z(m+1, n)\right] \qquad \text{IV. 11}$$

HATU (m, n) = total depth at the point U (m, n)

$$\text{HATU}(m, n) = \text{DEEPU}(m, n) + \text{ZATU}(m, n) \qquad \text{IV. 12}$$

HUX (m, n) = $(HU)_x$ at the point Z (m, n)

$$\text{HUX}(m, n) = \frac{\text{HATU}(m, n)\,U(m, n) - \text{HATU}(m-1, n)\,U(m-1, n)}{2 \Delta 1} \qquad \text{IV. 13}$$

where $\Delta 1$ is the grid length.
Note that 2 $\Delta 1$ is the spacing between two adjacent similar points. The variables above are so named only because they appear that way in the

computer program.

DEEPV (m, n) = equilibrium depth at the point V (m, n)
ZATV (m, n) = Z value at the point V (m, n)

$$ZATV\,(m, n) = \frac{1}{2}\left[Z\,(m, n) + Z\,(m, n-1)\right] \qquad \text{IV. 14}$$

HATV (m, n) = total depth at the point V (m, n)

$$HATV\,(m, n) = DEEPV\,(m, n) + ZATV\,(m, n) \qquad \text{IV. 15}$$

HVY (m, n) = $(HV)_y$ at the point Z (m, n)

$$HVY\,(m, n) = \frac{HATV\,(m, n)\,V\,(m, n) - HATV\,(m, n+1)\,V\,(m, n+1)}{2\;\Delta\;1} \qquad \text{IV. 16}$$

Now Equations III. 3 becomes

$$Z\,(m, n)^{(t+2)} = Z\,(m, n)^{(t)} - 2\;\Delta\;t\;\left[HUX\,(m, n)^{(t+1)} + HVY\,(m, n)^{(t+1)}\right]. \qquad \text{IV. 17}$$

One may notice that in order to evaluate HUX $(m, n)^{(t + 1)}$ and HVY $(m, n)^{(t + 1)}$ we need to know the value of Z $(m, n)^{(t + 1)}$. The values of Z $(m, n)^{(t + 1)}$ are not calculated and so, when needed, the Z $(m, n)^{(t + 1)}$ are approximated by Z $(m, n)^{(t)}$.

The error involved in this approximation is negligible; $Z^{t+2} - Z^{t+1}$ is at most several tenths of a foot, which is much less than the equilibrium depth.

For the U-point calculations, we have:

VATU (m, n) = V component of velocity at the point U (m, n)

$$VATU\,(m, n) = \frac{1}{4}\left[V\,(m-1, n) + V\,(m-1, n-1) + V\,(m, n) + V\,(m, n-1)\right] \qquad \text{IV. 18}$$

ZXATU (m, n) = Z_x at the point U (m, n)

$$ZXATU\,(m, n) = \frac{Z\,(m+1, n) - Z\,(m, n)}{2\;\Delta\;1} \qquad \text{IV. 19}$$

Now Equation III. 1 becomes

$$U(m,n)^{(t+1)} = U^{(t-1)} \qquad \text{IV. 20}$$

$$-2\,\Delta\, t\, r \left[(U(m,n)^{(t)})^2 + (V(m,n)^{(t)})^2 \right]^{\frac{1}{2}} \quad \frac{U(m,n)^{(t)}}{HATU(m,n)^{(t)}}$$

$$+2\,\Delta\, t\, f\, VATU(m,n)^{(t)} - 2\,\Delta\, t\, g\, ZXATU(m,n)^{(t)}.$$

In the second and third terms on the right hand side of IV. 20, values of $U(m, n)^t$ and $V(m, n)^t$ are required.

These are approximated by

$$U(m,n)^{(t)} \approx U(m,n)^{(t-1)}, \qquad \text{IV. 21}$$

and

$$V(m,n)^{(t)} \approx V(m,n)^{(t-1)}. \qquad \text{IV. 22}$$

Then, the sum of the first and second terms on the right of Equation IV. 20 becomes

$$U(m,n)^{(t-1)} \left[\frac{1 - 2\,\Delta\, t\, r \left[(U(m,n)^{(t-1)})^2 + (VATU(m,n)^{t-1})^2 \right]^{\frac{1}{2}}}{HATU(m,n)^{(t)}} \right]. \qquad \text{IV. 23}$$

At this stage, a stability factor is applied to the leading $U(m, n)^{(t-1)}$ factor.

$$U(m,n)^{(t-1)} \longrightarrow \overline{U(m,n)}^{(t-1)}, \qquad \text{IV. 24}$$

where IV. 25

$$\overline{U(m,n)}^{(t-1)} = a\, U(m,n)^{(t-1)}$$

$$+ \frac{(1-a)}{4} \left[\begin{array}{l} U(m+1,n)^{(t-1)} + U(m-1,n)^{(t-1)} \\ + U(m,n-1)^{(t-1)} + U(m,n+1)^{(t-1)} \end{array} \right]$$

$$= U(m,n)^{(t-1)} + \frac{(1-a)}{4} \quad (2\,\Delta\, 1)^2 \quad \nabla^2 U(m,n)^{(t-1)},$$

and where α is a stability factor.

The last term of IV. 25 is of the form A $\nabla^2 U$, where A is a coefficient of lateral diffusion of momentum (Fischer, 1965). For V point calculations, we have

UATV (m, n) = U component of velocity at the point V (m, n)

$$\mathrm{UATV}(m, n) = \frac{1}{4}\left[U(m-1, n) + U(m-1, n+1) + U(m, n) + U(m, n+1)\right] \qquad \text{IV. 26}$$

ZYATV (m, n) = Z_y at the point V (m, n)

$$\mathrm{ZYATV}(m, n) = \frac{Z(m, n) - Z(m, n+1)}{2\ \Delta\ 1} \qquad \text{IV. 27}$$

Equation IV. 2 becomes

IV. 28

$$\begin{aligned} V(m, n)^{(t+1)} &= V(m, n)^{(t-1)} \\ &- 2\,\Delta\, t\, r\left[(\mathrm{UATV}(m, n)^{(t)})^2 + (V(m, n)^{(t)})^2\right]^{\frac{1}{2}} \frac{V(m, n)^{(t)}}{\mathrm{HATV}(m, n)^{(t)}} \\ &- 2\ \Delta\ t f\, \mathrm{UATV}(m, n)^{(t)} - 2\ \Delta\ t g\, \mathrm{ZYATV}(m, n)^{(t)} \end{aligned}$$

By using the same technique as in the U-point calculations, we can also introduce an A $\nabla^2 V$ term into equation IV. 28 where

$$\overline{V(m, n)}^{(t-1)} = V(m, n)^{(t-1)} + \frac{(1-\alpha)}{4}(2\Delta 1)^2 \nabla^2 V(m, n)^{(t-1)} \qquad \text{IV. 29}$$

The finite difference approximation of the hydrodynamical equations becomes

IV. 30

$$Z(m, n)^{(t+2)} = \overline{Z(m, n)}^{(t)} - 2\ \Delta\ t\left[\mathrm{HUX}(m, n)^{(t+1)} + \mathrm{HVY}(m, n)^{(t+1)}\right],$$

IV. 31

$$U(m,n)^{(t+1)} = \overline{U(m,n)}^{(t-1)} \left[1 - 2\,\Delta\, t\, r \frac{\left[(U(m,n)^{(t-1)})^2 + (VATU(m,n)^{(t-1)})^2 \right]^{\frac{1}{2}}}{HATV(m,n)^{(t)}} \right]$$

$$+ 2\,\Delta\, t\, f\, VATU(m,n)^{(t-1)} - 2\,\Delta\, t\, g\, ZXATU(m,n)^{(t)},$$

and IV. 32

$$V(m,n)^{(t+1)} = \overline{V(m,n)}^{(t+1)} \left[1 - 2\,\Delta\, t r \frac{\left[(V(m,n)^{(t-1)})^2 + (V(m,n)^{(t-1)})^2 \right]^{\frac{1}{2}}}{HATV(m,n)^{(t)}} \right]$$

$$- 2\,\Delta\, t\, f\, UATV(m,n)^{(t-1)} - 2\,\Delta\, t\, g\, ZYATV(m,n)^{(t)}.$$

where r = friction constant
= .003,
α = stability factor
= .99,
$1-\alpha$ = .01,
Δt = 1 lunar minute
= 62.1030 solar seconds,
$\Delta 1$ = grid length (to be given),
φ = latitude (taken as a constant)
= 45 degrees north,
f = Coriolis parameter
= $2\,\Omega \sin\varphi$ (where Ω = angular speed of earth)
= 1.02820×10^{-4} rad./sec.,
and ω = angular speed of M_2 constituent
= .4880373 degrees/lunar minute
= .4880373 degrees/time step.

For our staggered grid system, the accepted criterion for numerical stability is

$$2\,\Delta\,1 > 2\,\Delta\, t \sqrt{2\, g\, D_{max}}\,, \qquad \text{IV. 33a}$$

$$2\,\Delta\,1 > 24000 \text{ feet}\,. \qquad \text{IV. 33b}$$

Calculations for the two dimensional grid were carried out on two systems of different grid length. One, identified as FUNDY 01, employed a grid length of 60,800 feet and the second, FUNDY 02, employed a grid length of 25,760 feet.

The initial values, at time zero of Z, were taken as the product of the observed amplitude and the cosine of the observed phase lag. The initial values of the U and V components of the velocity were assumed to be zero. This assumption was necessary since little is known about them. On the solid boundaries the normal component of the velocity is zero.

$$W_n = 0 . \qquad \text{IV. 34}$$

On the open boundaries, in this case the left, it is assumed that

$$\frac{\partial U}{\partial x} = 0 . \qquad \text{IV. 35}$$

This facilitates calculations for V on the open boundary in IV. 26.

In the various grid systems, and for various boundary conditions, we are faced with the problem of looking at and comparing the U, V and Z fields for a large number of points. To do this, it would be convenient to have steady-state solutions which were reasonably sinusoidal, so that we need only to look at the amplitude and phase lag at each point. This was done in the one-dimensional solution without explanation. In this way we can correlate the solutions at every grid point on one corange chart and one cotidal chart.

The steady state solution is not perfectly sinusoidal but is close enough to be approximated as a single harmonic. The amplitude was taken as the average of the high and low water heights. The phase lag was taken as the average of the high water phase lag and the low water phase lag with 180 degrees added to it. For this reason, the non-linear UU_x term was omitted from the equations of motion.

Although friction did not seem to distort the sine wave form it was left in the equations. The values of Z on the left boundary are inputted into the program so that energy is continually being supplied to the model. A principal symptomn of computational instability is a growth or decay in energy. Thus, a frictionless model might become unstable. This is why a relatively large friction constant has been used.

System FUNDY 01

In the first of the two-dimensional grids, FUNDY 01, a double grid length of $2 \Delta l = 60,800$ ft. was used (Fig. IV. 2 and Table IV. 1). Obviously the coast line approximation is not the best but should be sufficient to give reasonable cross stream distributions. The model does not extend into the far reaches of Chignecto Bay and Minas Basin, where the shoreline approximation would be very poor with such a large grid length. Jelesnianski (1965) used a patched grid system for storm surge calculations on a

continental shelf, with a smaller grid length for points near shore than for points far removed from the shore. Detailed calculations can then be limited to the near shore grid points. However, a patch grid system is not necessary for this study. Details in Minas Channel and Chignecto Bay will be studied in a finer grid system, FUNDY 02. The results of grid system FUNDY 01 will serve as a check on the results of grid system FUNDY 02.

Calculations FUNDY 01 A and FUNDY 01 B

The first two calculations with grid system FUNDY 01 were attempts to reproduce the observed M_2 configuration. In FUNDY 01 A the observed M_2 was imputted at columns m = 5 and m = 13. The assumption U (m, 4) = U (m, 5) allows easy calculation of V (5, n) in IV. 32. Calculation of $\nabla^2 U$, $\nabla^2 V$, $\nabla^2 Z$ is difficult for points adjacent to the solid boundary; for example, the central difference form of $\nabla^2 Z(6, 2)$ requires the value of Z (6, 1) which is undefined. In order to overcome this, it is necessary to take the backward difference for

$$\frac{\partial^2 Z(6, 2)}{\partial^2 y^2} \approx \frac{Z(6, 4) - 2Z(6, 3) + Z(6, 2)}{(2 \Delta 1)^2} . \qquad \text{IV. 36}$$

The point Z (6, 4) is more than half way across to the other side of the bay so that the backward approximation is poor. The only alternative is to neglect $\frac{\partial^2}{\partial x^2}$ and $\frac{\partial^2}{\partial y^2}$ wherever the central difference form is undefined.

In calculation FUNDY 01 A, off boundary values of Z were interpolated from charts of the observed M_2 surface and then used to calculate $\nabla^2 Z$. Values of $\nabla^2 U$ and $\nabla^2 V$ next to the solid boundary were assumed to be zero.

In calculation FUNDY 01 B, $\nabla^2 U$, $\nabla^2 U$ and $\nabla^2 Z$ were all neglected near the boundary. The amplitudes calculated in Fundy 01 A and in Fundy 01 B differ at most by 0. 1 ft. (Table IV. 2), and the phase lags by 1. 7 degrees. It is evident that neglecting the ∇^2 operator at points adjacent to the solid boundary is of little consequence.

The amplitudes calculated in Fundy 01 A and Fundy 01 B differ from the observed amplitude by no more than 1% (Table IV. 3). Figure IV. 3 demonstrates the error in judging the spacing and curvature of the "observed" lines in spite of the fact that we assumed the calculated and observed values to be identical at the mouth (column m = 5). From shallow water considerations the corange lines can be expected to be curved with the concave side towards the mouth, but in the centre of the model they are curved in the opposite direction. Despite this difference in curvature, the correlation between calculated and observed values is very good.

The agreement between the observed phase lag and the phase lag calculated in Fundy 01 A and Fundy 01 B (Fig. IV. 4) is not as good as that for the amplitude. This is understandable because the phase lag is generally a difficult quantity to determine accurately. The outstanding feature of the calculated cotidal lines is that they make a smaller angle with the axis or length of the bay than do the observed cotidal lines. The calculated difference in phase lag between points on opposite shores in the vicinity of Digby, N. S. is greater than expected. The curvature of the cotidal lines, a shallow water effect, is also greater than expected. The observed and calculated phase lags differ by 3 to 4 degrees near Digby and by 1 to 2 degrees on the opposite shore.

Little is known about the stability factor α , so a series of calculations was carried out in which α was varied between zero and one. The calculations became more stable as α approached 1. 0 and unstable as α approached 0. The value of α decided upon was . 99, the value used by Brettschneider (1963).

Calculation Fundy 01 C

The final calculation for the coarse grid system, Fundy 01C, was for a barrier at the mouth of Minas Channel. This meant setting U (12, 5) = 0.

The tide at the mouth of the bay is assumed to be unaffected by this barrier, but this assumption cannot be used for the tide at the entrance to Chignecto Bay which is too close to the barrier. Either the Chignecto Bay branch could be extended right up to its head (with zero flow), or a barrier could be erected at the entrance to both branches of the bay. The latter case was selected for Fundy 01 C.

The amplitude in front of the barrier with U (12, n) = 0. 0 dropped from 13. 5-14. 0 ft. down to 10. 9 ft. (Fig. IV. 5).

The entire corange surface agrees with the previous one-dimensional results in that the gradient of this surface decreases towards the barrier. The decrease in amplitude, as a percentage of the normal value, is 22% in Minas Channel and 18% in Chignecto Bay (Fig. IV. 7). This conforms to expectations that perturbations in the Minas Channel branch of the bay will have greater effect than those in Chignecto Bay.

The phase lag is now only 333 to 334 degrees at the barrier sites (Fig. IV. 6). Furthermore, the difference between the average phase lag at the mouth and the average value at the barrier sites is only 4 degrees. The 334° cotidal makes an angle of more more than 25° with the longitudinal axis of the bay. The tide exhibits strong standing wave character, expecially along the northwest shoreline where the difference in phase between mouth and barrier appears to be only 1 or 2 degrees. Along the southeast shore

the tide also displays standing wave character but to a lesser degree with a difference in phase between the mouth and barrier of 5 to 6 degrees.

The decrease in phase lag caused by the barrier is 9 degrees at the barrier site (Fig. IV. 8) and attenuates only gradually towards the mouth of the bay. Contrary to expectations, the decrease in phase lag is greater in front of Chignecto Bay than in front of Minas Channel. The calculations in the finer grid system, Fundy 02, will help to determine whether or not these decreases in phase lag are reasonable.

System Fundy 02

System Fundy 02 (Fig. IV. 9) has a double grid length of $2 \Delta 1 =$ 25, 760 ft., less than one-half that of system Fundy 01 and the depth is listed in Tables IV. 4 and IV. 5. Fundy 02 definitely approximates the shoreline much better than does Fundy 01, but it is not without fault either. The worst flaw in grid system Fundy 02 is its approximation to Minas Channel as a rectangle with a narrow opening at each end of width $2 \Delta 1$. The opening in the vicinity of U (20, 10) is smaller than reality and will cause larger than normal gradients in the M_2 surfaces at the point U (20, 10). This in turn will flatter the M_2 surfaces in Minas Channel. The model also does not see the "hook-like" shape of Cape Split since it cannot describe effects on a scale smaller than the grid length. The small scale variations in the shoreline can only be incorporated into the calculations by the use of a smaller grid length. This would further necessitate the use of a smaller time step. The purpose of this study is to look only at the overall tidal configuration, and the use of a finer grid length would be impractical.

The grid points in Fundy 02 are much closer than in Fundy 01. Whereas in Fundy 01 boundary values of $\frac{\partial^2}{\partial x^2}$ and $\frac{\partial^2}{\partial y^2}$ were neglected, in Fundy 02 they can now be approximated by the appropriate backward or forward difference approximation whenever the centre difference form cannot be obtained. For example, $\nabla^2 Z(15, 5)$ is approximated by

$$\nabla^2 Z(15, 5) = \left[Z(14, 5) - 2Z(15, 5) + Z(16, 5) \right] / (2 \Delta 1)^2 + \left[Z(15, 5) - 2Z(15, 6) + Z(15, 7) \right] / (2 \Delta 1)^2. \qquad \text{IV. 37}$$

With $2 \Delta t$ equal to 2 lunar minutes and $2 \Delta 1$ equal to 25, 760 ft., the criterion for computational stability is barely satisfied. To make the computations more stable, a smoothing operator is applied to the Z values. This technique has been used by Harris and Jelesnianski (1964). If S_n is an

operator, then the 9-point smoothing operator is defined as

$$S_9 \left[Z(m,n) \right] = \frac{1}{16} \left[\begin{array}{l} Z(m-1,n-1) + 2Z(m,n-1) + Z(m+1,n-1) \\ + 2Z(m-1,n) + 4Z(m,n) + 2Z(m+1,n) \\ + Z(m-1,n+1) + 2Z(m,n+1) + Z(m+1,n+1) \end{array} \right] \qquad \text{IV. 38}$$

It can be abbreviated as

$$S_9 \left[Z(m,n) \right] = \frac{1}{16} \begin{vmatrix} 1 & 2 & 1 \\ 2 & 4 & 2 \\ 1 & 2 & 1 \end{vmatrix} Z(m,n), \qquad \text{IV. 39}$$

where IV. 39 is the "filter factor form" of the 9-point smoothing operator. S_9 cannot always be used. For boundary grid points, some of the neighbours of the central point (m, n) do not exist and more restricted forms of the smoothing operator must be used. These are

$$S_5 \left[Z(m,n) \right] = \frac{1}{8} \begin{vmatrix} 0 & 1 & 0 \\ 1 & 4 & 1 \\ 0 & 1 & 0 \end{vmatrix} Z(m,n), \qquad \text{IV. 40}$$

and

$$S_3 \left[Z(m,n) \right] = \frac{1}{4} \begin{vmatrix} 1 & 2 & 1 \end{vmatrix} Z(m,n). \qquad \text{IV. 41}$$

S_3 can be applied to points along a boundary parallel to the x axis, or it can be rotated 90° and applied to points along a boundary parallel to the y axis. As examples, S_5 is applied to Z (4, 3), S_3 (rotated 90°) to Z (20, 8). Corner points such as Z (9, 3) are not smoothed at all and therefore become possible sources of instability.

Harris and Jelesnianski (1964) stated that the non-linear terms of the equations tend to divert energy from the principle harmonic to both higher and lower harmonics. The harmonic of wavelength 4 Δ l was found to be the most troublesome. S_{16}, S_9 and S_3 filter out this high frequency harmonic without changing the mean value of Z nor introducing a phase-shift.

<u>Fundy 02 A</u>

In this calculation and in calculation Fundy 02 B, the grid system shall extend only as far as the column Z (21, n). The first step is to reproduce the natural M_2 tidal configuration. The values of Z (21, n) are taken as the observed M_2 tide.

The calculated M_2 corange surface and the observed corange surface are plotted in Figure IV. 10. The difference between them is even greater than that found for the calculation of Fundy 01 A (Fig. IV. 3), the maximum difference being . 4 foot. The differences between the calculated curves of Figure IV. 3 and Figure IV. 10 are small, at most . 2 ft. The

important thing is the greater curvature of the corange lines in Figure IV. 10. In all calculations the variables are calculated only at a finite number of points. Values of these variables between grid points are found by rough linear interpolation. Since system Fundy 02 employs a finer grid length, the results from system Fundy 02 contain less uncertainty than those from Fundy 01, even though the surfaces agree very well.

The calculated phase lag of Fundy 02 A by as much as 4 degrees from the observed phase lags (Fig. IV. 11). This shows quite definitely that the chart of the "observed" phase lag in the Bay of Fundy was hydrodynamically incorrect.

The time relationship between the vertical displacement Z and the horizontal components of the velocity for the point (10, 7) is shown in Figure IV. 12(a). The wave form appears to be reasonably sinusoidal, supporting the method of correlating the tide at all the grid points from a simple harmonic point of view. The U component is slightly less than one quarter period in advance of high water. This difference, as much as 40 minutes, results from friction, (Fig. IV. 12(b)).

In numerical calculations for boundary value problems, it is always of interest to see how quickly the calculations reach steady state. The differences in the amplitude and phase lag for the time of first extremum and for steady state are at most . 3 ft. and 2 degrees (Fig. IV. 13 and IV. 14). Steady state was reached within three tidal cycles or 37 hours. For example, U (20, 10) only took 1. 5 tidal cycles (Fig. IV. 15). In calculation Fundy 02 B, it will be shown that whenever the boundary condition of no flow is used (as opposed to given values of Z) the calculations are less stable and thus take several tidal cycles longer to reach steady state.

In all the two-dimensional grid systems used here, U and V are calculated at different points in space. To obtain current ellipses, the two components must be combined vectorially at a common grid point. This is carried out by the following relations.

UATZ (m, n) = U component at the point Z (m, n)

$$\mathrm{UATZ}(m, n) = \frac{1}{2}\left[\mathrm{UATU}(m-1, n) + \mathrm{UATU}(m, n)\right], \qquad \text{IV. 42}$$

VATZ (m, n) = V component at the point Z (m, n)

$$\mathrm{VATZ}(m, n) = \frac{1}{2}\left[V(m, n-1) + V(m, n)\right]. \qquad \text{IV. 43}$$

We now have

$$\overrightarrow{W(m, n)} = \overrightarrow{\mathrm{VATZ}(m, n)} + \overrightarrow{\mathrm{UATZ}(m, n)}, \qquad \text{IV. 44}$$

where W (m, n) is the resultant velocity vector at the point Z (m, n).

Therefore

$$\left| W(m,n) \right| = \sqrt{VATZ(m,n)^2 + UATZ(m,n)^2} . \qquad \text{IV. 45}$$

In these solutions, VATZ (m, n) and UATZ (m, n) are taken as harmonic functions of the type

$$VATZ = VATZ_{max} \cos(\omega t - g) . \qquad \text{IV. 46}$$

Differentiation of IV. 45 with respect to t leads to the solution for the orientation, magnitude and phase lag of the major and minor axis of the current ellipses. The axes of these ellipses are plotted in Figure IV. 16. Over most of the Bay of Fundy, the tidal streams are of an alternating character. Only near the mouth, on the inward side of Grand Manan Island are the streams rotating. When the tidal streams do rotate, they rotate clockwise.

An example, for the point Z (3, 10), is found in Figure IV. 17. Most of the streams have their axes nearly parallel to the longitudinal axis of the bay. The largest streams are found in the vicinity of Minas Channel. The phase lags of the major axis of the current ellipses display a somewhat irregular pattern (Table IV. 6), particularly towards the mouth of the bay. The rotating nature of the currents there make it difficult to determine the orientation of the major axis accurately.

The co-amplitude lines of the U component of the velocity converge at the corners of the model as one would expect (Fig. IV. 18). The U distribution across the channel is very smooth and goes to zero quickly very close to the shore. The size of the grid length prevents close examination of the U contour near the shore.

The average value of U along cross section m = 2 is roughly 2. 7 ft. /sec. In the analytical model a value of 2. 5 ft. /sec. was found for the same cross section. The difference of 0. 2 ft. /sec. can by explained by the omission of friction in the analytical model. These values are also in general agreement with Forrester (1958).

The V component of the velocity is small generally except at the mouth of the bay, which makes it difficult to determine the time of maximum V. This uncertainty is probably another cause of the irregularities in the phase lags of the major axis of the current ellipses. Where the current is of an alternating character, the phase of V is either equal to or 180° out of phase with the phase of U. This causes the alternating current to be oriented at a small angle to the longitudinal axis

of the bay.

Calculation FUNDY 02 B

In calculation FUNDY 02 B, the entrances to Chignecto Bay and Minas Channel were closed by setting U (20, n) = 0, making calculation FUNDY 02 B very similar to calculation FUNDY 01 C. The gradients in the co-range surface decrease rapidly towards the barrier site (Fig. IV. 19), and in this case, the tidal wave behaves as a standing wave (Fig. IV. 20), as demonstrated by the 3 degree difference in phase lag between Grand Manan I. and Cape Chignecto.

The barriers in front of both channels of the bay are parallel, causing the lines of equal U amplitude to lie parallel to each other directly in front of the barrier (Fig. IV. 21). The values of Z at the mouth have been assumed to be unaffected by the barrier so that the perturbed U amplitude surface is similar to the normal U amplitude configuration (Fig. IV. 18). The main difference is that the average value of U across the mouth is now only 2. 0 ft. /sec. In the analytic solution the value of U at that cross section for the same boundary conditions was 2. 1 ft. /sec.

The percentage decrease in M_2 amplitude (Fig. IV. 22) (caused by setting U (20, n) = 0) are 21% and 27%, respectively, at the barrier sites in Chignecto Bay and Minas Basin.

Although the two sets of results differ in value, there are several similarities. Firstly, the ratio of the percentage decrease at the Chignecto Bay barrier site to that at the Minas Channel barrier site is the same for both calculations. Secondly, the shape of the surfaces in the two calculations is similar. It has been explained that any numerical approximation to the length or width of any body of water is limited to integral multiples of 2 Δ 1. The grid lengths for FUNDY 01 and FUNDY 02 differ by a factor of 2, so that their approximations to the physical size and shape of Minas Channel and Chignecto Bay also differ.

The surface representing the decrease in the M_2 phase lag appears to lie symmetrically about the longitudinal axis of the bay (Fig. IV. 23). Near both shores, the contours curve away from the barrier, giving the surface the shape of a trough slanted downwards towards the mouth of the bay.

Judging from Figure IV. 22 and IV. 23, the effects of the Chignecto Bay - Minas Channel barrier are relatively large. The perturbation attenuates at a constant rate between its large value at the barrier and its zero value at the mouth, indicating that the assumption of no effect upon Z at the mouth is not entirely valid. The outer boundary of the model should perhaps have been extended much farther out into the Gulf of Maine.

However, the tidal configuration is not known accurately there. A better choice may have been a line across the bay on the ocean side of Grand Manan I., but this would mean the inclusion of Passamaquoddy Bay where the narrow entrances would necessitate the use of a very small grid length.

Calculation FUNDY 02 C

This calculation is essentially the same as FUNDY 02 A except that the northeastern boundary has been extended in both channels. As expected, the M_2 corange surface (Fig. IV. 24) agrees with calculation FUNDY 02 A (Fig. IV. 10). The M_2 cotidal surface (Fig. IV. 25) also agrees with FUNDY 02 A. The large gradient in Minas Channel is caused partly by the blocking effect of Cape Split and partly from a crude approximation of the entrances to Minas Channel and Minas Basin.

Three additional cases will be considered, two of which include a single barrier, and the third both barriers. These cases will be designated FUNDY 02 D, E and F.

Calculation FUNDY 01 D

In the first of these calculations, a barrier was erected near Cape Split by setting

$$U(23, 10) = 0.0 \qquad \text{IV. 47}$$

The tide at the head of Chignecto Bay was assumed to be unaffected by this barrier: i. e. Z (24, 6) was taken as the observed M_2 tide. This is a simple but poor assumption since Z (24, 6) is close to the barrier site.

The resulting corange surface is plotted in Figure IV. 26. The tide has decreased almost 3 ft. in Minas Channel and the corange surface is almost flat. Between the entrance and the end of Minas Channel the difference in amplitude is roughly . 3 ft., whereas normally it is over 1. 5 ft. Over the rest of the bay there seems to be little change in the corange surface.

The difference in phase lag between the entrance and end of Minas Channel was also decreased appreciably, showing now a range of 2 or 3 degrees as compared to the normal range of 10 degrees (Fig. IV. 27).

The maximum decrease in amplitude is 14% at the barrier site. The effect is localized because of the constriction (in both width and depth) at the entrance to the channel. What little of the perturbation that does survive the constriction is attenuated quite quickly, although in the main part of the bay the gradient is not as large as in Minas Channel. Near the mouth of the bay the perturbation is barely felt.

The difference between the decrease in amplitude of 14% in FUNDY 02 D and the value of 20% in the analytic model is partly explained by the fact that the analytic model has a condition of no flow at the head of Chignecto Bay while this model (FUNDY 01 D) has no such condition,(see Fig. IV. 28).

The constriction at the entrance to Minas Channel also affects the decrease in phase lag (Fig. IV. 29). In fact, the gradient is larger at the constriction than it is at the barrier site. The effect of the barrier upon the phase lag is even more localized than the effect upon the amplitude, so that the assumption of no effect upon the vertical tide at the mouth of the bay is quite reasonable for calculation FUNDY 02 D.

Calculation FUNDY 02 E

In calculation FUNDY 02 E, a single barrier in Chignecto Bay is considered, with the boundary condition

$$U(24, 6) = 0.0 \qquad \text{IV. 48}$$

The tide at the entrance to Minas Basin (Z (24, 10) is inputted as the observed M_2 tide. At the barrier site, the amplitude is now 12. 5 ft., a decrease of about 1. 5 ft., and the corange surface becomes extremely flat. The resulting corange surface (Fig. IV. 31) is also very flat in Chignecto Bay. At the barrier site, the phase is less than 344 degrees, with little change from the normal configuration.

The maximum decrease in amplitude is 12-13% at the barrier site (Fig. IV. 32). Once again, this perturbation is localized, even more so than that for calculation FUNDY 02 D (Fig. IV. 28). The maximum decrease in phase lag is only 5 degrees (Fig. IV. 33). The perturbation does not propagate very far (the best example of localization in this study) and is an indication of the relative unimportance of Chignecto Bay in the Bay of Fundy system.

Calculation FUNDY 02 F

In this last calculation of barriers in the Bay of Fundy, the barriers of FUNDY 02 D and FUNDY 02 E are erected simultaneously by setting

$$U(24, 6) = U(24, 10) = 0.0 \qquad \text{IV. 49}$$

The corange surface (Fig. IV. 34) undergoes an appreciable decrease in amplitude but not as large a decrease as in calculation FUNDY B (Fig. IV. 19). In Chignecto Bay, the maximum amplitude is 11. 5 ft. and in Minas Channel, 11. 9 feet. The corange surface is again flat in front of the barriers, being flatter in Chignecto Bay than in Minas Channel.

The maximum phase lag is 334 degrees in Minas Channel and 334 - 335 degrees in Chignecto Bay. The tendency towards standing wave character between Grand Manan I. and Cape Chignecto is again apparent, with a phase difference of only 4 degrees, (Fig. IV. 35).

The percent decreases in amplitude are 19 - 20% and 20 - 21% directly in front of the Chignecto Bay and Minas Channel barrier sites, respectively (Fig. IV. 36). The 13% contour indicates that the effect from the Chignecto Bay barrier attenuates faster than does the effect from the Minas Channel barrier. This is also shown by the slope of the lines between 1% to 12%.

The greatest decreases in phase lag are 24 - 25 degrees in Minas Channel and 13 degrees in Chignecto Bay (Fig. IV. 37). This is a ratio of almost 2 to 1 and yet the phase lag perturbation from the Chignecto Bay barrier propagates further down the bay than does the effect from the Minas Channel barrier. The smaller effect on the southeast shore of the Bay of Fundy is again due to the constriction at the entrance to Minas Channel where we find an extremely large gradient in the surface of decrease in phase lag. The perturbation as a whole is large and travels right down the bay, again indicating that the assumption of no effect upon Z at the mouth is not good.

Correlation of FUNDY 02, C, D, E and F

In calculations FUNDY 02 D and E, the assumption was made that a barrier in one channel did not affect the vertical tide in the other channel and vice versa, an obviously incorrect assumption. For each of calculations FUNDY 02 D and FUNDY 02 E only one result can be taken as reasonably valid, namely the decreases as calculated for that area immediately in front of the barrier. We will now attempt to get an estimate of the effect of the barrier at each channel upon the tide at the end of the other channel. This crude estimate requires the results from calculation FUNDY 02 F, which included both the barriers at the same time. Only the percent decrease in amplitude will be discussed here.

In calculating the effect of the Minas Channel barrier at the barrier site, the following configuration was used. The "hash marks" indicate a barrier.

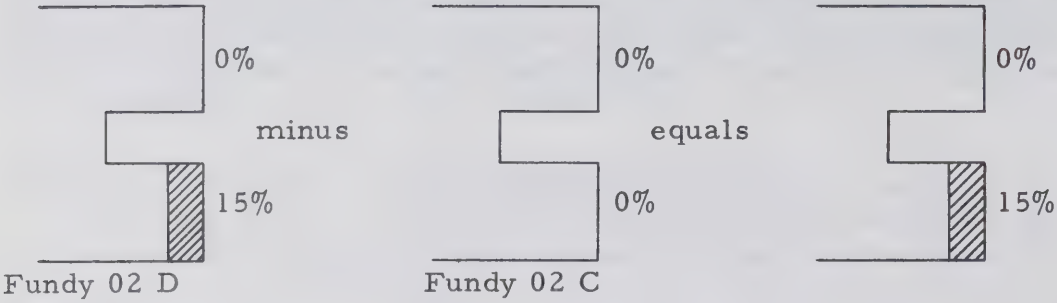

Fig. IV. 38

The maximum effect of the Minas Channel barrier at the end of the Chignecto Bay is estimated as follows:

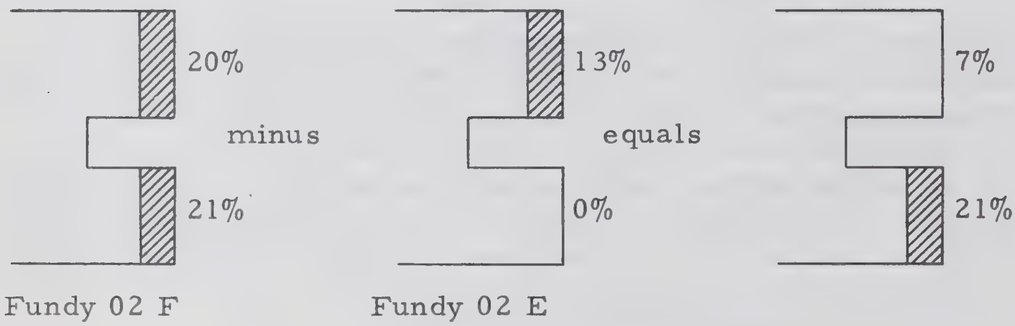

Fig. IV. 39

The maximum effect of the Chignecto Bay barrier upon the tide at the end of Minas Channel is estimated in similar manner.

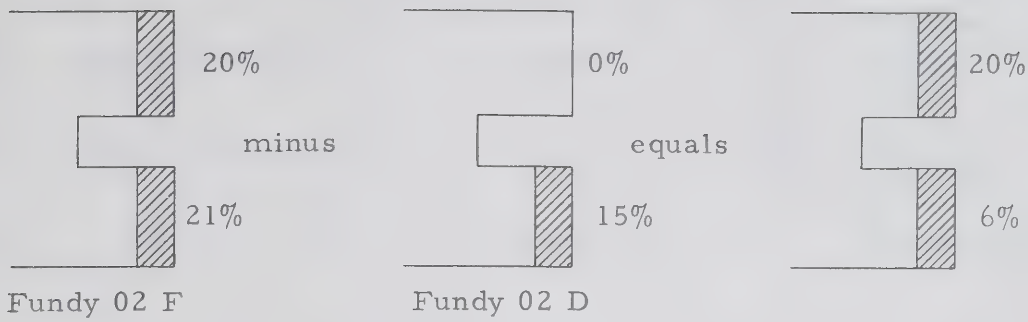

Fig. IV. 40

Admittedly, this is a weak method. These estimates should be regarded only as upper limits of the perturbation in the opposite channel, and in all probability, the real value is less than these maximum values. Similar reasoning was applied to the phase lags, and the results are listed below.

M_2 AMPLITUDE	Decrease in amplitude of ZATU (23, 10) (Minas Channel)	Decrease in amplitude of ZATU (23, 6) (Chignecto Bay)
U (23, 10) = 0 only (Minas Channel barrier)	15%	at most 7%
U (23, 6) = 0 only (Chignecto Bay barrier)	at most 6%	13%
U (23, 6) = 0 U (23, 10) = 0 (both barriers)	21%	20%

M_2 PHASE LAG	Decrease in phase lag of ZATU (23, 10)	Decrease in phase lag of ZATU (23, 6)
U (23, 10) = 0 only (Minas Channel barrier)	20 deg.	at most 8 deg.
U (23, 6) = 0 only (Chignecto Bay barrier)	at most 5 deg.	5 deg.
U (23, 6) = 0 U (23, 10) = 0 (both barriers)	25 deg.	13 deg.

The above results look very reasonable with one exception, the effect of the Chignecto Bay barrier upon the phase lag in Minas Channel is closer to zero rather than a 5% decrease.

Calculation FUNDY 02 G

UU_x, the largest advective term in the expansion of $\frac{dU}{dx}$, was previously neglected because of its non-linearity. It will now be included in calculation FUNDY 02 G. The boundary condition at the head of the bay is identical to FUNDY 02 F, that is, U (23, n) = 0.

A typical value of U, U (18, 7), is plotted as a function of time (Fig. IV. 41), one case with the UU_x term included in equation IV. 1 and the other with this term omitted. The inclusion of the UU_x term not only results in the displacement of the curve by . 1 ft. /sec. in the positive direction, but the time of maximum is advanced and the time of minimum delayed, both by not more than 15 - 20 minutes. The curve now has a slight "sawtooth" shape which can be interpreted as wave breaking.

Similar effects are seen in the Z values. In a comparison of Z (23, 6) in FUNDY 02 F and FUNDY 02 G, the time of maximum in FUNDY 02 G was found to be advanced by 20 minutes (Fig. IV. 42) and the maximum height was lowered by less than . 1 ft. The time of low water was delayed but the minimum was lowered by . 2 ft. (Fig. IV. 43), so that the Z values have also become slightly sawtooth and have been displaced in the negative direction (Table IV. 7).

The advancement of high water and delay of low water is found over the whole bay (Table IV. 8). Near the head of the bay, the absolute value of low water is substantially greater than the absolute value of high water. Furthermore, the time of low water plus 180° is much later than high water. Low water seems to display progressive wave characteristics while high water displays standing wave characteristics which implies that the difference in the time of low water between two stations should be greater than the difference in the time of high water between the same two stations. This was checked by examining tidal records for St. John and Grindstone I. The high water time differences are less than the low water time differences (Table IV. 9); the average value is 9 minutes less. A scrutiny of several other tidal records showed similar trends.

When the average amplitude and phase lag with UU_x included are compared with those values obtained without UU_x (Tables IV. 10 and 11), there seems to be only a slight difference at the head of the bay. The values with UU_x are at most 1/2 degrees earlier and . 07 ft. less than those values without UU_x.

FUNDY 02 H

In this calculation, all depths were set to the constant value of 240 ft., the average depth of the bay within the model. The boundary conditions are identical to FUNDY 02 G. The difference between the amplitudes of calculations FUNDY 02 H and FUNDY 02 G were calculated (Table IV. 12). Over most of the bay, the constant depth model gives larger amplitudes than with natural depth. The maximum difference is . 35 - . 40 ft. in the neighbourhood of columns m = 11 and 12. It is in this area that the normal depth averages about 240 ft.; towards the mouth, the depth is greater than 240 ft. and towards the head it is less. The effect of setting the depth constant to 240 ft. is to decrease the depth near the mouth and increase the depth near the head. The amplitude of Z has increased near the mouth and decreased near the head. It would seem that changes in depth have an inverse effect upon the amplitude of Z.

The difference in phase lag between FUNDY 02 G and FUNDY 02 H is also small (Table IV. 13), the maximum being only 2. 7 degrees. The pattern in Table IV. 13 is as expected; the tidal wave travels slower if depth is decreased and faster if depth is increased. This pattern cannot be determined accurately, the uncertainty in the values is ± (. 5 + . 5) = ± 1 degree.

V. POTENTIAL ENERGY IN THE BAY OF FUNDY

Energy can be expressed as

$$E = \frac{\rho}{2} \int_A \left[g Z^2 + (U^2 + V^2) H \right] dS \qquad \text{V. 1}$$

where S = surface area
A = region being considered
H = total depth

The Bay of Fundy has already been divided into a fine grid for our finite-difference solutions (grid system FUNDY 02), so that the above integral can be evaluated conveniently by numerical quadrature. The term gZ^2dS is assessed at the Z points, where dS is the square surface of area $(2 \Delta 1)^2$ centred on the Z point. U^2HdS and V^2HdS are evaluated similarly at the squares centred at the U points and V points, respectively.

For example, the maximum kinetic energy in the left most column (m = 2) in the x direction is

$$E_{kin} = \frac{\rho}{2} \sum_{n=2}^{11} \left[U(2, n)^2 H(2, n) (2 \Delta 1)^2 \right] \qquad \text{V. 2}$$

$$= 1.9 \times 10^{13} \text{ foot-pounds (ft.-lb.)}$$
$$= 7.2 \times 10^{6} \text{ kilowatt-hour (kw-hr.)}$$

The maximum potential energy * in the same column is

$$E_p = \frac{\rho}{2} \sum_{n=2}^{11} \left[32.17 \quad Z_{max} (2, n)^2 (2 \Delta 1)^2 \right] \qquad \text{V. 3}$$

$$= 1.4 \times 10^{13} \text{ ft.-lb.}$$
$$= 5.3 \times 10^{6} \text{ kw.-hr.}$$

These are approximate values because only the maximum values of U and Z were used, and the small phase lag differences were neglected. While the kinetic energy here is slightly larger than the potential energy, they are well within the same order of magnitude.

* Potential energy here is calculated with respect to local mean sea level.

By again neglecting the phase lags, the maximum potential energy of various sections of the Bay of Fundy system can be estimated. These values were found to be

Area	Potential Energy
Main part of Bay of Fundy	24.0×10^{13} ft.-lb.
Minas Channel	2.3×10^{13} ft.-lb.
Chignecto Bay	5.4×10^{13} ft.-lb.
Minas Basin	9.3×10^{13} ft.-lb.
Total =	41.0×10^{13} ft.-lb.
=	1.55×10^{8} kw.-hr.

In the event a barrier is built and water stored, it is the potential energy of the water behind the barrier which will determine the power output. The Minas Channel - Minas Basin system has more than twice the potential energy of Chignecto Bay. A dam built in the upper reaches of Chignecto Bay, such as the junction of Cumberland Basin and Shepody Bay, will have perhaps less than 1.0×10^{13} ft.-lb., but a dam at the entrance to Minas Basin (at Cape Sharp) will still have a potential of 9.3×10^{13} ft.-lb. Minas Basin also has much more potential than Passamaquoddy Bay, but the latter is suitable for a multi-pool project while Minas Basin is only suitable for a one-pool project.

Note: Since the potential energy is w. r. t. local mean sea level, the above values are estimates of the maximum power output of a dam only if: -

1. during flood tide the pool behind the barrier reaches the present normal maximum water level, and
2. during ebb tide, the pool is allowed to empty as low as the local mean sea level.

If low water in the pool is lower or higher than mean sea level, then the maximum power output will increase or decrease accordingly.

VI. SUMMARY AND REMARKS

The large tides in the Bay of Fundy appear to result from the shoaling effect (convergence of depth) and the partial resonance of the semi-diurnal tidal constituents. Since the M_2 represents 86% of the mean spring range where the ratio $(O_1 + K_1)/(M_2 + S_2)$ is only .08, it is reasonable to limit the study to the M_2. The M_2 is amplified by a factor of 3 from the Atlantic Ocean to Grand Manan I. and by a further factor of 2 from Grand Manan I. to Cape Split.

The first approach to the problem was a numerical solution to the one-dimensional hydrodynamical equations using finite-difference techniques, which predicted a 20% decrease in amplitude and 13 degree advance in phase lag at the barrier site for a barrier at Cape Sharp. Here, quadratic fiction was employed, but a frictionless, analytic solution for a similar schematization also predicted a 20% decrease.

Since the tidal configuration in the Bay of Fundy varies two-dimensionally, much of this study was carried out with several two-dimensional models, which also employed finite-differences. This permitted the inclusicn of the Coriolis accelleration. Calculations were carried out for various grid lengths and for various barriers in Chignecto Bay and Minas Basin, the results of which were in general agreement with the previous one-dimensional calculations. The models, of varying grid lengths, cannot give identical answers because they can only approximate the shoreline to integral multiples of the grid length. The use of finer grid lengths would not improve the accuracy of the results because the tide at the mouth of the bay has been assumed not altogether correctly to be unaffected by the barrier, besides which the computational time would also increase greatly.

Several other calculations were also included. The inclusion of the UU_x term in the equation of motion caused the tidal wave to break. Furthermore, the time of high water between two stations was less than the time of low water between the two stations, substantiated by the examination of tidal data for St. John, N. B. and Grindstone I. A calculation for a constant depth model indicated that shallower water causes larger amplitudes.

The effect of tidal barriers upon the phase lag is of minor importance while the effect upon the amplitude is the important issue. For a single-pool power dam, the water is allowed to enter and fill the pool behind the gates during flood tide and emptied through the turbines during ebb tide, so that the effects of the dam would probably be much less than those predicted for complete barriers. In view of the moderate decreases in amplitude found for complete barriers, we conclude that a power project at the head of the Bay of Fundy would not cause critical decreases in tidal

amplitude. On the basis of potential energy, Minas Basin is more desirable for power extraction than Chignecto Bay, but Minas Basin contains several deep trenches, which would increase construction costs. We have shown where the greatest energy potential is, but economic considerations are equally important; such judgement is beyond the scope of this study.

Several extentions of this study may prove very useful. Closure operations will cause the already large tidal current to increase astronomically so that models must be developed to provide tidal and current predictions during this transient state. Needless to say, these models will be very complex and development should begin well in advanced of construction. A study of storm surges must also be carried out to ensure that adequate allowance is made for extreme meteorological conditions.

VII. ACKNOWLEDGMENTS

The author would like to thank Dr. N. J. Campbell for the opportunity to carry out this study and for his criticism of this manuscript. Dr. G. Godin's advice and criticism on the mathematical and physical aspects of the study were also invaluable. Mr. F. G. Barber was boundless in his assistance of the assembling of this manuscript. This manuscript would not have been possible without Mr. M. Isabelle's expert preparation of the numerous diagrams.

VIII. LIST OF FIGURES AND TABLES

Figures

Tables

IX. REFERENCES

Anonymous, 1965. Atlantic coast tide and current tables. Canadian Hydrographic Service, Marine Sciences Branch, Dept. of Mines and Technical Surveys, Ottawa: 261 pp.

1959. International Passamaquoddy Fisheries Board. Report to International Joint Commission, Ottawa, Ontario, Washington, D. C. Appendix I, Oceanography.

1959. Investigation of the International Passamaquoddy Tidal Power Project. Report to the International Joint Commission by the International Passamaquoddy Engineering Board: 271 pp.

Brettschneider, G. 1963. Anwendung eines im Institut für Meereskunde der Universität Hamburg entwickelten Verfahrens zur numerischen Ermittlung von Gezeiten in Randmeeren auf die M_2 - Mitschwingungsgezeit der Nordsee. Als Diplomarbeit in Fach Ozeanographie des Mathematisch - Naturwissenshaftlichen Fakultät an der Universität Hamburg vorgelegt von Gottfried Brettschneider, Hamburg: 129 pp.

Dawson, W. B. 1917. Tides at the head of the Bay of Fundy. Dept. of Naval Service, Ottawa: 36 pp.

Defant, A. 1961. Physical Oceanography, Vol. II. Pergamon Press, London: 598 pp.

Dohler, G. 1965. Hydrographic tidal manual. Canadian Hydrographic Service, Marine Sciences Branch, Dept. of Mines and Technical Surveys, Ottawa: 143 pp.

Dronkers, J. J. 1964. Tidal Compulations in rivers and coastal waters. North-Holland Publishing Co., Amsterdam: 518 pp.

Farquharson, W. I. 1959. Causeway investigation, Northumberland Strait, report on tidal survey, 1958. Surveys and Mapping Branch, Dept. of Mines and Technical Surveys, Ottawa: 137 pp.

1965. Tidal stream and current surveys, evaluation of data. Report BIO-65-11, Bedford Institute of Oceanography, Dartmouth, N. S.: 66 pp.

Fischer, G. 1965. A survey of finite-difference approximations to the primitive equations. Monthly Weather Review, Vol. 93, No. 1: 1-10.

Forrester, W. D. 1958. Current measurements in Passamaquoddy Bay and the Bay of Fundy, 1957 and 1958. Tidal Publication No. 40, Canadian Hydrographic Service, Surveys and Mappings Branch, Dept. of Mines and Technical Surveys, Ottawa: 46 pp.

Godin, G. 1965. The M_2 tide in the Labrador Sea, Davis Strait and Baffin Bay. Deep-Sea Research, Vol. 12: 469-77.

1965. Some remarks on the tidal motion in a narrow rectangular sea of constant depth. Deep-Sea Research, Vol. 12: 461-468.

Hachey, H. B. 1934. The probable effect of tidal power development on Bay of Fundy tides. J. Franklin Inst., 217 (6): 747-756.

Hansen, W. Proceedings of the symposium on mathematical - hydrodynamical methods of physical oceanography. Institut für Meereskunde der Universität, Hamburg, 1962.

Hansen, W. 1956. Theorie zur errechnung des wasserstandes und der stromungen in randmeeren nebst anwendungen. Tellus 8, Nr. 3: 287-300.

Harris, D. L. and Jelesnianski, C. P. 1964. Some problems involved in the numerical solutions of tidal hydraulics equations. Monthly Weather Review, vol. 92, No. 9: 409-422 pp.

Ippen, A. T. and Harleman, D. R. F. 1958. Investigation of influence of proposed International Passamaquoddy Tidal Power Project on tides in the Bay of Fundy. Prepared for Passamaquoddy Tidal Power Survey, U. S. Army Engineer Division, New England Corps of Engineers, Boston, Massachussetts, under Contract No. DA-19-016-CIV-Eng-58-174: 31 pp.

Jelesnianski, C. P. 1965. A numerical calculation of storm tides induced by a tropical storm impinging on a continental shelf. Monthly Weather Review, vol. 93, No. 6: 343-358.

Kasahara, A. 1965. On certain finite-difference methods for fluid dynamics. Monthly Weather Review, vol. 93, No. 1: 27-31.

McLellan, H. J. 1958. Energy considerations in the Bay of Fundy system. J. Fish. Res. Bd. Canada, 15(2): 115-134.

Proudman, J. 1953. Dynamical oceanography. Methuen and Co. Ltd., London: 409 pp.

Rossiter, J. R. and Lennon, G. W. 1965. Computation of tidal conditions in the Thomas estuary by the initial value method. Institute civ. Engrs, vol. 31: 25-56.

Rouse, H. 1946. Elementary mechanics of fluids. John Wiley and Sons, New York: 444 pp.

Taylor, G. I. 1919. Tidal Friction in the Irish Sea. Philosophical Transactions of the Royal Society, A, vol. CCXX: 1-93.

X. FIGURES AND TABLES

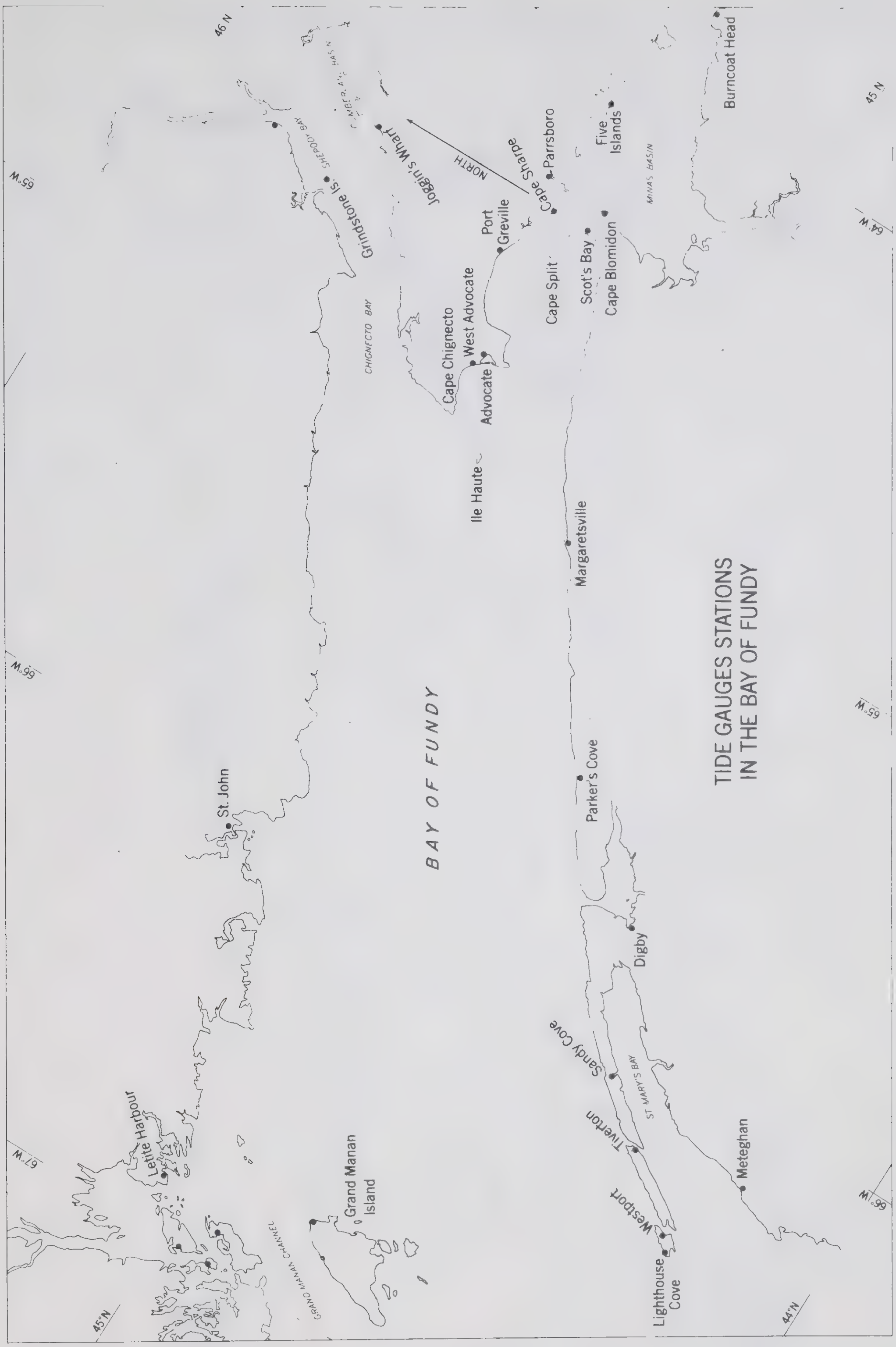
TIDE GAUGES STATIONS
IN THE BAY OF FUNDY
BAY OF FUNDY
CHIGNECTO BAY
SHEPODY BAY
MINAS BASIN
ST MARY'S BAY
GRAND MANAN CHANNEL
NORTH
St. John
Letite Harbour
Grand Manan Island
Lighthouse Cove
Westport
Tiverton
Sandy Cove
Meteghan
Digby
Parker's Cove
Margaretsville
Ile Haute
Advocate
West Advocate
Cape Chignecto
Port Greville
Cape Split
Scot's Bay
Cape Blomidon
Cape Sharpe
Parrsboro
Five Islands
Burncoat Head
Joggin's Wharf
Grindstone Is.
46°N
45°N
44°N
64°W
65°W
66°W
67°W

Figure I. 1

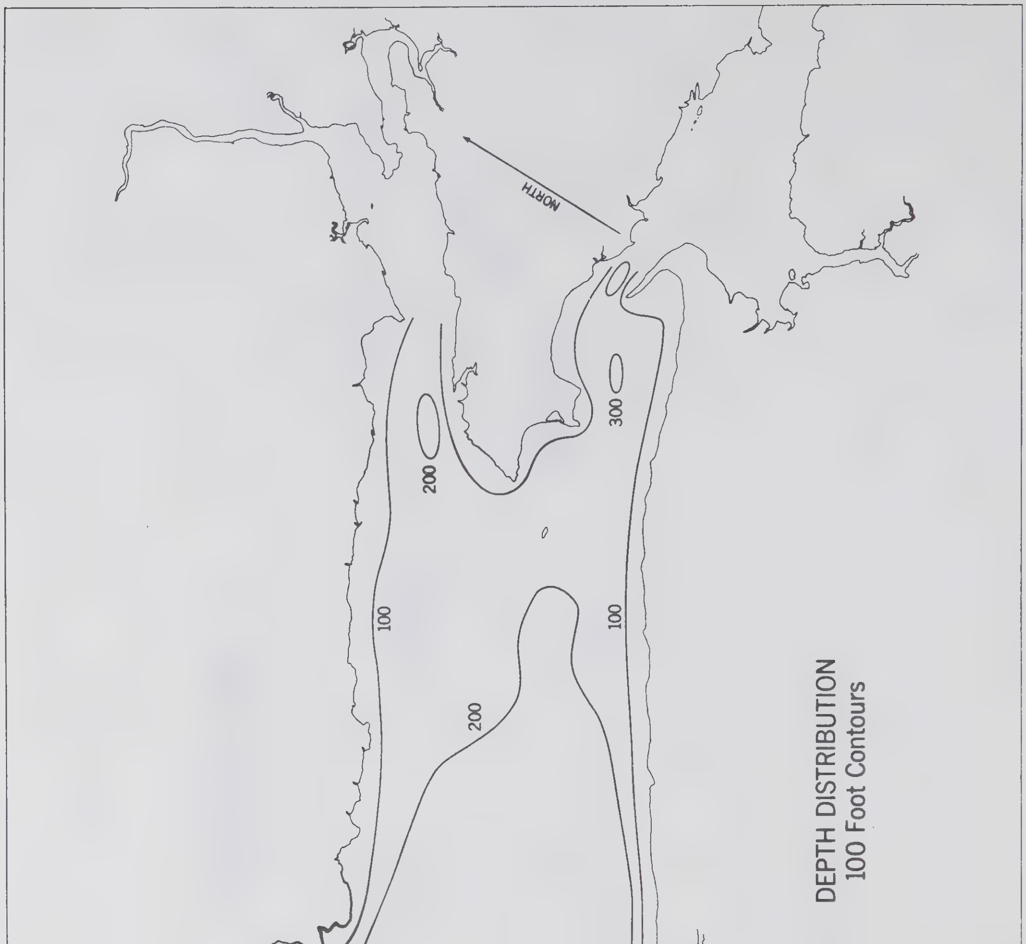
DEPTH DISTRIBUTION
100 Foot Contours
NORTH
100
100
200
200
200
300
300
400
500
600

Figure I. 2

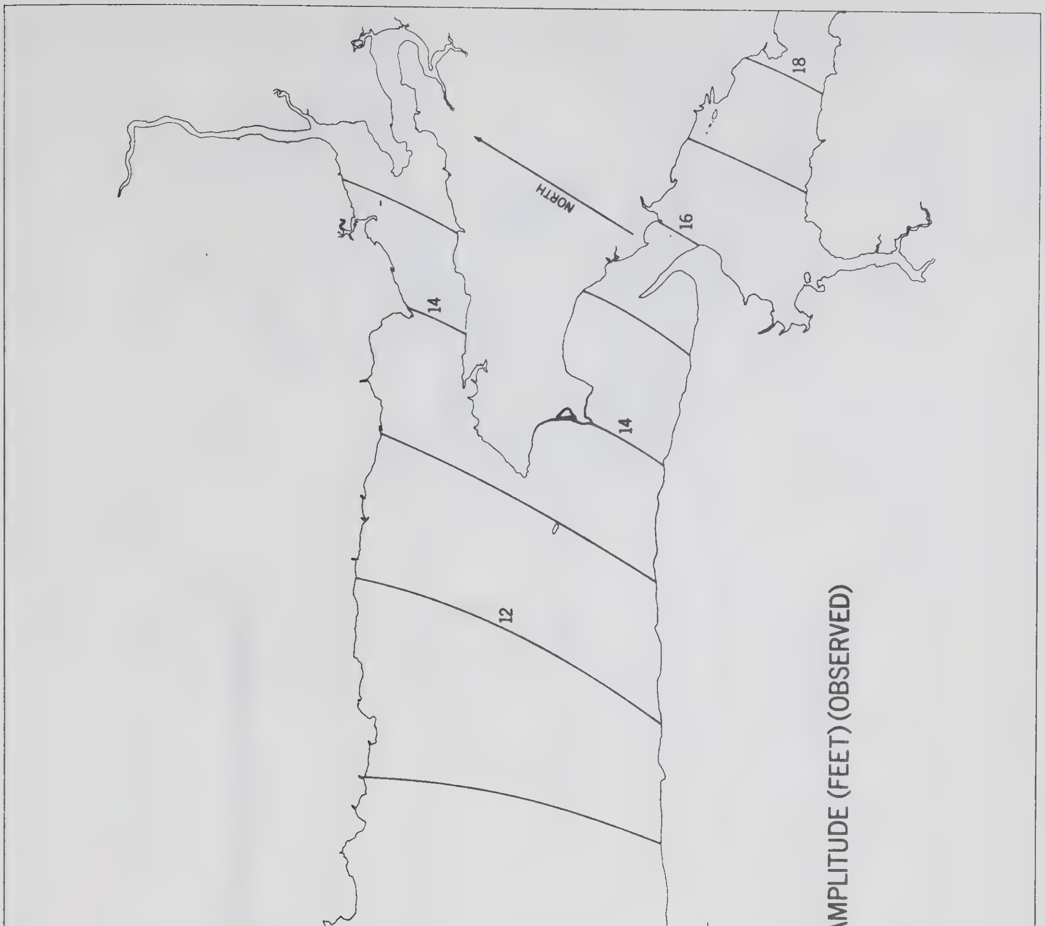

Figure I. 3

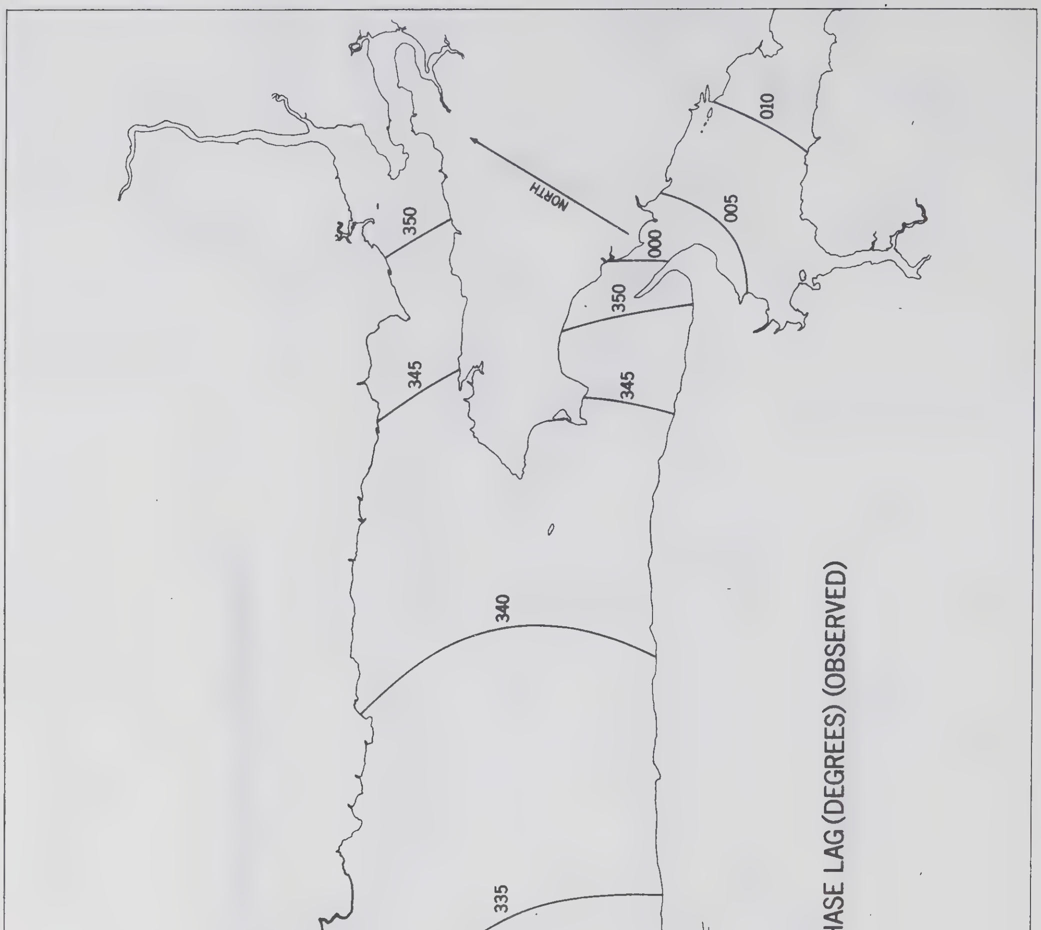
M$_2$ PHASE LAG (DEGREES) (OBSERVED)
NORTH
010
005
000
350
345
350
345
340
335
330
325

Figure I-4

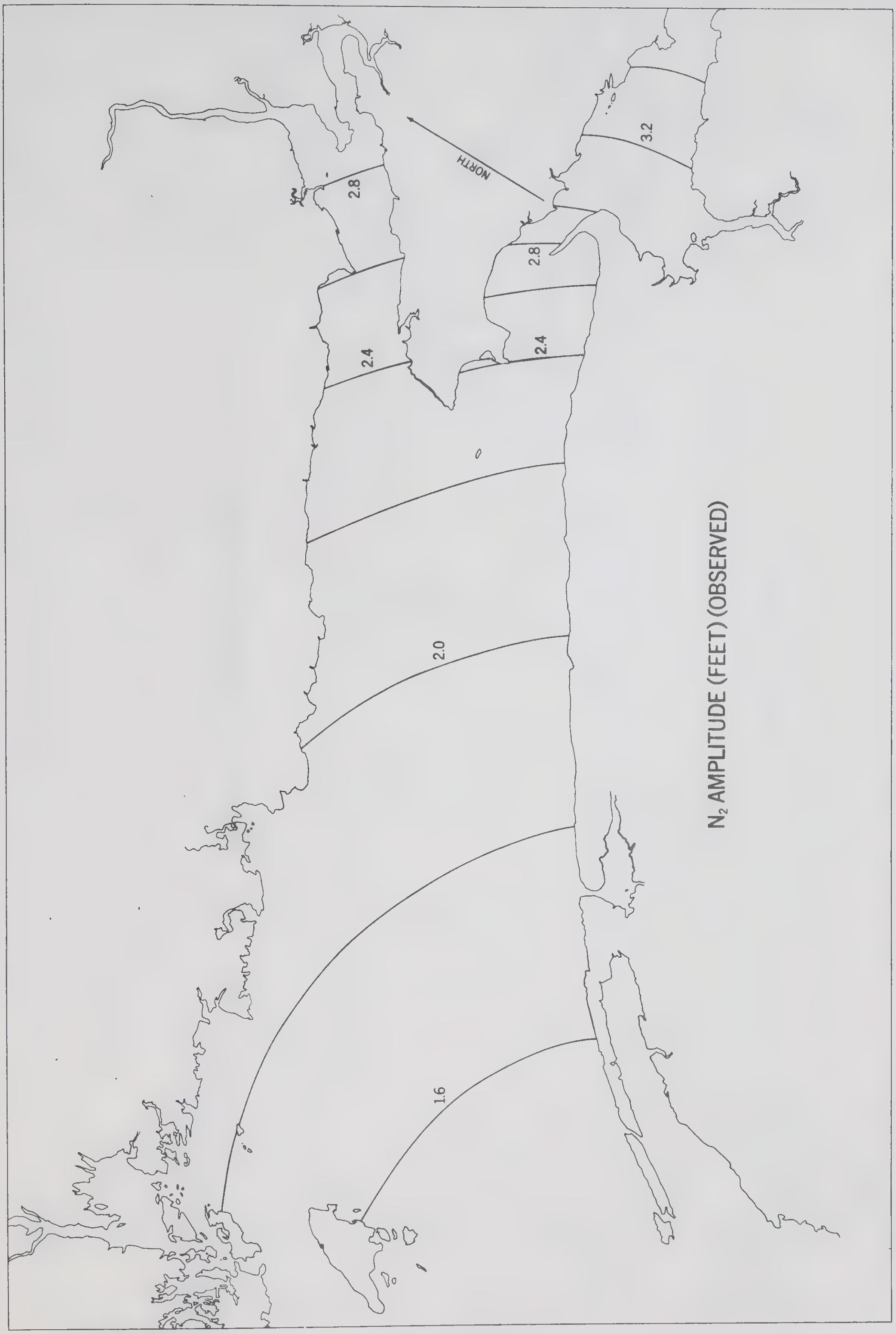

Figure I. 5

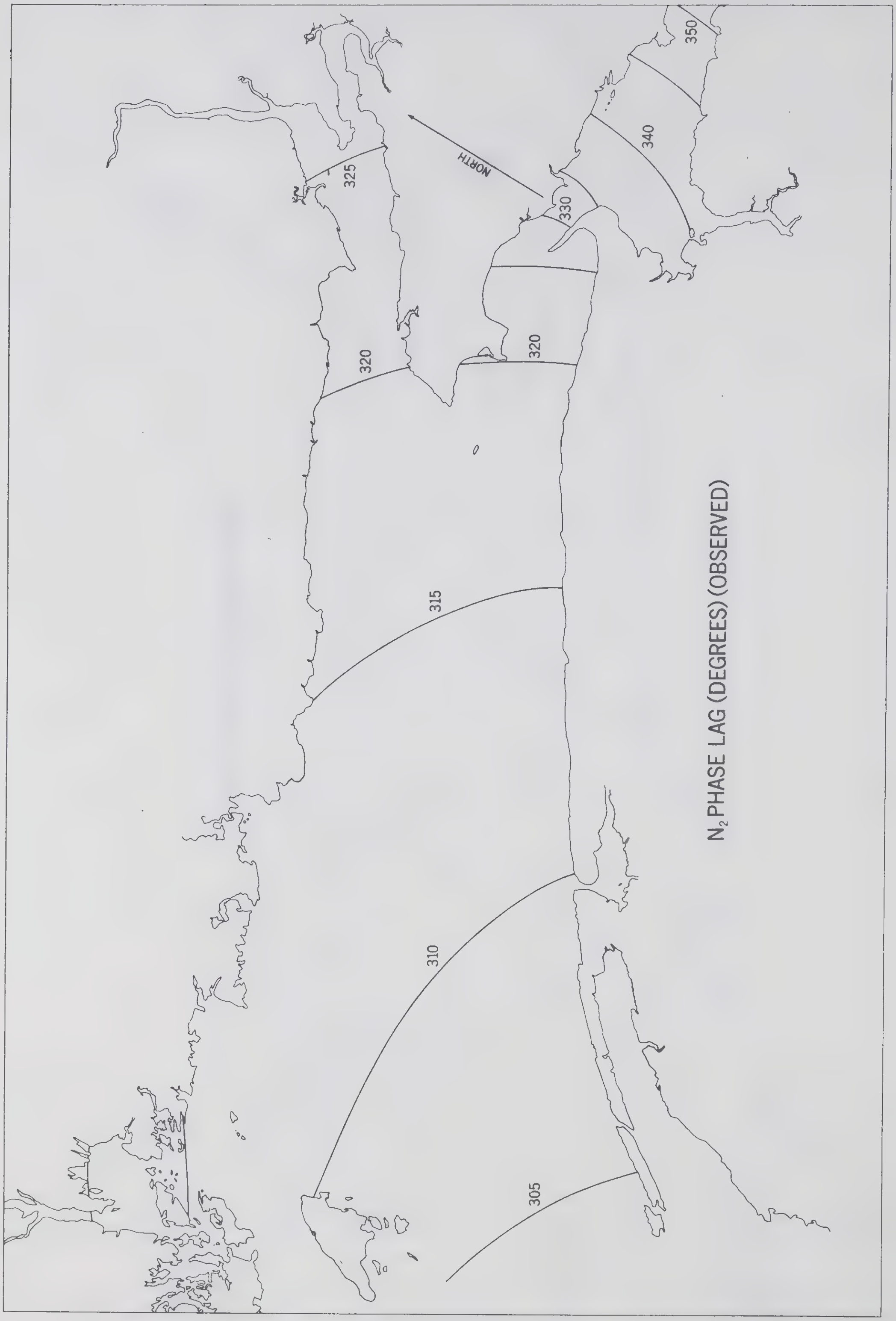
N$_2$ PHASE LAG (DEGREES) (OBSERVED)
NORTH
350
340
330
325
320
320
315
310
305

Figure I 6

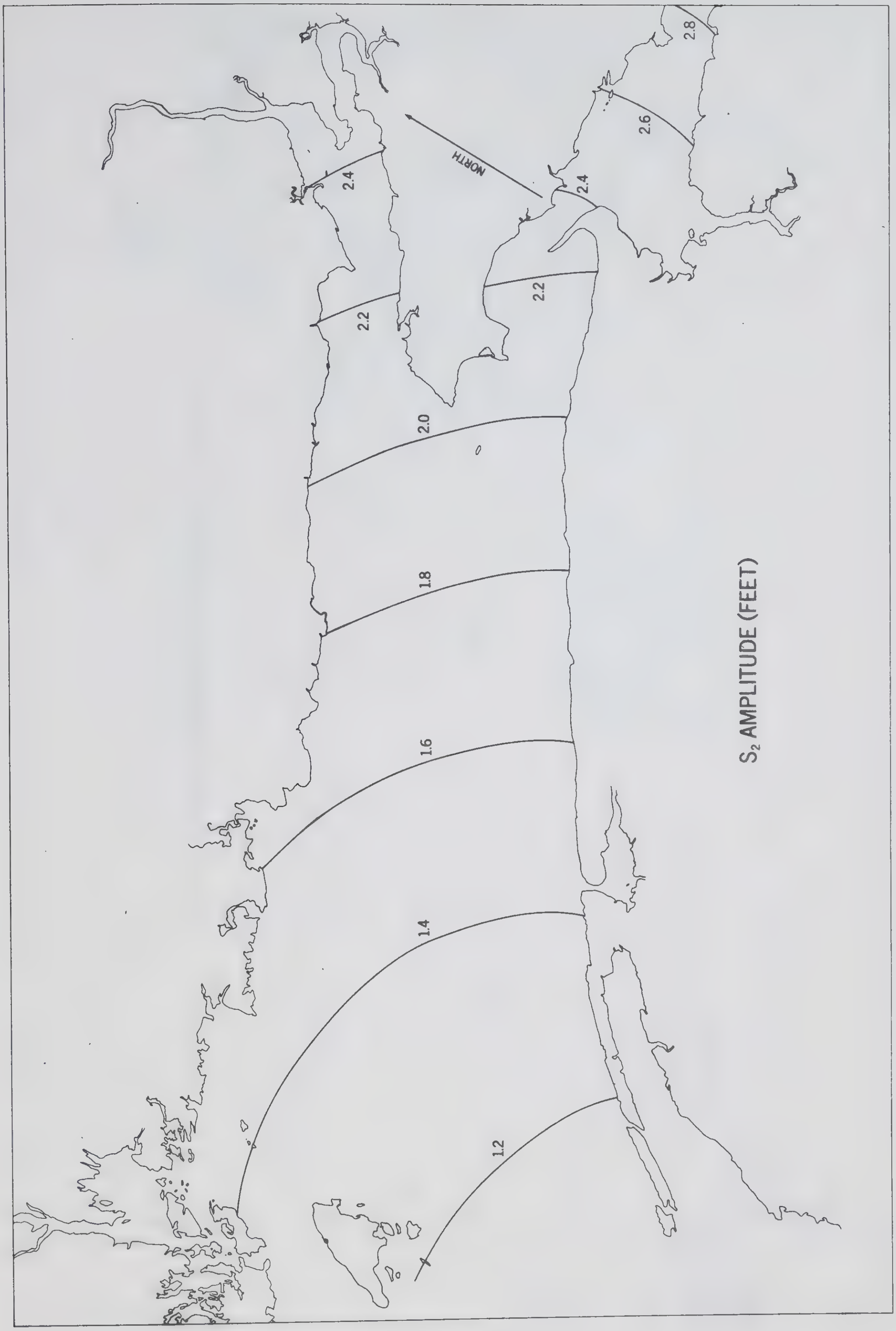

Figure I. 7

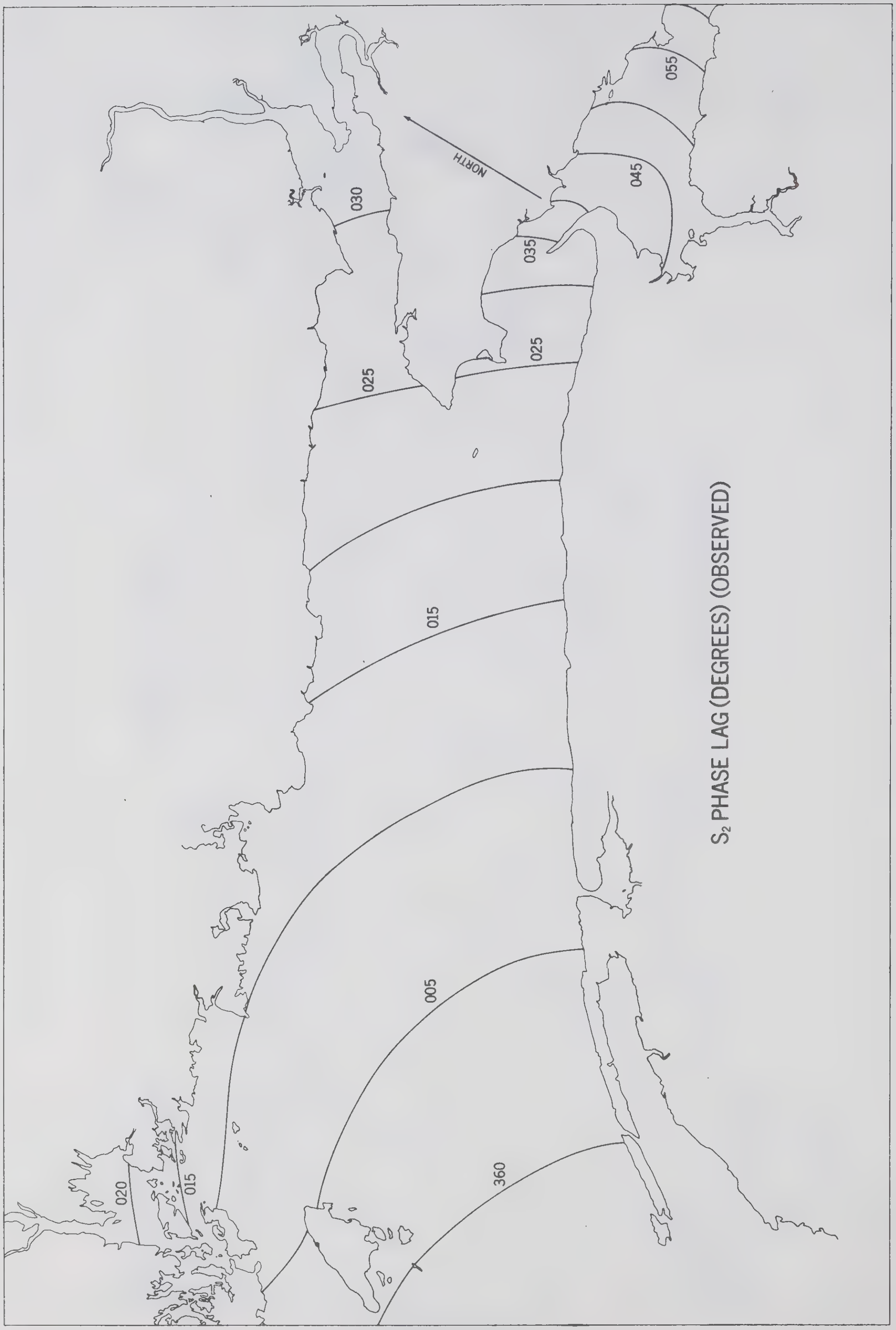

S_2 PHASE LAG (DEGREES) (OBSERVED)
NORTH
055
045
035
030
025
025
015
005
360
020
015

Figure I. 8

SCHEMATIZATION FOR ROSSITER'S ENERGY CALCULATIONS

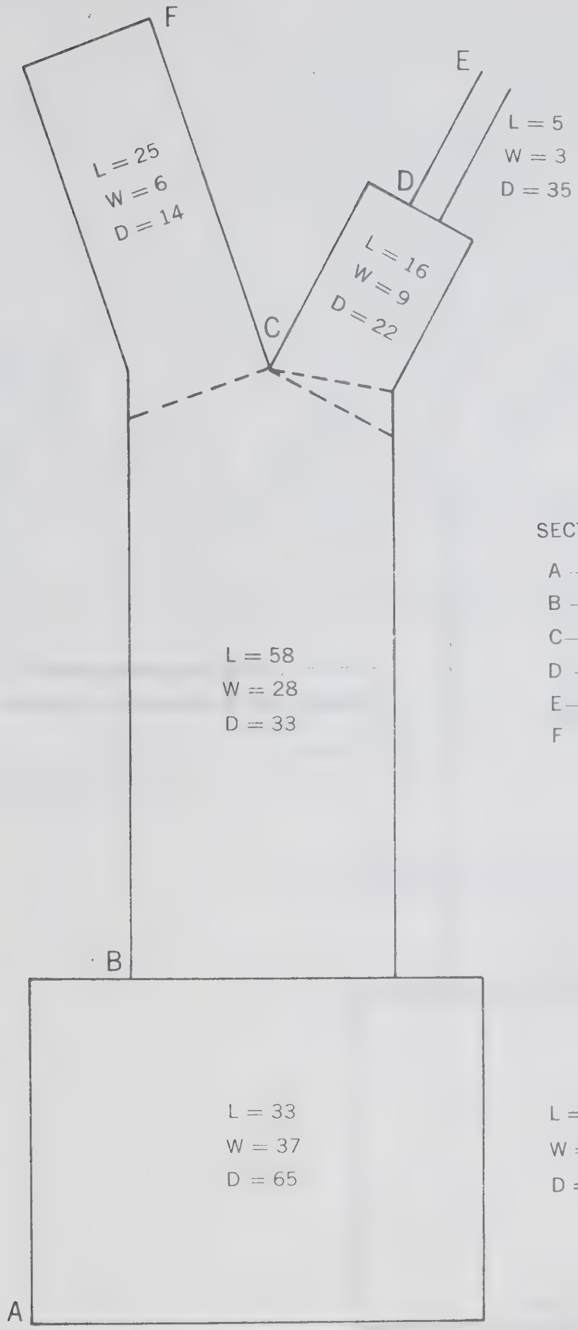

SECTION LOCATION

A --Brier Island
B --Campbell Point
C—Cape Chignecto
D -Point Greville
E—Cape Sharp
F Cape Maringouin

L = Length (Nautical miles)
W = Width (Nautical miles)
D = Depth (Fathoms)

Figure II. 1

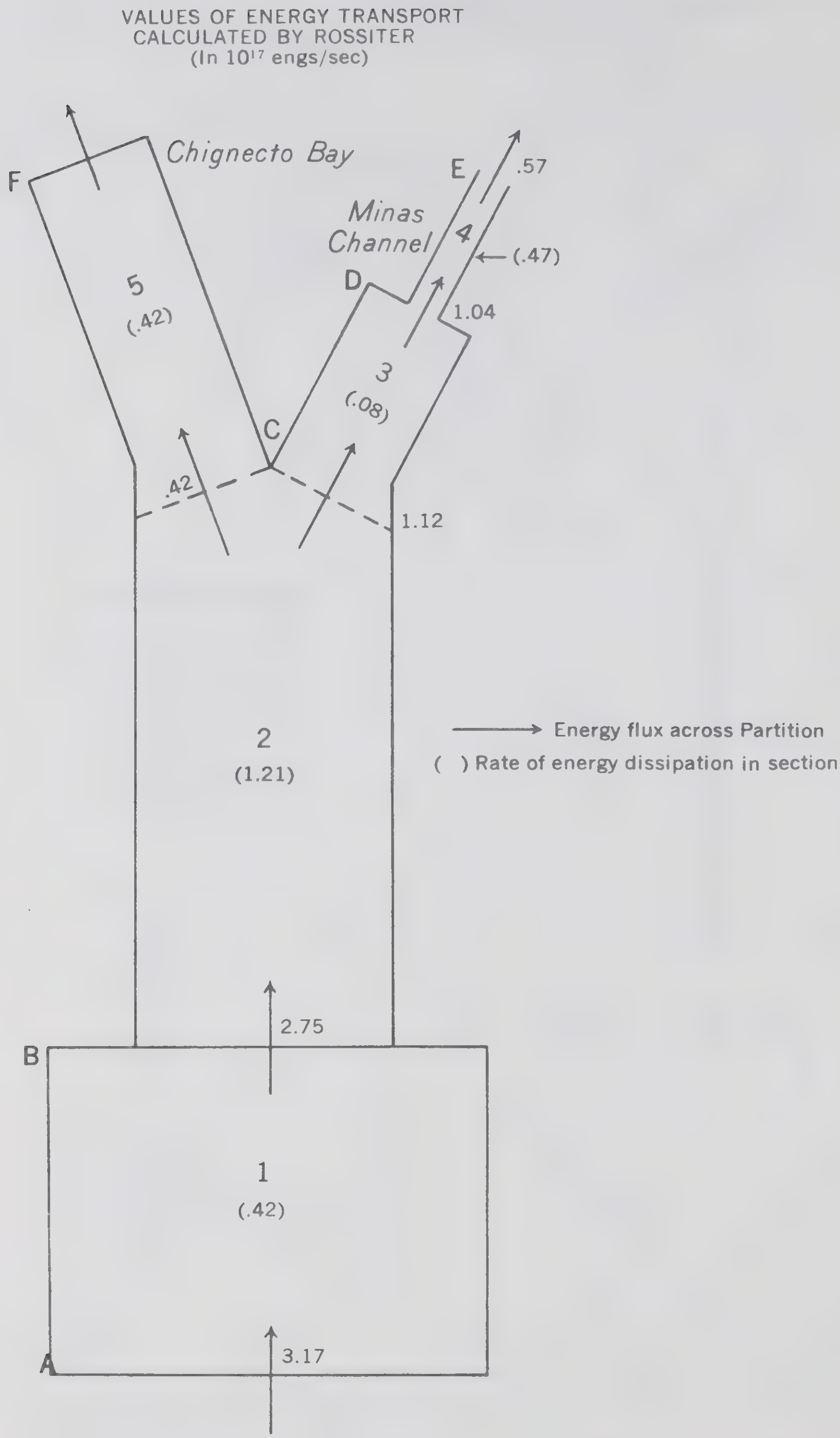

VALUES OF ENERGY TRANSPORT
CALCULATED BY ROSSITER
(In 10¹⁷ engs/sec)
Chignecto Bay
F
E
.57
Minas
Channel
4
(.47)
D
1.04
5
(.42)
3
(.08)
C
.42
1.12
2
(1.21)
Energy flux across Partition
( ) Rate of energy dissipation in section
2.75
B
1
(.42)
3.17
A

Figure II. 2

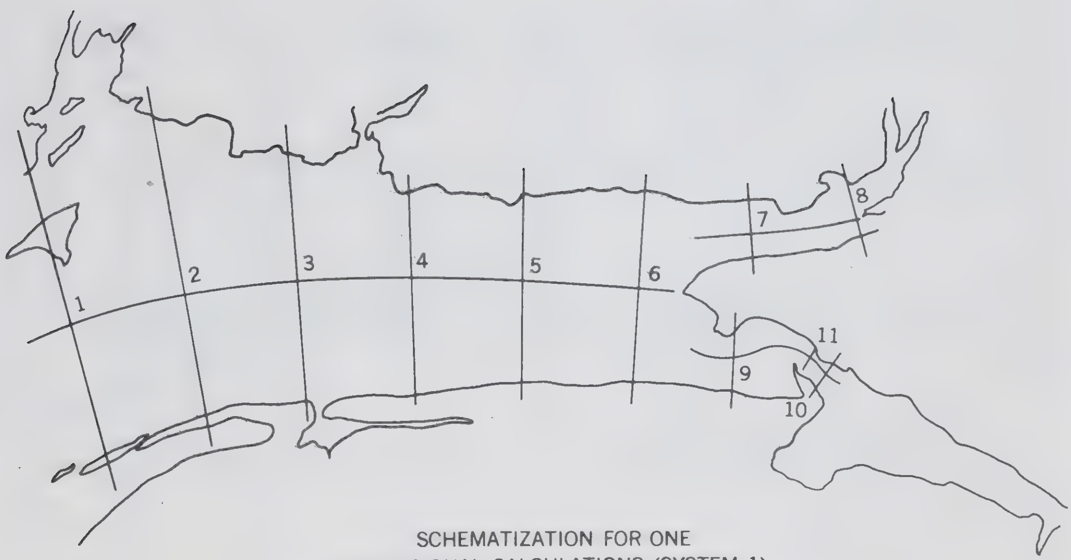

SCHEMATIZATION FOR ONE
DIMENSIONAL CALCULATIONS (SYSTEM 1)

Figure II. 3

STAGGERED GRID SYSTEM FOR
ONE DIMENSIONAL NUMERICAL SOLUTION

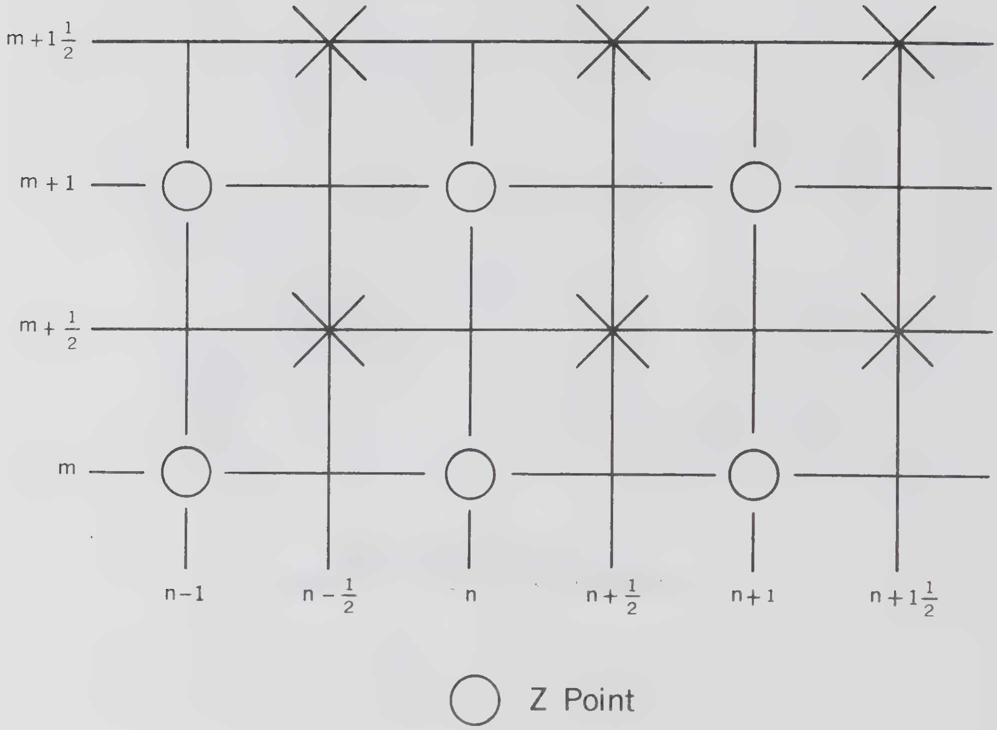

Figure II. 4

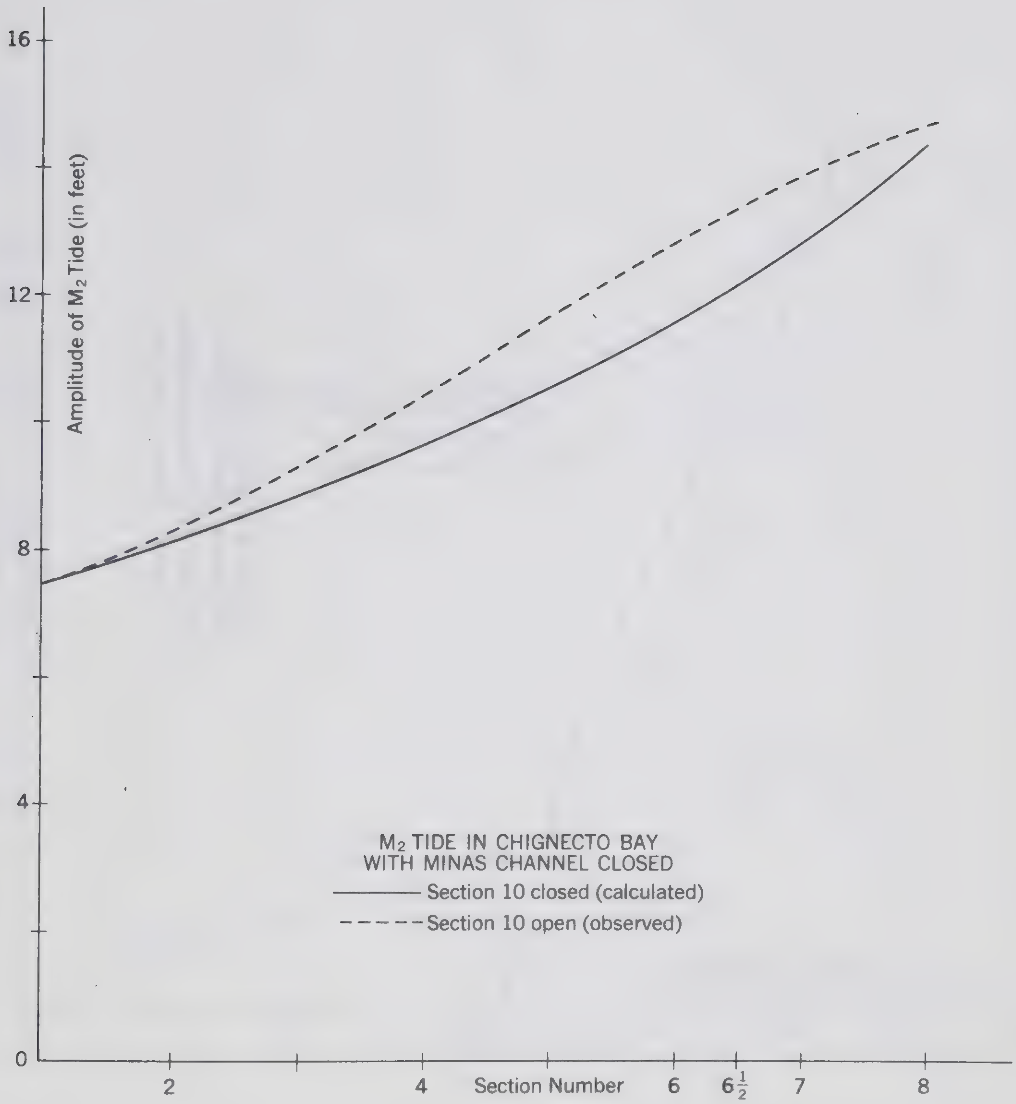

Amplitude of M_2 Tide (in feet)
16
12
8
4
0
2
4
Section Number
6
$6\frac{1}{2}$
7
8
M_2 TIDE IN CHIGNECTO BAY
WITH MINAS CHANNEL CLOSED
Section 10 closed (calculated)
Section 10 open (observed)

Figure II. 5

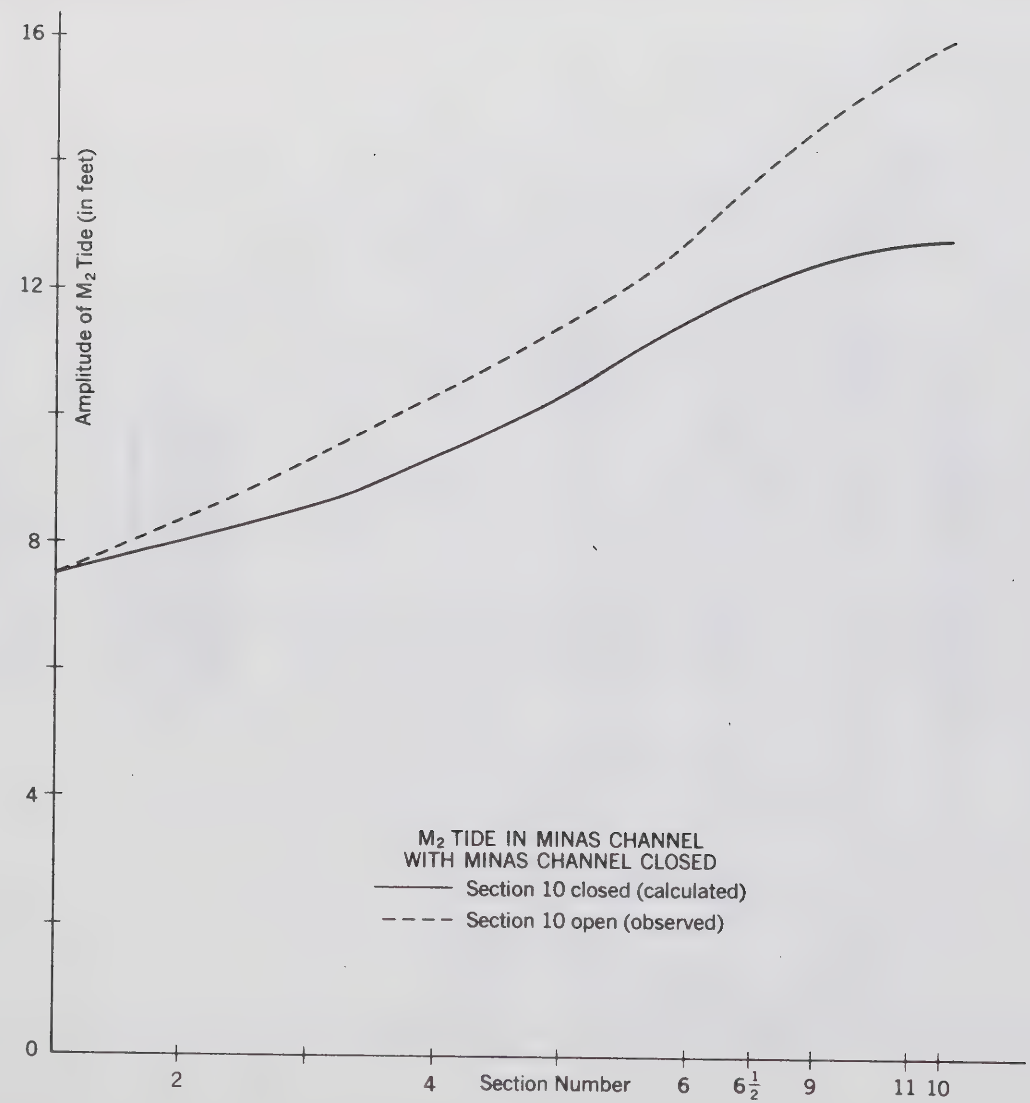

16
12
8
4
0
Amplitude of M2 Tide (in feet)
M2 TIDE IN MINAS CHANNEL
WITH MINAS CHANNEL CLOSED
Section 10 closed (calculated)
Section 10 open (observed)
2
4
Section Number
6
6 1/2
9
11 10

Figure II. 6

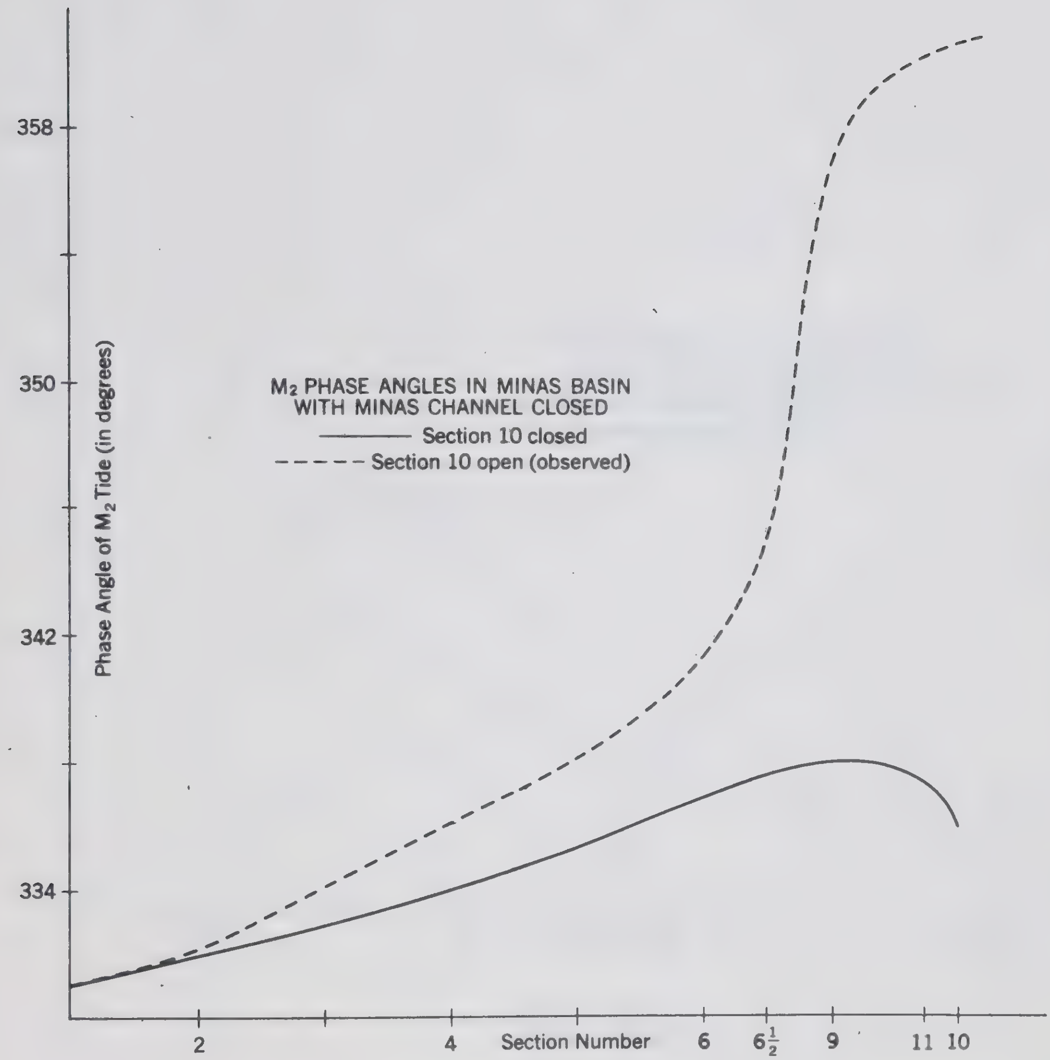

358
350
342
334
Phase Angle of M_2 Tide (in degrees)
M_2 PHASE ANGLES IN MINAS BASIN
WITH MINAS CHANNEL CLOSED
Section 10 closed
Section 10 open (observed)
2
4
Section Number
6
$6\frac{1}{2}$
9
11
10

Figure II. 7

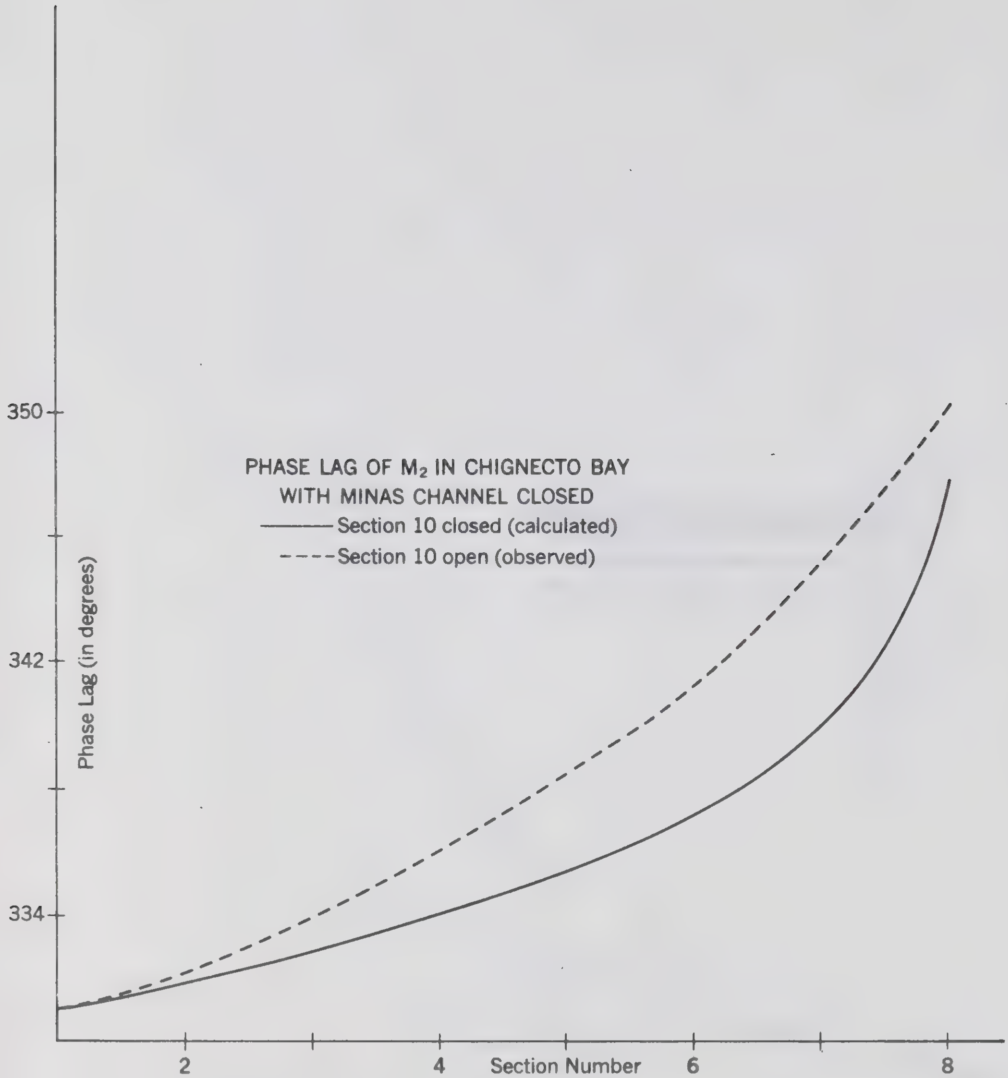

PHASE LAG OF M2 IN CHIGNECTO BAY
WITH MINAS CHANNEL CLOSED
Section 10 closed (calculated)
Section 10 open (observed)
Phase Lag (in degrees)
350
342
334
2
4
Section Number
6
8

Figure II. 8

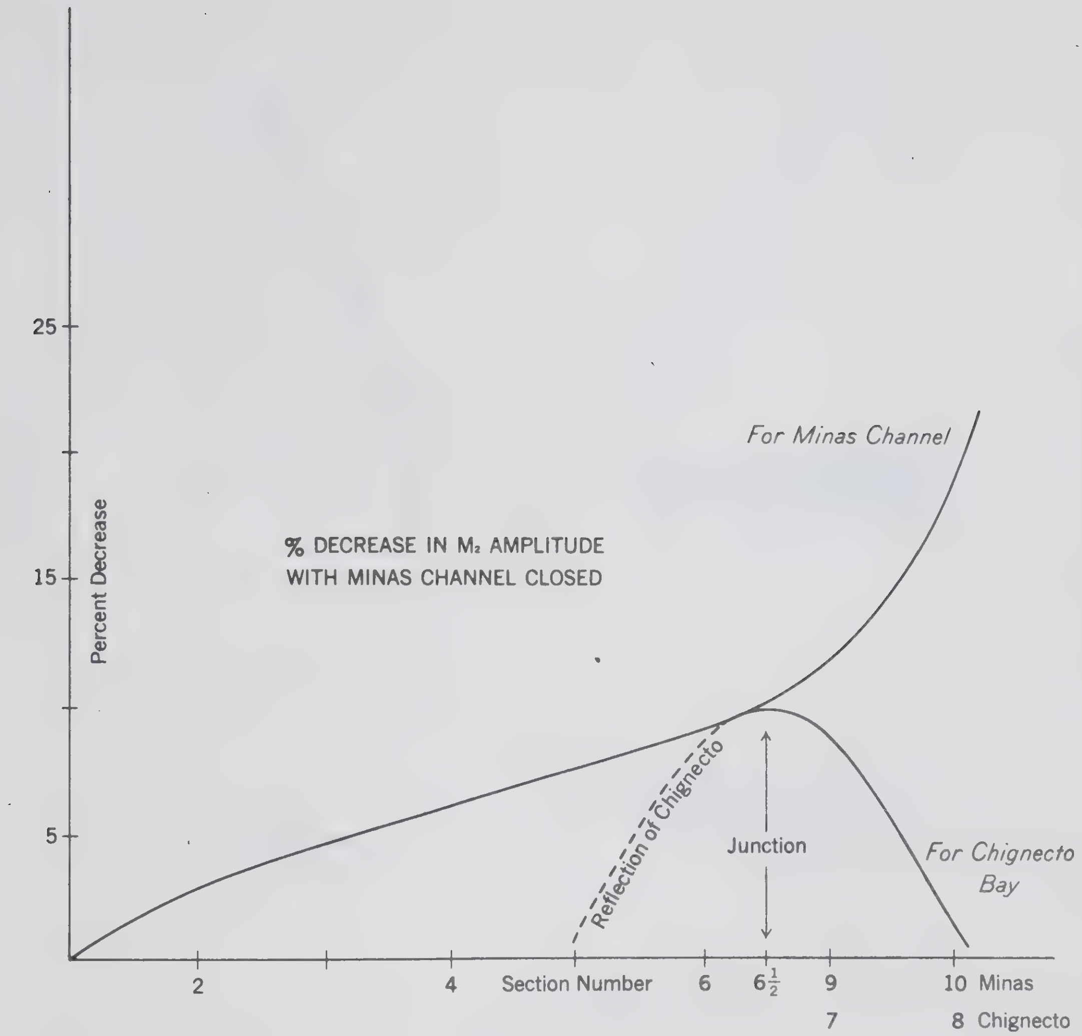

% DECREASE IN M₂ AMPLITUDE
WITH MINAS CHANNEL CLOSED
Percent Decrease
25
15
5
For Minas Channel
For Chignecto Bay
Reflection of Chignecto
Junction
2
4
Section Number
6
6½
9
10 Minas
7
8 Chignecto

Figure II. 9

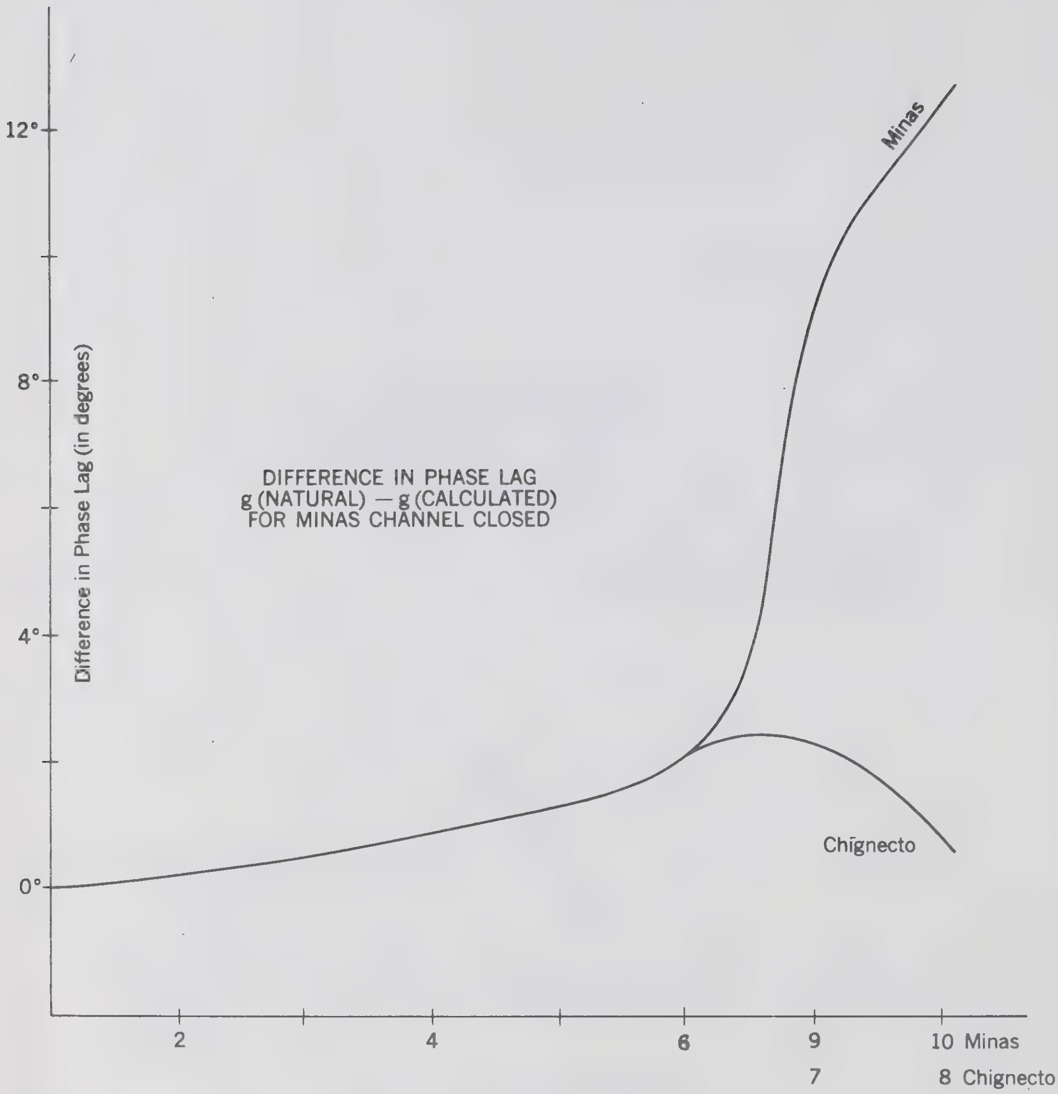

12°
8°
4°
0°
Difference in Phase Lag (in degrees)
DIFFERENCE IN PHASE LAG
g (NATURAL) — g (CALCULATED)
FOR MINAS CHANNEL CLOSED
Minas
Chignecto
2
4
6
9
10 Minas
7
8 Chignecto

Figure II. 10

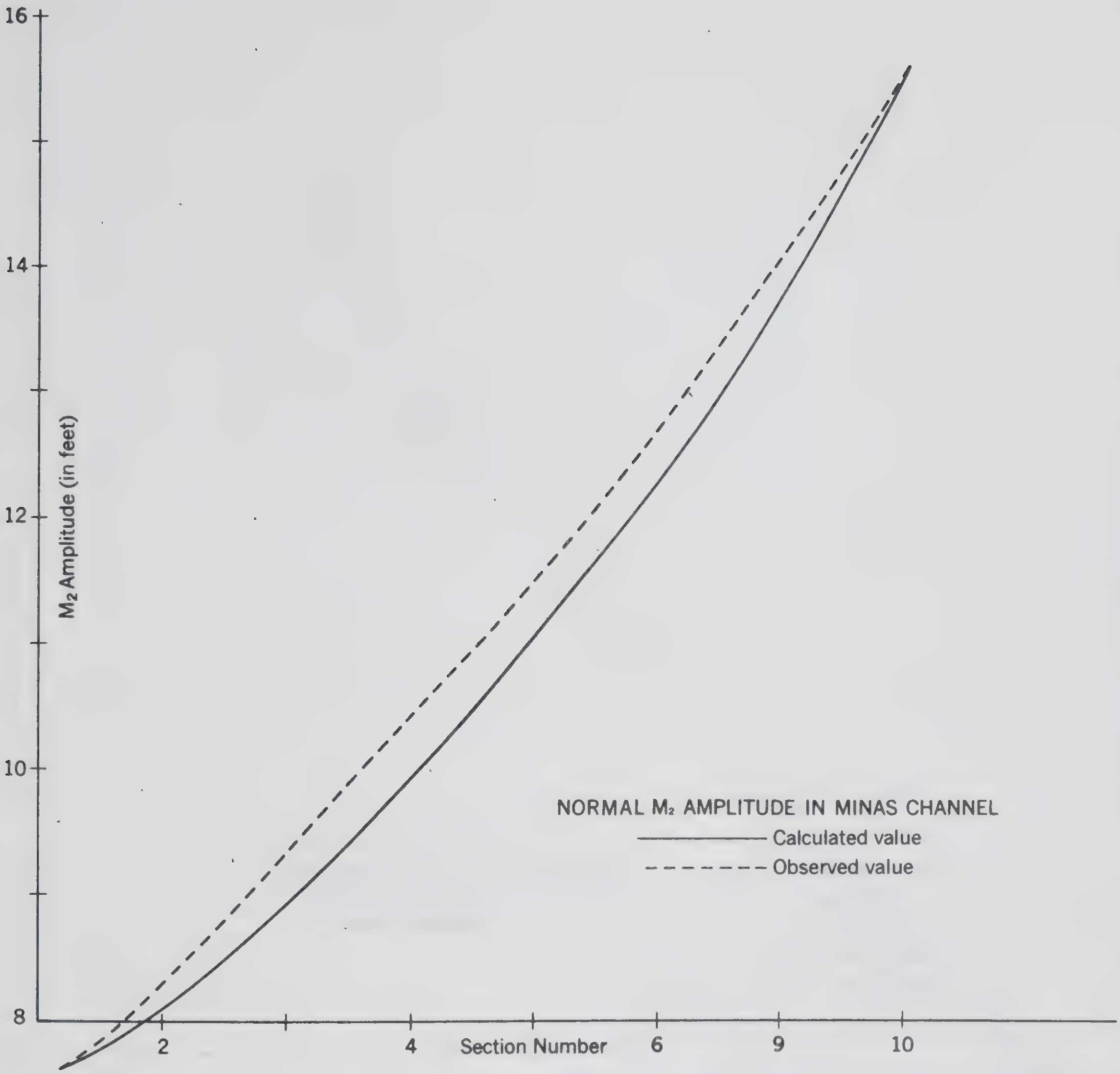

16
14
12
10
8
M_2 Amplitude (in feet)
2
4
Section Number
6
9
10
NORMAL M_2 AMPLITUDE IN MINAS CHANNEL
Calculated value
Observed value

Figure II. 11

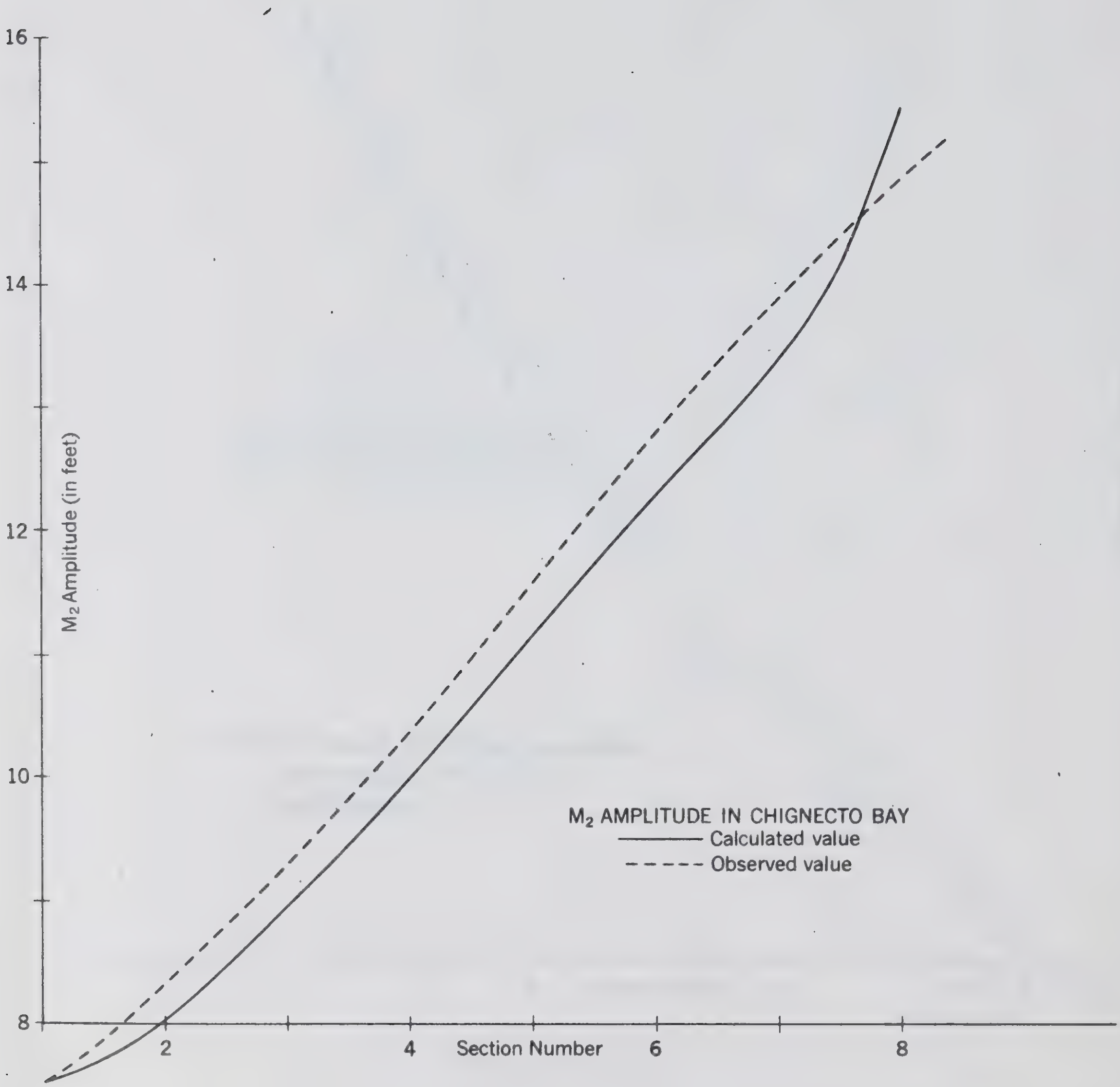
16
14
12
10
8
M_2 Amplitude (in feet)
2
4
Section Number
6
8
M_2 AMPLITUDE IN CHIGNECTO BAY
Calculated value
Observed value

Figure II. 12

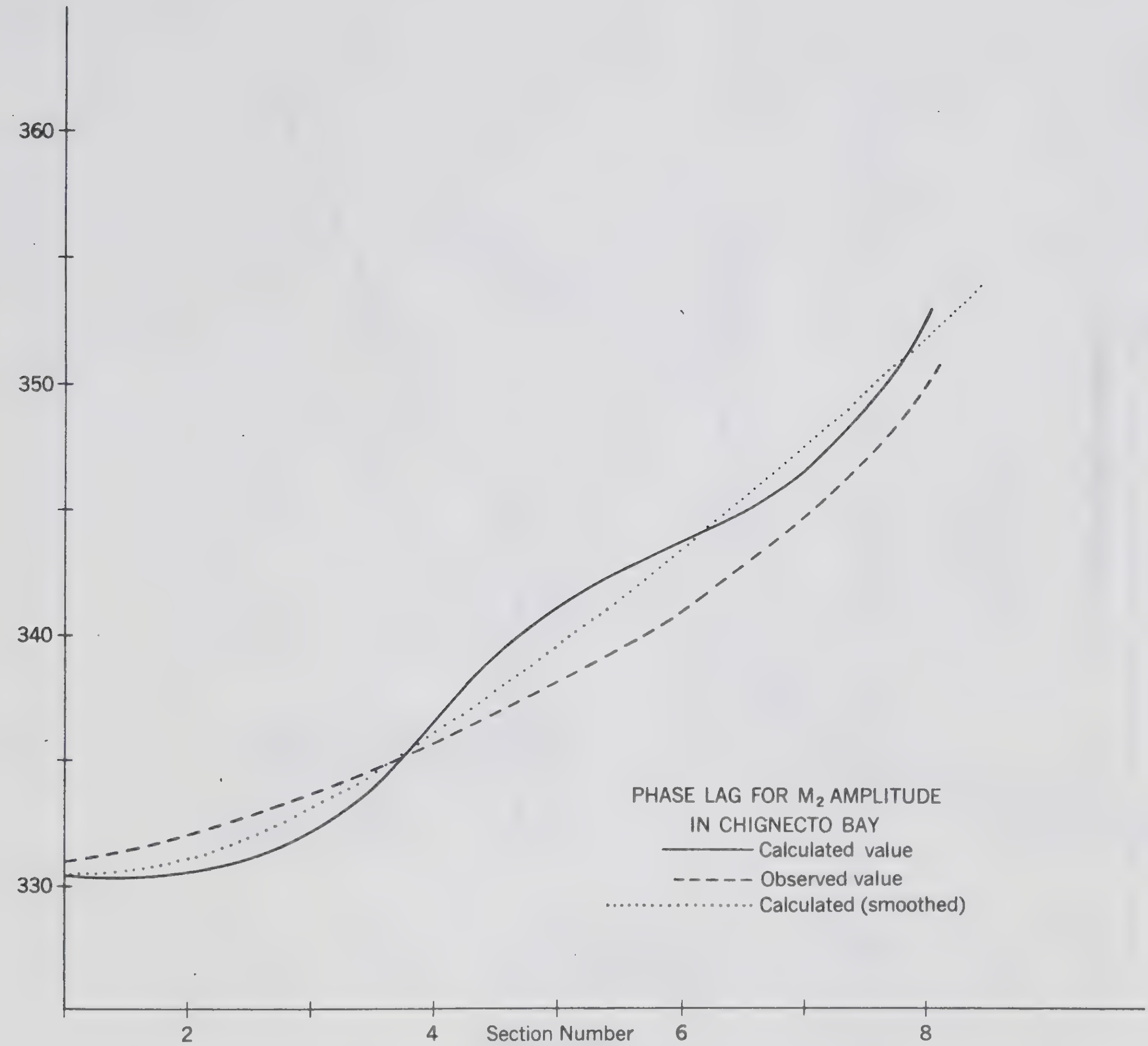
360
350
340
330
PHASE LAG FOR M_2 AMPLITUDE
IN CHIGNECTO BAY
Calculated value
Observed value
Calculated (smoothed)
2
4
Section Number
6
8

Figure II. 13

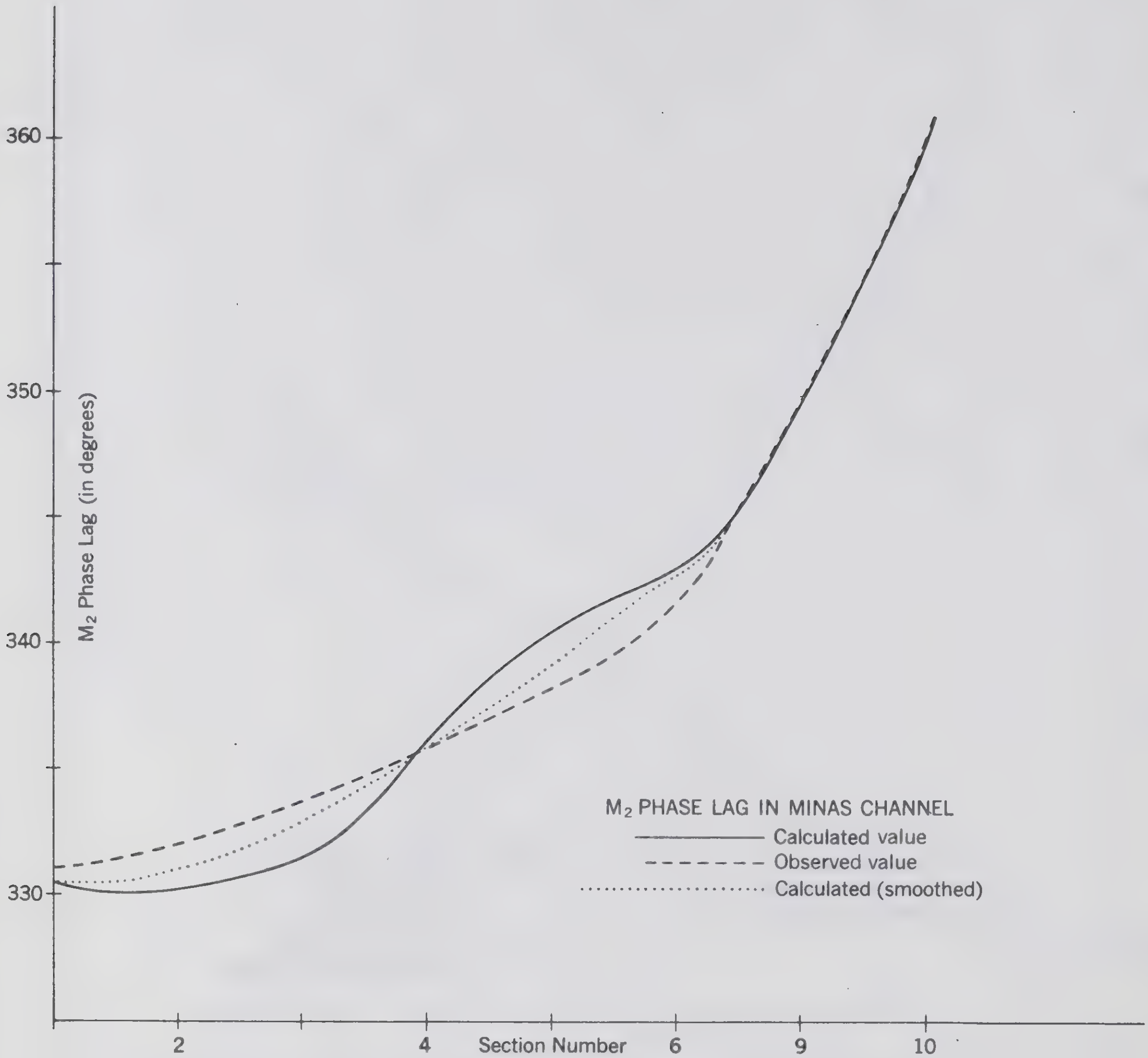

360
350
340
330
M_2 Phase Lag (in degrees)
2
4
Section Number
6
9
10
M_2 PHASE LAG IN MINAS CHANNEL
Calculated value
Observed value
Calculated (smoothed)

Figure II. 14

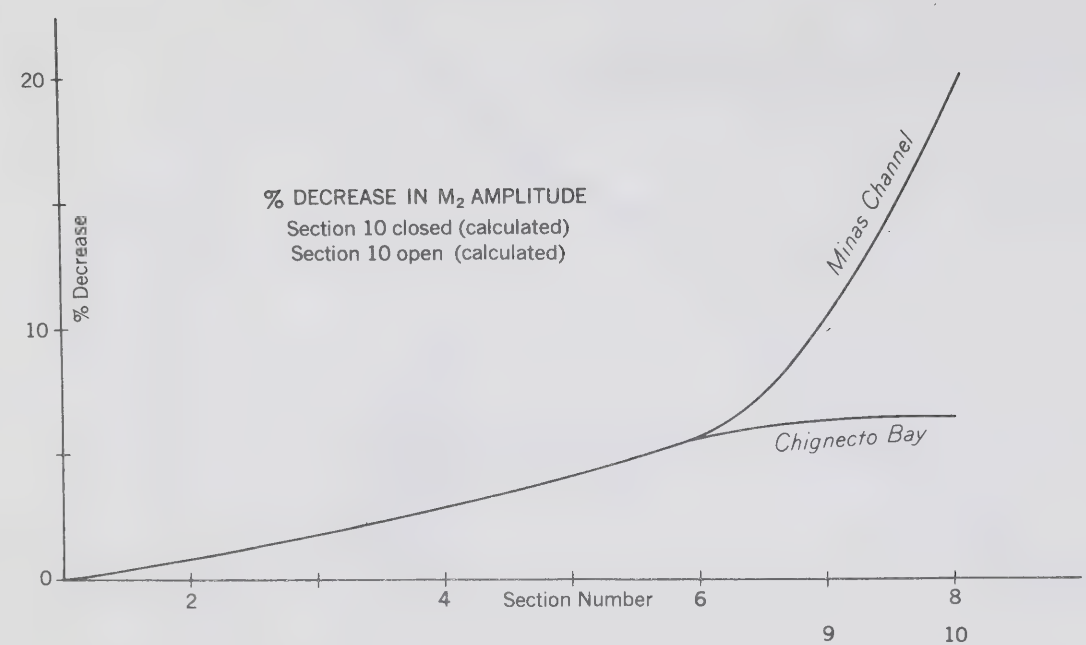
% DECREASE IN M2 AMPLITUDE
Section 10 closed (calculated)
Section 10 open (calculated)
% Decrease
20
10
0
2
4
Section Number
6
8
9
10
Minas Channel
Chignecto Bay

Figure II. 15

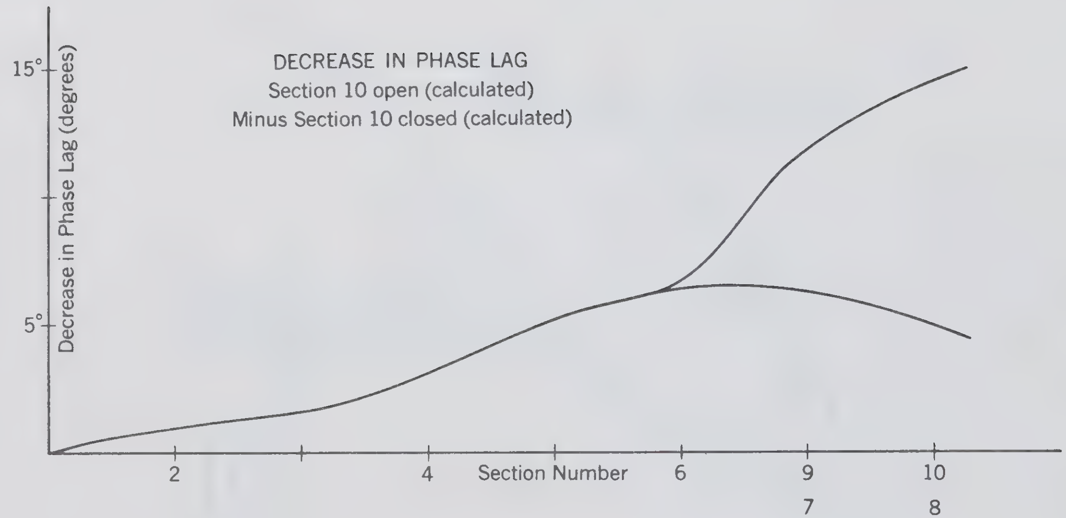
DECREASE IN PHASE LAG
Section 10 open (calculated)
Minus Section 10 closed (calculated)
Decrease in Phase Lag (degrees)
15°
5°
2
4
Section Number
6
9
10
7
8

Figure II. 16

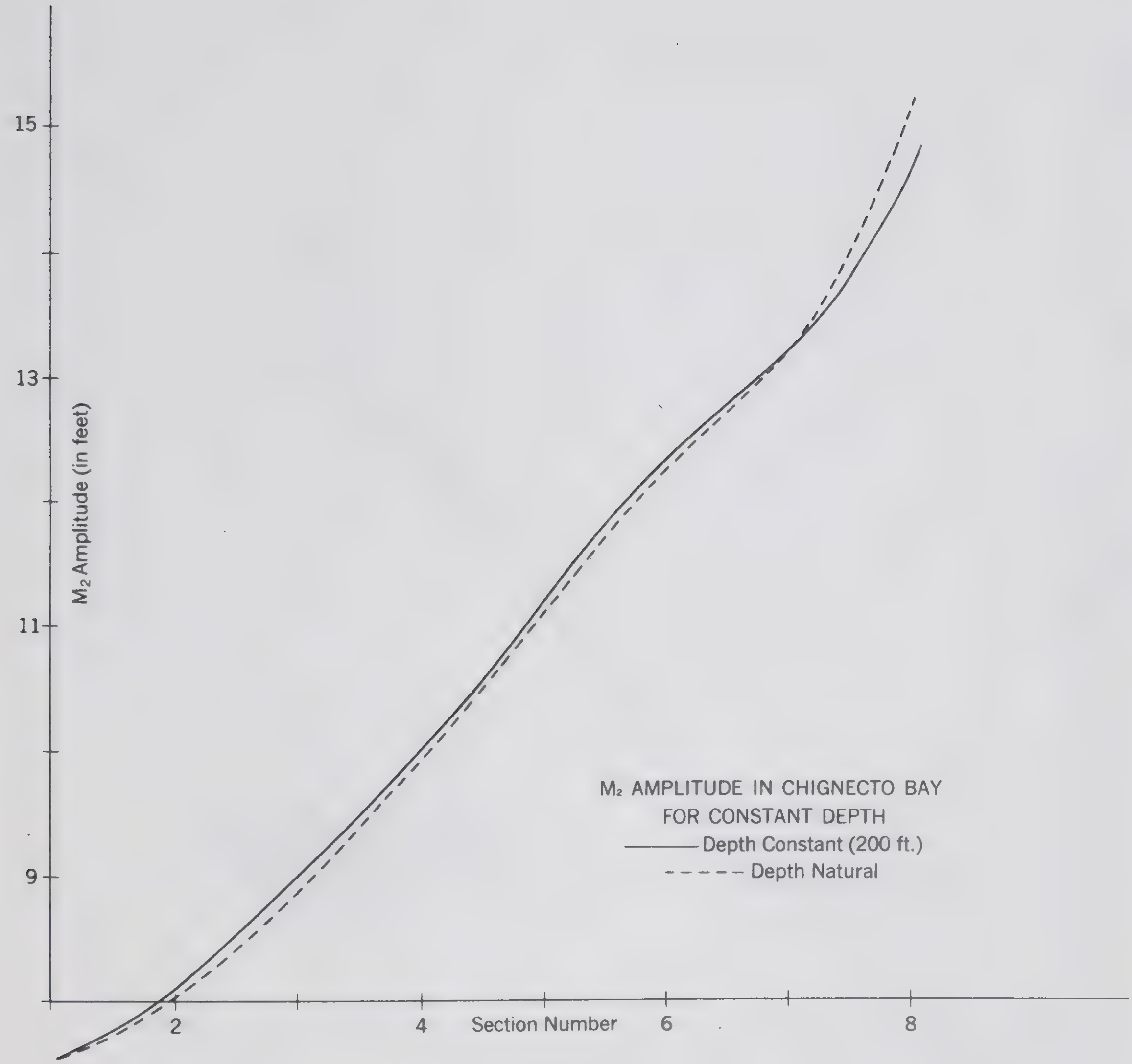

15
13
11
9
M_2 Amplitude (in feet)
2
4
Section Number
6
8
M_2 AMPLITUDE IN CHIGNECTO BAY
FOR CONSTANT DEPTH
Depth Constant (200 ft.)
Depth Natural

Figure II. 17

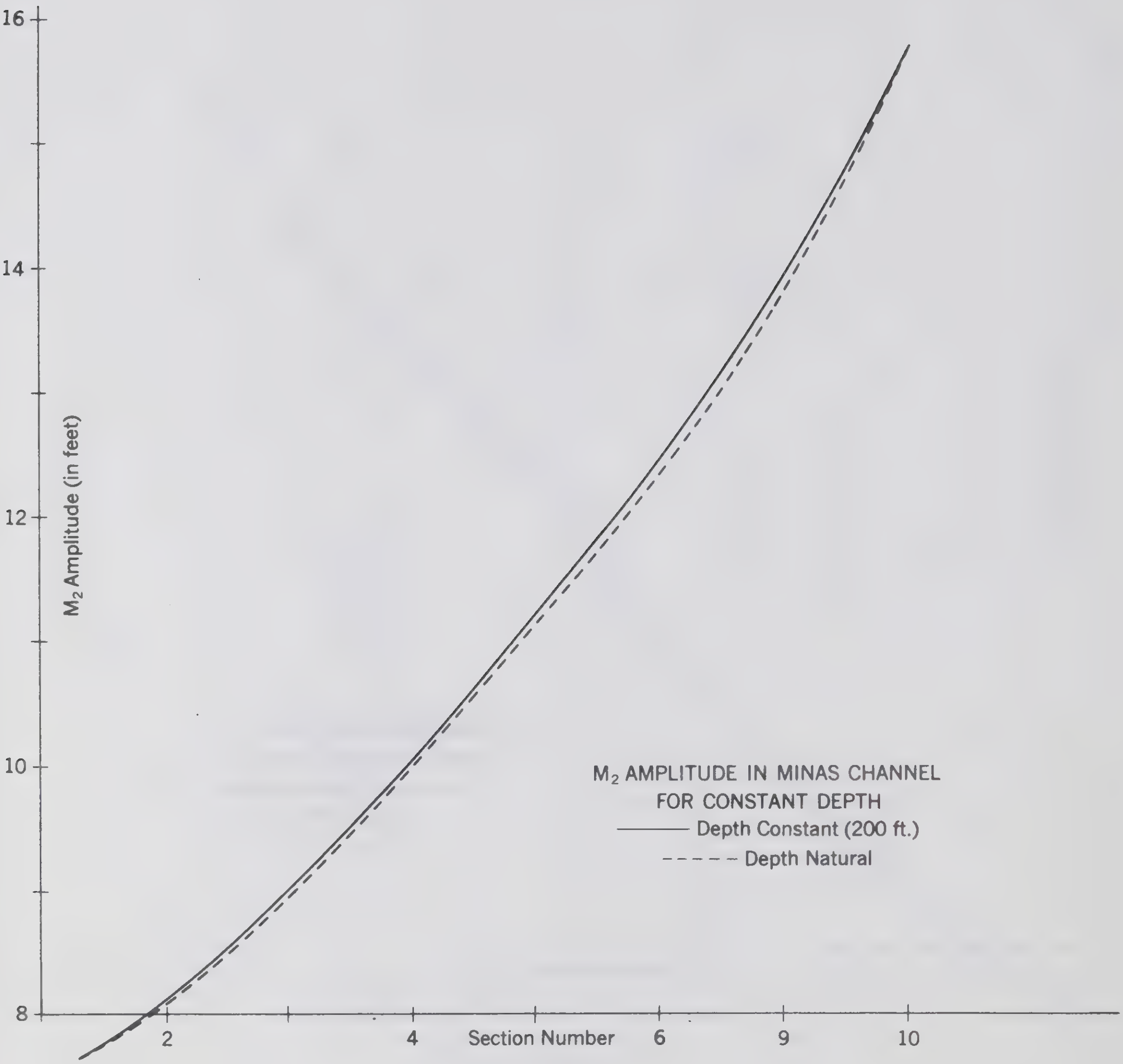

16
14
12
10
8
M_2 Amplitude (in feet)
2
4
Section Number
6
9
10
M_2 AMPLITUDE IN MINAS CHANNEL
FOR CONSTANT DEPTH
Depth Constant (200 ft.)
Depth Natural

Figure II. 18

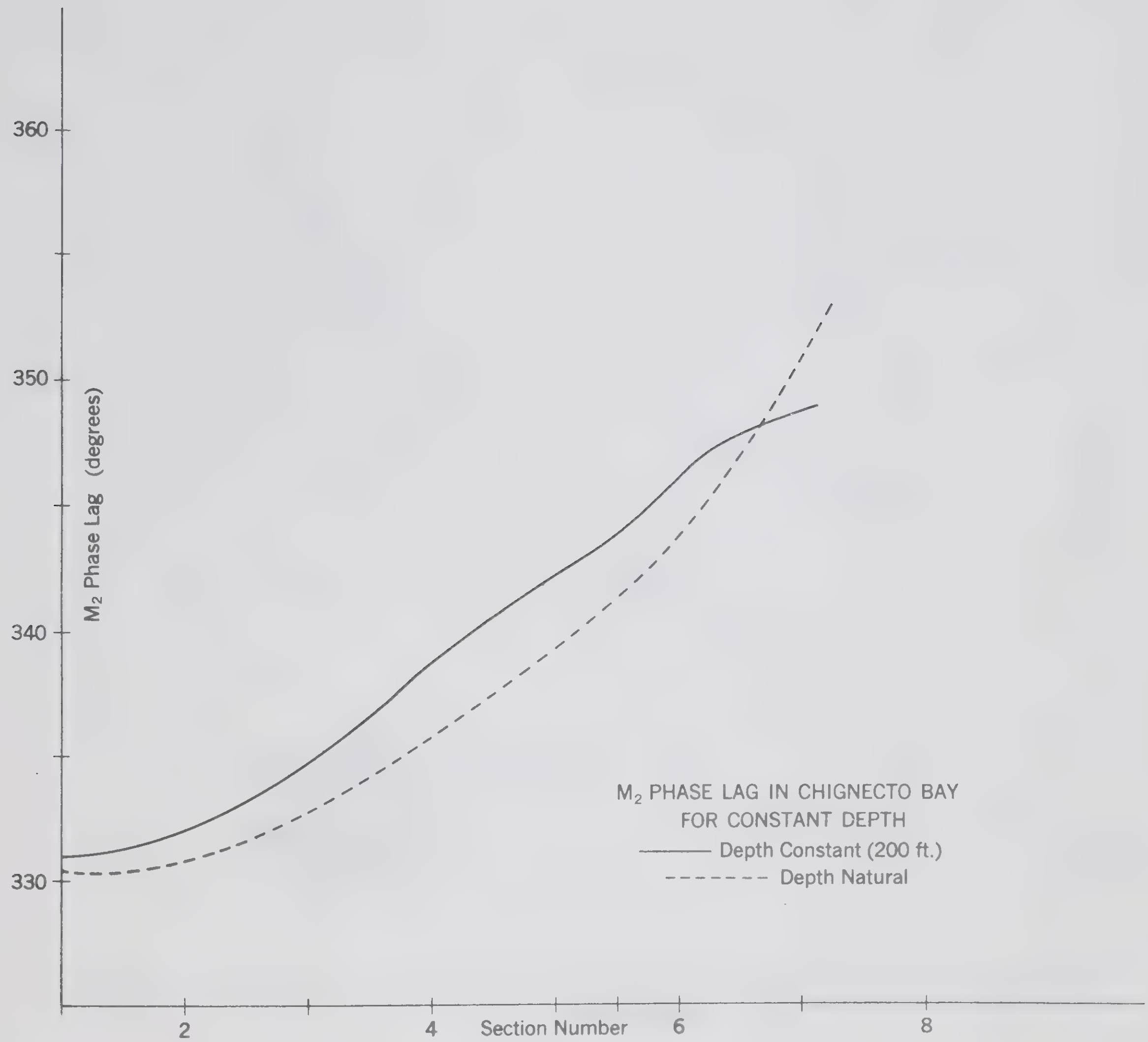
360
350
340
330
M_2 Phase Lag (degrees)
M_2 PHASE LAG IN CHIGNECTO BAY
FOR CONSTANT DEPTH
Depth Constant (200 ft.)
Depth Natural
2
4
Section Number
6
8

Figure II. 19

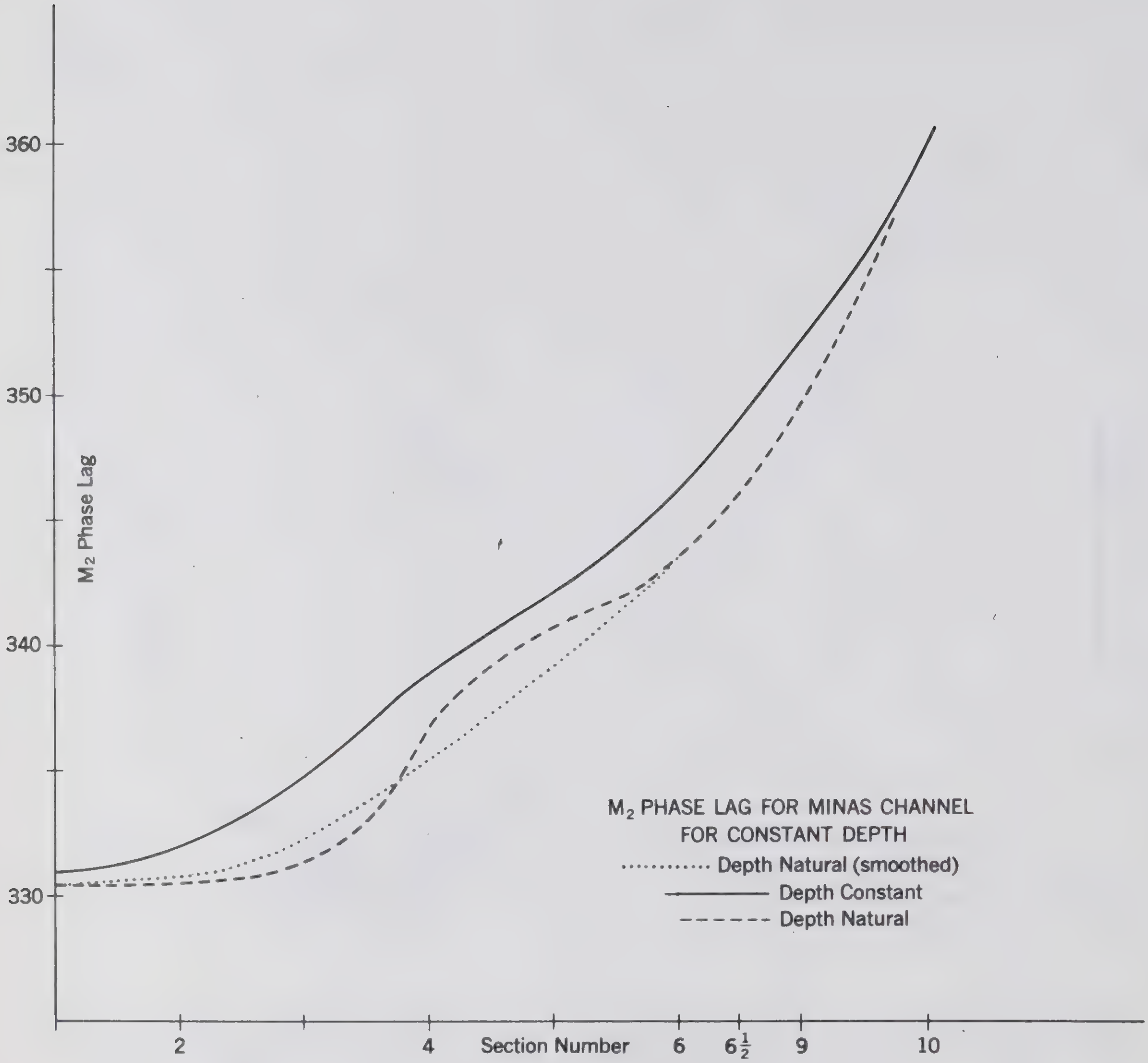

360
350
340
330
M_2 Phase Lag
M_2 PHASE LAG FOR MINAS CHANNEL
FOR CONSTANT DEPTH
Depth Natural (smoothed)
Depth Constant
Depth Natural
2
4
Section Number
6
$6\frac{1}{2}$
9
10

Figure II. 20

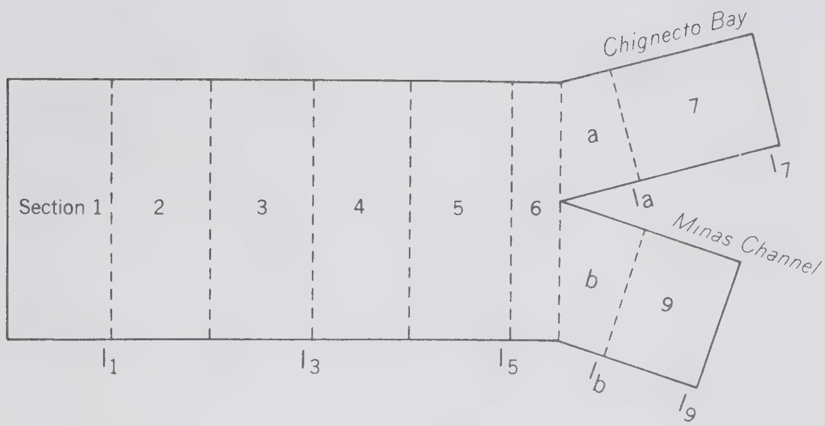

SCHEMATIZATION FOR CALCULATIONS
FOR ANALYTIC MODEL (NOT TO SCALE)

Figure III. 1

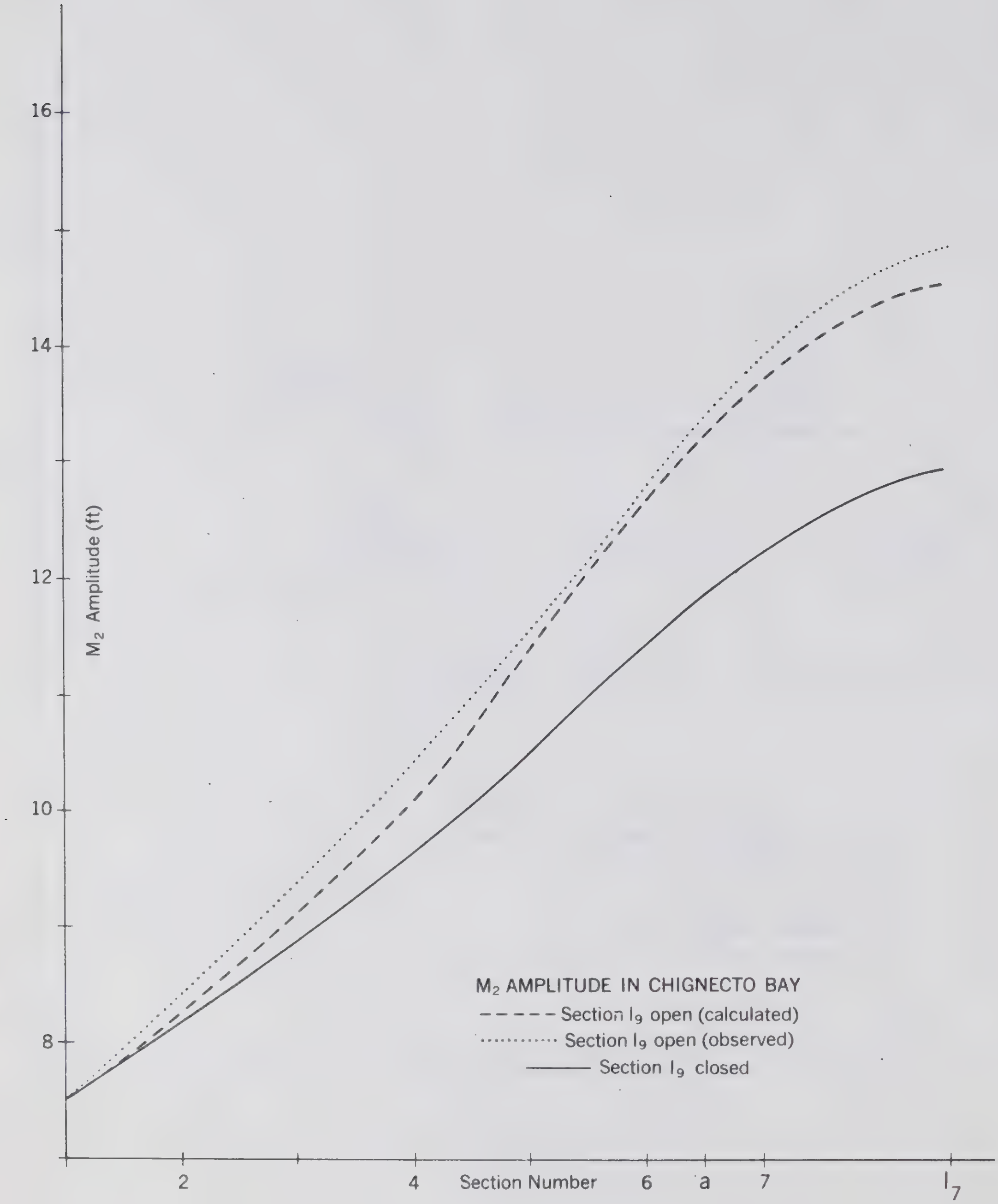
16
14
12
10
8
M₂ Amplitude (ft)
2
4
Section Number
6
a
7
I7
M₂ AMPLITUDE IN CHIGNECTO BAY
Section I9 open (calculated)
Section I9 open (observed)
Section I9 closed

Figure III. 2

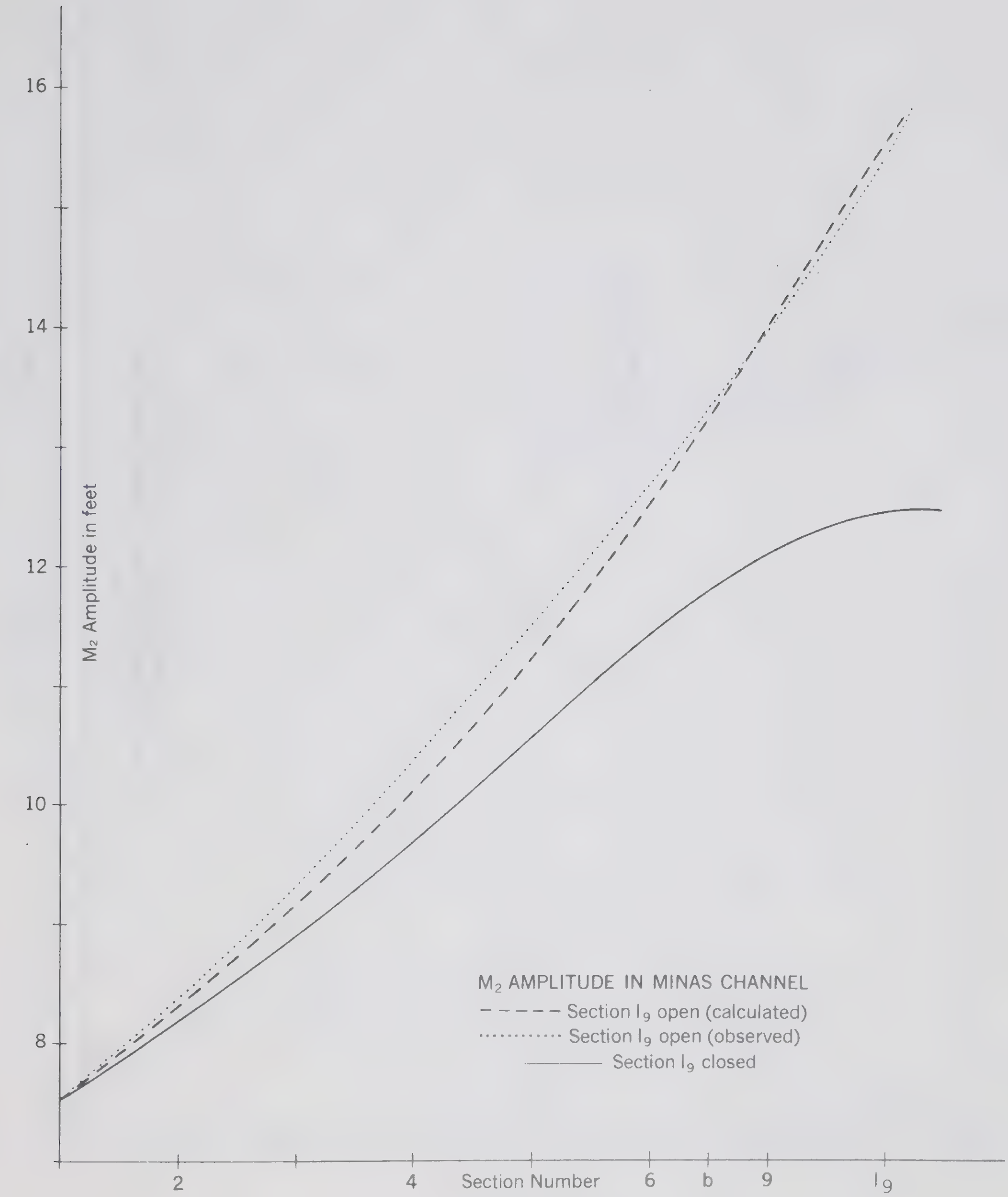

16
14
12
10
8
M₂ Amplitude in feet
2
4
Section Number
6
b
9
I9
M₂ AMPLITUDE IN MINAS CHANNEL
Section I9 open (calculated)
Section I9 open (observed)
Section I9 closed

Figure III. 3

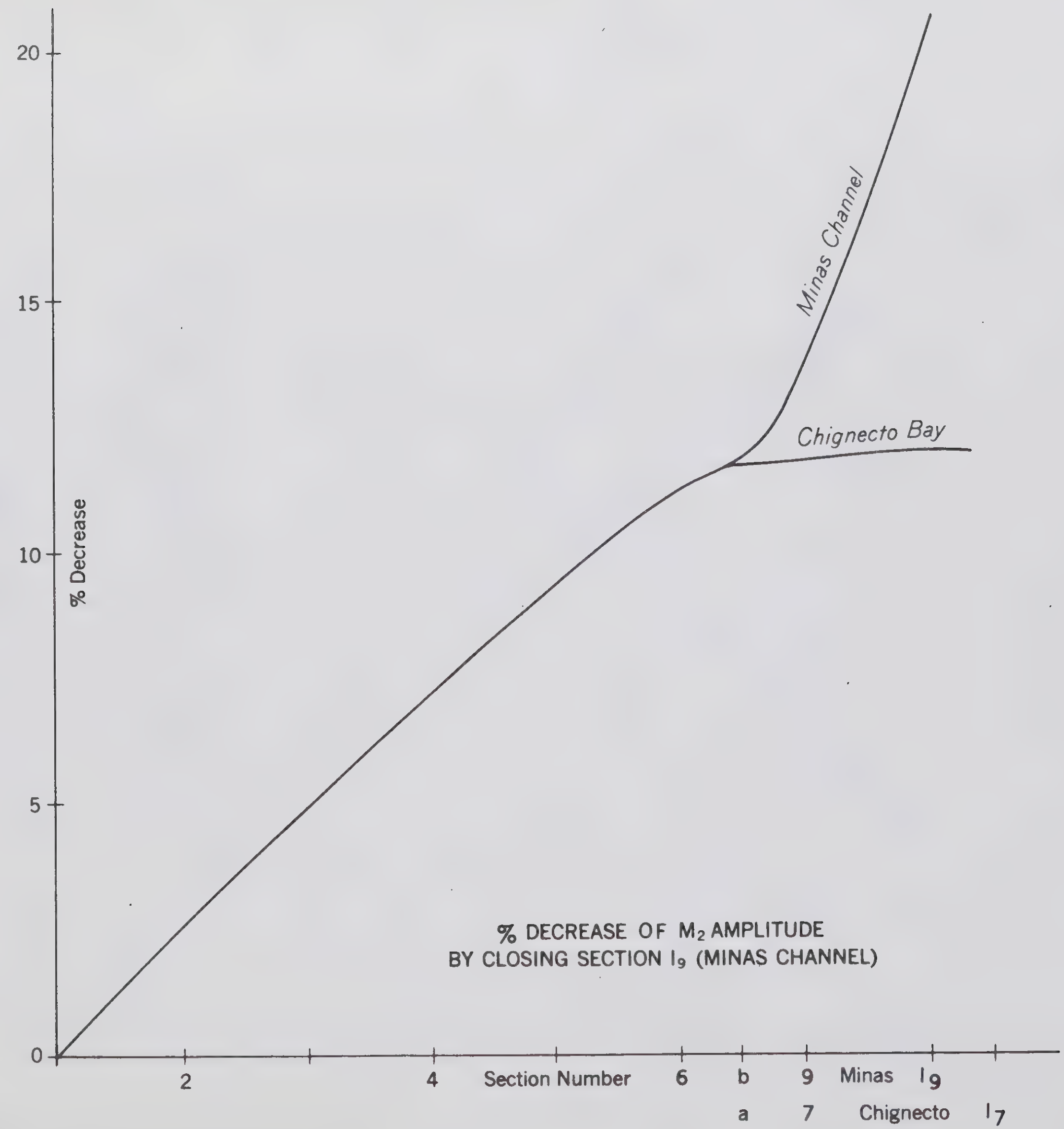
20
15
10
5
0
% Decrease
Minas Channel
Chignecto Bay
% DECREASE OF M_2 AMPLITUDE
BY CLOSING SECTION I_9 (MINAS CHANNEL)
2
4
Section Number
6
b
9
Minas
I_9
a
7
Chignecto
I_7

Figure III. 4

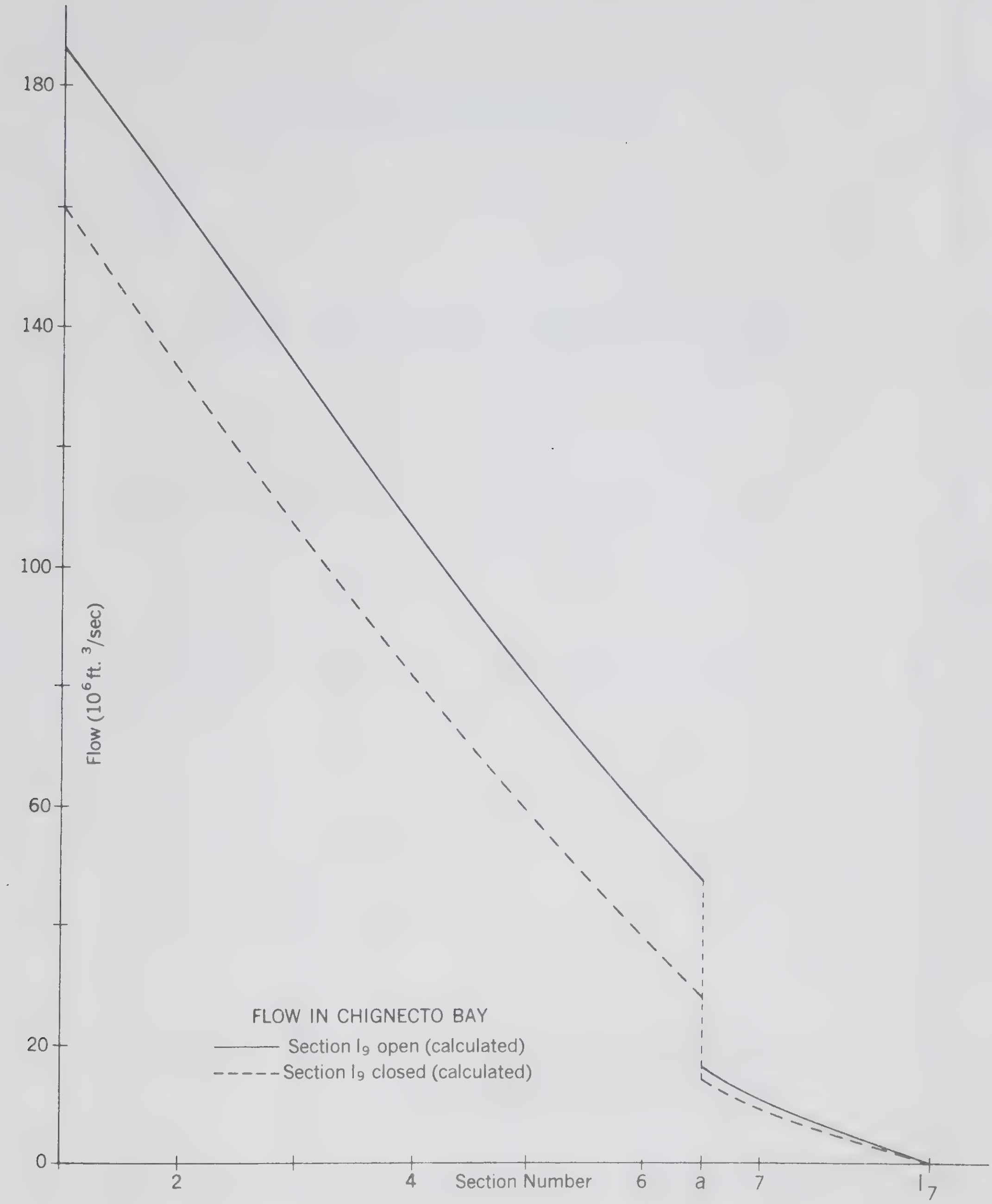

180
140
100
60
20
0
Flow (10^6 ft. ^{3}/sec)
FLOW IN CHIGNECTO BAY
Section I_9 open (calculated)
Section I_9 closed (calculated)
2
4
Section Number
6
a
7
I_7

Figure III. 5

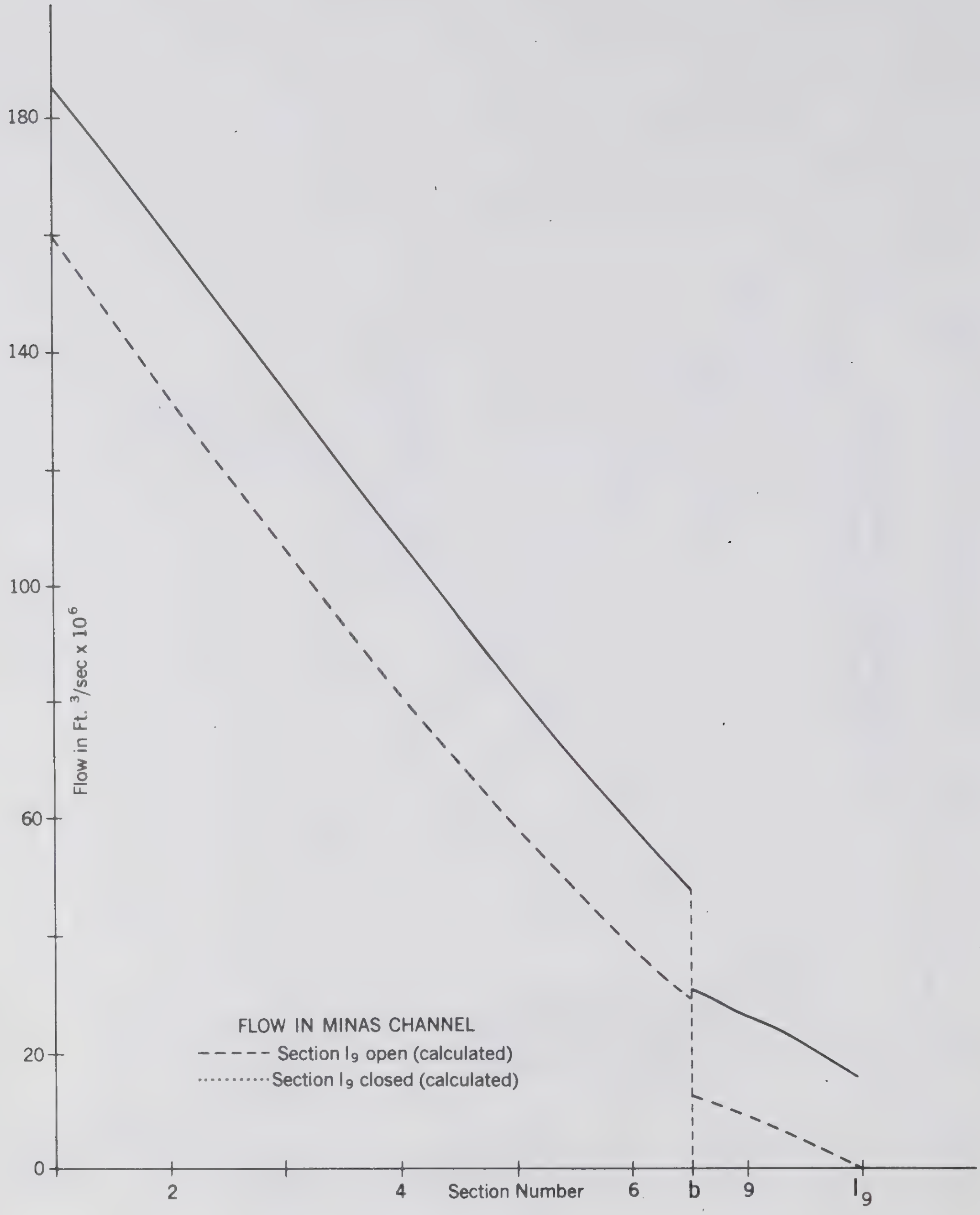
180
140
100
60
20
0
Flow in Ft. ^{3}/sec x 10^6
FLOW IN MINAS CHANNEL
Section I_9 open (calculated)
Section I_9 closed (calculated)
2
4
Section Number
6
b
9
I_9

Figure III. 6

NOTATION USED IN THE
RECTANGULAR CO-ORDINATE SYSTEMS

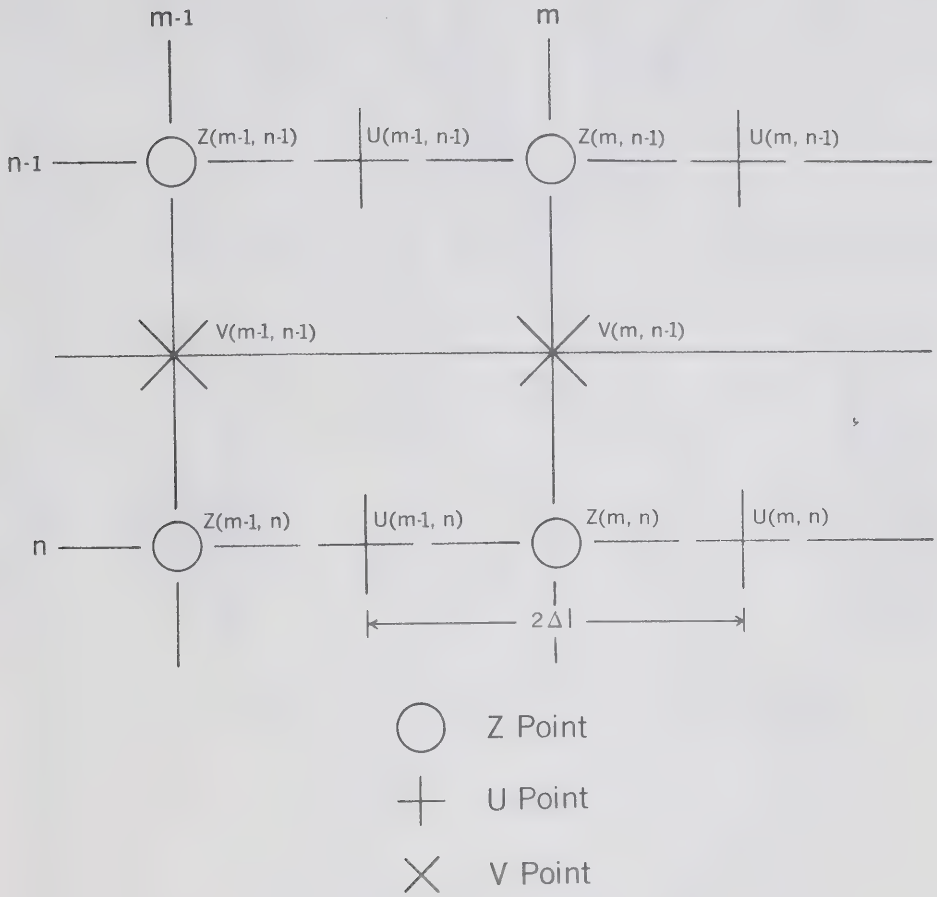

Figure IV. 1

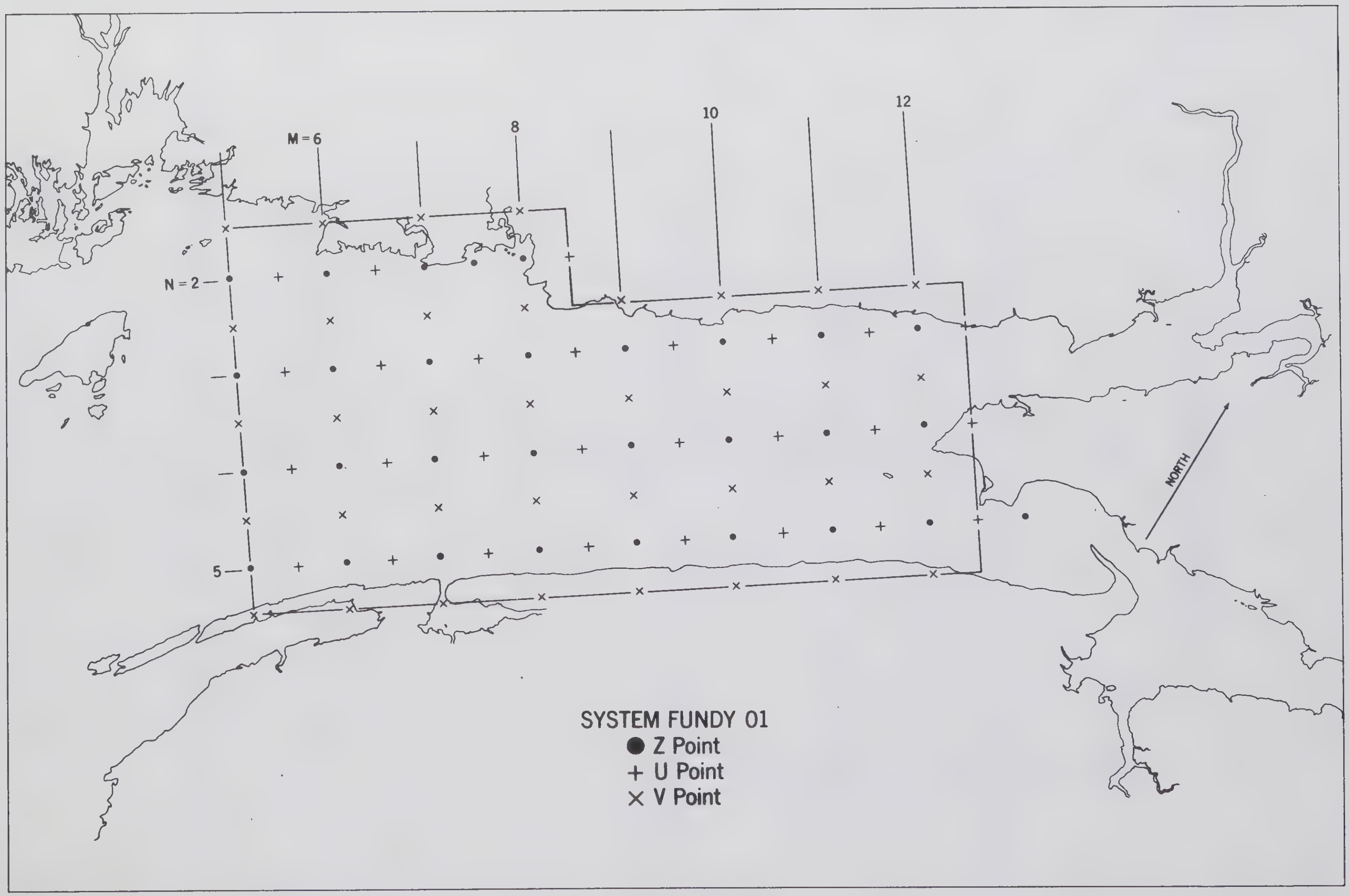

Figure IV. 2

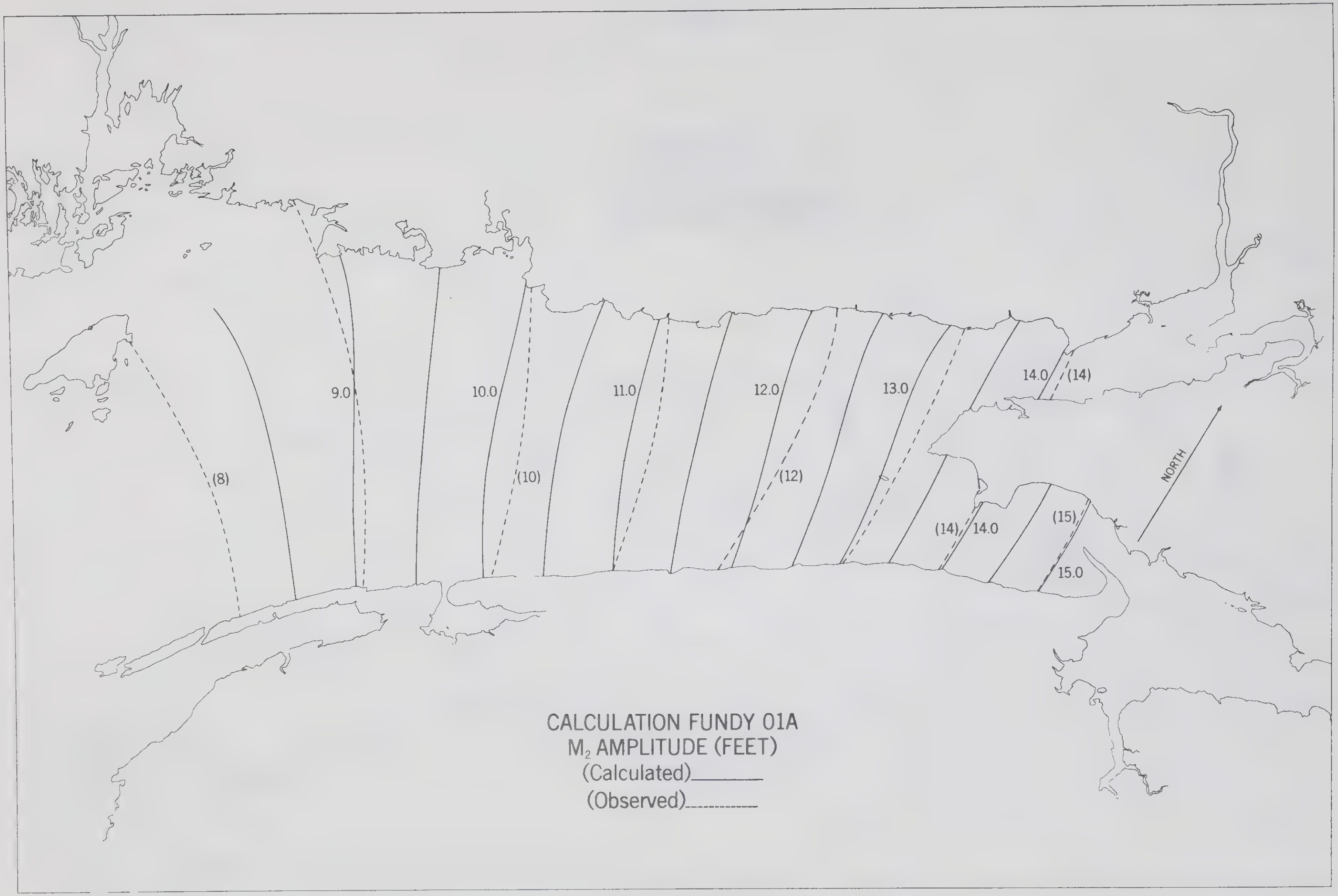
9.0
10.0
11.0
12.0
13.0
14.0
(14)
(8)
(10)
(12)
(14)
14.0
(15)
15.0
NORTH
CALCULATION FUNDY 01A
M_2 AMPLITUDE (FEET)
(Calculated)
(Observed)

Figure IV. 3

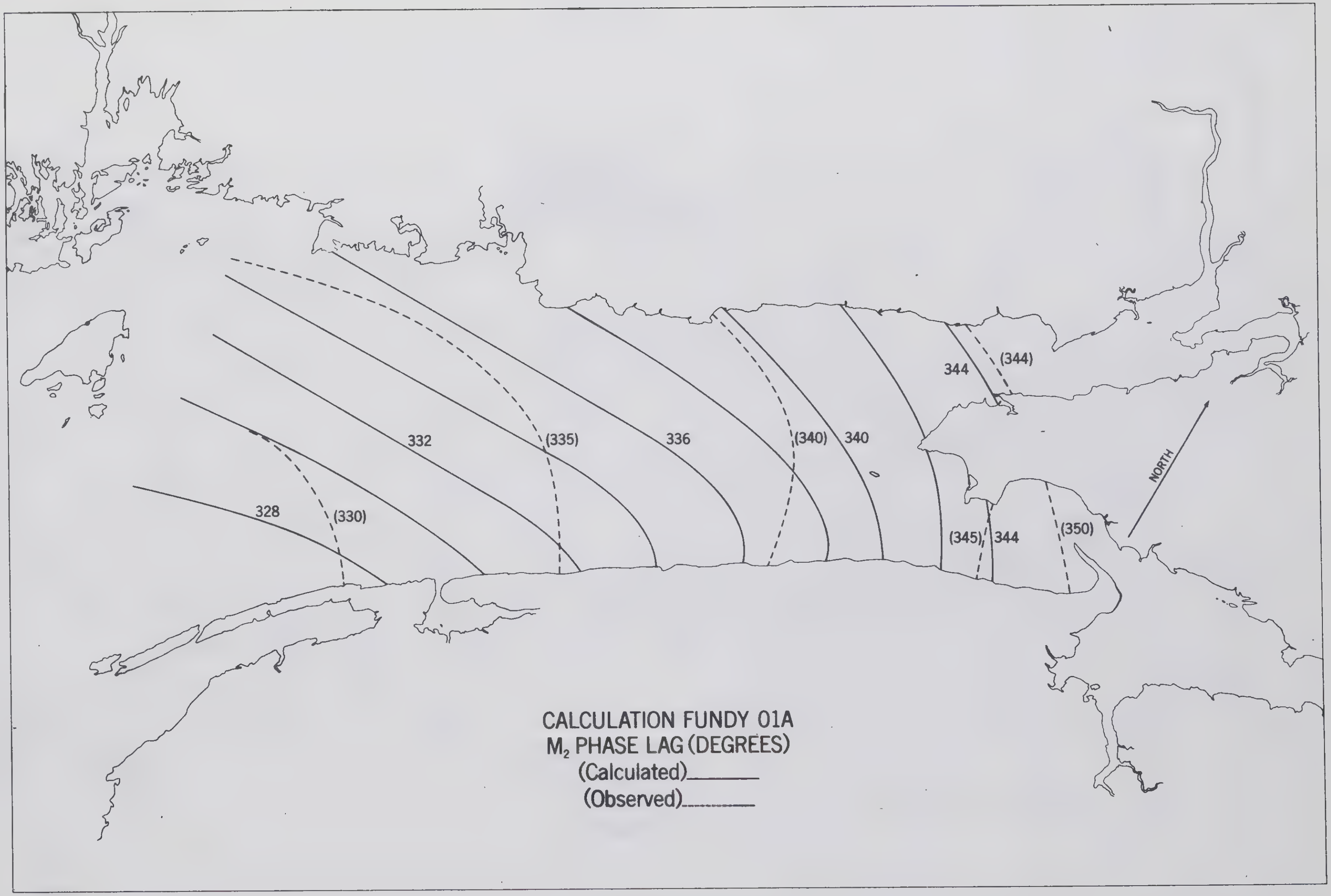
CALCULATION FUNDY 01A
M_2 PHASE LAG (DEGREES)
(Calculated)
(Observed)
NORTH
328
(330)
332
(335)
336
(340)
340
344
(344)
(345)
344
(350)

Figure IV. 4

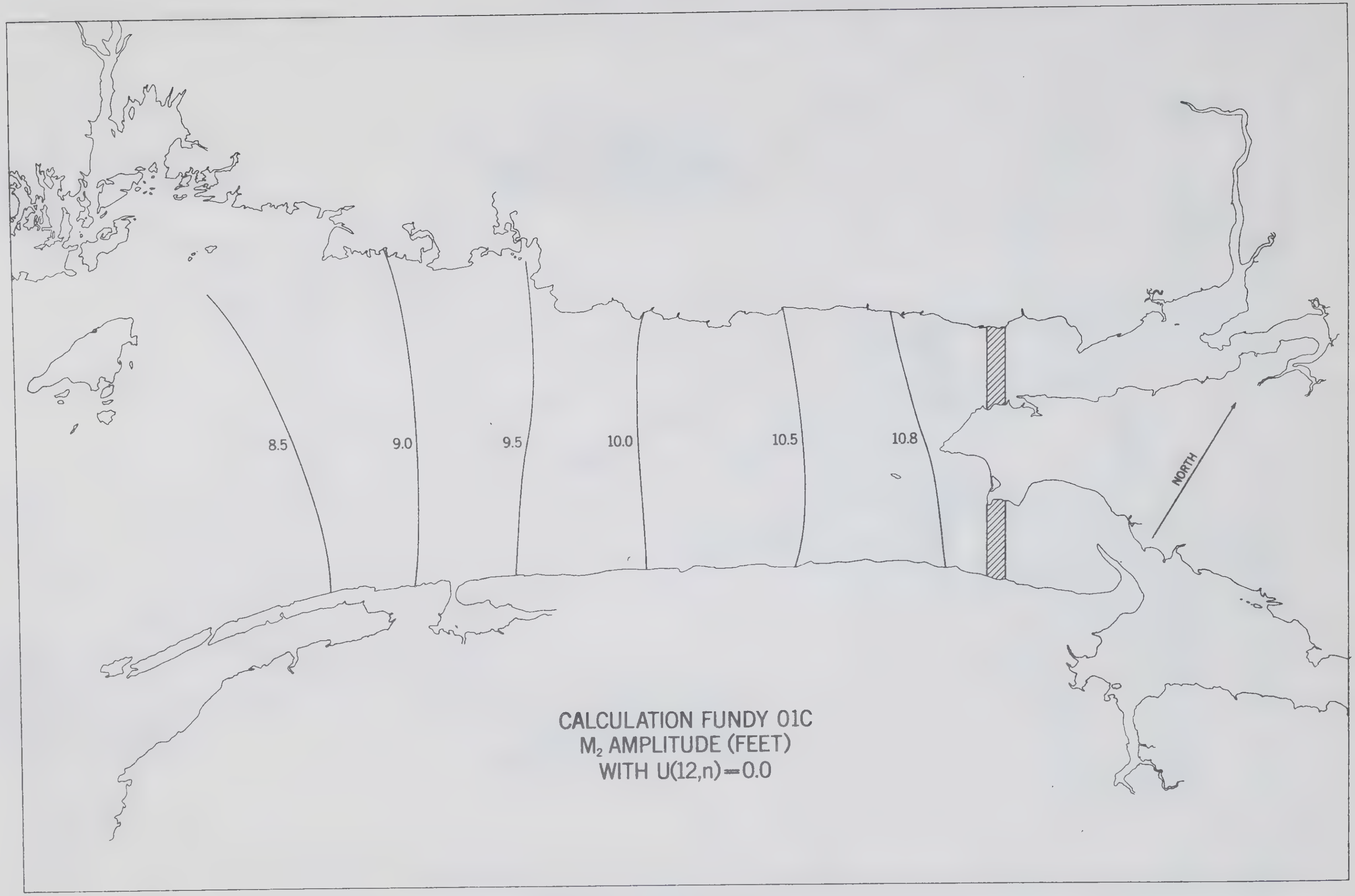
8.5
9.0
9.5
10.0
10.5
10.8
NORTH
CALCULATION FUNDY 01C
M_2 AMPLITUDE (FEET)
WITH U(12,n)=0.0

Figure IV. 5

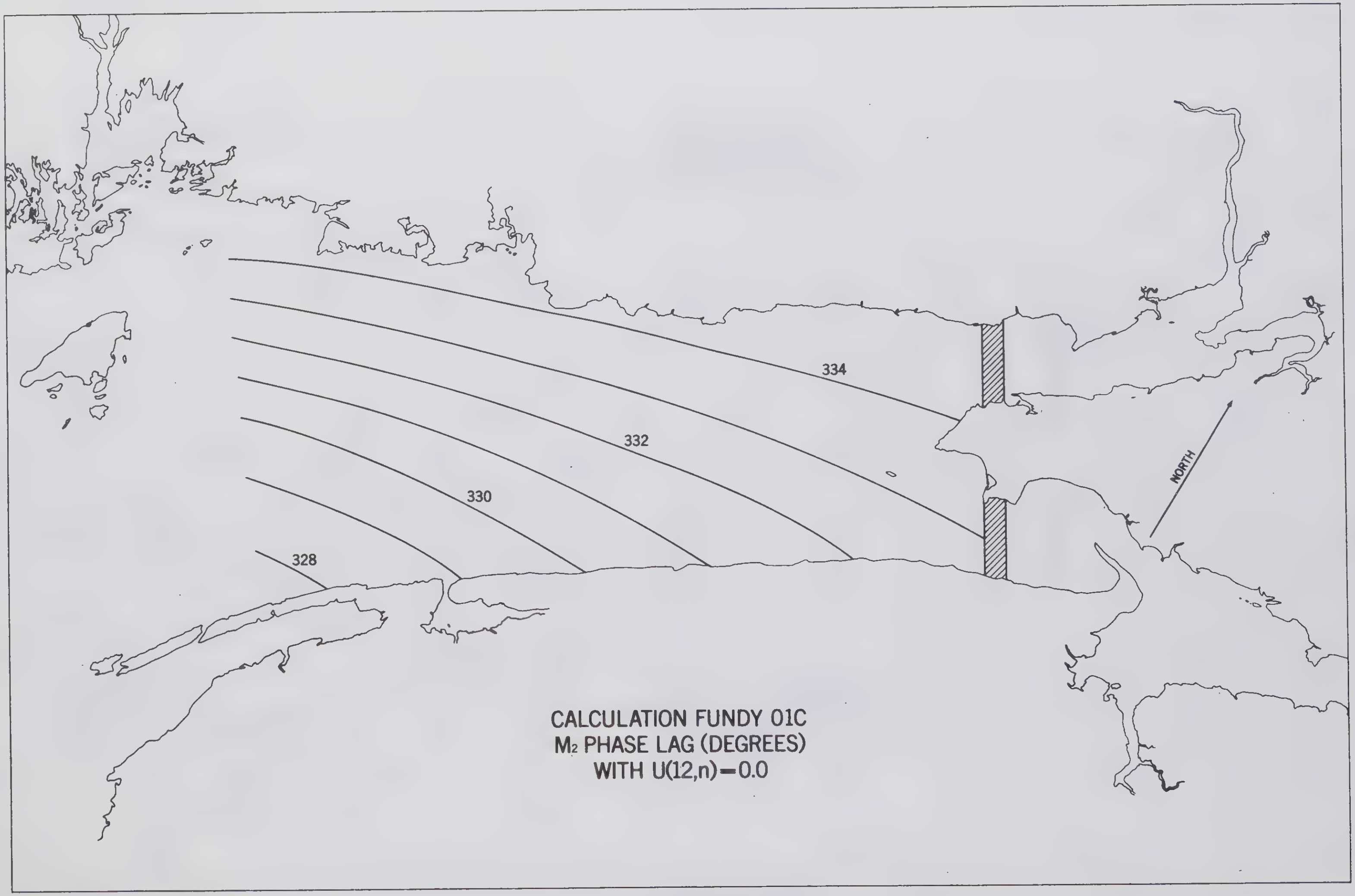
334
332
330
328
NORTH
CALCULATION FUNDY 01C
M2 PHASE LAG (DEGREES)
WITH U(12,n)—0.0

Figure IV. 6

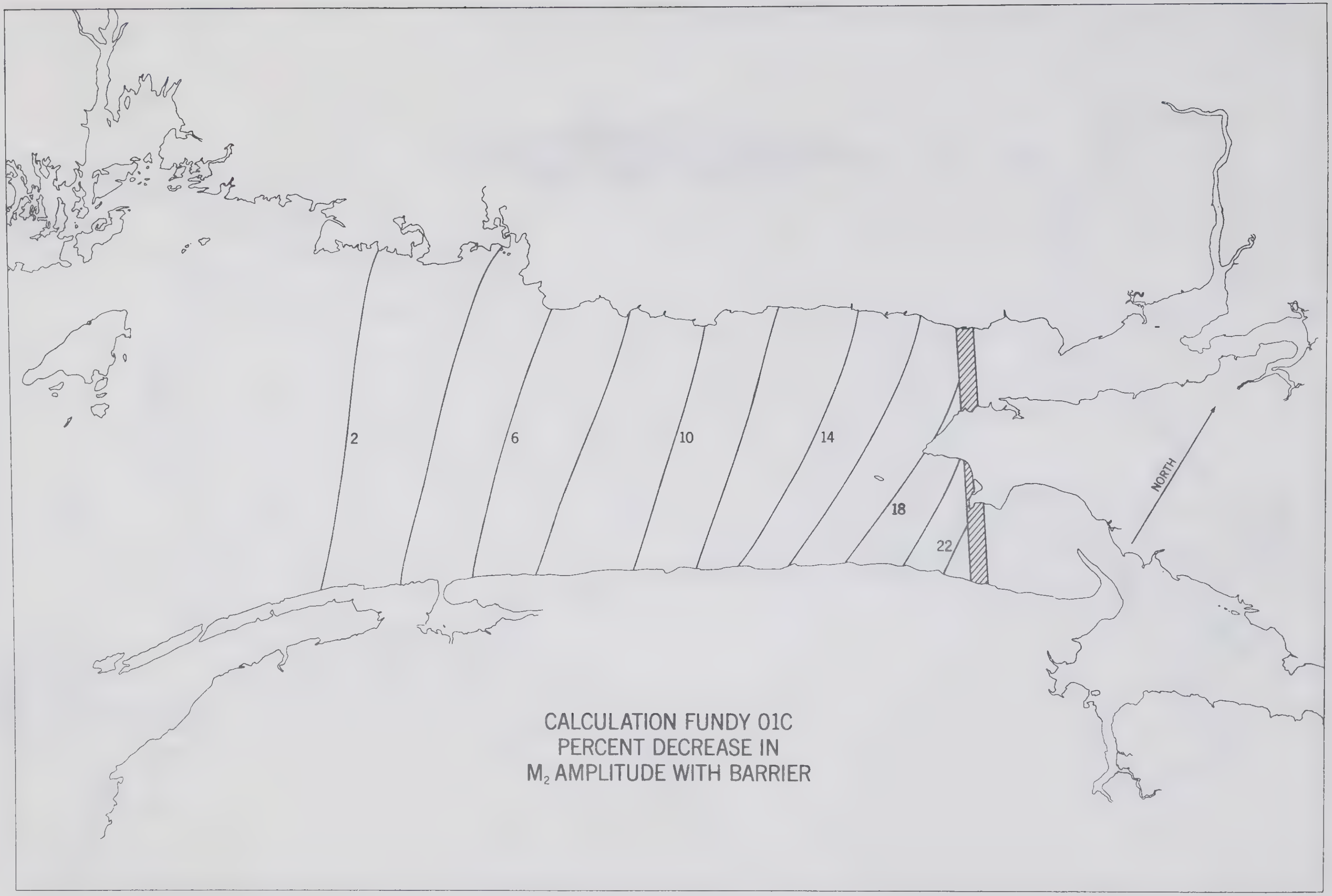
2
6
10
14
18
22
NORTH
CALCULATION FUNDY 01C
PERCENT DECREASE IN
M_2 AMPLITUDE WITH BARRIER

Figure IV. 7

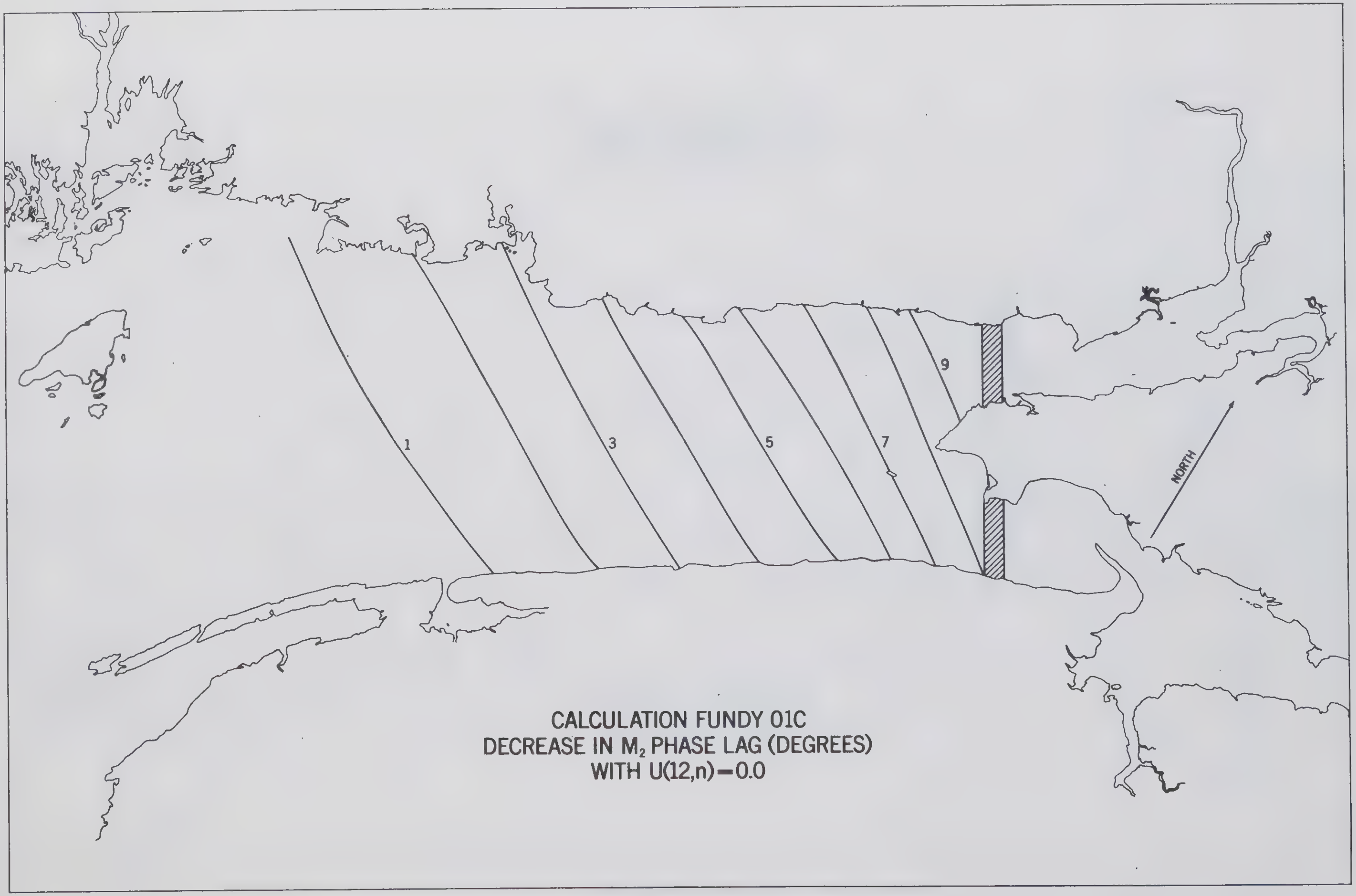
CALCULATION FUNDY 01C
DECREASE IN M_2 PHASE LAG (DEGREES)
WITH U(12,n)—0.0
NORTH
1
3
5
7
9

Figure IV. 8

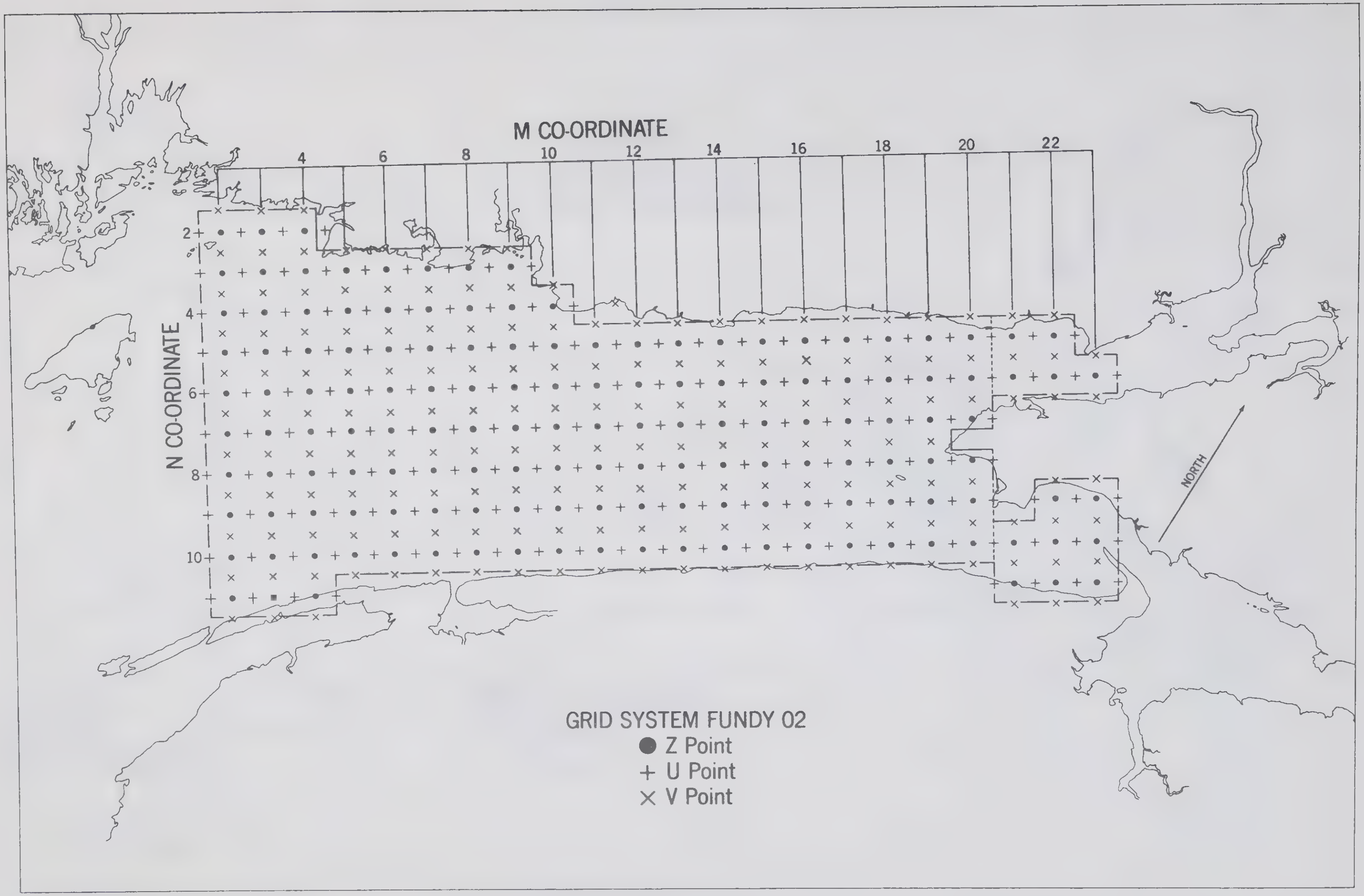
M CO-ORDINATE
4
6
8
10
12
14
16
18
20
22
N CO-ORDINATE
2
4
6
8
10
NORTH
GRID SYSTEM FUNDY 02
Z Point
U Point
V Point

Figure IV. 9

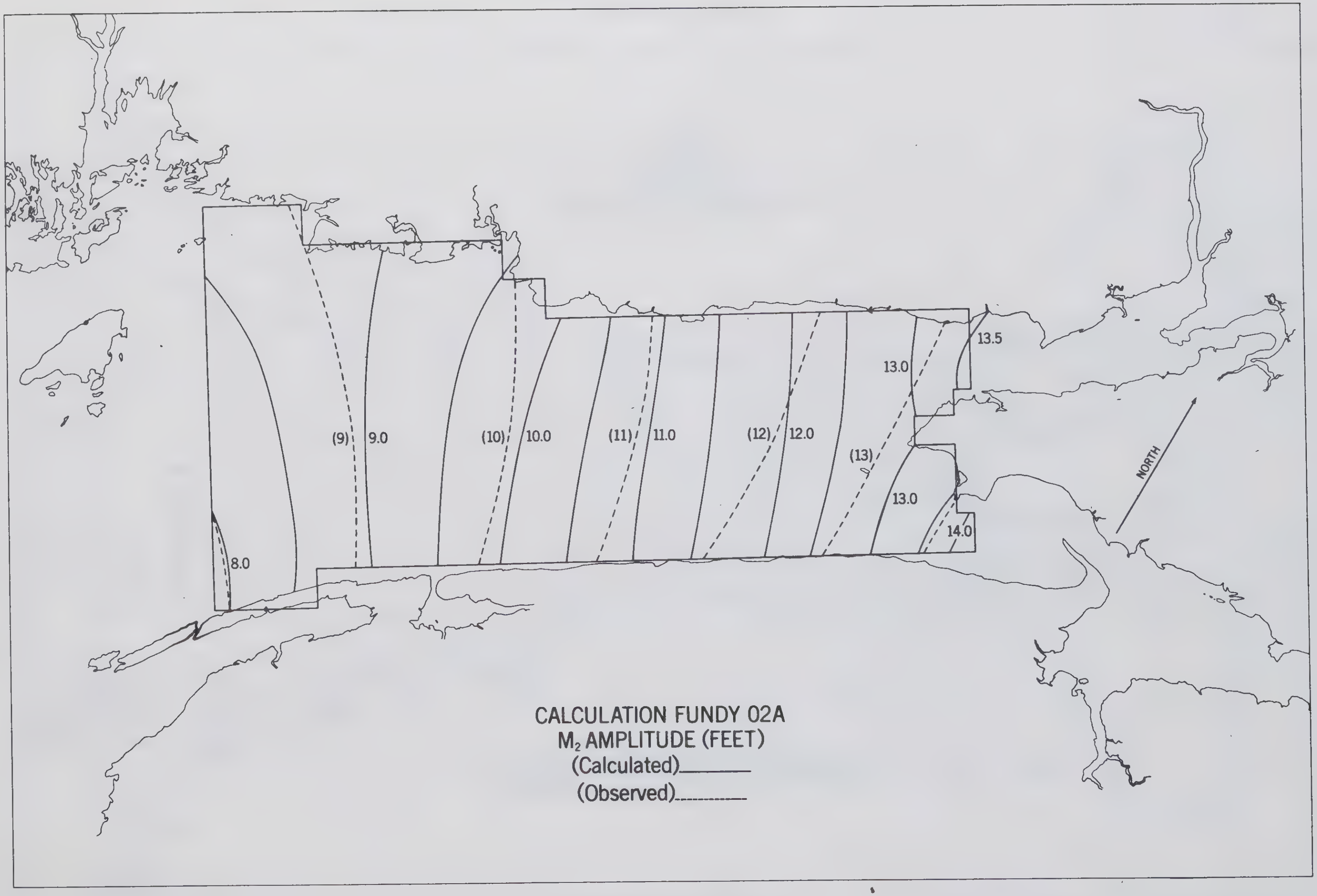

13.5
13.0
(9)
9.0
(10)
10.0
(11)
11.0
(12)
12.0
(13)
13.0
14.0
8.0
NORTH
CALCULATION FUNDY 02A
M_2 AMPLITUDE (FEET)
(Calculated)
(Observed)

Figure IV. 10

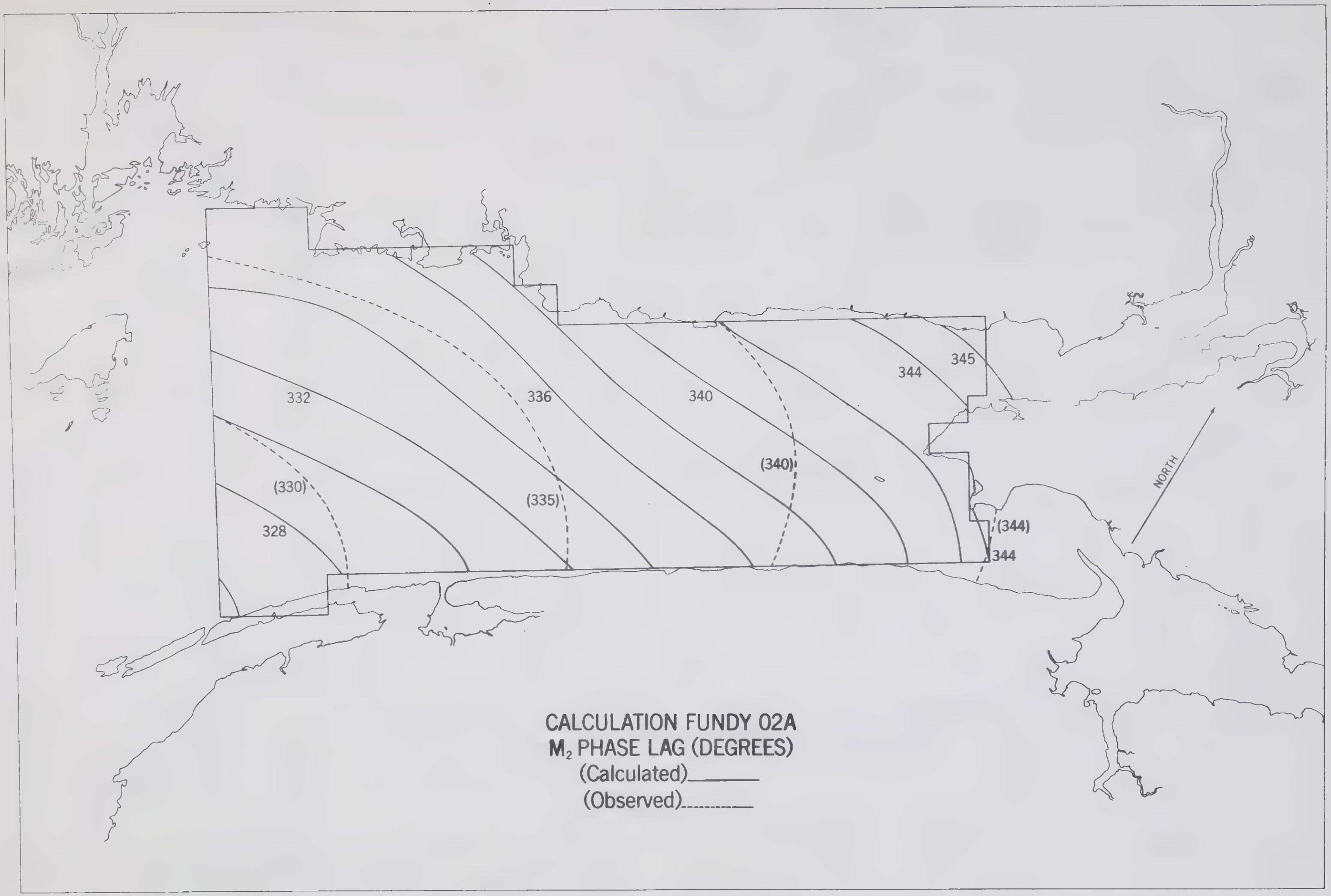
NORTH
345
344
340
336
332
328
(344)
344
(340)
(335)
(330)
CALCULATION FUNDY 02A
M_2 PHASE LAG (DEGREES)
(Calculated)
(Observed)

Figure IV. 11

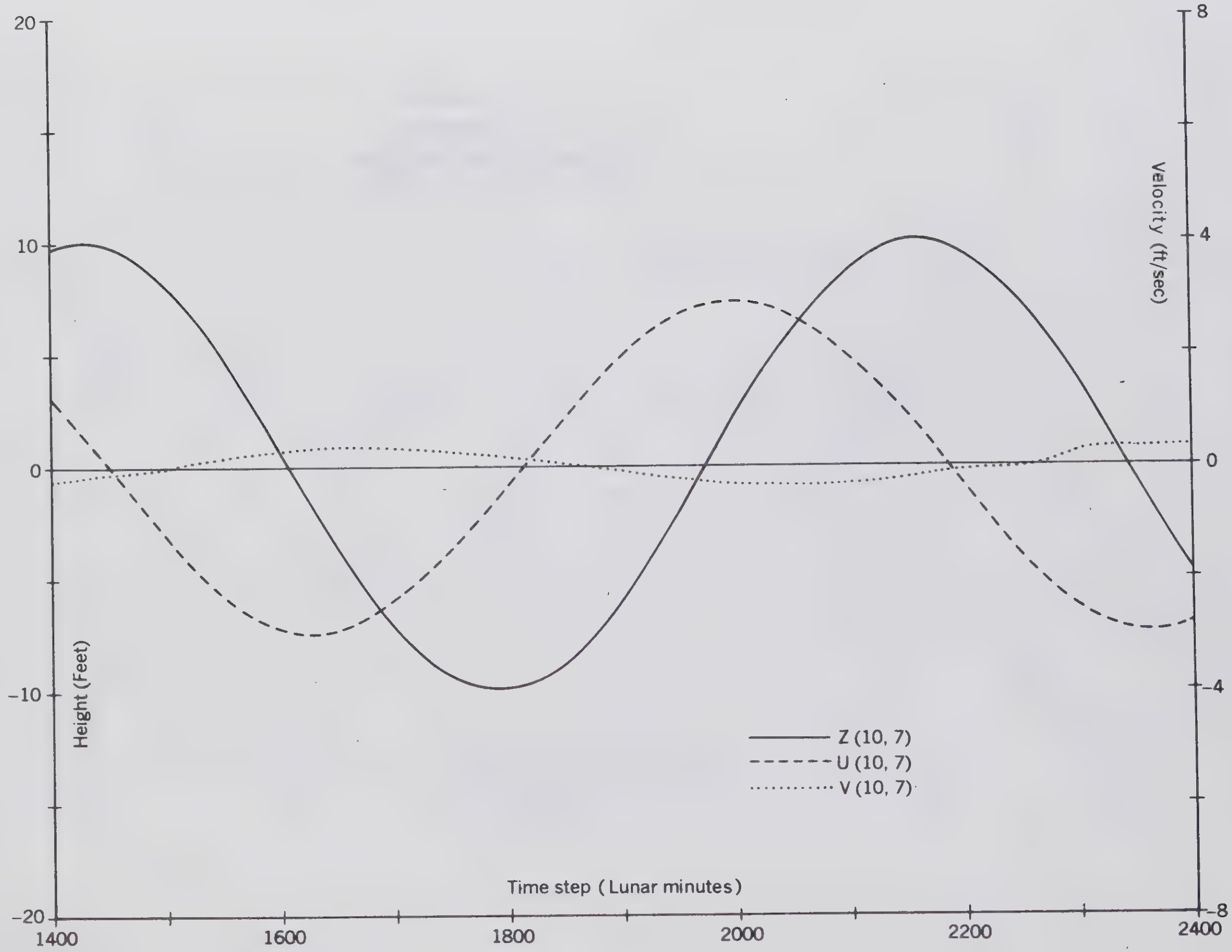

Figure IV. 12(a)

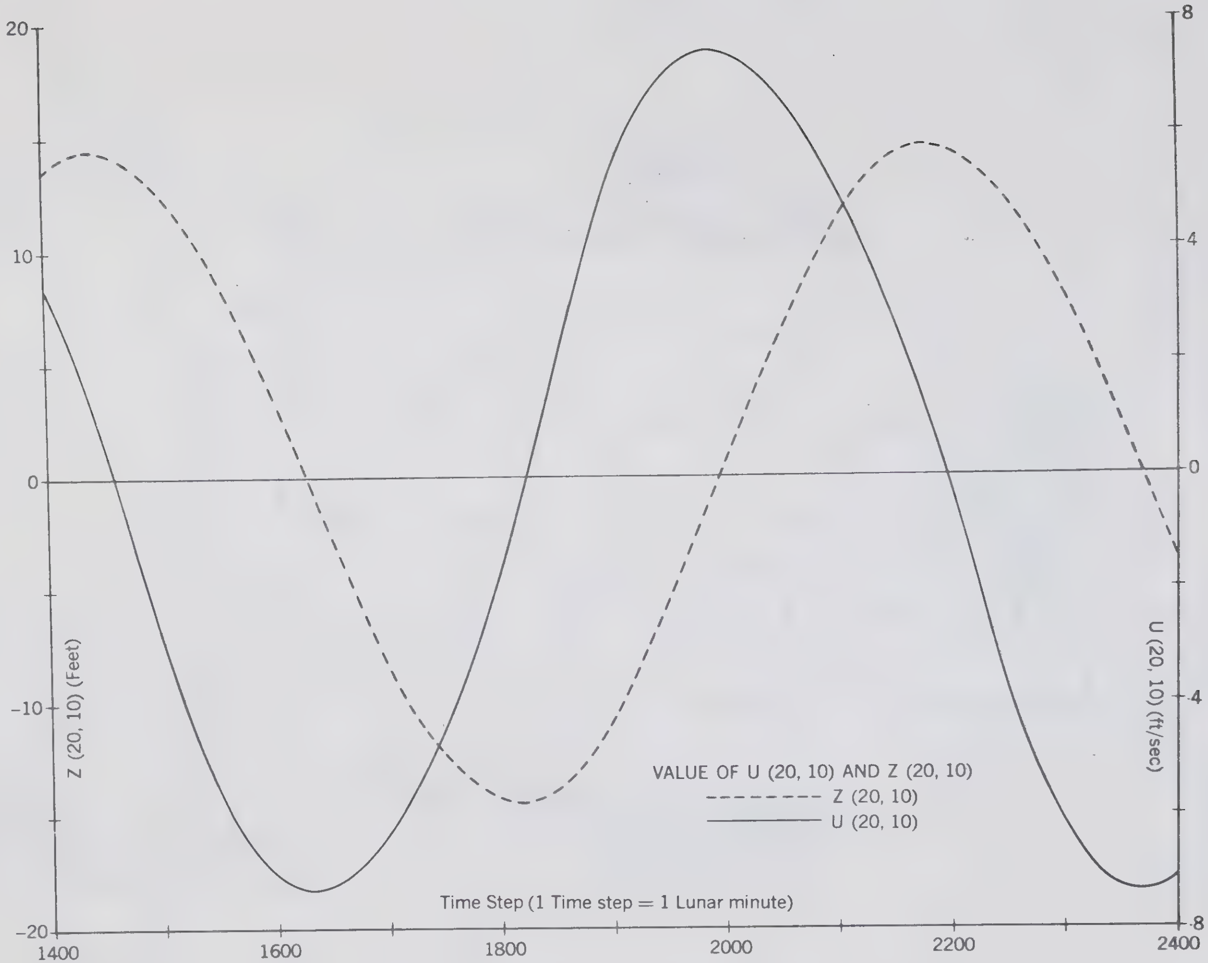

Figure IV. 12(b)

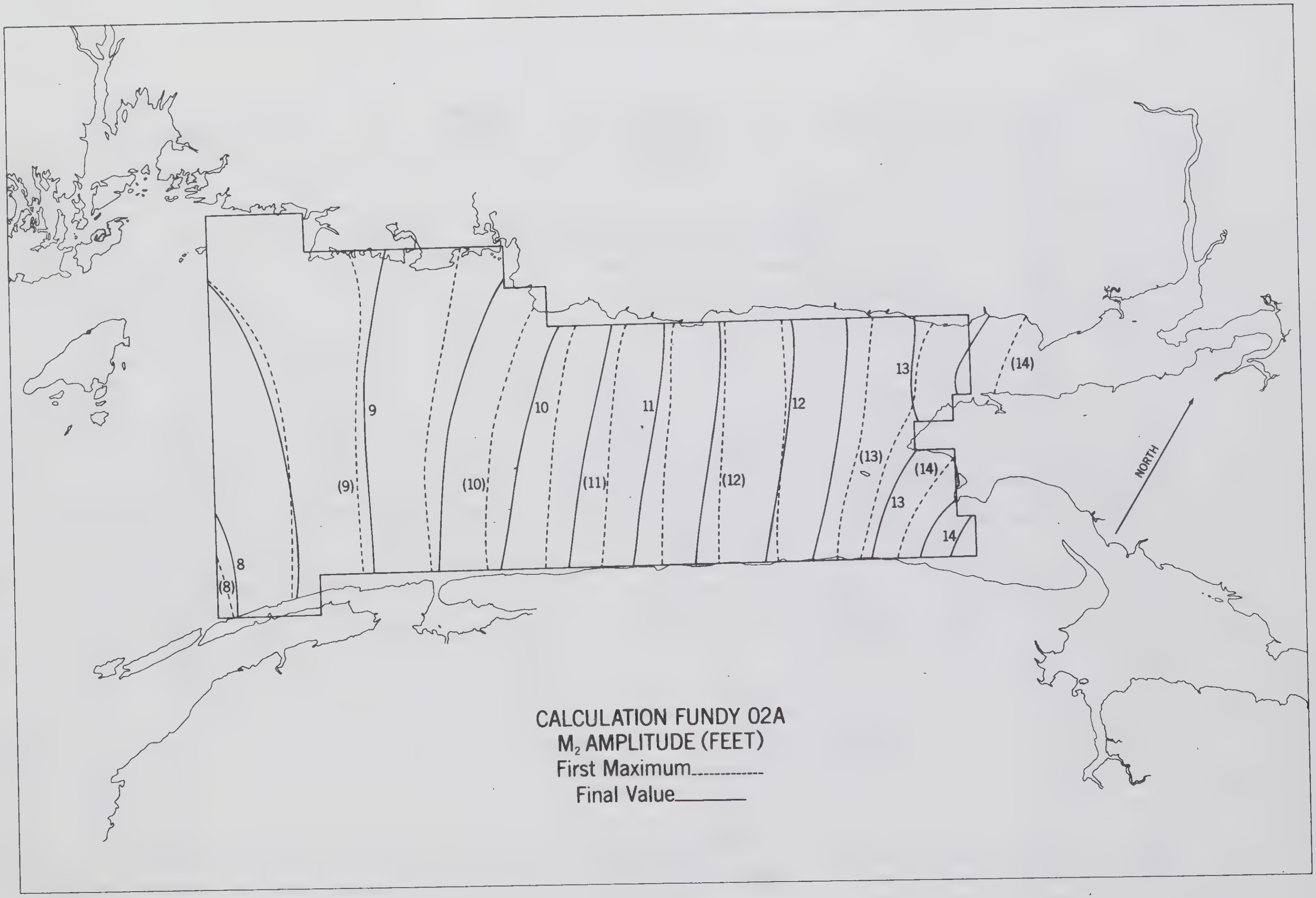
CALCULATION FUNDY 02A
M_2 AMPLITUDE (FEET)
First Maximum
Final Value
NORTH
8
(8)
9
(9)
10
(10)
11
(11)
12
(12)
13
(13)
14
(14)

Figure IV. 13

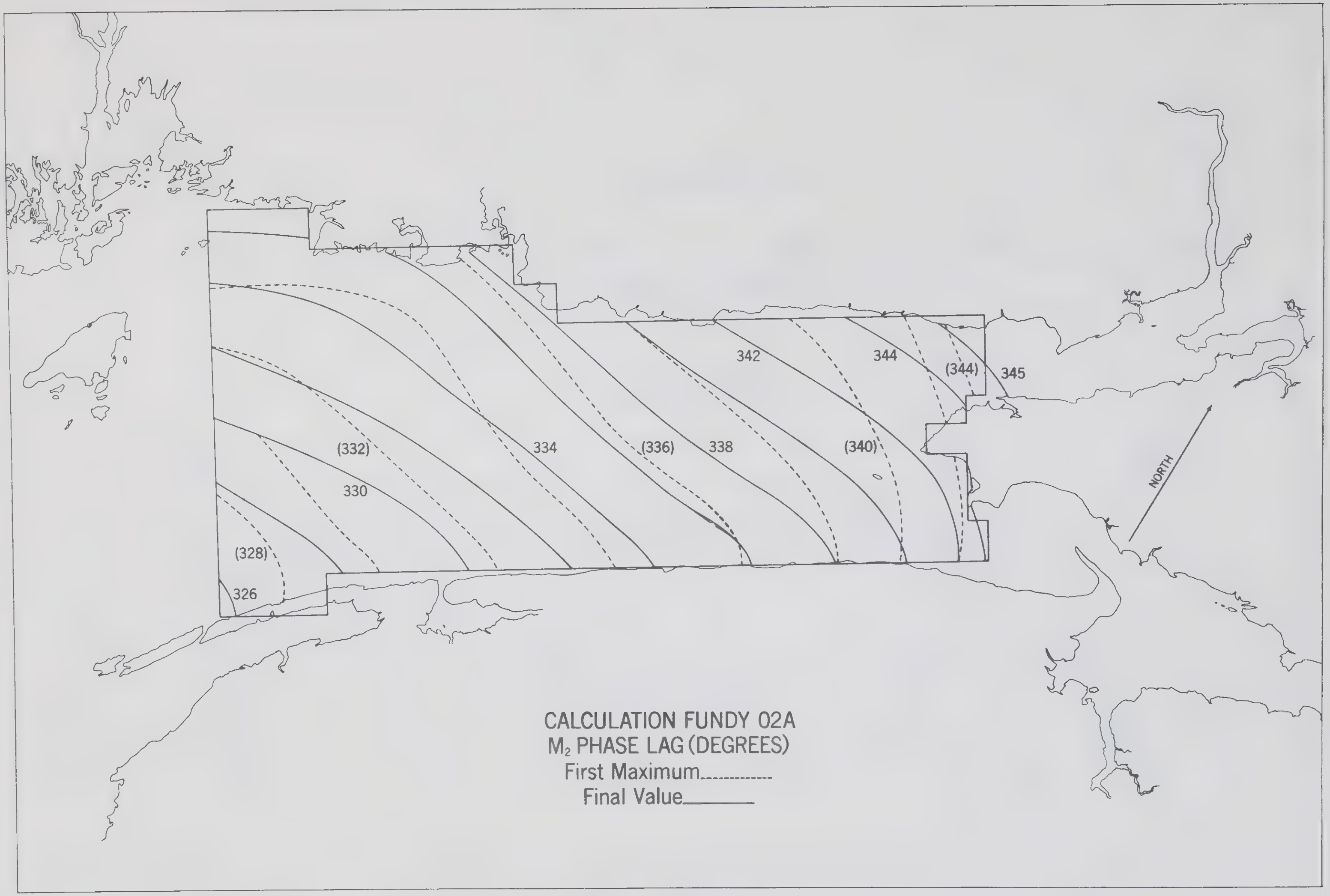
NORTH
345
(344)
344
342
(340)
338
(336)
334
(332)
330
(328)
326
CALCULATION FUNDY 02A
M2 PHASE LAG (DEGREES)
First Maximum
Final Value

Figure IV. 14

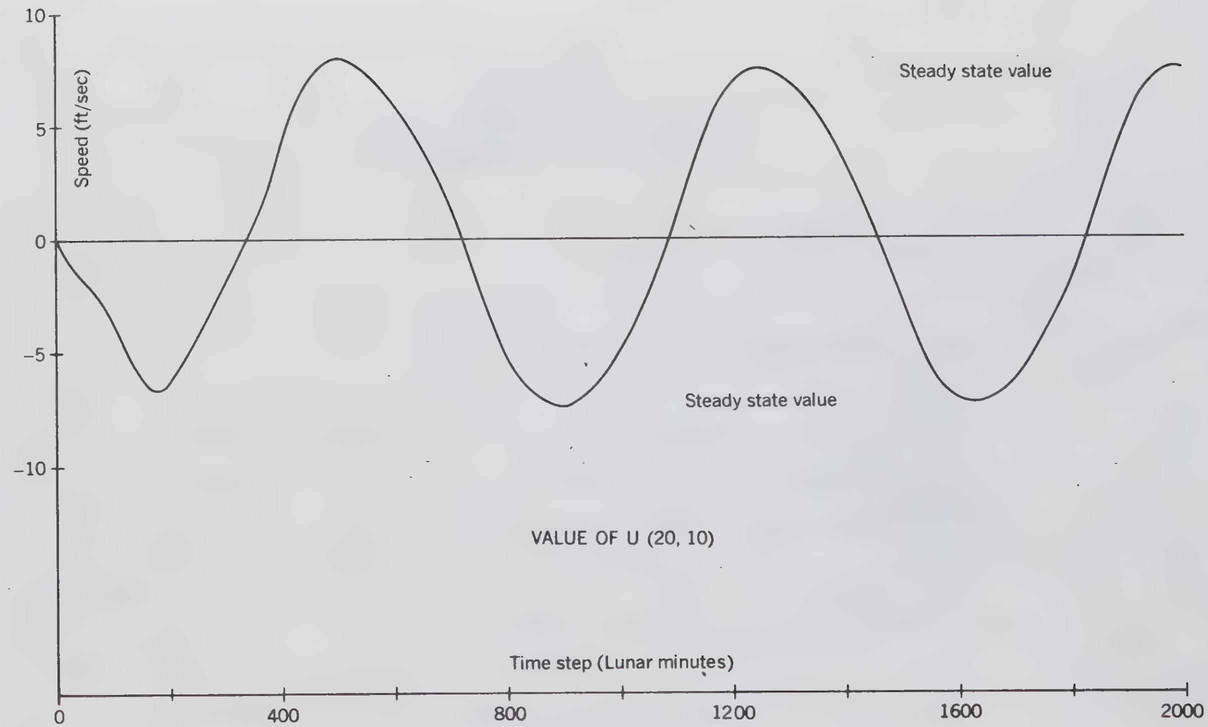
10
5
0
-5
-10
Speed (ft/sec)
Steady state value
Steady state value
VALUE OF U (20, 10)
Time step (Lunar minutes)
0
400
800
1200
1600
2000

Figure IV. 15

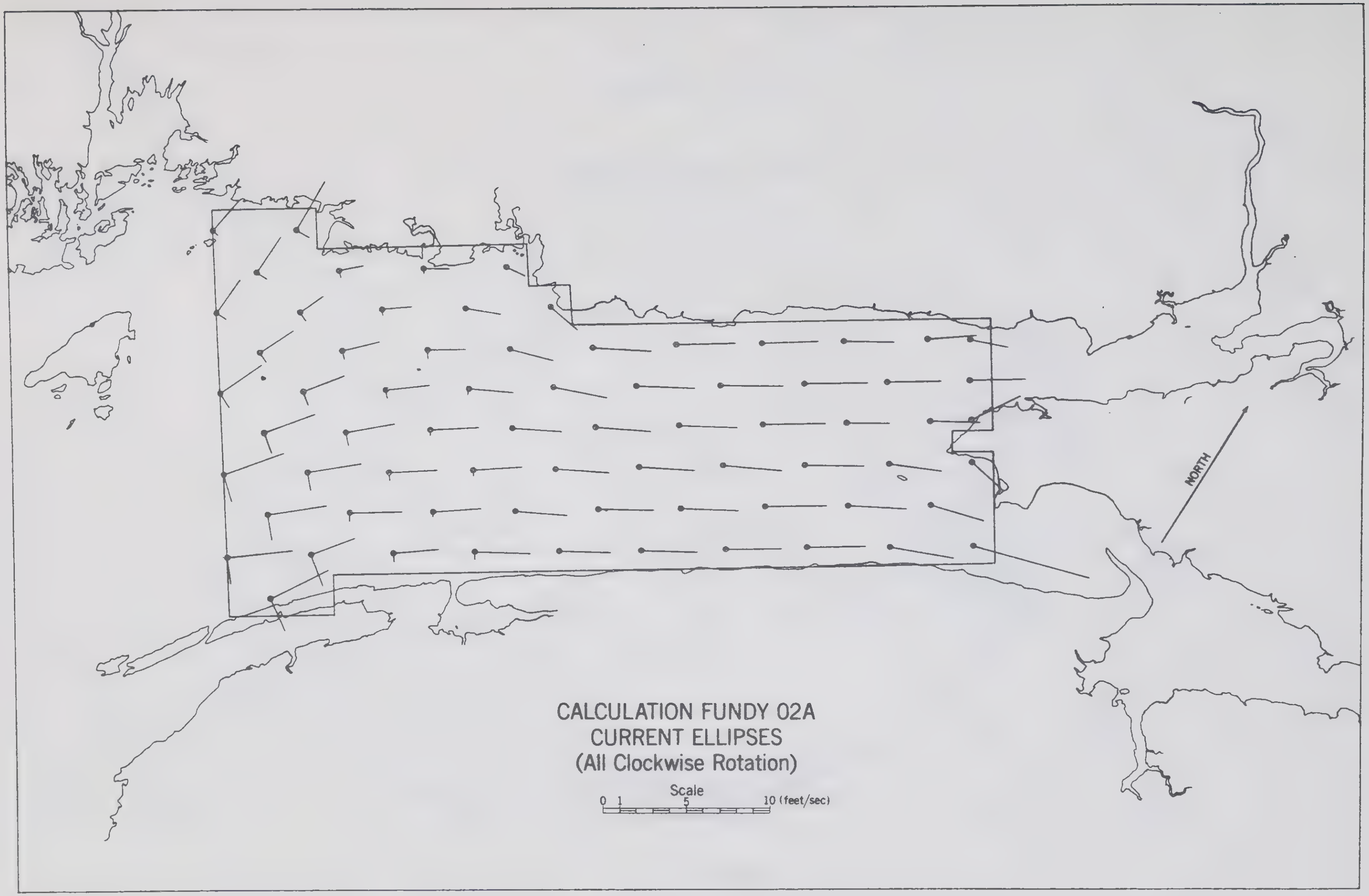
NORTH
CALCULATION FUNDY 02A
CURRENT ELLIPSES
(All Clockwise Rotation)
Scale
0 1 5 10 (feet/sec)

Figure IV. 16

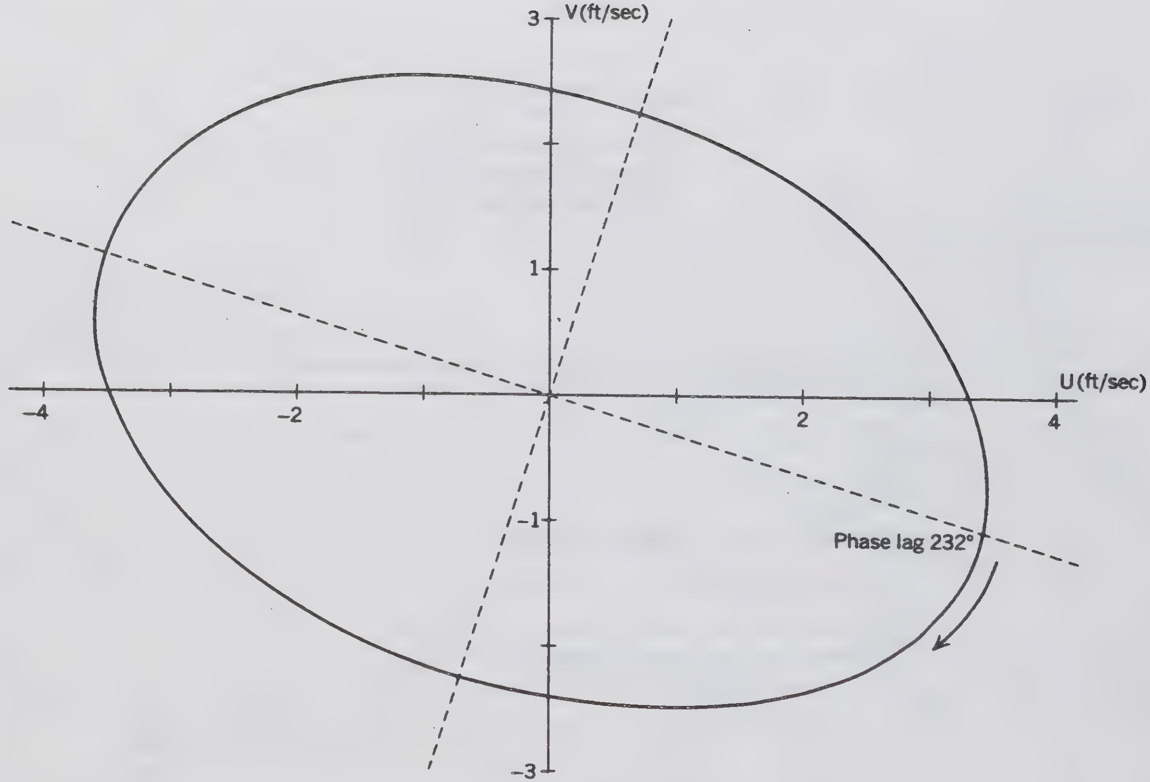

CURRENT ELLIPSE AT Z (3, 10)

Figure IV. 17

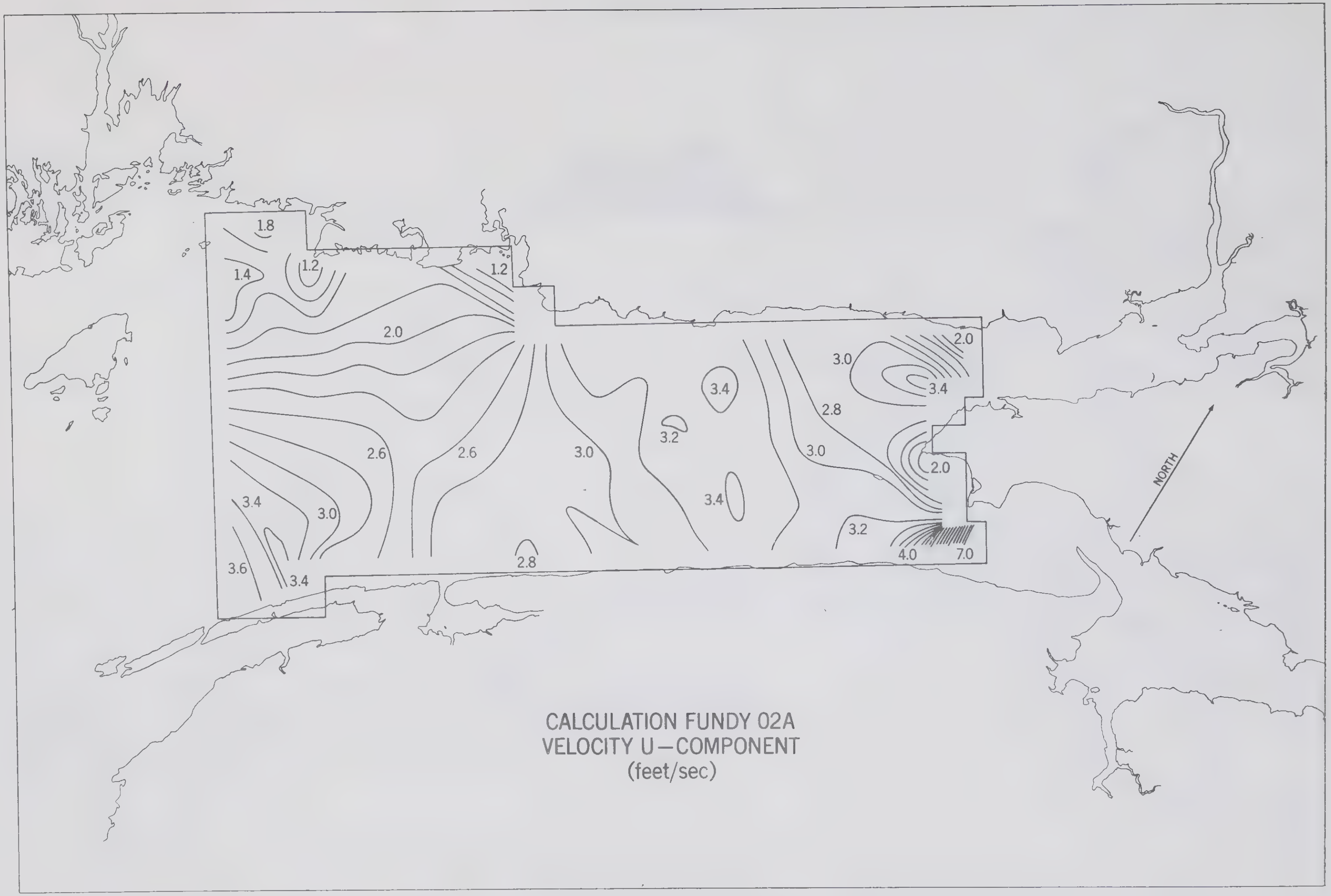

CALCULATION FUNDY 02A
VELOCITY U—COMPONENT
(feet/sec)

Figure IV. 18

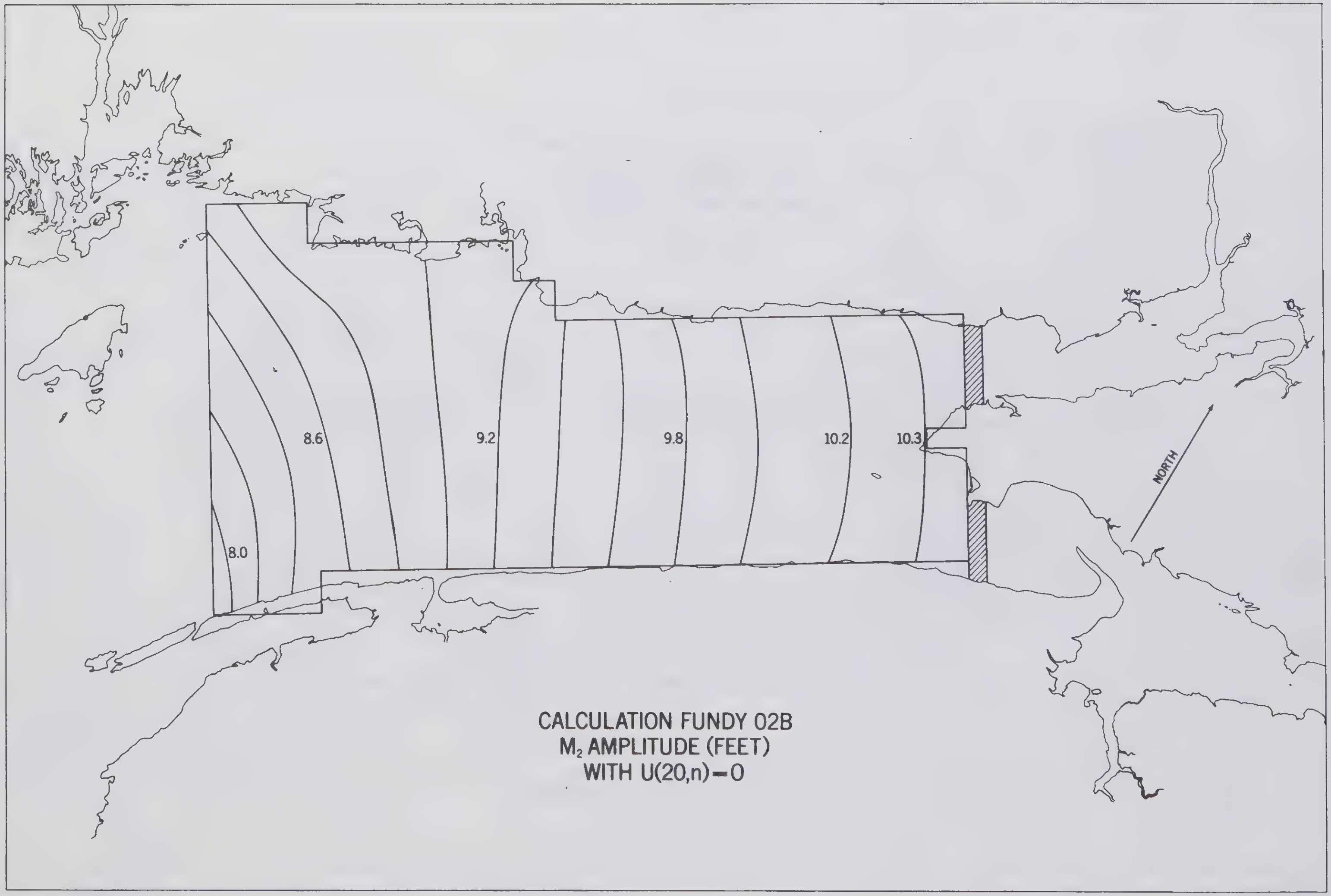
8.0
8.6
9.2
9.8
10.2
10.3
NORTH
CALCULATION FUNDY 02B
M_2 AMPLITUDE (FEET)
WITH U(20,n)=0

Figure IV. 19

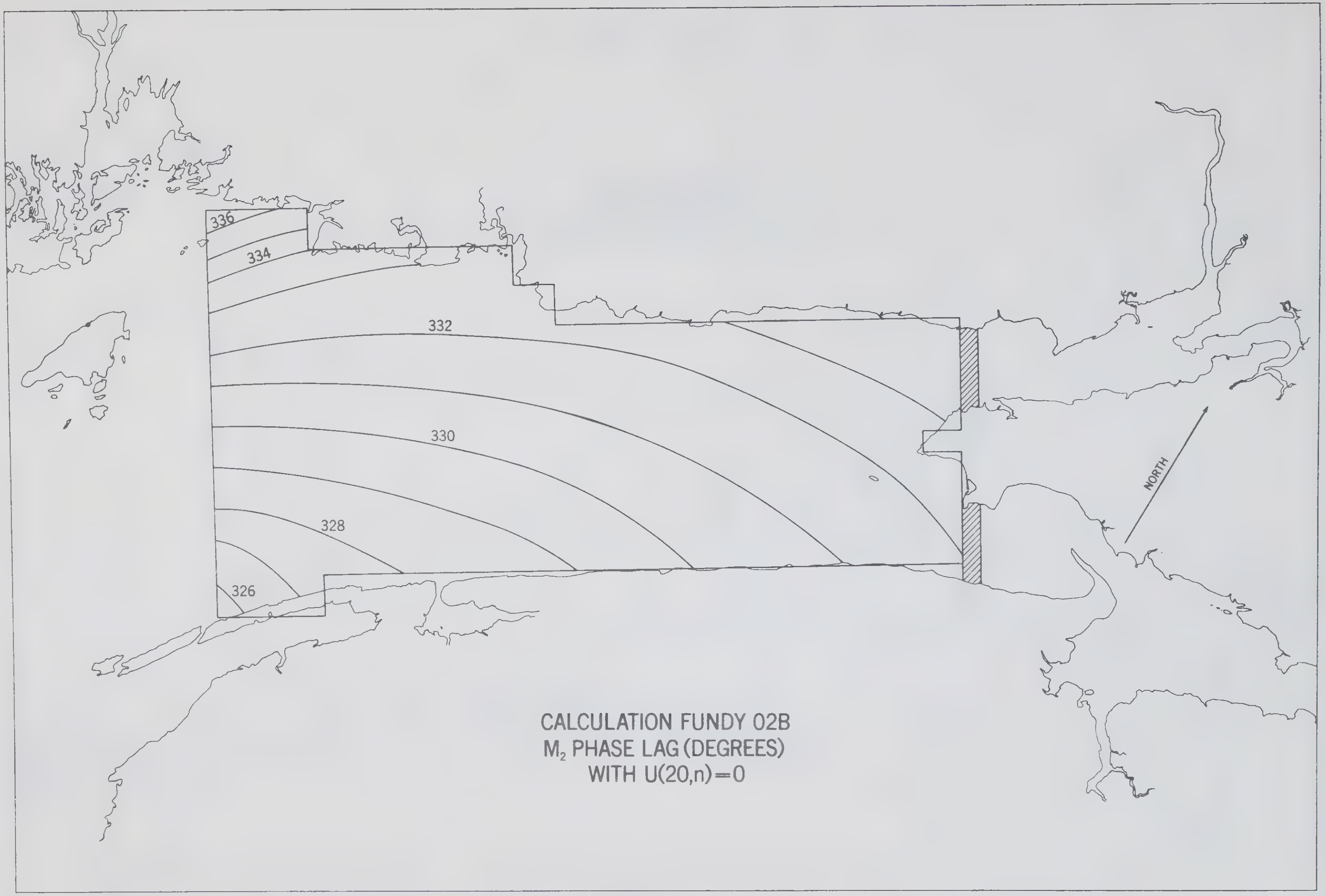

336
334
332
330
328
326
NORTH
CALCULATION FUNDY 02B
M2 PHASE LAG (DEGREES)
WITH U(20,n)=0

Figure IV. 20

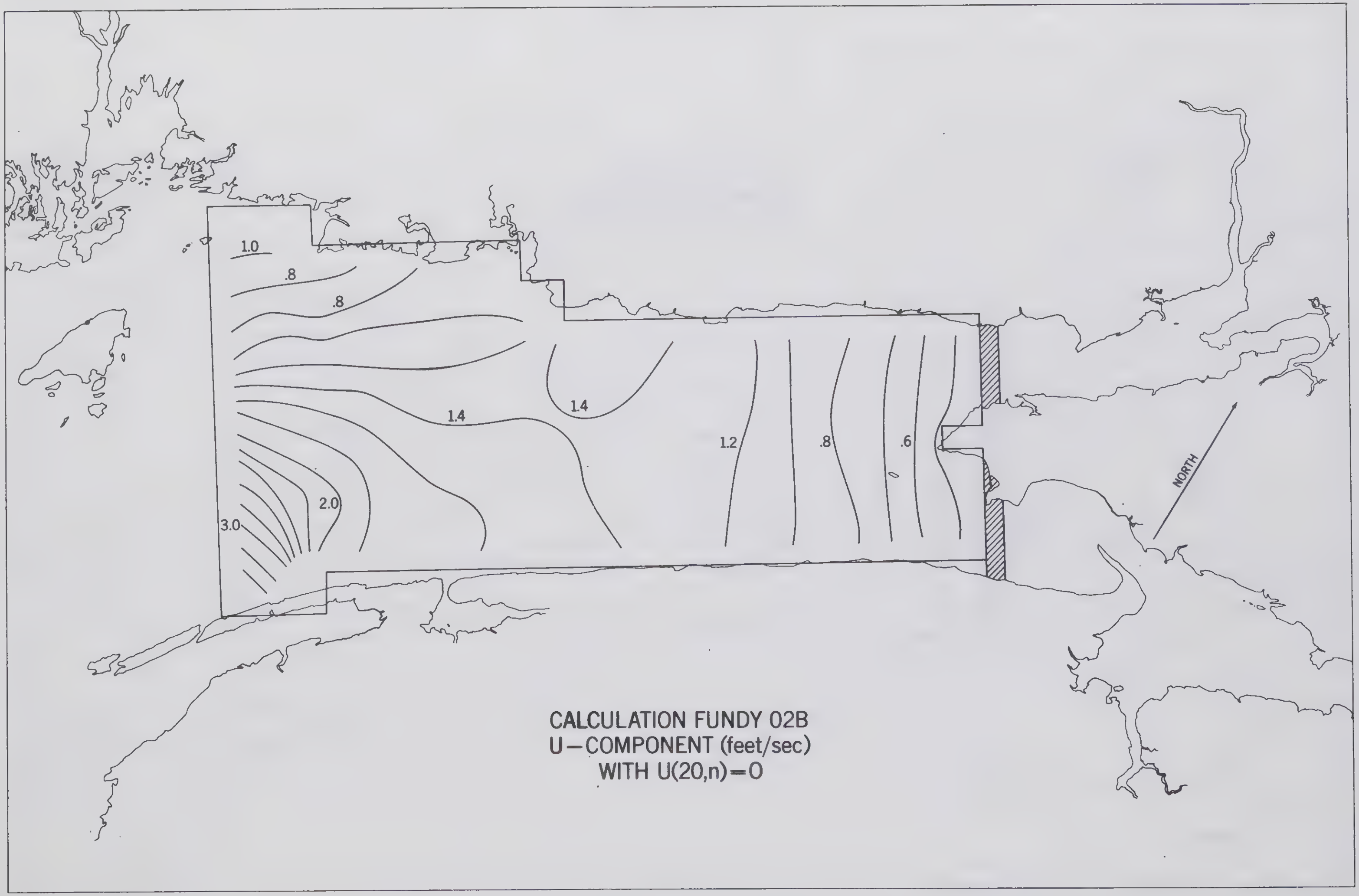
1.0
.8
.8
1.4
1.4
1.2
.8
.6
2.0
3.0
NORTH
CALCULATION FUNDY 02B
U—COMPONENT (feet/sec)
WITH U(20,n)=0

Figure IV. 21

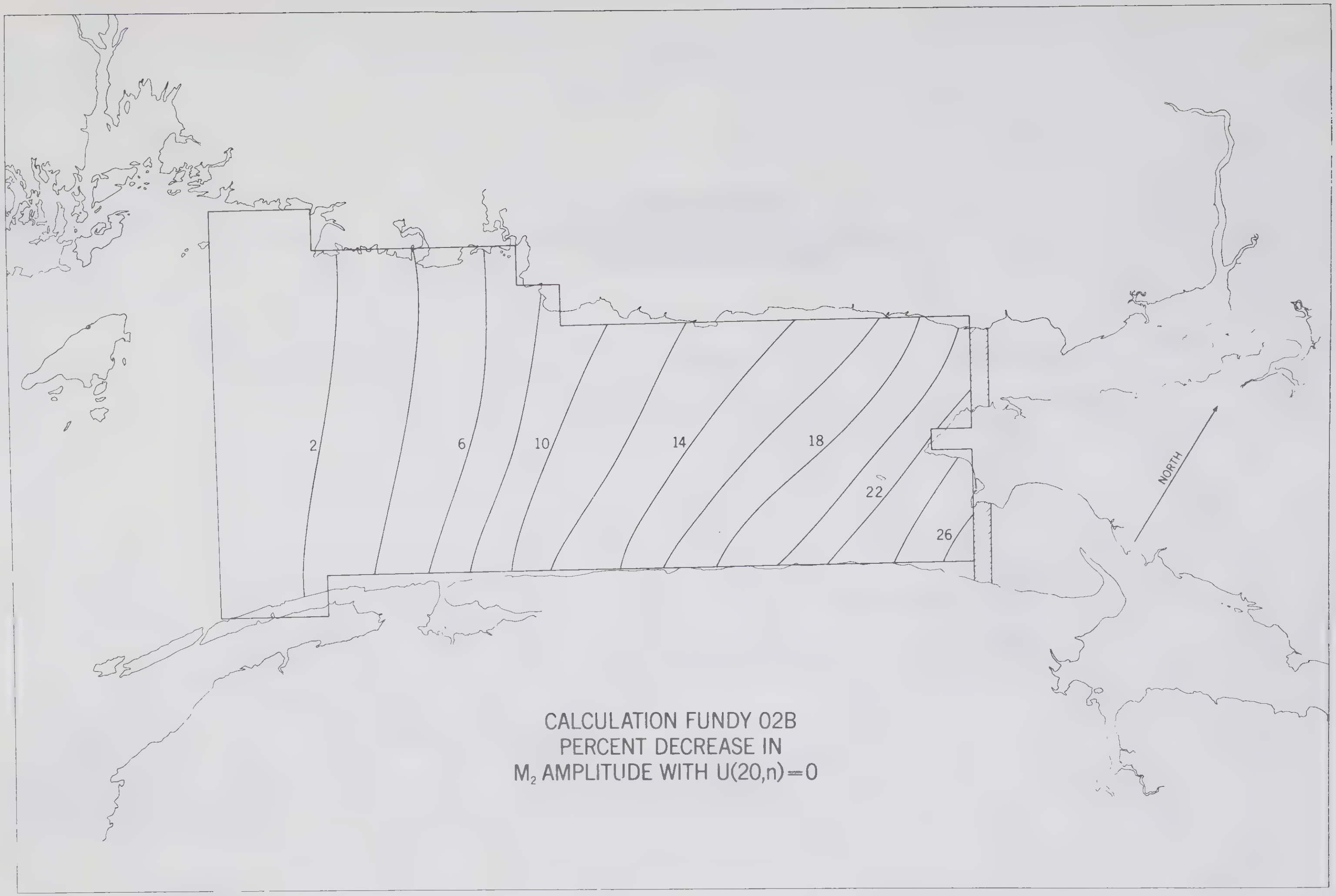
NORTH
2
6
10
14
18
22
26
CALCULATION FUNDY 02B
PERCENT DECREASE IN
M2 AMPLITUDE WITH U(20,n)=0

Figure IV. 22

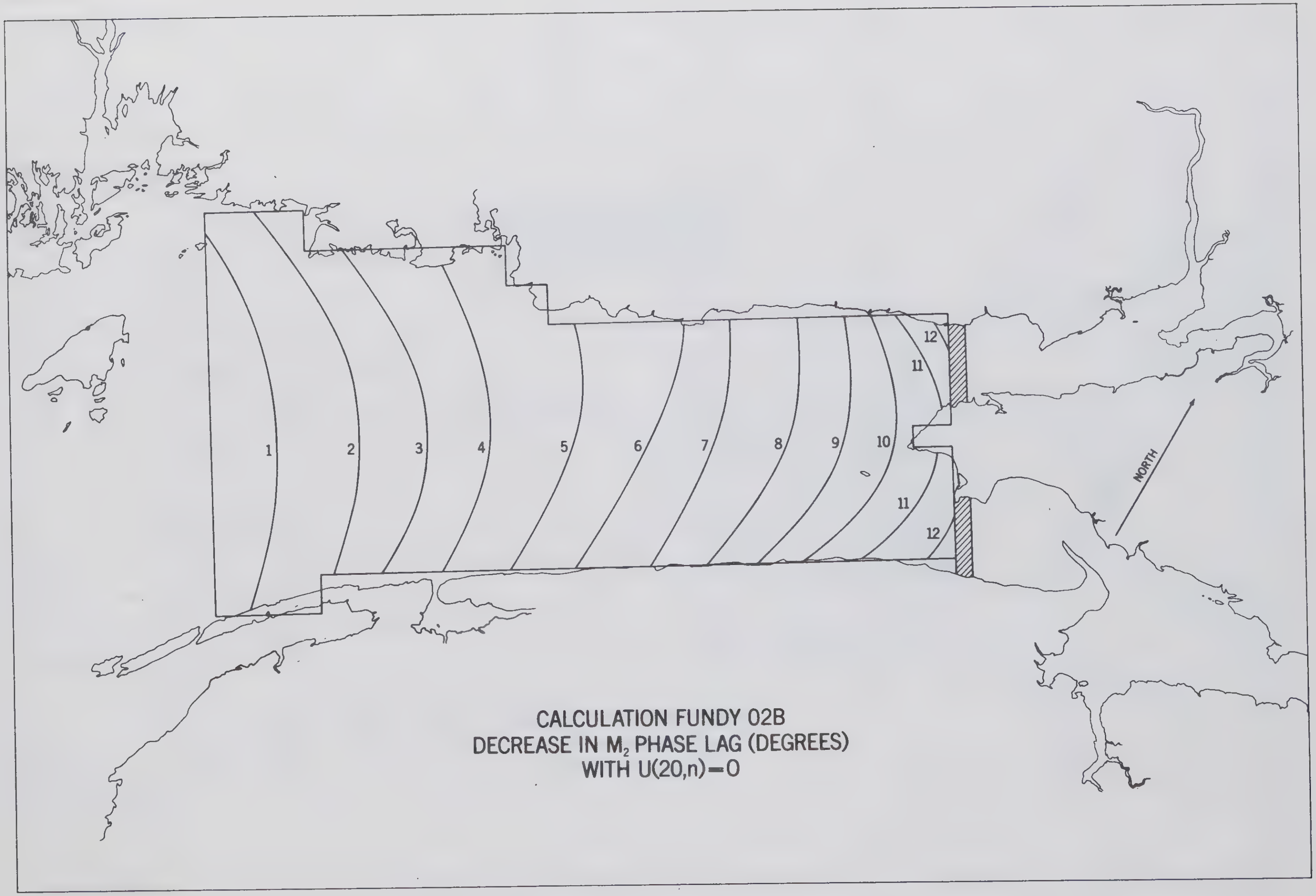
NORTH
1
2
3
4
5
6
7
8
9
10
11
12
11
12
CALCULATION FUNDY 02B
DECREASE IN M_2 PHASE LAG (DEGREES)
WITH U(20,n)=0

Figure IV. 23

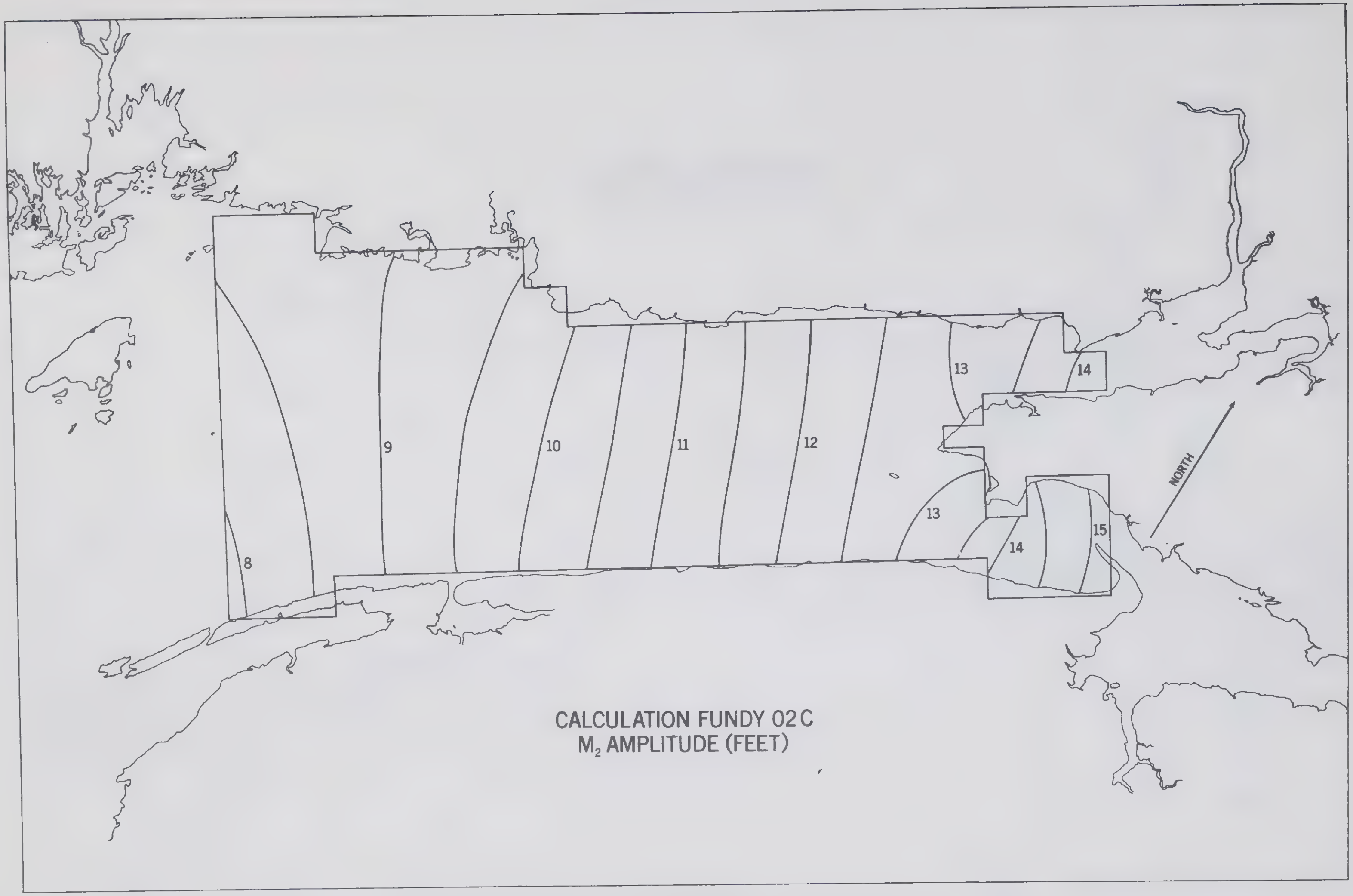
CALCULATION FUNDY 02C
M2 AMPLITUDE (FEET)
NORTH
8
9
10
11
12
13
13
14
14
15

Figure IV. 24

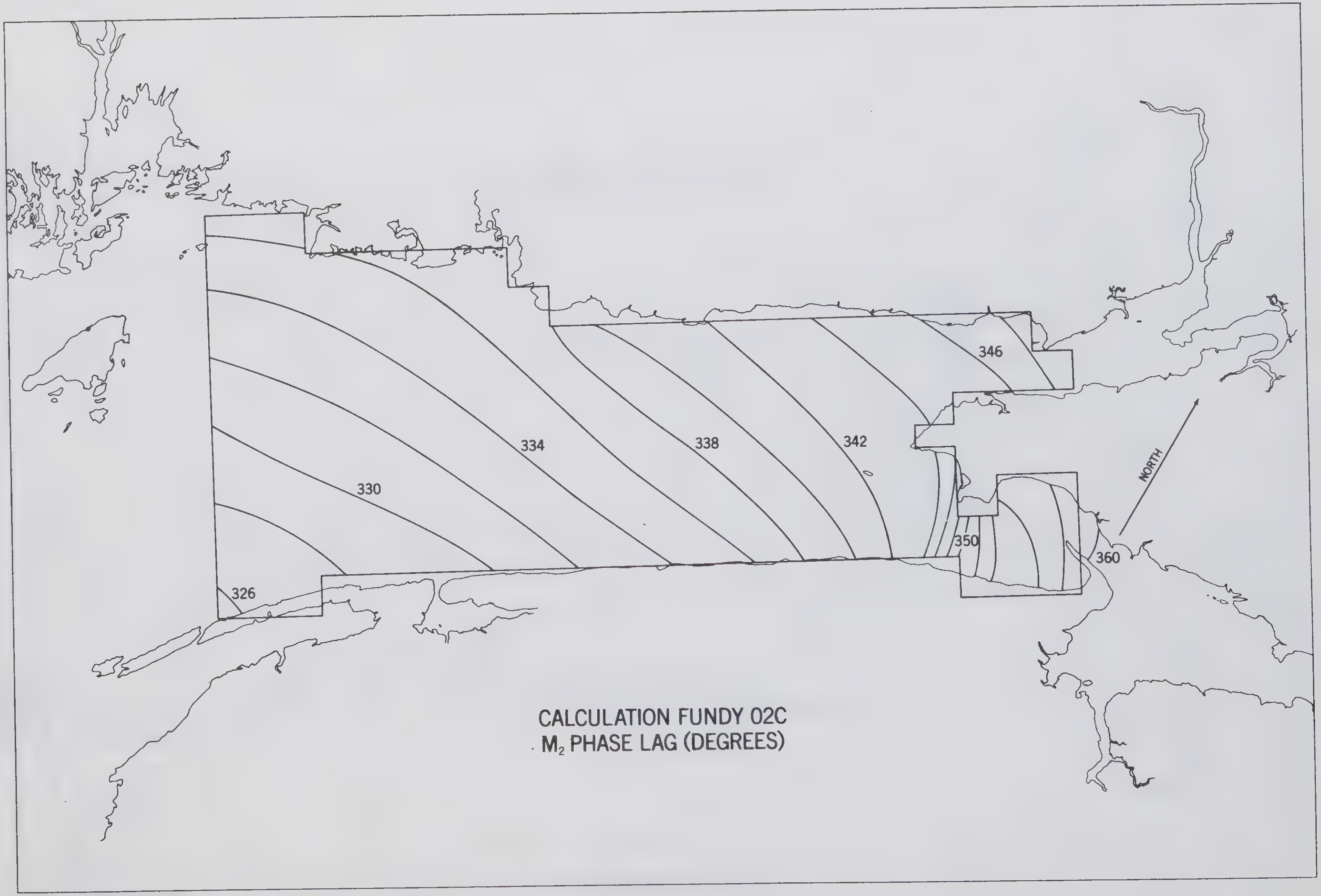
NORTH
326
330
334
338
342
346
350
360
CALCULATION FUNDY 02C
M2 PHASE LAG (DEGREES)

Figure IV. 25

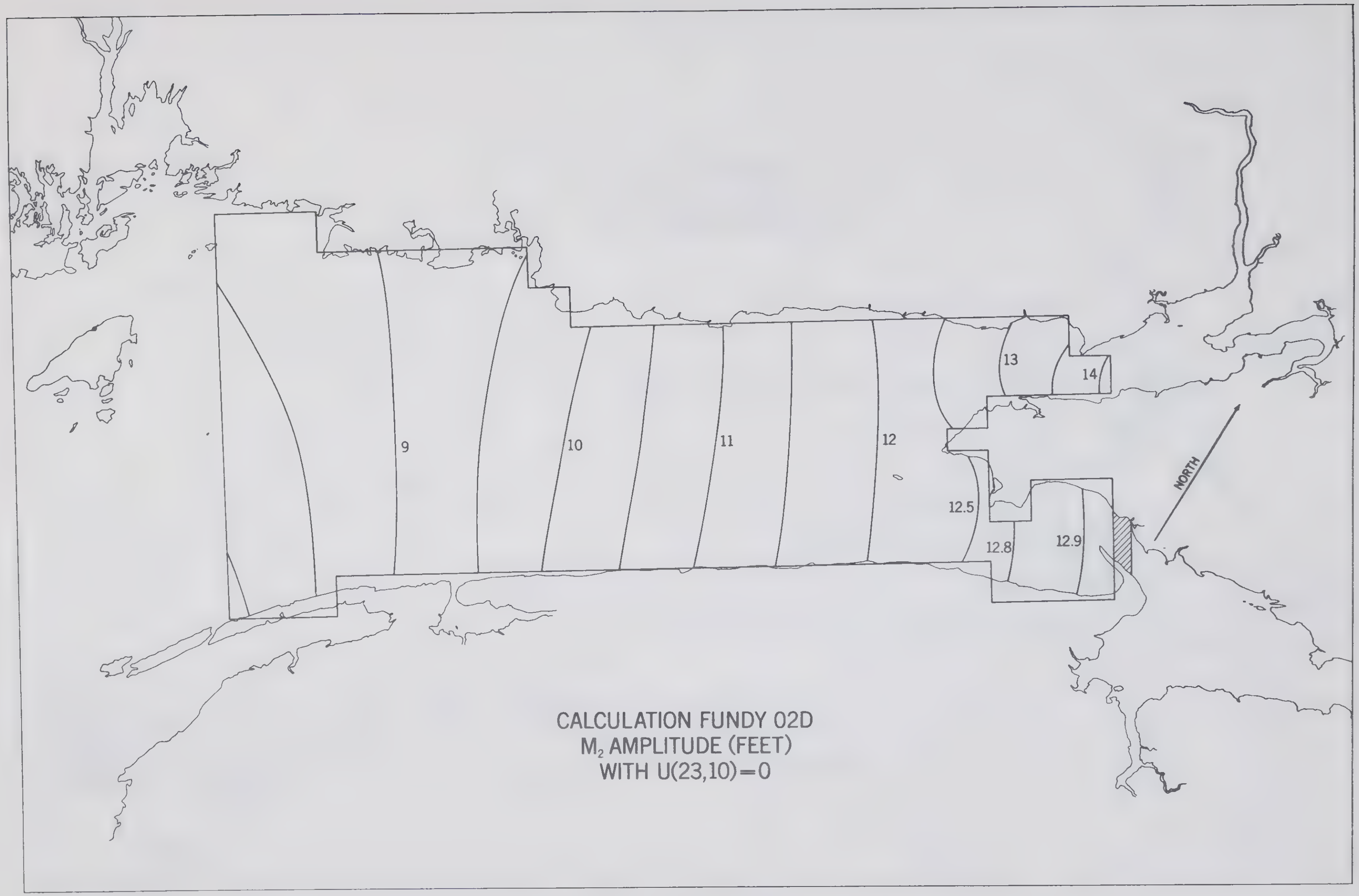

NORTH
9
10
11
12
12.5
12.8
12.9
13
14
CALCULATION FUNDY 02D
M_2 AMPLITUDE (FEET)
WITH U(23,10)=0

Figure IV. 26

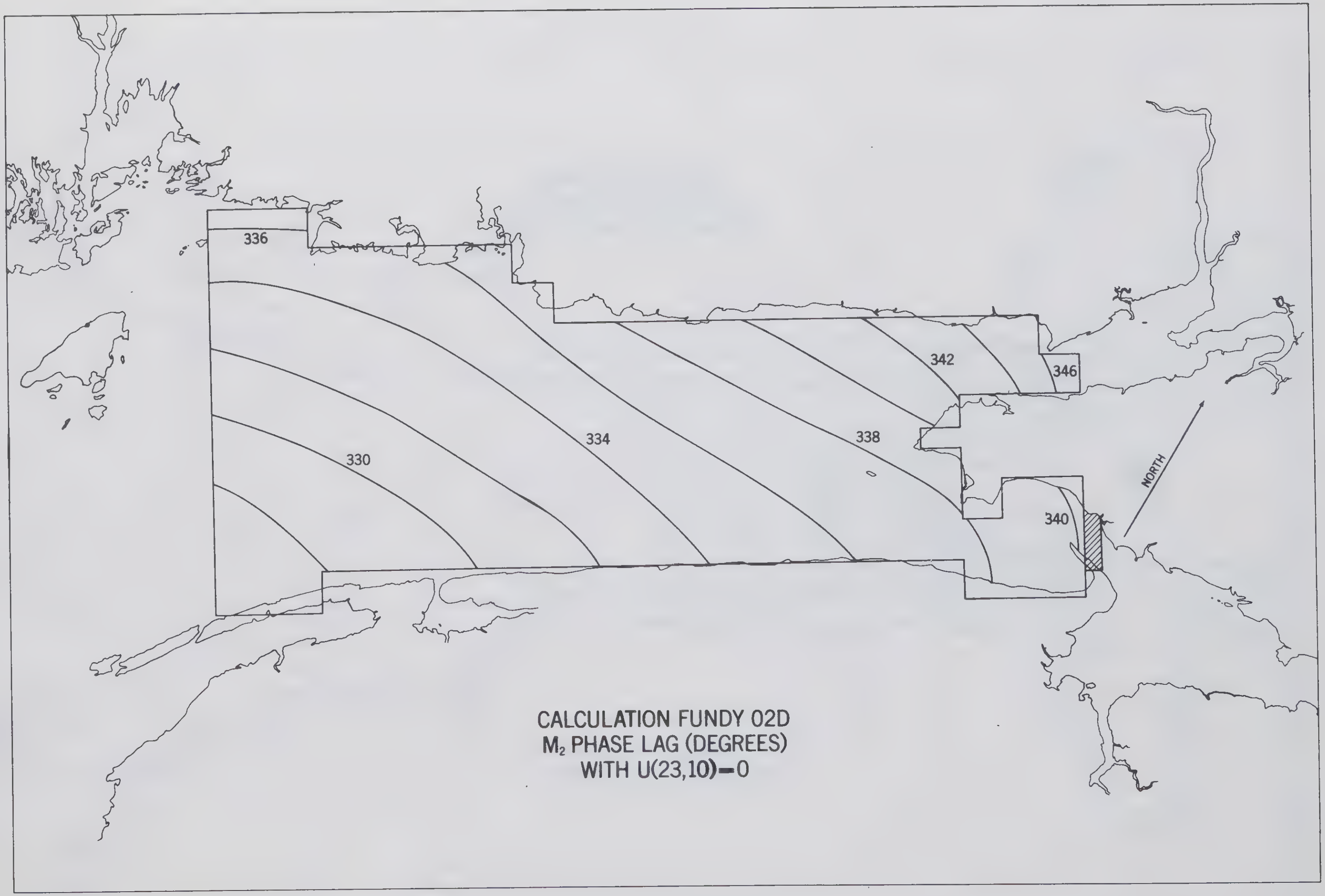
336
346
342
338
334
330
340
NORTH
CALCULATION FUNDY 02D
M_2 PHASE LAG (DEGREES)
WITH U(23,10)=0

Figure IV. 27

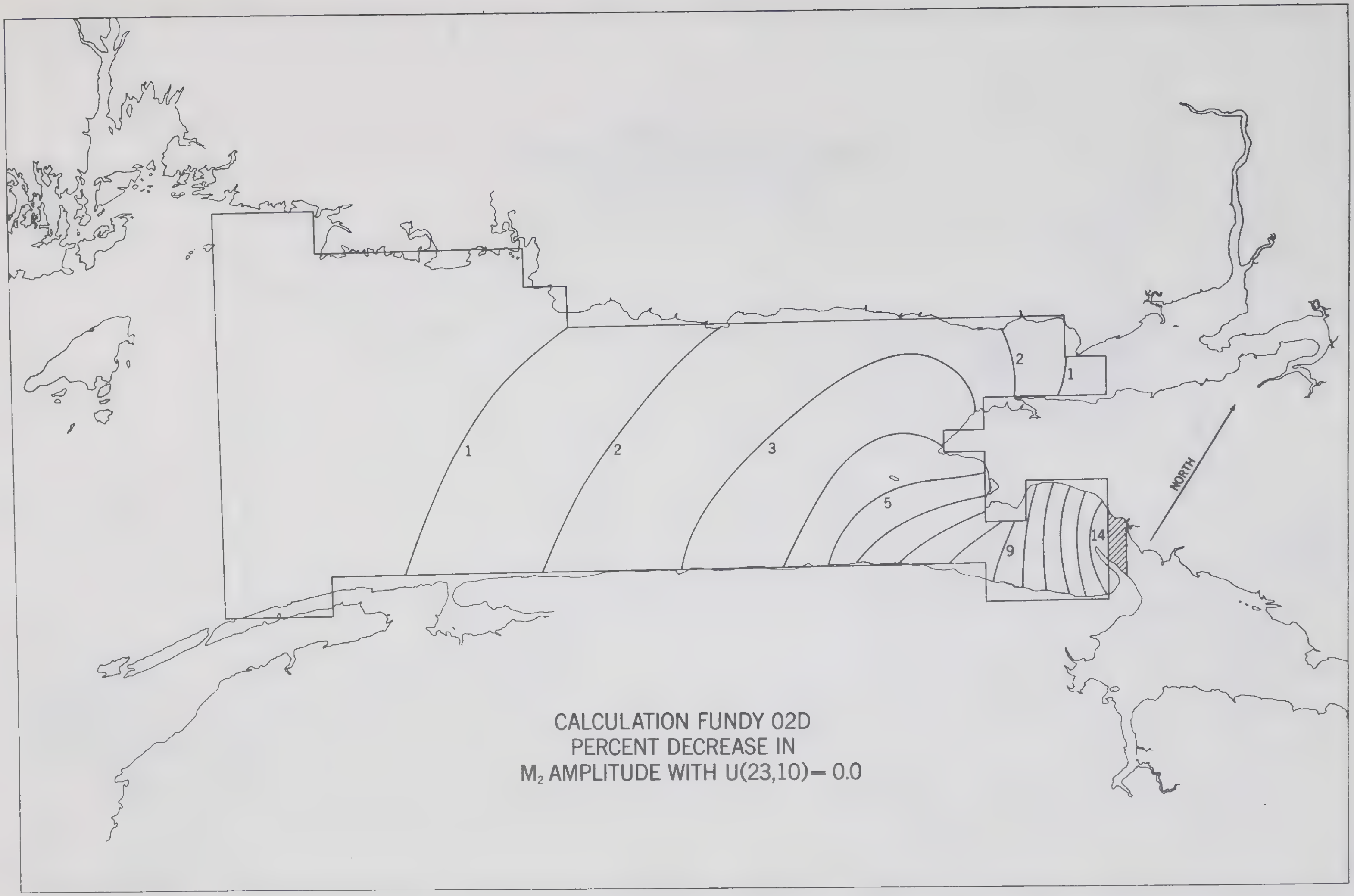
NORTH
1
2
3
5
9
14
2
1
CALCULATION FUNDY 02D
PERCENT DECREASE IN
M_2 AMPLITUDE WITH U(23,10)= 0.0

Figure IV. 28

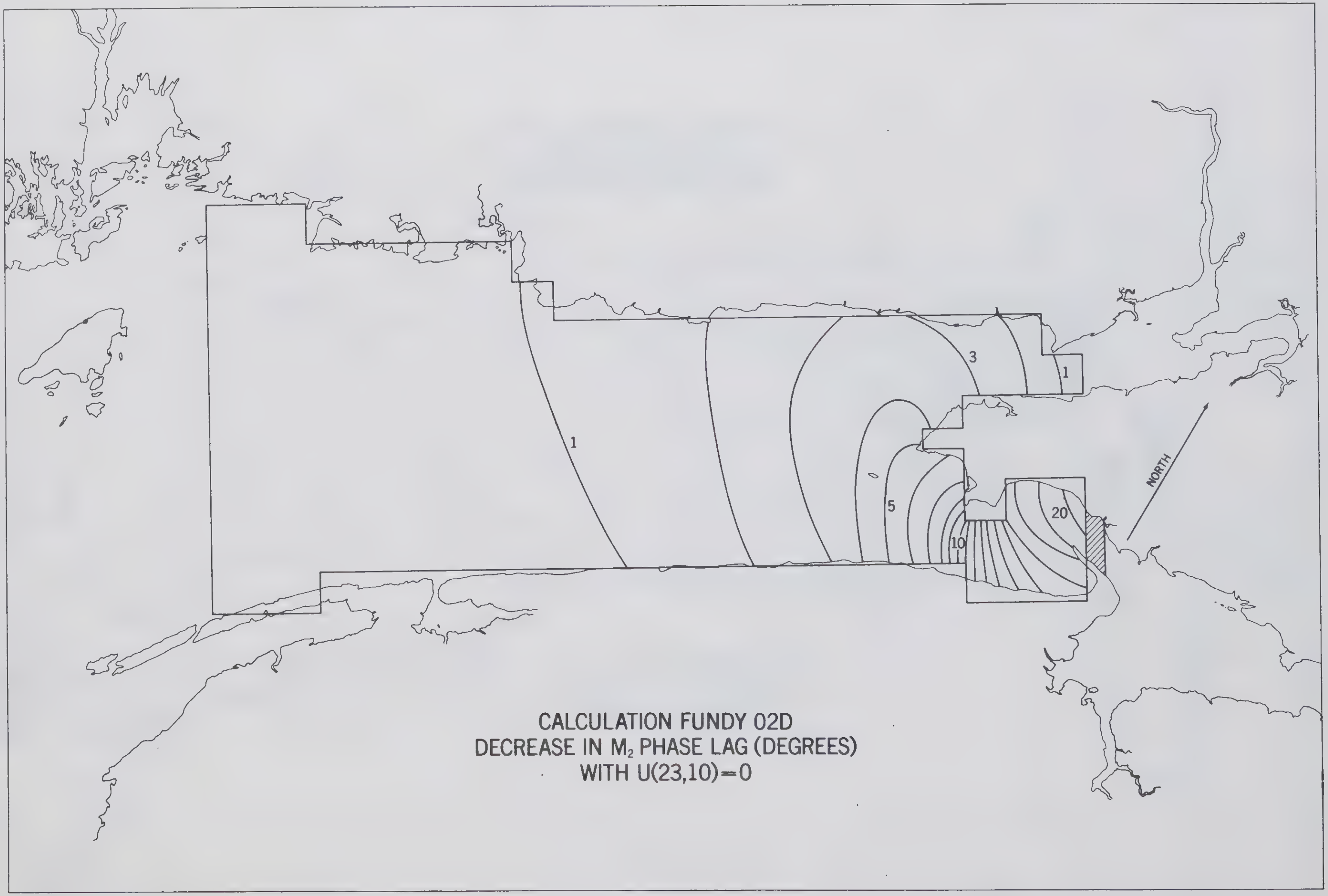
NORTH
1
3
5
10
20
1
CALCULATION FUNDY 02D
DECREASE IN M_2 PHASE LAG (DEGREES)
WITH U(23,10)=0

Figure IV. 29

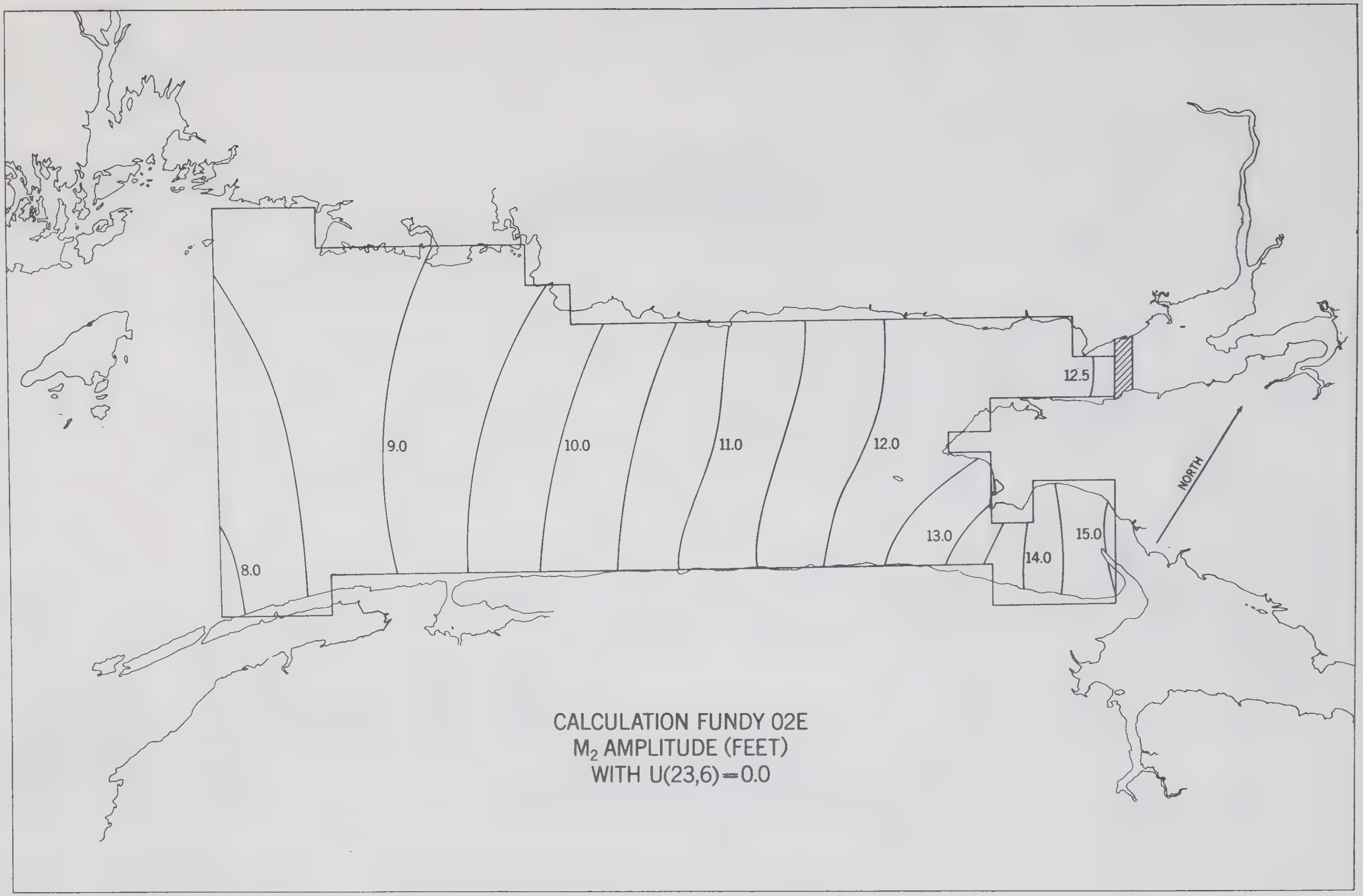

8.0
9.0
10.0
11.0
12.0
12.5
13.0
14.0
15.0
NORTH
CALCULATION FUNDY 02E
M2 AMPLITUDE (FEET)
WITH U(23,6)=0.0

Figure IV. 30

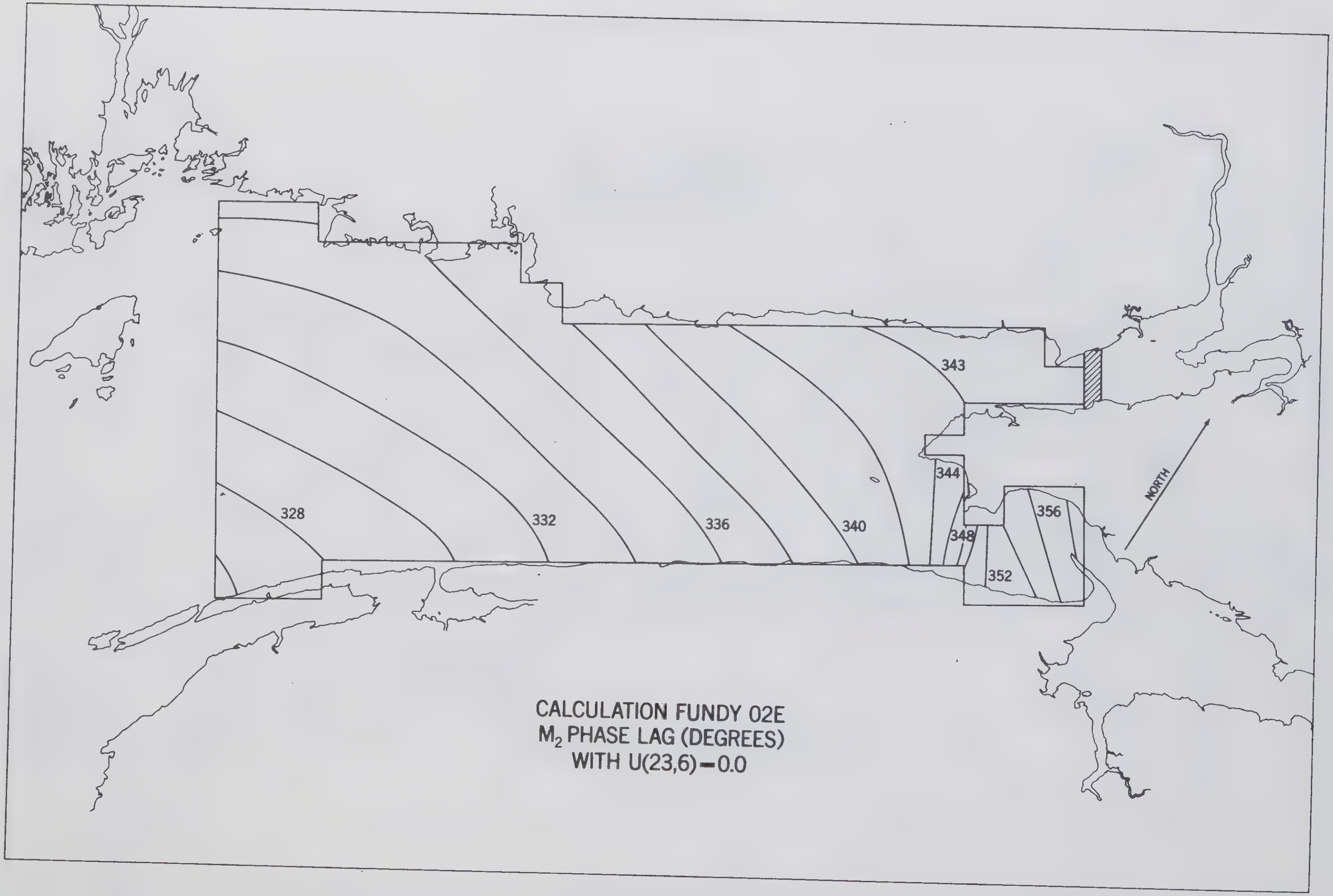
343
344
348
352
356
340
336
332
328
NORTH
CALCULATION FUNDY 02E
M2 PHASE LAG (DEGREES)
WITH U(23,6)—0.0

Figure IV. 31

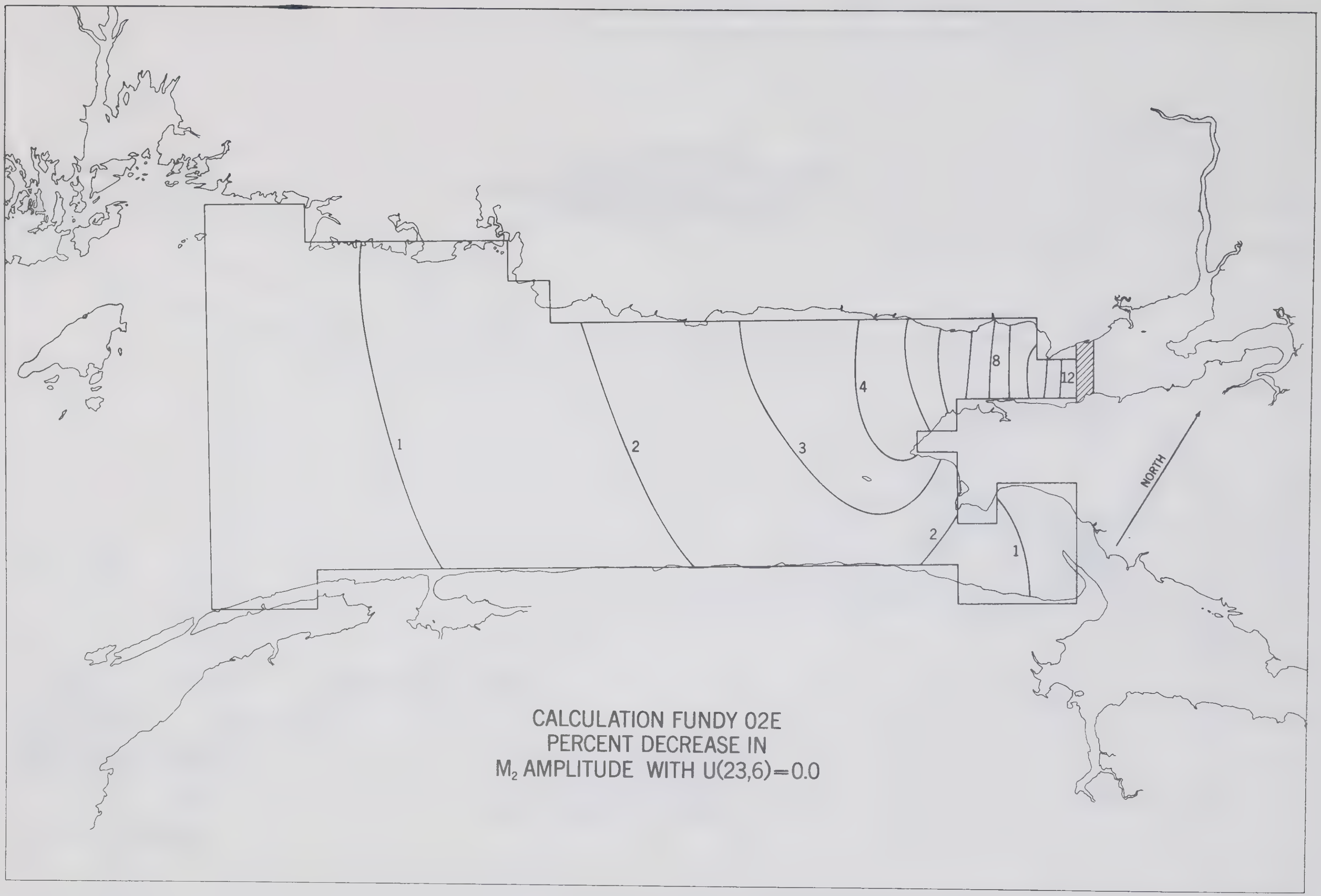
NORTH
1
2
3
4
8
12
2
1
CALCULATION FUNDY 02E
PERCENT DECREASE IN
M_2 AMPLITUDE WITH U(23,6)=0.0

Figure IV. 32

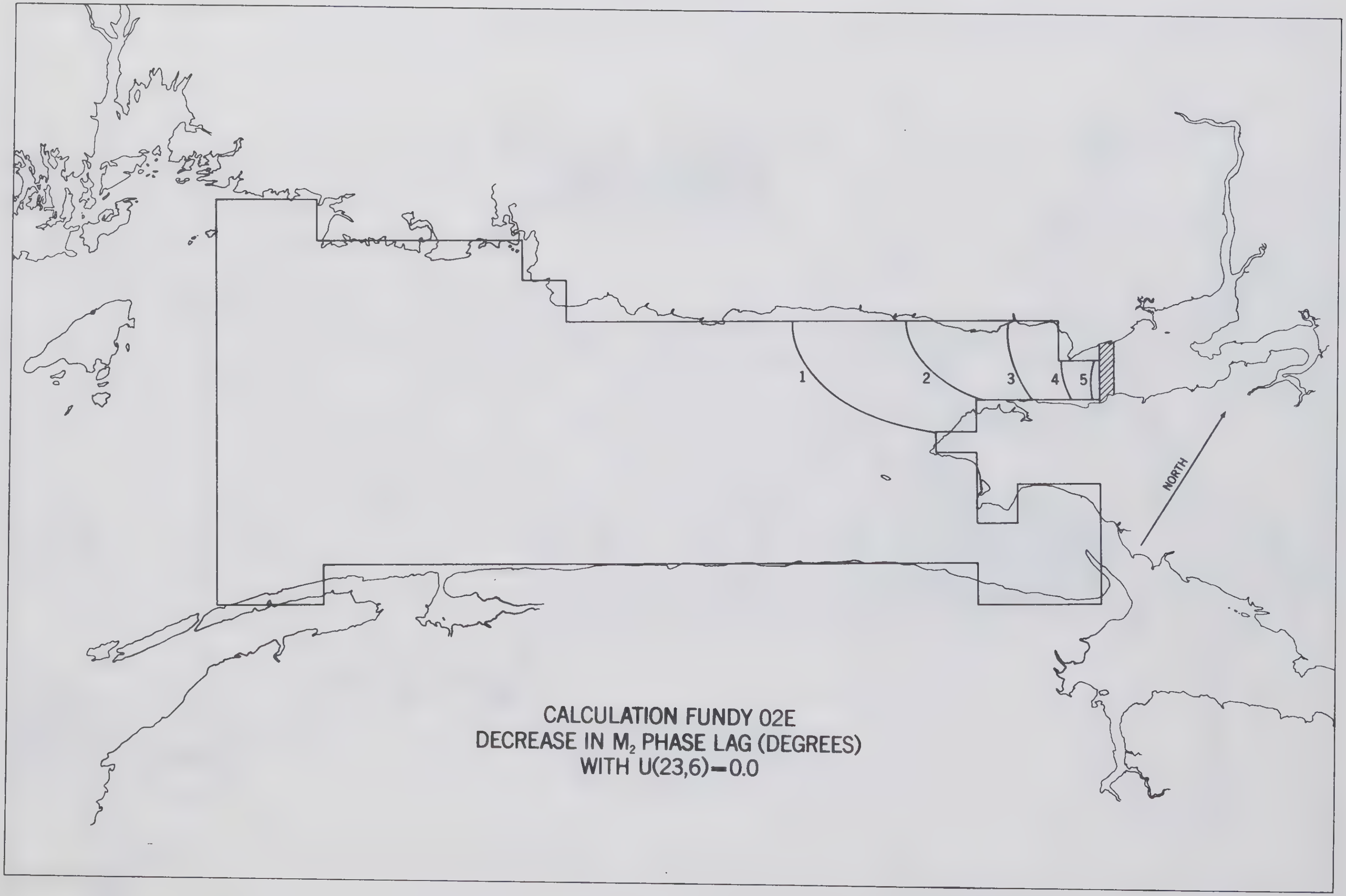
NORTH
1
2
3
4
5
CALCULATION FUNDY 02E
DECREASE IN M_2 PHASE LAG (DEGREES)
WITH U(23,6)—0.0

Figure IV. 33

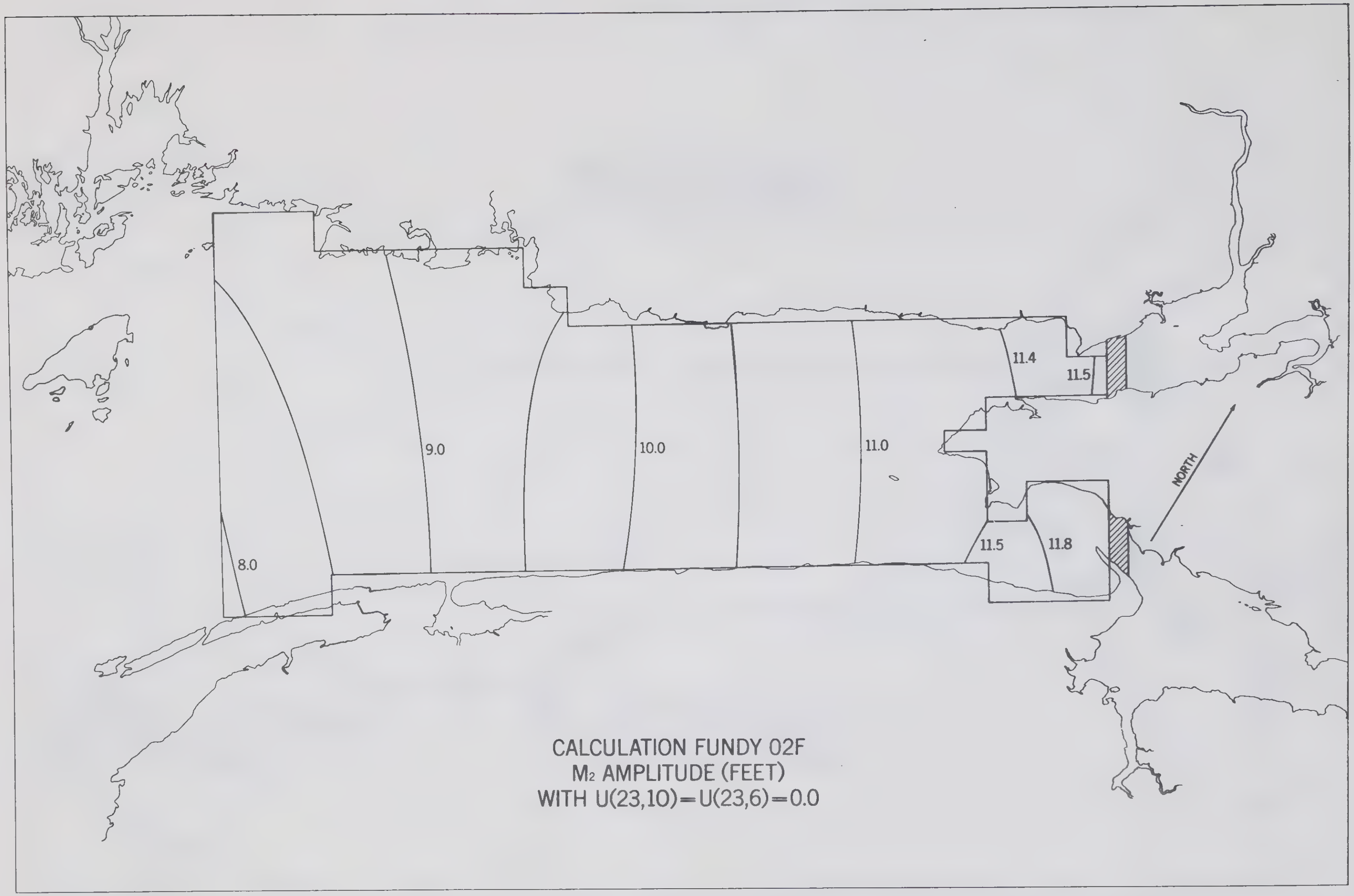

NORTH
11.4
11.5
11.5
11.8
11.0
10.0
9.0
8.0
CALCULATION FUNDY 02F
M2 AMPLITUDE (FEET)
WITH U(23,10)=U(23,6)=0.0

Figure IV. 34

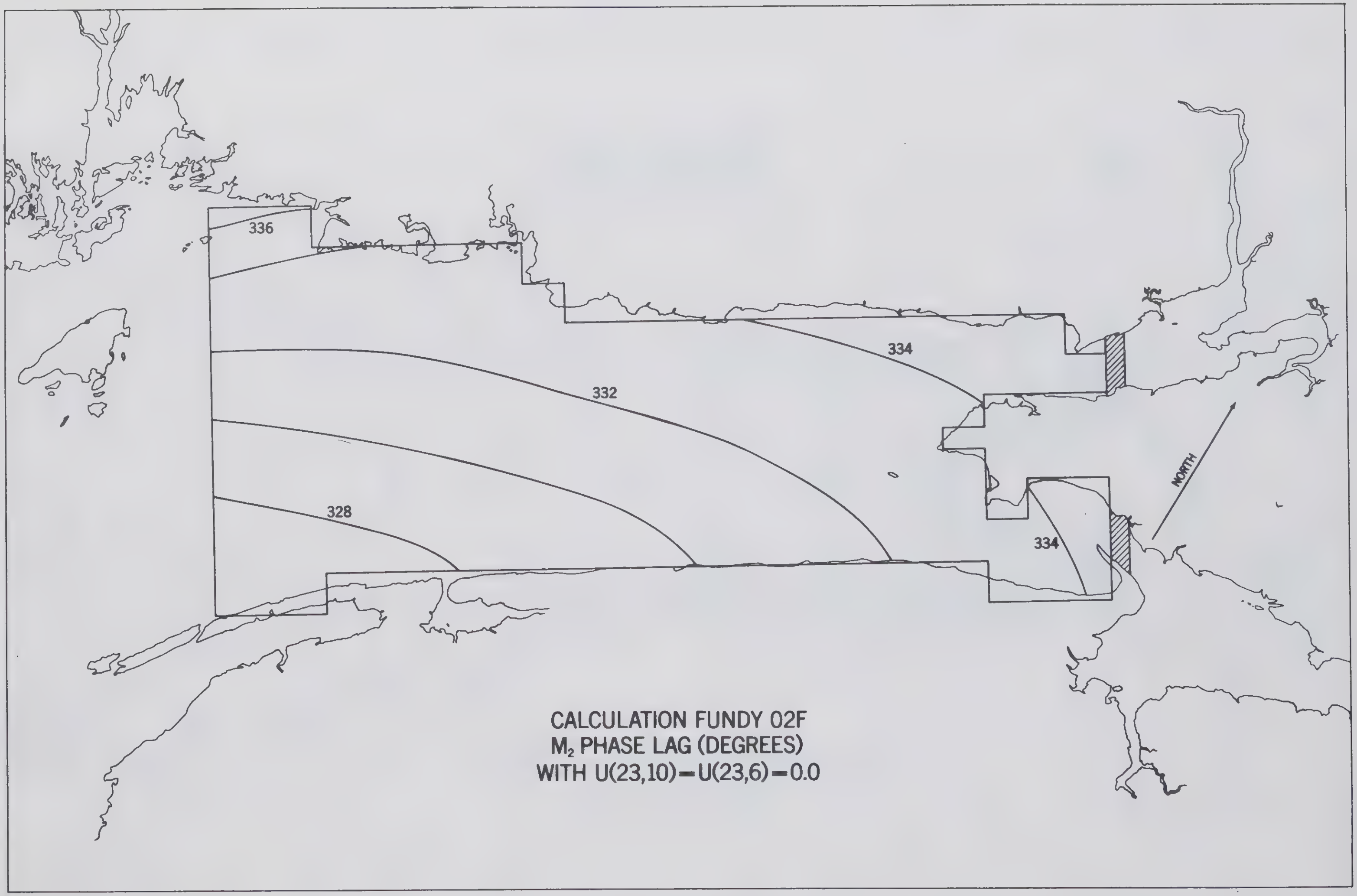
336
334
332
328
334
NORTH
CALCULATION FUNDY 02F
M2 PHASE LAG (DEGREES)
WITH U(23,10)—U(23,6)—0.0

Figure IV. 35

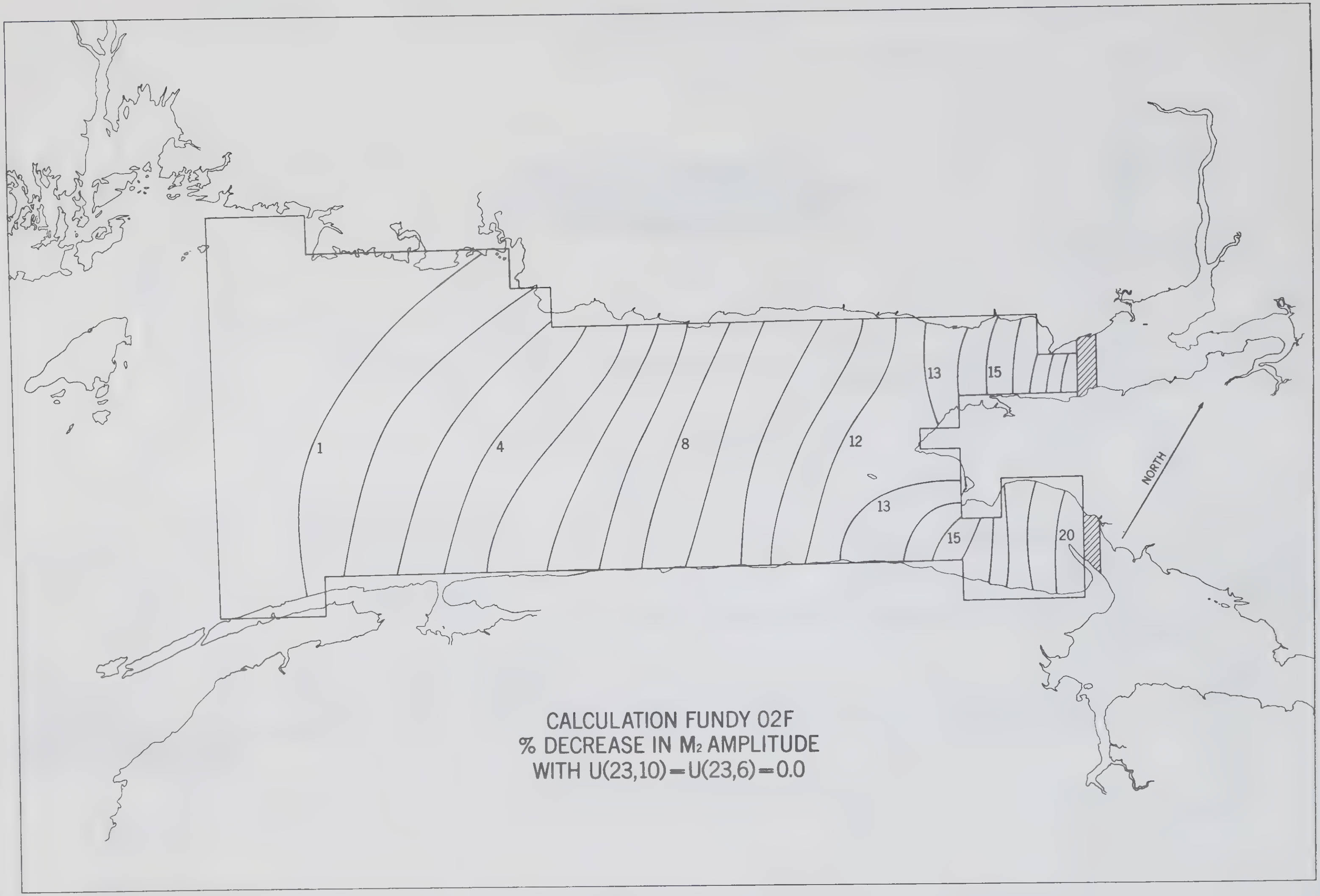
NORTH
1
4
8
12
13
15
13
15
20
CALCULATION FUNDY 02F
% DECREASE IN M2 AMPLITUDE
WITH U(23,10)=U(23,6)=0.0

Figure IV. 36

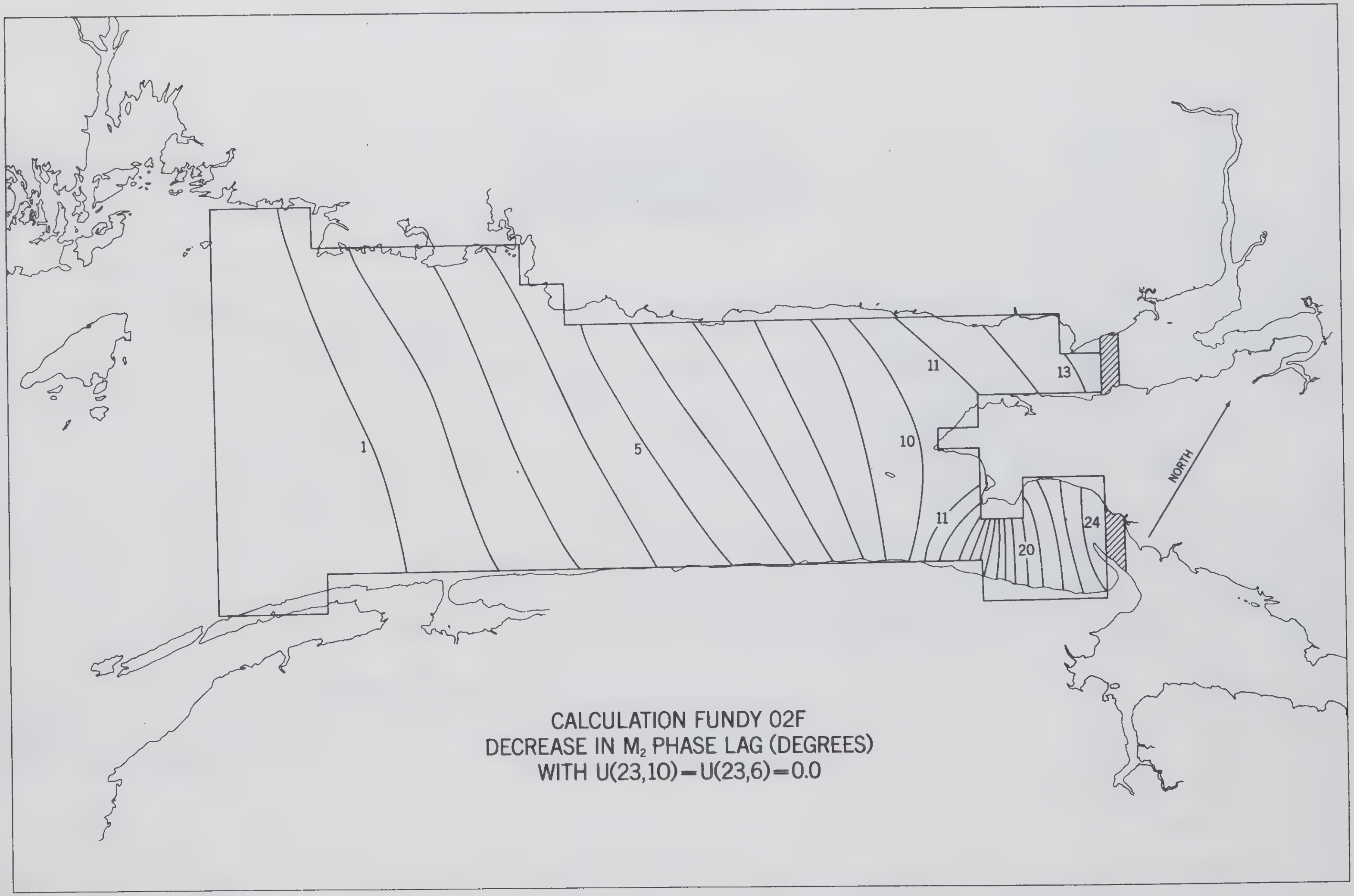

NORTH
1
5
10
11
11
13
20
24
CALCULATION FUNDY 02F
DECREASE IN M_2 PHASE LAG (DEGREES)
WITH U(23,10)=U(23,6)=0.0

Figure IV. 37

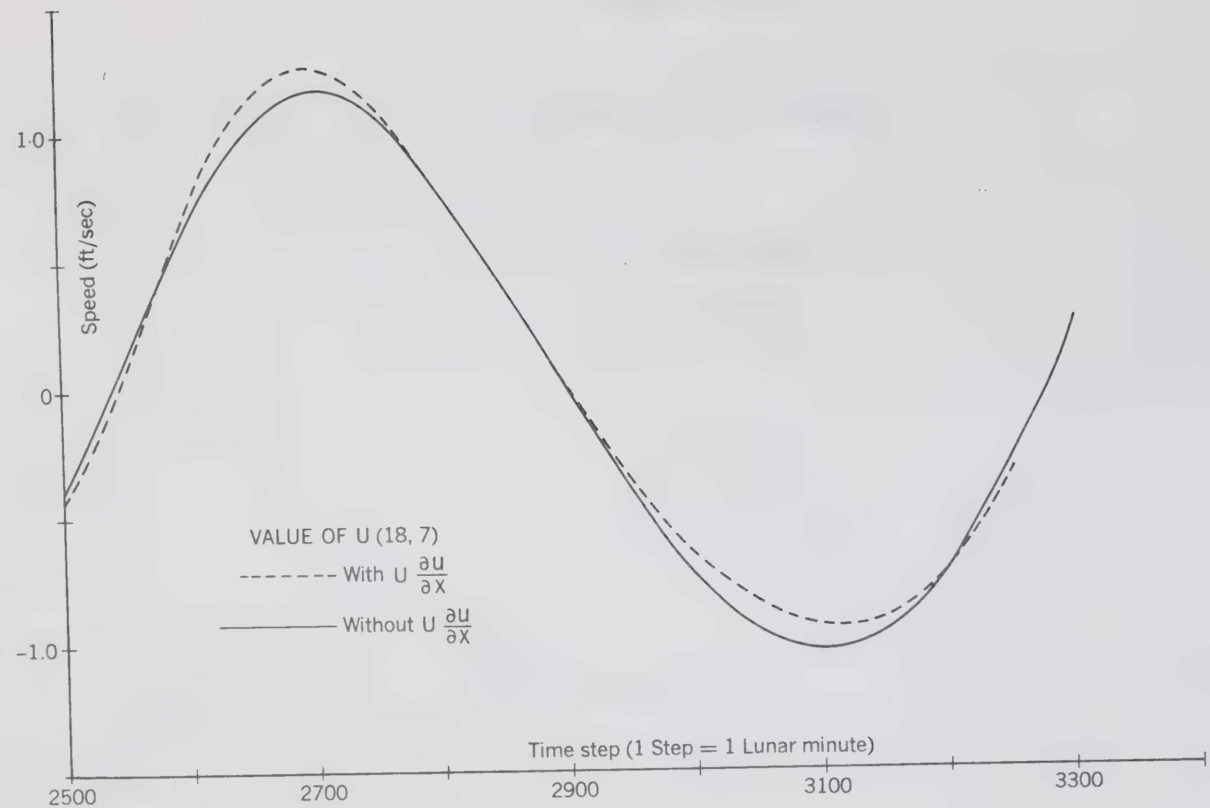

1.0
0
-1.0
Speed (ft/sec)
VALUE OF U (18, 7)
With $U \frac{\partial u}{\partial x}$
Without $U \frac{\partial u}{\partial x}$
Time step (1 Step = 1 Lunar minute)
2500
2700
2900
3100
3300

Figure IV. 41

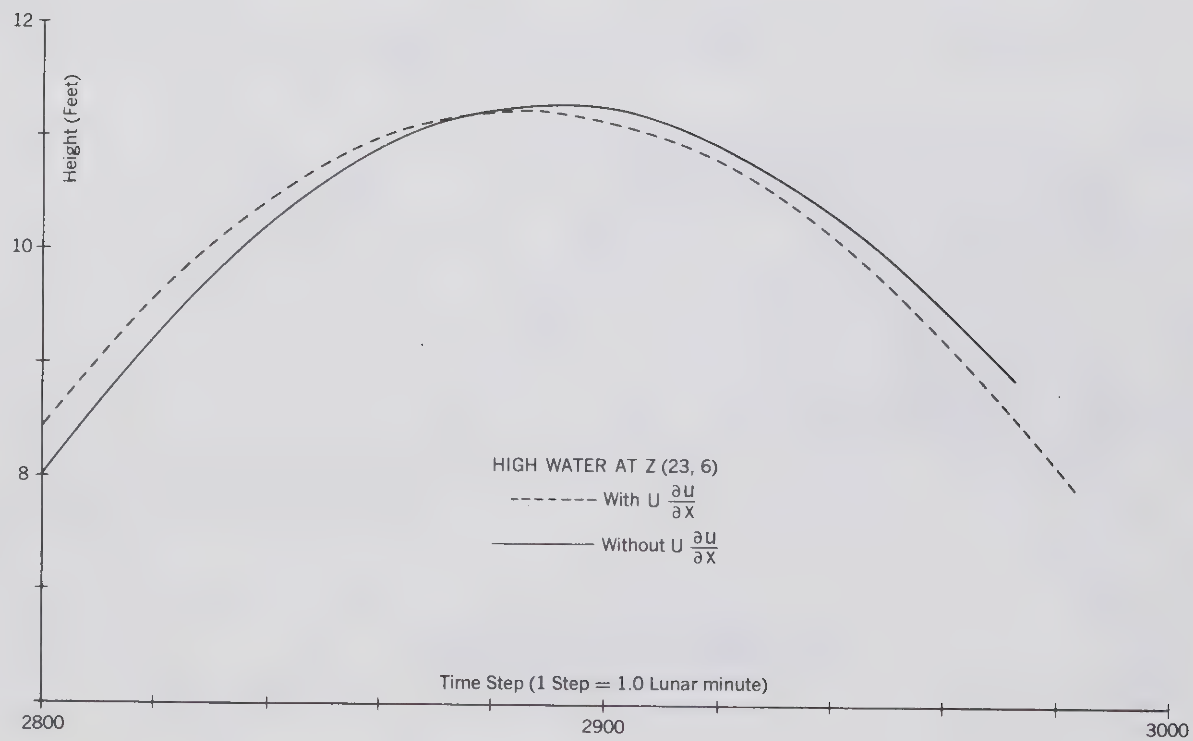
12
10
8
Height (Feet)
HIGH WATER AT Z (23, 6)
With U $\frac{\partial u}{\partial x}$
Without U $\frac{\partial u}{\partial x}$
Time Step (1 Step = 1.0 Lunar minute)
2800
2900
3000

Figure IV. 42

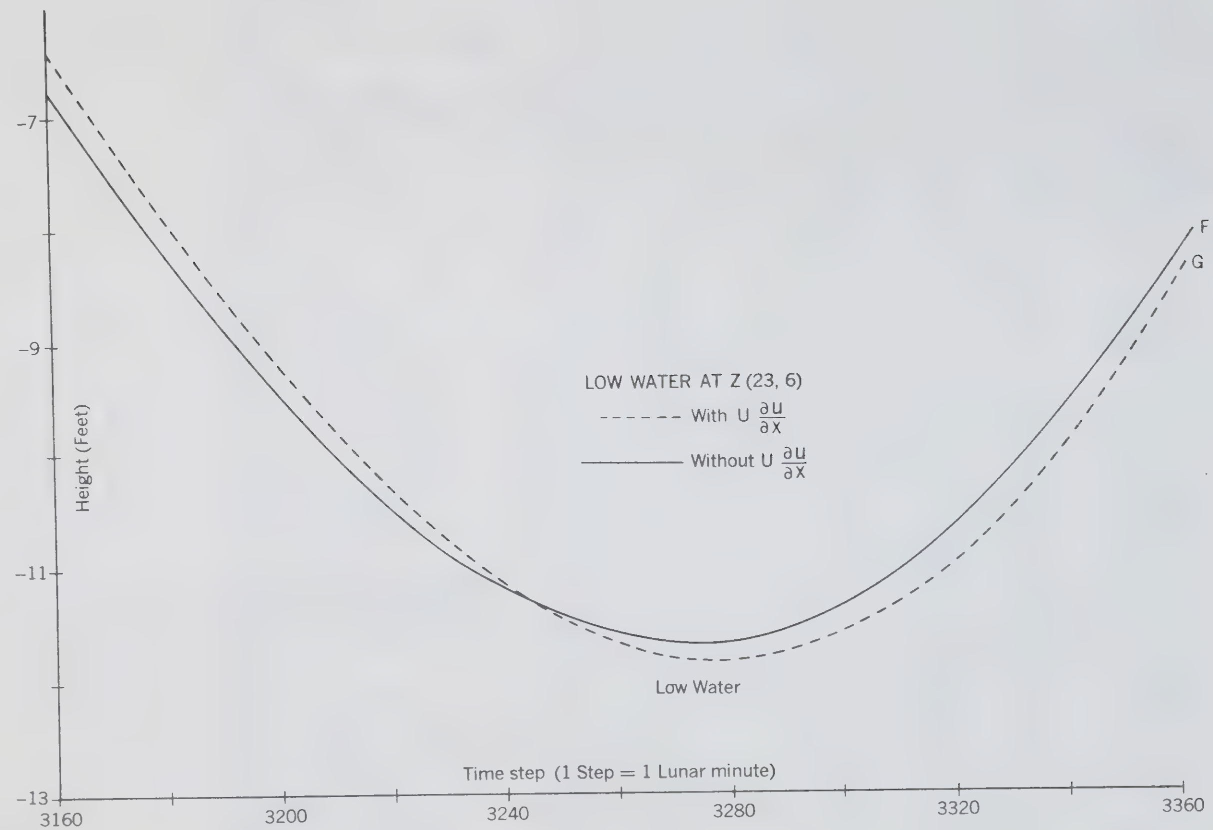

LOW WATER AT Z (23, 6)
With U ∂u/∂x
Without U ∂u/∂x
F
G
Low Water
Height (Feet)
-7
-9
-11
-13
Time step (1 Step = 1 Lunar minute)
3160
3200
3240
3280
3320
3360

Figure IV. 43

PRINCIPAL TIDAL CONSTITUENTS
IN THE
BAY OF FUNDY

LAT.=DEG.-MIN.
LONG.=DEG.-MIN.
H=AMPLITUDE(FEET)
G=PHASE LAG(DEGREES)

LOCATION OF TIDE GAUGE STATION	LONG.	LAT.	M2		N2		S2		K2		K1	
			H	G	H	G	H	G	H	G	H	G
PULPIT HARBOUR	44-09	68-53	4.90	313	1.05	284	0.78	343	0.21	344	.46	123
BAR HARBOUR	44-24	68-12	5.08	308	1.17	278	0.83	337	0.21	344	.46	120
LITTLE WOOD IS.	44-36	66-48	6.60	328	C.84	317	1.37	026	0.36	026	.41	116
NORTH HEAD,LONG IS.	44-46	66-45	8.25	339	1.62	312	1.28	015	0.35	015	.45	131
WELSH POOL	44-53	66-57	8.52	344	1.50	317	1.23	018	0.33	018	.49	136
WILSON BEACH	44-56	66-56	8.16	341	1.76	314	1.42	014	0.39	014	.62	133
FAIRHAVEN	44-58	67-01	8.78	346	1.95	316	1.48	018	0.40	024	.44	142
LETITE HARBOUR	45-03	66-52	8.33	340	2.00	312	1.47	013	0.40	013	.41	136
PORT ST. ANDREWS	45-04	67-03	8.92	349	2.03	318	1.44	022	0.39	022	.53	144
PARTRIDGE ISLANDS	45-14	66-03	10.12	337	1.96	308	1.67	009	0.45	009	.53	131
ST. JOHN	45-15	66-04	9.95	342	2.03	314	1.65	016	0.45	016	.51	134
HERRING COVE	45-35	64-58	13.60	351	2.58	322	2.18	026	0.59	026	.62	138
CAPE ENRAGE	45-36	64-46	14.02	352	2.65	323	2.25	027	0.61	027	.64	129
GRINDSTONE IS.	45-44	64-38	14.98	353	2.83	324	2.40	028	0.65	028	.66	134
HOPEWELL CAPE	45-52	64-35	15.92	354	3.00	325	2.55	029	0.68	029	.42	137
JOGGINS WHARF	45-41	66-28	16.00	351	2.52	321	2.35	031	0.64	031	.53	134
CAPE CAPSTAN	45-28	66-51	13.56	347	2.56	318	2.17	022	0.58	022	.62	134
WEST ADVOCATE	45-21	64-49	13.41	342	2.89	311	2.22	026	0.60	026	.59	122
ADVOCATE	45-20	64-47	13.80	343	2.78	317	2.36	026	0.64	026	.58	135
PORT GREVILLE	45-40	64-56	15.11	356	2.83	324	2.26	037	0.61	037	.57	136
CAPE SHARP	45-22	64-23	15.76	005	2.97	345	2.37	056	0.64	056	.52	140
PARRSBORO	45-22	64-20	16.57	005	2.78	337	2.47	049	0.67	049	.63	143
FIVE ISLANDS	45-23	64-08	17.39	011	3.21	345	2.60	053	0.70	053	.72	155
BURNCOAT HEAD	45-19	63-49	18.51	014	3.60	351	2.73	059	0.74	059	.47	154
CAPE BLOMIDON	45-16	64-21	16.50	004	3.30	336	2.40	044	0.65	044	.53	150
SCOT'S BAY	45-19	64-26	15.30	349	3.14	321	2.21	032	0.60	032	.53	138
MARGARETSVILLE	45-03	65-04	12.90	344	2.37	316	2.22	009	0.72	009	.54	123
PARKERS COVE	44-50	65-32	10.70	335	2.30	310	1.68	007	0.45	007	.64	135
DIGBY	44-38	65-45	10.20	337	1.90	309	1.80	005	0.49	005	.63	132
DEEP COVE,CULLODEN	44-40	65-50	9.74	334	1.98	314	1.44	006	0.39	006	.53	129
SANDY COVE	44-30	66-06	8.34	333	1.78	307	1.46	005	0.39	005	.55	132
TIVERTON	44-24	66-13	7.64	324	1.69	291	1.34	359	0.36	359	.54	123
WESTPORT	44-16	66-21	7.22	325	1.67	294	0.98	357	0.27	357	.47	130
LIGHTHOUSE COVE	44-15	66-24	7.06	325	1.48	297	1.12	357	0.30	357	.54	124

Table I. 1

DATA FOR ONE-DIMENSIONAL
NUMERICAL SOLUTION

A=CROSS-SECTIONAL AREA
(10 EXP(6) SQ.FT.)
H=DEPTH
(FEET)
S=SURFACE AREA
(10 EXP(9) SQ.FT.)
N=SECTION NUMBER

N	1	2	3	4	5	6	7	8	9	9-3/4	10
A	76.06	109.94	64.16	47.94	31.56	27.04	7.95	2.52	8.65		5.41
H		280	290	240	190	150	110	70	120		110
S		23.78	20.10	16.54	15.29	15.00	4.31	4.67	4.96	3.68	
M2 AMPLITUDE	7.50	8.30	9.4	10.4	11.6	12.8	13.8	14.8	14.1	15.3	16.0
M2 PHASE LAG	331	332	334	336	338	341	345	350	351	358	360

Table II. 2

DATA FOR 1-DIMENSIONAL ANALYTIC SOLUTION.

VARIABLE	UNITS	SECTION 1	2	3	4	5	6	A	7	B	9
B=BREADTH	10**4 FT.	25.8	23.2	21.0	16.8	16.8	11.0	6.0	3.6	5.7	5.4
A=CROSS-SECTION	10**6 SQ.FT.	109.9	64.2	47.9	31.6	27.0	14.1	6.2	2.5	7.2	5.4
H=DEPTH	FT	426	277	228	188	161	128	103	70	126	100
C*C=GA/B	SQ.FT/SQ.SEC	12200	9320	7720	6100	4820	4118	3314	2233	4054	3217
C	FT/SEC	110.0	96.5	87.9	78.0	69.3	64.2	57.6	47.1	63.7	56.7
K=W/C	RAD/FT.	1.287	1.467	1.611	1.816	2.044	2.210	2.460	3.01	2.22	2.50
L	NAUT.MILES	15.5	15.5	15.5	15.5	15.5	7.8	7.8	23.3	7.8	15.5
KL	RADIANS	.121	.138	.152	.171	.193	.104	.116	0.421	0.100	.236
COS(KL)	-----	.993	.990	.988	.985	.981	.995	.993	.911	.998	.972
SIN(KL)	-----	.121	.137	.151	.170	.192	.104	.116	.426	.100	.234
BC	10**6 SQ.FT/SEC	28.38	22.39	18.46	13.10	11.64	07.06	03.46	1.70	3.63	3.06
A/BC	SEC.	3.925	2.867	2.595	2.412	2.320	2.00	1.790	1.47	1.98	1.76

Table III. 1

ARBITRARY CONSTANTS FOR ANALYTIC SOLUTION

SECTION	A(N)	B(N)	C(N)	D(N)	
1	1.000	.000	1.000	.000	
2	.993	-0.475	1.700	-.053	
3	.962	-1.138	2.225	-.134	
4	.897	-1.996	3.233	-.286	
5	.768	-3.292	3.561	-.400	
6	.575	-4.815	6.280	-.887	
L(6)			5.999	-.913	
A	.388	-6.097	1.207	+.076	
7	.401	-6.305	1.994	+.125	CHIGNECTO BAY
L(7)	.423	-6.658	.000	.000	
B	.388	-6.097	10.709	-1.853	
9	.021	-8.205	13.869	-2.492	MINAS CHANNEL
L(9)	-1.006	-13.687	12.394	-2.419	

Table III. 2

DATA FOR GRID SYSTEM FUNDY01

DEPTH AT U-POINTS (FEET)

	M= 5	6	7	8	9	10	11	12	13
N= 2	229	133	080						
3	420	349	296	237	178	155	072		
4	432	193	278	279	262	185	150		
5	240	259	212	213	208	167	174	289	

DEPTH AT V-POINTS (FEET)

	M=5	6	7	8	9	10	11	12
N= 2	360	343	283	194				
3	498	372	331	108	219	166	173	138
4	456	282	289	284	243	274	215	168

Table IV. 1

COMPARISON OF FUNDY01-A AND FUNDY01-B

M2 AMPLITUDE (FEET)

TOP=FUNDY01 A
BOTTOM=FUNDY01 B

	M= 5	6	7	8	9	10	11	12
N= 2	8.60	8.86	9.38	9.94				
	8.60	8.87	9.37	9.90				
3	8.40	8.92	9.48	10.09	10.84	11.59	12.22	12.91
	8.40	8.92	9.47	10.06	10.80	11.54	12.16	12.78
4	8.30	8.89	9.71	10.36	11.03	11.70	12.33	13.03
	8.30	8.88	9.69	10.33	10.99	11.66	12.36	12.94
5	8.20	8.88	9.71	10.50	11.19	11.90	12.74	13.63
	8.20	8.90	9.69	10.46	11.16	11.85	12.68	13.56

Table IV. 2

COMPARISON OF FUNDY01-A AND FUNDY01-B

M2 PHASE LAG (DEGREES)

TOP FUNDY01-A
BOTTOM FUNDY01 B

	M= 5	6	7	8	9	10	11	12
N= 2	333.9	335.3	336.8	337.8				
	333.9	335.1	336.6	337.6				
3	330.9	332.7	334.6	336.1	338.1	339.5	341.0	342.5
	330.9	332.7	334.6	336.1	338.1	340.0	341.5	342.9
4	329.0	330.2	332.1	333.6	335.3	336.6	339.5	341.7
	329.0	330.3	332.7	334.2	335.6	336.6	339.5	342.0
5	328.0	328.8	329.3	331.2	333.2	335.6	337.3	341.2
	328.0	328.3	329.3	331.2	333.2	334.6	337.1	342.9

Table IV. 3

DEPTH FOR U POINTS (FEET)
FOR GRID SYSTEM FUNDY02

	M= 2	3	4	5	6	7	8	9	10	11	12	13	14	15	16	17	18	19	20	21	22	23
N= 2	187	103																				
3	252	193	223	145	145	100	080															
4	312	288	325	301	283	259	218	182														
5	406	402	[illegible]	[illegible]	367	337	290	284	224	201	159	160	136	143	149	126	84	115	91	61		
6	522	462	397	361	355	337	308	296	254	225	237	202	160	191	173	156	150	139	283	175	152	127
7	508	432	408	355	337	325	302	284	290	261	213	220	178	137	185	162	138	91				
8	414	372	372	319	349	325	308	272	278	267	255	202	226	209	203	192	150	139				
9	461	396	312	319	377	283	284	260	248	249	225	232	214	197	227	174	192	175			80	
10	431	330	288	265	265	193	200	224	208	195	195	184	148	149	131	120	132	139	151	200	140	231
11	215	162																		92	99	

Table IV. 4

DEPTH (FEET) FOR V POINTS
FOR GRID SYSTEM FUNDY02

	M= 2	3	4	5	6	7	8	9	10	11	12	13	14	15	16	17	18	19	20	21	22	23
N= 2	181	169	121																			
3	313	217	253	253	205	194	151	110														
4	402	373	349	349	313	302	272	242	182													
5	492	457	408	355	349	338	320	296	296	211	201	166	172	137	167	168	132	139	133	127	134	
6	428	493	419	385	373	350	344	314	272	273	219	250	172	197	179	174	150	139	145			
7	570	402	348	349	373	320	278	254	272	279	255	274	232	179	179	180	168	127	000			
8	432	450	420	349	331	343	326	280	290	279	255	250	256	245	239	204	144	156	121			
9	468	408	354	331	289	193	256	248	248	255	225	226	214	197	161	180	162	168	193	000	164	171
10	408	300	252																	140	119	089

Table IV. 5

PHASE LAG OF MAJOR AXIS
OF CURRENT ELLIPSE IN
THE POSITIVE X DIRECTION
(DEGREES)

CALCULATION FUNDY02 A
NORMAL CONFIGURATION

	M= 2	3	4	5	6	7	8	9	10	11	12	13	14	15	16	17	18	19	20
N= 2	263		264																
3		266		277		254		247											
4	271		265		264		258		254										
5		267		262		260		258		252		251		249		249		249	
6	262		258		257		258		256		255		254		255		258		264
7		254		251		253		255		256		255		254		256		261	
8	243		245		247		251		254		255		256		257		255		254
9		238		238		246		249		252		254		256		255		250	
10	228		236		234		242		248		250		250		248		246		251
11		247																	

Table IV. 6

M2 AMPLITUDE WITH U(23,6)=U(23,10)=0.0 (CALCULATION FUNDY02 G)

U DU/DX TERM INCLUDED IN THE EQUATIONS.

UPPER VALUE- HIGH WATER (FEET)
LOWER VALUE- LOW WATER (ABSOLUTE VALUE)

	M= 3	5	7	9	11	13	15	17	19	21	23
N= 4	8.56	8.82	9.05	9.30							
	8.55	8.84	9.08	9.34							
6	8.39	8.70	9.02	9.34	9.70	10.09	10.46	10.75	10.99	11.14	11.22
	8.42	8.78	9.10	9.44	9.85	10.30	10.77	11.17	11.52	11.74	11.85
8	8.26	8.62	9.00	9.36	9.73	10.10	10.46	10.76	11.00		
	8.30	8.71	9.09	9.49	9.91	10.33	10.77	11.17	11.50		
10	8.18	8.59	8.98	9.40	9.77	10.13	10.49	10.80	11.07	11.39	11.52
	8.21	8.65	9.06	9.53	9.95	10.37	10.81	11.21	11.59	12.08	12.30

Table IV. 7

M2 PHASE LAG , U(23,6)=U(23,10)=0.0 (CALCULATION FUNDY02 G)

U DU/DX TERM INCLUDED IN THE EQUATIONS

UPPER VALUE -PHASE OF HIGH WATER (DEGREES)
LOWER VALUE -PHASE OF LOW WATER + 180

	M= 3	5	7	9	11	13	15	17	19	21	23
N= 4	332.9	331.4	331.4	330.9							
	333.0	333.5	333.9	334.9							
6	330.9	330.0	329.5	329.5	329.5	329.0	328.5	328.5	328.5	328.0	328.0
	331.0	332.0	333.0	333.9	335.4	336.4	337.3	338.3	339.3	339.8	339.8
8	329.0	328.5	328.0	328.0	327.5	327.5	327.5	327.0	327.5		
	329.5	330.0	331.0	332.0	333.5	334.4	335.9	337.3	337.8		
10	327.5	327.0	326.0	326.5	326.0	326.0	326.0	326.0	326.0	326.5	326.5
	327.1	328.6	329.0	330.5	331.5	333.0	334.4	335.4	337.3	340.3	340.3

Table IV. 8

PROGRESSION OF THE TIDE
BETWEEN ST. JOHN AND GRINDSTONE IS.

DATE(1965)	GRINDSTONE (HOURS)		ST. JOHN (HOURS)	HIGH WATER, LAG (HOURS	LOW WATER LAG (HOURS)
JULY 25	0340	LOW	0217		0123
	0950	HIGH	0822	0128	
	1615		1441		0134
	2212		2044	0128	
26	0445		0310		0135
	1048		0923	0125	
	1715		1532		0143
	2310		2142	0128	
27	0545		0412		0133
	1150		1018	0132	
	1820		1637		0143
28	0005		2241	0124	
	0650		0508		0142
	1245		1113	0132	
	1915		1733		0142
29	0100		2339	0121	
	0730		0605		0125
	1345		1211	0134	
	2010		1823		0147
30	0200		0036	0124	
	0835		0659		0136
	1435		1304	0131	

Table IV. 9

AVERAGE M2 AMPLITUDE (FEET) WITH U(23,6)=U(23,10)=0.0

UPPER VALUE -WITH U DU/DX (CALCULATION G)
LOWER VALUE -WITHOUT U DU/DX (CALCULATION F)

M=	11	12	13	14	15	16	17	18	19	20	21	22	23
N=5	9.76	9.98	10.21	10.42	10.64	10.82	10.97	11.13	11.28	11.38	11.45	11.51	
	9.77	9.98	10.19	10.42	10.61	10.80	10.94	11.08	11.24	11.34	11.40	11.42	
6	9.78	9.99	10.20	10.40	10.62	10.77	10.96	11.11	11.26	11.38	11.44	11.50	11.53
	9.77	9.98	10.18	10.38	10.59	10.77	10.93	11.07	11.26	11.34	11.39	11.42	11.48
7	9.79	10.00	10.20	10.40	10.60	10.76	10.96	11.11	11.24	11.34			
	9.79	9.99	10.20	10.38	10.58	10.77	10.93	11.07	11.24	11.30			
8	9.82	10.02	10.22	10.42	10.62	10.78	10.96	11.10	11.25	11.36			
	9.82	10.00	10.21	10.40	10.59	10.77	10.93	11.08	11.26	11.31			
9	9.84	10.04	10.24	10.44	10.63	10.78	10.98	11.14	11.28	11.39		11.91	11.93
	9.84	10.03	10.23	10.42	10.60	10.79	10.92	11.10	11.29	11.35		11.85	11.87
10	9.86	10.06	10.25	10.45	10.65	10.81	11.00	11.18	11.33	11.50	11.74	11.85	11.91
	9.85	10.06	10.24	10.43	10.63	10.80	10.93	11.14	11.36	11.45	11.73	11.80	11.85
11											11.85	11.88	11.93
											11.76	11.82	11.86

Table IV. 10

AVERAGE M2 PHASE LAG (DEGREES) WITH U(23,6)=U(23,10)=0.0

UPPER VALUE -WITH U DU/DX (CALCULATION G)
LOWER VALUE -WITHOUT U DU/DX (CALCULATION F)

M=	12	13	14	15	16	17	18	19	20	21	22	23
N=5	333.7	333.9	333.8	334.4	333.9	334.2	334.1	334.2	334.2	334.0	334.4	
	333.9	334.3	334.4	334.3	334.7	334.4	334.2	334.4	334.4	334.4	334.6	
6	332.7	332.7	333.0	333.4	333.4	333.4	333.8	333.9	333.6	333.9	333.9	333.9
	332.9	333.2	333.2	334.4	333.9	333.7	333.9	334.3	334.2	334.1	334.4	334.4
7	331.5	332.0	332.2	332.5	332.7	332.9	332.9	332.6	333.2			
	332.2	332.2	332.4	332.9	333.2	333.3	333.4	333.4	333.9			
8	330.7	331.0	331.1	331.7	332.2	332.2	332.4	332.7	332.7			
	331.3	331.8	332.0	332.0	332.7	332.5	332.9	333.0	333.2			
9	330.0	330.5	330.7	331.2	331.2	331.5	331.7	332.4	332.2		333.7	333.7
	330.3	330.8	331.3	331.8	332.0	332.0	332.5	332.7	333.2		334.1	334.4
10	329.0	329.5	329.9	330.2	330.7	330.7	331.5	331.7	332.1	333.4	333.4	333.4
	329.8	330.0	330.2	330.5	331.5	331.5	332.0	332.2	332.7	333.6	334.1	333.8
11										333.4	333.4	333.7
										333.6	333.8	334.1

Table IV. 11

AMPLITUDE(FUNDY02 H) MINUS AMPLITUDE(FUNDY02 G)

(HUNDREDTHS OF A FOOT)

TO SHOW THE EFFECT OF CONSTANT DEPTH

	M=6	7	8	9	10	11	12	13	14	15	16	17	18	19	20	21	22	23
N= 3	17	22	24	24														
4	18	23	26	28	33													
5	19	23	27	30	34	39	40	37	34	28	24	21	16	08	05	03	00	
6	20	25	28	31	34	36	37	36	34	29	28	21	20	09	05	04	02	01
7	21	26	28	31	33	36	36	36	34	30	28	22	16	11	07			
8	20	25	30	32	33	36	36	35	33	28	27	22	18	12	09			
9	21	28	29	33	34	36	36	34	32	29	28	19	16	12	08		-8	-9
10	22	30	31	32	35	37	37	35	33	29	27	21	14	10	05	-3	-5	-8
11																-8	-7	-10

Table IV. 12

PHASE LAG(FUNDY02 H) MINUS PHASE LAG(FUNDY02 G)

PHASE LAG IN DEGREES

TO SHOW THE EFFECT OF CONSTANT DEPTH

M=	6	7	8	9	10	11	12	13	14	15	16	17	18	19	20	21	22	23
N=3	1.7	2.0	2.2	2.2														
4	1.8	1.7	1.7	2.0	2.7													
5	1.2	1.8	1.9	2.0	1.8	1.0	.9	.7	.6	.3	.7	.2	.1	-.1	.2	.4	-.5	
6	1.4	1.4	1.2	1.4	1.5	.7	1.0	1.4	.9	1.2	.3	.5	.1	.0	.3	.0	.2	.2
7	1.0	1.5	1.5	1.5	1.9	1.2	1.7	1.2	1.2	.7	.7	.8	.8	1.1	.5			
8	1.5	1.9	1.2	1.5	1.4	1.1	1.7	1.7	1.9	1.0	.5	.7	.5	.2	.7			
9	1.0	1.3	.7	1.9	1.7	.7	1.5	1.2	1.3	1.0	1.5	.9	1.2	.5	-.9		.2	.2
10	.5	1.3	1.2	1.8	2.2	1.7	1.7	1.7	1.6	1.3	1.3	1.3	.9	.7	.8	.0	.3	.0
11																-.3	.0	-.3

Table IV. 13

MANUSCRIPT REPORT SERIES No. 6

A Temperature-Salinity Plotting Program

J. R. WILSON

A Note on the Precision of Serial Temperature Data

F. G. BARBER

1967

Marine Sciences Branch,
Department of Energy, Mines and Resources, Ottawa

Manuscript Report Series No. 6

A TEMPERATURE-SALINITY PLOTTING PROGRAM

J. R. Wilson

A NOTE ON THE PRECISION OF SERIAL TEMPERATURE DATA

F. G. Barber

1967

ROGER DUHAMEL, F.R.S.C.
QUEEN'S PRINTER AND CONTROLLER OF STATIONERY
OTTAWA, 1967

CONTENTS

A TEMPERATURE-SALINITY PLOTTING PROGRAM

J.R. Wilson

The computer program described here provides for the production of temperature-salinity diagrams from serial oceanographic observations.

The program has been assigned the number G20409.

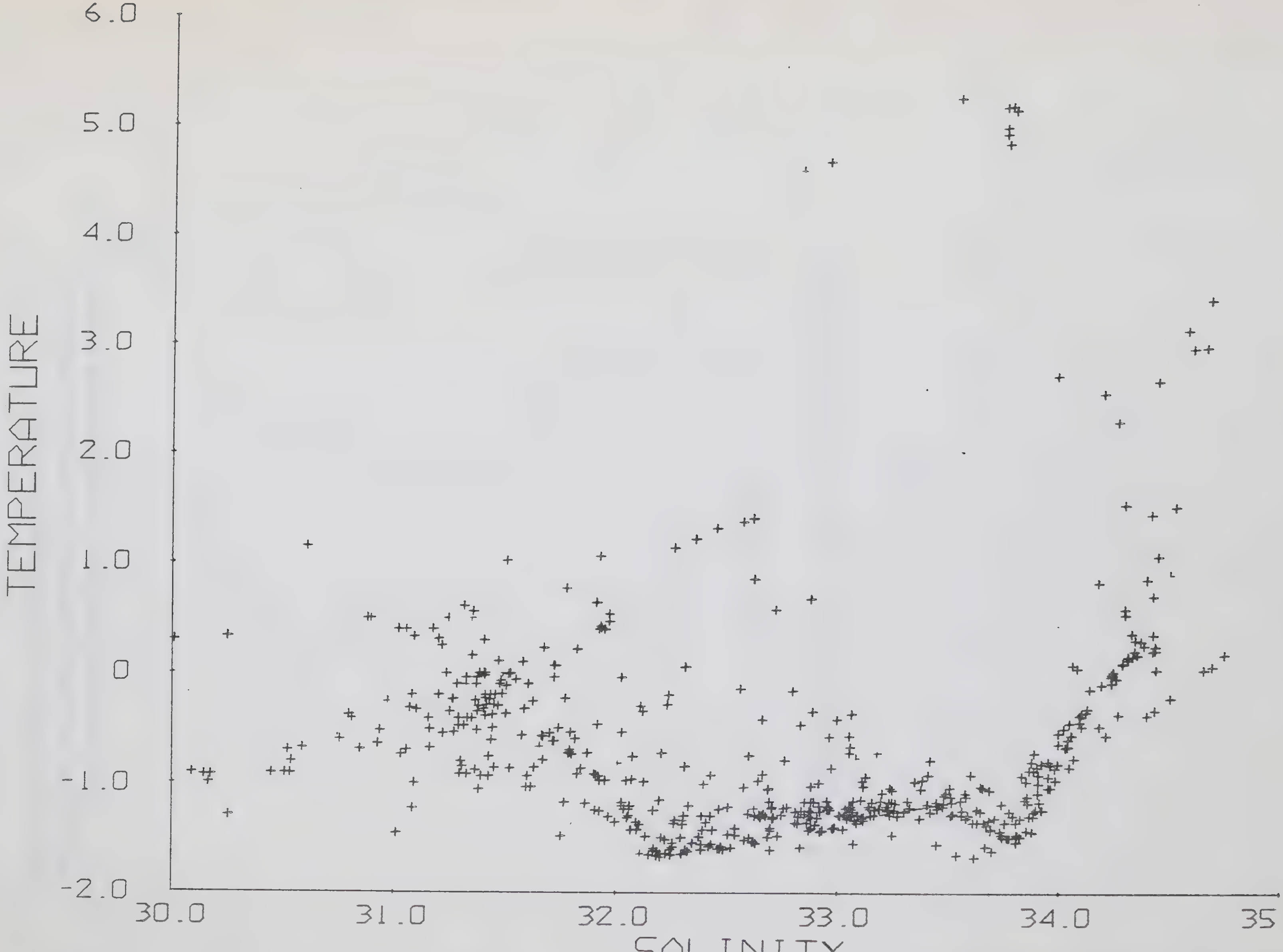

Figure 1. A photographic reproduction of a temperature-salinity diagram produced with the plot control card shown in Figure 2. A 0.02-mm liquid ink pen with black ink was used on the Calcomp 750 system. The diagram was not retouched in any way prior to photographing. The data were observed in 1961 in CCGS "Labrador" on a survey in Arctic waters and have been reported (Anon., 1966).

TEMPERATURE-SALINITY PLOTTING PROGRAM

Program Function

The program (Table 1) has been developed to produce standard oceanographic temperature-salinity diagrams (Fig. 1) using the Departmental Control Data Corporation 3100/Calcomp 750 plotting system. The dimensions of the plot, the ranges of the axes, and the code for the symbol to be drawn at each plotted point are read in from a card at program execution time. These parameters can therefore be changed by punching a new control card.

Temperature values having an illegal overpunch and points lying outside the range of the axes are not plotted but are logged on the on-line printer.

Table 1.

A compilation listing of the FORTRAN source program for the main program and the two subprograms.

```
                                      3200   FORTRAN     (2.1)            29/07/66

          PROGRAM MAIN
C         TEMPERATURE-SALINITY PLOTTING PROGRAM
C
C         J R WILSON
C         OCEANOGRAPHIC RESEARCH DIVISION
C         JULY 1966
C
          COMMON MBUFF(20),ICARD,LUN,NPRINTER,NPLOTI,TEMP,SAL,NPOINT,NPLOT,N
         1ERROR,SL,TL,SMIN,TMIN,SINC,TINC,SLNG,TLNG,IMARK,SMAX,TMAX
          ICARD = 60
          LUN = 01
          NPRINTER = 61
          NPLOTI = 1
          NPOINT = NPLOT = NERROR = 0
          READ (ICARD,2001) SL,TL,SMIN,TMIN,SINC,TINC,SLNG,TLNG,IMARK
          SMAX = SMIN + SLNG
          TMAX = TMIN + TLNG
       10 CALL READCTRL
          CALL PLOT
          GO TO 10
     2001 FORMAT (8F6.1,I4)
          END

            3200 FORTRAN DIAGNOSTIC RESULTS - FOR    MAIN

NO ERRORS

                                      3200   FORTRAN     (2.1)            29/07/66

          SUBROUTINE ERROR
          COMMON MBUFF(20),ICARD,LUN,NPRINTER,NPLOTI,TEMP,SAL,NPOINT,NPLOT,N
         1ERROR,SL,TL,SMIN,TMIN,SINC,TINC,SLNG,TLNG,IMARK,SMAX,TMAX
          WRITE (NPRINTER,4001) (MBUFF(I),I=1,20),TEMP,SAL
          NERROR = NERROR + 1
          RETURN
     4001 FORMAT (17H0INPUT DATA ERROR/1H ,20A4,2E12.3)
          END

            3200 FORTRAN DIAGNOSTIC RESULTS - FOR    ERROR

NO ERRORS
```

Table 1 (cont.)

```
                                 3200  FORTRAN    (2.1)           29/07/66
      SUBROUTINE READCTRL
      DIMENSION LARRY(3)
      COMMON MBUFF(20),ICARD,LUN,NPRINTER,NPLOTI,TEMP,SAL,NPOINT,NPLOT,N
     1ERROR,SL,TL,SMIN,TMIN,SINC,TINC,SLNG,TLNG,IMARK,SMAX,TMAX
    5 TEMP = SAL = 0.
      READ (ICARD,2001) (MBUFF(I),I=1,20)
      IF (MBUFF.EQ.4HENDP) 120,10
   10 IF (MBUFF.EQ.4HENDJ) 130,20
   20 DECODE (80,2002,MBUFF) NTEMP,NSAL,ITYPE
      IF (ITYPE.EQ.3) 30,5
   30 IF (NTEMP.EQ.60606060B.OR.NSAL.EQ.60606060B) 5,40
   40 DECODE (80,2003,MBUFF) NSTEMP,TEMPL,SALH,NSALL
      IF (NSTEMP.GT.11B) 50,70
   50 TEMPL = -TEMPL
      IF (NSTEMP.GE.40B.AND.NSTEMP.LE.51B) 65,55
   55 IF (NSTEMP.EQ.52B) 80,125
   65 NSTEMP = -(NSTEMP - 40B)
   70 TEMPL = NSTEMP*10 + TEMPL
   80 TEMP = TEMPL
      IF (NSALL.GT.11B) 100,110
  100 NSALL = 0
  110 SAL = SALH + NSALL/1000.
      RETURN
  120 CALL ENDPLOT (LUN)
      NPLOTI = 1
      GO TO 5
  125 CALL ERROR
      GO TO 5
  130 CALL ENDPLOT (LUN)
      WRITE (NPRINTER,4001) NPOINT,NPLOT,NERROR
      STOP
      ENTRY PLOT
      IF (TEMP.GE.TMIN.AND.TEMP.LE.TMAX.AND.SAL.GE.SMIN.AND.SAL.LE.SMAX)
     1135,195
  135 IF (NPLOTI.EQ.1) 140,190
  140 CALL AXISXY (LUN,SL,TL,SINC,SLNG,TLNG,SMIN,TMIN,SMIN,TMIN,TINC)
      SSCALE = SLNG/SL
      TSCALE = TLNG/TL
      XPOS = SMIN - SSCALE
      YPOS = TMIN - 0.08*TSCALE
      YPLOT = TMIN
  150 CALL PLOTXY (XPOS,YPOS,0,0)
      ENCODE (4,4002,LARRY) YPLOT
      CALL LABEL (4,2,0,LARRY)
      YPOS = YPOS + TINC
      YPLOT = YPLOT + TINC
      IF (YPOS.GT.TMAX) 160,150
  160 XPOS = SMIN - 1.25*SSCALE
      YPOS = TMIN + TLNG/2. - 1.35*TSCALE
      CALL PLOTXY (XPOS,YPOS,0,0)
      ENCODE (11,4003,LARRY)
      CALL LABEL (11,3,3,LARRY)
      XPOS = SMIN - 0.31*SSCALE
      YPOS = TMIN - 0.3*TSCALE
      YPLOT = SMIN
  170 CALL PLOTXY (XPOS,YPOS,0,0)
      ENCODE (4,4002,LARRY) YPLOT
      CALL LABEL (4,2,0,LARRY)
      XPOS = XPOS + SINC
      YPLOT = YPLOT + SINC
      IF (XPOS.GT.SMAX) 180,170
```

Table 1 (cont.)

```
  180 XPOS = SMIN + SLNG/2. - 0.9*SSCALE
      YPOS = TMIN - 0.8*TSCALE
      CALL PLOTXY (XPOS,YPOS,0,0)
      ENCODE (8,4004,LARRY)
      CALL LABEL (8,3,0,LARRY)
      NPLOTI = 0
      NPLOT = NPLOT + 1
  190 CALL PLOTXY (SAL,TEMP,0,IMARK)
      NPOINT = NPOINT + 1
      RETURN
  105 CALL ERROR
      RETURN
 2001 FORMAT (20A4)
 2002 FORMAT (32X,A4,1X,A4,38X,I1)
 2003 FORMAT (32X,R1,F3.2,1X,F4.2,R1)
 4001 FORMAT (1H1,I6,23H POINTS WERE PLOTTED ON,I3,8H GRAPHS./I6,51H ERR
     1ONEOUS OR OUT OF RANGE POINTS WERE ENCOUNTERED./12H END OF JOB.)
 4002 FORMAT (F4.1)
 4003 FORMAT (11HTEMPERATURE)
 4004 FORMAT (8HSALINITY)
      END

          3200 FORTRAN DIAGNOSTIC RESULTS - FOR    READCTRL

NO ERRORS
LOAD,56
RUN,10
```

Computer Configuration

The input is from the card reader. The output consists of error messages and an end-of-job summary on the on-line printer (Table 2) with a Calcomp plotter tape on logical unit 01.

It is unlikely that the program could be operated in unmodified form on other computer systems, including CDC-3100 systems, as they would not have compatible plotter subroutines.

Table 2.

A sample of the log of out-of-range data encountered and the end-of-job summary. For each out-of-range point encountered the phrase "INPUT DATA ERROR", an 80-column image of the data card, and the values of the temperature and salinity are printed. Only 4 of the 32 out-of-range points encountered in this job are shown in the table.

```
INPUT DATA ERROR
18137104009000026261091106500000A0020A29927     24034432                 3440493   2.000E-01   2.993E 01

INPUT DATA ERROR
1813710400900002626109110650008A0032A29926      24034439                 3440493   3.200E-01   2.993E 01

INPUT DATA ERROR
1813704800911802626109111130000A0003A29970      24084425                 3440513   3.000E-02   2.997E 01

INPUT DATA ERROR
1813704800911802626109111130008A0008A29972      24084428                 3440513   8.000E-02   2.997E 01


   1654 POINTS WERE PLOTTED ON   4 GRAPHS.
     32 ERRONEOUS OR OUT OF RANGE POINTS WERE ENCOUNTERED.
END OF JOB.
```

Input Deck Structure

${}^{7}_{9}$JOB, G20409, CODC, 10

${}^{7}_{9}$Equip, 01=MTCOEOU01

.
. (binary program deck)
.
.
.

${}^{7}_{9}$RUN, 10

(plot control card)

.
. (data deck containing temperature-salinity observations
. for first plot)
.
.
.

ENDP

.
. (data deck containing temperature-salinity observations
. for second plot)
.
.
.
ENDP
ENDJ

77
88

The JOB and EQUIP cards are explained fully in the Control Data Corporation 3200 Scope - Compass Reference Manual (Anon., 1964). The equipment assignment in the example above will result in the plotter tape being produced on channel 0 unit 1. The run card is also explained in the Scope-Compass Manual.

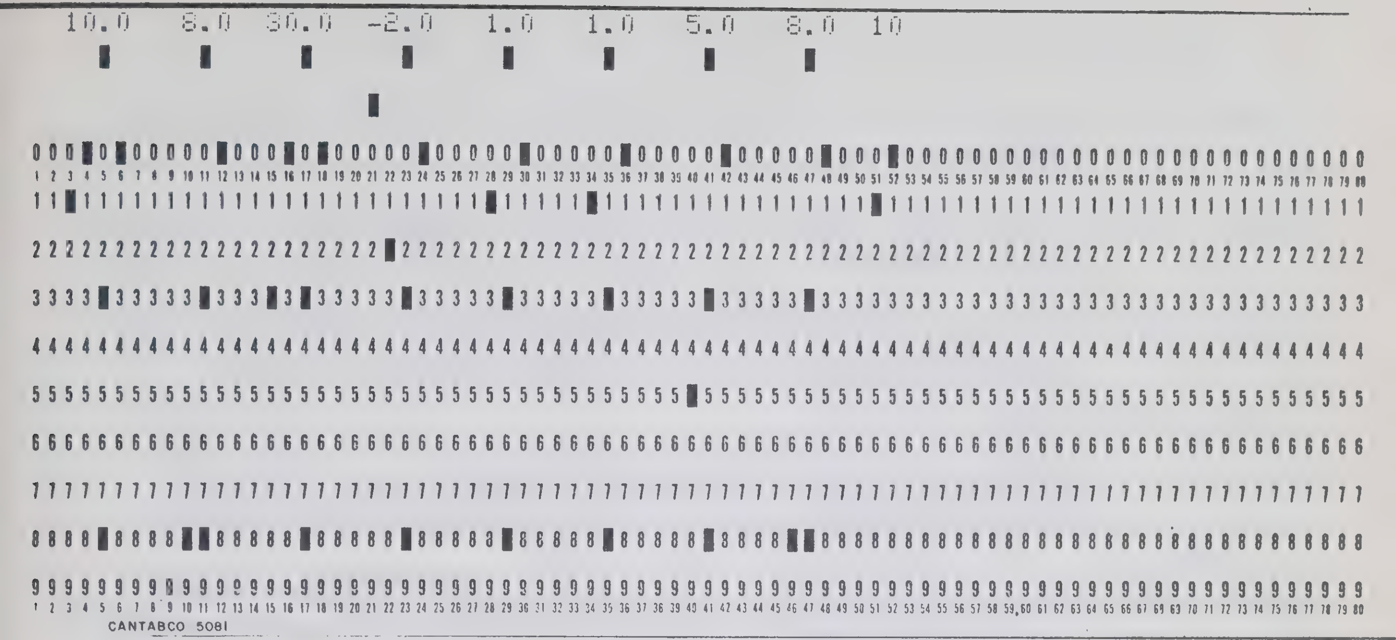

Figure 2. A photographic reproduction of a sample plot control card.

Field 1 specifies that the salinity or X-axis is to be 10 inches long.

Field 2 specifies that the temperature or Y-axis is to be 8 inches long.

Field 3 specifies that the minimum value of salinity is to be 30 parts per thousand.

Field 4 specifies that the minimum value of temperature to be plotted is -2 degrees.

Field 5 specifies that the salinity axis is to have a tick at 1-part-per-thousand intervals.

Field 6 specifies that the temperature axis is to have a tick at 1-degree intervals.

Field 7 specifies that the salinity axis is to be 5 parts per thousand in length.

Field 8 specifies that the temperature axis is to 8 degrees in length.

Field 9 specifies that a large vertical cross with the datum at its centre is to be drawn at each temperature-salinity point.

The format of the plot control card (Fig. 2) is as follows:

Columns 1-6. Length of the X-axis in inches to tenths of inches with the decimal point in column 5.

Columns 7-12. Length of the Y-axis in inches to tenths of inches with the decimal point in column 11.

Columns 13-18. Minimum value of the salinity to appear on the X-axis in parts per thousand to tenths of parts per thousand with decimal point in column 17.

Columns 19-24. Minimum value of the temperature to appear on the Y-axis in degrees to tenths of degrees with the decimal point in column 23.

Columns 25-30. The interval in parts per thousand to tenths of parts per thousand of salinity at which ticks are desired on the X-axis with the decimal point in column 29.

Columns 31-36. The interval in degrees to tenths of degrees at which ticks are desired on the Y-axis with the decimal point in column 35.

Columns 37-42. The length of the X-axis in parts per thousand of salinity to tenths of parts per thousand with the decimal point in column 41.

Columns 43-48. The length of the Y-axis in degrees to tenths of degrees with the decimal point appearing in column 47.

Columns 51-52. A two-digit code to indicate the symbol to be drawn at each plot temperature-salinity point.

The two-digit codes for the various symbols available are listed below. Odd numbers define small marks while even numbers define marks which compare to the odd-numbered marks but are about twice as long.

1-2. Up arrow, with datum at the point.
3-4. Right arrow, with datum at the point.
5-6. Down arrow, with datum at the point.
7-8. Left arrow, with datum at the point.
9-10. Vertical cross, with datum at its centre.
11-12. X within a box, with datum at its centre.
13-14. Hourglass-shaped dot, with datum at the lower left corner.

15-16. Diagonal cross, with datum at its centre.
17-18. Vertical carat, with datum at the point.
19-20. Horizontal carat, with datum at the point.
21-22. Right angle, with datum at intersection.
23-24. Right angle, turned 180 degrees, with datum at intersection.
25-26. Tee, on its side, with datum at intersection.
27-28. Tee, with datum at the intersection.
29-30. Vertical bar, with datum at its centre.
31-32. Horizontal bar, with datum at its centre.

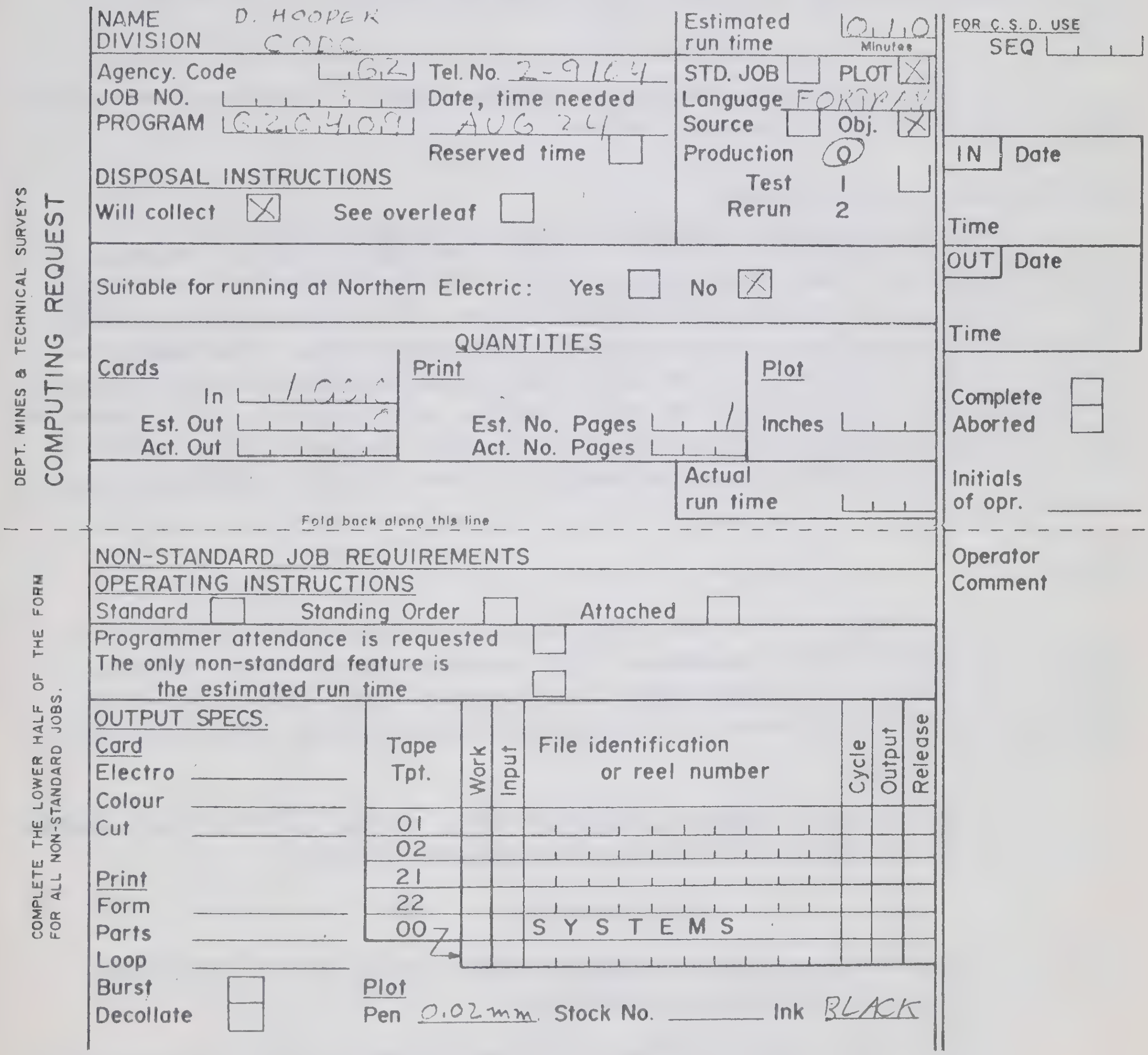

DEPT. MINES & TECHNICAL SURVEYS
COMPUTING REQUEST

NAME D. HOOPER
DIVISION CODC
Estimated run time 010 Minutes
FOR C.S.D. USE
SEQ

Agency. Code 62
Tel. No. 2-9164
STD. JOB
PLOT ☒
JOB NO.
Date, time needed
Language FORTRAN
PROGRAM G2G409
AUG 24
Source
Obj. ☒
Reserved time
Production 0
Test 1
Rerun 2
DISPOSAL INSTRUCTIONS
Will collect ☒
See overleaf

IN Date
Time
OUT Date
Time

Suitable for running at Northern Electric: Yes ☐ No ☒

QUANTITIES
Cards
In 1000
Est. Out
Act. Out
Print
Est. No. Pages 1
Act. No. Pages
Plot
Inches

Complete
Aborted

Actual run time
Initials of opr.

Fold back along this line

COMPLETE THE LOWER HALF OF THE FORM FOR ALL NON-STANDARD JOBS.

NON-STANDARD JOB REQUIREMENTS
OPERATING INSTRUCTIONS
Standard ☐ Standing Order ☐ Attached ☐
Programmer attendance is requested ☐
The only non-standard feature is the estimated run time ☐

Operator Comment

OUTPUT SPECS.
Card
Electro
Colour
Cut
Print
Form
Parts
Loop
Burst
Decollate

Tape Tpt.	Work	Input	File identification or reel number	Cycle	Output	Release
01						
02						
21						
22						
00			SYSTEMS			

Plot
Pen 0.02mm. Stock No. Ink BLACK

Figure 3. A photograph of a sample computing request form.

A completed computing request form (Fig. 3) is forwarded to the Computing Centre along with the program deck and data deck for each run of the program. The data decks consist of cards in the standard Canadian Oceanographic Data Centre format (Anon., 1965). All cards are ignored except the observed cards which contain a 3 punch in column 80.

There are two control cards which can be used to cause the computer to draw new axes or to indicate the end of job. These cards are ENDP and ENDJ. ENDP and ENDJ are punched in columns 1 through 4 of a card. The ENDP card can appear anywhere in a data deck and will cause all succeeding temperature-salinity points to be plotted on a new graph. The ENDJ card will appear as the last card in the data deck.

The card containing 7-8 punches in columns 1 and 2 is the normal end-of-job card required by the SCOPE monitor system.

Computations and Quality Control

All cards not having a 3 punch in column 80 are ignored by the program. Cards having a 3 in column 80 are checked so that both temperature and salinity are coded. If one or both are absent, the card is ignored. If both are present a check is performed to see that the values are within the range of the axes. If the values are outside the range of the axes or if the temperature field contains an illegal overpunch, an error message is generated on the printer and the card is ignored. If the values of temperature and salinity are within the range of the axes the plotter pen is moved to the correct location and the symbol indicated by columns 51 and 52 of the plot control card is drawn.

Output

Error messages and the end-of-job summary are generated on the on-line printer. The error message consists of an 80-column image of the card plus the values of temperature and salinity written in exponential form. If the cause of the error message was illegal overpunch in the temperature field, the temperature and salinity will be printed as 0.

The plotter tape is written on channel 0 unit 1. At the end of the job it should be removed and forwarded to the Calcomp 750 system for plotting.

REFERENCES

Anonymous, 1964. Reference Manual-3200 Computer System SCOPE/COMPASS. Control Data Publication 60057700.

1965. Form number MTS-146. Coding instructions for Canadian Oceanographic Data Centre cruisemaster questionnaire. Form Number MTS-149. Coding instructions for Canadian Oceanographic Data Centre station master and observed detail cards.

1966. Data record - Arctic 1961. Data record in press, Can. Oceanog. Data Centre.

A NOTE ON THE PRECISION OF SERIAL TEMPERATURE DATA

F. G. Barber

Serial oceanographic data obtained on a survey in Hudson Bay during the 1961 navigation season in the motor vessel "Theta" have been reported in a publication of the Canadian Oceanographic Data Centre (Anon., 1964). In this it was indicated that the tabulated temperature data are significant to 0.037C°; it will be shown that this value should have read 0.027C°. The values were calculated using a technique described by N. P. Fofonoff in an undated memorandum of the Pacific Oceanographic Group, and in a later (1963) discussion of the precision of oceanographic data relative to calculations of the speed of sound in sea water.

During the planning for the survey, it was considered that there would exist an opportunity to progress understanding of the precision of serial temperature observations. Upwards of two hundred station occupations in relatively shallow and generally cold water were proposed, and an adequate supply of both Richter & Wiese and Yoshino Factory protected reversing thermometers was available. It was decided that each reversing bottle (Knudsen type) be fitted with one each of a Richter & Wiese and a Yoshino thermometer, and that if possible, the arrangement would be adhered to throughout the survey. Each thermometer was to be read twice independently, and the readers were not to be aware of the experiment. A difficulty not foreseen prior to the survey relates to the level of training of the readers for, throughout the survey as well as at the start, a number of the readers were limited in experience.

The procedure was followed generally as outlined, and about 1,000 serial temperature observations derived from two readings of each of the two thermometers on each bottle. These were processed to obtain the value for each of the reading, functioning, and systematic errors presented in Table 1.

Table 1.
Calculated Value of the Standard Deviation for each of the Errors as Obtained from the "Theta" Material (Column a), and by Fofonoff (1963) (Column b)

Error Type	(a) (C°)	(b) (C°)
Reading	0.0100	0.0074
Functioning	0.0100	0.0055
Systematic	0.0064	0.0141

Using these values the precision of a single reading of one thermometer becomes 0.030C°, the average of two readings of two thermometers has a precision of 0.019C°, and the least significant difference of two averages (two tabulated values in the data report) becomes 0.027C°. Also shown in the table are the corresponding values obtained by Fofonoff (1963). As might have been anticipated his reading and functioning errors are smaller than those calculated for the Hudson Bay data. With regard to his value of the systematic error, he (personal communication) has indicated that the wording of his paper is misleading and has confirmed that the value of 0.0141C° refers to the individual systematic error and not to differences.

It is of interest that using the smaller of each of the tabulated values and in the situation that two thermometers on each reversing bottle are read twice, the average has a precision of 0.014C°. The estimate represents a precision higher than any of those shown in the tabulation of Fofonoff (1963, Table 1, p. 831).

Of additional interest in the present data is the distribution of the frequency of occurrence of the systematic differences between pairs of thermometers (Table 2). The manner of thermometer arrangement on the reversing bottles during the survey with Richter & Wiese instruments generally on the left in the reading position, led to a grouping not only with respect to the make of thermometer, but also with respect to the time of calibration.

Table 2.

Distribution of the Systematic Differences Between Paired Thermometers of Different Make, Rounded to the Second Decimal Place

Difference	-0.01	0.00	0.01	0.02
Frequency	1	4	5	3
Arithmetic mean		0.008C°		

This was carried out by the National Research Council; one make (R&W) was calibrated in 1960 on February 10, 11 and 12, the other on June 13 and 31, 1961. It seemed, therefore, that the arithmetic mean of 0.008C° of the distribution could be related to either the make or time of calibration, or both. This was tested using the "Student 't' test" which indicated that there was not sufficient evidence to support the hypothesis.

ACKNOWLEDGMENT

The author wishes to acknowledge the assistance of Messrs. B.J. Layton and T.B. Moodie in the preparation of the material.

REFERENCES

Anonymous, 1964. Data record. Hudson Bay Project - 1961. Can. Oceanog. Data Centre, 1964.

Fofonoff, N.P., 1963. Precision of oceanographic data for sound speed calculations. J. Acoust. Soc. Am. 35(6): 830-836.

MANUSCRIPT REPORT SERIES No. 7

Tuktoyaktuk Harbour - a data report

W. J. B. Kelly

1967
Marine Sciences Branch
Department of Energy, Mines and Resources, Ottawa

Manuscript Report Series No. 7

TUKTOYAKTUK HARBOUR - A DATA REPORT

W. J. B. Kelly

1967

ROGER DUHAMEL, F.R.S.C.
QUEEN'S PRINTER AND CONTROLLER OF STATIONERY
OTTAWA, 1967

CONTENTS

INTRODUCTION

The oceanographic data of this record were obtained in and adjacent to the waters of Tuktoyaktuk Harbour (Figure 1) during the period April 26, 1962 to September 16, 1963. The observations were made relative to a study by the National Research Council of Canada of the general problem of the applicability of air bubblers in a salt-water environment, particularly at Tuktoyaktuk. The air bubbler system used has been described by Dick (1961); Ince (1962) described the physical aspects of the environment at Tuktoyaktuk using part of the data reported here. For the purpose of this record the observational program has been divided into that carried out by personnel of the National Research Council in winter from ice cover (Figures 2,3,4,5) and that carried out during the summer of 1963 in the motor vessel "Richardson" of the Canadian Hydrographic Service (Figure 6).

The presentation of data in this report is subject to modification and possible correction at a later date. The usual errors including blunders are known to exist in the observed material but, in general, no attempt has been made to interpret or adjust values. It is noted that the depth of observation of the NRC material was feet and inches; in this record this is shown to the nearest foot. The depth of observation of the "Richardson" material is metres. The original records are on file at the Hydraulics Laboratory, Division of Mechanical Engineering, National Research Council, Ottawa and the Marine Sciences Branch, Ottawa.

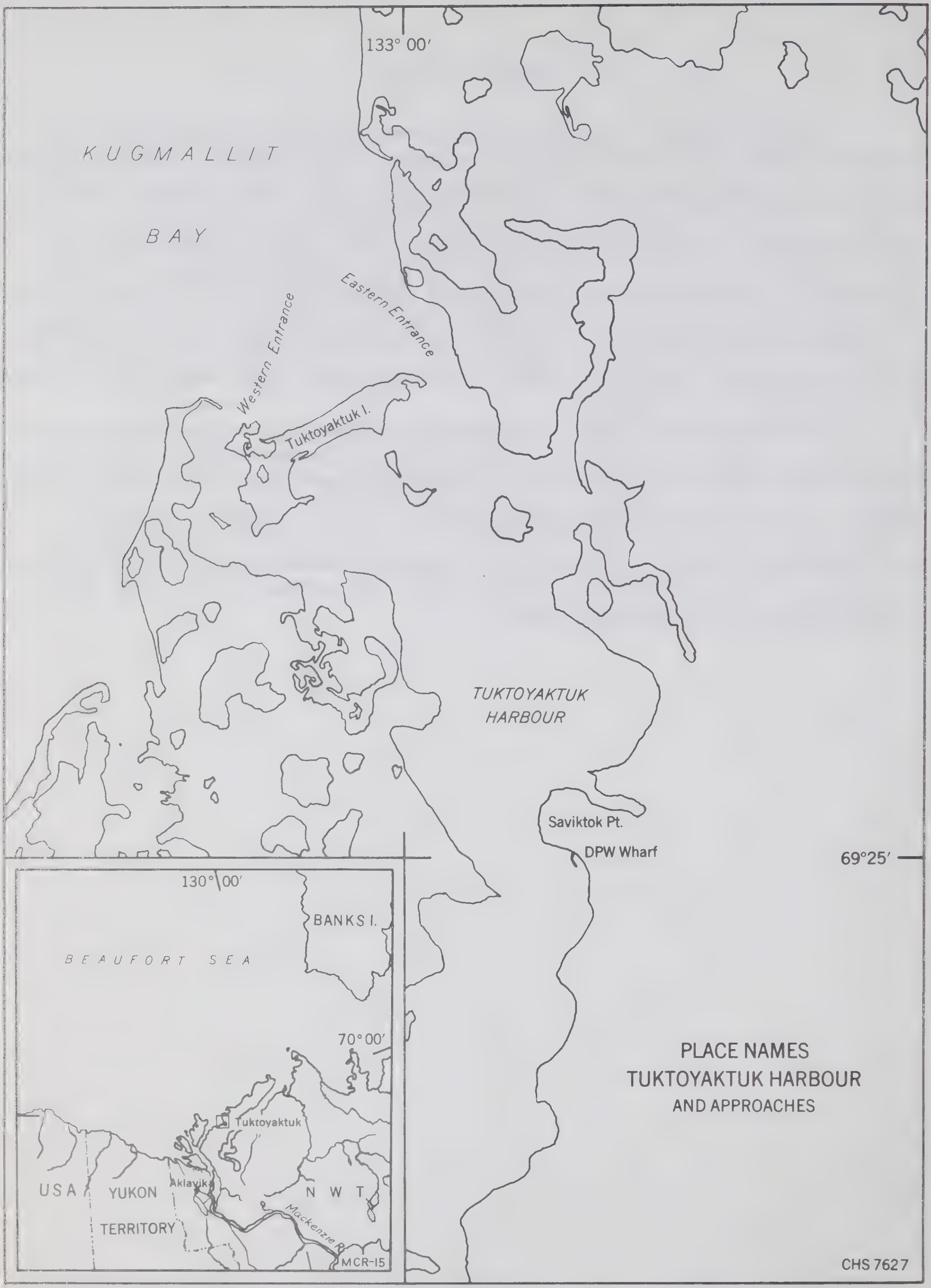

Figure 1. The location of Tuktoyaktuk Harbour with place names, indicating the location of the Department of Public Works wharf.

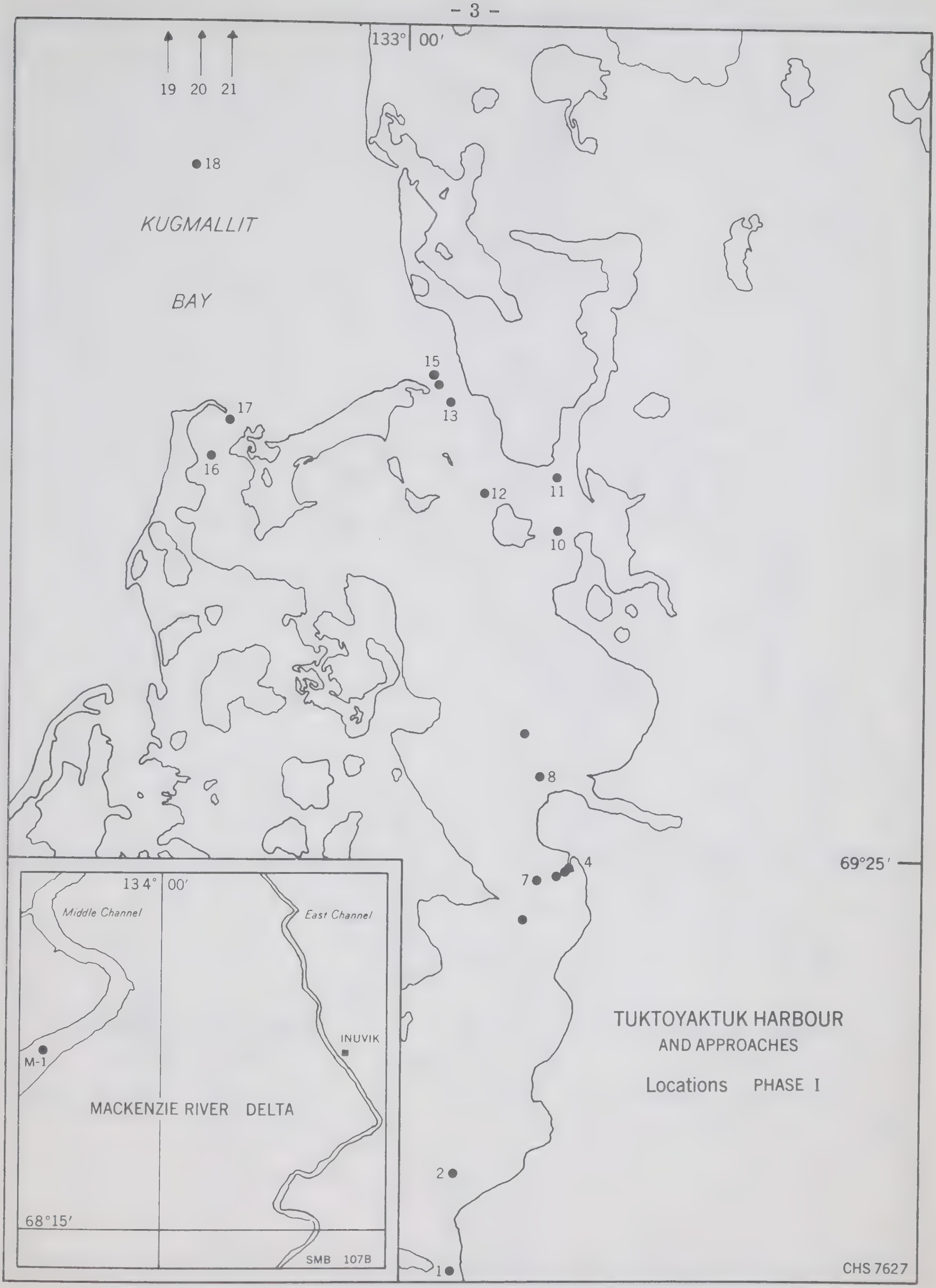

Figure 2. The location numbers of the observations of Phase I.

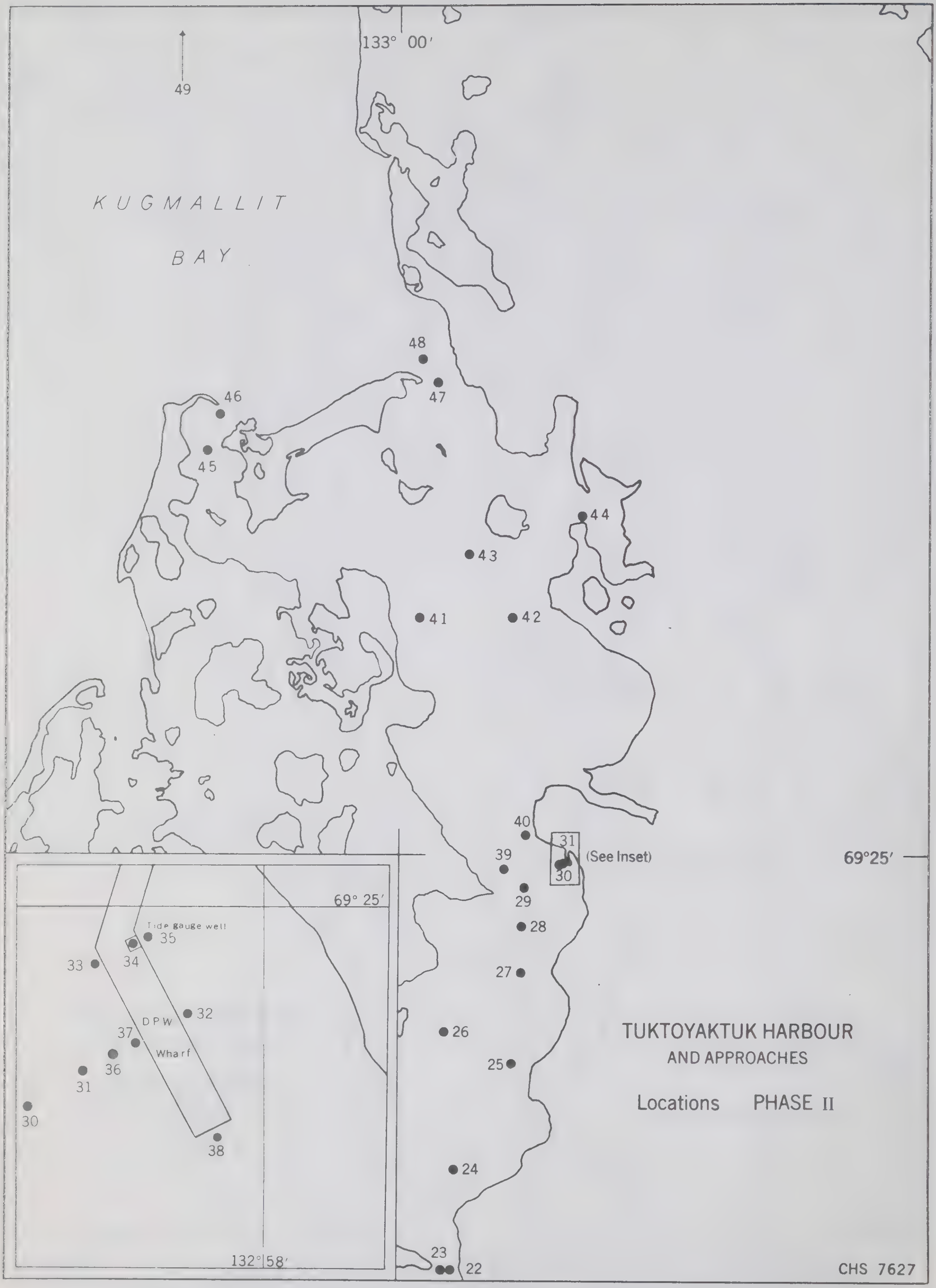

Figure 3. The location numbers of the observations of Phase II.

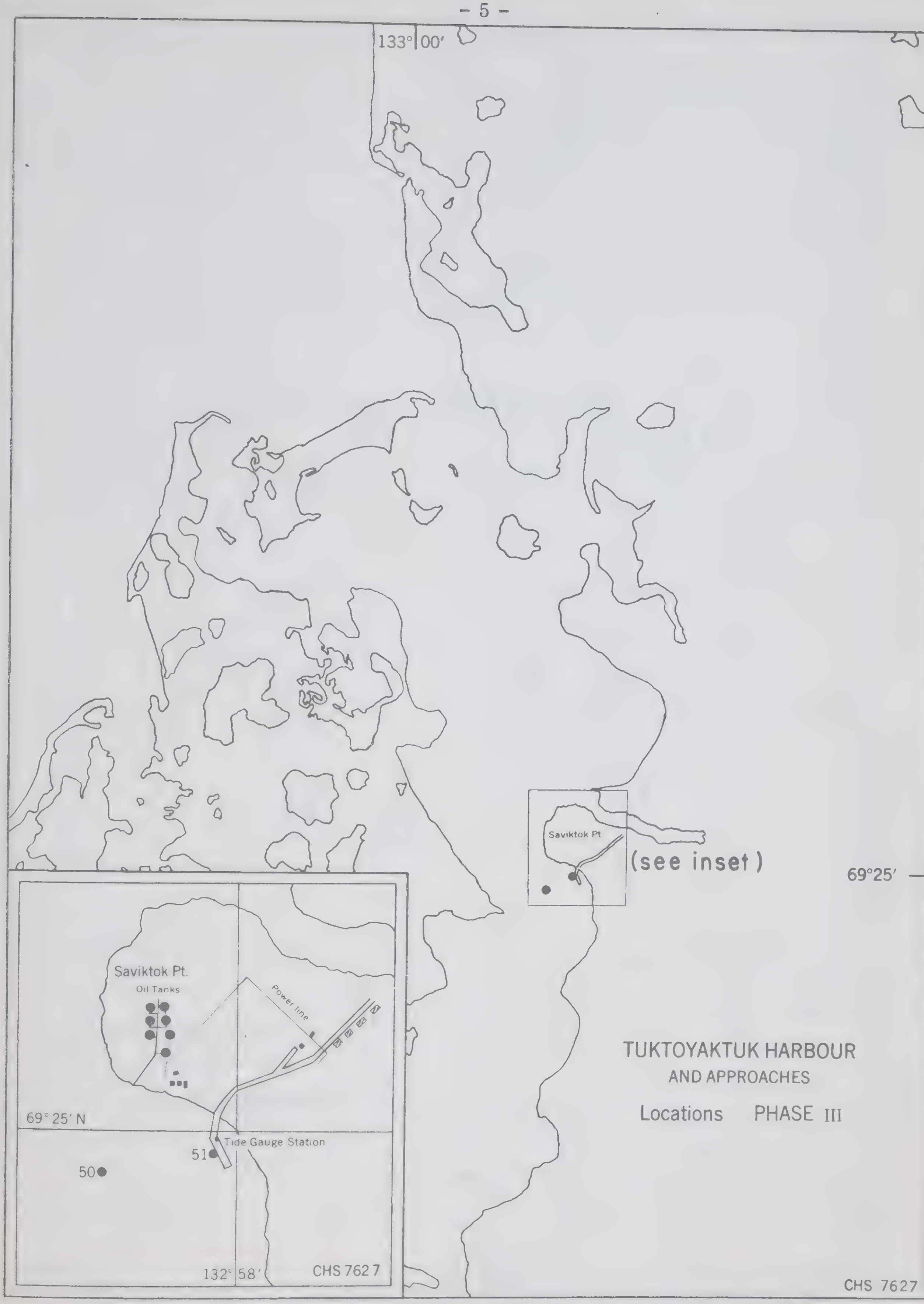

Figure 4. The location numbers of the observations of Phase III.

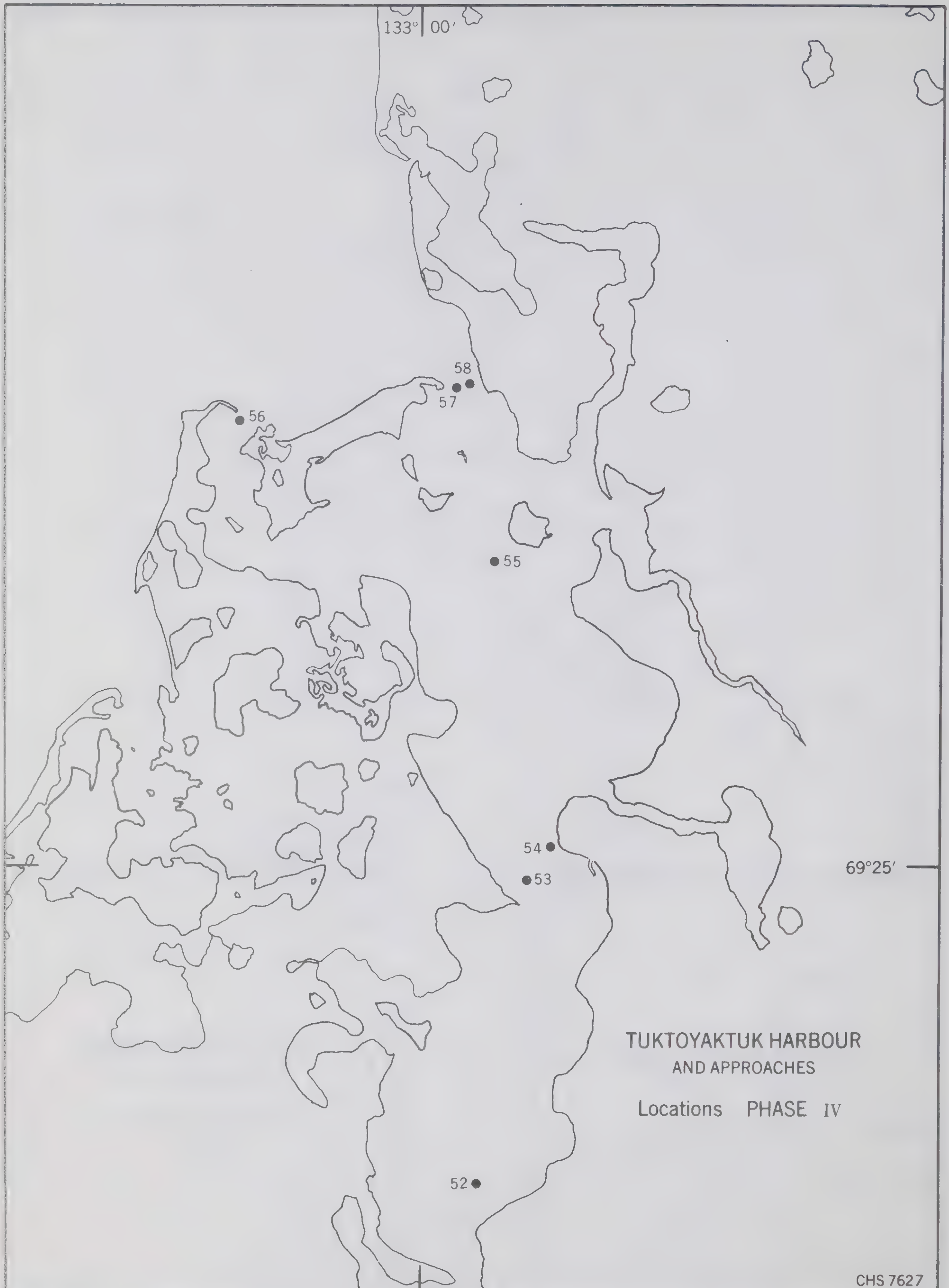

Figure 5. The location numbers of the observations of Phase IV.

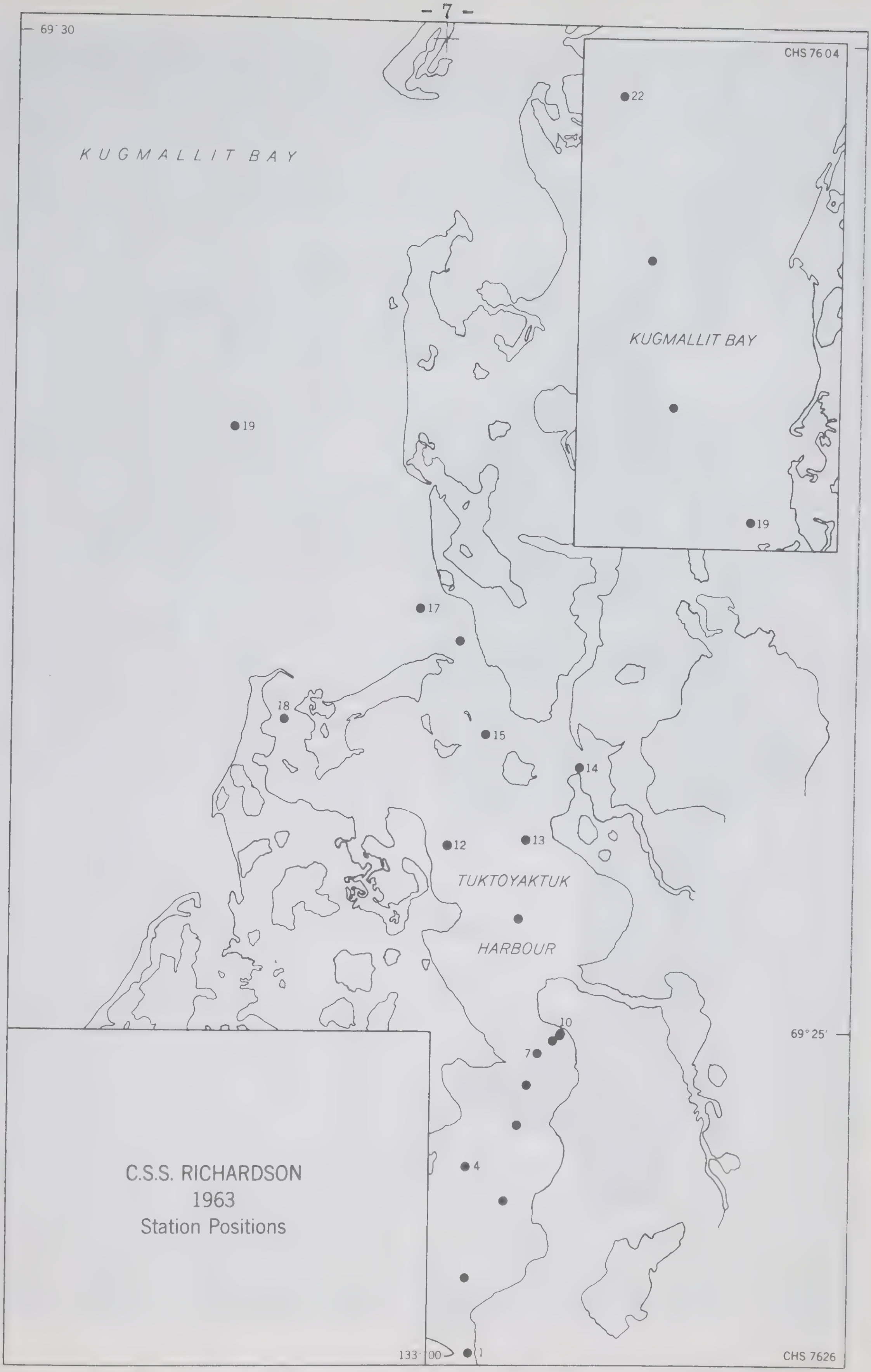

Figure 6. The approximate positions of stations occupied by "Richardson".

PROGRAMS

The NRC program

The program of NRC was subdivided into four phases as indicated in the following:

Phase I - April 26 to May 6, 1962 (Figure 2)
II - November 24 to December 10, 1962 (Figure 3)
III - December 14, 1962 to May 1, 1963 (Figure 4)
IV - April 19 to May 5, 1963 (Figure 5)

This subdivision is adhered to in the presentation of this record, and the extent of the data observed during each phase is shown in List 1. The listing also relates the consecutive number of the data headings of each phase to the location number in the figure for that phase. The consecutive numbers derive from machine processing carried out by the Canadian Oceanographic Data Centre, which agency provided the data in the form of machine print-outs. In the preparation of this record the print-out material was cropped and affixed to photocopy masters.

All of these observations were carried out from the ice cover, generally in a Bombardier Snowmobile chartered from a local resident, Mr. E. Gruben, who was employed as a guide and who carried out the observations of Phase III. The vehicle proved quite satisfactory both for transportation and for shelter while sampling.

Other observations made but not reported here include meteorological data, ice and snow thickness measurements and current observations; the latter have been utilized (Ince, 1962).

List 1: A tabulation of the NRC observations relating the consec number of the serial data to the location and to the consec slide number and showing the extent of the serial data.

PHASE I

Consec. No.	Location	Temp.	Sal.	Consec. No.	Location	Temp.	Sal.
1	12	X		46	17	X	
2	6	X		47	15	X	
3	7	X		48	17	X	
4	8	X		49	15	X	
5	9	X		50	17	X	
6	6	X	X	51	16	X	
7	6	X		52	15	X	
8	5	X		53	17	X	
9	6	X		54	16	X	
10	5	X	X	55	4	X	
11	5	X		56	7	X	
12	2		X	57	1	X	
13	6	X		58	2	X	
14	3		X	59	7	X	X
15	3	X		60	1	X	X
16	4	X		61	12	X	
17	16	X		62	12	X	
18	16	X	X	63	1	X	X
19	15	X	X	64	1	X	
20	12	X		65	4	X	
21	11	X		66	15	X	
22	11	X	X	67	15	X	X
23	10	X	X	68	19	X	
24	9	X	X	69	15	X	X
25	8	X	X	70	4	X	
26	6	X	X	71	15	X	
27	5	X	X	72	15	X	
28	4	X	X	73	19	X	X
29	7	X		74	19	X	
30	15	X		75	15	X	
31	15	X		76	15	X	
32	15	X		77	15	X	
33	16	X		78	4	X	
34	15	X		79	15	X	
35	16	X		80	3	X	
36	17	X		81	20	X	X
37	15	X		82	21	X	X
38	17	X		83	15	X	
39	16	X		84	15	X	
40	16	X		85	18	X	
41	17	X		86	13	X	
42	15	X		87	13	X	
43	16	X		88	13	X	
44	15	X		89	14	X	
45	16	X		90	15	X	

Consec. No.	Location	Temp.	Sal.	Consec. No.	Location	Temp.	Sal.
91	4	X	X	100	15	X	
92	2	X		101	15	X	
93	7	X		102	15	X	
94	9	X		103	15	X	
95	15	X		104	15	X	
96	4	X		105	15	X	
97	7	X		106	15	X	
98	2	X		107	4	X	
99	15	X		108	4	X	
				109	M-1	X	X

PHASE II

1	23	X	X	36	22	X	X
2	24	X	X	37	23	X	X
3	45	X	X	38	33	X	X
4	33	X	X	39	27	X	X
5	28	X	X	40	28	X	X
6	29	X	X	41	29	X	X
7	30	X	X	42	30	X	X
8	44	X	X	43	23	X	X
9	42	X	X	44	27	X	X
10	27	X	X	45	28	X	X
11	28	X	X	46	29	X	X
12	34		X	47	40	X	X
13	48	X	X	48	43	X	X
14	48	X	X	49	43	X	X
15	48	X	X	50	40	X	X
16	48	X	X	51	46	X	X
17	48	X	X	52	43	X	X
18	48	X	X	53	40	X	X
19	48	X	X	54	40	X	X
20	48	X	X	55	43	X	X
21	30	X	X	56	46	X	X
22	23	X	X	57	40	X	X
23	25	X	X	58	43	X	X
24	26	X	X	59	46	X	X
25	38	X	X	60	25	X	X
26	23	X	X	61	26	X	X
27	30	X	X	62	42	X	X
28	27	X	X	63	41	X	X
29	44	X	X	64	47	X	X
30	28	X	X	65	39	X	X
31	28		X	66	42	X	X
32	44		X	67	41	X	X
33	42		X	68	25	X	X
34	27		X	69	26	X	X
35	24		X	70	32		X

Consec. No.	Location	Temp.	Sal.	BT Slide	Consec. No.	Location	Temp.	Sal.	BT Slide
71	37		X	1	76	33	X	X	
72	37	X	X		77	28	X	X	
73	36	X	X		78	24	X	X	
74	31	X	X		79	28	X	X	
75	29		X	2	80	42	X	X	
					81	49	X	X	

PHASE III

1	51		X	3	15	50		X	17
2	50		X	4	16	51		X	18
3	51		X	5	17	50		X	19
4	50		X	6	18	51		X	20
5	50		X	7	19	51		X	21
6	51		X	8	20	50		X	22
7	50		X	9	21	50		X	23
8	51		X	10	22	51		X	24
9	50		X	11	23	50		X	25
10	51		X	12	24	51		X	26
11	50		X	13	25	50		X	27
12	51		X	14	26	50		X	28
13	50		X	15	27	51		X	29
14	51		X	16	28	50		X	
					29	51		X	30

PHASE IV

1	52	X	X		1	54	X	X	
2	52	X	X		2	54	X	X	
3	52	X	X		3	54	X	X	
4	52	X	X		4	54	X	X	
5	52	X	X		5	54	X	X	
6	52	X	X		6	54	X	X	
7	52	X	X		7	54	X	X	
8	52	X	X		8	54	X	X	
9	52	X	X		9	54	X	X	
1	53	X	X		1	55	X	X	
2	53	X	X		2	55	X	X	
3	53	X	X		3	55	X	X	
4	53	X	X		4	55	X	X	
5	53	X	X		5	55	X	X	
6	53	X	X		6	55	X	X	
7	53	X	X		7	55	X	X	
8	53	X	X		8	55	X	X	
9	53	X	X		9	55	X	X	

Consec. No.	Location	Temp.	Sal.
1	56	X	X
2	56	X	X
3	56	X	X
4	56	X	X
5	56	X	X
6	56	X	X
7	56	X	X
8	56	X	X
9	56	X	X
1	57	X	X
2	57	X	X
3	57	X	X
4	57	X	X

Consec. No.	Location	Temp.	Sal.
5	57	X	X
6	57	X	X
7	57	X	X
8	57	X	X
9	57	X	X
1	58	X	X
2	58	X	X
3	58	X	X
4	58	X	X
5	58	X	X
6	58	X	X
7	58	X	X
8	58	X	X
9	58	X	X

Procedures. During Phases I, II and IV each day's work was begun by recording tidal heights from the gauge at the wharf, and synchronizing watches with the clock on the gauge. At each location occupied, thermistor readings were taken first. Because of the shortage of storage bottles, salinity samples were taken only at selected locations. Measurements of currents were concentrated mainly in the harbour entrances. All depths were measured from the water surface, and for this purpose the suspension cables used on all the instruments were marked off at intervals of one foot.

During Phase IV simultaneous observations at two locations by two teams of observers were attempted; each team using a different type of "in situ" salinometer. The relation between the team, the locations occupied (Figure 5), the time interval and the type of meter used is shown below.

Team	Location	Interval GMT	Meter
1	55	16.8/2 - 04.8/3	RS-5
2	52	same	Wayne Kerr
1	54	16.1/2 - 04.03	RS-5
2	53	same	Wayne Kerr
1	57	15.5/4 - 03.5/5	RS-5
2	58	same	Wayne Kerr
1	56	16.0/4 - 04.0/5	RS-5

It was proposed that the observations of Phase III would comprise serial sampling for salinity and a BT lowering at two locations, close to the site of the bubbler every two weeks during the winter.

Temperature. Thermistor type thermometers designed and built by NRC were used in all the work except Phase III. At the end of each day's sampling, a zero point check was made on each thermistor. Reversing thermometers were used to make random, but unrecorded spot checks. A hand-lowered shallow range bathythermograph was utilized during Phases II and III.

Salinity. Determinations for salinity were carried out both by bottle sampling and by portable salinometer. The Phase I and III samples were obtained with Knudsen reversing bottles. Phase II salinities were determined "in situ" with a Wayne Kerr portable salinometer. At some of these locations reversing bottle samples were also taken; these appear in the text of the data to the right of the salinity column, followed by the abbreviation "KB" (Knudsen bottle). All the samples collected by reversing bottle were sent to the Bedford Institute of Oceanography for analysis where they were measured on an Auto-Lab Inductive Salinometer.

Phase IV salinities were again done "on location" using the Wayne Kerr meter of Phase II and an RS-5 instrument provided by the Marine Sciences Branch.

Listed below are extracts from the instruction manuals pertinent to each instrument, i.e., the manufacturer's statements of accuracy.

Wayne Kerr Portable Chlorinity Temperature Bridge #B441
Wayne Kerr Laboratories Ltd., Chessington, Surrey.

Chlorinity: 16-20 p.p.t. range 5° - 25°C,
accuracy: ± 0.05 p.p.t.
0-16 p.p.t. range 5° - 25°C,
accuracy: ± 0.1 p.p.t.
RS-5 Portable Salinometer
Industrial Instruments Inc., 89 Commerce Rd.,
Cedar Grove, N.J.

Salinity (direct reading) - 0-40°/°° ± 0.3°/°° (0-27°C)

Both instruments are battery operated and are fitted with approximately 300 feet of cable which is graduated for depth.

A presentation of a portion of the salinity values obtained using reversing bottles and using the "in situ" metres is shown in Figure 7.

Personnel. Personnel in the field comprised:

Phase I - S. Ince, J. Harron, G. Priest
II - S. Ince, R. Richardson, G. Priest
III - E. Gruben
IV - J. Harron, H. Caves, G. Priest

who, with the exception of Mr. E. Gruben, were members of the staff of the National Research Council, Ottawa.

Extract of Log

Phase I

April 26 - Party arrive Tuktoyaktuk
27 - Occupy locations 6, 7 and 12
28 - Occupy locations 2, 3, 5, 6, 8 and 9
29 - Occupy locations 4, 5, 6, 8, 9, 10, 11, 12, 15 and 16
30 - Occupy locations 7, 15, 16 and 17
May 1 - Occupy locations 1, 2, 4, 7, 12, 15, 16, 17
2 - Occupy locations 1, 4, 12, 15 and 16
3 - Occupy locations 2, 4, 13, 14, 15, 20 and 21
4 - Occupy locations 2, 4, 7, 9, 13, 14 and 15
5 - Occupy locations 4 and 15
6 - During the return flight to Inuvik, a landing was made on the Middle Channel of the Mackenzie River to occupy location M-1.

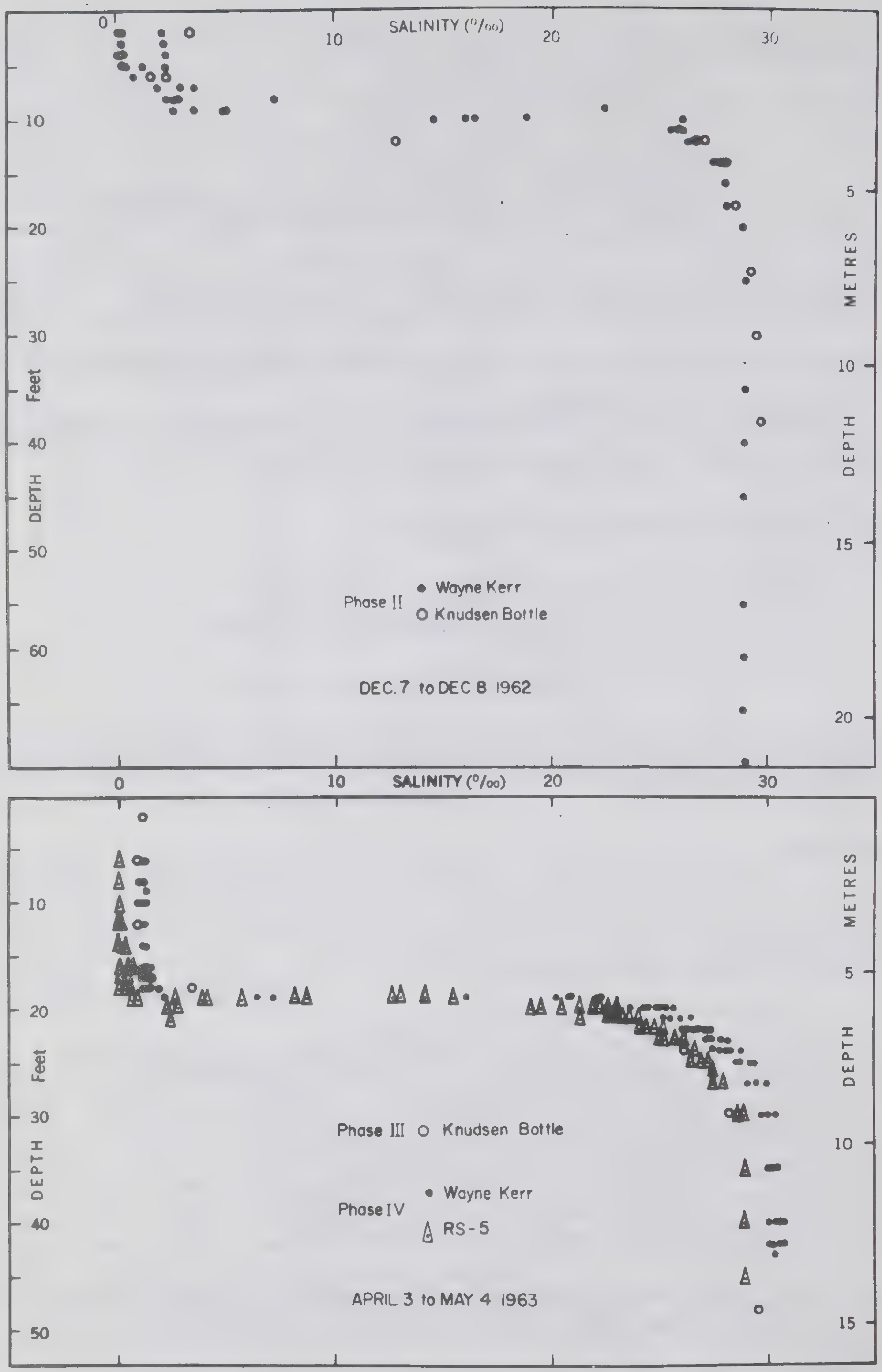

Figure 7. Distributions with depth (feet) of salinity(°/°°) near the Department of Public Works wharf. (a) From Phase II serial samples (consec numbers 71 and 75) and the Wayne Kerr instrument (consec numbers 70, 72, 73, 74 and 77). (b) From Phase III serial samples (consec numbers 28 and 29) and Phase IV RS-5 values (locations 54 and 55) and Wayne Kerr values (location 53).

Phase II

November	24	- Party arrive Tuktoyaktuk
	26	- Occupy locations 23, 24 and 45
	27	- Occupy locations 28, 29 and 33
	28	- Occupy locations 27, 28, 30, 42 and 44
	29	- Occupy locations 34 and 48
	30	- Occupy locations 23, 24, 25, 26, 27, 30, 48
December	1	- Occupy locations 28 and 44. Instruct E. Gruben in sampling procedures for winter program
	2	- Occupy locations 24, 27, 42 and 44
	3	- Occupy locations 22, 23, 27, 28, 29, 30 and 33
	4	- Occupy locations 23, 27, 28, 29, 40, 43 and 46
	5	- Occupy locations 25, 26, 39, 40, 41, 42, 43 and 46
	7	- Occupy locations 31, 32, 36 and 37. Check E. Gruben on procedure through one complete test run
	8	- Occupy locations 24, 28, 33 and 44
	9	- Occupy locations 49 in Kugmallit Bay
	10	- Party depart Tuktoyaktuk

Phase IV

April	19	- Party arrive Tuktoyaktuk
	20 -30	- Pilot experiment with NRC-designed bubbler
May	2	- Party divided into two groups, one occupy locations 52 and 55, other occupy locations 53 and 54
	3	- Occupy locations 52 and 55, 53 and 54
	4	- Occupy locations 56, 57 and 58
	5	- Occupy locations 56, 57 and 58
	7	- Depart Tuktoyaktuk

"Richardson" Program

Procedures. From July 26 until September 16, 1963, "Richardson" occupied 47 oceanographic stations (List 2) in Tuktoyaktuk Harbour and Kugmallit Bay. Samples for salinity were obtained by standard procedures and BT lowerings were carried out with the instrument used the previous winter during Phase III of the NRC program. Salinity samples were sent to the Bedford Institute of Oceanography for analysis. A meter block was used for the hydrographic casts; all depths are in metres.

Personnel. The personnel aboard "Richardson" for the survey were Messrs. T.D.W. McCulloch (Hydrographer-in-Charge) and R.W. Card.

List 2: A tabulation of the "Richardson" observations relating the consec number of the serial data to the station and to the consec slide number.

Consec. No.	Station	Consec. Slide No.	Consec No.	Station	Consec. Slide No.
1	1	1	24	6	24
2	2	2	25	6	25
3	3	3	26	22	26
4	4	4	27	21	27
5	5	5	28	20	28
6	6	6	29	19	29
7	7	7	30	17	30
8	8	8	31	16	31
9	18	9	32	18	32
10	15	10	33	15	33
11	14	11	34	14	34
12	13	12	35	13	35
13	12	13	36	12	36
14	11	14	37	11	37
15	9	15	38	7	38
16	10	16	39	8	39
17	16	17	40	6	40
18	17	18	41	5	41
19	19	19	42	4	42
20	20	20	43	3	43
21	21	21	44	2	44
22	22	22	45	1	45
23	6	23	46	9	46
			47	10	47

Extract of Log

July	26	- Occupy stations 1 to 4
	27	- Occupy stations 5, 6, 7, 8, 11, 12, 13, 14, 15 and 18
	28	- Occupy stations 9 and 10
	29	- Occupy stations 16, 17, 19, 20, 21 and 22
August	15	- Occupy station 6
	21	- Occupy station 6
September	6	- Occupy station 6
	13	- Occupy stations 19, 20, 21 and 22
	14	- Occupy stations 15, 16, 17 and 18
	15	- Occupy stations 1, 2, 3, 4, 5, 6, 7, 8, 11, 12, 13 and 14
	16	- Occupy stations 9 and 10

ACKNOWLEDGMENTS

The machine processing and the required data output were provided by the Canadian Oceanographic Data Centre. Mr. F.G. Barber critically reviewed the material.

REFERENCES

Dick, T.M. 1961. Description of air bubbling systems at Cambridge Bay and Tuktoyaktuk, N.W.T. Proceedings of the Symposium on Air Bubbling. Nat. Res. Council, Canada. Tech. Mem. No. 70.

Ince, S. 1962. Winter regime of a tidal inlet in the Arctic and the use of air bubblers for the protection of wharf structures. Eighth International Conference on Coastal Engineering, Mexico : 521-532.

Sauer, C.D. 1964. Bathythermograph data on aperture cards: a new approach to an old problem. J. Fish. Res. Bd. Canada, 21 (3) : 647-650.

DATA

NRC Serial Data

Explanation of data headings

Cons	The consecutive number of the stations occupied, in chronological order except for Phase IV. In Phase IV the consec number indicates the number and chronological order of sampling at the location.
Loc	Numbers assigned during the preparation of the record to provide an indication of the approximate location of the observation through reference to the appropriate figure.
Lat	The latitude
Long	The longitude
GMT	The Greenwich Mean Time of the observation.
Depth	The water depth in feet.
Depth	The depth in feet of the observation.
Temp	The observed temperature (°C) to two decimal places.
Sal	The salinity (°/°°) to two decimal places.

N R C Programme

Phase I

Serial data

Consecutive numbers 1 to 109

C R N 447

Cons	001 Loc 12
Lat	69° 26 28 N
Long	132° 59 06 W
GMT	19.0 27 iv
Depth	39 ft

DEPTH	TEMP
0005	-0003
0010	-0002
0015	0000
0018	0002
0019	0011
0020	0017
0025	0022
0026	0020
0027	0012
0028	0009
0029	0005

Cons	002 Loc 06
Lat	69° 24 57 N
Long	132° 58 13 W
GMT	21.0 27 iv
Depth	54 ft

DEPTH	TEMP
0010	-0006
0015	-0006
0018	-0002
0020	0012
0021	0018
0022	0024
0025	0025
0030	0010
0035	-0017
0040	-0021
0045	-0040
0050	-0042
0054	-0042

Cons	003 Loc 07
Lat	69° 24 56 N
Long	132° 58 26 W
GMT	22.5 27 iv
Depth	73 ft

DEPTH	TEMP
0007	-0003
0010	-0003
0015	-0002
0018	0002
0019	0006
0020	0011
0022	0023
0025	0025
0026	0025
0027	0017
0030	0006
0032	-0006
0035	-0012
0040	-0024
0045	-0041
0050	-0042
0055	-0044
0060	-0044
0065	-0044
0068	-0042

Cons	004 Loc 08
Lat	69° 25 21 N
Long	132° 58 23 W
GMT	00.0 28 iv
Depth	19 ft

DEPTH	TEMP
0006	-0006
0010	-0006
0015	-0004
0017	-0004
0018	0005
0019	0006

Cons	005 Loc 09
Lat	69° 25 29 N
Long	132° 58 38 W
GMT	01.0 28 iv
Depth	42 ft

DEPTH	TEMP
0005	-0009
0010	-0008
0015	-0009
0017	-0009
0019	-0002
0020	0000
0022	0011
0025	0014
0027	0009
0028	0005
0030	0008
0035	-0020
0040	-0023
0042	-0026

Cons 006 Loc 06
Lat 69° 24 57 N
Long 132° 58 13 W
GMT 15.0 28 iv
Depth 60 ft

DEPTH	TEMP	SAL
0008	-0003	
0010	-0003	
0014	-0003	
0015	-0003	
0016	-0003	
0017	-0002	
0018	-0002	
0019	0003	
0020	0008	2184
0021	0016	
0022	0019	
0023	0019	
0024	0022	
0025	0022	2664
0026	0019	
0027	0016	
0028	0009	
0029	0002	
0030	-0002	3022
0031	-0006	
0032	-0009	
0033	-0010	
0034	-0015	
0035	-0020	3075
0036	-0020	
0038	-0023	
0040	-0031	2999
0042	-0040	
0044	-0046	
0046	-0047	3045
0048	-0047	
0050	-0047	3065
0052	-0047	
0054	-0044	
0056	-0044	
0058	-0043	
0060	-0043	

Cons 007 Loc 06
Lat 69° 24 57 N
Long 132° 58 13 W
GMT 17.0 28 iv
Depth 60 ft

DEPTH	TEMP
0008	-0010
0010	-0018
0012	-0012
0015	-0012
0017	-0010
0019	0006
0020	0003
0021	0008
0022	0011
0023	0017
0024	0019
0025	0019
0026	0019
0027	0014
0028	0011
0029	0006
0030	0002
0031	-0004
0032	-0009
0033	-0012
0035	-0018
0038	-0024
0040	-0031
0044	-0046
0048	-0047
0050	-0049

Cons 008 Loc 05
Lat 69° 24 57 N
Long 132° 58 06 W
GMT 17.3 28 iv
Depth 50 ft

DEPTH	TEMP
0008	-0009
0010	-0008
0015	-0008
0017	-0006
0019	-0002
0020	0003
0021	0009
0022	0016
0023	0019
0024	0019
0025	0020
0026	0017
0027	0016
0028	0012
0029	0008
0030	0002
0031	-0002
0032	-0006
0033	-0010
0034	-0014
0035	-0017
0036	-0020
0038	-0024
0040	-0029
0042	-0038
0044	-0044

Cons 009 Loc 06
Lat 69° 24 57 N
Long 132° 58 13 W
GMT 18. 3 28 iv
Depth 60 ft

DEPTH	TEMP
0008	-0012
0010	-0008
0015	-0008
0019	-0008
0020	0003
0021	0009
0022	0016
0023	0016
0024	0019
0025	0020
0026	0019
0027	0016
0028	0012
0029	0006
0030	0003
0031	-0003
0032	-0006
0033	-0010
0035	-0017
0038	-0023
0040	-0029
0042	-0040
0044	-0045
0046	-0047
0048	-0055
0050	-0047
0054	-0049

Cons 010 Loc 05
Lat 69° 24 57 N
Long 132° 58 06 W
GMT 18. 8 28 iv
Depth 50 ft

DEPTH	TEMP	SAL
0008	-0009	0040
0010	-0008	
0015	-0008	0088
0017	-0002	
0019	-0006	
0020	-0003	
0021	0011	
0022	0017	
0023	0019	
0024	0019	
0025	0019	
0026	0019	
0027	0014	
0028	0011	
0029	0006	
0030	0002	
0031	-0002	
0032	-0006	
0033	-0010	
0034	-0014	
0035	-0017	
0036	-0020	
0038	-0023	
0040	-0031	
0042	-0040	
0044	-0044	

Cons 012 Loc 02
Lat 69° 23 47 N
Long 132° 59 21 W
GMT 22. 5 28 iv
Depth 33 ft

DEPTH	TEMP	SAL
0010		0079
0015		0098
0020		2160
0025		2803
0030		3039

Cons 011 Loc 05
Lat 69° 24 27 N
Long 132° 58 06 W
GMT 22. 2 28 iv
Depth 50 ft

DEPTH	TEMP
0008	-0009
0010	-0006
0015	-0006
0019	-0006
0020	-0004
0021	-0003
0022	0016
0023	0019
0024	0022
0025	0019
0026	0019
0027	0019
0028	0016
0029	0009
0030	0005
0031	-0004
0032	-0009
0033	-0012
0035	-0017
0038	-0018
0040	-0024
0042	-0029
0044	-0043
0050	-0043

Cons 013 Loc 06
Lat 69° 24 57 N
Long 132° 58 13 W
GMT 23.0 28 iv
Depth 60 ft

DEPTH	TEMP
0008	-0010
0010	-0010
0015	-0009
0019	0000
0020	0006
0021	0012
0022	0017
0023	0019
0024	0019
0025	0019
0026	0016
0027	0012
0028	0008
0029	0003
0030	0000
0031	-0008
0032	-0010
0033	-0015
0035	-0018
0040	-0028
0042	-0035
0044	-0044
0050	-0049

Cons 014 Loc 03
Lat 69° 24 44 N
Long 132° 58 37 W
GMT 23.2 28 iv
Depth 84 ft

DEPTH	SAL
0010	0048
0015	0092
0020	2213
0025	2710
0030	3051
0035	3080
0040	3106
0050	3125
0060	3130

Cons 015 Loc 03
Lat 69° 24 44 N
Long 132° 58 37 W
GMT 23.5 28 iv
Depth 84 ft

DEPTH	TEMP
0010	-0011
0015	-0008
0017	-0006
0019	0000
0020	0006
0021	0009
0022	0014
0023	0017
0024	0019
0025	0018
0026	0012
0027	0014
0028	0008
0030	-0004
0032	-0009
0034	-0018
0036	-0025
0038	-0026
0040	-0034
0044	-0050
0048	-0050
0050	-0054
0060	-0052
0070	-0050

Cons 016 Loc 04
Lat 69° 24 58 N
Long 132° 58 04 W
GMT 01.0 29 iv
Depth 17 ft

DEPTH	TEMP
0001	0011
0005	0009
0010	0011
0015	0009
0017	0009

Cons 017 Loc 16
Lat 69° 26 37 N
Long 133° 02 12 W
GMT 15.2 29 iv
Depth 56 ft

DEPTH	TEMP
0008	0000
0010	0002
0012	0002
0015	0003
0017	0003
0018	0002
0019	0014
0020	0025
0022	0037
0024	0044
0026	0048
0028	0053
0030	0056
0032	0056
0033	0056

Cons 018 Loc 16
Lat 69° 26 37 N
Long 133° 02 12 W
GMT 15.5 29 iv
Depth 56 ft

DEPTH	TEMP	SAL
0008	-0002	
0010	-0001	0025
0015	0001	0116
0018	0008	
0019	0014	
0020	0024	2802
0022	0035	2864
0028	0049	3087
0037	0055	

Cons 019 Loc 15
Lat 69° 26 57 N
Long 132° 59 42 W
GMT 16. 3 29 iv
Depth 30 ft

DEPTH	TEMP	SAL
0008	0000	
0010	0003	0014
0012	0000	
0015	0000	
0018	0000	0058
0019	0009	
0020	0016	2111
0022	0020	2182
0024	0019	
0026	0025	2277
0028	0025	
0029	0025	

Cons 021 Loc 11
Lat 69° 26 32 N
Long 132° 58 14 W
GMT 17. 6 29 iv
Depth 30 ft

DEPTH	TEMP
0008	0000
0010	0000
0015	0000
0017	0002
0018	0011
0019	0023
0020	0042
0021	0053
0022	0066
0023	0072
0024	0075
0025	0079

Cons 023 Loc 10
Lat 69° 26 20 N
Long 132° 58 16 W
GMT 18. 5 29 iv
Depth 16 ft

DEPTH	TEMP	SAL
0008	-0002	
0010	-0002	
0012		0071
0015	0000	
0016	0000	

Cons 020 Loc 12
Lat 69° 26 28 N
Long 132° 59 06 W
GMT 17. 3 29 iv
Depth 39 ft

DEPTH	TEMP
0008	-0002
0010	0000
0015	-0002
0018	-0002
0019	0002
0020	0009
0022	0019
0024	0023
0025	0022
0026	0019
0028	0009
0030	-0004
0035	-0010
0039	-0012

Cons 022 Loc 11
Lat 69° 26 32 N
Long 132° 58 14 W
GMT 17. 8 29 iv
Depth 30 ft

DEPTH	TEMP	SAL
0008	-0002	
0010	-0004	
0015	-0002	0095
0017	-0002	
0018	0007	1374
0019	0020	
0020	0033	
0021	0049	
0022	0062	3024
0023	0068	
0024	0071	
0025	0074	

Cons 024 Loc 09
Lat 69° 25 29 N
Long 132° 58 38 W
GMT 18. 8 29 iv
Depth 42 ft

DEPTH	TEMP	SAL
0008	-0002	
0010	0000	
0015	-0002	
0017	0000	0070
0018	0000	
0019	0005	
0020	0009	
0021	0017	2177
0022	0020	
0024	0023	
0026	0020	
0028	0011	
0030	0002	
0032	-0006	2931
0035	-0014	
0040	-0017	
0042	-0017	

Cons 025 Loc 08
Lat 69° 25 21 N
Long 132° 58 23 W
GMT 19.2 29 iv
Depth 19 ft

DEPTH	TEMP	SAL
0008	-0002	
0010	-0002	0082
0015	-0002	0083
0017	-0002	
0018	0003	
0019	0008	

Cons 026 Loc 06
Lat 69° 24 57 N
Long 132° 58 13 W
GMT 22.2 29 iv
Depth 60 ft

DEPTH	TEMP	SAL
0008	-0002	
0010	-0002	0071
0017	0002	0078
0019	0006	
0020	0012	
0021		2101
0022	0023	
0024	0026	
0026	0023	2752
0028	0016	
0030	0006	
0031	0002	2939
0032	-0004	
0035	-0014	
0036		2991
0038	-0017	
0040	-0022	
0041		3019
0045	-0040	
0050	-0041	

Cons 027 Loc 05
Lat 69° 24 57 N
Long 132° 58 06 W
GMT 23.0 29 iv
Depth 50 ft

DEPTH	TEMP	SAL
0010	-0002	
0015	-0002	
0017		0098
0018	0006	
0019	0009	
0020	0016	
0021	0022	2215
0022.	0025	
0024	0026	
0026	0022	2738
0028	0016	
0030	0003	
0032	-0006	
0035	-0014	
0040	-0020	

Cons 028 Loc 04
Lat 69° 24 58 N
Long 132° 58 04 W
GMT 23.5 29 iv
Depth 17 ft

DEPTH	TEMP	SAL
0000	0000	
0001	-0002	
0002	-0002	
0005	-0002	0124
0010	0000	
0015	0002	0091
0016	0002	
0017	0005	

Cons 029 Loc 07
Lat 69° 24 56 N
Long 132° 58 26 W
GMT 00.0 30 iv
Depth 73 ft

DEPTH	TEMP
0010	-0004
0015	-0005
0018	0001
0019	0005
0020	0012
0022	0020
0024	0020
0026	0016
0028	0008
0030	0000
0032	-0009
0035	-0016
0038	-0021
0040	-0024
0042	-0036
0045	-0042
0050	-0044
0060	-0045
0068	-0046

Cons 030 Loc 15
Lat 69° 26 57 N
Long 132° 59 42 W
GMT 15.5 30 iv
Depth 30 ft

DEPTH	TEMP
0002	-0004
0004	-0003
0006	-0002
0008	-0002
0010	0000
0015	0000
0017	0000
0018	0010
0019	0016
0020	0022
0022	0025
0024	0026
0026	0028
0028	0030
0029	0030

Cons 031 Loc 15
Lat 69° 26 57 N
Long 132° 59 42 W
GMT 16. 2 30 iv
Depth 30 ft

DEPTH	TEMP
0006	0000
0008	0000
0010	0000
0015	0000
0017	0000
0018	0004
0019	0014
0020	0018
0025	0025

Cons 032 Loc 15
Lat 69° 26 57 N
Long 132° 59 42 W
GMT 16. 9 30 iv
Depth 30 ft

DEPTH	TEMP
0006	0000
0008	0000
0010	0000
0012	0000
0014	0000
0016	0000
0017	0000
0018	0002
0019	0014
0020	0019
0022	0022
0025	0023

Cons 033 Loc 16
Lat 69° 26 37 N
Long 133° 02 12 W
GMT 17. 3 30 iv
Depth 56 ft

DEPTH	TEMP
0006	-0002
0010	0000
0016	0002
0017	0002
0018	0003
0019	0016
0020	0022
0022	0034
0024	0040
0026	0045
0028	0048
0030	0053
0032	0055

Cons 034 Loc 15
Lat 69° 26 57 N
Long 132° 59 42 W
GMT 17. 9 30 iv
Depth 30 ft

DEPTH	TEMP
0006	-0002
0010	-0002
0016	0000
0018	0000
0019	0005
0020	0014
0022	0020
0024	0022
0026	0025
0028	0025

Cons 035 Loc 16
Lat 69° 26 37 N
Long 133° 02 12 W
GMT 18. 3 30 iv
Depth 56 ft

DEPTH	TEMP
0006	0000
0010	0000
0016	0002
0018	0003
0019	0012
0020	0022
0022	0033
0026	0045
0030	0053

Cons 036 Loc 17
Lat 69° 26 45 N
Long 133° 02 02 W
GMT 19. 2 30 iv
Depth 10 ft

DEPTH	TEMP
0006	0000
0008	0000
0010	0000

Cons 037 Loc 15
Lat 69° 26 57 N
Long 132° 59 42 W
GMT 19. 5 30 iv
Depth 30 ft

DEPTH	TEMP
0006	-0002
0010	-0002
0016	0000
0018	0000
0019	0004
0020	0012
0022	0016
0024	0022
0028	0025

Cons 038 Loc 17
Lat 69° 26 45N
Long 133° 02 02W
GMT 19.8 30 iv
Depth 10 ft

DEPTH	TEMP
0008	0000

Cons 039 Loc 16
Lat 69° 26 37N
Long 133° 02 12W
GMT 20.0 30 iv
Depth 56 ft

DEPTH	TEMP
0019	0011

Cons 040 Loc 16
Lat 69° 26 37N
Long 133° 02 12W
GMT 21.4 30 iv
Depth 56 ft

DEPTH	TEMP
0008	0000
0010	0000
0012	0000
0016	0002
0017	0003
0018	0007
0019	0012
0020	0022
0022	0033
0026	0047
0030	0055

Cons 041 Loc 17
Lat 69° 26 45N
Long 133° 02 02W
GMT 21.8 30 iv
Depth 10 ft

DEPTH	TEMP
0007	0000
0008	0002
0009	0003

Cons 042 Loc 15
Lat 69° 26 57N
Long 132° 59 42W
GMT 22.1 30 iv
Depth 30 ft

DEPTH	TEMP
0008	0000
0012	0000
0016	0000
0018	0000
0019	0003
0020	0015
0021	0017
0022	0019
0024	0020
0026	0023
0028	0028

Cons 043 Loc 16
Lat 69° 26 37N
Long 133° 02 12W
GMT 22.7 30 iv
Depth 56 ft

DEPTH	TEMP
0008	0000
0010	0002
0012	0002
0014	0003
0016	0003
0017	0003
0018	0005
0019	0014
0020	0022
0022	0036
0024	0042
0026	0045
0030	0053

Cons 044 Loc 15
Lat 69° 26 57N
Long 132° 59 42W
GMT 23.4 30 iv
Depth 30 ft

DEPTH	TEMP
0008	0000
0012	0000
0016	0000
0017	0000
0018	0000
0019	0012
0020	0019
0021	0020
0022	0019
0024	0020
0028	0025

Cons 045 Loc 16
Lat 69° 26 37N
Long 133° 02 12W
GMT 00.2 01 v
Depth 56 ft

DEPTH	TEMP
0008	0000
0012	0000
0016	0002
0017	0003
0018	0006
0019	0016
0020	0023
0022	0034
0024	0042
0026	0045
0030	0056

Cons 046 Loc 017
Lat 69° 26 45N
Long 133° 02 02W
GMT 00.4 01 v
Depth 10 ft

DEPTH	TEMP
0007	0000
0008	0002
0009	0002
0010	0003

Cons 047 Loc 15
Lat 69° 26 57 N
Long 132° 59 42 W
GMT 00.8 01 v
Depth 30 ft

DEPTH	TEMP
0008	0000
0012	0000
0016	0000
0017	0000
0018	0003
0019	0014
0020	0017
0021	0022
0022	0020
0024	0020
0028	0025

Cons 048 Loc 17
Lat 69° 26 45 N
Long 133° 02 02 W
GMT 02.8 01 v
Depth 10 ft

DEPTH	TEMP
0007	0000
0008	0002
0009	0002

Cons 049 Loc 15
Lat 69° 26 57 N
Long 132° 59 42 W
GMT 02.9 01 v
Depth 30 ft

DEPTH	TEMP
0008	-0002
0012	0002
0016	0002
0017	0002
0018	0013
0019	0017
0020	0019
0022	0022
0028	0023

Cons 050 Loc 17
Lat 69° 26 45 N
Long 133° 02 02 W
GMT 03.8 01 v
Depth 10 ft

DEPTH	TEMP
0007	0000
0008	0000
0009	0000

Cons 051 Loc 16
Lat 69° 26 37 N
Long 133° 02 12 W
GMT 04.1 01 v
Depth 56 ft

DEPTH	TEMP
0008	-0002
0012	0000
0016	0002
0017	0003
0018	0006
0019	0017
0020	0023
0022	0034
0024	0040
0026	0045
0028	0053
0030	0055
0033	0053

Cons 052 Loc 15
Lat 69° 26 57 N
Long 132° 59 42 W
GMT 05.2 01 v
Depth 30 ft

DEPTH	TEMP
0008	0000
0012	0000
0016	0000
0017	-0002
0018	0011
0019	0016
0020	0019
0022	0022
0024	0023
0028	0028

Cons 053 Loc 17
Lat 69° 26 45 N
Long 133° 02 02 W
GMT 05.7 01 v
Depth 10 ft

DEPTH	TEMP
0007	-0002
0008	-0002
0009	-0002

Cons 054 Loc 16
Lat 69° 26 37 N
Long 133° 02 12 W
GMT 05.8 01 v
Depth 56 ft

DEPTH	TEMP
0008	-0003
0010	-0002
0012	0000
0016	0001
0017	0002
0018	0003
0019	0017
0020	0023
0022	0034
0024	0040
0026	0044
0028	0050
0030	0053

Cons 055 Loc 04
Lat 69° 24 58 N
Long 132° 58 04 W
GMT 17.0 01 v
Depth 17 ft

DEPTH	TEMP
0001	0000
0002	0000
0004	0000
0006	0000
0008	0000
0010	0002
0012	0002
0014	0001
0016	0003

Cons 056 Loc 07
Lat 69° 24 56 N
Long 132° 58 26 W
GMT 17.8 01 v
Depth 73 ft

DEPTH	TEMP
0008	-0005
0010	-0007
0012	-0004
0014	-0003
0016	-0003
0018	0002
0020	0012
0022	0020
0025	0020
0030	-0002
0035	-0018
0040	-0028
0045	-0044
0050	-0044
0055	-0046
0060	-0044
0065	-0044

Cons 057 Loc 01
Lat 69° 23 20 N
Long 132° 59 25 W
GMT 19.0 01 v
Depth 23 ft

DEPTH	TEMP
0006	-0003
0008	-0003
0010	-0003
0016	-0002
0017	-0003
0018	-0002
0019	0016
0020	0020
0021	0020
0022	0022
0023	0023

Cons 058 Loc 02
Lat 69° 23 47 N
Long 132° 59 21 W
GMT 19.5 01 v
Depth 33 ft

DEPTH	TEMP
0006	-0003
0008	-0004
0010	-0004
0012	-0003
0014	-0002
0016	0000
0017	0000
0018	0002
0019	0011
0020	0019
0022	0026
0024	0028
0026	0026
0028	0020
0030	0011
0031	0009
0032	0010

Cons 060 Loc 01
Lat 69° 23 20 N
Long 132° 59 25 W
GMT 22.4 01 v
Depth 23 ft

DEPTH	TEMP	SAL
0006	-0003	
0008	-0002	0052
0010	-0003	
0013		0087
0016	-0002	
0018	-0002	0240
0019	-0002	
0020	0019	2116
0021	0023	
0022	0025	
0023	0026	

Cons 059 Loc 07
Lat 69° 24 56 N
Long 132° 58 26 W
GMT 21.2 01 v
Depth 73 ft

DEPTH	TEMP	SAL
0006	-0004	
0007		0084
0008	-0002	
0010	-0003	
0011		0065
0012	-0002	
0014	-0002	
0015		0079
0016	0002	
0017		0071
0018	0002	
0019	0006	
0020	0011	
0021		2130
0022	0020	
0025	0022	2557
0028	0012	
0030	0003	3008
0035	-0014	3053
0040	-0026	3089
0042	-0041	
0045	-0040	3110
0050	-0041	3114
0055		3122
0060	-0041	3108
0065		3118
0068	-0041	

Cons 061 Loc 12
Lat 69° 26 28 N
Long 132° 59 06 W
GMT 23.5 01 v
Depth 39 ft

DEPTH	TEMP
0000	0002
0002	-0002
0004	-0002
0006	-0002
0008	-0002
0010	-0001
0012	-0002
0014	-0003
0016	0003
0017	0002

Cons 062 Loc 12
Lat 69° 26 28 N
Long 132° 59 06 W
GMT 00.2 02 v
Depth 39 ft

DEPTH	TEMP
0000	0000
0002	-0003
0004	-0004
0006	-0003
0008	-0003
0010	-0003
0012	-0003
0014	-0003
0016	0000
0017	0002

Cons 063 Loc 01
Lat 69° 23 20 N
Long 132° 59 25 W
GMT 00.6 02 v
Depth 23 ft

DEPTH	TEMP	SAL
0006	-0008	
0008	-0003	
0010	-0006	
0012	-0006	0069
0014	-0006	
0016	-0004	
0018	-0002	1384
0019	0002	
0020	0016	2194
0021	0020	
0022	0025	
0023	0026	

Cons 064 Loc 01
Lat 69° 23 20 N
Long 132° 59 25 W
GMT 00.8 02 v
Depth 23 ft

DEPTH	TEMP
0006	-0008
0008	-0008
0010	-0008
0012	-0008
0014	-0008
0016	-0007
0018	-0005
0019	-0006
0020	0015
0021	0019
0022	0021
0023	0023

Cons 065 Loc 04
Lat 69° 24 58 N
Long 132° 58 04 W
GMT 01.7 02 v
Depth 17 ft

DEPTH	TEMP
0000	-0003
0002	-0002
0004	-0003
0006	-0003
0008	-0003
0010	-0003
0012	-0003
0014	-0002
0016	-0003

Cons 066 Loc 15
Lat 69° 26 57 N
Long 132° 59 42 W
GMT 15.5 02 v
Depth 30 ft

DEPTH	TEMP
0006	0000
0008	0000
0010	0000
0012	0000
0014	0000
0016	0000
0017	0000
0018	0006
0019	0017
0020	0019
0021	0020
0022	0022
0024	0023
0026	0026
0028	0030

Cons 067 Loc 15
Lat 69° 26 57 N
Long 132° 59 42 W
GMT 16.8 02 v
Depth 30 ft

DEPTH	TEMP	SAL
0006	-0003	
0008	-0003	
0010	-0002	0052
0012	-0003	
0014	-0003	
0016	-0002	
0017	0000	
0018	0010	1995
0019	0019	
0020	0020	
0022	0020	
0023		2245
0026	0025	

Cons 069 Loc 15
Lat 69° 26 57 N
Long 132° 59 42 W
GMT 18.1 02 v
Depth 30 ft

DEPTH	TEMP	SAL
0006	-0003	
0008	-0004	
0010	-0003	0035
0012	-0003	
0014	-0003	
0016	0000	
0017	0000	
0018	0013	2050
0019	0019	
0020	0020	
0022	0022	
0023		2204
0026	0026	

Cons 071 Loc 15
Lat 69° 26 57 N
Long 132° 59 42 W
GMT 19.7 02 v
Depth 30 ft

DEPTH	TEMP
0006	-0003
0008	-0003
0010	-0003
0012	-0003
0014	-0003
0016	-0003
0017	-0003
0018	-0001
0019	0010
0020	0017
0022	0020
0026	0031

Cons 068 Loc 19
Lat 69° 27 46 N
Long 133° 02 24 W
GMT 17.8 02 v
Depth 16 ft

DEPTH	TEMP
0006	-0002
0008	-0002
0010	-0002
0012	-0002
0014	-0002
0015	0000

Cons 070 Loc 04
Lat 69° 24 58 N
Long 132° 58 04 W
GMT 19.4 02 v
Depth 17 ft

DEPTH	TEMP
0000	-0002
0002	-0004
0004	-0003
0006	-0003
0008	-0003
0010	-0003
0012	-0003
0014	-0002
0016	-0003

Cons 072 Loc 15
Lat 69° 26 57 N
Long 132° 59 42 W
GMT 21.2 02 v
Depth 30 ft

DEPTH	TEMP
0006	0000
0008	0000
0010	0000
0012	0000
0014	0000
0016	-0002
0017	-0002
0018	0000
0019	-0002
0020	0014
0022	0019
0024	0022
0026	0026
0029	0028

Cons 073 Loc 19
Lat 69° 27 46 N
Long 133° 02 24 W
GMT 21.8 02 v
Depth 16 ft

DEPTH	TEMP	SAL
0006	-0003	
0008	-0002	0007
0010	-0002	
0012	0002	
0013	0000	
0014	0002	0027
0015	0002	
0016	0002	

Cons 074 Loc 19
Lat 69° 27 46 N
Long 133° 02 24 W
GMT 22.4 02 v
Depth 16 ft

DEPTH	TEMP
0006	-0003
0008	-0002
0010	-0002
0012	-0002
0014	0000
0015	0000
0016	0003

Cons 075 Loc 15
Lat 69° 26 57 N
Long 132° 59 42 W
GMT 22.7 02 v
Depth 30 ft

DEPTH	TEMP
0006	-0002
0008	-0002
0010	-0002
0012	-0002
0014	0000
0016	-0002
0017	-0002
0018	-0002
0019	0002
0020	0006
0021	0011
0022	0012
0024	0020
0026	0026
0029	0028

Cons 076 Loc 15
Lat 69° 26 57 N
Long 132° 59 42 W
GMT 23.4 02 v
Depth 30 ft

DEPTH	TEMP
0016	-0003
0018	-0003
0019	-0002
0020	0003
0021	0006
0022	0014
0023	0019
0024	0021

Cons 077 Loc 15
Lat 69° 26 57 N
Long 132° 59 42 W
GMT 00.0 03 v
Depth 30 ft

DEPTH	TEMP
0006	-0003
0008	-0004
0010	-0003
0012	-0002
0014	-0002
0016	-0003
0017	-0003
0018	-0003
0019	-0002
0020	0006
0021	0014
0022	0017
0024	0019
0026	0025
0029	0030

Cons 078 Loc 04
Lat 69° 24 58 N
Long 132° 58 04 W
GMT 01.0 03 v
Depth 17 ft

DEPTH	TEMP
0000	-0002
0002	-0002
0004	-0003
0006	-0003
0008	-0003
0010	-0002
0012	-0003
0014	-0003
0016	-0003
0017	0000

Cons 079 Loc 15
Lat 69° 26 57N
Long 132° 59 42W
GMT 01.2 03 v
Depth 30 ft

DEPTH	TEMP
0006	-0004
0008	-0004
0010	-0004
0012	-0004
0014	-0004
0016	-0004
0018	-0003
0019	0002
0020	0012
0021	0016
0022	0017
0024	0019
0026	0020
0029	0023

Cons 081 Loc 20
Lat 69° 38 10N
Long 133° 14 30W
GMT 15.7 03 v
Depth 18 ft

DEPTH	TEMP	SAL
0006	-0004	0215
0008	-0004	
0010	-0004	0073
0012	-0004	
0014	-0004	
0015		0077
0016	-0003	
0017	-0003	
0018	-0004	

Cons 083 Loc 15
Lat 69° 26 57N
Long 132° 59 42W
GMT 19.7 03 v
Depth 30 ft

DEPTH	TEMP
0006	-0002
0008	-0002
0010	-0002
0012	-0002
0014	-0002
0016	-0002
0017	-0002
0018	0000
0019	0012
0020	0020
0022	0023
0024	0023
0026	0028
0029	0031

Cons 080 Loc 03
Lat 69° 24 44N
Long 132° 58 37W
GMT 03.5 03 v
Depth 84 ft

DEPTH	TEMP
0006	-0004
0008	-0003
0010	-0004
0012	-0004
0014	-0003
0016	-0002
0017	-0003
0018	-0002
0019	0014
0020	0016
0021	0017
0023	0019
0024	0020
0026	0020

Cons 082 Loc 21
Lat 69° 42 50N
Long 133° 20 30W
GMT 17.1 03 v
Depth 25 ft

DEPTH	TEMP	SAL
0006	-0010	0035
0008	-0010	
0010	-0010	0164
0012	-0012	
0014	-0012	0200
0016	-0014	0205
0017	-0022	
0018	-0024	0210
0019	-0028	
0020	-0037	0809
0021	-0046	
0022	-0056	1106
0023	-0059	
0024	-0059	
0025	-0061	

Cons 084 Loc 15
Lat 69° 26 57N
Long 132° 59 42W
GMT 21.8 03 v
Depth 30 ft

DEPTH	TEMP
0006	0000
0008	0000
0010	0000
0012	0000
0014	0000
0016	-0002
0017	-0002
0018	-0002
0019	-0002
0020	0008
0021	0017
0024	0023
0029	0030

Cons 085 Loc 18
Lat 69° 27 12N
Long 133° 00 20W
GMT 22.1 03 v
Depth 23 ft

DEPTH	TEMP
0006	0000
0008	0000
0010	-0002
0012	0000
0014	0002
0016	0000
0017	0000
0018	-0002
0019	0000
0020	0009
0021	0014
0022	0016
0023	0020

Cons 086 Loc 13
Lat 69° 26 51N
Long 132° 59 30W
GMT 22.4 03 v
Depth 18 ft

DEPTH	TEMP
0006	0000
0008	0000
0010	0000
0012	0000
0014	0000
0016	0000
0017	-0002
0018	0000

Cons 087 Loc 13
Lat 69° 26 51N
Long 132° 59 30W
GMT 23.4 03 v
Depth 18 ft

DEPTH	TEMP
0006	0000
0008	0000
0010	0000
0012	0000
0014	-0002
0016	-0002
0017	0000
0018	0001

Cons 088 Loc 13
Lat 69° 26 51N
Long 132° 59 30W
GMT 00.1 04 v
Depth 18 ft

DEPTH	TEMP
0006	0000
0008	0000
0010	0000
0011	-0002
0012	-0002
0013	-0002
0014	0000
0015	0000
0016	-0003
0017	0000
0018	0000

Cons 089 Loc 14
Lat 69° 26 56N
Long 132° 59 39W
GMT 00.6 04 v
Depth 30 ft

DEPTH	TEMP
0006	0000
0008	-0002
0010	-0002
0012	-0002
0013	-0002
0014	-0003
0015	-0002
0016	-0002
0017	-0002
0018	0000
0019	0002
0020	0000
0021	0011
0022	0017
0023	0019

Cons 090 Loc 15
Lat 69° 26 57N
Long 132° 59 42W
GMT 00.8 04 v
Depth 30 ft

DEPTH	TEMP
0006	-0002
0008	-0003
0010	-0003
0012	-0003
0014	-0003
0015	-0002
0016	0000
0017	-0002
0018	-0002
0019	0000
0020	0005
0021	0017
0022	0017
0023	0020
0024	0022
0026	0025
0029	0030

Cons 091 Loc 04
Lat 69° 24 58 N
Long 132° 58 04 W
GMT 03.8 04 v
Depth 17 ft

DEPTH	TEMP	SAL
0000	-0004	
0002	-0004	
0004	-0003	
0005		0076
0006	-0003	
0008	-0003	
0010	-0003	0077
0012	-0003	
0014	-0003	
0016	-0003	
0017	-0002	

Cons 092 Loc 02
Lat 69° 23 47 N
Long 132° 59 21 W
GMT 04.5 04 v
Depth 33 ft

DEPTH	TEMP
0006	-0006
0008	-0004
0010	-0004
0012	-0003
0014	-0003
0016	-0003
0018	0000
0019	0009
0020	0017
0022	0025
0024	0026
0026	0026
0028	0019
0030	0011
0032	0009

Cons 093 Loc 07
Lat 69° 24 56 N
Long 132° 58 26 W
GMT 04.8 04 v
Depth 73 ft

DEPTH	TEMP
0006	-0004
0008	-0004
0010	-0003
0012	-0003
0014	-0003
0016	-0002
0018	0000
0019	0006
0020	0014
0022	0022
0024	0023
0026	0020
0028	0011
0030	0000
0032	-0006
0034	-0012
0036	-0017
0038	-0018
0040	-0024
0045	-0041
0050	-0043
0060	-0041
0065	-0041
0067	-0041

Cons 094 Loc 09
Lat 69° 25 29 N
Long 132° 58 38 W
GMT 05.0 04 v
Depth 42 ft

DEPTH	TEMP
0006	-0002
0008	-0003
0010	-0003
0012	-0002
0014	-0002
0016	0000
0018	-0002
0019	0006
0020	0016
0022	0020
0024	0023
0026	0019
0028	0009
0030	0000
0032	-0009
0034	-0012
0036	-0017
0038	-0017
0040	-0018

Cons 095 Loc 15
Lat 69° 26 57 N
Long 132° 59 42 W
GMT 05.4 04 v
Depth 30 ft

DEPTH	TEMP
0006	0003
0008	0003
0010	0002
0012	0002
0014	0002
0016	0002
0018	0002
0019	0014
0020	0017
0022	0017
0023	0019
0024	0019
0026	0020
0027	0026
0028	0026

Cons	096 Loc 04
Lat	69° 24 58 N
Long	132° 58 04 W
GMT	18.9 04 v
Depth	17 ft

DEPTH	TEMP
0000	0002
0002	0002
0004	0002
0006	-0002
0008	0000
0010	0002
0012	0002
0014	0003
0016	0005

Cons	097 Loc 07
Lat	69° 24 56 N
Long	132° 58 26 W
GMT	19.2 04 v
Depth	73 ft

DEPTH	TEMP
0006	0000
0008	0000
0010	-0002
0012	0000
0014	0002
0016	0002
0017	0003
0018	0006
0019	0014
0020	0019
0022	0022
0024	0025
0026	0019
0028	0011
0030	0002
0032	-0009
0034	-0012
0036	-0014
0038	-0020
0040	-0028
0042	-0037
0045	-0040
0050	-0040
0055	-0040
0060	-0040
0065	-0041
0067	-0041

Cons	098 Loc 02
Lat	69° 23 47 N
Long	132° 59 21 W
GMT	19.5 04 v
Depth	33 ft

DEPTH	TEMP
0006	0002
0008	-0002
0010	-0002
0012	-0003
0014	-0002
0016	-0003
0017	-0002
0018	0008
0019	0014
0020	0020
0022	0030
0024	0031
0026	0028
0028	0020
0030	0012
0031	0011

Cons	099 Loc 15
Lat	69° 26 57 N
Long	132° 59 42 W
GMT	20.0 04 v
Depth	30 ft

DEPTH	TEMP
0006	0000
0008	-0002
0010	-0002
0012	-0002
0014	-0002
0016	-0002
0017	0002
0018	0012
0019	0019
0020	0019
0021	0019
0022	0019
0024	0023
0026	0030
0028	0030

Cons	100 Loc 15
Lat	69° 26 57 N
Long	132° 59 42 W
GMT	23.3 04 v
Depth	30 ft

DEPTH	TEMP
0006	0003
0008	0003
0010	0003
0012	0003
0014	0003
0016	0005
0017	0005
0018	0006
0019	0005
0020	0014
0021	0023
0022	0025
0024	0031
0026	0042

Cons	101 Loc 15
Lat	69° 26 57 N
Long	132° 59 42 W
GMT	23.8 04 v
Depth	30 ft

DEPTH	TEMP
0006	0009
0008	0009
0010	0009
0012	0006
0014	0008
0016	0008
0017	0005
0018	0005
0019	0012
0020	0008
0021	0017
0022	0022
0024	0030
0026	0036

Cons 102 Loc 15
Lat 69° 26 57N
Long 132° 59 42W
GMT 00.0 05 v
Depth 30 ft

DEPTH	TEMP
0006	0006
0008	0006
0010	0006
0012	0006
0014	0006
0016	0006
0017	0006
0018	0006
0019	0009
0020	0008
0021	0017
0022	0019
0024	0030
0026	0034

Cons 103 Loc 15
Lat 69° 26 57N
Long 132° 59 42W
GMT 00.3 05 v
Depth 30 ft

DEPTH	TEMP
0006	0009
0008	0006
0010	0008
0012	0005
0014	0006
0016	0005
0017	0005
0018	0006
0019	0006
0020	0005
0021	0017
0022	0017

Cons 104 Loc 15
Lat 69° 26 57N
Long 132° 59 42W
GMT 00.7 05 v
Depth 30 ft

DEPTH	TEMP
0006	0003
0008	0005
0010	0006
0012	0005
0014	0005
0016	0005
0017	0005
0018	0003
0019	0005
0020	0006
0021	0017
0022	0020
0024	0028
0026	0034
0029	0039

Cons 105 Loc 15
Lat 69° 26 57N
Long 132° 59 42W
GMT 01.0 05 v
Depth 30 ft

DEPTH	TEMP
0006	0008
0008	0006
0010	0005
0012	0005
0014	0005
0016	0005
0017	0005
0018	0006
0019	0006
0020	0006
0021	0020
0022	0023
0024	0030
0026	0031

Cons 106 Loc 15
Lat 69° 26 57N
Long 132° 59 42W
GMT 01.3 05 v
Depth 30 ft

DEPTH	TEMP
0006	0006
0008	0006
0010	0006
0012	0006
0014	0006
0016	0005
0017	0005
0018	0006
0019	0006
0020	0005
0021	0019
0022	0023
0023	0026
0024	0028
0025	0030
0026	0031
0027	0033

Cons 107 Loc 04
Lat 69° 24 58N
Long 132° 58 04W
GMT 02.0 05 v
Depth 17 ft

DEPTH	TEMP
0000	0006
0002	0005
0004	0005
0006	0006
0008	0005
0010	0003
0012	0005
0014	0006
0016	0006

Cons 108 Loc 04
Lat 69° 24 58 N
Long 132° 58 04 W
GMT 16.9 05 v
Depth 17 ft

DEPTH	TEMP
0002	0003
0004	0003
0006	0003
0008	0004
0010	0004
0012	0006
0014	0006
0016	0006

Cons 109 Loc M-1
Lat 68° 21 00 N
Long 134° 11 00 W
GMT 02.2 06 v
DEPTH 60

DEPTH	TEMP	SAL
0000		0.15KB
0005	-0004	
0006	-0004	
0008	-0004	
0010	-0004	
0012	-0002	
0014	-0004	
0016	-0002	
0018	-0002	
0020	-0002	
0025	-0002	
0030	-0002	
0035	-0004	
0040	-0004	
0045	-0002	
0050	-0002	
0055	-0004	
0058	-0004	

N R C Programme

Phase II

Serial data

Consecutive numbers 1 to 81

C R N 448

Cons	001	Loc 23	
Lat	69°	23	22 N
Long	132°	59	26 W
GMT	18.5	26	xi
Depth	23 ft		

DEPTH	TEMP	SAL
0002	-0021	0230
0003	-0021	0240
0004	-0024	0270
0005	-0024	0340
0006	-0020	0650
0007	-0012	0960
0008	-0008	1770
0009	-0008	1920
0010	-0010	2570
0011	-0011	
0012	-0012	2660
0013	-0012	
0014	-0014	2700
0015	-0012	
0016	-0010	2730
0017	-0008	
0018	-0007	2780
0019	-0005	
0020	-0004	2820
0021	-0004	
0022	-0003	2840
0023	0001	

Cons	002	Loc 24	
Lat	69°	23	45 N
Long	132°	59	23 W
GMT	19.5	26	xi
Depth	35 ft		

DEPTH	TEMP	SAL
0002	-0005	0220
0003	-0007	0210
0004	-0012	0310
0005	-0012	0370
0006	-0010	0600
0007	-0005	1140
0008	0001	2150
0009	-0001	2540
0010	-0001	2480
0012	-0009	2710
0014	-0009	2770
0015	-0002	
0016	0002	2800
0018	-0005	2840
0020	-0002	2860
0022	-0008	2890
0024	-0009	
0026	-0010	
0028	-0008	
0030	-0005	2900

Cons 003 Loc 45
Lat 69° 26 35 N
Long 133° 02 11 W
GMT 22.1 26 xi
Depth 34 ft

DEPTH	TEMP	SAL
0002	0007	
0004	0002	0060
0006	0001	0155
0007		1530
0008	-0017	2420
0009	-0035	2580
0010	-0038	2680
0012	-0048	2730
0014	-0052	2770
0016	-0055	2760
0018	-0054	
0020	-0053	2790
0022	-0052	
0024	-0051	2805
0026	-0050	2810
0028	-0049	2810
0030	-0049	2840
0032	-0046	
0034	-0043	

Cons 004 Loc 33
Lat 69° 24 58N
Long 132° 58 05W
GMT 00.3 27 xi
Depth 15 ft

DEPTH	TEMP	SAL
0001	-0025	0300
0002	-0025	0280
0003	-0027	0320
0004	-0027	0330
0005	-0027	0340
0006	-0027	0370
0007	-0035	1000
0008	-0036	1490
0009	-0040	2030
0010	-0031	2570
0011	-0038	2650
0012	-0059	2710
0013	-0062	2720
0014	-0057	2740
0015	-0057	2710

Cons 005 Loc 28
Lat 69° 24 43 N
Long 132° 58 37 W
GMT 18.0 27 xi
Depth 85 ft

DEPTH	TEMP	SAL	
0002	-0002	0090	1.37KB
0003	-0004	0100	
0004	-0011	0330	1.37KB
0005	-0012	0400	4.02KB
0006	-0015	0640	
0007	-0016	1100	4.07KB
0008	-0012	1900	25.05KB
0009	-0007	2480	
0010	-0013	2660	24.96KB
0012	-0036	2740	
0014	-0031	2770	
0016	-0021	2810	
0017	-0036	2840	
0018	-0025	2840	
0019	-0050	2850	
0020	-0050	2890	
0025	-0056	2900	29.59KB
0030	-0068	2900	
0035	-0065		29.68KB
0040	-0056	2900	
0045	-0059	2900	
0050	-0062	2900	
0055	-0067		
0060	-0064	2900	
0065		2910	
0070	-0062	2900	
0071		2900	
0072		2900	
0073		2900	
0074		2900	
0075		2900	
0076		2900	
0077	0006	2340	

Cons	006	Loc 29	
Lat	69°	24	53 N
Long	132°	58	35 W
GMT	23.0	27	xi
Depth	64 ft		

DEPTH	TEMP	SAL
0002	-0007	0090
0003	-0007	0100
0004	-0008	0110
0005	-0009	0180
0006	-0012	0550
0007	-0018	0840
0008	-0022	1580
0009	-0023	2500
0010	-0022	2620
0012	-0041	2720
0014	-0044	2740
0016	-0040	2800
0018	-0047	2840
0020	-0065	2880
0025	-0075	2900
0030	-0074	2900
0035	-0062	2900
0040	-0066	2900
0044	-0069	
0045	-0068	

Cons	007	Loc 30	
Lat	69°	24	58 N
Long	132°	58	10 W
GMT	00.0	28	xi
Depth	55 ft		

DEPTH	TEMP	SAL
0002	-0004	
0003	-0006	0090
0004	-0006	0110
0005	-0008	0210
0006	-0010	0380
0007	-0014	0520
0008	-0017	1500
0009	-0026	2410
0010	-0027	2580
0012	-0047	2740
0014	-0041	2760
0016	-0041	2720
0018	-0050	2800
0020	-0059	2820
0025	-0077	2900
0030	-0078	2900
0035	-0067	
0040	-0068	2900
0045	-0070	
0050	-0075	2900
0055	-0068	

Cons	008	Loc 44	
Lat	69°	26	20 N
Long	132°	57	55 W
GMT	17.8	28	xi
Depth	27 ft		

DEPTH	TEMP	SAL	
0002	0002	0000	
0003	0001	0000	0.46KB
0004	-0001	0000	
0005	0000	0050	3.47KB
0006	0003	0320	
0007	0018	0760	3.39KB
0008	0035	1530	

Cons 009 Loc 42
Lat 69° 25 58 N
Long 132° 58 45 W
GMT 18.8 28 xi
Depth 69 ft

DEPTH	TEMP	SAL	
0002	-0002	0050	1.04KB
0003	-0003	0070	
0004	-0001	0080	0.93KB
0005	-0004	0170	
0006	-0010	0570	6.06KB
0007	-0012	0690	
0008	-0017	1100	6.08KB
0009	-0019	2220	
0010	-0027	2570	
0012	-0036	2700	
0014	-0052	2780	27.41KB
0015			
0016	-0050	2800	27.50KB
0018	-0052	2830	
0020	-0058	2840	
0025	-0066	2900	
0028	-0057		

Cons 010 Loc 27
Lat 69° 24 32 N
Long 132° 58 39 W
GMT 22.2 28 xi
Depth 70 ft

DEPTH	TEMP	SAL
0002	0012	0100
0003	0008	0130
0004	0003	
0005	0000	0340
0006		0400
0007	-0004	0540
0008		1030
0009		2320
0010	-0003	2600
0012	-0017	2710
0014	-0026	
0016	-0013	2820
0018	-0017	
0020	-0028	2880
0025	-0048	2870
0030	-0069	2900
0035	-0047	
0040	-0036	
0050	-0057	2900
0060	-0048	
0069		2900

Cons 011 Loc 28
Lat 69° 24 43 N
Long 132° 58 37 W
GMT 23.5 28 xi
Depth 85 ft

DEPTH	TEMP	SAL
0002	0014	
0004	0008	0060
0006	0001	0340
0008		0730
0010	-0006	2250
0012	-0016	2510
0020	-0049	2780
0030	-0061	2900
0040	-0052	
0050	-0064	
0060	-0050	
0070	-0040	
0075	-0024	
0076	-0026	
0077	-0008	
0078	0001	2580

Cons 012 Loc 34
Lat 69° 24 59N
Long 132° 58 03W
GMT 00.5 29 xi
Depth 6 ft

DEPTH	TEMP	SAL
0001		0380
0002		0420
0003		0400
0004		0490
0005		0500
0006		0520

Cons 013 Loc 48
Lat 69° 26 58N
Long 132° 59 43W
GMT 18.3 29 xi
Depth 28 ft

DEPTH	TEMP	SAL
0002	0000	0040
0003	0000	0040
0004	0000	0030
0005	-0001	0030
0006	-0001	0030
0007	-0001	0040
0008	-0008	0280
0009	-0025	1820
0010	-0040	2650
0011	-0048	2780
0012	-0048	2800
0014	-0048	2800
0016	-0051	2870
0018	-0050	2870
0020	-0051	2890
0025	-0051	2900
0027	-0052	2910

Cons 014 Loc 48
Lat 69° 26 58N
Long 132° 59 43W
GMT 19.7 29 xi
Depth 28 ft

DEPTH	TEMP	SAL
0002	0017	0000
0003	0011	0000
0004	0009	0000
0005	0005	0030
0006	0004	0040
0007	0002	0090
0008	-0005	0490
0009	-0026	2460
0010	-0040	2660
0011	-0049	2770
0016	-0054	2800

Cons 015 Loc 48
Lat 69° 26 58N
Long 132° 59 43W
GMT 21.3 29 xi
Depth 28 ft

DEPTH	TEMP	SAL
0002	0010	0000
0003	0008	0000
0004	0004	0000
0005	0003	0000
0006	0003	0000
0007	0001	0020
0008	-0001	0050
0009	-0029	1500
0010	-0038	2530
0011	-0044	2740
0012	-0048	2800
0016	-0052	2860
0020	-0056	2900
0025	-0056	2920

Cons 016 Loc 48
Lat 69° 26 58 N
Long 132° 59 43 W
GMT 22.8 29 xi
Depth 28 ft

DEPTH	TEMP	SAL
0002	0009	0000
0003	0006	0000
0004	0003	0000
0006	0001	0000
0007	0001	0020
0008	-0001	0030
0009	-0025	2080
0010	-0034	2470
0011	-0034	2620
0012	-0039	2690
0014	-0046	2750
0016	-0048	2830
0020	-0053	2870
0025	-0054	2900

Cons 017 Loc 48
Lat 69° 26 58 N
Long 132° 59 43 W
GMT 01.2 30 xi
Depth 28 ft

DEPTH	TEMP	SAL
0002	0003	0000
0003	0002	0020
0004	-0001	0030
0005	-0002	0040
0006	-0002	0040
0007	-0003	0040
0008	-0008	0190
0009	-0020	1200
0010	-0033	1910
0011	-0042	2520
0012	-0044	2640
0014	-0050	2770
0016	-0054	2850
0020	-0056	2900
0025	-0056	2900

Cons 018 Loc 48
Lat 69° 26 58 N
Long 132° 59 43 W
GMT 04.0 30 xi
Depth 28 ft

DEPTH	TEMP	SAL
0002	-0001	0020
0003	-0001	0020
0004	-0002	0020
0005	-0002	0030
0006	-0003	0030
0007	-0003	0020
0008	-0009	0320
0009	-0016	0840
0010	-0034	2150
0011	-0035	2550
0012	-0045	2630
0014	-0053	2850
0016	-0055	2870
0018	-0058	2900
0020	-0058	2900
0022	-0058	2900

Cons 019 Loc 48
Lat 69° 26 58 N
Long 132° 59 43 W
GMT 05.5 30 xi
Depth 28 ft

DEPTH	TEMP	SAL
0002	0001	0000
0003	-0001	0000
0004	-0003	0020
0005	-0003	0020
0006	-0003	0030
0007	-0003	0030
0008	-0011	0380
0009	-0016	0830
0010	-0040	2530
0011	-0044	2730
0012	-0048	2790
0014	-0052	2830
0016	-0058	2890
0018	-0059	2900
0020	-0060	2900
0025	-0062	2900

Cons 020 Loc 48
Lat 69° 26 58 N
Long 132° 59 43 W
GMT 06.5 30 xi
Depth 28 ft

DEPTH	TEMP	SAL
0002	-0001	0000
0003	-0002	0000
0005	-0003	0000
0007	-0003	0030
0008	-0006	0250
0009	-0025	2440
0010	-0043	2660
0011	-0047	2740
0012	-0053	2790
0014	-0059	2900
0020	-0060	2900

Cons 021 Loc 30
Lat 69° 24 58 N
Long 132° 58 10 W
GMT 18.4 30 xi
Depth 55 ft

DEPTH	TEMP	SAL
0002	-0001	0080
0003	-0001	0110
0004	-0001	0140
0005	-0003	0360
0006	-0003	0400
0007	-0005	0570
0008	-0006	0820
0009	-0012	1450
0010	-0012	2650
0011	-0011	2700
0012	-0014	2740
0014	-0021	2780
0016	-0021	2820
0018	-0023	2830
0020	-0028	2830
0025	-0052	2900
0030	-0054	2910
0035	-0046	2920
0040	-0048	2910
0045	-0043	2910
0050	-0040	

Cons 022 Loc 23
Lat 69° 23 22 N
Long 132° 59 26 W
GMT 19.3 30 xi
Depth 23 ft

DEPTH	TEMP	SAL
0002	-0010	0600
0003	-0005	0600
0004	-0010	0800
0005	-0010	1000
0006	-0015	2000
0007	-0016	2200
0008	-0016	2440
0009	-0018	2610
0010	-0018	2670
0011	-0023	2680
0012	-0032	2690
0014	-0027	2600
0016	-0026	2610

Cons 023 Loc 25
Lat 69° 24 10 N
Long 132° 58 46 W
GMT 19.9 30 xi
Depth 34 ft

DEPTH	TEMP	SAL
0002	-0001	0370
0003	-0001	0370
0004	-0001	0360
0005	-0002	0360
0006	-0002	0350
0007	-0003	0360
0008	-0006	0700
0009	-0018	1620
0010	-0018	2280
0011	-0024	2660
0012	-0028	2710

Cons 024 Loc 26
Lat 69° 24 18 N
Long 132° 59 30 W
GMT 20.5 30 xi
Depth 53 ft

DEPTH	TEMP	SAL
0002	-0007	0400
0004	-0004	0370
0006	-0004	0370
0007	-0004	0370
0008	-0008	0620
0009	-0018	1650
0010	-0014	2560
0011	-0017	2380

Cons 025 Loc 38
Lat 69° 24 57 N
Long 132° 58 02 W
GMT 20.6 30 xi
Depth 16 ft

DEPTH	TEMP	SAL
0002	-0003	0280
0004	-0003	0300
0006	-0004	0330
0007	-0005	0360
0008	-0012	1010
0009	-0018	1690
0010	-0020	2480
0011	-0018	2660
0012	-0022	2670
0014	-0022	2740
0015	-0036	2770
0016	-0035	2790

Cons 026 Loc 23
Lat 69° 23 22 N
Long 132° 59 26 W
GMT 22.6 30 xi
Depth 23 ft

DEPTH	TEMP	SAL
0002	-0003	0260
0003	-0004	0220
0004	-0004	0250
0005	-0004	0300
0006	-0004	0290
0007	-0005	0410
0008	-0012	0900
0009	-0018	1320
0010	-0019	2430
0011	-0020	2610
0012	-0029	2680

Cons 027 Loc 30
Lat 69° 24 58 N
Long 132° 58 10 W
GMT 23.2 30 xi
Depth 55 ft

DEPTH	TEMP	SAL
0002	-0001	0050
0003	-0002	0050
0004	-0003	0050
0005	-0006	0260
0006	-0006	0310
0007	-0009	0560
0008	-0016	1180
0009	-0017	1530
0010	-0019	2410
0011	-0012	2630
0012	-0022	2680
0014	-0032	2740
0016	-0034	2780
0020	-0053	2830
0025	-0065	2870
0030	-0070	2900
0040	-0059	2900

Cons 028 Loc 27
Lat 69° 24 32N
Long 132° 58 39W
GMT 23.9 30 xi
Depth 70 ft

DEPTH	TEMP	SAL
0002	-0001	0080
0003	-0004	0070
0004	-0004	0070
0005	-0004	0060
0006	-0008	0210
0007	-0008	0280
0008	-0011	0510
0009	-0012	1100
0010	-0008	2430
0011	-0012	2620
0012	-0017	2670
0014	-0031	2730
0016	-0034	2780
0020	-0052	2820
0025	-0046	2880
0030	-0062	2900
0035	-0044	2900
0040	-0040	2900
0050	-0060	2900
0070	-0032	2410

Cons 029 Loc 44
Lat 69° 26 20N
Long 132° 57 55W
GMT 00.8 01 xii
Depth 27 ft

DEPTH	TEMP	SAL
0002	0004	0000
0003	0000	0020
0004	-0002	0040
0005	-0003	0050
0006	-0002	0060
0007	0005	0200
0008	0018	0600
0009	0032	1000

Cons 030 Loc 28
Lat 69° 24 43N
Long 132° 58 37W
GMT 18.9 01 xii
Depth 85 ft

DEPTH	TEMP	SAL
0002	0007	0060
0003	-0004	0070
0004	-0004	0070
0005	-0006	0100
0006	-0008	0300
0007	-0008	0320
0008	-0010	0720
0009	-0014	1290
0010	-0012	2340
0011	-0012	2590
0012	-0014	2660
0014	-0024	2740
0016	-0031	2760
0018	-0037	2820
0020	-0045	2840
0025	-0061	2900
0030	-0058	2900
0033	-0051	
0035	-0040	2900
0037	-0047	
0040	-0054	2930
0045	-0058	2910
0050	-0059	2900
0055	-0058	2910
0060	-0057	2910
0065	-0050	2910
0070	-0044	2900
0075	-0041	2900
0076	-0040	2900
0077	-0040	2900
0080	-0036	1960

Cons 031 Loc 28
Lat 69° 24 43N
Long 132° 58 37W
GMT 23.0 01 xii
Depth 85 ft

DEPTH	TEMP	SAL
0005		0191
0010		2419
0015		2774
0020		2840
0030		2940
0050		2963

KB

Cons 032 Loc 44
Lat 69° 26 20N
Long 132° 57 55W
GMT 12.0 02 xii
Depth 27 ft

DEPTH	TEMP	SAL
0000		0050 KB

Cons 033 Loc 42
Lat 69° 25 58N
Long 132° 58 45W
GMT 12.2 02 xii
Depth 69 ft

DEPTH	TEMP	SAL
0000		0117 KB

Cons 034 Loc 27
Lat 69° 24 32N
Long 132° 58 39W
GMT 12.3 02 xii
Depth 70 ft

DEPTH	TEMP	SAL
0000		0129 KB

Cons 035 Loc 24
Lat 69° 23 45N
Long 132° 59 23W
GMT 12.5 02 xii
Depth 35 ft

DEPTH	TEMP	SAL
0000		0155 KB

Cons 036 Loc 22
Lat 69° 23 22 N
Long 132° 59 19 W
GMT 18.5 03 xii
Depth 26 ft

DEPTH	TEMP	SAL
0002	-0008	0090
0003	-0009	0090
0004	-0010	0100
0005	-0010	0100
0006	-0013	0270
0007	-0014	0310
0008	-0014	0300
0009	-0012	0530
0010	-0008	1140
0011	0000	2500
0012	0000	2540
0013	0000	2650
0014	-0004	2710
0016	-0004	2730
0018	-0010	2740
0020	-0016	2790
0025	-0025	2820
0028	-0026	2840

Cons	037		Loc 23
Lat	69°	23	22 N
Long	132°	59	26 W
GMT	19.2	03	xii
Depth	23 ft		

DEPTH	TEMP	SAL
0002	-0006	0050
0003	-0006	0060
0004	-0006	0060
0005	-0007	0060
0006	-0008	0260
0007	-0009	0330
0008	-0010	0390
0009	-0012	0740
0010	-0020	1750
0011	-0013	2600
0012	-0011	2550
0013	-0014	2700

Cons	038		Loc 33
Lat	69°	24	58 N
Long	132°	58	05 W
GMT	19.6	03	xii
Depth	23 ft		

DEPTH	TEMP	SAL
0002	-0006	0070
0003	-0007	0070
0004	-0007	0070
0005	-0007	0110
0006	-0008	0290
0007	-0011	0370
0008	-0011	0530
0009	-0015	0950
0010	-0018	2230
0011	-0011	2590
0012	-0011	2670
0013	-0015	2700

Cons	039		Loc 27
Lat	69°	24	32 N
Long	132°	58	39 W
GMT	21.5	03	xii
Depth	70 ft		

DEPTH	TEMP	SAL
0002	-0006	0070
0003	-0006	0060
0004	-0007	0060
0005	-0008	0110
0006	-0008	0270
0007	-0009	0310
0008	-0010	0420
0009	-0014	1060
0010	-0016	2370
0011	-0011	2620
0012	-0013	2670
0013	-0019	2710
0014	-0025	1520

Cons	040		Loc 28
Lat	69°	24	43 N
Long	132°	58	37 W
GMT	22.0	03	xii
Depth	85 ft		

DEPTH	TEMP	SAL
0002	-0006	0050
0003	-0006	0050
0004	-0007	0050
0005	-0008	0090
0006	-0008	0250
0007	-0009	0300
0008	-0010	0380
0009	-0015	1060
0010	-0016	2310
0011	-0011	2610
0012	-0013	2670
0013	-0018	2710
0014	-0028	2720
0015	-0031	2750

Cons 041 Loc 29
Lat 69° 24 53 N
Long 132° 58 35 W
GMT 22. 2 03 xii
Depth 64 ft

DEPTH	TEMP	SAL
0002	-0006	0050
0003	-0006	0060
0004	-0007	0060
0005		0100
0006	-0008	0220
0007	-0009	0310
0008	-0011	0410
0009	-0015	1070
0010	-0016	2350
0011	-0011	2600
0012	-0013	2670
0015	-0035	2740

Cons 042 Loc 30
Lat 69° 24 58 N
Long 132° 58 10 W
GMT 23. 2 03 xii
Depth 55 ft

DEPTH	TEMP	SAL
0002	-0005	0040
0003	-0006	0040
0004	-0006	0030
0005	-0007	0030
0006	-0010	0110
0007	-0011	0220
0008	-0022	0290
0009	-0017	0720
0010	-0014	1370
0011	-0009	1690
0012	-0010	1930
0013	-0015	2540
0014	-0025	2670
0015	-0031	2720
0016	-0040	2740
0020	-0060	2800

Cons 043 Loc 23
Lat 69° 23 22 N
Long 132° 59 26 W
GMT 00. 0 04 xii
Depth 23 ft

DEPTH	TEMP	SAL
0002	-0008	0150
0003	-0010	0120
0004	-0008	0230
0005	-0008	0260
0006	-0008	0240
0007	-0009	0270
0008	-0009	0310
0009	-0012	0870
0010	-0016	1600
0011	-0012	2250
0012	-0012	2530
0013	-0016	2680

Cons 044 Loc 27
Lat 69° 24 32 N
Long 132° 58 39 W
GMT 00. 2 04 xii
Depth 70 ft

DEPTH	TEMP	SAL
0002	-0005	0060
0003	-0006	0050
0004	-0007	0140
0005	-0008	0210
0006	-0008	0230
0007	-0008	0280
0008	-0008	0450
0009	-0010	0640
0010	-0014	2290
0011	-0011	2600
0012	-0011	2670
0013	-0015	2700
0014	-0019	2730

Cons 045 Loc 28
Lat 69° 24 43 N
Long 132° 58 37 W
GMT 00.4 04 xii
Depth 85 ft

DEPTH	TEMP	SAL
0002	-0006	0080
0003	-0007	0070
0004	-0007	0070
0005	-0007	0180
0006	-0012	0230
0007	-0008	0280
0008	-0009	0430
0009	-0011	0960
0010	-0015	2150
0011	-0009	2580
0012	-0011	2650
0013	-0015	2690
0014	-0022	2740
0015	-0029	2760

Cons 046 Loc 29
Lat 69° 24 53 N
Long 132° 58 35 W
GMT 00.7 04 xii
Depth 64 ft

DEPTH	TEMP	SAL
0002	-0006	0080
0003	-0005	0070
0004	-0005	0070
0005	-0008	0080
0006	-0008	0210
0007	-0007	0310
0008	-0009	0430
0009	-0009	0820
0010	-0015	2070
0011	-0011	2570
0012	-0009	2670
0013	-0017	2700
0014	-0021	2750
0015	-0032	2760

Cons 047 Loc 40
Lat 69° 25 05 N
Long 132° 58 33 W
GMT 17.6 04 xii
Depth 22 ft

DEPTH	TEMP	SAL
0002	0003	0000
0003	-0001	0000
0004	-0002	0000
0005	-0002	0000
0006	-0002	0000
0007	-0002	0020
0008	-0006	0040
0009	-0011	0500
0010	-0012	1100
0011	-0025	2500
0012	-0038	2700
0013	-0043	2760
0014	-0045	2780
0015	-0043	2800
0016	-0043	2820

Cons 048 Loc 43
Lat 69° 26 12 N
Long 132° 59 13 W
GMT 17.9 04 xii
Depth 46 ft

DEPTH	TEMP	SAL
0002	-0002	0000
0003	-0002	0000
0004	-0003	0000
0005	-0003	0000
0006	-0003	0000
0007	-0004	0030
0008	-0008	0260
0009	-0011	0340
0010	-0015	1840
0011	-0028	2380
0012	-0034	2540
0013	-0041	2680
0014	-0043	2720
0015	-0045	2800
0016	-0044	2820
0017	-0047	2880
0018	-0047	2900
0019	-0047	2900
0020	-0047	2900
0021	-0047	2900

Cons	049		Loc 43
Lat	69°	26	12 N
Long	132°	59	13 W
GMT	19.0	04	xii
Depth	46 ft		

DEPTH	TEMP	SAL
0002	-0001	0000
0003	-0002	0000
0004	-0002	0000
0005	-0002	0000
0006	-0002	0000
0007	-0004	0060
0008	-0007	0280
0009	-0009	0420
0010	-0014	1510
0011	-0027	2600
0012	-0040	2620
0013	-0042	2680
0014	-0044	2750
0015	-0045	2880

Cons	050		Loc 40
Lat	69°	25	05 N
Long	132°	58	33 W
GMT	19.3	04	xii
Depth	22 ft		

DEPTH	TEMP	SAL
0002	-0001	0000
0003	-0002	0000
0004	-0002	0000
0005	-0002	0010
0006	-0002	0020
0007	-0002	0030
0008	-0007	0120
0009	-0011	0750
0010	-0013	1300
0011	-0025	2480
0012	-0037	2630
0013	-0044	2770
0014	-0045	2800
0015	-0044	2840
0016	-0046	2840
0017	-0046	2900
0018	-0047	2900
0019	-0046	2900
0020	-0046	2900
0021	-0047	2900

Cons	051		Loc 46
Lat	69°	26	46 N
Long	133	02	03 W
GMT	20.3	04	xii
Depth	33 ft		

DEPTH	TEMP	SAL
0002	0002	0000
0003	-0001	0000
0004	-0001	0000
0005	-0001	0010
0006	-0002	0040
0007	-0003	0100
0008	-0007	0400
0009	-0012	0990
0010	-0023	2260
0011	-0033	2580
0012	-0042	2680
0014	-0052	2740
0016	-0054	2800
0018	-0053	2830
0020	-0053	2800
0024	-0051	2800
0030	-0051	2820
0033	-0051	2800

Cons	052		Loc 43
Lat	69°	26	12 N
Long	132°	59	13 W
GMT	22.0	04	xii
Depth	46 ft		

DEPTH	TEMP	SAL
0002	0004	0020
0004	-0001	0010
0006	-0002	0020
0007	-0003	0050
0008	-0006	0270
0009	-0009	0400
0010	-0019	2040
0011	-0023	2530
0012	-0031	2630
0014	-0044	2760
0015	-0046	2840

Cons 053 Loc 40
Lat 69° 25 05 N
Long 132° 58 33 W
GMT 22. 2 04 xii
Depth 22 ft

DEPTH	TEMP	SAL
0002	0001	0030
0004	0000	0020
0006	-0001	0100
0007	-0003	0160
0008	-0005	0330
0009	-0008	0550
0010	-0018	1960
0011	-0027	2570
0012	-0037	2700
0014	-0043	2780
0016	-0044	2800
0018	-0045	2860
0020	-0046	2890

Cons 054 Loc 40
Lat 69° 25 05 N
Long 132° 58 33 W
GMT 00. 1 05 xii
Depth 22 ft

DEPTH	TEMP	SAL
0002	0001	0000
0004	0000	0000
0006	0000	0000
0007	-0003	0040
0008	-0005	0190
0009	-0009	0650
0010	-0013	1450
0011	-0029	2430
0012	-0035	2600
0014	-0046	2780
0016	-0047	2880
0018	-0049	2900
0020	-0049	2900
0021	-0049	2900

Cons 055 Loc 43
Lat 69° 26 12 N
Long 132° 59 13 W
GMT 00. 6 05 xii
Depth 46 ft

DEPTH	TEMP	SAL
0002	-0001	0000
0004	-0001	0000
0006	-0002	0020
0007	-0002	0010
0008	-0003	0020
0009	-0010	0600
0010	-0015	1400
0011	-0038	2540
0012	-0042	2720
0014	-0048	2880
0016	-0049	2900

Cons 056 Loc 46
Lat 69° 26 46 N
Long 133° 02 03 W
GMT 01. 1 05 xii
Depth 33 ft

DEPTH	TEMP	SAL
0002	-0001	0000
0003		0000
0004	-0002	0000
0006	-0002	0020
0007	-0002	0020
0008	-0003	0040
0009	-0009	0420
0010	-0019	1500
0011	-0029	2410
0012	-0041	2600
0014	-0052	2720
0016	-0055	2760
0018	-0055	2780
0020	-0055	2780
0025	-0053	2780
0030	-0053	2800
0033	-0050	2800

Cons 057 Loc 40
Lat 69° 25 05 N
Long 132° 58 33 W
GMT 03. 7 05 xii
Depth 22 ft

DEPTH	TEMP	SAL
0004	-0001	0000
0006		0000
0007		0000
0008	-0005	0030
0009	-0010	0400
0010	-0019	1400
0011	-0033	2420
0012	-0037	2700
0014	-0039	2760
0016	-0044	2800
0020	-0049	2900

Cons 058 Loc 43
Lat 69° 26 12 N
Long 132° 59 13 W
GMT 04. 2 05 xii
Depth 46 ft

DEPTH	TEMP	SAL
0004	-0005	0000
0006	-0004	0000
0007	-0003	0000
0008	-0004	0020
0009	-0008	0060
0010	-0020	1800
0011	-0030	2410
0012	-0034	2570
0014	-0047	2820

Cons 059 Loc 46
Lat 69° 26 46 N
Long 133° 02 03 W
GMT 04. 8 05 xii
Depth 33 ft

DEPTH	TEMP	SAL
0003	-0001	0000
0004	-0002	0000
0006	-0002	0000
0007	-0003	0000
0008	-0006	0270
0009	-0015	0940
0010	-0025	2240
0011	-0037	2600
0012	-0044	2680
0014	-0053	2760
0016	-0056	2800
0018	-0056	2800
0020	-0056	2800
0025	-0055	2800

Cons 060 Loc 25
Lat 69° 24 10 N
Long 132° 58 46 W
GMT 17. 4 05 xii
Depth 34 ft

DEPTH	TEMP	SAL
0002	-0003	0080
0004	-0008	0050
0006	-0009	0100
0007	-0011	0240
0008	-0012	0320
0009	-0012	0430
0010	-0009	0920
0011	-0004	2420
0012	-0004	2610
0014	-0010	2730
0016	-0026	2770
0018	-0037	2800
0020	-0037	2820
0025	-0040	2880
0030	-0038	2900
0034	-0020	2180

Cons 061 Loc 26
Lat 69° 24 18 N
Long 132° 59 30 W
GMT 18.0 05 xii
Depth 53 ft

DEPTH	TEMP	SAL
0002	-0006	0080
0004		0070
0006		0080
0007	-0008	0220
0008		0260
0009	-0006	0520
0010	-0008	0980
0011	-0005	2410
0012	-0003	2590
0016	-0018	2760
0020	-0048	2820
0025	-0049	2870
0030	-0042	2900
0035	-0036	2900
0040	-0036	2900
0045	-0035	2900
0050	-0032	2900
0053	-0016	2260

Cons 062 Loc 42
Lat 69° 25 58 N
Long 132° 58 45 W
GMT 18.6 05 xii
Depth 69 ft

DEPTH	TEMP	SAL
0002	0006	0020
0004	-0004	0010
0006	-0004	0030
0007	-0008	0220
0008	-0009	0270
0009	-0010	0430
0010	-0013	1410
0011	-0020	2500
0012	-0021	2640
0014	-0042	2760
0016	-0053	2790
0018	-0057	2830
0020	-0059	2840
0025	-0058	2880
0029	-0053	2010

Cons 063 Loc 41
Lat 69° 25 58 N
Long 132° 59 47 W
GMT 19.2 05 xii
Depth 35 ft

DEPTH	TEMP	SAL
0002	0005	0020
0003	-0002	0010
0004	-0004	0010
0005	-0004	0010
0006	-0004	0010
0007	-0008	0200
0008	-0010	0280
0009	-0011	0490
0010	-0020	1450
0011	-0017	2450
0012	-0020	2580
0014	-0042	2720
0016	-0054	2750
0018	-0055	2770
0020	-0054	2800
0025	-0052	2860
0030	-0053	2890
0035	-0058	2210

Cons 064 Loc 47
Lat 69° 26 53 N
Long 132° 59 36 W
GMT 20.5 05 xii
Depth 15 ft

DEPTH	TEMP	SAL
0003	-0002	0000
0004	-0003	0000
0006	-0005	0010
0007	-0007	0240
0008	-0007	0280
0009	-0010	0420
0010	-0014	0710
0011	-0024	2210
0012	-0037	2620
0014	-0048	2880
0015	-0047	2900

Cons 065 Loc 39
Lat 69° 24 59 N
Long 132° 58 51 W
GMT 20. 7 05 xii
Depth 40 ft

DEPTH	TEMP	SAL
0003	-0001	0000
0004	-0002	0001
0006	-0002	0002
0007	-0004	0120
0008	-0005	0240
0009	-0007	0260
0010	-0014	1430
0011	-0032	2510
0012	-0035	2650
0014	-0043	2740
0015	-0044	2800

Cons 066 Loc 42
Lat 69° 25 58 N
Long 132° 58 45 W
GMT 21. 6 05 xii
Depth 69 ft

DEPTH	TEMP	SAL
0003	-0003	0020
0004	-0004	0020
0006	-0006	0040
0007	-0007	0170
0008	-0010	0240
0009	-0012	0520
0010	-0012	0560
0011	-0016	2530
0012	-0023	2650
0014	-0035	2730
0016	-0052	2770
0018	-0056	2800
0020	-0055	2830
0025	-0058	2870

Cons 067 Loc 41
Lat 69° 25 58 N
Long 132° 59 47 W
GMT 22. 0 05 xii
Depth 35 ft

DEPTH	TEMP	SAL
0003	-0005	0000
0004	-0004	0000
0006	-0005	0030
0007	-0008	0160
0008	-0010	0290
0009	-0011	0620
0010	-0014	1920
0011	-0017	2570
0012	-0021	2650
0014	-0036	2720
0016	-0049	2780
0018	-0056	2800
0020	-0053	2830
0025	-0051	2880

Cons 068 Loc 25
Lat 69° 24 10 N
Long 132° 58 46 W
GMT 22. 4 05 xii
Depth 34 ft

DEPTH	TEMP	SAL
0003	-0002	0070
0004	-0006	0070
0006	-0007	0110
0007	-0009	0260
0008	-0011	0330
0009	-0009	0700
0010	-0004	1710
0011	-0001	2540
0012	-0005	2690
0014	-0011	2750
0016	0000	2780
0018	-0033	2820
0020	-0045	2840
0025	-0037	2890

Cons 069 Loc 26
Lat 69° 24 18 N
Long 132° 59 30 W
GMT 22. 8 05 xii
Depth 53 ft

DEPTH	TEMP	SAL
0003	-0003	0060
0004	-0005	0060
0006	-0007	0100
0007	-0008	0240
0008	-0014	0330
0009	-0010	0820
0010	-0005	2050
0011	-0002	2570
0012	-0005	2690
0014	-0013	2750
0016	-0025	2780
0018	-0044	2820
0020	-0046	2840
0025	-0046	2900

Cons 070 Loc 32
Lat 69° 24 59 N
Long 132° 58 02 W
GMT 18. 2 07 xii
Depth 13 ft

DEPTH	TEMP	SAL
0002		0220
0003		0230
0004		0230
0005		0230
0006		0230
0007		0300
0008		0290
0009		0360
0010		1470
0011		2580
0012		2630

Cons 071 Loc 37
Lat 69° 24 58 N
Long 132° 58 04 W
GMT 18. 8 07 xii
Depth 15 ft

DEPTH	TEMP	SAL	
0002		0348	KB
0006		0239	KB
0012		1285	KB

Cons 072 Loc 37
Lat 69° 24 58 N
Long 132° 58 04 W
GMT 22. 2 07 xii
Depth 15 ft

DEPTH	TEMP	SAL
0002	-0005	0020
0004	-0006	0030
0005	-0007	0130
0006	-0008	0160
0007	-0008	0190
0008	-0008	0230
0009	-0009	0270
0010	-0018	1620
0011	-0011	2550
0012	-0017	2650
0014	-0025	2760

Cons 073 Loc 36
Lat 69° 24 59 N
Long 132° 58 01 W
GMT 23. 0 07 xii
Depth 15 ft

DEPTH	TEMP	SAL
0002	-0008	0020
0003	-0006	0030
0004	-0006	0040
0005	-0008	0060
0006	-0008	0160
0007	-0008	0200
0008	-0012	0270
0009	-0010	0520
0010	-0018	1650
0011	-0009	2590
0012	-0016	2650
0014	-0028	2760
0015	-0011	1090

Cons	074		Loc 31
Lat	69°	24	58 N
Long	132°	58	06 W
GMT	23. 1	07	xii
Depth	18 ft		

DEPTH	TEMP	SAL
0002	-0006	0020
0003	-0007	0030
0004	-0006	0020
0005	-0007	0030
0006	-0008	0170
0007	-0008	0190
0008	-0008	0270
0009	-0009	0500
0010	-0018	1890
0011	-0008	2580
0012	-0017	2670
0014	-0038	2780
0016	-0048	2800
0018	-0049	2810

Cons	075		Loc 29
Lat	69°	24	53 N
Long	132°	58	35 W
GMT	23. 5	07	xii
Depth	64 ft		

DEPTH	TEMP	SAL	
0006		0157	KB
0012		2706	
0018		2850	
0024		2932	
0030		2954	
0048		2975	

Cons	076		Loc 033
Lat	69°	24	58 N
Long	132°	58	05 W
GMT	00. 5	08	xii
Depth	23 ft		

DEPTH	TEMP	SAL
0002	– 0008	0340
0003	– 0008	0260
0004	– 0008	0220
0006	– 0008	0260
0007	– 0008	0250
0008	– 0008	0260
0009	– 0011	1050
0010	– 0017	2300
0011	– 0009	2640
0012	– 0018	2680

Cons	077		Loc 28
Lat	69°	24	43 N
Long	132°	58	37 W
GMT	00. 8	08	xii
Depth	85 ft		

DEPTH	TEMP	SAL
0002	-0006	0040
0003	-0006	0040
0004	-0007	0050
0005	-0007	0040
0006	-0009	0080
0007	-0011	0370
0008	-0009	0730
0009	-0005	2250
0010	-0004	2610
0011	-0005	2720
0012	-0011	2770
0014	-0028	2820
0016	-0038	2810
0018	-0050	2860
0020	-0063	2880
0025	-0058	2900
0030	-0067	2900
0035	-0044	2900
0040	-0065	2900
0045	-0067	2900
0050	-0067	2920
0055	-0067	2910
0060	-0065	2920
0065	-0063	2900
0070	-0059	2920

Cons 078 Loc 24
Lat 69° 23 45 N
Long 132° 59 23 W
GMT 17.8 08 xii
Depth 35 ft

DEPTH	TEMP	SAL
0003	-0007	0070
0005	-0008	0080
0006	-0009	0100
0007	-0010	0260
0008	-0011	0360
0009	-0009	0660
0010	-0004	2360
0011	-0003	2630
0012	-0006	2740
0014	-0016	2790
0016	-0011	2810
0018	-0035	2840
0020	-0031	2870
0025	-0038	2900
0030	-0023	2900
0035	-0021	2400

Cons 079 Loc 28
Lat 69° 24 43 N
Long 132° 58 37 W
GMT 19.4 08 xii
Depth 85 ft

DEPTH	TEMP	SAL
0003	-0005	0030
0005	-0007	0040
0006	-0007	0030
0007	-0008	0130
0008	-0009	0230
0009	-0010	0420
0010	-0014	1400
0011	-0005	2570
0012	-0007	2680
0014	-0030	2750
0016	-0040	2790
0018	-0059	2850
0020	-0065	2860
0025	-0061	2900
0030	-0061	2900
0035	-0049	2900
0040	-0061	2900

Cons 080 Loc 42
Lat 69° 25 58 N
Long 132° 58 45 W
GMT 19.8 08 xii
Depth 69 ft

DEPTH	TEMP	SAL
0003	-0005	0020
0005	-0005	0020
0006	-0005	0050
0007	-0006	0080
0008	-0007	0170
0009	-0007	0440
0010	-0014	1290
0011	-0020	2500
0012	-0028	2680
0014	-0043	2760
0016	-0053	2790
0018	-0053	2830
0020	-0053	2870
0025	-0058	2890
0028	-0049	2900

Cons 081 Loc 49
Lat 69° 38 10 N
Long 133° 14 20 W
GMT 19.0 09 xii
Depth 14 ft

DEPTH	TEMP	SAL
0003	-0002	0000
0004	-0003	0000
0005	-0004	0010
0006	-0004	0010
0007	-0004	0000
0008	-0004	0000
0009	-0003	0000
0010	0002	0005
0011	0010	2460
0012	-0005	2820
0013	-0028	2880
0014	-0020	2900

N R C Programme

Phase III

Serial data

Consecutive numbers 1 to 29

C R N 449

Cons 001 Loc 51
Lat 69° 24 58 N
Long 132° 58 04 W
GMT 20. 5 14 xii
Depth 15 ft

DEPTH	TEMP	SAL
0002		2478
0006		0229
0012		0223

Cons 002 Loc 50
Lat 69° 24 57 N
Long 132° 58 27 W
GMT 21. 8 14 xii
Depth 64 ft

DEPTH	TEMP	SAL
0006		2965
0012		2934
0018		2890
0024		2790
0030		2370
0048		0098

Cons 003 Loc 51
Lat 69° 24 58 N
Long 132° 58 04 W
GMT 21. 0 24 xii
Depth 15 ft

DEPTH	TEMP	SAL
0002		0081
0006		0088
0012		

Cons 004 Loc 50
Lat 69° 24 57 N
Long 132° 58 27 W
GMT 22. 3 24 xii
Depth 64 ft

DEPTH	TEMP	SAL
0006		2744
0012		0071
0018		0301
0024		2838
0030		2907
0048		2979

Cons 005 Loc 50
Lat 69° 24 57 N
Long 132° 58 27 W
GMT 21. 5 01 i 63
Depth 64 ft

DEPTH	TEMP	SAL
0006		0079
0012		0247
0018		2716
0024		2834
0030		
0048		3011

Cons 006 Loc 51
Lat 69° 24 58 N
Long 132° 58 04 W
GMT 22. 9 01 i
Depth 15 ft

DEPTH	TEMP	SAL
0002		0220
0006		0170
0012		0239

Cons 007 Loc 50
Lat 69° 24 57 N
Long 132° 58 27 W
GMT 23. 0 10 i
Depth 64 ft

DEPTH	TEMP	SAL
0006		0084
0012		0105
0018		2543
0024		2733
0030		2858
0048		2961

Cons 008 Loc 51
Lat 69° 24 58 N
Long 132° 58 04 W
GMT 00. 1 11 i
Depth 15 ft

DEPTH	TEMP	SAL
0002		0194
0012		0162

Cons	009	Loc 50	
Lat	69°	24	57 N
Long	132°	58	27 W
GMT	20.0	18	i
Depth	64 ft		

DEPTH	TEMP	SAL
0006		0086
0012		0092
0018		2479
0024		2704
0030		2841
0048		2967

Cons	010	Loc 51	
Lat	69°	24	58 N
Long	132°	58	04 W
GMT	20.8	18	i
Depth	15 ft		

DEPTH	TEMP	SAL
0002		0173
0006		0164
0012		0169

Cons	011	Loc 050	
Lat	69°	24	57 N
Long	132°	58	27 W
GMT	21.0	27	i
Depth	64 ft		

DEPTH	TEMP	SAL
0006		0092
0012		0107
0018		2799
0024		2921
0030		2629
0048		3032

Cons	012	Loc 51	
Lat	69°	24	58 N
Long	132°	58	04 W
GMT	23.0	27	i
Depth	15 ft		

DEPTH	TEMP	SAL
0002		0186
0006		0168
0012		0159

Cons	013	Loc 50	
Lat	69°	24	57 N
Long	132°	58	27 W
GMT	21.2	07	ii
Depth	64 ft		

DEPTH	TEMP	SAL
0006		0072
0012		0173
0018		2489
0024		2678
0030		2849
0048		2960

Cons	014	Loc 51	
Lat	69°	24	58 N
Long	132°	58	04 W
GMT	23.0	07	ii
Depth	15 ft		

DEPTH	TEMP	SAL
0002		0117
0006		0121
0012		0127

Cons	015	Loc 50	
Lat	69°	24	57 N
Long	132°	58	27 W
GMT	21.2	11	ii
Depth	64 ft		

DEPTH	TEMP	SAL
0006		0091
0012		0099
0018		2711
0024		2610
0030		2754
0048		2964

Cons	016	Loc 51	
Lat	69°	24	58 N
Long	132°	58	04 W
GMT	23.0	11	ii
Depth	15 ft		

DEPTH	TEMP	SAL
0002		0141
0006		0140
0012		0136

Cons 017 Loc 50
Lat 69° 24 57 N
Long 132° 58 27 W
GMT 20. 0 24 ii
Depth 64 ft

DEPTH	TEMP	SAL
0006		0075
0012		0088
0018		2502
0024		2702
0030		2856
0048		2666

Cons 018 Loc 51
Lat 69° 24 58 N
Long 132° 58 04 W
GMT 21. 5 24 ii
Depth 15 ft

DEPTH	TEMP	SAL
0002		0129
0006		0126
0012		0123

Cons 019 Loc 51
Lat 69° 24 58 N
Long 132° 58 04 W
GMT 20. 8 07 iii
Depth 15 ft

DEPTH	TEMP	SAL
0002		0094
0006		0089
0012		0099

Cons 020 Loc 50
Lat 69° 24 57 N
Long 132° 58 27 W
GMT 00. 5 08 iii
Depth 64 ft

DEPTH	TEMP	SAL
0006		0067
0012		0084
0018		2234
0024		2723
0030		2877
0048		2958

Cons 021 Loc 50
Lat 69° 24 57 N
Long 132° 58 27 W
GMT 21. 5 17 iii
Depth 64 ft

DEPTH	TEMP	SAL
0006		0084
0012		0083
0018		2158
0024		2642
0030		2810
0048		2970

Cons 022 Loc 51
Lat 69° 24 58 N
Long 132° 58 04 W
GMT 00. 0 18 iii
Depth 15 ft

DEPTH	TEMP	SAL
0002		0096
0006		0093
0012		0089

Cons 023 Loc 50
Lat 69° 24 57 N
Long 132° 58 27 W
GMT 21. 8 25 iii
Depth 64 ft

DEPTH	TEMP	SAL
0006		0067
0012		0071
0018		0205
0024		0265
0030		2782
0048		2931

Cons 024 Loc 51
Lat 69° 24 58 N
Long 132° 58 27 W
GMT 23. 2 25 iii
Depth 15 ft

DEPTH	TEMP	SAL
0002		0065
0006		0075
0012		0067

Cons	025	Loc 50	
Lat	69°	24	57 N
Long	132°	58	27 W
GMT	21. 8	03	iv
Depth	64 ft		

DEPTH	TEMP	SAL
0006		0091
0012		0078
0018		0546
0024		2588
0030		2819
0048		2919

Cons	026	Loc 50	
Lat	69°	24	57 N
Long	132°	58	27 W
GMT	21. 5	09	iv
Depth	64 ft		

DEPTH	TEMP	SAL
0006		0077
0012		0072
0018		0414
0024		0129
0030		2741
0048		2931

Cons	027	Loc 51	
Lat	69°	24	58 N
Long	132°	58	04 W
GMT	22. 3	09	iv
Depth	15 ft		

DEPTH	TEMP	SAL
0002		0074
0006		0068
0012		0068

Cons	028	Loc 50	
Lat	69°	24	57 N
Long	132°	58	27 W
GMT	17. 3	01	v
Depth	64 ft		

DEPTH	TEMP	SAL
0006		0085
0012		0080
0018		0342
0024		2623
0030		2834
0048		2956

Cons	029	Loc 51	
Lat	69°	24	58 N
Long	132°	58	04 W
GMT	17. 9	01	v
Depth	15 ft		

DEPTH	TEMP	SAL
0002		0107
0006		0087
0012		0087

NRC Programme

Phase IV

Serial data

Consecutive numbers 1 to 9

(Time-series study Locations 52 to 58)

CRN 13 - 63 - 004

Cons	001		Loc 55
Lat	69°	26	12 N
Long	132°	59	13 W
GMT	16. 8	02	v
Depth	45 ft		

DEPTH	TEMP	SAL
0006	-0005	0000
0008	-0003	0000
0010	-0003	0000
0012	-0002	0000
0014	-0002	0020
0016	-0002	0020
0017	-0002	0050
0018	-0002	0040
0019	-0001	0060
0020	0000	1920
0021	0001	2140
0022	0002	2420
0023	0001	2500
0024	-0001	2600
0025	-0004	2650
0027	-0008	2750
0030	-0020	2880
0035	-0030	2900
0040	-0033	2900
0045	-0034	2900

Cons	002		Loc 55
Lat	69°	26	12 N
Long	132°	59	13 W
GMT	18. 2	02	v
Depth	45 ft		

DEPTH	TEMP	SAL
0006	-0003	0000
0008	-0003	
0010	-0003	
0012	-0003	
0014	-0003	0020
0016	-0003	0040
0017	-0003	0040
0018	-0002	0040
0019	-0001	0400
0020	0001	2200
0021	0002	2410
0022	0001	2510
0023	0000	2590
0024	-0003	2690
0025	-0006	2740
0027	-0013	2820
0030	-0021	2870
0035	-0030	2900
0040	-0034	2900
0045	-0034	2900

Cons	003		Loc 55
Lat	69°	26	12 N
Long	132°	59	13 W
GMT	19. 8	02	v
Depth	45 ft		

DEPTH	TEMP	SAL
0006	0009	0000
0008	-0002	0000
0010	-0002	0000
0012	-0002	0020
0014	-0003	0040
0016	-0002	0040
0017	-0002	0040
0018	-0002	0040
0019	-0001	0260
0020	0000	0270
0021	0001	2270
0022	0002	2440
0023	0000	2580
0024	-0002	2660
0025	-0006	2740
0027	-0013	2820
0030	-0021	2870
0035	-0029	2900
0040	-0033	2900
0045	-0034	2900

Cons	004		Loc 55
Lat	69°	26	12 N
Long	132°	59	13 W
GMT	20. 8	02	v
Depth	45 ft		

DEPTH	TEMP	SAL
0006	-0003	0000
0008	-0003	0000
0010	-0003	0000
0012	-0003	0020
0014	-0003	0030
0016	-0003	0020
0017	-0003	0030
0018	-0002	0040
0019	-0001	0870
0020	0001	2210
0021	0002	2410
0022	0001	2470
0023	-0001	2570
0024	-0003	2660
0025	-0006	2740
0027	-0014	2850
0030	-0018	2880
0035	-0026	2900
0040	-0033	2900
0045	-0034	2900

Cons	005		Loc 55
Lat	69°	26	12 N
Long	132°	59	13 W
GMT	21. 2	02	v
Depth	45 ft		

DEPTH	TEMP	SAL
0006	-0003	0000
0007	-0003	0000
0008	-0004	0000
0010	-0002	0000
0012	-0003	0010
0014	-0002	0030
0016	-0002	0040
0017	-0002	0040
0018	-0001	0040
0019	-0001	0810
0020	0001	2250
0021	0002	2410
0022	0001	2530
0023	-0001	2600
0024	-0003	2650
0025	-0006	2760
0027	-0013	2810
0030	-0021	2880
0035	-0029	2900
0040	-0033	2900
0045	-0034	2900

Cons	006		Loc 55
Lat	69°	26	12 N
Long	132°	59	13 W
GMT	00. 2	03	v
Depth	45 ft		

DEPTH	TEMP	SAL
0006	0000	0000
0008	-0003	0000
0010	-0003	0000
0012	-0003	0020
0014	-0003	0030
0016	-0002	0040
0017	-0002	0030
0018	-0002	0040
0019	0000	1300
0020	0001	2240
0021	0002	2350
0022	0001	2470
0023	-0001	2620
0024	-0004	2660
0025	-0006	2730
0027	-0013	2800
0030	-0022	2890
0035	-0028	2900
0040	-0032	2900
0045	-0034	2900

Cons	007	Loc 55	
Lat	69°	26	12 N
Long	132°	59	13 W
GMT	01. 8	03	v
Depth	45 ft		

DEPTH	TEMP	SAL
0006	-0002	0000
0008	-0002	0000
0010	-0003	0000
0012	-0002	0000
0014	-0002	0010
0016	-0002	0000
0017	-0002	0000
0018	-0002	0050
0019	0000	1420
0020	0002	2230
0021	0002	2330
0022	0001	2440
0023	0000	2590
0024	-0004	2650
0025	-0006	2700
0027	-0012	2800
0030	-0020	2870
0035	-0029	2900
0040	-0032	2900
0045	-0034	2900

Cons	008	Loc 55	
Lat	69°	26	12 N
Long	132°	59	13 W
GMT	03. 2	03	v
Depth	45 ft		

DEPTH	TEMP	SAL
0006	-0003	0000
0008	-0003	0000
0010	-0003	0000
0012	-0002	0020
0014	-0002	0020
0016	-0002	0040
0017	-0002	0040
0018	-0002	0040
0019	0000	0570
0020	0001	2130
0021	0001	2300
0022	0002	2530
0023	0000	2600
0024	-0002	2630
0025	-0005	2720
0027	-0011	2810
0030	-0020	2860
0035	-0028	2900
0040	-0033	2900
0045	-0034	2900

Cons 009 Loc 55
Lat 69° 26 12 N
Long 132° 59 13 W
GMT 04. 8 03 v
Depth 45 ft

DEPTH	TEMP	SAL
0006	-0003	0000
0008	-0003	0000
0010	-0002	0000
0012	-0002	0020
0014	-0002	0030
0016	-0002	0040
0017	-0002	0040
0018	-0002	0040
0019	-0001	0060
0020	0001	2060
0021	0002	2270
0022	0002	2460
0023	0000	2580
0024	-0002	2650
0025	-0005	2700
0027	-0011	2750
0030	-0020	2830
0035	-0030	2900
0040	-0033	2900
0045	-0034	2900

Cons 001 Loc 52
Lat 69° 23 45 N
Long 132° 59 23 W
GMT 16. 8 02 v
Depth 29 ft

DEPTH	TEMP	SAL
0006	-0009	0092
0008	-0010	0092
0010	-0010	0092
0012	-0010	0104
0014	-0010	0104
0016	-0011	0112
0017	-0011	0112
0018	-0012	0128
0019	-0019	1112
0020	-0123	2456
0021	-0114	2540
0022	-0067	2672
0023	-0005	2776
0024	0000	2844
0025	-0001	2904
0027	-0004	2968
0029	-0005	2960

Cons 002 Loc 52
Lat 69° 23 45 N
Long 132° 59 23 W
GMT 18. 2 02 v
Depth 29 ft

DEPTH	TEMP	SAL
0006	-0005	0056
0008	-0007	0080
0010	-0007	0092
0012	-0007	0092
0014	-0007	0096
0016	-0007	0104
0017	-0007	0104
0018	-0006	0120
0019	-0006	0192
0020	0002	2356
0021	0004	2520
0022	0004	2592
0023	0003	2692
0024	0001	2776
0025	-0001	2868
0027	-0003	2924
0029	-0006	2976

Cons 003 Loc 52
Lat 69° 23 45 N
Long 132° 59 23 W
GMT 19. 8 02 v
Depth 29 ft

DEPTH	TEMP	SAL
0006	0051	0080
0008	-0006	0084
0010	-0006	0088
0012	-0006	0088
0014	-0006	0100
0016	-0006	0108
0017	-0006	0120
0018	-0006	0124
0019	-0004	0432
0020	0001	2348
0021	0004	2568
0022	0005	2624
0023	0003	2704
0024	0002	2772
0025	0001	2884
0027	-0001	2904
0029	-0005	2960

Cons 004 Loc 52
Lat 69° 23 45 N
Long 132° 59 23 W
GMT 21. 2 02 v
Depth 29 ft

DEPTH	TEMP	SAL
0006	-0006	0084
0008	-0008	0112
0010	-0009	0120
0012	-0010	0128
0014	-0010	0128
0016	-0010	0128
0017	-0011	0132
0018	-0012	0136
0019	-0031	0700
0020	-0072	2508
0021	-0053	2584
0022	-0033	2676
0023	-0004	2764
0024	0001	2840
0025	0000	2844
0027	-0003	2924
0029	-0006	2980

Cons 005 Loc 52
Lat 69° 23 45 N
Long 132° 59 23 W
GMT 22. 8 02 v
Depth 29 ft

DEPTH	TEMP	SAL
0006	0017	0076
0008	-0004	0100
0010	-0006	0100
0012	-0006	0108
0014	-0006	0120
0016	-0006	0124
0017	-0007	0128
0018	-0006	0136
0019	-0002	1940
0020	0002	2456
0021	0005	2604
0022	0004	2672
0023	0002	2788
0024	0001	2848
0025	-0001	2888
0027	-0003	2988
0029	-0007	2984

Cons 006 Loc 52
Lat 69° 23 45 N
Long 132° 59 23 W
GMT 00. 2 03 v
Depth 29 ft

DEPTH	TEMP	SAL
0006	-0006	0092
0008	-0001	0092
0010	-0005	0100
0012	-0006	0108
0014	-0007	0112
0016	-0007	0116
0017	-0006	0128
0018	-0006	0140
0019	0000	2328
0020	0004	2564
0021	0005	2584
0022	0002	2764
0023	0001	2788
0024	0000	2860
0025	-0001	2932
0027	-0005	2960
0029	-0007	2960

Cons 007 Loc 52
Lat 69° 23 45 N
Long 132° 59 23 W
GMT 01. 8 03 v
Depth 29 ft

DEPTH	TEMP	SAL
0006	0032	0092
0008	-0004	0112
0010	-0005	0116
0012	-0006	0116
0014	-0007	0124
0016	-0007	0132
0017	-0006	0140
0018	-0006	0148
0019	0001	2400
0020	0004	2532
0021	0005	2624
0022	0004	2724
0023	0001	2804
0024	0000	2864
0025	-0002	2932
0027	-0004	2976
0029	-0007	2988

Cons 008 Loc 52
Lat 69° 23 45 N
Long 132° 59 23 W
GMT 03. 2 03 v
Depth 29 ft

DEPTH	TEMP	SAL
0006	-0003	0116
0008	-0007	0120
0010	-0009	0128
0012	-0009	0128
0014	-0008	0128
0016	-0009	0132
0017	-0010	0152
0018	-0010	0164
0019	-0065	2444
0020	-0050	2588
0021	-0049	2680
0022	-0006	2772
0023	-0000	2860
0024	-0001	2884
0025	-0002	2928
0027	-0004	3000
0029	-0006	3052

Cons	009		Loc 52
Lat	69°	23	45 N
Long	132°	59	23 W
GMT	04. 8	03	v
Depth	29 ft		

DEPTH	TEMP	SAL
0006	-0002	0132
0008	-0007	0132
0010	-0008	0136
0012	-0008	0144
0014	-0009	0152
0016	-0007	0160
0017	-0007	0168
0018	-0006	0176
0019	-0002	1620
0020	0002	2580
0021	0003	2652
0022	0002	2808
0023	0002	2844
0024	0000	2940
0025	-0001	2968
0027	-0003	3040
0029	-0008	3048

Cons 001 Loc 54
Lat 69° 25 05 N
Long 132° 58 33 W
GMT 16.1 02 v
Depth 24 ft

DEPTH	TEMP	SAL
0006	-0005	0000
0008	-0004	0000
0010	-0005	0000
0012	-0004	0020
0014	-0004	0000
0016	-0004	0000
0017	-0004	0000
0018	-0003	0000
0019	-0002	0080
0020	-0001	1950
0021	0001	2340
0022	0001	2440
0023	0000	2530
0024	-0002	2600

Cons 002 Loc 54
Lat 69° 25 05 N
Long 132° 58 33 W
GMT 17.6 02 v
Depth 24 ft

DEPTH	TEMP	SAL
0006	-0003	0000
0008	-0003	0000
0010	-0004	0000
0012	-0004	0000
0014	-0004	0000
0016	-0003	0002
0017	-0003	0003
0018	-0001	0003
0019	-0002	0270
0020	0001	2220
0021	0003	2360
0022	0001	2480
0023	-0002	2620
0024	-0004	2670

Cons 003 Loc 54
Lat 69° 25 05 N
Long 132° 58 33 W
GMT 17.6 02 v
Depth 24 ft

DEPTH	TEMP	SAL
0006	0000	0000
0008	0001	0000
0010	-0004	0000
0012	-0004	0000
0014	-0004	0002
0016	-0004	0002
0017	-0003	0005
0018	-0002	0005
0019	-0001	0380
0020	0000	2210
0021	0001	2380
0022	0000	2510
0023	-0002	2610
0024	-0004	2670

Cons 004 Loc 54
Lat 69° 25 05 N
Long 132° 58 33 W
GMT 20.5 02 v
Depth 24 ft

DEPTH	TEMP	SAL
0006	-0004	0000
0008	-0004	0000
0010	-0005	0000
0012	-0004	0020
0014	-0004	0030
0016	-0002	0060
0017	-0002	0050
0018	-0002	0050
0019	-0001	0190
0020	0000	0220
0021	0001	0240
0022	0000	2460
0023	-0002	2600
0024	-0004	2670

Cons 005 Loc 54
Lat 69° 25 05 N
Long 132° 58 33 W
GMT 22.0 02 v
Depth 24 ft

DEPTH	TEMP	SAL
0006	-0005	0000
0008	-0005	0000
0010	-0005	0000
0012	-0004	0000
0014	-0003	0000
0016	-0002	0005
0017	-0002	0004
0018	-0002	0004
0019	-0002	0004
0020	0000	2230
0021	0001	2360
0022	0000	2520
0023	-0002	2590
0024	-0005	2680

Cons 006 Loc 54
Lat 69° 25 05 N
Long 132° 58 33 W
GMT 23.5 02 v
Depth 24 ft

DEPTH	TEMP	SAL
0006	-0004	0000
0008	-0004	0000
0010	-0004	0000
0012	-0004	0020
0014	-0004	0020
0016	-0003	0030
0017	-0003	0030
0018	-0003	0030
0019	-0001	1440
0020	0000	2310
0021	0001	2400
0022	0000	2520
0023	-0002	2640
0024	-0004	2650

Cons 007 Loc 54
Lat 69° 25 05 N
Long 132° 58 33 W
GMT 01.0 03 v
Depth 24 ft

DEPTH	TEMP	SAL
0006	-0003	0000
0008	-0003	0000
0010	-0003	0000
0012	-0003	0000
0014	-0004	0010
0016	-0004	0030
0017	-0002	0040
0018	-0002	0030
0019	-0001	1550
0020	0001	2320
0021	0001	2380
0022	0000	2520
0023	-0003	2590
0024	-0005	2700

Cons 008 Loc 54
Lat 69° 25 05 N
Long 132° 58 33 W
GMT 02.5 03 v
Depth 24 ft

DEPTH	TEMP	SAL
0006	-0004	0000
0008	-0003	0000
0010	-0003	0000
0012	-0003	0000
0014	-0003	0030
0016	-0003	0040
0017	-0002	0030
0018	-0005	0050
0019	0000	1270
0020	0001	2270
0021	0001	2370
0022	0000	2460
0023	-0002	2580
0024	-0004	2650

Cons	009		Loc 54
Lat	69°	25	05 N
Long	132°	58	33 W
GMT	04.0	03	v
Depth	24 ft		

DEPTH	TEMP	SAL
0006	-0004	0000
0008	-0004	0000
0010	-0004	0000
0012	-0004	0020
0014	-0004	0020
0016	-0004	0030
0017	-0004	0040
0018	-0002	0060
0019	-0001	0580
0020	0001	2240
0021	0001	2380
0022	0000	2520
0023	-0002	2570
0024	-0004	2680

Cons	001		Loc 53
Lat	69°	24	59 N
Long	132°	58	51 W
GMT	16.1	02	v
Depth	43 ft		

DEPTH	TEMP	SAL
0006	-0009	0100
0008	-0009	0100
0010	-0009	0112
0012	-0009	0112
0014	-0008	0120
0016	-0007	0132
0017	-0006	0140
0018	-0006	0152
0019	-0004	1612
0020	-0004	2532
0021	-0004	2624
0022	-0005	2744
0023	-0007	2784
0024	-0010	2856
0025	-0012	2940
0027	-0019	3000
0030	-0026	3056
0035	-0033	3080
0040	-0037	3080
0042	-0037	3088

Cons	002		Loc 53
Lat	69°	24	59 N
Long	132°	58	51 W
GMT	17.5	02	v
Depth	43 ft		

DEPTH	TEMP	SAL
0006	-0009	0076
0008	-0009	0088
0010	-0009	0088
0012	-0009	0096
0014	-0008	0108
0016	-0007	0132
0017	-0006	0124
0018	-0006	0132
0019	-0005	0632
0020	-0004	2436
0021	-0004	2560
0022	-0004	2620
0023	-0007	2748
0024	-0010	2808
0025	-0013	2856
0027	-0019	2960
0030	-0026	2972
0035	-0034	3032
0040	-0037	3052
0042	-0038	3052

Cons 003 Loc 53
Lat 69° 24 59 N
Long 132° 58 51 W
GMT 19.0 02 v
Depth 43 ft

DEPTH	TEMP	SAL
0006	0005	0084
0008	-0008	0092
0010	-0009	0096
0012	-0009	0096
0014	-0008	0100
0016	-0007	0104
0017	-0005	0104
0018	-0005	0112
0019	-0008	0200
0020	-0008	2376
0021	-0003	2528
0022	-0004	2640
0023	-0006	2732
0024	-0008	2752
0025	-0010	2868
0027	-0019	2960
0030	-0027	2988
0035	-0034	3020
0040	-0037	3024
0042	-0038	3020

Cons 004 Loc 53
Lat 69° 24 59 N
Long 132° 58 51 W
GMT 20.5 02 v
Depth 43 ft

DEPTH	TEMP	SAL
0006	-0002	0080
0008	-0007	0092
0010	-0009	0092
0012	-0008	0092
0014	-0007	0120
0016	-0007	0120
0017	-0007	0120
0018	-0006	0124
0019	-0005	0712
0020	-0005	2456
0021	-0005	2560
0022	-0004	2644
0023	-0009	2736
0024	-0006	2816
0025	-0011	2872
0027	-0019	2936
0030	-0024	2980
0035	-0033	3020
0040	-0037	3048
0043	-0037	3048

Cons 005 Loc 53
Lat 69° 24 59 N
Long 132° 58 51 W
GMT 22.0 02 v
Depth 43 ft

DEPTH	TEMP	SAL
0006	-0006	0116
0008	-0008	0124
0010	-0009	0112
0012	-0008	0120
0014	-0007	0124
0016	-0006	0132
0017	-0006	0132
0018	-0006	0152
0019	-0004	2036
0020	-0004	2496
0021	-0004	2608
0022	-0004	2664
0023	-0006	2788
0024	-0010	2848
0025	-0012	2936
0027	-0019	3008
0030	-0025	3004
0035	-0033	3024
0040	-0036	3024
0042	-0037	3024

Cons 006 Loc 53
Lat 69° 24 59 N
Long 132° 58 51 W
GMT 23.5 02 v
Depth 43 ft

DEPTH	TEMP	SAL
0006	0019	0088
0008	0005	0088
0010	-0008	0088
0012	-0008	0088
0014	-0008	0108
0016	-0006	0116
0017	-0006	0124
0018	-0006	0160
0019	-0004	2244
0020	-0003	2516
0021	-0004	2624
0022	-0006	2696
0023	-0007	2760
0024	-0010	2832
0025	-0012	2864
0027	-0018	2920
0030	-0026	2972
0035	-0033	3020
0040	-0036	3028
0042	-0037	3028

Cons	007	Loc 53	
Lat	69°	24	59 N
Long	132°	58	51 W
GMT	01. 1	03	v
Depth	43 ft		

DEPTH	TEMP	SAL
0006	-0008	0088
0008	-0007	0092
0010	-0008	0104
0012	-0008	0104
0014	-0008	0104
0016	-0006	0128
0017	-0006	0136
0018	-0005	0152
0019	-0005	2220
0020	-0005	2544
0021	-0005	2612
0022	-0006	2728
0023	-0008	2768
0024	-0011	2828
0025	-0011	2856
0027	-0019	2960
0030	-0026	2980
0035	-0034	3000
0040	-0037	3012
0042	-0037	3016

Cons	008	Loc 53	
Lat	69°	24	59 N
Long	132°	58	51 W
GMT	02. 5	03	v
Depth	43 ft		

DEPTH	TEMP	SAL
0006	-0006	0124
0008	-0008	0124
0010	-0009	0132
0012	-0009	0132
0014	-0009	0132
0016	-0008	0152
0017	-0008	0156
0018	-0005	0184
0019	-0005	2088
0020	-0012	2560
0021	-0008	2656
0022	-0006	2752
0023	-0009	2824
0024	-0012	2888
0025	-0015	2948
0027	-0019	3008
0030	-0027	3040
0035	-0034	3068
0040	-0036	3080
0042	-0037	3080

Cons	009	Loc 53	
Lat	69°	24	59 N
Long	132°	58	51 W
GMT	4.0	03	v
Depth	43 ft		

DEPTH	TEMP	SAL
0006	-0009	0116
0008	-0009	0120
0010	-0009	0120
0012	-0010	0120
0014	-0010	0136
0016	-0010	0144
0017	-0009	0148
0018	-0007	0156
0019	-0003	2104
0020	-0006	2572
0021	-0005	2604
0022	-0006	2728
0023	-0010	2828
0024	-0012	2892
0025	-0014	2952
0027	-0019	2992
0030	-0026	3040
0035	-0035	3044
0040	-0037	3068
0042	-0038	3068

Cons 001 Loc 57
Lat 69° 26 53 N
Long 132° 59 36 W
GMT 15. 5 04 v
Depth 21 ft

DEPTH	TEMP	SAL
0006	-0003	0000
0008	-0003	0000
0010	-0002	0000
0012	-0002	0000
0014	-0002	0020
0016	-0002	0000
0017	-0002	0020
0018	0000	1420
0019	0001	2220
0020	0002	2300

Cons 002 Loc 57
Lat 69° 26 53 N
Long 132° 59 36 W
GMT 17. 0 04 v
Depth 21 ft

DEPTH	TEMP	SAL
0006	-0002	0000
0008	-0002	0000
0010	-0002	0000
0012	-0002	0000
0014	-0002	0010
0016	-0002	0010
0017	-0002	0020
0018	-0002	0040
0019	-0002	0180
0020	0000	1830
0021	0001	2280

Cons 003 Loc 57
Lat 69° 26 53 N
Long 132° 59 36 W
GMT 18. 3 04 v
Depth 21 ft

DEPTH	TEMP	SAL
0006	-0001	0000
0008	-0001	0000
0010	-0002	0000
0012	-0002	0000
0014	-0002	0000
0016	-0002	0000
0017	-0002	0020
0018	-0002	0020
0019	-0002	0060
0020	-0002	0340
0021	0001	2400

Cons 004 Loc 57
Lat 69° 26 53 N
Long 132° 59 36 W
GMT 20. 0 04 v
Depth 21 ft

DEPTH	TEMP	SAL
0006	-0001	0000
0008	-0001	0000
0010	-0002	0000
0012	-0002	0000
0014	-0002	0000
0016	-0002	0010
0017	-0002	0030
0018	-0002	0070
0019	-0002	0220
0020	0000	2120
0021	0001	2380

Cons 005 Loc 57
Lat 69° 26 53 N
Long 132° 59 36 W
GMT 21.5 04 v
Depth 21 ft

DEPTH	TEMP	SAL
0006	-0001	0000
0008	0000	0000
0010	-0002	0000
0012	-0002	0000
0014	-0002	0000
0016	-0001	0030
0017	-0002	0100
0018	-0002	0250
0019	0000	2140
0020	0001	2460
0021	0000	2660

Cons 006 Loc 57
Lat 69° 26 53 N
Long 132° 59 36 W
GMT 23.0 04 v
Depth 21 ft

DEPTH	TEMP	SAL
0006	-0002	0000
0008	-0002	0000
0010	-0002	0000
0012	-0002	0000
0014	-0002	0000
0016	-0002	0000
0017	-0002	0000
0018	-0002	0080
0019		1940
0020		2470
0021		2660

Cons 007 Loc 57
Lat 69° 26 53 N
Long 132° 59 36 W
GMT 00.5 05 v
Depth 21 ft

DEPTH	TEMP	SAL
0006	-0002	0000
0008	-0002	0000
0010	-0002	0000
0012	-0002	0000
0014	-0002	0000
0016	-0002	0000
0017	-0002	0000
0018	-0001	0130
0019	0000	2200
0020	0000	2420
0021	0001	2500

Cons 008 Loc 57
Lat 69° 26 53 N
Long 132° 59 36 W
GMT 02.0 05 v
Depth 21 ft

DEPTH	TEMP	SAL
0006	-0002	0000
0008	-0002	0000
0010	-0002	0000
0012	-0002	0000
0014	-0002	0000
0016	-0002	0000
0017	-0002	0000
0018	-0001	0000
0019	-0001	0820
0020	0000	1840
0021	0002	2040

Cons	009	Loc 57	
Lat	69°	26	53 N
Long	132°	59	36 W
GMT	03. 5	05	v
Depth	21 ft		

DEPTH	TEMP	SAL
0006	-0002	0000
0008	-0002	0000
0010	-0002	0000
0012	-0002	0000
0014	-0002	0000
0016	-0002	0000
0017	-0002	0000
0018	-0002	0000
0019	0000	1340
0020	0000	1800
0021	0001	1980

Cons	001	Loc 58	
Lat	69°	26	54 N
Long	132°	59	30 W
GMT	15. 5	04	v
Depth	13 ft		

DEPTH	TEMP	SAL
0006	-0007	0164
0007	-0007	0168
0008	-0007	0168
0009	-0007	0176
0010	-0007	0176
0011	-0006	0184
0012	-0006	0184
0013	-0006	0188

Cons	002	Loc 58	
Lat	69°	26	54 N
Long	132°	59	30 W
GMT	17. 0	04	v
Depth	13 ft		

DEPTH	TEMP	SAL
0006	-0007	0112
0007	-0007	0112
0008	-0007	0112
0009	-0007	0132
0010	-0007	0132
0011	-0007	0132
0012	-0007	0132
0013	-0007	0132

Cons	003	Loc 58	
Lat	69°	26	54 N
Long	132°	59	30 W
GMT	18. 3	04	v
Depth	13 ft		

DEPTH	TEMP	SAL
0006	-0006	0088
0007	-0006	0088
0008	-0006	0088
0009	-0006	0100
0010	-0006	0104
0011	-0006	0108
0012	-0007	0108
0013	-0006	0108

Cons	004	Loc 58	
Lat	69°	26	54 N
Long	132°	59	30 W
GMT	20. 0	04	v
Depth	13 ft		

DEPTH	TEMP	SAL
0006	-0006	0092
0007	-0006	0080
0008	-0006	0096
0009	-0006	0096
0010	-0006	0096
0011	-0007	0108
0012	-0007	0120
0013	-0007	0120

Cons	005	Loc 58	
Lat	69°	26	54 N
Long	132°	59	30 W
GMT	21. 5	04	v
Depth	13 ft		

DEPTH	TEMP	SAL
0006	-0005	0080
0007	-0006	0080
0008	-0006	0088
0009	-0006	0088
0010	-0006	0092
0011	-0007	0112
0012	-0007	0112
0013	-0006	128

Cons	006	Loc 58	
Lat	69°	26	54 N
Long	132°	59	30 W
GMT	23. 0	04	v
Depth	13 ft		

DEPTH	TEMP	SAL
0006	-0007	0096
0007	-0007	0096
0008	-0007	0096
0009	-0007	0096
0010	-0007	0120
0011	-0007	0120
0012	-0007	0128
0013	-0007	0136

Cons	007		Loc 58
Lat	69°	26	54 N
Long	132°	59	30 W
GMT	00.5	05	v
Depth	13 ft		

DEPTH	TEMP	SAL
0006	-0006	0112
0007	-0006	0112
0008	-0006	0112
0009	-0006	0112
0010	-0006	0112
0011	-0006	0120
0012	-0006	0132
0013	-0006	0140

Cons	008		Loc 58
Lat	69°	26	54 N
Long	132°	59	30 W
GMT	02.0	05	v
Depth	13 ft		

DEPTH	TEMP	SAL
0006	-0006	0104
0007	-0007	0120
0008	-0007	0100
0009	-0007	0104
0010	-0007	0104
0011	-0007	0112
0012	-0007	0128
0013	-0007	0128

Cons	009		Loc 58
Lat	69°	26	54 N
Long	132°	59	30 W
GMT	03.5	05	v
Depth	13 ft		

DEPTH	TEMP	SAL
0006	-0007	0116
0007	-0007	0140
0008	-0006	0140
0009	-0007	0140
0010	-0007	0140
0011	-0007	0140
0012	-0007	0140
0013	-0007	0156

Cons 001 Loc 56
Lat 69° 26 46 N
Long 133° 02 03 W
GMT 16. 0 04 v
Depth 10 ft

DEPTH	TEMP	SAL
0006	-0005	0116

Cons 002 Loc 56
Lat 69° 26 46 N
Long 133° 02 03 W
GMT 17. 3 04 v
Depth 10 ft

DEPTH	TEMP	SAL
0006	-0005	0068

Cons 003 Loc 56
Lat 69° 26 46 N
Long 133° 02 03 W
GMT 18. 8 04 v
Depth 10 ft

DEPTH	TEMP	SAL
0006	-0005	0112

Cons 004 Loc 56
Lat 69° 26 46 N
Long 133° 02 03 W
GMT 20. 3 04 v
Depth 10 ft

DEPTH	TEMP	SAL
0006	-0005	0064

Cons 005 Loc 56
Lat 69° 26 46 N
Long 133° 02 03 W
GMT 21. 8 04 v
Depth 10 ft

DEPTH	TEMP	SAL
0006	-0005	0108

Cons 006 Loc 56
Lat 69° 26 46 N
Long 133° 02 03 W
GMT 23. 3 04 v
Depth 10 ft

DEPTH	TEMP	SAL
0006	-0005	0100

Cons 007 Loc 56
Lat 69° 26 46 N
Long 133° 02 03 W
GMT 00. 9 05 v
Depth 10 ft

DEPTH	TEMP	SAL
0006	-0005	0104

Cons 008 Loc 56
Lat 69° 26 46 N
Long 133° 02 03 W
GMT 02. 3 05 v
Depth 10 ft

DEPTH	TEMP	SAL
0006	-0006	0116

Cons 009 Loc 56
Lat 69° 26 46 N
Long 133° 02 03 W
GMT 04. 0 05 v
Depth 10 ft

DEPTH	TEMP	SAL
0006	-0005	0080

DATA (continued)

"Richardson" Serial Data

Note

The presentation of serial data in this section derives directly from methods used at the Canadian Oceanographic Data Centre.

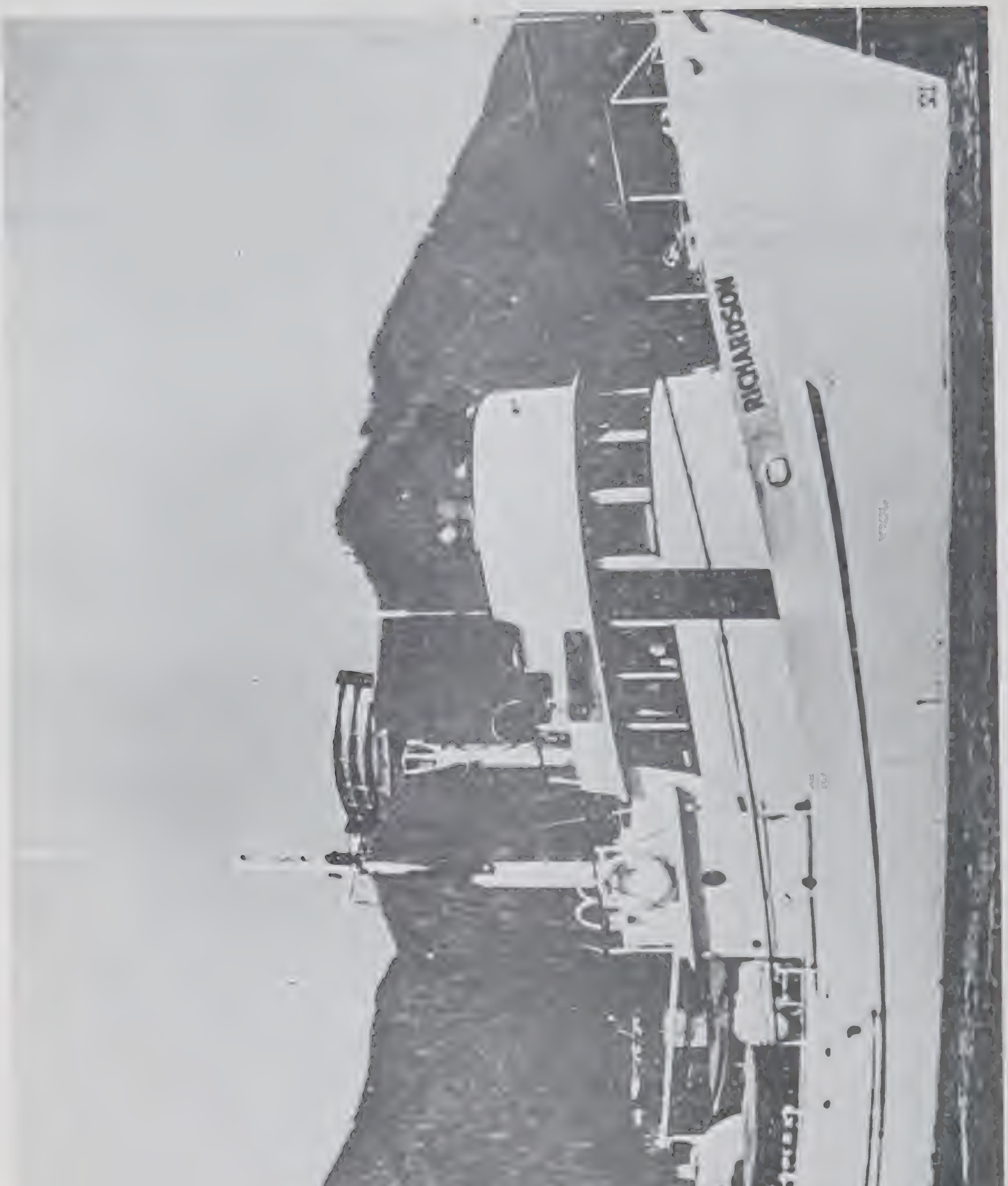
RICHARDSON

"RICHARDSON" SERIAL DATA

AND

EXPLANATION OF DATA RECORD HEADINGS

EXPLANATION OF DATA RECORD HEADINGS

MASTER HEADINGS

(1) C-REF-NO	(6) YR	(11) DEPTH	(16) WAVES 1	(21) AIR T	(26) VIS
(2) CONS. NO	(7) MONTH	(12) MXSAMPD	(17) WAVES 2	(22) WET B	(27) STN
(3) LAT	(8) DAY	(13) NO. DPTH	(18) WND-DIR	(23) ww-CODE	
(4) LON	(9) HR	(14) W-COLOR	(19) WND-FCE	(24) CLD-TPE	
(5) MARSD SQ	(10) C/I	(15) W-TRNSP	(20) BARO	(25) CLD-AMT	(28) HW

(1) CRUISE REFERENCE NUMBER: Assigned by the Institute. Commences with 001 at the beginning of each year (effective Jan. 1, 1963). Prior to that date the CRN was a number designated by CODC.

(2) CONSECUTIVE NUMBER: Indicates the chronological order in which the stations were occupied.

(3) LATITUDE:

(4) LONGITUDE: Indicate the position of the platform at the time of observation.

(5) MARSDEN SQUARE: Designates the geographic area code of the observation.

(6) YEAR:

(7) MONTH:

(8) DAY:

(9) HOUR: The time (Greenwich Mean Time) at which the surface environmental data were recorded. It is reported to tenths of hours.
If an "X" precedes the value for HOUR, (prior to Jan. 1, 1963) it indicates that the reported time is doubtful.

(10) COUNTRY/INSTITUTE: The International Geophysical Year (IGY) Country Code/ Institute Code.

(11) DEPTH: The sounding reported in metres.

(12) MAXIMUM SAMPLING DEPTH: A code to indicate the deepest sampling depth

00m - 50m = 00
51m - 150m = 01
151m - 250m = 02
etc.

(13) NUMBER OF DEPTH:	The number of levels observed at each station
(14) WATER COLOUR:	The Forel-Ule Code
(15) WATER TRANSPARENCY:	The depth in metres at which a Secchi disc (white disc, 30 cm. in diameter) just disappears from view, or the optical density expressed in percentage;
(16) WAVES 1 ($d_W d_W P_W H_W$-code):	The direction, period and height of the wind-propagated wave system (See Tables 3 and 4.) Ref: World Meteorological Organization Codes 0885, 3155, 1555.
(17) WAVES 2 ($d_W d_W P_W H_W$-code):	The direction, period and height of the predominant non-wind-propagated wave system. (See Tables 3 and 4.) Ref: World Meteorological Organization Codes 0885, 315 1555.
(18) WIND DIRECTION:	The true direction to the nearest 10 degrees from which the wind is blowing (wind direction 990 means:- wind variable or direction unknown).
(19) WIND FORCE (WND-FCE):	Beaufort notation
WIND SPEED (WND-SPD):	Estimated in nautical miles per hour
(20) BAROMETER:	The barometric pressure reported in millibars
(21) AIR TEMPERATURE:	(°F)
(22) WET BULB:	(°F)
(23) ww CODE:	Present Weather Code (See Table 8) Ref: WMO Code 467
(24) CLOUD TYPE:	The type of predominating clouds (See Table 5). Ref: WMO Code 0500.
(25) CLOUD AMOUNT:	The sky coverage in eighths (See Table 6). Ref: WMO Code 2700.
(26) VISIBILITY:	Visibility at the surface (See Table 7). Ref: WMO Code 4300.
(27) STATION:	A station reference number, assigned by the institute prior to, or during the survey.
(28) HOURS AFTER HIGH WATER:	Indicates the state of the tide for nearshore observations

OBSERVED DATA HEADINGS

DEPTH:	The depth in metres at the moment the oceanographic bottle reversed.
SALINITY :	The salinity as reported in a. 1/100 parts per 1000 or b. 1/1000 parts per 1000 In case a: a NON-significant third place decimal is reported as zero. In case b: the 3rd place of decimals is significant

Table 1

CONVERSION MINUTES TO $^1/_{10}$ HRS.

Minutes	Tenths Hrs.
00–03	0
04–08	1
09–15	2
16–20	3
21–27	4
28–32	5
33–39	6
40–44	7
45–51	8
52–56	9
57–59	0 (next HR.)

Table 2 DIRECTION CODE (dd)

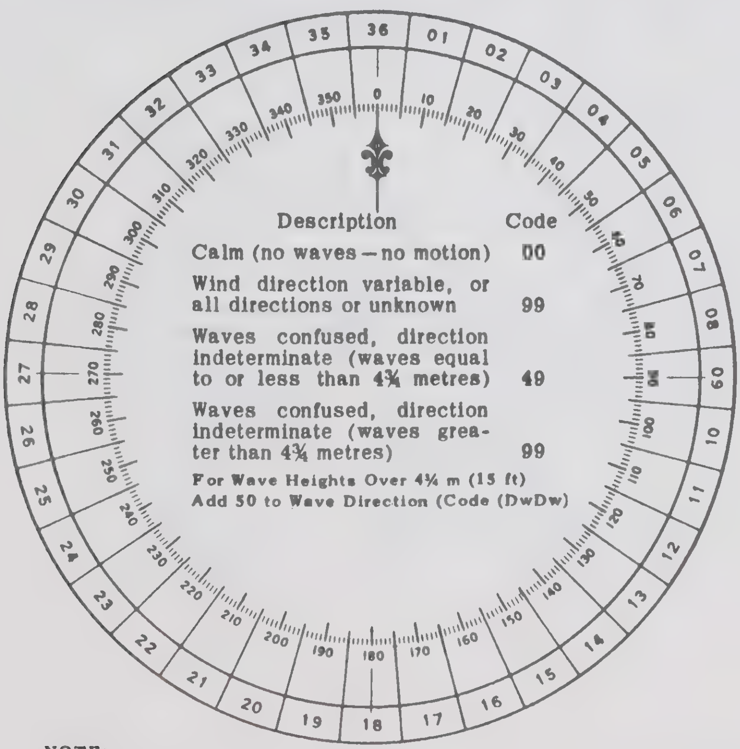

Description	Code
Calm (no waves – no motion)	00
Wind direction variable, or all directions or unknown	99
Waves confused, direction indeterminate (waves equal to or less than 4¾ metres)	49
Waves confused, direction indeterminate (waves greater than 4¾ metres)	99

For Wave Heights Over 4¾ m (15 ft)
Add 50 to Wave Direction (Code (DwDw)

NOTE:
Always use the true direction from which the wind is blowing, or the direction from which Waves I (sea), or Waves II (swell) come.

Table 3 PERIOD OF THE WAVES (Pw)

(Measure to the Nearest Second)

Code:	Period in Seconds:	Code:	Period in Seconds:
2	5 sec. or less	8	16 or 17 sec.
3	6 or 7 sec.	9	18 or 19 sec.
4	8 or 9 sec.	0	20 or 21 sec.
5	10 or 11 sec.	1	Over 21 sec.
6	12 or 13 sec.	X	Calm, or period not determined
7	14 or 15 sec.		

Table 4 HEIGHT OF THE WAVES (Hw)

- The average value of the wave height (vertical distance between trough and crest) is reported, as obtained from the larger well formed waves of the wave system being observed.
- Each code figure provides for reporting a range of heights. For example: 1 = ¼ m (1 ft) to ¾ m (2½ ft); 5 = 2¼ m (7 ft) to 2¾ m (9 ft); 9 = 4¼ m (13½ ft) to 4¾ m (15 ft), etc.
- If a wave height comes exactly midway between the heights corresponding to two code figures, the lower code figure is reported; e.g. a height of 2¾ m is reported by code figure 5.

Code			Code	
0	Less than ¼ m (1 ft)		0	5 m (16 ft)
1	½ m (1½ ft)		1	5½ m (17½ ft)
2	1 m (3 ft)		2	6 m (19 ft)
3	1½ m (5 ft)	Add	3	6½ m (21 ft)
4	2 m (6½ ft)	50	4	7 m (22½ ft)
5	2½ m (8 ft)	to	5	7½ m (24 ft)
6	3 m (9½ ft)	Dw Dw	6	8 m (25½ ft)
7	3½ m (11 ft)		7	8½ m (27 ft)
8	4 m (13 ft)		8	9 m (29 ft)
9	4½ m (14 ft)		9	9½ m (30½ ft) or more
x	Height not determined			

Table 5 CLOUD TYPE CODE

Code	Cloud Type		Code	Cloud Type	
0	Cirrus	Ci	5	Nimbostratus	Ns
1	Cirrocumulus	Cc	6	Stratocumulus	Sc
2	Cirrostratus	Cs	7	Stratus	St
3	Altocumulus........	Ac	8	Cumulus	Cu
4	Altostratus.........	As	9	Cumulonimbus	Cb
x	Cloud not visible owing to darkness, fog, duststorm, sandstorm, or other analogous phenomena				

Table 6 CLOUD AMOUNT CODE

Code	Cloud Cover	Code	Cloud Cover
0	0	6	6 oktas
1	1 okta or less, but not zero	7	7 oktas or more, but not 8 oktas
2	2 oktas	8	8 oktas
3	3 oktas	9	Sky obscured, or cloud amount cannot be estimated
4	4 oktas		
5	5 oktas		

Note: 1 okta = $\frac{1}{8}$ of the sky covered

Table 7 VISIBILITY

Code	Estimate of hor. Visibility	
0	Less than 50 metres	(less than 55 yards)
1	50—200 metres	(approx. 55—220 yards)
2	200—500 metres	(approx. 220—550 yards)
3	500—1,000 metres	(approx. 550 yards— $\frac{5}{8}$ n.m.)
4	1—2 km	(approx. $\frac{5}{8}$—1 n.m.)
5	2—4 km	(approx. 1—2 n.m.)
6	4—10 km	(approx. 2—6 n.m.)
7	10—20 km	(approx. 6—12 n.m.)
8	20—50 km	(approx. 12—30 n.m.)
9	50 km or more	(30 n.m. or more)

Note: n.m. = nautical mile

Table 8 PRESENT WEATHER

W.W. CODE

NO PRECIPITATION ON STATION AT TIME OF OBSERVATION

Group	Code figure ww	Description	
No meteors except photometeors	00	Cloud development not observed or not observable	characteristic change of the state of sky during the past hour
	01	Clouds generally dissolving or becoming less developed	
	02	State of sky on the whole unchanged	
	03	Clouds generally forming or developing	
Haze, dust, sand or smoke	04	Visibility reduced by smoke, e.g. veldt or forest fires, industrial smoke or volcanic ashes	
	05	Haze	
	06	Widespread dust in suspension in the air, not raised by wind at or near the station at the time of observation	
	07	Dust or sand raised by wind at or near the station at the time of observation, but no well developed dust whirl(s) or sand whirl(s), and no duststorm or sandstorm seen	
	08	Well developed dust whirl(s) or sand whirl(s) seen at or near the station during the preceding hour or at the time of observation, but no dustorm or sandstorm	
	09	Duststorm or sandstorm within sight at the time of observation, or at the station during the preceding hour	
	10	Mist	
	11	Patches of	shallow fog or ice fog at the station, whether on land or sea, not deeper than about 2 metres on land or 10 metres at sea
	12	More of less continuous	
	13	Lightning visible, no thunder heard	
	14	Precipitation within sight, not reaching the ground or the surface of the sea	
	15	Precipitation within sight, reaching the ground or the surface of the sea, but distant (i.e. estimated to be more than 5 km) from the station	
	16	Precipitation within sight, reaching the ground or the surface of the sea, near to, but not at the station	
	17	Thunderstorm, but no precepitation at the time of observation	
	18	Squalls	at or within sight of the station during the preceding hour or at the time of observation
	19	Funnel clouds	

ww = 20 – 29 Precipitation, fog, ice fog or thunderstorm at the station during the preceding hour but not at the time of observation

Code	Description	
20	Drizzle (not freezing) or snow grains	not falling as shower(s)
21	Rain (not freezing)	
22	Snow	
23	Rain and snow or ice pellets, type (a)	
24	Freezing drizzle or freezing rain	
25	Shower(s) of rain	
26	Shower(s) of snow, or of rain and snow	
27	Shower(s) of hail, or of rain and hail	
28	Fog or ice fog	
29	Thunderstorm (with or without precipitation)	

ww = 30 – 39 Duststorm, sandstorm, drifting or blowing snow

Code	Description	
30	Slight or moderate duststorm or sandstorm	– has decreased during the preceding hour
31		– no appreciable change during the preceding hour
32		– has begun or has increased during the preceding hour
33	Severe duststorm or sandstorm	– has decreased during the preceding hour
34		– no appreciable change during the preceding hour
35		– has begun or has increased during the preceding hour
36	Slight or moderate blowing snow	generally low (below eye level)
37	Heavy drifting snow	
38	Slight or moderate blowing snow	generally high (above eye level)
39	Heavy blowing snow	

ww = 40 – 49 Fog or ice fog at the time of observation

Code	Description	
40	Fog or ice fog at a distance at the time of observation, but not at the station during the preceding hour, the fog or ice fog extending to a level above that of the observer	
41	Fog or ice fog in patches	
42	Fog or ice fog, sky visible	has become thinner during the preceding hour
43	Fog or ice fog, sky invisible	
44	Fog or ice fog, sky visible	no appreciable change during the preceding hour
45	Fog or ice fog, sky invisible	
46	Fog or ice fog, sky visible	has begun or has become thicker during the preceding hour
47	Fog or ice fog, sky invisible	
48	Fog, depositing rime, sky visible	
49	Fog, depositing rime, sky invisible	

NO PRECIPITATION ON STATION AT TIME OF OBSERVATION

Table 8 (CONT'D)

PRECIPITATION ON STATION AT TIME OF OBSERVATION

ww = 50 – 59	Drizzle	
50	Drizzle, not freezing, intermittent	slight at time of observation
51	Drizzle, not freezing, continuous	
52	Drizzle, not freezing, intermittent	moderate at time of observation
53	Drizzle, not freezing, continuous	
54	Drizzle, not freezing, intermittent	heavy (dense) at time of observation
55	Drizzle, not freezing, continuous	
56	Drizzle, freezing, slight	
57	Drizzle, freezing, moderate or heavy (dense)	
58	Drizzle and rain, slight	
59	Drizzle and rain, moderate or heavy	

ww = 60 – 69	Rain	
60	Rain, not freezing, intermittent	slight at time of observation
61	Rain, not freezing, continuous	
62	Rain, not freezing, intermittent	moderate at time of observation
63	Rain, not freezing, continuous	
64	Rain, not freezing, intermittent	heavy at time of observation
65	Rain, not freezing, continuous	
66	Rain, freezing, slight	
67	Rain, freezing, moderate or heavy	
68	Rain or drizzle and snow, slight	
69	Rain or drizzle and snow, moderate or heavy	

70 – 79	Solid precipitation not in showers	
ww		
70	Intermittent fall of snow flakes	slight at time of observation
71	Continuous fall of snow flakes	
72	Intermittent fall of snow flakes	moderate at time of observation
73	Continuous fall of snow flakes	
74	Intermittent fall of snow flakes	heavy at time of observation
75	Continuous fall of snow flakes	
76	Ice prisms (with or without fog)	
77	Snow grains (with or without fog)	
78	Isolated starlike snow crystals (with or without fog)	
79	Ice pellets, type (a)	

ww = 80 – 99	Showery precipitation, or precipitation with current or recent thunderstorm	
80	Rain shower(s), slight	
81	Rain shower(s), moderate or heavy	
82	Rain shower(s), violent	
83	Shower(s) of rain and snow mixed, slight	
84	Shower(s) of rain and snow mixed, moderate or heavy	
85	Snow shower(s), slight	
86	Snow shower(s), moderate or heavy	
87	Shower(s) of snow pellets or ice pellets, type (b), with or without rain or rain and snow mixed	– slight
88		– moderate or heavy
89	Shower(s) of hail, with or without rain or rain and snow mixed, not associated with thunder	– slight
90		– moderate or heavy
91	Slight rain at time of observation	thunderstorm during the preceding hour but not at time of observation
92	Moderate or heavy rain at time of observation	
93	Slight snow, or rain and snow mixed or hail at time of observation	
94	Moderate or heavy snow, or rain and snow mixed or hail at time of observation	
95	Thunderstorm, slight or moderate, without hail, but with rain and/or snow at time of observation	thunderstorm at time of observation
96	Thunderstorm, slight or moderate, with hail at time of observation	
97	Thunderstorm, heavy, without hail, but with rain and/or snow at time of observation	
98	Thunderstorm, combined with duststorm or sandstorm at time of observation	
99	Thunderstorm, heavy, with hail at time of observation	

PRECIPITATION ON STATION AT TIME OF OBSERVATION

"Richardson" Programme

Serial data

Consecutive numbers 1 to 47

C-REF-NO 002	YR 1963	DEPTH 10	WAVES 1 22XX	AIR T 68.0	VIS 7
CONS. NO 001	MONTH 7	MXSAMPD	WAVES 2 22X1	WET B 60.0	STN 001
LAT 69-234N	DAY 26	NO.DPTH 5	WND-DIR 220	WW-CODE 03	
LON 132-595W	HR 20.8	W-COLOR	WND-SPD 15	CLD-TPE 8	
MARSD SQ	C/I 1813	W-TRNSP	BARO 1000.5	CLD-AMT 2	HW

DEPTH	T E M P	S A L
0000		08700
0002		23533
0004		25127
0006		22757
0008		25168

C-REF-NO 002	YR 1963	DEPTH 10	WAVES 1 22XX	AIR T 68.0	VIS 7
CONS. NO 002	MONTH 7	MXSAMPD	WAVES 2 22X1	WET B 60.0	STN 002
LAT 69-238N	DAY 26	NO.DPTH 5	WND-DIR 220	WW-CODE 03	
LON 132-595W	HR 21.[illegible]	W-COLOR	WND-SPD 15	CLD-TPE 8	
MARSD SQ	C/I 1813	W-TRNSP	BARO 1000.5	CLD-AMT 2	HW

DEPTH	T E M P	S A L
0000		07310
0002		07950
0004		24296
0006		26609
0008		27235

C-REF-NO 002	YR 1963	DEPTH 13	WAVES 1 22XX	AIR T 68.0	VIS 7
CONS. NO 003	MONTH 7	MXSAMPD	WAVES 2 22X1	WET B 60.0	STN 003
LAT 69-241N	DAY 26	NO.DPTH 7	WND-DIR 220	WW-CODE 03	
LON 132-589W	HR 22.8	W-COLOR	WND-SPD 15	CLD-TPE 8	
MARSD SQ	C/I 1813	W-TRNSP	BARO 1000.5	CLD-AMT 2	HW

DEPTH	T E M P	S A L
0000		07400
0002		21973
0004		26046
0006		26753
0008		27650
0010		26673
0012		27395

C-REF-NO 002	YR 1963	DEPTH 13	WAVES 1 22XX	AIR T 68.0	VIS 7
CONS. NO 004	MONTH 7	MXSAMPD	WAVES 2 22X1	WET B 60.0	STN 004
LAT 69-243N	DAY 26	NO.DPTH 7	WND-DIR 220	WW-CODE 03	
LON 132-595W	HR 23.8	W-COLOR	WND-SPD 20	CLD-TPE 8	
MARSD SQ	C/I 1813	W-TRNSP	BARO 1000.5	CLD-AMT 3	HW

DEPTH	T E M P	S A L
0000		05880
0002		05970
0004		20044
0006		25350
0008		26918
0010		27713
0012		28585

C-REF-NO 002	YR 1963	DEPTH	25	WAVES 1	22XX	AIR T	68.0	VIS	
CONS. NO 005	MONTH 7	MXSAMPD		WAVES 2	22X1	WET B	60.0	STN	005
LAT 69-245N	DAY 27	NO.DPTH	8	WND-DIR	220	WW-CODE	03		
LON 132-587W	HR 00.5	W-COLOR		WND-SPD	20	CLD-TPE	8		
MARSD SQ	C/I 1813	W-TRNSP		BARO	1000.5	CLD-AMT	4	HW	

DEPTH	T E M P	S A L
0000		05000
0002		05400
0004		06650
0006		22154
0008		25079
0010		26594
0015		28817
0020		29286

C-REF-NO 002	YR 1963	DEPTH	27	WAVES 1	22XX	AIR T	68.0	VIS	7
CONS. NO 006	MONTH 7	MXSAMPD		WAVES 2	22X1	WET B	60.0	STN	006
LAT 69-247N	DAY 27	NO.DPTH	7	WND-DIR	220	WW-CODE	03		
LON 132-586W	HR 01.7	W-COLOR		WND-SPD	20	CLD-TPE	8		
MARSD SQ	C/I 1813	W-TRNSP		BARO	1000.5	CLD-AMT	5	HW	

DEPTH	T E M P	S A L
0000		05090
0002		06160
0006		25342
0008		26778
0010		27760
0018		29228
0024		29305

C-REF-NO 002	YR	1963	DEPTH	21	WAVES 1	22XX	AIR T	65.0	VIS	7
CONS. NO 007	MONTH	7	MXSAMPD		WAVES 2	22X1	WET B	59.0	STN	007
LAT 69-249N	DAY	27	NO.DPTH	7	WND-DIR	220	WW-CODE	03		
LON 132-585W	HR	02.2	W-COLOR		WND-SPD	20	CLD-TPE	8		
MARSD SQ	C/I	1813	W-TRNSP		BARO	1000.5	CLD-AMT	6	HW	

DEPTH	T E M P	S A L
0000		04770
0002		04950
0004		18520
0006		25200
0008		26392
0011		27989
0018		29287

C-REF-NO 002	YR	1963	DEPTH	17	WAVES 1	22XX	AIR T	65.0	VIS	7
CONS. NO 008	MONTH	7	MXSAMPD		WAVES 2	22X1	WET B	59.0	STN	008
LAT 69-250N	DAY	27	NO.DPTH	7	WND-DIR	220	WW-CODE	03		
LON 132-582W	HR	02.7	W-COLOR		WND-SPD	20	CLD-TPE	8		
MARSD SQ	C/I	1813	W-TRNSP		BARO	1000.5	CLD-AMT	6	HW	

DEPTH	T E M P	S A L
0000		04910
0002		04820
0004		11750
0006		24335
0008		26127
0010		27159
0015		29189

C-REF-NO 002	YR 1963	DEPTH	11	WAVES 1 32XX	AIR T 58.0	VIS 6
CONS. NO 009	MONTH 7	MXSAMPD		WAVES 2 32X2	WET B 56.0	STN 018
LAT 69-266N	DAY 27	NO.DPTH	6	WND-DIR 320	WW-CODE 64	
LON 132-022W	HR 16.3	W-COLOR		WND-SPD 15	CLD-TPE 6	
MARSD SQ	C/I 1813	W-TRNSP		BARO 1000.9	CLD-AMT 9	HW

DEPTH	T E M P	S A L
0000		03910
0002		03820
0003		05820
0004		22795
0006		25165
0010		25521

C-REF-NO 002	YR 1963	DEPTH	13	WAVES 1 32XX	AIR T 58.0	VIS 6
CONS. NO 010	MONTH 7	MXSAMPD		WAVES 2 32X2	WET B 56.0	STN 015
LAT 69-265N	DAY 27	NO.DPTH	7	WND-DIR 320	WW-CODE 59	
LON 132-593W	HR 17.0	W-COLOR		WND-SPD 25	CLD-TPE 6	
MARSD SQ	C/I 1813	W-TRNSP		BARO 1000.9	CLD-AMT 9	HW

DEPTH	T E M P	S A L
0000		04030
0002		04430
0004		04390
0006		22432
0008		25239
0010		26964
0012		28031

C-REF-NO 002	YR 1963	DEPTH	5	WAVES 1 32XX	AIR T 58.0	VIS 6
CONS. NO 011	MONTH 7	MXSAMPD		WAVES 2 32X2	WET B 56.0	STN 014
LAT 69-264N	DAY 27	NO.DPTH	3	WND-DIR 320	WW-CODE 59	
LON 132-579W	HR 17.4	W-COLOR		WND-SPD 25	CLD-TPE 6	
MARSD SQ	C/I 1813	W-TRNSP		BARO 1000.9	CLD-AMT 9	HW

DEPTH	T E M P	S A L
0000		02050
0001		02140
0004		02070

C-REF-NO 002	YR 1963	DEPTH 9	WAVES 1 32XX	AIR T 58.0	VIS 6
CONS. NO 012	MONTH 7	MXSAMPD	WAVES 2 32X2	WET B 50.0	STN 013
LAT 69-260N	DAY 27	NO.DPTH 5	WND-DIR 320	WW-CODE 02	
LON 132-587W	HR 17.9	W-COLOR	WND-SPD 20	CLD-TPE 6	
MARSD SQ	C/I 1813	W-TRNSP	BARO 1000.9	CLD-AMT 9	HW

DEPTH	TEMP	SAL
0000		03860
0002		03750
0003		03750
0004		04090
0007		26011

C-REF-NO 002	YR 1963	DEPTH 10	WAVES 1 32XX	AIR T 58.0	VIS 8
CONS. NO 013	MONTH 7	MXSAMPD	WAVES 2 32X2	WET B 50.0	STN 012
LAT 69-260N	DAY 27	NO.DPTH 6	WND-DIR 320	WW-CODE 02	
LON 132-598W	HR 18.4	W-COLOR	WND-SPD 30	CLD-TPE 6	
MARSD SQ	C/I 1813	W-TRNSP	BARO 1000.9	CLD-AMT 9	HW

DEPTH	TEMP	SAL
0000		04300
0002		04030
0003		04300
0005		21328
0007		25377
0008		26647

C-REF-NO 002	YR 1963	DEPTH 22	WAVES 1 32XX	AIR T 58.0	VIS 8
CONS. NO 014	MONTH 7	MXSAMPD	WAVES 2 32X2	WET B 50.0	STN 011
LAT 69-255N	DAY 27	NO.DPTH 8	WND-DIR 320	WW-CODE 02	
LON 132-587W	HR 20.5	W-COLOR	WND-SPD 30	CLD-TPE 6	
MARSD SQ	C/I 1813	W-TRNSP	BARO 1000.9	CLD-AMT 9	HW

DEPTH	TEMP	SAL
0000		04880
0002		04750
0004		04860
0006		24098
0008		26062
0010		27445
0014		28757
0020		29853

C-REF-NO 002	YR 1963	DEPTH 16	WAVES 1 32XX	AIR T 58.0	VIS	
CONS. NO 015	MONTH 7	MXSAMPD	WAVES 2 32X2	WET B 50.0	STN 009	
LAT 69-250N	DAY 28	NO.DPTH 7	WND-DIR 320	WW-CODE 02		
LON 132-581W	HR 02.4	W-COLOR	WND-SPD 35	CLD-TPE 6		
MARSD SQ	C/I 1813	W-TRNSP	BARO 1000.9	CLD-AMT 9	HW	

DEPTH	TEMP	SAL
0000		04930
0002		04800
0004		04880
0006		22654
0009		26008
0012		28120
0016		28026

C-REF-NO 002	YR 1963	DEPTH 5	WAVES 1 32XX	AIR T 58.0	VIS 8
CONS. NO 016	MONTH 7	MXSAMPD	WAVES 2 32X2	WET B 50.0	STN 010
LAT 69-250N	DAY 28	NO.DPTH 3	WND-DIR 320	WW-CODE 02	
LON 132-581W	HR 02.9	W-COLOR	WND-SPD 35	CLD-TPE 6	
MARSD SQ	C/I 1813	W-TRNSP	BARO 1000.8	CLD-AMT 9	HW

DEPTH	TEMP	SAL
0000		04860
0002		04950
0004		05310

C-REF-NO 002	YR 1963	DEPTH 4	WAVES 1 27XX	AIR T 50.0	VIS 7
CONS. NO 017	MONTH 7	MXSAMPD	WAVES 2 27X2	WET B 48.0	STN 016
LAT 69-270N	DAY 29	NO.DPTH 3	WND-DIR 270	WW-CODE 52	
LON 132-596W	HR 00.7	W-COLOR	WND-SPD 20	CLD-TPE 6	
MARSD SQ	C/I 1813	W-TRNSP	BARO 1001.0	CLD-AMT 9	HW

DEPTH	TEMP	SAL
0000		03770
0002		03770
0004		03860

C-REF-NO 002	YR 1963	DEPTH 9	WAVES 1 27XX	AIR T 50.0	VIS 7
CONS. NO 018	MONTH 7	MXSAMPD	WAVES 2 27X2	WET B 48.0	STN 017
LAT 69-271N	DAY 29	NO.DPTH 5	WND-DIR 270	WW-CODE 52	
LON 133-002W	HR 01.2	W-COLOR	WND-SPD 20	CLD-TPE 6	
MARSD SQ	C/I 1813	W-TRNSP	BARO 1001.0	CLD-AMT 9	HW

DEPTH	T E M P	S A L
0000		03840
0002		03770
0003		03770
0004		03780
0006		19590

C-REF-NO 002	YR 1963	DEPTH 4	WAVES 1 27XX	AIR T 50.0	VIS 7
CONS. NO 019	MONTH 7	MXSAMPD	WAVES 2 27X3	WET B 48.0	STN 019
LAT 69-281N	DAY 29	NO.DPTH 3	WND-DIR 270	WW-CODE 02	
LON 133-029W	HR 01.7	W-COLOR	WND-SPD 20	CLD-TPE 6	
MARSD SQ	C/I 1813	W-TRNSP	BARO 1001.0	CLD-AMT 9	HW

DEPTH	T E M P	S A L
0000		04030
0002		04110
0004		04270

C-REF-NO 002	YR 1963	DEPTH 4	WAVES 1 27XX	AIR T 50.0	VIS 7
CONS. NO 020	MONTH 7	MXSAMPD	WAVES 2 27X3	WET B 48.0	STN 020
LAT 69-308N	DAY 29	NO.DPTH 3	WND-DIR 270	WW-CODE 02	
LON 133-086W	HR 02.2	W-COLOR	WND-SPD 20	CLD-TPE 6	
MARSD SQ	C/I 1813	W-TRNSP	BARO 1001.0	CLD-AMT 9	HW

DEPTH	T E M P	S A L
0000		06180
0002		07630
0004		08580

C-REF-NO 002	YR 1963	DEPTH	4	WAVES 1 27XX	AIR T 50.0	VIS 7
CONS. NO 021	MONTH 7	MXSAMPD		WAVES 2 27X3	WET B 48.0	STN 021
LAT 69-346N	DAY 29	NO.DPTH	3	WND-DIR 270	WW-CODE 02	
LON 133-104W	HR 02.7	W-COLOR		WND-SPD 20	CLD-TPE 6	
MARSD SQ	C/I 1813	W-TRNSP		BARO 1001.0	CLD-AMT 9	HW

DEPTH	T E M P	S A L
0000		02400
0002		02600
0003		03200

C-REF-NO 002	YR 1963	DEPTH	5	WAVES 1 27XX	AIR T 50.0	VIS 7
CONS. NO 022	MONTH 7	MXSAMPD		WAVES 2 27X3	WET B 48.0	STN 022
LAT 69-387N	DAY 29	NO.DPTH	4	WND-DIR 270	WW-CODE 02	
LON 133-125W	HR 03.2	W-COLOR		WND-SPD 20	CLD-TPE 6	
MARSD SQ	C/I 1813	W-TRNSP		BARO 1001.0	CLD-AMT 9	HW

DEPTH	T E M P	S A L
0000		01750
0002		01750
0003		01800
0005		01810

C-REF-NO 002	YR 1963	DEPTH	27	WAVES 1 22XX	AIR T 55.0	VIS 9
CONS. NO 023	MONTH 8	MXSAMPD		WAVES 2 22X1	WET B 50.0	STN 006
LAT 69-247N	DAY 15	NO.DPTH	8	WND-DIR 220	WW-CODE 02	
LON 132-586W	HR 23.8	W-COLOR		WND-SPD 15	CLD-TPE 6	
MARSD SQ	C/I 1813	W-TRNSP		BARO 1000.0	CLD-AMT 6	HW

DEPTH	T E M P	S A L
0000		02700
0002		02600
0006		02100
0008		22200
0010		26761
0012		28006
0018		28784
0024		28909

C-REF-NO 002	YR 1963	DEPTH 27	WAVES 1 22XX	AIR T 59.0	VIS 9
CONS. NO 024	MONTH 8	MXSAMPD	WAVES 2 22X1	WET B 53.0	STN 006
LAT 69-247N	DAY 21	NO.DPTH	WND-DIR 220	WW-CODE 01	
LON 132-586W	HR 23.5	W-COLOR	WND-SPD 10	CLD-TPE 6	
MARSD SQ	C/I 1813	W-TRNSP	BARO 1002.1	CLD-AMT 5	HW

Bathythermograph lowering only.

C-REF-NO 002	YR 1963	DEPTH 27	WAVES 1 09XX	AIR T 35.0	VIS 8
CONS. NO 025	MONTH 9	MXSAMPD	WAVES 2 09X1	WET B 34.0	STN 006
LAT 69-247N	DAY 06	NO.DPTH	WND-DIR 090	WW-CODE 03	
LON 132-586W	HR 20.2	W-COLOR	WND-SPD 15	CLD-TPE 6	
MARSD SQ	C/I 1813	W-TRNSP	BARO 1002.0	CLD-AMT 9	HW

Bathythermograph lowering only.

C-REF-NO 002	YR 1963	DEPTH 6	WAVES 1 36XX	AIR T 29.5	VIS 8
CONS. NO 026	MONTH 9	MXSAMPD	WAVES 2 36X2	WET B 28.0	STN 022
LAT 69-387N	DAY 13	NO.DPTH 4	WND-DIR 360	WW-CODE 02	
LON 133-125W	HR 21.7	W-COLOR	WND-SPD 15	CLD-TPE 8	
MARSD SQ	C/I 1813	W-TRNSP	BARO 1002.0	CLD-AMT 9	HW

DEPTH	TEMP	SAL
0000		31300
0002		31300
0004		31320
0005		31406

C-REF-NO 002	YR 1963	DEPTH 4	WAVES 1 36XX	AIR T 29.5	VIS 8
CONS. NO 027	MONTH 9	MXSAMPD	WAVES 2 36X2	WET B 28.0	STN 021
LAT 69-346N	DAY 13	NO.DPTH 3	WND-DIR 360	WW-CODE 02	
LON 133-104W	HR 22.4	W-COLOR	WND-SPD 15	CLD-TPE 8	
MARSD SQ	C/I 1813	W-TRNSP	BARO 1002.0	CLD-AMT 9	HW

DEPTH	TEMP	SAL
0000		10400
0002		28870
0004		30130

C-REF-NO 002	YR 1963	DEPTH 4	WAVES 1 36XX	AIR T 30.0	VIS 8
CONS. NO 028	MONTH 9	MXSAMPD	WAVES 2 36X2	WET B 29.0	STN 020
LAT 69-308N	DAY 13	NO.DPTH 3	WND-DIR 360	WW-CODE 02	
LON 133-086W	HR 23.2	W-COLOR	WND-SPD 15	CLD-TPE 8	
MARSD SQ	C/I 1813	W-TRNSP	BARO 1002.0	CLD-AMT 9	HW

DEPTH	TEMP	SAL
0000		03300
0002		25060
0004		28830

C-REF-NO 002	YR 1963	DEPTH 4	WAVES 1 36XX	AIR T 30.0	VIS 8
CONS. NO 029	MONTH 9	MXSAMPD	WAVES 2 36X2	WET B 29.0	STN 019
LAT 69-280N	DAY 13	NO.DPTH 3	WND-DIR 360	WW-CODE 02	
LON 133-029W	HR 23.8	W-COLOR	WND-SPD 15	CLD-TPE 8	
MARSD SQ	C/I 1813	W-TRNSP	BARO 1002.0	CLD-AMT 9	HW

DEPTH	TEMP	SAL
0000		01150
0002		00910
0003		12740

C-REF-NO 002	YR 1963	DEPTH 9	WAVES 1 36XX	AIR T 30.0	VIS 8
CONS. NO 030	MONTH 9	MXSAMPD	WAVES 2 36X2	WET B 29.0	STN 017
LAT 69-271N	DAY 14	NO.DPTH 4	WND-DIR 360	WW-CODE 02	
LON 133-002W	HR 00.4	W-COLOR	WND-SPD 15	CLD-TPE 8	
MARSD SQ	C/I 1813	W-TRNSP	BARO 1002.0	CLD-AMT 9	HW

DEPTH	TEMP	SAL
0000		00950
0002		02120
0004		10660
0006		26451

C-REF-NO 002	YR 1963	DEPTH 4	WAVES 1 36XX	AIR T 30.0	VIS 8
CONS. NO 031	MONTH 9	MXSAMPD	WAVES 2 36X2	WET B 29.0	STN 016
LAT 69-270N	DAY 14	NO.DPTH 3	WND-DIR 360	WW-CODE 02	
LON 132-596W	HR 01.3	W-COLOR	WND-SPD 15	CLD-TPE 8	
MARSD SQ	C/I 1813	W-TRNSP	BARO 1002.0	CLD-AMT 9	HW

DEPTH	T E M P	S A L
0000		01670
0002		04300
0004		18780

C-REF-NO 002	YR 1963	DEPTH 11	WAVES 1 14XX	AIR T 33.0	VIS 9
CONS. NO 032	MONTH 9	MXSAMPD	WAVES 2 14X2	WET B 32.0	STN 018
LAT 69-266N	DAY 14	NO.DPTH 6	WND-DIR 140	WW-CODE 03	
LON 133-022W	HR 20.6	W-COLOR	WND-SPD 25	CLD-TPE 6	
MARSD SQ	C/I 1813	W-TRNSP	BARO 1002.0	CLD-AMT 6	HW

DEPTH	T E M P	S A L
0000		02930
0002		05480
0004		18040
0006		26290
0008		27817
0009		28050

C-REF-NO 002	YR 1963	DEPTH 14	WAVES 1 14XX	AIR T 33.0	VIS 9
CONS. NO 033	MONTH 9	MXSAMPD	WAVES 2 14X2	WET B 32.0	STN 015
LAT 69-265N	DAY 14	NO.DPTH 7	WND-DIR 140	WW-CODE 03	
LON 132-593W	HR 21.2	W-COLOR	WND-SPD 25	CLD-TPE 6	
MARSD SQ	C/I 1813	W-TRNSP	BARO 1002.0	CLD-AMT 6	HW

DEPTH	T E M P	S A L
0000		04000
0002		12620
0004		24890
0006		27235
0008		27553
0010		28799
0014		29521

C-REF-NO 002	YR 1963	DEPTH 5	WAVES 1 18XX	AIR T 30.5	VIS 9
CONS. NO 034	MONTH 9	MXSAMPD	WAVES 2 18X1	WET B 30.5	STN 014
LAT 69-264N	DAY 15	NO.DPTH 3	WND-DIR 180	WW-CODE 02	
LON 132-579W	HR 15.3	W-COLOR	WND-SPD 20	CLD-TPE 6	
MARSD SQ	C/I 1813	W-TRNSP	BARO 1001.5	CLD-AMT 5	HW

DEPTH	T E M P	S A L
0000		08600
0001		08240
0003		09220

C-REF-NO 002	YR 1963	DEPTH 9	WAVES 1 18XX	AIR T 30.5	VIS 9
CONS. NO 035	MONTH 9	MXSAMPD	WAVES 2 18X1	WET B 30.5	STN 013
LAT 69-260N	DAY 15	NO.DPTH 5	WND-DIR 180	WW-CODE 02	
LON 132-587W	HR 15.7	W-COLOR	WND-SPD 20	CLD-TPE 6	
MARSD SQ	C/I 1813	W-TRNSP	BARO 1001.5	CLD-AMT 5	HW

DEPTH	T E M P	S A L
0000		08880
0002		08970
0004		21610
0005		25960
0007		27345

C-REF-NO 002	YR 1963	DEPTH 10	WAVES 1 18XX	AIR T 30.5	VIS 9
CONS. NO 036	MONTH 9	MXSAMPD	WAVES 2 18X1	WET B 30.5	STN 012
LAT 69-260N	DAY 15	NO.DPTH 6	WND-DIR 180	WW-CODE 02	
LON 132-598W	HR 16.1	W-COLOR	WND-SPD 20	CLD-TPE 6	
MARSD SQ	C/I 1813	W-TRNSP	BARO 1001.5	CLD-AMT 5	HW

DEPTH	T E M P	S A L
0000		09680
0002		09950
0004		21680
0006		25091
0008		27097
0009		28193

C-REF-NO 002	YR 1963	DEPTH 22	WAVES 1 99XX	AIR T 30.5	VIS 9
CONS. NO 037	MONTH 9	MXSAMPD	WAVES 2 99X1	WET B 30.5	STN 011
LAT 69-256N	DAY 15	NO.DPTH 8	WND-DIR 180	WW-CODE 02	
LON 132-588W	HR 16.7	W-COLOR	WND-SPD 20	CLD-TPE 6	
MARSD SQ	C/I 1813	W-TRNSP	BARO 1001.5	CLD-AMT 5	HW

DEPTH	T E M P	S A L
0000		10450
0002		09770
0004		22340
0006		26598
0008		27803
0010		28469
0015		29090
0020		29130

C-REF-NO 002	YR 1963	DEPTH 20	WAVES 1 18XX	AIR T 33.0	VIS 9
CONS. NO 038	MONTH 9	MXSAMPD	WAVES 2 18X1	WET B 32.0	STN 007
LAT 69-249N	DAY 15	NO.DPTH 7	WND-DIR 180	WW-CODE 01	
LON 132-585W	HR 17.7	W-COLOR	WND-SPD 20	CLD-TPE 6	
MARSD SQ	C/I 1813	W-TRNSP	BARO 1001.5	CLD-AMT 4	HW

DEPTH	T E M P	S A L
0000		13720
0002		15290
0004		25390
0006		26650
0008		27497
0010		28509
0018		28685

C-REF-NO 002	YR 1963	DEPTH	17	WAVES 1 18XX	AIR T 33.0	VIS 9
CONS. NO 039	MONTH 9	MXSAMPD		WAVES 2 18X1	WET B 32.0	STN 008
LAT 69-250N	DAY 15	NO.DPTH	7	WND-DIR 180	WW-CODE 01	
LON 132-582W	HR 18.2	W-COLOR		WND-SPD 20	CLD-TPE 6	
MARSD SQ	C/I 1813	W-TRNSP		BARO 1001.5	CLD-AMT 3	HW

DEPTH	T E M P	S A L
0000		12440
0002		11020
0004		23210
0006		25782
0008		27604
0010		28285
0015		28649

C-REF-NO 002	YR 1963	DEPTH	27	WAVES 1 18XX	AIR T 33.0	VIS 9
CONS. NO 040	MONTH 9	MXSAMPD		WAVES 2 18X1	WET B 32.0	STN 006
LAT 69-247N	DAY 15	NO.DPTH	8	WND-DIR 180	WW-CODE 01	
LON 132-586W	HR 18.8	W-COLOR		WND-SPD 20	CLD-TPE 6	
MARSD SQ	C/I 1813	W-TRNSP		BARO 1001.5	CLD-AMT 3	HW

DEPTH	T E M P	S A L
0000		12710
0002		13040
0004		18590
0006		24991
0008		26866
0010		28043
0016		28577
0024		28680

C-REF-NO 002	YR 1963	DEPTH	25	WAVES 1 18XX	AIR T 39.0	VIS 9
CONS. NO 041	MONTH 9	MXSAMPD		WAVES 2 18X1	WET B 37.0	STN 005
LAT 69-245N	DAY 15	NO.DPTH	8	WND-DIR 180	WW-CODE 01	
LON 132-587W	HR 21.8	W-COLOR		WND-SPD 20	CLD-TPE 6	
MARSD SQ	C/I 1813	W-TRNSP		BARO 1001.5	CLD-AMT 2	HW

DEPTH	T E M P	S A L
0000		18480
0002		15200
0004		21990
0006		24668
0008		27239
0010		28054
0016		28532
0021		28563

C-REF-NO 002	YR 1963	DEPTH	13	WAVES 1 XX	AIR T 39.0	VIS 9
CONS. NO 042	MONTH 9	MXSAMPD		WAVES 2 X1	WET B 37.0	STN 004
LAT 64-243N	DAY 15	NO.DPTH	7	WND-DIR 180	WW-CODE 01	
LON 132-595W	HR 22.3	W-COLOR		WND-SPD 20	CLD-TPE 6	
MARSD SQ	C/I 1813	W-TRNSP		BARO 1001.5	CLD-AMT 2	HW

DEPTH	T E M P	S A L
0000		17580
0002		17580
0004		18940
0006		25984
0008		27031
0010		27292
0012		27702

C-REF-NO 002	YR 1963	DEPTH	13	WAVES 1 18XX	AIR T 39.0	VIS 9
CONS. NO 043	MONTH 9	MXSAMPD		WAVES 2 18X1	WET B 37.0	STN 003
LAT 69-241N	DAY 15	NO.DPTH	7	WND-DIR 180	WW-CODE 01	
LON 132-589W	HR 22.8	W-COLOR		WND-SPD 20	CLD-TPE 6	
MARSD SQ	C/I 1813	W-TRNSP		BARO 1001.5	CLD-AMT 1	HW

DEPTH	T E M P	S A L
0000		16930
0002		18430
0004		22430
0006		25137
0008		26840
0010		26818
0012		27642

C-REF-NO 002	YR 1963	DEPTH	10	WAVES 1 18XX	AIR T 39.0	VIS 9
CONS. NO 044	MONTH 9	MXSAMPD		WAVES 2 18X1	WET B 37.0	STN 002
LAT 69-238N	DAY 15	NO.DPTH	5	WND-DIR 180	WW-CODE 01	
LON 132-595W	HR 23.3	W-COLOR		WND-SPD 20	CLD-TPE 6	
MARSD SQ	C/I 1813	W-TRNSP		BARO 1001.5	CLD-AMT 1	HW

DEPTH	T E M P	S A L
0000		21640
0002		21540
0004		23420
0006		25894
0008		27100

C-REF-NO 002	YR 1963	DEPTH	10	WAVES 1 18XX	AIR T 39.0	VIS 9
CONS. NO 045	MONTH 9	MXSAMPD		WAVES 2 18X1	WET B 37.0	STN 001
LAT 69-234N	DAY 15	NO.DPTH	5	WND-DIR 180	WW-CODE 01	
LON 132-594W	HR 23.8	W-COLOR		WND-SPD 20	CLD-TPE 6	
MARSD SQ	C/I 1813	W-TRNSP		BARO 1001.5	CLD-AMT 1	HW

DEPTH	T E M P	S A L
0000		19800
0002		24140
0004		25340
0006		26333
0008		26857

C-REF-NO 002	YR 1963	DEPTH	12	WAVES 1	18XX	AIR T	33.0	VIS	8
CONS. NO 046	MONTH 9	MXSAMPD		WAVES 2	18X1	WET B	32.0	STN	009
LAT 69-250N	DAY 16	NO.DPTH	7	WND-DIR	180	WW-CODE	02		
LON 132-581W	HR 15.7	W-COLOR		WND-SPD	15	CLD-TPE	6		
MARSD SQ	C/I 1813	W-TRNSP		BARO	1001.2	CLD-AMT	6	HW	

DEPTH	T E M P	S A L
0000		14690
0002		17510
0004		23160
0006		25357
0008		27472
0010		27018
0011		28055

C-REF-NO 002	YR 1963	DEPTH	5	WAVES 1	18XX	AIR T	33.0	VIS	8
CONS. NO 047	MONTH 9	MXSAMPD		WAVES 2	18XX	WET B	32.0	STN	010
LAT 69-250N	DAY 16	NO.DPTH	3	WND-DIR	180	WW-CODE	02		
LON 132-581W	HR 16.2	W-COLOR		WND-SPD	15	CLD-TPE	6		
MARSD SQ	C/I 1813	W-TRNSP		BARO	1001.2	CLD-AMT	6	HW	

GMT	DEPTH	T E M P	S A L
162	0000		14690
162	0002		15220
162	0004		23690

DATA (continued)

Bathythermograms

The bathythermograph lowerings were made with one BT.

The traces were reproduced by hand on preprinted grids and are in chronological order. The circled number on each reproduction is the consec slide number and relates the trace to Lists 1 and 2. The slides are held at the Canadian Oceanographic Data Centre and are available there in the form of aperture cards (Sauer, 1964).

BATHYTHERMOGRAMS

PHASES II AND III, AND "RICHARDSON"

LOWERINGS

N R C Programme

"Bathythermograms"

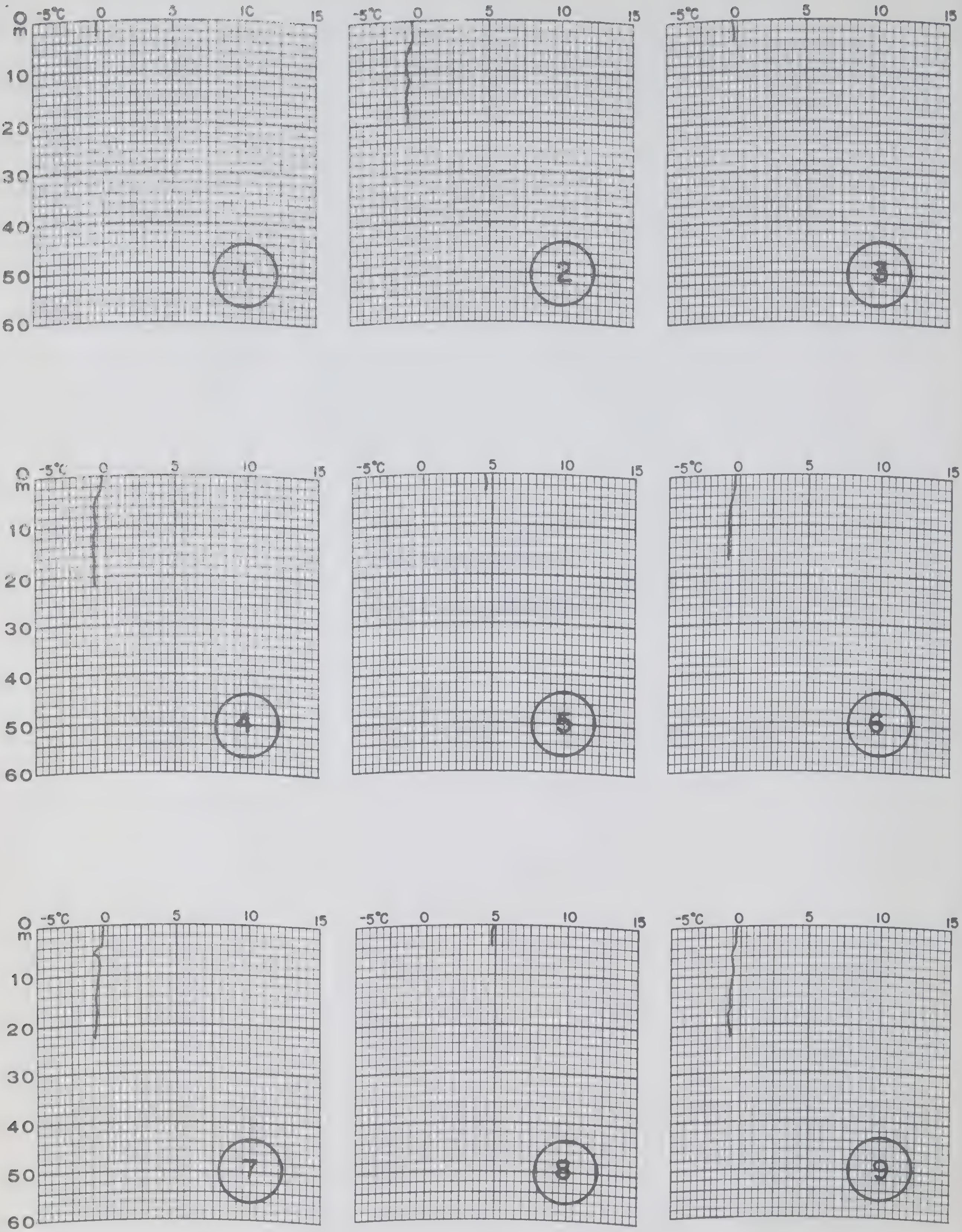
-5°C 0 5 10 15
0 m 10 20 30 40 50 60
1
2
3
4
5
6
7
8
9

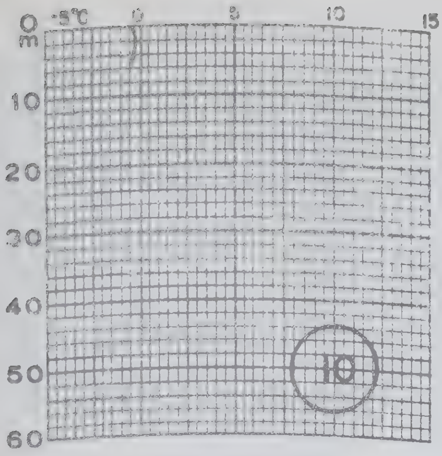
-5°C 0 5 10 15
0 m 10 20 30 40 50 60
10

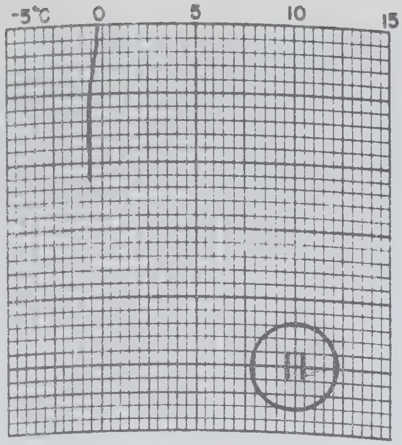
-5°C 0 5 10 15
11

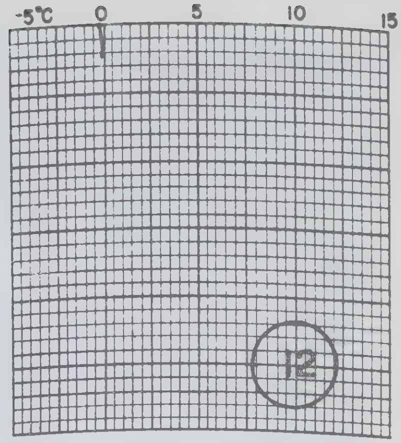
-5°C 0 5 10 15
12

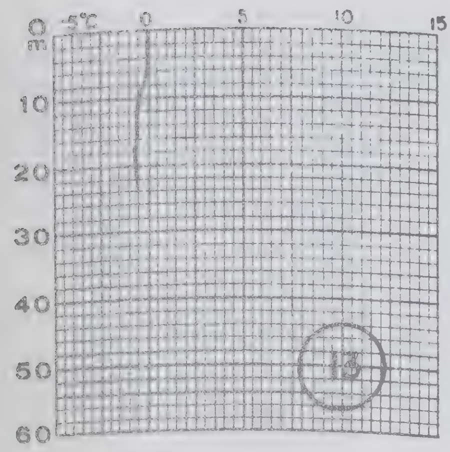
-5°C 0 5 10 15
0 m 10 20 30 40 50 60
13

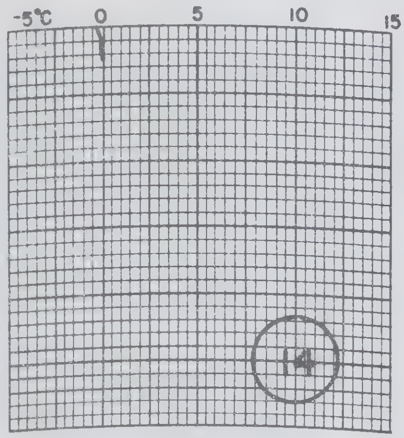
-5°C 0 5 10 15
14

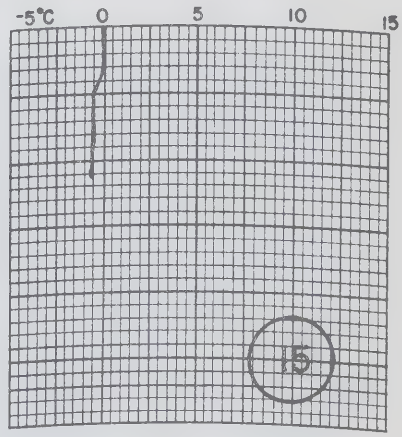
-5°C 0 5 10 15
15

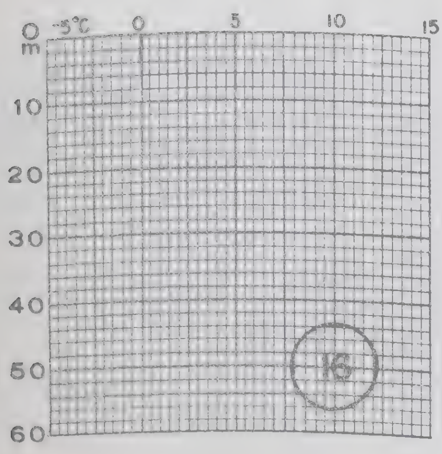
-5°C 0 5 10 15
0 m 10 20 30 40 50 60
16

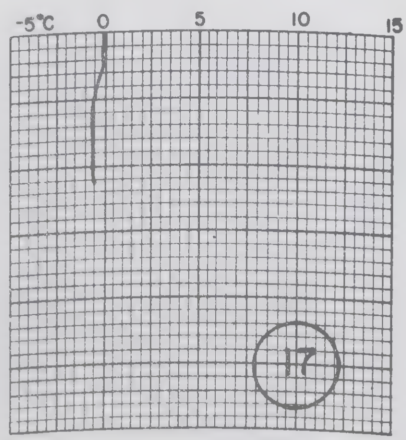
-5°C 0 5 10 15
17

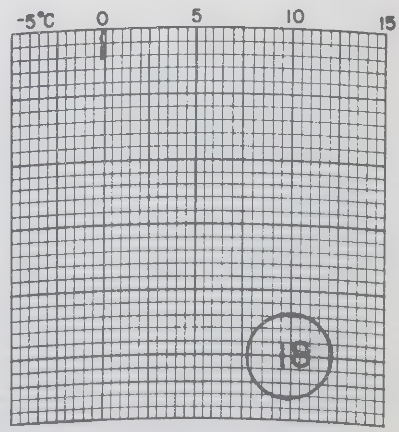
-5°C 0 5 10 15
18

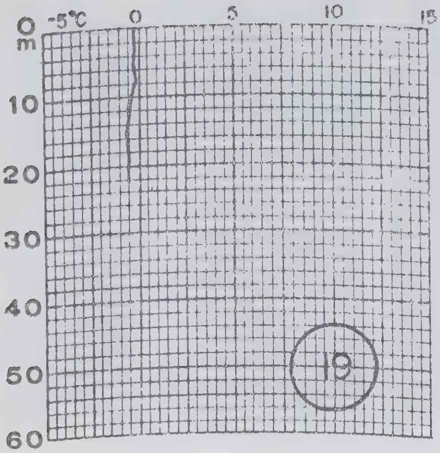
-5°C 0 5 10 15
0 m 10 20 30 40 50 60
19

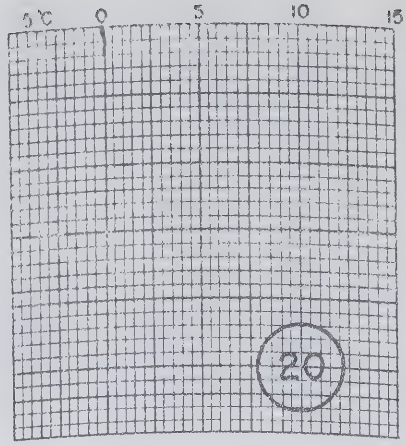
5°C 0 5 10 15
20

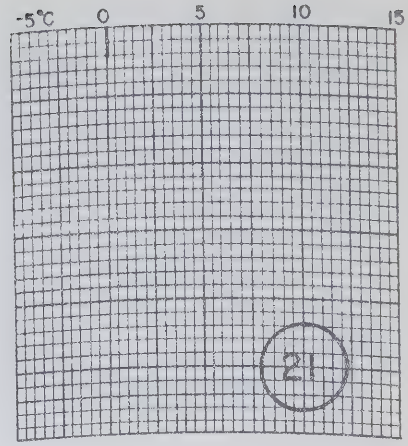
-5°C 0 5 10 15
21

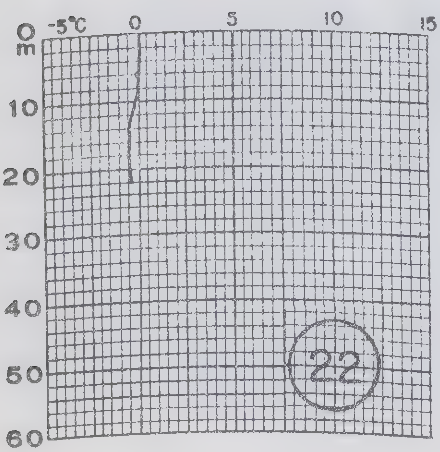
-5°C 0 5 10 15
0 m 10 20 30 40 50 60
22

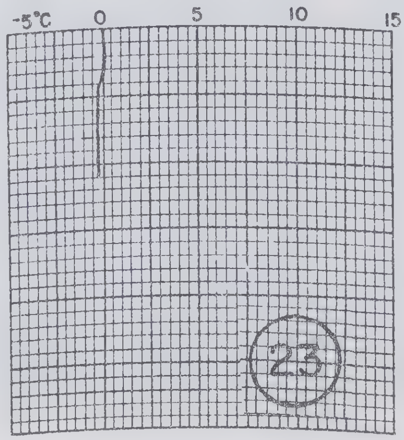
-5°C 0 5 10 15
23

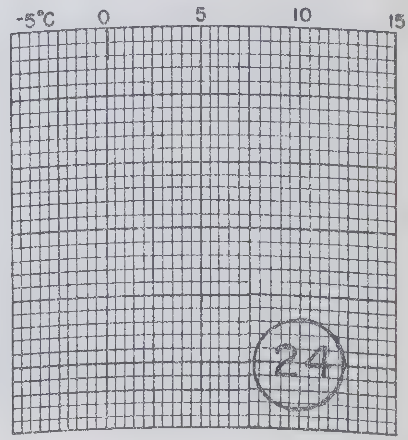
-5°C 0 5 10 15
24

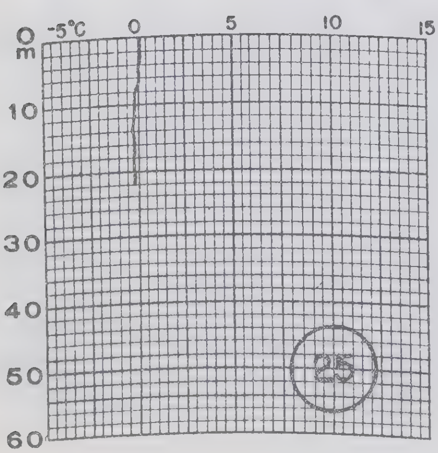
-5°C 0 5 10 15
0 m 10 20 30 40 50 60
25

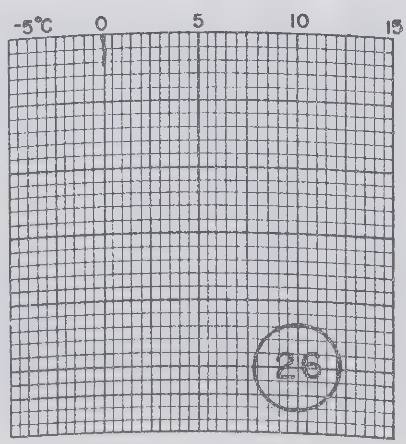
-5°C 0 5 10 15
26

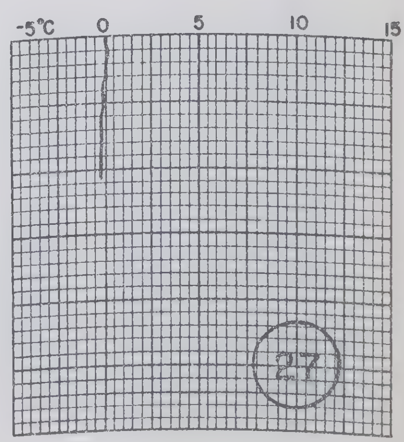
-5°C 0 5 10 15
27

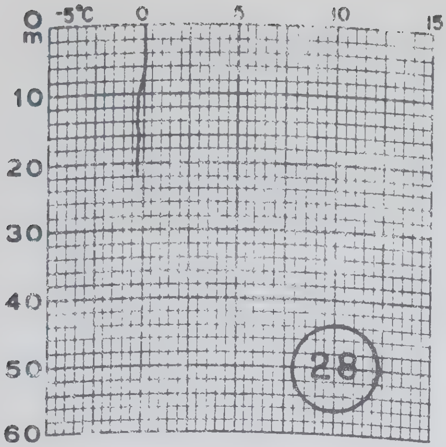
-5°C 0 5 10 15
0 m
10
20
30
40
50
60
28

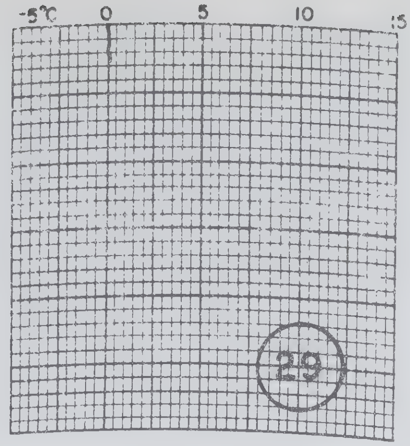
-5°C 0 5 10 15
29

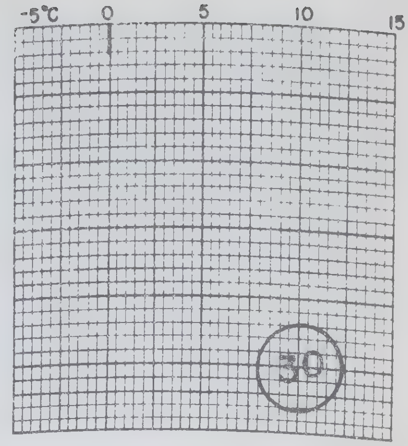
-5°C 0 5 10 15
30

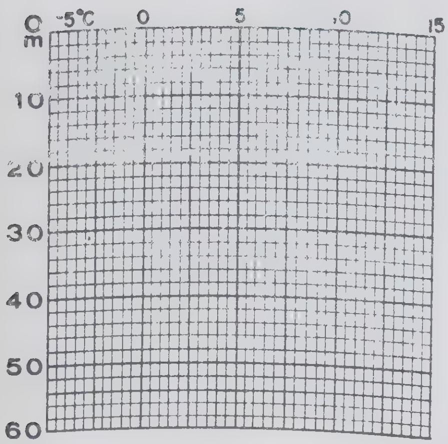
-5°C 0 5 10 15
0 m
10
20
30
40
50
60

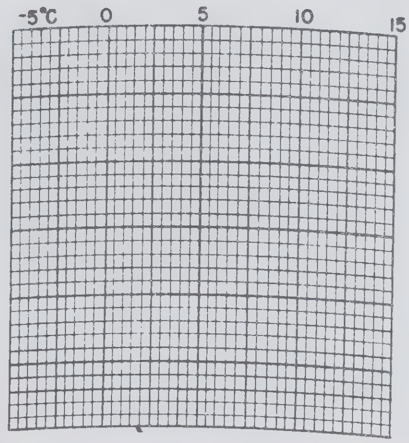
-5°C 0 5 10 15

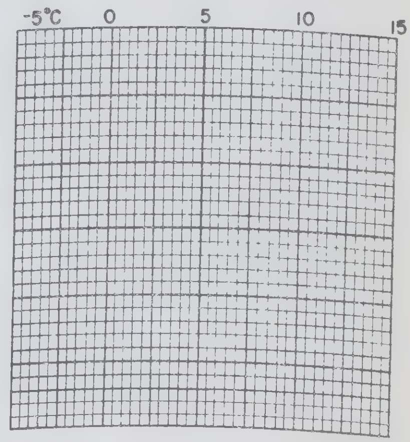
-5°C 0 5 10 15

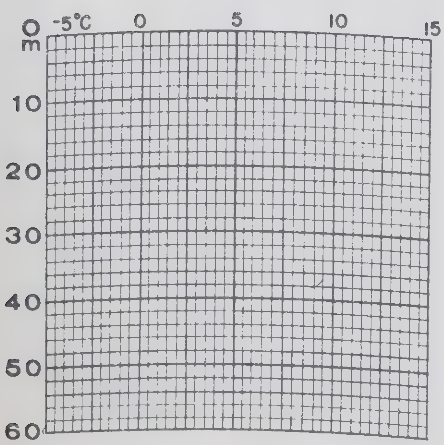
-5°C 0 5 10 15
0 m
10
20
30
40
50
60

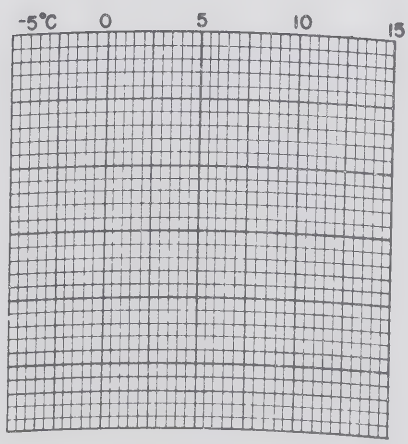
-5°C 0 5 10 15

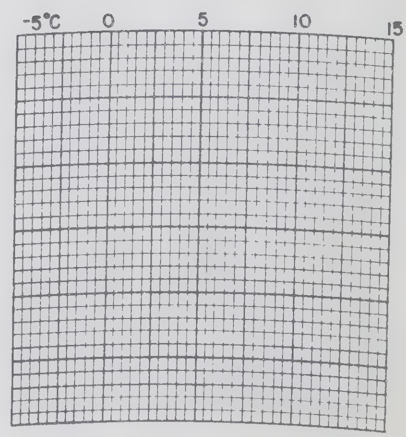
-5°C 0 5 10 15

"Richardson" Programme

"Bathythermograms"

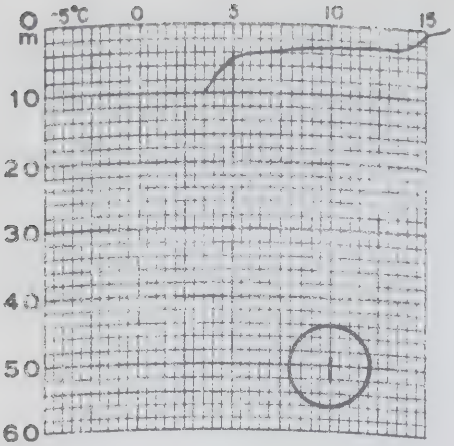
-5°C 0 5 10 15
0 m 10 20 30 40 50 60
1

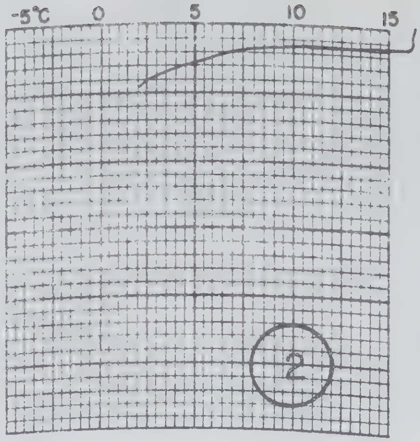
-5°C 0 5 10 15
2

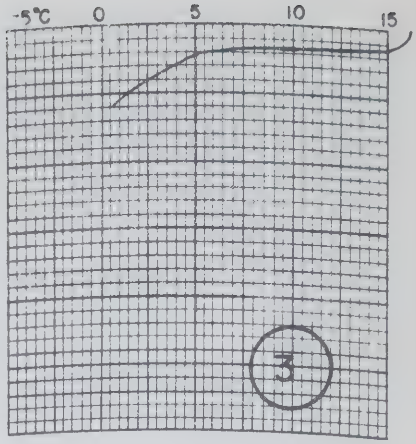
-5°C 0 5 10 15
3

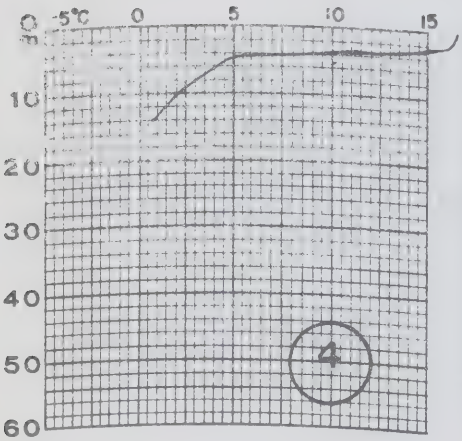
-5°C 0 5 10 15
0 m 10 20 30 40 50 60
4

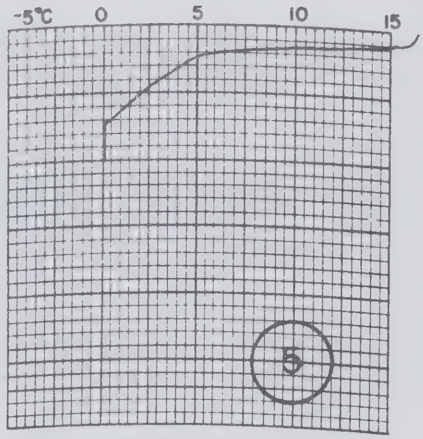
-5°C 0 5 10 15
5

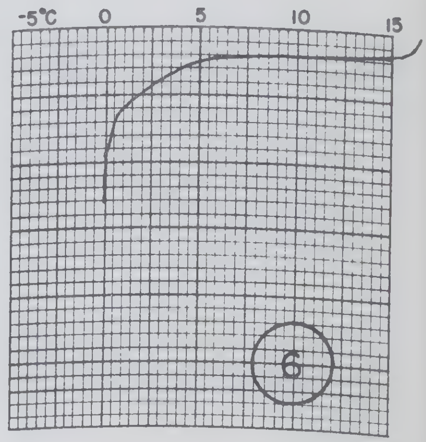
-5°C 0 5 10 15
6

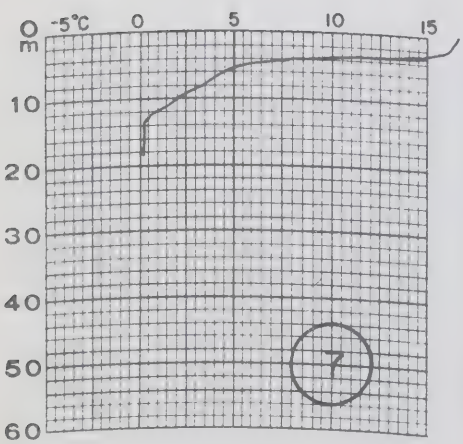
-5°C 0 5 10 15
0 m 10 20 30 40 50 60
7

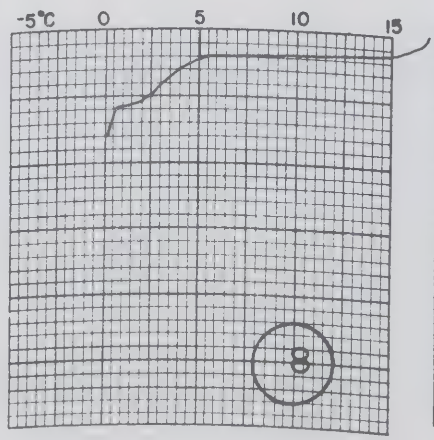
-5°C 0 5 10 15
8

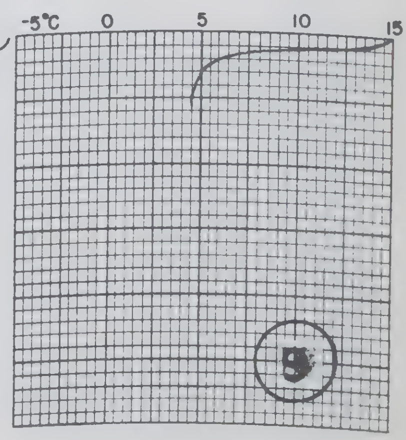
-5°C 0 5 10 15

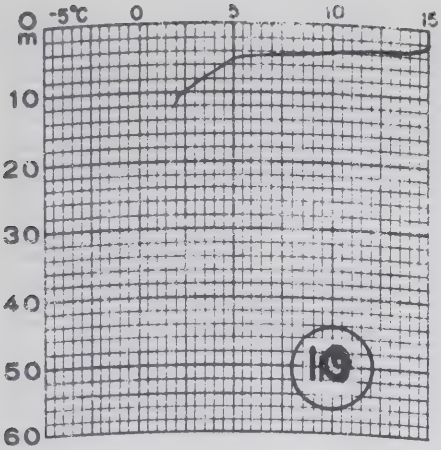
-5°C 0 5 10 15
0 m
10
20
30
40
50
60

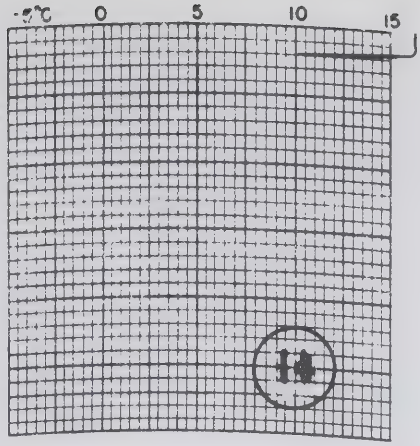
-5°C 0 5 10 15

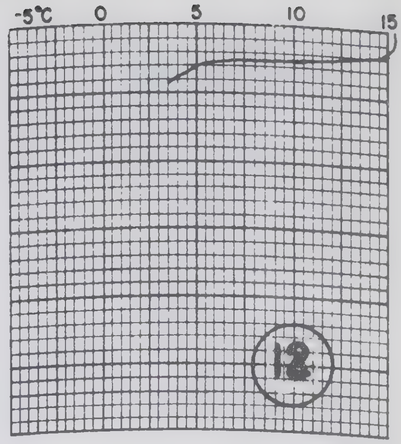
-5°C 0 5 10 15

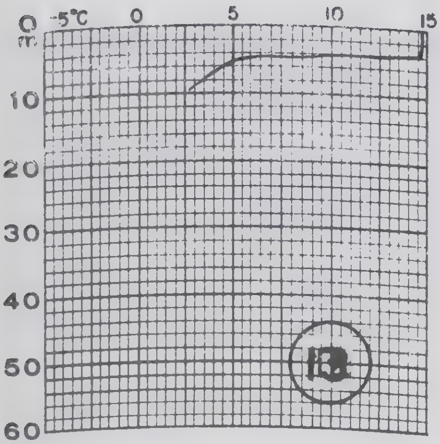
-5°C 0 5 10 15
0 m
10
20
30
40
50
60

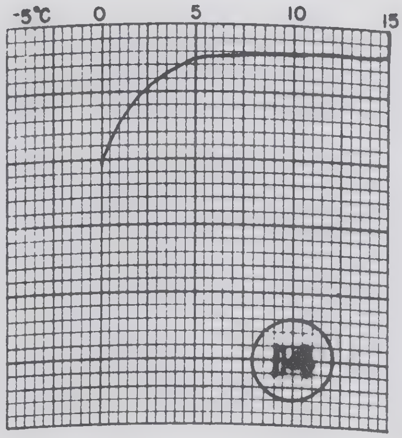
-5°C 0 5 10 15

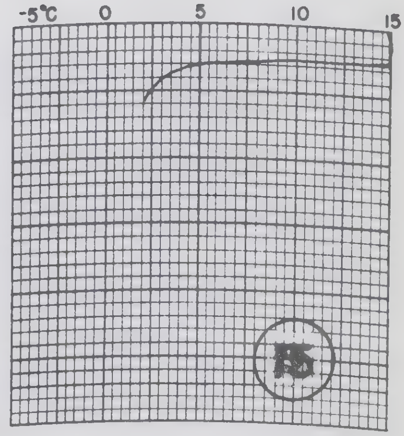
-5°C 0 5 10 15

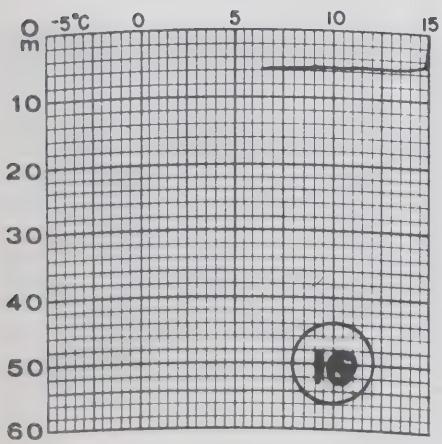
-5°C 0 5 10 15
0 m
10
20
30
40
50
60

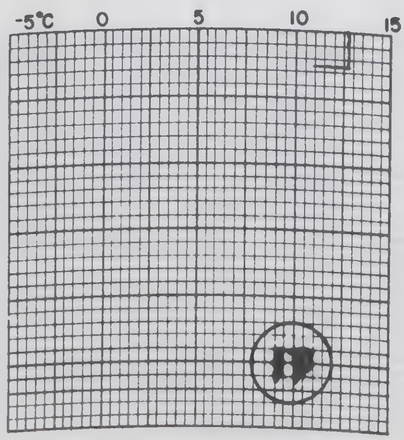
-5°C 0 5 10 15

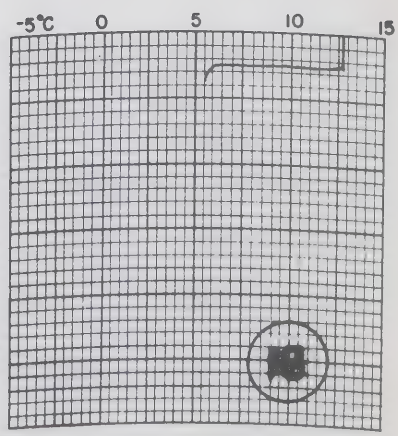
-5°C 0 5 10 15

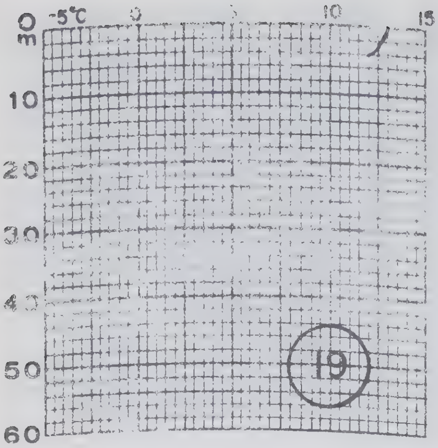
-5°C
0
5
10
15
0 m
10
20
30
40
50
60
19

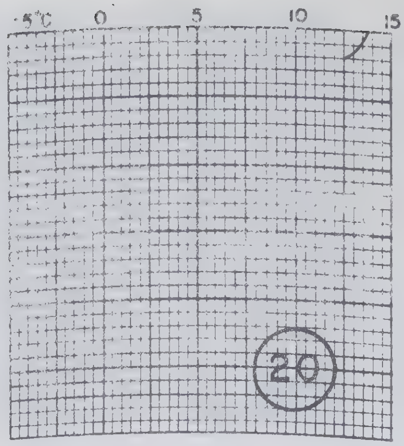
-5°C
0
5
10
15
20

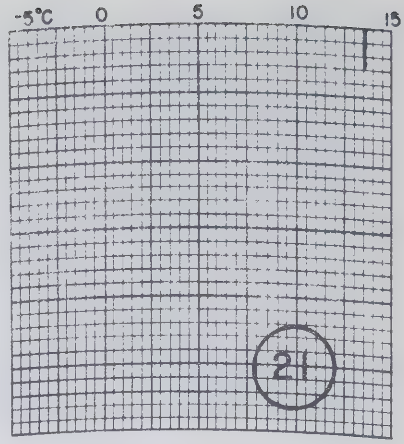
-5°C
0
5
10
15
21

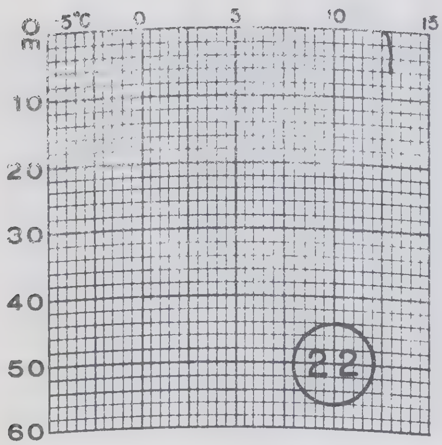
-5°C
0
5
10
15
0 m
10
20
30
40
50
60
22

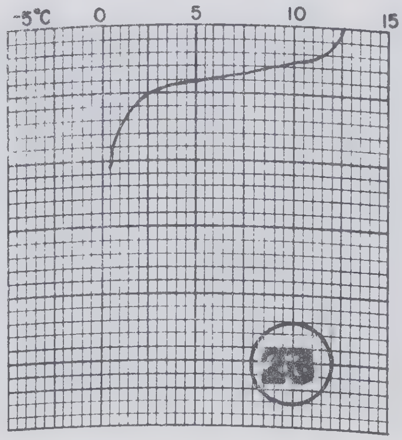
-5°C
0
5
10
15
23

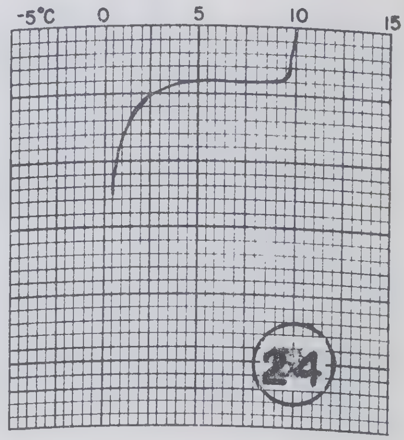
-5°C
0
5
10
15
24

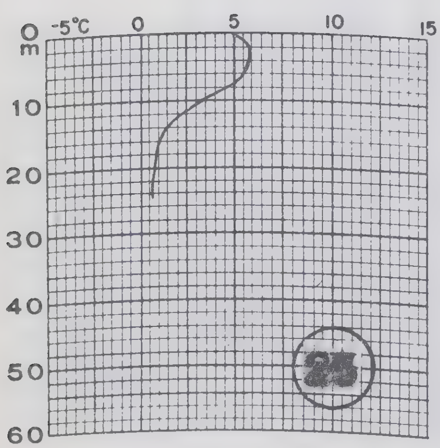
-5°C
0
5
10
15
0 m
10
20
30
40
50
60
25

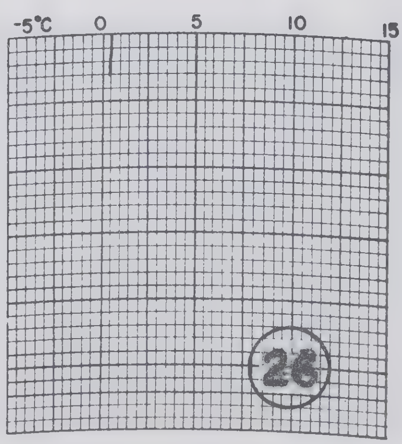
-5°C
0
5
10
15
26

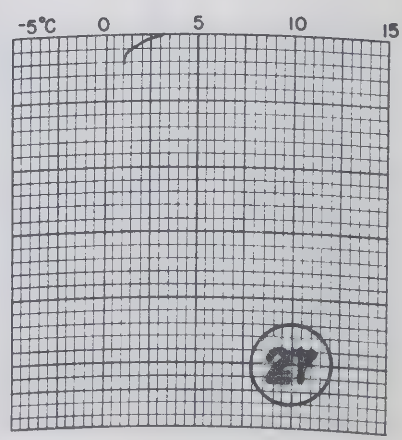
-5°C
0
5
10
15
27

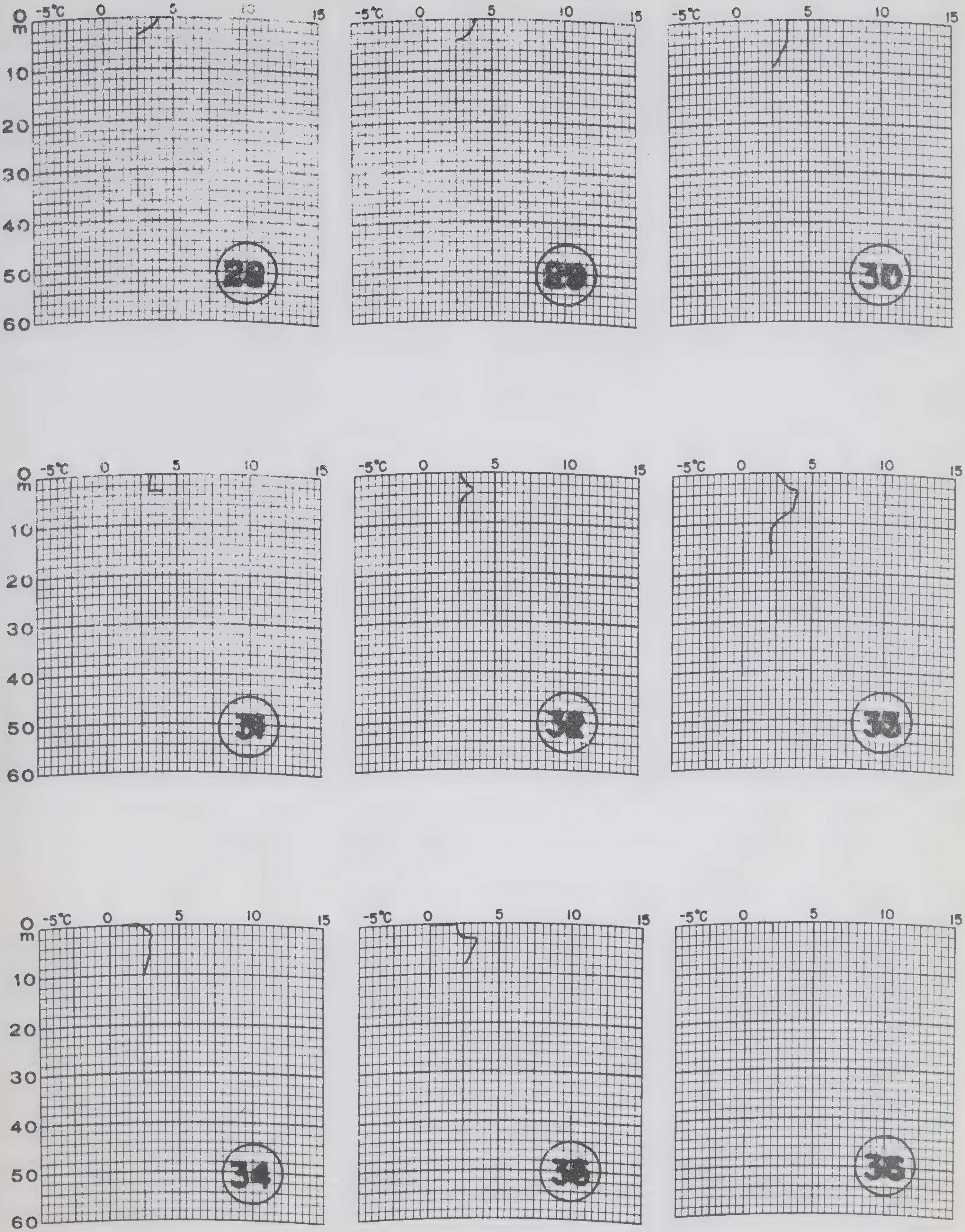
-5°C
0
5
10
15
0 m
10
20
30
40
50
60
30
33
34

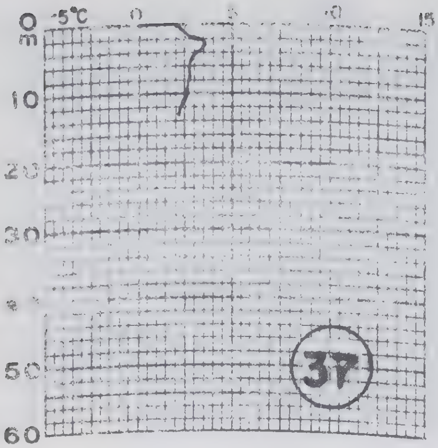
-5°C 0 5 10 15
0 m 10 20 30 50 60
37

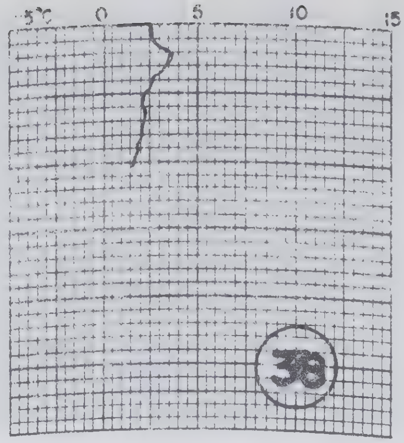
-5°C 0 5 10 15
38

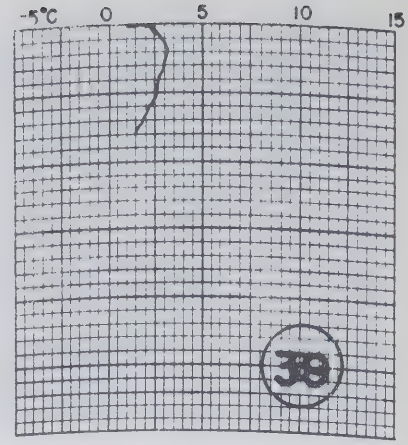
-5°C 0 5 10 15
39

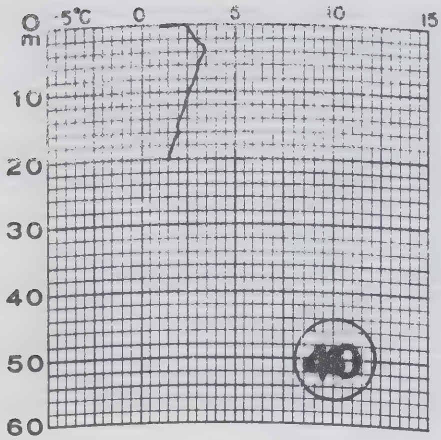
-5°C 0 5 10 15
0 m 10 20 30 40 50 60
40

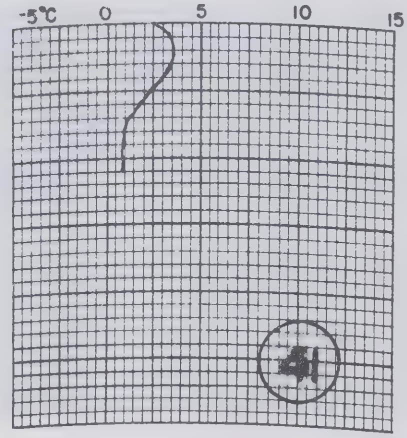
-5°C 0 5 10 15
41

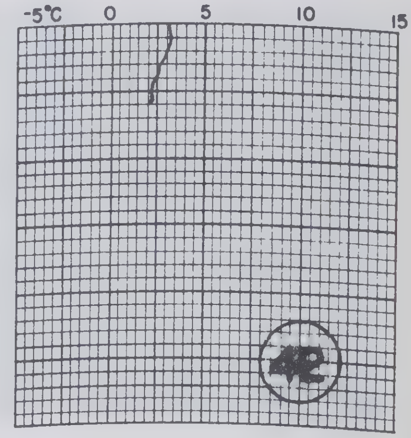
-5°C 0 5 10 15
42

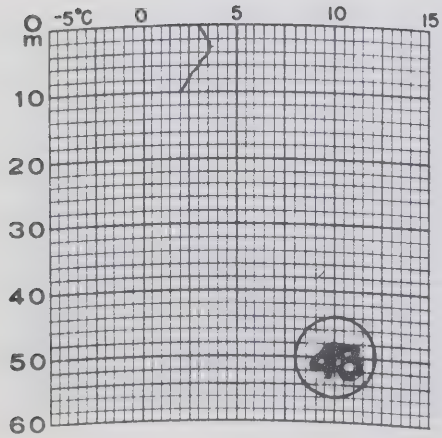
-5°C 0 5 10 15
0 m 10 20 30 40 50 60
43

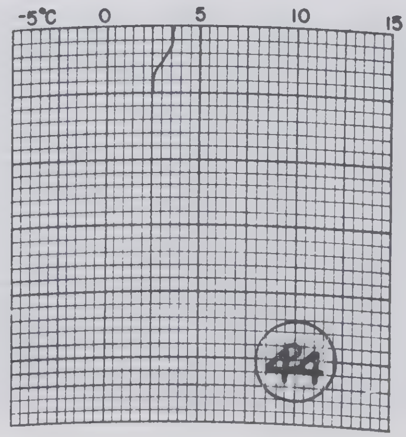
-5°C 0 5 10 15
44

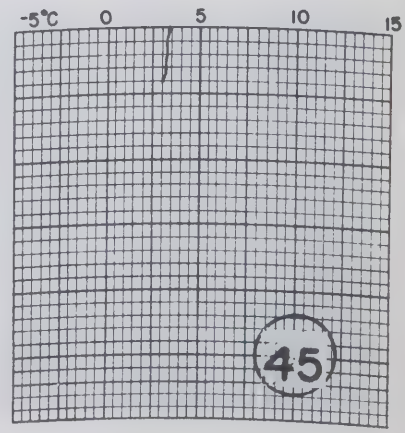
-5°C 0 5 10 15
45

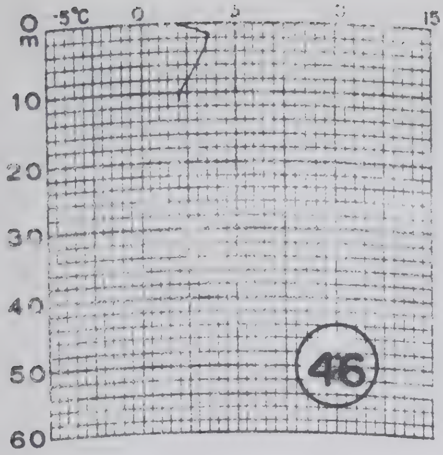
-5°C 0 5 10 15
0 m 10 20 30 40 50 60
46

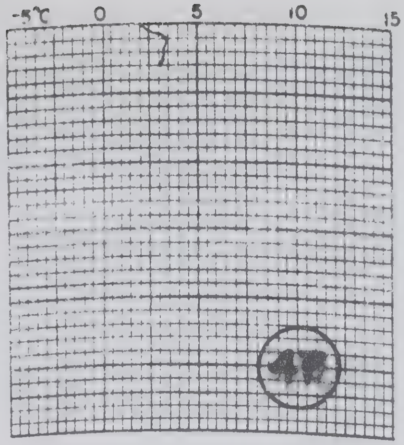
-5°C 0 5 10 15

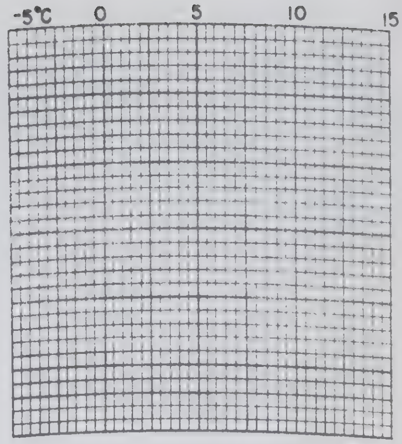
-5°C 0 5 10 15

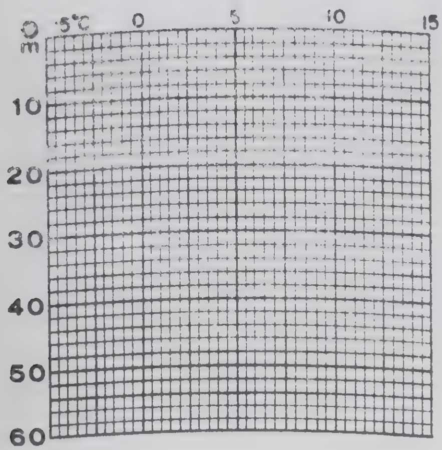
-5°C 0 5 10 15
0 m 10 20 30 40 50 60

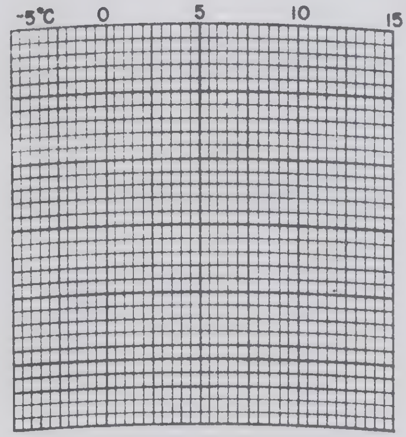
-5°C 0 5 10 15

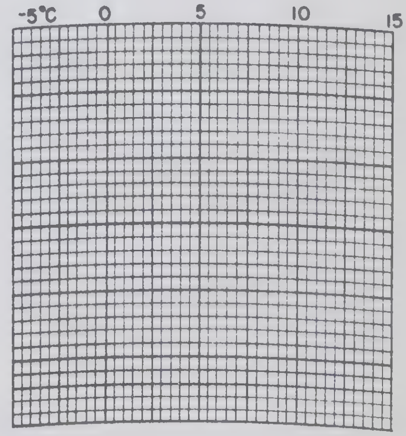
-5°C 0 5 10 15

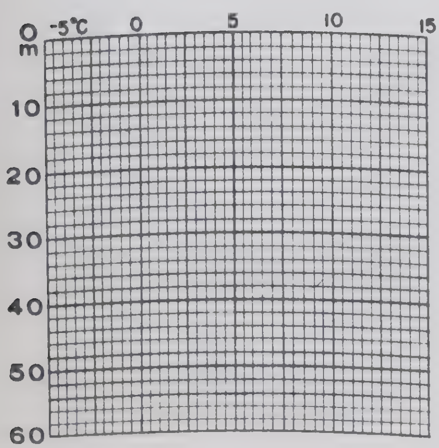
-5°C 0 5 10 15
0 m 10 20 30 40 50 60

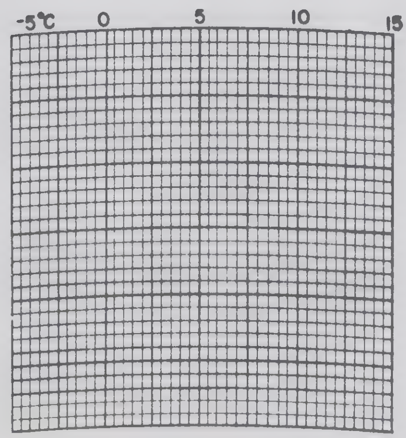
-5°C 0 5 10 15

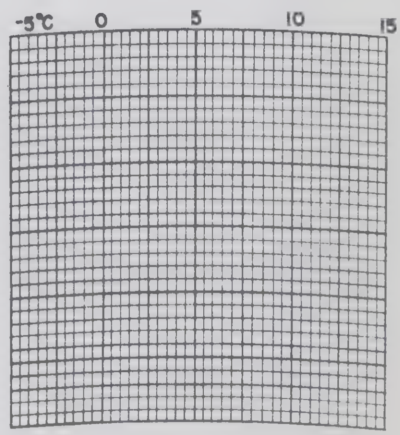
-5°C 0 5 10 15

MANUSCRIPT
REPORT SERIES **No. 8**

The 1965 Current Survey of the Bay of Fundy - A New Analysis of the Data and an Interpretation of the Results

Gabriel Godin

1968

Marine Sciences Branch
Department of Energy, Mines and Resources, Ottawa

Manuscript Report Series No. 8

THE 1965 CURRENT SURVEY OF THE BAY OF FUNDY - A NEW ANALYSIS OF THE DATA AND AN INTERPRETATION OF THE RESULTS

Gabriel Godin

1968

CONTENTS

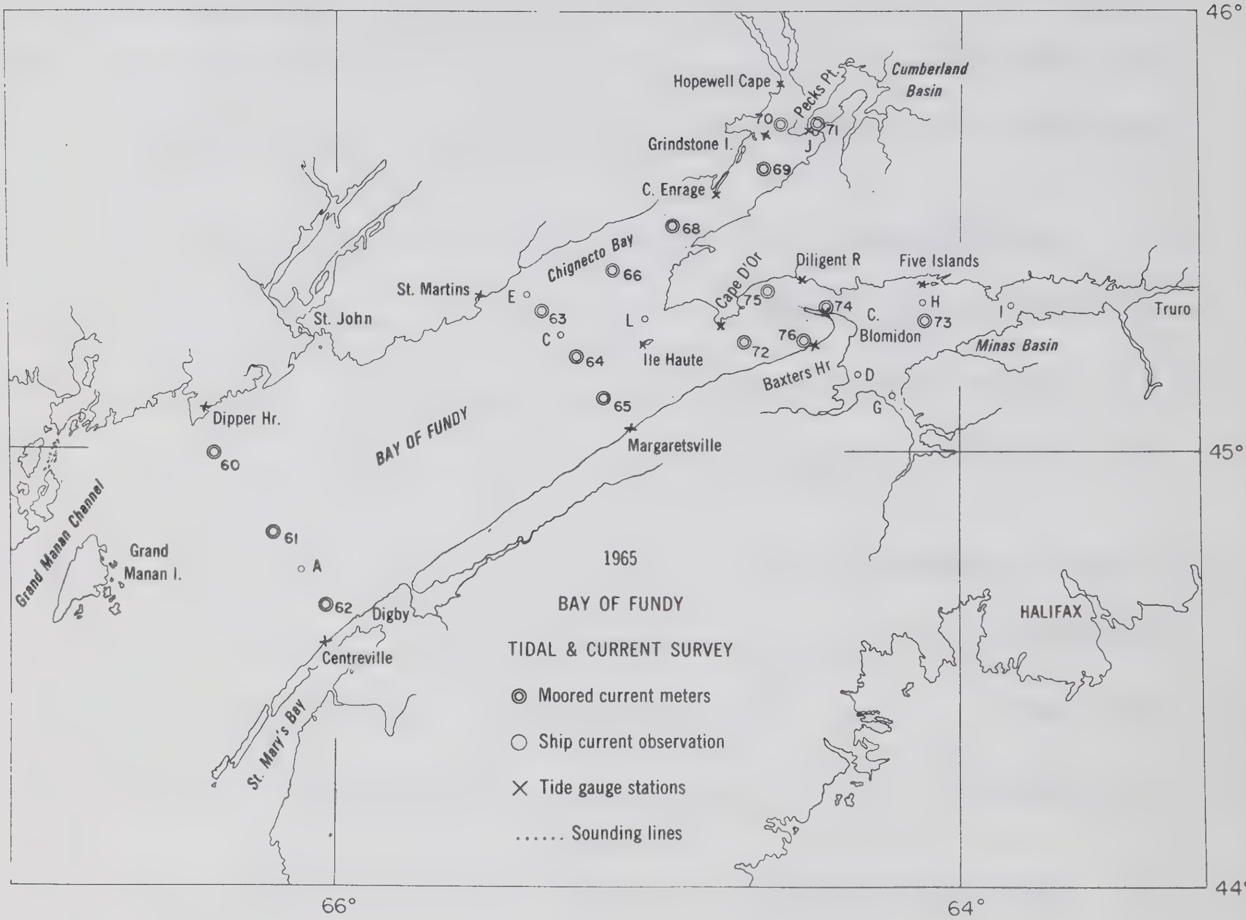

Frontispiece. The location of the stations for the 1965 current survey.

1. INTRODUCTION

The current survey of 1965 carried out by Mr. C.J. Langford and his group in the Bay of Fundy has yielded a very large amount of data (Anon., 1966). Since that time we have developed a technique of current analysis (Godin, 1967) which we were anxious to put to test. The material on the Bay of Fundy seemed ideal for such an application and with the assistance of the Bedford Institute of Oceanography which has supplied us with the data, we have proceeded with the analyses.

The analyses indicate that the semidiurnal constituents are by far the dominant ones of the horizontal motion. In the case of short intervals of observation however, the contribution of the individual semidiurnal constituents could not be ascertained accurately on account of the presence of L_2. This constituent is partly of shallow water origin (resulting from the interaction of M_2 and S_2), partly of astronomical origin; it happens to have the same order of magnitude as S_2 and N_2 and it cannot be separated for observations covering an interval of 15 days. The results of the analyses for S_2 and even M_2, in such instances, are blurred by the presence of this hidden constituent.

The low passing of the data reveals in a certain measure the variation of the residual current in time. These variations naturally can be interpreted in many ways, but over the body of the bay they seem to confirm the surface circulation pattern deduced by Bumpus and Lauzier (1965) from the drift of bottles.

The residual currents measured in Minas Channel are extremely large (1 to 1.5 knots). But we must remember that they were obtained from spot observations and these observations do not necessarily imply that there is a net steady inflow across the whole section. We interpret rather these apparent residual currents in the following way. Due to the configuration of the channel and the bottom topography, the incoming flood current does not have a uniform value across the section; it may contain zones of larger and of smaller velocities. During the ebb flow the velocity pattern may be quite different. The net result is that the measurement of the current at one point yields a tidal stream of a given strength and phase as well as a residual current; the measurement of current at another point of the same section would yield a tidal stream of approximately the same strength and phase, but in addition a markedly different residual current. If the density of the sample points is large enough across the section, one will deduce that the net flow in and out of the section during a tidal cycle is exactly equal to zero. But the results of the observations at a single sample point must be handled with caution and one cannot assume that the net residual current measured at the point is the same all over the section; it may simply reflect the horizontal and vertical inhomogeneities of the tidal flow.

We had to accept the data obtained during the survey at their face values on account of the long time elapsed between the survey and our analyses and on account as well of the absence of Mr. C.J. Langford.

However we have taken the freedom to correct three very obvious mistakes in the observations:

(1) the frame of reference for station 73 has been rotated by 90°,

(2) the clock time for station 74 has been advanced by 1 hour, and
(3) the clock time for station 76 has been advanced by 2 hours.

2. THE ANALYSES

A current observation may be represented by a rate and a direction or by two components of velocity along two mutually perpendicular directions; the latter representation is more convenient for the purpose of analysis.

The choice of a particular frame of reference is immaterial but the most rational choice consists in taking the x axis to run along the east while the y axis runs along the north. The data which have been supplied to us had already been decomposed into two components. Unfortunately the frame of reference chosen was right-handed (or geographical) in which standard trigonometric calculations are impossible and it differed for almost each station (a very unnecessary complication). We made the frame of reference left-handed by changing the sign of the x component. Also all the inclinations and directions quoted in the results are referred to an x axis running toward the east, the angles being measured counterclockwise from it. The directions shown in the plots (see Appendices) however had to refer to the particular frame of reference chosen for the given station. Table 1 gives the orientation of the x axis of the particular frame of reference chosen for a given station with respect to the east.

Table 1

Orientation of the Frames of Reference Chosen for the Various Stations at which Observations were Collected

Station	Orientation of the x axis of the particular frame of reference with respect to the east
60-61-62	034°
63-64-65	034°
66-67-68	034°
69-71	052°
70	073°
72	018°
73	270°
74	349°
75-76	034°

The analysis consists first in smoothing the observations taken at intervals of five minutes in our case. The smoothing eliminates almost completely any accidental error in reading or in punching which we may note here and there in the raw data shown in the plots under the labels X and Y. The smoothing also eliminates the high frequency oscillations which become very conspicuous in Minas Channel (Plots corresponding to stations 72, 74, 75 and 76). The smoothed data (labelled X-SM and Y-SM) can be sampled afterwards at the more practical time interval of one hour.

The smoothed data are then low passed, and the results of the low passing, labelled X-LP and Y-LP in the plots, show the x and y components of the residual currents. The results of the low passing are replotted in a new set of plots (Plots 25 to 48) which show as well the equivalent rates and directions which are physically more intuitive. As said already all the orientations mentioned in the plots refer to the particular frame of reference identified in Table 1. X-LP and Y-LP are removed from the smoothed data and what is left, called X-R and Y-R in the plots, is subjected to a harmonic analysis.

The choice of the constituents which may be separated from a given set of observations depends on the number 2N+1 of these hourly observations and on the difference in frequency of the given pair of constituents whose separability we wish to investigate, according to the formula:

$$N \left| \sigma_K - \sigma_{K+1} \right| \geqq .8 \qquad (1)$$

σ_k is the frequency of the dominant constituent of the pair, in cycles per hour, σ_{k+1}, that of the smaller constituent. Strictly speaking the criterion of separability should be:

$$\left| \sigma_K - \sigma_{K+1} \right| N \geqq 1$$

but it turns out to be a bit too stringent for the type of observations that occupies us.

Table 2 shows the pair arrangement which we have used in order to set up a list of the constituents which may be separated from a given set of observations.

In the actual punched cards fed to the computer, the frequencies identify the constituent quoted in the above table.

The choice of the constituents is done in the following way: the quantity $|\sigma_k - \sigma_{k+1}|N$ is computed. If it is equal to or larger than .8, the second constituent of the pair is retained; if it is not, one goes to the next pair.

We have been compelled to add M_3 and M_6 to the list of constituents in order to represent the strong six-diurnal oscillations which are found at the stations located at the head of the bay.

Table 2

Pair Arrangement for the Elaboration of a List of Constituents which may be Separated from a Given Set of Observations

	σ_k Name	σ_{k+1} Name	Frequency cycles/hour
1	ZERO	M_2	.0805114007
2	M_2	S_2	.0833333333
3	S_2	L_2	.0820235526
4	M_2	N_2	.0789992487
5	N_2	μ_2	.0776894680
6	M_2	K_1	.0417807462
7	K_1	O_1	.0387306544
8	O_1	NO_1	.0402685943
9	O_1	Q_1	.0372185025
10	K_1	OO_1	.0448308380
11	K_1	J_1	.0432928982
12	M_2	M_4	.1610228013
13	M_4	MS_4	.1638447340
14	M_4	MN_4	.1595106494
15	M_4	M_8	.3220456025
16	M_4	M_3	.1207671011
17	M_4	M_6	.2415342021

The complex amplitude of the analyzable constituents is evaluated by applying to the sequence of observations the least square requirement:

$$\sum_{j=-N}^{N} \left| \sum_{\kappa=-n}^{n} a_\kappa \, e^{2\pi i \sigma_\kappa j} - Z(j) \right|^2 = \text{Min} \tag{2}$$

m is the number of constituents analyzed, z(j) represents the velocity at time j which has been smoothed and from which the residual current has been removed. z(j) is represented by X-R and Y-R in the plots. a_k is the complex amplitude searched for.

Once the a_k's are obtained the constituents to be inferred are found and the complex amplitude of the main constituent is readjusted. For this purpose we write:

$$a_K = a_K^t + \frac{\sin(N+\frac{1}{2})\,\pi\,(\sigma_K - \sigma_{KK'})}{(N+\frac{1}{2})\sin\pi\,(\sigma_K - \sigma_{KK'})} \quad a_{KK'} \tag{3}$$

and we assume

$$a_{KK'} = R_{KK'}\, a_K^t$$

In the above forumlas, a_k^t stands for the undistorted complex amplitude of the main constituent, $a_{kk'}$, the amplitude of a constituent located in the vicinity of the constituent k and which cannot be separated from it in the given analysis. $R_{kk'}$ is an empirical constant of proportionality obtained from a set of yearly analysis of coastal observations. Table 3 gives the magnitude and the phase of the $R_{kk'}$ s which are of relevance in our analysis.

Table 3

Amplitude and Phase of the Empirical Complex Constant of Proportionality $R_{kk'}$ Used for the Inference of Unanalyzable Constituents in the Bay of Fundy

k	k'	$R_{kk'}$	arg $R_{kk'}$
M_2	N_2	.20	28.1°
O_1	Q_1	.17	22.4°
K_1	P_1	.33	.7°
S_2	K_2	.27	-.5°
N_2	ν_2	.23	-6.0°

The knowledge of the mid-time allows us to calculate the corrections f_k and u_k to the nodal modulations as well as the astronomical arguments. We write

$$\begin{aligned} a_k &\equiv f_k \left| a_k \right| e^{2\pi i (V_k + u_k - G_k^+)} \\ a_{-k} &\equiv f_k \left| a_{-k} \right| e^{-2\pi i (V_k + u_k - G_k^-)} \end{aligned} \tag{4}$$

The lengths of the semimajor and semiminor axes, M_k and m_k of the constituent ellipses are then given by

$$\begin{aligned} M_k &= |a_k| + |a_{-k}| \\ m_k &= |a_k| - |a_{-k}| \end{aligned} \qquad (5)$$

If m_k is negative, this indicates that the current vector rotates clockwise around the constituent ellipse.

The inclination of the major axis to the x axis is given by

$$\theta_K = \frac{1}{2}(G_K^- - G_K^+) \qquad (6)$$

while the Greenwich phase lag is given by

$$g_K = \frac{1}{2}(G_K^+ + G_K^-) \qquad (7)$$

There is an ambiguity of 1/2 cycle (180°, π radians) in θ_k and g_k. It has no practical importance since only G_k^+ and G_k^- are actually used in the representation of the observations. We choose θ_k to fall between O and 1/2 cycle (O and 180°, O and π radians) and we pick g_k to fall approximately 1/4 cycle behind the g_k of the coastal observations, taking as positive the currents which move towards the head of the bay.

The probable error on the magnitude and the phase of a given constituent is given by

$$\Delta \cong 2(\bar{\Delta}_x + \bar{\Delta}_y)(2N+1)^{-\frac{1}{2}} \qquad (8)$$

and

$$\Delta G \cong 2(\bar{\Delta}_x + \bar{\Delta}_y) M_K^{-1} (2N+1)^{-\frac{1}{2}} \qquad (9)$$

where $\overline{\Delta x}$ and $\overline{\Delta y}$ are the root mean square deviation in the x and y directions.

Unfortunately the true error on a given constituent is much more sensitive to the presence of constituents hiding in its vicinity than to the root mean square deviation. This can be noted for instance for the diurnals which, according to (8) and (9), are smaller or equal to the background noise although the values obtained are sensible and pretty uniform while on the other hand the actual error on S_2 is certainly greater than the one indicated by (8) and (9) in view of the scatter of values whenever L_2 cannot be isolated. We must note as well that formulas (8) and (9) are based on the assumption of the randomness of the error while in fact an inspection of the actual residues, labelled X-ER and Y-ER in the plots, do not exhibit a random character and reflect rather the interference of one or more hidden constituents.

We test the success of the technique of inference by calculating the residues from

$$Z(j)-\sum_{\kappa=-n}^{n} a_\kappa \, e^{2\pi i\sigma_\kappa j}$$

as well as from

$$Z(j)-\sum_{\kappa=-n}^{n} a_\kappa^t \, e^{2\pi i\sigma_\kappa j}-\sum_{\kappa'=-n'}^{n'} a_{\kappa\kappa'} \, e^{2\pi i\sigma_{\kappa\kappa'} j}$$

in some instances which are shown in Plots 1 to 24. The success of the inference using the assumed relationship $a_{kk'} = R_{kk'} a_k^t$ is doubtful in many instances and we certainly prefer a direct analysis of the constituents whenever this is feasible.

For this purpose we have made a single analysis of all the data which were available at a given depth even though they were separated by a time gap. This was the case for the following stations:

Stn.	Depth
61	13m
64	25m
65	25m
68	25m
71	5m
72	25m

In this fashion the resolution is finer and the perturbing influence of L_2 on M_2 and S_2 is eliminated; the results are then more stable. All the data pertaining to the analyses are found in the Appendix.

3. DISCUSSION OF THE RESULTS

3.1 The Constituents

The results of the analyses which are displayed in the latter pages of this report show plainly that M_2 is the most important of all constituents; M_3, M_4, M_6 and M_8 which become large at the head of the bay are created by M_2 in order of magnitude.

The diurnals are small all over the bay and their analysis turned out to be an academic exercise more than anything else.

Table 4 gives the semimajor and semiminor axes of the constituent M_2 as well as its Greenwich phase lag. The values in brackets result from analyses from which L_2 could not be separated.

Table 4

The Results of the Analyses for M_2

	Depth								
	5 or 13 Metres			25 Metres			50 Metres		
Station	M knots	m knots	g o	M knots	m knots	g o	M knots	m knots	g o
60	1.30	-.15	271.1						
61	1.54	-.14	266.2				(1.78	-.06	259.9)
62	2.08	-.21	262.1						
63				1.77	.03	264.4			
64	2.29	-.22	265.2	1.88	.02	271.6			
65				2.17	-.04	265.7			
66				(1.61	-.07	259.5)			
68				1.68	.07	265.2			
69	(1.92	-.02	264.3)						
70	(2.84	.03	272.7)						
71	2.26	-.08	268.5						
72				4.07	.23	279.0			
73	(2.58	-.03	289.5)						
74	3.27	-.23	288.4						
75	(2.97	.05	284.8)						
76	(1.49	-.11	289.6)						

The values listed in Table 4 are displayed graphically in Figure 1. The major axis is oriented along the direction given by the analysis; the length of the axis is proportional to the intensity of the M_2 stream at this point. The cotidal lines are drawn at intervals of 10° of phase ($\longrightarrow$ 20 minutes in time).

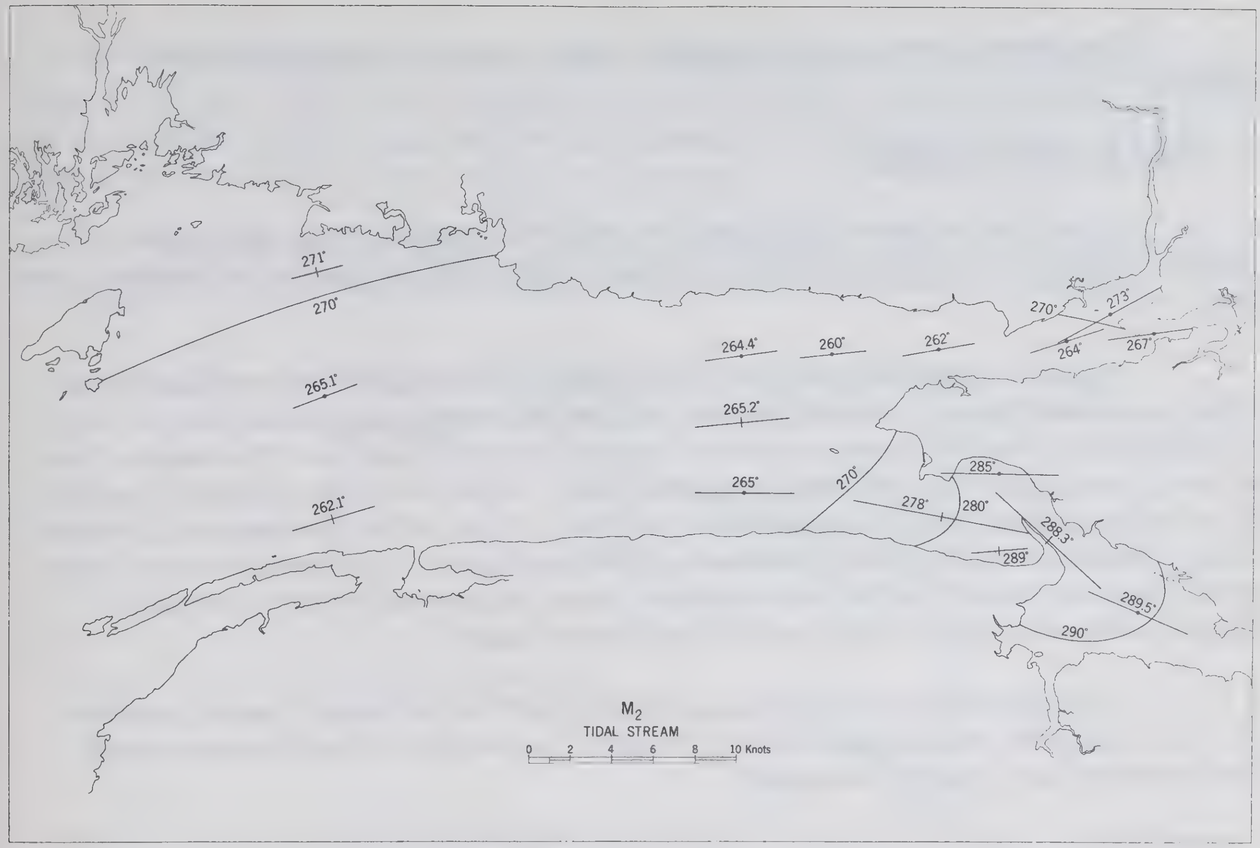

Figure 1. The major and minor axes of the M_2 tidal stream ellipses as well as the Greenwich phase lag of the stream vector.

We note that within the accuracy of the analysis the M_2 stream is nearly simultaneous over the body of the Bay; it becomes progressive in Minas Channel and in Cumberland Basin. There is obvious evidence of some horizontal gradients in the phase of the streams at the mouth of the bay. These gradients disappear farther inside the bay.

The tidal streams are essentially rectilinear with a slight tendency to turn clockwise; the only certain counterclockwise rotation takes place at station 72. The minor axis of the ellipse amounts to at most 10 per cent of the major axis; most often it is negligibly small. The shallow water constituents such as M_3, M_4, M_6 etc. increase in importance towards the head of the bay. There they become larger than the diurnals and are of the same order of magnitude as many semidiurnals. The plot of residues X-ER and Y-ER indicate that other high frequency shallow water constituents are present besides the ones searched for in the analyses. The short duration of the interval of observation prevented our investigating these constituents more closely.

The high frequency oscillations present in the raw data for station 72 onwards indicate strong turbulent motion with vertical and horizontal eddies. The instantaneous rates may therefore at times be much larger than the smoothed rates.

According to theory (Proudman, 1953) the streams should turn earlier near the bottom. Station 61 obeys this rule, but the reverse occurs for station 64. The peculiar bottom topography at the latter station might explain this anomaly.

The diurnal streams are negligibly small, and do not warrant further discussion.

3.2 The Residual Currents

Plots 25 to 48 show on a magnified scale the results of the low passing. The scale of magnitude extends to 2 knots and one notch on the vertical scale indicates one knot.

Figure 2 illustrates the mean and range of the information contained in the latter mentioned plots. The full arrows indicate the drifts near the surface (5, 10 or 13 metres); the dashed arrows show the drifts at 25 or 50 metres. The length of the arrow is proportional to the intensity of the drift. A pair of arrows joined by an arc of a circle indicates that the direction of the flow varied during the interval of observations between the directions indicated. In Minas Channel the directions were very steady but the intensity of the flow varied in time; the notched interval indicates approximately the limits within which the flow oscillated.

We discuss first the residual currents observed in Minas Channel (stations 72, 74, 75 and 76) which appear rather peculiar and which can lead to extravagant conclusions if not properly assessed.

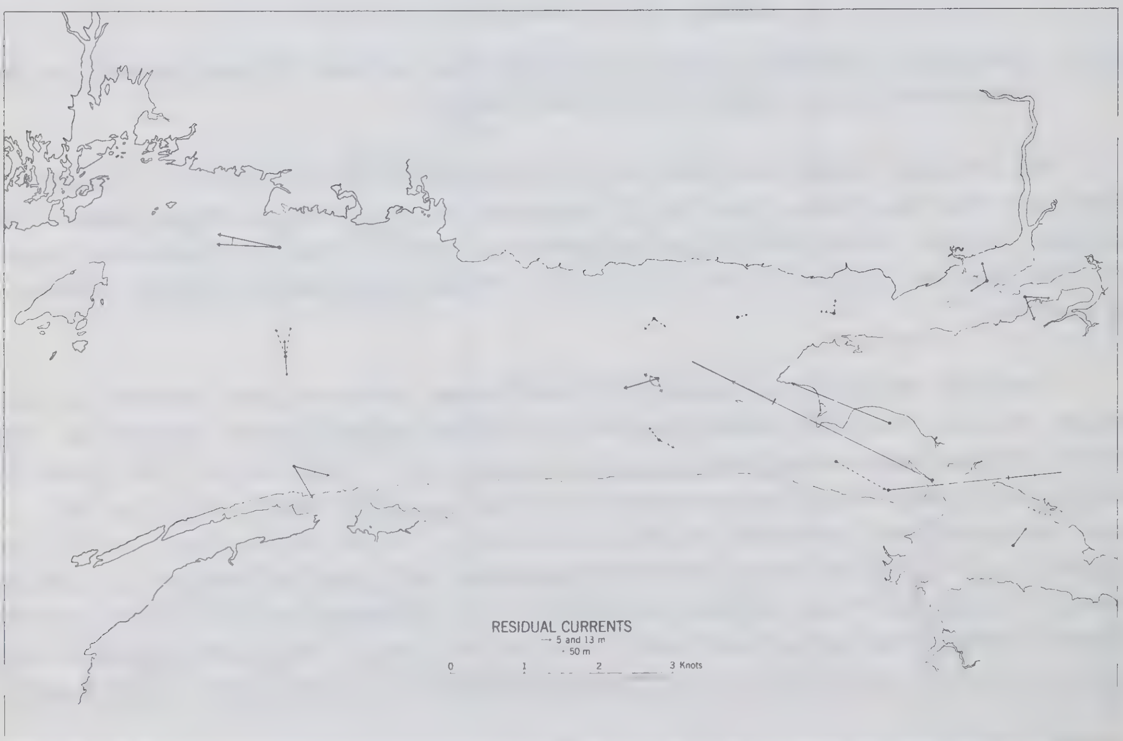

Figure 2. The direction and magnitude of the residual current plotted on a uniform scale. The dashed arrows pertain to the 25 or 50 m depth. Two arrows joined by an arc of a circle indicate that the residual current oscillated between the directions shown during the interval of observation. The bar across some arrows indicates that the current oscillated in magnitude in the same direction and the bar indicates the smallest magnitude of the current.

The magnitude of these currents is unbelievably large and they seem to have a very constant orientation. If we take them at face value, Minas Basin should have emptied itself centuries ago while Minas Channel would always overflow. We must therefore search for a more sensible explanation.

First the outward drift of 1.5 knots at station 74 must be compensated by an inward drift of equal magnitude on the northern side of the narrow channel; so:

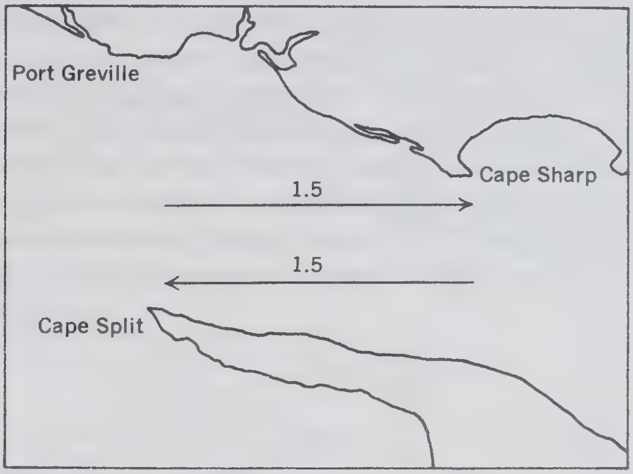

Taking M_2 as well as the residual current, the following velocity distribution will be found at flood and at ebb:

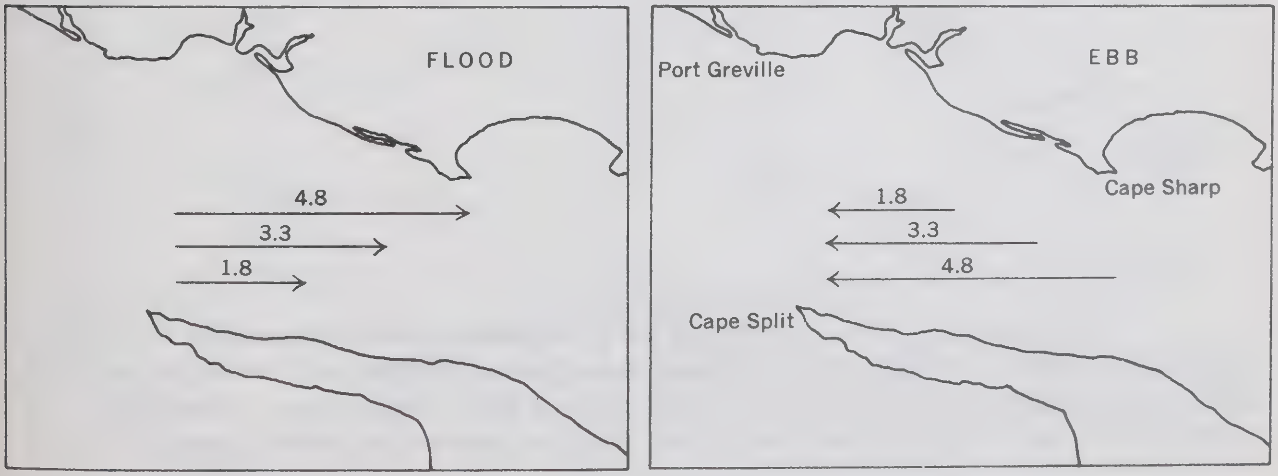

We see that the projection of Cape Split causes large inward currents in the northern portion of the channel on account of its impeding presence, while at ebb the situation is reversed: the flow is faster around Cape Split. The apparent residual current simply indicates the presence of horizontal gradients in a north south direction of the tidal flow at flood and at ebb; they have nothing to do with a true circulation.

If we look at the whole of Minas Channel, fortified by this observation, we have the following picture at flood and at ebb situations:

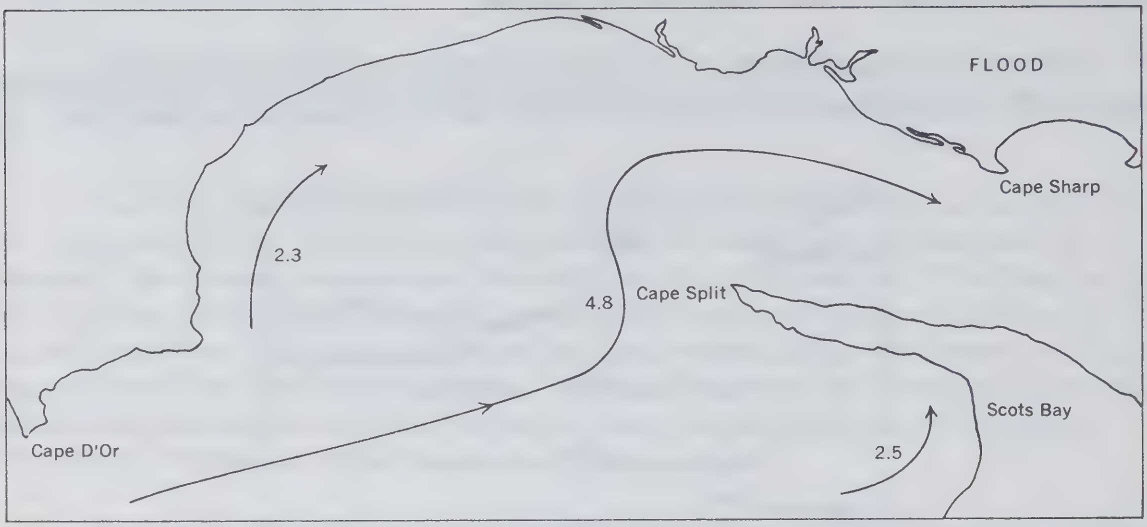

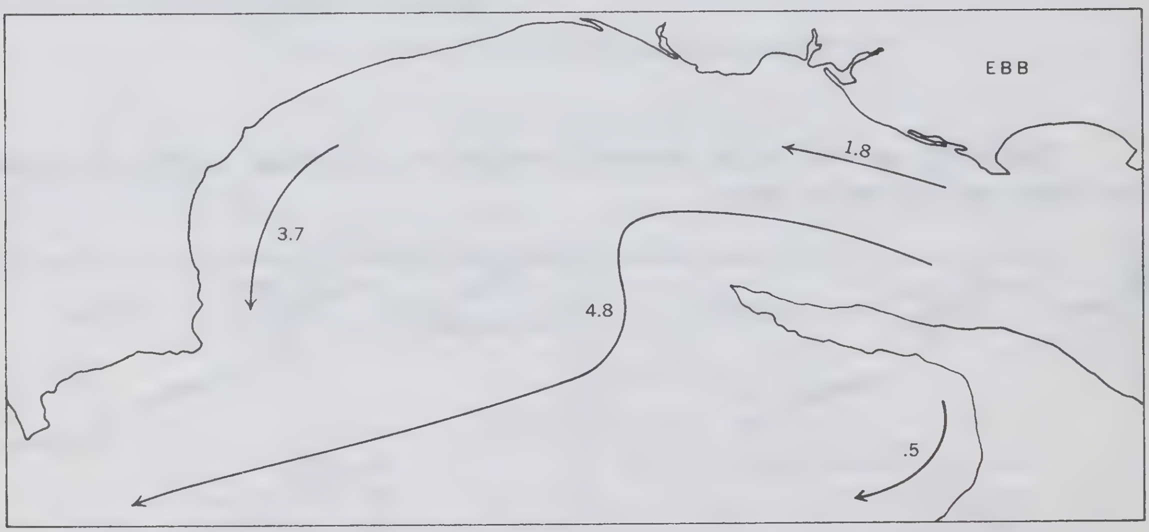

The projection of Cape Split causes at all times small currents in the embayment of Scots Bay. However the currents there have a chance to be stronger at flood than at ebb because they are created ahead of Cape Split while at ebb, Cape Split deflects the main portion of the flow to the southern portion of Minas Channel.

Similarly the encroachment of Cape d'Or causes smaller currents at flood than at ebb in its vicinity.

The band of strong currents which is located approximately in the middle of the bed ahead of Minas Channel is deflected northward at flood and southward at ebb.

The presence of Cape d'Or and Cape Split should cause the formation of appreciable horizontal eddies. We have observed the flood and ebb flows in the small scale model of the Bay of Fundy which is now located in the Tides and Water Levels

Section of the Inland Waters Branch in Ottawa. We have noted that an eddy forms past Cape d'Or at flood; this eddy is not stationary but it moves along the flow and it eventually disappears in Minas Basin as the flood flow weakens. At ebb, a large eddy forms to the west of Cape Split in the embayment of Scots Bay. This eddy has large horizontal dimensions (the size of the embayment) and it does not change its position. It is then possible, if we believe the model, that the picture we give of the flow in Minas Channel is complicated by the presence of these eddies.

The presence of an eddy at ebb in the embayment would be reflected in the measurement registered by a current meter at a given point close to the shore as a weak oscillatory current over which is superimposed a steady inward flow. This is exactly what has been observed at station 76. Unfortunately there is an ambiguity of two hours at this station. We have assumed the clock reading on the meter to be two hours behind the correct time in view of the coastal observations which show that the time of high water is approximately simultaneous between Cape d'Or and Scots Bay; this could not be reconciled with a delay of two hours in the maximum tidal streams. However a turn of the current two hours ahead at Scots Bay could be very well fitted with the eddy picture; thus:

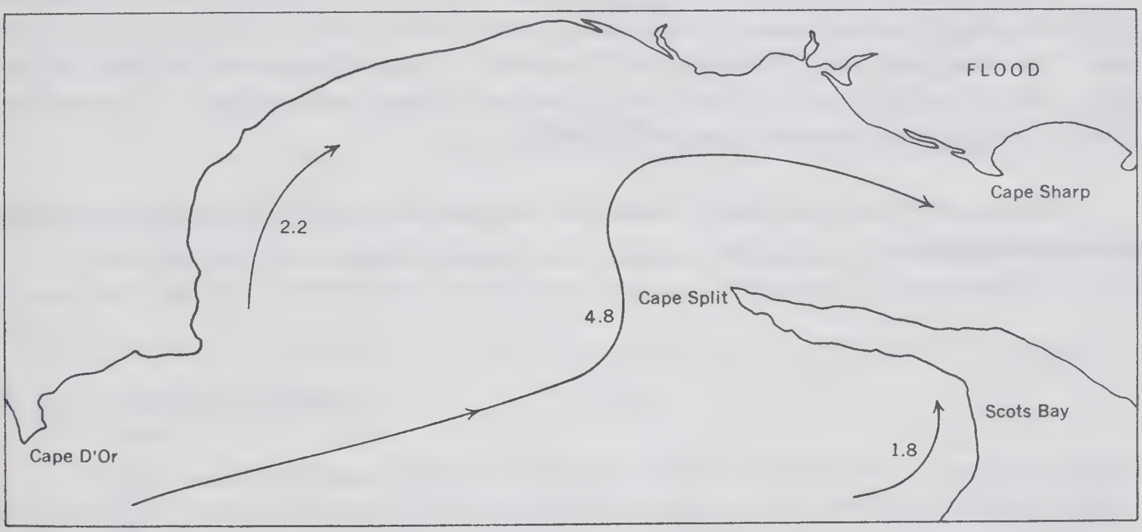

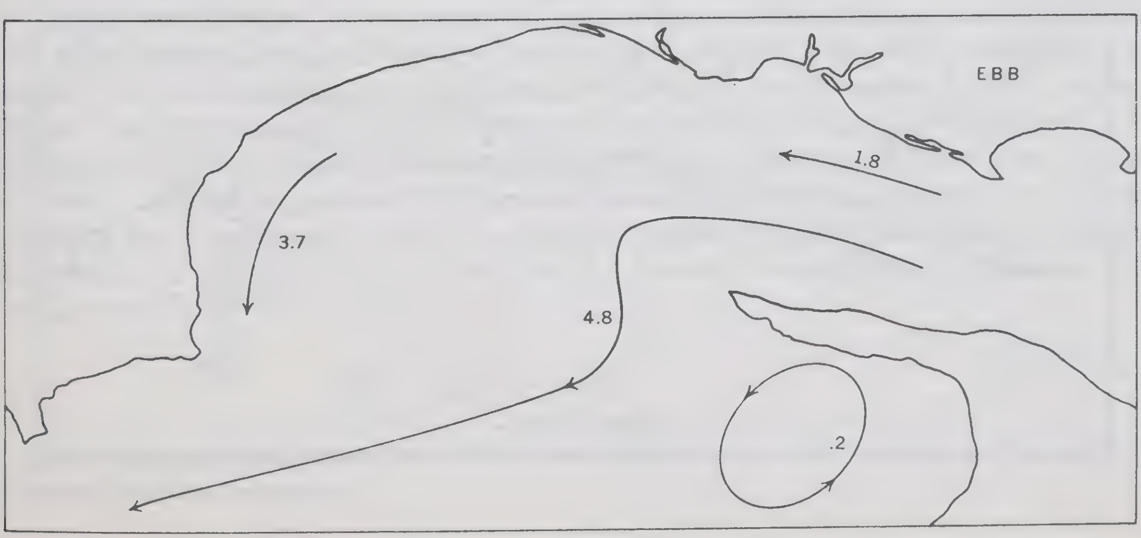

It is therefore too bad that we cannot ascertain whether the meter clock was right or two hours behind at station 76 since by now we are too far removed from the operational details of the survey.

In any case however we are quite convinced that the apparent circulation revealed by the residual currents in Minas Channel is created by the horizontal gradients in the strength of the tidal flow and that it would disappear altogether without tidal motion.

We note in Plot 46 that in the magnitude of the residual current at station 74, there are two well marked minima located approximately 14 days apart. The minima reflect the neap tides of the 7th and of the 21st of April, 1965.

We have no ready explanation for the northeast drift of .3 knot observed at station 73 in the centre of Minas Basin (Plot 45). It may indicate a genuine counter-clockwise circulation in the basin or it may once again reflect the presence of horizontal gradients in the flood and ebb.

Over the main body of the bay, stations 60 and 62 (Plots 25 and 29) indicate clearly an outward and an inward drift at 13 metres along the northern and the southern shores. The observations at station 61 (Plots 26, 27 and 28) are not as easy to interpret. At 13 metres, the drift may be directed against both shores; at 50 metres, the drift is definitely directed against the north shore.

We may fit the spot observations at stations 60 to 66 by assuming the following circulation pattern:

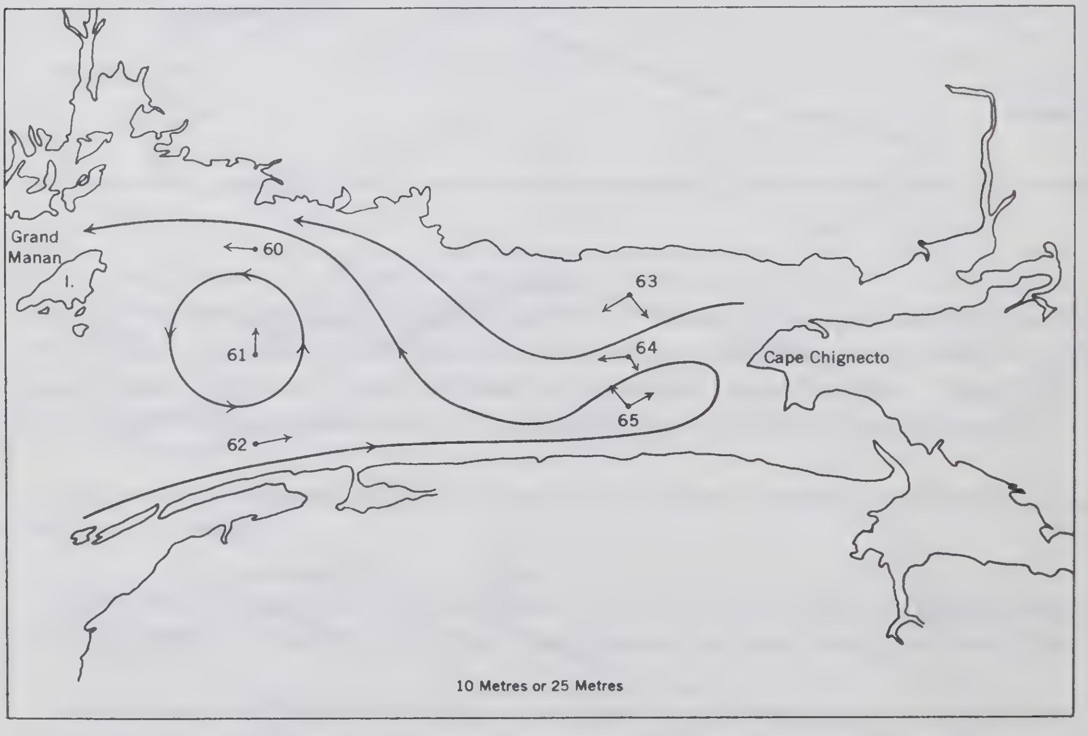

The gyre at station 61 might shift its position in time near the surface resulting in the following pattern:

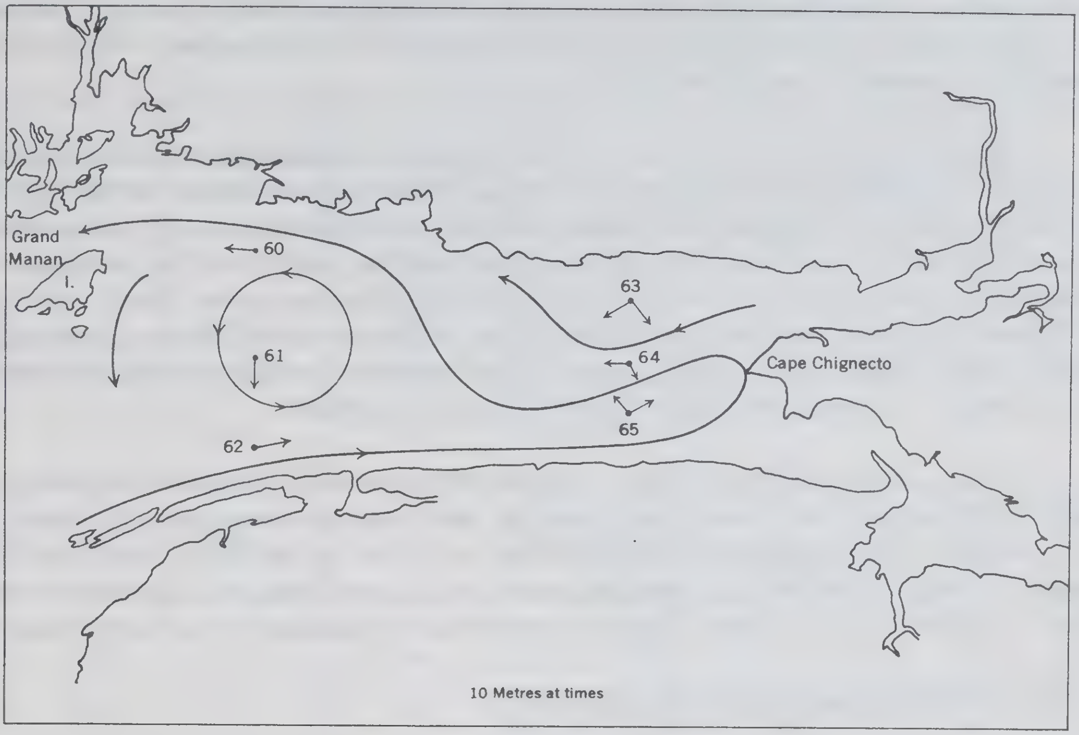

The patterns we assume agree in substance with the circulation deduced by Bumpus and Lauzier (1965) by observing the recovery pattern of drift bottles released in the bay.

3.3 The Maximum Currents

There being so many tales of fierce currents in the Bay of Fundy, it is good to sit down and evaluate soberly from the observations that are now available, the maximum currents that are liable to occur.

It is not difficult to estimate the probable maximum tidal streams. We may safely assume that these will occur when the moon and the sun are in conjunction or in opposition, when they have their largest declination and when the moon is in perigee. Then the constituents M_2, S_2, K_2 and N_2 will be in phase. The remaining small constituents will have random phases under average conditions and will tend to cancel each other. It is also preferable to ignore the shallow water constituents which tend to diminish the maximum values of the streams since they represent the resistance of the bottom to the tidal motion. We take the probable maximum tidal stream to have value

$$M_2 + S_2 + K_2 + N_2 + \Delta \tag{10}$$

Δ represents the unexplained portion of the tidal motion and it is measured by the root mean square deviation.

It is not as easy to estimate the maximum currents liable to occur at a given point. The wind stress and the pressure gradients create the residual currents and we must know the response of the bay to such forces before we may predict in detail these currents. At the present, the dynamics of the Bay of Fundy has not yet been sufficiently studied and we cannot rely on this source of information. We have to rely instead on the observational material.

During the 1965 survey, the weather was calm and settled and we assume that the residual currents observed indicate a situation of rest and peace in the bay. We may set up a table of expected maximum currents under conditions of calm with some feeling of confidence. However we are not in a position to predict the maximum currents that may occur when a severe weather disturbance makes itself felt over the bay. Table 5 lists the maximum expected tidal streams as well as the maximum currents under conditions of calm. The + sign indicates inward moving currents; -, the reverse. $\pm$ means that the current is purely periodic.

We may note that it was new moon at 05 hours June 29, that the moon was at perigee at 00 hours June 30 and that it had its maximum declination at 01 hours June 29; accordingly, near maximum tidal streams occurred at the end of June and the beginning of July. Similarly it was new moon at 12 hours July 28, the moon was at perigee at 09 hours July 28 and it had its maximum declination at 23 hours July 26.

3.4 The Volumes Displaced by the M_2 Tide

It is possible to obtain an idea of the M_2 tidal streams necessary to raise by 30 to 34 feet the levels in Minas Channel and in Minas Basin, by calculating the volume of water that has to be transported across a given section over half a tidal cycle.

If at a given section, the maximum tidal stream has a speed of u_o metres/hour, its average value over half a tidal cycle is $2u_o/\Pi$. The volume of water transported during the half cycle amounts to

$$\frac{12\ u_o A}{\Pi}$$

where A is the area of the cross section, since the duration of a half tidal cycle is six lunar hours.

The surface of Minas Channel and Minas Basin covers about $1.63 \times 10^9 m^2$ and the volume of water necessary to raise the level by about 30 feet (9.15 m) equals

$$V = 14.9 \times 10^9 m^3$$

We take the cross section at station 72 to measure $4.6 \times 10^5 m^2$ so that at station 72,

$$u_o = \frac{\Pi V}{12\ A} = \frac{3.1416 \times 14.9 \times 10^9 m^3}{12 \times 4.6 \times 10^5 m^2 \text{ hour}} = 8.4 \times 10^3 m/\text{lunar hour} \sim 4.4 \text{ knots}$$

which compares favourably with the observed value of 4.35 knots.

Table 5

The Maximum Expected Tidal Streams and the Maximum Expected Currents under Conditions of Calm

Station	Depth metres	Tidal Stream knots	Max observed knots	Time	Current knots	Max observed knots	Time
60	13	2.04	1.88	4.5 1/7/65	-2.44	-2.31	4.5 1/7/65
61	13	2.38	2.05	9.5 29/7/65	+2.38		
61	50	2.47	2.21	2.5 29/6/65	+2.47		
62	13	3.03	2.78	5.5 2/7/65	+3.26	+2.87	10.5 2/7/65
63	25	2.52	2.17	4.5 30/7/65	+2.52		
64	10	3.03	2.75	4.5 1/7/65	-3.25	-2.92	4.5 1/7/65
64	25	2.78	2.40	4.5 1/7/65	-2.90	-2.50	4.5 1/7/65
64	25	2.75	2.33	4.5 30/7/65	-2.81	-2.36	4.5 30/7/65
65	25	3.36	2.79	4.5 30/6/65	+3.44	+2.85	9.5 30/6/65
65	25	3.01	2.78	4.5 30/7/65	+3.11	+2.46	10.5 30/7/65
66	25	2.46	1.95	22.5 30/7/65	+2.53	+2.04	22.5 30/7/65
68	25	2.58	2.05	21.5 30/6/65	-2.67	-2.19	5.5 2/7/65
68	25	2.52	2.15	21.5 29/7/65	-2.64	-2.07	4.5 30/7/65
69	10	2.79	2.37	20.5 28/7/65	+2.79		
70	5	4.25	3.64	4.5 30/6/65	-4.37	-3.58	4.5 30/6/65
71	5	3.75	3.05	21.5 29/6/65	+3.90	+3.29	21.5 29/6/65
71	5	3.18	2.74	10.5 30/7/65	+3.34	+2.98	10.5 30/7/65
72	25	6.43	4.95	4.5 1/7/65	+6.74	+5.14	22.5 30/6/65
72	25	6.60	4.28	4.5 15/7/65	+6.88	+4.25	10.5 14/7/65
73	10	3.56	2.80	7.5 3/7/65	+3.56		
74	5	4.69	4.21	3.5 29/7/65	-6.20	-4.91	3.5 29/7/65
75	10	4.90	3.11	5.5 14/8/65	-5.60	-3.81	5.5 14/8/65
76	10	2.41	2.11	16.5 31/7/65	+3.38	+2.78	22.5 31/7/65

The cross section at station 74 has a value of $2.8 \times 10^5 m^2$ while we estimate the surface of Minas Basin to amount to $8.5 \times 10^8 m^2$. The average of the M_2 range in the basin is 34 feet (10.36 m). The volume of water necessary to bring about this increase in level amounts to $8.81 \times 10^9 m^3$; this in turn requires a maximum M_2 stream of 4.6 knots at station 74. The actually observed value is 3.3 knots far below the estimate. One must note however that the meter at this station was located at a depth of five metres and very close to the south shore, most likely for the practical reason that it was the only place where it could be safely moored. The streams are likely to be stronger farther away from the coast.

4. ACKNOWLEDGMENTS

Mr. J.D. Taylor has written the programs for the analysis of the current observations. The Bedford Institute of Oceanography has supplied all the current observations collected during the 1965 survey as well as all other relevant information.

Commander W.I. Farquharson (rt'd) and Dr. W.D. Forrester read the manuscript and made valuable comments.

5. REFERENCES

Anonymous. MS 1966. Bay of Fundy, data report, tidal and current survey, 1965. Bedford Institute of Oceanography Unpublished Manuscript. Data Series 66-2-D.

Proudman, J., 1953. Dynamical oceanography. 311. Methuen.

Bumpus, D.F. and Lauzier, L.M., 1965. Serial atlas of the marine environment. Folio 7, Plate 4. American Geographical Society.

Godin, G., 1967. The analysis of current observations. International Hydrographic Review, 44, No. 1, 149-165.

6. GLOSSARY

Amplitude:	A pure harmonic oscillation of frequency σ_k may be represented mathematically by $a_k e^{2\pi i \sigma_k j}$ or, less conveniently, by $A_k \cos(2\pi \sigma_k j - \alpha_k)$. Both a_k and A_k are called the amplitude. a_k is a complex number which has magnitude A_k and phase $-\alpha_k$. A_k is a real number.
Constituent:	A pure harmonic oscillation of tidal origin.
Current:	The rate of displacement of fluid particles along a certain direction at a fixed point in space.
Current observation:	An instantaneous measurement of the current.
Declination:	The angular elevation of a celestial body above the celestial equator.

Perigee: The point at which a celestial body is closest to the earth.

Residual current: A current observation contains the contribution of the tidal streams and of some other type of motion. What is left in the current observation, once the tidal streams are removed, is the residual current. Such currents may vary in time but not harmonically.

Residues: What is left in a current observation after the tidal streams and the residual current are removed. It represents the portion of the current observation which escaped the analysis.

Tidal streams: Purely periodic currents created by the tidal forces.

7. APPENDICES

7.1 Results of the analysis of the current observations collected during the 1965 survey of the Bay of Fundy

The analysis gives the length of the semimajor and semiminor axes of the constituent ellipses, the probable error on these values (the same for all), the inclination of the major axis to the east, the phase angles G^+ and G^-, the Greenwich phase lag g and the probable error on these quantities, all in degrees. This error is not given when the magnitude of the constituent is smaller than the background noise.

The constituents to which a number is affixed have been analyzed directly. The constituent which follows and which does not have a number has been inferred from the preceding one.

The x and y components (in the original frame of reference) of the mean residual current (which may have some meaning at times) denoted by x_0 and y_0, are given at the bottom. We supply as well the equivalent rates and direction of this mean residual current, the orientation being referred this time to an axis running along the east. $\overline{\Delta x}$ and $\overline{\Delta y}$ are the root mean square deviations in the x and y directions of the original frame of reference.

The number of hourly observations available for the analysis is denoted by 2N+1 and is given in the heading. The mid-time which is useful for checking is also tabulated.

Station 60 Depth 13 m 10 hours 15/6/65 to 3 hours 27/7/65

Mid-time 18.5 hours 3/7/65

2N+1=809

	Major knots	Minor knots	Δ	Inc. °	G^+ °	G^- °	g °	ΔG °
1 M_2	1.30	-.15	±.020	42.0	263.1	279.1	271.1	±.9
2 S_2	.26	-.06		38.9	307.3	317.0	312.2	4.4
K_2	.07	-.02		38.9	307.8	317.5	312.7	16.0
3 L_2	.07	.02		37.9	77.2	85.0	81.1	16.0
4 N_2	.30	-.05		48.2	225.5	253.9	239.7	3.8
ν_2	.07	-.01		48.2	231.5	259.5	245.7	16.0
5 μ_2	.04	-.01		125.6	229.1	53.1	283.0	28.7
6 K_1	.02	-.01		70.2	39.2	111.5	75.4	-
P_1	.01	-.01		70.2	38.5	110.8	74.6	-
7 O_1	.02	.00		169.1	9.8	280.0	324.9	-
8 NO_1	.02	.01		159.3	307.7	198.3	253.0	-
9 Q_1	.01	.00		110.4	81.4	234.2	337.8	-
10 OO_1	.02	.01		12.0	311.8	267.8	289.8	-
11 J_1	.02	.00		175.9	67.1	350.9	29.0	-
12 M_4	.10	-.00		2.5	64.6	1.5	33.0	11.5
13 MS_4	.05	-.01		9.2	80.5	30.9	55.7	22.9
14 MN_4	.06	-.01		179.4	47.6	338.4	193.0	18.9
15 M_8	.01	-.00		90.0	226.0	338.6	282.6	-

$x_o, y = -.40, .08 \longleftrightarrow .41 \quad 203^\circ$

$\Delta x = .14$

$\Delta y = .14$

Station 61 Depth 13 m   14 hours 15/6/65 to 12 hours 1/7/65

Mid-Time=12.5 hours 23/6/65

2N+1=309

	Major knots	Minor knots	Δ knots	Inc. °	G^{+} °	G^{-} °	g °	ΔG °
1 M_2	1.52	-.10	------	49.4	246.0	276.9	261.5	------
N_2	.31	-.02		49.4	217.9	248.8	233.4	
2 S_2	.14	-.04		49.4	249.3	280.1	264.7	
K_2	.04	-.01		49.4	249.8	280.6	265.2	
3 K_1	.04	-.01		25.8	48.4	32.0	40.2	
P_1	.01	-.00		25.8	47.7	31.3	39.5	
4 O_1	.03	.01		34.9	27.3	29.1	28.2	
Q_1	.00	.00		34.9	4.9	6.7	5.8	
5 OO_1	.01	-.01		86.3	265.2	9.8	317.5	
6 M_4	.04	.02		.4	213.5	146.2	179.9	
7 MS_4	.03	-.02		28.0	110.8	98.9	104.9	
8 M_8	.01	-.00		144.4	170.3	31.1	100.7	

$x_o, y_o = .08, -.02 \longleftrightarrow .08 \quad 020^{\circ}$

Station 61 Depth 13 m 16 hours 22/7-65 to 5 hours 21/8-65

Mid-Time = 10.5 hours 6/8-65

2N+1=637

	Major	Minor	Δ	Inc.	G^+	G^-	g	ΔG
1 M_2	1.62	-.16	±.017	49.4	249.7	280.5	265.1	±.6
2 S_2	.21	-.01		59.2	286.3	336.6	311.5	4.6
K_2	.06	-.00		59.2	286.8	337.1	312.0	16.0
3 L_2	.16	-.04		57.0	94.3	140.3	117.3	6.1
4 N_2	.37	-.06		44.1	228.9	249.1	239.0	2.6
ν_2	.09	-.01		44.1	234.9	255.1	245.0	10.3
5 μ_2	.06	.01		60.6	287.5	340.6	314.1	16.0
6 K_1	.03	-.01		43.5	20.3	39.4	29.9	32.1
P_1	.01	-.00		43.5	19.6	38.7	29.2	-
7 O_1	.02	-.01		30.0	52.3	44.3	48.3	-
8 NO_1	.01	-.00		146.9	313.0	178.4	245.9	-
9 Q_1	.01	-.00		71.2	296.9	11.2	334.1	-
10 OO_1	.01	-.00		159.2	114.1	4.5	239.3	-
11 J_1	.01	.01		21.6	174.3	149.5	341.9	-
12 M_4	.07	-.01		70.9	105.8	178.7	141.8	13.8
13 MS_4	.03	.01		92.5	127.7	244.6	186.2	32.1
14 MN_4	.07	-.04		61.0	63.2	117.3	90.3	13.8
15 M_8	.01	-.01		14.8	187.2	148.8	168.0	-

x_o, y = .01,.13 ↔ .13 123°

Δx = .16

Δy = .10

Station 61 Depth 13 m Combined Analysis of the Two Previous Sets of Data

Mid-Time=2.22 hours 23/7/65

2N+1=309+637=946

	Major knots	Minor knots	Inc	G^+	G^-	g
			°	°	°	°
1 M_2	1.54	-.14	49.5	250.6	281.7	266.2
2 S_2	.20	-.02	53.7	293.0	332.5	312.8
3 L_2	.12	-.02	56.2	92.4	136.8	114.6
4 N_2	.41	-.07	44.5	226.0	247.0	236.5
5 μ_2	.03	-.01	73.9	311.9	31.8	351.9
6 K_1	.04	-.01	33.4	45.0	43.7	44.4
7 O_1	.02	-.01	34.6	41.6	42.9	42.3
8 NO_1	.01	-.00	131.7	317.9	153.3	235.6
9 Q_1	.01	-.01	57.3	343.7	30.3	7.0
10 OO_1	.01	.00	141.3	151.4	6.1	258.8
11 J_1	.01	.01	55.9	182.3	226.1	24.2
12 M_4	.05	-.01	59.4	133.4	184.2	158.8
13 MS_4	.02	.01	78.2	123.0	211.3	167.2
14 MN_4	.05	-.02	76.9	29.3	115.2	72.3
15 M_8	.01	.00	171.9	190.1	105.9	148.0

Station 61 Depth 50 m 14 hours 15/6/65 to 12 hours 1/7/65

Mid-Time = 12.5 hours 23/6/65

2N+1=309

	Major	Minor	Δ	Inc	G^+	G^-	g	ΔG
1 M_2	1.78	-.06	±.026	45.3	248.6	271.2	259.9	±.9
N_2	.36	-.01		45.3	220.5	243.1	231.8	4.3
2 S_2	.15	-.04		35.0	283.0	284.9	283.9	10.4
K_2	.04	-.01		35.0	283.5	285.4	284.4	38.2
3 K_1	.03	.00		57.7	51.6	99.0	75.3	45.1
P_1	.01	.00		57.7	50.9	98.3	74.6	-
4 O_1	.02	-.00		57.8	40.6	88.2	64.4	-
Q_1	.00	-.00		57.8	18.2	65.8	42.0	-
5 OO_1	.02	-.01		40.8	48.8	62.3	55.6	-
6 M_4	.06	.03		55.0	30.7	72.8	51.8	31.0
7 MS_4	.02	.02		62.0	314.6	10.7	342.7	-
8 M_8	.01	-.00		17.5	342.2	309.2	325.7	-

$x_o, y_o = -.03, .20 \leftrightarrow .21 \quad 125^o$

$\Delta x = .14$

$\Delta y - .09$

Station 62 Depth 13 m 17 hours 15/6/65 to 10 hours 22/7/65

Mid-Time = 1.5 hours 4/7/65

2N+1=809

	Major	Minor	Δ	Inc.	G^+	G^-	g	ΔG
1 M_2	2.08	-.21	±.015	44.5	251.6	272.6	262.1	±.4
2 S_2	.33	-.10		47.8	193.8	285.6	299.4	2.6
K_2	.09	-.03		47.8	286.1	313.7	299.9	9.7
3 L_2	.11	-.07		91.8	70.7	186.3	128.5	7.8
4 N_2	.43	-.03		42.7	220.0	237.4	228.7	1.9
ν_2	.10	-.01		42.7	226.0	243.4	234.7	8.6
5 μ_2	.10	-.06		12.7	231.3	188.7	30.0	8.6
6 K_1	.04	-.01		25.3	36.6	19.2	27.9	21.2
P_1	.02	-.00		25.3	35.9	18.5	27.2	-
7 O_1	.03	-.01		52.4	359.3	36.2	17.8	28.7
8 NO_1	.01	.00		88.7	332.5	82.0	207.3	-
9 Q_1	.01	.00		107.2	287.0	73.3	0.2	-
10 OO_1	.02	-.00		96.0	319.4	83.5	11.5	-
11 J_1	.01	.00		21.6	2.1	337.2	349.7	-
12 M_4	.05	-.04		179.8	189.8	121.5	155.7	17.2
13 MS_4	.04	-.02		128.1	358.9	187.9	93.1	21.2
14 MN_4	.04	.01		142.1	227.8	83.9	335.9	21.2
15 M_8	.03	-.01		166.6	179.8	85.0	312.4	28.7

x_o, y_o =.18,-.15 .23 354^o

Δx = .10

Δy = .12

Station 63 Depth 25m 20 hours 16/6/65 to 15 hours 5/8/65

Mid-Time=17.5 hours 11/7/65

2N+1=1123

	Major	Minor	Δ	Inc	G^+	G^-	g	ΔG
1 M_2	1.77	.03	±.008	37.2	261.1	267.6	264.4	±.3
2 S_2	.25	-.02		32.4	317.8	314.6	316.2	1.8
K_2	.07	-.01		32.4	318.3	315.1	316.7	6.5
3 L_2	.13	-.01		33.3	92.0	90.7	91.4	3.5
4 N_2	.34	-.01		36.1	236.6	240.7	238.7	1.3
ν_2	.08	-.00		86.1	242.6	246.7	244.7	5.7
5 μ_2	.05	-.03		48.5	234.1	263.2	68.7	9.2
6 K_1	.04	.00		39.7	47.5	59.0	53.3	11.5
P_1	.01	.00		39.7	46.8	58.3	52.6	-
7 O_1	.03	-.01		29.4	33.7	24.5	29.1	15.5
8 NO_1	.00	.00		173.3	349.2	267.8	128.5	-
9 Q_1	.00	-.00		52.9	311.8	349.6	330.7	-
10 OO_1	.00	-.00		34.9	316.5	318.4	317.5	-
11 J_1	.00	-.00		24.5	111.1	92.0	101.6	-
12 M_4	.05	-.04		105.3	296.4	79.1	7.8	9.2
13 MS_4	.03	-.01		133.8	338.0	177.6	77.8	15.5
14 MN_4	.02	-.01		79.0	317.6	47.6	2.6	22.9
15 M_8	.01	-.00		147.5	178.8	45.8	292.3	-

$x_o, y_o = .00, -.05 \longleftrightarrow .05 \quad 304^o$

$\Delta x = .09$

$\Delta y = .04$

Station 64 Depth 10 m 22 hours 16/6/65 to 14 hours 17/7/65

Mid-Time=5.5 hours 2/7/65

2N+1=663

	Major	Minor	Δ	Inc.	G^+	G^-	g	ΔG
1 M_2	2.29	-.22	±.014	35.2	264.0	266.3	265.2	±.3
2 S_2	.31	.02		32.7	300.8	298.3	299.6	2.6
K_2	.08	.00		32.7	301.3	298.8	300.1	9.7
3 L_2	.05	-.02		92.6	323.1	80.3	21.7	16.0
4 N_2	.25	-.01		41.8	237.8	253.4	245.6	32.1
ν_2	.06	-.00		41.8	243.8	259.4	251.6	13.2
5 μ_2	.07	-.01		135.1	161.5	3.7	82.6	11.5
6 K_1	.05	.00		35.2	42.7	45.0	43.9	16.0
P_1	.02	.00		35.2	42.0	44.3	43.2	40.1
7 O_1	.03	-.01		21.1	78.1	52.4	65.3	26.4
8 NO_1	.02	.00		173.4	321.9	240.6	101.3	40.1
9 Q_1	.01	.00		145.6	248.5	111.6	0.0	-
10 OO_1	.02	-.00		165.9	249.6	153.4	21.5	40.1
11 J_1	.02	.00		169.5	347.7	258.6	303.2	40.1
12 M_4	.12	-.04		158.0	190.2	78.9	314.6	6.7
13 MS_4	.03	-.02		130.8	245.3	79.0	342.2	26.4
14 MN_4	.02	.01		58.6	146.0	195.2	170.6	40.1
15 M_8	.01	-.01		176.2	177.6	102.0	139.8	-

x_o,y_o=.-.22,-.04 ↔ .22 224°

Δx = .10

Δy = .08

Station 64 Depth 25 m 22 hours 16/6/65 to 22 hours 6/7/65

Mid-Time= 21.5 hours 26/6/65

2N+1=407

	Major	Minor	Δ	Inc.	G^+	G^-	g	ΔG
1 M_2	2.00	-.01	$\pm$.016	35.4	266.7	269.5	268.1	±.4
N_2	.40	-.00		35.4	238.6	241.4	240.0	2.4
2 S_2	.21	.02		31.0	320.5	314.5	317.5	4.4
K_2	.06	.00		31.0	321.0	315.0	318.0	16.2
3 K_1	.04	.00		40.2	42.4	54.7	48.6	22.6
P_1	.01	.00		40.2	41.7	54.0	47.9	-
4 O_1	.03	-.00		39.6	56.2	67.5	61.9	26.6
Q_1	.01	-.00		39.6	33.8	45.1	39.5	-
5 OO_1	.01	.00		13.4	343.4	302.3	322.9	-
6 M_4	.11	-.02		51.1	81.0	115.3	98.2	9.8
7 MS_4	.02	-.00		40.6	51.4	64.5	58.0	-
8 M_8	.01	.00		45.3	157.4	180.1	168.8	-

x_o, y_o=-.12, .03 $\longleftrightarrow$ .12 200°

Δx=.11

Δy=.05

Station 64 Depth 25 m 18 hours 21/7/65 to 10 hours 22/8/65

Mid-Time 13.5 hours 6/8/65

2N+1=687

	Major	Minor	Δ	Inc	G^+	G^-	g	ΔG
1 M_2	1.92	.03	$\pm$.008	37.0	268.2	274.2	271.2	$\pm$.2
2 S_2	.32	-.02		38.8	309.8	319.5	314.7	1.4
K_2	.09	-.01		38.8	310.3	320.0	315.2	5.0
3 L_2	.18	.00		41.5	106.3	121.3	113.8	2.5
4 N_2	.35	.01		33.0	241.8	239.9	240.9	1.3
ν_2	.08	.00		33.0	247.8	245.9	246.9	5.7
5 μ_2	.08	-.01		20.9	311.7	285.5	118.6	5.7
6 K_1	.04	-.00		38.0	50.8	58.7	54.8	11.5
P_1	.02	-.00		38.0	50.1	58.0	54.1	22.9
7 O_1	.04	-.00		38.1	41.8	50.1	46.0	11.5
8 NO_1	.01	.00		62.8	269.0	326.6	297.8	-
9 Q_1	.01	-.00		34.5	34.8	35.9	35.4	-
10 OO_1	.01	.00		60.3	151.0	203.5	177.3	-
11 J_1	.01	.00		164.2	122.4	22.7	72.6	-
12 M_4	.06	-.02		61.9	86.4	142.1	114.3	7.6
13 MS_4	.02	-.02		26.6	172.6	184.6	177.2	22.9
14 MN_4	.04	.00		55.7	43.1	86.5	64.8	11.5
15 M_8	.02	.00		27.1	155.5	141.6	148.6	22.9

$x_o, y_o = -.06, -.01 \longleftrightarrow .06 \quad 223^\circ$

$\Delta x = .07$

$\Delta y = .04$

Station 64 Depth 25 m Combined Analysis of the Two Previous Sets of Data

Mid-Time=10.40 hours 22/7/65

2N+1=407+687=1094

	Major knots	Minor knots	Inc. °	G^+ °	G^- °	g °
1 M_2	1.88	.02	36.4	269.1	274.0	271.6
2 S_2	.28	-.01	38.7	318.2	327.6	322.9
3 L_2	.16	-.01	41.9	105.7	121.6	113.7
4 N_2	.41	.00	35.6	241.6	244.9	243.3
5 μ_2	.06	-.02	25.5	313.8	296.8	125.3
6 K_1	.05	.00	41.2	56.2	70.7	63.5
7 O_1	.04	-.00	40.8	45.6	59.1	52.4
8 NO_1	.01	-.00	61.3	267.5	322.0	294.8
9 Q_1	.01	-.00	49.1	11.9	42.1	27.0
10 OO_1	.00	.00	36.5	131.8	136.8	134.3
11 J_1	.01	-.00	138.0	138.0	345.9	62.0
12 M_4	.07	-.01	55.2	90.4	132.7	111.6
13 MS_4	.01	-.01	42.6	139.7	157.0	148.4
14 MN_4	.03	.00	76.8	35.3	120.9	78.1
15 M_8	.01	.00	31.2	155.0	149.3	152.2

Station 65 Depth 25 m 8 hours 17/6/65 to 10 hours 4/7/65

Mid-Time= 20.5 hours 25/6/65

2N+1=337

	Major	Minor	Δ	Inc	G^+	G^-	g	ΔG
1 M_2	2.35	-.04	$\pm$.016	30.1	268.4	260.6	264.5	$\pm$ .4
N_2	.47	-.01		30.1	240.3	232.5	236.4	2.0
2 S_2	.33	.00		31.2	321.2	315.5	318.4	3.0
K_2	.09	.00		31.2	321.7	316.0	318.9	11.0
3 K_1	.04	.00		33.7	35.5	35.0	35.3	23.4
P_1	.01	.00		33.7	34.8	34.3	34.6	-
4 O_1	.03	-.00		37.4	23.8	30.6	27.2	33.6
Q_1	.00	-.00		37.4	1.4	8.2	4.8	-
5 OO_1	.01	-.00		43.2	243.9	262.4	253.2	-
6 M_4	.06	-.03		145.4	215.6	78.3	327.0	-
7 MS_4	.02	-.01		29.7	121.2	112.5	116.9	43.6
8 M_8	.02	-.01		90.9	293.3	47.1	350.2	-

$x_o, y_o = .06, -.05 \leftrightarrow .08 \quad 354^o$

$\Delta x = .12$

$\Delta y = .03$

Station 65 Depth 25 21 hours 21/7/65 to 9 hours 6/7/65

Mid-Time=14.5 hours 29/7/65

2N+1=299

	Major	Minor	Δ	Inc.	G^+	G^-	g	ΔG
1 M_2	2.17	-.05	$\pm$.026	30.9	269.4	263.3	266.4	$\pm$ .7
N_2	.43	-.01		30.9	241.3	235.2	238.3	3.6
2 S_2	.19	-.01		32.4	56.4	53.1	54.8	8.3
K_2	.05	-.00		32.4	56.9	53.6	55.3	30.9
3 K_1	.04	.00		35.4	17.6	20.4	19.0	39.0
P_1	.01	.00		35.4	16.9	19.7	18.3	-
4 O_1	.04	.01		35.8	26.2	29.8	28.0	36.1
Q_1	.01	.00		35.8	3.8	7.4	5.6	-
5 OO_1	.02	.00		19.4	73.1	43.8	58.5	-
6 M_4	.10	.04		1.6	74.8	10.1	42.5	16.6
7 MS_4	.03	.01		81.6	158.9	254.1	206.5	-
8 M_8	.03	.01		32.6	145.0	142.2	143.6	-

x_o, y_o=-.07,.10 .12 159^o

Δx =.17

Δy =.06

Station 65 Depth 25 Combined Analysis of the Two Previous Sets of Data

Mid-time=17.30 hours 11/7/65

2N+1=337+299=636

	Major knots	Minor knots	Inc °	G^+ °	G^- °	g °
1 M_2	2.17	-.04	30.5	269.2	262.2	265.7
2 S_2	.21	.00	30.0	321.6	313.6	317.6
3 L_2	.12	-.01	27.9	105.9	93.6	99.8
4 N_2	.40	-.02	31.2	256.3	250.8	253.6
5 μ_2	.11	.01	31.0	226.7	220.8	43.8
6 K_1	.06	-.00	38.4	46.7	55.4	51.1
7 O_1	.03	-.00	47.0	24.1	50.1	37.1
8 NO_1	.01	-.00	163.3	56.0	312.7	184.4
9 Q_1	.01	-.00	177.9	48.6	336.4	12.5
10 OO_1	.00	.00	119.6	17.2	288.4	202.8
11 J_1	.01	-.00	39.3	98.8	209.5	204.2
12 M_4	.06	.01	176.4	125.9	50.8	88.4
13 MS_4	.01	.01	7.2	129.7	76.1	102.9
14 MN_4	.05	.04	118.8	11.0	180.5	95.8
15 M_8	.01	.00	173.8	161.5	80.2	120.9

Station 66 Depth 25 m 8 hours 20/7/65 to 8 hours 4/8/65

Mid-Time=19.5 hours 27/7/65

2N+1=287

	Major	Minor	Δ	Inc.	G^+	G^-	g	ΔG
1 M_2	1.61	-.07	±.022	37.1	256.4	262.6	259.5	±.8
N_2	.32	-.01		37.1	228.3	234.5	231.4	4.1
2 S_2	.31	-.03		39.1	353.3	3.5	358.4	4.2
K_2	.08	-.01		39.1	353.8	4.0	358.9	15.5
3 K_1	.04	-.00		51.4	61.2	95.9	78.6	29.2
P_1	.01	-.00		51.4	60.5	95.2	77.9	-
4 O_1	.03	-.00		51.7	328.0	3.3	345.7	41.8
Q_1	.01	-.00		51.7	305.6	340.9	323.3	-
5 OO_1	.02	.00		34.5	158.5	159.4	159.0	-
6 M_4	.11	.07		88.1	56.4	164.6	110.5	13.1
7 MS_4	.04	.01		74.6	180.5	261.7	221.1	36.1
8 M_8	.02	-.01		36.9	180.2	65.9	303.1	-

$x_o, y_o = .07, .02 \longleftrightarrow .07 \quad 50^\circ$

$\Delta x = .14$

$\Delta y = .05$

Station 68 Depth 25 m 10 hours 18/6/65 to 12 hours 4/7/65

Mid-Time=10.5 hours 26/6/65

2N+1=313

	Major	Minor	Δ	Inc.	G^+	G^-	g	ΔG
1 M_2	1.70	.06	$\pm$.017	39.1	255.4	265.7	260.6	$\pm$ .7
N_2	.34	.01		39.1	227.3	237.6	232.5	3.5
2 S_2	.33	-.03		41.7	318.2	333.7	326.0	3.6
K_2	.09	-.01		41.7	318.7	334.2	326.5	13.5
3 K_1	.04	.01		35.1	39.4	41.6	40.5	26.6
P_1	.01	.00		35.1	38.7	40.9	39.8	-
4 O_1	.03	-.01		14.2	69.8	30.1	50.0	-
Q_1	.00	-.00		14.2	47.4	7.7	27.6	-
5 OO_1	.02	-.00		37.9	271.6	279.3	275.5	-
6 M_4	.14	-.02		49.4	101.8	132.7	117.3	9.2
7 MS_4	.04	.01		43.6	148.8	168.1	158.5	30.2
8 M_8	.05	.00		168.5	6.1	275.1	140.9	-

x_o, y_o=.-.06,.08 $\longleftrightarrow$ .09 161°

Δx = .12

Δy = .03

Station 68 Depth 25 12 hours 21/7/65 to 12 hours 5/8/65

Mid-Time = 23.4 hours 28/7/65

2N+1=287

	Major	Minor	Δ	Inc.	G^+	G^-	g	ΔG
1 M_2	1.70	.05	$\pm$.022	40.5	257.8	270.8	264.3	$\pm$ .8
N_2	.34	.01		40.5	229.7	242.7	236.2	3.8
2 S_2	.25	-.01		37.5	15.6	22.6	19.1	5.2
K_2	.07	-.00		37.5	16.1	23.1	19.6	18.9
3 K_1	.05	-.01		37.0	62.3	68.4	65.4	26.4
P_1	.02	-.00		37.0	61.6	67.7	64.7	-
4 O_1	.04	-.01		24.6	46.2	27.3	36.8	32.7
Q_1	.01	-.00		24.6	23.8	4.9	14.4	-
5 OO_1	.01	-.00		43.1	196.3	214.4	205.4	-
6 M_4	.19	-.00		45.9	106.0	129.8	117.9	7.4
7 MS_4	.05	-.05		60.2	222.6	275.1	248.9	29.2
8 M_8	.03	-.02		25.9	292.6	276.5	284.6	-

$x_o, y_o = -.09,\ .08 \leftrightarrow .12 \quad 173^o$

$\Delta x = .16$

$\Delta y = .03$

Station 68 Depth 25 m Combined Analysis of the Two Previous Sets of Data

Mid-Time= .08 hours 12/7/65

2N+1=313+287=600

	Major knots	Minor knots	Inc. °	G^+ °	G^- °	g °
1 M_2	1.68	.07	39.5	259.7	270.7	265.2
2 S_2	.21	-.01	39.0	307.0	317.0	312.0
3 L_2	.14	.00	33.2	82.9	81.4	82.2
4 N_2	.34	-.01	44.6	223.1	244.3	233.7
5 μ_2	.09	.00	40.7	261.5	274.8	88.2
6 K_1	.04	.01	24.6	38.5	19.7	29.1
7 O_1	.03	-.00	21.5	33.4	8.5	21.0
8 NO_1	.03	-.01	13.0	155.7	113.7	134.7
9 Q_1	.01	-.01	37.4	45.2	52.1	48.7
10 OO_1	.01	-.00	111.5	330.5	125.6	228.1
11 J_1	.02	-.01	11.1	141.6	95.7	118.7
12 M_4	.12	-.02	44.6	125.7	147.0	136.4
13 MS_4	.02	.01	84.2	152.9	253.3	203.1
14 MN_4	.07	.01	41.1	83.8	98.0	90.9
15 M_8	.02	-.01	171.3	1.9	276.4	139.2

Station 69 Depth 10 m 15 hours 20/7/65 to 15 hours 4/8/65

Mid-Time=2.5 hours 28/7/65

2N+1=287

	Major	Minor	Δ	Inc.	G^+	G^-	g	ΔG
1 M_2	1.92	-.02	±.028	50.6	265.7	262.9	264.3	± .9
N_2	.38	-.00		50.6	237.6	234.8	236.2	4.4
2 S_2	.24	-.01		55.2	357.2	3.5	360.4	6.9
K_2	.07	-.00		55.2	357.7	4.0	360.9	25.2
3 K_1	.06	.00		45.0	40.8	26.8	33.8	27.5
P_1	.02	.00		45.0	40.1	26.1	33.1	-
4 O_1	.02	-.01		58.0	82.4	94.3	88.4	-
Q_1	.00	-.00		58.0	60.0	71.9	66.0	-
5 OO_1	.03	.00		43.0	108.9	90.8	99.9	48.1
6 M_4	.23	-.01		56.0	106.6	114.5	110.6	8.2
7 MS_4	.01	.01		93.4	261.9	344.7	303.3	-
8 M_8	.04	-.00		184.9	142.4	28.2	265.3	-

$x_o, y_o = .02, .01 \leftrightarrow .02 \quad 60^\circ$

$\Delta x = .18$

$\Delta y = .06$

Station 70 Depth 5 13 hours 18/6/65 to 9 hours 5/7/65

Mid-Time=22.5 hours 26/6/65

2N+1=331

	Major	Minor	Δ	Inc.	G^+	G^-	g	ΔG
1 M_2	2.84	.03	$\pm$.038	71.3	274.4	271.0	272.7	$\pm$ .8
N_2	.57	.01		71.3	246.3	242.9	244.6	4.0
2 S_2	.45	.02		77.5	302.0	311.0	306.5	5.0
K_2	.12	.01		77.5	302.5	311.5	307.0	18.5
3 K_1	.04	.01		85.2	48.4	72.8	60.6	-
P_1	.01	.00		85.2	47.7	72.1	59.9	45.7
4 O_1	.05	-.01		72.2	6.3	4.7	5.5	-
Q_1	.01	0-.00		72.2	343.9	342.3	343.1	-
5 OO_1	.01	.00		157.0	83.7	251.8	167.8	-
6 M_4	.52	-.11		58.4	110.2	80.9	95.6	4.8
7 MS_4	.06	-.02		53.5	172.9	133.8	153.4	42.4
8 M_8	.15	-.04		89.9	316.2	350.0	333.1	26.4
9 M_3	.03	.00		84.8	100.2	129.7	111.9	-
10 M_6	.39	-.04		80.2	240.1	254.5	247.3	5.6

$x_o, y_o = -.09, .10 \longleftrightarrow .13 \quad 166^o$

$\Delta x = .27$

$\Delta y = .08$

Station 71 Depth 5 m 16 hours 18/6/65 to 12 hours 5/7/65

Mid-Time=1.5 hours 27/6/65

2N+1=331

	Major	Minor	Δ	Inc.	G^+	G^-	g	ΔG
1 M_2	2.44	-.06	±.042	41.3	274.8	253.4	264.1	±1.0
N_2	.49	-.01		41.3	246.7	225.3	236.0	5.1
2 S_2	.40	-.02		45.1	337.2	323.4	330.3	6.2
K_2	.11	-.01		45.1	337.7	323.9	330.8	22.9
3 K_1	.05	-.01		48.5	56.7	49.7	53.2	50.1
P_1	.02	-.00		48.5	56.0	49.0	52.5	-
4 O_1	.04	-.01		56.4	58.0	66.8	62.4	-
Q_1	.01	-.00		56.4	35.6	44.4	40.0	-
5 OO_1	.02	-.00		95.4	271.8	358.6	315.2	-
6 M_4	.29	-.07		43.9	161.7	145.5	153.6	9.7
7 MS_4	.08	-.00		62.8	173.5	195.1	184.3	33.2
8 M_8	.08	-.03		35.3	198.2	164.8	181.5	-
9 M_3	.05	.01		46.8	78.3	68.0	73.1	50.5
10 M_6	.31	-.03		29.8	251.9	207.5	229.7	7.9

$x_o, y_o = .12, -.09 \leftrightarrow .15 \quad 357^o$

$\Delta x = .31$

$\Delta y = .07$

Station 71 Depth 5 m 8 hours 21/7/65 to 8 hours 9/8/65

Mid-Time = 19.5 hours 30/7/65

2N+1=383

	Major	Minor	Δ	Inc.	G^+	G^-	g	ΔG
1 M_2	2.18	-.10	$\pm$.051	40.0	282.5	258.6	270.6	$\pm$ 1.4
N_2	.44	-.02		40.0	254.4	230.5	242.5	6.9
2 S_2	.13	.01		26.7	355.5	304.9	330.2	22.9
K_2	.04	.00		26.7	356.0	305.4	330.7	-
3 K_1	.03	-.01		57.7	349.0	.5	354.8	-
P_1	.01	-.00		57.7	348.3	359.8	354.1	-
4 O_1	.02	-.00		64.4	334.2	359.0	346.6	-
Q_1	.00	-.00		64.4	311.8	336.6	324.2	-
5 OO_1	.01	.00		118.0	138.8	270.8	204.8	-
6 M_4	.28	-.06		41.0	200.0	177.9	189.0	11.9
7 MS_4	.02	.02		93.4	203.7	286.4	245.1	-
8 M_8	.05	-.03		165.0	301.8	167.9	54.9	-
9 M_3	.03	-.01		46.4	71.5	60.2	65.9	-
10 M_6	.30	-.02		33.0	293.1	255.1	274.2	9.6

x_o, y_o = .11,-.12 $\leftrightarrow$ .16 347^o

Δx =.39

Δy =.11

Station 71 Depth 5 m   Combined Analysis of the Two Previous Sets of Data

Mid-Time=4.00 hours 15/7/65

2N+1=331+383=714

	Major knots	Minor= knots	Inc. o	G^+ o	G^- o	g o
1 M_2	2.26	-.08	40.6	279.8	257.1	268.5
2 S_2	.31	-.00	38.6	337.8	311.1	324.5
3 L_2	.17	.00	37.4	125.8	96.7	111.3
4 N_2	.45	-.02	39.3	262.2	236.8	249.5
5 μ_2	.13	-.01	43.5	228.8	211.7	220.3
6 K_1	.04	-.01	58.0	19.6	31.6	25.6
7 O_1	.02	-.00	95.7	342.4	69.8	26.1
8 NO_1	.02	-.00	18.6	148.4	81.6	115.0
9 Q_1	.01	.00	7.6	115.3	26.6	71.0
10 OO_1	.01	-.00	150.0	185.3	21.2	283.3
11 J_1	.02	.00	22.3	96.0	36.7	66.4
12 M_4	.20	-.04	40.5	191.4	168.4	179.9
13 MS_4	.03	.01	59.1	174.6	188.8	181.7
14 MN_4	.10	-.03	53.4	148.3	151.0	149.7
15 M_8	.03	-.02	16.9	235.9	165.6	200.8
16 M_3	.03	-.00	46.0	79.9	67.8	73.9
17 M_6	.20	-.01	31.2	273.3	231.8	252.6

Station 72 Depth 25 m 12 hours 17/6/65 to 8 hours 3/7/65

Mid-Time=9.5 hours 25/6/65

2N+1=307

	Major	Minor	Δ	Inc.	G^+	G^-	g	ΔG
1 M_2	4.35	.22	$\pm$.059	18.0	274.3	274.2	274.3	$\pm$ .8
N_2	.87	.04		18.0	246.2	246.1	246.1	4.0
2 S_2	.62	.10		19.5	313.2	316.1	314.7	5.6
K_2	.17	.03		19.5	313.7	316.6	315.2	20.9
3 K_1	.08	.00		31.4	42.9	69.7	56.3	44.1
P_1	.03	.00		31.4	42.2	69.0	55.6	-
4 O_1	.06	.00		40.8	28.9	74.5	51.7	-
Q_1	.01	.00		40.8	6.5	52.1	29.3	-
5 OO_1	.02	.00		40.3	226.2	270.8	248.5	-
6 M_4	.21	.19		90.9	291.0	76.7	3.9	19.0
7 MS_4	.08	-.01		126.5	326.6	183.6	75.1	48.2
8 M_8	.04	-.03		6.2	47.3	23.7	35.5	-
9 M_3	.03	.00		175.2	350.1	304.4	327.2	-
10 M_6	.15	.05		46.0	317.3	13.4	345.3	22.1

$x_o, y_o = .23, -.21 \leftrightarrow .31 \quad 352^\circ$

$\Delta x = .42$

$\Delta y - .10$

Station 72   Depth 25 m   15 hours 4/7/65 to 8 hours 20/7/65

Mid-Time=11.5 hours 12/7/65

2N+1=305

	Major	Minor	Δ	Inc.	G^+	G^-	g	ΔG
1 M_2	4.34	.23	±.056	18.4	281.5	282.2	281.9	± .8
N_2	.87	.05		18.4	253.4	254.1	253.8	3.8
2 S_2	.78	.03		19.5	286.0	289.0	287.5	4.2
K_2	.21	.01		19.5	286.5	289.5	288.0	15.5
3 K_1	.07	.01		20.3	41.3	45.9	43.6	43.5
P_1	.03	.00		20.3	40.6	45.2	42.9	-
4 O_1	.05	.01		29.8	52.6	76.3	64.5	-
Q_1	.01	.00		29.8	30.2	53.9	42.1	-
5 OO_1	.01	-.00		41.3	281.4	327.9	304.7	-
6 M_4	.23	.21		56.9	326.1	43.9	15.0	16.1
7 MS_4	.08	.05		49.1	345.3	47.5	16.4	44.7
8 M_8	.05	-.01		88.0	18.3	158.3	88.3	-
9 M_3	.02	-.00		31.8	92.2	119.9	106.1	-
10 M_6	.11	.08		48.8	17.6	79.1	48.3	29.2

$x_o, y_o = .24, -.15 \longleftrightarrow .28 \quad 002^{o}$

$\Delta x = .40$

$\Delta y = .09$

Station 72 Depth 25 m Combined Analysis of the two Previous Sets of Data

Mid-Time=21.83 hours 3/7/65

2N+1=307+305=612

	Major knots	Minor knots	Inc. °	G^+ °	G^- °	g °
1 M_2	4.07	.23	18.1	278.9	279.0	279.0
2 S_2	.43	.04	18.8	322.9	324.5	323.7
3 L_2	.27	-.02	21.1	109.0	115.3	112.2
4 N_2	.89	.06	18.5	258.6	259.6	259.1
5 μ_2	.03	.01	40.1	292.6	337.0	314.8
6 K_1	.10	.01	25.2	53.6	67.9	60.8
7 O_1	.05	.01	33.5	30.0	61.1	45.6
8 NO_1	.01	-.00	67.0	8.2	106.2	57.2
9 Q_1	.01	.00	46.8	181.8	76.4	47.6
10 OO_1	.01	-.00	153.7	90.2	1.6	318.5
11 J_1	.01	-.00	159.1	177.4	99.5	138.5
12 M_4	.20	.18	90.5	309.9	94.8	202.4
13 MS_4	.06	.03	115.3	355.1	189.8	272.5
14 MN_4	.08	.06	120.5	280.0	125.0	202.5
15 M_8	.01	.00	45.8	23.4	78.9	51.2
16 M_3	.01	-.00	74.1	61.4	173.6	117.5
17 M_6	.09	.04	39.0	347.5	29.5	8.5

Station 73 Depth 10 m 16 hours 17/6/65 to 15 hours 23/7/65

Mid-Time=15.5 hours 5/7/65

2N+1=791

	Major	Minor	Δ	Inc.	G^+	G^-	g	ΔG
1 M_2	2.58	-.03	$\pm$.015	10.3	189.2	29.8	289.5	$\pm$ .3
2 S_2	.40	-.01		10.7	243.3	84.7	344.0	2.2
K_2	.11	-.00		10.7	243.8	85.2	344.5	8.0
3 L_2	.15	-.01		.9	350.4	172.1	81.3	6.1
4 N_2	.41	.03		12.2	176.7	21.1	278.9	2.2
ν_2	.09	.01		12.2	182.7	27.1	284.9	9.2
5 μ_2	.13	-.02		16.8	244.4	98.1	351.3	6.9
6 K_1	.04	.00		14.2	303.4	151.8	47.6	21.2
P_1	.01	.00		14.2	302.7	151.1	46.9	-
7 O_1	.02	-.00		16.4	291.5	144.3	37.9	37.2
8 NO_1	.01	.00		4.9	184.2	13.9	279.1	-
9 Q_1	.00	-.00		111.6	132.9	176.2	154.6	-
10 OO_1	.01	.00		20.6	158.3	19.4	268.9	-
11 J_1	.01	.00		20.1	224.8	86.2	335.5	-
12 M_4	.11	-.02		2.4	36.7	221.5	129.1	9.2
13 MS_4	.04	-.01		14.0	74.2	282.2	178.2	26.3
14 MN_4	.03	-.02		1.3	49.3	231.9	140.6	32.7
15 M_8	.01	-.01		1.2	231.1	53.4	322.3	-
16 M_3	.02	.00		5.2	.9	191.3	96.1	-
17 M_6	.20	.01		15.2	241.0	91.3	346.2	4.3

$x_o, y_o = -.07,\ .12 \leftrightarrow .14 \quad 64^{o}$

$\Delta x = .06$

$\Delta y = .15$

Station 74 Depth 5 m 13 hours 26/7/65 to 9 hours 25/8/65

Mid-Time 10.5 hours 10/8/65

2N+1=643

	Major	Minor	Δ	Inc.	G^+	G^-	g	ΔG
1 M_2	3.27	-.23	$\pm$.029	168.8	288.6	288.1	288.4	$\pm$ .5
2 S_2	.45	-.03		173.2	338.5	346.8	342.7	3.8
K_2	.12	-.01		173.2	339.1	347.4	343.3	14.3
3 L_2	.28	-.03		164.6	117.4	108.6	113.0	6.2
4 N_2	.61	-.03		168.5	259.2	258.3	258.8	2.8
ν_2	.14	-.01		168.5	265.3	264.4	264.9	12.2
5 μ_2	.17	-.03		174.8	323.3	334.9	329.1	10.1
6 K_1	.07	.01		170.0	46.9	49.0	48.1	23.4
P_1	.02	.00		170.0	46.2	48.3	47.3	-
7 O_1	.07	.00		164.5	42.7	33.7	38.2	22.3
8 NO_1	.02	-.00		152.9	11.6	334.9	355.5	-
9 Q_1	.02	-.01		14.7	353.1	44.5	18.8	-
10 OO_1	.01	.01		121.0	170.2	74.4	302.3	-
11 J_1	.01	-.00		122.8	163.8	71.3	297.6	-
12 M_4	.68	-.10		1.1	97.7	121.8	109.8	2.8
13 MS_4	.18	-.06		.2	164.8	187.2	176.0	10.5
14 MN_4	.28	-.05		6.2	57.2	91.7	74.6	7.2
15 M_8	.16	.01		11.3	235.2	279.7	257.5	18.9
16 M_3	.01	-.01		76.9	267.4	83.1	355.2	-
17 M_6	.29	-.10		164.7	47.4	38.7	43.0	6.0

$x_o, y_o = -1.46, -.37 \leftrightarrow 1.51 \quad 183^\circ$

$\Delta x = .24$

$\Delta y = .13$

Station 75 Depth 10 m   10 hours 8/8/65 to 10 hours 23/8/65

Mid-Time = 21.5 hours 15/8/65

2N+1=287

	Major	Minor	Δ	Inc.	G^+	G^-	g	ΔG
1 M_2	2.97	.05	$\pm$.045	31.0	287.8	281.8	284.8	$\pm$ .9
N_2	.59	.01		31.0	259.7	253.7	256.7	4.5
2 S_2	.80	.01		31.1	348.5	342.7	345.6	3.3
K_2	.22	.00		31.1	349.0	343.2	346.1	12.3
3 K_1	.07	.00		30.9	81.9	75.6	78.8	38.4
P_1	.02	.00		30.9	81.2	74.9	78.1	-
4 O_1	.06	.00		22.6	78.6	55.8	67.2	47.6
Q_1	.01	.00		22.6	56.2	33.4	44.8	-
5 OO_1	.01	.00		45.2	304.4	326.9	315.7	-
6 M_4	.24	.03		178.4	121.4	50.2	85.8	12.5
7 MS_4	.18	-.00		174.8	202.0	123.6	162.8	17.2
8 M_8	.04	.02		31.6	241.3	236.6	238.9	-
9 M_3	.05	.01		31.9	32.4	28.2	30.3	-
10 M_6	.15	.04		38.1	19.5	27.8	23.7	17.5

$x_o, y_o = -.61,\ .32 \leftrightarrow .70 \quad 187^\circ$

$\Delta x = .32$

$\Delta y = .06$

Station 76 Depth 10 m 20 hours 29/7/65 to 8 hours 21/8/65

Mid-Time = 1.5 hours 10/8/65

2N+1=467

		Major	Minor	Δ	Inc.	G^+	G^-	g	ΔG
1	M_2	1.49	-.11	±.032	36.4	287.2	292.0	289.6	±1.3
	N_2	.30	-.02		36.4	258.0	262.8	260.5	6.4
2	S_2	.28	-.03		40.4	312.3	325.2	318.8	6.9
	K_2	.08	-.01		40.4	313.0	325.9	319.5	25.2
3	K_1	.03	.00		59.2	288.4	338.8	313.6	-
	P_1	.01	.00		59.2	287.5	337.9	312.7	-
4	O_1	.03	.00		49.0	277.2	307.3	292.3	-
	Q_1	.01	.00		49.0	253.7	283.8	268.8	-
5	OO_1	.01	.00		31.5	130.5	125.5	128.0	-
6	M_4	.34	.01		76.5	28.7	113.7	71.2	6.3
7	MS_4	.15	.01		66.7	62.7	128.2	95.5	14.0
8	M_8	.07	-.01		77.4	346.9	73.7	30.3	45.8
9	M_3	.01	.00		81.9	347.5	83.3	85.4	-
10	M_6	.20	.04		43.3	138.0	156.5	147.2	9.3

$x_o, y_o = .97, .01 \leftrightarrow .97 \quad 35^\circ$

$\Delta x = .26$

$\Delta y = .09$

7.2 Plots

Plots 1 to 24 show first the x and y components of the current observations taken at intervals of five minutes; these are labelled by X and Y in the diagrams. X-SM and Y-SM are the plots of the smoothed x and y components sampled at intervals of one hour.

X-LP and Y-LP are the low passes of the smoothed x and y sequences. X-R and Y-R are the differences between X-SM and X-LP, and Y-SM and Y-LP; X-R and Y-R are the quantities subjected to a harmonic analysis.

X-PR and Y-PR represent the functions fitted to X-R and Y-R with the help of the least squares to which there have been added X-LP and Y-LP.

X-ER and Y-ER are the differences between X-SM and X-PR, and Y-SM and Y-PR; they represent the portion of the observations which escaped the analysis.

For short sequences of observations there are marked oscillations in X-ER and Y-ER which are due to the presence of some unanalyzable constituents such as N_2. In this case X-ER and Y-ER are evaluated anew after the hidden constituents have been inferred and a second plot is shown for the same set of data.

Plots 25 to 48 show the magnitude and direction as well as the x and y components of the residual current (low pass). The direction is with respect to the original frame of reference whose orientations are given in Table 1.

Plot 1

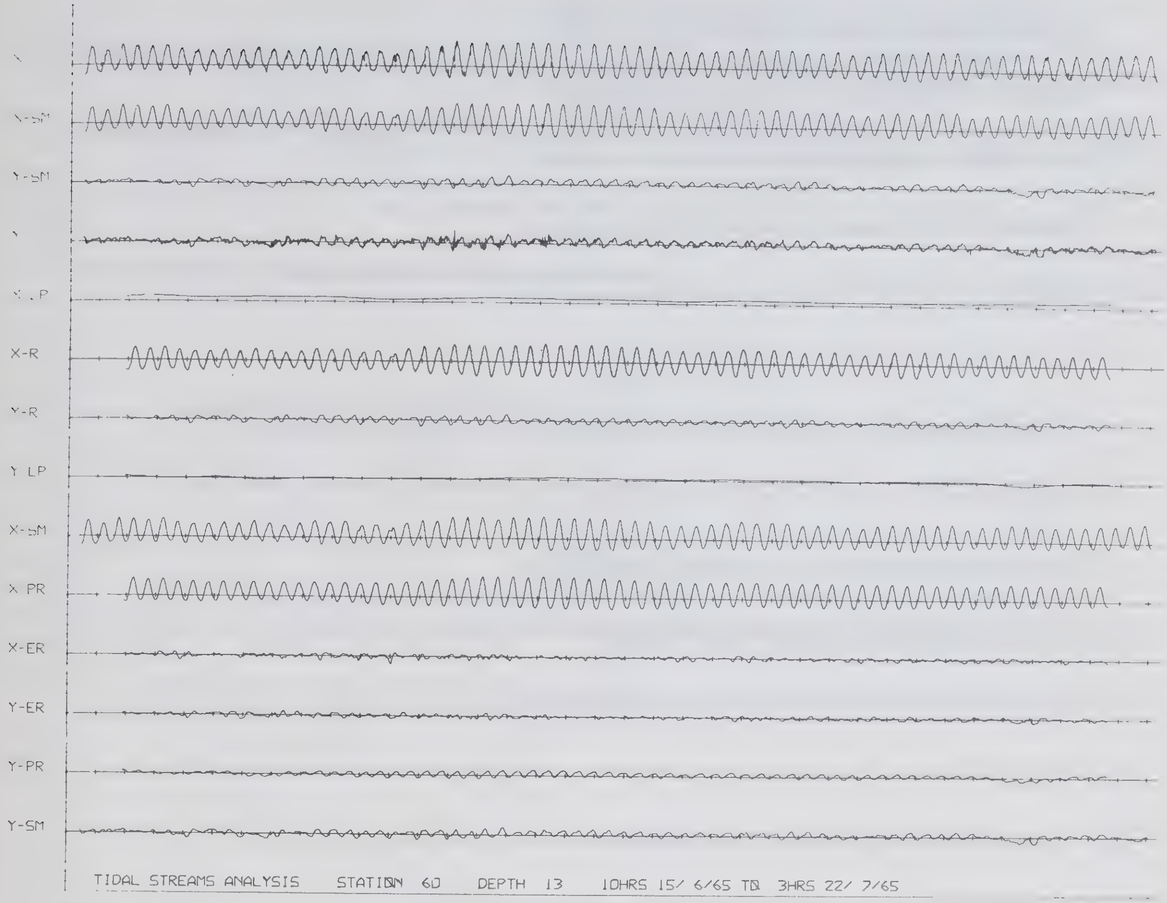
X-SM
Y-SM
X-R
Y-R
Y LP
X-SM
X PR
X-ER
Y-ER
Y-PR
Y-SM
TIDAL STREAMS ANALYSIS STATION 60 DEPTH 13 10HRS 15/ 6/65 TO 3HRS 22/ 7/65

Plot 2(a)

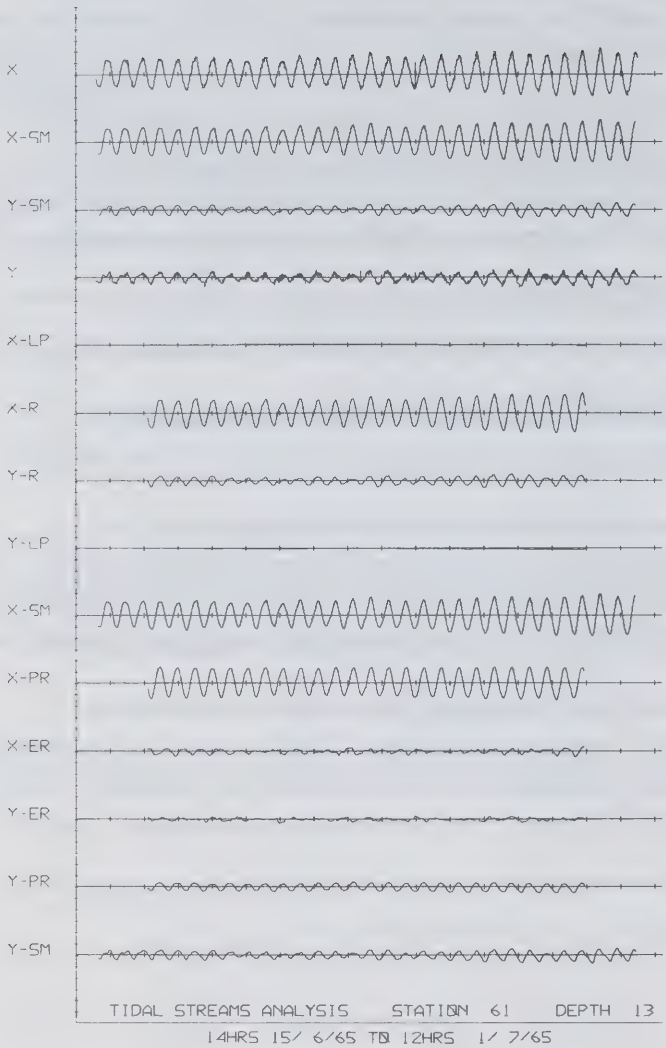

Plot 2(b)

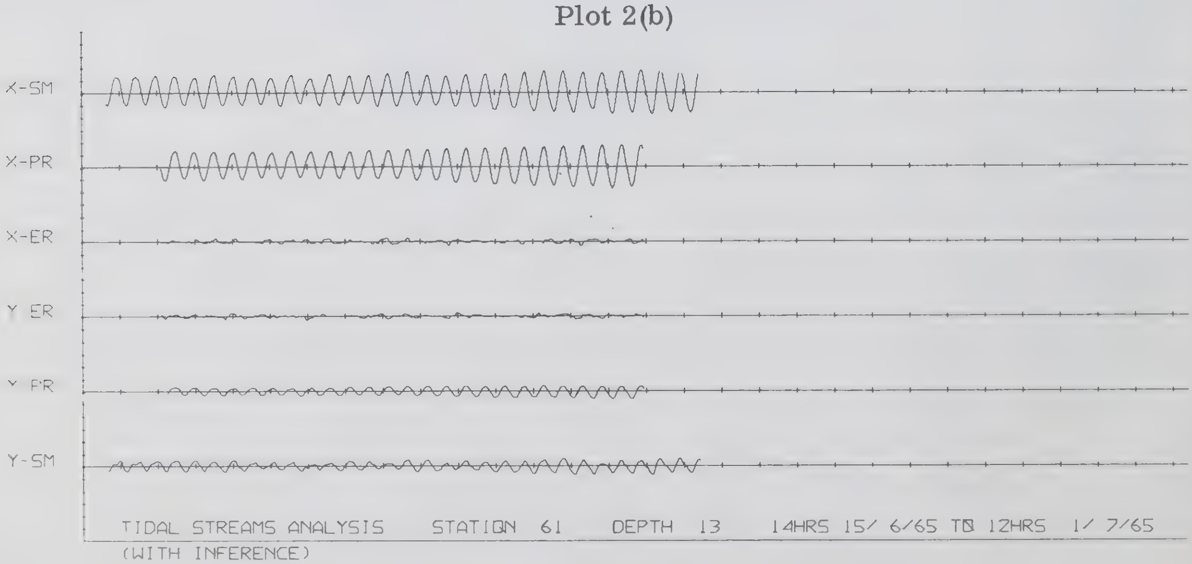

Plot 3

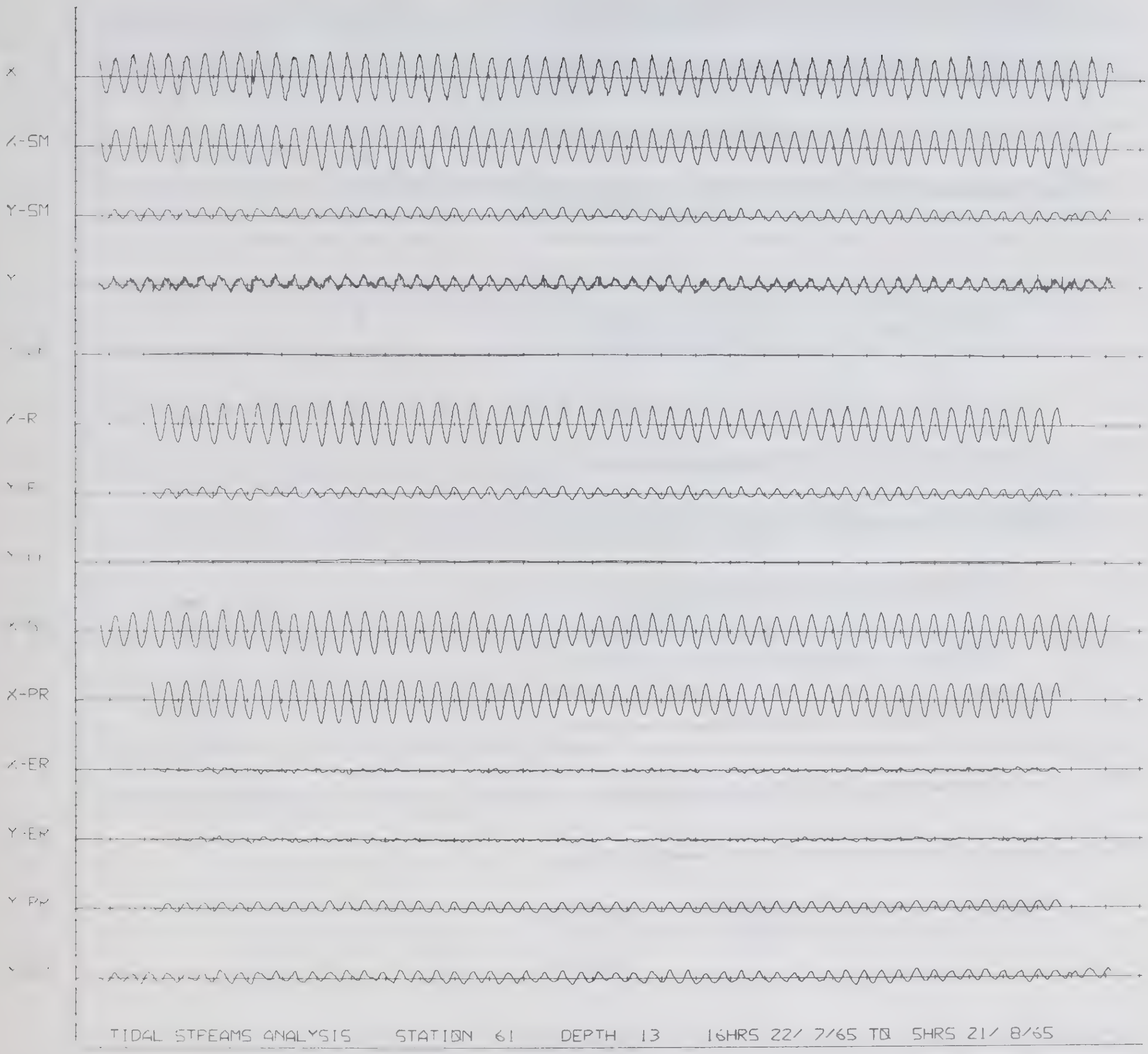
X
X-SM
Y-SM
X-PR
X-ER
Y-ER
TIDAL STREAMS ANALYSIS STATION 61 DEPTH 13 16HRS 22/ 7/65 TO 5HRS 21/ 8/65

Plot 4(a)

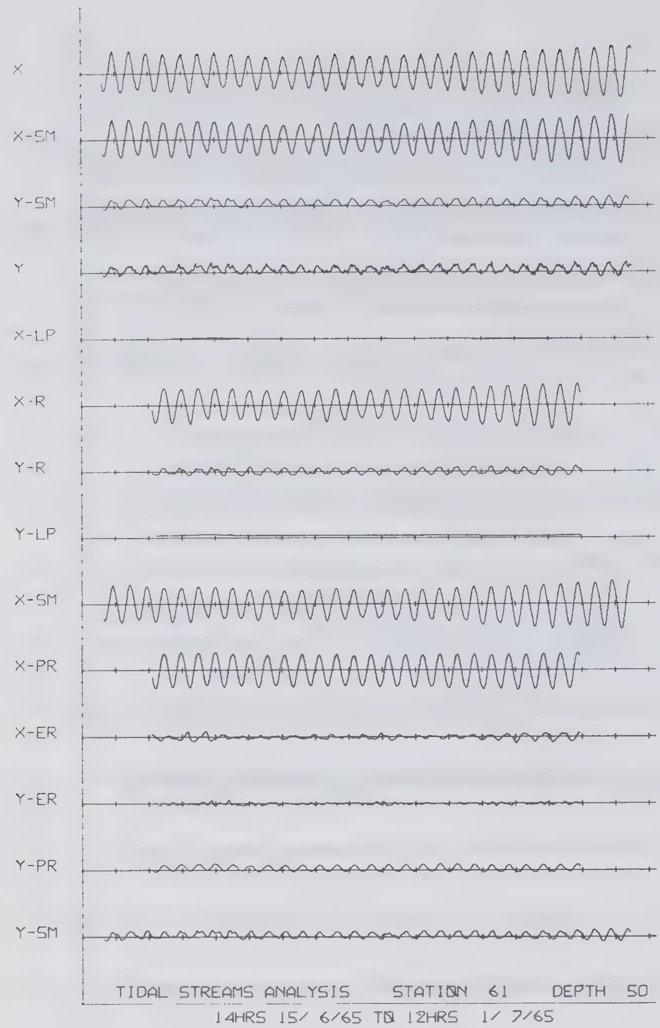

Plot 4(b)

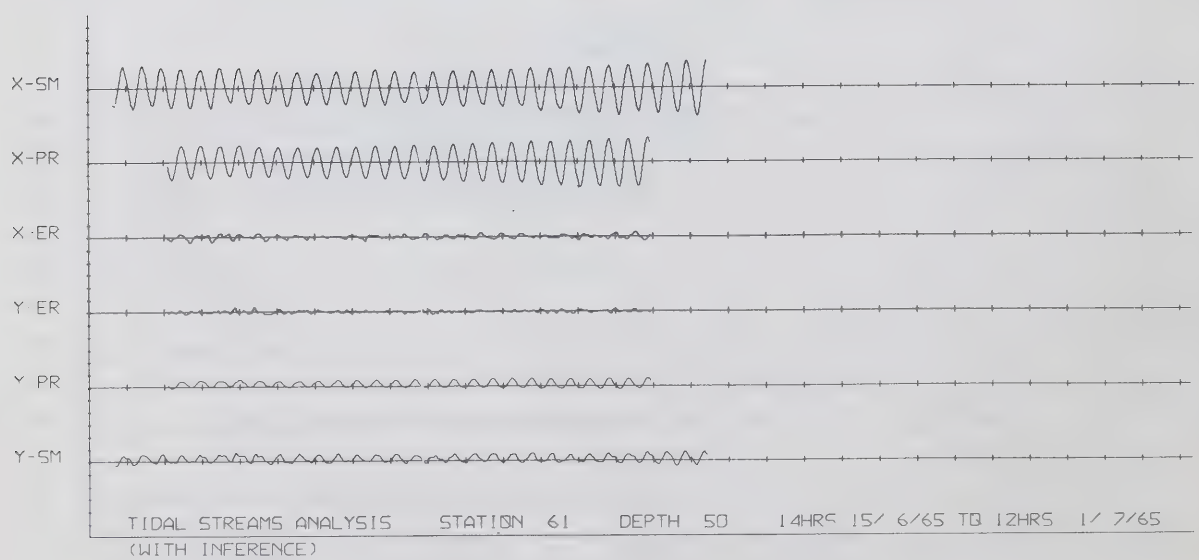

Plot 5

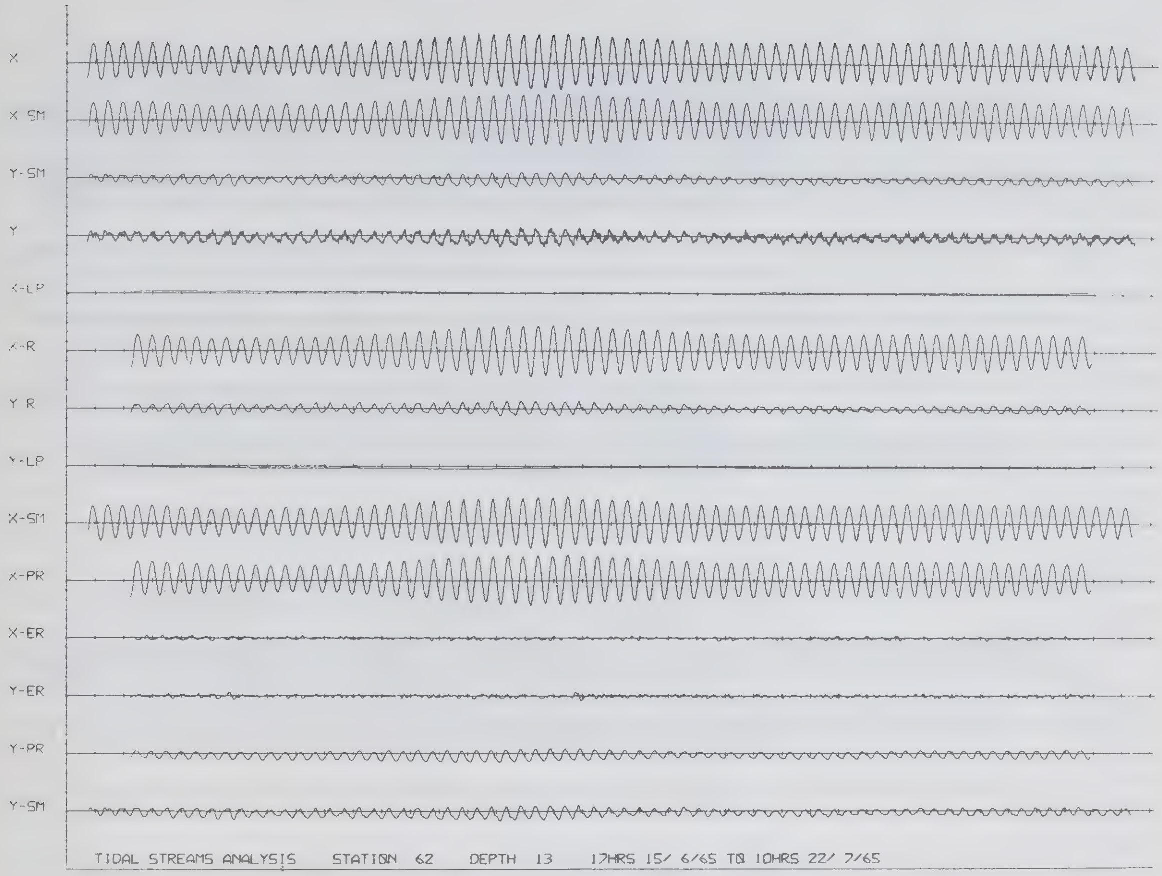
X
X SM
Y-SM
Y
X-LP
X-R
Y R
Y-LP
X-SM
X-PR
X-ER
Y-ER
Y-PR
Y-SM
TIDAL STREAMS ANALYSIS STATION 62 DEPTH 13 17HRS 15/ 6/65 TO 10HRS 22/ 7/65

Plot 6

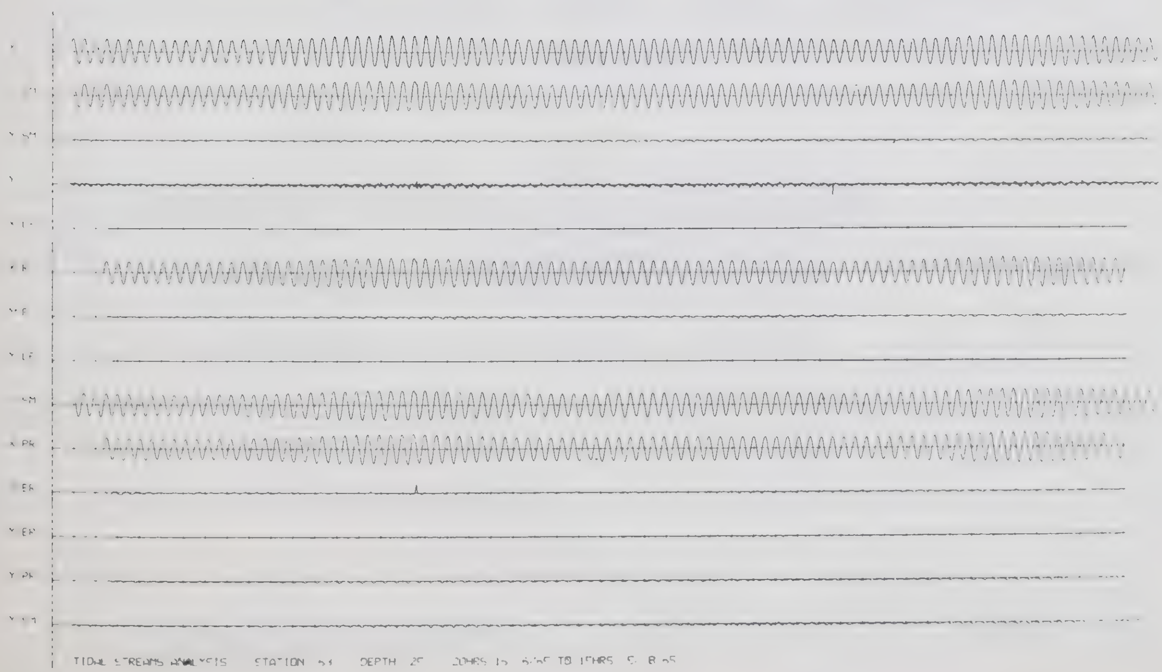
TIDAL STREAMS ANALYSIS STATION DEPTH

Plot 7

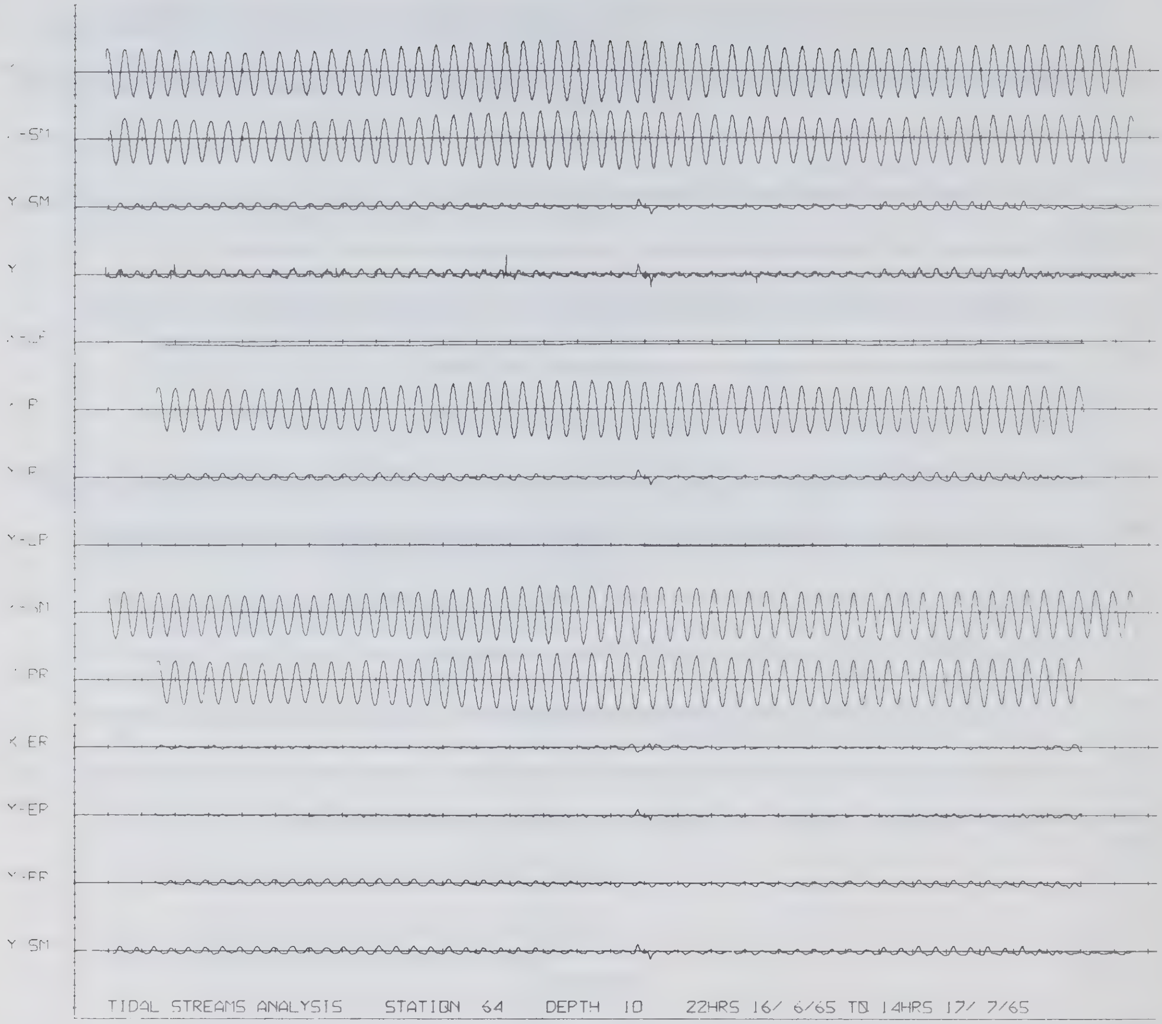

-SM
Y SM
Y
P
Y-LP
PR
ER
Y-EP
Y-EF
Y SM
TIDAL STREAMS ANALYSIS STATION 64 DEPTH 10 22HRS 16/ 6/65 TO 14HRS 17/ 7/65

Plot 8(a)

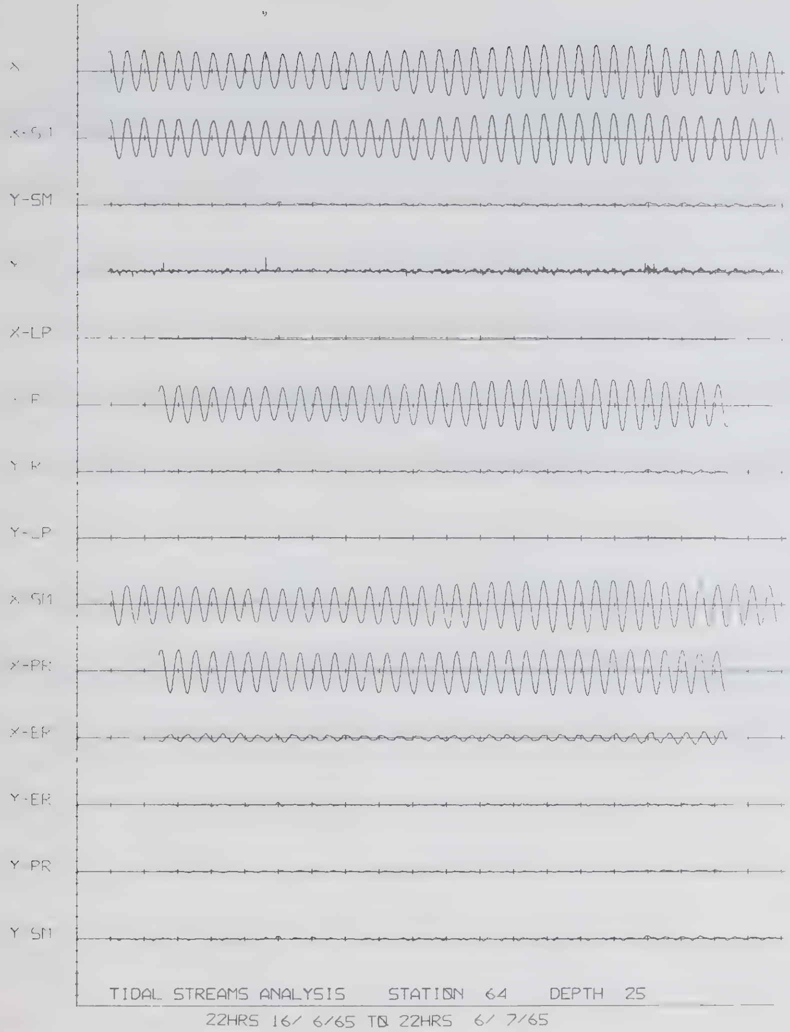

Plot 8(b)

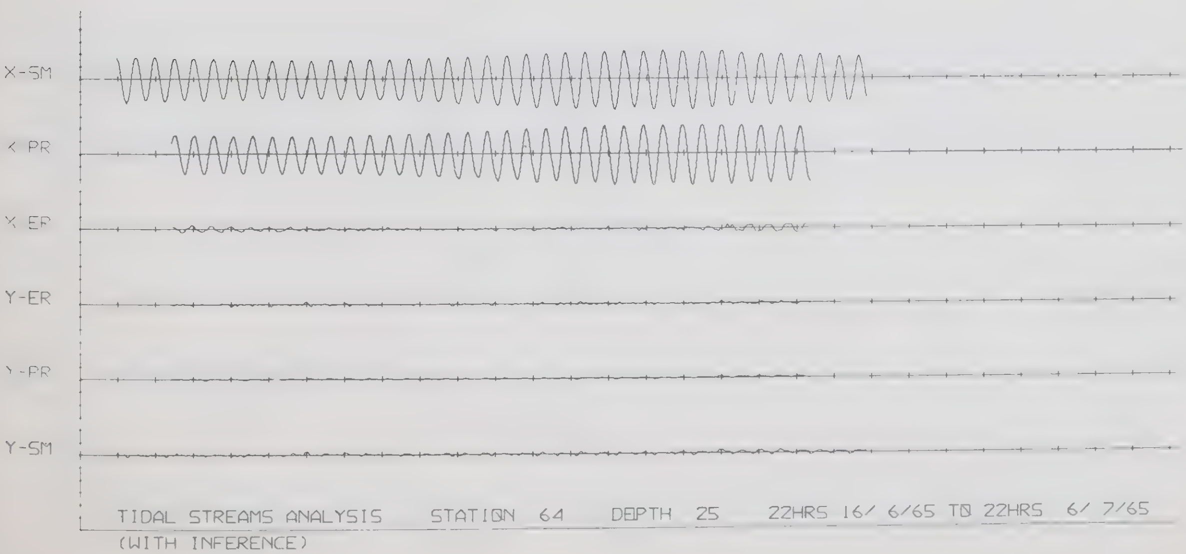

Plot 9

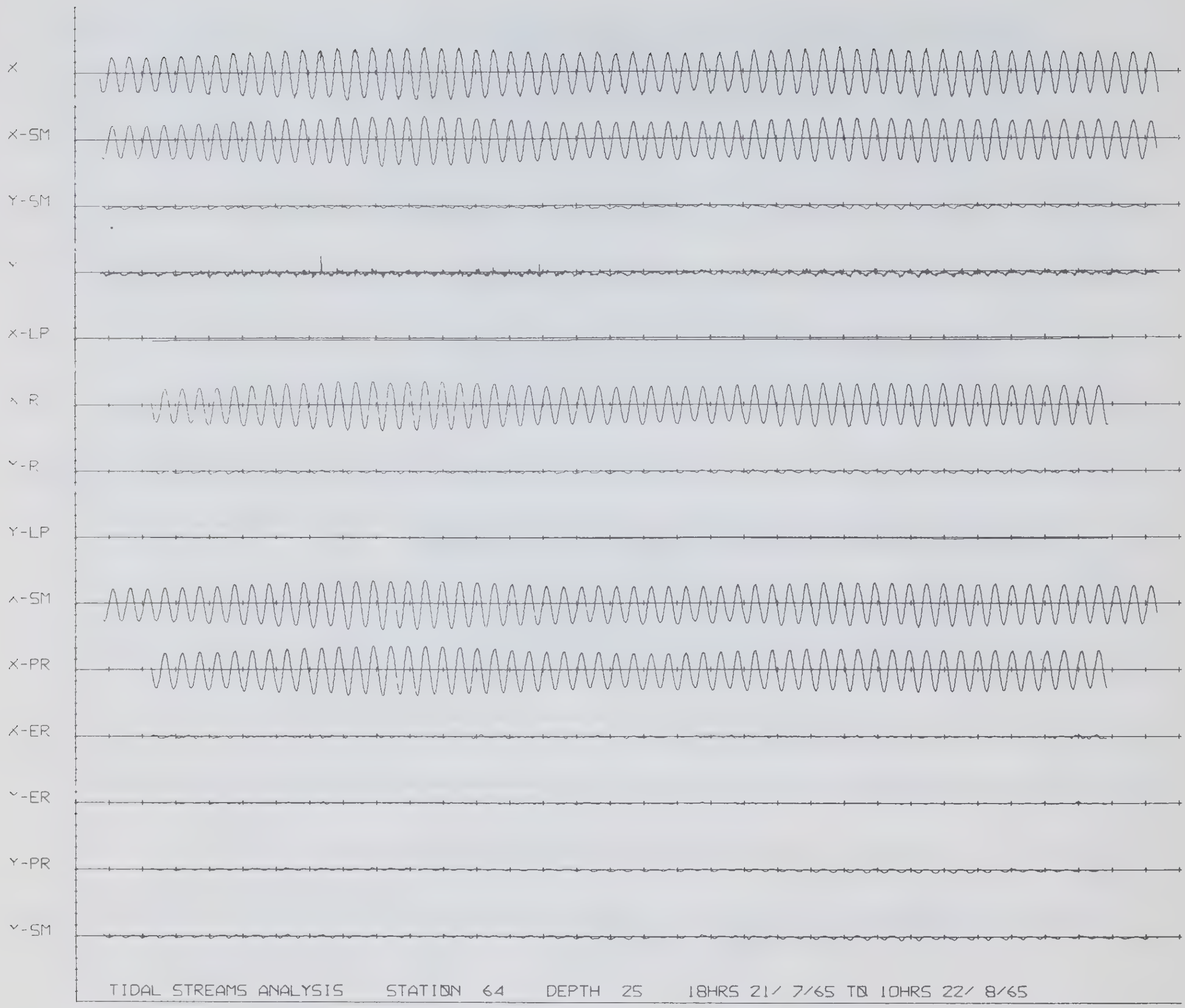
X
X-SM
Y-SM
Y
X-LP
X-R
Y-R
Y-LP
X-SM
X-PR
X-ER
Y-ER
Y-PR
Y-SM
TIDAL STREAMS ANALYSIS STATION 64 DEPTH 25 18HRS 21/ 7/65 TO 10HRS 22/ 8/65

Plot 10(a)

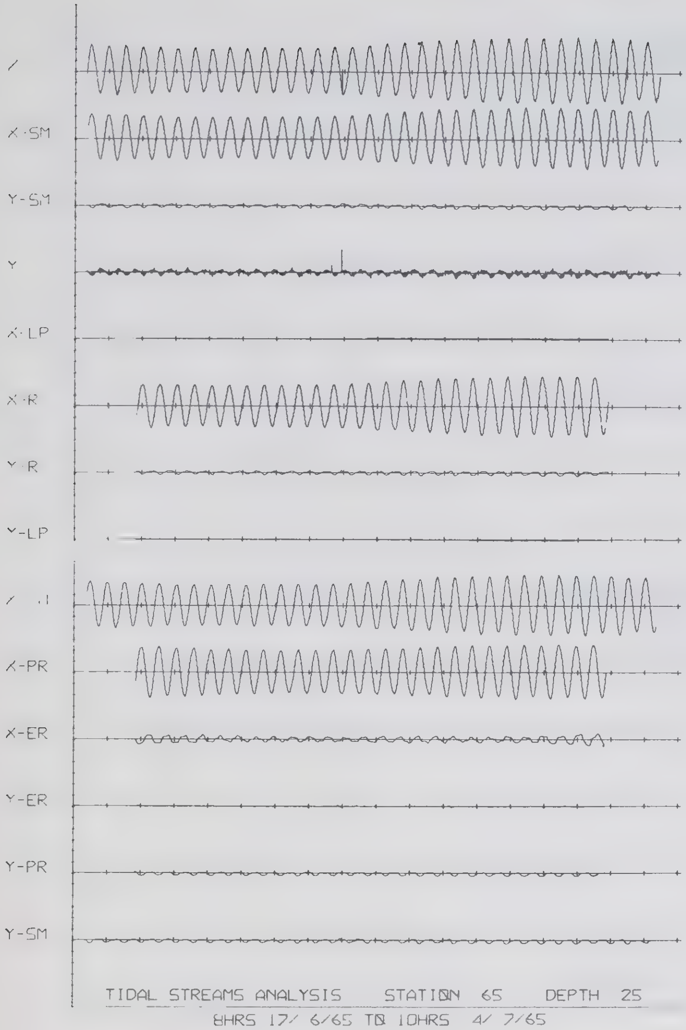

Plot 10(b)

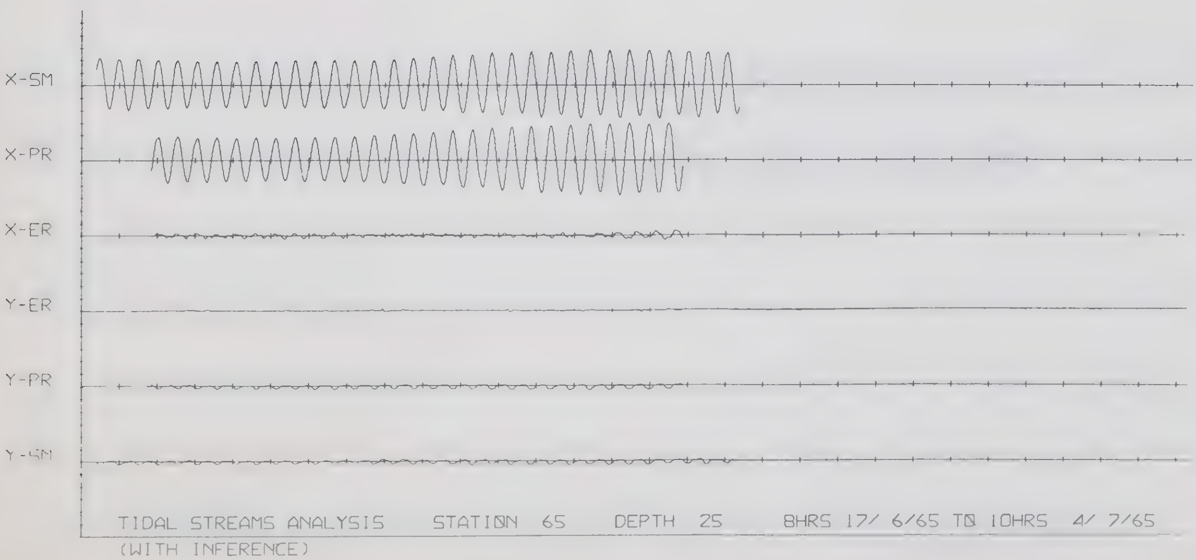

Plot 11(a)

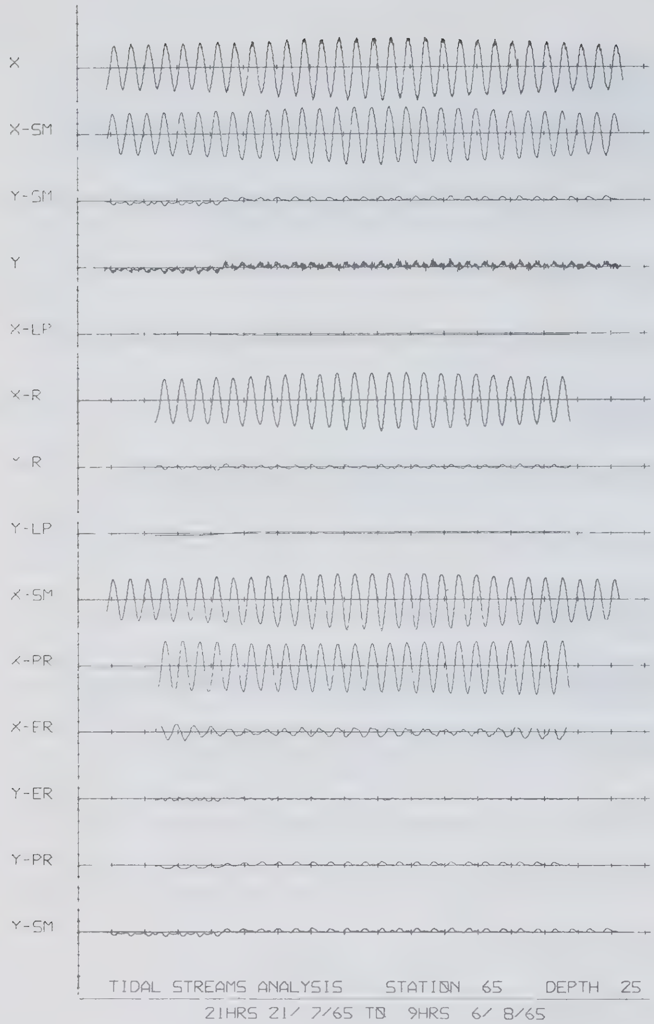

Plot 11(b)

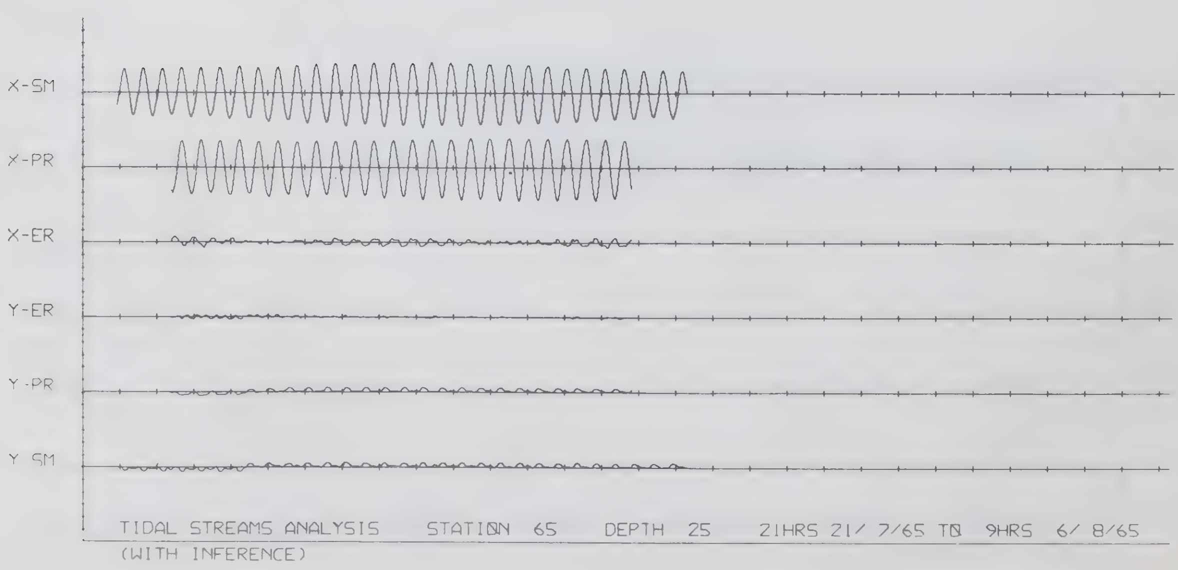

Plot 12(a)

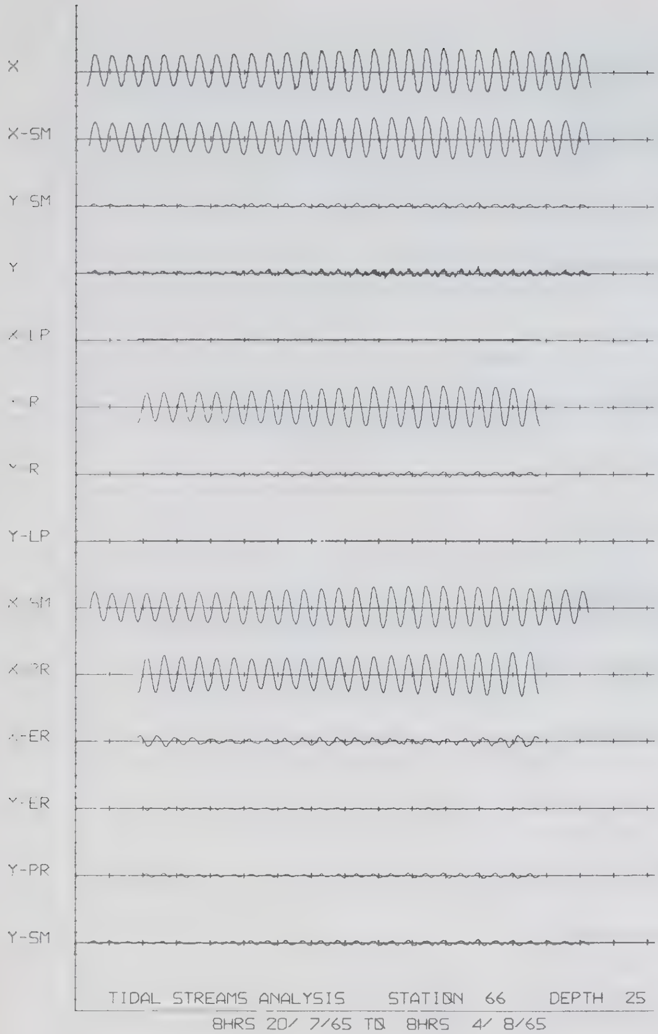

Plot 12(b)

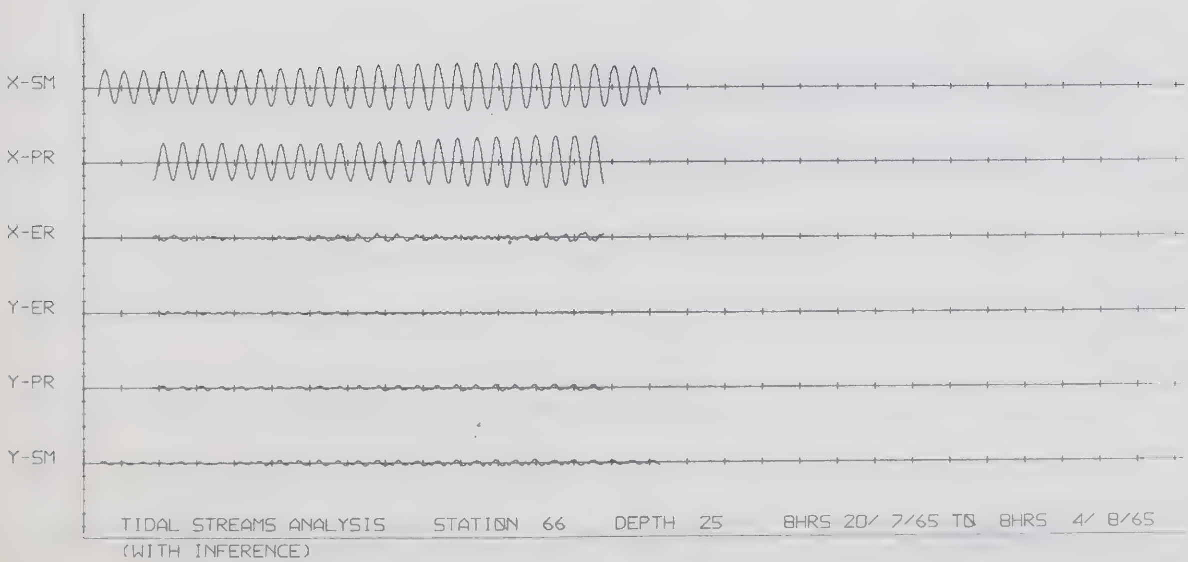

Plot 13(a)

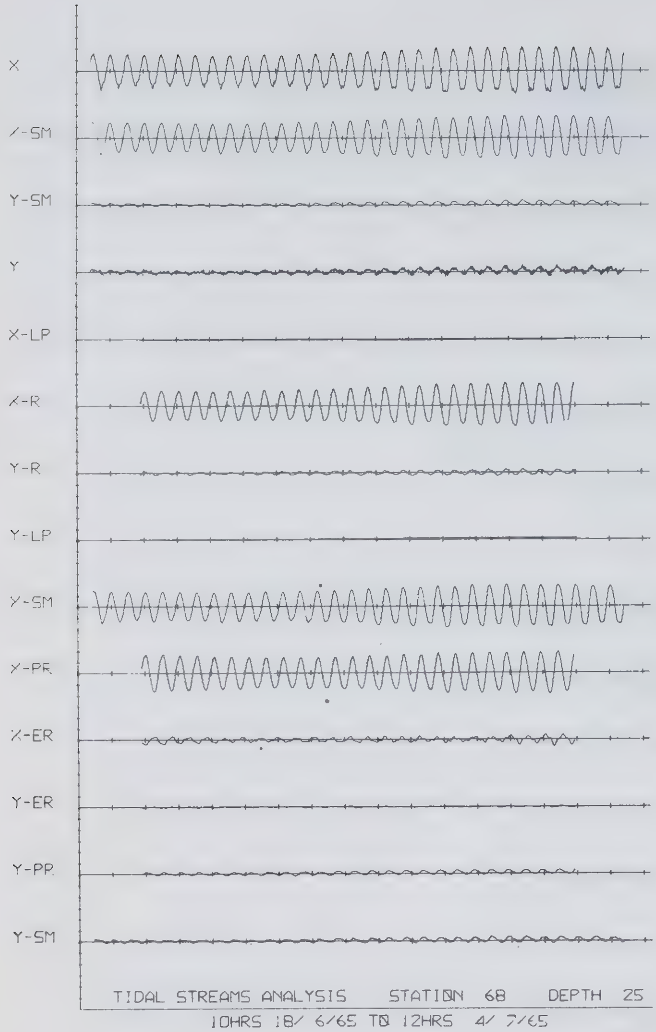

Plot 13(b)

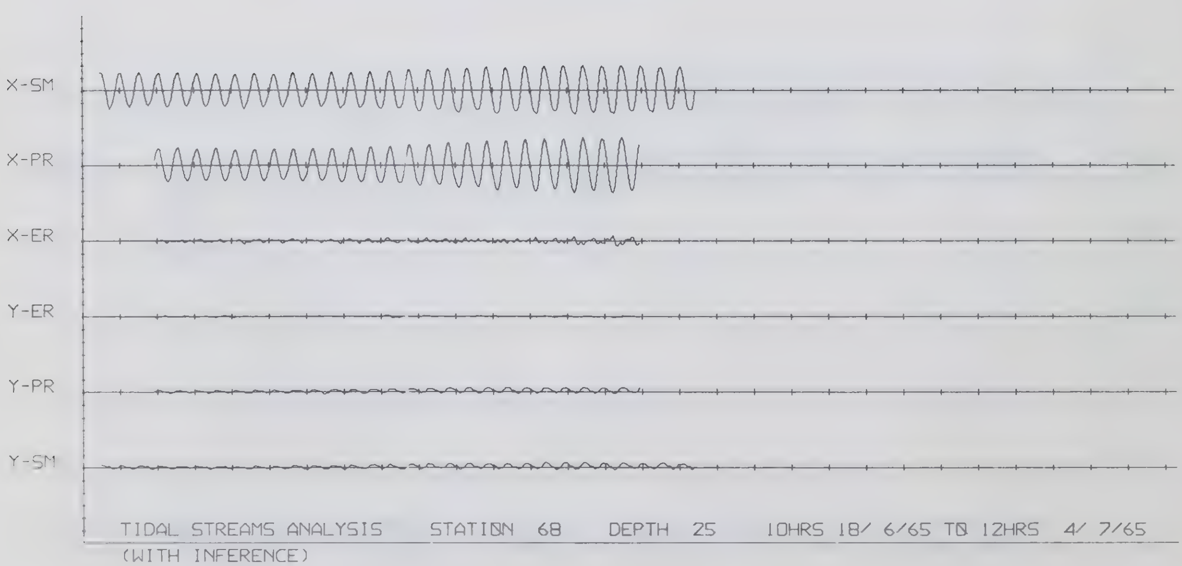

Plot 14(a)

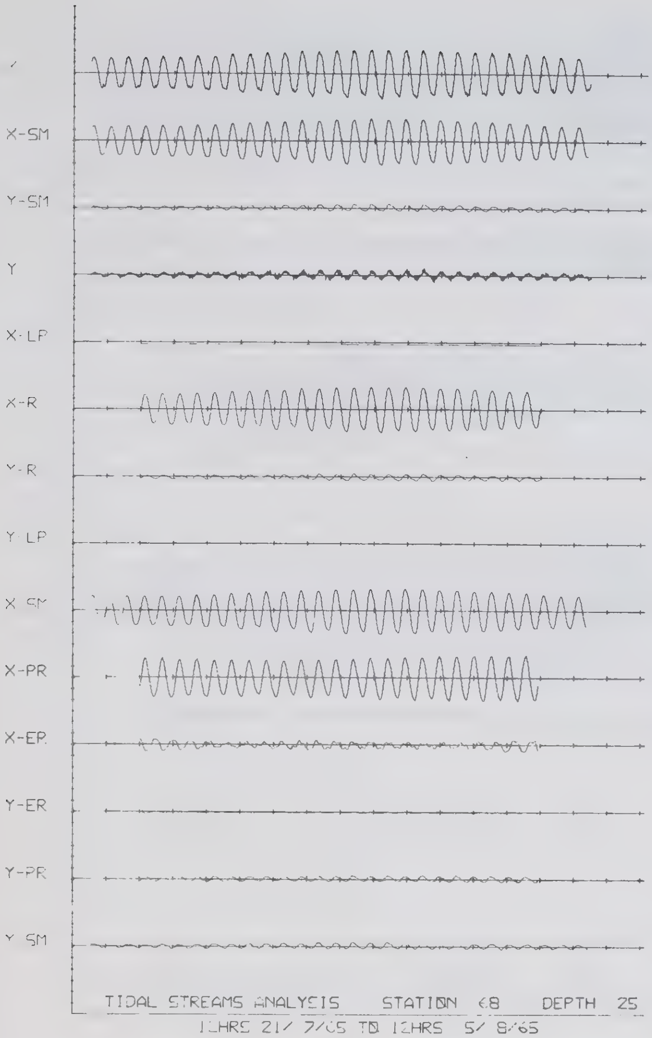

Plot 14(b)

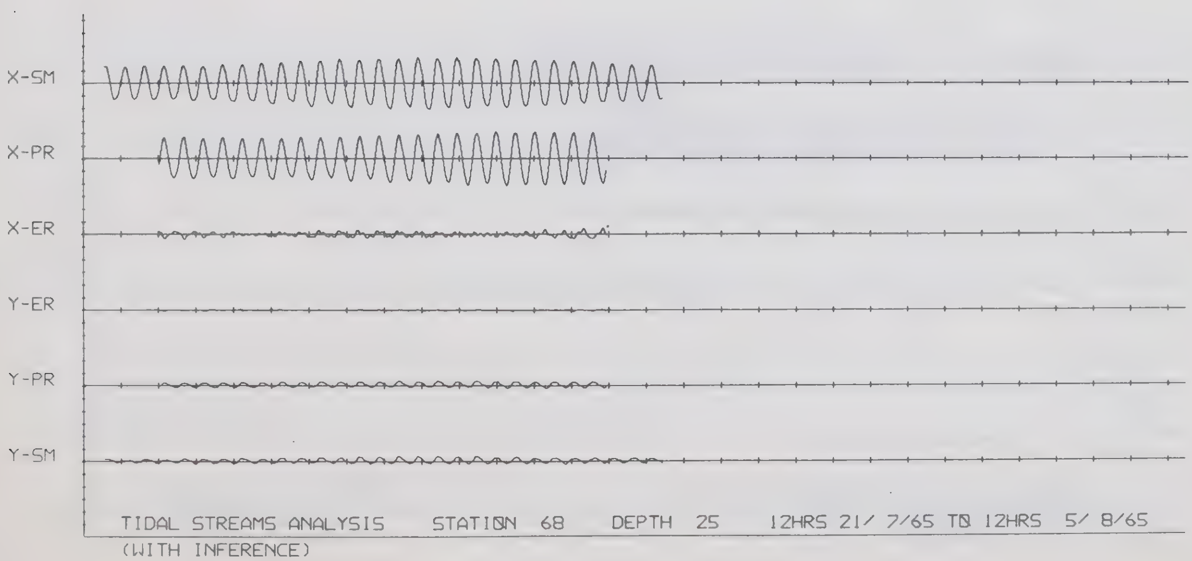

Plot 15(a)

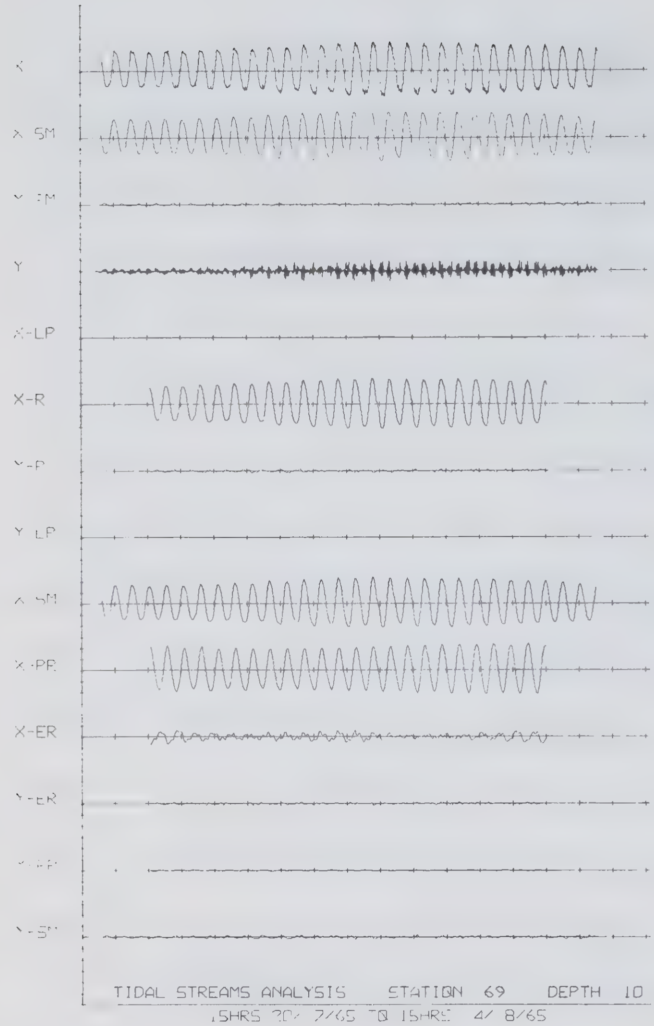

Plot 15(b)

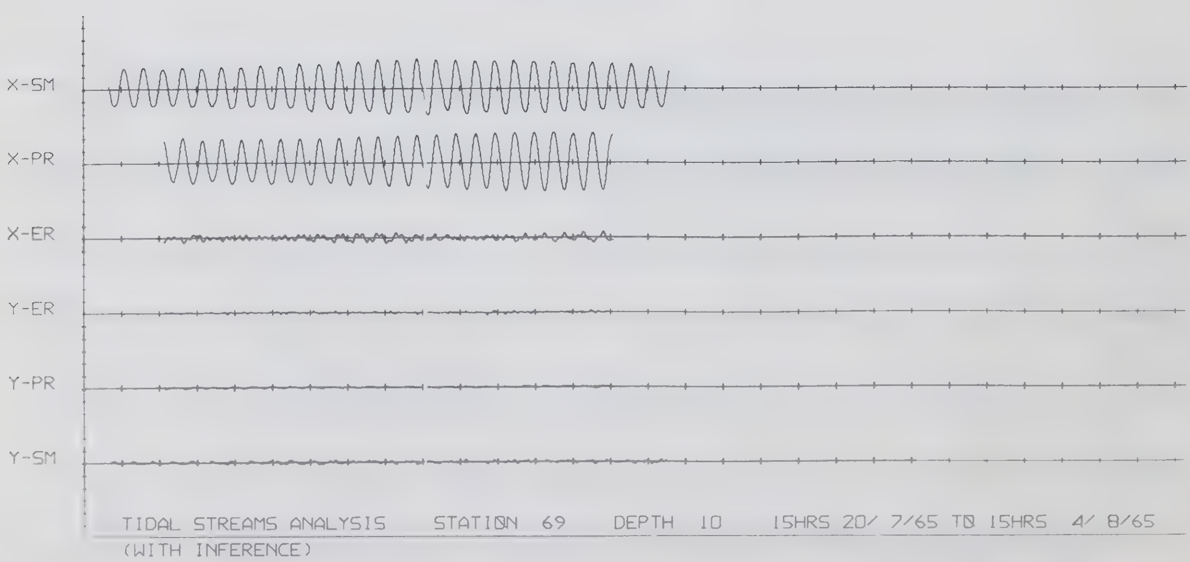

Plot 16(a)

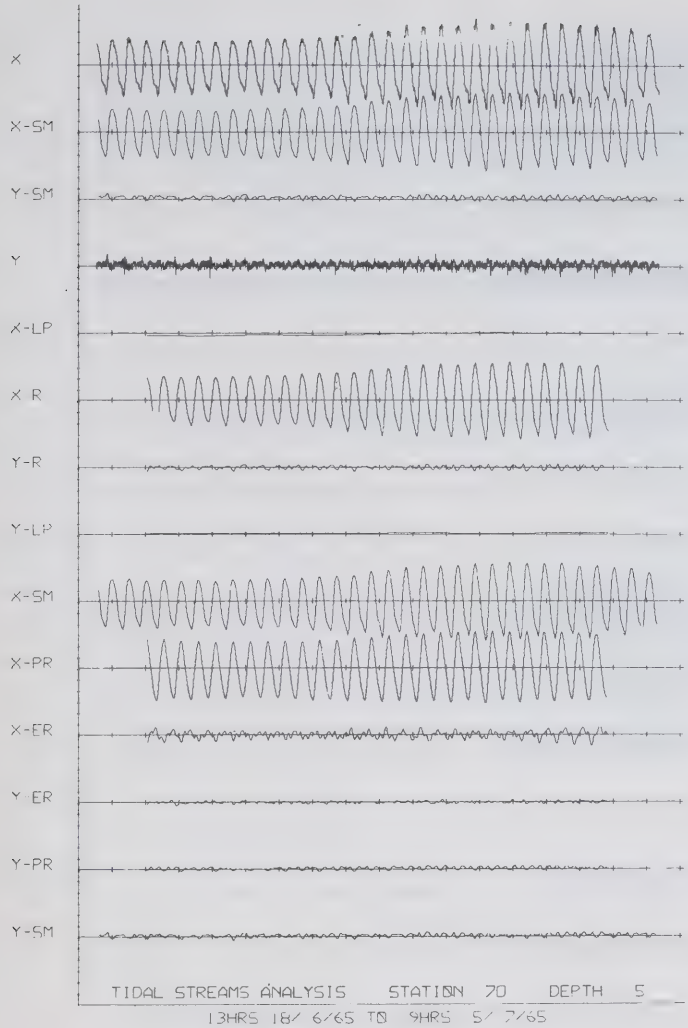

Plot 16(b)

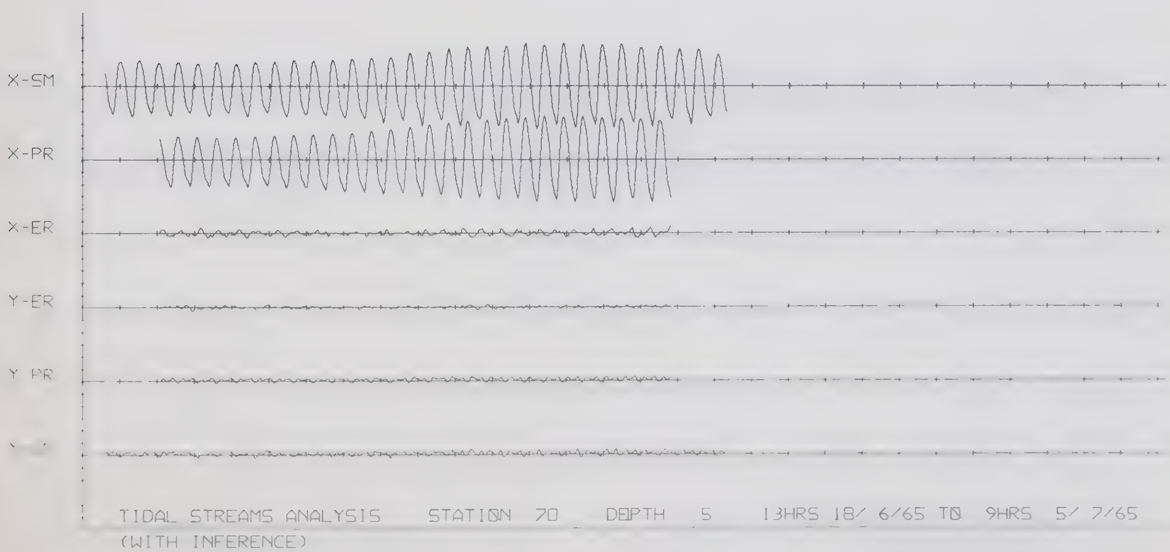

Plot 17(a)

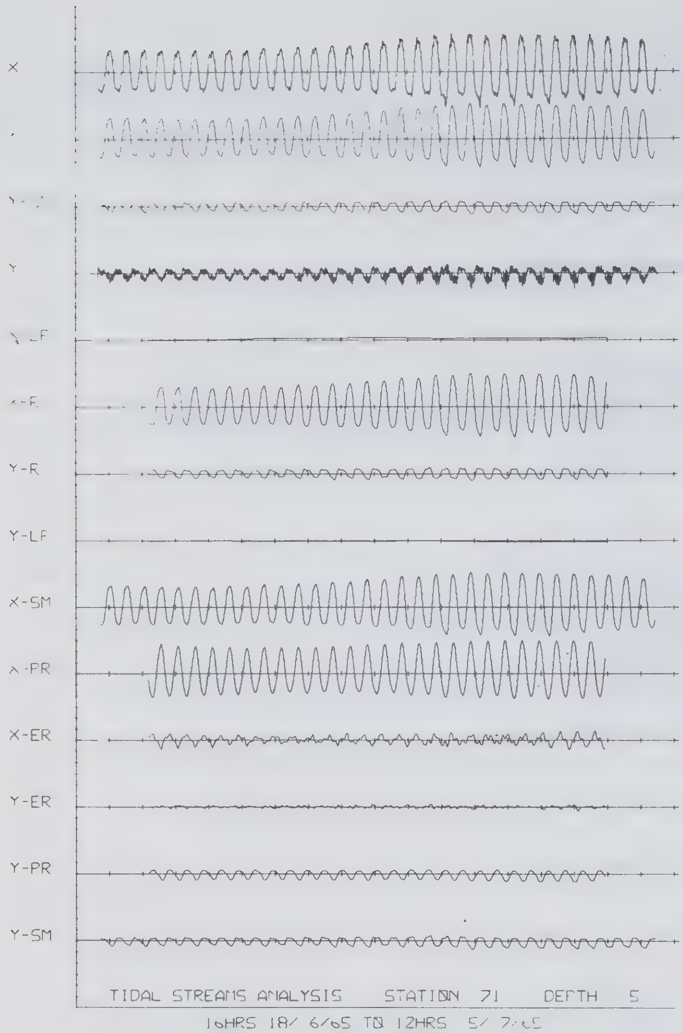

Plot 17(b)

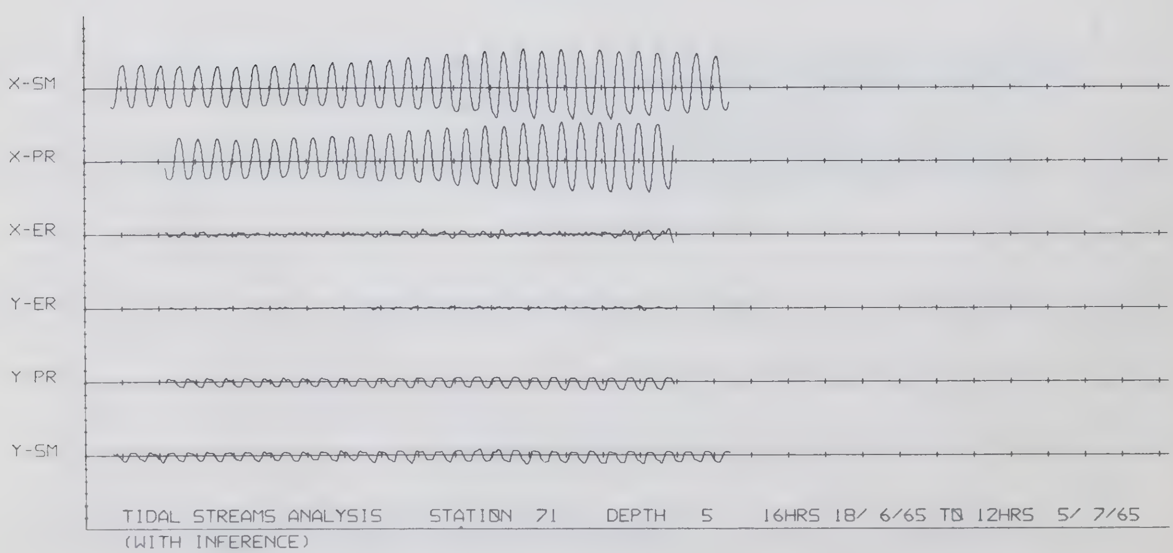

Plot 18(a)

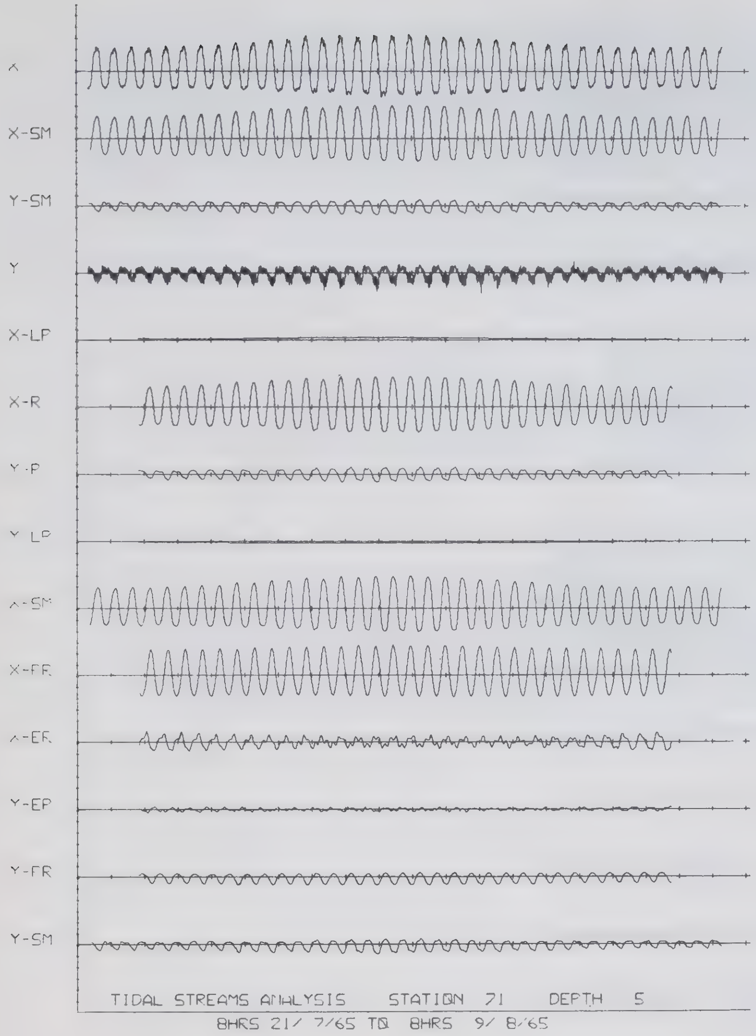

Plot 18(b)

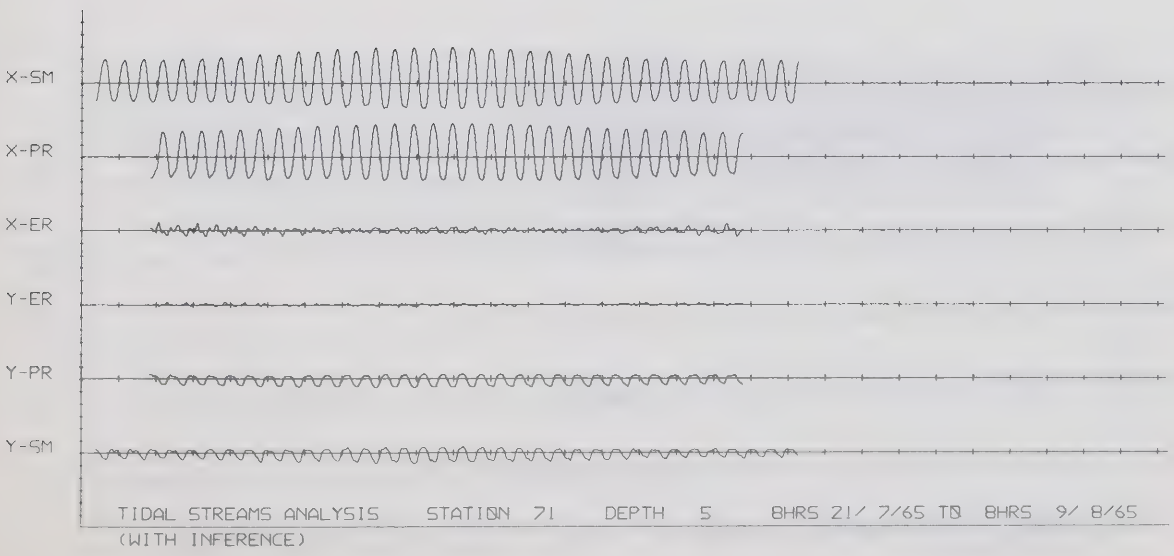

Plot 19(a)

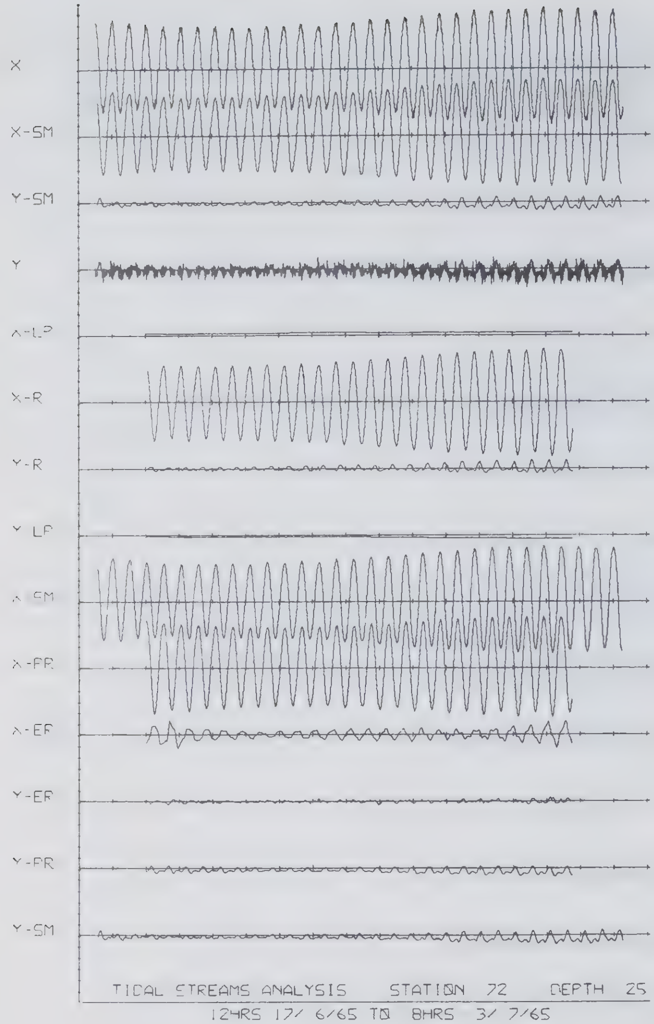

Plot 19(b)

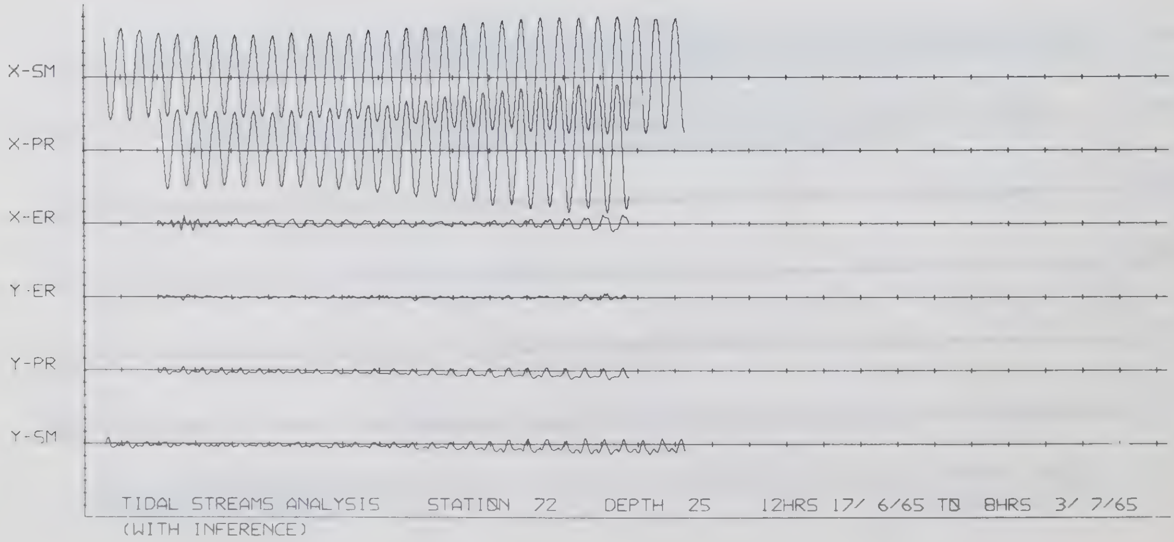

Plot 20(a)

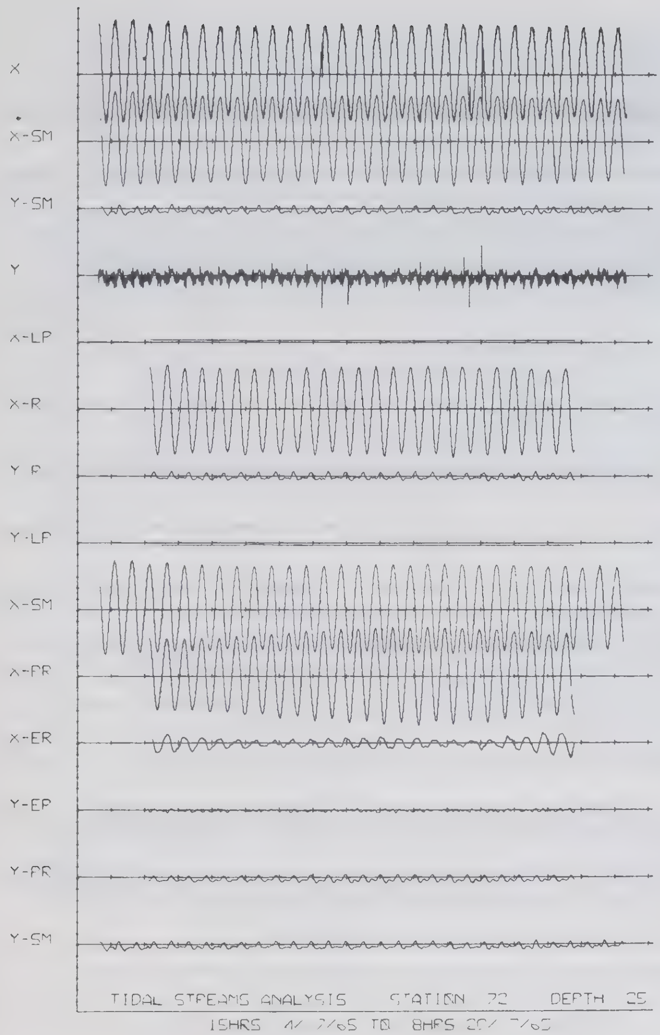

Plot 20(b)

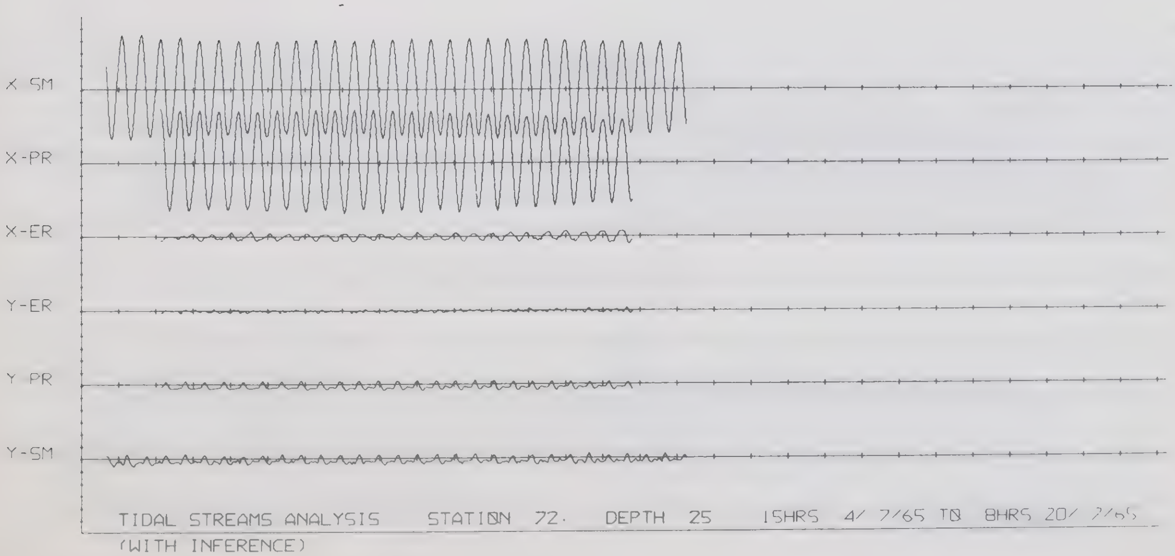

Plot 21(a)

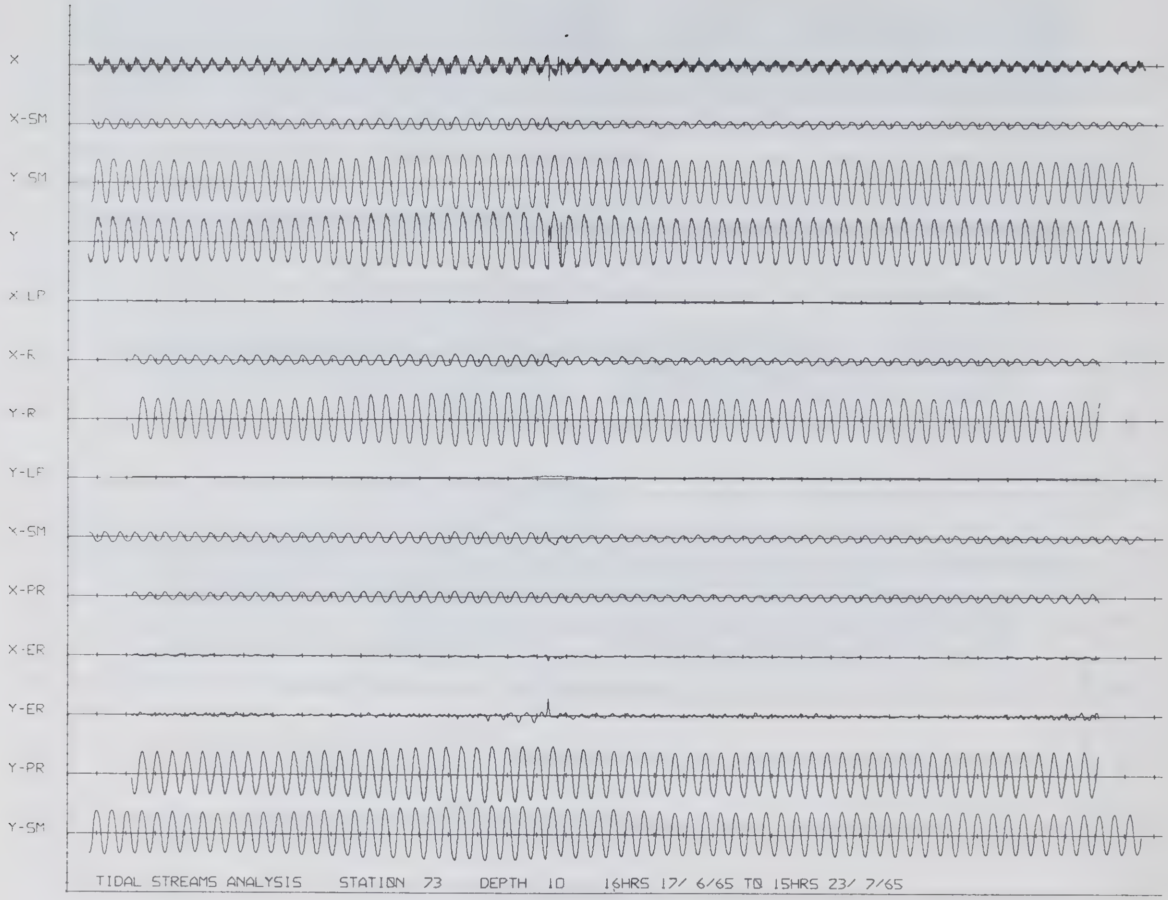

Plot 21(b)

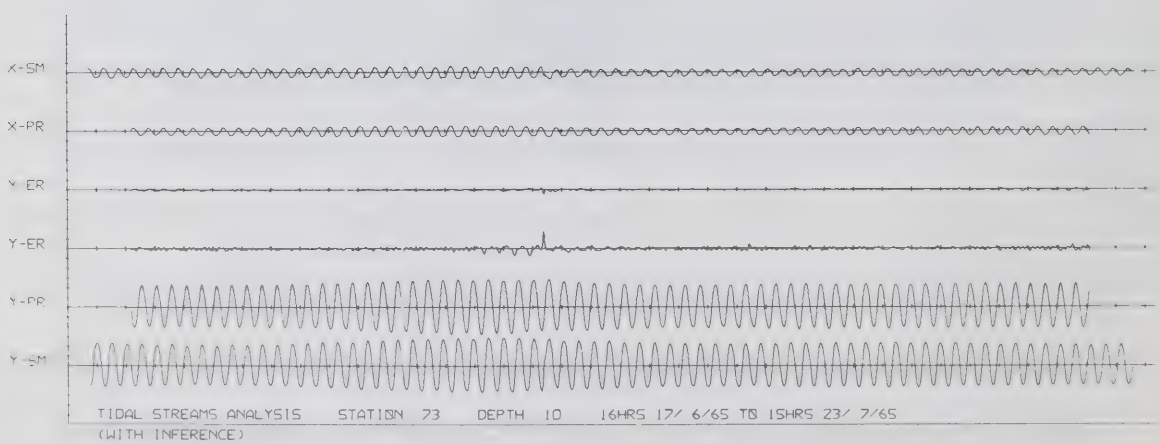

Plot 22(a)

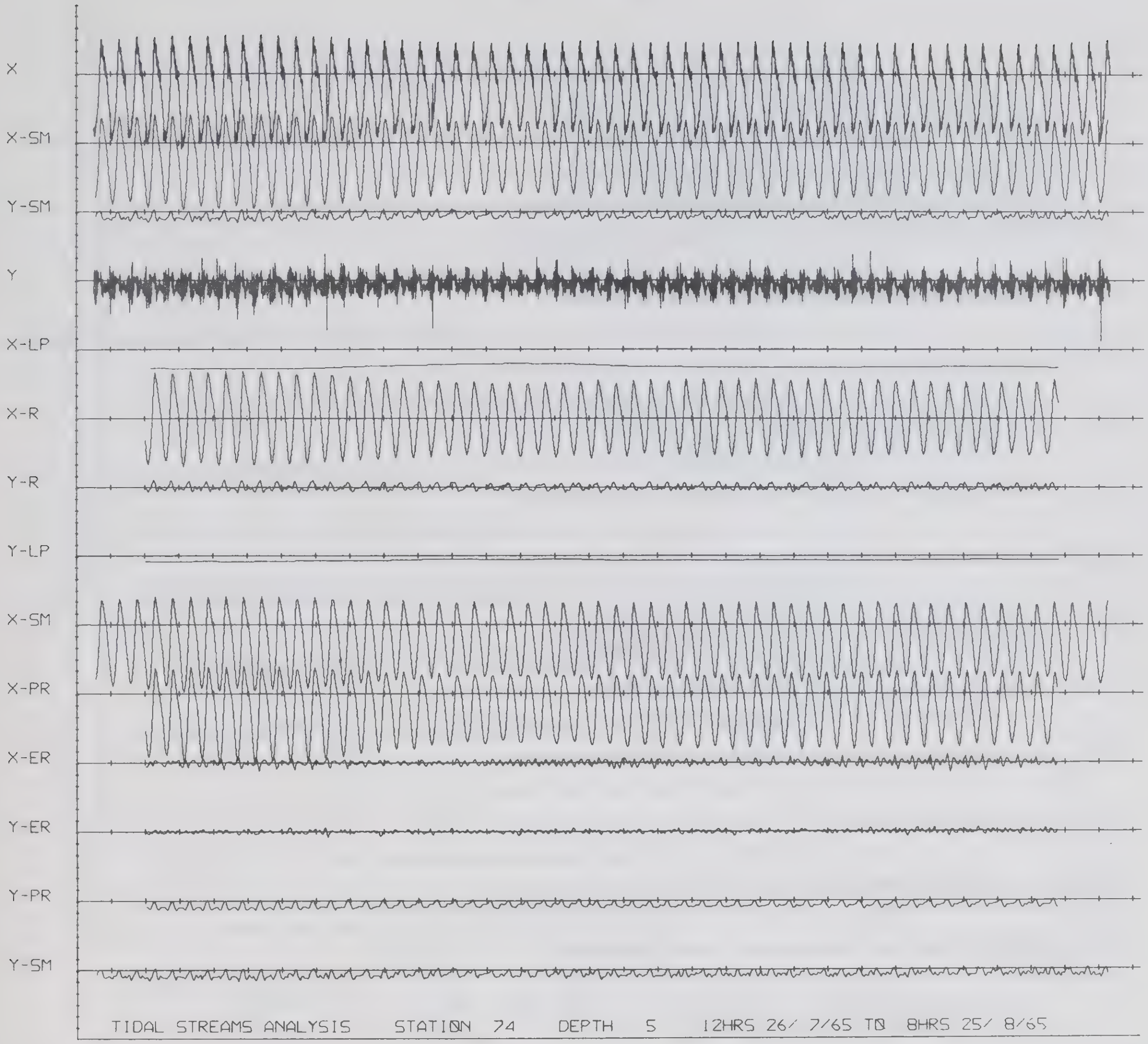

Plot 22(b)

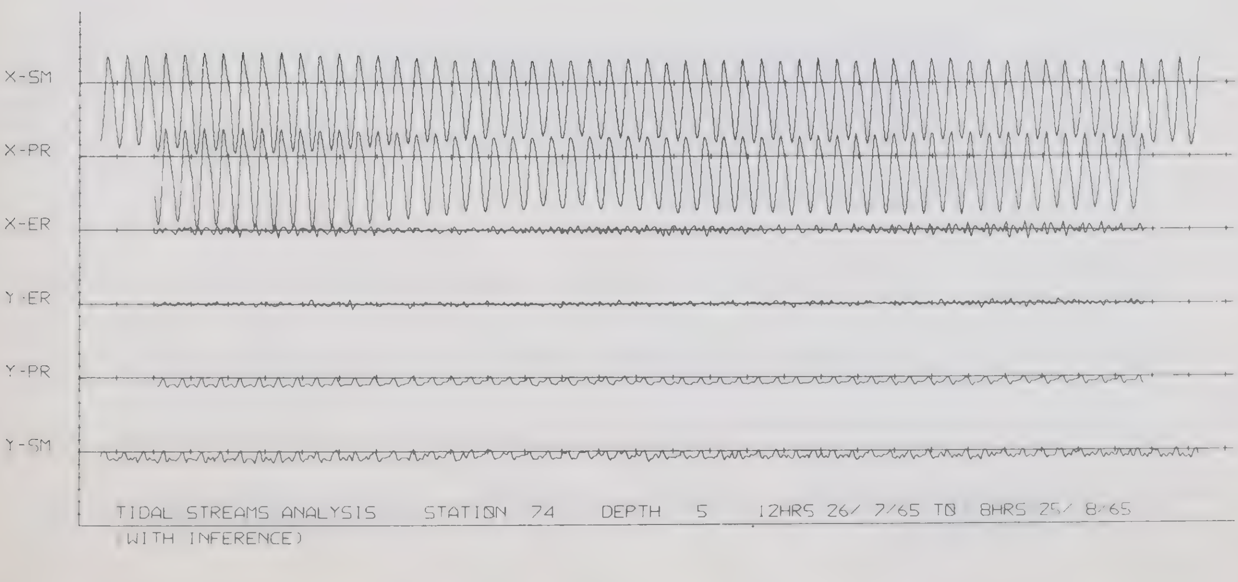

Plot 23(a)

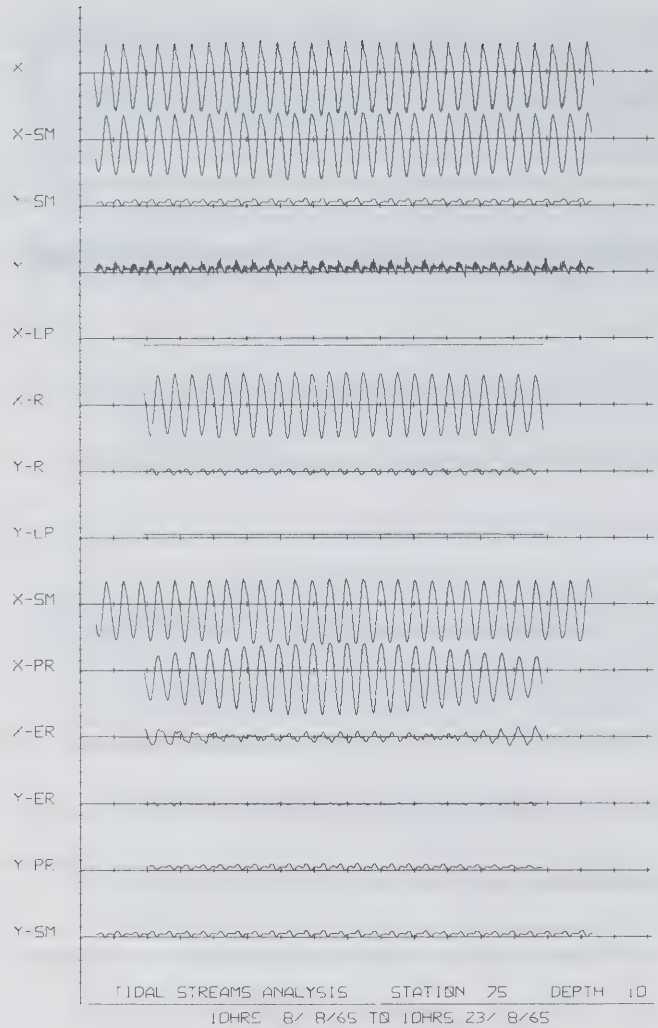

Plot 23(b)

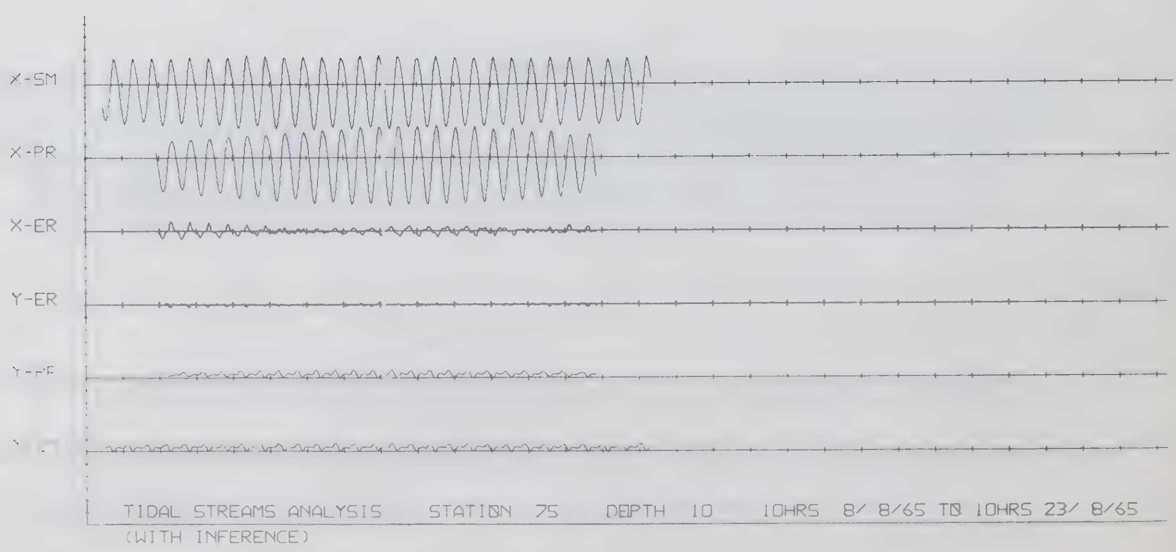

Plot 24(a)

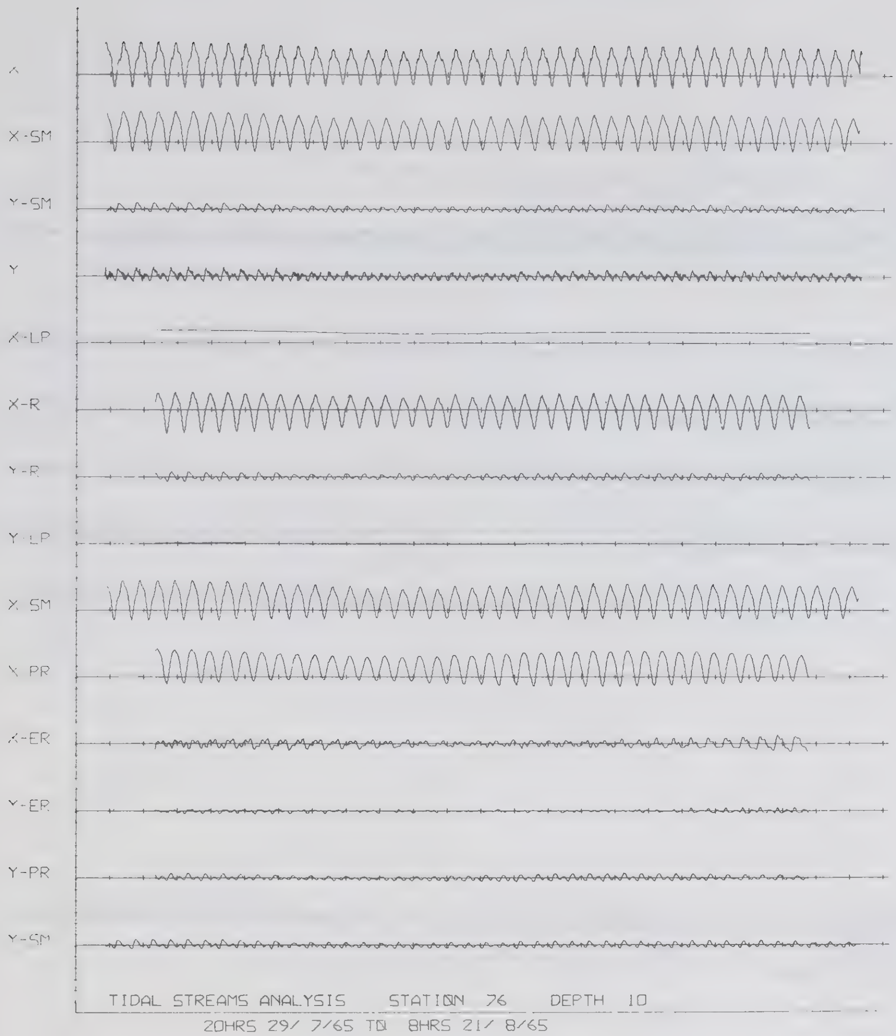

Plot 24(b)

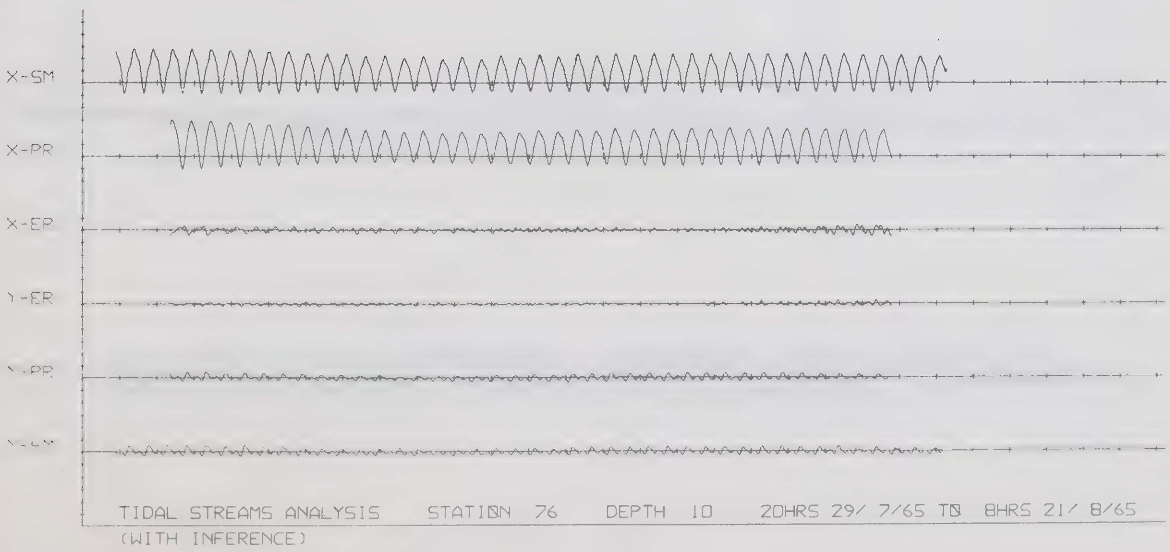

Plot 25

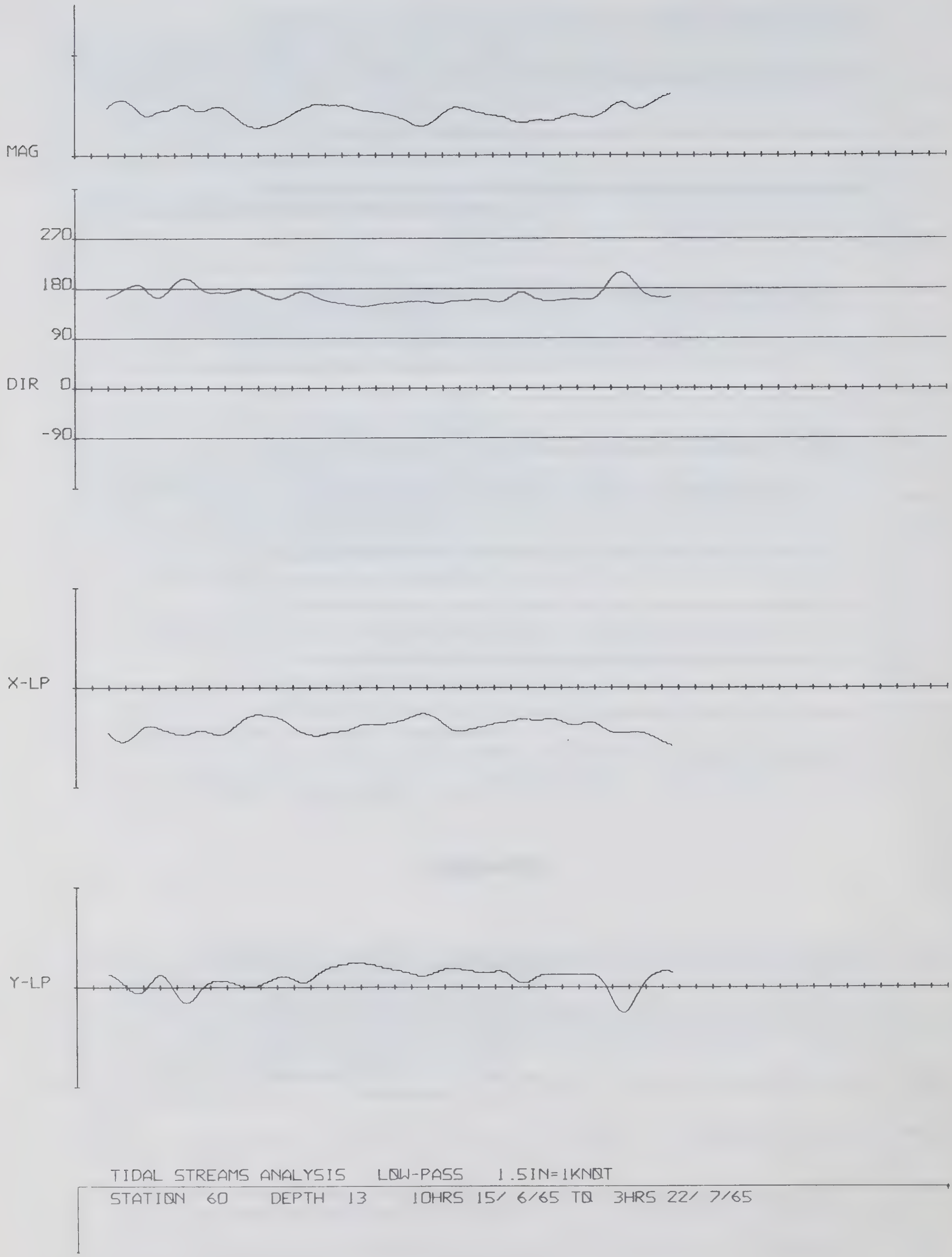
MAG
270
180
90
DIR 0
-90
X-LP
Y-LP
TIDAL STREAMS ANALYSIS LOW-PASS 1.5IN=1KNOT
STATION 60 DEPTH 13 10HRS 15/ 6/65 TO 3HRS 22/ 7/65

Plot 26

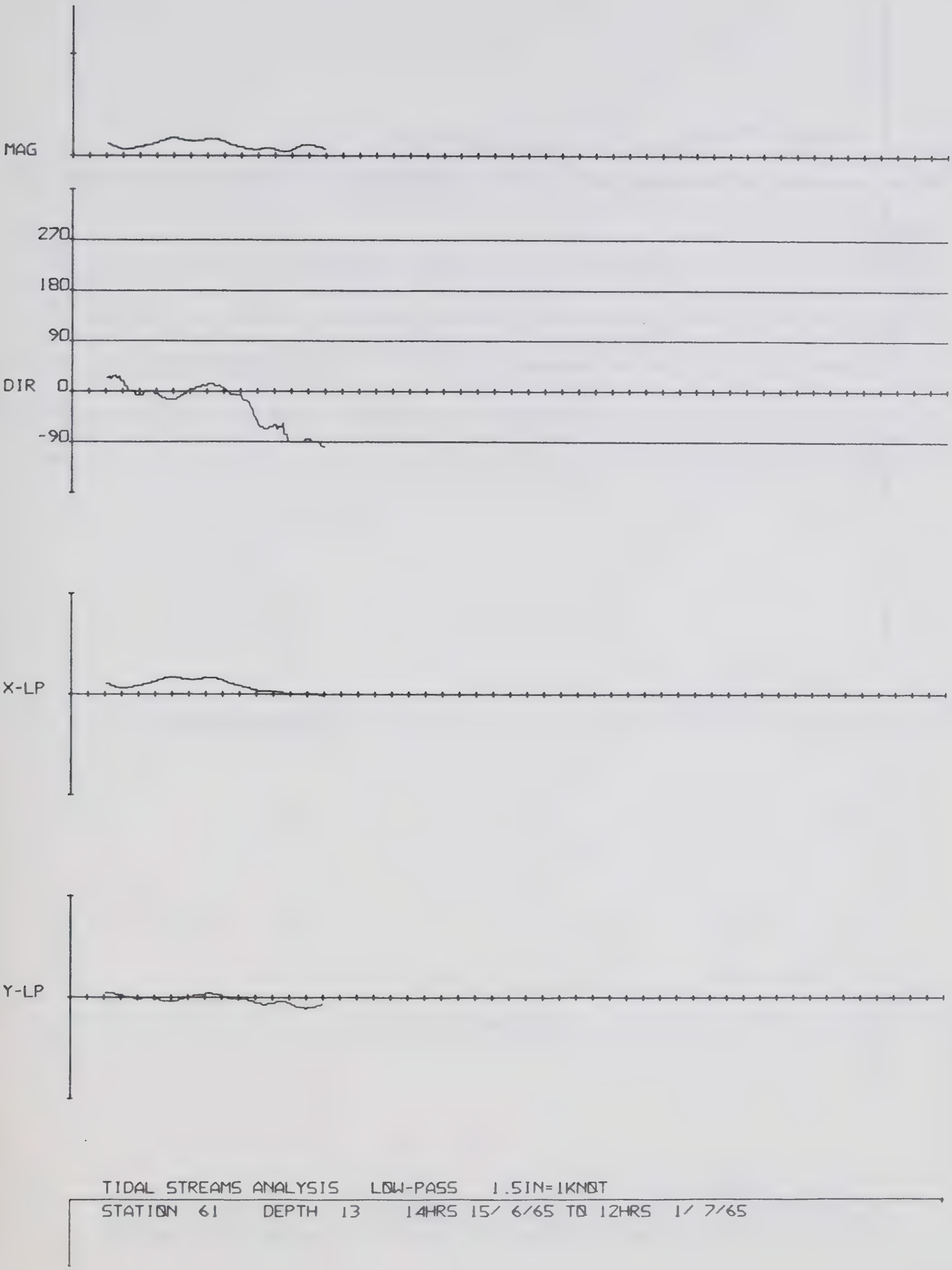
MAG
270
180
90
DIR 0
-90
X-LP
Y-LP
TIDAL STREAMS ANALYSIS LOW-PASS 1.5IN=1KNOT
STATION 61 DEPTH 13 14HRS 15/ 6/65 TO 12HRS 1/ 7/65

Plot 27

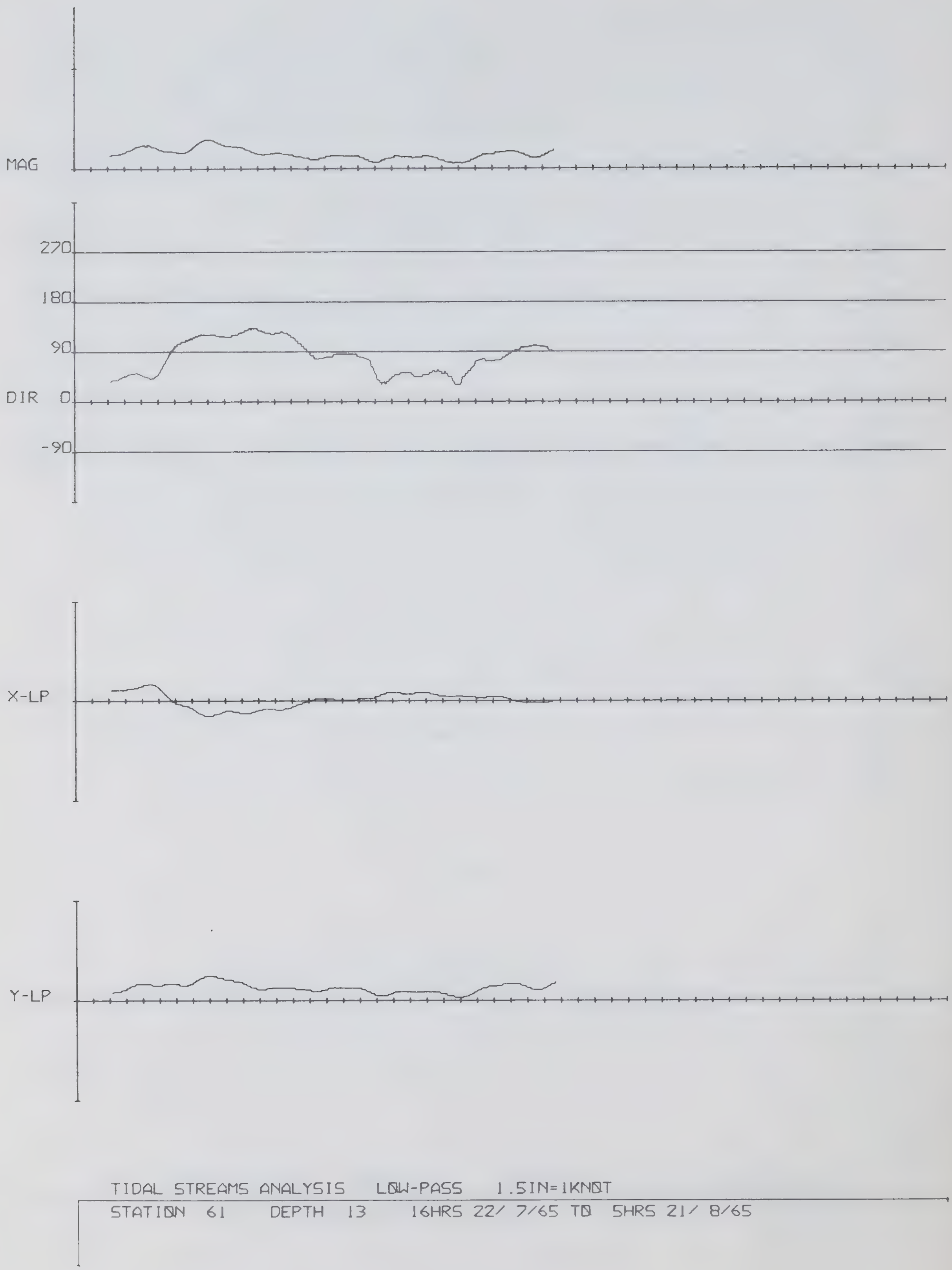
MAG
270
180
90
DIR 0
-90
X-LP
Y-LP
TIDAL STREAMS ANALYSIS LOW-PASS 1.5IN=1KNOT
STATION 61 DEPTH 13 16HRS 22/ 7/65 TO 5HRS 21/ 8/65

Plot 28

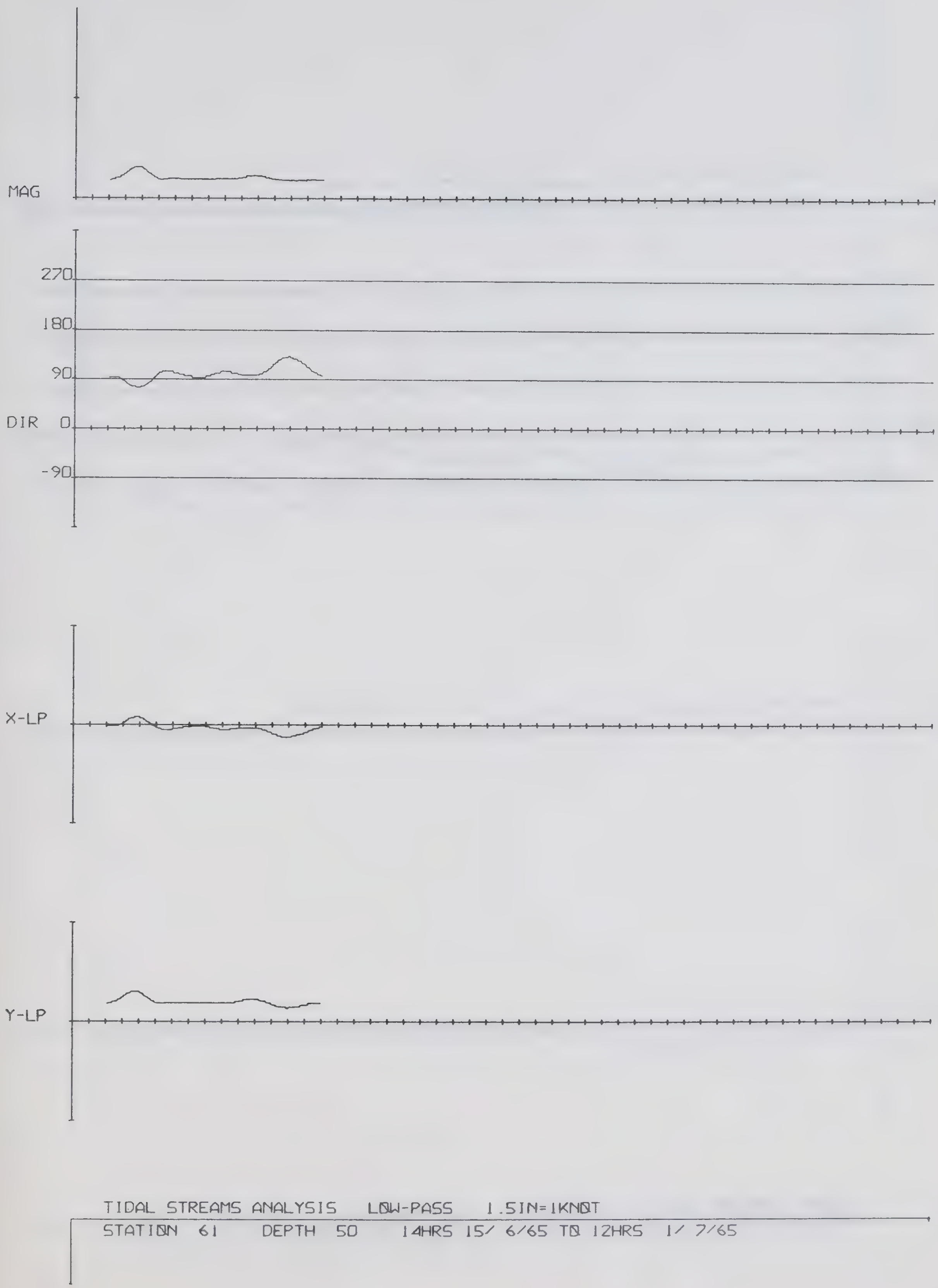
MAG
270
180
90
DIR 0
-90
X-LP
Y-LP
TIDAL STREAMS ANALYSIS LOW-PASS 1.5IN=1KNOT
STATION 61 DEPTH 50 14HRS 15/ 6/65 TO 12HRS 1/ 7/65

Plot 29

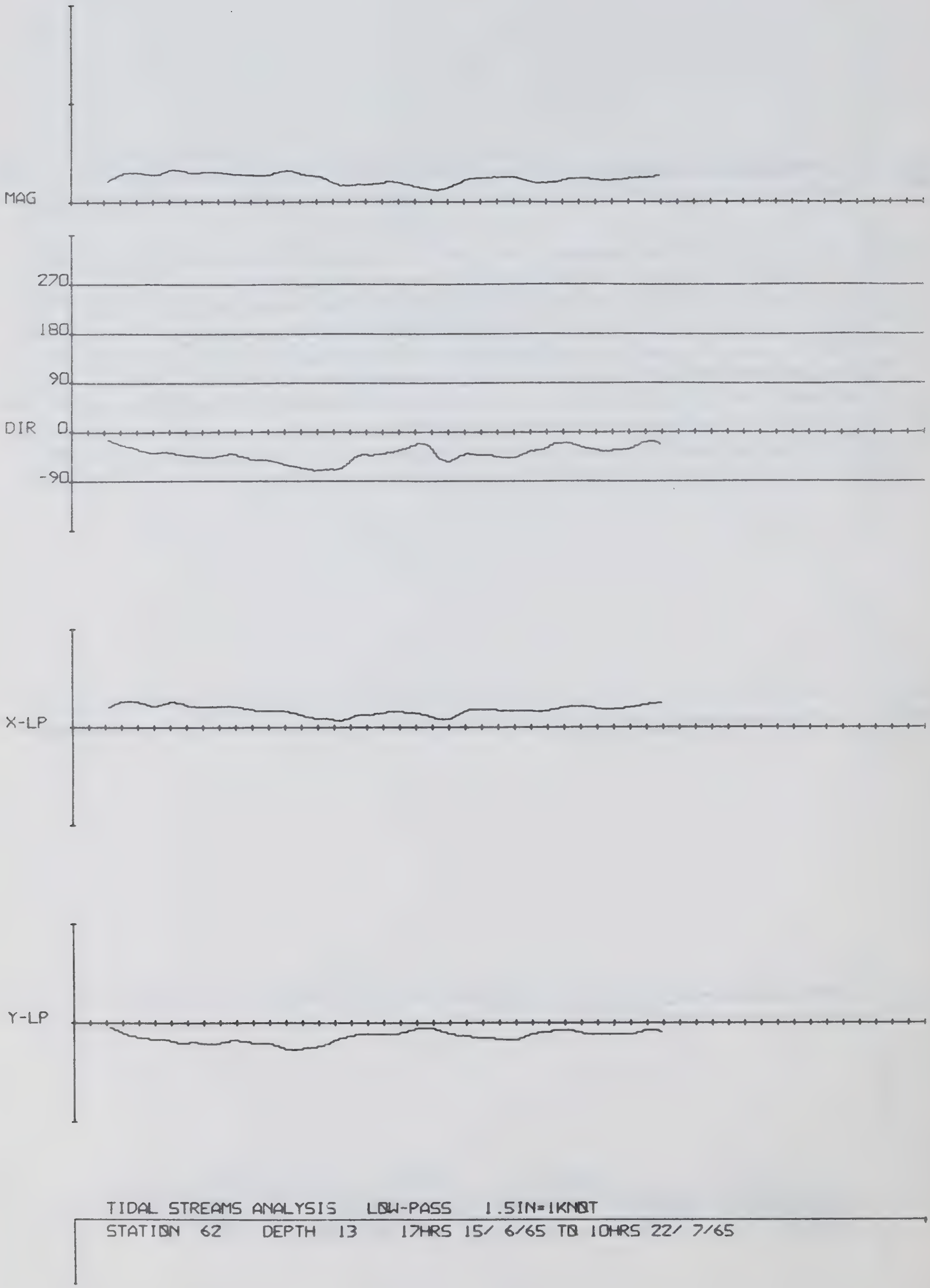
MAG
270
180
90
DIR 0
-90
X-LP
Y-LP
TIDAL STREAMS ANALYSIS LOW-PASS 1.5IN=1KNOT
STATION 62 DEPTH 13 17HRS 15/ 6/65 TO 10HRS 22/ 7/65

Plot 30

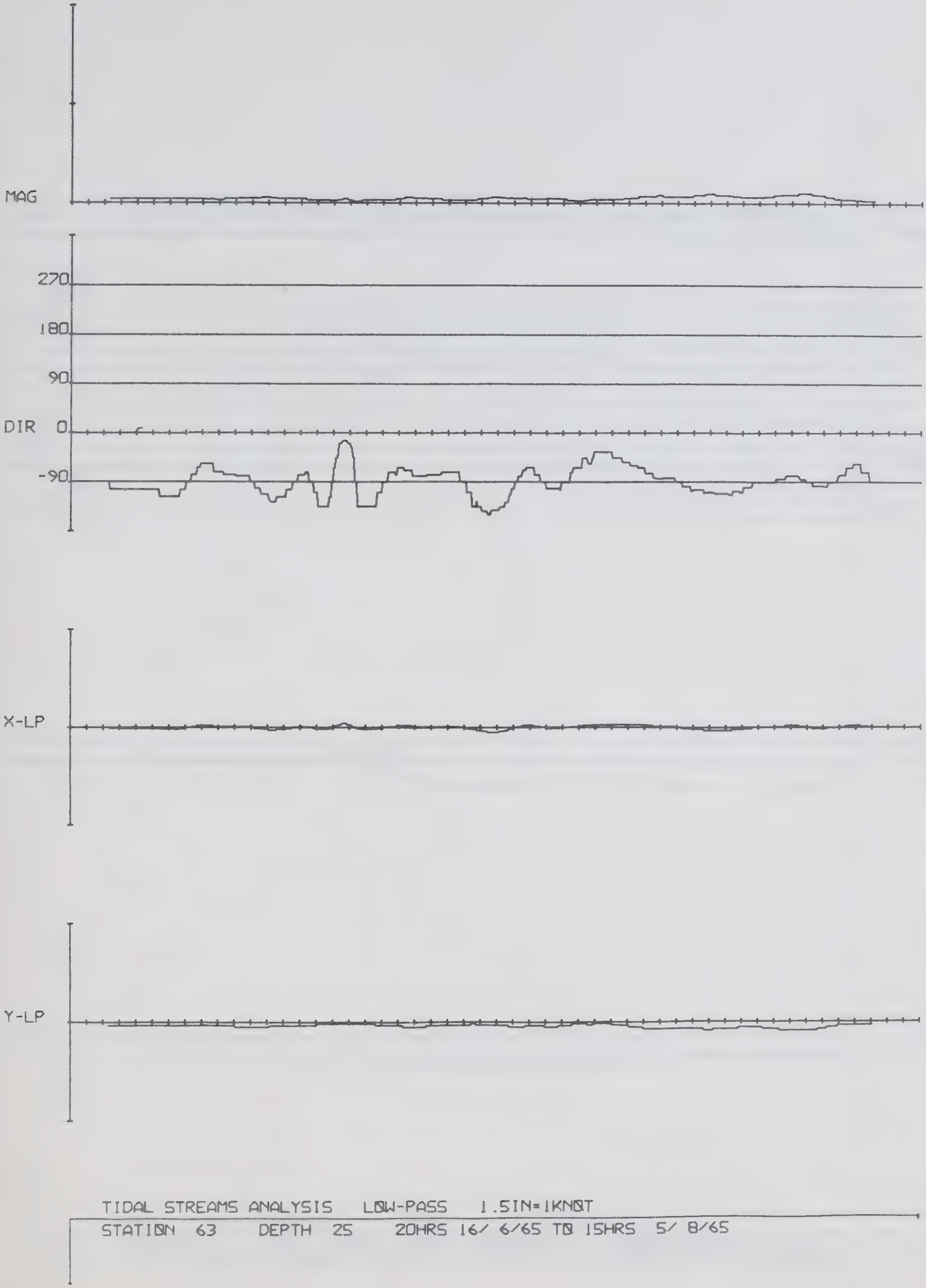
MAG
270
180
90
DIR 0
-90
X-LP
Y-LP
TIDAL STREAMS ANALYSIS LOW-PASS 1.5IN=1KNOT
STATION 63 DEPTH 25 20HRS 16/ 6/65 TO 15HRS 5/ 8/65

Plot 31

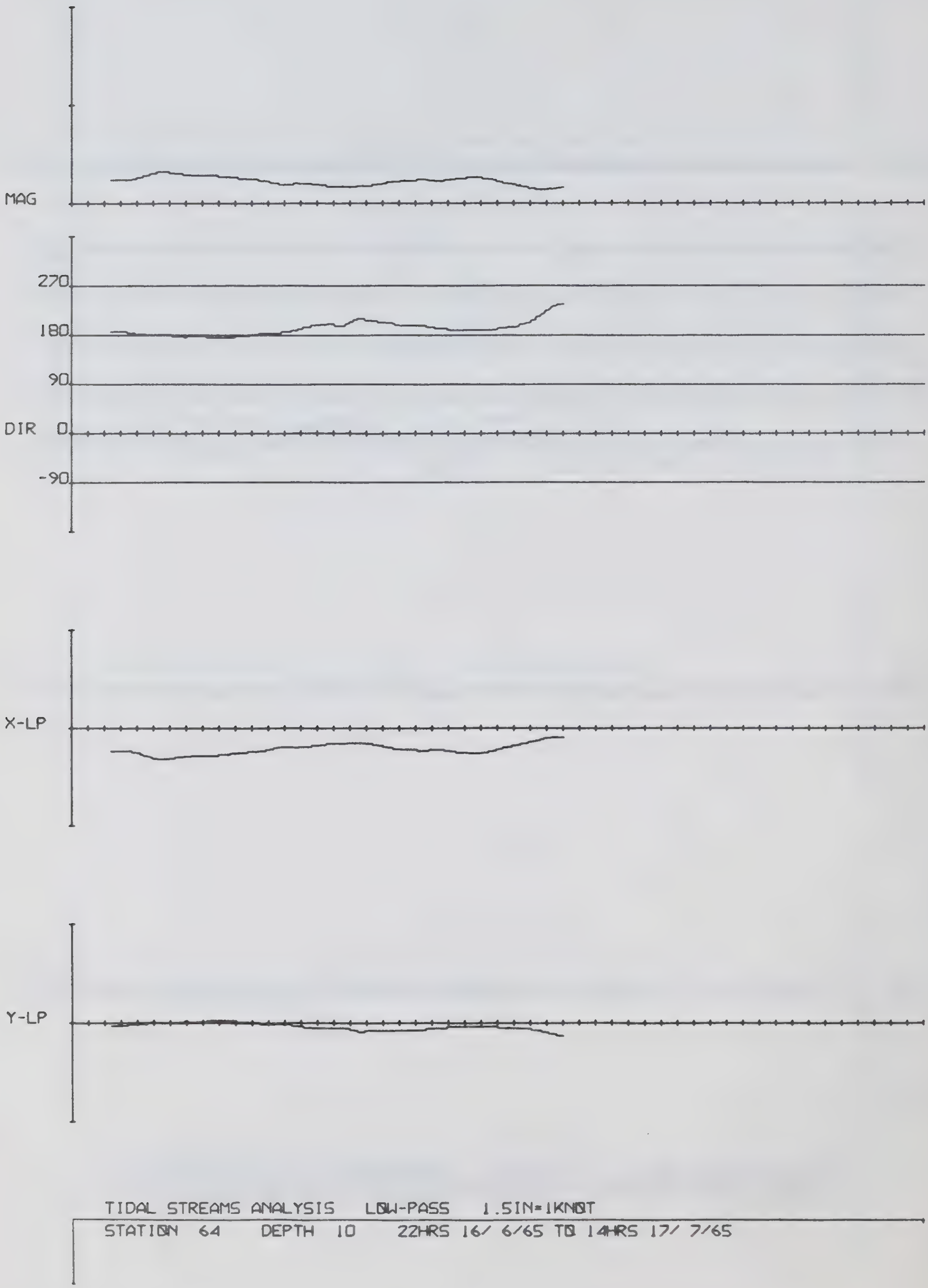
MAG
270
180
90
DIR 0
-90
X-LP
Y-LP
TIDAL STREAMS ANALYSIS LOW-PASS 1.5IN=1KNOT
STATION 64 DEPTH 10 22HRS 16/ 6/65 TO 14HRS 17/ 7/65

Plot 32

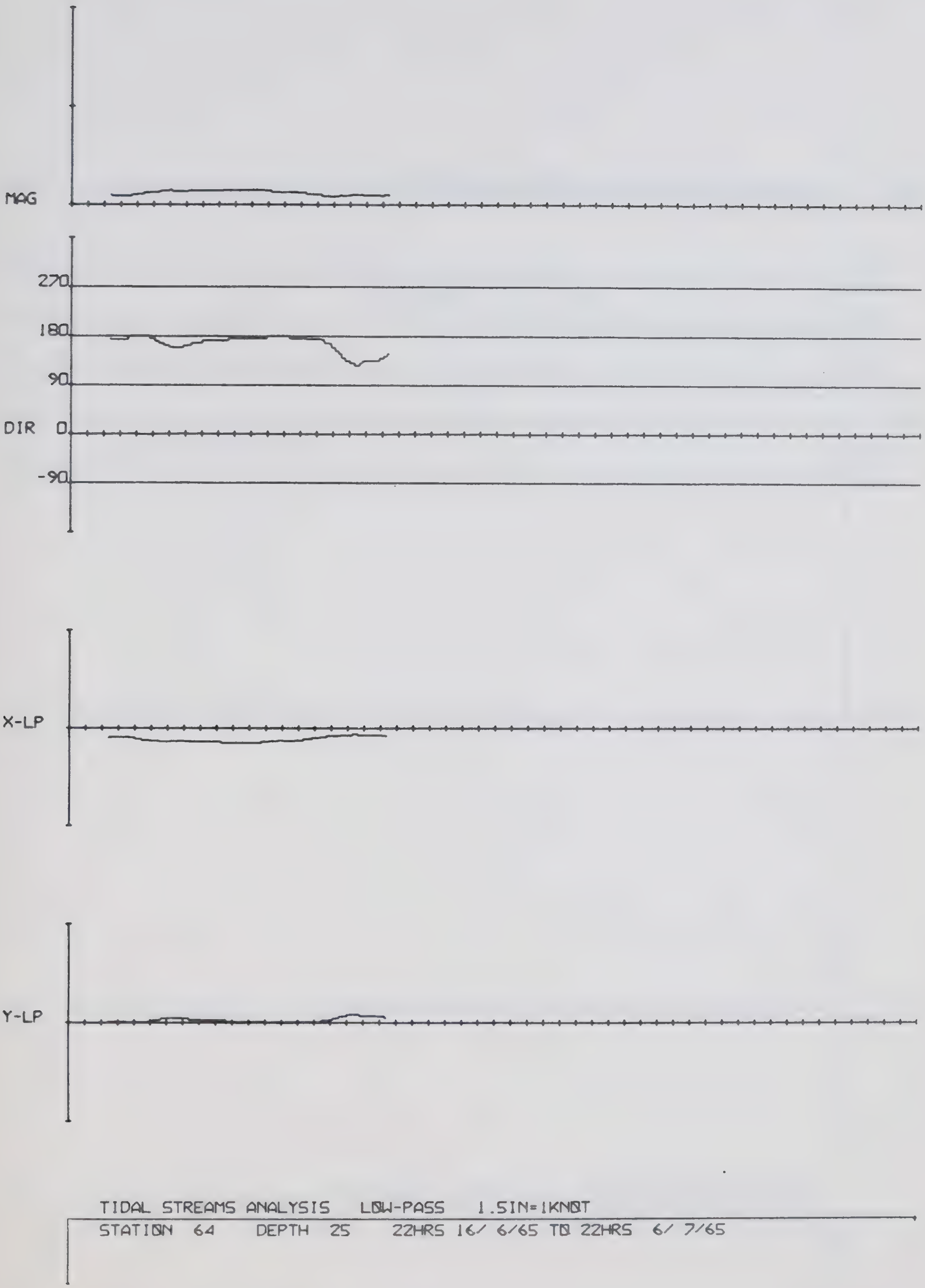
MAG
270
180
90
DIR 0
-90
X-LP
Y-LP
TIDAL STREAMS ANALYSIS LOW-PASS 1.5IN=1KNOT
STATION 64 DEPTH 25 22HRS 16/ 6/65 TO 22HRS 6/ 7/65

Plot 33

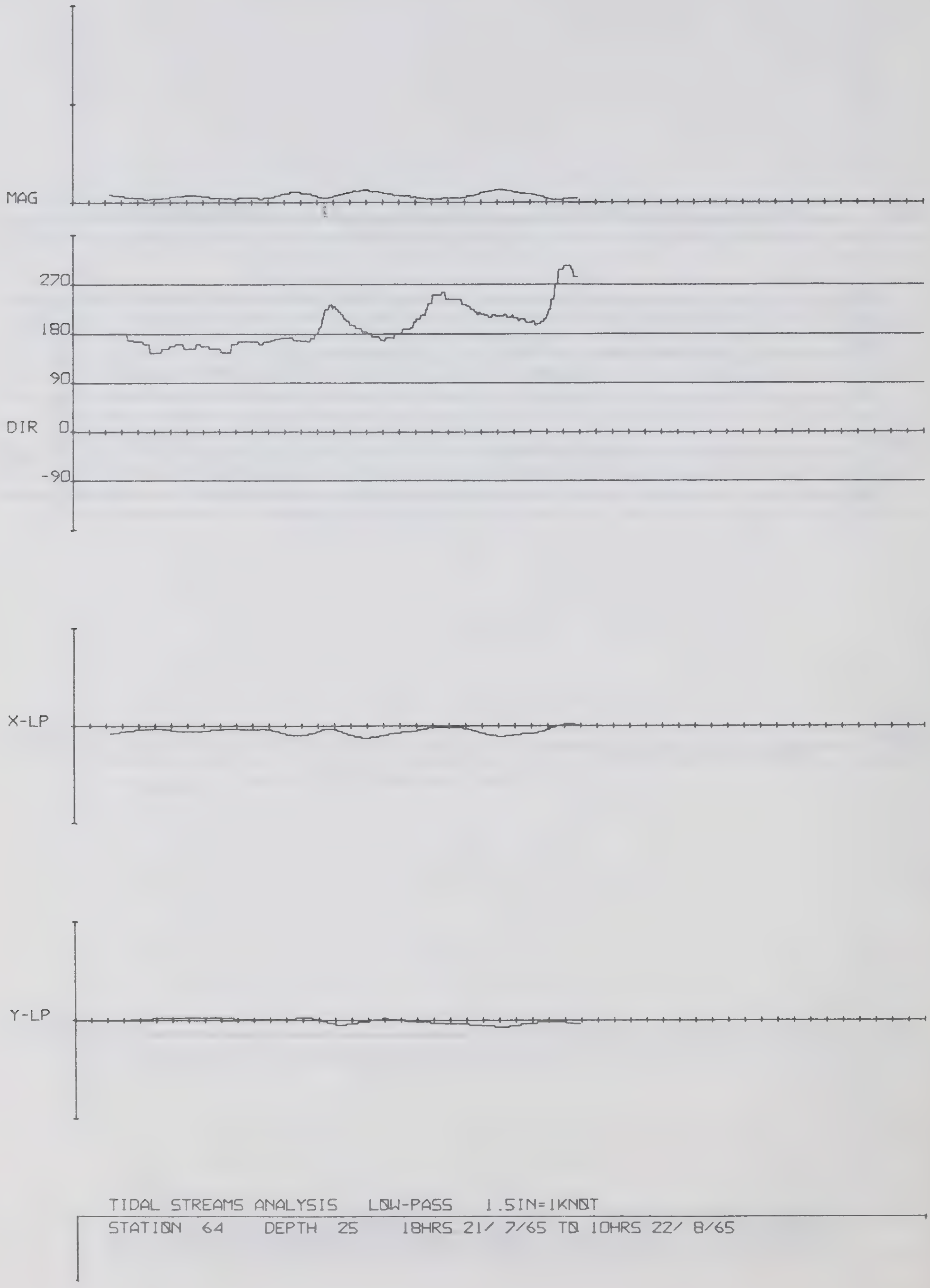
MAG
270
180
90
DIR 0
-90
X-LP
Y-LP
TIDAL STREAMS ANALYSIS LOW-PASS 1.5IN=1KNOT
STATION 64 DEPTH 25 18HRS 21/ 7/65 TO 10HRS 22/ 8/65

Plot 34

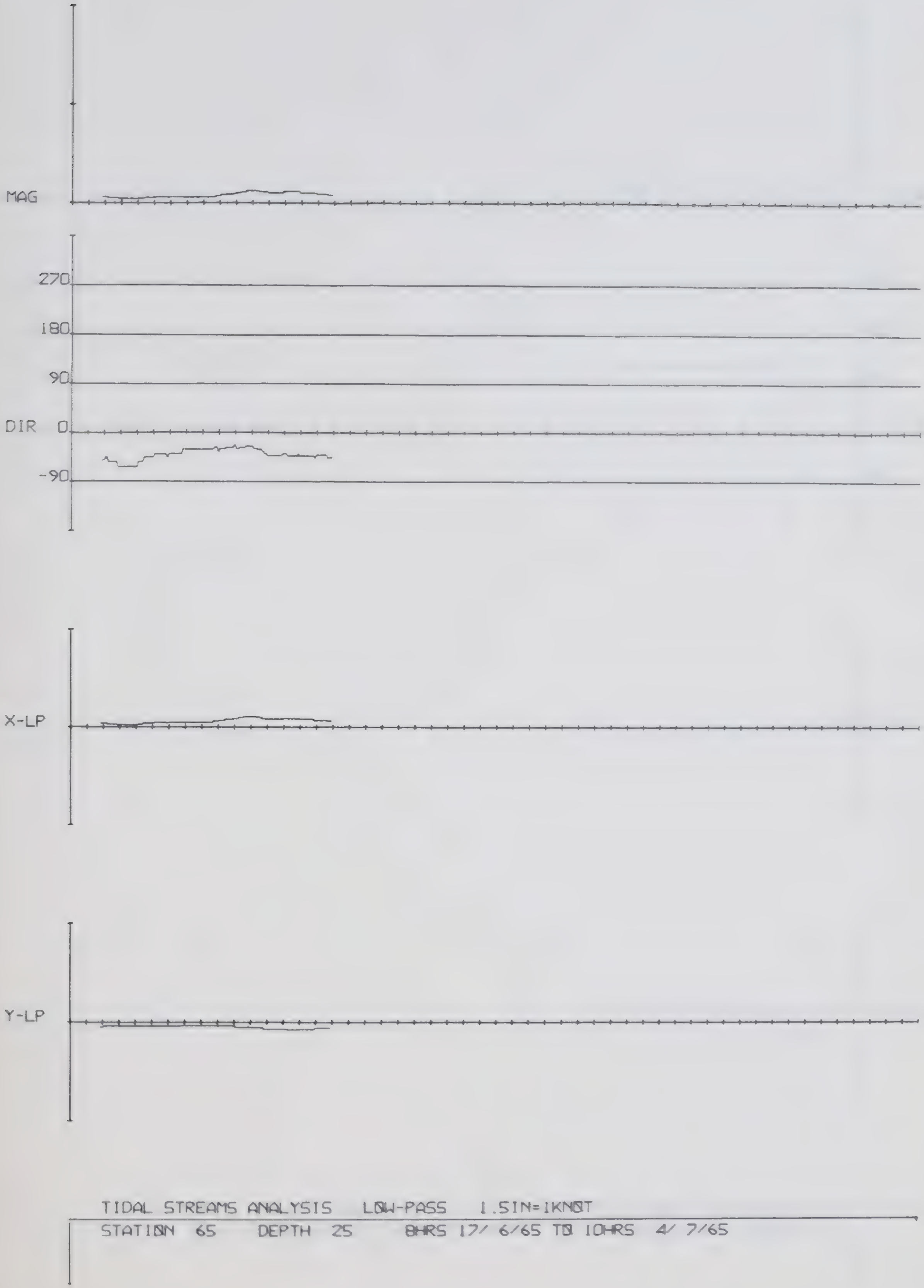

MAG
270
180
90
DIR 0
-90
X-LP
Y-LP
TIDAL STREAMS ANALYSIS LOW-PASS 1.5IN=1KNOT
STATION 65 DEPTH 25 8HRS 17/ 6/65 TO 10HRS 4/ 7/65

Plot 35

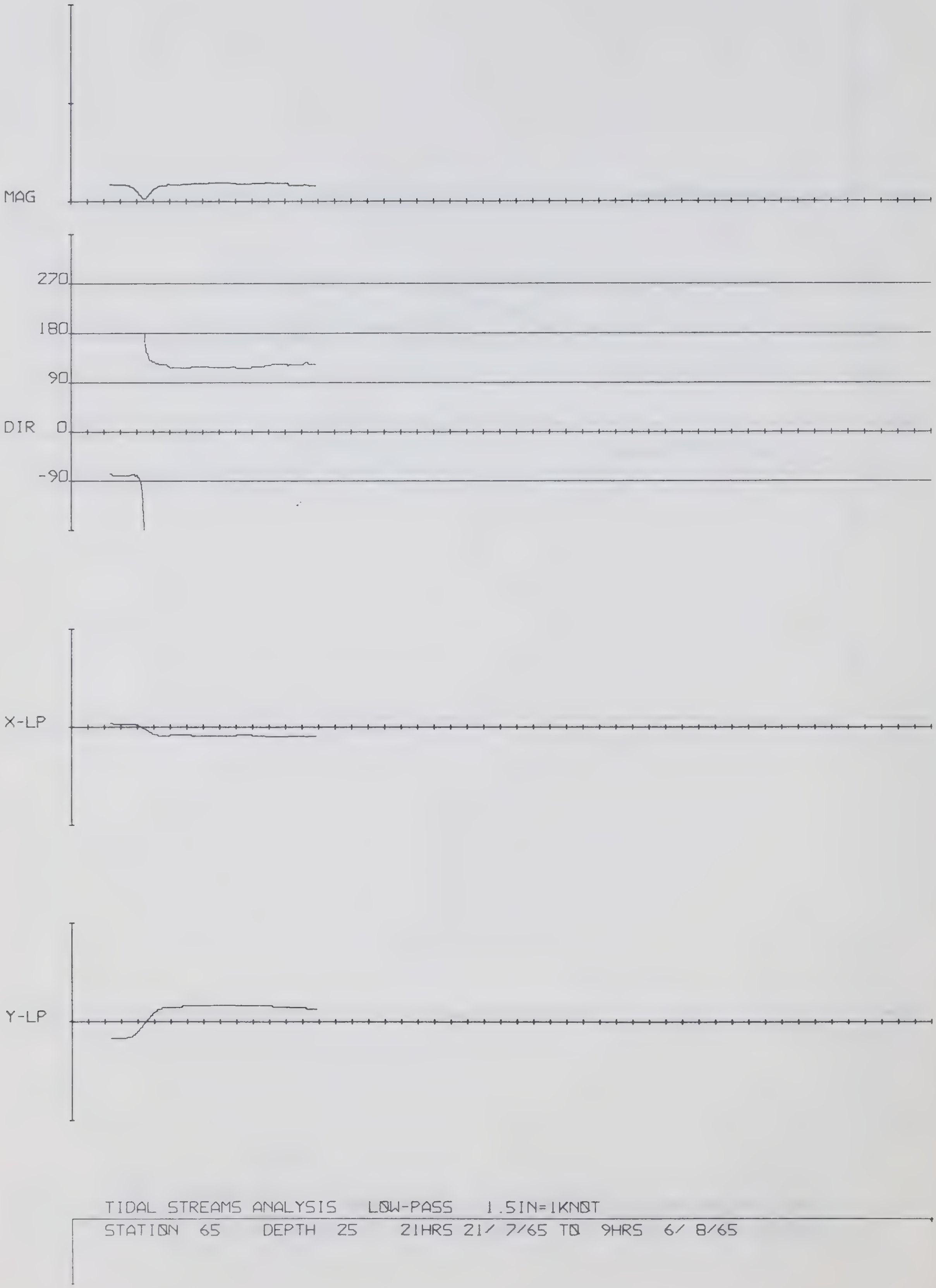
MAG
270
180
90
DIR 0
-90
X-LP
Y-LP
TIDAL STREAMS ANALYSIS LOW-PASS 1.5IN=1KNOT
STATION 65 DEPTH 25 21HRS 21/ 7/65 TO 9HRS 6/ 8/65

Plot 36

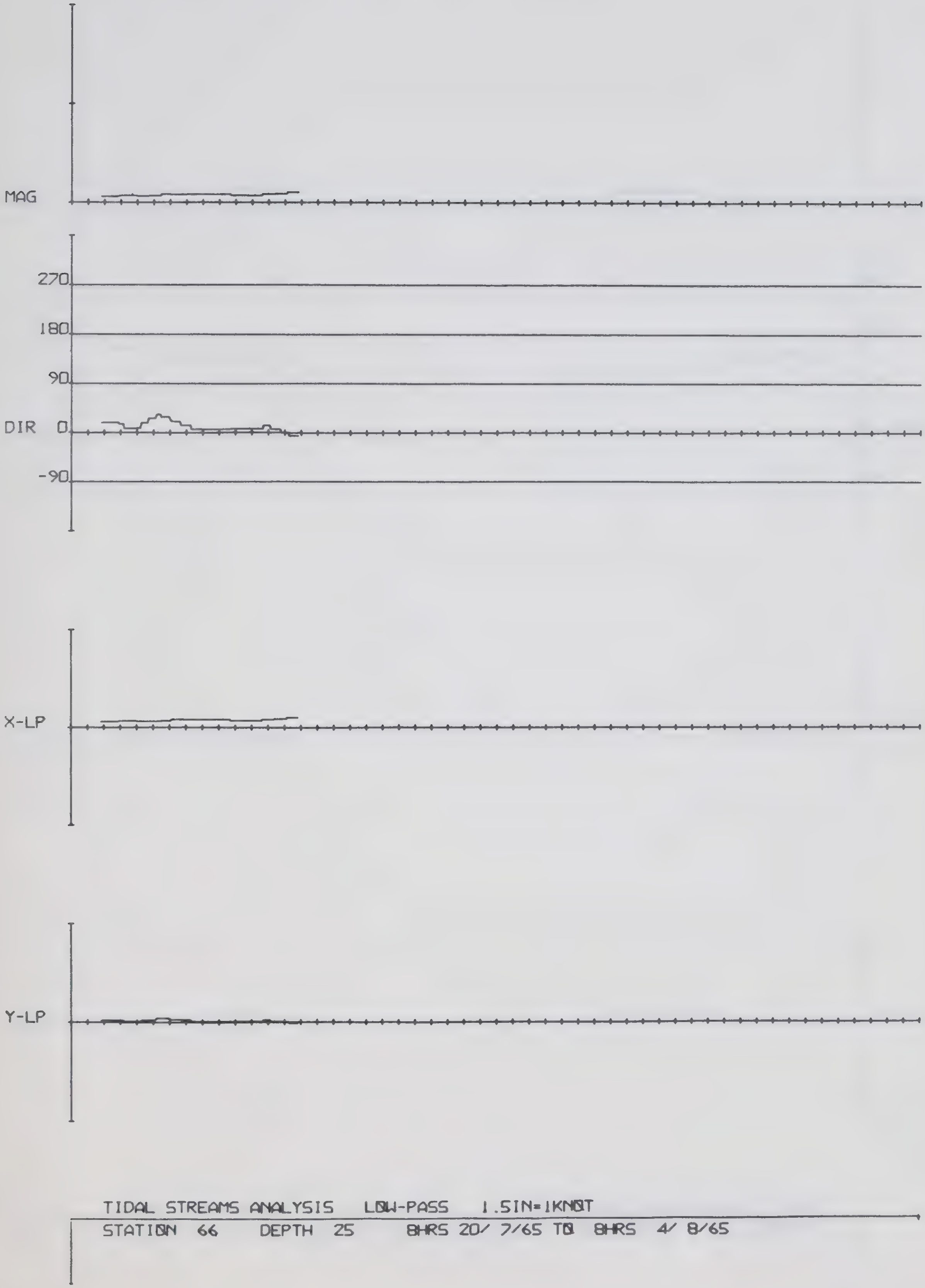
MAG
270
180
90
DIR 0
-90
X-LP
Y-LP
TIDAL STREAMS ANALYSIS LOW-PASS 1.5IN=1KNOT
STATION 66 DEPTH 25 8HRS 20/ 7/65 TO 8HRS 4/ 8/65

Plot 37

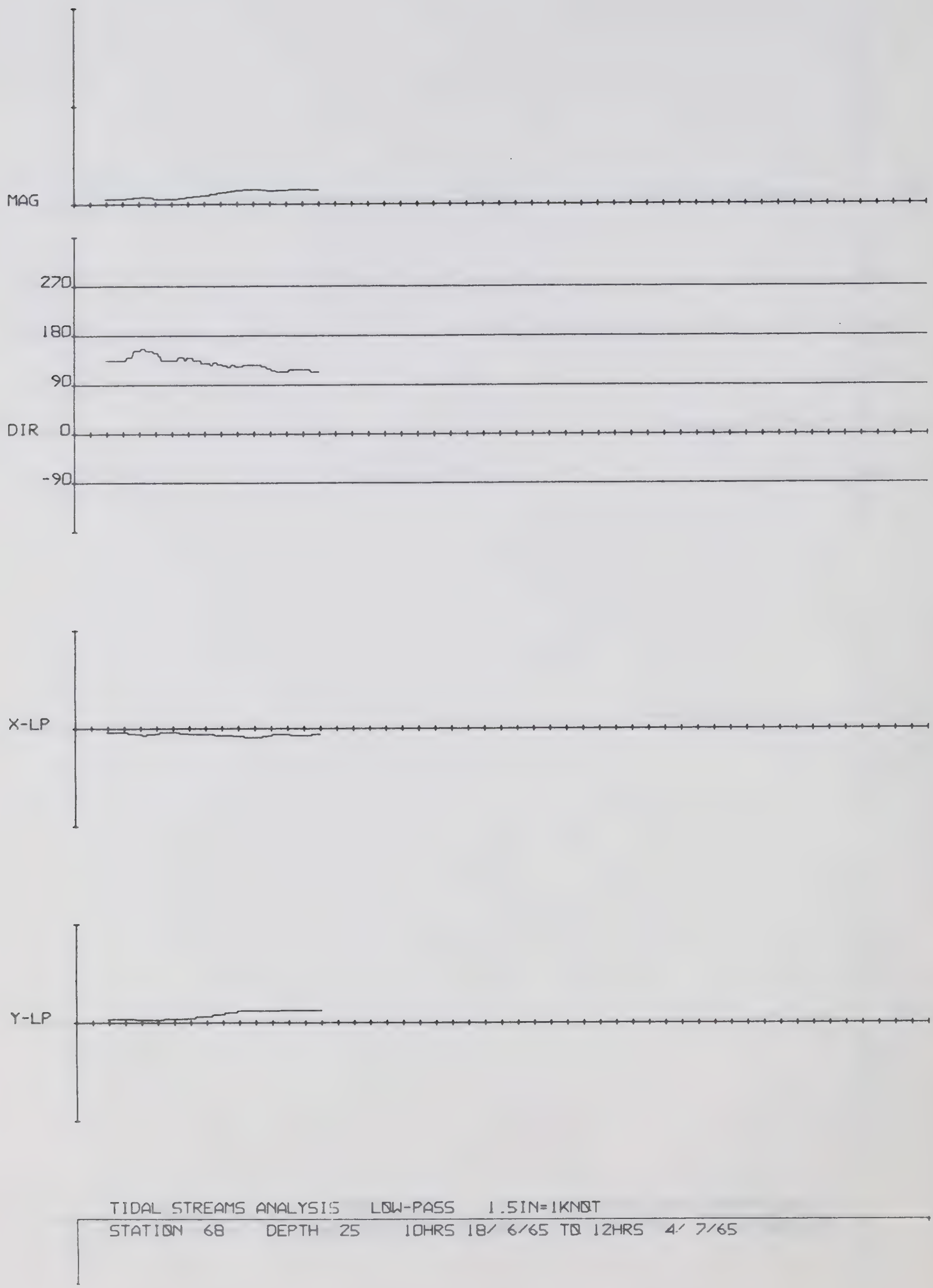
MAG
270
180
90
DIR 0
-90
X-LP
Y-LP
TIDAL STREAMS ANALYSIS LOW-PASS 1.5IN=1KNOT
STATION 68 DEPTH 25 10HRS 18/ 6/65 TO 12HRS 4/ 7/65

Plot 38

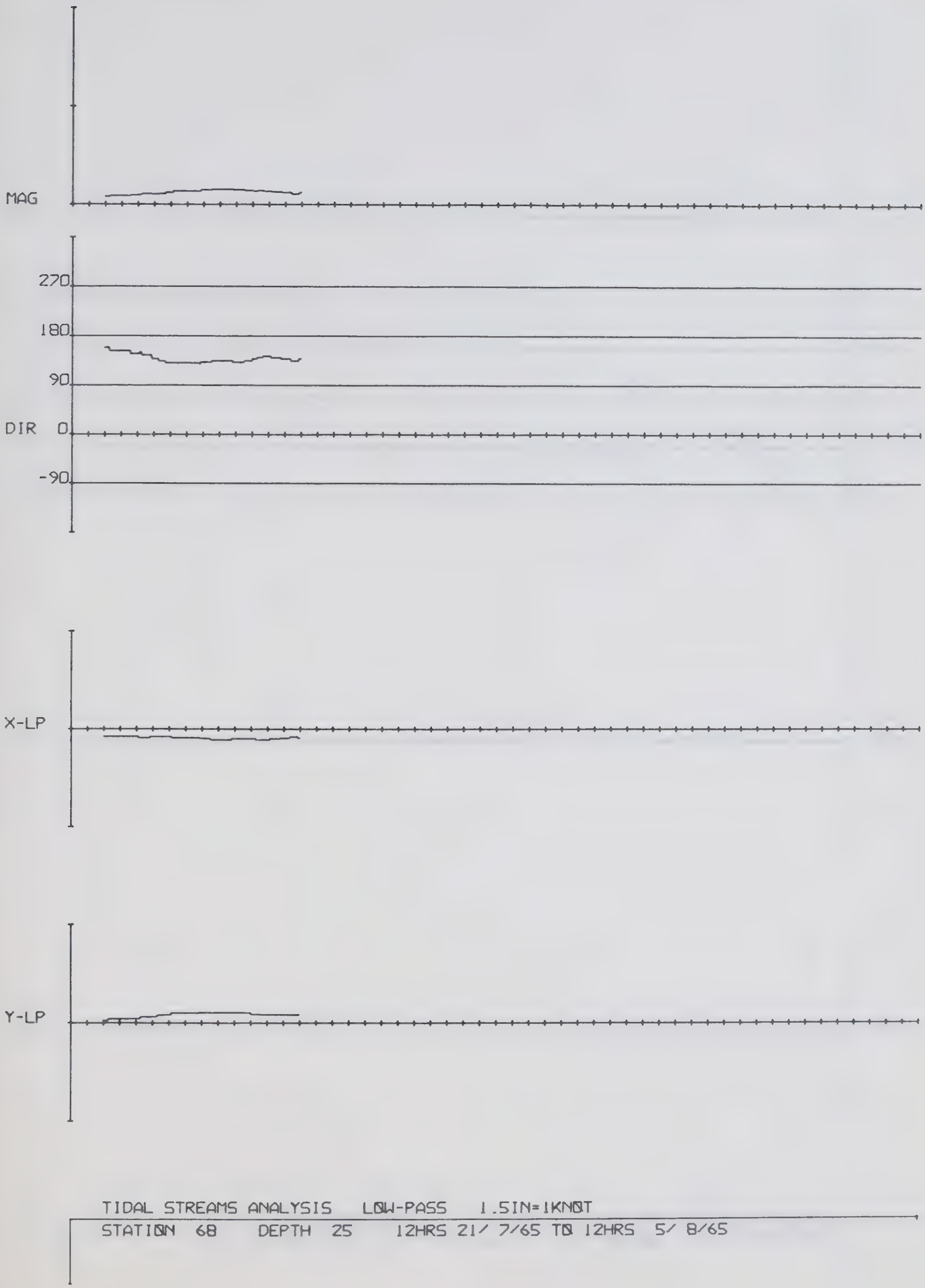
MAG
270
180
90
DIR 0
-90
X-LP
Y-LP
TIDAL STREAMS ANALYSIS LOW-PASS 1.5IN=1KNOT
STATION 68 DEPTH 25 12HRS 21/ 7/65 TO 12HRS 5/ 8/65

Plot 39

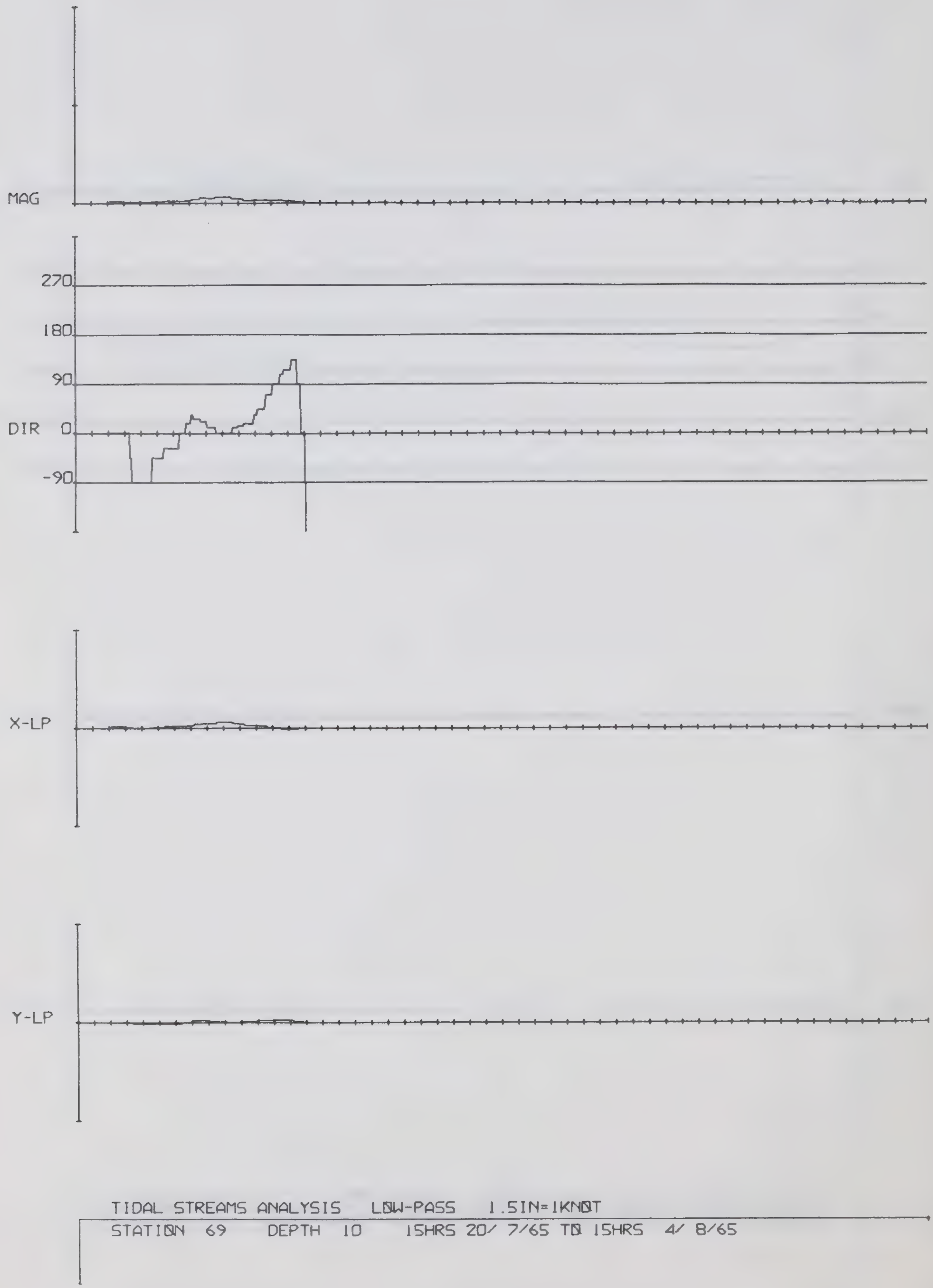
MAG
270
180
90
DIR 0
-90
X-LP
Y-LP
TIDAL STREAMS ANALYSIS LOW-PASS 1.5IN=1KNOT
STATION 69 DEPTH 10 15HRS 20/ 7/65 TO 15HRS 4/ 8/65

Plot 40

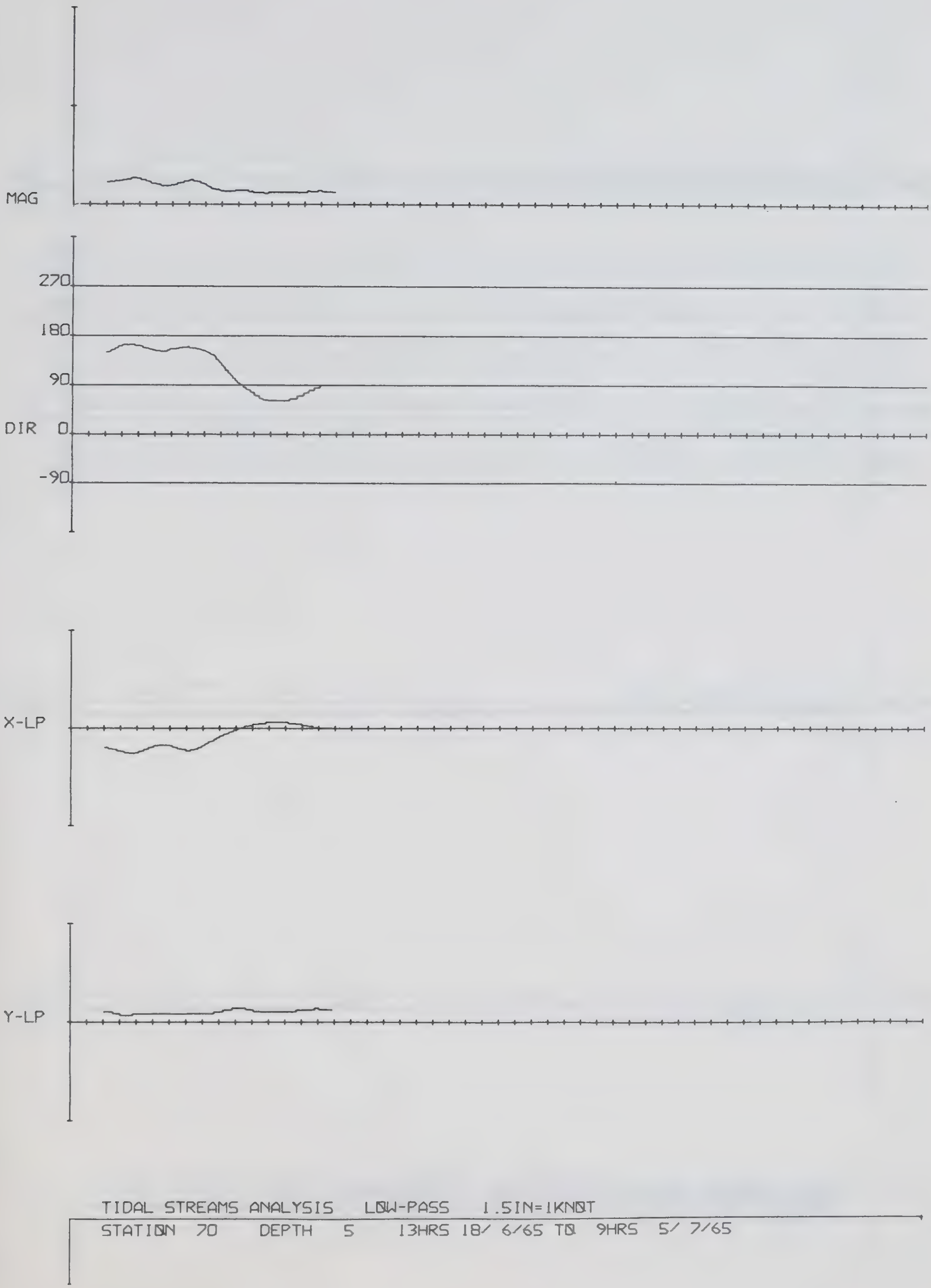
MAG
270
180
90
DIR 0
-90
X-LP
Y-LP
TIDAL STREAMS ANALYSIS LOW-PASS 1.5IN=1KNOT
STATION 70 DEPTH 5 13HRS 18/ 6/65 TO 9HRS 5/ 7/65

Plot 41

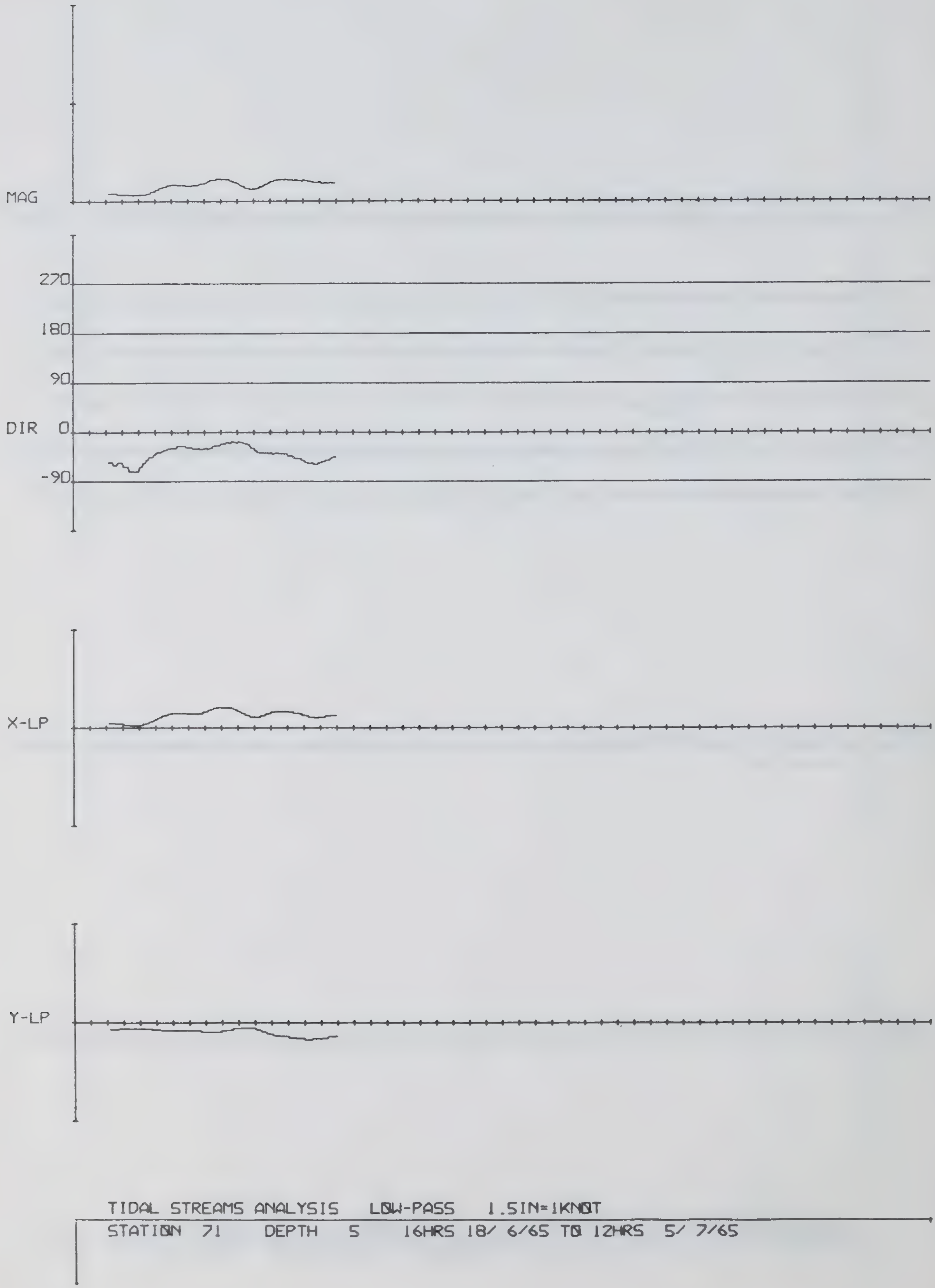
MAG
270
180
90
DIR 0
-90
X-LP
Y-LP
TIDAL STREAMS ANALYSIS LOW-PASS 1.5IN=1KNOT
STATION 71 DEPTH 5 16HRS 18/ 6/65 TO 12HRS 5/ 7/65

Plot 42

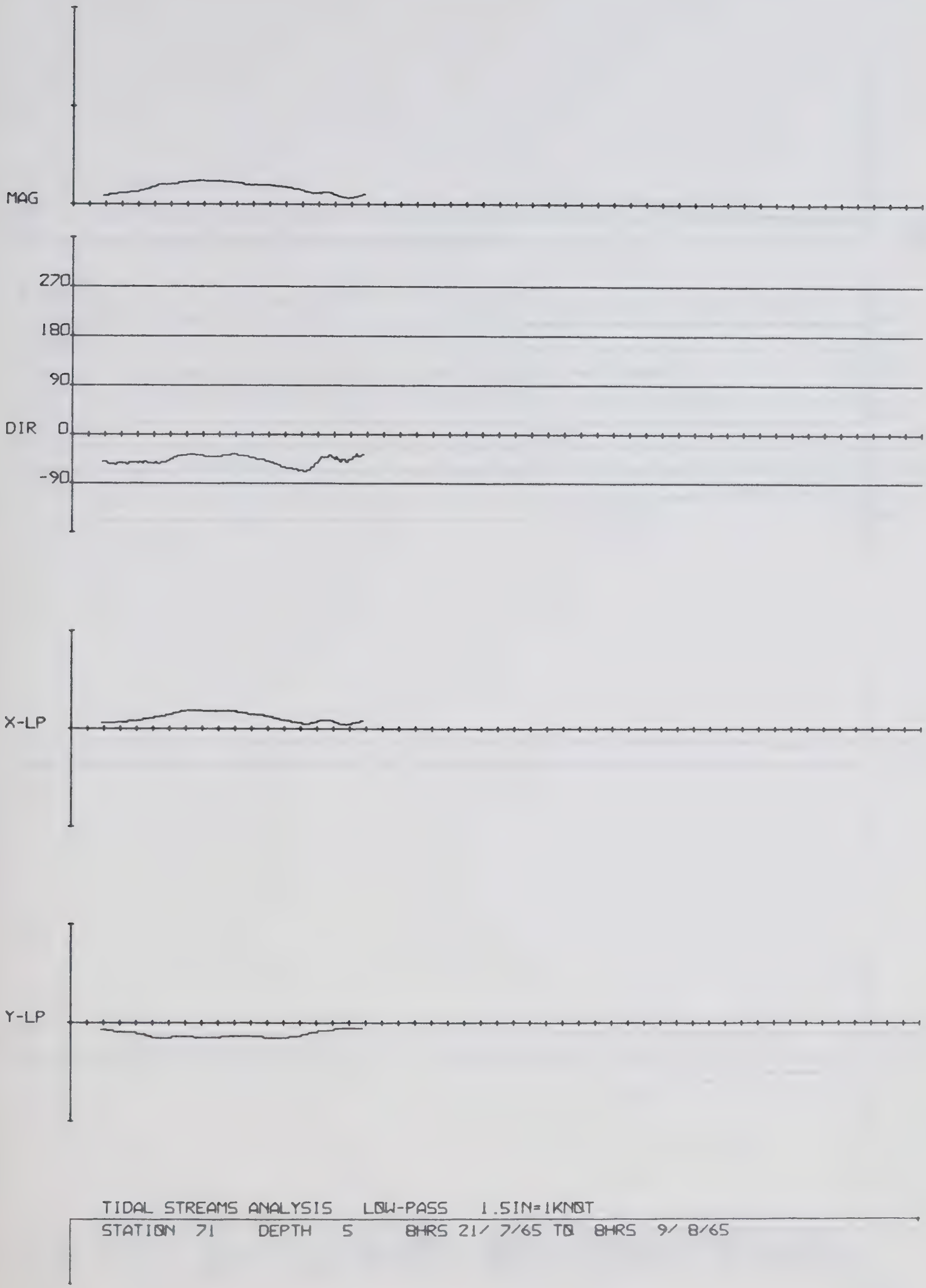
MAG
270
180
90
DIR 0
-90
X-LP
Y-LP
TIDAL STREAMS ANALYSIS LOW-PASS 1.5IN=1KNOT
STATION 71 DEPTH 5 8HRS 21/ 7/65 TO 8HRS 9/ 8/65

Plot 43

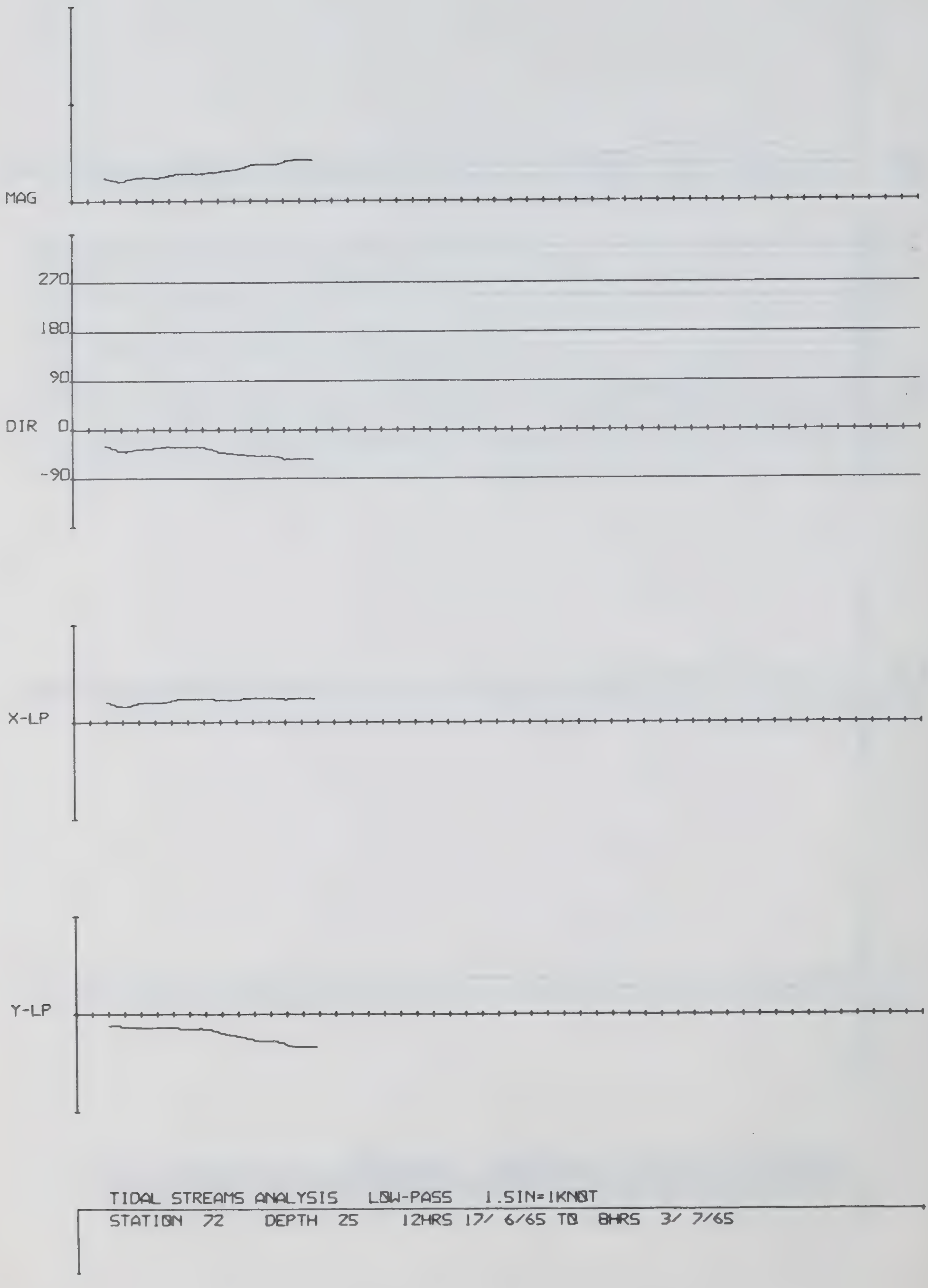
MAG
270
180
90
DIR 0
-90
X-LP
Y-LP
TIDAL STREAMS ANALYSIS LOW-PASS 1.5IN=1KNOT
STATION 72 DEPTH 25 12HRS 17/ 6/65 TO 8HRS 3/ 7/65

Plot 44

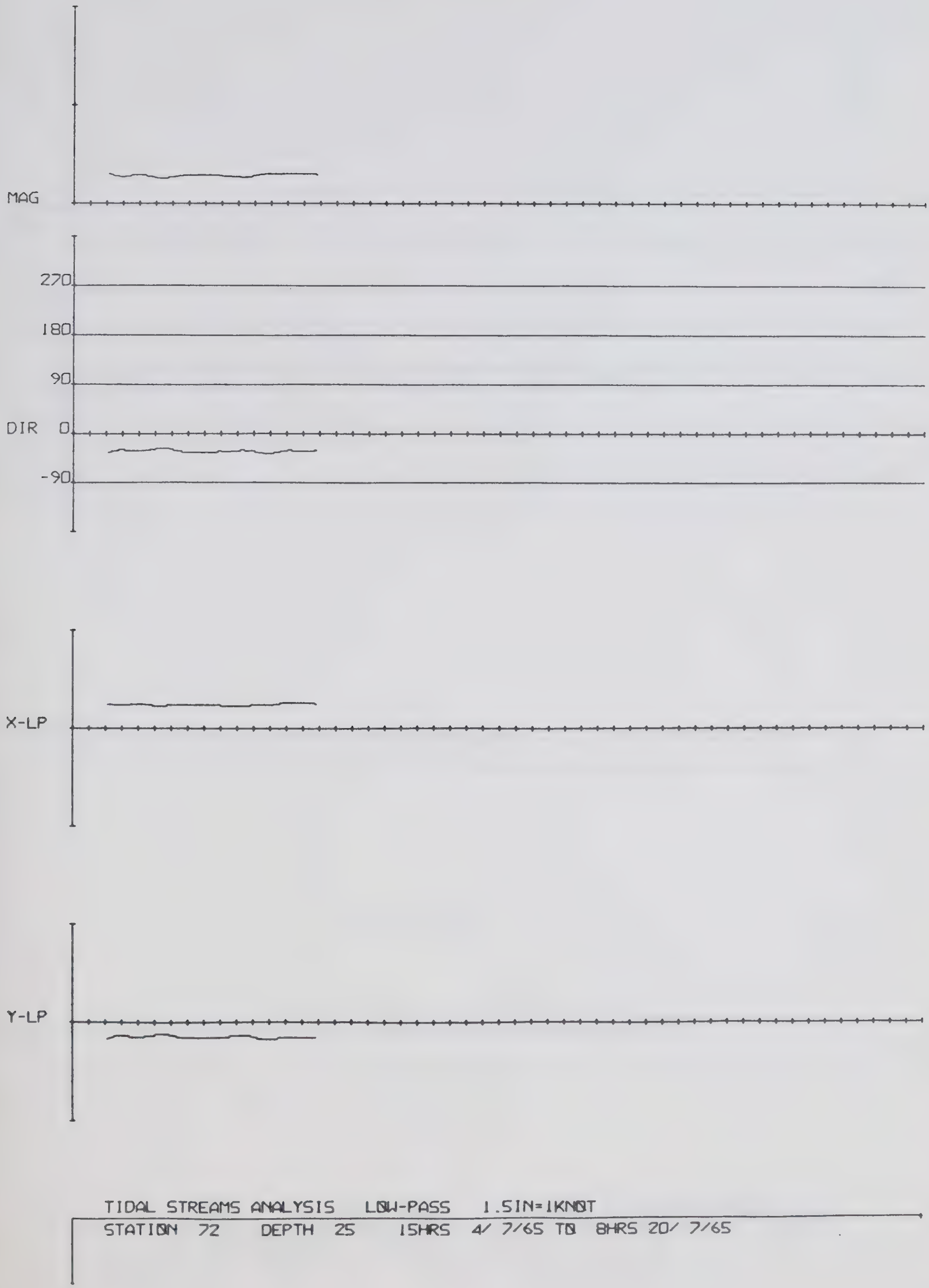
MAG
270
180
90
DIR 0
-90
X-LP
Y-LP
TIDAL STREAMS ANALYSIS LOW-PASS 1.5IN=1KNOT
STATION 72 DEPTH 25 15HRS 4/ 7/65 TO 8HRS 20/ 7/65

Plot 45

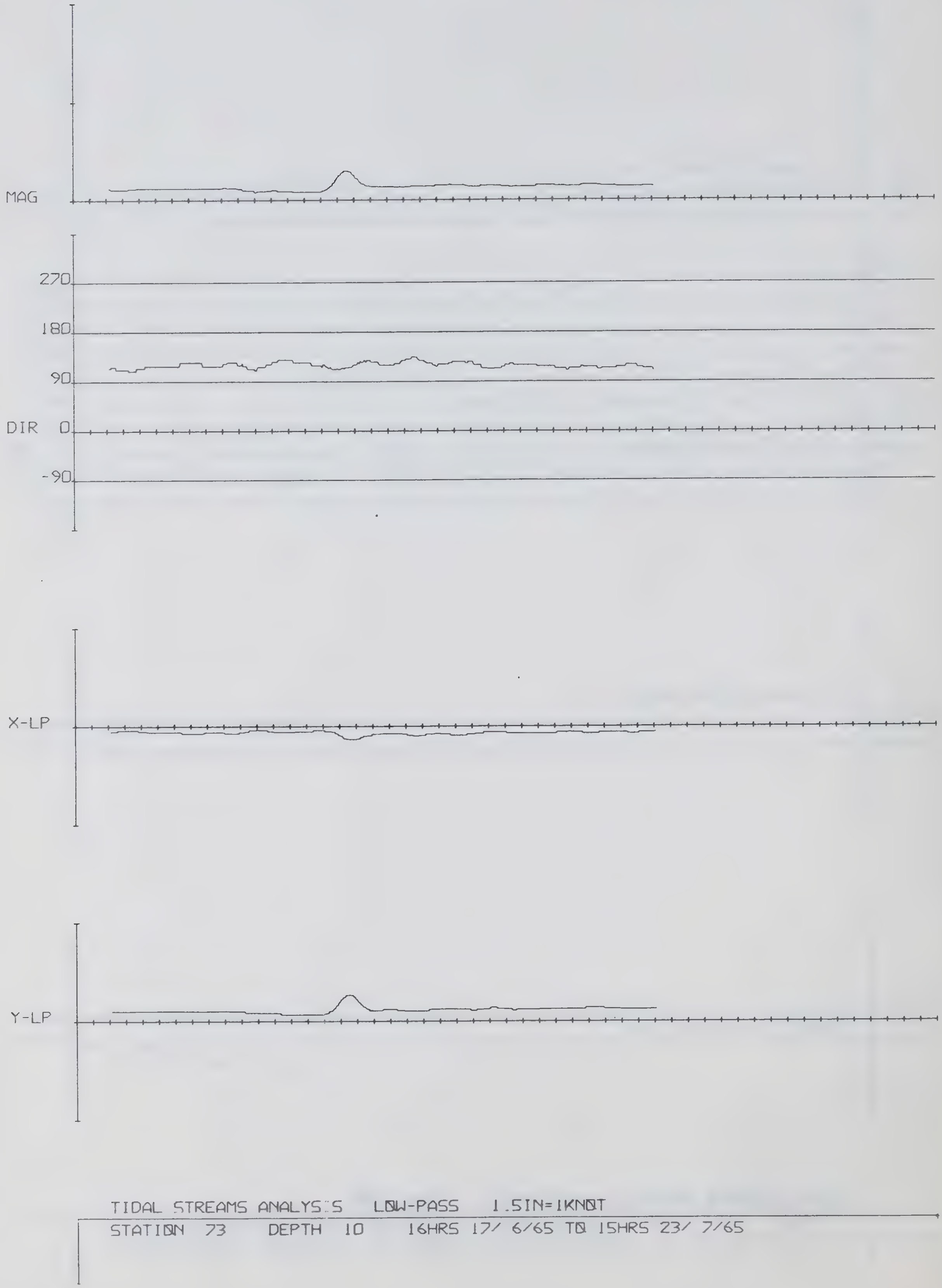
MAG
270
180
90
DIR 0
-90
X-LP
Y-LP
TIDAL STREAMS ANALYSIS LOW-PASS 1.5IN=1KNOT
STATION 73 DEPTH 10 16HRS 17/ 6/65 TO 15HRS 23/ 7/65

Plot 46

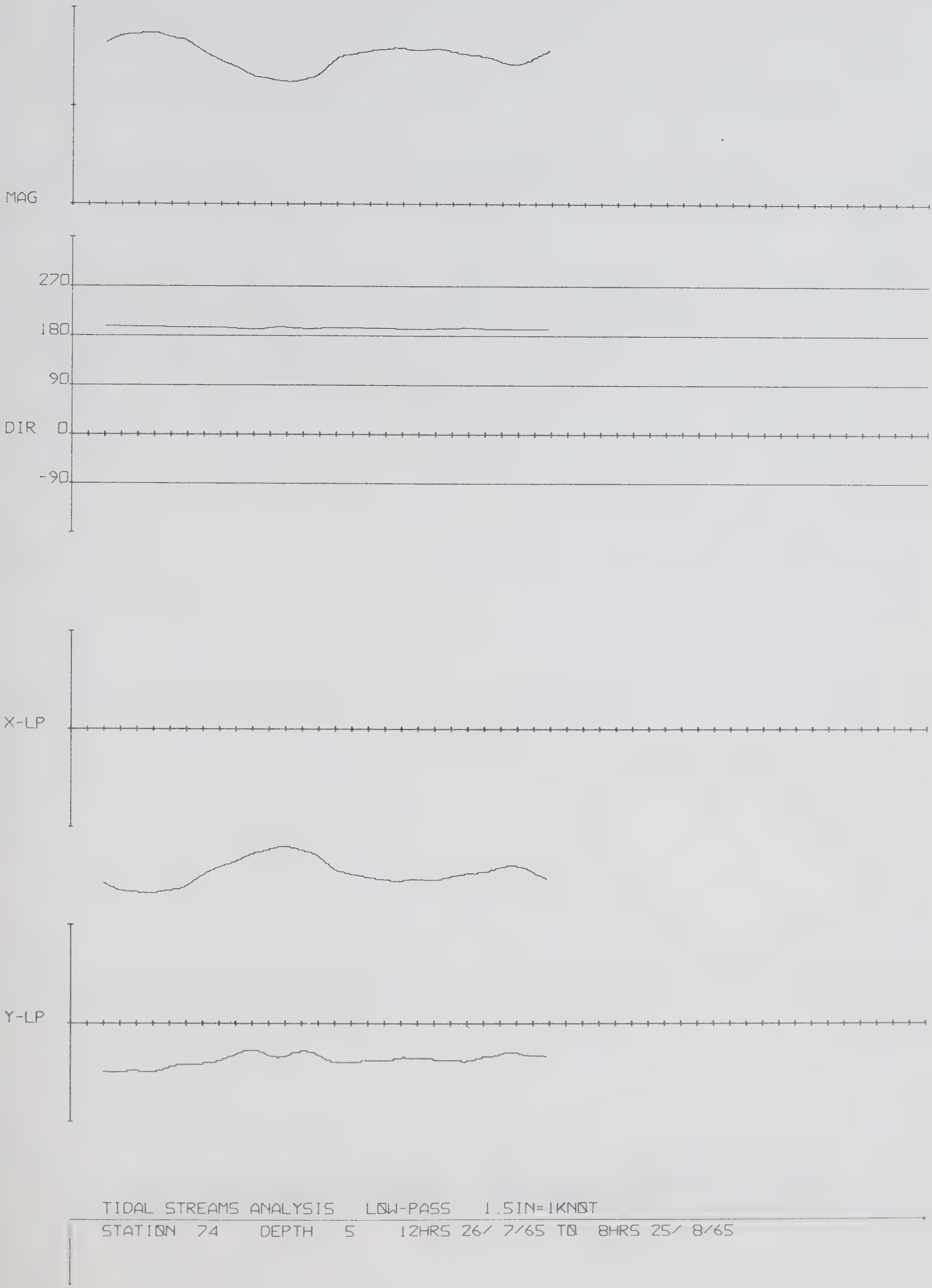
MAG
270
180
90
DIR 0
-90
X-LP
Y-LP
TIDAL STREAMS ANALYSIS LOW-PASS 1.5IN=1KNOT
STATION 74 DEPTH 5 12HRS 26/ 7/65 TO 8HRS 25/ 8/65

Plot 47

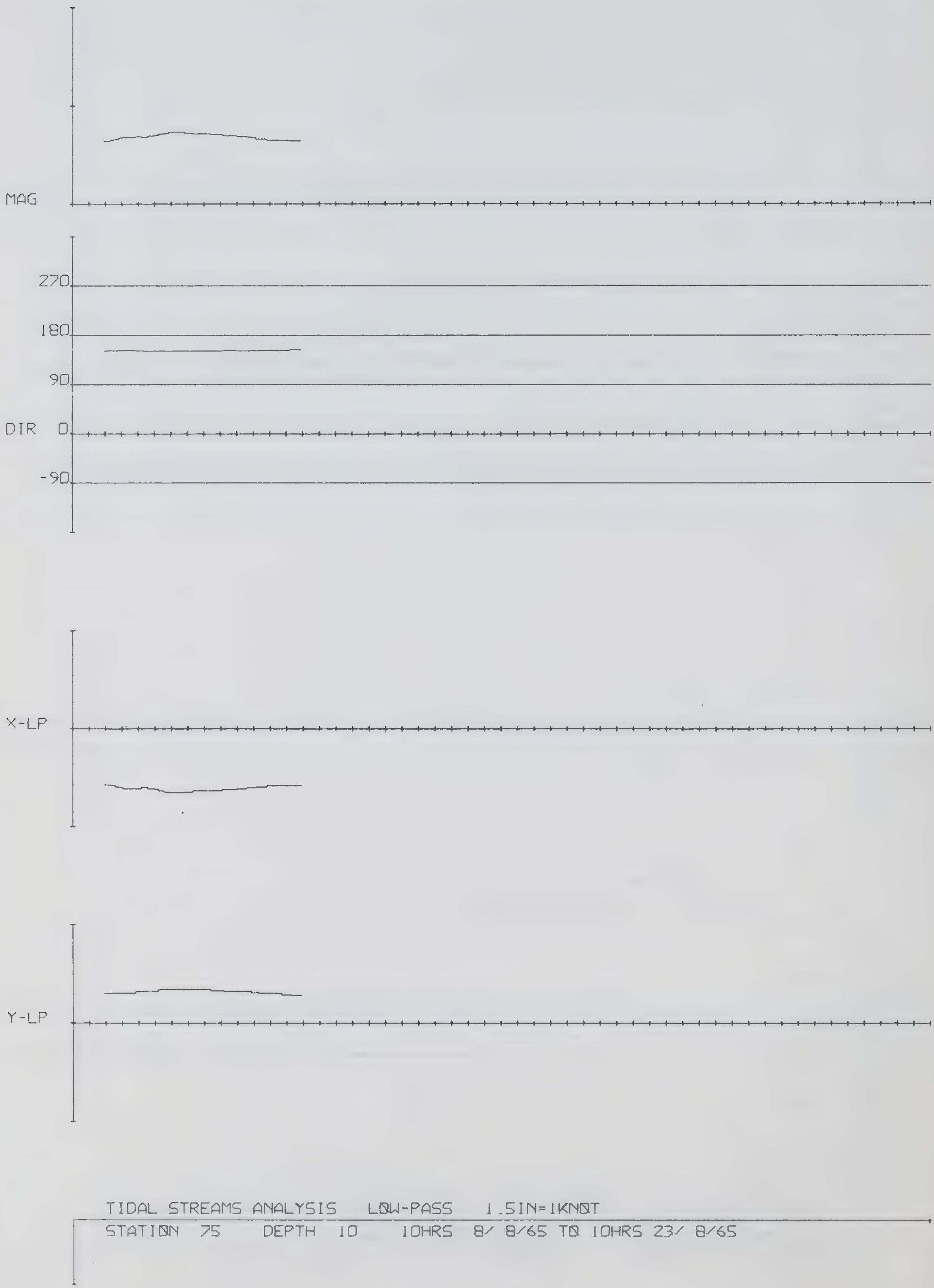
MAG
270
180
90
DIR 0
-90
X-LP
Y-LP
TIDAL STREAMS ANALYSIS LOW-PASS 1.5IN=1KNOT
STATION 75 DEPTH 10 10HRS 8/ 8/65 TO 10HRS 23/ 8/65

Plot 48

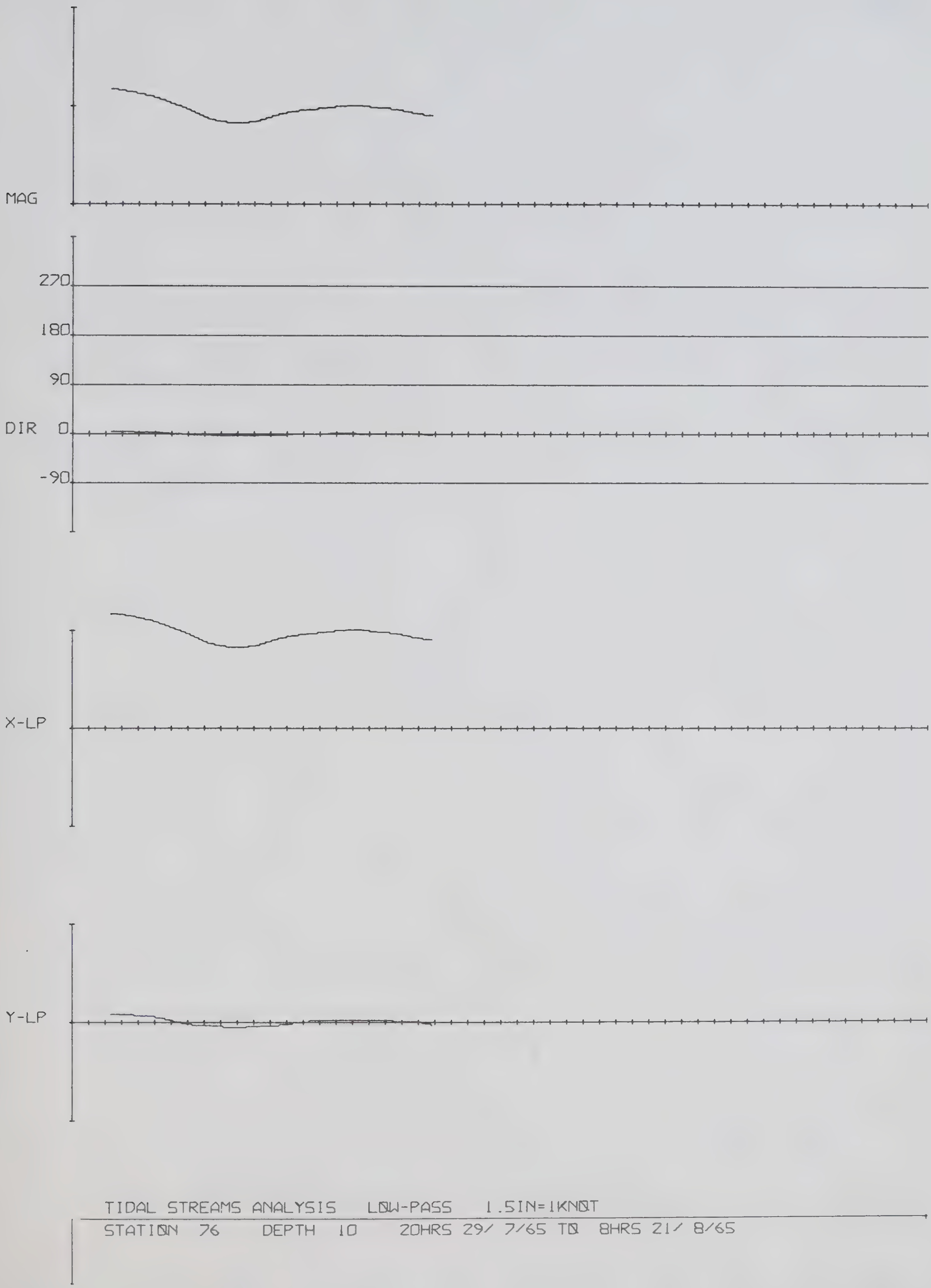
MAG
270
180
90
DIR 0
-90
X-LP
Y-LP
TIDAL STREAMS ANALYSIS LOW-PASS 1.5IN=1KNOT
STATION 76 DEPTH 10 20HRS 29/ 7/65 TO 8HRS 21/ 8/65

MANUSCRIPT
REPORT SERIES

No. 9

On the water of Tuktoyaktuk Harbour

F.G. Barber

1968

Marine Sciences Branch
Department of Energy, Mines and Resources, Ottawa

Manuscript Report Series

No. 9

ON THE WATER OF TUKTOYAKTUK HARBOUR

F. G. Barber

1968

CONTENTS

Abstract

A series of oceanographic observations from ice cover and from shipboard in Tuktoyaktuk Harbour are described. A coarse winter energy budget of the water with and without ice cover is examined. Water exchange due to estuarine and tidal mechanisms is suggested and the significance of conditions in the seaward approach discussed. A model of the influence of the tidal mechanism is developed and given quantitative consideration.

INTRODUCTION

The author will describe certain major features of oceanographic data obtained in and adjacent to Tuktoyaktuk Harbour in 1962 and 1963. The observations were made relative to the operation of an air bubbler system in the harbour during the winter; part of the data have been reported by Kelly (1967). Dick (1961) described the bubbler installation and Ince (1962) described the winter environment in the water of Tuktoyaktuk Harbour and some of the more important factors which determine the property distributions there.

Early in the work, the author was interested in examining the energy budget of the harbour water and how far the influence of the bubbler might be observed there. Subsequently, and after the gross features of the budget had been established, interest centred on the observed change of salinity during the period of ice cover and the probable relation of this change to a tidal influence. As mentioned in a later section a similar influence is believed to have been detected in observations made in the vicinity of Fury and Hecla Strait in 1960. Other examples have not been found in the literature, although it seems certain that the effect occurs elsewhere and likely leads to significant variations in those areas. Possibly the mechanism is best observed in the Arctic and perhaps in the vicinity of northern Foxe Basin and the Mackenzie River.

A description of the harbour and approaches is available in the Pilots (Canada. Dept. Mines and Tech. Surv.; 1958, 1961) and detailed depth information is available for much of the harbour in charts of the Canadian Hydrographic Service, although a portion has not yet been surveyed. Considerable oceanographic data were obtained in 1952 in the seaward approach to the harbour and these have been discussed (Cameron, 1953).

The harbour (Figure 1) is on the eastern edge of the delta of the Mackenzie River (Mackay, 1963). It is about 6.5 km long and up to 1.8 km wide. Over much of the length of the harbour, depths in excess of 10m are frequent; less frequent are depths to 20m and these occur in relatively small isolated depressions. The maximum depth is about 26m and a limiting depth of about 4m exists in Kugmallit Bay close to Eastern Entrance. In Kugmallit Bay the depth does not attain 6m (19.7 feet) within a distance seaward of the harbour of 22 km.

The normal range of the tide, which was described as semidiurnal (Dohler, 1964), is about 0.4m. Local wind effects can lead apparently to long stands at a high or low water, particularly during the ice-free season which extends from the end of June to early October.

Surface runoff into the harbour during the spring and summer is believed to be significant but has not been quantitatively assessed; winter runoff is not likely significant. Direct current data observed by Ince (1962, his Figure 10) indicate that in Eastern Entrance maximum speeds of 24 cm sec^{-1} can occur. With his data and an estimate

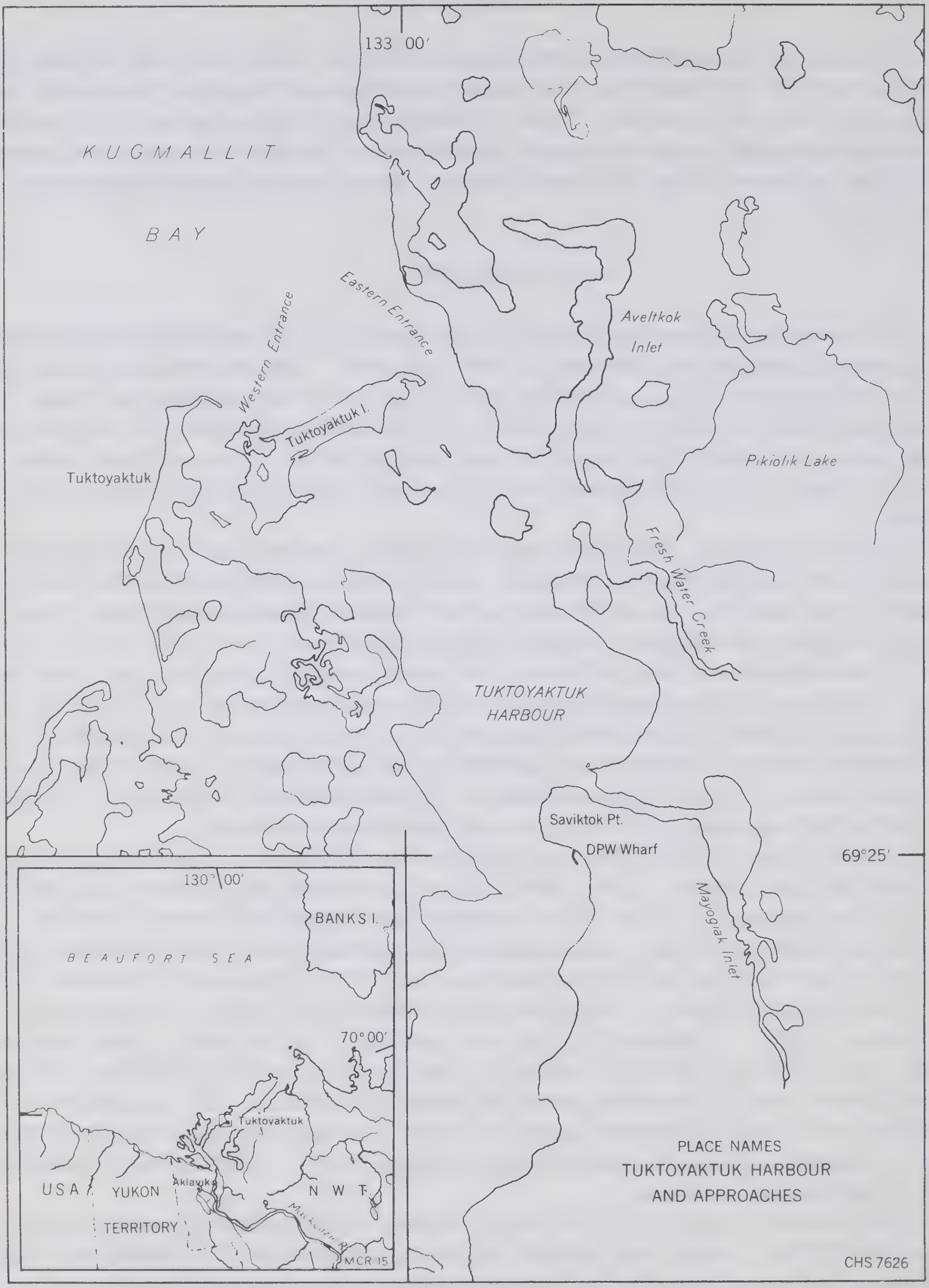

Figure 1(a). Tuktoyaktuk Harbour. Location and place names.

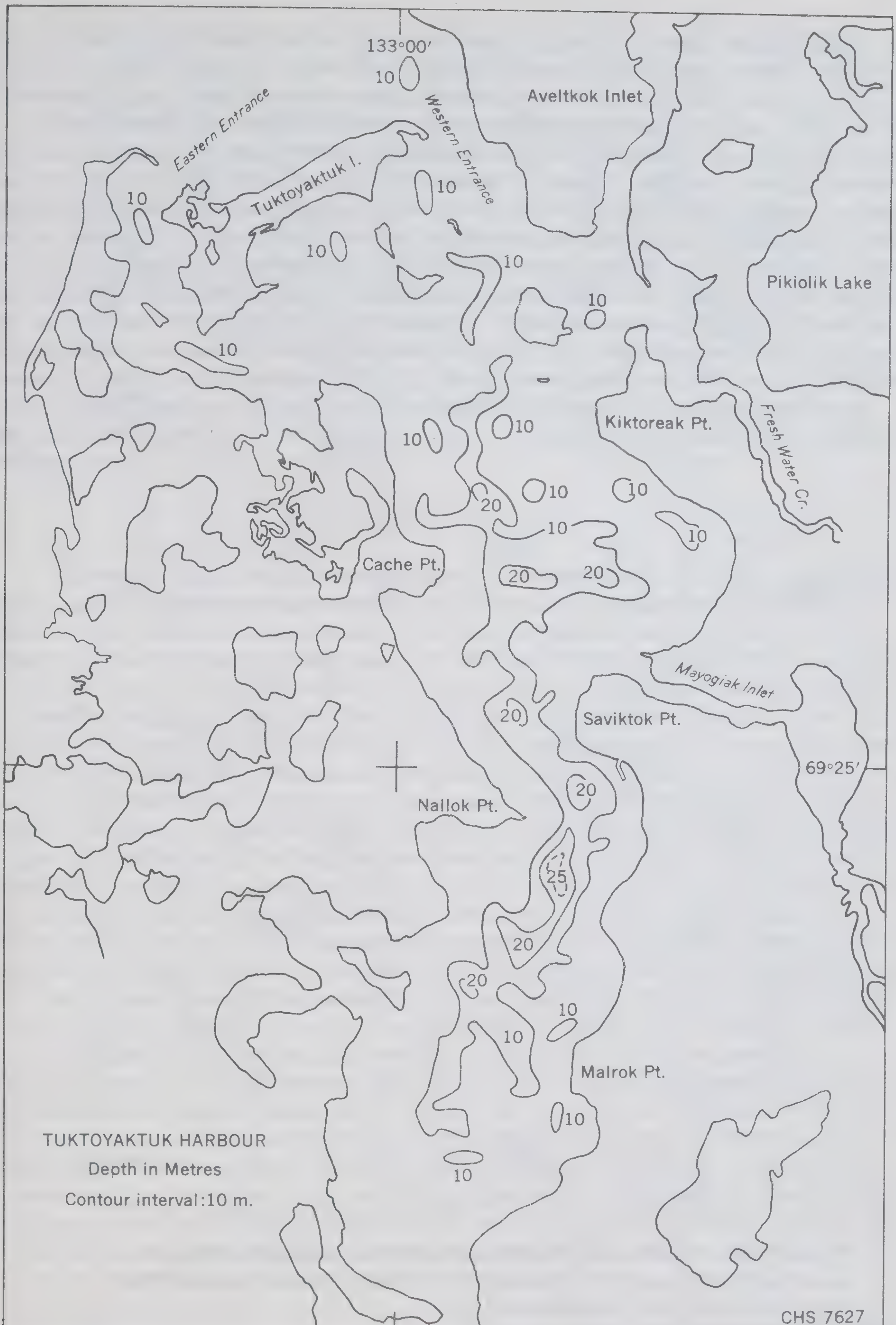

Figure 1(b). Tuktoyaktuk Harbour. Gross features of the bathymetry in metres.

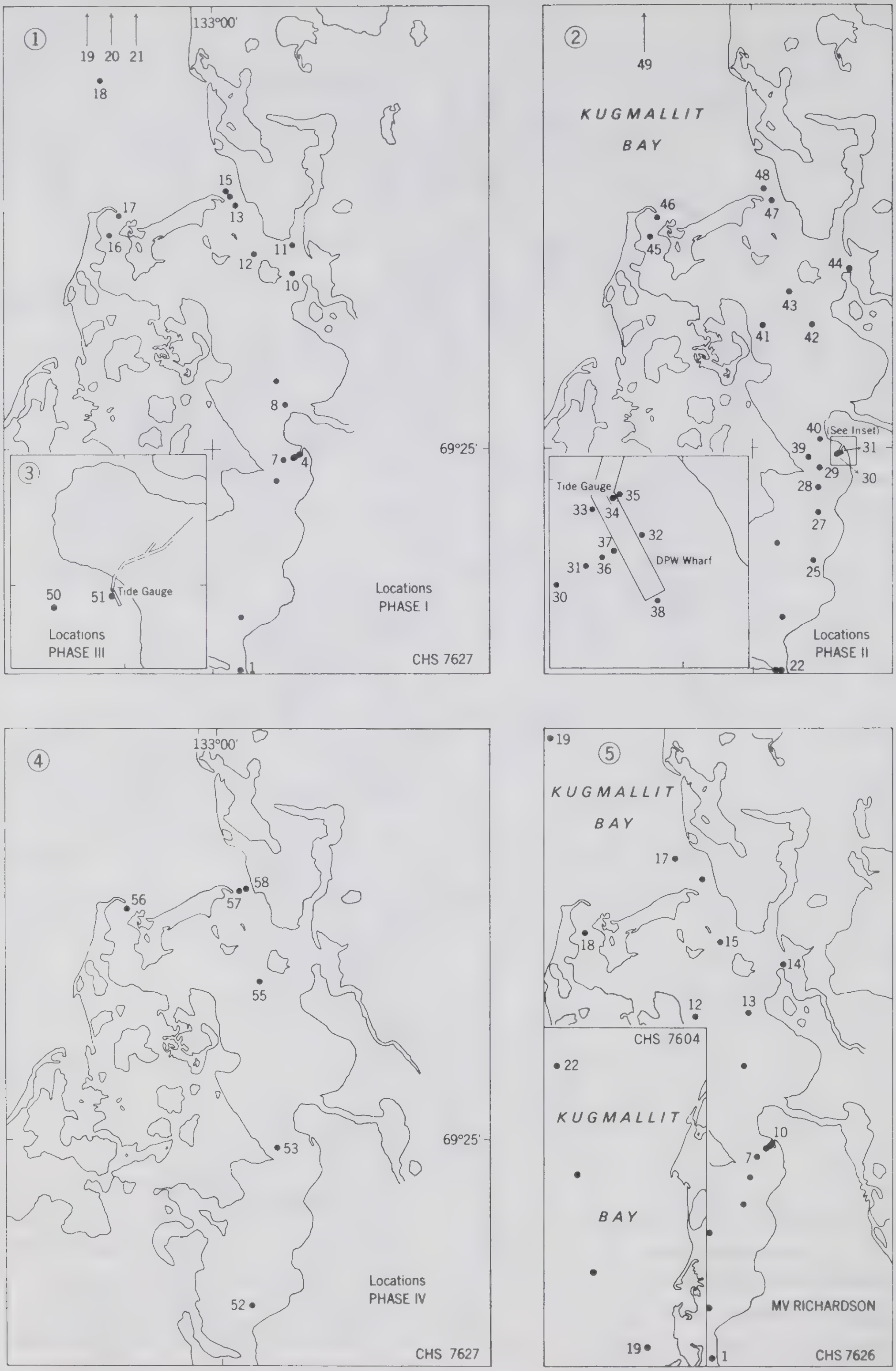

Figure 1(c). Number and location of positions occupied from ice cover during Phase I (1), Phase II (2), Phase III (inset 3) and Phase IV (4) and from MV "Richardson" (5).

of the volume required each tide to raise the level, it may be shown that the water movement in Western Entrance is in phase with that in Eastern Entrance. With an rms value of 15 cm sec^{-1} the excursion each tide is determined to be about 3400 m.

Tuktoyaktuk lies within the permafrost region of Canada (Brown, 1966) but data on the distribution of temperature in the ground are not available. As sea level there has not been at a higher level for many thousands of years a relatively deep permafrost may be anticipated (J. Ross Mackay, personal communication). It is recognized that bodies of water which remain unfrozen at depth markedly influence permafrost distributions in their vicinity (Lachenbruch, 1957; Brown, et al., 1964); they constitute relatively warm regions at the surface of the ground and consequently contribute heat to the ground which is eventually given off to the atmosphere. The temperature in the harbour subbottom would be similar to that in the harbour water so that during part of a year some unfrozen ground (ground warmer than 0°C) would occur, perhaps to some well-defined horizon. Under these circumstances a contribution of ground water to the harbour might occur but is not likely sufficient to cause a recognizable change in the salinity distribution there.

REVIEW

Cameron (1953) studied oceanographic data obtained in 1952 and showed that a marked change occurred in the distribution of temperature and salinity seaward of Kugmallit Bay. He related the change to the interaction between the fresh water discharged from the Mackenzie River and the wind. Ince (1962)* indicated that under the ice cover in Kugmallit Bay the water "is practically fresh Mackenzie water" and he associated the condition directly to the mechanism described by Cameron. The description of events obtained from local residents (Ince, 1962) suggests that the mechanism likely occurs every year. The essential feature of the mechanism is an offshore transport of surface water which occurs as a secondary effect of an easterly wind in the absence of ice cover. Because of this transport in late August 1952 the surface salinity in Kugmallit Bay exceeded 30°/oo and the distribution of density in a seaward section indicated an upwelling condition close to the coast. Earlier in August an accumulation of low-salinity water in Kugmallit Bay was indicated. Thus the combined works of Cameron (1953) and Ince (1962) indicate the existence of an extensive accumulation of fresh water in Kugmallit Bay in spring which decreases markedly during the summer.

In spring a remarkable stratification was observed within the harbour under the ice cover (Ince, 1962 his Figure 12; and Figure 4 here). This comprised a freshwater layer about 6m thick overlying another in which the salinity exceeded 30°/oo. The temperature in the fresh-water layer was close to the freezing point and in the deeper high-salinity layer it was about -0.5°C. A well-defined inversion of temperature to 0.3°C occurred in the intense salinity gradient (halocline) between the two layers. Somewhat higher temperatures were observed at locations within the harbour where some isolation due to internal sills occurred. Ince (1962) suggested that the distributions in these areas represented conditions which existed in the harbour at freeze-up. Also, and because of the successful operation of the bubbler system during the winter, he theorized that the halocline was shallower during that time.

*The temperature and salinity data described by Ince (1962) were observed during the period April 27 - May 6, 1962 and are listed here in Table I.

The data to be discussed indicate that the latter situation actually occurred but in the discussion this is not attributed to the influence of the bubbler, although it is suggested that the salinity of the surface layer close to the bubbler site during the 1962-63 winter may reflect such influence. The energy budget estimates of a later section indicate that changes in the environment due to the bubbler need not be measurable by the techniques used. In these estimates it was assumed that the loss of heat at the bubbler site comprised sensible heat only and was not met through formation of frazil ice or other effect. One such effect was described by Pounder (1961) in discussing the influence of salinity gradients (his page 42) where he remarked, "the water column ... could melt sufficient ice to reduce its mean salinity to $32°/_{oo}$ without change of temperature." It was then estimated that 9.09cm of water equivalent of ice could be melted. The heat * required for this, 500 g cal cm^{-2}, would be derived from a system which started at -1.72°C and ended at -1.72°C without additional source of heat.

Of course there is an error. It lies in the part sentence quoted above, the statement therein being false. It seems to have been derived from the observation that the freezing point of the column would be reduced by 0.05C° on mixing. The result would be a salinity throughout of $33°/_{oo}$ at a temperature of -1.72°C. Then followed the calculation of the amount of ice which when melted would reduce the salinity of the column to $32°/_{oo}$ still at -1.72°C. But this could only be accomplished were there a heat input from an external source to cause the ice to melt.

DESCRIPTION OF THE DATA

Remarks concerning the data

The extent of the data described here is shown in Table I and the locations at which stations were occupied are shown in Figure 1(c). With the exception of the data obtained in the MV "Richardson" of the Canadian Hydrographic Service the observations were obtained from ice cover by the National Research Council of Canada. Three phases (I, II, and IV) of the latter program represent periods of relatively intense field activity by NRC staff from Ottawa. To a degree the detail of the program of observations represents an attempt to test various items of equipment in the Arctic environment but, as it was recognized relatively early in the program that the conventional techniques and instruments used would allow only a gross evaluation of the environment, at least in relation to the influence of the bubbler, no serious instrument trials were completed. The decision was partly influenced by the conclusions reached from a budget study, reported briefly in later section, to the effect that ample sensible heat existed in the harbour to meet the loss at the bubbler site.

Three methods were used to obtain the salinity data; these were:

(1) reversing bottles and laboratory determination after sample storage,
(2) portable conductive meter and hand-lowered cell, and
(3) portable inductive meter and hand-lowered cell.

---

*Assuming the ice to be at the freezing point and taking the latent heat as 55 cal gm^{-1} (Pounder, 1961 p. 45) then the heat required is equal to the water equivalent of ice (9.09) times the latent heat (55) and is 500 g cal.

Table I (a)

A listing of the data indicating the date observed and a brief description. Most of the observations, Phases I to IV, were carried out from ice cover by personnel of the National Research Council of Canada, the observations in summer in the motor vessel "Richardson" of the Canadian Hydrographic Service. The approximate location of the stations occupied may be obtained from Figure 1 which is a modification of that in the data report (Kelly, 1967).

Phase I	April 27 - May 6, 1962; temperature and some salinity data; previously described by Ince (1962). 109 consec numbers in all.
Phase II	Nov. 26 - Dec. 9, 1963; temperature and salinity. 81 consec numbers.
Phase III	Dec. 14, 1962 - May 1, 1963; serial salinity and BT lowerings weekly at two locations. 29 consec numbers.
Phase IV	May 2-5, 1963; temperature and salinity. 63 consec numbers.
"Richardson"	July 26 - Sept. 16, 1963; serial salinity and BT lowerings. 47 consec numbers.

Relatively large differences exist in this material particularly during Phase IV and appear mainly between the conductive meter on one hand and the inductive meter and sampling bottles on the other. It did not appear possible to determine the nature of these differences but it is believed that they are not significant to the work as it is presented here.

The quality of the tabulated temperatures in the data report (Kelly, 1967) appears to be good but it has not been possible to provide an estimate of the significant difference between the tabulated values. For the material utilized it is assumed this difference is smaller than 0.01C°.

General features

Figure 2 shows the distribution of salinity during the entire period as inferred from observations with reversing bottles at about one position. Prominent in this is the marked salinity gradient or halocline in which the salinity increased from very low values to about 25°/oo over a short depth interval. Above the halocline in a surface layer the salinity was extremely low, less than 1°/oo, during the period of ice cover and increased to at least 13.7°/oo during the ice-free period. At this time in the deep water below the halocline, the salinity was about 29.0°/oo. Higher salinity occurred there during the winter months, 30°/oo during the 1962-63 winter and 31°/oo earlier in April of 1962. Thus the data suggest the existence in the deep water of a salinity variation with annual period.

Table I (b)

A listing by date of the locations occupied in Tuktoyaktuk Harbour and Kugmallit Bay during Phases I, II and IV.

Phase I

location \ day	April 1962 27	28	29	30	May 1	2	3	4	5
	12	8	4	7	16	12	15	13	15
	6	9	16	15	17	1	4	14	14
	7	6	16	15	15	1	15	15	15
		6	15	15	17	4	3	4	15
		5	12	16	15	15	20	2	14
		6	11	15	17	15	21	7	4
		5	11	16	16	19	15	9	4
		5	10	17	15	15	14	15	
		2	9	15	17	4	14	4	
		6	8	17	16	15	18	7	
		3	6	16	3	15	13	2	
		3	5	16	7	19	13	15	
			4	17	1	19		15	
				15	2	15		15	
				16	7	15			
				15	1				
					12				

Phase II

November 1962 26	27	28	29	30	December 1	2	3	4	5	6	7	8	9
23	35	30	34	48	44	44	22	23	40		32	33	49
24	28	44	48	48	28	42	23	27	43		37	28	
45	29	42	48	48	28	27	33	28	46		37	24	
		27	48	48		24	27	29	40		36	28	
		28	48	30			28	40	43		31	42	
				23			29	43	46		29		
				25			30	43	25				
				26				40	26				
				38				46	42				
				23				43	41				
				30				40	47				
				27					39				
									42				
									41				
									25				
									26				

Phase IV

May 1963 2	3	4	5
53,54	52,55	57,58	57,58
52,55	53,54	56	56
53,54	52,55	57,58	57,58
52,55	53,54	56	56
53,54	52,55	57,58	57,58
52,55	53,54	56	56
53,54	52,55	57,58	
52,55		56	
53,54		57,58	
52,55		56	
53,54		57,58	
		56	

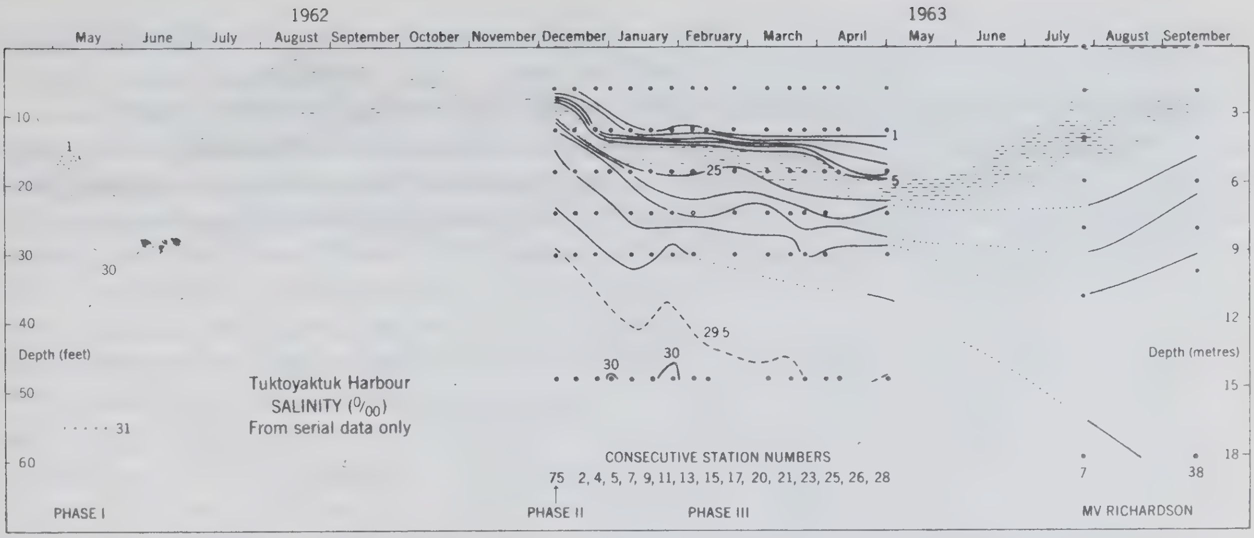

Figure 2. Salinity distribution based on samples obtained with reversing bottles during the period April, 1962 to September, 1963. The shaded portion indicates the depth over which the change was 20°/oo. Data used comprise all Phase I, Phase II consec number 75, Phase III consec numbers 2, 4, 5, 7, 9, 11, 13, 15, 17, 20, 21, 23, 25, 26, and 28, and "Richardson" consec numbers 7 and 38.

A similar period is apparent in the depth of the surface layer which appears minimum in early December and at a maximum at some time during the spring. The observations from the ice cover indicate that the depth of the layer increased by a factor of two and, as the salinity of the layer did not change significantly during this time, the depth increase represents an increase of fresh water in the surface layer, also by a factor of two. As it would appear reasonable to assume that such a local contribution of fresh water could not occur during the winter it may be concluded that the fresh water comes from the Mackenzie River. It would seem too, that the accumulation over shallow Kugmallit Bay would prevent any movement into the harbour from seaward so that the high-salinity deeper water must intrude there at another time. This consideration envisages a rapid accumulation of the fresh water in Kugmallit Bay with a much slower increase in the harbour due probably to tidal influences and the relative depth of mixed layer and sill.

The maximum observed depth of the mixed layer is close to that of the sill and was attained in May. Because it is close to sill depth it probably represents the deepest extent of the mixed layer throughout the period of ice cover. It is visualized that the condition persists relatively unchanged to the end of June at which time, and in association with removal of the ice cover, the trend toward the observed late summer distributions is established.

The distribution at freeze-up was not observed so that the surface salinity at the time is also a subject for conjecture. It seems possible that the change to lower salinities occurred * prior to ice formation so that when the ice cover began to form

*The only evidence which supports this possibility appears to be the temperature values in the halocline. As shown in the subsequent description, particularly of Phases I and II, the temperatures there tend to be generally warmer then the freezing point, whereas values closer to the freezing point could be expected to some depth within the halocline had the water there been recently influenced by freezing at the surface.

it did so in a water nearly fresh. This is a useful supposition for it provides an origin, 0°C, for heat storage estimates in the surface layer. The "Richardson" data (Figure 3) indicate that such seasonal storage does occur for by the end of July the surface temperature exceeded 15°C and the storage at one position was estimated to be 9.4 kg cal cm^{-2}. This level of storage appears to have continued there through mid-August to about August 21, declining to 2.5 kg cal cm^{-2} by mid-September and presumably to zero in a surface layer by the time of ice formation.

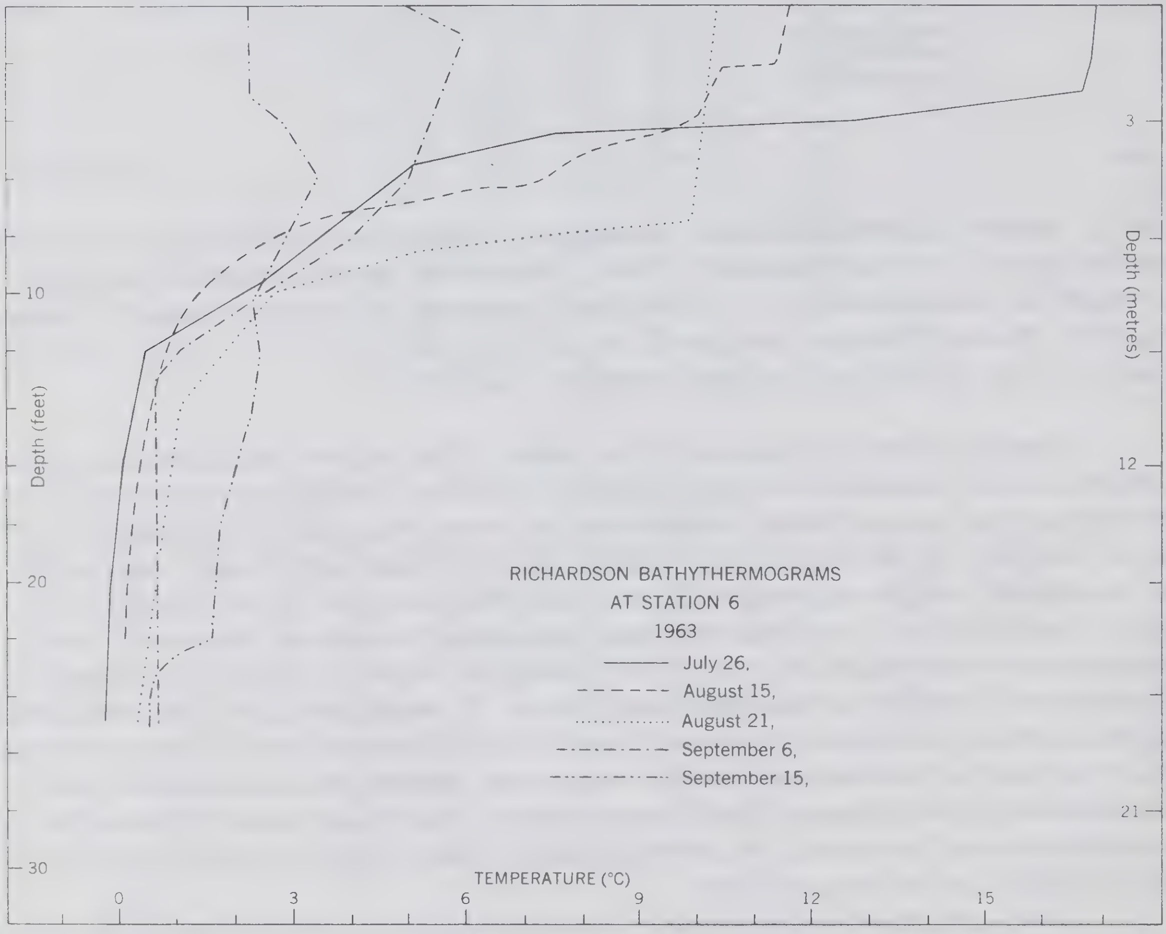

Figure 3. Distribution of temperature at "Richardson" location 6 from BT data indicating the date observed. With 0°C as the origin the seasonal heat storage for each was calculated to be 9.4, 8.5, 9.1, 5.2 and 2.5 kg cal cm^{-2}, respectively.

The stability of the heat storage in the surface layer to August 21 is of interest as it coincides with an increase of surface salinity there (Figure 2). Both aspects are compatible with the advective influence of the estuarine circulation which occurs at this time due to surface runoff into the harbour and with the existence of a water of oceanic salinity in the near approaches. However, the efficiency of the coupling provided by the estuarine circulation cannot be evaluated for not only are the data minimal but also another exchange mechanism is believed to be significant.

From ice cover

Phase I (April 27 - May 6, 1962). Two structural characteristics of widespread occurrence in Arctic waters are evident in the observations in Tuktoyaktuk. One is the halocline, the other the temperature maximum within the halocline. That these can occur (apparently the temperature maximum is not a persistent feature) is demonstrated by Phase I data (Figure 4) which indicate the existence of the maximum toward the bottom of an extremely strong halocline. Above the halocline in the surface layer, to about 6m depth, the salinity was less than 1°/oo and the temperature close to the freezing point. Below the halocline the salinity increased to the bottom to about 31°/oo where the temperature was between -0.5 and -0.4°C. At 25 feet (7.6m), a depth likely close to the bottom of the halocline throughout the harbour, the temperature varied about 0.65C° (Figure 5). It seems that this relatively wide range of temperature may be brought about by a number of influences including isolation of the deeper water (as at location 16 and perhaps at location 11) by variation of depth within the harbour as suggested by Ince (1962).

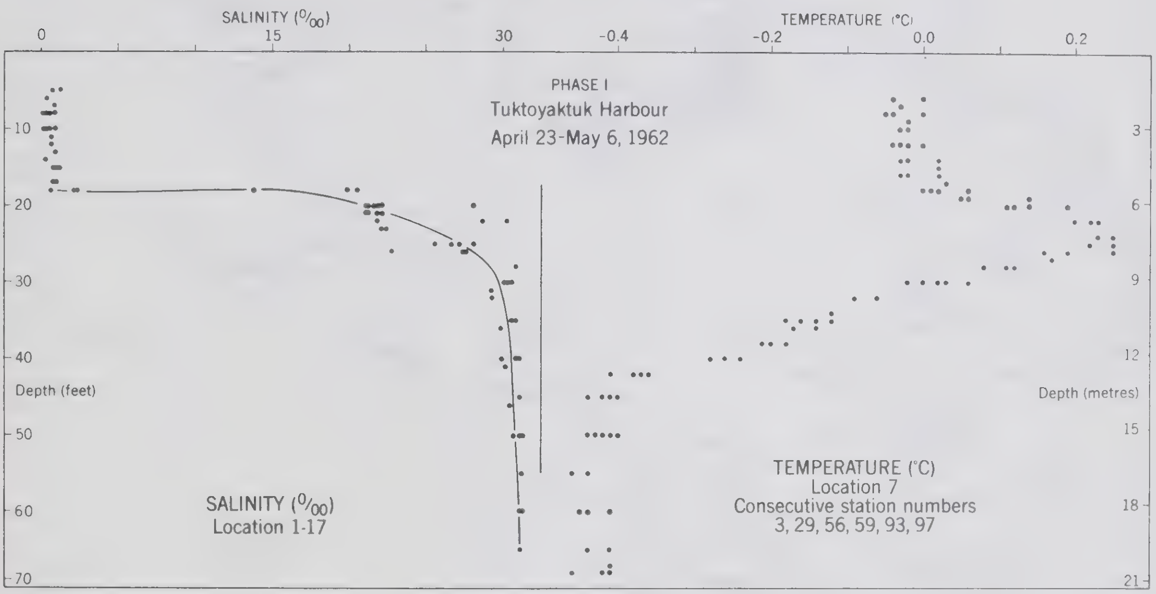

Figure 4. The structure of salinity and temperature during Phase I. All of the observed salinity values are shown. The temperature values were observed at location 7, consec numbers 3, 29, 56, 59, 93 and 97.

Data in the harbour approach during Phase I, although few, indicate (Figure 6) the existence of a low-salinity layer to about 18 feet (5.5m) and, while not sufficient to allow proper definition of the deeper salinity structure, suggest that the halocline may be less intense there than in the harbour. The suggestion is supported by the fact that a maximum in the temperature structure below the surface layer was not observed at the extreme seaward position (location 21). At this position the coldest, to -0.61°C, water of Phase I was observed close to the bottom at 25 feet (7.6m).

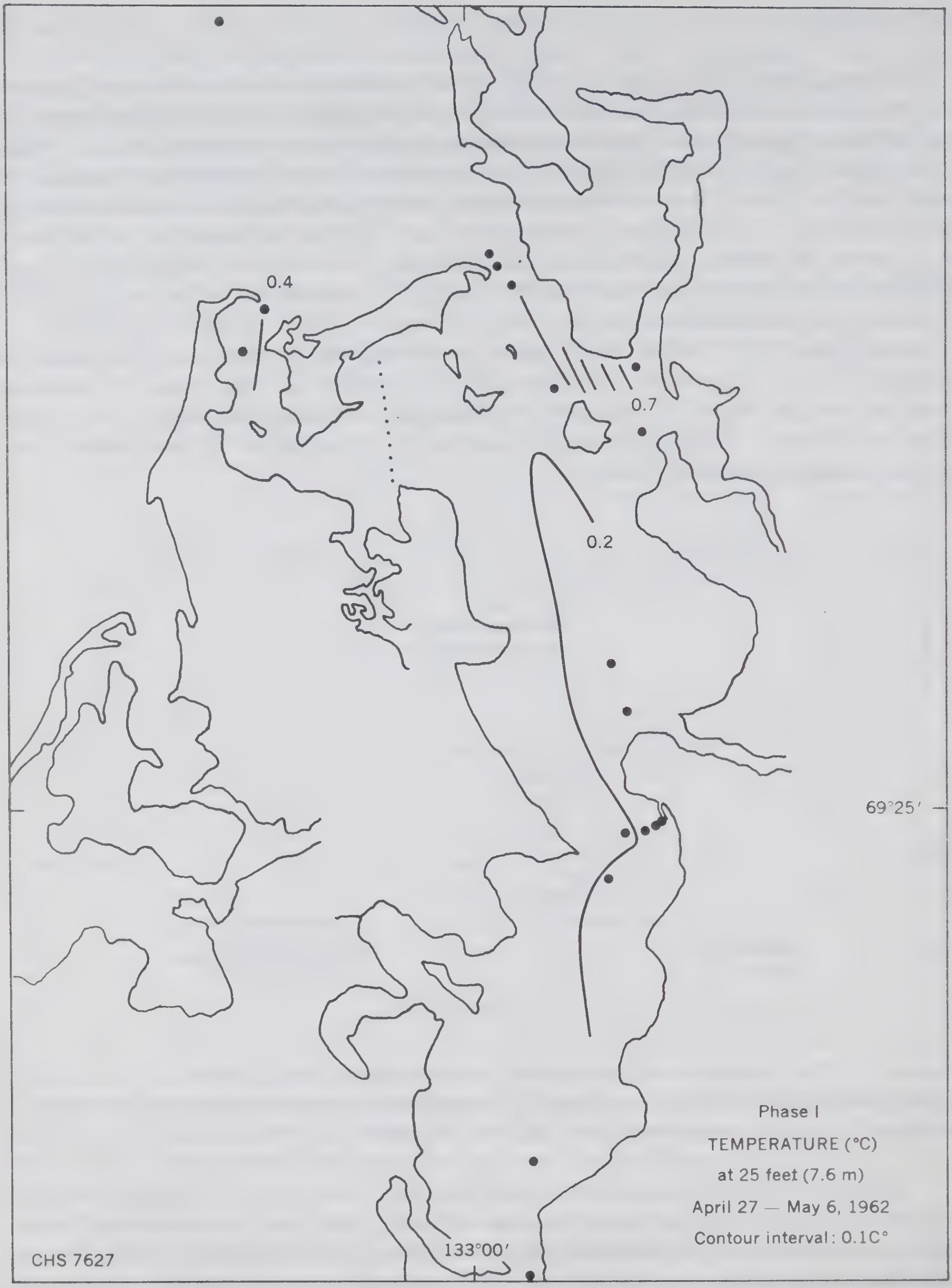

Figure 5. Distribution of temperature (°C) at 25 feet (7.6m) during Phase I (consec numbers 1, 2, 3, 5, 10, 15, 17, 19, 20, 21, 57 and 58). In all of the presentations of horizontal distributions an open circle indicates a location where data were observed, a closed circle indicates a location where data there were used in the interpretation.

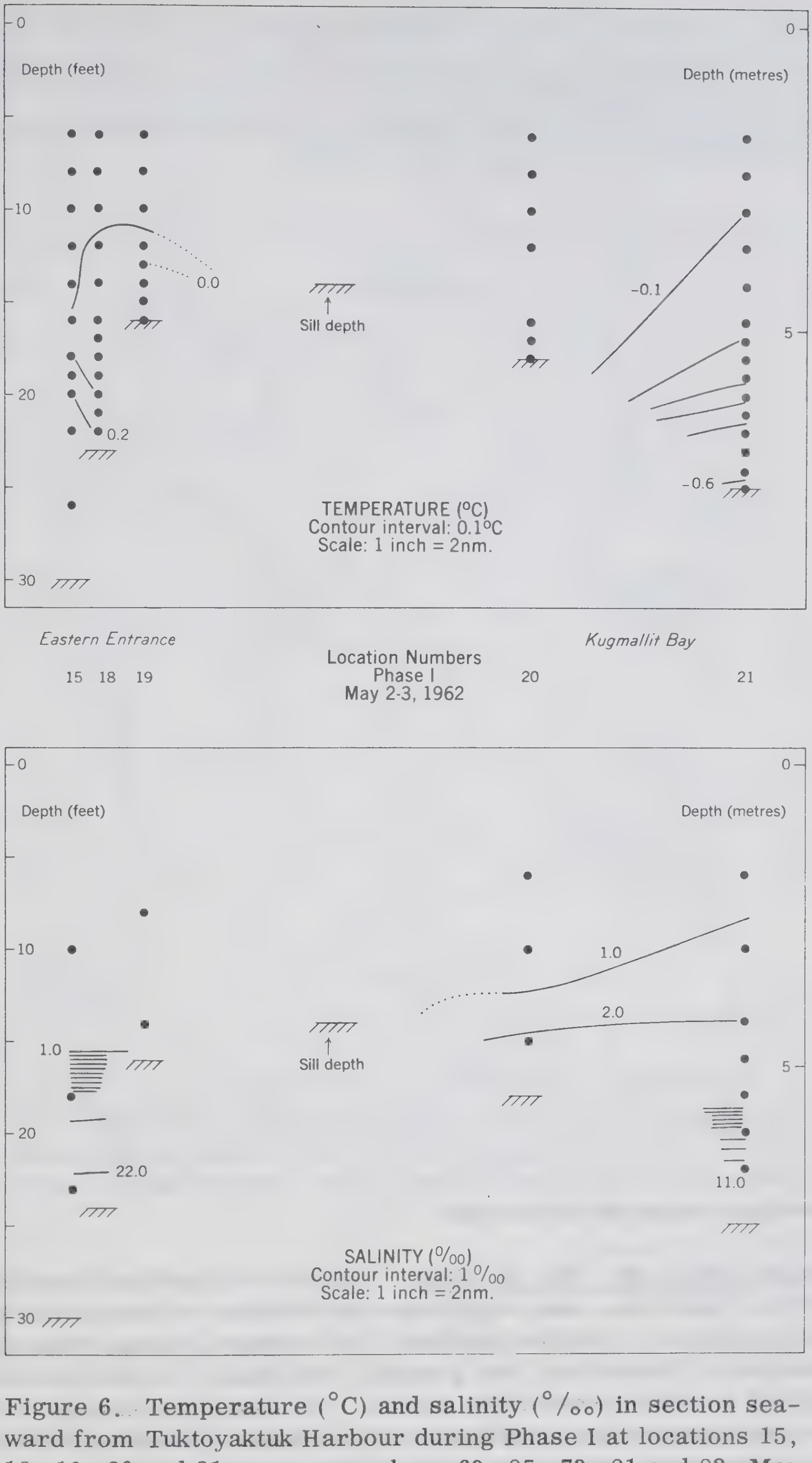

Figure 6. Temperature (°C) and salinity (°/₀₀) in section seaward from Tuktoyaktuk Harbour during Phase I at locations 15, 18, 19, 20 and 21, consec numbers 69, 85, 73, 81 and 82, May 2-3, 1962.

During the period a position in Eastern Entrance (location 15) was occupied on 29 occasions. The temperature data observed at 20 feet (6.1m) at the position and the observed relative change of sea level within the harbour are shown in Figure 7. A temperature variation of tidal period of about 0.2C° is indicated such that a cold water occurred at high tide and a warmer water at low tide.

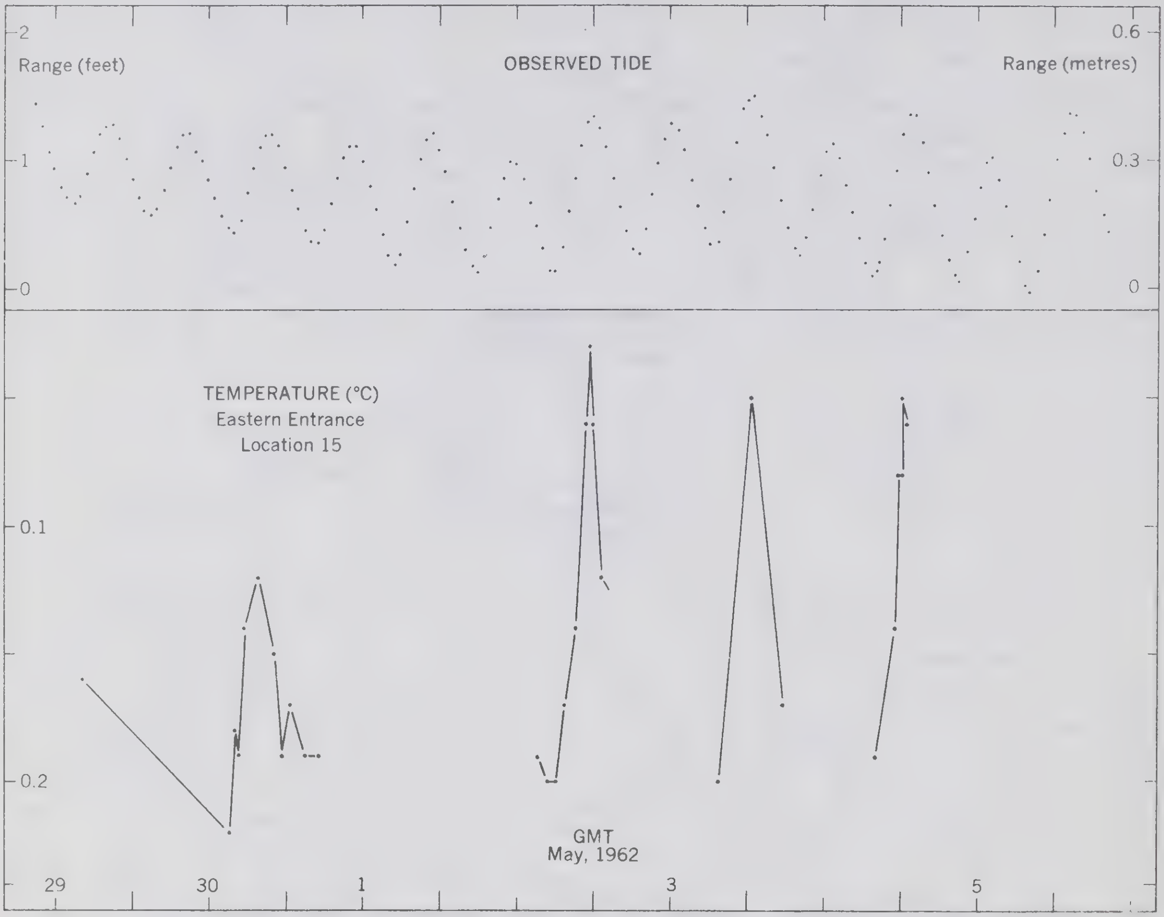

Figure 7. Temperature (°C) at 20 feet (6.1m) at location 15 in Eastern Entrance during the period April 29 - May 5, 1962 and the observed range of the tide which was provided in the form of hourly values by the Canadian Hydrographic Service. A systematic error of one hour may exist in the tidal information and if it does the time shown is late by this amount.

Phase II (Nov. 26 - Dec. 9, 1962). The effect of isolation described above may on occasion be of more than usual significance as the data for these periods suggest a strong time-dependence in the distributions. For example, during Phase II the salinity of the surface layer (Figure 8(a)) was generally less than 1°/oo except in the vicinity of the wharf and toward the head of the harbour. As mentioned on page 17 the values close to the wharf may reflect an influence of the bubbler. However the increase up the harbour is presumably due to changing conditions in Kugmallit Bay subsequent to the formation of an ice cover there. The temperature distribution at depth (Figure 8(b)) also suggests changing conditions with generally warmer values upharbour from about the location of the wharf.

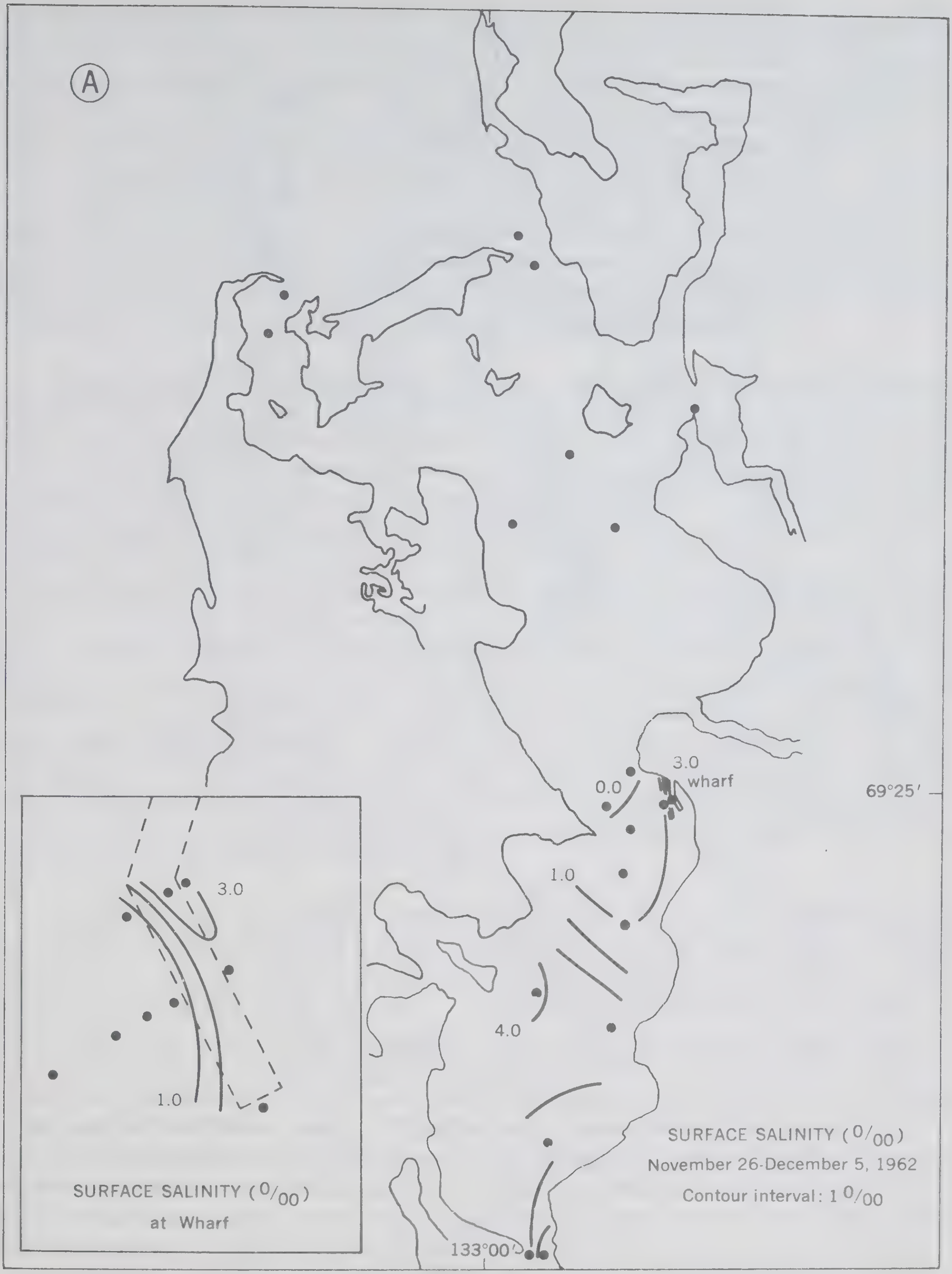

Figure 8(a). Distribution of salinity (°/₀₀) in Tuktoyaktuk Harbour during period Nov. 26 - Dec. 5, 1962 of Phase II. In surface layer from consec numbers 1, 2, 3, 5, 6, 8, 9, 10, 13, 21, 23, 24, 36, 47, 48, 50, 51, 63, 64 and 65. Inset shows distribution in vicinity of wharf from consec numbers 4, 12, 25, 38, 42, 70, 72, 73 and 74 (see Figure 1 for station locations in vicinity of wharf).

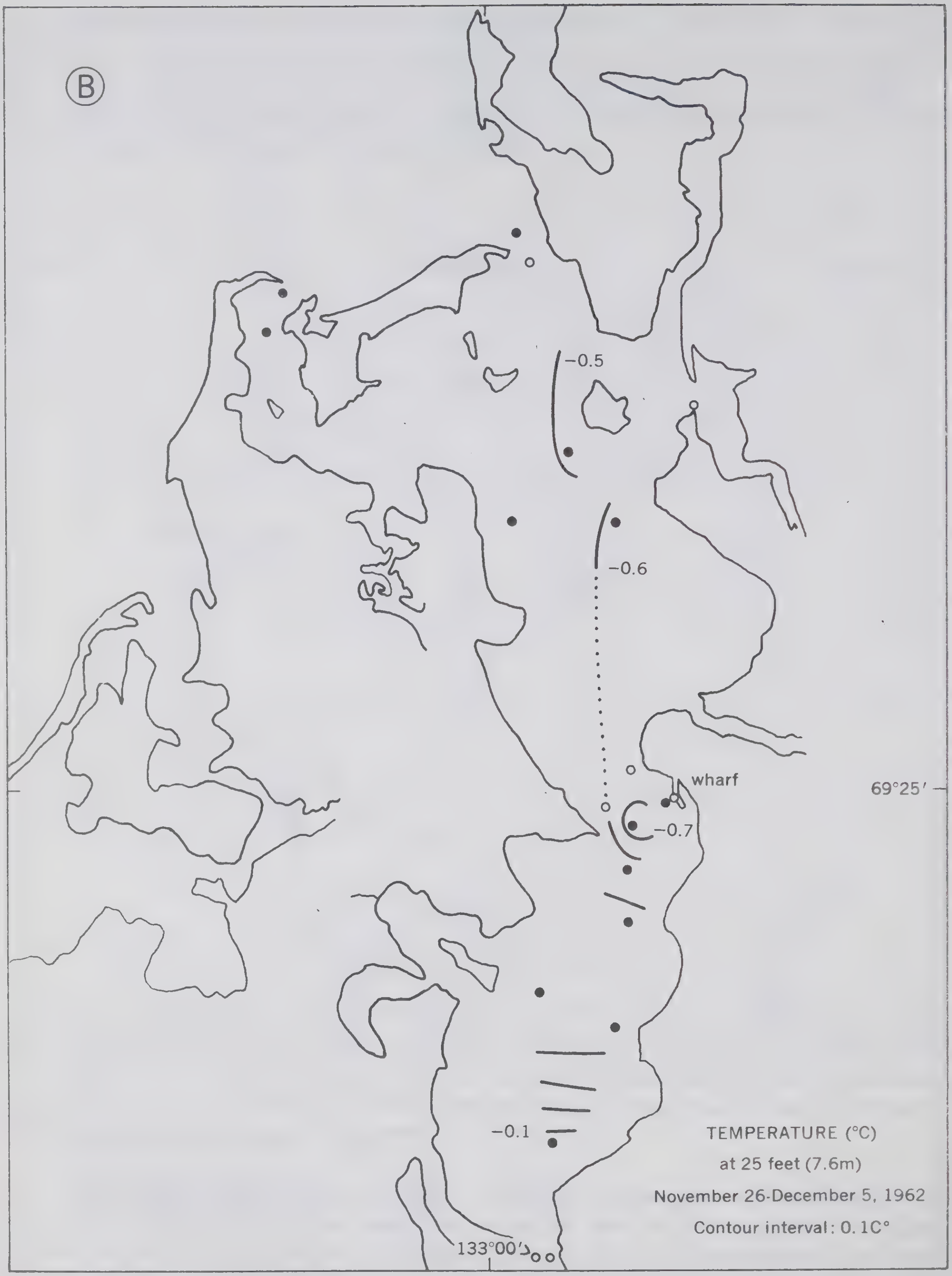

Figure 8(b). Temperature distribution (°C) at 25 feet (7.6m) from consec numbers 1, 2, 3, 5, 6, 7, 9, 10, 13, 51, 52, 60, 61 and 63. Same details as Figure 8(a).

The salinity data of this phase were based on one of the in situ salinometers and on a smaller number of bottle samples. The distribution of salinity with depth at one position (location 28) derived from data of both types obtained there (Figure 9(a)) indicates a reasonable agreement in these data which for the purpose was deemed adequate; maximum salinity determined during this phase from bottle samples was 29.75°/oo (consec 75) and 29.30°/oo with the field salinometer (consec 30). The distribution in time of the temperature at this location (Figure 9(b)) does not indicate the inversion observed in the halocline during Phase I, although a slight secondary maximum, to -0.4°C, occurred below the halocline at consec number 30 and less at the other numbers. At consec 11 an increase to -0.1°C occurred close to the bottom, an increase which appears to have been general at locations farther up the harbour.

Phase III (Dec. 14, 1962 - May 1, 1963). The salinity observations made at location 50 (Figure 1(c), inset 3) are presented here in Figure 2 and described on page 7 where it was shown that the surface layer increased from a depth of 10 feet to 18 feet. Dick (1961, his Figure 1(b)) showed that the air bubbler was positioned about the wharf in this range of depth, so that for part of the period the bubbler was operating within the halocline depth and consequently a flux of salt to the surface would occur. There is some evidence that this influence was observed. Salinity observations at a location (51) close to the face of the wharf (Figure 10) indicate that near-surface values there were higher than observed in the surface layer away from the wharf (Figure 2). Also the observed gradual decrease of salinity close to the wharf indicated in Figure 10 is compatible with the observed increase in thickness of the surface layer relative to the depth of the bubbler, i.e., there would be progressively less upward salt flux as the layer extended deeper than the bubbler. This increase of depth of an isothermal (0°C) surface layer is indicated in the bathythermograph observations made during this phase (not shown here), but there is no indication in the BT observations close to the wharf of an effect which might be due to the bubbler. A temperature inversion in the halocline does not appear in the BT data for this phase.

Phase IV (May 2-5, 1963). Salinity observations during this phase with in situ salinometers of two types (Figure 11) agree in general with the distributions toward the end of Phase III (Figure 2); in particular the depth and salinity of the surface layer indicated in all the material are the same. The temperature observations indicate a structure similar to that of Phase I (Figure 3) but without the marked temperature inversion within the depth of the halocline observed a year earlier. Temperatures at the maximum depth observed (45 feet or 13.7m) were between -0.4 and -0.3°C and suggest some warming of the deeper water during the period since Phase II of about 0.3C°. The warming is compatible with the observed decrease in salinity of the deeper water during the interval between Phases II and IV, assuming that it is surface water which is mixed into the deeper water; however, the increase of temperature is slightly larger than should have occurred under this circumstance alone.

From MV "Richardson" (July 26 - Sept. 16, 1963). In addition to the series of BT lowerings at station 6 described earlier in the assessment of the seasonal heat storage (Figure 3) two series of salinity observations were made over the area, one at the end of July the other at mid-September. Some of the latter observations were utilized to prepare Figure 2 and indicate an increase of surface salinity and a salinity

Figure 9(a). Salinity (°/oo) at location 28 during Phase II from consec numbers 5, 11, 30, 40, 45, 77 and 79. A number (not shown) of the deepest salinity observations appear to be in error (they are unreasonably low) and it is surmised that the cell was located on or too close to the bottom. Shown is the envelope of values from the portable salinometer as well as open circles from reversing bottle samples at location (consec number 31).

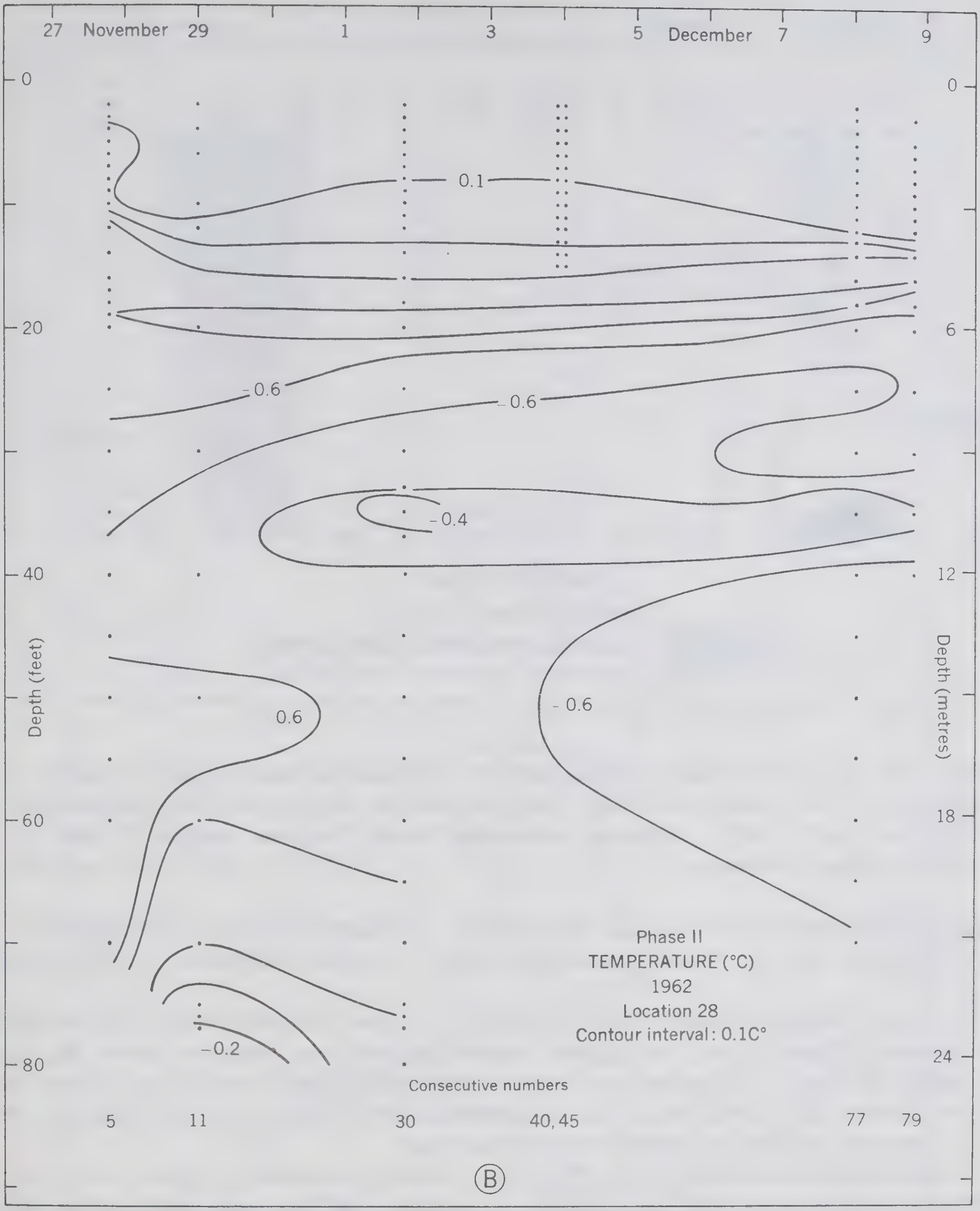

Figure 9(b). Temperature (°C) distribution with depth and time. Same detail as Figure 9(a). The deeper temperature values at consec number 11 may be in error, but see text.

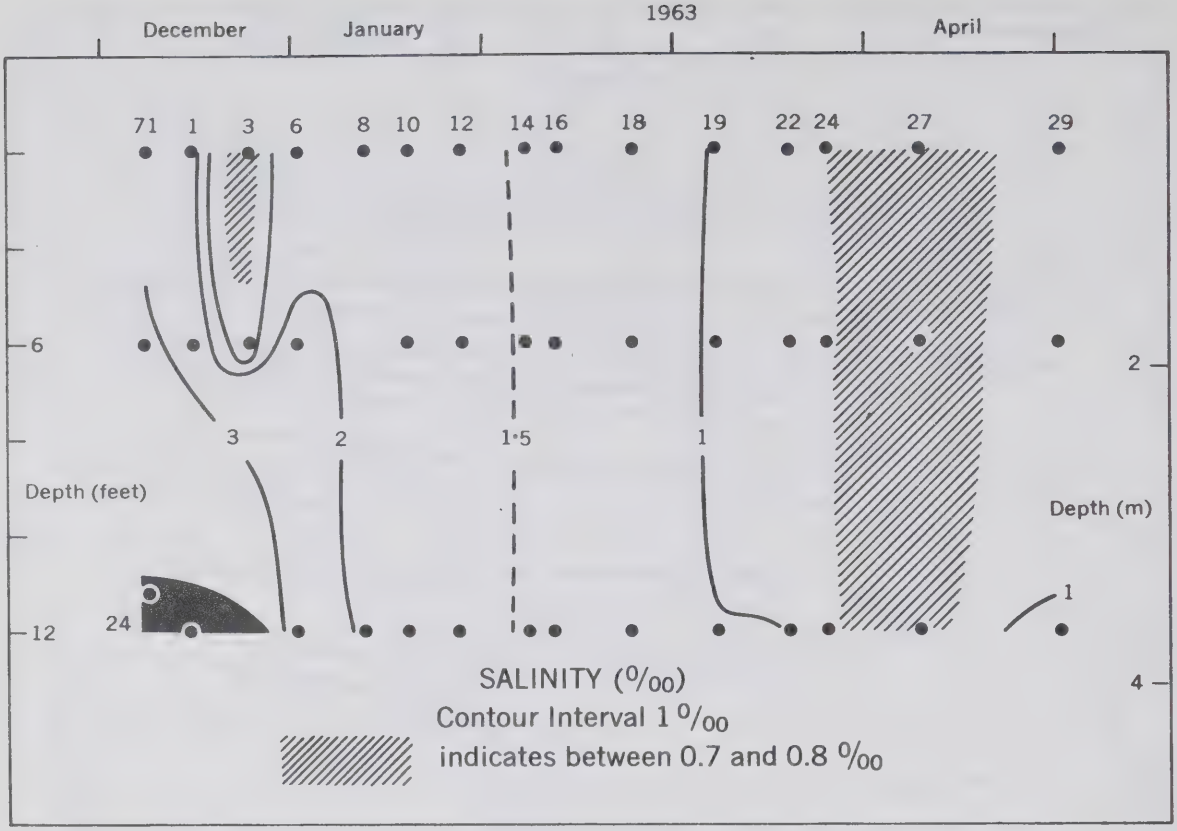

Figure 10. An interpretation of the salinity distribution based on data obtained close to the dock (location 51) with reversing bottles during the period December 7, 1962 to May 1, 1963. Data used comprise Phase II consec number 71 and Phase III consec numbers 1, 3, 6, 8, 10, 12, 14, 16, 18, 19, 22, 24, 27 and 29.

decrease in the deeper water during the interval. In Kugmallit Bay at "Richardson" station 22, depth 5m, the water was isohaline at 2°/oo on July 29 and 31°/oo on September 13.

In July slightly higher salinity, over 5°/oo, was observed inshore of station 22 at the surface (Figure 12(a)); the highest surface salinity was observed within the harbour toward the head. In September (Figure 12(b)) values decreased sharply from the 31°/oo at station 22 to less than 5°/oo in Eastern Entrance; again a relatively high value, 20°/oo, occurred within the harbour toward the head.

In July the highest salinity, 29.9°/oo, within the harbour (Figure 13(a)) was observed at station 11 at 20m and a number of values to 29°/oo were observed at about the same time. In mid-September a value greater than 29.5°/oo (Figure 13(b)) was not observed and the region of highest salinity had been 'displaced' toward the entrance since July. The decrease of salinity in the deeper water interpreted from Figure 2 might be due to such a water movement, although the nature of the exchange during the period of runoff could lead to reduced salinity in the deeper water (see page 27).

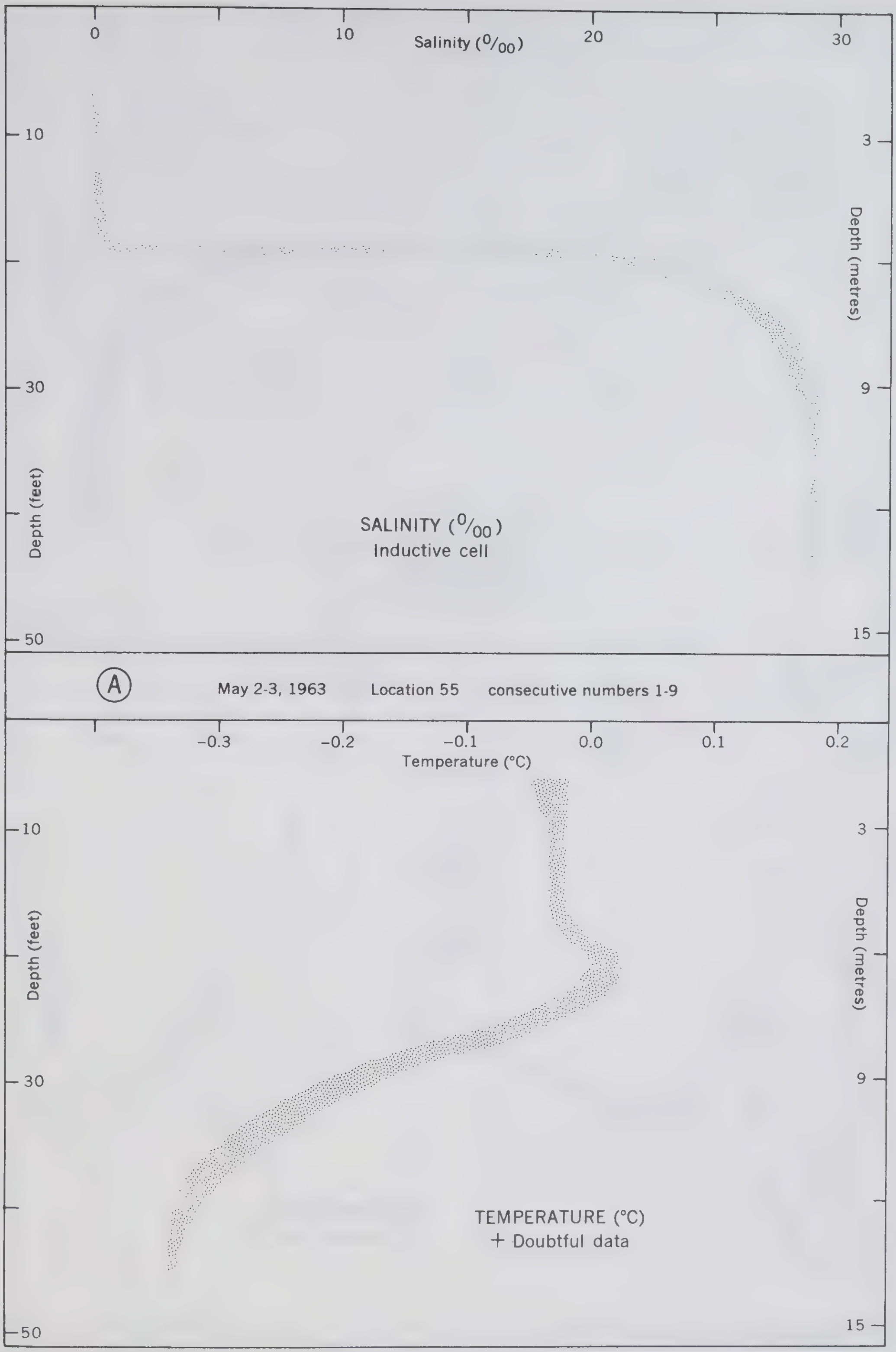

Figure 11(a). An interpretation of temperature and salinity data observed on Phase IV in Tuktoyaktuk Harbour at location 55 consec numbers 1-9, May 2-3, 1963. Also indicated are the salinity observations made at the same position (location 28) on May 1 of Phase III.

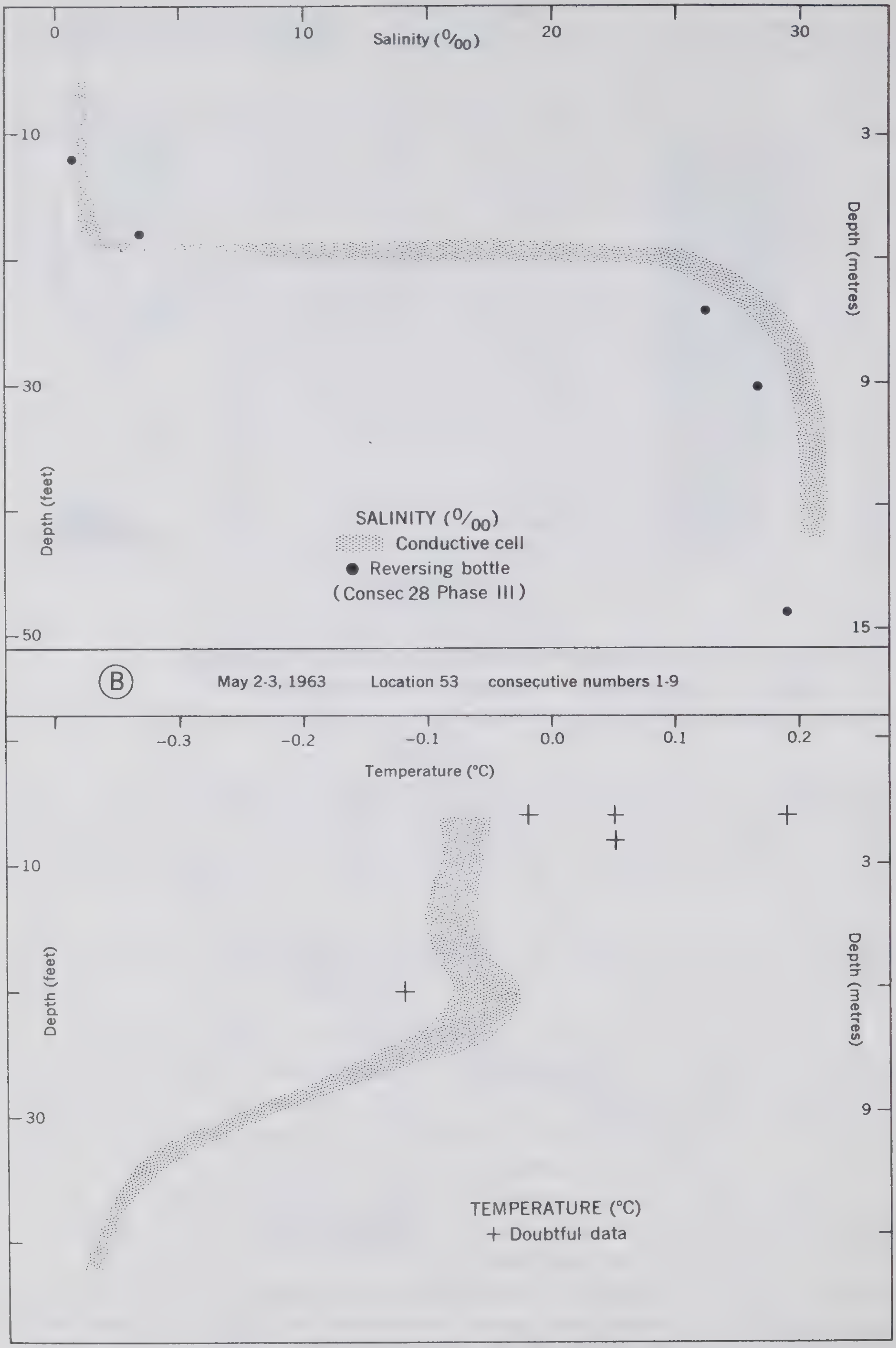

Figure 11(b). Salinity and temperature at location 53 consec numbers 1-9, same dates as Figure 11(a).

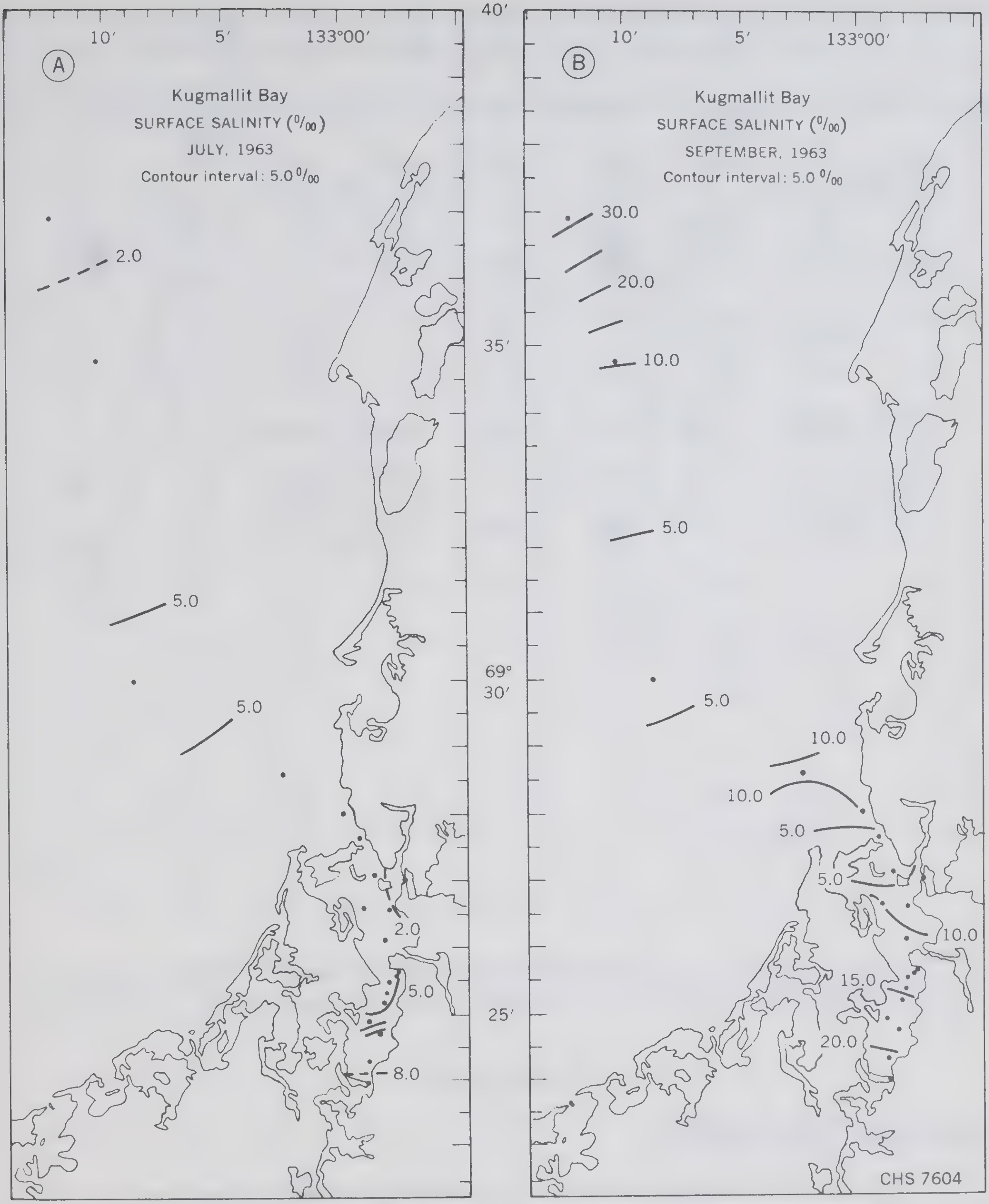

Figure 12. Surface salinity (°/₀₀) in Tuktoyaktuk Harbour and Kugmallit Bay from MV "Richardson" observations in 1963. (a) July 26–29. (b) September 13–16.

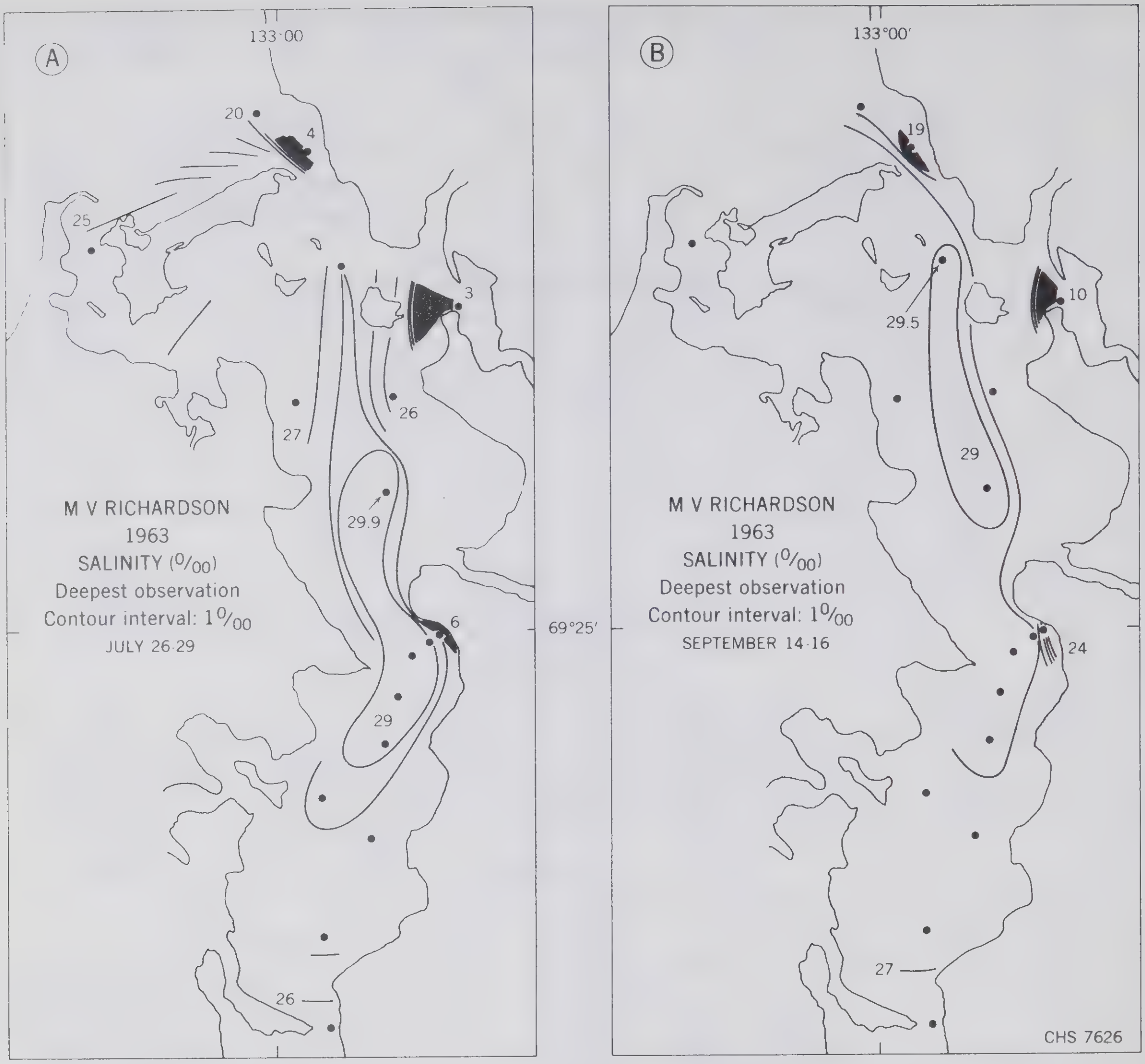

Figure 13. Salinity (°/oo) in Tuktoyaktuk Harbour at depth of deepest observation from MV "Richardson" observations in 1963. (a) July 26-29. (b) September 13-16.

DISCUSSION

A comparative winter heat loss

The radiative and flux terms of the heat budget equation (Sverdrup, et al., 1942, p. 100) were evaluated for a column of water in Tuktoyaktuk Harbour at each midmonth during the 1962-63 winter. The terms were estimated under two surface conditions, one for a normal ice and snow cover (Table II), the other for open water (Table III), and followed a similar derivation for a region in Hudson Bay (Barber, 1967). For the purpose here and within the stated conclusions, the two major characteristics of the budget, the value of the sensible heat storage and the difference in heat loss with and without an ice cover, are of such size that there would be little point in providing detail of the estimate beyond that given below and in the tables. The meteorological data were obtained from publications of the Meteorological Branch, Canada Department of Transport.

Table II

Calculated midmonthly values, October to May, of terms of energy budget (g cal cm^{-2} day^{-1}) under conditions of normal ice and snow cover. Net loss is sum of $Q_b + Q_e - Q_s + Q_r + Q_h$.

	Oct	Nov	Dec	Jan	Feb	Mar	Apr	May
Q_{os}	100	15	0	3	67	225	470	690
C	8.5	5.0	6.1	3.6	4.7	4.3	7.0	8.0
Q_s	43	13	0	3.0	60	209	322	364
Q_r	14.5	12	0	1	44	154	209	171
T_a	-3.6	-17.8	-21.3	-29.9	-28.1	-27.3	-12.1	-2.3
e_a	4	1	1	0.3	0.4	0.3	2	4.6
e_w	5	1	1	0.4	0.5	0.5	2	5
U_5	7	6.3	7.9	5.6	6.3	5.4	6.3	4.9
Q_b	74	87	84	87	79	83	86	91
Q_e	21	17	11	3	3	7	12	18
Q_h	-	-	-	-	-	-	-	-
net loss	66.5	103	95	88	66	35	-15	-84

Q_{os} = mean solar radiation incident on the sea surface under a clear sky (Mateer, 1955).

C = daylight cloud cover in tenths of sky covered.

Q_s = estimated solar radiation incident on the sea surface.

Q_r = mean value of the solar radiation reflected from the sea surface.

T_a = air temperature (°C).

e_a, e_w = vapour pressure (mb) at the sea surface and at a height of 'a' metres.

U_5 = wind speed (m s^{-1}) at a height of 5 metres.

Q_b = effective long wave back radiation.

Q_e = evaporation

Q_h - sensible heat conduction.

Table III

Calculated midmonthly values, October to May, of terms of the energy budget (g cal cm^{-2} day^{-1}) under open-water conditions. The values of Q_s and U_5 are the same as in Table II.

	Oct	Nov	Dec	Jan	Feb	Mar	Apr	May
Q_s	43	13	0	3.0	6.0	209	322	364
Q_r	5	12	0	1	28	48	47	42
T_a	-3.6	-17.8	-21.3	-29.9	-28.1	-27.3	-12.1	-2.31
T_s	0	0	0	0	0	0	0	0
e_a	4	1	1	0.3	0.4	0.3	2	4.6
e_w	6	6	6	6	6	6	6	6
U_5	7	6.3	7.9	5.6	6.3	5.4	6.3	4.9
Q_e	108	245	319	243	271	234	190	54
Q_b	82	184	228	188	203	185	143	33
Q_h	118	523	787	780	828	688	354	53
net loss	270	951	1334	1209	1207	946	412	-182

T_s = surface water temperature ($^{\circ}$C).

The tabulations of Tables II and III indicate that the heat loss under the condition of open water is 10 to 20 times that under the condition of an ice cover. During the period October to April the total loss of heat over an open area $20m^2$ would be 3×10^{10} g cal.

The amount of sensible heat in the water column, assuming the freezing point as the origin for the estimate, was calculated* to be 1600 g cal cm^{-2} in the deeper water adjacent to the bubbler site. An estimate of the total sensible heat in the harbour followed and was determined to be two to three orders of magnitude greater than the total heat loss at an open-water site of area mentioned above. As the area is about the size maintained by the air bubbler it may be concluded that if the heat loss was met out of the total mass of water the resulting change of temperature would not have been measurable.

*For the estimate an approximation to the temperature distribution observed at location 7 during April 27 - May 6, 1962 (Figure 4) was used such that in the depth interval 6m to 21m the average temperature was -0.4°C and the freezing point -1.5°C. It was assumed that significant sensible heat did not exist at depth shallower than 6m.

Some consideration was given the possibility that the heat loss was provided through formation of frazil ice at the bubbler site. Williams (1961, p. 7) noted that frazil formation would result when the "thermal reserve is exhausted" and suggested that such formation might be used to advantage, apparently, through utilization of the bubbler technique. It was envisaged that the frazil ice would be advected away from the site by the action of the bubbler and would become part of the existing ice cover. If the total loss of heat estimated for the site at Tuktoyaktuk were met in this way an amount of about 4×10^8 grams of ice would form. This would be a volume (assuming an ice density of 0.9 gm cc^{-1}) of $4 \times 10^2 m^3$ or a thickness of 0.02 cm over the area of the harbour. An indication that a portion of the heat loss at the bubbler site was met in this manner was given by Ince (1962, p. 5) from ice thickness measurements; apparently frazil ice deposited at the bottom surface of the ice cover close to the site.

Although this energy budget does not provide information of specific value to the problem of bubbler operation, it is possible that Tuktoyaktuk Harbour could prove a useful site for further experiment. For example, it is conceivable that an area of open water could be maintained for a time and of a size that the heat loss would lead to measurable change. Other experiments might be based on the peculiar water structure under the ice cover (fresh and saline water in the same column) and might consider the influence of a bubbler, or other device, operated below the halocline in the deepest part of the harbour. A redistribution of the water could occur which, if ascertained, might provide further insight into specific problems of bubbler operation in the control of ice cover. A difficulty is that of the coupling of the water of the harbour and of Kugmallit Bay, i.e., to what extent and in what manner does exchange occur? Some consideration is given to this in the next section where it is shown that tidal exchange is considerable. The definition of an experiment must recognize this; indeed, it is possible that stronger evidence in the data of the bubbler effect does not exist because the effect is removed by this tidal exchange.

An elementary examination of the exchange mechanisms

As is usual in Arctic areas it is the salinity data which provide the main material for assessment and definition of the structure and of the dominant processes. In the following section an attempt is made to establish the nature of the exchange mechanisms and to define qualitatively the influence of each as interpreted from the salinity data.

Without ice cover. During the summer period of ice and snow melt and runoff an estuarine type of circulation likely occurs. This would comprise a seaward flow of mixed fresh and salt water in a surface layer and a compensating subsurface flow of saline water into the harbour. It seems possible that during times of maximum runoff the subsurface flow may not provide a salt balance so that part of the salt in the surface layer would be derived from the deeper water. This would explain the apparent decrease of salinity in the deeper waters during the summer. However, by mid-September the runoff is probably at a lower level so that the condition would not occur. At this time the salinity immediately seaward of the harbour can exceed 31°/oo and it would seem probable that a high salinity water moves into the harbour due to the coupling of the estuarine circulation. However the data are not sufficient to confirm this interpretation. One other exchange mechanism appears capable of providing the required coupling and the evidence which allowed some evaluation of the nature and significance of the mechanism was obtained after freeze-up.

With ice cover. An interesting aspect of the salinity data observed from the ice cover is that a portion was obtained at closely spaced depth intervals. Examples described indicate the existence of an extremely intense halocline bounded at the top by a near discontinuity between the halocline and the homogeneous surface layer, the latter being nearly devoid of salt. The condition prevailed even though the amount of fresh water in the surface layer was increasing, that is the layer was increasing in thickness without an increase of salinity. It is concluded that very little mixing between the layers was occurring. This is of interest for it suggests little shear and hence a small advective term; quite a different situation than is usually encountered. It seems that the fresh water which occurs in the harbour at this time, or much of it, is associated with that occurring to seaward and enters from that direction. As a result an estuarine type of circulation is not generated and a net outflow in the surface layer with return flow and upward transport does not occur. Also, as the water of the surface layer at this time is virtually fresh, surface cooling at temperatures close to freezing would lead to stability as in a lake, rather than instability as in the ocean. Furthermore, as the salinity is low the amount of salt made available to the surface layer through freezing would be negligible. Thus, the evolution* of the surface mixed layer through the winter would not relate to the formation of denser water at the ice-water interface. But the increase of fresh-water content, that is, the increase in depth of the mixed layer, was accompanied by a decrease of salinity at depth below the halocline. It is believed that both results are due to a tidal effect over the period of duration of the ice cover. A somewhat similar influence is believed to have been observed in the distributions in Fury and Hecla Strait in 1960 (Barber, 1965), and it is here conjectured that the peculiar distributions in Tofino and Bedwell Inlets described by Pickard (1963, p. 1128) may also have been the result of a tidal influence.

The essential feature of the influence is that the water of the ebb is not entirely the same water which comprised the flood, although the volume of each is the same. The extent to which such a volume exchange occurs at Tuktoyaktuk is determined by a number of factors including the amplitude of the tidal current, shape of the basin, degree of vertical mixing, stability and bottom roughness. The influence of the exchange is quite marked initially because it takes place in the circumstance that the surface water of Kugmallit Bay is maintained as fresh water while the surface water of the harbour is saline. Subsequently the surface water of the harbour becomes fresh so that although the volume exchange likely continues unaltered a result is not as apparent.

A loss of sensible heat would be associated with this loss of salt as the salt water is warmer than the freezing point and the fresh water is at the freezing point. The effect would lead to the existence of slightly higher temperatures in the deeper water by the end of the period of ice cover. This occurred (Phase II to Phase IV) but to greater extent than would be expected from the observed salinity reduction. The explanation may lie in the fact that localized areas of relatively warm water at depth indicated early in the period of ice cover (Figure 9(b), consec 5) become mixed into the mass of deeper water by the end of the period of ice cover.

---

*This feature as well as the lack of an estuarine type of circulation during the period of ice cover are considered as further evidence that the environment at Tuktoyaktuk may be particularly suited to experiment based on the distribution of salinity.

A model of the exchange. For the purpose of the discussion in this section it will be assumed that for periods multiples of tidal a net volume transport due to tidal effects does not occur. It will also be assumed that gradients of pressure due to wind stress, variations of atmospheric pressure and density differences are so small as to be not significant.

It would appear that of those factors which influence the exchange the amplitude of the tidal current and the shape of the basin would be most important. At the entrance, the flood movement into the harbour is surface water of Kugmallit Bay, while the ebb movement out of the harbour comprises both* the surface and deeper water there. Thus, the purely tidal advective motions would alone lead to an exchange.

Within the harbour, exchange would be accomplished by tidal turbulence and mixing, including relatively large scale and persistent (recurring) eddy formations resulting from horizontal gradients due to the tide. Tidal mixing would be influenced by the density of the water of the flood relative to that in the harbour. Whether this difference can be sufficiently large to cause significant variation in the size of the volume exchange per tide is not directly evident in the observations. It will be suggested that in at least one circumstance the volume exchange could be very much larger than usual.

First, it is emphasized that the non-time-dependent factors determine that a definite volume exchange will take place each tide. This will be expressed as a fraction of the flood volume retained in the harbour. In the event that all of the water in the region was the same, that is, all fresh water or a water at some particular salinity, the exchange would occur but of course would not be recognized through measurements of salinity. If salinity differences exist an exchange factor could be established in terms of changes of concentration each tide. However, the situation at Tuktoyaktuk is somewhat simpler as it is possible to estimate the volume exchange directly from the change of fresh-water content. For example, it was the interpretation of Figure 2 that the volume of fresh water in the harbour at the end of December was about twice the amount there at the beginning of December. The actual volume increase appears to have been $2 \times 10^7 m^3$**, which over the interval of 31 days of semidiurnal tide indicates a calculable retention of fresh water per tide (actually $3 \times 10^5 m^3$). A further calculation allows the estimate that at least one twelfth of the intertidal volume is exchanged each tide.

During the period January to April, and after the depth of fresh water in the harbour attained sill depth, a much smaller increase in the amount of fresh water in the harbour is indicated. It is estimated that the actual increase over the total depth, assuming a base salinity of 30°/oo, was about 1m over the area. Thus a change in the rate of increase of fresh water occurred from 2m a month to 1m each 4 months, that is by a factor of 8, after sill depth was attained. During this entire period it is considered that the exchange factor remained unchanged at one twelfth.

---

*The data upon which Figure 7 is based is considered as qualitative evidence that this occurs.

**The area is about $10^7 m^2$ and the depth increase of fresh water was about 2m.

Were the net seaward flux of salt to continue the harbour would eventually become salt free. This does not occur because the fresh water from the Mackenzie River flowing eastward past the harbour entrance in winter is replaced in summer by water of oceanic salinity. In this circumstance a net salt flux into the harbour could occur due to tidal exchange. However, at this time a net volume transport out of the harbour occurs due to surface runoff into the harbour which in turn could lead to a movement of salt into the harbour. It does not appear possible to determine from present data the extent to which the estuarine circulation couples the harbour water to that of Kugmallit Bay, so that the relative significance of the tidal and estuarine exchange mechanisms cannot be assessed. It does appear, however, that in a steady state situation in summer (constant runoff and constant salinity distribution in Kugmallit Bay) a portion of the salt balance in the harbour could be due to tidal exchange. Indeed it seems possible that in general the subsurface or up-estuary flow required to maintain the salt balance in an inlet may be due entirely to the tidal exchange mechanism.

In Tuktoyaktuk Harbour we recognize that in late summer and autumn a net salt flux occurs into the harbour so that annually a balance is likely maintained. At some time during this period the water of the flood may comprise a water heavier (saltier) than in the harbour. Were all the flood retained through exchange with deeper water, complete exchange would require about 10 tides, i.e., about 5 days. The calculation is useful only in that it suggests that extreme change could occur through a single extreme event, such as a storm.

According to the Pilot (Canada. Dept. Mines and Tech. Surv., 1961, p. 18) 'westerly gales have caused a high tide to rise from 4 to 5 feet (1.2 to 1.5m) above normal'. The volume of water contributing to this increase of sea level would come from Kugmallit Bay where it is known that the salinity of the water varies with annual period from near zero to at least $31.4^{\circ}/_{\circ\circ}$. The high-salinity water occurred within 18 km of Tuktoyaktuk and it seems likely that water of higher salinity would be observed even closer to the harbour on occasion. Were this circumstance to coincide with a 'westerly gale' then a significant portion of the volume increase of the harbour water could comprise a high-salinity water which might in turn be sufficiently salt to replace the deeper water there. The most likely time for the occurrence of such a circumstance seems to be during September and early October and while adequate sea-level data (e.g., Canada. Dept. Mines and Tech. Surv., 1964) and meteorological data (e.g., Canada. Dept. Transport, undated) appear to be available for the period, oceanographic data are not.

The situation then with regard to the influence of a storm is similar to that for the estuarine circulation in that neither can be evaluated from present data. On the other hand, the extent to which the water of the harbour is coupled to that of Kugmallit Bay by a secondary effect of the tide is sufficiently well indicated that a quantitative estimate of the resulting exchange is possible. The emphasis in the result lies in the fact that a marked variation with a period of a year occurs in the water in Kugmallit Bay. This result, in turn, is due to a secondary effect of the wind of annual period in the presence of a winter ice cover and the proximity of a large river and the ocean.

ACKNOWLEDGMENTS

Mr. W.J.B. Kelly assisted with data preparation and Mr. M. Isabelle provided the line drawings. Examination of terms of the energy budget was carried out by Messrs. R.A. Clarke and T.B. Moodie while summer assistants. Mrs. Annette Regimbald typed drafts of the manuscript. Dr. G.L. Pickard critically reviewed the manuscript.

REFERENCES

Barber, F.G. 1965. Current observations in Fury and Hecla Straits. J. Fish. Res. Bd. Can. 22(1) : 225-229.
1967. A Contribution to the Oceanography of Hudson Bay. Canada. Dept Energy, Mines and Res. Mar. Sc. Br. MS Rep. Ser. No. 4.

Brown, R.J.E. 1966. Relation between mean annual air and ground temperatures in the permafrost region of Canada. Proceedings Permafrost International Conference, Lafayette, Indiana, November 1963. NAS-NRC Pub. No. 1287 : 241-47.

Brown, W.G., G.H. Johnston, and R.J.E. Brown. 1964. Comparison of observed and calculated ground temperatures with permafrost distribution under a northern lake. Can. Geotech. J. 1(3) : 147-54.

Cameron, W.M. 1953. Hydrographic and Oceanographic Observations of Southeast Beaufort Sea 1952. Inst. Oceanog. U.B.C.

Canada. Dept Mines and Tech. Surv., Can. Hydrograph. Serv. 1958. Great Slave Lake and Mackenzie River Pilot. pp. 1-85.
1961. Pilot of Arctic Canada. 3 : 1-370.
1964. Water Levels 1963.

Canada. Dept Transport, Met. Br. Undated. Monthly Record Meteorological Observations in Canada for September and October 1963.

Dick, T.M. 1961. Description of air bubbler systems at Cambridge Bay and Tuktoyaktuk, NWT. Proceedings of the Symposium on Air Bubbling. NRC Canada. Tech. Mem. No. 70.

Dohler, G. 1964. Tides in Canadian waters. Unpublished. Canada. Dept Mines and Tech. Surv.

Ince, S. 1962. Winter regime of a tidal inlet in the Arctic and the use of air bubblers for the protection of wharf structures. Eighth International Conference on Coastal Engineering, Mexico. pp. 521-532.

Kelly, W.J.B. 1967. Tuktoyaktuk Harbour - a data report. Canada. Dept Energy, Mines and Res. Mar. Sc. Br. MS Rep. Ser. No. 7.

Lachenbruch, A.H. 1957. Thermal effects of the ocean on permafrost. Bull. Geol. Soc. Am. 68 : 1515-29.

Mackay, J. Ross. 1963. The Mackenzie delta area, N.W.T. Canada. Dept. Mines and Tech. Surv. Geogr. Br. Mem. 8 : 202.

Mateer, C.L. 1955. Average insolation in Canada during cloudless days. Can. J. Technol. 33 : 12-32.

Pickard, G.L. 1963. Oceanographic characteristics of inlets of Vancouver Island, British Columbia. J. Fish. Res. Bd. Canada, 20(5) : 1109-1144.

Pounder, E.R. 1961. Thermodynamic considerations on the use of air bubbling systems in salt water. Proceedings of the Symposium on Air Bubbling. NRC Canada. Tech. Mem. No. 70.

Sverdrup, H.U., M.W. Johnson, and R.H. Fleming. 1942. The Oceans. New York. Prentice-Hall.

Williams, G.P. 1961. Thermal regime of lakes and rivers with reference to air bubbling systems. Proceedings of the Symposium on Air Bubbling. NRC Canada. Tech. Mem. No. 70.

MANUSCRIPT
REPORT SERIES
No. 10

Structure, Dynamics and Chemistry of Lake Ontario

Investigations Based on Monitor Cruises in 1966 and 1967

H. E. Sweers

1969

Marine Sciences Branch
Department of Energy, Mines and Resources
Ottawa, Canada

Manuscript Report Series

No. 10

STRUCTURE, DYNAMICS AND CHEMISTRY OF LAKE ONTARIO

Investigations Based on Monitor Cruises in 1966 and 1967

H. E. Sweers

1969

The Queen's Printer, Ottawa, Canada, 1969

ABSTRACT

Data obtained from a series of monitor cruises on Lake Ontario during the 1966 and 1967 field seasons are analyzed in detail, and the findings placed in the context of existing knowledge. After a brief and fairly general outline of the thermal regime throughout the year, the reliability of the data is discussed, employing an infrequently used technique to determine the relation between natural (geographical or temporal) and random variability in the data. The thermal structure and its temporal changes during late spring, summer and early fall are then described in more detail, with special emphasis on development, intensity and decay of the stratification, upwelling, regional temperature anomalies in relation to wind and river flows, and persistent deviations of the actual structure from an equilibrium situation defined as the expected structure in the absence of external forces. The results are used extensively to perform calculations on water movements, response times to external forcing conditions and mixing processes in the lake.

Rainey's flushing model is refined, predicting a 20 year response time of the composition of lake water to a change in the input concentration of a conservative parameter. A new method to calculate the vertical coefficient of eddy diffusivity in the thermocline layer is developed, and compared with a classical method. K_z is found to be approximately 0.12 cm^2/sec in the layer of maximal vertical temperature gradient. An attempt is made to use geostrophic calculations to define water movements, and it is found that the method has only limited applicability; transports deduced from the calculations are 5 to 10 times too large. Seasonal changes in heat content are calculated and used to draw conclusions on advective water movements within the lake.

The horizontal and vertical distributions and seasonal variations of oxygen, specific conductance, pH, total alkalinity, hardness and chloride are studied in relation to the thermal structure, and persistent local anomalies are pointed out. It is found that these are usually surprisingly small in areal extent, which supports one of the major conclusions of this report: For the period studied, that is for the months of June through October, the lake is essentially well mixed horizontally, and there is little or no evidence of a confined eastward transport along the southern shore of water carrying with it a good percentage of all admixtures entering the lake from that side.

CONTENTS

APPENDICES

LIST OF TABLES

LIST OF FIGURES

LIST OF SYNOPTIC CHARTS

(All in Appendix F)

1. INTRODUCTION

1.1 General Remarks

During the summers of 1966 and 1967 the Canada Centre for Inland Waters, Department of Energy, Mines and Resources, undertook an intensive program of limnological cruises on Lake Ontario. The cruises were organized in close cooperation with other branches of the same department and with the Public Health Engineering Division of the Department of National Health and Welfare. In both years a regular series of monitor cruises covering the whole lake were made at two-week intervals, sampling such parameters as temperature, oxygen, specific conductance, pH, hardness, chloride, total alkalinity, various nutrients, turbidity and some bacteriological parameters, at a number of standard depths. The field seasons extended from early June to late September in 1966 and from mid-June to late October in 1967, and the ships used were the M.V. Brandal and the M.V. Theron respectively.

The present report contains the results of an extensive literature survey and an analysis of data sampled in 1966 and 1967. In the first chapter the thermal regime of the lake is discussed in general terms; it serves as a background for later, more detailed discussions. In Chapter 2 the methods of sampling and analysing the data are outlined and their representativeness discussed. The thermal regime during late spring, summer and early fall then is worked out in more detail, paying special attention to such phenomena as stratification, upwelling and persistent local anomalies in the temperature structure. In Chapter 4 seasonal variations in heat content and the importance of internal, advective water movements in the redistribution of heat are discussed. This is followed by a general chapter on the horizontal and vertical distributions of and seasonal changes in the concentrations of various chemical parameters. The major function of this chapter is to illustrate the close relationship between the distributions of temperature and of chemical parameters, leading to some conclusions on circulation and mixing processes in the lake. In Chapter 7 the results of the foregoing chapters are used for some numerical calculations on vertical eddy diffusivity in the thermocline region, geostrophic currents, and the response of the lake to varying wind conditions. Some remarks are also made on internal waves. Finally the residence time in the lake of a conservative parameter will be calculated using a model lake based on conclusions reached in earlier chapters.

To acquaint the reader with the shape and dimension of the Lake Ontario basin, a recently published bathymetric chart (Canadian Hydrographic Service) is reproduced in Fig. 0.

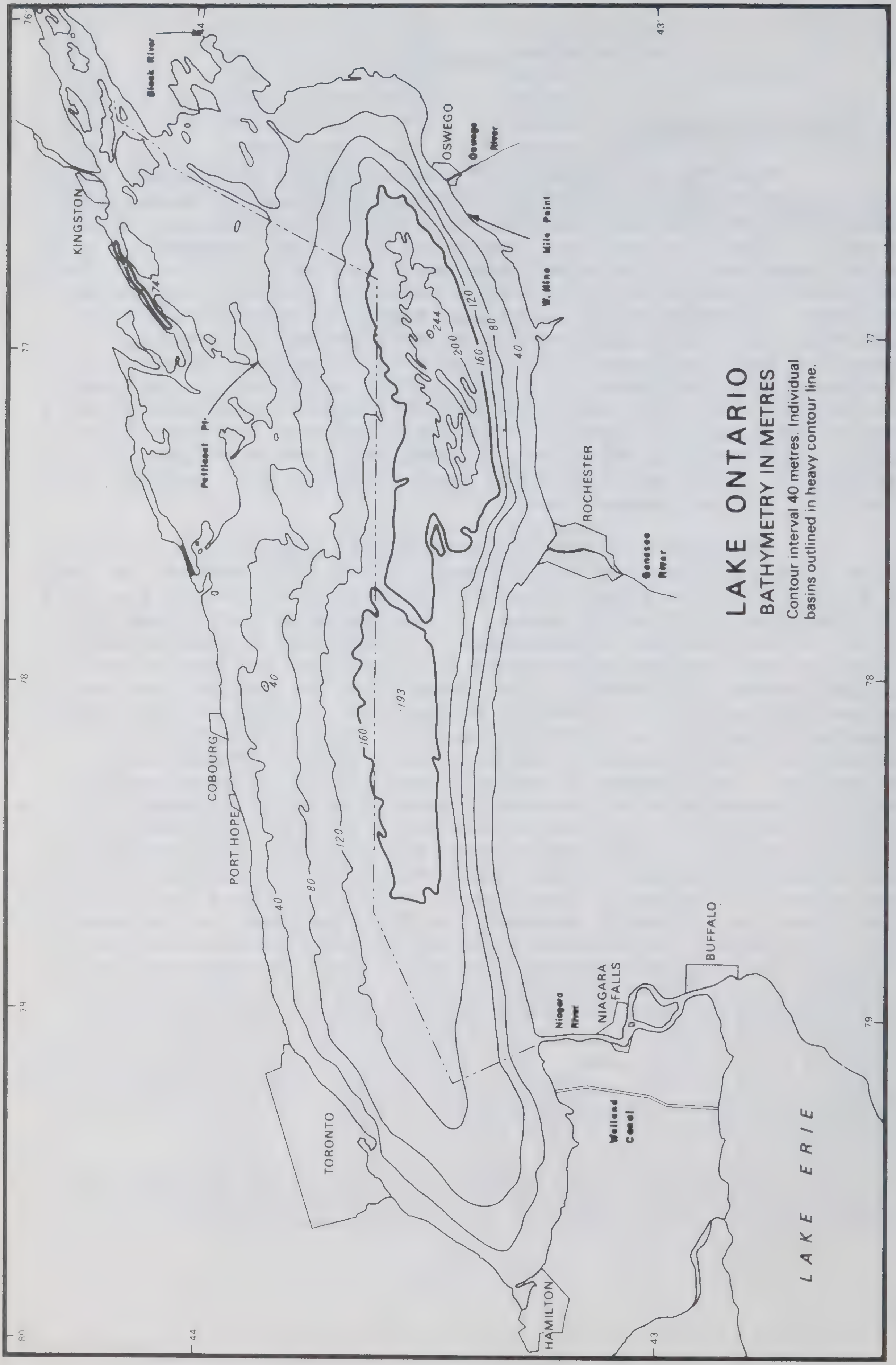
LAKE ONTARIO
BATHYMETRY IN METRES
Contour interval 40 metres. Individual basins outlined in heavy contour line.
KINGSTON
Black River
OSWEGO
Oswego River
W. Nine Mile Point
ROCHESTER
Genesee River
Petticoat Pt.
COBOURG
PORT HOPE
TORONTO
HAMILTON
NIAGARA FALLS
Niagara River
BUFFALO
Welland Canal
LAKE ERIE

Fig. 0

1.2 Thermal Regime[1]

In this section a general outline will be given of seasonal variations in the thermal structure of the lake, and some of the consequences for mixing and circulation briefly mentioned. The description is partially based on the results of a literature survey, partially on conclusions substantiated in the remainder of this report, where a detailed study is made of the data collected in 1966 and 1967.

1.2.1 Time Scale of Variations

The thermal structure of Lake Ontario is continuously in a state of flux. The greatest changes are generated by the yearly cycle; superimposed thereon are many types of periodic and random disturbances of higher frequencies. The yearly cycle itself, in turn, can be considered as a perturbation on long term variations induced by changes in climate and aging of the lake.

Long term changes in the lake temperature have not been studied in detail. Evidence from Lake Erie water intake temperature records seems to indicate a slight increase in mean surface temperature of about 0.2C° per decade over the past half a century (USDI, 1967-a), which is of the same order of magnitude as the increase in the yearly mean air temperature reported for stations in southern Ontario (Thomas, 1957). Further studies are necessary, however, before any natural long term trends can be established beyond doubt.

The higher frequency disturbances in the thermal structure, those which are superimposed on the yearly cycle, are induced by natural climatological variations. Strong winds, for example, may cause upwelling at the windward shores by causing a displacement of surface waters in an offshore direction, and, in summer, a tilting of the thermocline. This effect is most noticeable when the lake is well stratified; and it may, in summer, cause temporary local reductions in surface temperature by as much as 12 to 15C° to a low of 4°C. Changes in wind-stress or barometric pressure may set up both surface and internal oscillations. Dominant among the internal oscillations, which manifest themselves as fluctuations in thermocline depth over a range of up to 8 metres or more (Mortimer, 1968),

---

[1] The text for this subsection is partially taken from a paper submitted to the International Joint Commission by the present author.

are frequencies around and above the intertial period of 17.4 hours (Verber, 1966; Hamblin and Rodgers, 1967), and, to a lesser extent, those with a period of 4 to 8 days related to the passage of weather systems (Section 6.3). These oscillations are coupled with large internal displacements of the water and are, together with wind induced turbulence and residual currents, effective agents in increasing the intensity of mixing over the entire area of the lake.

The yearly cycle is the most important perturbation determining the thermal structure of the lake. It consists of two phases, a heating phase lasting roughly from mid-March to mid-September, and a cooling phase during the remaining part of the year (Rodgers and Anderson, 1961; Rodgers and Anderson, 1963). Processes taking place during these phases are mainly determined by, or related to, the heat balance. Changes in thermal structure throughout the year can be described in terms of the four seasons of a lake-climatology, which correspond in time roughly to the four calendar seasons.

1.2.2 Spring

The heating phase begins by mid-March. In winter all water cools to a temperature below the temperature of maximum density of 4°C. In late March or early April the surface temperature starts rising in the shallower, nearshore waters. The onset of spring can, in a lake-climatological sense, be defined by the appearance of a ring of water with a temperature above 4°C along the shores in late April or early May. The transition zone between these warmer nearshore waters and the colder mid-lake waters is called the thermal bar (Rodgers, 1966-I). This is a convergence zone, extending from surface to bottom, and it is characterized by strong horizontal temperature gradients at the lake surface (gradients up to 7C° over 100 metres have been reported by Rodgers, 1966-I). On the nearshore side of the thermal bar a thermocline develops, separating the rapidly warming surface water from the deeper water, which remains at a temperature close to the temperature of maximum density. The thermal bar moves gradually but steadily towards the middle until it dissipates, in late May or early June, due to heating of the mid-lake surface water to a temperature above that of maximum density. Relatively strong horizontal gradients around a temperature minimum somewhere over the deeper parts of the lake may persist until the end of June. Typical surface temperature distributions for these phases are shown in Figs. 1 and F. 4.

The duration of the thermal bar period has been estimated by Rodgers (1966-II) to be roughly 4 to 8 weeks. Data available to the present author seem to indicate that this estimate may be somewhat on the low side. Charts of the thermal structures in 1959 (Rodgers and Anderson, 1963), 1965 (Rodgers, 1966-II) and 1968 (DOT, Lakes Investigation Unit, airborne

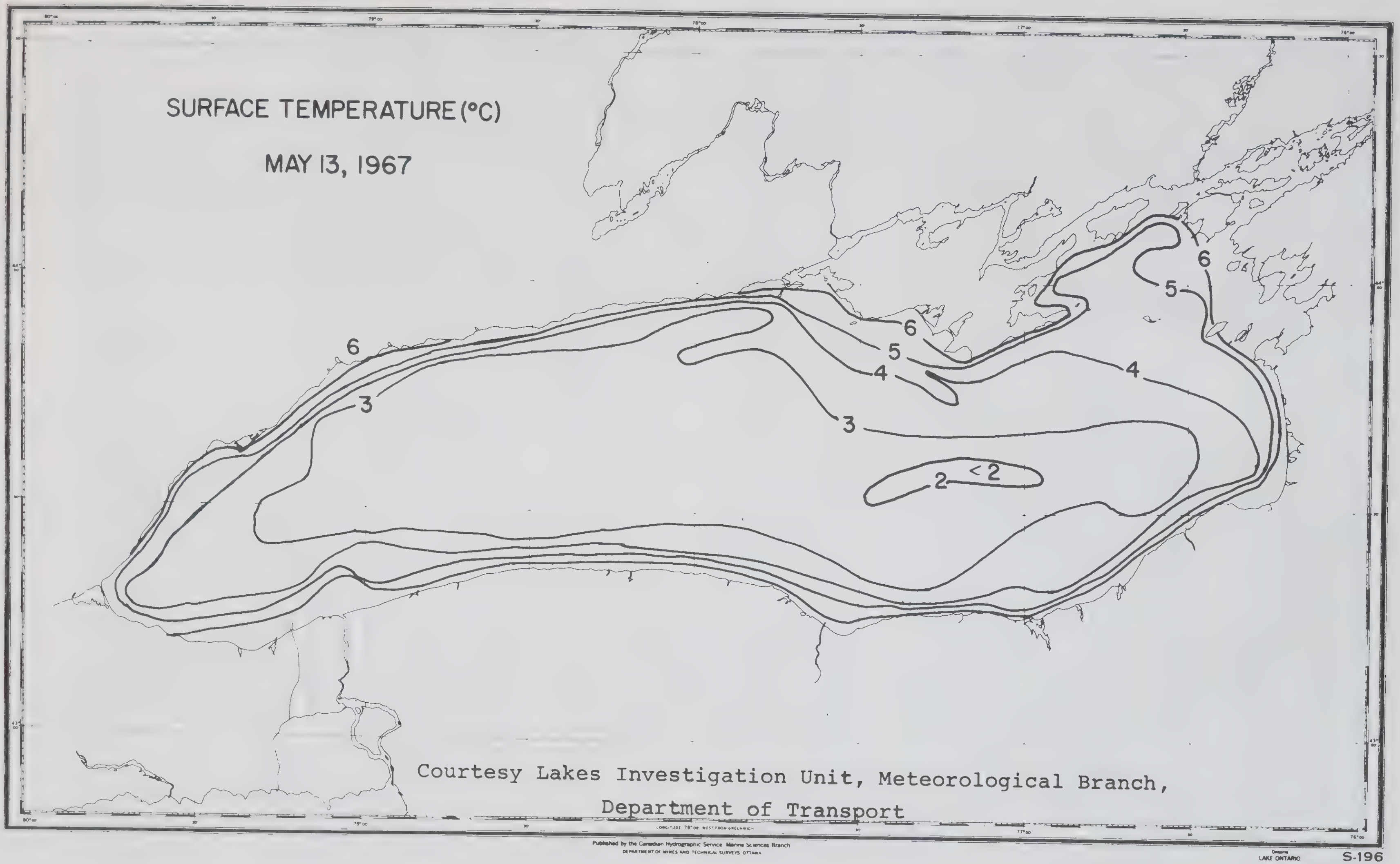

Fig. 1 Surface temperature distribution in early spring, shortly after development of the thermal bar.

radiometer charts) indicate for the onset of the thermal bar the approximate dates of May 1, May 10 and April 23 respectively and for the dissipation June 25, June 20 and June 14 respectively. The average duration of the thermal bar period for these years is about 7 to 8 weeks rather than 4 to 8 weeks. Upon dissipation of the thermal bar it still takes 3 to 4 weeks before the mid-lake temperature minimum disappears (Section 3.1.1).

On the offshore side of the thermal bar vertical mixing extends from surface to bottom, but on the nearshore side it is restricted to within the epilimnion (Rodgers, 1966-II) by the development of the thermocline. The areal extent over which pollutants entering the lake can be mixed is temporarily reduced when the thermal bar separates the nearshore waters from the main body of the lake. Its offshore movement, however, is fairly rapid and the nearshore ring of water will cover at least half the area of the lake within 4 weeks after the emergence of the thermal bar.

1.2.3 Summer

The beginning of the summer season in Lake Ontario can be defined by the disappearance of the offshore temperature minimum in late June, early July[1], by the combined effects of continued heating and advection of nearshore surface waters towards the middle of the lake. Surface temperature minima occurring during the summer are always related to upwelling phenomena and are, consequently, very close to shore. Typical summer distributions are shown in Figs. F.10 and F.23; the first of these is characteristic for a period with strong westerly winds, the second for a period with weaker or more variable winds. The isotherms tend to run in a ENE - WSW direction and are usually not related to the depth contours. The epilimnion is separated from the hypolimnion by a strong thermocline, the average gradient of which is between 1 and 2.5C° per metre over a temperature interval of 6 to 8C°, and the average depth of which is about 17 metres. The lake mean surface temperature does not vary much during the summer and usually remains between 18 and 21°C; the hypolimnion temperature varies slightly with depth, but, in this season, not with time, and ranges between 4.0 and 3.8°C. The downward rate of displacement of the thermocline is strongly dependent on wind induced turbulence, and thus on wind strength, and is, after its initial establishment, fairly low throughout the summer.

---

[1] The information presented in this paragraph is based on data from 1966 to 1967, but can be considered to be representative for conditions in most summers (Section 2.3 and Chapter 3).

Local characteristics of the thermal structure are to a large extent determined by the residual eastward component of the winds (about 150 cm/sec for Toronto International Airport). As a result the average surface temperature is about 6C° lower in the vicinity of Toronto than in the southeastern end of the lake, and the thermocline slopes by about 5.5 cm/km over the longitudinal axis of the lake, being on the average about 13 metres deeper near the southeastern shore than near Toronto. A typical summer-mean temperature distribution is shown in Figs. 13 and 18, which are based on data collected at two-week intervals in 1966 and confirmed by material collected in 1967. The mean surface temperature distribution is shown in Fig. 13, and the mean thickness of the epilimnion, as defined by the depth of the 10°C isotherm, is shown in Fig. 18.

Vertical mixing is confined to the epilimnion, which, in the summer, contains about 10 to 20 percent of the volume of water in the lake. Evidence from the horizontal distributions of temperature and of various chemical parameters suggests that the lake is horizontally well mixed throughout this period (Chapters 3 and 4). These distribution patterns show no evidence for the hypothesis that pollutants released along the southern shore are retained in an eastward water movement along this shore, but indicate that the water carried in this current becomes well mixed with the surrounding surface waters before it reaches the northeastern section of the lake.

1.2.4 Fall

The cooling phase starts in the second part of September. In particular, the onset of autumn in a lake-climatological sense is characterized by a relatively sudden drop in the mean surface temperature to a value well below 17°C, coupled with an increase in the rate of descent of the thermocline and a decrease in the intensity of the maximum vertical temperature gradient. This usually occurs after a period of hard winds in late September or early October, but the basic cause is the cooling and subsequent sinking of the surface water when the heating season gives way to the cooling season. Some of the processes taking place in autumn are similar to those in spring (Rodgers, 1966-I). Nearshore waters cool faster than those in the centre of the lake, eventually giving rise to the appearance of a "reversed" thermal bar in late fall, when nearshore waters have cooled to below the temperature of maximum density and mid-lake waters have remained relatively warm. The fall thermal bar, which has a much weaker gradient than the spring thermal bar, will again move in an offshore direction until it eventually dissipates in January, when all surface water has cooled to below 4°C. A typical temperature distribution for autumn shows the situation shortly before the emergence of the weak (reversed) thermal bar (Fig. 2).

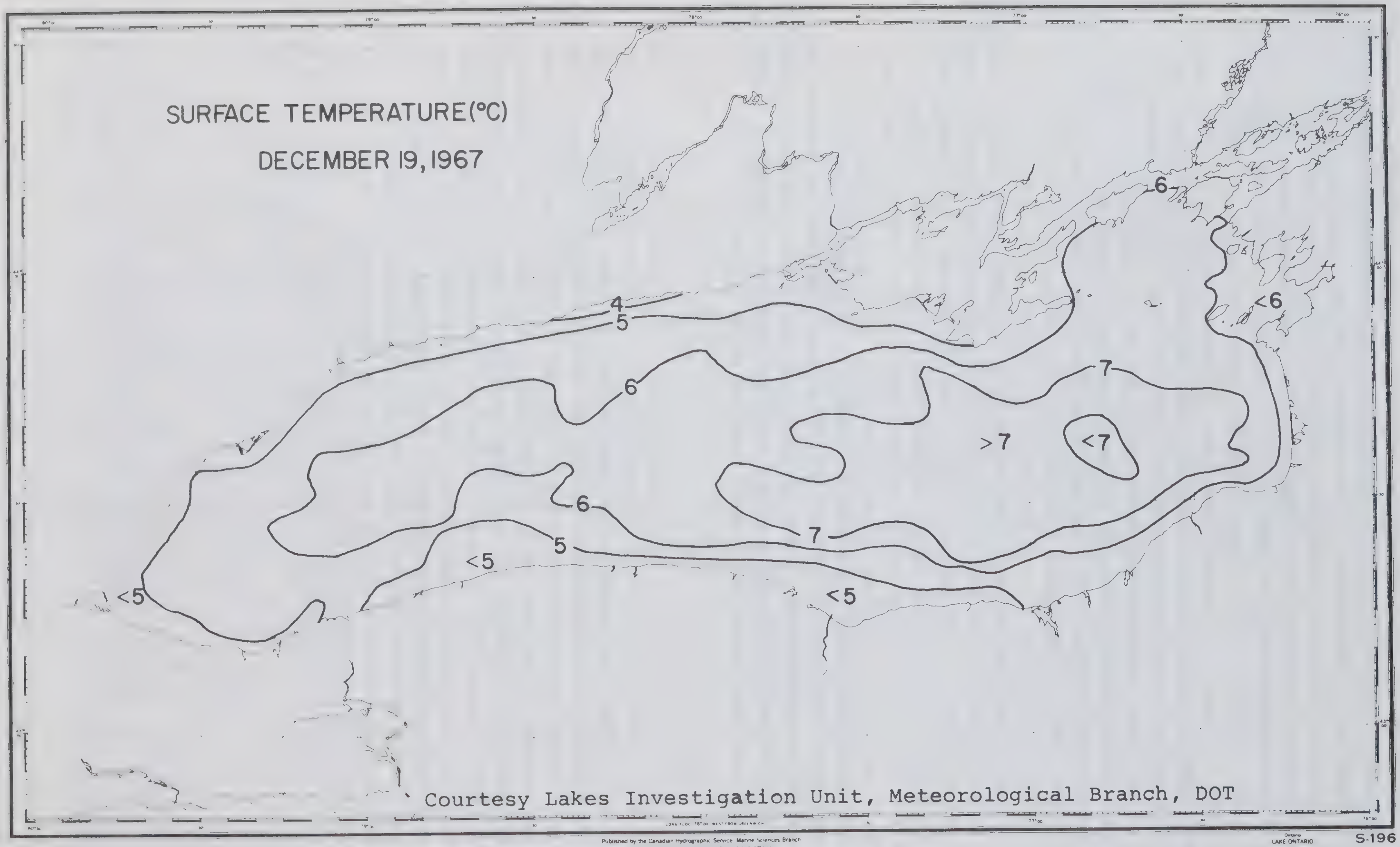

Fig. 2 Surface temperature distribution in fall.

The depth to which vertical circulation is effective increases with the rapidly increasing depth of the thermocline and reaches the bottom when the surface temperature drops to near the temperature of maximum density. The fall thermal bar may temporarily interrupt mixing over the total area of the lake, but its effect on the rate of dilution of a pollutant is even less important than that of the spring thermal bar. This is due to its lesser intensity as well as to the fact that water on the nearshore side of the fall thermal bar is not stratified.

1.2.5 Winter

The onset of winter can be defined, in a lake-climatological sense, by the cooling of all surface water to a temperature below 4°C. Surface isotherms tend to be parallel to the depth contours in this season and the water temperature is vertically uniform or increases slightly with depth (Rodgers and Anderson, 1963). Cooling thus proceeds by a loss of heat from all depths, and the temperature maximum occurs near or over the deepest part of the lake. Vertical circulation extends, at least occasionally, to a depth of 100 metres or more, as is evidenced by the decrease in hypolimnion temperatures throughout the winter. Ice may develop in the nearshore regions, and expecially in the relatively shallow region north of Main Duck Island, but it seldom covers more than a small fraction of the lake surface (Anderson et al, 1961; Wilshaw et al, 1965; Rondy, 1967). A typical temperature distribution for late winter, just before the appearance of the spring thermal bar, is shown in Fig. 3.

1.2.6 Consequences for Mixing and Flushing

The lake is, in general, well mixed over its total volume during late fall, winter and early spring, as is evidenced by the fact that seasonal temperature variations are reflected at all depths. Vertical circulation probably reaches a maximum intensity during the spring and fall overturns in early spring and late fall respectively. During the remaining part of the year, when the lake is stratified, the epilimnion and hypolimnion each appear to be well mixed over the total area of the lake. The epilimnion, however, is separated from the hypolimnion by the thermocline, which acts as a "diffusion floor".

Finally, it may be mentioned that lake stratification during part of the year hardly affects the natural displacement rate of a conservative pollutant in the water. A conservative pollutant is one which neither disintegrates nor participates in bio- or geochemical processes. If a large amount of such a pollutant were injected into the lake, a period of 20 years would be required for a 90% reduction of the amount of material initially injected, regardless of whether the lake were

stratified in the summer or not (Chapter 7). This time, however, could be prolonged considerably if the material in question were to enter cyclical reactions of a biochemical or geochemical nature.

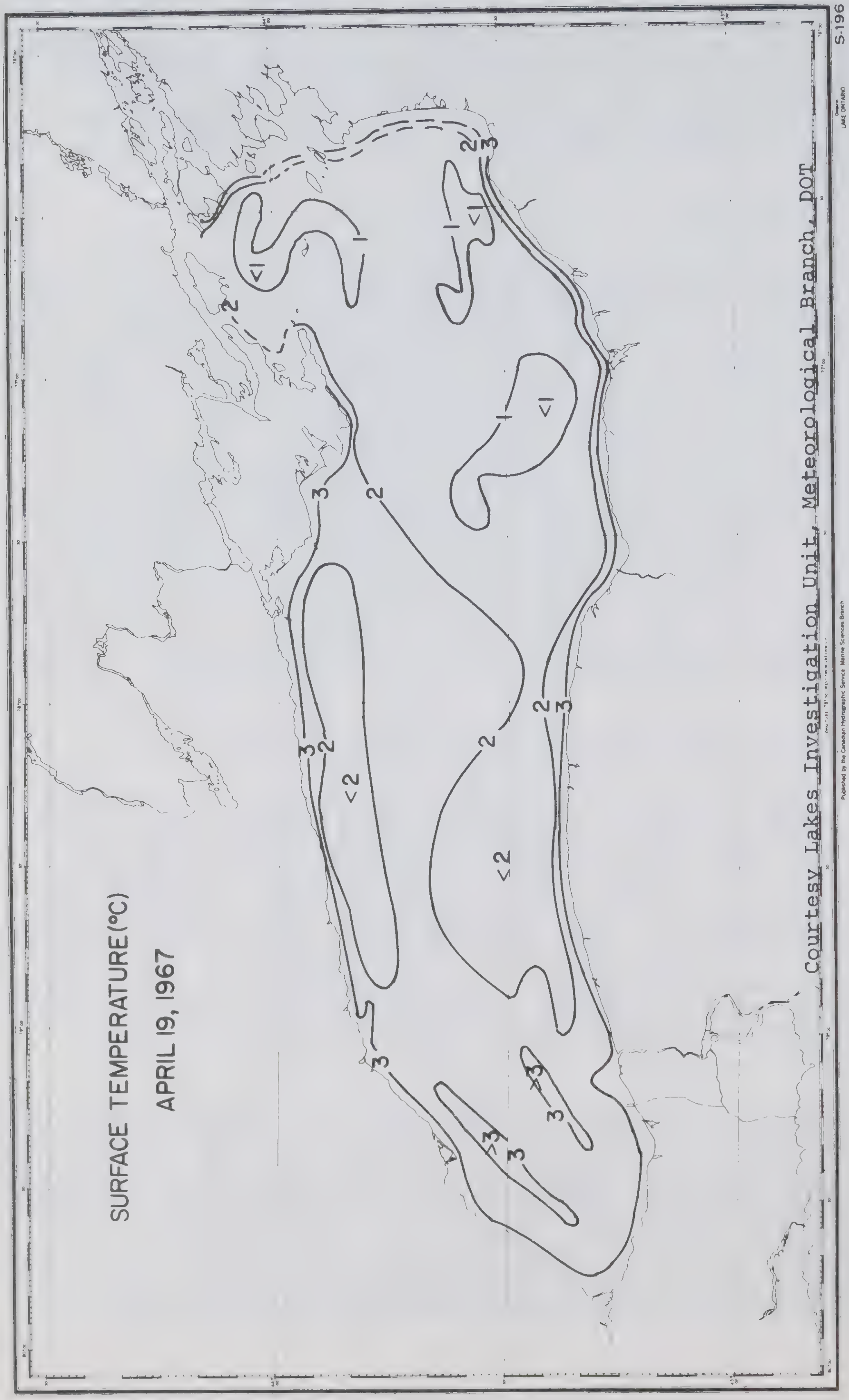

Fig. 3 Surface temperature distribution in late winter.

2. DATA AND METHODS

2.1 Limnological Data

2.1.1 Sampling Program

In 1966 a series of 9 monitor cruises were made at regular bi-weekly intervals between June 9 and September 30. On each of these cruises the same 47 stations, distributed evenly over the lake in a triangular pattern with distances of 22 km between stations (Fig. 4), were sampled at standard depths of 1, 10, 20, 30, 50, 75, 100, 150 and 200 metres. The 1967 field season was somewhat longer, and a total of eleven monitor cruises were made between June 12 and November 1. The station pattern was redesigned and chosen to give an optimum amount of information on the horizontal distribution in areas with relatively large fluctuations and strong horizontal gradients (Fig. 5). Sampling depths were similar to those in 1966.

All samples were analysed for about 15 different parameters, such as temperature, oxygen, specific conductance, pH hardness, chloride, total alkalinity, various nutrients, turbidity and some bacteriological parameters. In the present report only the first seven of these will be discussed.

In addition to this two other types of measurements were made: (1) vertical temperature profiles on each station, using a bathythermograph, and (2) continuous surface temperature records, using a towed thermister suspended from a boom extending a few metres beyond the side of the ship and towed at a depth of 0.5 metres below the surface.

2.1.2 Methods and Instrumentation

Some of the methods used to determine the concentrations of the chemical parameters have been described in a report by the Working Committee on Methodology of the International Joint Commission (1966). Other methods, which have not yet been described in detail, are adaptations with only minor modifications of methods described elsewhere.

Oxygen was determined by the Winkler Method (Strickland and Parsons, 1965) and expressed in mg O_2 per liter. The percentage saturation of oxygen was read from graphs giving the relation between temperature, dissolved oxygen and percentage saturation oxygen for distilled water at a pressure equal to the average barometric pressure at the surface of Lake Ontario (Dobson, 1968). Specific conductance was measured in μ mhos/cm with a Wheatstone bridge (ASTM, 1966) and the measurements have been corrected to a reference temperature of 18 and 25°C respectively for the 1966 and 1967 observations. Hardness was determined by titration with EDTA (Standard

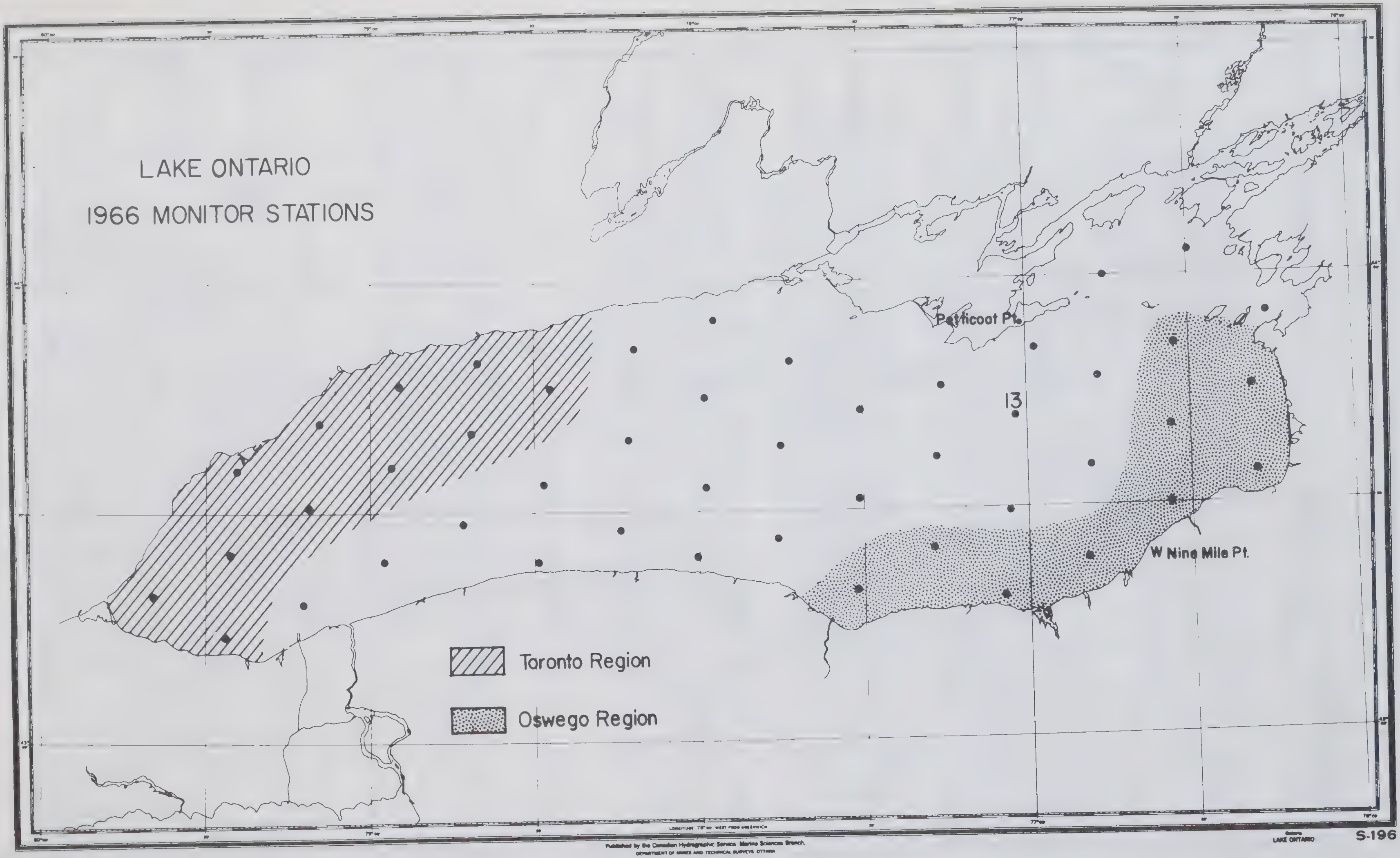

Fig. 4 Locations of the 1966 monitor stations.

Methods, p. 147; APHA, 1965) and total alkalinity by titration with sulfuric acid to the equivalence pH of carbonic acid dissociation (Thomas and Lynch, 1960). The units for both are mg $CaCO_3$/l. Chloride was measured colorimetrically (ASTM, 1966) and expressed in mg Cl/l. The techniques for measuring the last three parameters were adapted to a Technicon auto-analyser; details of these adaptations are described in the report by the Working Committee on Methodology of the International Joint Commission. In 1966 all analyses were carried out on board ship, in 1967 samples were taken back to shore for hardness and total alkalinity.

Temperature profiles were measured using reversing thermometers and bathythermographs. The surface temperature was measured with a thermistor and recorded on paper strip chart installed in the laboratory. The latter equipment did not function properly during a large part of the 1967 field season. The sampling depth was measured with a meterwheel.

2.1.3 Confidence Limits for the Data

In Table 1 a summary is given of the 95% confidence limits (2 standard deviations) of the data. These are based on estimates of the precision of the measurements by the agencies responsible for the analyses. In the last two columns similar statistics are given for 1966 and 1967, but based on an analyses of the variability of the hypolimnion data by the author. The variability is defined as twice the mean standard deviation of all the 75 and 100 metre level observations for each field season, and the statistic thus is a measure of purely random errors as well as natural variability and geographical gradients in the data. In most cases the variability is somewhat higher than the precision estimate, as can be expected. Differences between the estimated precisions for the two years are largely incidental, and are probably caused by minor variations in instrumentation and by the difference in personnel involved in the measurements.

The 95% confidence limits of cruise-mean hypolimnion values can be calculated from the variability of the data by dividing the latter by the square root of the number of observations. This relation, however, is valid only if the variability is of a Gaussian random nature; it does not hold in the presence of natural horizontal gradients or time dependent errors. The cruise to cruise variations in the mean hypolimnion values of total alkalinity, hardness and chloride in 1966 and of pH and specific conductance in 1967, however, are far too large to be explained as due to random errors and too erratic and mutually unrelated to be explained as natural time dependent fluctuations (see numbers in the Figs. 47 and 50). In the opinion of the author, these variations are largely artificial and are caused by the use of inaccurate standards and by changes in the sensitivity of the equipment. The arguments leading to this conclusion are substantiated in Appendix A.

	units	estimated precision (2 SD)		variability hypol. data (2 SD)	
year		1966	1967	1966	1967
depth	m	1.5 [1]	[1]		
temperature (B.T.)	°C	0.5 [1]	[1]		
temp. (rev. therm.)	°C	0.02-0.05 [1,7]	0.02-0.05 [1,7]	.32 [4]	.16 [4]
sp. conductance	μmhos/cm at 25°C	3. [2]	3. [2]	4.0 [5]	14. [6]
hardness	mg $CaCO_3$/l	1. [3]	1. [3]	3.	4.
total alkalinity	mg $CaCO_3$/l	1. [3]	5. [3]	3.	7.
chloride	mg Cl/l	1. [3]	1. [3]	2.0	2.0
pH	pH units	0.04 [2]	0.1 [3]	0.08	0.3
diss. oxygen	mg O_2/l	0.05 [2]	0.1 [3]	1.2	1.4

1) estimate by the present author
2) personal communication by H. Dobson, Canada Centre for Inland Waters
3) personal communication by R. Orr, Dept. of National Health and Welfare
4) 0.1 at a depth of 150 metres in both years
5) 3.4 for measuremetns adjusted to 18°C
6) 9 for the last four cruises in 1967
7) estimate of precision depends on range of thermometer used

Table 1 Estimated precision (95% confidence limits) of the measurements and calculated variability (2 standard deviations) of the hypolimnion data.

In this appendix it is shown that the variability in the measurements of some parameters cannot be explained in terms of Gaussian random errors and natural geographical and temporal effects only. In some instances the variability is to a large extent caused by so called "quasi-random" errors, caused by slow changes in sensitivity and/or calibration of the equipment. These quasi-random errors seriously limit the usefulness of the data affected for the study of horizontal distribution patterns, because they may give rise to artificial horizontal gradients, as is explained in Appendix A.

Temperature and oxygen data are relatively or completely free of quasi-random errors, and so are specific conductance and pH data for 1966. In 1967, however, the latter two have been measured less accurately (Table 1), and natural geographical gradients are often partially or completely masked by fictitious gradients caused by quasi-random errors. The distributions of hardness, total alkalinity and chloride are for most cruises of doubtful value. In Appendix F the horizontal distributions of all but the latter three parameters have been shown for all cruises for which the data are meaningful.

The cruise mean values of hardness, total alkalinity and chloride, however, have been used. Under the assumption that the hypolimnion concentrations are almost constant throughout the summer, as is, for example, the case with temperature, conductance and pH in 1966, seasonal variations of the epilimnion concentrations can be calculated by subtracting the two averages. The results are shown in the Figs. 47 and 50, and discussed in Section 5.2.

2.1.4 Processing of the Data

The data have been analysed in various ways. Four of the basic procedures used are:

1. Cruise by cruise plots of the horizontal distributions at various levels.

2. Computations of cruise average profiles, by taking, unless otherwise specified, weighted means at the standard depths.

3. Time series studies of the means for the whole lake, and for parts of the lake, at the surface and at various subsurface levels.

4. Computations of mean horizontal distributions for the summer.

Horizontal means of the 1967 data have been calculated using weighing factors proportional to the area for which each station is considered to be representative (Fig. 5). No

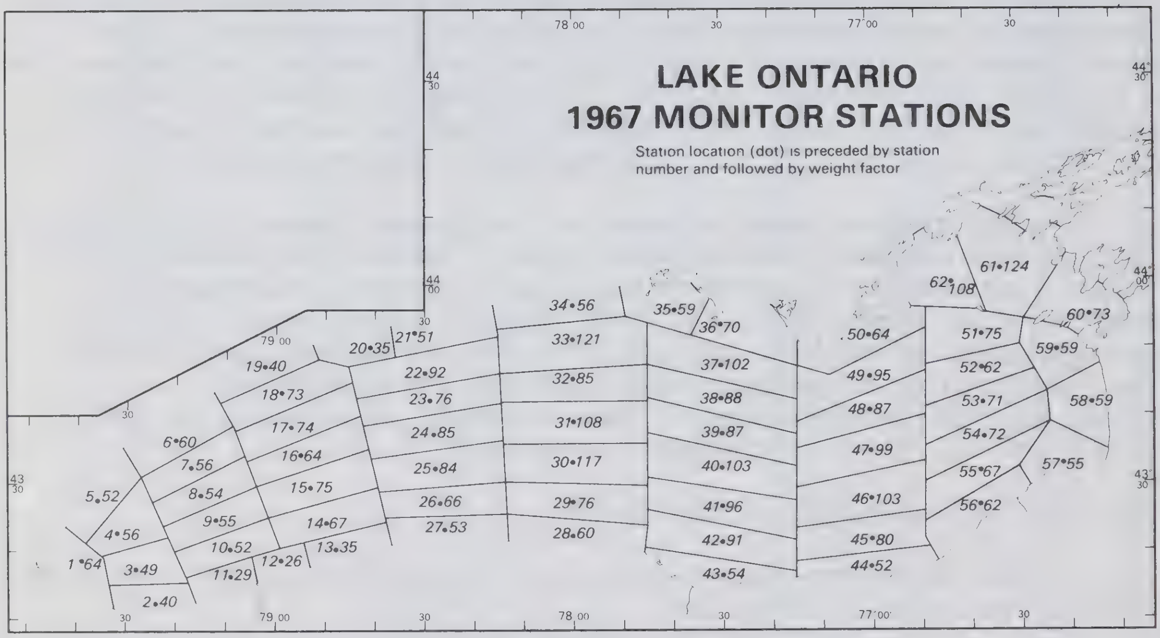

Fig. 5 Locations and weight factors of the 1967 monitor stations.

weighing factors have been applied to the 1966 data, since the monitor stations are distributed much more evenly over the lake.

The temperature data have also been used for a number of other calculations, such as heat storage, vertical eddy diffusivity, characteristics of the vertical temperature gradient in the thermocline layer, cyclic variations in thermocline depth, and horizontal water movements. The computational techniques used will be outlined in the respective sections. One technique, however, will be discussed here since reference to it is made throughout the report.

The mean vertical temperature profile of a number of data can be defined in two ways. The first, and most commonly used, definition consists of defining a mean profile $\overline{T}(z)$ by averaging all observations at each level:

$$\overline{T}(z) = \frac{1}{N} \sum_{i=1}^{N} w_i T_i(z) \qquad (2.1.a)$$

where w_i and $T_i(z)$, $i = 1,2,\ldots,N$, are the weight factors and the observed temperature profiles respectively. Chemical profiles have only been determined using this equation. The second definition, which has been discussed in detail in a recent paper by the author (1969), consists of averaging the depths of the isotherms. The individual temperature curves in this case have to be described by a function $Z_i(\theta)$, where the depth Z is the dependent variable and the temperature θ the independent variable. The mean profile is then defined by:

$$\overline{Z}(\theta) = \frac{1}{N} \sum_{i=1}^{N} w_i Z_i(\theta) \qquad (2.1.b)$$

(Capitals T and Z denote dependent variables, lower case letters z and θ independent variables). This technique can only be used if $Z_i(\theta)$ is unique for every value of θ, that is, if the temperature is a monotone decreasing function of depth. This is the case during the summer, when Lake Ontario is stratified. The function $\overline{Z}(\theta)$ has a number of characteristics that are of importance in the following discussions:

(i) The maximum gradient of $\overline{Z}(\theta)$ is roughly equal to the average of the maximum gradients of the temperature profiles at each of the stations, and gradients at other points (z,θ) of the curve are about equal to the mean gradient of the individual observations at the corresponding temperature. The maximum gradient of $\overline{T}(z)$ is in general much smaller than the average of the maximum gradients of the individual curves.

(ii) The depth below the surface of any point of $\overline{Z}(\theta)$ is directly proportional to the amount of water in the lake with a temperature equal to or higher than the temperature of that point.

(iii) $\overline{Z}(\theta)$ reaches the surface at a temperature equal to the highest temperature observed during any particular cruise and intersects the function $\overline{T}(z)$ near the depth maximum gradient. Above this depth $\overline{Z}(\theta)$ indicates higher temperatures, below this depth lower temperatures than $\overline{T}(z)$. In a situation where the depth of the thermocline is disturbed by internal waves only, the difference is roughly proportional to a product of the amplitude of the internal waves with the second derivate of the vertical temperature gradient at this level.

(iv) The mean depth of an isotherm is, unlike the mean temperature at any level, in first approximation independent of internal wave action.

Both the $\overline{T}(z)$ and the $\overline{Z}(\theta)$ profiles for each cruise have been calculated. The former are given with the horizontal temperature distribution charts in Appendix F, the latter have been plotted in Figs. 26 and 27. Both are used for calculations of the vertical coefficient of eddy diffusivity, and $\overline{Z}(\theta)$ has also been used to describe the mean vertical temperature gradient in the lake.

2.2 Other data

Meteorological data were taken from the Monthly Meteorological Summaries for Toronto International Airport, published by the Department of Transport, and from records of the weather observations carried out on board the M.V. Brandal in 1966 and the M.V. Theron in 1967. The wind data for the shore-based meteorological station consist of observations once every hour of the mean wind speed during the past hour and the instantaneous direction at the moment of observation. Daily, weekly and monthly means have been computed by taking vector averages of the hourly wind speed and direction observations. Shipboard weather observations are taken once every three hours and reflect conditions at the time of observation.

Water intake data from four public utility plants, three in the vicinity of Toronto and one near Rochester, were kindly made available by the sampling agencies (Table 2) and obtained with help of the University of Toronto and of the Rochester Program Office, FWPCA, respectively.

2.3 Representativeness of the Data

The spacial distribution of most parameters is closely related to the thermal structure of the lake. This, in turn, is

water intake station	approximate position	distance offshore (m)	depth (m)	code
R.C. Harris	13 km east of Toronto Island	2900	11.4	T_1
New Island Plant (W)	off Toronto Island	800	19.2	T_2
Old Island Plant (E)	off Toronto Island	1000	9.0	T_3
Monroe County	Rochester	1800	12.0	T_4

Table 2 Location and depth of water intakes for which temperature data have been analyzed.

largely determined by external factors such as winds and the exchange of energy through the air-water interface. The representativeness of the lake-wide distribution patterns of most parameters thus can be judged to a large extent from the representativeness of the meteorological conditions.

The 1966 and 1967 wind data for Toronto International Airport are summarized in Table 3 and compared with 10-year averages for the period of 1956 through 1965 (DOT, 1966). Data for a shore-based meteorological station are not completely representative for conditions in the open lake (Richards et al, 1966). It may be assumed, however, that the year-to-year variations in the climate over the lake and over the surrounding land areas are similar, since both reflect the overall weather conditions in the area.

Table 3 shows that the frequency of winds with an eastward or westward component is almost normal in both years, but that the residual wind has a higher than average component towards the east in 1966 and, especially in June and July, a lower than average eastward component in 1967. The mean wind speed is close to average in 1966, but is considerably lower in 1967. The largest difference occurs during the months of July and August, when the mean wind speed reaches record low since meteorological observations started at this location in 1938 (DOT, 1967), being 281 cm/sec versus a 30-year mean of 375 cm/sec. This difference is examplified by the fact that strong winds were extremely rare in this period: winds exceeding 580 cm/sec (Beaufort speed 5 or over) and 850 cm/sec (Beaufort speed 6 and over) occurred only 9.0 and 0.5% of the time as compared with 20% and 3.4% respectively in the period of 1956 through 1965. In 1966, on the other hand, the frequency of occurrence of strong winds was about normal. The effect on the lake of these differences in the wind conditions may be larger than suggested by Table 3, since the windstress is proportional to the square of the wind speed. The summer mean windstress in 1967 is just over half of the mean windstress in 1966 (Table 10).

The thermal structure thus can be expected to be close to "normal" in 1966, but there may be important differences between the patterns observed in 1966 and 1967.

The representativity of the 1966 data has also been studied by comparing the monitor cruise data with continuous temperature observations obtained from two water intakes, located near Toronto and Rochester respectively (Fig. 6). The summer-mean temperature of the Rochester water intake, situated

			June	July	Aug.	Sept.	Oct.
frequency (%) of winds with a component towards	E	'66		56	58	53	
		'67	39	50	53	51	48
		'56-'65	45	46	47	41	46
	W	'66		9	19	20	
		'67	33	15	17	13	28
		'56-'65	18	17	18	20	21
residual winds (cm/sec) towards	E	'66	135	160	143	103	
		'67	6	80	99	125	94
		'56-'65	131	119	115	103	123
	S	'66	-33	54	31	60	
		'67	-22	-52	36	87	-67
		'56-'65	19	21	9	-12	28
mean windspeed (cm/sec)		'66	351	391	355	386	440
		'67	315	257	307	377	386
		'56-'65	391	364	364	382	404

Table 3 A comparison of the 1966 and 1967 wind data for Toronto International Airport with 10-year mean data for the period of 1956 through 1965. The percentage of winds blowing towards the east includes all winds blowing from NW, W and SW.

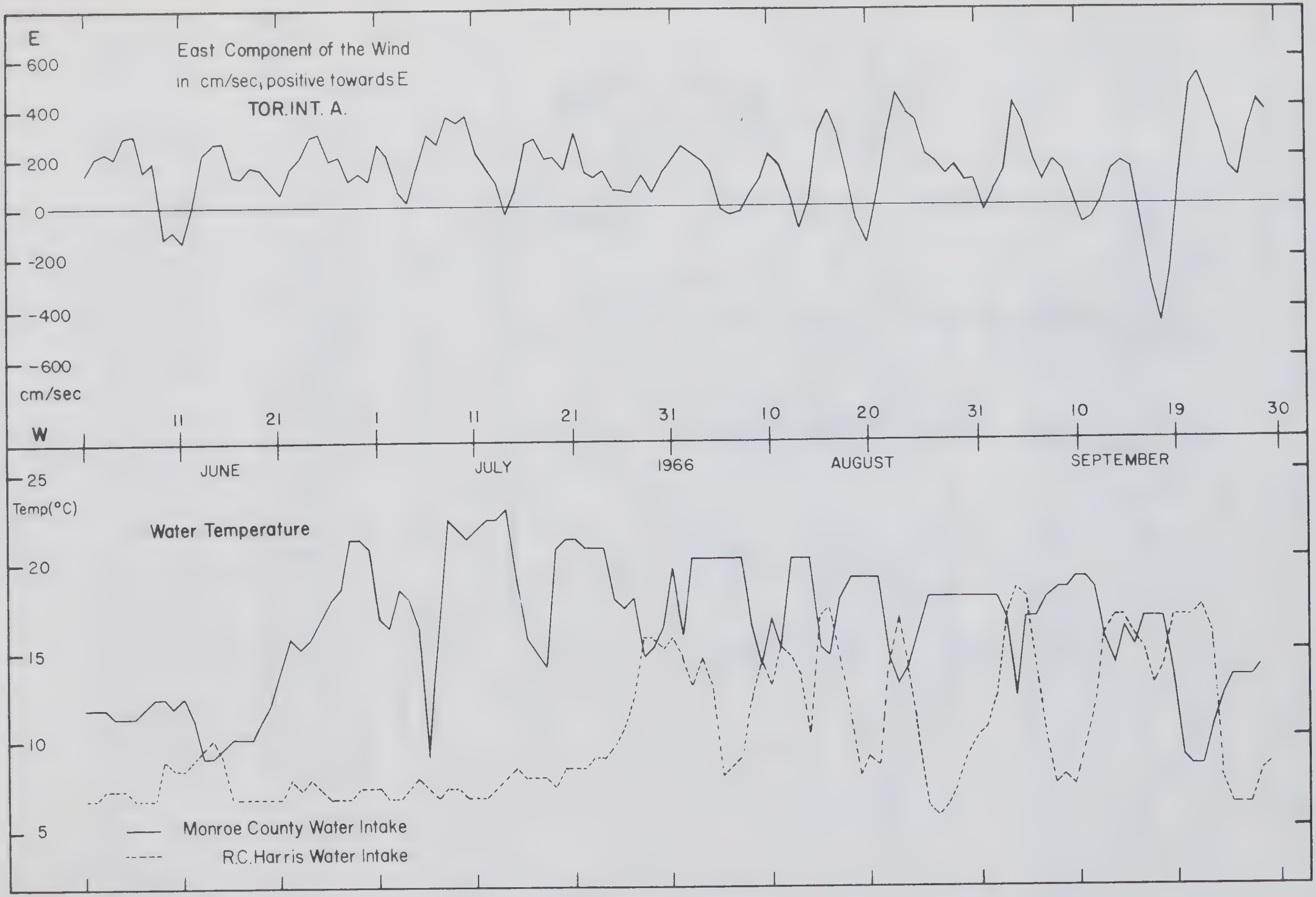

Fig. 6 East component of the wind (Toronto International Airport) versus water intake temperatures in Toronto (R.C. Harris plant) and Rochester (Monroe County water intake), summer 1966.

1800 metres offshore at a depth of about 12 metres, is 17.7°C. The mean temperature for the RC Harris water intake near Toronto, situated 2900 metres offshore at a depth of 11 metres, is 10.8°C. The average of the temperatures measured at these stations during the cruises made in the same period deviates by less than 0.2C° from the overall averages, indicating that the cruises form a representative sample of the summer.

In Section 3.6 the representativeness of the 1966 and 1967 data will be discussed in the light of earlier observations (such as those of Rodgers and Anderson, 1963).

2.4 Definitions

Some of the definitions used in this report differ from the generally accepted definitions. The reason for this is that they have been adapted to the analytical procedures used in studying the data. For practical purposes the difference is usually not important, although the definitions presented below may seem to be less accurate from a theoretical point of view.

The thermocline, unless otherwise indicated, is defined as the depth of the 10°C isotherm rather than as the depth of maximum vertical gradient. This simplifies the analysis of the data, since the depth of the 10°C isotherm is less dependent on transient effects than the depth of the maximum gradient. The latter may, for example, shift up and down not only with internal waves but also with the intermittent formation of secondary thermoclines. In Lake Ontario the two levels are usually very close together, at least in the summer, and the two terms will be used interchangeably in this report. On a few cruises in early spring or late fall, however, the proposed definition is not satisfactory, and the depth of the thermocline is approximated by the depth of, for example, the 7°C isothermal surface.

The epilimnion is usually defined as a layer above the thermocline with small or no vertical temperature gradients, the hypolimnion as a similar layer below the thermocline. The transition zone, in which there is a strong vertical temperature gradient, is called the thermocline region. The terms epilimnion and hypolimnion will occasionally be used loosely to refer to all water above and below the thermocline respectively.

3. THERMAL REGIME IN 1966 AND 1967

In the introduction it was pointed out that the thermal regime can conveniently be described in terms of the four seasons of a lake-climatology, and definitions were proposed to mark the beginning and end of each of these seasons in terms of characteristic aspects of the temporal changes in thermal structure and mean temperature. It was concluded that the seasons thus defined correspond in time closely to the four calendar seasons. In the present chapter the 1966 and 1967 data will be discussed in view of this classification, and the choice of definitions delineating the seasons substantiated.

In both years the field season commenced in late spring and continued until early fall. For the purpose of the following discussion the cruises will therefore be grouped into three classes: late spring, summer and early fall. The thermal structure in these seasons, and especially in summer, will be described in detail.

The thermal regime is strongly influenced not only by seasonal changes in the climate, but also by winds immediately prior to and during the period of observation. For that reason winds prior to and during each cruise have been plotted on the thermocline depth charts in Appendix F. The weekly vector-mean winds for Toronto International Airport are shown in Figs. 7 and 8, which illustrate the consistency of eastward winds over the lake throughout both field seasons. Especially in 1966 the vector-mean wind varies little from week to week.

3.1 Horizontal Distributions

The horizontal temperature distribution and depth-of-the-thermocline charts for all cruises are presented in Appendix F. In the top lefthand corner of the charts the lake-mean temperature profiles, T(z), and the daily mean wind vectors respectively are shown.

3.1.1 Late Spring

The first cruise in 1966 (Figs. F. 1 and F. 2) shows the situation shortly after dissipation of the thermal bar proper; a minimum surface temperature of about 4.5°C occurs over the deepest part of the lake. A large area with cold surface water, temperatures of 8°C and lower, extends over most of the deeper parts of the lake, covering about 25 to 30% of its area, and the isotherms run roughly parallel to the depth contours. The depth of the thermocline, which is approximated by the 7°C isotherm for this cruise, is very shallow over most of the lake. Near the shores it dips down to a depth of 10 metres or more, reaching a maximum depth of 25 metres in the far southeastern corner of the lake.

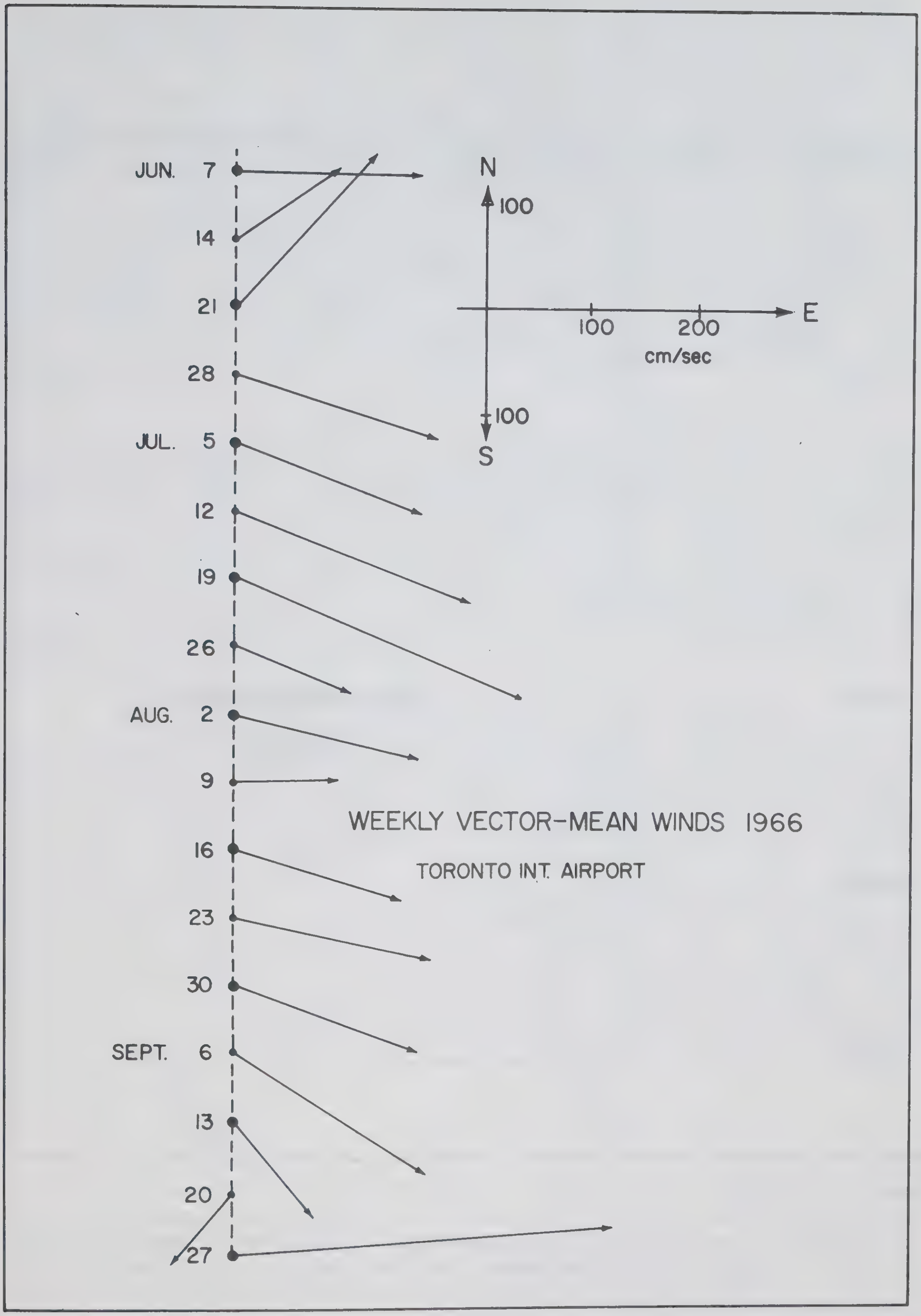

Fig. 7 Weekly vector-mean winds for Toronto International Airport during the 1966 field season.

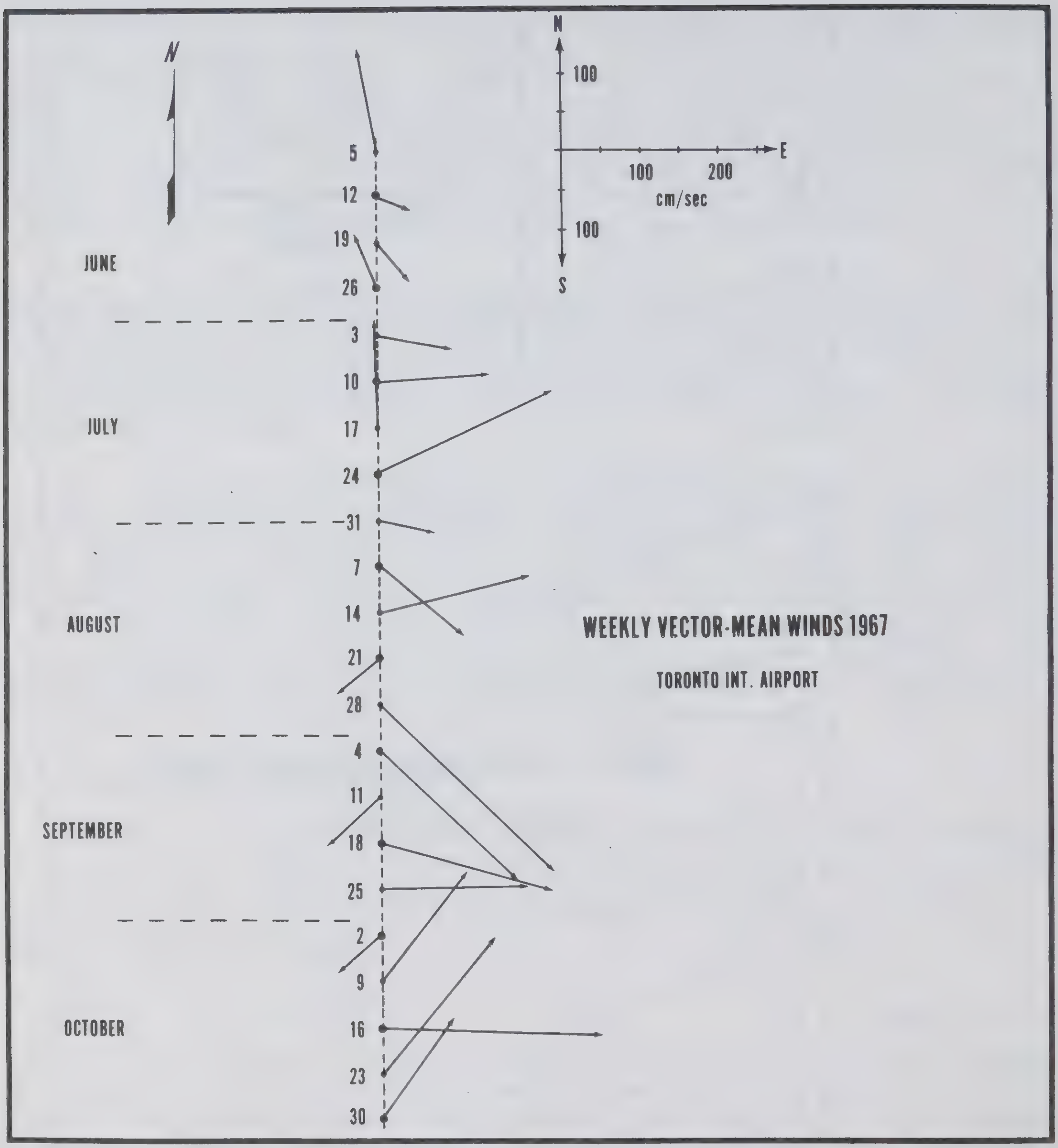

Fig. 8 Weekly vector-mean winds for Toronto International Airport during the 1967 field season.

Two weeks later, by the end of June, the surface temperature (Fig. F. 4) has risen considerably and the extent of the temperature minimum is reduced to about 12% of the total area of the lake. Vertical circulation decreases rapidly in intensity upon formation of a thermocline in the mid-lake minimum in early June, and the location of this minimum consequently is influenced to a much larger extent by external forces, such as windstress, than during the thermal bar period earlier in spring. Under the influence of prevailing westerly winds it has been moved closer towards the eastern shore, and the isotherms are no longer parallel to the depth contours. The thermocline (Fig. F. 5), which for this and all later cruises is approximated by the depth of the 10°C isotherm, is still shallow over a large part of the lake, again dipping down near the shores and reaching a maximum depth of 20 metres in the far southeastern corner.

The first cruise in 1967 (mid-June, Figs. F.56 and F.57) shows a pattern roughly similar to that of the early June 1966 cruise, with a temperature minimum of 8°C over the deepest part of the lake, an area with low surface temperatures extending over most of the deeper parts of the lake covering about 25% of its area, and a shallow thermocline sloping downwards near the shores. The early June 1966 cruise shows the situation a few days after dissipation of the thermal bar, the mid-June 1967 cruise, however, follows about one to two weeks after its dissipation.

During the late June 1967 cruise (Figs. F.61 and F.62) the thermal structure is very complicated. The mid-lake temperature minimum has a very complex configuration, and a second minimum, caused by upwelling, appears near Toronto. In both areas the surface temperature drops to about 10°C, elsewhere in the lake temperatures are 17°C or over. This pattern is reflected in the distribution of the thermocline depth, which is about 10 metres over most of the lake, showing two minima of less than 5 metres corresponding in location to the temperature minima, and sloping downwards to a maximum of 30 metres just east of the mouth of the Niagara River. The concurrent appearance of two minima and the rather complicated distribution of the surface temperature are related to the variable, but relatively strong, winds in the period immediately prior to and during the cruise.

3.1.2 Summer

The next six cruises in both years, sampled between early July and mid-September, show thermal patterns that are typical for the summer. The temperature minimum, with the exception of a short period in late July 1967 (Fig. F.72), is always close to the northwestern shore, the maximum close to the opposite shore. The direction of the isotherms is no longer related to the direction of the shorelines or to the depth contours, and the lake-mean surface temperature is fairly constant, fluctuating between 18 and 21°C (Figs. 9 and 10). The

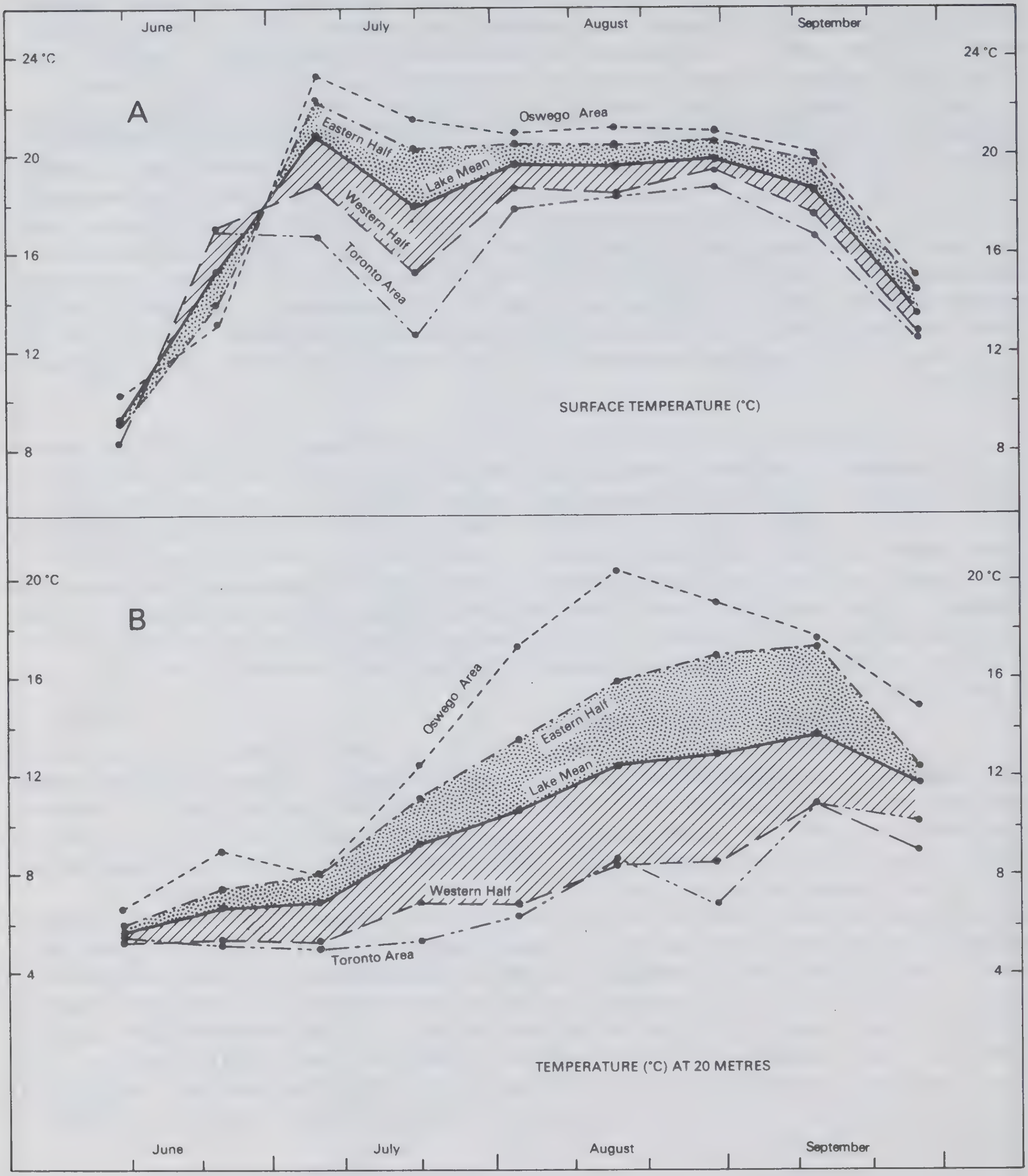

Fig. 9 Cruise mean temperatures for the period of June through September 1966 at the surface and at a depth of 20 metres, compared with mean temperatures for the eastern and western halves of the lake and with means for a group of stations in the Oswego and Toronto regions respectively.

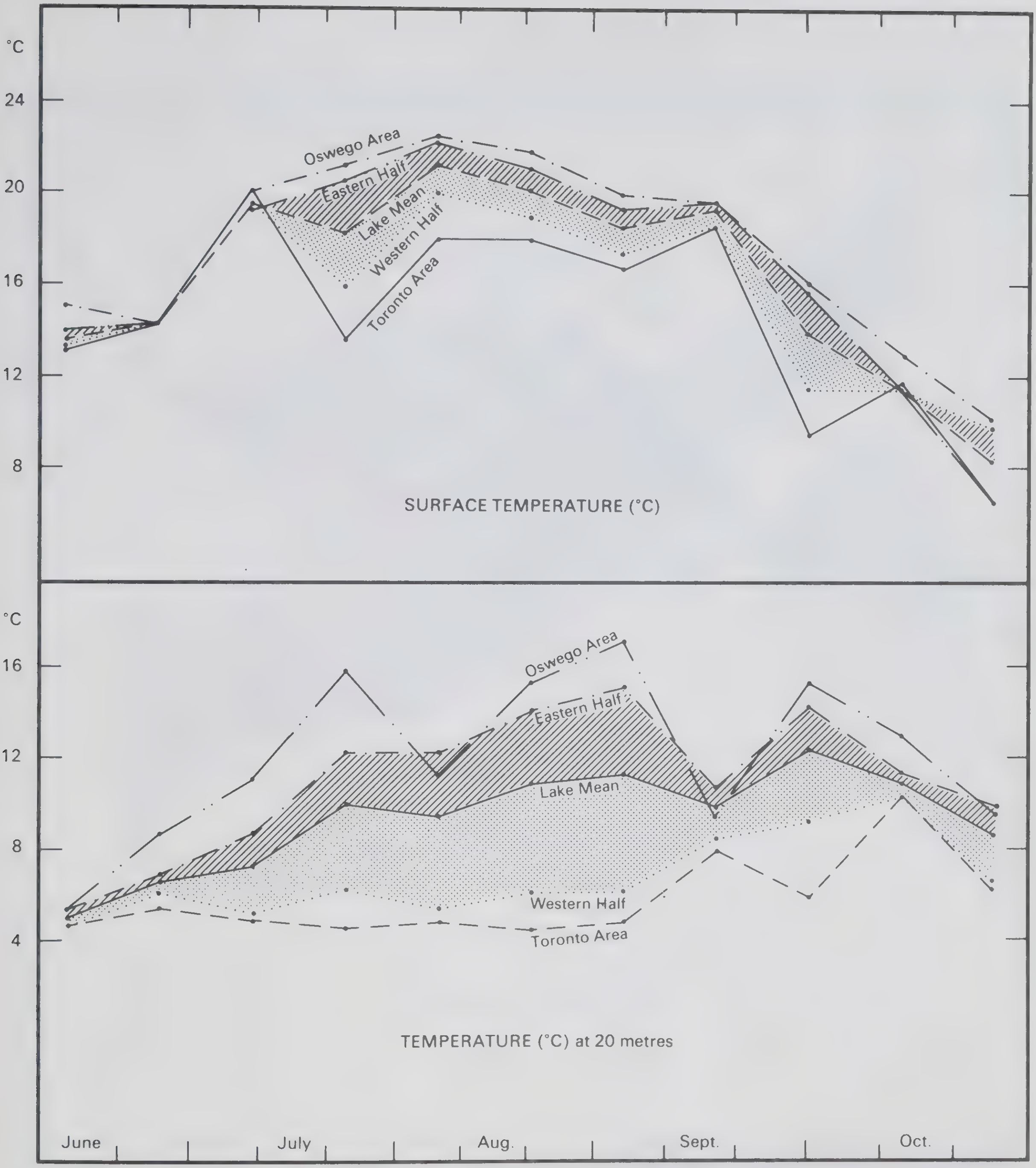

Fig. 10 Cruise mean temperatures for the period of June through October 1967 at the surface and at a depth of 20 metres, compared with the mean temperatures for the eastern and western halves of the lake.

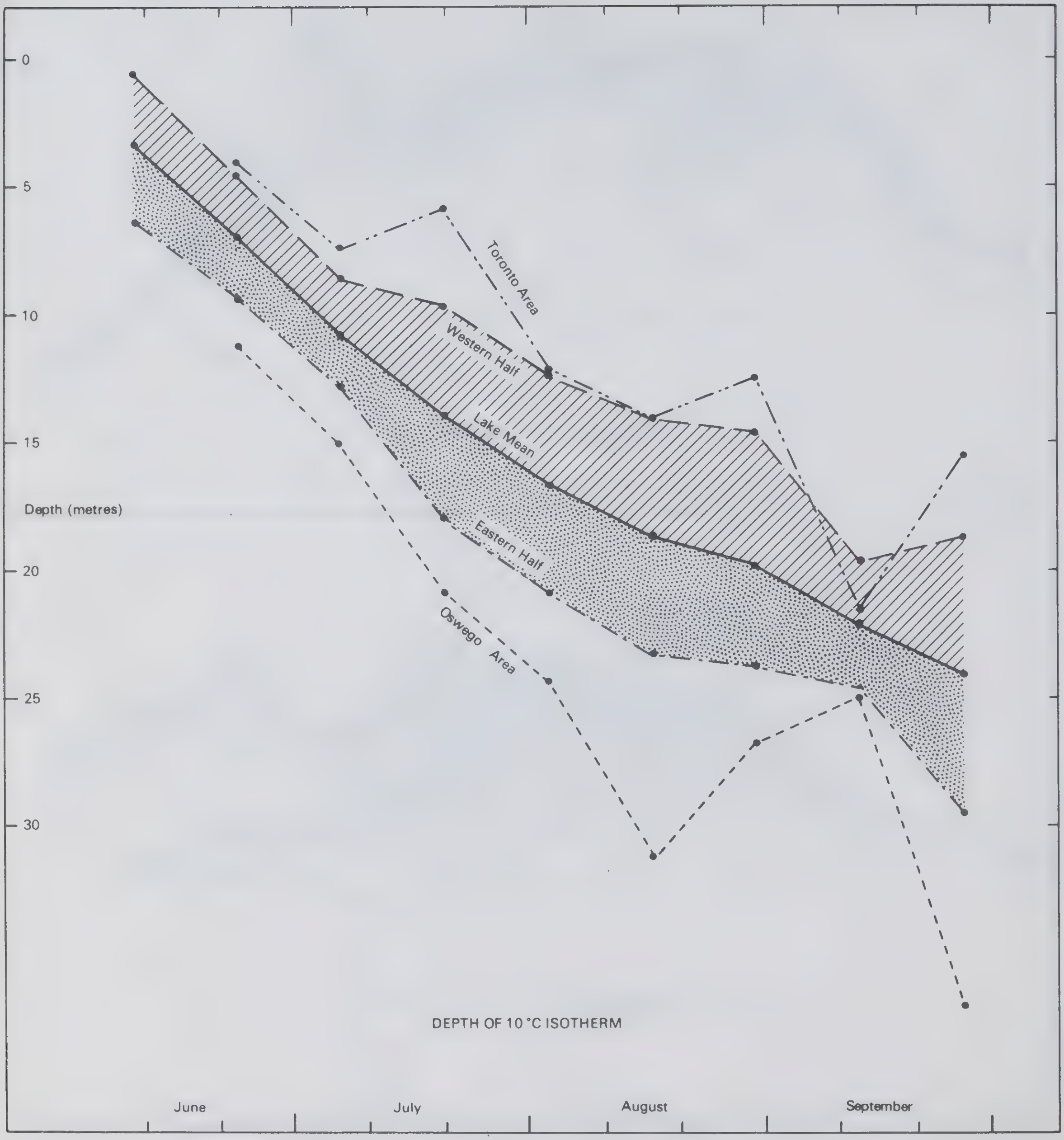

Fig. 11 Mean depth of the 10°C isotherm for the period of June through September 1966, compared with the same for the eastern and western halves of the lake and for the Toronto and Oswego regions.

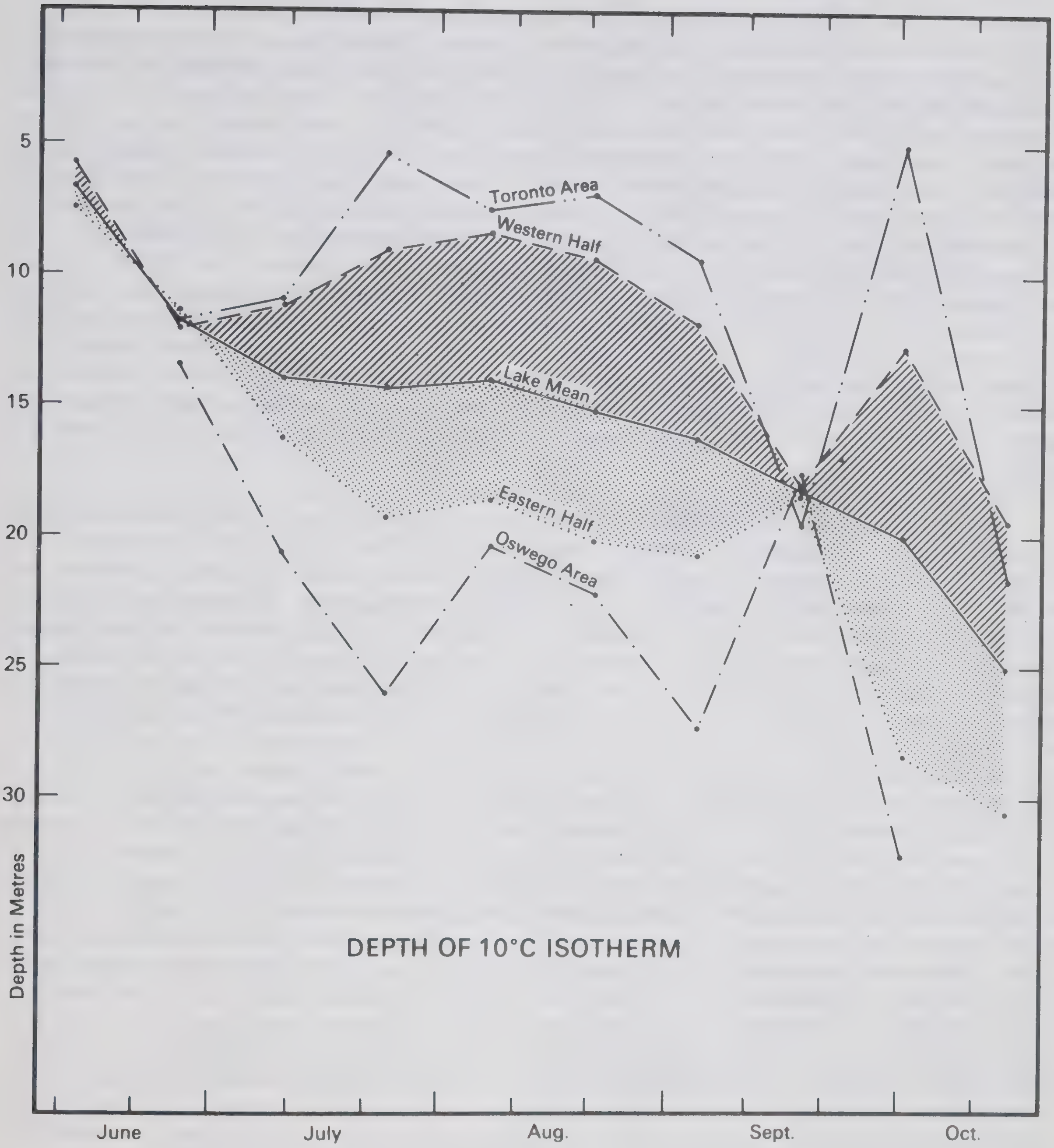

Fig. 12 Mean depth of the 10°C isotherm for the period of June through October 1967, compared with the same for the eastern and western halves of the lake.

thermocline depth (Figs. 11 and 12) likewise usually reaches a minimum in the northwestern part of the lake and slopes downwards towards the southeastern end.

In early September 1966 (Fig. F.42) a secondary maximum in thermocline depth appears near Hamilton, but it covers only a relatively small area and the surface temperature shows no corresponding minimum. During the early part of this cruise the wind direction changed from a generally eastward to a westward direction. This, perhaps together with a strong internal seiche, may have caused the second maximum in thermocline depth, which, however, is confined to a narrow strip along the shore. Adjacent to this strip is a large area where the thermocline is at a minimum depth, and the mean thermocline depth in the western half of the lake is still much less than that in the eastern half (Fig. 11). The reversal of wind direction thus is sufficient to cause a local convergence of water on the western shore, but the westward wind is not strong and/or persistent enough to cause a complete redistribution of epilimnion water and a reversal of the east-west slope of the thermocline (see also Chapter 4).

In mid-September 1967 an interesting, elongated area of minimum thermocline depth occurs off the southern shore (Fig. F.94). Around this area the thermocline slopes downwards from a minimum of 6 metres to a depth of 12 to 20 metres or more. The pattern may reflect a temporary gyre with a confined, perhaps almost jet-like, eastward current along the southern shore. In early August a curious temperature minimum of small areal extent occurs in the middle of the lake between Toronto and Niagara (Fig. F.78). This coldspot, in which the surface temperature drops to a minimum of 10°C[1], may have originated in the vicinity of Toronto during the previous upwelling period. During a seven day period immediately preceding the cruise the winds were very weak and variable, and it therefore seems likely that the coldspot is at least a week old. It may have originated in the previous upwelling period and drifted southwards. In this case, however, it is not clear how a small area like the one observed can maintain such a low minimum temperature in its core over so long a period, unless it is the centre of a counter-clockwise gyre. The author has no plausible explanation for either the apparent longevity of the observed coldspot, if it developed before, or for its origin, if it developed during the one week period in which the winds were weak and variable. No evidence for even the slightest temperature minimum in this region is found on any of the other cruises.

---

[1] This coldspot is obvious from reversing thermometer observations as well as from the towed thermister record.

The magnitude of the east-west gradients in temperature and in thermocline depth vary considerably from cruise to cruise. Very strong upwelling with surface temperatures in some locations dropping to below 14°C, and sometimes as low as 8 to 10°C, is observed on roughly half of the cruises, spread out more or less evenly over the summer. The median dates of these cruises are 7 July, 22 July and 31 August 1966, and 27 July, 23 August and 7 September 1967 respectively (Figs. F.10, F.17, F.35, F.72, F.83 and F.88). Under influence of the dominantly eastward component of the wind the coldest surface water is in all these cases found in the vicinity of Toronto or elsewhere along the northwestern shore. The thermocline (Figs. F.11, F.18, F.36, F.73, F.84 and F.89) also shows a strong east-west tilt, sloping downwards towards the east, sometimes reaching a maximum depth as high as 45 metres in the vicinity of Oswego, while reaching the surface at the opposite side of the lake.

During the other six cruises the surface temperature distribution (Figs. F.23, F.29, F.41, F.67, F.78 and F.93) is relatively uniform, and the thermocline slope (Figs. F.24, F.30, F.42, F.68, F.79 and F.94) generally much less, although temperatures are consistently lower and the thermocline shallower in the western section of the lake than in the eastern section.

The spacial distribution of temperature during the summer season is summarized in Figs. 13 through 24, showing the mean temperature distribution at various levels and the mean depth of the thermocline for the period of early July to mid-September in 1966 and 1967 respectively. The patterns for the two years are almost identical.

The surface temperature near Toronto is usually well below the lake-mean surface temperature, as was pointed out before. The magnitude of this phenomenon is clearly illustrated by Figs. 13 and 19, showing a difference in the summer-mean temperatures near Toronto and near Oswego respectively of about 7C°. This difference extends downwards to the lower end of the range of depths over which the thermocline fluctuates, and it is still noticeable at a depth of 50 metres. It can be explained in terms of a tilt of the thermocline due to the forcing effects of the predominantly westerly winds. The thermocline itself is about 16 metres deeper near Oswego than near Toronto, which corresponds to a mean slope of 5.6 cm/km over the longitudinal axis of the lake.

The surface isotherms in the western end tend to run parallel to the northwest shores. Elsewhere they also follow a generally NE-SW direction, with a tendency to become approximately parallel to the shores close to the southern and eastern boundaries of the lake. Isotherms at the deeper levels, however, show a stronger tendency to run parallel to the depth contours, as do the iso-depth lines of the 10°C isotherm.

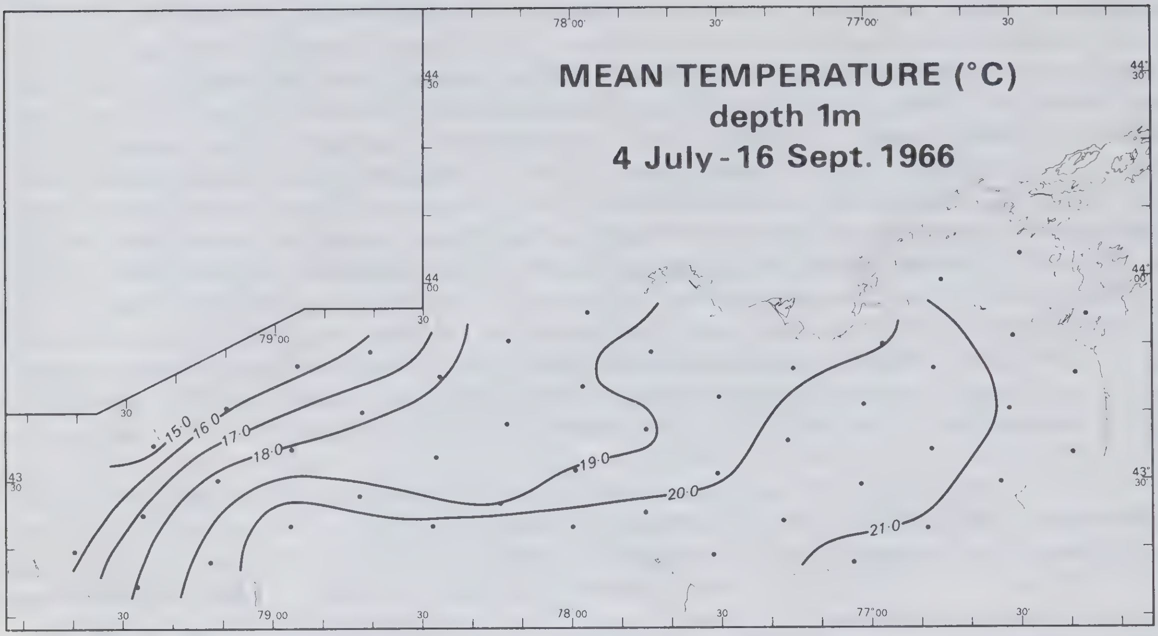

Fig. 13 Summer-mean surface temperature distribution in 1966.

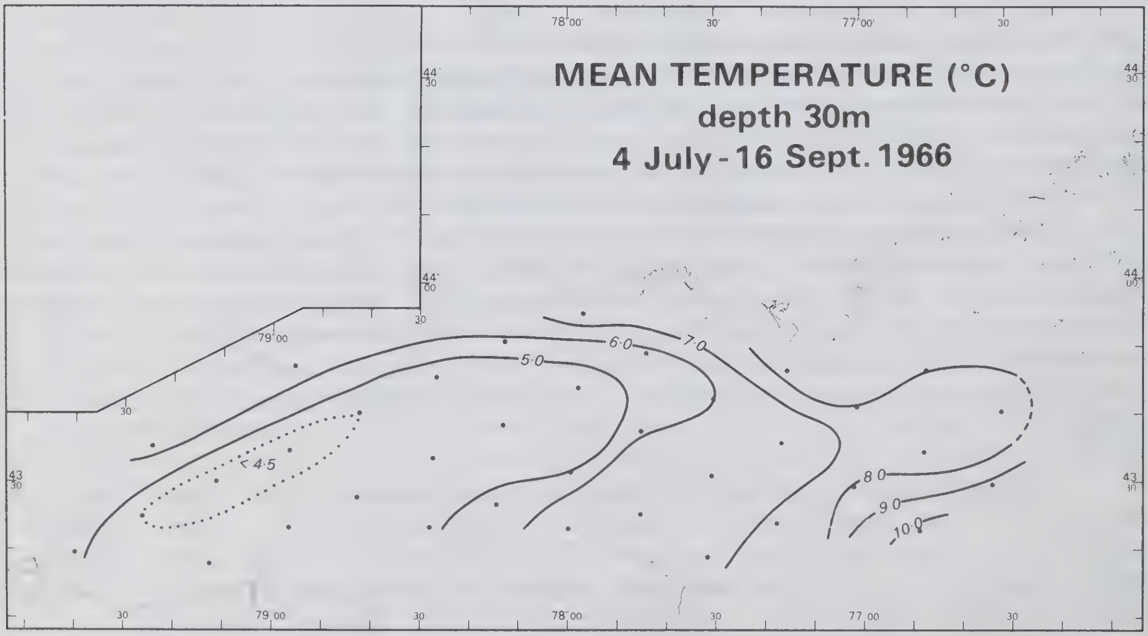

Fig. 14 Summer-mean temperature distribution at the 30-metre level in 1966.

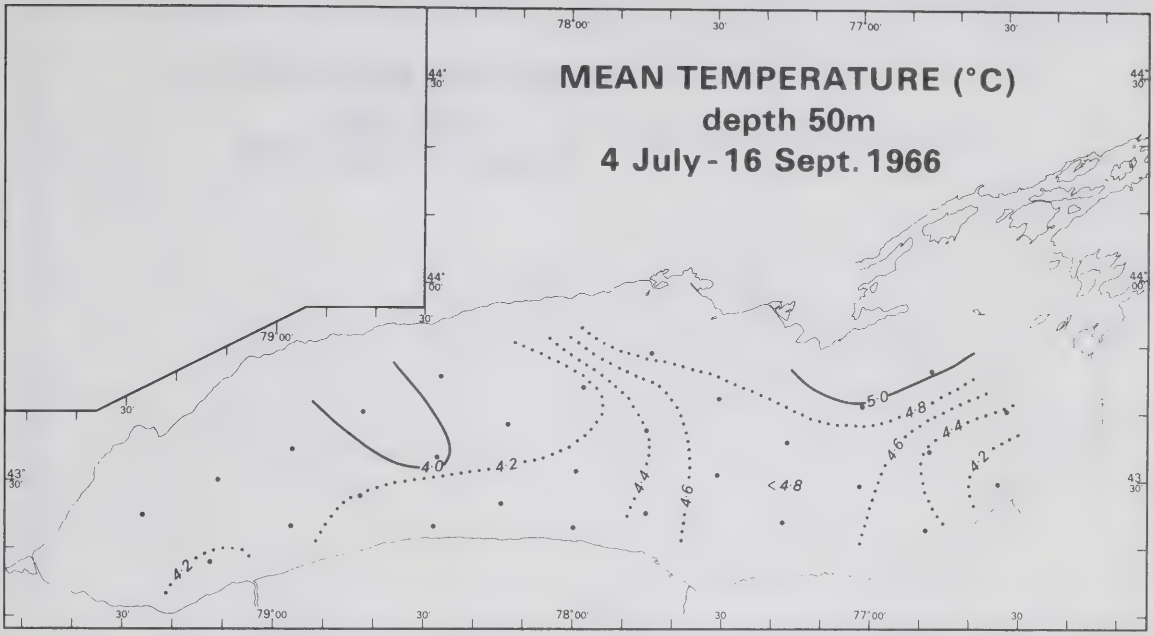

Fig. 15 Summer-mean temperature distribution at the 50-metre level in 1966.

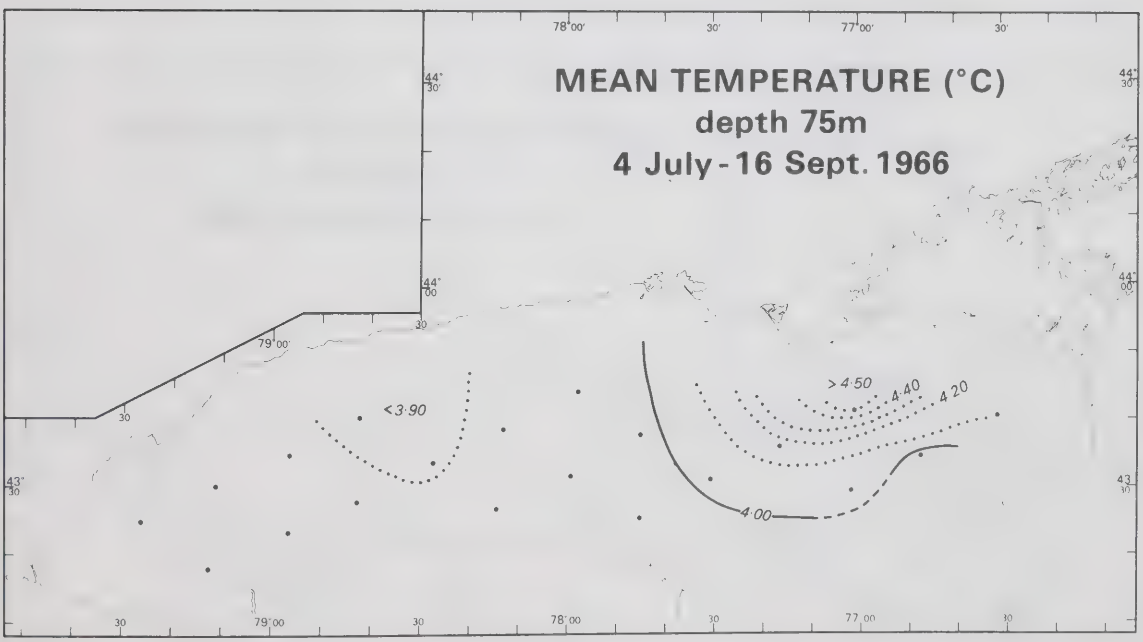

Fig. 16 Summer-mean temperature distribution at the 75-metre level in 1966.

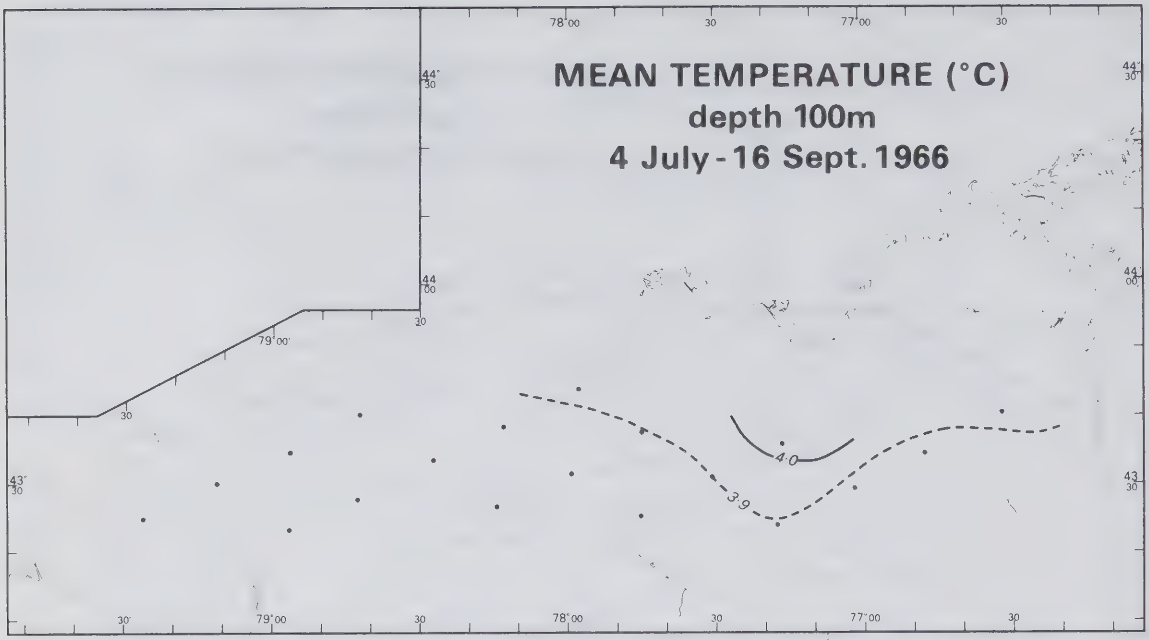

Fig. 17 Summer-mean temperature distribution at the 100-metre level in 1966.

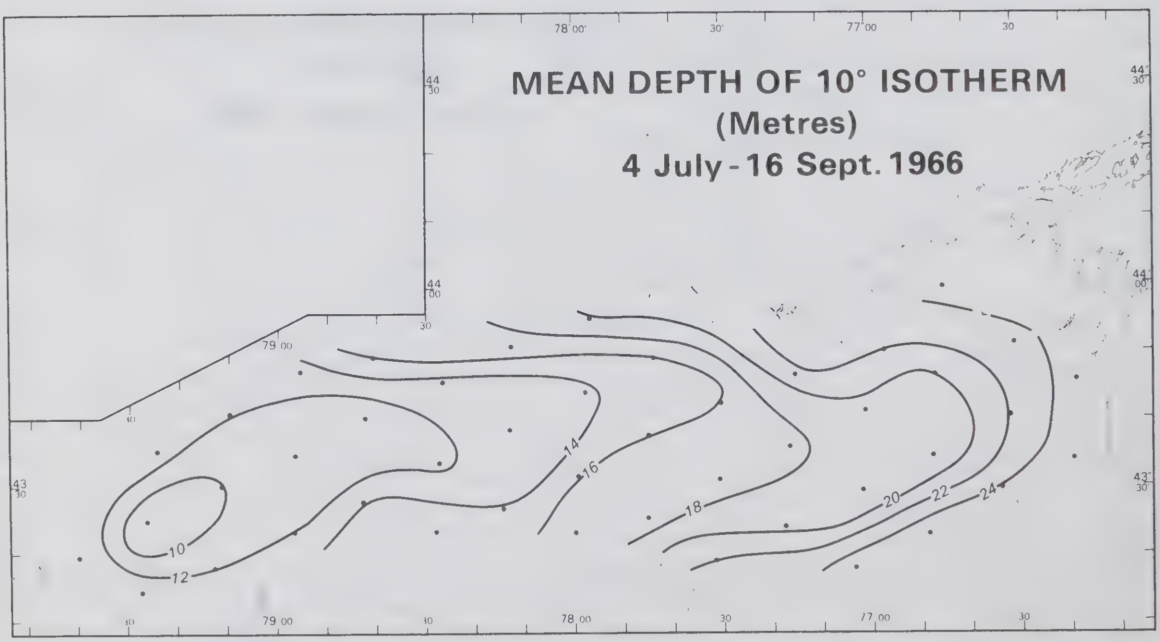

Fig. 18 Summer-mean distribution of the depth of the 10°C isotherm in 1966.

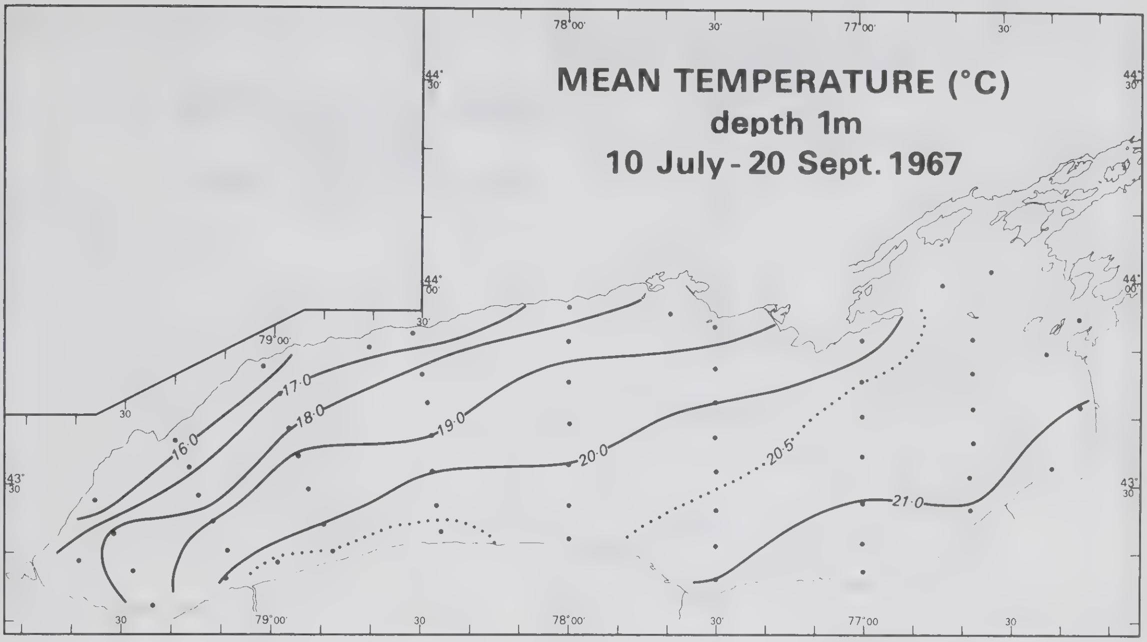

Fig. 19 Summer-mean surface temperature distribution in 1967.

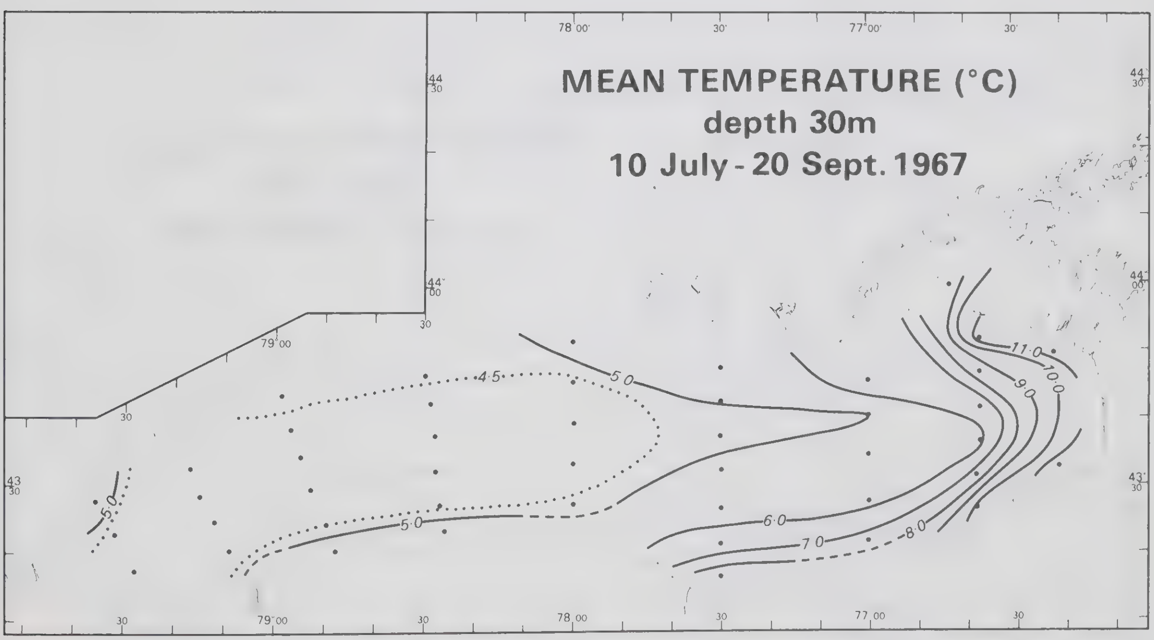

Fig. 20 Summer-mean temperature distribution at the 30-metre level in 1967.

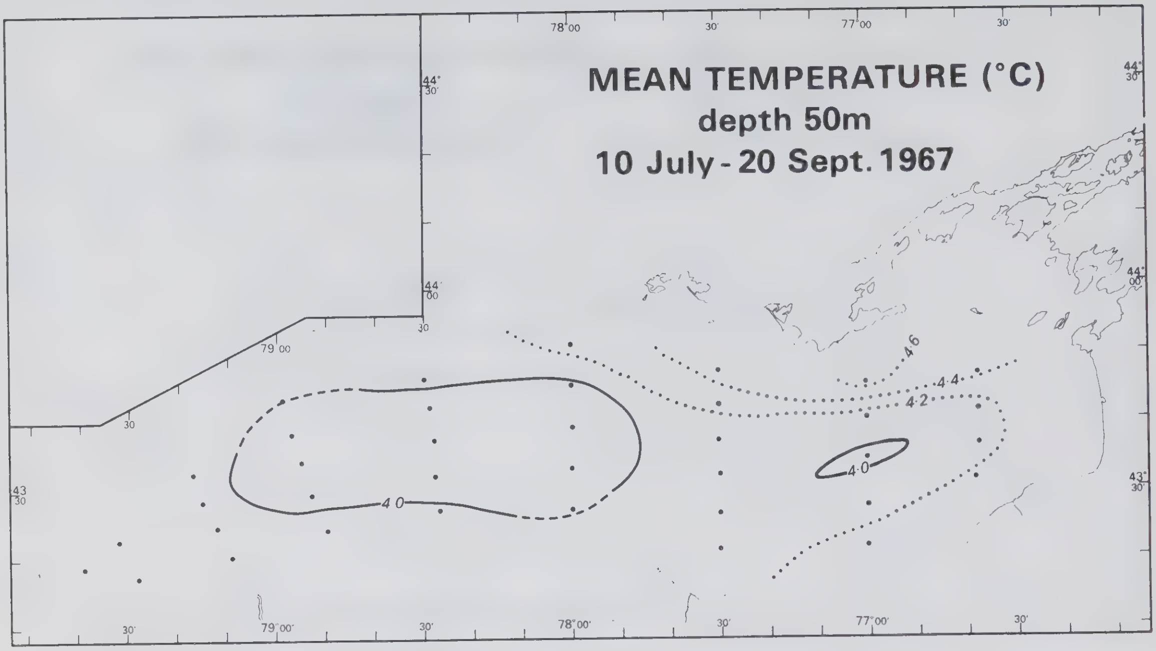

Fig. 21 Summer-mean temperature distribution at the 50 metre level in 1967.

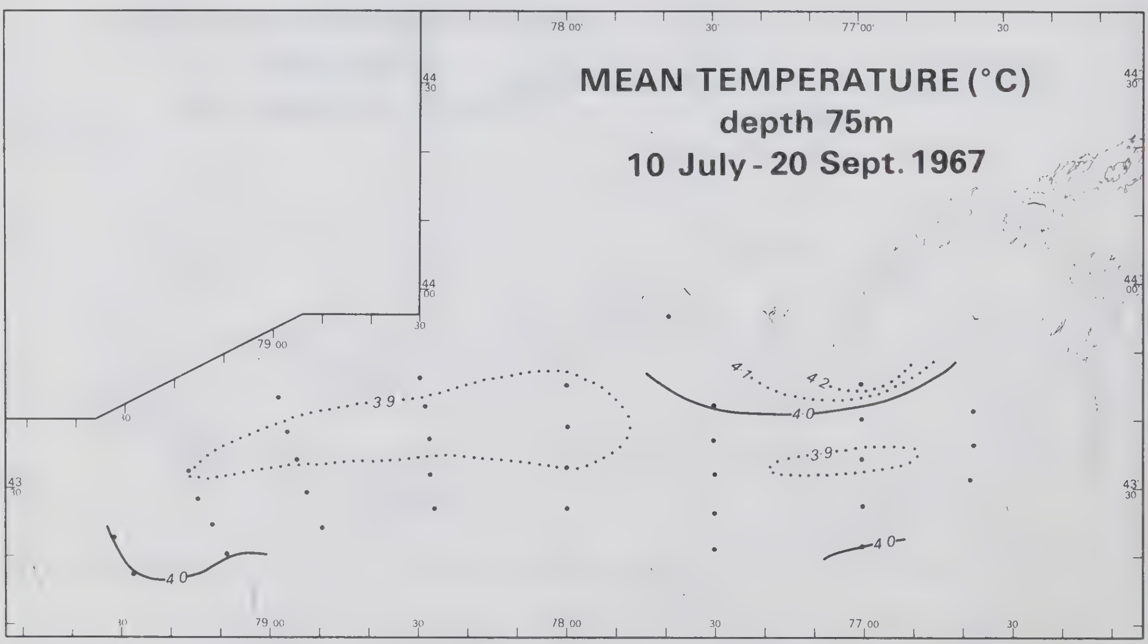

Fig. 22 Summer-mean temperature distribution at the 75-metre level in 1967.

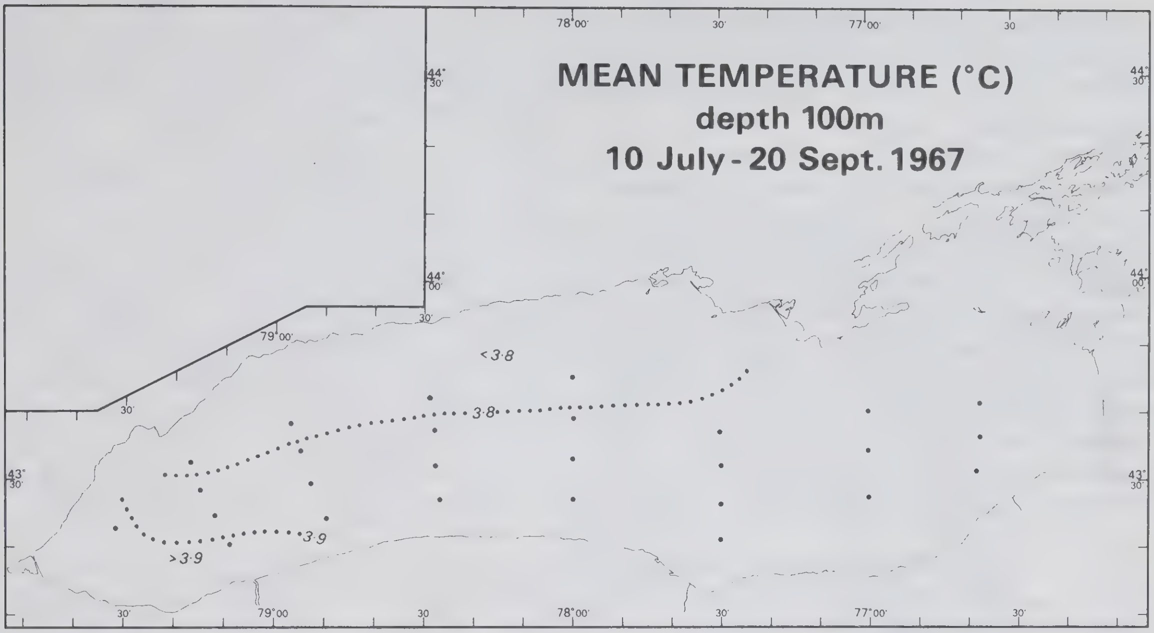

Fig. 23 Summer-mean temperature distribution at the 100-metre level in 1967.

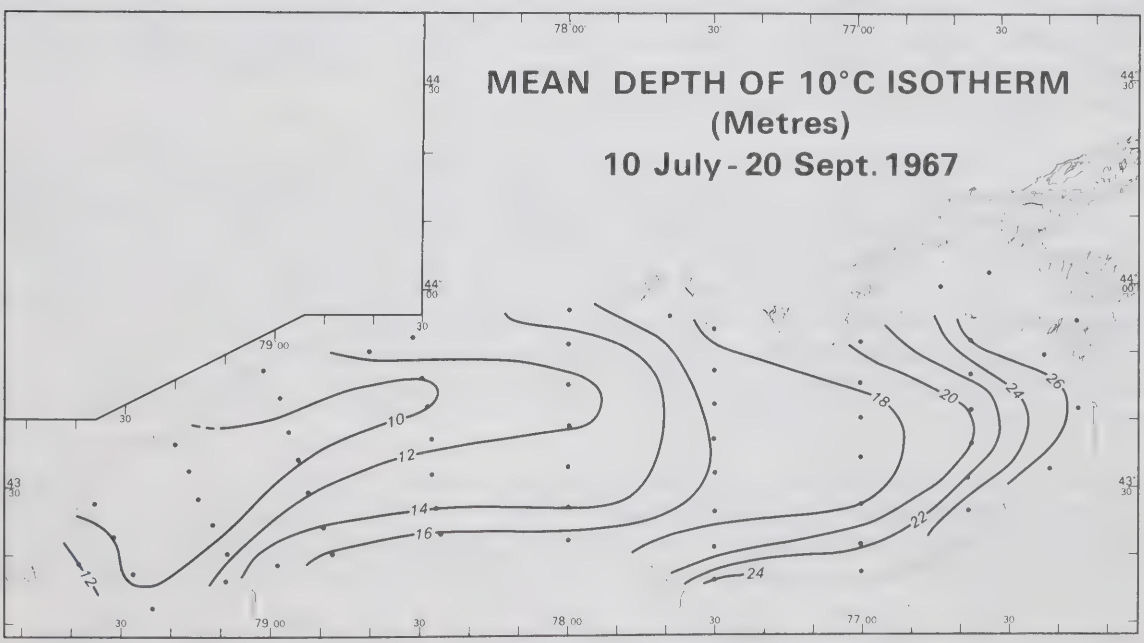

Fig. 24 Summer-mean distribution of the depth of the 10°C isotherm in 1967.

The location of the temperature minimum in the western end of the lake changes with depth. At the surface and 10 metre levels it occurs close to the Toronto shore, at the 20 and 30 metre levels it has shifted towards the middle of the lake and is separated from all shores by a band of warmer water. At the 30 metre level, for example, the minimum temperature in both years is reached midway between Toronto and the mouth of the Niagara River. Temperatures near the Toronto side are up to 2C° higher, near the Niagara side up to 0.5C° higher than in the middle. This mid-lake temperature minimum is also reflected by the average depth of the 10° isotherm, which in the centre is 9 metres, a few metres less than near the Toronto and Hamilton shores, and about 4 metres less than near the southern shore. Increased vertical mixing in shallow water can depress the thermocline near the shores, but this is usually a more local effect than suggested by the observed patterns (Figs. 18 and 24), and thus cannot completely explain the observed distribution.

The mid-lake temperature minimum at intermediate depths suggests the possible existence of a fairly consistent, counter-clockwise rotation of waters in the layers above the thermocline, causing a westward current along the northern shore and an eastward current along the southern shore.

The mid-lake temperature minimum is most obvious in the west end of the lake. The fact, however, that both the isotherms in the deeper levels and the iso-depth lines of the thermocline tend to run parallel to the shores, suggests that the mid-lake temperature minimum would extend over most of the deeper parts of the lake if this were not masked by the overall east-west slope of the thermocline. This, in turn, may indicate that the counter-clockwise rotation may circle the whole lake rather than only the far western corner.

In the hypolimnion the horizontal temperature gradients are greatly reduced, and at the 150 metre level the temperature is so nearly homogeneous that the available data do not indicate any significant horizontal temperature gradients. At intermediate depths, notably at the 75 and 100 metre levels, a very interesting temperature maximum is found at a station 14 km south of Prince Edwards Point (Station 13, see Fig. 4, and Station 49, Fig. 5), which will be discussed in more detail in Section 3.4.2.

The persistency of the east-west gradients in temperature and thermocline depth is related to the predomination of eastward winds throughout the two summers. This is illustrated well by Figs. 7 and 8, showing the weekly mean vector winds for Toronto International Airport. Periods with westward winds never lasted long enough to reverse the direction of these overall gradients, although they may have considerable local influence, as was pointed out. In the Sections 6.2 and 6.3 some

calculations are made relating the east-west slope of thermocline depth to mean wind strength and to the time needed for the lake to respond to a change in wind conditions by a complete reversal of east-west gradients.

3.1.3 Early fall

The last cruise in 1966 (late September) indicates the onset of fall in the thermal regime, which is characterized by a rapid turbulent downward mixing of the thermocline and a rapid decrease of the average surface temperature. Within a two week period the average surface temperature drops by almost 5C° to 13.9°C, and the intensity of the vertical temperature gradient in the thermocline region decreases to half its original value (Section 3.3). The onset of the fall regime coincides with a reversal of the net heat flow through the surface of the lake from a gain into a loss. The resulting convective downward mixing of the cooled surface waters causes an "erosion" of the thermocline (Tully and Giovando, 1963). This effect is strengthened by a period with strong winds just prior to the cruise.

In 1967 the onset of the fall regime becomes obvious in the early October cruise, which also shows a drop in mean surface temperature of 5C° from an average of 19°C during the previous cruise. The maximum vertical temperature gradient decreases considerably, and the thermocline depth ranges over an interval of more than 43 metres. Both this cruise and the late September 1966 cruise show strong upwelling along the northwestern shore, caused by strong winds immediately prior to the start of the cruises.

The trends indicated by the results of the early October cruise in 1967 continue during the mid and late October cruises. The thermal structure is irregular and strongly inclueneced by the wind, and upwelling seems to be a regular feature. Theoretically, the cooling should proceed more rapidly in the shallow, nearshore waters than in the middle of the lake, and the isotherms should align themselves more or less with the shorelines and depth contours. This effect, however, is completely masked by other phenomena, such as upwelling. It probably does not become dominant until the thermocline has descended much deeper. Neither of the two field seasons studied extended late enough in fall to observe this, but Rodgers and Anderson's (1961) data and the ART temperature charts of the Lakes Investigation Unit (DOT, 1968) illustrate that the isotherms tend to align themselves with the shores later in fall.

3.2 Mean Temperature and Thermocline Depth

Some of the characteristics of seasonal variations in the thermal structure arise very clearly from a study of the cruise-to-cruise variations in the lake-mean temperature and

thermocline depth and by comparing these with means for the eastern and western halves and for groups of stations in the Toronto and Oswego regions respectively (Figs. 9, 10, 11 and 12). The eastern and western sections are separated by a north-south line dividing the area of the lake approximately into two equal parts; the position of the stations chosen as being characteristic for the Toronto and Oswego regions respectively shown in Fig. 5. The vertical axis in Figs. 11 and 12 indicates both depth and the ratio, in percent, of the volume of lake water above that depth to the total volume of the lake[1]. The latter scale can be used, for example, to define the volume of epilimnion water, or of a water mass within certain temperature limits.

3.2.1 Late Spring

The average surface temperature rises rapidly during late spring: about 0.2°C per day in 1966 and 0.4°C/day in 1967 over the four week period between the first and third cruises, and the lake-mean depth of the 10°C isotherm increases at a rate of about 25 cm per day from 3 to 11 metres in 1966 and from 7 to 14 metres in 1967. The difference in mean thermocline depth between the two years is partially due to a difference in the dates of the cruises, but its mean depth at comparable dates is somewhat larger in 1967 than in 1966. The temperature at the 20 metre level increases only slightly during this period. The mean surface temperature in the eastern and western halves of the lake is about equal, but the thermocline is in both years somewhat deeper in the eastern section.

3.2.2 Summer

In 1966 the mean surface temperature reaches its maximum of 20.6°C very early in the summer (around July 10). In 1967 a slightly higher maximum, 21.3°C, is reached a month later. The mean temperature at the 20 metre level increases much more slowly, and does not reach its peak of about 13°C until late September. Decreases of the average surface temperature, such as during the second part of July 1966 and in mid-July, August and late September 1967 respectively, are coupled with relatively rapid increases in both the temperature at the 20 metre level and the tilt of the thermocline (Figs. 9, 10, 11 and 12). This is not surprising, since an increase in thermocline tilt will cause an increase in the lake-mean temperature at levels below, and a decrease above its mean depth (Fig. 25). Variations in the mean surface temperature throughout the summer season thus are to a large extent determined by

---

[1] These have been calculated from the area-depth curves given by Anderson (1961).

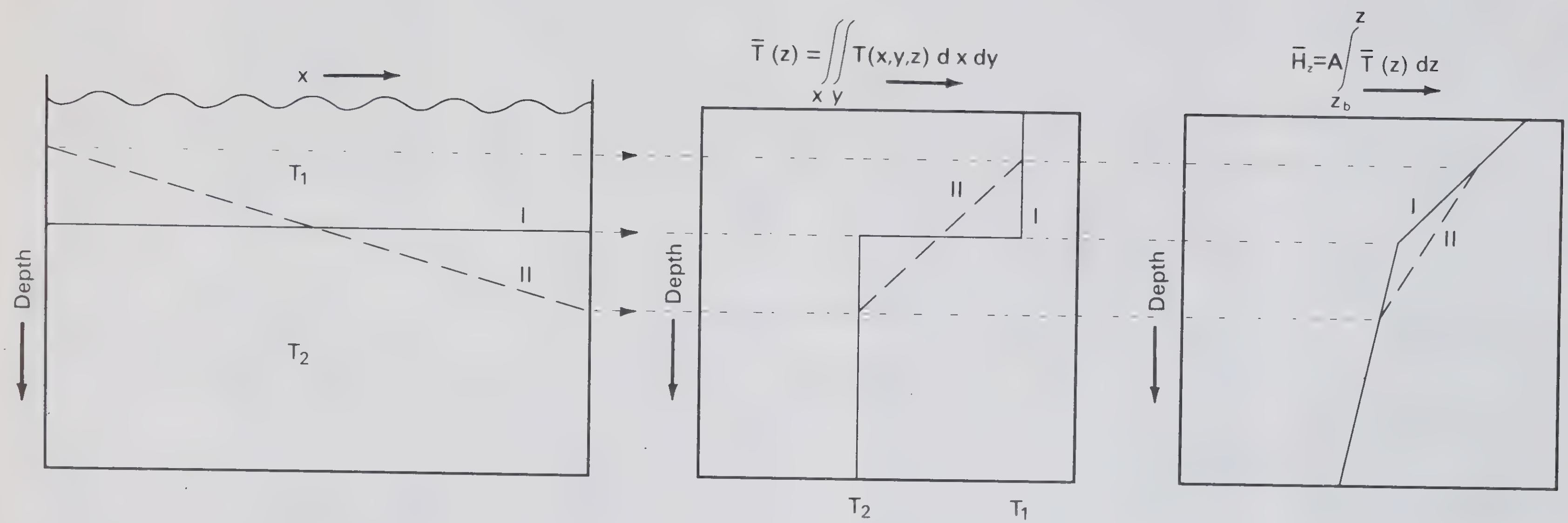

Fig. 25 Lengthwise section of a two-layered model lake showing the interface between the two layers before (I) and after (II) tilting. The next two diagrams show the mean temperature and the mean heat content below each level respectively as a function of depth before (I) and after (II) tilting, illustrating the resulting reversible, convective downward transport of heat.

changes in the tilt of the thermocline, and minima will occur during periods of strong upwelling. The observed differences in time and temperature of the maxima in the two years may thus not be significant in terms of the climatology of the lake.

The surface temperature at individual stations usually ranges between 18 and 22°C, only dipping below this in upwelling areas and increasing above this under exceptionally quiet periods or near the shores in relatively sheltered areas. The highest surface temperature observed locally in the open lake during the two summers is just over 24°C, off the mouth of the Niagara River in mid-July 1966 (Fig. F.16).

A comparison of the Figs. 11 and 12 reveals an interesting difference between the thermal regimes in the two summers. The summer-mean thermocline depth is slightly less in 1967 than in 1966 (15.7 versus 16.9 metres). The mean volume of the epilimnion, defined by the volume of water above the 10°C isothermal surface, thus is 17 and 18% respectively in the two years. More important, however, is that the mean depth increases gradually throughout the summer of 1966, at a rate of approximately 15 cm/day, whereas it is almost constant during the months of July and August in 1967. This difference is probably related to differences in the wind patterns in the two years. The mean wind strength, and especially the frequency of occurrence of strong winds, windforce 5 or over, is exceptionally low in the summer of 1967 (Table 3, Section 2.3).

The depth of the thermocline is dependent on various factors, such as convective downward mixing and wind induced turbulence (Tully and Giovando, 1963). During the heating season the latter is the most important factor, and the relation between wind strength and thermocline depth in the summer is discussed in more detail in Appendix C. Variations in the depth of a seasonal thermocline are especially sensitive to the force of the strongest winds during the period of observation, and the lack of strong winds during the summer of 1967 may thus well explain its stationarity throughout the months of July and August. The first day with a daily mean squared wind velocity[1] corresponding to an average wind strength of windforce 4 or over occurred in late August (root mean square wind speed of 630 cm/sec). During the summer of 1966, on the other hand, winds with a comparable strength occurred regularly, at least once every two or three weeks. According to Tabata's equation (Appendix C) a 12-hour mean wind speed of 700 cm/sec can increase the depth of the mixed layer to 10.4 metres which corresponds to a depth of roughly 14.4 metres of the 10°C isotherm. This is close to the average thermocline depth, and

---

[1]All wind speeds quoted are for Toronto International Airport; a correction can be made to obtain a better estimate of wind speeds over the lake by multiplying them by the lake breeze index (Richards, 1964), which averages 1.39 over the summer.

winds of this force may thus influence its mean depth, especially since the actual thermocline depth may vary a great deal over the area of the lake.

It has already been pointed out that the summer-mean surface temperature is much lower in the vicinity of Toronto (14.5°C) than in the southeastern end of the lake (21.5°C). The persistency of this difference is also well illustrated by Figs. 9 and 10, showing a difference in the mean temperatures for groups of stations in these areas decreasing from 6C° in July to 2C° by mid-September. The only exception to this pattern is during the mid-July 1967 cruise, in which the surface temperature is almost uniform over the total area of the lake.

The decrease in magnitude of the east-west temperature gradient later in the summer might suggest a significant difference in the thermal structures of early and late summer. A comparison with the depth of the thermocline (solid line in Figs. 11 and 12), however, shows that it merely is a reflection of the steady increase in the mean depth of the latter. A tilt of the thermocline will have its largest effect on the east-west temperature gradient at the surface when its average depth is small. If, on the other hand, its mean depth is closer to the 20 metre level, the largest horizontal temperature gradients will result at this depth. The Figs. 9 and 10 clearly illustrate this point, showing that the difference between the 20 metre temperatures at opposite sides of the lake increases gradually throughout the summer, reaching a maximum of 12C° in the late August, early September.

Throughout the summer the thermocline slopes downwards towards the east at a rate of between 8 cm/km and 2 cm/km, averaging 5.6 cm/km. This slope is never reversed or levelled out, not even during prolonged periods of weak winds (Figs. 11 and 12). In Section 6.3 it will be shown that even a westward wind will not be able to reverse the existing slope unless it is both fairly strong and very consistent. Rough calculations indicate that a strong westward wind of at least 2.5 days duration (or an average wind of 7.3 days duration) is needed to reverse the thermocline.

The difference in the mean thermocline depth in the eastern and western halves is, after its initial establishment in late June or early July, fairly constant throughout the summer, averaging 7.4 and 8.4 metres respectively (Tables 5 and 6) over the two summers. The mean surface and 20 metre level temperatures differ in both years by about 2.7 and 5.7C° respectively. These differences indicate a large east-west gradient in the heat storage per cm^2 surface area; the consequences of this on circulation in the lake will be discussed in Chapter 4.

3.2.3 Fall

In the second part of September the direction of heat flow reverses and the lake starts cooling. As a result the surface temperature decreases again and, partially due to convective downward mixing of cooled surface waters and partially due to the increased frequency of strong winds in fall, the thermocline is "eroded" and increases in depth more rapidly than before. In both years the surface temperature drops by 5C° from 19 to 14°C over a two week period and the mean thermocline depth increases by 2 metres. In early October 1967 the rate of descent of the thermocline increases to 5 metres per fortnight. Even more striking is the decrease in the intensity of the thermocline, which will be discussed in Section 3.3.

The volume of the epilimnion increases rapidly from 18 to 26% by mid-October in 1967, and the mean temperature of waters in the 30 to 50 metre depth range starts increasing in October from an average of 4.4°C throughout the summer to 8 to 5°C, depending on depth, by the end of the field season in late October (Fig. F.105). The maximum temperature at these levels, however, is probably not reached until much later. In 1959 Rodgers (1961) measured a maximum temperature of 9°C at both the 30 and 60 metre levels by the end of November.

3.3 Intensity of the Thermocline in the Summer

In Section 2.1.4 two techniques for calculating a lake-mean temperature profile have been outlined, and it is pointed out that the function $\overline{Z}(\theta)$ has certain advantages in a study of the thermocline. The temperature profiles shown in Figs. 26 and 27 are cruise averages of all bathythermograph data extending beyond a depth of 40 metres. The abscissa gives temperature, the ordinate depth below the surface as well as the relative volume of water above each level (with reference to a total volume of 1620 km^3; Anderson, 1961).

The intensity of the thermocline is, for the purpose of the following description, defined as the maximum vertical temperature gradient over a 6C° interval and is expressed in units of Celcius degrees per metre. The $\overline{Z}(\theta)$ curves for the spring cruises only indicate the relative volume of water above certain isothermal surfaces, but do not give an accurate estimate of the intensity of the thermocline, since only part of the lake is stratified (Sweers, 1968). During the summer, however, the intensity indicated by the $\overline{Z}(\theta)$ curves is approximately equal to the mean of the intensities of the individual temperature profiles, and the temperature gradients almost always reach a maximum between the 10 and 14°C isothermal surfaces.

The cruise-mean intensity fluctuates between 1.5 and 3.5 C°/m, and averages 2.6 C°/m in 1966 and 2.3 C°/m in 1967 (Figs. 26 and 27 respectively). There is no obvious correlation

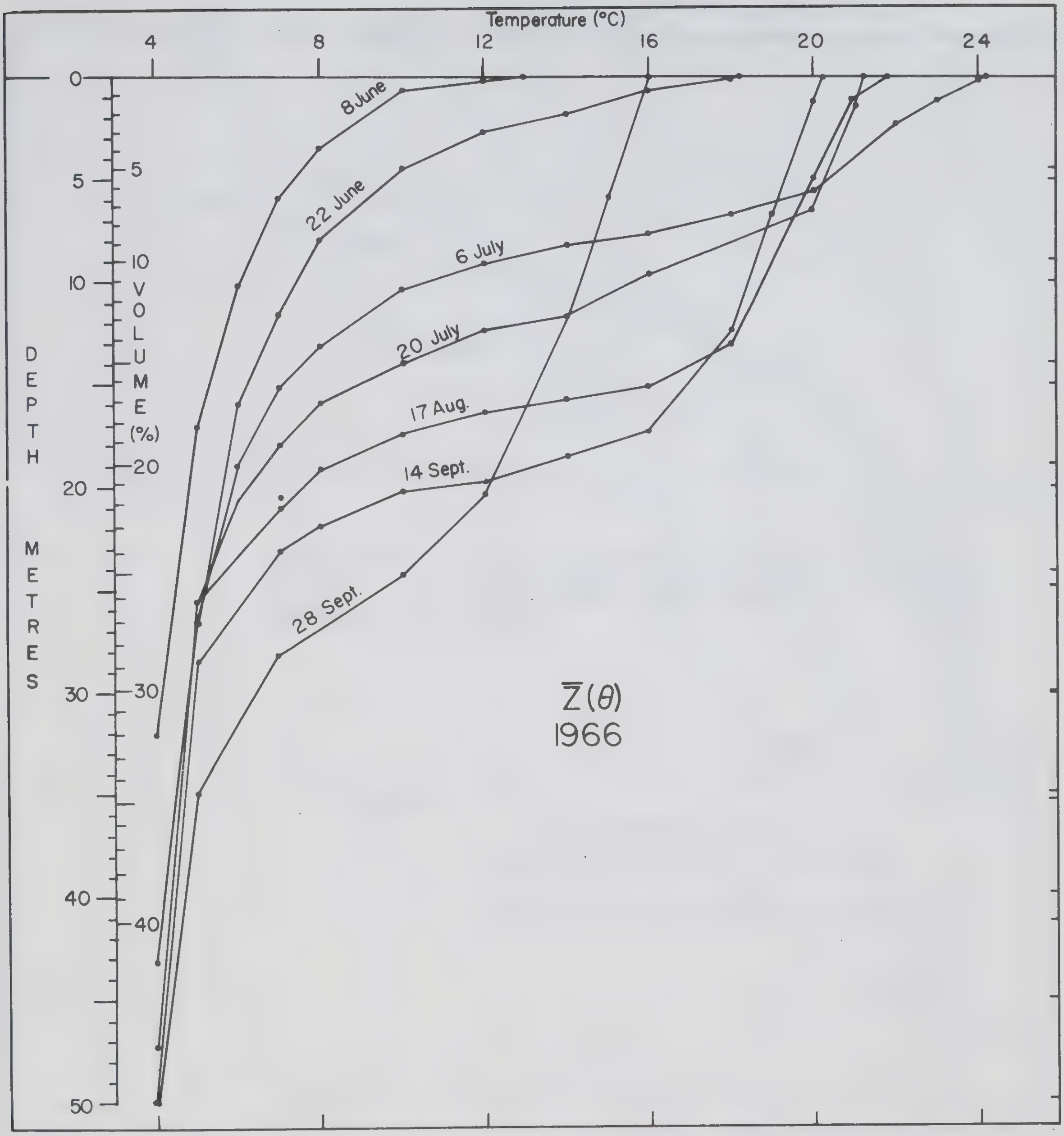

Fig. 26 Mean vertical temperature profiles $\bar{Z}(\theta)$ for the 1966 cruises.

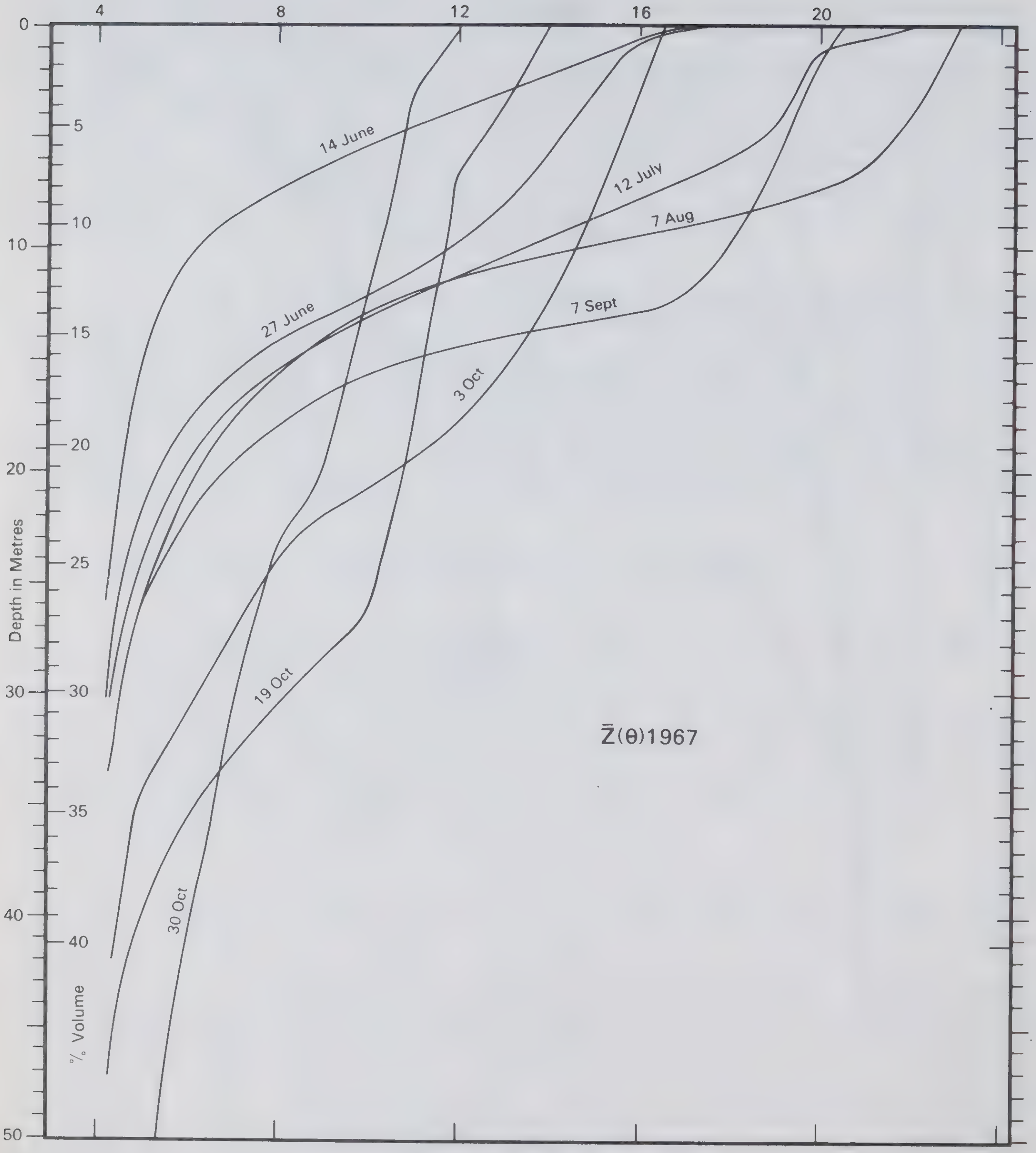

Fig. 27 Mean vertical temperature profiles $\bar{\bar{Z}}(\theta)$ for the 1967 cruises.

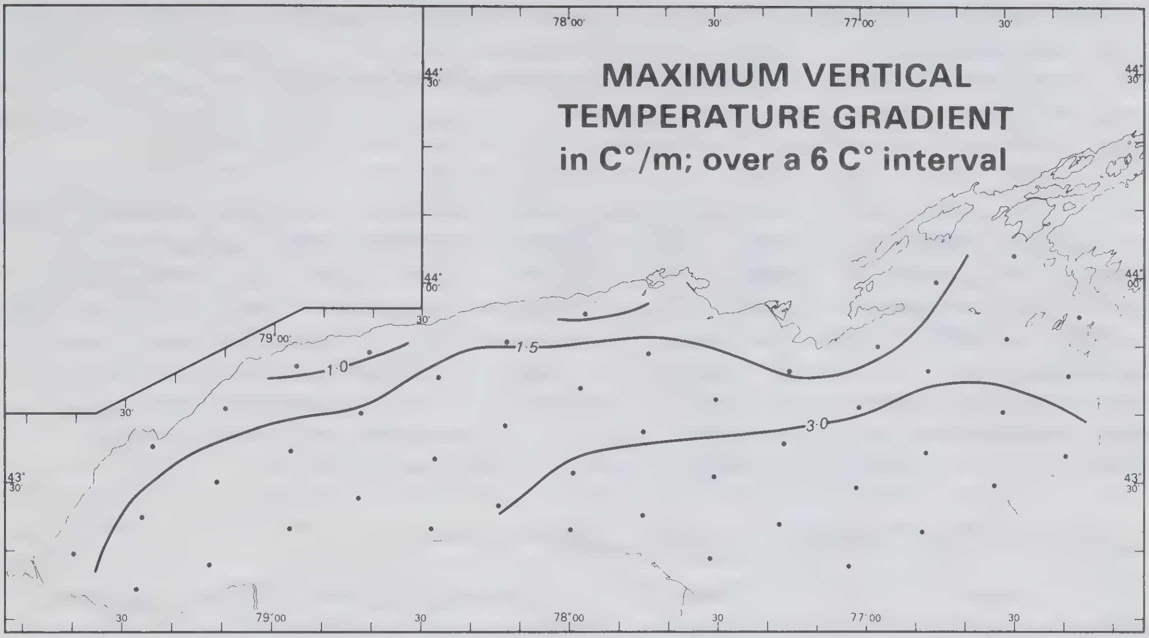

Fig. 28 Maximum vertical temperature gradient over a 6C° interval; mean distribution for the summer of 1966.

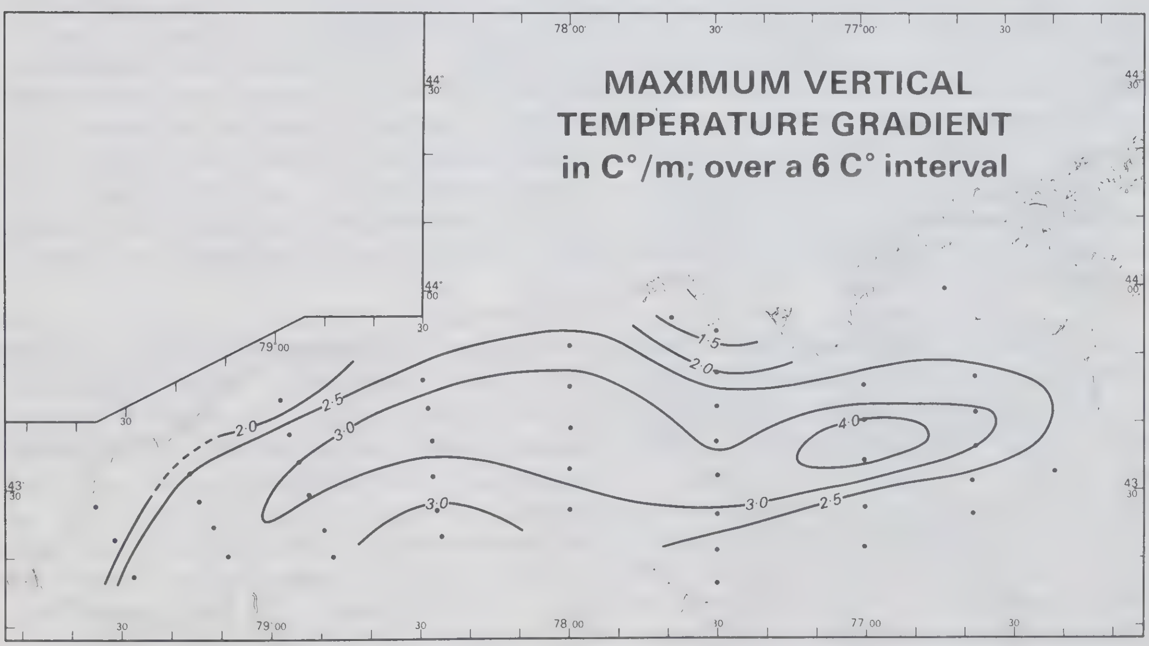

Fig. 29 Maximum vertical temperature gradient over a 6C° interval; mean distribution for the summer of 1967.

between the mean maximum vertical temperature gradient and either the wind strength prior to the time of observation or the depth of the thermocline. During the second part of September in both years the thermocline intensity decreases rapidly to about 1°C/m by the end of the month, marking the onset of fall in the thermal regime.

A study of the spacial distribution of the summer-mean thermocline intensity for the individual stations reveals no consistent patterns (Figs. 28 and 29). In 1966 the intensity ranges from about 4 C°/m in the western section to 1.2 C°/m near Toronto, in 1967 the steepest gradients (3.5 C°/m) occur over the deeper parts of the lake and there is no indication of a consistent east-west gradient. There is no obvious relation between the mean thermocline depth at any location and the maximum of the vertical temperature gradient.

3.4 Consistent Regional Anomalies

Some of the lake-wide characteristics of the thermal structure have been discussed in previous sections. In this section a number of local phenomena will be discussed in more detail.

3.4.1 Niagara River

The Niagara River is the major tributary to Lake Ontario, supplying about 80% of the total influx of water. Its influence on the thermal structure is clearly visible, both in the surface temperature distribution and in the thermocline depth. Throughout the 1966 and 1967 field seasons the surface temperature near the mouth of the Niagara River is above the lake-mean surface temperature, sometimes by as much as several degrees, but it is usually close to the temperature in the area north of Main Duck Island which feeds the St. Lawrence River. (see for example the summer mean temperature distributions, Figs. 13 and 19). This confirms the conclusion reached earlier by Rodgers and Anderson (1963), based on river temperature data, that the net advective term of the overall heat budget of the lake is very small.

The thermocline usually slopes downwards rather steeply towards the river outfall from the north and west, but remains deep in a narrow band extending eastwards along the shore (for example Figs. 18 and 24). The summer-mean temperature distributions (Figs. 13 and 19) show a tongue of relatively warm water extending eastwards along the southern shore from its mouth. A study of the distribution patterns during the individual cruises, however, reveals that the core of this high temperature area is rather variable in shape and extent. Sometimes it follows the southern shore (Figs. F.10 and F.93), but on other occasions (see for example Figs. F.16, F.23 and F.67) it extends towards the north or even northwest into the lake. The areal extent of

the temperature maximum is never very large, suggesting a fairly rapid mixing of Niagara River water with the lake water.

3.4.2 Deep Maximum South of Prince Edward Peninsula

In both years a very interesting, and statistically highly significant, temperature maximum has been observed in the hypolimnion at 14 to 21 km south of Prince Edward Peninsula (at Station 13, Fig. 4, and Station 49, Fig. 5, respectively). Its location and depth are slightly different in the two years. In 1966 the maximum is most obvious at the 75 metre level 21 km south of Prince Edward Point; in 1967 it is more obvious somewhat closer to the shore, 14 km offshore, at the 50 metre level (Figs. 15 through 17 and 21 through 23). The summer-mean deviation of the maximum temperature from the average temperature at the same level is about 0.5C° in both years. Under the assumption that temperature observations in the hypolimnion can be considered as random samples taken from a Gaussian population, the probability of such a deviation arising by chance is less than 0.01%! The location of the maximum varies slightly from cruise to cruise, but it is always in the general area indicated by the charts giving summer-mean temperature distributions at the 50, 75 and 100 metre levels in the two years respectively. Temperatures at a depth of 75 metres at Station 13, in 1966,and at a depth of 50 metres at Station 47, in 1967, are for every single cruise above the lake means for these depths respectively.

There is no direct relation between temperature distributions at higher levels and the location of the hypolimnion maximum. The surface temperature, and especially the thermocline depth, are much less south of the Prince Edward Peninsula than in the far southeastern section of the lake, and there are no obvious topographical features that could be used to explain a temperature anomaly in the hypolimnion of this magnitude and consistency. It therefore appears that the maximum cannot be explained by a downward movement or increased downward mixing of epilimnion water. This impression is strengthened by the fact that in 1966 the mean conductance of water in the temperature maximum is 3 μmhos/cm higher (about 1%) and the average pH is 0.05 units lower than their lake-mean values at the corresponding level, whereas the epilimnion values deviate in the opposite direction from the mean hypolimnion values (Table 4). The differences are significant to better than 95%. The 1967 data unfortunately cannot be used to confirm this difference in conductance and pH, due to their lower precision (Table 1).

		hypolimnion	epilimnion	absolute difference (epil.-hypol.)	percentage difference	95% confidence limits of mean
mean for summer 1966						
hardness	mg $CaCO_3$/l	132.9	127.6	-5.3	-4.0	0.4
total alkalinity	mg $CaCO_3$/l	90.2	85.8	-4.4	-4.8	0.4
chloride	mg Cl/l	25.3	25.8	+0.5	+1.8	0.3
specific conductance	μmhos/cm	279.5	271.1	-8.4	-3.0	0.6
mean for summer 1967						
hardness	mg $CaCO_3$/l	134.3	129.0	-5.3	-3.9	0.5
total alkalinity	mg $CaCO_3$/l	86.3	81.4	-4.9	-5.7	0.9
chloride	mg Cl/l	26.3	26.8	+0.5	+1.9	0.3
specific conductance	μmhos/cm	323.6	315.4	-8.2	-2.5	1.8

Table 4 A comparison of the difference between the mean epilimnion and hypolimnion values of hardness, total alkalinity, chloride and specific conductance. The 95% confidence limits give an indication of the significance of these differences, and are based on the variability of the hypolimnion data (Table 1). They are a measure of the accuracy of the difference, but not of the reliability of the absolute values.

Both temperature and chemical data thus confirm the statistical significance of the deviations observed in the 50 to 100 metre levels south of the Prince Edward Peninsula. Further research needs to be done to pinpoint the causes of this phenomenon[1].

3.5 Details of an Upwelling Episode off Rochester

In the second half of September 1966 an extremely strong incidence of upwelling was observed along the south shore of Lake Ontario. Surface temperatures in the Rochester area dropped from an average of 20°C to a low of 8°C within 41 hours. Due to a fortunate coincidence the area was sampled twice during this upwelling episode, the first time 41 hours after the onset of a strong easterly wind, and again two days later. The winds prior to and during these sampling periods are shown in Fig. 30, the horizontal temperature distributions in Fig. 31.

The first indications of upwelling were observed in the vicinity of Oswego, about 36 hours after the change of the wind. When the Rochester area was sampled, about 5 hours later, the upwelling was firmly established and the minimum surface temperature had dropped to below 8°C (Fig. 31). During the second visit 42 hours later, a full twelve hours after the wind had reversed again, the upwelling was even stronger and the minimum surface temperatures had decreased to less that 6°C. Water intake temperatures of the Monroe County water works near Rochester (1,800 metres offshore at a depth of 12 metres) indicate a marked decrease in temperature, from 17 to 9°C within a few hours, about 30 hours after the reversal of the wind. The response time at the surface is somewhat longer, since the change at the surface will lag behind the subsurface temperature decrease, and is estimated to be 36 to 40 hours.

The upward and offshore movement of the isotherms is also clearly illustrated in Fig. 32, which gives changes in the temperature distribution along a section perpendicular to the shore. The isotherms move upwards over a distance of 10 metres

---

[1] Since writing the report, data from 5 monitor cruises and 1 special cruise in 1968 have been analysed. These do not show a similar temperature maximum in the region south of Prince Edward Peninsula. The difference between 1968 and the preceding years could be due to a difference in the station positions. It is more likely, however, that the intensity of the maximum varies from year to year, indicating that it may not be as persistent a feature as suggested by the earlier data.

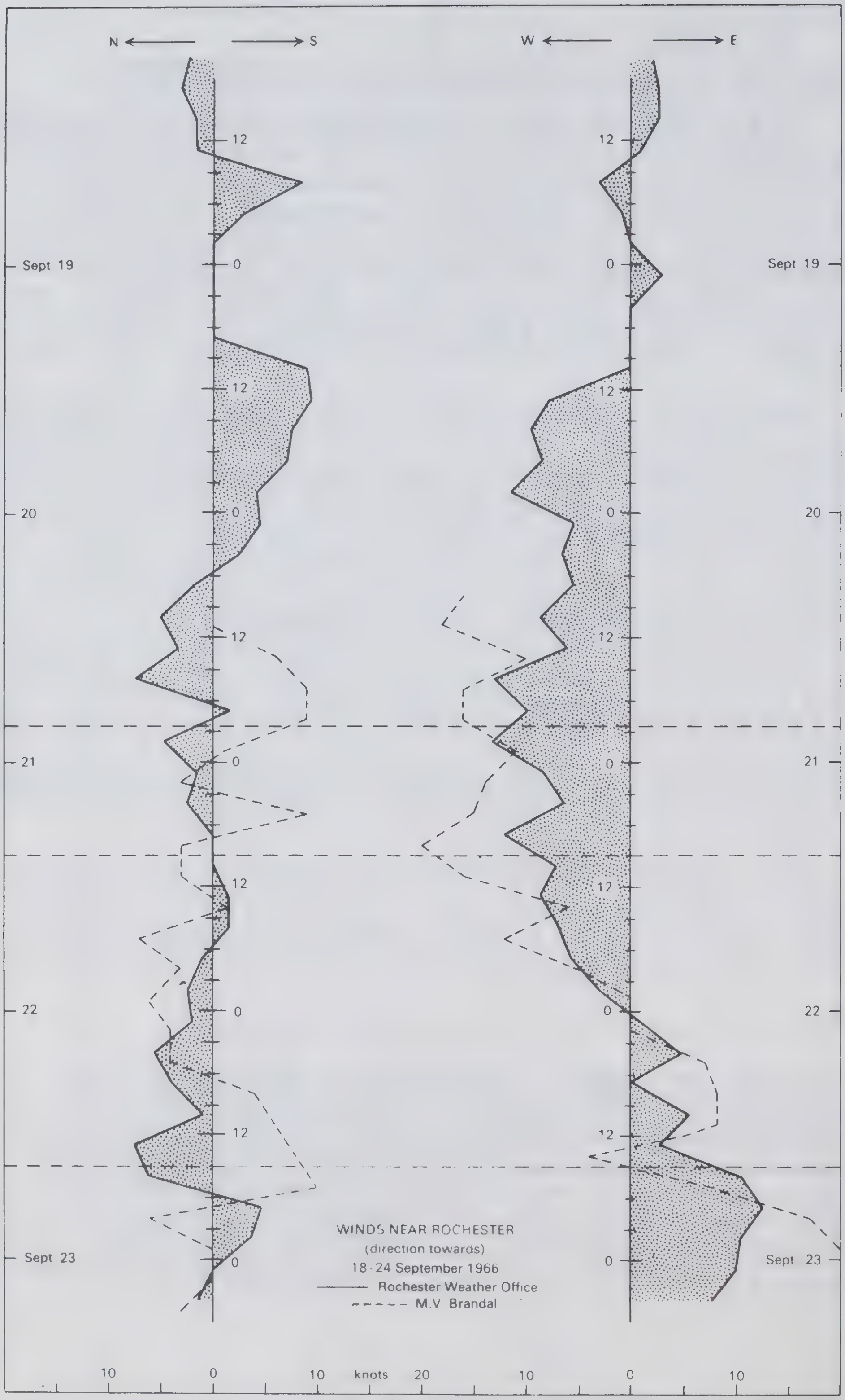

Fig. 30 Winds in the Rochester area during a period of strong upwelling, September 18-24, 1966.

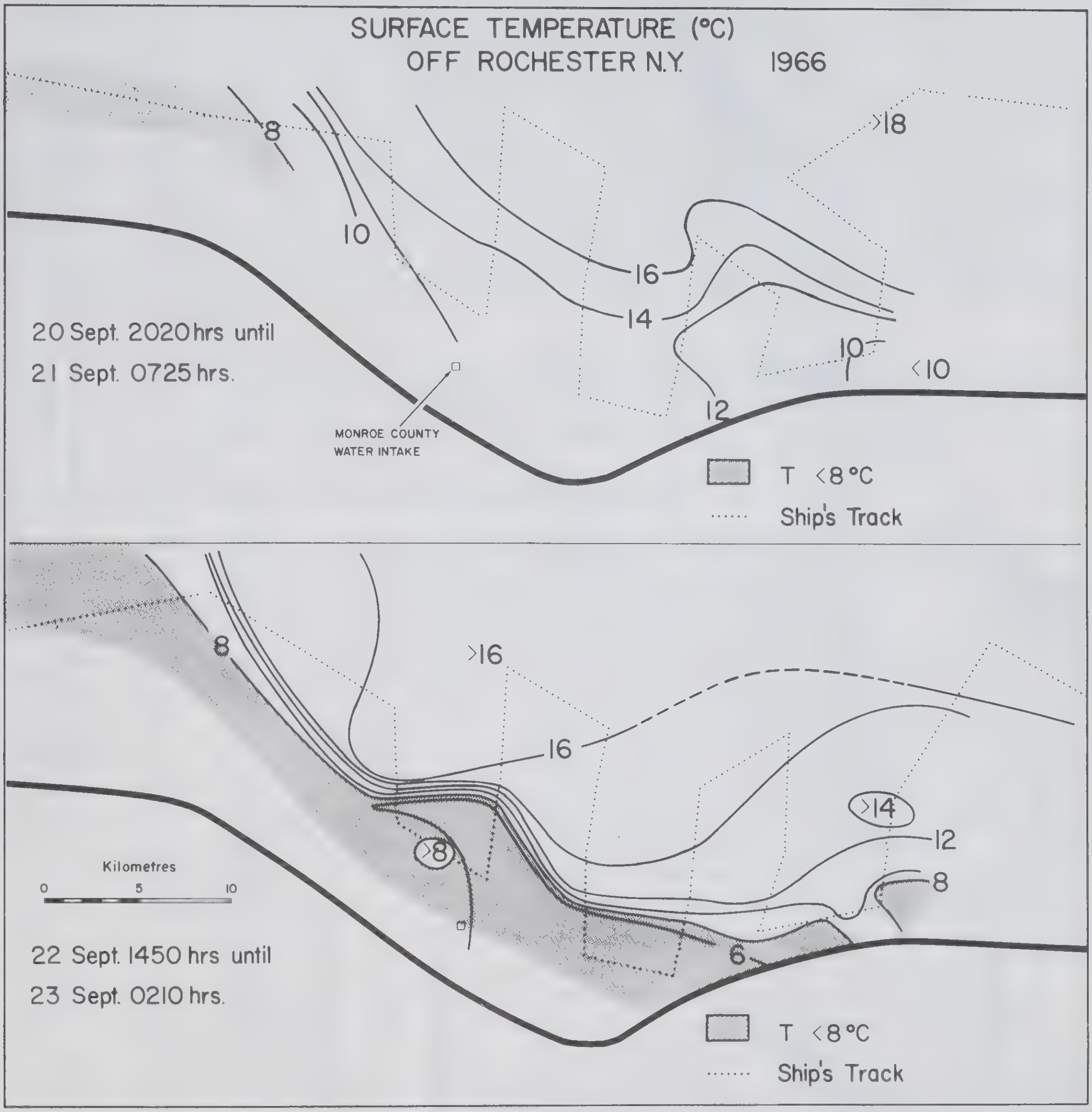

Fig. 31 Surface temperature distribution in the Rochester area during a period of strong upwelling.

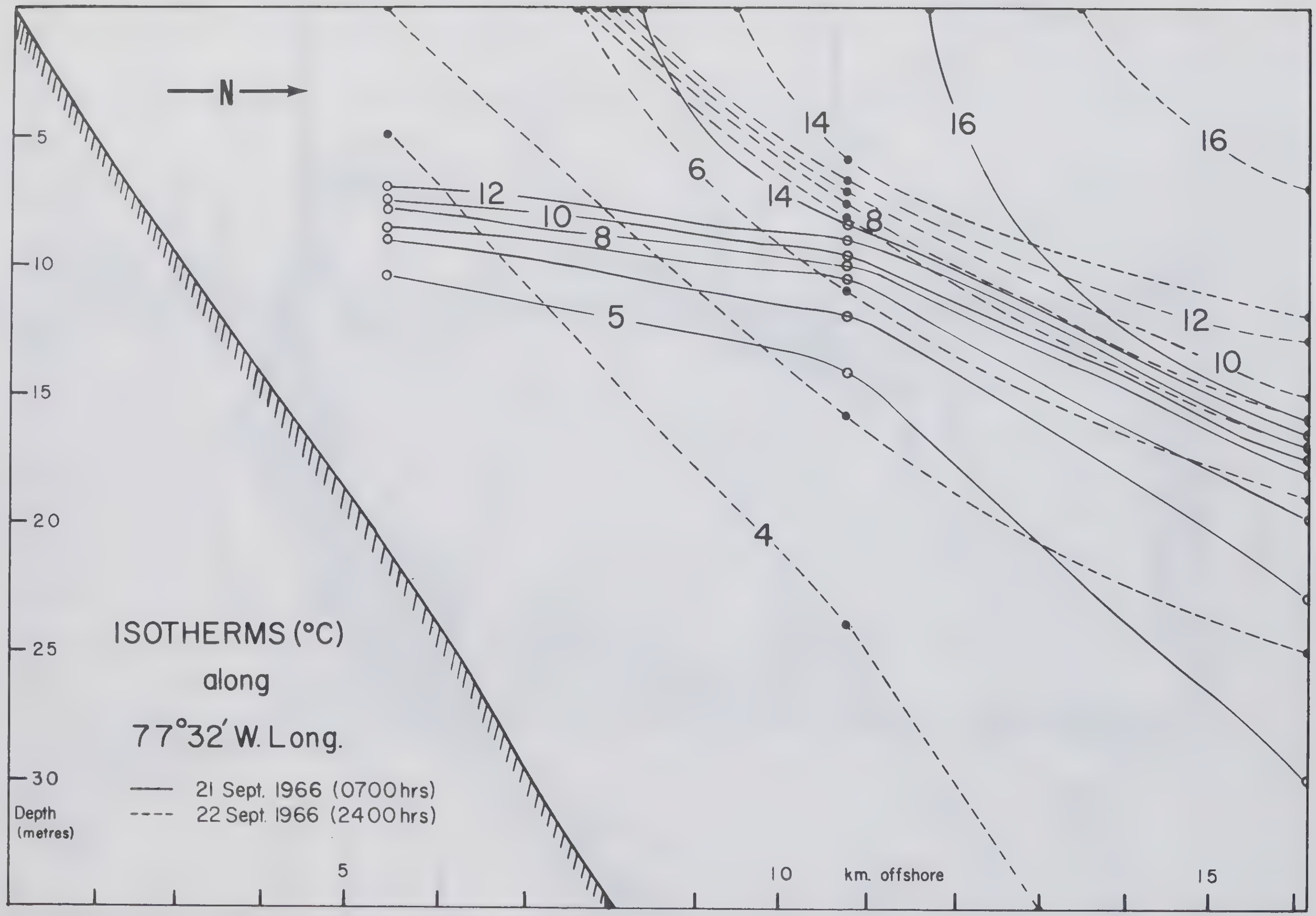

Fig. 32 Change in position over a 41-hour interval of the isotherms in a cross section perpendicular to the Rochester shore during a period of strong upwelling.

and offshore over a distance of 8 km in a time interval of 42 hours. This information can be used to obtain an estimate of vertical and offshore velocities of the water by a technique described by Smith et al (1966). Assume that there is no displacement of the isotherms due to along-shore transport, and that the exchange of heat through the surface of the water is negligible. The first assumption is at least partially supported by the fact that the surface isotherms run more or less parallel to the shore (Fig. 31), the second by the fact that the net heat input into the lake is about zero in the second part of September. The observed change in the position of the isotherms then corresponds to an upward velocity of 7×10^{-3} cm/sec and an offshore velocity of 5 cm/sec. This is only a crude estimate, since the available data are insufficient to define the changes in the thermal structure in detail, but it illustrates the order of magnitude of horizontal and vertical velocities during the upwelling episode.

Unfortunately, the cruise only covered the southern shore of the lake, and changes in thermal structure in other parts of the lake have not been observed.

3.6 A Comparison with Earlier Findings

An early attempt to describe the thermal structure of Lake Ontario was made by Millar (1952), based on data collected in the period of 1936 to 1946. He studies temperature records collected in the cooling water intakes of a number of commercial vessels crossing the lake along fixed routes, which provide only partial coverage of the lake. No data were available for the southeastern part and only few for the western sections. His conclusions nevertheless have been largely confirmed by Rodgers and Anderson (1963). The latter authors made an extensive analysis of the thermal structure during 1959 and 1960, based on a series of monitor cruises at one to two month intervals. Some of the conclusions of their work have been cited in the introduction. In this section a brief comparison between characteristics of the thermal structure observed during the summers of 1966 and 1967 and the results of the Miller and Rodgers et al will be made. Miller finds a 10 year summer-mean difference between the temperatures near Rochester and Cobourg of 3.4C°, measured at the depth of the cooling water intakes of the ships which is 4.5 to 6 metres below the surface. The estimated mean temperature difference over the summers of 1966 and 1967 at this depth is 3.2C°.

Rodgers and Anderson find a summer-mean difference between the surface temperatures near Toronto and Oswego respectively of 4.5C° (based on four cruises), which corresponds reasonably well to the mean of 6C° for the years 1966 and 1967. The mean downward slope from east to west of the thermocline is 5 cm/km in the summers of 1959 and 1960, which compares with 5.6 cm/km in 1966 and 1967.

A qualitative comparison of the surface temperature distributions observed by Miller and by Rodgers et al with the present data shows a high degree of similarity, not only during the summer, but also during late spring and early fall.

4. HEAT CONTENT

The lake-mean heat content per cm^2 surface area has been calculated from bathythermograph data by integrating the temperature-minus-four over depth from the surface to a maximum depth of 50 metres or to the bottom, whichever is shallower. Temperatures below this depth do not change enough to affect changes in heat storage by more than a few percent, which is less than the estimated reliability of the calculations. In early fall, however, a measurable amount of heat is transported to deeper layers, and the data presented in the present report have been corrected by taking this into account. In all calculations the specific heat is approximated by one, and no weight factors have been applied. The number of BT data for the last two cruises in 1967 is insufficient for accurate calculations, and these will therefore not be discussed.

The lake-mean heat content per cruise is given in Figs. 33 and 34 (for 1966 and 1967 respectively), the rate of change in heat storage between pairs of consecutive cruises in Fig. 35. The mean daily heat input decreases gradually from 450 cal/cm^2 in June to zero by the middle of September, when the cooling season starts. The 1966 data are in fairly good agreement with values published by Rodgers and Anderson (1961), based on observations in 1958 and 1959, which are indicated by the dotted line in Fig. 35. In 1967 the heat input seems to fluctuate much more erratically, and the total heat content remains nearly constant during July and August.

The total heat content in the top 50 metres reaches a maximum of 32.5 kcal/cm^2 by late September 1966, and a much lower maximum, 28.3 kcal/cm^2, in late August 1967. The summer-mean heat content is also higher in 1966, although the difference is smaller than that for the maxima, being 27.1 versus 25.4 kcal/cm^2 in 1967. The difference between the two years is caused by the low rate of heat input during the months of July and August in 1967.

In Section 3.2.2 the difference in wind conditions between the two summers has been discussed in relation to thermocline depth. It is not clear whether this also has been a factor in the difference in heating of the lake. It is interesting to note, however, that the mean epilimnion temperature, defined as the mean temperature of all water above the 10°C isothermal surface, remains almost constant at 17.5°C throughout the summer of 1966, but rises steadily throughout July and August 1967 from 14.8 to 18.9°C. The thermocline depth, on the other hand, increases at a rate of 7 cm/day in 1966, but remains almost constant in 1967, and the increase in heat content in the latter year thus is parallel to an increase in the mean hypolimnion temperature rather than to a gradual descent of the thermocline (as it was in 1966).

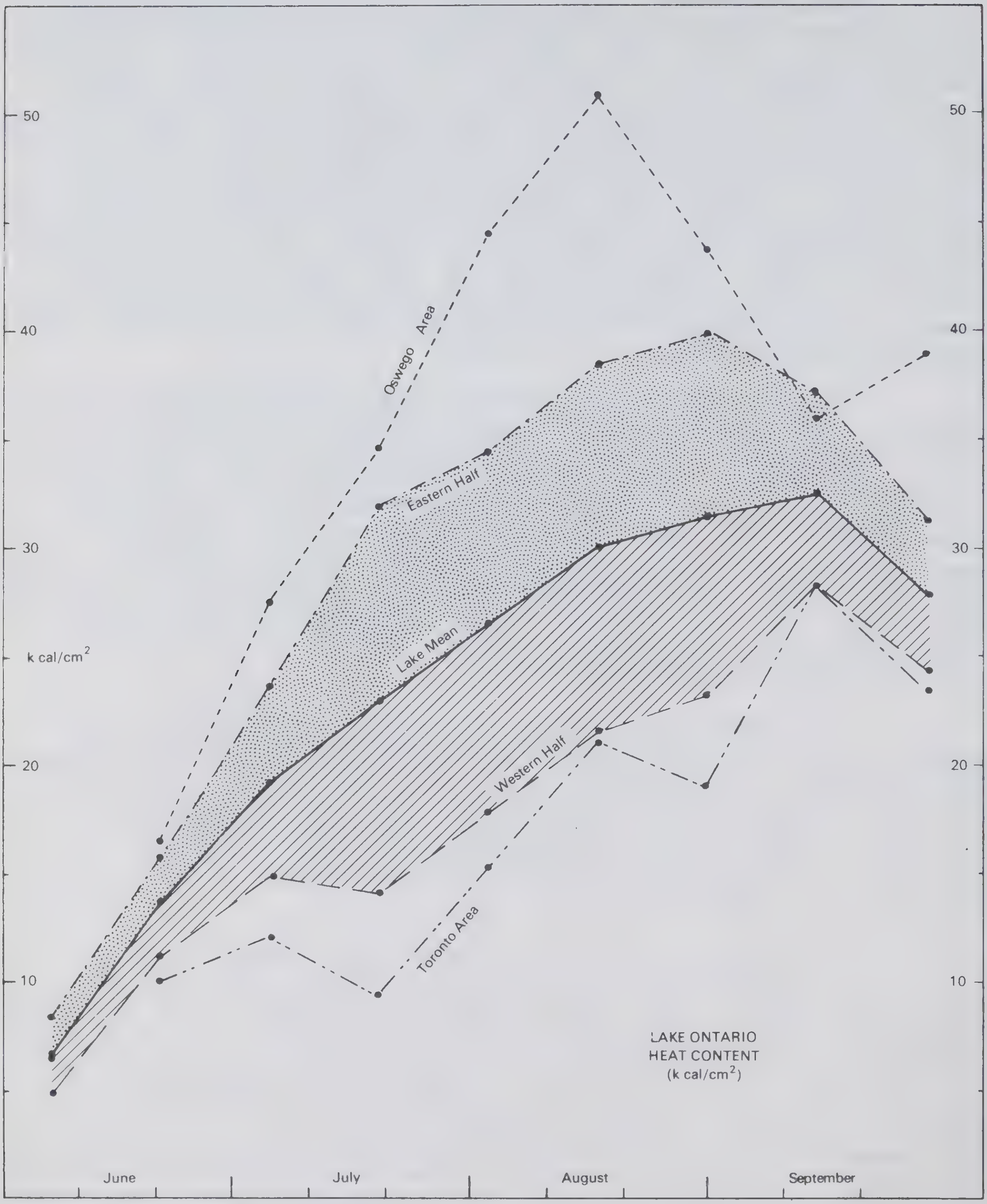

Fig. 33 Lake-mean heat content for the period of June through September 1966, compared with the means for the eastern and western halves of the lake and for the Toronto and Oswego regions respectively.

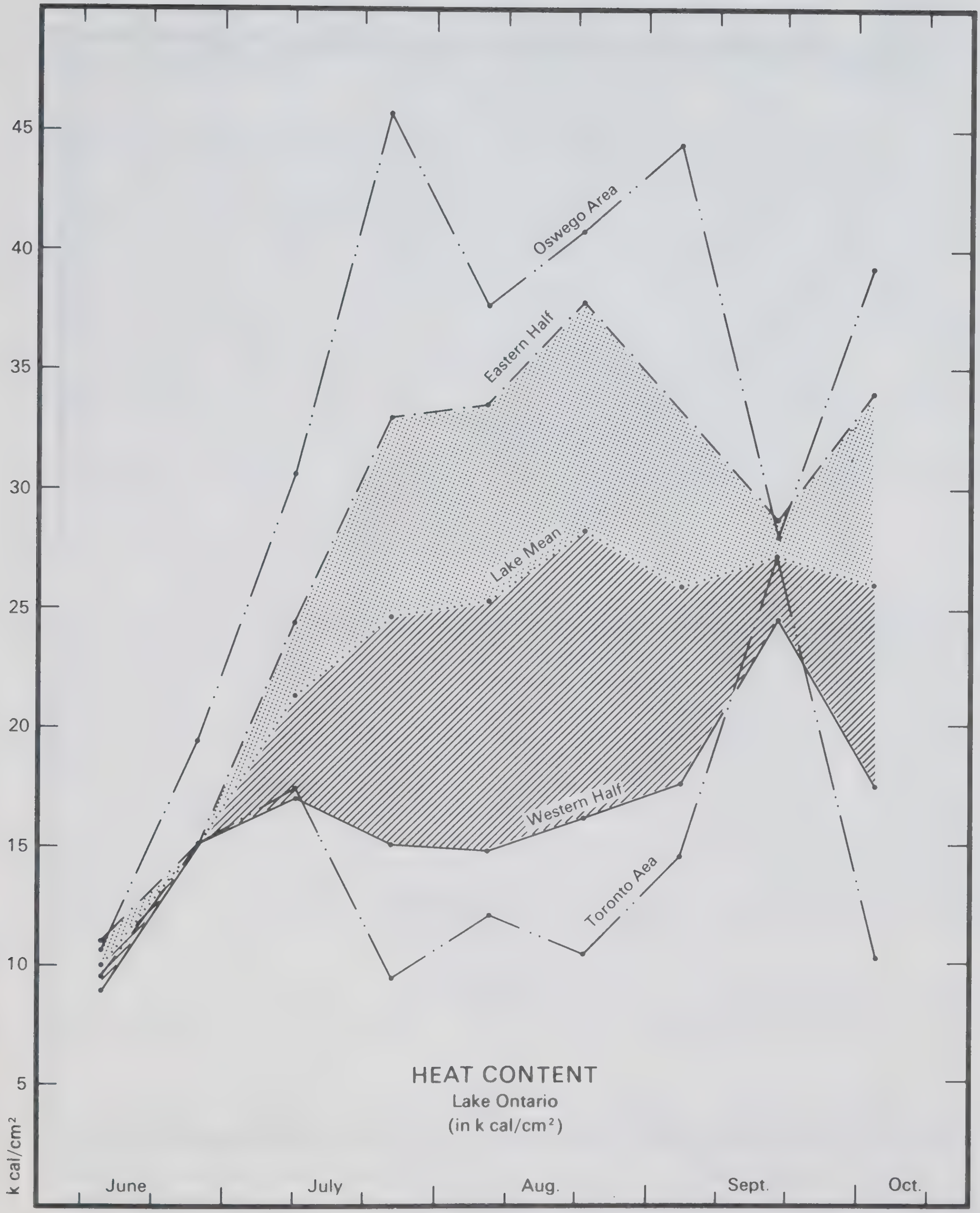

Fig. 34 Lake-mean heat content for the period of June through October 1967, compared with the means for the eastern and western halves of the lake.

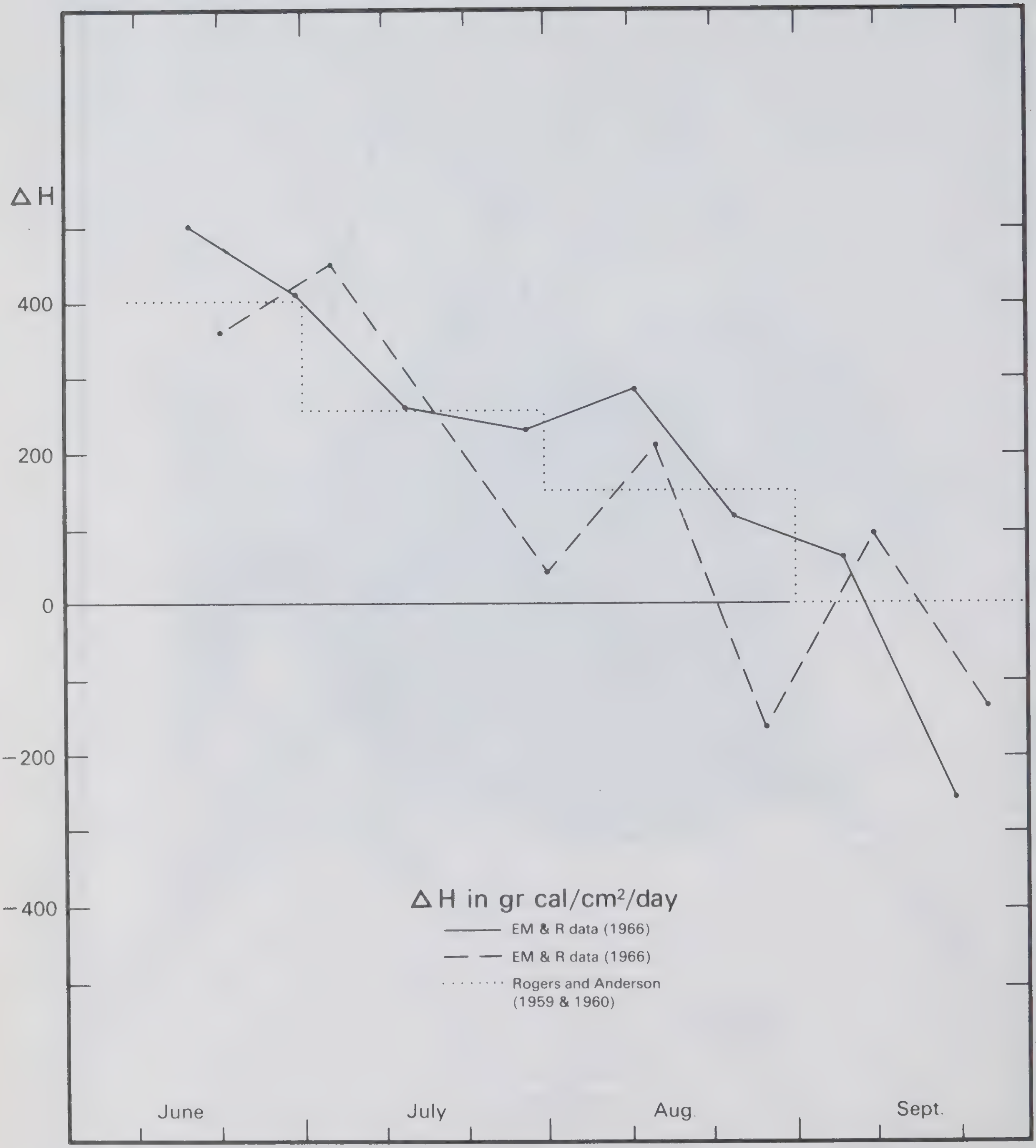

Fig. 35 Mean net heat input for the period of June through September 1966 (solid line), and for June through October 1967 (dashed line), compared with the monthly means for the years 1959 and 1960 (dotted line) published by Rodgers and Anderson.

Fluctuations in the heat content during consecutive two week periods are quite large, but these can probably to a large extent be explained by an insufficient density of the station network and by non-synopticity of the data. During a five day cruise conditions on the lake can sometimes change quite considerably. A good example of this is the apparent secondary peak in the heat input in August 1966. For a period of 1 1/2 days prior to the mid-August 1966 cruise the wind is blowing towards that side of the lake where the cruise starts; shortly afterwards, however, it shifts around and blows towards the east for the remaining four days. As a result maxima in the depth of the thermocline are observed both shortly after the start of the cruise, near Hamilton, and by the end of the cruise, near Oswego (Fig. F.30). The change in wind results apparently in a net eastward transport of epilimnion water during the cruise, which, in turn, gives rise to an imaginary peak in the heat input. During the next cruise winds are more stationary, and the measured heat content therefore is a better approximation of the real value; the heat input during the two week period preceding the late August cruise therefore is lower than could be expected. Similar explanations can account at least partially for the large fluctuations in heat input during consecutive two week periods in 1967.

4.1 Internal Advection of Heat

The rate of increase in heat content is not only a function of time, but also of location. In Figs. 33 and 34 the lake-mean heat content per cm^2 is compared with averages for the eastern and western halves (shaded areas) and for small areas near Oswego and Toronto. The average heat content of the eastern section is consistently much higher than that of the western section. During both summers the difference ranges between approximately 6 and 20 $kcal/cm^2$ and averages 14 $kcal/cm^2$, as compared with a lake-mean heat content over the summer of 25 $kcal/cm^2$! Discrepancies are even larger if the lake-mean is compared with the heat content of small areas near Toronto and Oswego. The maximum mean heat content over an area near Oswego covering 15 to 20% of the lake, for example, is up to 75% higher than the lake-mean for the same cruise.

The spacial patterns of lines connecting points with equal heat content per cm^2 are closely related to the distribution of thermocline depth as is to be expected.

The horizontal gradients in heat content are far too large to be explained by local variations in the rate of energy exchange through the lake surface. It thus is obvious that internal advection currents must play an important role in the redistribution of heat throughout the summer. This phenomenon has been discussed earlier by Rodgers (1966) in connection with the dissipation of the mid-lake temperature minimum after the disappearance of the thermal bar. He pointed out that the

subsequent rapid rise in heat content at mid-lake stations could be explained only by taking into account the advection of warmer nearshore water towards the centre of the lake. The present data indicate the continuing importance of advection throughout the summer, although the transport appears to be in a predominantly east-west direction rather than towards the centre of the lake.

The magnitude of the east-west advection term, and the associated horizontal current velocities, can be calculated from changes in the distribution of energy in the lake. The general equation relating the heat content h(z,y,z,t) in a unit volume of water to the sum of a source term q(x,y,z,t) and the advective terms is:

$$\frac{\partial h(x,y,z,t)}{\partial t} = q(x,y,z,t) - \operatorname{div}\left\{h(x,y,z,t)\cdot\vec{v}\right\} \qquad (4.1.a)$$

where $\vec{v}$ is the velocity vector and t the time.

An estimate of the east-west velocity can easily be made in a greatly simplified case. Consider the lake as a two-layered system, an epilimnion and a hypolimnion, divided by a sharp interface. Assume that all heat absorbed by the lake remains in the epilimnion, and that the temperature, and consequently the heat content per cm^3, is independent of depth within each of the two layers. The heat content below 1 cm^2 of the surface, H(x,y,t), then is equal to:

$$H(x,y,t) = h(x,y,z,t) \times Z(x,y,t) \qquad (4.1.b)$$

where $Z(x,y,t) = Z_e$ is the thickness of the epilimnion. The source term per cm^2 of the lake surface, furthermore, is assumed to be independent of location and equal to the lake-average rate of increase in heat content:

$$\mathcal{Q}(t) = \frac{1}{A}\int_0^{z_e}\int^{A} q(x,y,z,t)\,dx\,dy\,dz = \frac{\partial \bar{H}(t)}{\partial t} \qquad (4.1.c)$$

where $\bar{H}(t)$ is the average heat content below 1 cm^2 of the surface at any moment t, and A the area of the lake. The lake is split along a north-south line into two sections with equal surface areas. Longitudinal water movements in the epilimnion now can be calculated using a simplified form of equation (a), which can be obtained by integration over depth and over the area of each of the sections. For a finite interval of time Δ t between cruises this becomes:

$$\frac{1}{2} A\varphi(t) = \frac{1}{2} A \frac{\Delta \bar{H}_w(t)}{\Delta t} + \bar{h}_w(t) Z(t) uy \qquad (4.1.d)$$

where, $\bar{H}_w(t)$ is the average heat content per cm^2 in the western section of the lake, $\bar{h}_w(t) = \bar{H}_w(t)/\bar{Z}_w(t)$ is the mean heat content per cm^3, $\bar{Z}_w(t)$ the average thickness of the epilimnion in the western section, $\bar{Z}$ the lake average thickness of the epilimnion, u the advective velocity, and y the width of the cross-section. This equation can be solved for u:

$$u = \frac{\frac{1}{2} A \left(\frac{\Delta \bar{H}(t)}{\Delta t} - \frac{\Delta \bar{H}_w(t)}{\Delta t} \right)}{\bar{h}_w(t) Z(t) y} = \frac{\Delta \bar{H}(t) - \Delta \bar{H}_w(t)}{\Delta t \bar{H}_w(t)} \times \frac{A}{2y} \times \frac{\bar{Z}_w(t)}{\bar{Z}(t)} \qquad (4.1.e)$$

Equation 4.1.e has been applied to the present data; the results are summarized in the Tables 5 and 6. During June, transports in an east-west direction are small. Throughout July, in both years, however, there is a large transport of epilimnion water towards the eastern section of the lake. Early in July the temperature minimum in the eastern section disappears completely and is replaced by a minimum near Toronto, caused by upwelling, and a considerable amount of surface water moves towards the east. A maximum two week mean eastward velocity of 3.0 cm/sec is reached by the middle of July in both years. (The mean eastward epilimnion velocity due to the flow of water through the lake is 0.3 cm/sec). Assuming the rate of downward movement of the thermocline due to eddy diffusion processes to be constant over the lake, this would correspond to a maximum return flow of 0.5 cm/sec in the hypolimnion.

Later in the summer conditions are more stationary, but by the middle of September the direction of transport is reversed and there is a net flow of epilimnion water towards the west. The return flow reaches a maximum two week mean velocity of 1.5 cm/sec in 1966 and 3.3 cm/sec in 1967.

For the purpose of these calculations it was assumed that the rate of heat exchange through the surface of the lake is independent of location. This is only true in a first approximation. Various terms of the heat budget, such as long

cruise	median date	$\overline{H}$	$\overline{H}_w$	$\overline{H}-\overline{H}_w$	$\Delta(\overline{H}-\overline{H}_w)$	$\overline{Z}$	$\overline{Z}_w$	$\overline{Z}-\overline{Z}_w$	u
			kcal/cm^2				cm		cm/sec
2	8 Jun.	6.5	4.4	2.1	0.3	340	50	290	0.2
4	22 Jun.	13.5	11.2	2.4	2.0	700	480	220	1.4
6	6 Jul.	19.2	14.8	4.4	4.6	1080	880	200	2.9
8	20 Jul.	23.1	14.2	8.9	-0.7	1390	970	420	-0.4
10	3 Aug.	26.3	18.0	8.3	0.1	1660	1240	420	0.0
12	17 Aug.	30.0	21.6	8.4	0.0	1870	1410	460	0.0
14	31 Aug.	31.6	23.2	8.4	-3.9	1980	1480	500	-1.5
16	14 Sept.	32.7	28.2	4.5	-1.0	2220	1980	240	-0.4
18	28 Sept.	28.1	24.6	3.5		2410	1880	530	
summer means		27.1	20.0	7.1		1700	1330	370	

Table 5 Calculation of an east-west advection term from the heat budget in 1966. The symbols are explained in the text, u has been calculated from equation 4.1.e, using A=18,250 km^2 and y=65 km, and is positive towards the east.

cruise	median date	$\bar{H}$	$\bar{H}_w$	$\bar{H}-\bar{H}_w$	$\Delta(\bar{H}-\bar{H}_w)$	$\bar{Z}$	$\bar{Z}_w$	$\bar{Z}-\bar{Z}_w$	u
				kcal/cm^2			cm		cm/sec
1	14 Jun.	10.1	9.1	1.1		670	580	0.9	
3	27 Jun.	14.1	14.8	-0.6	-1.7	1150	1150	0.0	-1.7
5	12 Jul.	21.3	17.1	4.2	+4.9	1390	1090	3.0	+2.8
7	27 Jul.	24.6	15.1	9.5	+5.3	1430	930	5.0	+3.0
9	7 Aug.	25.2	14.8	10.4	+0.9	1410	850	5.7	+0.6
11	23 Aug.	28.3	16.2	12.2	+1.8	1520	940	5.8	+0.7
13	7 Sept.	25.9	17.6	8.3	-3.9	1600	1150	4.5	-1.7
15	18 Sept.	27.3	24.6	2.6	-5.7	1760	1660	1.0	-3.3
17	3 Oct.	25.3	16.7	8.6	+6.0	1970	1220	7.7	+2.6
summer means		25.5	17.6	7.9		1520	1100	4.2	

Table 6 Calculation of an east-west advection term from the heat budget in 1967. The symbols are explained in the text, u has been calculated from equation 4.1.e , using A=18,250 km^2 and y=65 km, and is positive towards the east.

wave back radiation, evaporation and conduction, are, for example, dependent on surface temperature. Energy losses due to these terms will, under similar atmospheric conditions be lower, the lower surface temperature. It consequently can be expected that some of these terms are lower in the western section of the lake than in the eastern section, because of the difference in the surface temperatures for the two areas. This means that the actual transport towards the east may even be somewhat larger than the calculated transport indicated in Tables 5 and 6.

5. DISTRIBUTION OF CHEMICAL PARAMETERS

In Appendix F the surface distributions of oxygen are shown for all cruises, those of conductance and pH only for the cruises for which the data are accurate enough to yield meaningful results (see Appendix A). The hardness, total alkalinity and chloride data for most cruises are too inaccurate to give meaningful horizontal distribution patterns, and therefore are not included in Appendix F, but have been used only in a study of seasonal trends. In the top lefthand corner of all charts the lake-mean profiles have been plotted, and on some of these the mean profile for a number of stations in an upwelling area has also been indicated (dashed lines). Seasonal changes in the lake-mean profiles are shown in the Figs. 43 through 50.

5.1 Spacial Distributions

The spacial distribution of the major chemical parameters, such as specific conductance, pH, dissolved oxygen, total alkalinity, hardness and chloride, is usually closely related to the thermal structure of the lake. Local variations, due to river outflows etc., may be more marked than in the temperature distribution pattern, but they are seldom more extensive. A study of the charts presented in Appendix F illustrates these points very well. A complete discussion of the gross features of the horizontal distribution patterns would to a large extent duplicate the description of thermal structure, and will, therefore, not be undertaken. The general relationship between the distributions of temperature and of some of the chemical parameters, however, will be studied in more detail in the next section and some of the more conspicuous, recurrent local anomalies will be studied in Section 5.3. In the present section the summer-mean horizontal distributions of conductance, pH and oxygen will be discussed. The charts are based on averages of six cruises in the period of early July through mid-September.

5.1.1 Specific Conductance

The summer-mean specific conductance distribution at the surface (Figs. 36 and 40) shows similar patterns in the two summers. In both years the conductance ranges from a minimum

of about 308 μmhos/cm (at 25°C)[1] near the middle of the lake to a maximum of 320 mhos/cm in the Toronto-Hamilton area. Over most of the eastern half the conductance remains low, but the patterns show a secondary maximum in a small area near the mouth of the Oswego River. This secondary maximum is higher in 1967 (320 μmhos/cm) than in 1966 (311 μmhos/cm), but is obvious in both years; its cause will be discussed in more detail in Section 5.3. The maximum in the western section coincides with the area of minimum surface temperature (Figs. 13 and 19). A study of the distribution patterns shows that the surface conductance usually is lower, the lower the temperature in an area, and that it approaches the hypolimnion mean for temperatures dropping to a value close to the hypolimnion mean of 3.9°C. Upwelling thus affects conductance as well as temperature.

The iso-lines of specific conductance generally tend to be parallel to the isotherms, although this is not as obvious in the summer-mean pattern for 1967 as in that for 1966. The apparent irregularity of the 1967 pattern is probably due to the lower accuracy of the conductance data in that year (Table 1).

Horizontal gradients in conductance below the thermocline region are small, and disappear in a background of random variations in the measurements. In 1966 the summer-mean conductance at the 75 metre level, for example, ranges in a fairly random manner between 320 and 323 μmhos/cm (at 25°C), with the exception of a few slightly higher values around the area south of Prince Edward Peninsula, where a maximum summer-mean of 325 μmhos/cm is reached at Station 13. The 1967 data, although less accurate, also indicate that horizontal gradients in the hypolimnion are considerably smaller than those in the epilimnion.

---

[1]To convert specific conductance values from a reference temperature of 18°C to one of 25°C, multiply by a factor 1.15 (Standard Methods, APHA, 1965). A study by Rodgers (1962) on waters of the Great Lakes indicates a slightly higher conversion factor of 1.18. A comparison of the summer-mean conductances for 1966 and 1967, measured at 18 and 25°C respectively, suggests a conversion factor in between these two values of 1.16. If the 1966 and 1967 values are corrected for a mean yearly increase of 0.4% (Dobson, 1968), the conversion factor would become even closer to the value of 1.15 used in the present report.

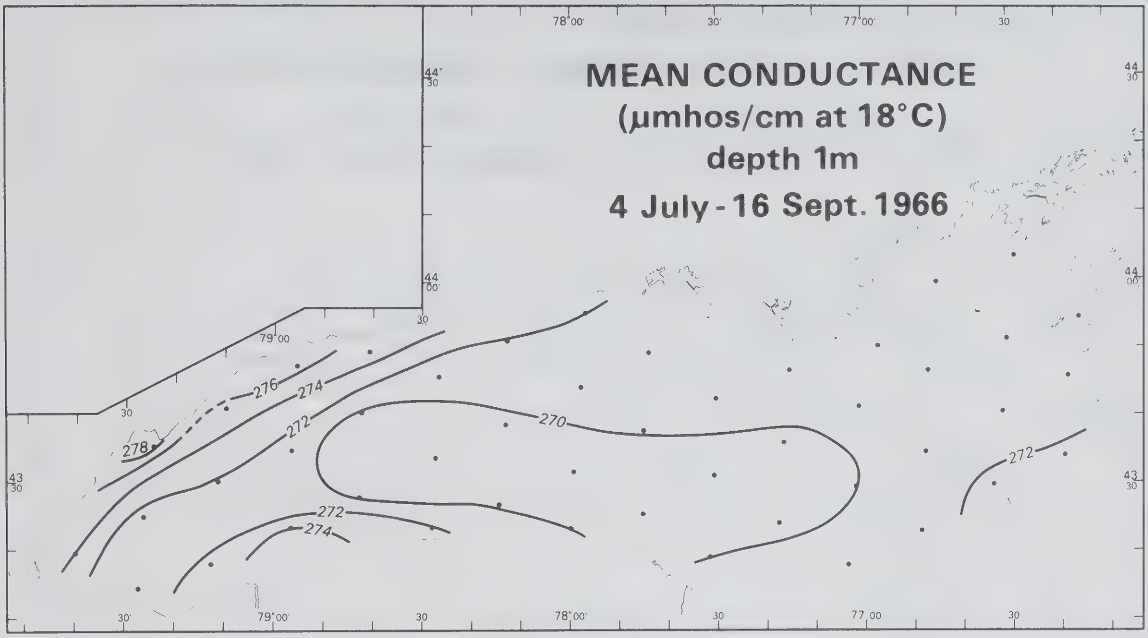

Fig. 36 Summer-mean specific conductance distribution at a depth of 1 metre in 1966.

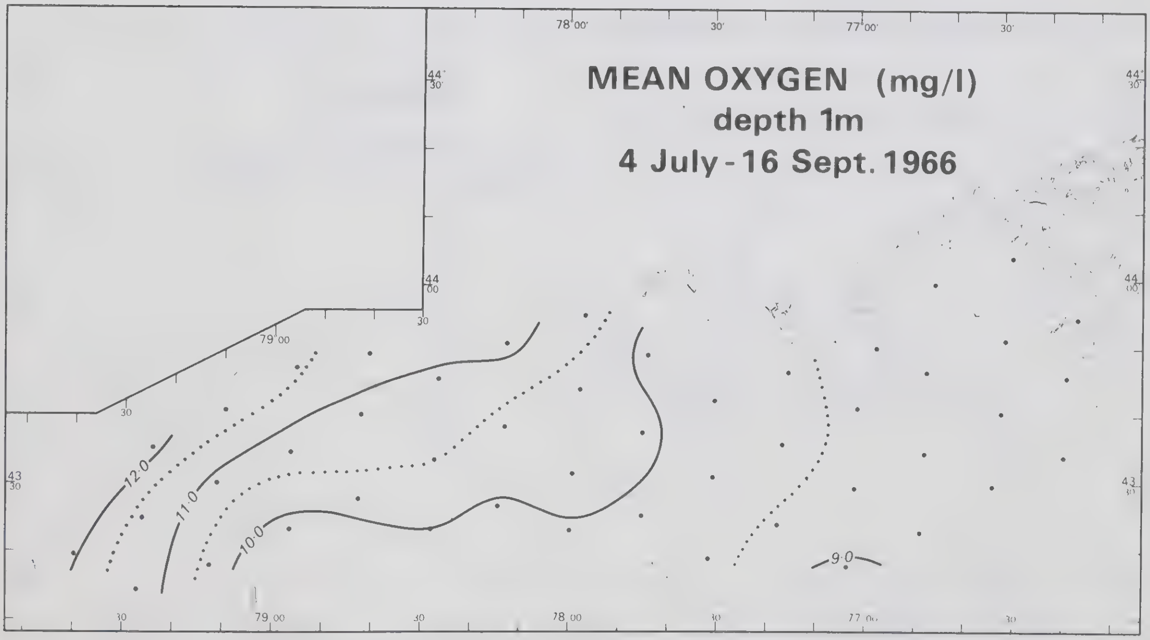

Fig. 37 Summer-mean dissolved oxygen distribution at a depth of 1 metre in 1966.

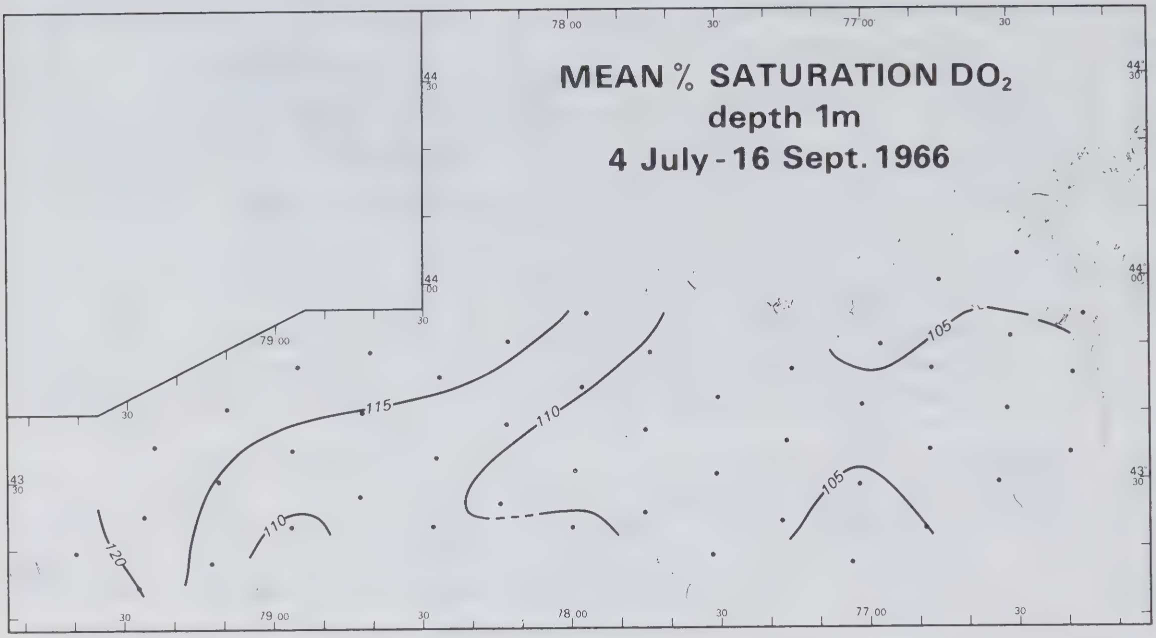

Fig. 38 Summer-mean distribution of the percentage saturation of oxygen at a depth of 1 metre in 1966.

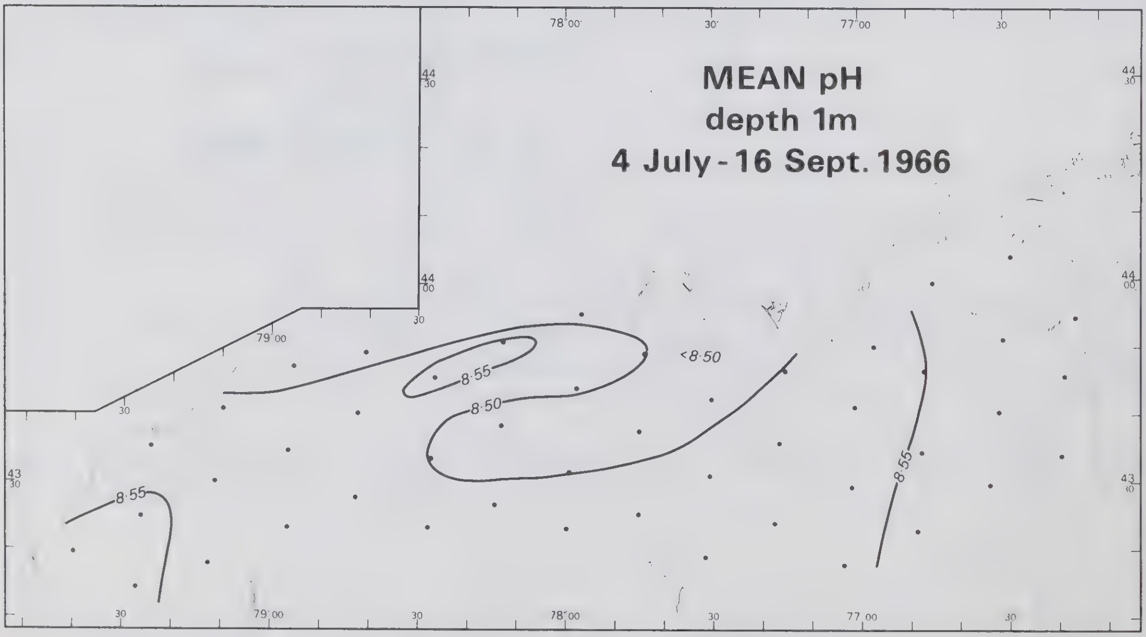

Fig. 39 Summer-mean pH distribution at a depth of 1 metre in 1966.

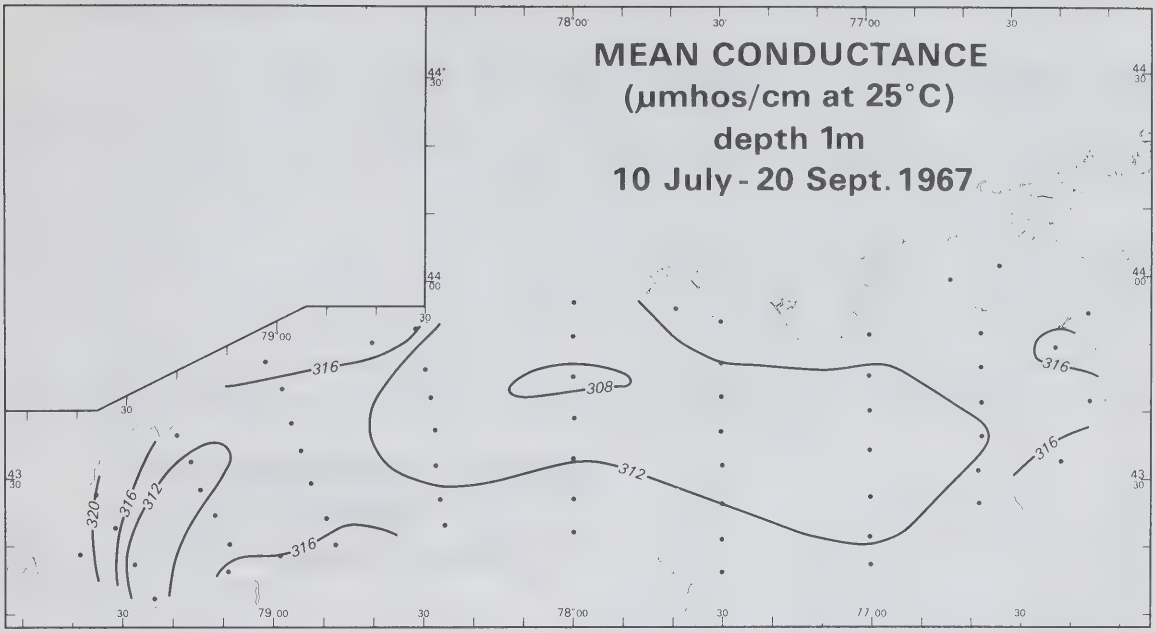

Fig. 40 Summer-mean specific conductance distribution at a depth of 1 metre in 1967.

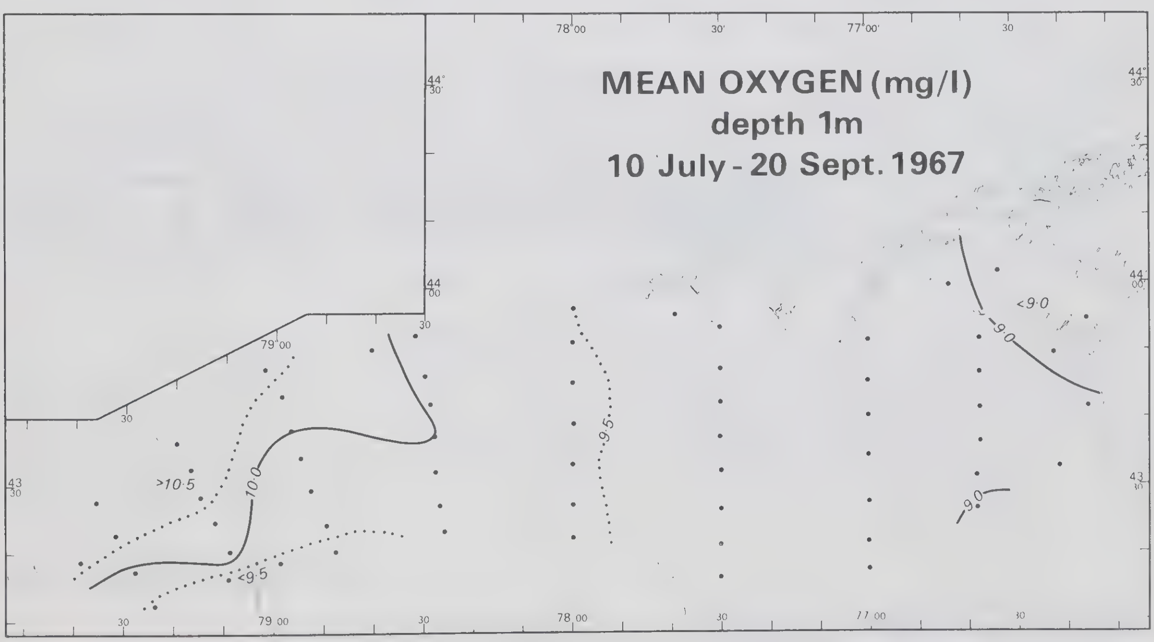

Fig. 41 Summer-mean dissolved oxygen distribution at a depth of 1 metre in 1967.

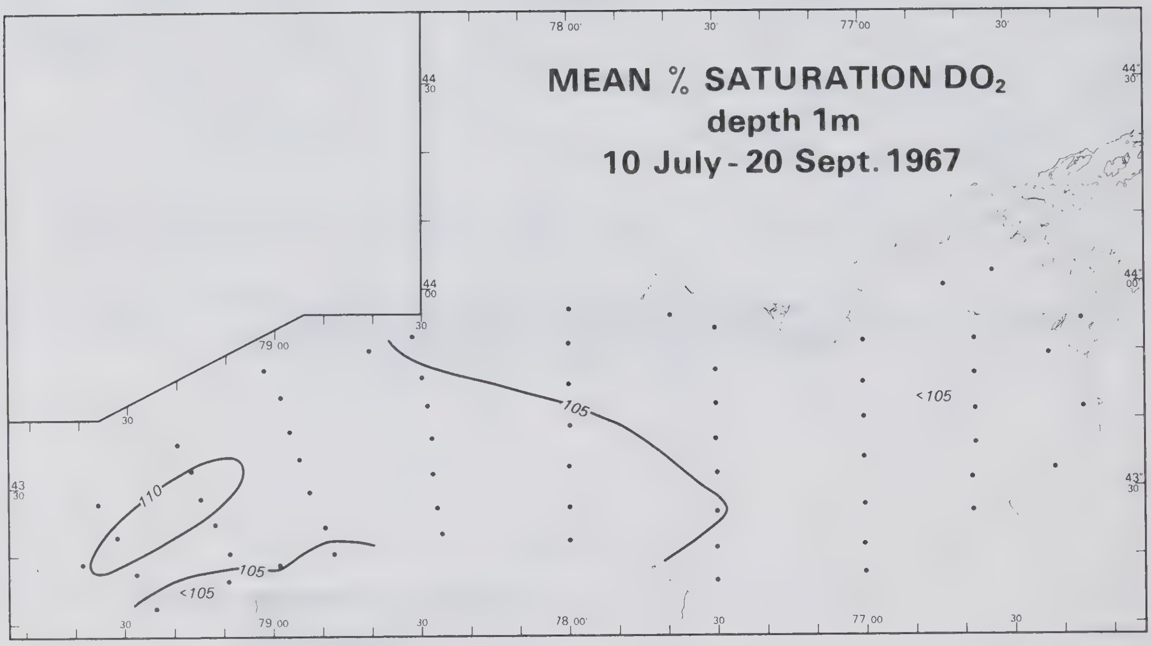

Fig. 42 Summer-mean distribution of the percentage saturation of oxygen at a depth of 1 metre in 1967.

5.1.2 Oxygen

The summer-mean dissolved oxygen and percentage saturation oxygen charts (Figs. 37, 38, 41 and 42) also show a striking similarity to the temperature charts. The oxygen content varies from a maximum of 11 to 12 mg/l near the northwestern shore to a minimum of 9 mg/l in the eastern half of the lake, with a secondary minimum, also of 9 mg/l, off the mouth of the Niagara River. The percentage saturation of oxygen also is higher near Toronto (112-122%) than elsewhere in the lake, although the summer-mean concentration remains well above the 100% saturation level at every station. The maxima are somewhat higher in 1966 than in 1967, the minima, however, are about equal in both years, and the distribution patterns are closely related.

The east-west gradients in both the total oxygen content and the percentage saturation seem to indicate a somewhat higher level of algal activity in the western half of the lake than in the eastern half. Algal activity appears to be highest near the northwestern shores, especially during the frequently occurring upwelling episodes. This will be discussed in more detail in Section 5.4.

The summer-mean oxygen content at the 75 metre level shows only small horizontal variations, ranging between 13.0 and 11.5 mg/l, and tending to be closer to the lower limits of this range, the smaller the distance between sampling depth and bottom.

5.1.3 pH

The horizontal distribution of pH (Fig. 39) is completely different from any of the patterns discussed so far. The summer-mean pH is almost constant over the lake, ranging in 1966 in a largely random manner between 8.43 and 8.61. The influence of upwelling near Toronto can barely be recognized, as the surface pH, even near the centre of an upwelling area, usually is well above its mean hypolimnion value of 8.1.

In 1966 the summer-mean pH in the hypolimnion ranges between 8.0 and 8.1, tending to be close to the lower limits of this range in the vicinity of the bottom. Horizontal gradients are much smaller than those at the surface, and are, to a large extent, overshadowed by apparently random geographical or incidental variations.

5.2 Seasonal Trends

The cruise-mean profiles of oxygen, specific conductance (in 1966) and pH (in 1966) have been summarized in time-depth diagrams (Figs. 43 through 46, 48 and 49). The total alkalinity, hardness, chloride, specific conductance (in 1967) and pH (in 1967) data are not accurate enough to give meaningful

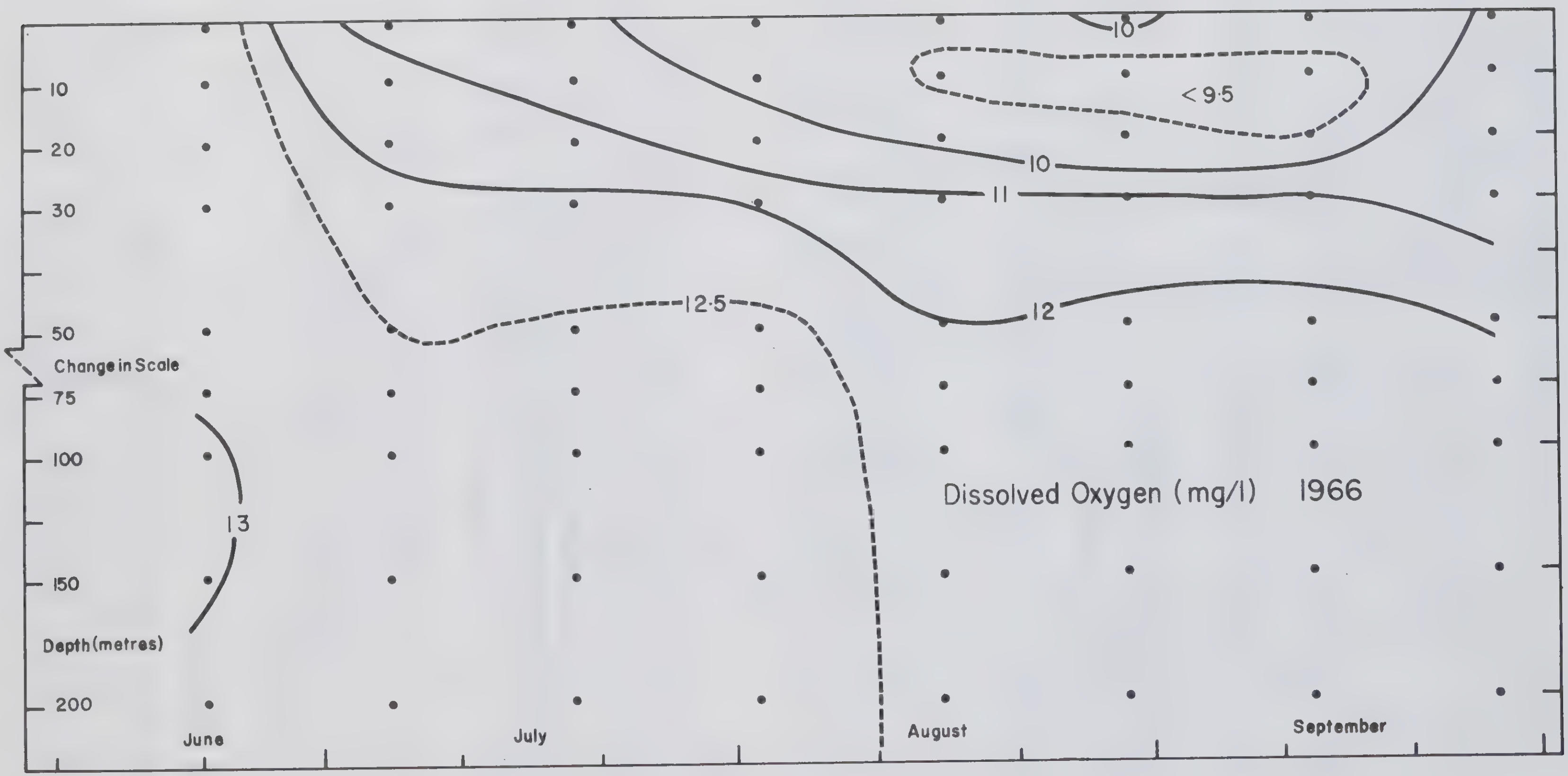

Fig. 43 Dissolved oxygen; changes in the mean profile throughout the 1966 field season.

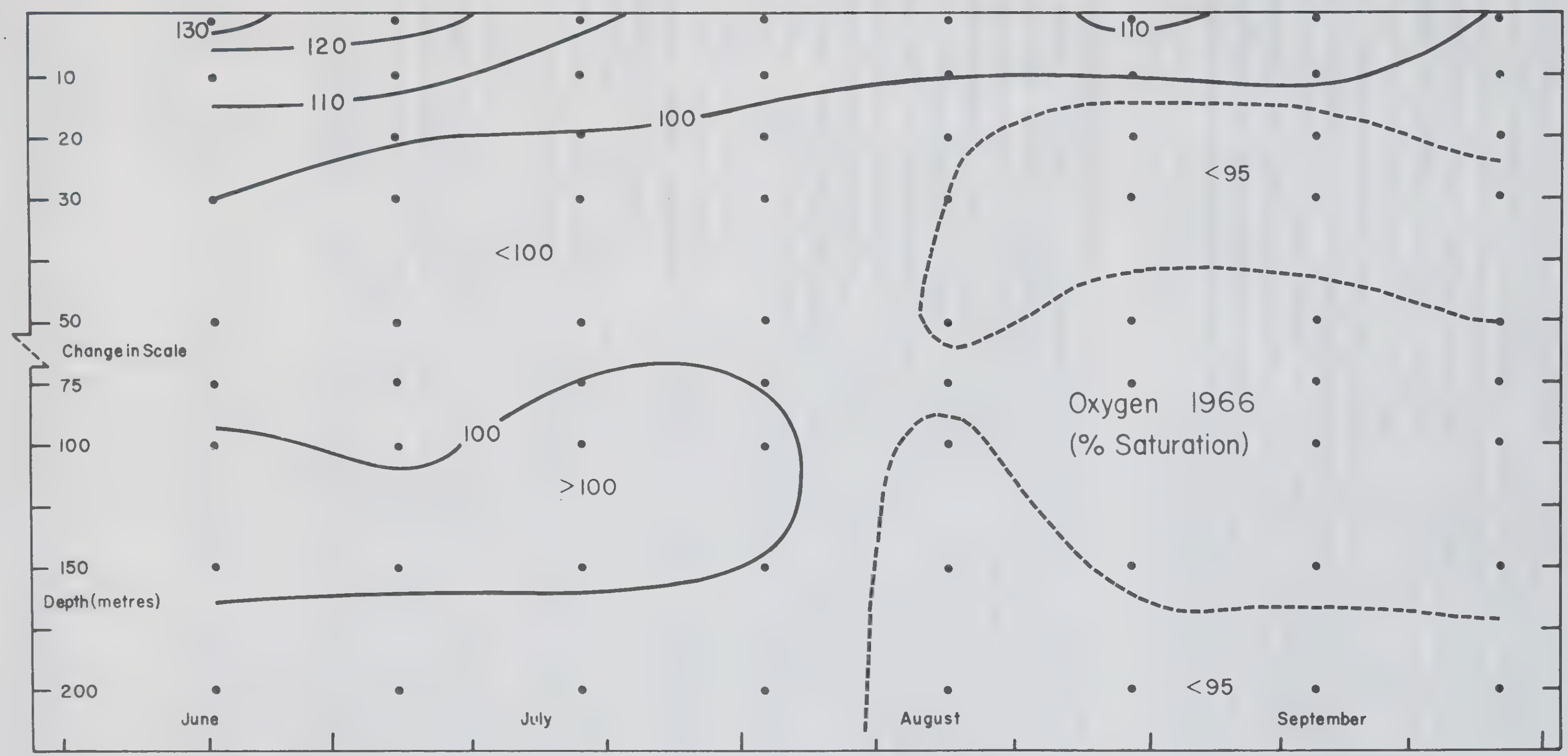

Fig. 44 Percentage saturation oxygen; changes in the mean profile throughout the 1966 field season.

time-depth diagrams due to quasi-random errors (Appendix A). An estimate of changes throughout the season of the epilimnion concentrations, however, can still be made. The specific conductance and pH data for 1966 strongly suggest that the mean hypolimnion values remain essentially constant, or, at least, that temporal fluctuations are much smaller than those in the epilimnion. Assuming that this is true for all major parameters (except perhaps oxygen), variations in the epilimnion can be determined by adjusting the measurements for apparent fluctuations in the hypolimnion. This has been done, and the results are presented in Figs. 47 and 50. The measured cruise-mean hypolimnion values are also indicated to give the reader an impression of the randomness of the cruise to cruise variations.

5.2.1 Specific Conductance

The vertical distribution of specific conductance in 1966 (Fig. 45) is practically homogeneous in early June. By late June a vertical stratification develops, and throughout the summer surface conductance values are about 3% lower than hypolimnion values (313 versus 322 μ mhos/cm). The low-conductance layer increases in thickness as the summer progresses, and the depth of maximum vertical gradient of conductance corresponds to the depth of the thermocline. In late September the surface conductance increases again, probably as a result of mixing with deeper waters. Conductance in the hypolimnion, on the other hand, remains almost constant throughout the field season and is 322 μ mhos/cm (reference temperature 25°C).

Changes in 1967 are parallel to those in 1966 (Fig. 50). Late in June the mean epilimnion conductance starts decreasing and it remains about 3% below the mean hypolimnion value throughout the summer. By late September the difference starts decreasing, and by the end of October the mean epilimnion and hypolimnion values are roughly equal again.

Variations in specific conductance are caused by variations in the concentrations of various conducting ions. Table 4 shows that the decrease in the summer-mean specific conductance in the epilimnion is parallel to decreases in hardness and total alkalinity, but inversely related to a (percentage wise smaller) change in chloride. The numerical relation between these parameters is given by (Appendix B):

$$\text{cond.} \approx 1.02 \times [\text{hard.}] + 0.864 \times [\text{t. alk}] + 2.14\,[\text{Cl}] \qquad (5.a)$$

where the terms between square brackets stand for the values of hardness, total alkalinity and chloride respectively. Together the three terms on the righthand side account for 79% of the specific conductance of Lake Ontario water. Application of

equation a to the data given in Table 4 shows that the variations in the epilimnion conductance can fully be accounted for by changes in total alkalinity, hardness and chloride: the calculated changes are -8.0 and -8.4 μmhos/cm (at 25°C) respectively in 1966 and 1967, as compared with measured changes of -8.4 and -8.2 μ mhos/cm.

The last column in Table 4 indicates the significance of the measured differences between the mean epilimnion and hypolimnion concentrations. They are always larger than twice the standard deviation of the variability of the hypolimnion data divided by the square root of the number of observations. The difference, therefore, cannot be explained in terms of errors in the data or variability of the hypolimnion observations, and must be considered to be real.

5.2.2 Oxygen

The mean epilimnion oxygen content decreases gradually from a maximum of 132% saturation in late June to 105% in late September 1966 (Figs. 44 and 49). Changes in 1967 are similar, although the saturation level tends to be slightly lower. In late October 1967 the percentage saturation of oxygen reaches a minimum of 94%. In both years the percentage saturation shows a secondary peak of about 110% in late August, early September. The absolute oxygen content decreases rapidly in late spring with increasing surface temperatures, remains relatively constant at between 9 and 10 mg/l throughout the summer, and rises slightly again in early fall. The high oxygen levels in June, and the secondary maximum in August, can probably be explained by a primary and secondary peak in algal growth (see also Section 5.4).

The mean oxygen concentration in the hypolimnion decreases gradually throughout each of the two field seasons at a rate of approximately 0.007 mg/liter/day[1], which amounts to a 5% decrease in the percentage saturation from 100% to 95%, or 96 to 91%, in 1966 and 1967 respectively. The cause of the difference between the 1966 and 1967 data is not clear; it could perhaps be caused, however, by a difference in the methods used in the two years. In 1966 all oxygens were determined by titrations (Winkler method, Strickland and Parsons, 1965), whereas an oxygen probe was used on most of the cruises in 1967.

In the thermocline region an interesting, although very slight, oxygen minimum develops during the latter part of August, with oxygen concentrations about 0.4 to 0.7 mg/l lower than at the surface.

---

[1] Estimate based on an analysis of the 1966 data by Dobson (1968), confirmed by the present study of data from the 1967 field season as well as of those of 1966.

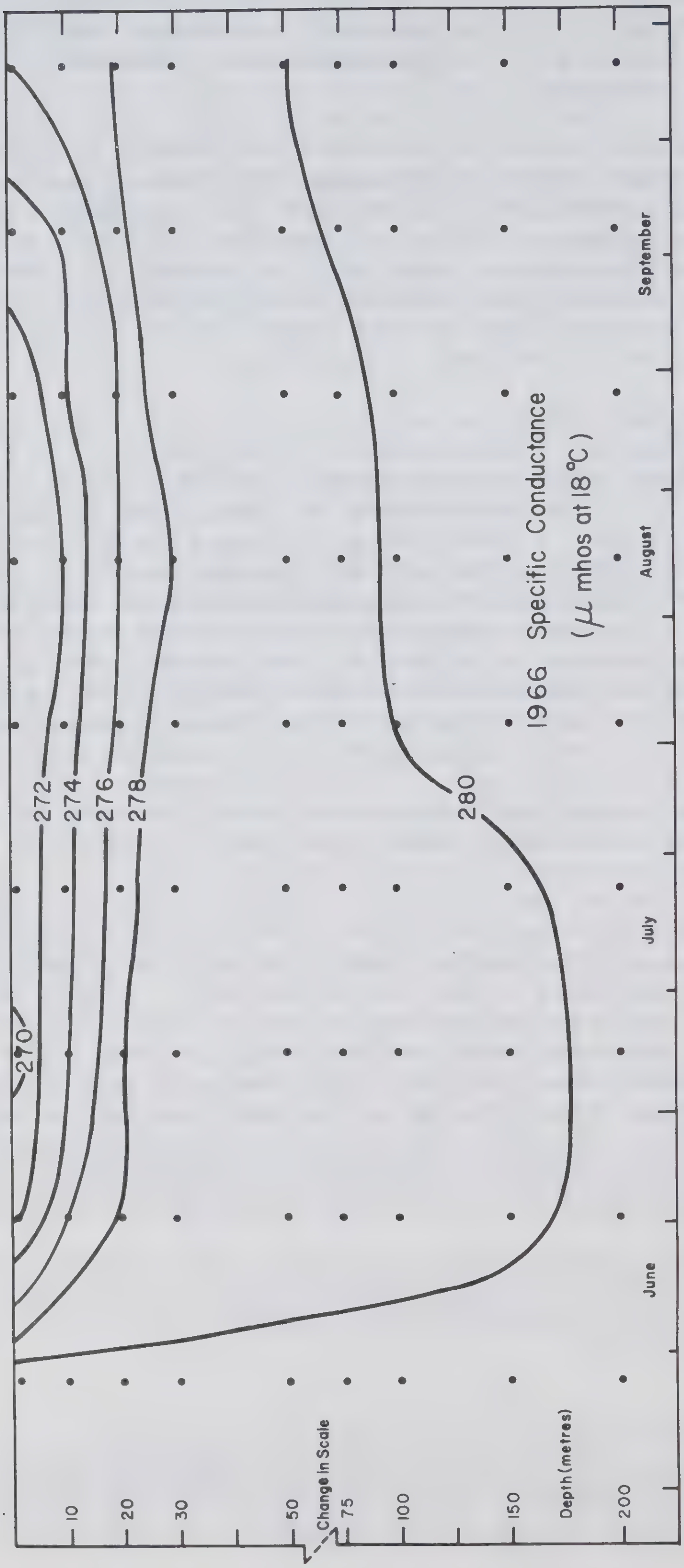

Fig. 45 Specific conductance; changes in the mean profile throughout the 1966 field season.

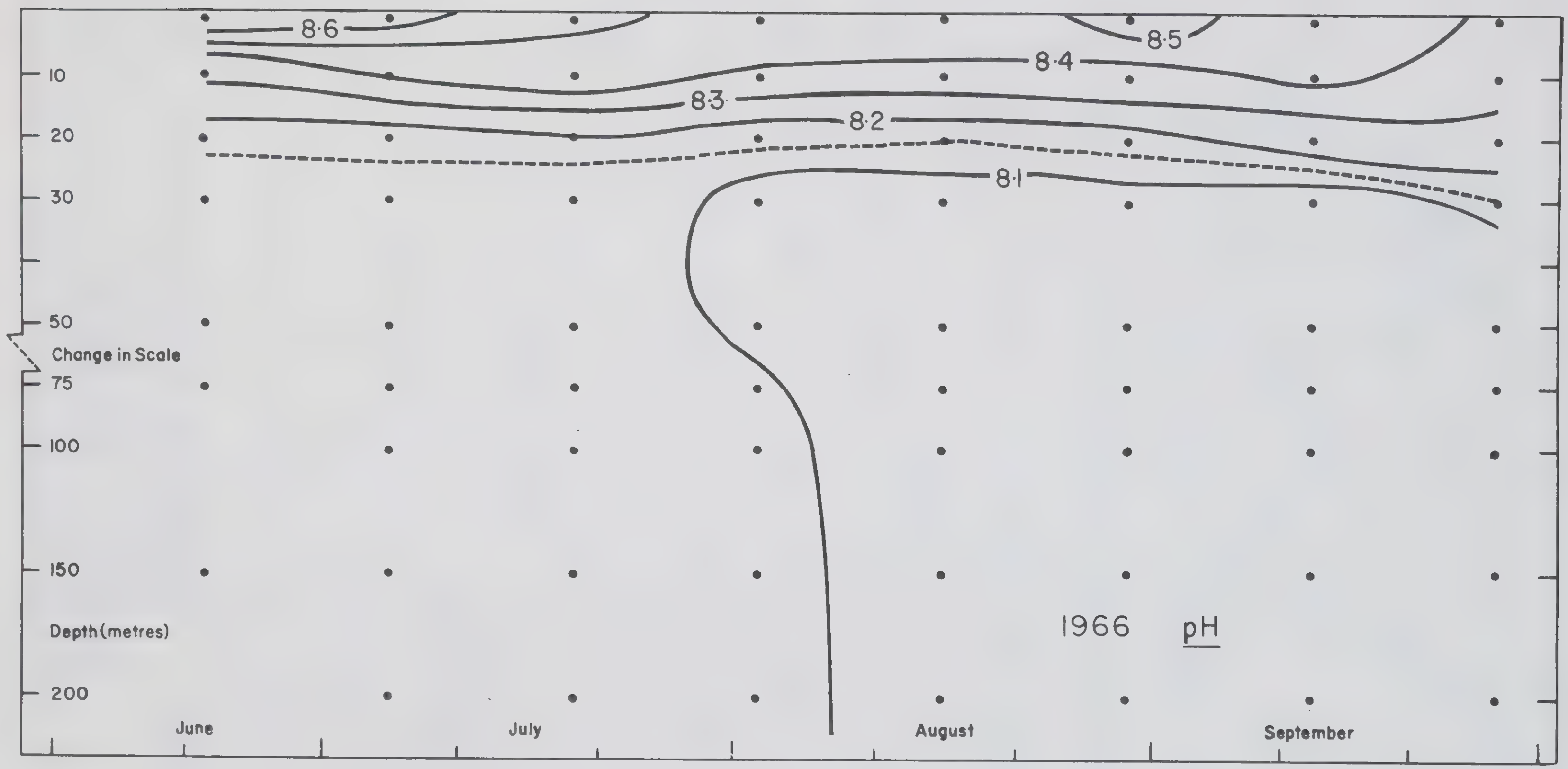

Fig. 46 pH; changes in the mean profile throughout the 1966 field season.

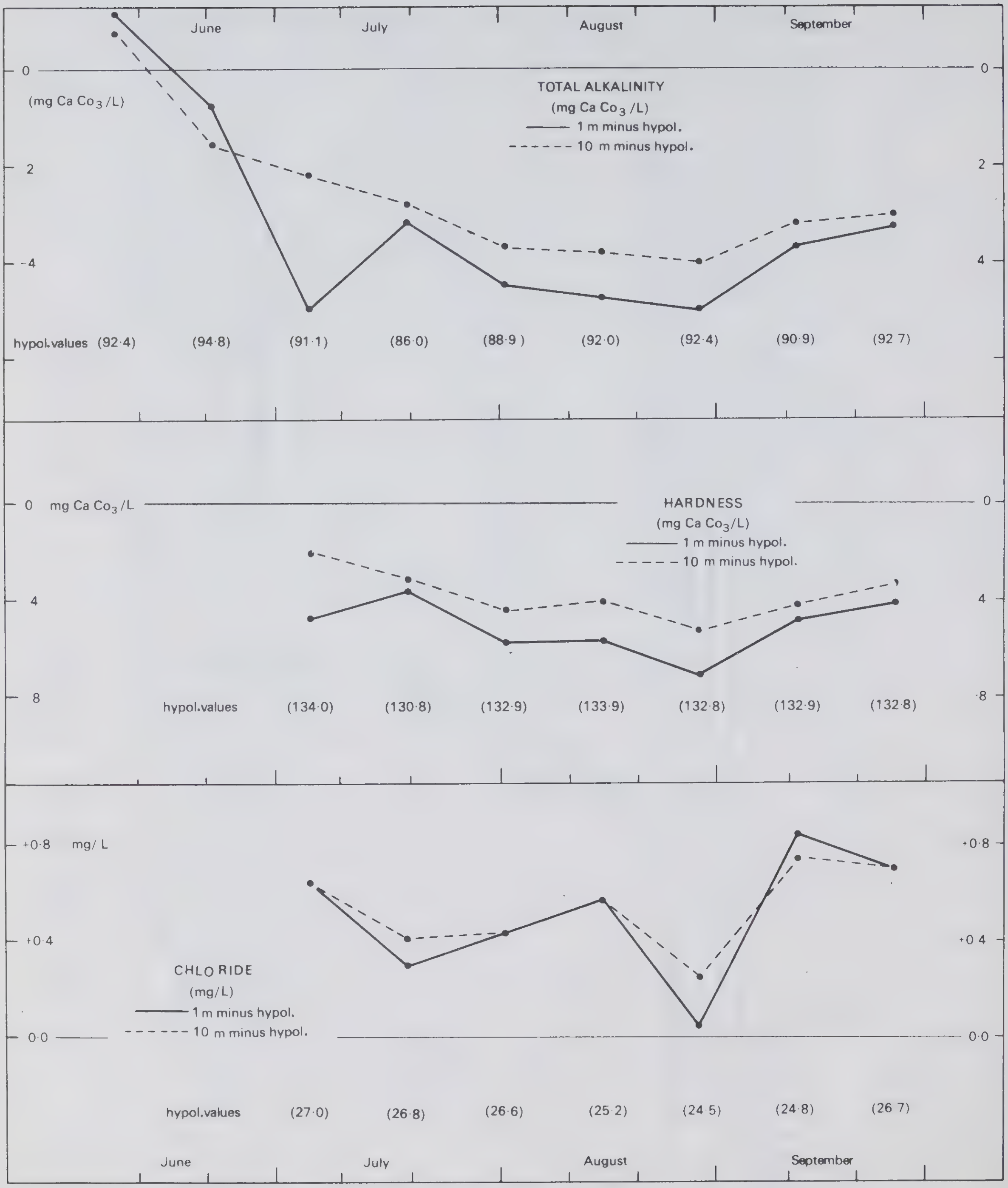

Fig. 47 Differences in the epilimnion and the hypolimnion concentrations of total alkalinity, hardness and chloride during the 1966 field season. Between brackets the measured cruise mean hypolimnion values; see text for a discussion of their accuracy.

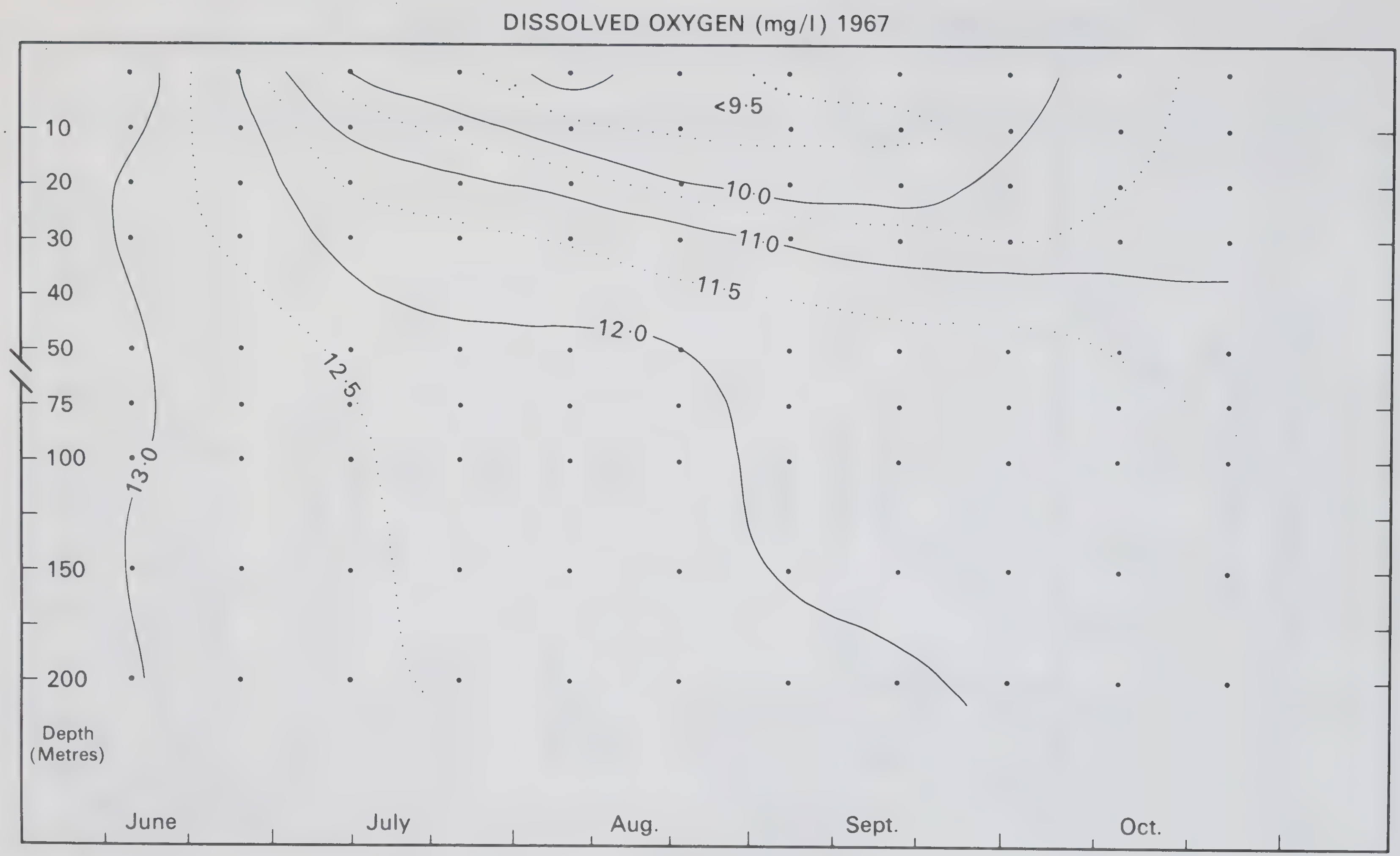

Fig. 48 Dissolved oxygen, changes in the mean profile throughout the 1967 field season.

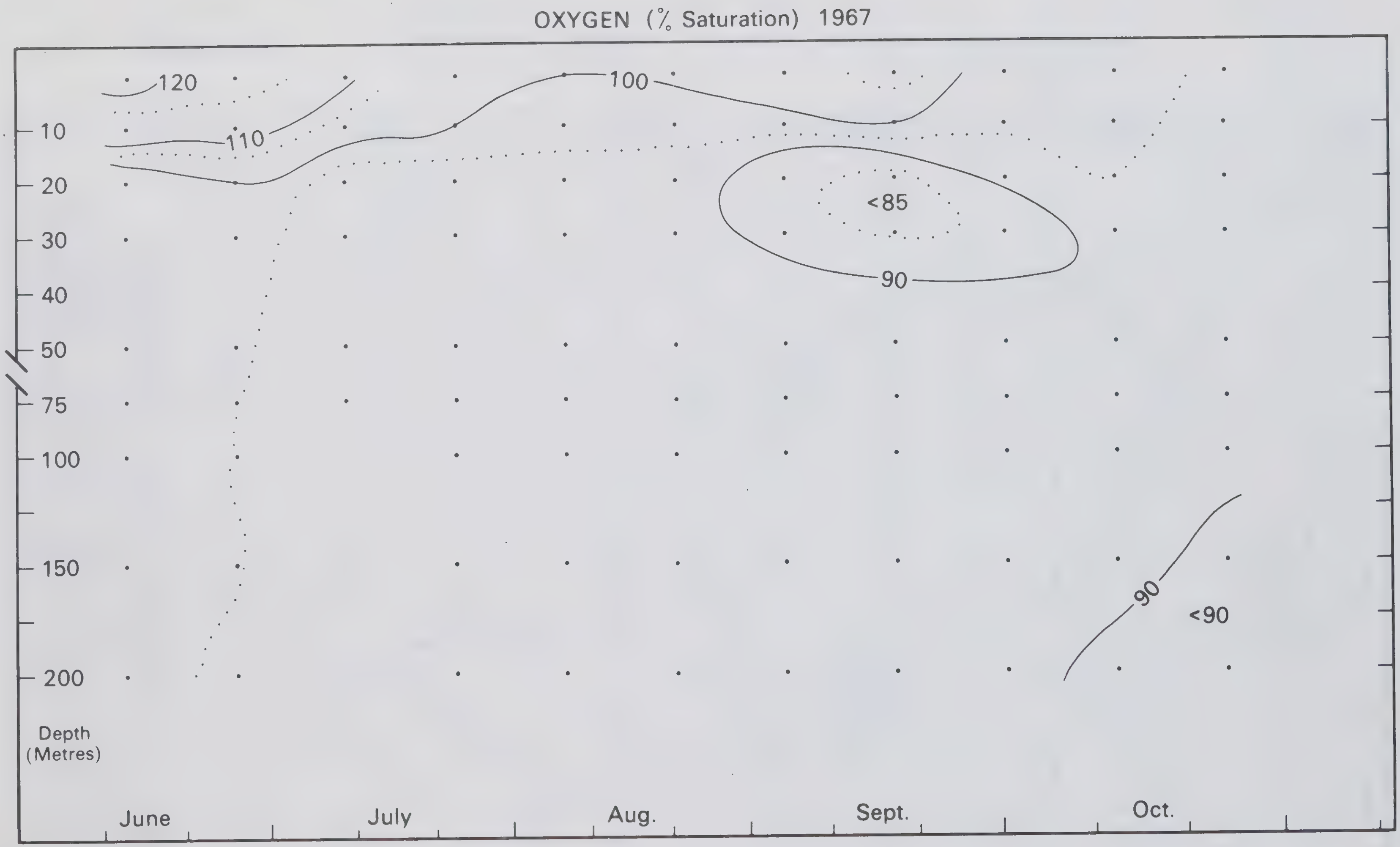

Fig. 49 Percentage saturation oxygen; changes in the mean profile throughout the 1967 field season.

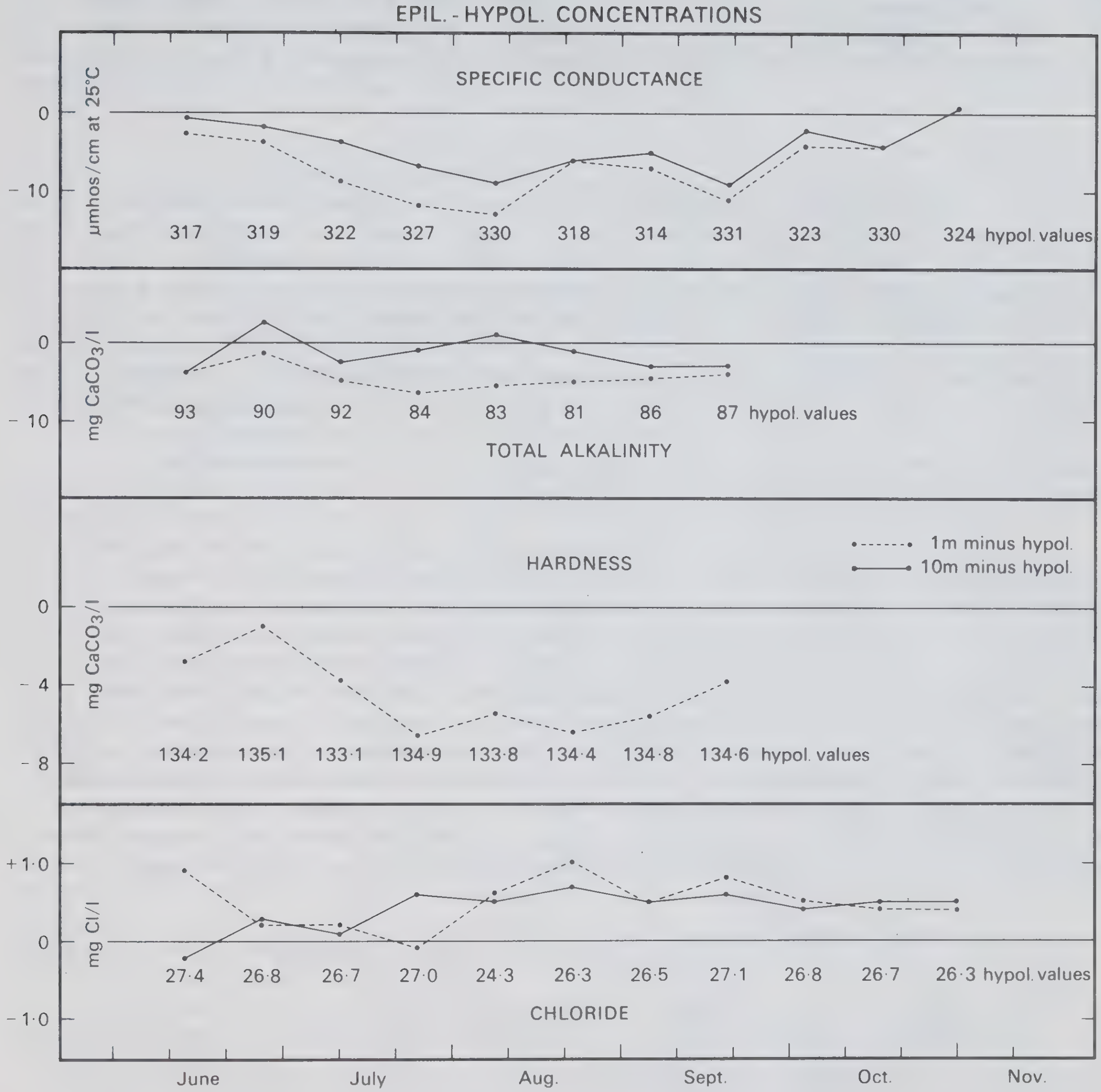

Fig. 50 Differences in the epilimnion and the hypolimnion values of specific conductance, total alkalinity, hardness and chloride during the 1967 field season. Between brackets the measured cruise mean hypolimnion values; see text for a discussion of their accuracy.

In general the oxygen content tends to decrease slightly near the bottom, but almost all observations indicate a saturation level well above the 80 percent. The lowest oxygen values have been observed in the area north of Main Duck Island, with summer-means at the 30 metre level of 6.9 mg/l (68%) in 1966 and 8.4 mg/l (73%) in 1967, and with absolute minima in late August of both years of 4.2 mg/l (41%) and 6.9 mg/l (61%) respectively.

5.2.3 pH

Throughout the 1966 field season, the pH profile shows a strong stratification (Fig. 46). The mean pH at the surface decreases slowly from a high of 8.7 in late June to 8.4 by late September, showing a small secondary peak of 8.6 in late August. The mean hypolimnion pH remains almost constant, decreasing only from a mean of 8.12 to 8.07 over the same period. The depth of maximum vertical gradient of pH differs markedly from that of the other parameters discussed in this report: It does not descend with the thermocline, but remains almost constant at a depth of 10 to 20 metres throughout the entire field season.

The pH is generally linked with biological activity and tends to increase with increasing algal growth and to decrease with increasing concentrations of carbon dioxide in the water. The two peaks in the surface pH thus suggest primary and secondary surges in algal growth in late June and late August respectively, confirming the deductions based on seasonal changes of the lake-mean oxygen content, and the slight decrease in the hypolimnion pH may be related to an increase in carbon dioxide content due to the oxidation of settling organic material. No attempt will be made to explain the difference in the profiles of pH and those of the other parameters. The 1967 data (Fig. 50), although less accurate, confirm the seasonal cycles observed in 1966.

5.2.4 Total Alkalinity, Hardness and Chloride

Under the assumption that variations in the hypolimnion concentrations of total alkalinity, hardness and chloride are small or negligible, seasonal variations in the epilimnion can be studied (Figs. 47 and 50). The mean vertical distribution of these parameters is almost uniform in June. In July, however, the epilimnion concentrations of hardness and total alkalinity decrease by 4 to 5%, whereas the measured chloride content increases by almost 2%. In late September the mean epilimnion concentrations start increasing again, except chloride, which decreases. Mean differences during the summers of 1966 and 1967 are summarized in Table 4.

The early July and late August 1966 lows in total alkalinity near the surface may be related to the primary and secondary maxima in plankton growth. The lows in total alkalinity, however, are not nearly as marked as the primary and secondary maxima in pH and oxygen saturation level. The generally lower alkalinity in the epilimnion, throughout the summer, is also related to a shift in the $CaCO_3$ - CO_2 - H_2O equilibrium with temperature (Kramer, 1964).

To explain seasonal variations in epilimnion hardness, a detailed study of the ionic balance has to be undertaken. One possible explanation for the decrease in the surface layers could be a shift in the $CaCO_3$ - CO_2 - H_2O equilibrium due to the rise in temperature, which also affects the total alkalinity (Kramer, 1964). The observed variation, however, definitely cannot be explained in terms of a seasonal cycle in the average hardness of tributaries to the lake; the rate of decrease in early summer is too fast, and the amount of material involved too large.

The apparent increase during the summer of the epilimnion chloride content is unexpected. It cannot be explained in terms of evaporation: a 1.8% increase in chloride in the epilimnion over a period of one month would require an average daily evaporation of 1 cm/day in excess over the precipitation, as compared with an estimated daily evaporation in June and July of less than 0.1 cm (Richards and Rodgers, 1964). Neither can it be explained in terms of varying chloride contents in the tributaries; this would, for example, require an increase in the chloride concentration of the Niagara River to at least 40 mg/l during the summer, which is not the case. Measured chloride concentrations in the Niagara River are roughly similar to those in Lake Ontario (Table 7). To the author's knowledge chloride does not participate to any appreciable extent in naturally occurring biochemical or geochemical reactions, and it therefore seems unlikely that such reactions could cause the observed seasonal changes. The only explanation, that appears to be plausible at present, is that the measured vertical gradient in the mean chloride distribution is artificial, and is introduced by as yet unknown sensitivities of the analytical techniques used to other properties of the water. The samples are not filtered before analysis, and differing concentrations of suspended organic or inorganic particles, as well as differences in other properties of epilimnion and hypolimnion water, could cause a systematic dependence of the results of chloride measurements on other characteristics of the water.

5.3 Consistent Regional Anomalies

Little is known about the composition of water carried to the lake by its major tributaries. Some measurements have been made by the Ontario Water Resources Commission and by the U.S. Geological Survey, but these are insufficient to derive

	units	L. Ontario, surface water (1966)	Niagara River	Genesee River	Oswego River	Black River
diss. O_2	mg/l	9.6	9.6	3.3	6.3	5.4
conductance	μmhos/cm at 18°C.	272	271	440	1135	150
hardness	mg $CaCO_3$/l	128	135	200	326	-
chloride	mg Cl/l	26	26	43	326	4.5
average flow	m^3/sec	-	4,900	21.4	76.9	36.7
data from the year(s)		'66	'59,'65	'55, '65	'56,'57 '65,'66	'65

Table 7 Summer average composition of selected major tributaries. River data are based on samples taken in the years indicated, with the exception of oxygen which has been sampled in 1965 only. The calculated means are seldom based on more than 10 observations and thus have a limited reliability.

seasonal fluctuations or even yearly mean concentrations of the rivers concerned. The available information is summarized in Table 7, which is based on data published in the "Water Quality Report" series of the U.S. Geological Survey and in a report by the Ontario Water Resources Commission (1967).

The influence of the major tributaries on the surface distribution patterns of various parameters is often clearly discernible, although only in the vicinity of their mouths. The nature of these local anomalies is usually consistent with the information given in Table 7, however scanty the data on which it is based may be.

5.3.1 Niagara River

The Niagara River supplies about 80% of the total influx of water, including precipitation, into Lake Ontario. The composition of its water is basically the same as that of Lake Erie water, which feeds the Niagara River, although modified to some extent due to human activities (release of effluents, etc.). Few measurements have been made to determine its mean composition near the mouth, but the available data indicate a high degree of similarity between Niagara River and Lake Ontario water (Table 7).

The summer-mean conductance in 1966 (Fig. 45) shows a maximum off the Niagara River, extending over a small distance eastwards from its mouth. The distributions for the individual cruises, however, are, like the temperature patterns, much more variable, and indicate a tongue of Niagara water extending into the lake in varying directions, although seldom westwards (Figs. F.14, F.33 and F.39).

Patterns for any individual cruise are, of course, strongly influenced by winds prior to the moment of observation. The variability of the patterns, however, suggests that there is no hydrodynamically determined, semi-consistent and confined eastward current along the southern shore. The data are more consistent with the hypotheses of a diffuse rather than of a jet-like nature, permitting intense horizontal mixing instead of confining Niagara River water to a narrow band along the shore and isolating it from the main body of the lake.

The distribution patterns of oxygen and pH show similar characteristics, and confirm the conclusions derived from the conductance patterns.

5.3.2 Oswego River

The Oswego River is the third largest source of water, after the Niagara River and precipitation, and contributes about 2.5% of the yearly flow into the lake. The composition of its water deviates considerably from that of the lake; specific

conductance is 4 times higher, hardness 2.3 times higher and chloride more than 12 times higher (Table 7). These high values are mainly due to geological conditions in the drainage basin of the Oswego River. Temperature, on the other hand, is about equal to the average temperature in the eastern section of the lake, and oxygen somewhat lower in the summer.

The dissolved solids content, although high, is not high enough to offset the influence of temperature on the density of the water, at least in the summer. Water from the Oswego River therefore mixes with the epilimnion, when the lake is stratified, and does not sink down into the hypolimnion.

The influence of the anomalous concentrations of various parameters is clearly discernible on the surface distribution charts for the individual cruises. The conductance charts, for example, indicate a general eastward movement of water along the southern shore (Fig. 40). The shape and extent of the area over which Oswego water can be distinguished, however, is rather variable, which seems to indicate that currents in the lake are of a relatively diffuse and variable character. In early July, 1966, the tongue of high conductance water extends over a long distance along the southern and eastern shores (Fig. F.14). In early June and late July, 1966, on the other hand, it extends due north and northwest respectively from the mouth of the river (Figs. F. 3 and F.21), and the early August and early September cruises in 1966 (Figs. F.27 and F.39) indicate a tendency for an along-shore eastward movement of the water and a rapid loss of its identity.

The distributions of hardness and chloride, which are, for reasons discussed elsewhere, not shown in this report, substantially support the conclusions that can be drawn from the conductance patterns.

5.3.3 Black River

The third biggest tributary, the Black River, has a mean discharge amounting to 1 1/2% of the flow through the lake. It carries a low load of dissolved solids: specific conductance is about half and chloride only 20% of the lake-mean (Table 7). The oxygen content (5.4 mg/l) is also below the lake average, but its mean temperature is about equal to the mean surface temperature in the area north of Main Duck Island.

Horizontal gradients of conductance and oxygen fan out from the river mouth and are almost negligible outside Black River Bay. Local details in the distribution patterns therefore do not give much information about water movements in this area of the lake. The northeastern corner of the lake has been sampled in detail on a few cruises, but even these data do not allow any identification of Black River water outside the bay.

5.3.4 Genesee River

The Genesee River (1% of the total flow into the lake) likewise only has a very local influence on the observed distribution patterns. The composition of its water is relatively close to that of the lake, and it is not surprising therefore, that the station pattern usually was too coarse to detect anomalies due to Genesee River water. On the early and late July 1966 cruises a detailed study has been made of the area, showing small tongues of water with a somewhat lower salinity extending into the lake and over a short distance eastwards along the shore respectively.

5.3.5 Local Anomalies and Eastward Transport

The influence of all tributaries, with the possible exception of the Niagara River, on the horizontal distribution patterns is essentially of a local nature. Waters from the Niagara, Oswego, Black and Genesee Rivers can be recognized in the lake as anomalies in the lakewide distribution patterns of several parameters, but the areal extent of these anomalies is usually small, and their shape and location variable. It, therefore, appears that horizontal mixing processes are strong enough to rapidly disperse all inflows, and there is little or no evidence for the existence of a confined or more or less isolated eastward current along the southern shores, carrying water with anomalous concentrations of any substance from the tributaries (and sewage outfalls) directly to the St. Lawrence River. The observations rather suggest a diffuse eastward movement of water along the southern shore, in which nearshore waters are continuously mixed with offshore waters.

The existing large-scale surface gradients discussed earlier are caused by lakewide horizontal and vertical circulation patterns, and are related to differences between the composition of epilimnion and hypolimnion waters rather than to the nature of water flowing into the lake from external sources. Horizontal gradients disappear largely in periods with little upwelling, and are strongest during periods with strong upwelling.

5.4 Chemical Profiles in an Upwelling Area

In the preceding sections the close relationship between thermal structure and the distribution of various other parameters has been discussed. It was pointed out that the surface concentration of most parameters tends to be closest to the mean hypolimnion value in areas with strong upwelling. In this section, a more detailed analysis of the profiles in these areas will be made. Average profiles, for groups of 4 to 7 stations in upwelling areas, have been computed for temperature, pH, oxygen, specific conductance and, in one instance, hardness, and are, for a number of cruises,

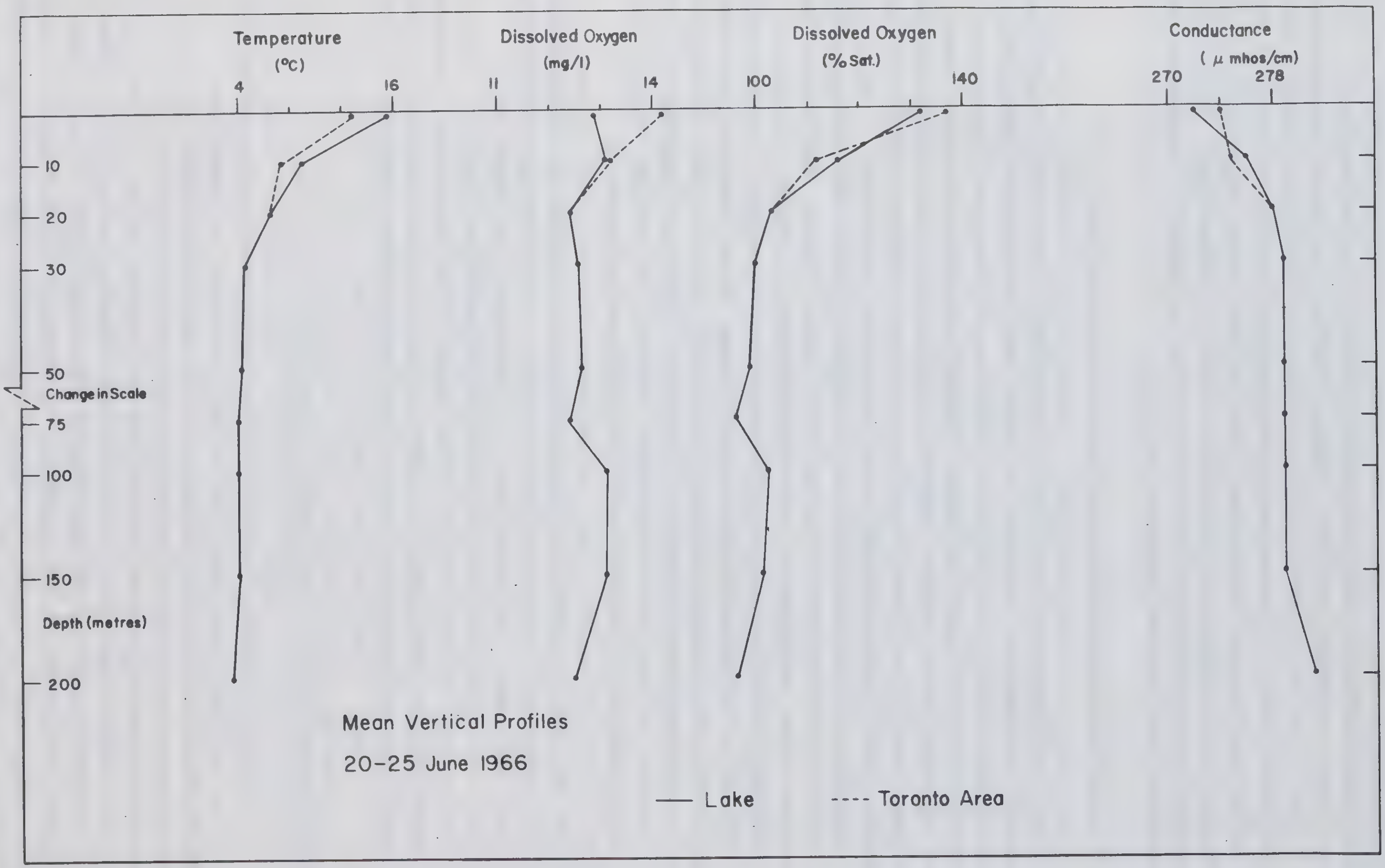

Fig. 51 Mean vertical profiles of temperature, oxygen, pH and conductance in an upwelling area (dashed lines) compared with their lake mean profiles (solid lines), June 20-25, 1966.

compared with their lake-mean profiles (Figs. 52 through 55). The same has also been done for data from the mid-lake temperature minimum in late spring 1966 (Fig. 51). Data for the individual stations show essentially the same characteristics, but are more difficult to interpret due to a larger degree of scatter. The highest degree of oxygen supersaturation usually occurs in areas with strong upwelling or the coldest surface water (Figs. F. 4 and F.10), at least in late spring and early summer. The mean percentage saturation in these areas is 5 to 20% above the lake-mean (Figs. F. 7 and F.13), rising as high as 140% in late June and early July. The absolute oxygen content below the 30 metre level is almost independent of depth or location, ranging between 12.5 and 13.0 mg/l, and decreasing near the surface to an average of 10.5 mg/l in July. In upwelling areas, on the other hand, it increases to more than 14 mg/l.

In a recent study of seasonal changes in the oxygen distribution, Dobson (1968) points out that the relatively high oxygen saturation levels in the epilimnion during late spring and early summer may be caused by a combination of two factors: the rapid rise in temperature of cold, oxygen rich waters, in combination with a strong photosynthetic oxygen production by algae. The mean oxygen profiles in the cold central part of the lake in late June (Fig. 51), and in the nearshore upwelling areas in July (Figs. 52 and 53), confirm his conclusions and serve to emphasize the importance of the latter factor.

The rate of increase of pH in water brought to the surface by upwelling in late spring or early summer is also very high, and the surface pH in these areas may rise to its lake-mean level or even higher (Fig. 53). This also indicates a rapid increase in algal activity as soon as the water rises into the trophogenic zone.

The specific conductance and hardness values near the surface, on the other hand, increase much more slowly, and their averages in upwelling areas are somewhere between their lake-mean hypolimnion and epilimnion values. The surface distribution charts given in Appendix F indicate that they reach their maxima at a fairly large distance from the centre of an upwelling area.

In late summer and early fall, the vertical profiles in an upwelling area show distinctly different characteristics (Figs. 54[1] and 55). The oxygen content near the surface is

---

[1]This cruise is not a monitor cruise, and the solid line represents the mean profile for a number of stations outside the upwelling area rather than a lake-mean profile.

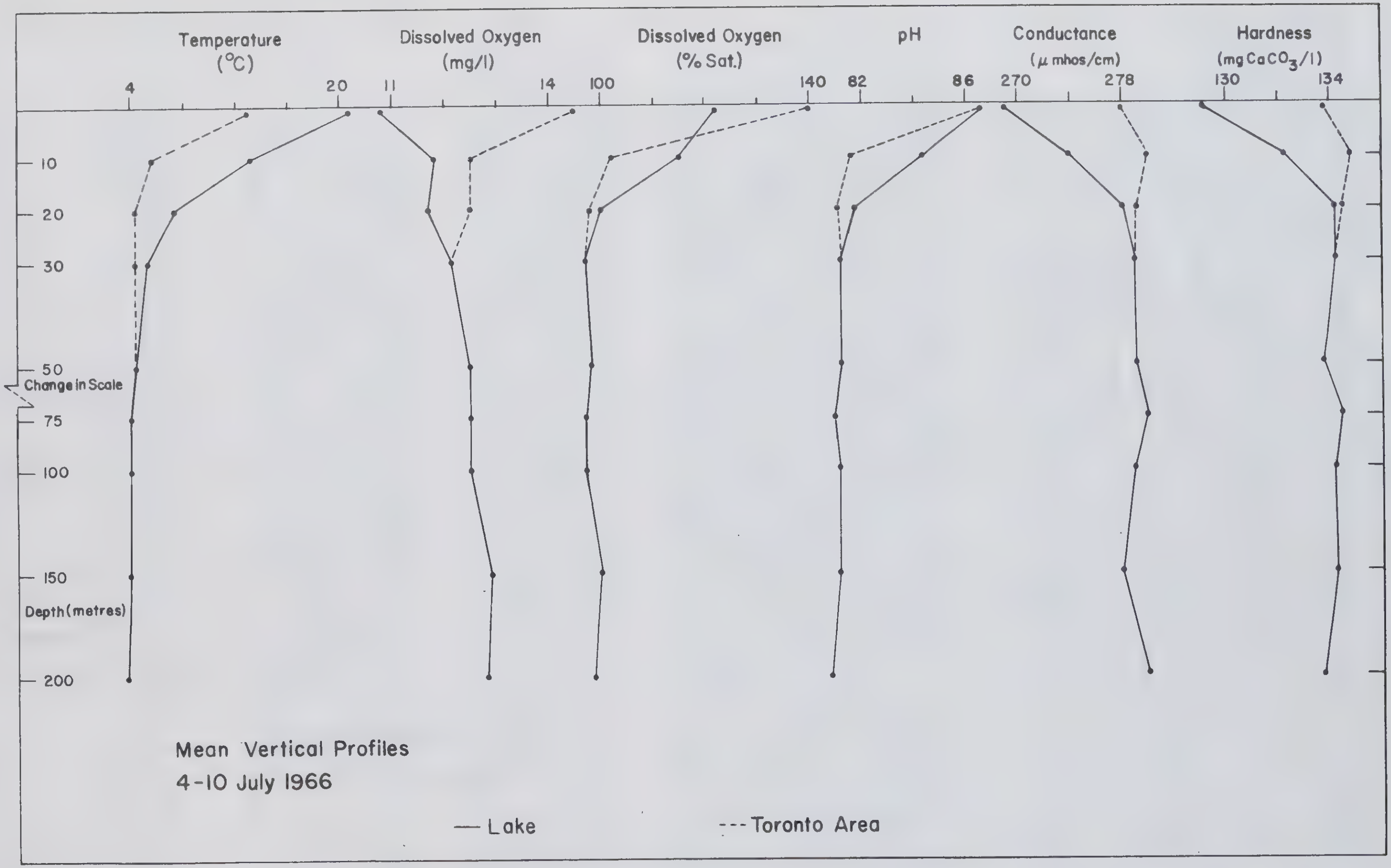

Fig. 52 Mean vertical profiles of temperature, oxygen, pH, conductance and hardness in an upwelling area (dashed lines) compared with their lake mean profiles (solid lines), July 4-10, 1966.

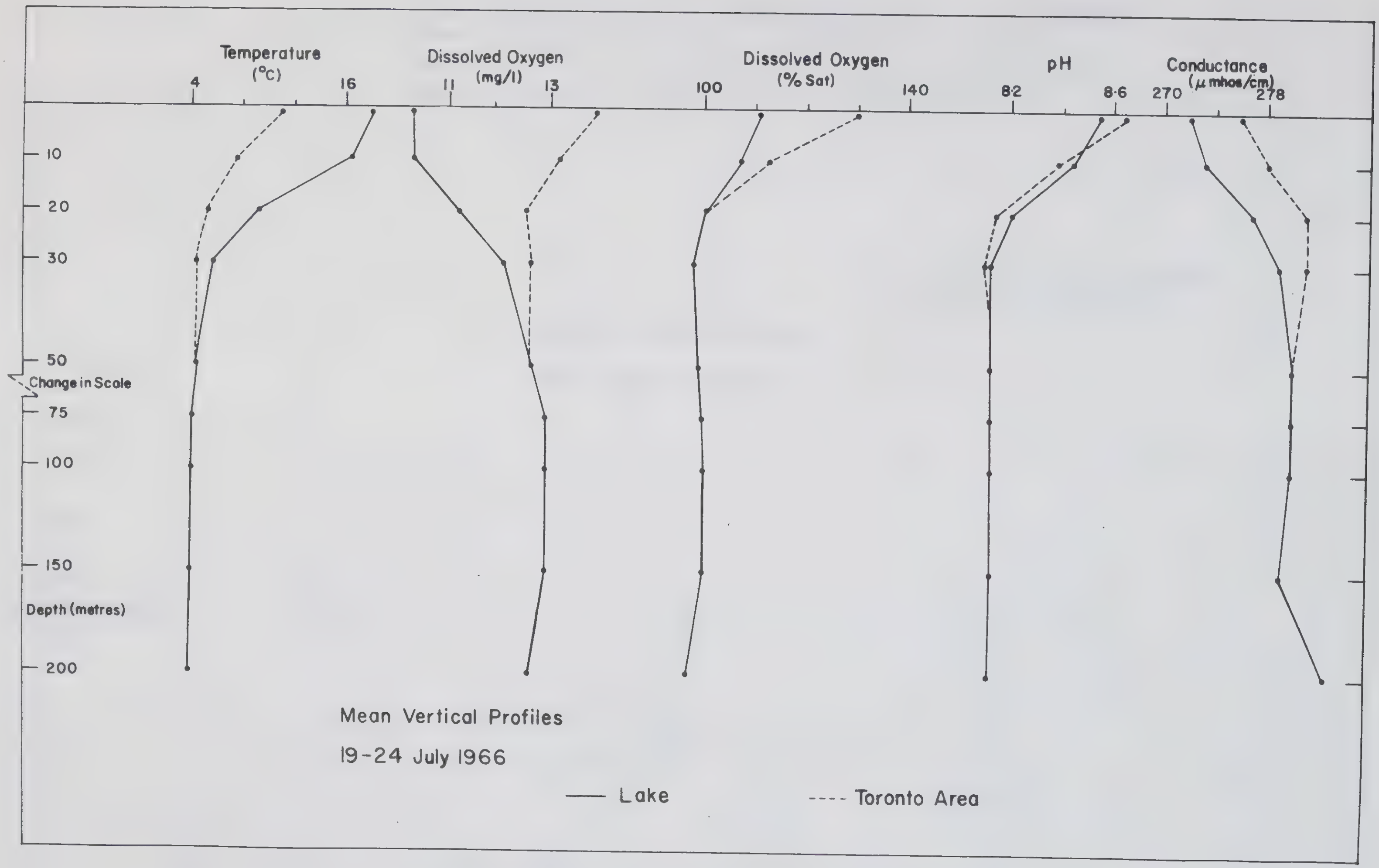

Fig. 53 Mean vertical profiles of temperature, oxygen, pH and conductance in an upwelling area (dashed lines) compared with their lake mean profiles (solid lines), July 19-24, 1966.

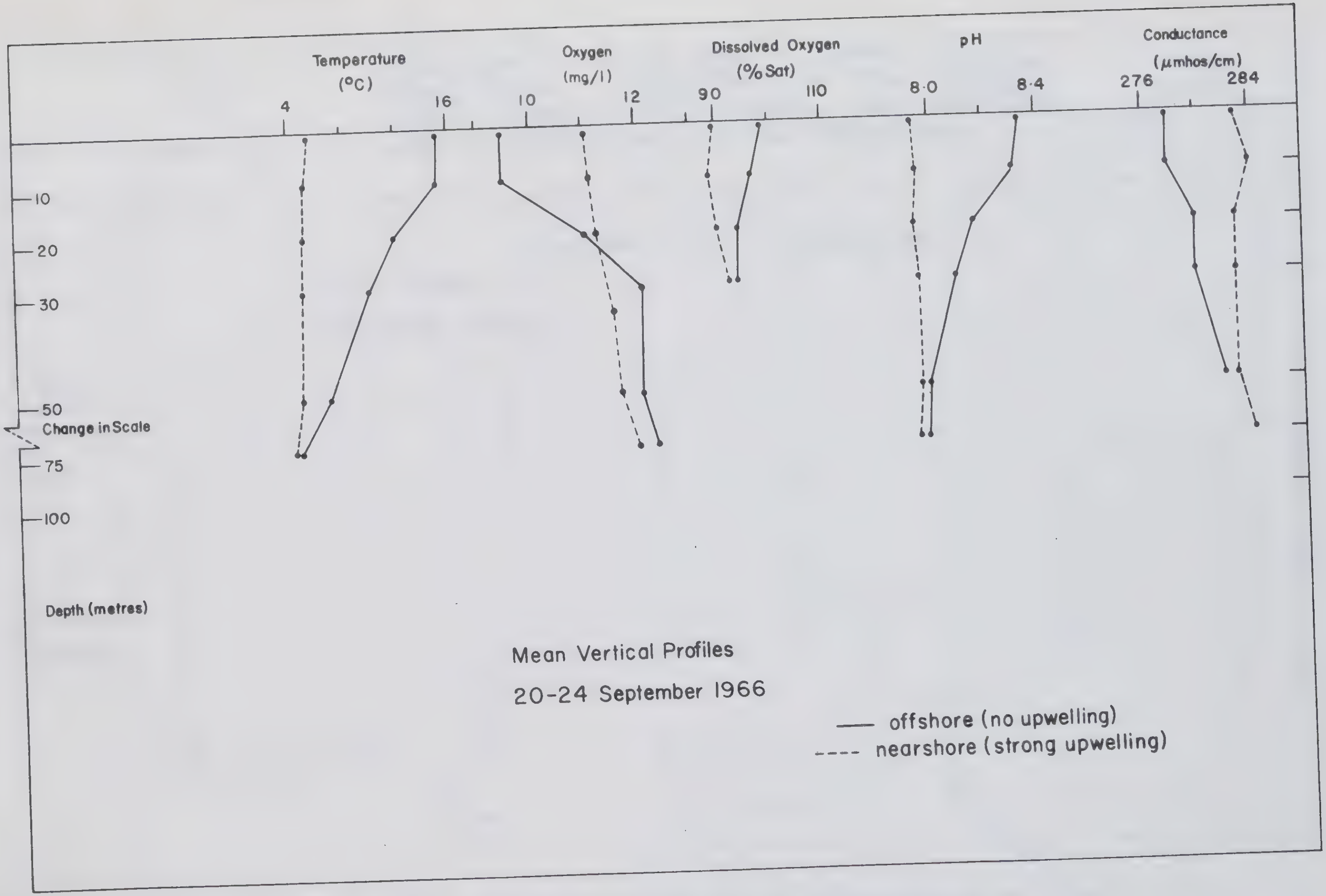

Fig. 54 Mean vertical profiles of temperature, oxygen, pH and conductance in an upwelling area (dashed lines) compared with their lake mean profiles (solid lines), September 20-24, 1966.

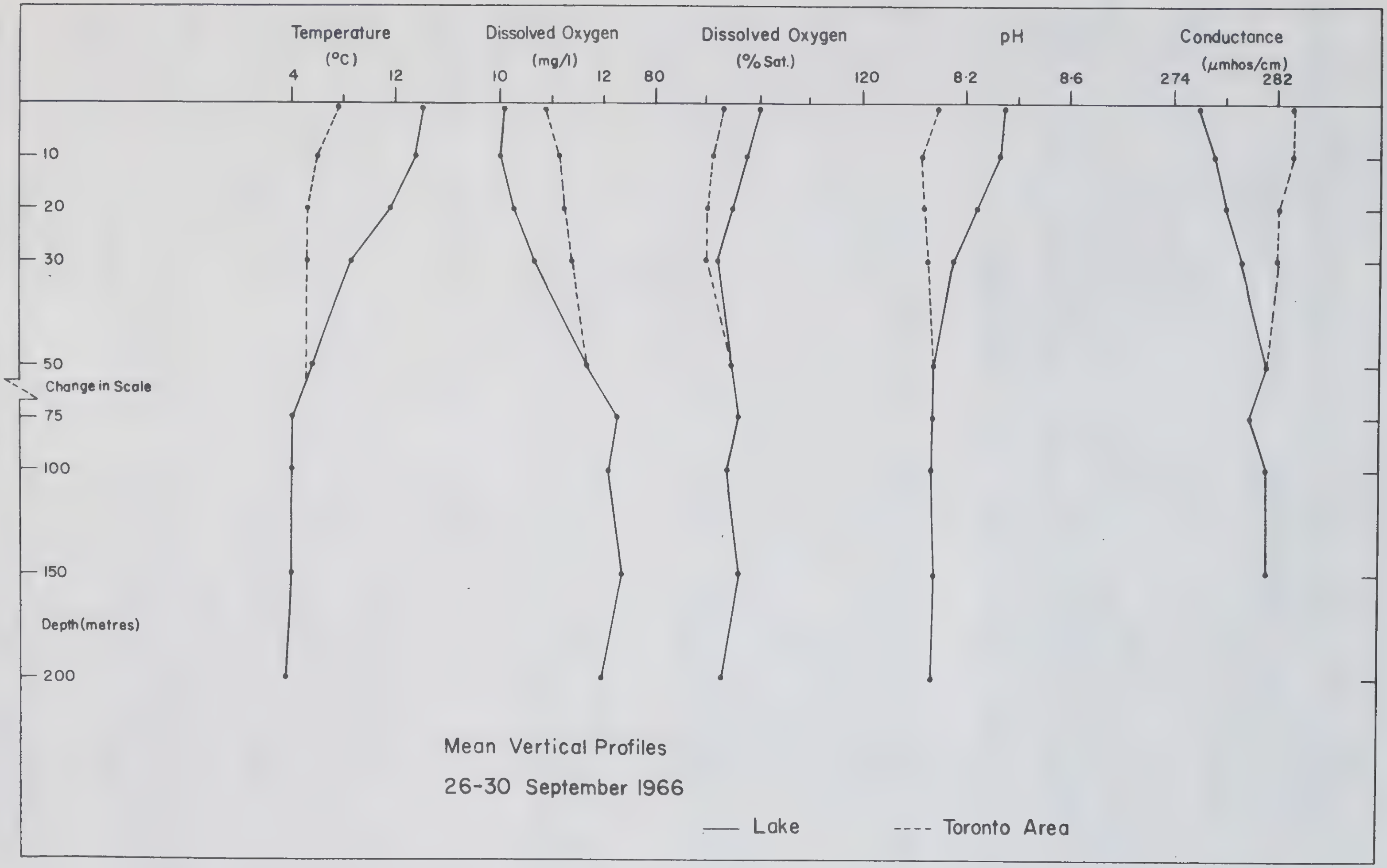

Fig. 55 Mean vertical profiles of temperature, oxygen, pH and conductance in an upwelling area (dashed lines) compared with their lake mean profiles (solid lines), September 26-30, 1966.

lower than in the hypolimnion, even in the coldest parts of the lake, and the percentage saturation is almost independent of depth in the centre of the upwelling areas. Outside these areas it rises from about 90% in the hypolimnion to close to 100% near the surface. Conductance and pH have similar distributions, being vertically homogeneous in upwelling areas and rising to 8.4 or decreasing to 318 μmhos/cm (at 25°C) respectively further offshore.

Upwelling thus has an influence on processes in the lake which varies with time. In late spring and early summer, when light conditions are optimal, the replenishment of nutrients stimulates a vigorous algal growth as is evidenced by a rapid rise in oxygen content and pH. In late summer and early fall, on the other hand, algal growth in these areas is much slower, and the oxygen content and pH rise only very slowly to their equilibrium values.

6. CALCULATIONS BASED ON TEMPERATURE OBSERVATIONS

6.1 Vertical Eddy Diffusivity in the Thermocline Region

The coefficient of vertical eddy diffusivity, K_z, has been estimated from the present data by two different techniques, both based on changes with time of the lake-mean temperature profile. Derivation of the respective equations is outlined in Appendix D.

First of all, K_z can be calculated as a function of the rate of downward transport of heat through a horizontal surface and the vertical temperature coefficient:

$$\frac{\partial H_z}{\partial t} = -K_z \frac{\partial \overline{T}(z)}{\partial z} \qquad (6.a)$$

where $\overline{H}_z$ is the lake-mean heat content per cm^2 below a depth z, t the time, K_z the vertical coefficient of eddy diffusivity at a depth z, and $\overline{T}(z)$ the lake-mean temperature at a depth z. A slightly different form of equation a, using data for individual stations instead of lake-means, has often been used to calculate K_z (see, for example, Hutchinson, 1957). By using lake-mean profiles, however, the effect of transient changes in the distribution of thermocline depth and surface temperature are reduced, although not completely avoided. This will be discussed in more detail below.

Alternately, a coefficient of vertical eddy diffusivity K_z' can be calculated from the rate of downward displacement of the isotherms, in combination with the vertical temperature gradient:

$$\overline{w}'\left(\overline{T}(z_b') - \overline{T}(z')\right) = -K_z' \frac{\partial \overline{T}(z')}{\partial z'} \qquad (6.b)$$

where $\overline{w}'$ is the rate of downward displacement of the lake-mean depth of the isotherm considered, z' its lake-mean depth at the time of observation and T(z') its temperature, and where $\overline{T}(z_b')$ is the temperature at the bottom, K_z' the calculated eddy diffusion and $\frac{\partial \overline{T}(z')}{\partial z}$ the vertical temperature gradient at a depth z'.

Equation b has been developed by the present author in an effort to obtain a more accurate estimate of the mean coefficient of vertical eddy diffusivity in the thermocline region; this equation is less sensitive to variations in thermal structure than equation a.

The equations a and b have been applied to intermediate depths only. Close to the surface they are not valid, due to the fact that increases in temperature are caused by the absorption of radiative energy as well as by downward

1966			1967		
period	K_z	K'_z	period	K_z	K'_z
7 July - 22 July	0.23	0.16	12 July - 26 July	0.231	0.051
23 July - 4 Aug.	0.12	0.15	27 July - 7 Aug.	-0.001	-0.018
5 Aug. - 17 Aug.	0.32	0.12	8 Aug. - 23 Aug.	-0.033	0.059
18 Aug. - 31 Aug.	0.04	0.04	24 Aug. - 6 Sept.	0.078	0.028
1 Sept.- 14 Sept.	-0.07	0.14	7 Sept - 18 Sept.	-0.102	0.044
15 Sept.- 28 Sept.	0.49	0.12			
mean	0.19	0.12		0.036	0.033
SD	0.18	0.05		0.042	0.014

Table 8 Vertical diffusion coefficients (cm^2/sec) in the thermocline layer computed from $\overline{T}(z)$ and $\overline{Z}(\theta)$ respectively. On the lower two lines the summer means and the standard deviations are given.

mixing. The trophogenic zone (the layer in which 99% of all incoming radiation is absorbed) varies in thickness from cruise to cruise. Data on the penetration of light in Lake Ontario are scarce; some measurements, however, have been made by the Rochester Program Office (US Dept. of Interior, FWPCA, 1967) indicating that the trophogenic zone in the summer of 1965 varied in thickness between 10 and 25 metres, depending on time and location, and averaged about 20 metres on the cruise with the clearest water.

At depths well below the thermocline, the vertical temperature gradient, and changes in heat content, become so small that the equations a and b cannot be applied successfully to the present data. For these reasons, both K_z and $K_z^{\prime}$ have been calculated only in the thermocline region. The results are summarized in Table 8, K_z has been determined for every 5 metres down to 40 metres, $K_z^{\prime}$ for values of z corresponding to the lake-mean depth of the isothermal surfaces between 5 and 15°C. In both cases the table only gives mean values of the eddy diffusivity coefficient for a value of z equal to the lake-mean thermocline depth over the corresponding two week period.

In the following paragraphs the results obtained by the equations a and b will be compared, and arguments presented to support the usefulness of equation b. In the final paragraphs of this chapter the striking difference between the summer-mean values in 1966 and 1967 of both K_z and $K_z^{\prime}$ (0.19 and 0.12 cm^2/sec in 1966 and 0.036 and 0.033 cm^2/sec in 1967 respectively), will be discussed and an effort made to explain this difference.

The standard deviation of the computed values of K_z is as much as four times as large as that of $K_z^{\prime}$ (Table 8), indicating that the summer-mean of the latter may be a more reliable estimate of the vertical diffusivity coefficient. The reason for the magnitude of the standard deviation of K_z is that the vertical transport term $\overline{wf}$, which has been neglected in the derivation of equation D.e (see Appendix D), is not always insignificantly small. Changes in the distribution of heat within the lake may cause reversible upward or downward fluxes of heat. This is illustrated in Fig. 25 for the case of a two layered model lake with an infinitely sharp boundary separating the two layers. An increase in the tilt of the thermocline, for example, causes an upward flux of heat on one side and a downward flux on the other side of the lake. As a result the lake-mean heat content below a unit area at depth z increases for all depths over which the thermocline ranges. The net downward transport of heat thus is reversible, since the original distribution of heat can be restored if the tilt of the thermocline decreases to its original level.

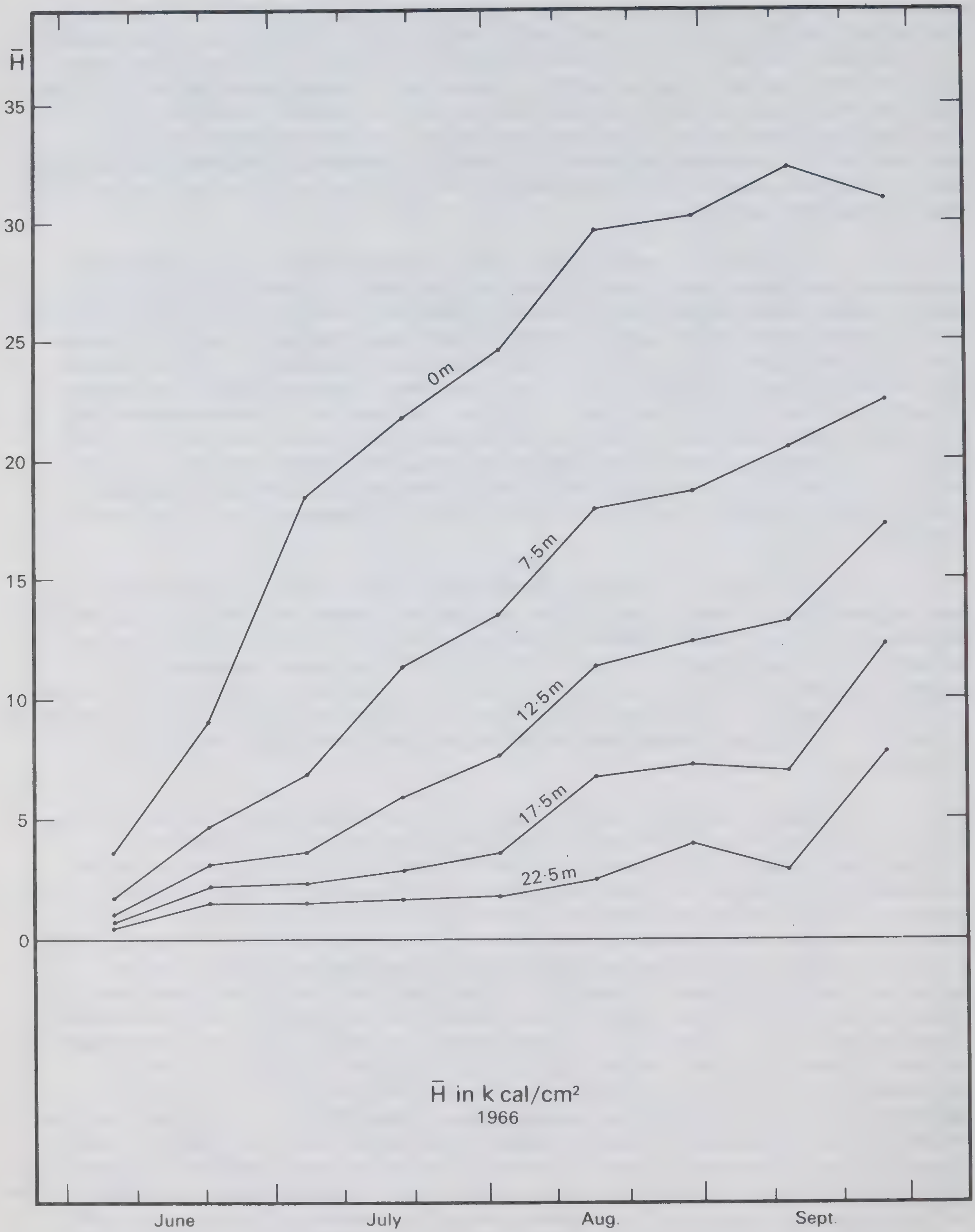

Fig. 56 Heat content below the surface and below four subsurface levels relative to a column of water of 4°C extending from each of these levels to a depth of 50 metres in 1966.

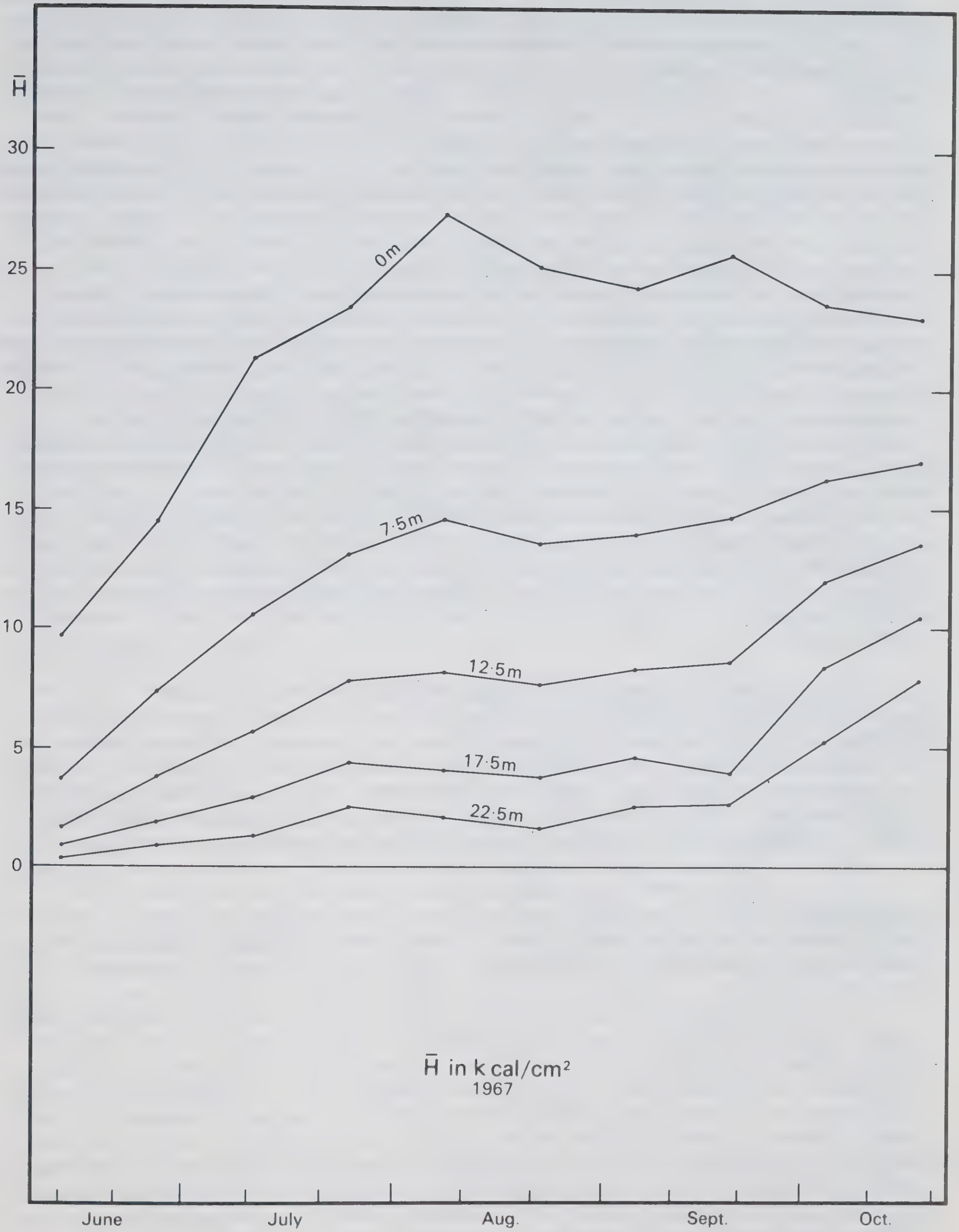

Fig. 57 Heat content below the surface and below four subsurface levels relative to a column of water of 4°C extending from each of these levels to a depth of 50 metres in 1967.

The importance of the reversible convective redistribution of heat in the actual lake is illustrated in the Figs. 56 and 57, which show fluctuations in the mean heat content of the lake below certain levels during the 1966 and 1967 field seasons. In the middle of July 1966, for example, the heat content below the 7.5 metre level increases much faster than the total heat content of the lake, and in early September of the same year the heat content below 17.5 metre level decreases temporarily while the total heat content is still increasing. In both cases the slope of the thermocline shows sudden variations, increasing and decreasing markedly, and the computed values of K_z are unrealistically high and low respectively. An increase in thermocline slope, for example, may cause warm epilimnion water to locally penetrate to depths normally occupied by cold hypolimnion water, thereby increasing the lake-mean heat content at this level. Similar features are brought out by the 1967 data, where K_z even turns negative in three instances due to an apparent upward flux of heat. These irregularities are caused by the fact that the vertical transport term $\overline{wf}$ in equation D.d obviously cannot be neglected in the samples given. In the derivation of equation b, on the other hand, this term has been taken into account implicitely by referencing the equation to a coordinate system moving up and down with elements of the thermal structure. The computed values of K_z' consequently are more reliable than those of K_z, which is also brought out by the difference in their standard deviations.

The difference in the mean values of K_z and K_z' is caused by a different mechanism. K_z, the mean vertical eddy diffusivity at a constant depth z, is based on the gradient of $\overline{T}(z)$, which is calculated by averaging the observed temperatures at each level. K_z', on the other hand, is based on the gradient of $\overline{Z}(\theta)$, which is usually larger than the gradient of $\overline{T}(z)$. Consequently, K_z' will be somewhat smaller than K_z.

For these two reasons the author feels that the estimates of the coefficient of vertical eddy diffusion given by K_z' are more accurate than those given by K_z, and in the remaining part of this section only K_z' will be discussed.

Attention has already been drawn to the unexpectedly large difference between the summer mean values of K_z' in the two summers studied, K_z' being 0.12 and 0.03 cm^2/sec in 1966 and 1967 respectively. This is undoubtedly related to the difference in weather conditions during the two summers. Wind conditions in particular are significantly different, as was discussed in Section 2.3. The magnitude of the coefficient of eddy diffusivity in the thermocline region is directly proportional to its rate of downward displacement (see equation b). This, in turn, is strongly dependent on wind strength, especially on the strength of the strongest winds occurring during the period of observation by Appendix C, and the lack of strong

winds in July and August 1967 may thus explain the low value of K_z' for this year. More experiments are needed, however, to determine whether the wind alone can account quantitatively for the differences between the two years, or whether other factors should be considered as well.

In view of the foregoing arguments the author considers the 1966 values of K_z' to be more representative than the 1967 values for conditions in the lake during the majority of years.

Csanady (1964) has published the results of a series of dye experiments in the Lakes Erie and Huron, undertaken to determine the coefficients of horizontal and vertical eddy diffusivity in the epilimnion. He indicates as typical values for the horizontal and vertical diffusivities in this layer: $K_{xe}=1000$ cm^2/sec and $K_{ze}=7$ cm^2/sec respectively. These results may not be directly comparable with the value of K_z' in the thermocline region of approximately 0.1 cm^2/sec, due to the difference in techniques used, but the order of magnitude of the difference between K_{ze} and K_z', and between K_{xe} and K_z', is certainly significant. The thermocline consequently acts as a "diffusion" floor, at least in the summer, greatly reducing the diffusive penetration into the hypolimnion of any substances dissolved in the epilimnion.

6.2 Dynamic Height

The use of dynamic height calculations to deduce circulation patterns in a large lake is a risky procedure, since lakes seldom are large enough to warrant neglect of the effect of their boundaries in the basic equations. The technique has been applied with some success, however, to Lake Huron by Ayers (1956) and to Lake Superior by Ragotzkie (1966). Recently it has also been used on Lake Michigan (Bellaire and Ayers, 1967; Noble, 1967) and on Lake Ontario (Scott and Lansing, 1967).

Scott studied data from a number of cross sections in eastern Lake Ontario. He used the dynamic height method to calculate currents, assuming a geostrophic balance, and taking the 45 metre level as the depth of no motion. The current is given by:

$$V = \frac{10^3 \sin \varphi}{1.45 \times 10^{-4} \sin \alpha} \quad [\text{cm/sec}] \qquad (6.2.a)$$

where φ is the angle between a surface of constant dynamic height anomaly and the horizontal, and α the latitude of observation. Scott estimated that the influence of centripetal accelerations, caused by the curvature of lake boundaries, on the geostrophically calculated current is not more than 15 percent, and he therefore neglected this effect in his calculations. The choice

of the depth of the level of no motion is not critical, as long as it remains below the thermocline, since the computed dynamic height gradients are hardly affected by the small horizontal temperature gradients occurring in the hypolimnion, where all water is about 3.9 °C. His major conclusions are:

(i) a relatively strong gradient current (speeds up to 30 cm/sec) moves in a counter-clockwise direction along the southern and eastern shores;

(ii) a weak counter-current flows westwards along the northern shore;

(iii) these currents are a regular feature in the eastern part of the lake, at least in late spring and early summer.

Very few direct current measurements have been made, however, to support these conclusions, and the applicability of the geostrophic method to calculate the numerical strength of these currents is insufficiently substantiated.

The present author calculated net transport through the three N-S sections from Petticoat Point to W. Nine Mile Point (Fig. 4) from data presented in Scott's paper by integrating the currents over the cross-sectional area. The respective transports for cruises on July 13, 1965; June 3, 1966; and July 8, 1966, are 14 x 10^6, 8.4 x 10^6 and 46 x 10^6 liters/sec towards the east (Table 9), much in excess over the summer-mean net eastward flow of 6.4 x 10^6 liters/sec through the lake to the mouth of the St. Lawrence River (DEMR). This discrepancy cannot be explained by assuming a return flow in the hypolimnion balancing the difference between geostrophic and net eastward flow, since this would involve an unrealistically large rate of thermocline descent in the eastern section of the lake. An excess flow of 10 x 10^6 liters/sec, for example, would cause the thermocline in this section to increase in depth at a rate of 24 cm/day, up and above the natural rate of increase due to downward mixing. Neither can the choice of a different level of no notion solve the problem, since temperatures in the hypolimnion are so nearly uniform that variations in depth of the reference level hardly affect the geostrophic calculations, unless the reference level falls partially within the epilimnion. The temperature distribution, however, does not provide any clues to help define a level of no motion within the epilimnion, and thus does not support this assumption. It appears, therefore, that the current velocities and transports deduced from Scott's data cannot be real, unless they are transient rather than persistent features.

To test their consistency, geostrophic transports have been calculated from summer-mean thermal distributions to reduce the influence of transients. All calculations are made with reference to an assumed level of no motion at a depth of

location	time	flow
outflow St. Lawrence River	yearly mean	6.8×10^6
eastward flow through cross section	mean 4 Jul.-16 Sept. 1966	48×10^6
	mean 10 Jul.-21 Sept. 1967	35×10^6
	13 Jul. 1965 (Scott)	14×10^6
	8 Jul. 1966 (Scott)	46×10^6

Table 9 Yearly mean outflow through the St. Lawrence River, compared with the flow through a N-S cross section along 77°00'W calculated from summer-mean dynamic height patterns in 1966 and 1967. For comparison, the instantaneous transport for two cruises in 1965 and 1966, based on dynamic height patterns by Scott and Lansing (1967), are also shown. Flows are given in liters per second.

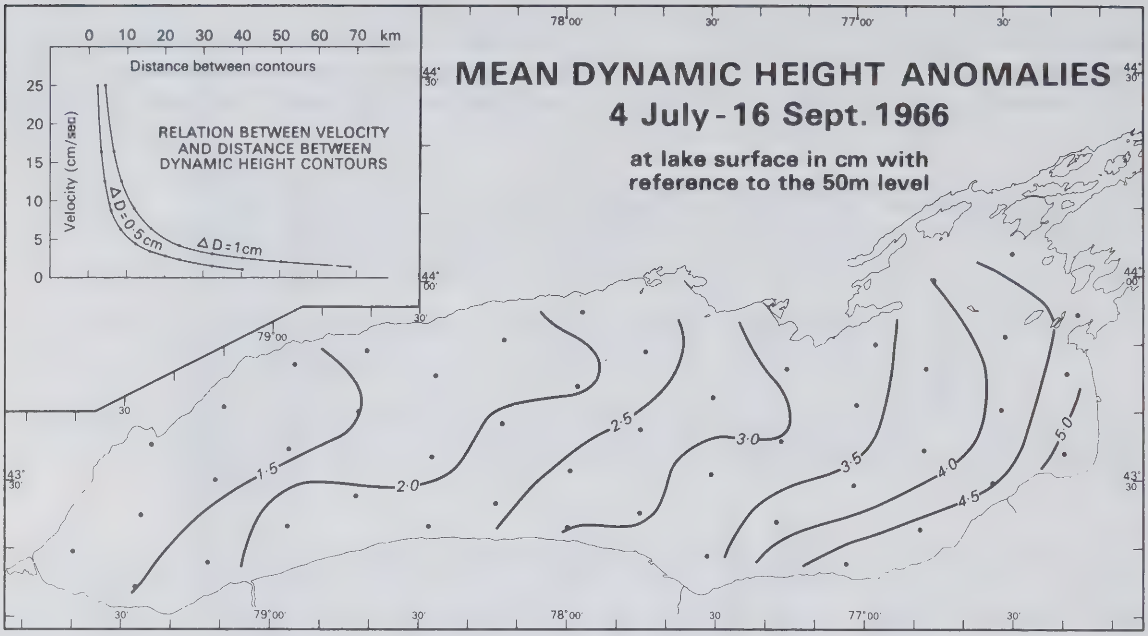

Fig. 58 Summer-mean dynamic height anomalies in cm in 1966.

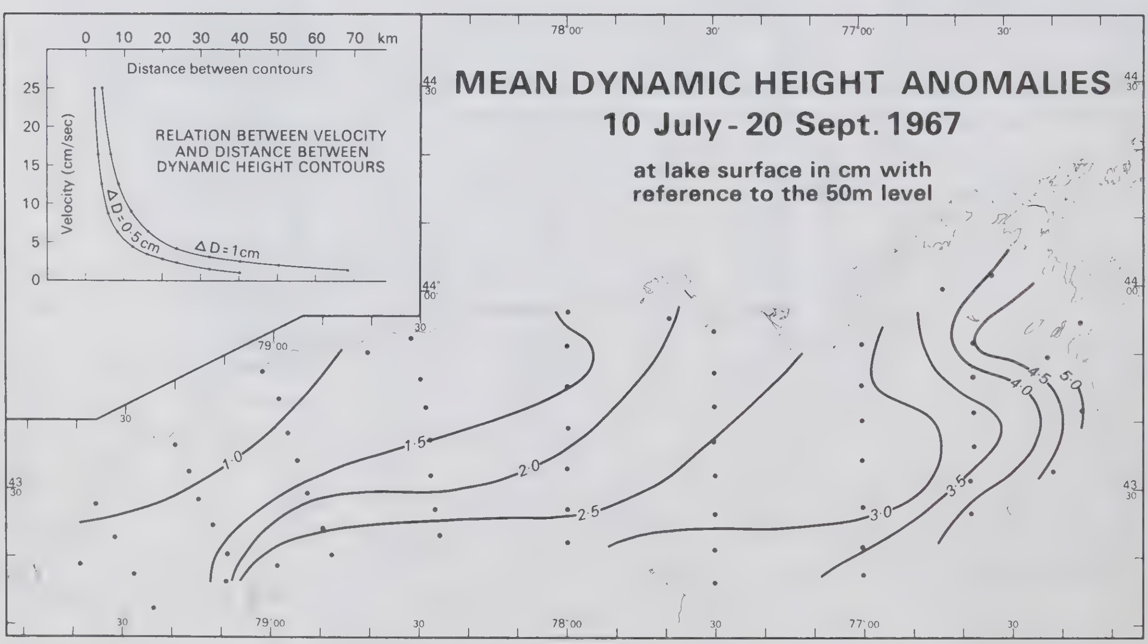

Fig. 59 Summer-mean dynamic height anomalies in cm in 1967.

50 metres. The summer-mean dynamic height patterns for 1966 and 1967 (Figs. 58 and 59) are essentially similar, showing in both years a maximum near the southeastern shore and a minimum in the Toronto region, and indicating a strong eastward flow along the southern, and a weak return flow along the northern shore. The geostrophically calculated strength of this current is approximately 5 cm/sec over a 20 km wide zone. Speeds could be much higher, however, if the current were to be concentrated in a narrow zone along the shore; the present station network regrettably is too coarse to resolve this.

Interpretation of the data is complicated by the fact that the contours of equal dynamic height are seldom closed in themselves, but tend to run from shore to shore. Assuming a layer of no motion below the thermocline, or at the bottom, the mean eastward transports through a N-S cross-section from Petticoat Point to West Nine Mile Point is 48 x 10^6 and 35 x 10^6 liters/sec in 1966 and 1967 respectively. This is of the same order of magnitude as the values calculated from Scott's data, thus confirming his original conclusion that the calculated geostrophic currents are consistent rather than transient features during the summer. The discrepancy between net eastward flow and calculated geostrophic transport, however, is also confirmed, and the conclusion that equation a cannot be used to calculate the numerical strength of currents in the eastern section of Lake Ontario thus seems inevitable.

The basic reasons for the breakdown of the geostrophic method in Lake Ontario are probably twofold. First of all, it may not be correct to neglect boundary conditions in a relatively small lake, like Lake Ontario, not only because of the effect of centripetal accelerations of the currents due to the curvature of the boundaries, but also because of the increased importance of other effects, such as lateral and bottom friction. Secondly, the relatively persistant eastward component of the wind exerts a strong, only occasionally interrupted, horizontal force on the lake, which must be taken into account in setting up the dynamic equations. This has not been done in the derivation of equation a.

The foregoing does not imply that the geostrophic method is useless as a tool in studying flow patterns in the Great Lakes. The general circulation pattern, found by Scott in the eastern section of Lake Ontario, has been qualitatively substantiated by direct current measurements (FWPCA, 1967) and drift object studies (Hamblin and Rodgers, 1967). The flow patterns deduced for other lakes by the dynamic height method also have been supported by various other measurements, and all authors quoted above give good evidence for the qualitative applicability of the method. Ayers (1956), however, pointed out that the computed transport through a section in Lake Huron was about twice as high as the outflow of the St. Clair River, but he attributed this to inaccuracies inherent to the necessary

interpolations of the observations and to the choice of the reference level (the level of no motion).

One of the reasons for the breakdown of the numerical applicability of the geostrophic method is the fact that wind induced currents are not taken into account. The wind over Lake Ontario has a relatively consistent eastward component, which will generate a southward drift current along the eastern shore counteracting the northward dynamic current. Proudman (1953, page 179), described a situation in an unbounded ocean consisting of a two layer system, without friction between the layers, where a wind drift is combined with a gradient current in such a manner, that there is no resultant transport. In this case the wind blows approximately parallel to the lines of greatest gradient of dynamic height, in an "uphill" direction. The relation between windforce and the dynamic height gradient is then given by:

$$k \rho_a u_a^2 = g \rho_w h \sin \varphi \qquad (6.2.b)$$

where k = wind-shear stress coefficient,
ρ_a = density of air,
u_a = wind velocity relative to the water,
g = acceleration of gravity,
ρ_w = density of water in the upper layer,
h = depth of the upper layer of water, and
φ = angle between the water surface and the horizontal.

In this model the dynamic height gradient is proportional to the angle φ, due to the uniformity of temperature within each of the two layers, and is, in the upper layer, given by $\rho_w \varphi$ Substitution of the constants, $k = 2.5 \times 10^{-3}$, $\rho_a = 1.25 \times 10^{-3}$ gm/cm^3, $\rho_w = 1.00$, and $g = 980$ cm/sec^2 (Proudman), gives:

$$h \sin \varphi = 3.19 \times 10^{-9} u_a^2 \qquad (6.2.c)$$

In a stationary condition, and in the absence of currents in the lower layer, the relation between the surface slope φ and the slope φ' of the interface is given by:

$$tg\, \varphi' = \frac{\rho_w}{\rho_w' - \rho_w}\, tg\, \varphi \qquad (6.2.d)$$

where ρ_w' is the density of the hypolimnion water. For small angles φ and φ' equation (d) can be approximated by:

$$\sin \varphi' = \frac{1}{\rho_w' - \rho_w} \sin \varphi \qquad (6.2.e)$$

Substitution of (e) in (c) gives for the relation between thermocline slope and wind stress:

$$h(\rho_w' - \rho_w)\sin\varphi' = 3.19 \times 10^{-9} u_a^{2} \qquad (6.2.f)$$

Equation f can be applied to estimate the magnitude of a mean dynamic height gradient that would balance the wind drift. The author realizes that, in applying this equation to Lake Ontario, he is open to the same criticism as given above on the applicability of geostrophic methods developed for an unbounded ocean, the lake is of limited dimensions. It is nevertheless felt that (f) can give an indication of the order of magnitude of the wind drift factor.

The mean windstress at Toronto International Airport in the summer of 1966 has eastward and southward components of k x 80 x 10^3 and k x 33 x 10^3 (cm/sec)^2 respectively, where k is the windstress coefficient. Windstresses on the lake surface will be somewhat higher, and can be estimated from shore based observations using the lake breeze index (Richards, 1964, quoted in Richards et al, 1966), which averages 1.39 over the summer. This gives for the eastward and southward windstress components over the open lake values of k x 155 x 10^3 and k x 64 x 10^3 (cm/sec)^2 respectively. Substituting this in equation f, taking for the mean thermocline depth in the eastern half a value of 22 metres and for the density difference between epilimnion and hypolimnion a value of 1.77 x 10^{-3} (corresponding to temperatures of 20 and 4°C respectively), the equilibrium slope of the thermocline in the direction of the wind is found to be 19 cm/km. In other words, in an unbounded ocean an average windstress of 2.5 x 10^{-3} x 155 x 10^3 = 387 cm^2/sec^2 would roughly compensate for the geostrophic transport due to a dynamic height gradient of 3.3 x 10^{-3} cm/km (which, for an epilimnion temperature of 20°C, corresponds to the observed slope of the interface of 19 cm/km). The actually observed slope, in a direction perpendicular to the eastern shore, is in the order of 20 cm/km (Fig. 58), increasing to a maximum of 27 cm/km in the vicinity of Rochester. The mean slope of the interface along the longitudinal axis of the lake is 7 cm/km.

The mean windstress for 1967 is about 30% smaller than that for 1966 (Table 10). The slope of the interface, and the dynamic height gradient, on the other hand, are roughly equal to those in 1966. Application of equation f to the 1967 data gives for a thermocline slope balancing the mean windstress a value of 12 cm/km. Both the calculated and observed thermocline slopes thus are of the same order of magnitude as in 1966.

It has been shown that, for the model of an unbounded, two-layered ocean, the transport due to a wind drift current, set up by an eastbound wind equal in magnitude to the residual wind over the lake, will largely compensate the geostrophic transport due to a dynamic height gradient of the magnitude generally

parameter	units	summer 1966	summer 1967
wind			
component towards east	cm/sec	195	145
component towards north	cm/sec	-75	42
wind square			
component towards east	$(cm/sec)^2$	155×10^3	93×10^3
component towards north	$(cm/sec)^2$	-64×10^3	19×10^3
mean		174×10^3	108×10^3
thermocline slope			
calculated	cm/km	19	12
max. over 20 km near E. shore	cm/km	27	27
mean over longitudinal axis	cm/km	7.5	7
thickness epilimnion			
lake mean	cm	18×10^2	18×10^2
mean near eastern shore	cm	22×10^2	22×10^2

Table 10 A comparison of mean wind data, mean thermocline slope, and calculated thermocline slope in the case of zero net transport along the eastern shore (see text Section 6.2), for the summers of 1966 and 1967. The mean winds are based on observations at Toronto International Airport, adjusted for conditions over the open lake by multiplication with the lake breeze index.

observed in Lake Ontario. The influence of boundary conditions on calculations such as those made above cannot be neglected, but it seems nevertheless likely that windstresses can seriously hamper any attempt to estimate transports or current velocities by purely geostrophic calculations. This does not affect the value of the geostrophic method in deducing general current patterns from temperature observations, as was pointed out above, but in a quantitative calculation of actual transports the windstress must be taken into account.

6.3 Response to the Lake to Winds

The thermal structure of the lake is subject to variable external forces acting on its surface, causing both oscillatory and semi-permanent deviations from an equilibrium. The equilibrium structure is, for the purpose of the following arguments, characterized by the absence of horizontal gradients. The vertical temperature profile then is determined by such factors as the exchange of energy through the air-water interface and turbulence. Oscillatory deviations from the equilibrium can be triggered by air pressure fluctuations and by variations in the wind field. Semi-permanent deviations are mainly caused by residual winds over extended periods of time, and by effects related to the rotation of the basin.

The response of the lake to variations in external forces is rather complicated. It may be useful to introduce the term "response time" to indicate the lag between a change in external forces and the response to this change. The response time is a function of the rate and the amplitude of changes in the forcing agent as well as of location within the lake and of the property involved. It is, for example, obvious that a noticeable change in the thermal structure must be preceded by a change in currents; the response time for the latter thus is shorter than that for changes in the thermal distribution.

6.3.1 Response Time of Currents

Currents can respond fairly rapidly to changes in the wind direction. In a preliminary report by the Rochester Program Office, Federal Water Pollution Control Administration (1967), it is indicated that surface currents often respond in less than 6 hours to a wind-shift. Nearshore currents may respond even faster. These conclusions are based on current measurements in 1965 on a network of buoy stations distributed over the whole lake. Hamblin and Rodgers (1967) studied nearshore currents in the Toronto Region, but they did not feel that enough data had been collected to formulate definite conclusions about the response time. Data presented in their report, however, seem to suggest a much longer response time to a complete reversal of the wind, in the order of 24 hours. Their measurements have been collected from an instrument tower, situated about 1,400 metres offshore in the vicinity of Toronto

in a water depth of 10 metres. Currents in this location are almost always parallel to the wind. A reversal of the wind direction is usually, but not always, followed by a reversal of the surface current after 20 to 30 hours.

The difference between the results quoted depends partially on the location, partially on a difference in the method of analysis of the data. Both estimates are based on visual scanning of the records. The FWPCA records have been scanned for the response of current to rapid changes in the wind direction under storm conditions (personal communication from D. Casey), whereas the present author scanned the Great Lakes Institute records (Hamblin and Rodgers, 1967) for a reversal of the current caused by any reversal of wind direction lasting long enough to affect the current, regardless of wind strength. It is obvious, however, that the stronger the wind, the faster the currents will respond, and the difference in scanning techniques may thus partially explain the difference in the estimated response times. The available information can be summarized as follows: both the speed and the direction of currents in the lake respond to changes in the windfield within a period of 6 to 24 hours. The response time depends on the rate of change of the winds as well as on the location of the point of observation, and tends to be shorter for stronger winds and near the shores.

6.3.2 Response Time of Thermal Structure

The spacial distribution of temperature responds much more slowly to changes in the windfield, since a change in current has to persist for some time to transport a volume of water large enough to cause a significant change in thermal structure. To obtain an impression of the response time in local, nearshore areas, temperature records for a number of water intake stations have been analyzed and correlated with winds. Three of the stations are in the vicinity of Toronto, one near Rochester (Table 2).

In Fig. 6, noon-hour temperatures observed at the R.C. Harris plant near Toronto and at the Monroe County water intake near Rochester are compared with each other, and with the east-west component of the three-day mean wind vector. This figure clearly illustrates the negative correlation between the temperatures at opposite sides of the lake and the strong dependence of both on the wind. These relations have been studied in more detail by correlation and spectral analyses of series of wind and temperature data, sampled at 6 hour intervals starting midnight on May 31, 1966, and ending on September 30 of the same year. The wind data are 6 hour vector-mean winds for Toronto International Airport, centered around the time of observation of the temperatures.

The results of the correlation analyses are given in Fig. 60, the dotted lines indicate the 95 percent limits for a correlation r not differing significantly from zero (r=0.09). Water temperatures near Toronto are correlated negatively with the east component of the wind, those near Rochester positively. The correlation is barely significant for lag 0, but increases rapidly and reaches a maximum of 0.3 to 0.4 after 36 to 48 yours. After 4 1/2 days the correlation becomes insignificant and it remains so for longer lags. Correlation with the north component of the wind is very low, never more than 0.15 for the Toronto stations, and only for short lags up to 0.2 for the Rochester station. A further study of the data shows that correlation of the observed temperatures with the east component of the wind is better than with either the northeast or southeast components. The correlation analysis confirms the response time of about 48 hours that can be estimated by a visual comparison of the traces in Fig. 6.

In the second part of September a cruise has been made in the Rochester area during the only period in the summer of 1966 with strong easterly winds lasting more that 24 hours. Extensive upwelling is found in the Rochester area about 44 hours after the winds shifted in Toronto, but only a slight onset of upwelling in the Oswego area, sampled 12 hours earlier. Monroe County water intake data, sampled at a depth of 12 metres, show a marked drop in temperature about 30 hours after the start, and a return to near normal values 48 hours after termination of this spell of easterly winds, again confirming a response time of the thermal structure in the order of 36 to 48 hours.

The response time discussed in the preceding paragraphs is based on local, nearshore observations of the thermal structure. The average east-west tilt of the thermocline, however, was never reversed throughout the summer (see Figs. 11 and 12), even though large fluctuations in the nearshore depth of the thermocline often occurred. It is interesting to compare the observed response times with the time needed to obtain a complete reversal of the thermocline tilt. The latter can easily be calculated from the mean epilimnion depth in the western ($\overline{Z}_w$) and eastern ($\overline{Z}_e$) sections of the lake (Table 5) in combination with an assumed average horizontal velocity v. The time t needed to complete reversal is given by:

$$t v \overline{Z} y = (\overline{Z}_e - \overline{Z}_w) . \frac{1}{2} A$$

where $\overline{Z}$ is the lake average depth of the thermocline, y the width of a north-south cross-section through the lake, and 1/2 A the area of the eastern or western half of the lake. Substitution of summer mean values ($\overline{Z}$ = 17.0 m, $\overline{Z}_w$ = 13.2 m, $\overline{Z}_e$ = 20.8 m), and of A = 18,250 km^2, y = 80 km and a mean velocity of 10

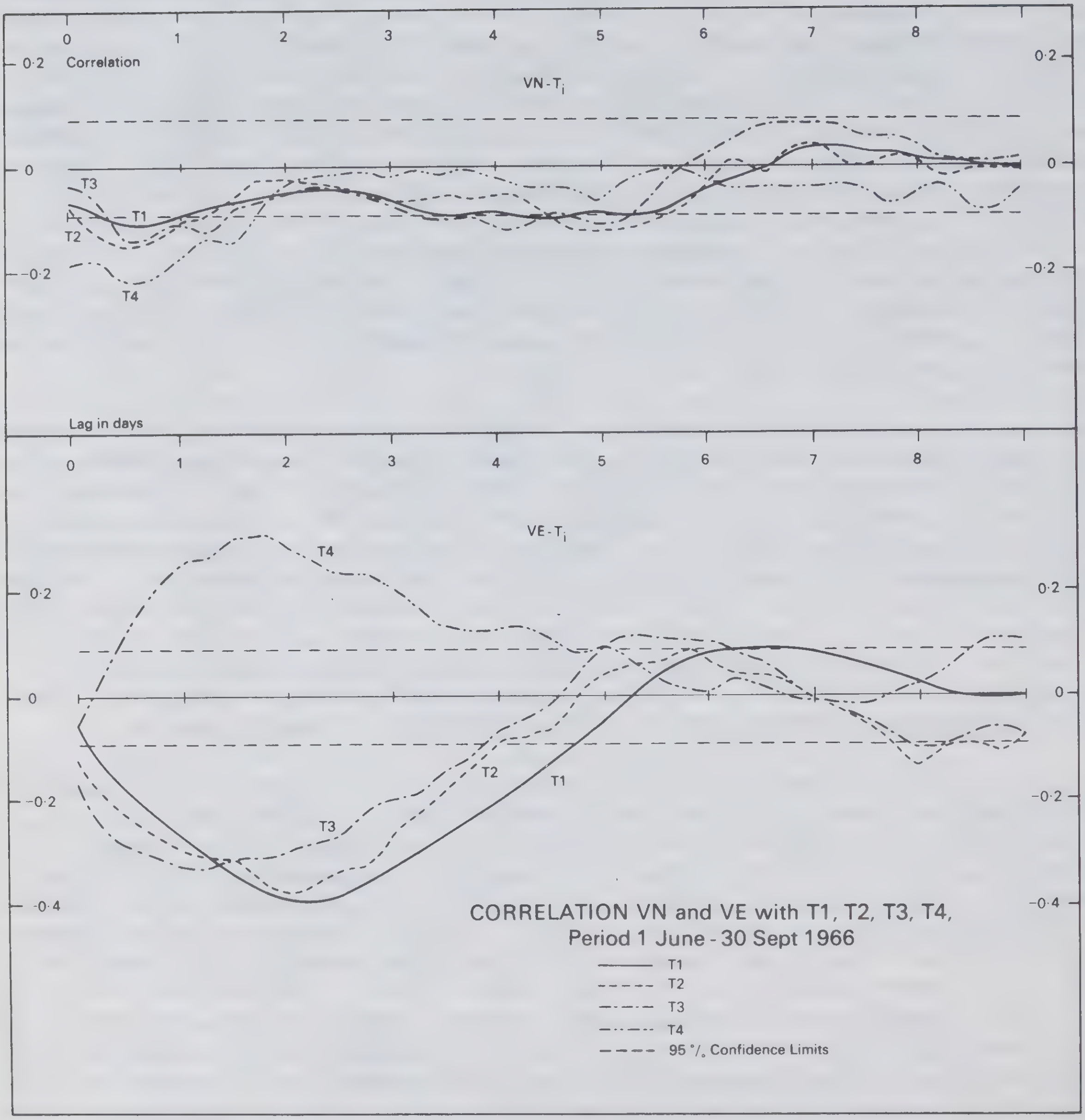

Fig. 60 Correlation between the east and north components of the wind and water intake temperatures from four different stations for the 1966 field season. For the location of the stations see Table 2.

cm/sec[1]) gives a reversal time of 7.3 days. Even assuming a westward current, in the middle of the lake, averaging 30 cm/sec over the cross-sectional area of the epilimnion, the reversal time would be 2 1/2 days! Currents of this strength, however, can and do occur locally, but it seems unlikely that they would occur over the whole width of the lake.

The length of the calculated response time of the overall thermal structure explains why no reversals of the east-west tilt of the thermocline were observed during the summers of 1966 and 1967. At no time during those two summers did winds blow from the east for a period long enough to cause a complete reversal of the tilt.

6.4 Auto and Cross Spectra of Water Intake Temperatures and Winds

Various authors have analyzed periodicities in series of temperature or current data on the Great Lakes. Csanady (1967) recently studied the oscillations from a theoretical point of view. He computed the types of internal and surface modes that occur in a "Model Great Lake", which he defined as a circular basin of constant depth containing two layers of fluid of slightly different density and having a diameter comparable to the dimensions of the Great Lakes. He suggests the existence of two types of internal oscillations with finite frequencies:

1. slow, counter-clockwise rotating internal waves with periods of many times the half pendulum day ("Kelvin waves"), and

2. internal seiches rotating in either direction with periods up to or within a small fraction of the inertial period,

and a third type of "oscillation" with a frequency zero, which may manifest itself as a jet-type current along the shores.

Mortimer (1963) has found some experimental evidence for the first two types of oscillations in water intake data from a number of stations around Lake Michigan. Verber (1966) found evidence of periodicities of about 17.4 hours, which is near the inertial period, in power spectra of current records sampled in the same lake. Progressive vector diagrams of the current, especially in the open lake, sometimes show a very clear rotary movement of the water with this period. A similar

---

[1]The Rochester Program Office (1967) reports an average net transport velocity of 5 cm/sec and an average speed of 15 cm/sec in the epilimnion throughout the summer of 1965.

peaking in current spectra of Lake Ontario has recently been reported by Hamblin and Rodgers (1967). They also found a diurnal peak in the power spectra, which is highly correlated with diurnal fluctuations of wind. This peak is not obvious in the power spectrum published by Verber, but that may be due to the fact that his data were sampled much further offshore than Hamblin and Rodgers' data. The latter authors also carried out a cross spectral analysis between currents and winds. Slow variations in the currents (periods over 30 hours) are well correlated with the east-west component of the wind, but their correlation with the north-south component, which is almost perpendicular to the shore at the observation site, remains below the 95 percent significance level. Diurnal current fluctuations, on the other hand, are well correlated with the north-south component of the wind, but in this case the correlation with the east-west component remains below the 95 percent significance level.

The water intake data collected by the present author have also been subjected to spectral analysis. The data series consist of about 500 points, read off the original data records at 6-hour intervals, and covering the period of June 1 through September 30, 1966[1]; the location of the water intakes is summarized in Table 2. Auto and cross spectra have been determined for wind data from Toronto International Airport and for the water intake temperatures.

6.4.1 Auto Spectra

Power spectra of both the winds and the temperatures are presented in Fig. 61; the 95 percent confidence limits have been indicated by an arrow on the righthand side (Munk et al, 1959). The temperature spectra show a large peak near the inertial period of 16.5 hours, but relatively little energy is present in the diurnal period. This does not contradict Hamblin and Rodgers' finding of a diurnal peak in the current spectra, since changes in the thermal structure are secondary to changes in the current, and thus may be much smaller. Another, less conspicuous, concentration of energy shows up as a slight bulge in the spectrum for periods of 5 to 8 days.

Wind spectra show a peak for a period of 4 to 8 days and two peaks on either side of the diurnal period. The fact that the diurnal peak is split into two peaks may be due to insufficient length of the record analysed or to aliasing caused by the low sampling frequency. For periods over 10 days, the power in the wind spectrum decreases with increasing periods, whereas power in the water temperature spectra keeps increasing over the full range of frequencies analyzed. The difference is

---

[1] The 1967 water intake data records have not been studied.

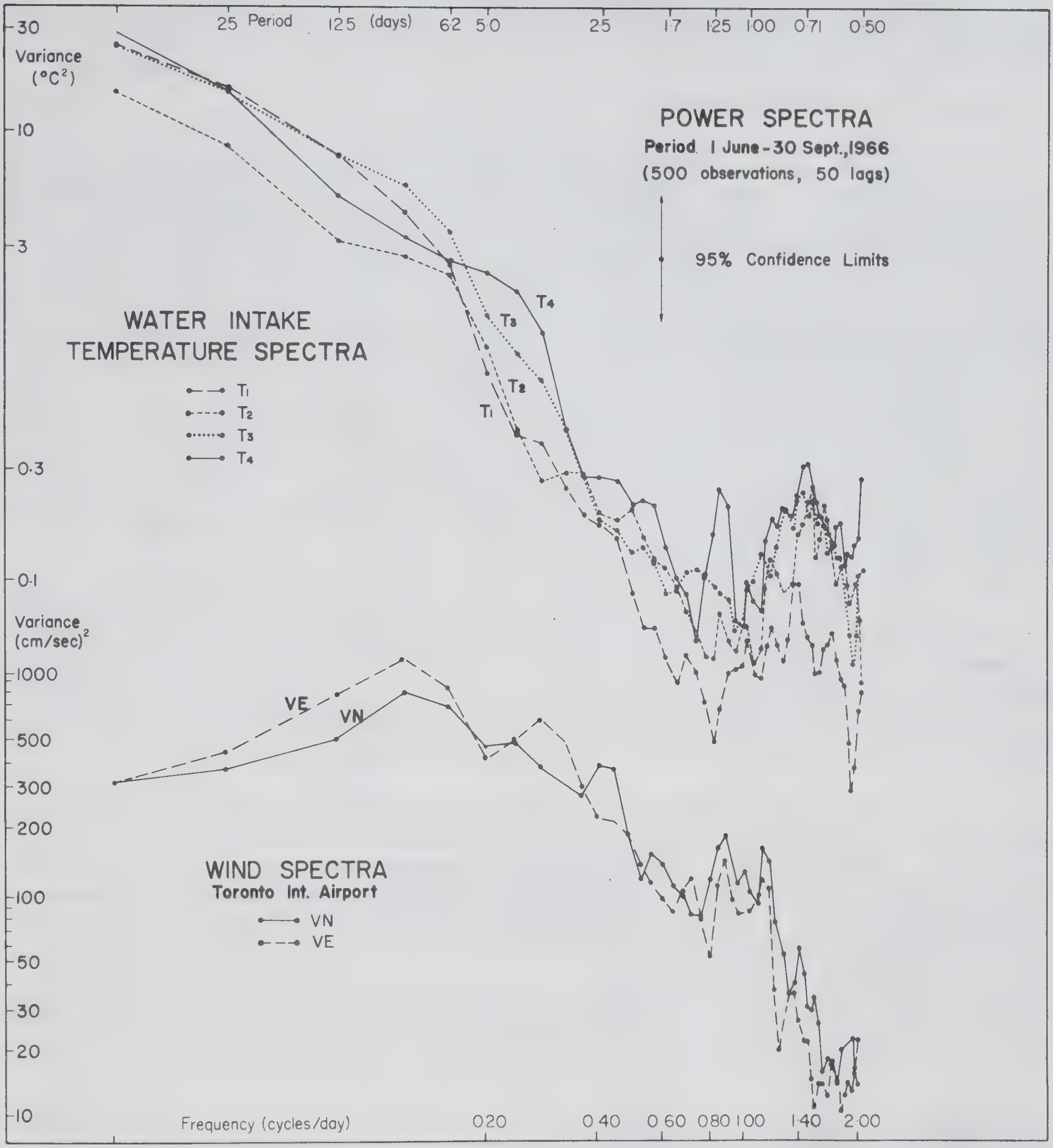

Fig. 61 Power spectra of the water intake temperatures of four different stations, and of the north and east components of the wind, for the period of June through September 1966.

probably due to the influence of seasonal changes in temperature and also to the strong dependence of the latter on heat exchange and residual winds. The energy in the low frequency range may also be increased by the natural response frequency of the lake: the first order longitudinal internal wave has a period of about 15 days[1].

6.4.2 Cross spectra

Cross correlation spectra have been calculated for 12 and for 50 lags. The latter calculations give a better resolution of the peaks, but are subject to larger random errors and the resulting spectra consequently fluctuate more than those for 12 lags. In the spectra presented, the results of the high resolution analysis are given whenever they are significant; but when they hover around the 95 percent significance level, usually at the high frequency end of the spectrum, the results of the low resolution analysis are presented. The transition is marked by a discontinuity in the curves and an arrow along the frequency axis. Dotted lines indicate the 95 percent confidence limits of a coherence differing from zero (Appendix E). The phase has been omitted whenever the coherence remains consistently insignificant for a frequency interval.

In the illustrations, lags are expressed in degrees and indicated as positive if the first data series is ahead of the second series by up to half a period, negative if it lags behind the second series by up to half a period. The coherence is a measure analogous to the actual correlation (not to the square of the correlation) between two series of data.

The cross spectra between the three water intake temperature records sampled near Toronto are presented in Fig. 62. They show a very high level of correlation (0.9) for low frequencies, even though one station is almost twice as deep as the other two. For periods shorter than 5 days, however, the coherence decreases rapidly, becoming barely significant for periods between 1 and 2 days. A secondary peak marks the inertial period of 16.5 hours. The coherence between the two shallow water intake stations, R.C. Harris (T_1) and the Old

---

[1]This can be calculated (Proudman, 1953) from

$$T = 2L\left\{\frac{\rho'}{\rho'-\rho}\cdot\frac{1}{g}\left(\frac{1}{h}+\frac{1}{h'}\right)\right\}^{\frac{1}{2}}$$

where T is the oscillation period, L the length of the basin, g the gravity acceleration, h and h' the thickness of the upper and lower layers and ρ and ρ' their densities.

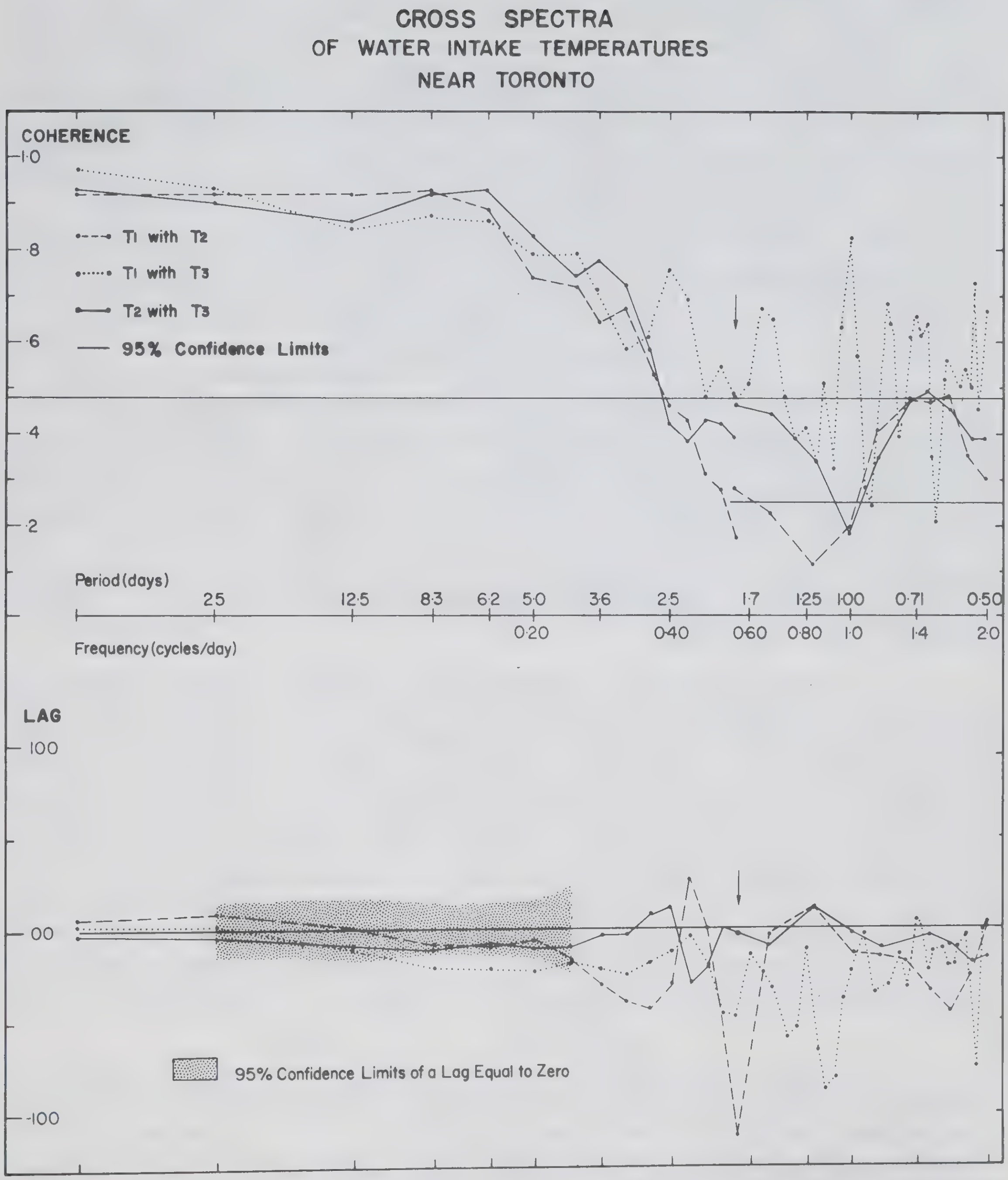

Fig. 62 Coherence and phase lag between temperature data from three water intake stations in the Toronto region. In the high frequency region the number of lags used in the analysis is reduced from 50 to 12 in two of the three data series (T_1 with T_2 and T_2 with T_3).

Eastern Island Plant (T_3), also shows a peak for the diurnal fluctuation. This peak, which barely can be recognized in their power spectra, is highly significant in a statistical sense, and may be related to the diurnal periodicity in the winds. The phase relation between these two stations indicates a lead of the western station over the eastern for almost all frequencies, suggesting a clockwise rotation of the internal waves. The 95 percent confidence limits of a phase lag differing from zero has been calculated (Appendix E) for the mean coherence of the three stations and is indicated by the shaded area in Fig. 62. The "clockwise" lag between the Old (Eastern) Toronto Island Plant data (T_3) and the R.C. Harris data (T_1), 13 km east of the former, is statistically significant for periods of 6 to 8 days and corresponds to an eastward speed of the internal waves of 0.7 km/hour. These observations do not agree with the counter-clockwise rotation found by Mortimer (1963) for internal waves moving around the basin with a similar velocity (1.8 km/hour). His data, however, are based on a study of individual occurrences of slowly rotating waves with a large amplitude, whereas the present data are based on a statistical analysis of a continuous series of data. The presently observed clockwise rotation can perhaps be explained by the generally eastward movement of meteorological disturbances over the lake.

The coherence between the Toronto water intake temperatures and the Monroe County data (Fig. 63) is below the 95 percent significance level for almost all frequencies, with the exception of a marked peak for a period of about 8 days. Coherence in this peak rises to between 0.6 and 0.7, the phase lag between the opposite sides of the lake is roughly 180°. The power spectra of temperatures and winds, and the correlation spectrum between temperature and the east component of the latter, also reflect a peak for the same period. More data are needed to decide whether this correlation is due to a rotating internal wave or whether it is an indirect effect caused by the correlation between temperatures anywhere in the lake with the wind.

The correlation between winds and water intake temperatures is shown in Figs. 64 and 65. Temperatures are strongly correlated with the east-west component of the wind for periods longer than 5 days (up to 0.8), and, to a lesser extent, for periods down to one day. For diurnal and shorter periods the coherence is well below the 95 percent confidence limits. Correlation with the north-south component of the wind, on the other hand, is much lower, fluctuating around the 95 percent confidence limits and showing a few peaks up to 0.4 for periods of about 2 and 4 days in the Toronto region and a similar peak for a 6-day period in the Rochester area. Nearshore temperatures thus are much more dependent on winds blowing longitudinally over the lake than on winds across the lake. The reason

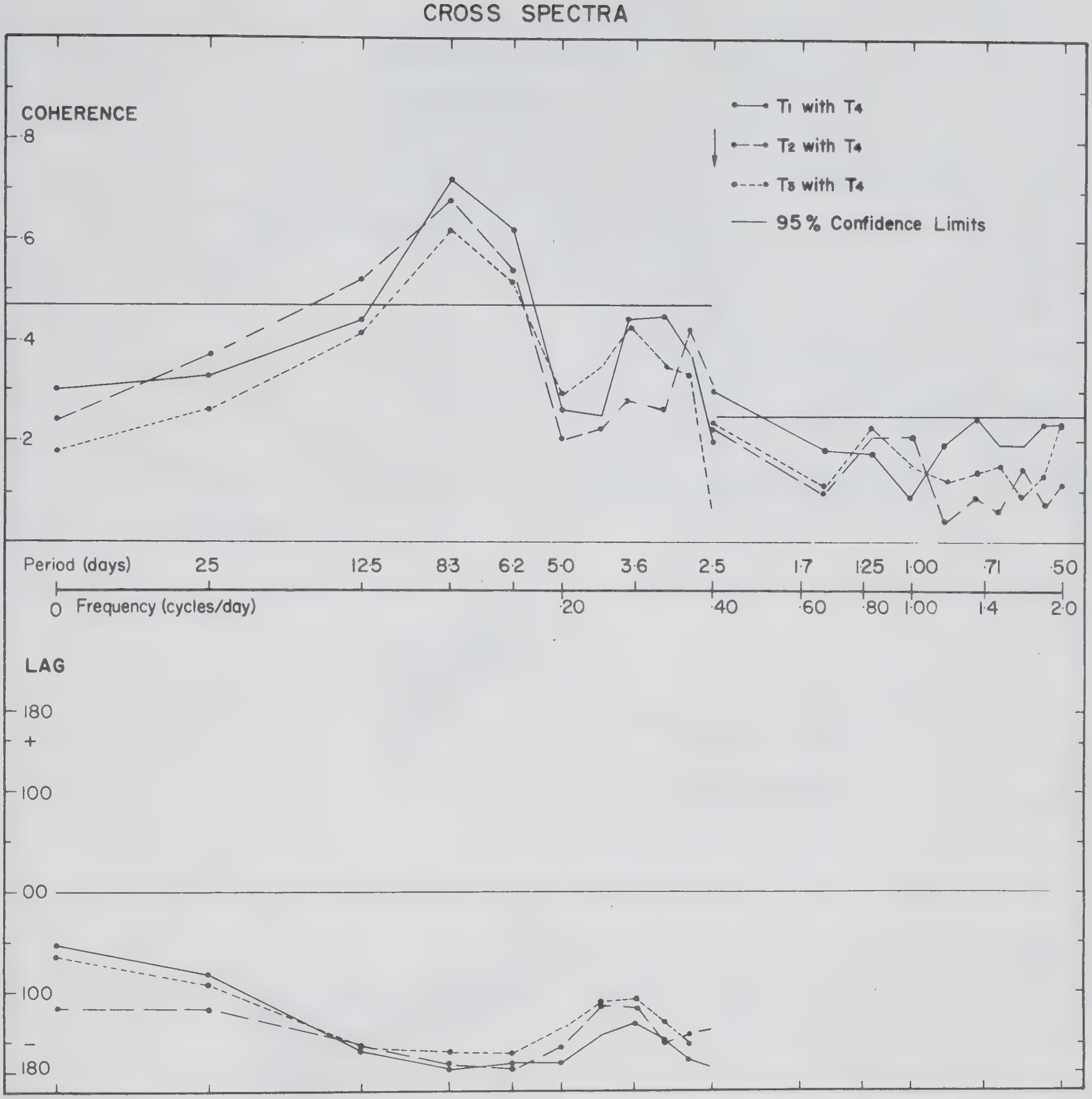

Fig. 63 Coherence and phase lag between temperature data from each of three water intake stations in the Toronto region and data from a station near Rochester. In the high frequency region the number of lags used in the analysis is reduced from 50 to 12.

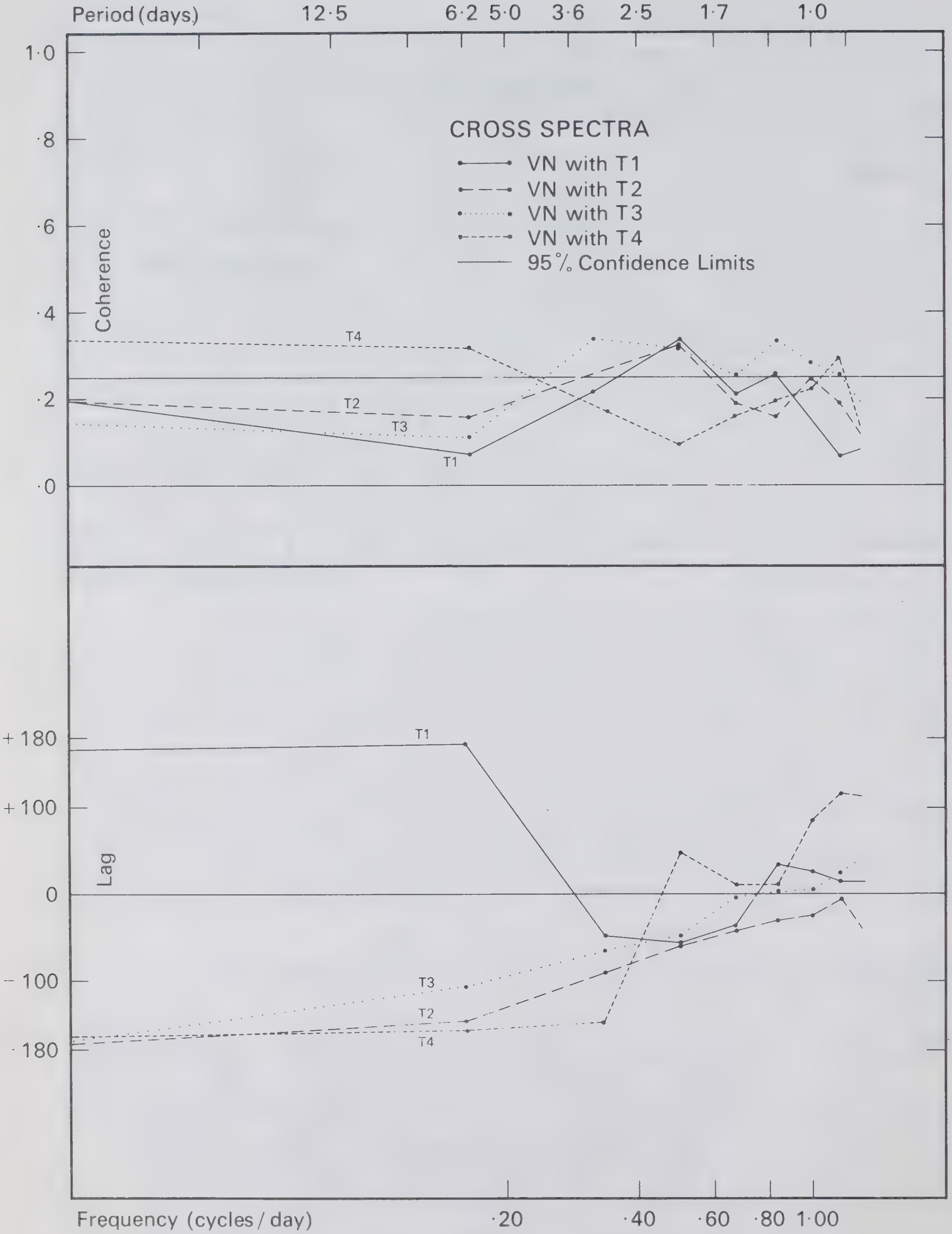

Fig. 64 Coherence and phase lag between the north component of the wind (Toronto International Airport) and the temperature data from each of four water intake stations. The data are analysed for 12 lags only.

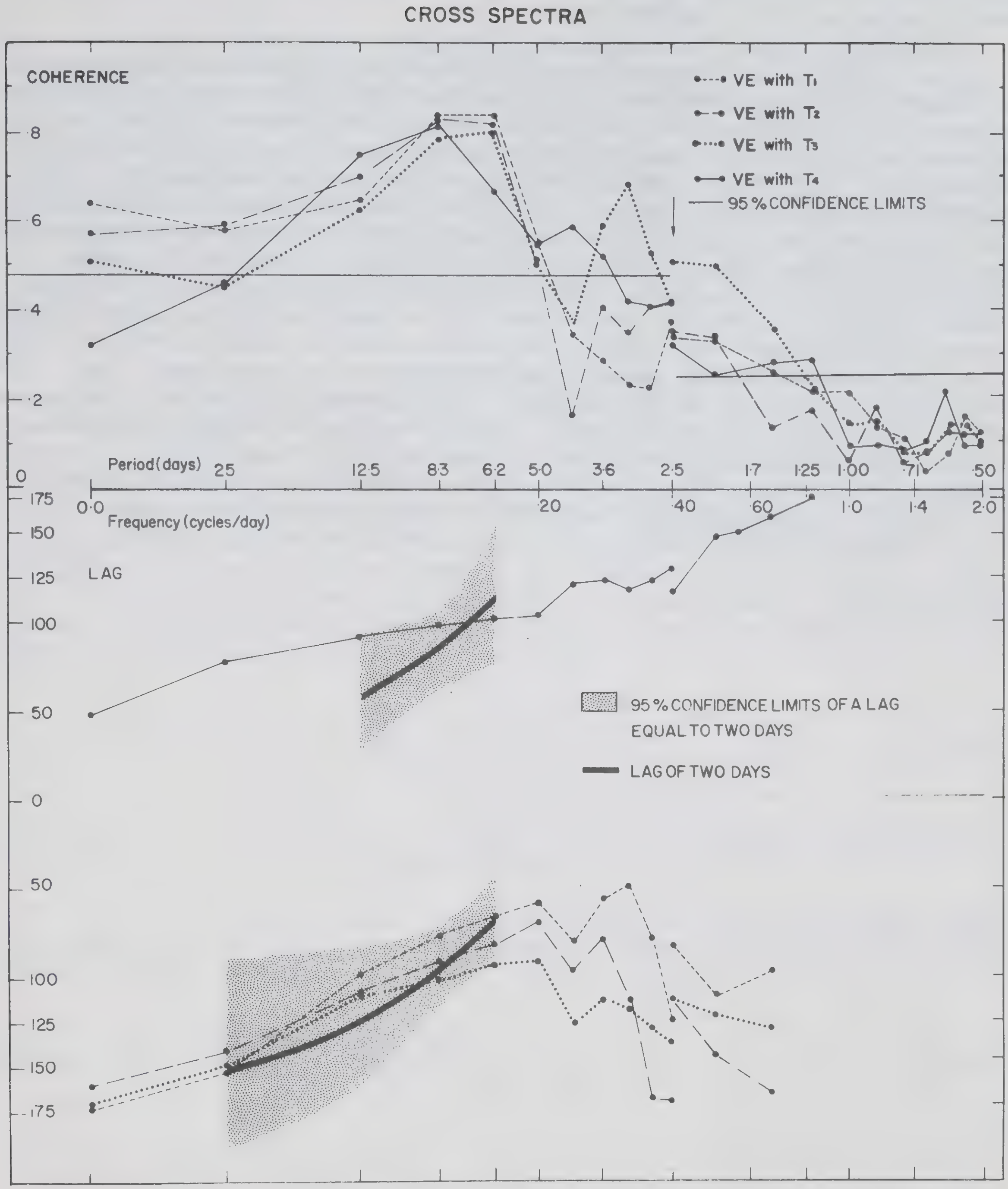

Fig. 65 Coherence and phase lag between the east component of the wind and temperature data from each of four water intake stations. In the high frequency region the number of lags used in the analyses is reduced from 50 to 12.

for this is not immediately evident, but it may be related to the location of the stations or to the consistency of the east-west slope in the thermocline.

A wind blowing towards the east is positively correlated with a temperature decrease near Toronto and with a temperature increase in the vicinity of Rochester. The lag between winds and temperatures for a very slow oscillation consequently is 180° near Toronto and 0° near Rochester, if the response time is negligibly small in relation to the period of the oscillation. In a preceding section evidence was presented for a response time in the order of 36 to 48 hours for slow oscillations. The phase lag corresponding to a hypothetical 2-day response time is indicated by a heavy line in Fig. 65 for those frequencies for which the coherence is sufficiently high to allow a reasonably accurate estimate of the actual lag. The shaded area indicates 95 percent confidence limits of the phase around the hypothetical 2-day lag, calculated from the mean coherence for the corresponding period (equation D.e). For periods between 6 and 25 days, the observed lags correspond within the 95% confidence limits to the assumed two-day lag, thus confirming the conclusions of the preceding section.

7. RESIDENCE TIME OF THE WATER

The study of the effectiveness of anti-pollution measures on the Great Lakes is complicated both by the large volume of these lakes and by a lack of knowledge about the fate of many of the pollutants discarded into them. An increased efficiency of waste removal from sewage consequently will only become noticeable after a number of years, even for conservative parameters, such as chloride, that are hardly or not at all affected by geochemical or biochemical processes. For chemically active substances the retention time may be even longer or, in some instances, almost indefinite when they are deposited on the bottom.

The effect of a stepwise decrease in the input of a conservative parameter on its concentration in the lake has been calculated by Rainey (1967). He used a simplified lake model and assumed (i) the precipitation on the lake equals the evaporation, (ii) the flow rates R into and from the lake are equal and constant in time, (iii) the concentration C_1 of pollutants in the streams entering the lake and the rate of addition Q of pollutants from other sources are constant and (iv) all pollutants are distributed so that their concentration $C_2(t)$ is uniform throughout the lake. The concentration in the lake at an arbitrary time t then is:

$$C_2(t) = C_2(0) + \left\{ C_1 + \frac{Q}{R} - C_2(0) \right\} \cdot \left\{ 1 - e^{-\tau t} \right\} \qquad (7.a)$$

where the time-constant τ =R/V, V is the volume of the lake, and $C_2(0)$ the initial concentration.

The adaption of concentrations in the lake to a stepwise change in input concentration is given by the "reduction" factor γ (t):

$$\gamma(t) = 1 - \frac{C_2(t) - C_2(0)}{C_1 + \frac{Q}{R} - C_2(0)} \qquad (7.b)$$

Combining (a) and (b) gives:

$$\gamma(t) = e^{-\tau t} \qquad (7.c)$$

The factor γ (t) is reduced to 10 percent after a length of time given by $t\tau$ = 2.3. For Lake Ontario the ratio of yearly flow over volume, τ , is 0.128, and the time t needed for a reduction

of $\gamma(t)$ to 10 percent, the "retention" time, thus is equal to $2.3/\tau$ or 18 years.

The lake model used by Rainey does not take the summer stratification into account. The present author repeated Rainey's calculations, changing only the last assumption, assuming that the lake is well mixed in the winter and stratified in the summer. Any pollutants entering in the winter then are mixed evenly over the total volume of the lake, but those entering during the summer are mixed only with the epilimnion water. No pollutants penetrate to the hypolimnion during this period, and the outflow of the lake is fed by the epilimnion only. Hypolimnion concentrations consequently are constant throughout the summer. During the fall overturn the two water masses are mixed, and the concentration $C_2(t)$ becomes uniform over the whole lake.

Equation c, relating $\gamma(t)$ to the time-constant τ, is independent of the origin of the time axis, and the relative change in concentration over a time t therefore can also be written as a product of the reduction factors over a number of time intervals Δt_i, if $t = \sum_{i=1}^{n} \Delta t_i$:

$$\gamma(t) = \prod_{i=1}^{n} \gamma(\Delta t_i) \qquad (7.d)$$

Rainey's equation, in a slightly modified version, thus can be applied to subsequent stratified and non-stratified periods, and an overall reduction factor for a stratified period can be defined by:

$$\gamma_0(t) = \frac{\gamma_1(t)\, V_1 + \gamma_2(t)\, V_2}{V_1 + V_2} \qquad (7.e)$$

where $\gamma_1(t)$ and $\gamma_2(t)$ are the reduction factors and V_1 and V_2 the volumes of the two layers respectively. The function $\gamma_0(t)$ gives the mean concentration that would result from instantaneous mixing of the two layers at the moment t, and thus is directly proportional to the total quantity within the lake of the parameter concerned.

Assume the lake to be stratified from June through October, with an average epilimnion thickness of 15 metres, and vertically well mixed during the remaining 7 months. The time constant τ for the epilimnion then is 0.80, and the reduction factors for the epilimnion and the hypolimnion after a stratified season are 0.7363 and 1.000 respectively, giving a value of 0.9540 for the composite reduction factor γ_0. The

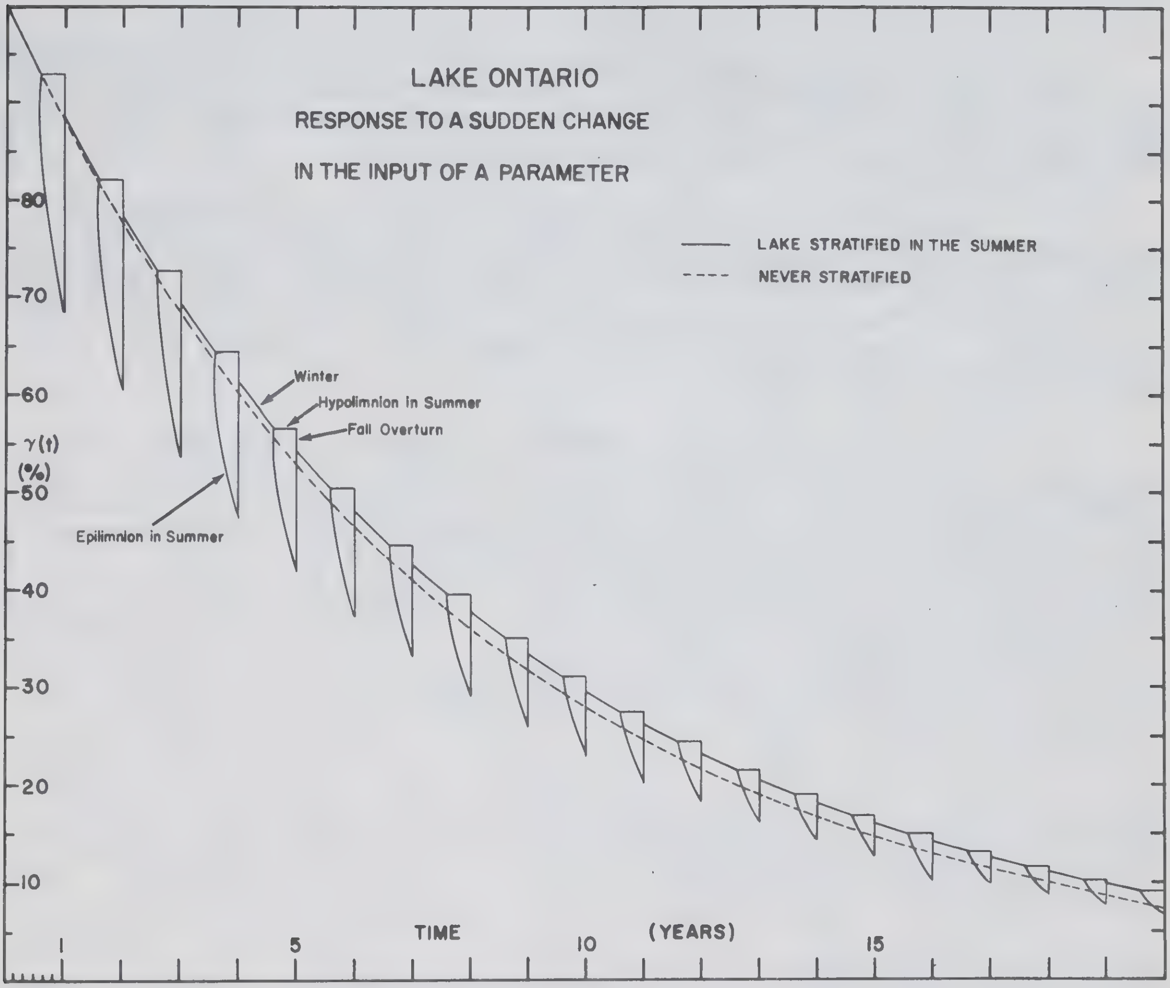

Fig. 66 Response of the concentration of a parameter P to a stepwise change in the rate of input of that parameter into the lake. The function γ (t) gives the percentage change relative to the total change in the rate of input.

reduction factor after a non-stratified season can likewise be calculated (equation c), and is 0.9279, and the yearly reduction factor is 0.9540 x 0.9279 = 0.8852. Substitution of this in equation d shows that $\gamma(t)$ is reduced to 10% after a period of approximately 19 years, which is only slightly higher than the retention time calculated according to Rainey's original assumptions.

This rather surprising result is mainly caused by the fact that the flushing time of the whole lake, 7.8 years, as well as that of the epilimnion, 1.2 years, both are much longer than the duration of the stratified period.

Changes of concentrations in the lake computed according to either method are illustrated in Fig. 66. It may be interesting to note that the curves also can be interpreted as cumulative "age" distributions: of the water mass present at any time, for example, 90% is less than 19 years old, 50% less than 10 years, etc.

In the foregoing it thus has been shown that the presence of vertical stratification during a part of the year hardly affects the retention time of a conservative pollutant. The essential assumptions are the effectiveness of horizontal mixing in the epilimnion during the stratified period, and of both horizontal and vertical mixing throughout the total volume of the lake during the remaining part of the year. Evidence for the first assumption has been presented in the Chapters 3 and 5, where it was shown that water with anomalous concentrations entering the lake from rivers is rapidly dispersed and mixed with surrounding waters. Mixing processes during the winter have not been studied in this report, but the effectiveness of vertical mixing is evidenced by the well documented replenishment of oxygen (for example Dobson, 1968) and the presence of a strong seasonal temperature cycle (Rodgers and Anderson, 1963) at all depths. Vertical mixing may not be equally effective at all times throughout the non-stratified period, but intermittent incidences occur frequently enough to maintain an almost uniform distribution of a parameter throughout the lake, due to the magnitude of the ratio of volume over flow. The relatively brief interruptions of horizontal mixing during the thermal bar periods may cause a slight increase in retention time, but the author feels that a good maximum estimate for the retention time of a conservative parameter is in the order of 25 years.

8. CONCLUSIONS

In the present paper an analysis is presented of a large number of Lake Ontario limnological data, sampled mainly in the summers of 1966 and 1967, and an attempt is made to interpret the data in terms of thermal structure and of circulation and mixing processes. A general description is given of seasonal variations in thermal structure, mainly based on an extensive literature survey, and the processes taking place during late spring, summer, and early fall are described in more detail than has hitherto been possible. Although the paper does not deal with pollution per se, the fate of any conservative substance entering the lake is discussed in terms of dilution, distribution and residence time. The results can be summarized as follows (all conclusions are valid for the stratified season only, unless otherwise specified):

1. From late October or early November until the middle of spring the lake can be considered as a fairly homogeneous body of water which is relatively well mixed over most or all of its volume. From late June until early fall the lake consists of a two layered system with a sharp interface, the thermocline. Within each of these layers the water is relatively well mixed. In spring and fall there are transition periods when the lake is only partially stratified, near the shores in spring and in the middle during fall, the two parts of the lake being separated by an area with strong horizontal gradients, the thermal bar.

2. In the summer any substance entering the lake near or at the surface is mixed almost homogeneously over the total area of the lake and over the total volume of the epilimnion.

3. There is evidence for a fairly consistent net eastward transport of water along the southern shore, but the current is neither strong nor confined enough to carry a significant part of the admixtures, originating on the southern and eastern shores, directly towards the St. Lawrence River. Chemical distribution patterns in the epilimnion indicate that any water with anomalous concentrations of any parameter is rapidly dispersed and mixed with surrounding surface waters.

4. Circulation patterns in the lake are strongly dependent on the winds: currents respond within 6 to 24 hours to changes in the wind field. The lake-wide distribution of water masses, however, responds much more slowly. Locally the thermal distribution may respond

in 36 to 48 hours, but a lake-wide redistribution of water masses, such as would be required for a reversal of the tilt of the thermocline, takes 5 to 7 days, and does not occur during the 1966 and 1967 field seasons.

5. The thermocline starts to develop in May but does not extend over the whole of the lake until late June. Throughout the summer it remains at a mean depth of 12 to 20 metres, and in late September, early October the rate of descent of the thermocline increases again with the onset of fall cooling.

6. The thermocline is usually much deeper in the eastern end of the lake than in the western end. The mean slope is 5.6 cm/km, the lowest observed slope on any cruise in July, August or September is 2 cm/km. Surface temperatures show a similar east-west gradient, being on the average about 6C° higher near Oswego than in the vicinity of Toronto. This is mainly caused by the predominance of eastward winds.

7. The actual depth of the thermocline at any one location is also subject to seiche and internal wave action. Dominant periods in the spectrum of nearshore water intake temperatures, which reflect variations in the depth of the thermocline, are a band around the inertial period of 17.4 hours and, to a lesser extent, periods in the order of 5 to 8 days which may be correlated with similar variations in the wind field.

8. The areal distribution of heat content per cm^2 surface area indicates that internal advection remains an important factor in the redistribution of heat, not only during dissipation of the thermal bar but throughout most of the summer. In July of both years the centre of cold water shifts from the centre of the eastern half of the lake towards the northwestern shores. The eastward currents in the epilimnion, corresponding to this redistribution of heat, reach a maximum mean velocity over the cross-sectional area of the epilimnion of 3 cm/sec over a 14-day period in July of both years. In August and early September these advective currents are smaller and more variable, but later in September of both years a similar, although somewhat smaller, transport takes place in the opposite direction.

9. The lake-mean vertical temperature gradient in the summer averages 2C°/m over a depth interval of 3 to 4 metres, the maximum may be as high as 3 to 4C°/m over a depth interval of 2 to 3 metres.

10. Upwelling is a regular feature in the lake, and can occur anywhere near the shores under offshore wind conditions. It occurs most frequently, however, in the vicinity of Toronto and elsewhere along the northwestern shores. Water velocities during a period of strong upwelling may be as high as 5 cm/sec in an offshore direction and 7 x 10^{-3} cm/sec in a vertical direction towards the surface.

11. The vertical coefficient of eddy diffusivity, K_z, has been calculated with reference to a coordinate system fixed in space as well as with reference to a coordinate system fixed relative to the thermocline. The latter technique, recently developed by the author, gives lower but more accurate estimates of K_z in the thermocline region. The summer-mean vertical coefficient of eddy diffusivity in the thermocline region, 0.12 cm^2/sec, is almost two orders of magnitude smaller than that in the epilimnion (7 cm^2/sec) and about 4 orders of magnitude smaller than the horizontal diffusivity coefficient in the epilimnion (2000 cm^2/sec). Diffusive transport down into the hypolimnion of any substance dissolved in the epilimnion thus is very small throughout the summer, and the thermocline acts as a "diffusion floor".

12. Geostrophic calculations are not useful as a tool to calculate the numerical strength of currents from dynamic height gradients. The technique does, however, give an indication of general current patterns. The slope of the thermocline in a hypothetical two-layer system, in which the geostrophic current is balanced by a wind-drift current, is, for the prevailing wind conditions, equal to the slope actually observed near the western shore of the lake.

13. The residence time of a conservative parameter, that is a parameter not participating in cyclic or other chemical or biological processes, is hardly influenced by the summer stratification. A 90 percent adaption of its lake-mean concentration to a sudden change in the rate of input is reached after a period of about 19 years.

14. The spacial distribution of various chemical parameters, such as specific conductance, oxygen and pH, is related to the thermal structure of the lake. For most parameters the mean hypolimnion values are significantly different from the mean epilimnion values.

15. The mean oxygen content is higher in the hypolimnion than in the epilimnion at any time during the summer, but the percentage saturation is highest close to the

surface, decreasing from 130 to 100 percent in the epilimnion and from 100 to 95 percent (96 to 91 percent in 1967) in the hypolimnion between late June and late September. Oxygen values tend to be somewhat lower in samples taken close to the bottom, but values below 70 percent have only been found in Prince Edward Bay, where a minimum of 41 percent was observed in late August 1966. In areas with strong upwelling, the surface-oxygen concentration rises to a maximum, and the percentage saturation occasionally reaches as high as 150 or 160 percent, indicating vigorous photosynthetic activity. Areas with strong horizontal temperature gradients usually also show horizontal gradients in both the absolute oxygen content and in the percentage saturation, both tending to be lower at higher temperatures. A subsurface minimum in the oxygen content has been observed only in late August, early September of both years.

16. The pH decreases from a mean of about 8.6 near the surface to 8.1 in the hypolimnion. Surface values reach a maximum of 8.7 in early summer, indicating vigorous algal growth, and decrease gradually to about 8.5 in September. A secondary peak in pH (and in oxygen) in late August gives some indication for a secondary upswing in plankton growth at this time.

17. The spacial distribution of specific conductance is very closely related to the thermal structure. The conductance decreases from an average of 322 μ mhos/cm in the hypolimnion (adjusted to a reference temperature of 25°C) to 313 μ mhos/cm in the epilimnion. In areas of strong upwelling the surface values are close to the hypolimnion value, decreasing gradually to 313 μ mhos/cm as the water warms up.

18. The conductivity of lake water is mainly a function of total alkalinity, hardness and chloride. Relative differences between the epilimnion and the hypolimnion values of the first two are of the same order of magnitude as those for conductance, being about 4 percent. The mean hypolimnion values for hardness and total alkalinity are 133 mg $CaCO_3$/l and 88 mg $CaCO_3$/l respectively.

19. The chloride data are not as accurate as the observations of total alkalinity or hardness, but the data seem to indicate a significant difference between the mean epilimnion and hypolimnion values of 2 percent. The sign of this difference, however, does not correspond with that of specific conductance,

epilimnion values being higher rather than lower than the hypolimnion values. The difference is too large to be explained by simple chloride-budget considerations.

20. The outflows of some rivers are clearly reflected by local anomalies in the concentrations of various parameters, but the areal extent of these anomalies is usually small and variable. A good example is a tongue of high conductance water often extending from the mouth of the Genesee River into the lake. The shape and distribution of these anomalies confirm that the lake is essentially well mixed, and that there is no evidence of a confined eastward transport along the southern shore of water carrying with it a good percentage of all admixtures entering the lake from that side.

21. The Niagara River is the only river that influences the thermal structure of the lake to a considerable extent. The course of the isotherms and other iso-lines suggests that its water, although rapidly loosing identity, moves as a diffuse current eastward along the southern shore.

22. A comparison of data from the two years with each other, and with the results of previous studies, indicates that the above findings are probably representative for most summers. This view is supported by a study of the wind data.

9. ACKNOWLEDGEMENTS

The author is indebted to all individuals involved in the sampling and the analysis of the data. These include employees of the Great Lakes and Water Quality Divisions of the Inland Waters Branch, DEMR; the Hydrographic Service, Central Region, and the Canadian Oceanographic Data Centre of the Marine Sciences Branch, Department of Energy, Mines and Resources, and the Public Health Engineering Division, Department of National Health and Welfare. The author is especially grateful for the stimulating discussions on chemical problems, encountered in the study of the data, with Mr. R.C.T. Orr and Mr. H.H. Dobson, and for discussions on physical problems with Mr. P.F. Hamblin. The technique used to derive the vertical coefficient of eddy diffusion has been formulated with help of Dr. D.B. Rao; for his assistance not only with this section, but also in the development of some of the other mathematical tools used in this report, the author is especially grateful.

The study of the vast volume of data was greatly facilitated by the programming and computer processing assistance by Mr. H.R. Steeves and some of his staff, notably Mr. R.T. Moore, and Mr. J.D. Taylor. The author is also indebted to the Data Processing Group of the Great Lakes Division, first headed by Mr. R. Chevier and later by Mr. W. Nagel, for the manual analysis of certain parts of the data; to Mr. J.D. Bradford and Mr. H.A.C. Jones, for their assistance in editing this report and preparing the drawings, and to Mr. B. Kelly and Mr. G.W. Gough for the drafting of the illustrations.

Last but not least the author wants to express his gratitude to the Marine Sciences Branch for allowing him to continue working on this report after his transfer from the Inland Waters Branch in July 1966.

10. BIBLIOGRAPHY

AMERICAN PUBLIC HEALTH ASSOCIATION. 1965. Standard methods for the examination of water and wastewater, 12th. ed. Am. Public Health Assoc., New York. 769 p.

AMERICAN SOCIETY FOR TESTING AND MATERIALS. 1966. Book of ASTM Standards, Part 23. Industrial water; atmospheric analysis. Am. Soc. For Testing and Materials, Philadelphia; 882 p.

ANDERSON, D.V. 1961. A note on the morphology of the basins of the Great Lakes. J. Fish. Res. Bd. Canada 18(2); pp 273-277.

ANDERSON, D.V., J.P. BRUCE, U. SPORNS and G.K. RODGERS. 1961. Winter research on Lake Ontario. U. of Michigan, Great Lakes Res. Div.; Pub. 7; pp 185-198.

ARLEY, N. and K.R. BUCH. 1950. Introduction to the theory of probability and statistics. John Wiley, New York. 238 p.

AYERS, J.C. 1956. A dynamic height method for the determination of currents in deep lakes. Limnol. and Oceanogr. 1(3); pp 150-161.

BELLAIRE, F.R., and J.C. AYERS. 1967. Current patterns and lake slope. In Proceedings, 10th Conference on Great Lakes Research; Int. Assoc. for Great Lakes Res., Ann Arbor; pp 251-263.

CHAWLA, V.K. and W.J. TRAVERSY. 1968. Methods of analyses on Great Lakes waters. Presented at 11th Conf. on Great Lakes Res.; Milwaukee, Wisc.; 18-20 April.

CSANADY, G.T. 1964. Turbulence and diffusion in the Great Lakes. U. of Michigan. Great Lakes Res. Div., Pub. 10; pp 59-69.

CSANADY, G.T. 1967. Large-scale motion in the Great Lakes. J. Geophys. Res. 72(16); pp 4151-4162.

DEPARTMENT OF ENERGY, MINES & RESOURCES, Canada; Water Resources Papers, St. Lawrence and southern Hudson Bay drainage. Inland Waters Branch. Before 1964 published by Department of Northern Affairs.

DEPARTMENT OF TRANSPORT, Canada; Lakes Investigation Unit. Surface water temperature by ART survey, Lake Ontario. Unpublished chart series.

DEPARTMENT OF TRANSPORT, Canada; Meteorological Branch. 1966. Wind frequency tables for Vancouver, Toronto and Montreal. Pub. CDS 8-66.

DEPARTMENT OF TRANSPORT, Canada; Meteorological Branch. 1967. Annual meteorological summary for Toronto International Airport, Ontario, 1966.

DEPARTMENT OF TRANSPORT, Canada; Meteological Branch. 1968. Annual meteorological summary for Toronto International Airport, Ontario, 1967.

DOBSON, H.H. 1968. Principal ions and dissolved oxygen in Lake Ontario. In Proceedings, 10th Conference on Great Lakes Research. Int. Assoc. for Great Lakes Res., Ann Arbor; pp 337-356.

GOODMAN, N.R. 1957. On the joint estimation of the spectra, co-spectrum and quadrature spectrum of a two-dimensional stationary Gaussian Process. Scientific Paper 10; Engineering Statistics Lab., New York, N.Y.

HAMBLIN, P.F. and G.K. RODGERS. 1967. The currents in the Toronto region of Lake Ontario, U. of Toronto, Great Lakes Inst. Pub. PR 29; 133 p.

HUTCHINSON, G.E. 1957. A treatise on limnology. Vol. I, John Wiley and Sons, New York. 1015 p.

INTERNATIONAL JOINT COMMISSION, Working Committee on Methodology. 1966. A digest of analytical methods employed by laboratories associated with International Joint Commission research on the Great Lakes. 120 p.

KRAMER, J.R. 1964. Theoretical model for the chemical composition of fresh water with application to the Great Lakes. U. of Michigan. Great Lakes Res. Div., Pub. 11, pp 147-160.

MILLAR, F.G. 1952. Surface temperatures of the Great Lakes. J. Fish. Res. Bd. Can. 9(7), pp 329-376.

MORTIMER, C.H. 1963. Frontiers in physical limnology with particular reference to long waves in rotating basins. U. of Michigan. Great Lakes Res. Div., Pub. 10; pp 9-42.

MORTIMER, C.H. 1968. Internal waves and associated currents observed in Lake Michigan during the summer of 1963. U. of Wisconsin - Milwaukee, Center for Great Lakes Studies; Sp. Rep. 1; 111 p.

MUNK, W.H., F.E. SNODGRASS and M.J. TUCKER. 1959. Spectra of low frequency ocean waves. Bull Scripps Inst. of Oceanogr., U. of California, 7(4); pp 283-362.

NOBLE, V.E. 1967. Evidences of geostrophically defined circulation in Lake Michigan. In Proceedings, 10th Conference on Great Lakes Research. Int. Assoc. for Great Lakes Res., Ann Arbor; pp 289-298.

ONTARIO WATER RESOURCES COMMISSION. 1967. Water Quality Data 1964-65, Vol. I. Ont. Water Resources Comm. Toronto. 287 p.

PANOFSKY, H.A. and S.W. BRIAR. 1965. Some applications of statistics to meteorology. Penn. State Univ. Press. U.S.A.

PROUDMAN, J. 1953. Dynamical oceanography. Methuen & Co., London. 409 p.

RAGOTZKIE, R.A. 1966. The Keweenaw current, a regular feature of summer circulation of Lake Superior, U. of Wisconsin. Techn. Rep. 29; 29 p.

RAINEY, R.H. 1967. Natural displacement of pollution from the Great Lakes. Science 155(3767); pp 1242-1243.

RICHARDS, T.L. 1964. Recent developments in the field of Great Lakes evaporation. Verhandlungen, Intern. Verein. Limnologie, Stuttgart, 15; pp 247-256.

RICHARDS, T.L. and G.K. RODGERS. 1964. An investigation of the extremes of annual and monthly evaporation from Lake Ontario. U. of Mich; Great Lakes Res. Div.; Publ. 11; pp 283-293.

RICHARDS, T.L., H. DRAGERT and D.R. McINTYRE. 1966. Influence of atmospheric stability and over-water fetch on winds over the lower Great Lakes. Monthly Weather Rev. 94(7); pp 448-453.

RODGERS, G.K. and D.V. ANDERSON. 1961. A preliminary study of the energy budget of Lake Ontario. J. Fish. Bd. Canada 18(4); pp 617-636.

RODGERS, G.K. 1962. Temperature adjustment of conductance measurements in waters of the Great Lakes. Great Lakes Inst., U. of Toronto, Interim Rept.

RODGERS, G.K. and D.V. ANDERSON. 1963. The thermal structure of Lake Ontario. U. of Michigan, Great Lakes Res. Div; Pub. 10; pp 59-69.

RODGERS, G.K. 1966-I. The thermal bar in Lake Ontario, spring 1965 and winter 1965-66. U. of Michigan, Great Lakes Res. Div.; Pub. 15; pp 369-374.

RODGERS, G.K. 1966-II. A note on thermocline development and the thermal bar in Lake Ontario. I.A.S.H. symposium in Garda; Pub. 70; pp 401-405.

RONDY, D.R. 1967. Great Lakes ice cover, winter 1966-67. U.S. Lake Survey; Basic Data Report 5-3; 60 p.

SCOTT, J.T. and L. LANSING. 1967. Gradient circulation in eastern Lake Ontario. In Proceedings, 10th Conference on Great Lakes Research. Int. Assoc. for Great Lakes Res. Ann Arbor. pp 322-336.

SMITH, R.L., J.G. PATTULLO and R.K. LANE. 1966. An investigation of the early stages of upwelling along the Oregon coast, J. of Geophys. Res. 71(4); pp 1135-1140.

STRICKLAND, J.D.H. and T.R. PARSONS. 1965. A manual of sea-water analysis. Fish. Res. Bd., Canada; Bull. No. 125 2nd ed.; 203 p.

SWEERS, H.E. 1969. Two methods of describing the "average" vertical temperature distribution of a lake. J. Fish. Res. Bd. Canada; 25(9); pp 1911-1922.

TABATA, S., N.E.J. BOSTON and F.M. BOYCE. 1965. The relation between wind speed and summer isothermal surface layer of water at Ocean Station P in the eastern subarctic Pacific Ocean. J. Geophys. Res. 70(16); pp 3867-3878.

THOMAS, J.F.J. and J.J. LYNCH. 1960. Determination of carbonate alkalinity in natural waters. J. AWWA; vol. 52; pp 259-268.

THOMAS, M.K. 1957. Changes in the climate of Ontario. Pub. in: Changes in the fauna of Ontario; edited by F.A. Urquhart; U. of Toronto Press; pp 56-75.

TULLY, J.P. and L.F. GIOVANDO. 1963. Seasonal temperature structure in the eastern subarctic Pacific Ocean. Marine Distributions; ed. by M.J. Dunbar; Roy. Soc. Can. Spec. Pub. 5; U. of Toronto Press; pp 10-36.

U.S. DEPARTMENT OF THE INTERIOR. Water Resources data series. U.S. Geol. Surv., Washington.

U.S. DEPARTMENT OF THE INTERIOR. 1967. A report on chemical biological, and physical findings in Lake Ontario; (Manuscript Report). Fed. Water Poll. Control Admin., Rochester.

U.S. DEPARTMENT OF THE INTERIOR. 1967-a. Report Lake Erie Enforcement Conference Technical Committee. Federal Water Pollution Control Administration, Chicago, U.S.A.

VAN NOSTRAND, D. 1960. The international dictionary of applied mathematics. D. Van Nostrand, Toronto. Ed.: W.F. Freiberger.

VERBER, J.L. 1966. Inertial currents in the Great Lakes. U. of Michigan, Great Lakes Res. Div.; Pub. 15; pp 375-379.

WILSHAW, R.E. and D.R. RONDY. 1965. Great Lakes ice cover, winter 1964-65. U.S. Lake Survey; Research Rep. 5-1; 79 p.

APPENDIX A

ACCURACY OF THE DATA

This appendix may be longer than strictly necessary, but the author feels that a more complete outline of the reasoning behind the selection of data to be discussed or omitted in this report may be useful for future reference. In the first four subsections the types of errors affecting the data, and their consequences, are defined in general terms, and the statistics used are formulated. In the last two subsections this is applied to a discussion of the reliability of the present data.

A.1 Definitions and Statistics

The best method to determine the reliability of measurements is by "letting the errors occur", that is, by interspersing a sufficient number of duplicate and known samples with the material sent down to the laboratory for analysis. The laboratory personnel should not be able to recognize these samples as test samples, and they should be handled in exactly the same manner as the actual lake-water samples. A program of this nature, however, has not been carried out on a regular basis during the 1966 and 1967 field seasons, and variations in the cruise to cruise reliability of the measurements thus have not been monitored. Large fluctuations in the variability of data sampled on different cruises, however, did occur, and the author thus had to develop a method, based on the internal and mutual consistency of the measurements, to estimate their reliability.

Internal consistency of the data can be defined as the degree of compatibility with certain basic hypotheses of the observations of one and the same parameter, sampled on one cruise at different depths or at the same level on subsequent cruises, and mutual consistency as the degree of compatibility between measurements of different, often interrelated, parameters.

A.1.1. Definitions

The data discussed in this report are subject to various types of errors, which can be classified into four groups: random, quasi-random, systematic and gross errors. These can be defined as follows:

Let a series of samples be taken from a homogeneous medium. The result of any measurements x_i can be regarded as being composed of two terms:

$x_i = \mu + \nu_i$

where μ , usually called the "true" value, is a numerical constant common to all members of the series x_i, and v_i, the random error, is an unpredictable deviation from μ for any particular measurement (Van Nostrand, 1960). The unpredictability of v_i is an essential aspect of the randomness of an error. This, of course, should not be confused with the fact that the probability of occurrence of certain values of x_i often can be predicted. The distribution of the errors may, depending on the type of experiment and the parameter measured, be Gaussian, binomial or otherwise. In the following sections it will be assumed, however, that the distribution is Gaussian, unless otherwise noted.

If, on the other hand, the actual value of v_i can be predicted from errors in the measurements immediately preceding x_i, the error is not purely random. It will be called a "quasi-random" error:

$$x_i = \mu + fct(v_{i-1}, v_{i-2}, \ldots..)$$

The quasi-random error thus affects groups of consecutive measurements rather than individual determinations, and the degree of dependence of the error in two determinations is lower, the longer the time interval between them. This type of error is usually not distinguished in the theory of errors, but its usefulness in a study of the reliability of the present data will become obvious.

For the third type of error, the systematic error, the value of v_i can be predicted from the "true" value μ :

$$x_i = \mu + fct(\mu)$$

The systematic error is related to the quasi-random error in the sense that, if v_i can be predicted from μ , it can also be predicted from v_{i-1}, v_{i-2}, etc., although the reverse generally will not be true.

The gross error is caused by unpredictable, occasionally occurring, mistakes by the human factor involved in conducting the experiment, and in the reading and recording of the results. It will normally affect a small percentage of the data only.

In chemical terminology, the reliability of a measurement if often indicated by its accuracy and precision. These can be defined in terms of the errors discussed above.

Precision denotes the reproducibility of the determinations; it is a measure of the combined effects of the random and quasi-random errors. The precision thus is only a meaningful

statistic if it has been determined under the same conditions as those under which the data were sampled. (The reproducibility of a series of measurements may be much lower under actual field conditions than under carefully controlled, idealized laboratory conditions). Under the assumption that the distribution of errors is approximately Gaussian, the precision can be defined as twice the standard deviation, which corresponds to the 95% confidence limits.

Accuracy is a measure of the systematic error, and of that part of the quasi-random error which shows variations over a period much longer than the duration of a cruise. It is not always possible to separate the "long term" quasi-random effects from the systematic errors.

A.1.2 Classification of Errors

In an actual set of data several or all of the four types of errors defined above may occur, and they can originate in the sampling, analysing and data-processing stages of handling the data. Some of the major sources of error in each of the four groups are summarized below; a few are listed more than once if they contribute significantly to more than one class of error:

Class A. Random errors in:

1. sample coordinates
   a. position
   b. time
   c. depth

2. sample collection
   a. insufficient flushing of sample bottle
   b. presence of particulate matter (the occasional trapping of large zooplankton organisms, for example, may affect the results of the analyses unless the samples are filtered immediately)

3. sample handling
   a. improper rinsing of containers
   b. improper preservation or storage of samples (these factors can also lead to quasi-random or systematic errors)

4. sample analysis (the magnitude of this error depends on the analytical procedure, the equipment used and on the initial concentration of the parameter).

Class B. Quasi-random errors, caused by:

1. use of inaccurate or non-stable standards for calibration.

2. insufficient rinsing of equipment between samples; this may especially affect automated and semi-automated analyses, for example, due to:
   a. gradual changes in the sensitivity of an electrode due to deposits on its surface
   b. variations in the transparency of containers used for colorimetric methods due to deposits

3. variations in temperature and humidity of the laboratory may affect the performance of the equipment or reaction rates.

4. changes in the sensitivity of electronic sensors, due to variations in voltage and/or frequency of the power supply, may become serious sources of error on board of a ship if its power supply is insufficiently stabilized[1].

5. variations in the time lapse between the moment of sampling and the beginning of the analysis, which may:
   a. affect the concentration of a parameter due to chemical or physical processes
   b. cause the samples to be analyzed at different temperatures, if the time interval is too short to allow them to reach equilibrium with the temperature in the laboratory

Class C. Systematic errors due to:

1. insufficient calibration of the analytical method or equipment.

2. undetected influences of admixtures in the sample on the analytical results.

Class D. Gross errors, due to mistakes in:

1. labelling of samples.

2. entering the results on the basic data sheets.

3. copying the data onto the data summary sheets.

4. keypunching or other data processing stages.

---

[1] Estimated ranges of fluctuation on board the Brandal in 1966 are plus or minus 10 to 15 Hertz and plus or minus 20 Volts.

A.1.3 Reduction and Consequences of Various Classes of Errors

Purely random errors are largely unavoidable, although their magnitude can be reduced to a certain extent by choosing the most suitable analytical procedure, by duplicating sampling and/or analyses procedures whenever possible, and by placing more emphasis on the quality of data than on their quantity. Purely random errors will increase the spread of the observations, thus reducing both the reliability of the individual observations and, if the number of samples is fixed, that of their mean.

Gross errors can largely be avoided by measures similar to those that can reduce the purely random error. Under actual field conditions, and particularly in bad weather, however, it may be very hard to completely avoid making gross errors, but proper quality control during subsequent data processing stages can be helpful in spotting and eliminating most, or all, of the more serious gross errors slipping into the data during the sampling and analysis stages.

The quasi-random error, by definition, differs from the purely random error in that it affects groups of consecutive measurements rather than individual determinations. As a result, the error in one measurement depends partially on the error in the preceding measurement, the degree of dependence being lower, the longer the time interval between the determinations. The quasi-random error thus may influence both the standard deviation and the mean of groups of observations; the latter influence may become especially serious for small groups of data. For a very large population of data on the other hand, or for a series of data sampled at long time intervals, its effect on the mean, and on a histogram of the observations, is often similar to that of a purely random error. Under certain conditions, however, the two types of errors can be distinguished by statistical techniques that will be outlined below. Another, very serious, effect of the quasi-random error is that it may give rise to fictitious horizontal or vertical gradients on plots of the data (Fig. A.1).

The importance of random, quasi-random and gross errors in a series of data can sometimes be established by a study of the internal consistency of the observations, as will be shown in the following subsections. The possible presence of systematic errors, on the other hand, can be found only by comparing the results obtained by different authors, by using different analytical techniques, or by mixing especially prepared solutions in varying ratio's with the samples (ASTM, 1965). A discussion of this type of error will not be attempted, since it would carry beyond the scope of the present report, requiring a thorough study of the analytical procedures from a chemical point of view.

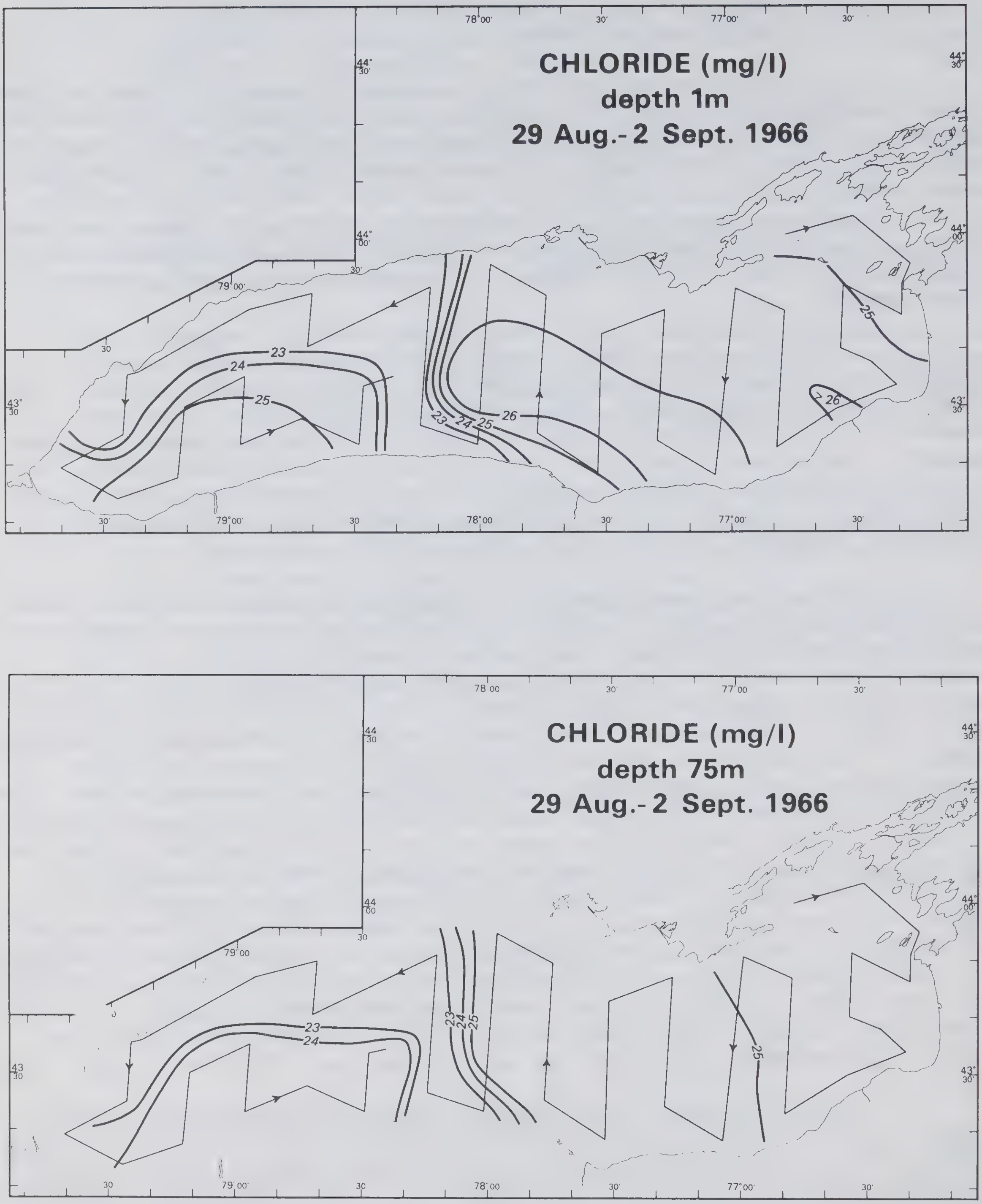

Fig. A1 Fictitious horizontal distributions of chloride at the 1 and 50 metre levels, suggested by data sampled on a cruise in late August 1966.

The borderline between quasi-random errors and systematic errors is sometimes difficult to pinpoint, as was mentioned before. Analysis of the data of one cruise, for example, may indicate that there are no important quasi-random errors, whereas a comparison of the mean values for subsequent cruises may strongly suggest an inconsistency in the calibrations. Some examples of this type of a "long-term" quasi-random error will be given.

In summary then, it can be concluded that of the four types of errors discussed above only one, the purely random error, is inherent to the data, although even this error can be reduced to a certain extent by indealizing the sampling and analytical procedures. Gross errors can largely be avoided, but, if present, can usually be detected while the data are processed, and the observations concerned can be rejected. Quasi-random errors, which may affect a large percentage of the data, can seldom be corrected for, due to the difficulty in establishing their time dependence. In principle, however, they can be avoided by a proper quality control of the analyses. Systematic errors are of importance mainly in the intercalibration of methods, or in a study involving data collected by various authors and/or techniques. Theoretically, the data can be corrected for systematic errors if they can be defined.

A.1.4 Statistical Calculations

Let x_i and y_i $(i=1,2,\ldots,N)$ be two series of measurements with means M_x and M_y, and with standard deviations SD_x and SD_y. It can be tested whether or not these two series can be considered as subsamples from the same population by using Student's t-test (for the means) and Snedecor's F-test (for the standard deviations).

The following statistics then have to be calculated:

$$M_x = \frac{1}{N}\sum_i x_i \qquad M_y = \frac{1}{N}\sum_i y_i \tag{A.a}$$

$$SD_x = \sqrt{\frac{\sum (x_i - M_x)^2}{N}} \qquad SD_y = \sqrt{\frac{\sum (y_i - M_y)^2}{N}} \tag{A.b}$$

$$t = \sqrt{\frac{N}{2}} \cdot \frac{M_x - M_y}{SD_{x,y}} = \sqrt{N} \cdot \frac{M_x - M_y}{SD_x^2 + SD_y^2} \tag{A.c}$$

$$F = \frac{SD_x^2}{SD_y^2} \tag{A.d}$$

where $SD_{x,y}$, the best estimate of the standard deviation of the parent population, is defined in equation f given below.

Tables for t and F are given in most textbooks on statistics (for example; Arley and Buch, 1950); the tables for F have to be entered with the reciprocal of F if its calculated value is less than one. If, for example, N=24 (50), the 95 percent confidence limits for x_i and y_i to have been sampled from the same population are t = 2.1 (2.0) and F = 2.0 (1.7) respectively.

Let it now be assumed that the series x_i and y_i, i = 1,2,....,N, have been sampled from one and the same population in the following sequence: $x_1, y_1, x_2, y_2, \ldots, x_N, y_N$. In this case the means and standard deviations of the two series will be similar, and a best estimate of the overall mean, $M_{x,y}$, and standard deviation $SD_{x,y}$, can be calculated:

$$M_{x,y} = \frac{M_x + M_y}{2} \qquad (A.e)$$

$$SD_{x,y} = \sqrt{\frac{SD_x^2 + SD_y^2}{2}} \qquad (A.f)$$

From the two series, x_i and y_i, a third series can be derived by taking the differences between pairs of samples x_i and y_i for each value of i:

$$z_i = x_i - y_i \quad (i = 1, \ldots\ldots, N)$$

The mean M_z and standard deviation SD_z are related to the means and standard deviations of the parent series (Arley and Buch, 1950):

$$M_z = M_x - M_y \simeq 0 \qquad (A.g)$$

$$SD_z = \sqrt{SD_x^2 + SD_y^2} \simeq SD_x . \sqrt{2} \simeq SD_{x,y} . \sqrt{2} \quad (A.h)$$

for sufficiently large N, which means that, in a statistical sense, M_z is equal to zero, and SD_z to $SD_x\sqrt{2}$, within the chosen confidence limits.

Essential in the derivation of the equations g and h is that the series x_i and y_i originate from the same parent population, and that the measurements are subject to Gaussian random errors only. If, on the other hand, the errors were to be of a quasi-random nature, the equations would not be valid. In that case the errors in subsequent values x_i and y_i would no longer be independent, and it can be expected that the standard deviation SD_z of the series z_i becomes smaller in relation to $SD_{x,y}$ than predicted by equation h. The mean M_z, however, would still be equal to zero within the chosen confidence limits. Combining the equations h and d, the statistical significance of the difference between SD_z and SD_x can be tested:

$$F = 2 \frac{SD_x^2}{SD_z^2}$$

It will be assumed that quasi-random errors are present if F exceeds the 95% confidence limits.

In an actual set of lake data, variations between the measurements are, of course, not only due to errors, but also to naturally occurring geographical or temporal effects. In the second part of this appendix it will be assumed that the internal consistency of the data is not affected by systematic errors, that the data have been corrected for gross errors, and that observations taken on the same cruise can be considered as synoptic. Fluctuations within the set of data collected during a cruise then are caused by three factors: random and/or quasi-random errors and natural geographical effects (depth and location). An effort will now be made to estimate the relative importance of the two types of errors and to compare their magnitude with the range of naturally occurring variations.

A.2 Application to the Present Data

A.2.1 Mutual and Internal Consistency

In the summer the lake is divided into a two-layered system by a sharp interface, the thermocline. Any water entering the lake from the rivers and sewage outflows will be mixed with the upper layer. Due to the density difference between the two layers and the stability of the thermocline, very little, if any, of the dissolved admixtures will be transported down into the hypolimnion. For this reason it is to be expected that horizontal gradients in the concentration of many parameters will be much smaller in the hypolimnion than in the epilimnion.

The horizontal gradients of pH and specific conductance at a depth of 50 or 75 metres are usually largely, if not completely, masked by random variations in the measurements, whether these be due to random errors or to naturally occurring random fluctuations in their concentrations. At the surface, on the other hand, geographically determined gradients are more prominent and do not disappear in a background of random fluctuations. On some cruises, however, the data appear to indicate large horizontal gradients in the deeper water. These gradients are, in the author's opinion, fallacious for the following reasons:

1. The data are not internally consistent. In every instance where a large horizontal gradient in the hypolimnion concentration of these parameters is observed, a similar, equally large gradient appears in the surface data, as is, for example, illustrated in Fig. A.1. (The reverse is not true; surface gradients are not always coupled to gradients in the hypolimnion). This is suspicious, especially since the arising patterns seem to be closer related to the actual track made by the ship than to the geography of the lake, and do not recur on other cruises in similar locations. A possible explanation lies in the fact that the data have been analyzed in the sequence in which they were sampled. A gradual or sudden, change in the sensitivity of the analytical equipment, or in its calibration, thus will show up as an apparent horizontal gradient in both deep and shallow data. The resulting apparent horizontal distribution patterns consequently will seem to be related to the ships track.

2. The observations of different parameters are not mutually consistent. Theoretically there is a definite numerical relationship between specific conductance and the concentrations of the major ionic species in the water (Appendix B). Near the surface the horizontal distributions of conductance, on the one hand, and of total alkalinity, hardness and chloride, on the other hand, are usually closely related (Chapter 5). In the hypolimnion, however, the horizontal gradients that appear occasionally in the distributions of any of these parameters are never related to similar gradients in distributions of the others.

These two points are obvious from a study of the horizontal distribution patterns, but they can also be demonstrated in a different manner. In Fig. A.2 the pH, total alkalinity, conductance, chloride and hardness observations made at the 1 and 50 metre levels in a mid-summer cruise in 1966 are shown as time series. Observations at the 10 and 75 metre

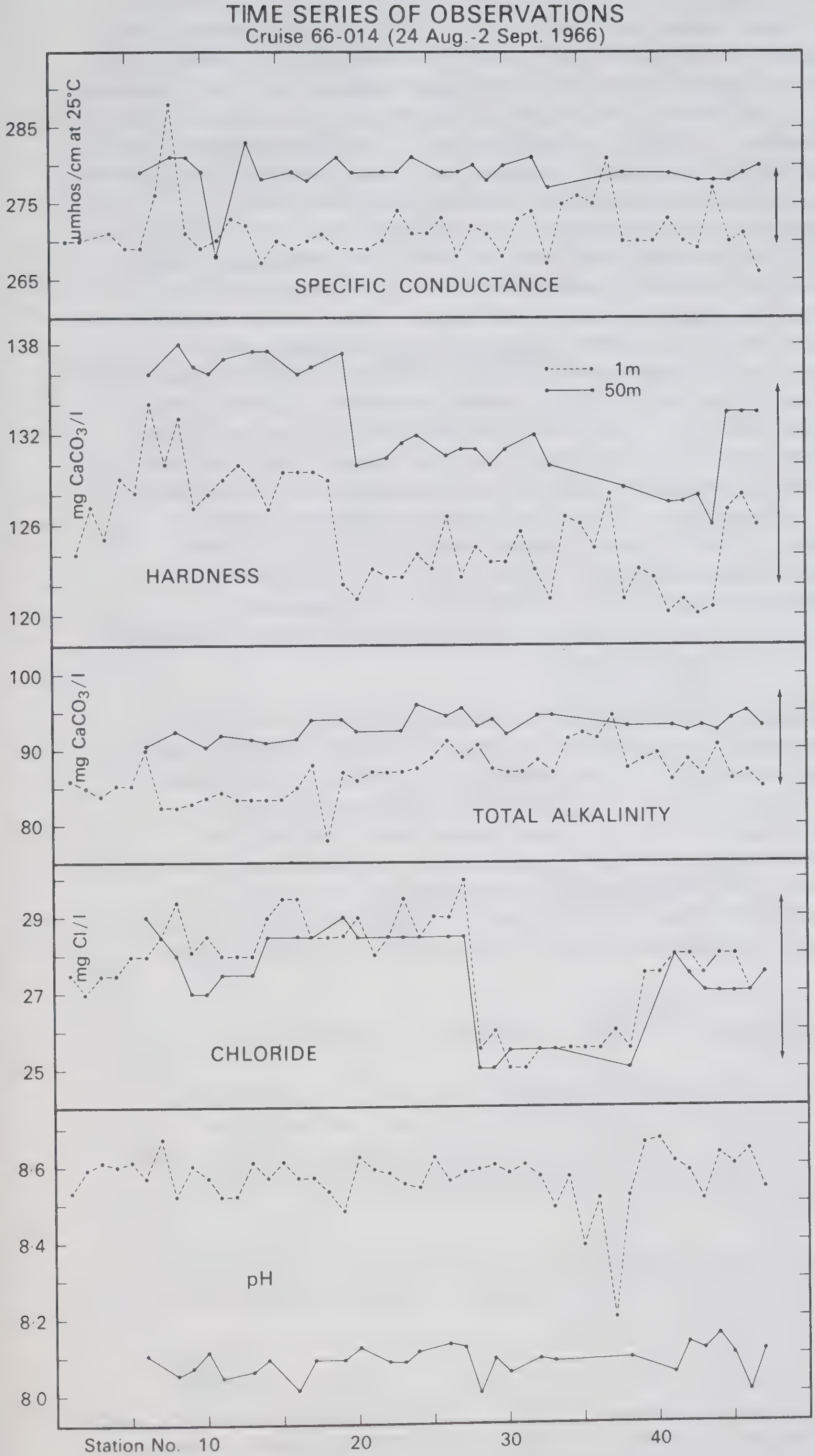

Fig. A2

A comparison of the time series of measurements of different parameters sampled during a monitor cruise in late August 1966. Subsequent points along the horizontal axis denote samples taken at consecutive stations. The arrows on the right hand side indicate the magnitude of a change in the concentration of the respective parameters that would cause a variation of 10 µmhos/cm in the conductance, provided that the concentration of all other parameters remains constant.

levels are essentially similar to those at the 1 and 50 metre levels respectively. The data are entered in the sequence in which they were analyzed; all points along a vertical refer to the same station. It is seen that the conductance and pH traces show no trends or major discontinuities for groups of stations while the cruise proceeds. Total alkalinity, on the other hand, shows a small trend towards higher values as the cruise proceeds, while hardness and chloride both show quite erratic and unrelated jumps downwards and upwards in the middle of the cruise. In Appendix B the numerical relation between specific conductance and the three latter parameters is discussed in detail. At present, it is sufficient to note that the trend in total alkalinity, as well as the jumps in hardness and chloride, are so large that they definitely should correspond to simultaneous measurable changes in the conductance, provided that they are real. The arrows on the righthand side of Fig. A.2 show the changes in total alkalinity, hardness and chloride that would correspond to a change of 10 μmhos/cm in specific conductance. Similar anomalies for the data sampled during a cruise in late August, 1967, are shown in Fig. A.3. The observed phenomena could perhaps be explained by large fluctuations in the concentrations of some of the minor constituents in the water, but this is speculative and, in the opinion of the author, highly unlikely.

In some instances the quasi-random error is large enough to completely mask the natural geographical distribution patterns in the epilimnion, as, for example, in the hardness distributions shown in Fig. A.1. In 1966 this occurred regularly for the total alkalinity, hardness and chloride distributions, and these consequently are not presented in the present report. In 1967 this happened occasionally for the specific conductance and pH distributions. (The areal distribution of the first three parameters has not been studied for 1967).

A.2.2 Statistical Study of the Internal Consistency

The occurrence of quasi-random errors in the data can also be studied by means of the statistical technique outlined earlier. For this purpose the following assumptions concerning the horizontal and vertical distributions of a parameter P will be made:

1. The epilimnion and the hypolimnion can be considered as two distinct water masses with not necessarily equal concentrations of P.

2. Vertical gradients are small within each of these two layers, but may be larger in the thermocline region. (The validity of this assumption for most parameters discussed in this report is illustrated in the Chapters 3 and 5).

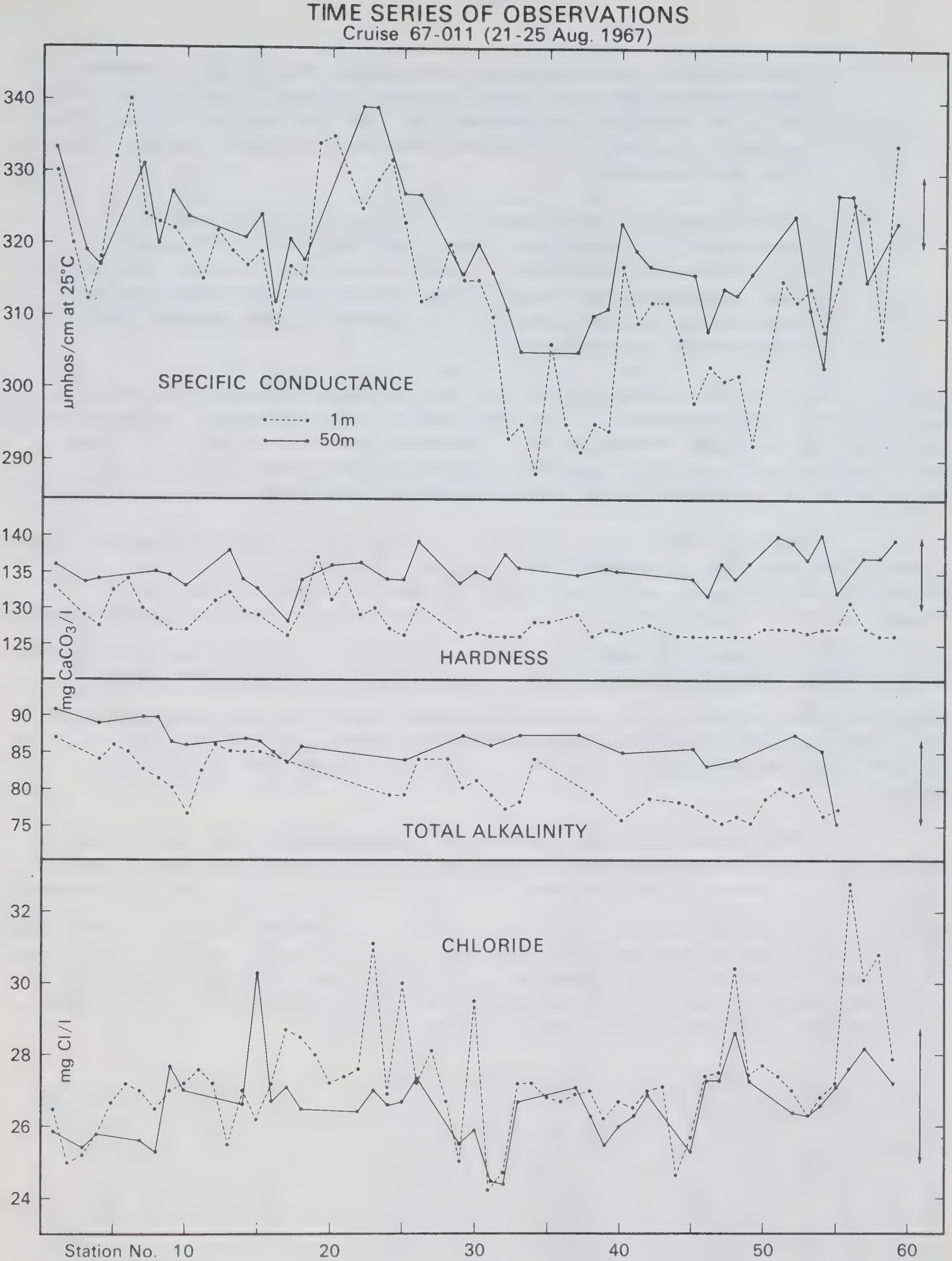

Fig. A3. A comparison of the time series of measurements of different paramenters sampled during a monitor cruise in late August 1967. Subsequent points along the horizontal axis denote samples taken at consecutive stations. The arrows on the right hand side indicate the magnitude of a change in the concentration of the respective parameters that would cause a variation of 10 μmhos/cm in the conductance, provided that the concentration of all other parameters remains constant.

3. Horizontal gradients in the epilimnion are larger than those in the hypolimnion, since the latter is not, or hardly, affected by the inflow of rivers and is much larger in volume (about 4 times larger than the epilimnion).

4. Distribution patterns in the two layers are not necessarily parallel, nor do they have to show horizontal gradients of the same magnitude, although the patterns may show some relation to each other. The reasons are similar to those cited under the preceding assumption.

These assumptions obviously will not hold for all parameters, and may not hold within a few metres of the bottom. Temperature, however, is a good example of a parameter for which all four assumptions are valid, but for oxygen, and especially for nutrients, the second and third assumptions may not be correct.

Values for the statistic F for various parameters have been computed for a number of cruises (Table A.1). The standard deviations of the 1 and 75 metre level data are compared with each other (F^{1}_{75}), and with that of the difference population formed by subtracting for each station the 50 and 75 metre level observations, (F^{1}_{50-75} and F^{75}_{50-75} respectively). Underscored values of F indicate that there is no significant difference (95% confidence limits) between the standard deviations concerned. Table A.1 illustrates the following points:

The standard deviation of temperature at the 1 metre level is in all cases much larger than that in the hypolimnion, resulting in very high values of F^{1}_{75} and F^{1}_{50-75}. The difference between the standard deviations of the 75 metre observations and of the difference population is not significant, which indicates that there are no quasi-random errors or natural geographical effects large enough to dominate the purely random errors and the natural random variations in the medium.

The specific conductance observations show an essentially different situation. For the first cruise (66-14) all three F values indicate significant differences in the standard deviations. The standard deviation at the 1 metre level, however, is still significantly larger than that at the 75 metre level, and it can be concluded that quasi-random errors, or natural geographical effects in the hypolimnion, are smaller than the geographical effects at the surface. For the two 1967 cruises the situation is different. The standard deviation of the surface samples is of the same order of magnitude as that of the hypolimnion samples, while the standard deviation of the difference population is considerably smaller, as is shown by F^{75}_{50-75}. This could hypothetically be explained by assuming that

cruise no.	median date	parameter	SD_1	SD_{10}	SD_{50}	SD_{75}	SD_{50-75}	F^1_{75}	F^1_{50-75}	F^{75}_{50-75}
66-14	31/8/66	temp.	.75	3.17	.33	.17	.29	20.	13.4	$\underline{1.6}$
		sp. cond.	4.0	3.7	2.3	1.2	1.1	3.8	8.9	2.3
		hard.	4.0	3.3	3.6	3.1	1.0	$\underline{1.6}$	32.	18.
		t. alk.	1.8	2.3	1.1	1.3	0.5	$\underline{2.0}$	24.	12.
		pH	0.040	0.171	0.037	0.054	0.051	$\underline{1.8}$	$\underline{1.2}$	2.2
		Cl	1.7	1.3	1.3	1.3	.4	$\underline{1.1}$	29.	26.
67-11	23/8/67	temp.	1.07	5.71	.22	.14	.16	60.	80.	$\underline{1.5}$
		sp. cond.	10.4	11.9	8.2	9.5	7.5	1.2	3.9	3.3
		pH	.177	.155	.123	.114	.080	2.5	10.	4.8
		Cl	1.3	1.0	1.1	1.2	1.2	$\underline{1.1}$	2.4	$\underline{2.0}$
67-15	18/9/67	temp.	.56	2.47	.52	.08	.13	50.	37.	$\underline{1.4}$
		sp. cond.	4.6	6.0	5.0	4.5	2.4	$\underline{1.0}$	7.4	7.5
		pH	.117	.183	.090	.074	.041	2.4	16.	13.
		Cl	0.72	0.62	0.67	0.69	0.26	$\underline{1.1}$	15.	14.

Table A1 Standard deviations of the observations of a number of parameters for three cruises at the depths of 1, 10, 50 and 75 metres. In the eighth column the standard deviation of the differences between the 50 and 75-metre level observations for each station is given, and in the last three columns the significance of the differences between the standard deviations at various levels is tested with the F test. Underscored values indicate that the standard deviations for the two populations concerned do not differ significantly.

the surface and 75 metre level distributions show similar natural patterns and gradients of the same magnitude. This, however, is extremely unlikely in view of the isolation of the hypolimnion from the influence of tributaries by the thermocline, and also because of the large ratio of hypolimnion to epilimnion volume. A much more likely explanation is the presence of quasi-random errors in the data.

For chloride, the situation is similar to that of specific conductance. In this case the data for the cruises 66-17 and 67-15 reveal large internal inconsistencies caused by quasi-random errors, whereas the data for cruise 67-11 indicate a much smaller quasi-random error, which may be of roughly the same order of magnitude as effects due to geographically determined gradients.

On cruise 66-14 enough hardness and total alkalinity data were collected for a statistical analysis, and these also indicate the presence of large quasi-random errors. In 1967 these parameters have been sampled at fewer depths, and not enough data are available for a complete analysis of their internal consistency.

The F values for pH have been included in the table, since the method proved to be useful in some instances to eliminate cruises with bad pH data. The results are not as obvious as for the parameters discussed above, but they seem to indicate that quasi-random errors may have been an important factor for the 1967 cruises. A closer comparison of the horizontal distributions of pH in the epilimnion with those in the hypolimnion confirms that pH values are less reliable in 1967 than in 1966, and the distributions for most 1967 cruises have, for that reason, not been presented in Appendix F.

The standard deviation of the different parameters for the 1, 10, 50, and 75 metre levels, and for the difference population of the 50 minus the 75 metre level samples of each station, have, for comparison, also been given in Table A.1. Differences between the standard deviations at the 1 and 10 metre levels are related to the mean depth of the thermocline, relative to these levels, and to thermocline tilt. These factors are discussed in more detail in the Chapters 3 and 5. Differences between the standard deviations at the 50 and 75 metre levels reflect the fact that the water tends to become more homogeneous with increasing depth below the thermocline. Interesting to note is the inconsistency of the variability calculated for each of the parameters on the different cruises. The standard deviation of conductance at the 50 and 75 metre levels, for example, is five times as high for cruise 67-11, for which the data are considered to be subject to serious quasi-random errors, than for cruise 66-14. Similar differences occur for pH and chloride, and they usually reflect variations in the accuracy with which data have been collected, although

changes in natural variability may, in the upper layers of the lake, also occasionally play a role. The standard deviation of temperature in the hypolimnion is fairly constant, indicating a consistent accuracy of the measurements throughout the two field seasons.

The "F technique" thus has proven to be a useful tool to aid the detection of a special type of error, defined as quasi-random error, in the measurements of some parameters. It may not be as useful, however, for such parameters as oxygen and nutrients, which are strongly affected by biochemical processes, and no attempt has been made to apply the F technique to these parameters. The rejection of many of the specific conductance, pH, hardness, total alkalinity and chloride data, sampled in 1966 and 1967 but not shown in this report, is based on a statistical analysis of their internal consistency with the "F technique". (Rejection for the present study, of course, does not imply that the data could not give valuable information for other types of studies).

ion	conductance factor per mg/l (ASTM, 1965)	concentration in mg/l (Dobson, 1968)	calculated conductance (µmhos/cm at 25°C)	% of total calc. conductance
Ca^{++}	2.60	42.9	111.4	32.2
Mg^{++}	3.82	6.4	24.4	7.1
Na^{+}	2.13	12.2	26.0	7.5
K^{+}	1.84	1.44	2.7	0.8
HCO_3^{-}	0.715	115.	82.2	23.8
SO_4^{--}	1.54	27.1	41.7	12.1
Cl^{-}	2.14	26.7	57.1	16.5
total calculated conductance			345.5	100.0
measured conductance			315	91.5

Table B1 Relative conductance of some of the major ions in Lake Ontario water, and a comparison of computed and measured conductances.

APPENDIX B

SPECIFIC CONDUCTANCE AS A FUNCTION OF IONIC CONCENTRATIONS

Specific conductance is a function of ionic concentrations in the water, and it can be calculated if the composition of a sample is known:

$$C = \sum \rho_i A_i \qquad (B.a)$$

where C is the specific conductance in μmhos/cm at 25°C, ρ_i the conductance factor and A_i the concentration in mg/l of the ionic species i. Using the conductance factors given in "Standard Methods" (APHA, 1965), this can be written as:

$$C = 2.60 \times [Ca] + 3.82 \times [Mg] + 2.13 \times [Na] + 1.84 \times [K] +$$

$$+ 2.14 \times [Cl] + 0.715 \times [HCO_3] + 1.54 \times [SO_4] + \ldots . \qquad (B.b)$$

where the symbols between square brackets stand for the concentrations of calcium, magnesium, sodium, potassium, chloride, bicarbonate and sulfate respectively, and the dots for any other ions that may be present in the water.

In Lake Ontario the conductance is for more than 99% determined by the concentration of seven ions: calcium (32%), magnesium (7%), sodium (7 1/2%), potassium (1%), bicarbonate (24%), sulfate (12%) and chloride (16 1/2%) (Table B.1). These percentages have been calculated, using equation b, from the results of a comprehensive analysis of 14 mid-lake samples (Dobson, 1968). It must be noted, however, that equation b, when applied to these samples, yields a conductance of 341 μmhos/cm (at 25°C), which is 8.2% above the measured conductance. This discrepancy cannot be accounted for by a lack of precision of the measurements, which is 1.2%[1]. The cause for the difference between measured and observed conductance values is not clear, but it could perhaps be due to the fact that unfiltered samples were used for the analyses. All samples are left undisturbed for some time before subsamples for the actual analyses are carefully decanted, without stirring up the sediment. Small suspended particles thus may have been present in the subsamples, and ions attached thereon could have been released during the chemical analysis. Some ions may also

---

[1] Calculated from standard deviation estimates given in Chawla and Traversy (1968), which are representative also for these analyses (personal communication by Traversy).

have been attached to organic molecules or in colloids. In all these cases the ions concerned cannot, or only partially, contribute to the conductivity of a sample, but they may be liberated during the analysis of the individual ionic species, and equation b therefore may predict somewhat too high a value for the conductance.

Calcium and magnesium have been measured as hardness on all monitor stations; their absolute concentrations have only been measured occasionally. Using a ratio of 6.8:1 (Dobson, 1968) of their relative concentrations, however, their contributions to the conductance can be estimated from the hardness determinations:

$$68 \text{ mg Ca/l} \equiv \frac{100}{40} \times 68 \text{ mg } CaCO_3/l = 170 \text{ mg } CaCO_3/l$$

$$10 \text{ mg Mg/l} \equiv \frac{40}{24} \times \frac{100}{40} \text{ mg } CaCO_3/l = 42 \text{ mg } CaCO_3/l$$

$$\text{measurable hardness} = 212 \text{ mg } CaCO_3/l$$

This corresponds to a conductance factor per mg $CaCO_3/l$ hardness of:

$$\mu = \frac{68}{78} \times 2.60 + \frac{10}{78} \times 3.82 = 1.02 \mu\text{mhos/cm (at 25°C)}$$

Similarly, the bicarbonate concentration has not been measured independently, but as total alkalinity. In the normally observed pH range of 7.9 to 8.7, more than 99% of the dissolved carbonates is present in the form of bicarbonate. Its contribution to the conductance can be calculated from the observed total alkalinity using a conductance factor of 0.864 μmhos/cm at 25°C per mg $CaCO_3/l$.

Equation b can now be rewritten in terms of hardness and total alkalinity instead of Ca, Mg and HCO_3:

$$C = 1.02 \times [\text{hard}] + 0.864 \times [\text{t alk}] + 2.14 \times [Cl] +$$
$$+ 2.13 \times [Na] + 1.84 \times [K] + 1.54 \times [SO_4] \qquad (B.c)$$

where the symbols between the square brackets denote the concentrations in mg $CaCO_3/l$ of hardness and total alkalinity, and in mg-ion/l of the other four parameters. The first three terms, hardness, total alkalinity and chloride, are the only parameters that have been measured routinely for all monitor stations; they account for roughly 39, 24 and 16 1/2% of the calculated conductance respectively. Assuming the relative contributions

of the various ions to the conductance to be constant, equation c can now be written in terms of the three routinely measured parameters:

$$C = \frac{100}{79.5} \times \left\{ 1.02 \times [\text{hard}] + 0.864 \times [\text{t alk}] + 2.14 \times [\text{Cl}] \right\} \quad (B.d)$$

Application of equation d to the summer mean concentrations of hardness, total alkalinity and chloride also gives values for the specific conductance that are higher than the actually measured conductance (4.5 and 4% respectively in 1966 and 1967). This discrepancy is probably due to similar causes as suggested above for the 14 comprehensive analyses, and perhaps also partially to not yet detected systematic errors or interactions between the parameters or to possible inaccuracies in the conductance factors used. The agreement, however, is good enough for a study of the correlation between observed distributions of the routinely measured parameters.

APPENDIX C

WIND STRENGTH AND THERMOCLINE DEPTH

The relation between wind strength and thermocline depth has, among others, been studied by Tully and Giovando (1963) and by Tabata, Boston and Boyce (1965). Tully and Giovando show that the depth of the thermocline is mainly determined by wind strength, during the heating season, and by convective mixing, resulting from heat losses at the surface during the cooling season. Their studies are based on data collected in the eastern subarctic Pacific Ocean, especially on those from Ocean Weather Station P, but their conclusions are probably applicable to other large bodies of water in temperate regions as well.

Tabata et al define a mixed layer depth D_L as the depth of a zone with uniform temperature between the surface and the first intermediate thermocline, and they find for the heating season the following relation between D_L and the mean wind strength u during the preceding 12 hours:

$$D_L = 4.1 + 0.129\, u^2 \qquad (C.a)$$

where u is expressed in metres per second and D_L in metres. This relation is also based on a study of Ocean Weather Station P data. Tabata et al also formulate a linear relation between D_L and u, predicting the mixed layer depth with the same accuracy. The standard deviation of the difference between measured and calculated values of D_L is 5.8 in both cases.

The mixed layer depth will usually be shallower than the seasonal thermocline, but during periods of strong winds all intermediate thermoclines descent and may eventually merge with the latter. The mean depth of the seasonal thermocline thus is relatively insensitive to weak and moderate winds, but may change considerably under the influence of prolonged periods of strong winds.

In the present paper the depth of the thermocline has been defined as the depth of the 10°C surface. This is on the average four metres below the top of the thermocline region, which, in turn, corresponds to the bottom of the mixed layer, as defined by Tabata et al, in the absence of intermediate thermoclines. Even with this correction, equation a may not be directly applicable to conditions in Lake Ontario, since the thermocline depth varies considerably with location, and since the lake is of limited dimensions as compared with the ocean. The equation, however, does give an indication of the depth to which wind induced vertical turbulence may be strong enough to

erode the thermocline, and it also shows that the mean thermocline depth is to a large extent determined by the strongest winds, rather than by mean wind strength, during the period between the formation of the seasonal thermocline and the time of observation.

APPENDIX D

VERTICAL EDDY DIFFUSIVITY

The vertical coefficient of eddy diffusivity K_z can be calculated from a knowledge of the vertical gradient and the time derivate of a property with a concentration f . The basic diffusion equation, in the absence of sources and sinks, is:

$$\frac{\partial f}{\partial t} + u\frac{\partial f}{\partial x} + v\frac{\partial f}{\partial y} + w\frac{\partial f}{\partial z} = \tag{D.a}$$

$$= \frac{\partial}{\partial x}\left(K_x\frac{\partial f}{\partial x}\right) + \frac{\partial}{\partial y}\left(K_y\frac{\partial f}{\partial y}\right) + \frac{\partial}{\partial z}\left(K_z\frac{\partial f}{\partial z}\right)$$

where x, y and z are the two horizontal and the vertical axis of a rectangular coordinate system with its origin at the surface; and where u, v and w are the velocity components and K_x, K_y and K_z the diffusivity coefficients in these directions respectively. The vertical axis is measured positive in a downward direction. This equation is valid only for "conservative" parameters, that is, for parameters that are not affected by chemical reactions or other processes that could change their concentrations in the absence of diffusive or advective transport. Consequently, it cannot be used for such parameters as pH, temperature at any level at which a measurable amount of radiation is absorbed, or dissolved oxygen.

The parameter f is carried by water, which for practical purposes can be assumed to be an incompressible fluid:

$$\frac{\partial u}{\partial x} + \frac{\partial u}{\partial y} + \frac{\partial w}{\partial z} = 0 \tag{D.b}$$

Combining (a) and (b), the diffusion equation can be written:

$$\frac{\partial f}{\partial t} + \frac{\partial}{\partial x}(uf) + \frac{\partial}{\partial y}(vf) + \frac{\partial}{\partial z}(wf) = \tag{D.c}$$

$$= \frac{\partial}{\partial x}\left(K_x\frac{\partial f}{\partial x}\right) + \frac{\partial}{\partial y}\left(K_y\frac{\partial f}{\partial y}\right) + \frac{\partial}{\partial z}\left(K_z\frac{\partial f}{\partial z}\right)$$

A mean value K_z of the vertical diffusivity coefficient can be derived from changes in the lake-mean profile of f, $\bar{f}(z)$, assuming that there is no transport through the boundaries of the lake and that $K_z = \hat{K}_z$ is a function of depth only. Integration of (c) over the area A of the lake then gives:

$$\frac{\partial \bar{f}}{\partial t} + \frac{\partial}{\partial z}(\overline{wf}) = \frac{\partial}{\partial z}\left(\hat{K}_z \frac{\partial \bar{f}}{\partial z}\right) \qquad (D.d)$$

where

$$\bar{f} = \frac{1}{A}\int^{A} f\,dx\,dy$$

and

$$\overline{wf} = \frac{1}{A}\int^{A} (wf)\,dx\,dy$$

The second term in equation d is usually neglected, being of higher order than the other terms, and the diffusion equation becomes:

$$\frac{\partial \bar{f}}{\partial t} = \frac{\partial}{\partial z}\left(\hat{K}_z \frac{\partial \bar{f}}{\partial z}\right) \qquad (D.e)$$

In the following the cap over K_z will be omitted.

Application of (e) to the temperature data and integration over depth from a depth z to the bottom z_b, assuming that there is no diffusive transport of heat through the bottom, gives:

$$\int_{z}^{z_b} \frac{\partial \bar{T}(z)}{\partial t}\,dz = \frac{\partial \bar{H}_z}{\partial t} = -K_z \frac{\partial \bar{T}(z)}{\partial z} \qquad (D.f)$$

where $\bar{H}_z$ is the mean heat content below a unit area at depth z and $\bar{T}(z)$ the mean temperature at a depth z. In the transfer from (e) to (f), it has been assumed that the coefficient of eddy diffusivity for a chemical parameter f is approximately equal to the coefficient of eddy conductivity for temperature, and K_z will henceforth in both cases be called the coefficient of eddy diffusivity.

In the derivation of equation (f), it has been assumed that K_z is independent of location for any given depth. This is not strictly true, since K_z is inversely related to the stability $\frac{1}{\rho}\frac{\partial \rho}{\partial z}$, where ρ is the density, and this is maximal at or near the thermocline. The depth of the corresponding minimum of K_z thus depends on the depth of the thermocline, which is a function of location and time. It has furthermore been assumed that the term $\frac{\partial}{\partial z}(\overline{wf})$ can be neglected. This is not strictly true either, since the continuous variations in the tilt of the thermocline cause an apparent advective vertical transport of heat, as is discussed in more detail in Chapter 6 (see also Fig. 25). This suggests that it may be more realistic, at least when spacially averaged data are used, to calculate K_z with reference to a coordinate system fixed with respect to characteristic points of the thermal structure rather than with respect to the surface of the water.

The author developed a technique to calculate the vertical coefficient of eddy diffusivity in the thermocline region, using a coordinate system fixed with respect to the thermocline. The origin of this system moves downward with the downward progression of the "heatwave", and its distance below the surface is given by $z_e(t)$, where $z_e(t)$ is the mean depth of the thermocline at the time t.

The processing of a series of data, defining the spacial temperature distribution in a lake, is done in two distinct steps. First of all, the "mean depth" curve $\overline{Z}(\theta)$ (see Section 2.1.4) is calculated. This curve is then used to define a model temperature distribution in the lake in such a manner, that all isotherms are horizontal and at a depth below the surface given by $\overline{Z}(\theta)$. The two mean profiles $\overline{Z}(\theta)$ and $\overline{T}(z)$ are identical in this model, and $T(z) = \overline{T}(z)$ is independent of x and y. The new coordinate system is now defined with respect to the depth $z_e(t)$ of the 10°C isotherm, and the depth z(t) below the surface of a point z' in this system is given by:

$$z(t) = z' + z_e(t)$$

In this model the diffusion equation d can be written with respect to the moving coordinate system; substitution of the temperature $\overline{T}(z)$ for the function $\overline{f}$ gives:

$$\frac{\partial}{\partial z'}\left(\overline{w'\overline{T}(z')}\right) = \frac{\partial}{\partial z'}\left(K_z' \frac{\partial \overline{T}(z')}{\partial z'}\right) \qquad (D.g)$$

The time dependent term $\frac{\partial \overline{T}(z')}{\partial t}$ on the lefthand side of (d) vanishes by definition for z' = 0, and is small in the vicinity of the thermocline, because the coordinate system travels downward with the 10°C isotherm. Since $T(z) = \overline{T}(z)$ is independent of x and y, equation (g) can be rewritten:

$$\frac{\partial}{\partial z'}\left(\overline{w'}\,\overline{T}(z')\right) = \frac{\partial}{\partial z'}\left(K_z' \frac{\partial \overline{T}(z')}{\partial z'}\right)$$

where $\overline{w}'$ is the mean vertical velocity, which is equal to the rate of downward movement of the thermocline. Integration over depth from z' to the bottom gives:

$$\overline{w'}\left(\overline{T}(z_b') - \overline{T}(z')\right) = -K_z' \frac{\partial \overline{T}(z')}{\partial z'} \qquad (D.h)$$

again assuming that there is no downward eddy diffusion through the bottom. This equation can be used to derive K_z' from the rate of downward movement of the thermocline and the temperature gradient given by $\overline{Z}(\theta)$.

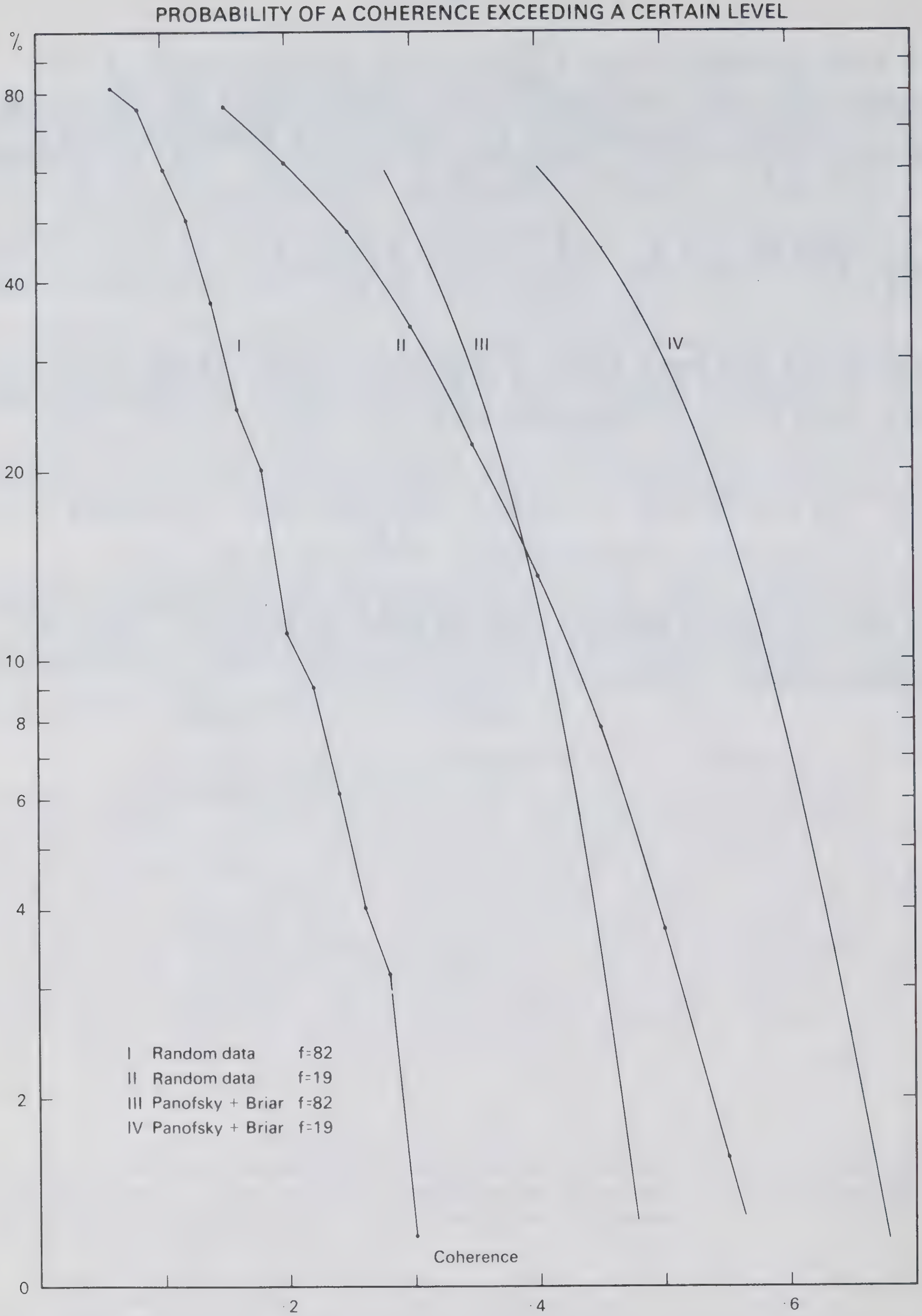

Fig. E1 Comparison of significance limits of the coherence between two random Gaussian series of data with the limits quoted by Panofsky and Briar. Curves I and II are based on Tuckey type power spectrum analyses of 25 pairs of random data series with N = 500, m = 12, f = 82 and N = 500, m = 50, f = 19 respectively.

APPENDIX E

CONFIDENCE LIMITS OF COHERENCE AND PHASE LAG

The 95% confidence limits of coherence can be derived from an equation by Goodman (1957), quoted by Panofsky and Briar (1965), giving the confidence limits β of the coherence squared as a function of the number of degrees of freedom f and the probability level p:

$$\beta = \left[1 - p^{1/(f-1)}\right]^{1/2} \qquad (E.a)$$

where f is a function of the length N of the data series and of the maximum number of lags m used in the analysis:

$$f = 2\frac{N}{m} - \frac{1}{2}$$

This equation, however, does not correspond well with the results of a test analysis of the coherence between two series of Gaussian random data. In Fig. E.1 calculated values of the square root of β for different probability levels are compared with confidence limits determined experimentally by analysing the coherence of 25 pairs of random number series consisting of 500 elements each. It is obvious that equation a underestimates the reliability of the results, and the 95% confidence limits indicated by dashed lines in the illustrations therefore have been based on the latter calculations rather than on this equation.

The confidence limits $\Delta\theta$ of the phase θ are a function of the coherence R_∞ of an infinitely long series of data and of the number of degrees of freedom, and can for large f be calculated using an equation given by Goodman (1957), quoted by Munk et al (1959):

$$\sin^2 \Delta\theta \simeq \frac{1 - R_\infty^2}{R_\infty^2} \cdot \frac{6}{f} \qquad (E.b)$$

In Fig. E.2 this equation is plotted for 19 and 82 degrees of freedom, which corresponds to 50 and 12 lags respectively in a data series of 500.

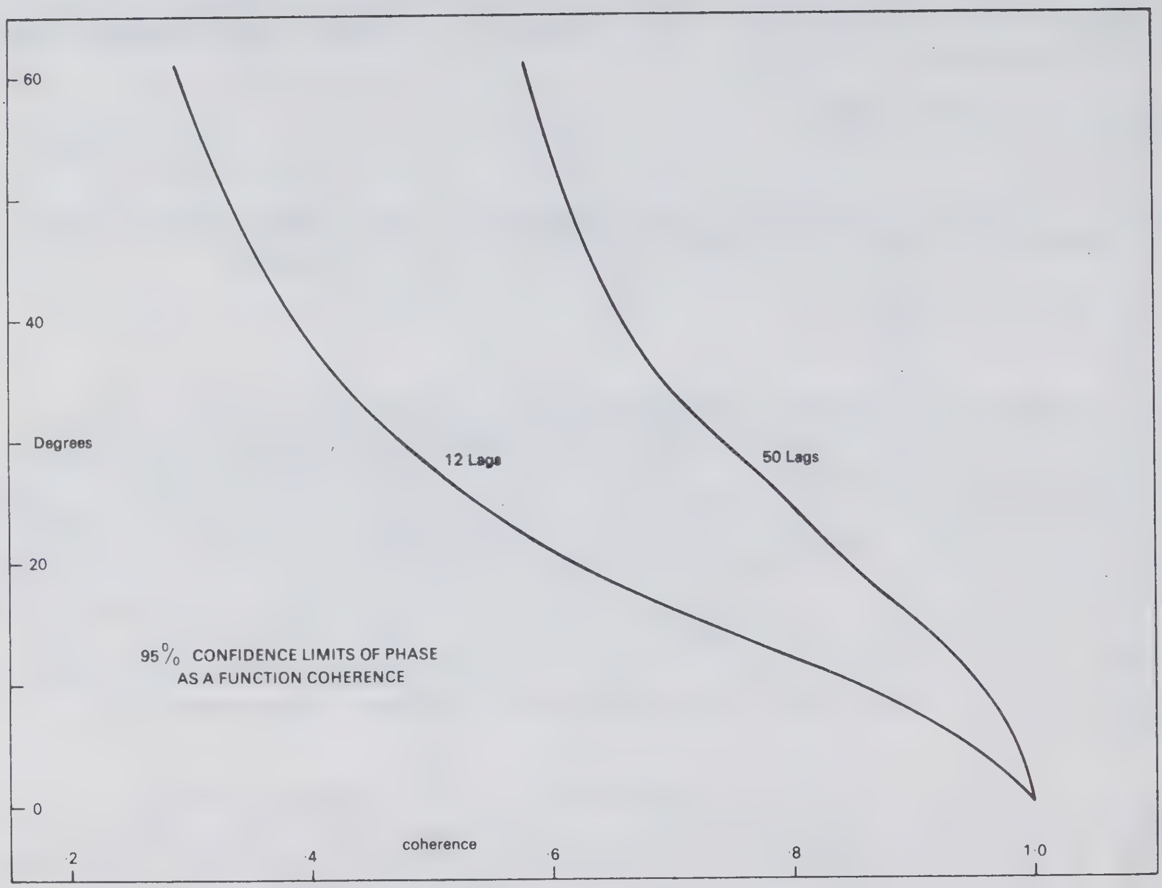

Fig. E2 The 95 percent confidence limits of phase as a function of coherence for 82 and 19 degrees of freedom (12 and 50 lags in a data series of 500 respectively).

APPENDIX F

CRUISE BY CRUISE HORIZONTAL DISTRIBUTION CHARTS

Cruise by cruise charts for thermal structure and the distribution of oxygen, pH and conductance during the field seasons of 1966 and 1967 are presented. All horizontal distributions are for the surface (0.5 or 1.0m). The profiles in the top lefthand corners of most charts are lake-means over all monitor station data for any cruise (solid lines), or means over a group of stations in an upwelling area (dotted lines). The wind tracks, in the top lefthand corners of the thermocline-depth charts, have been constructed from hourly observations at Toronto International Airport by taking daily vector means.

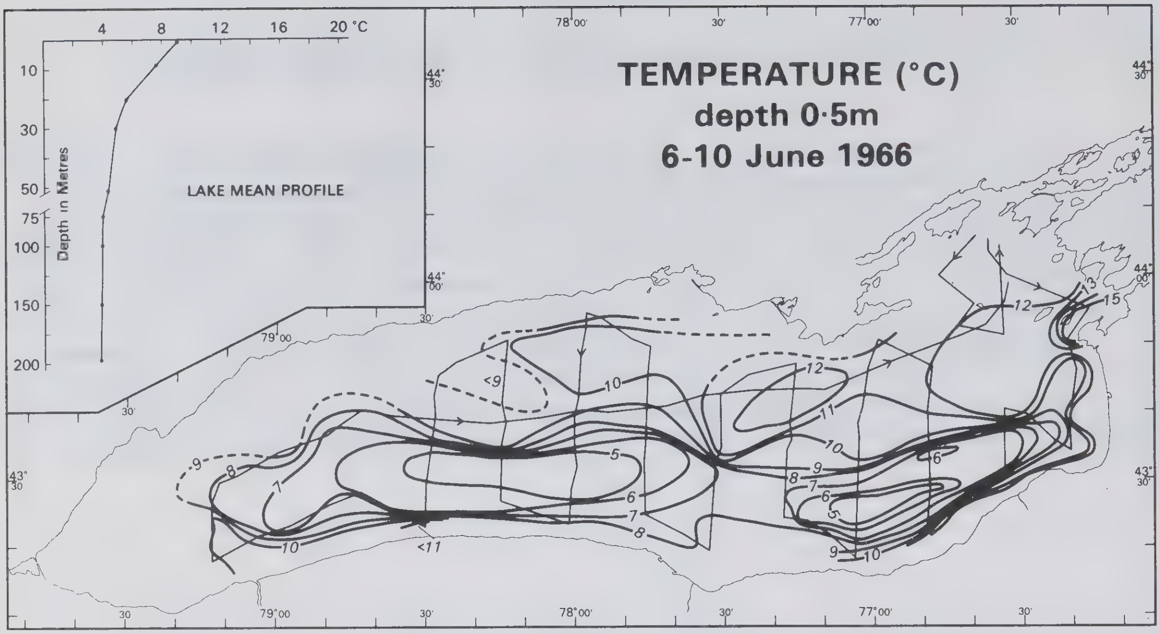

Figure F.1

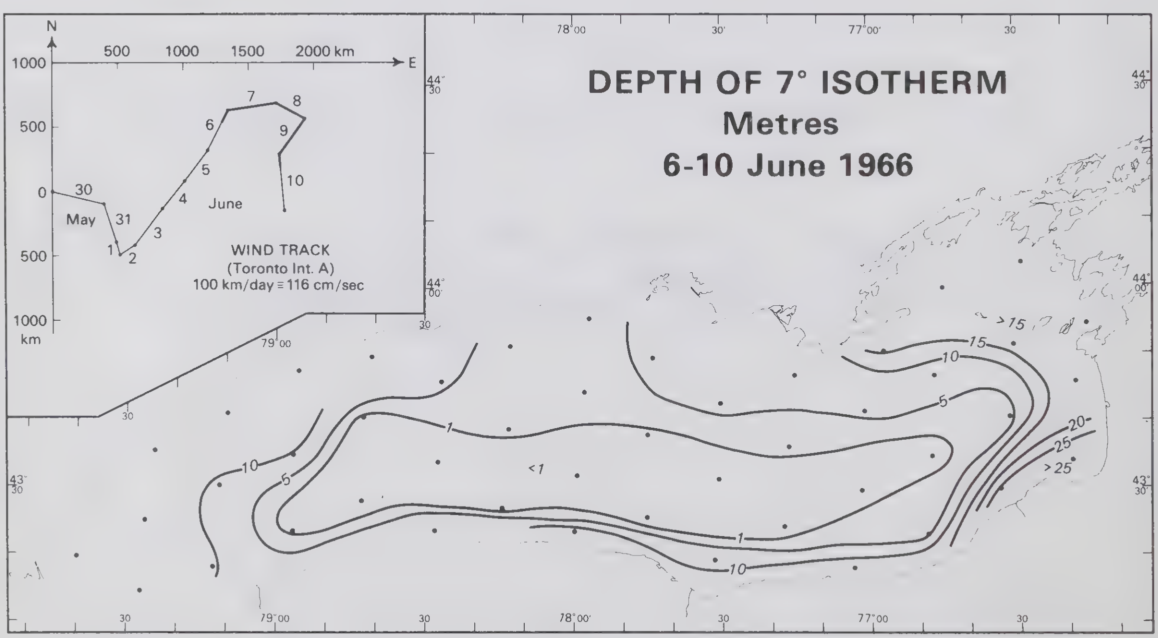

Figure F.2

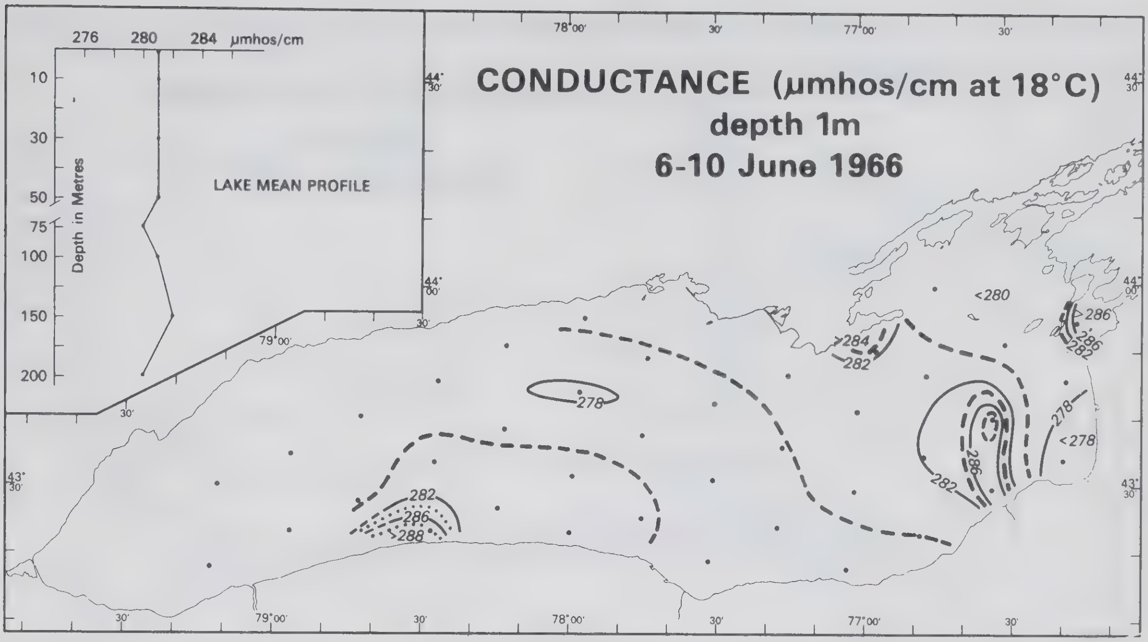

Figure F.3

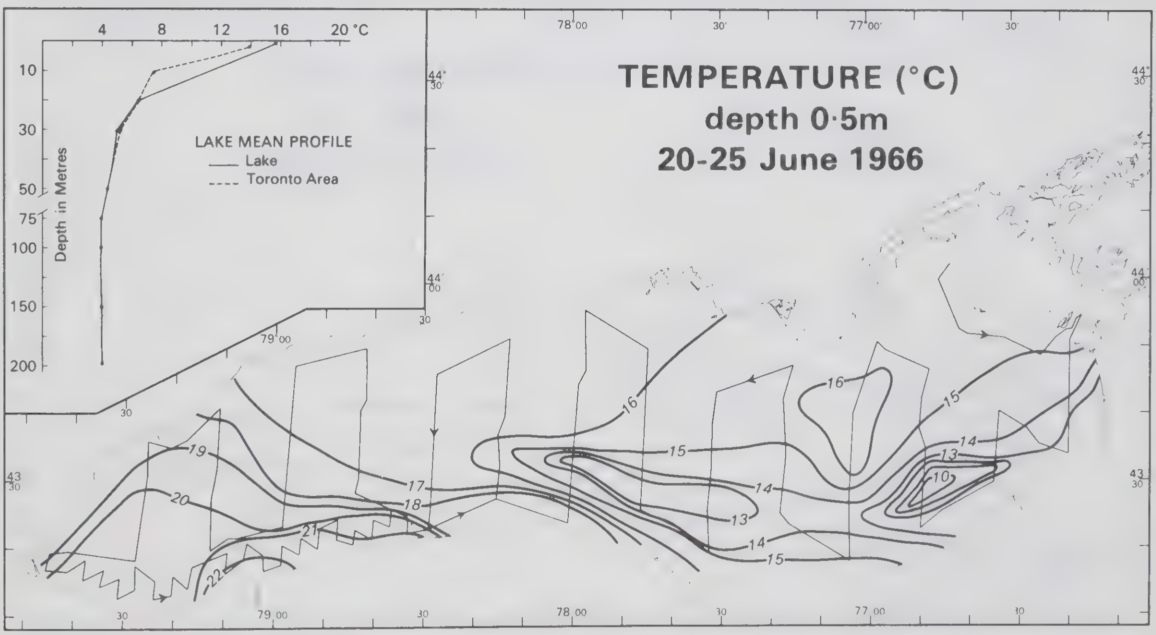

Figure F.4

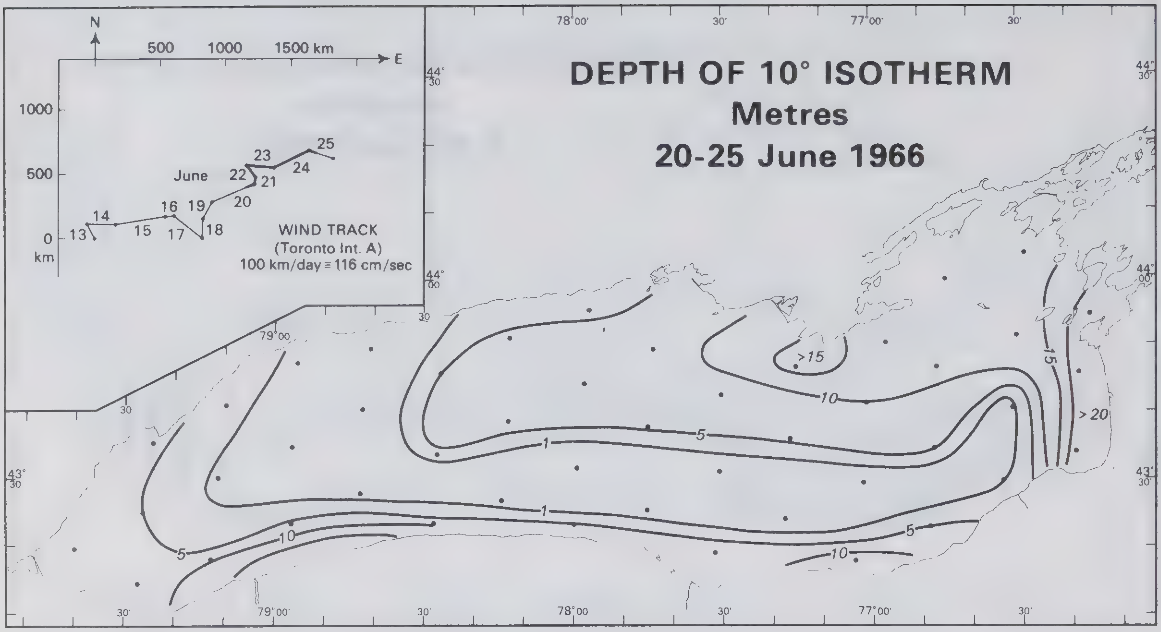

Figure F.5

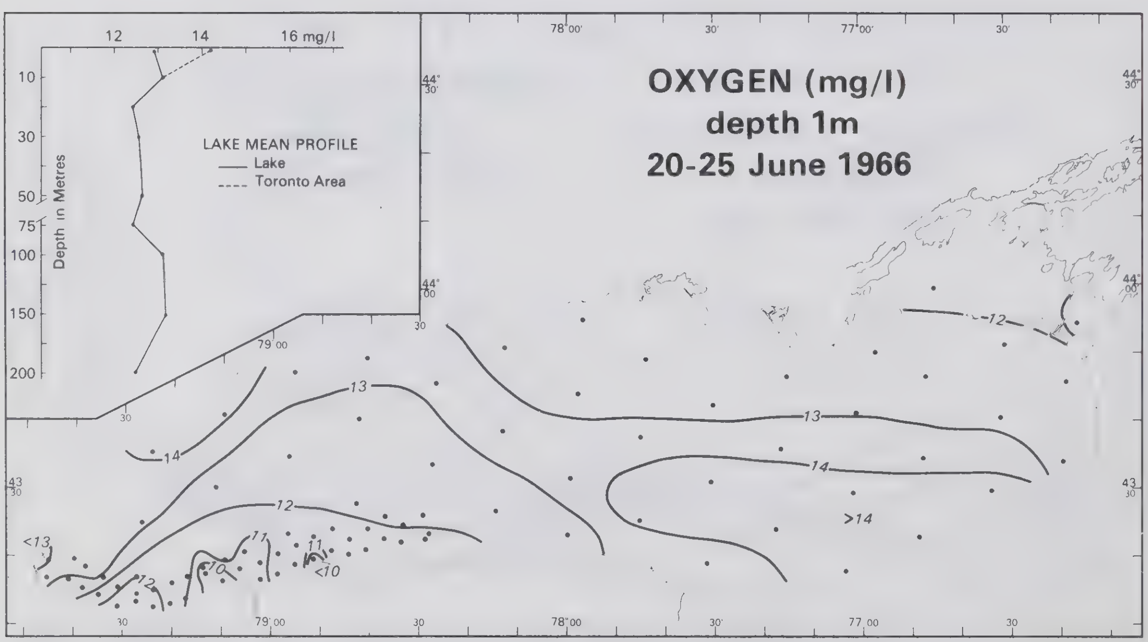

Figure F.6

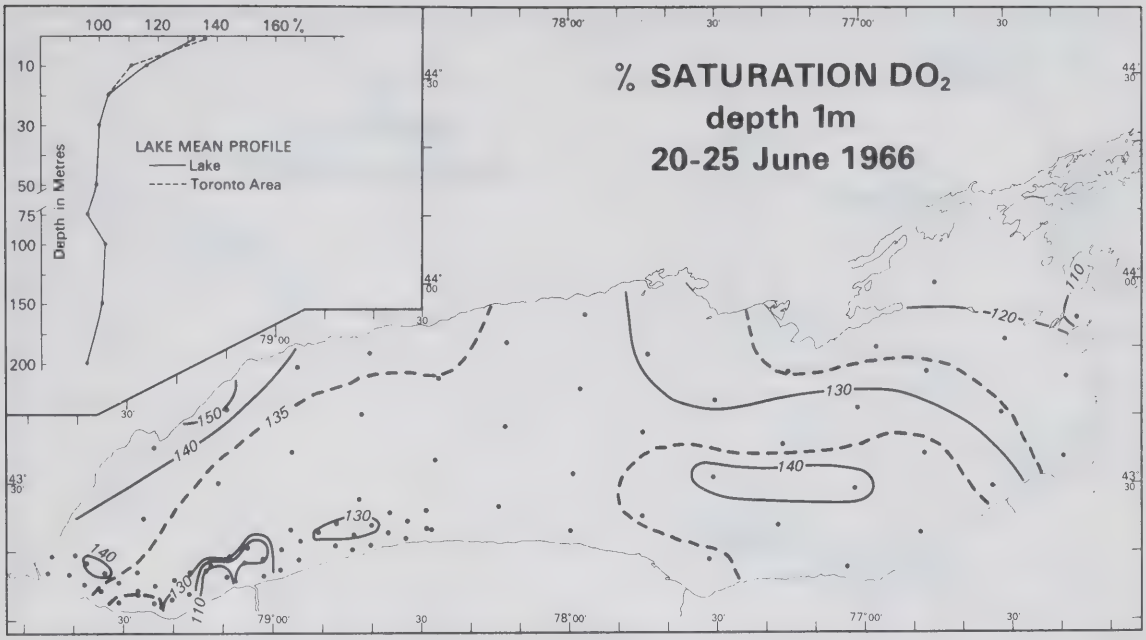

Figure F.7

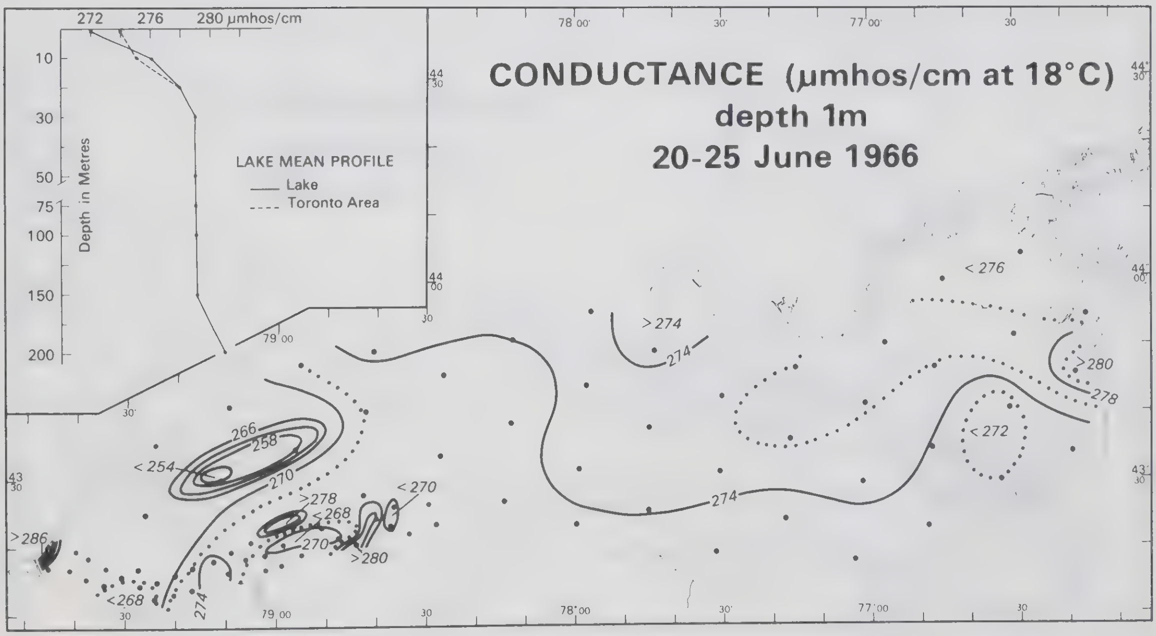

Figure F.8

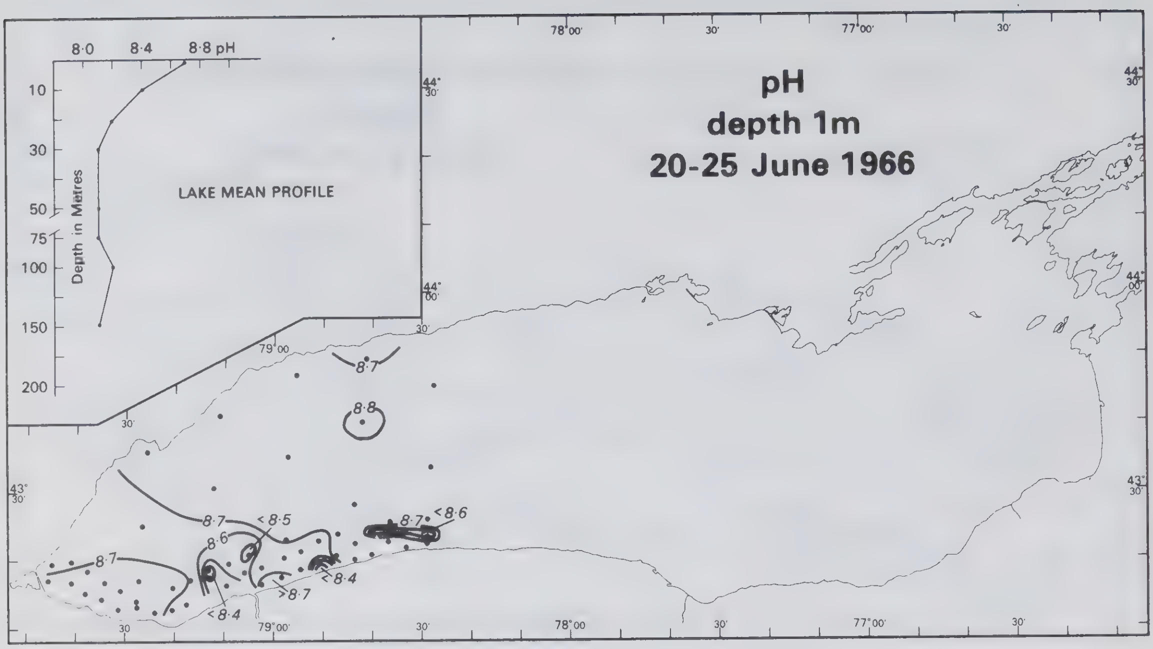

Figure F.9

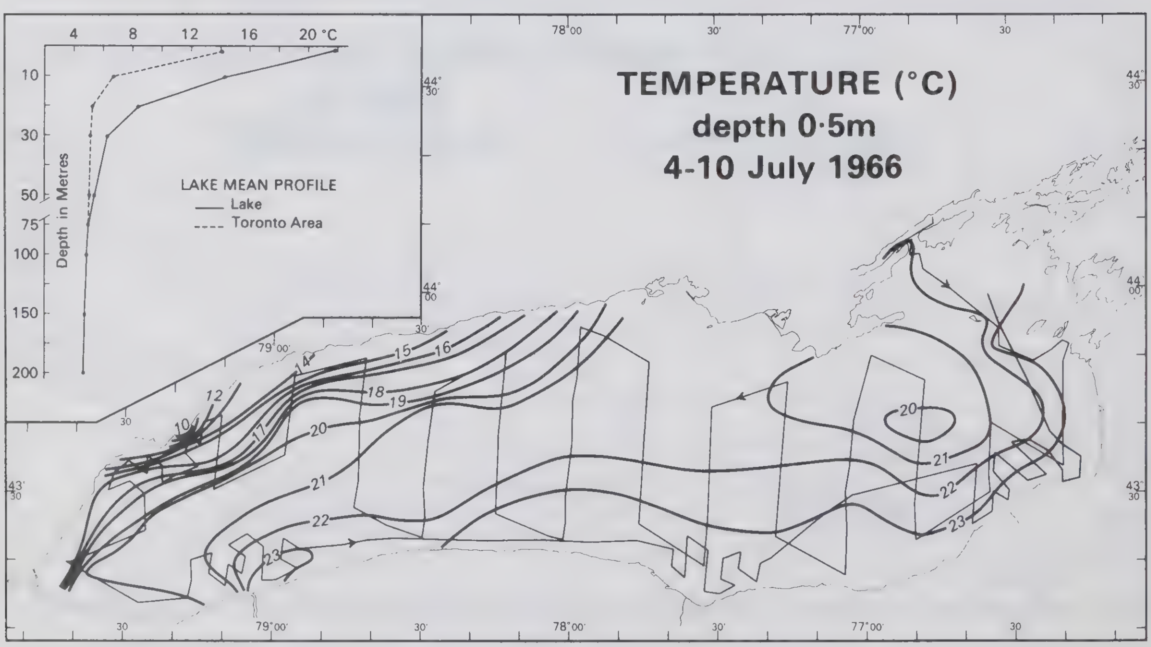

Figure F.10

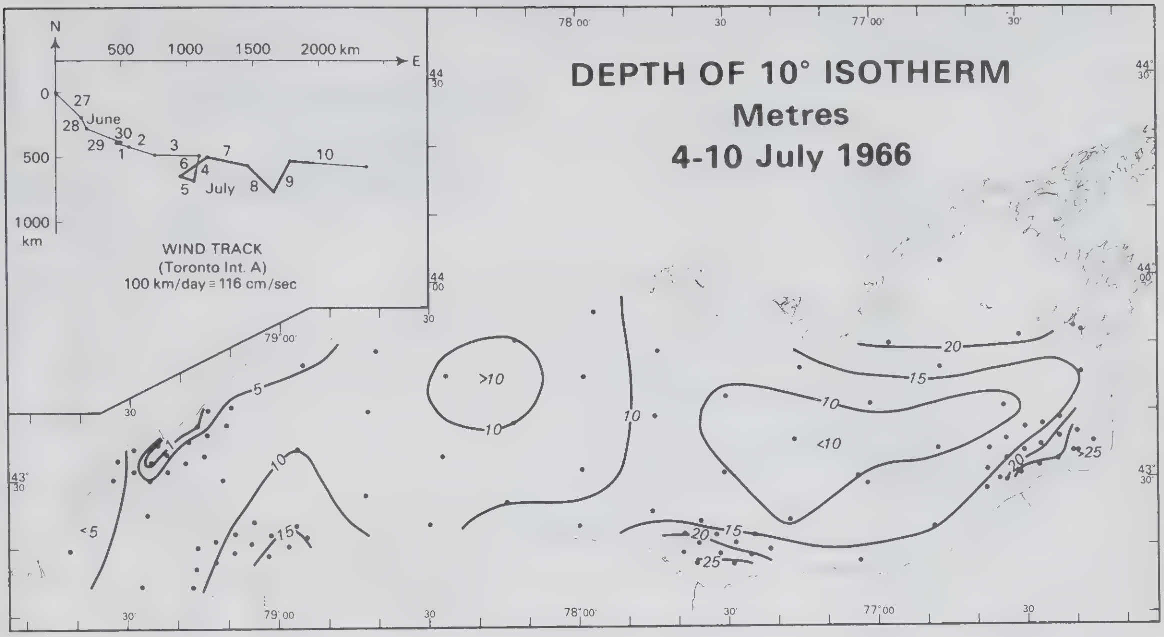

Figure F.11

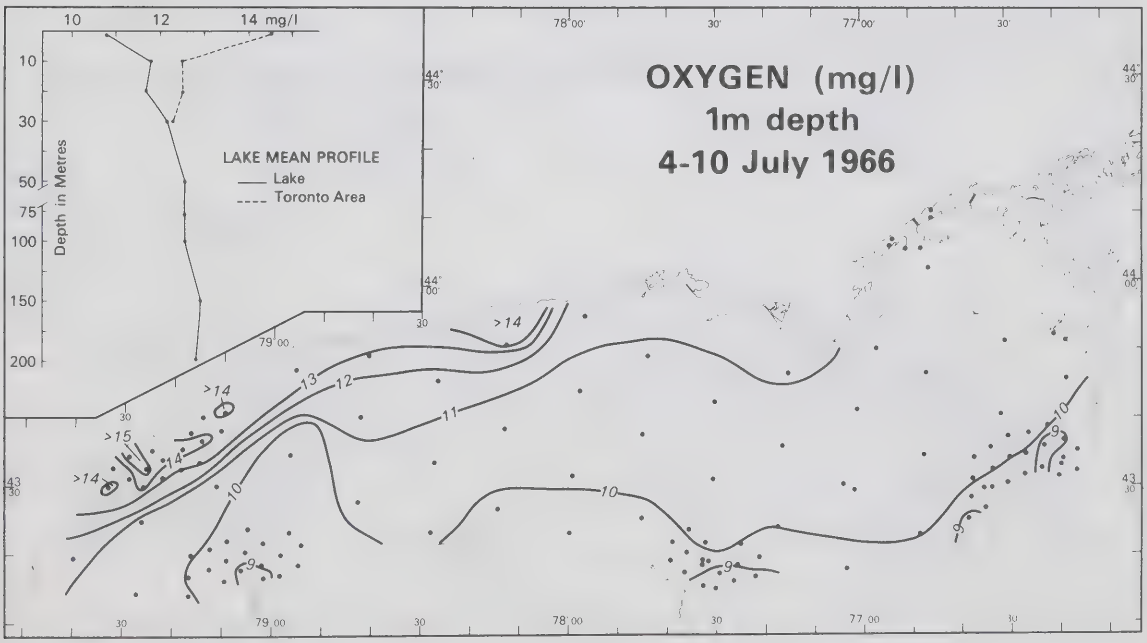

Figure F.12

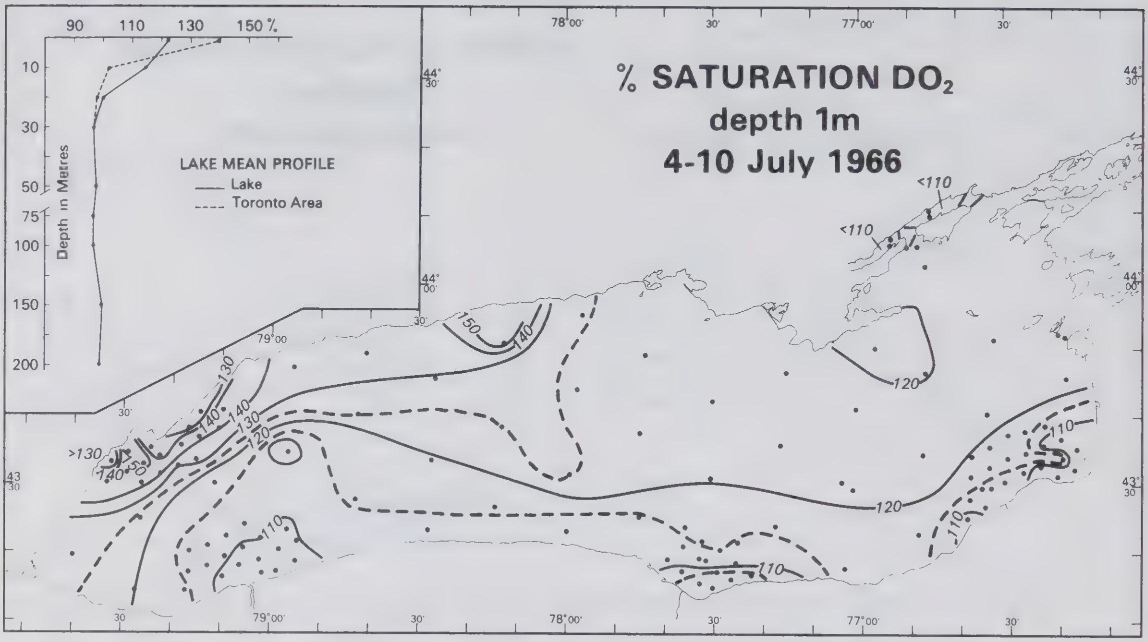

Figure F.13

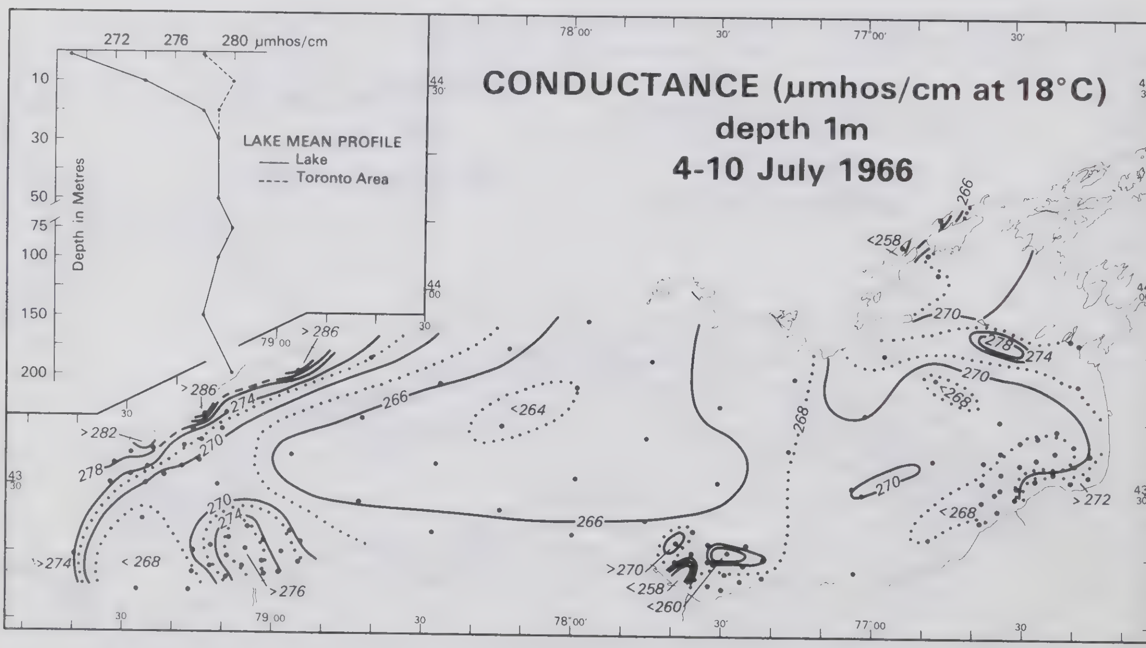

Figure F.14

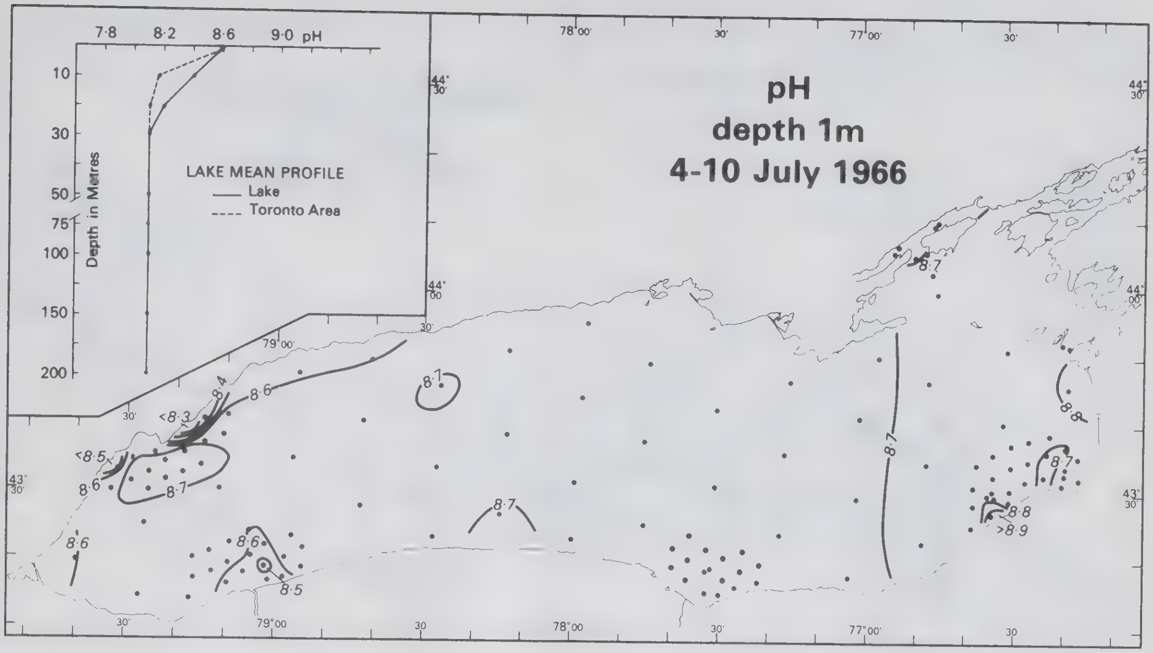

Figure F.15

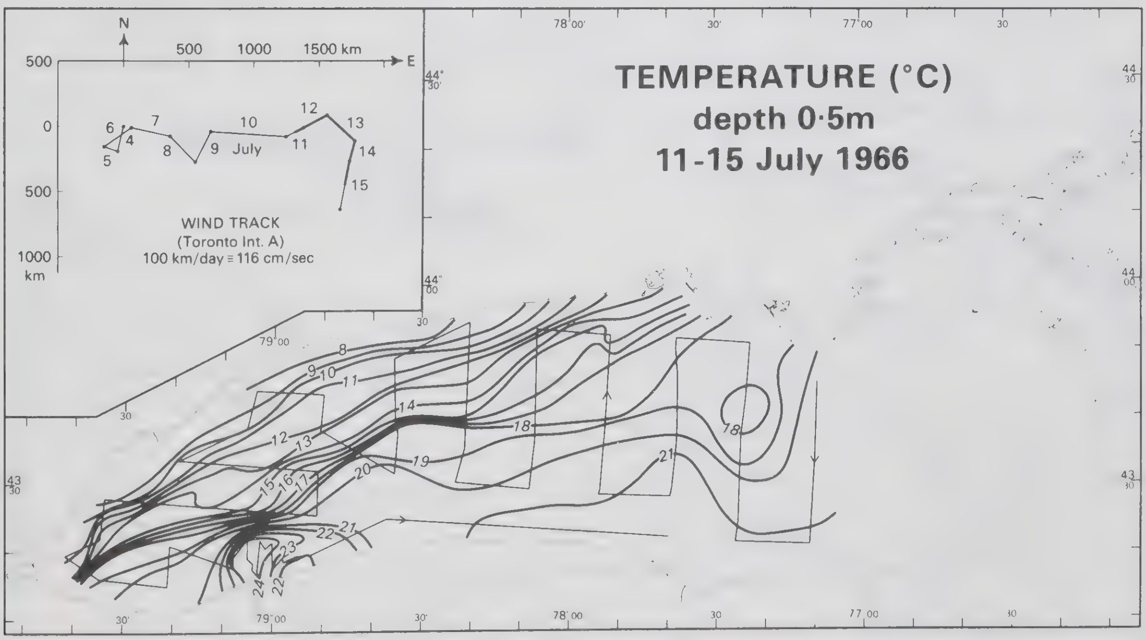

Figure F.16

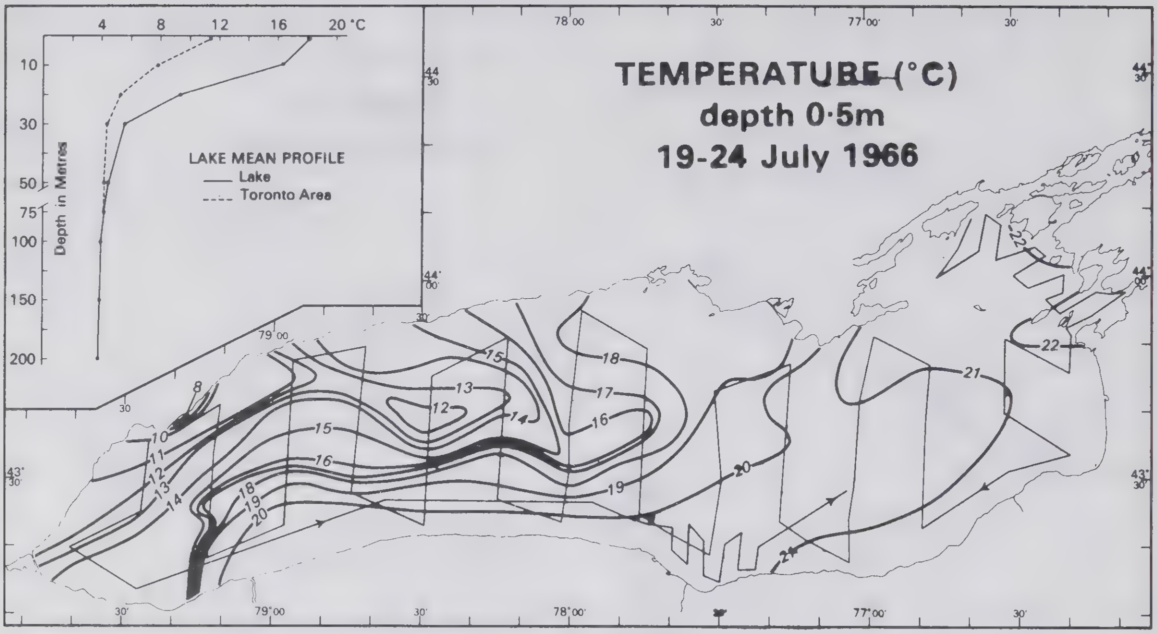

Figure F. 17

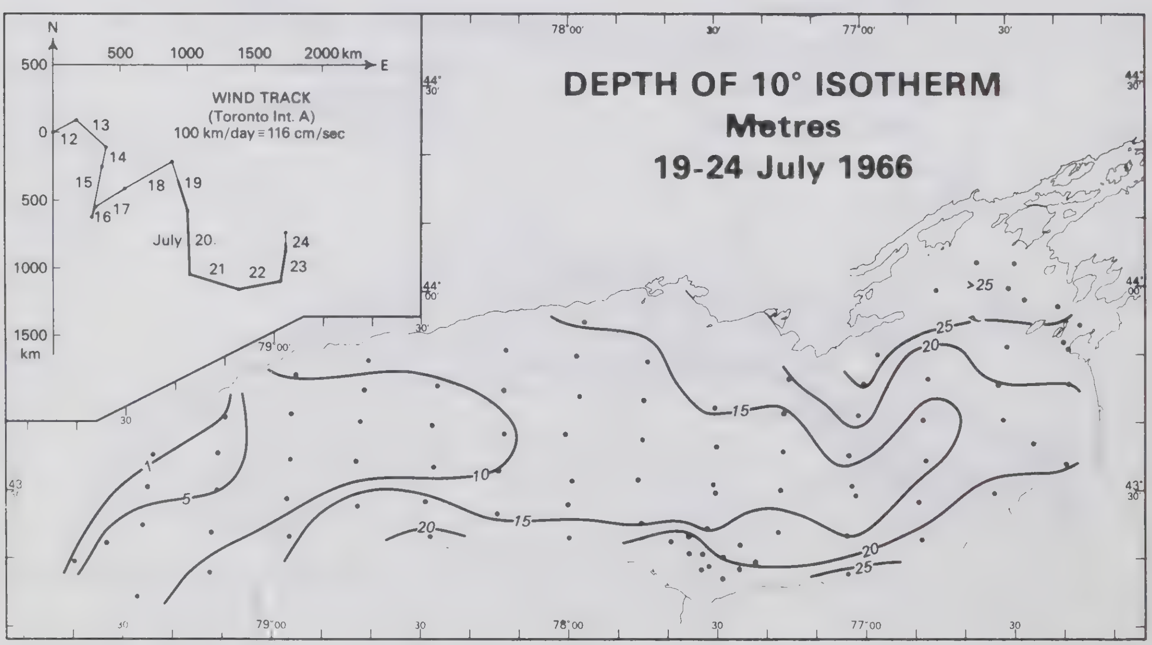

Figure F. 18

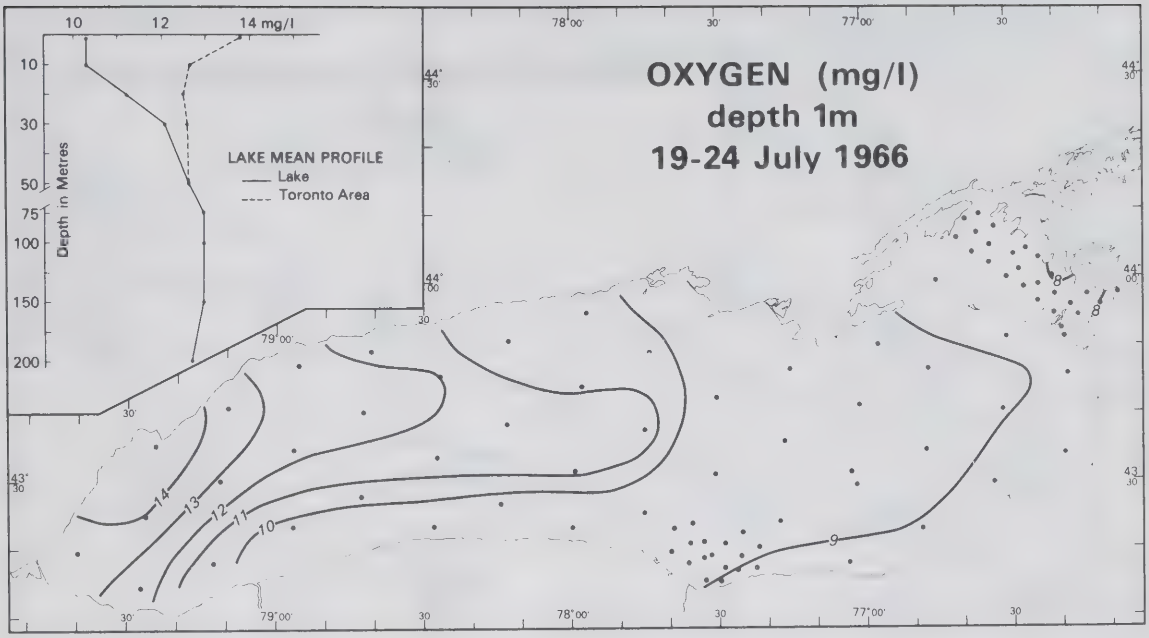

Figure F.19

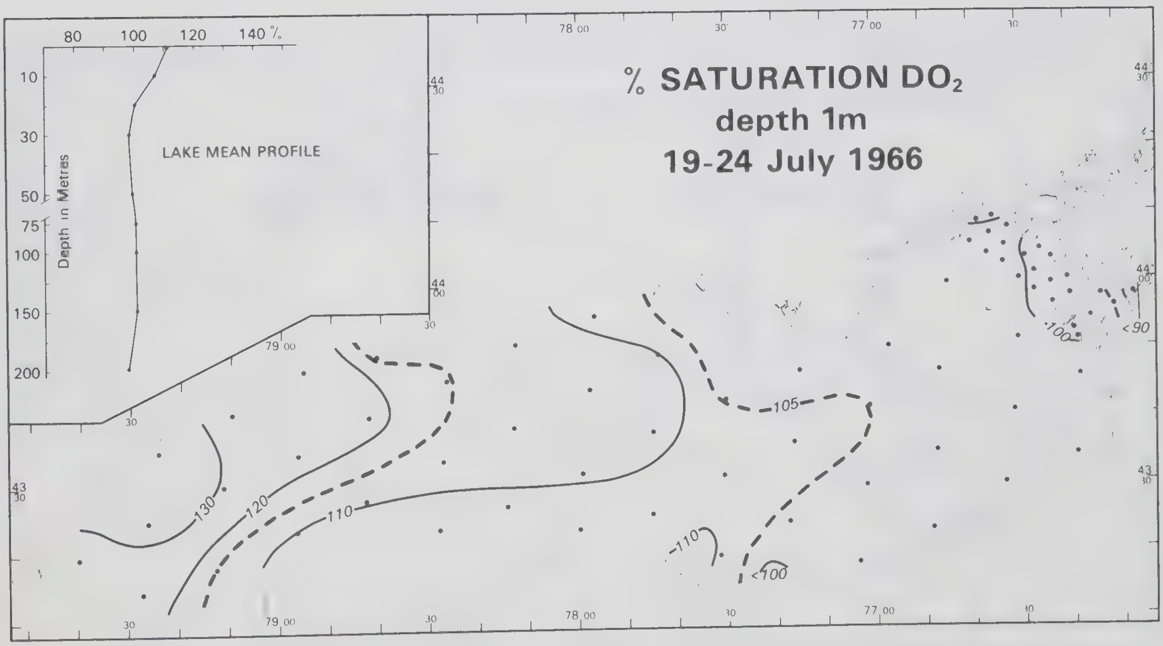

Figure F.20

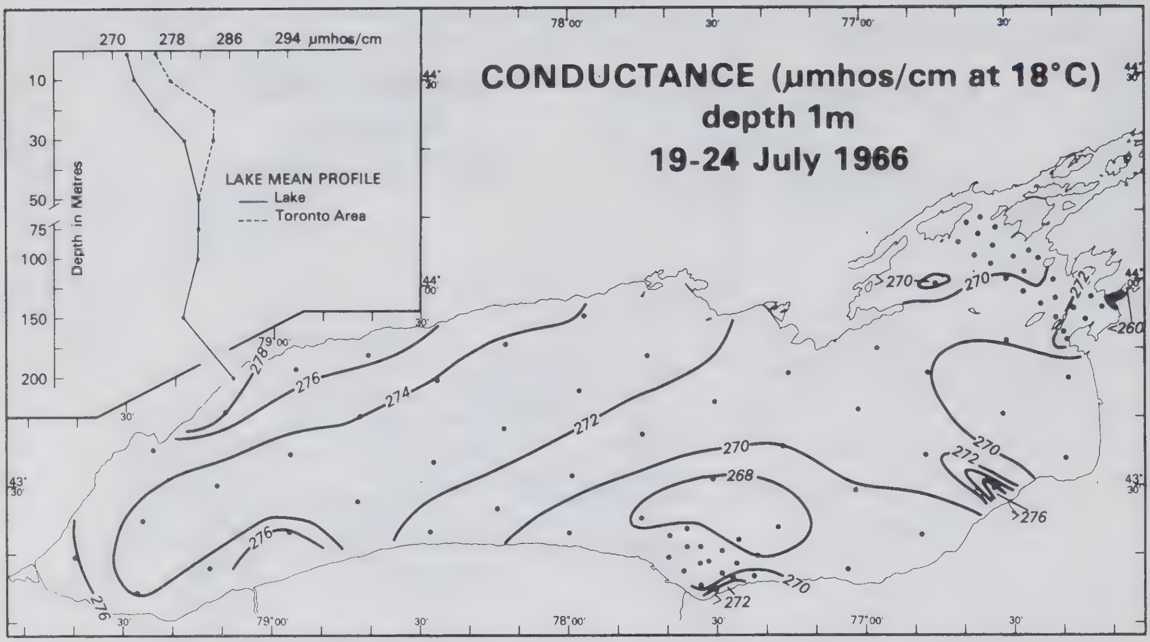

Figure F.21

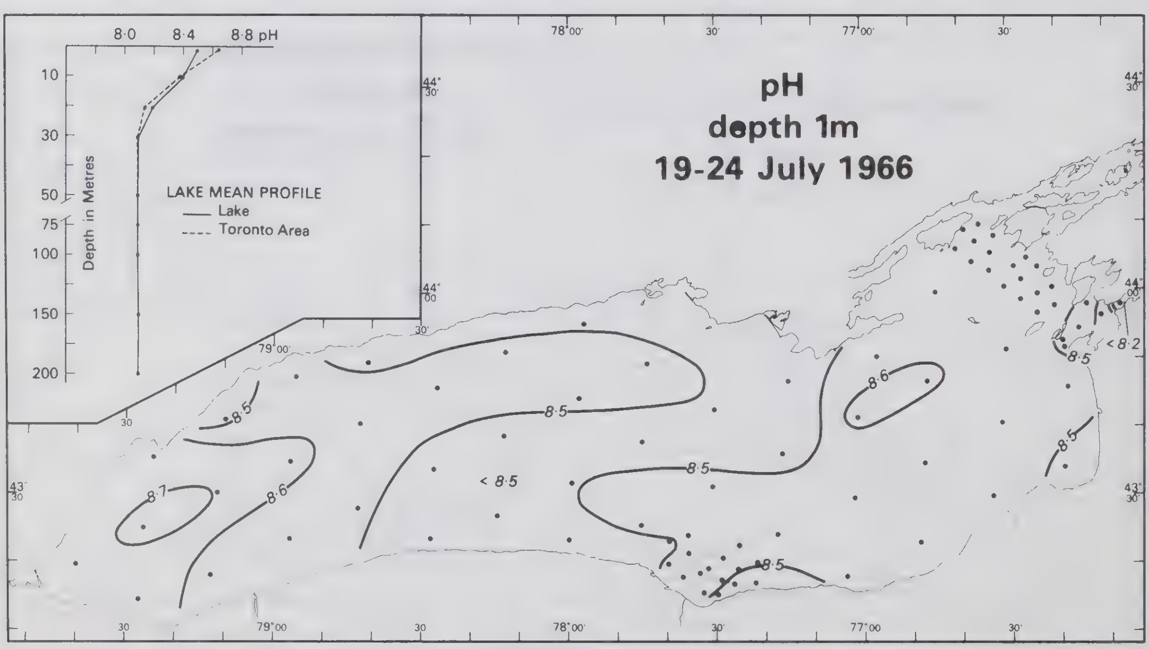

Figure F.22

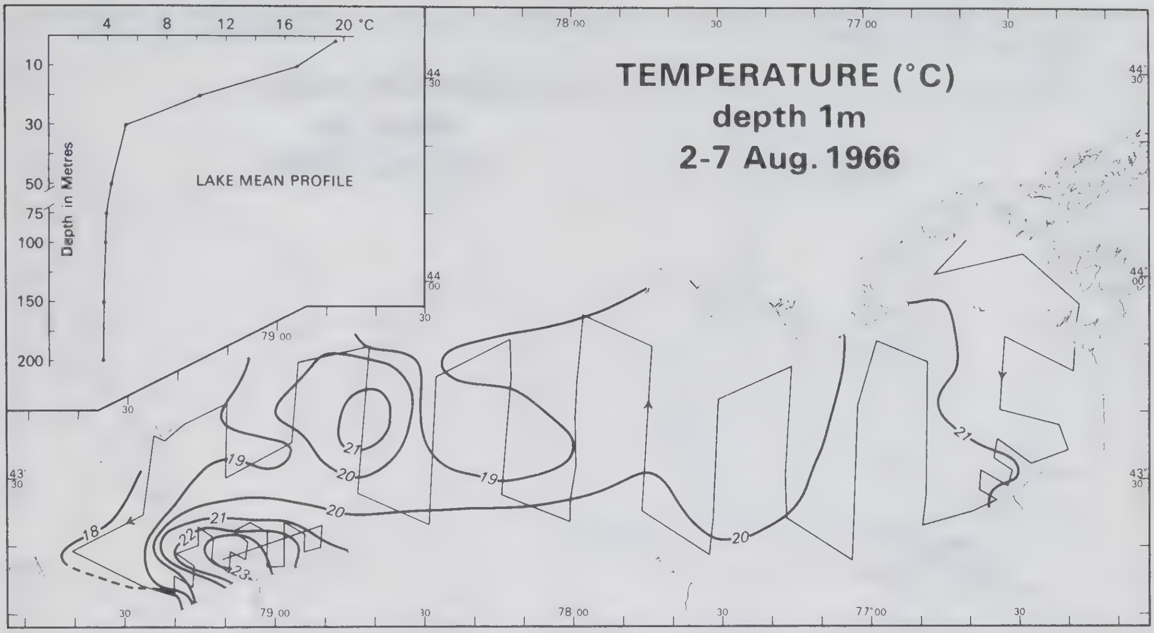

Figure F.23

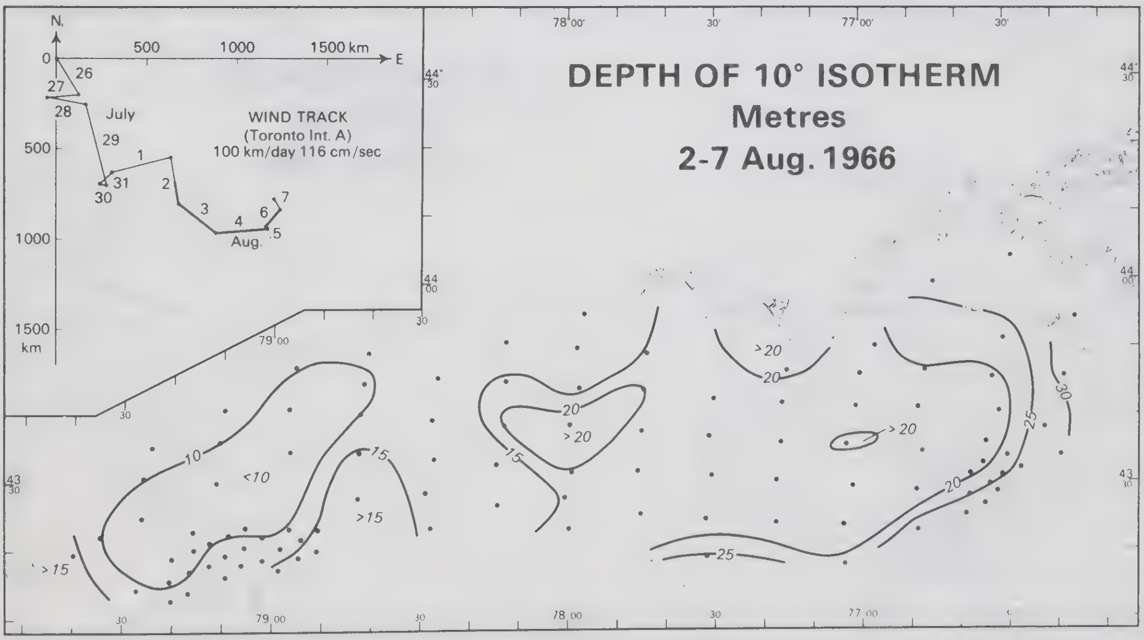

Figure F.24

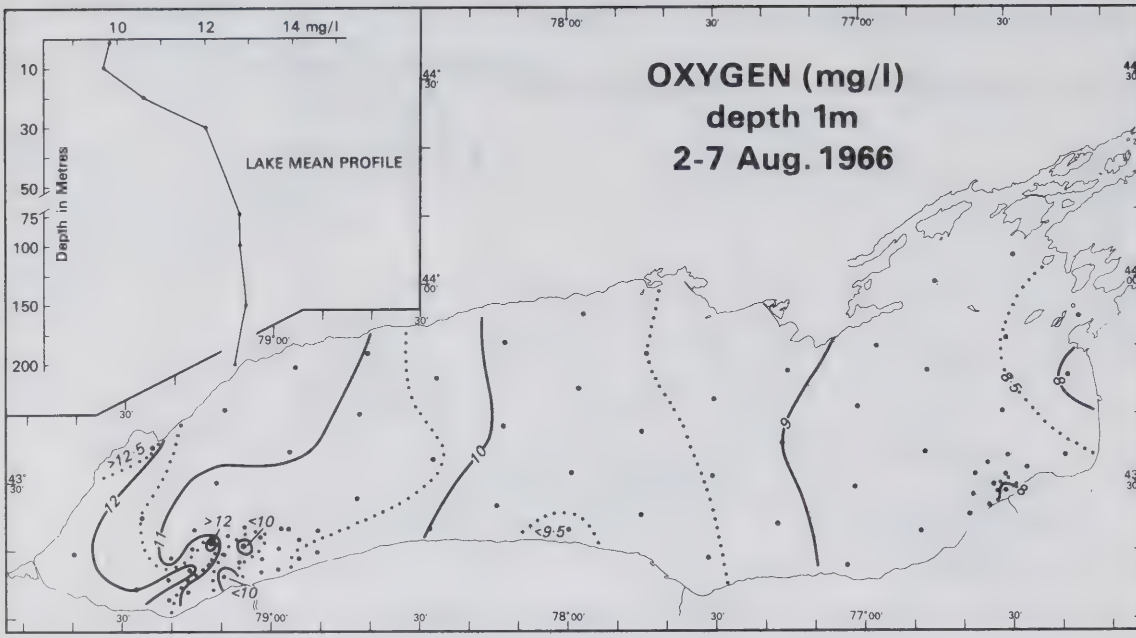

Figure F.25

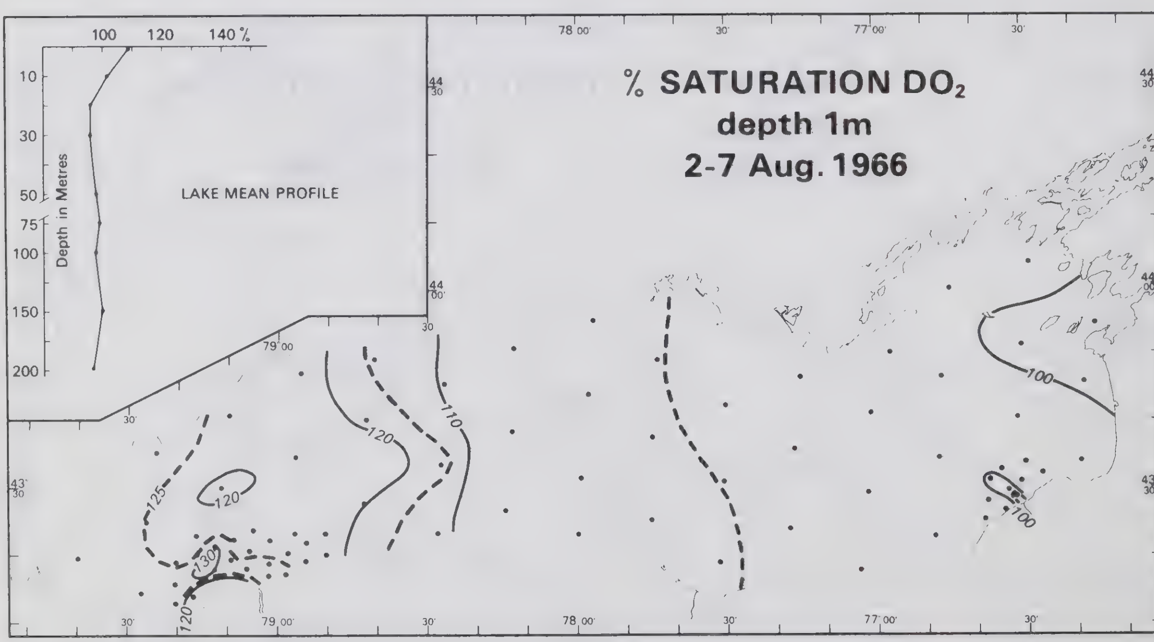

Figure F.26

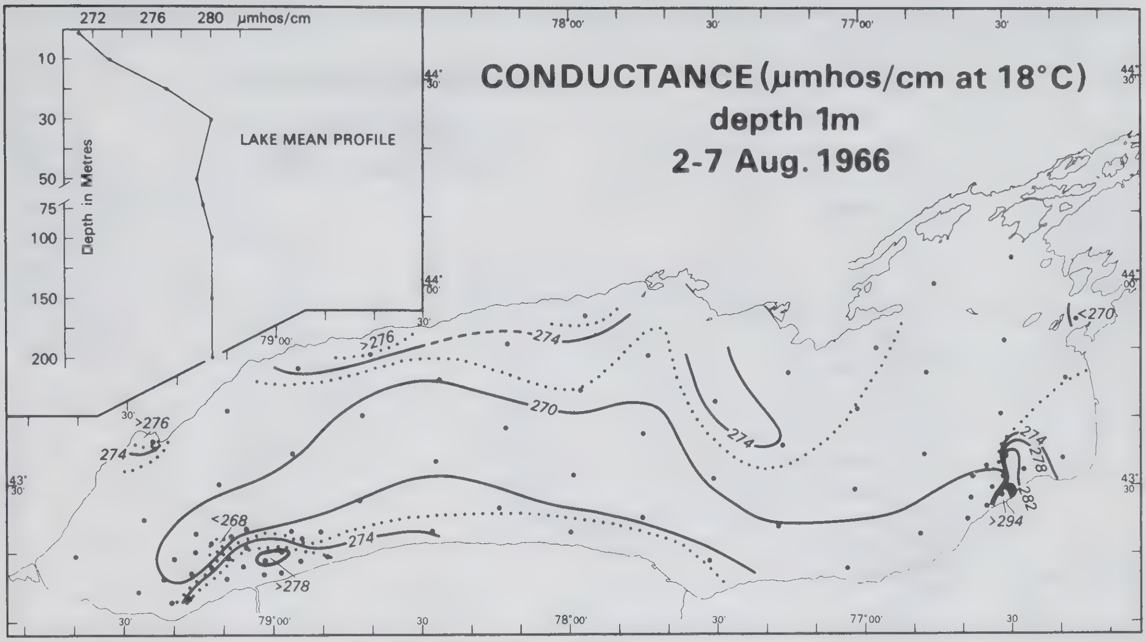

Figure F.27

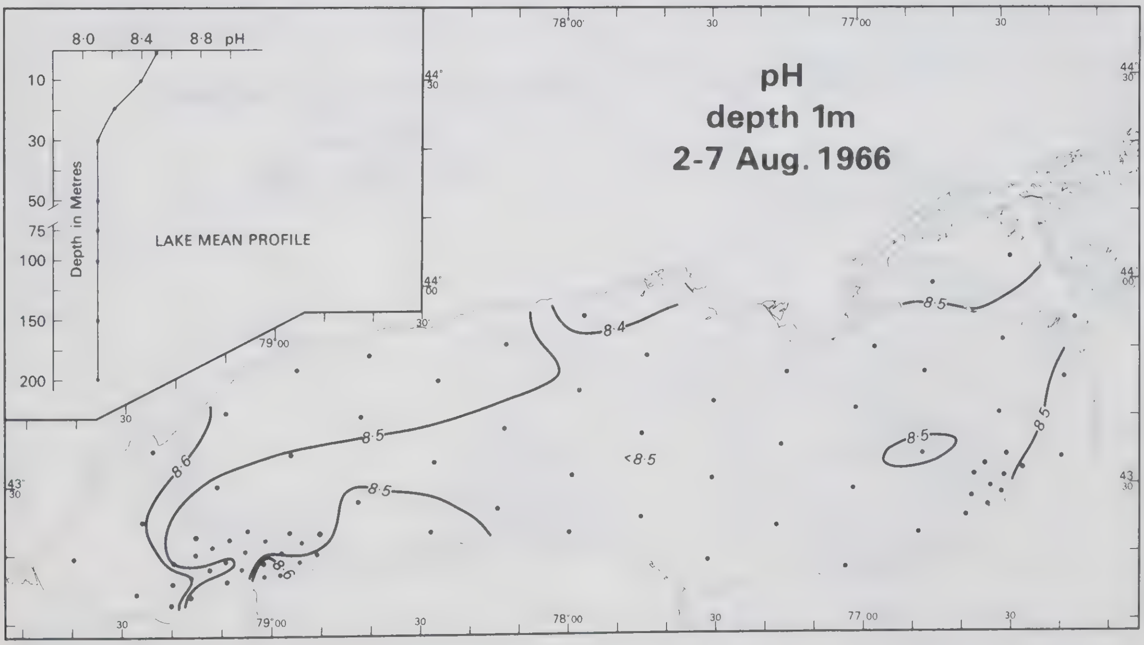

Figure F.28

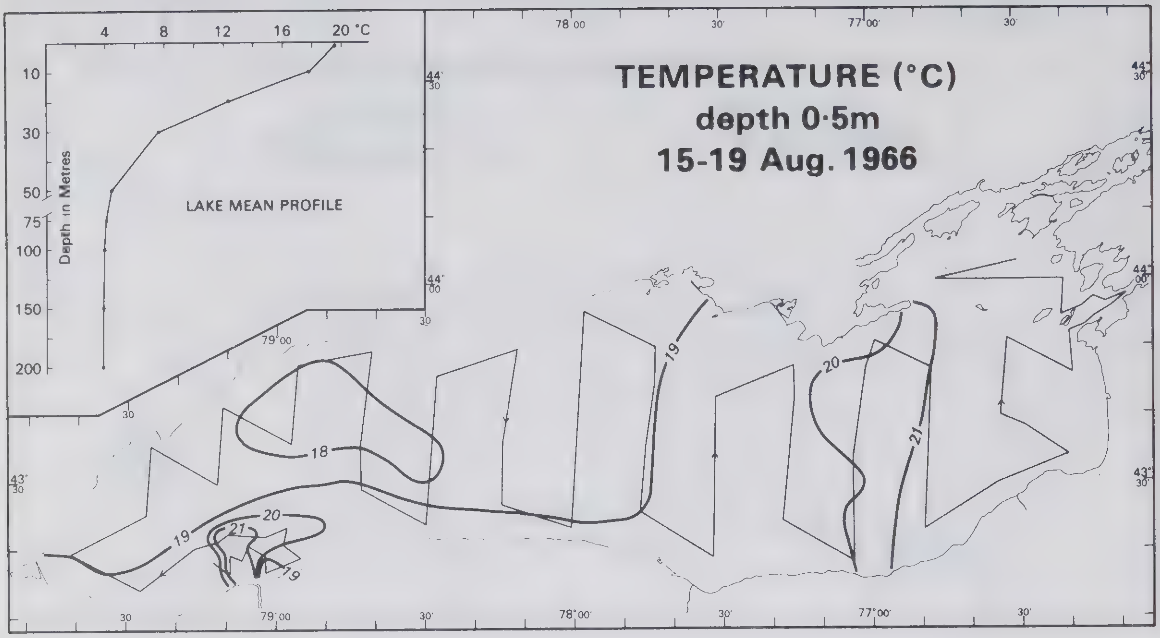

Figure F.29

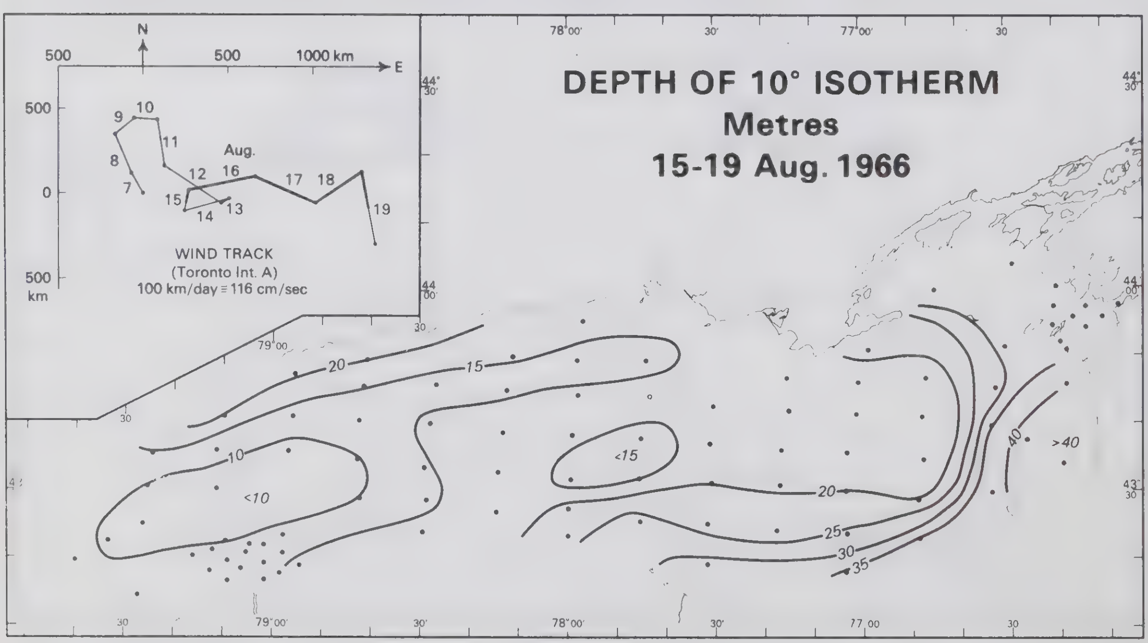

Figure F.30

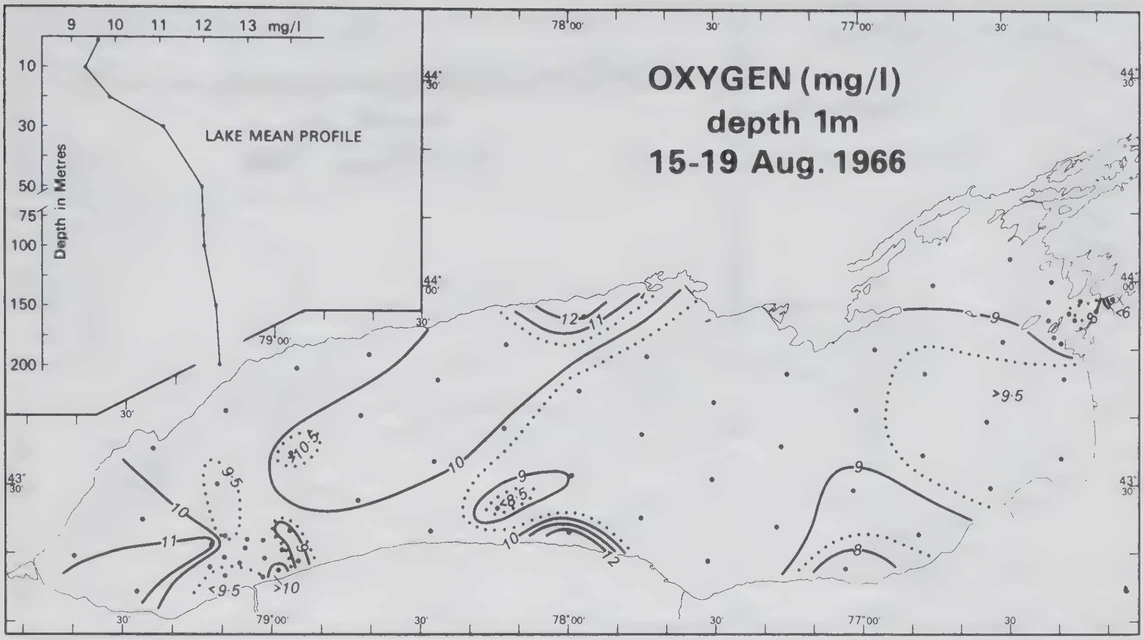

Figure F.31

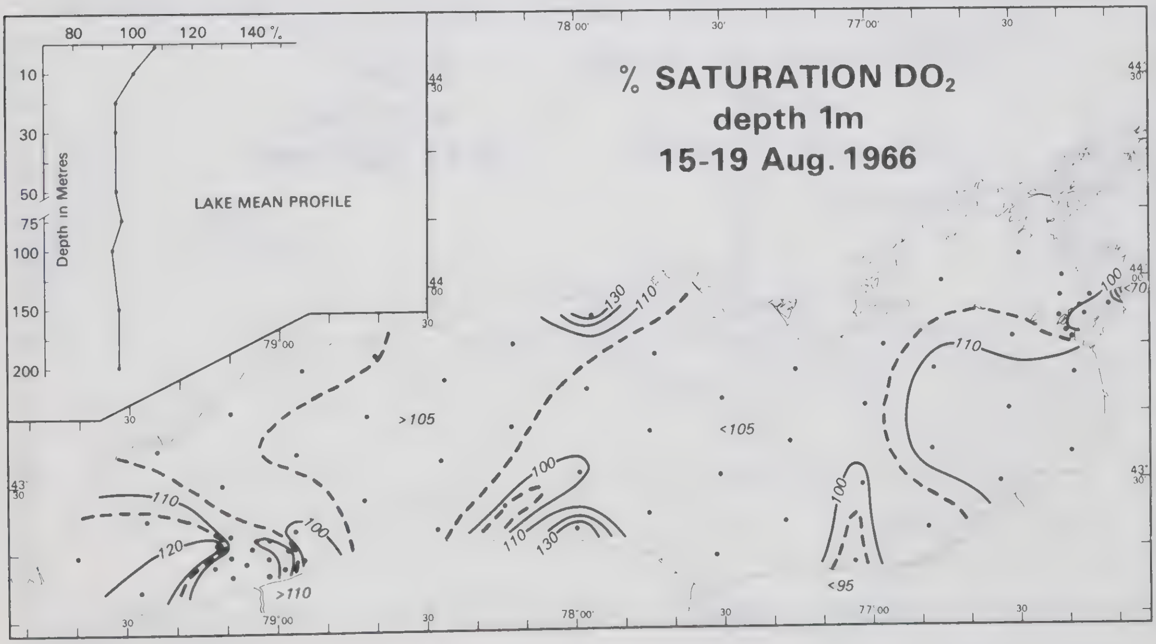

Figure F.32

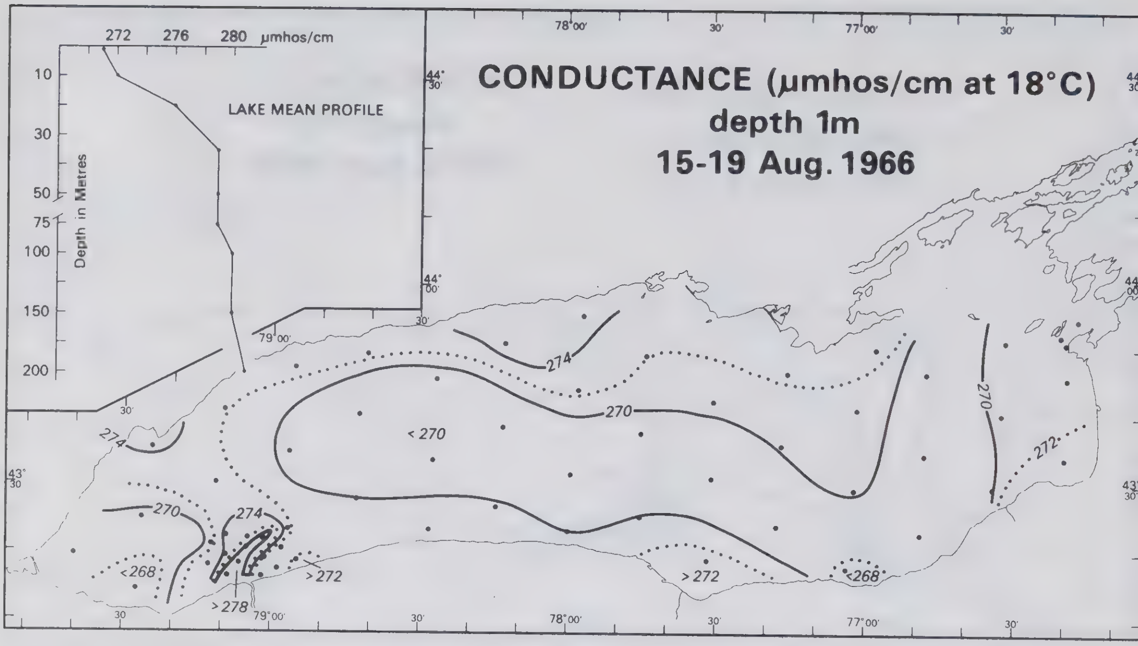

Figure F.33

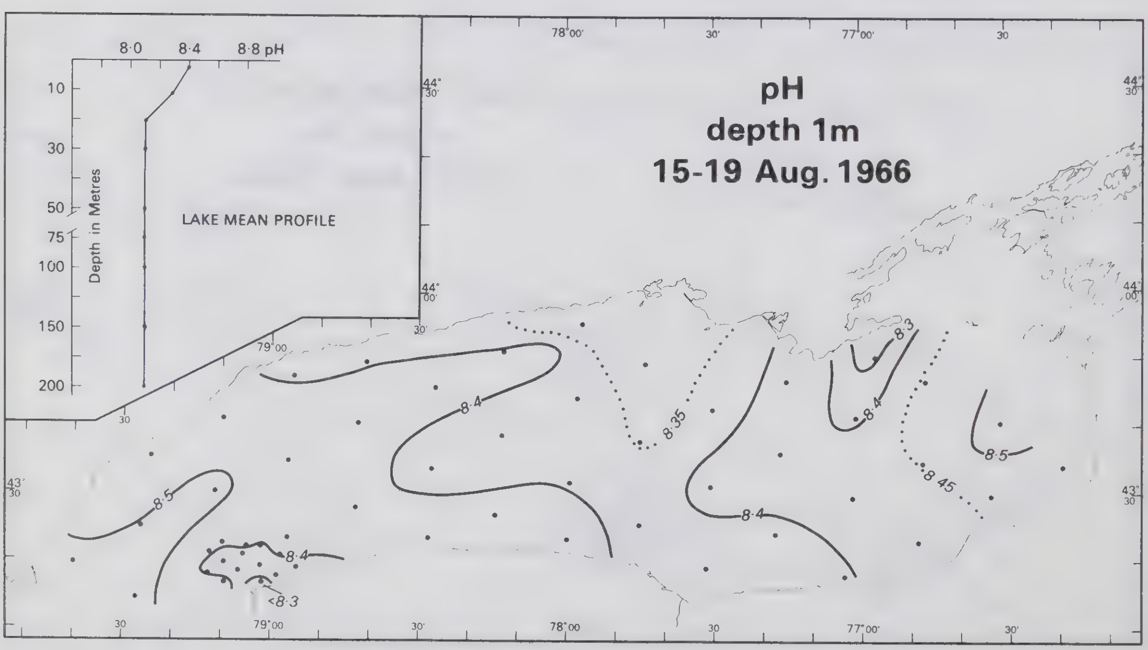

Figure F.34

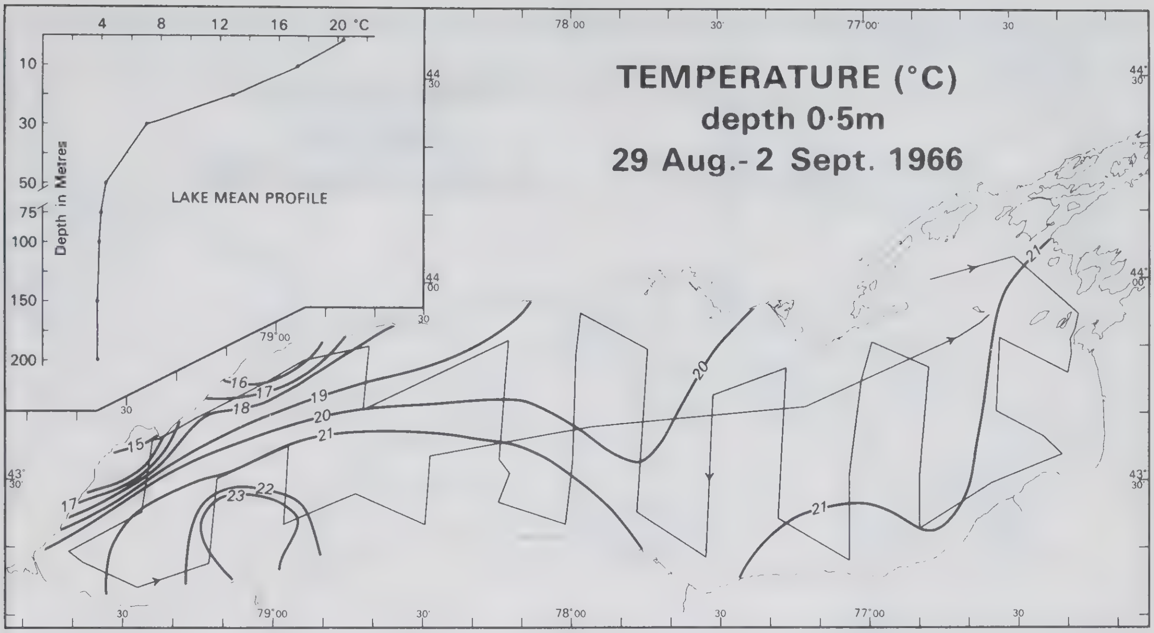

Figure F.35

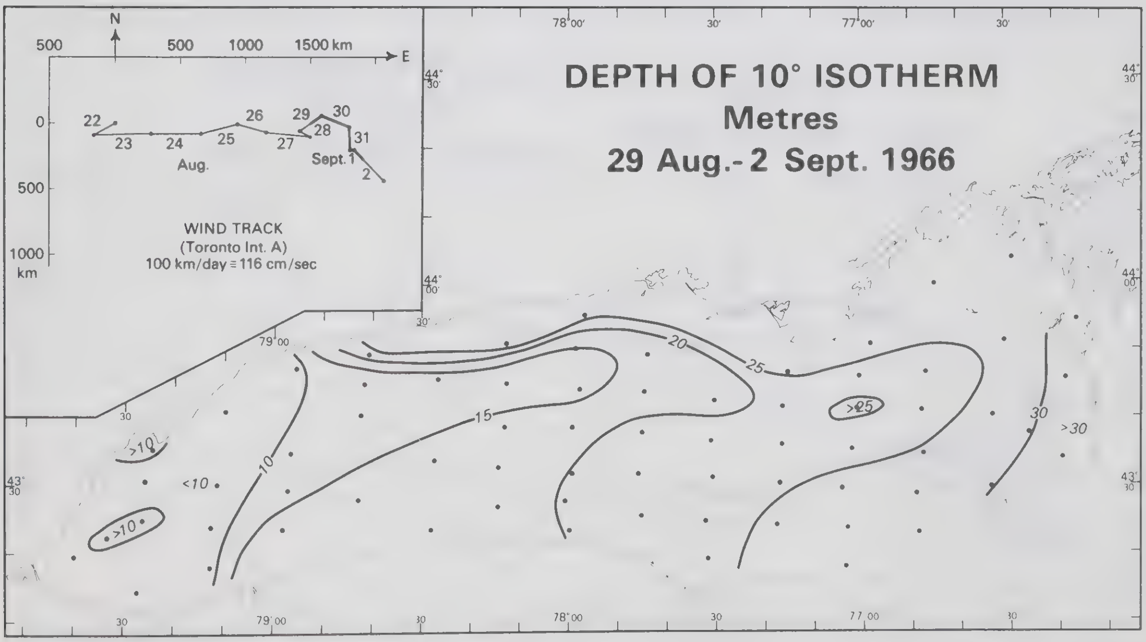

Figure F.36

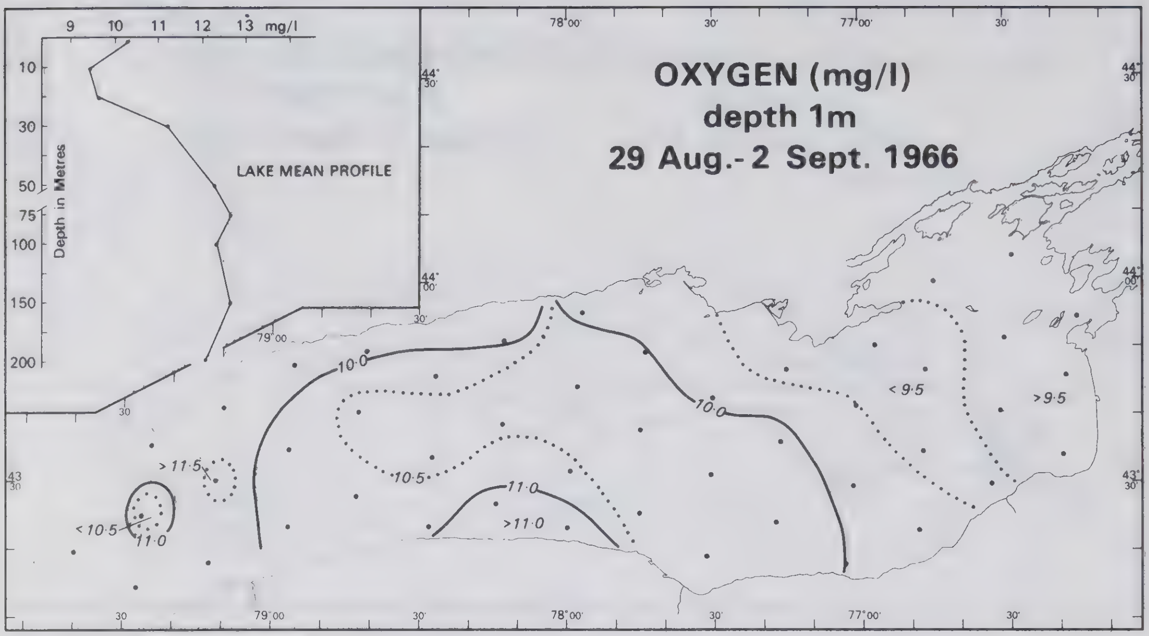

Figure F.37

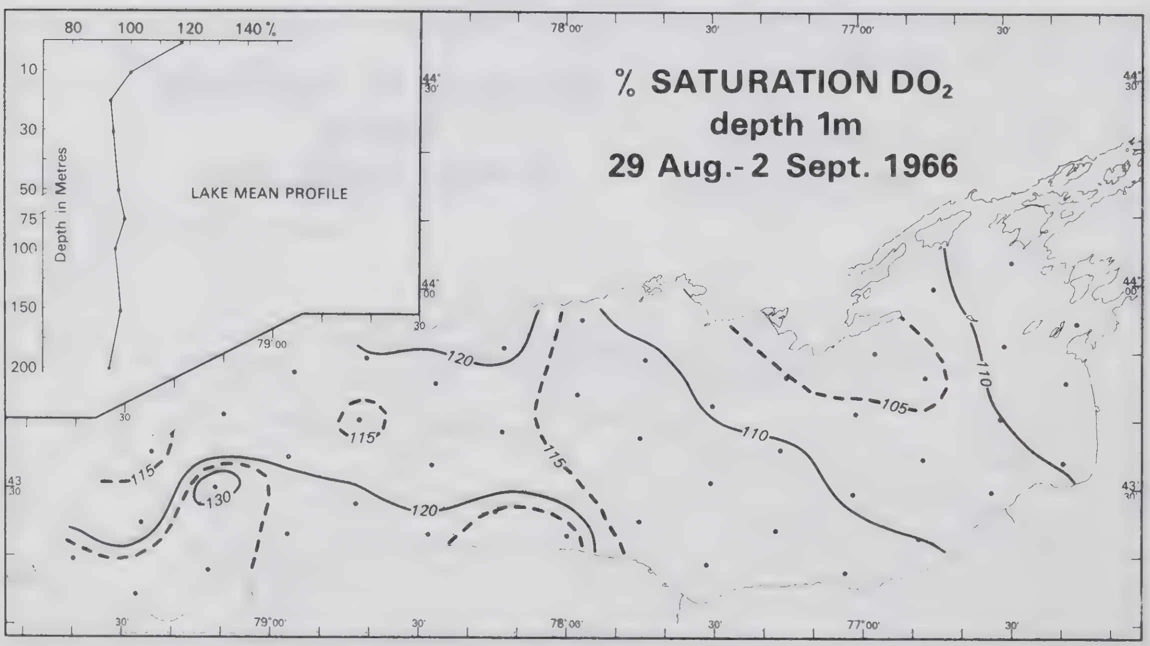

Figure F.38

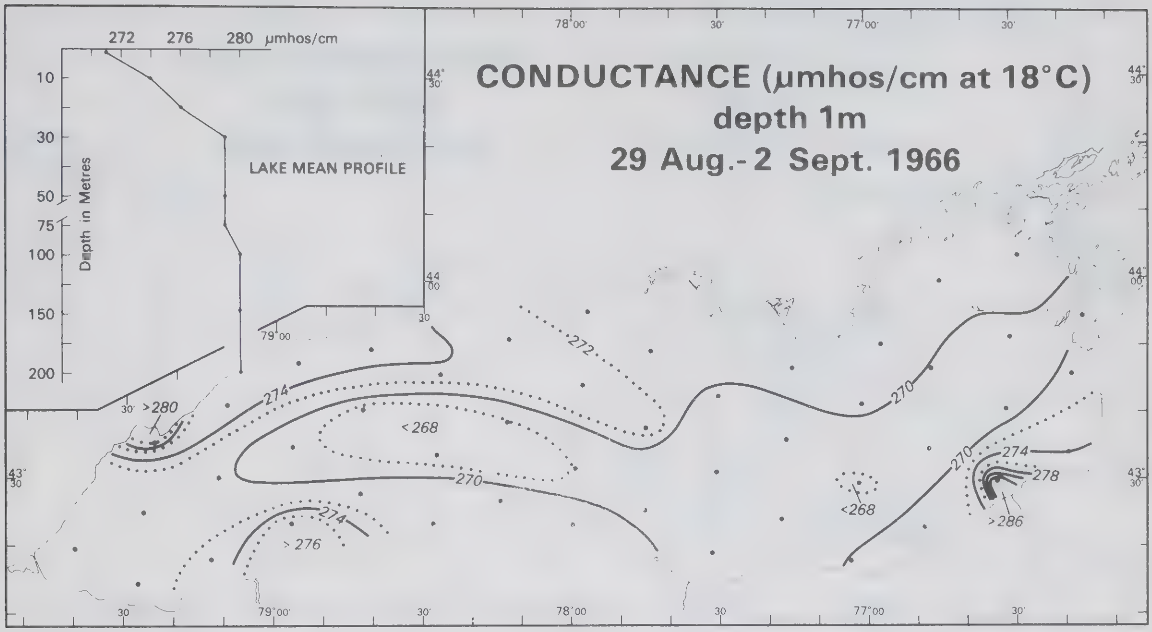

Figure F.39

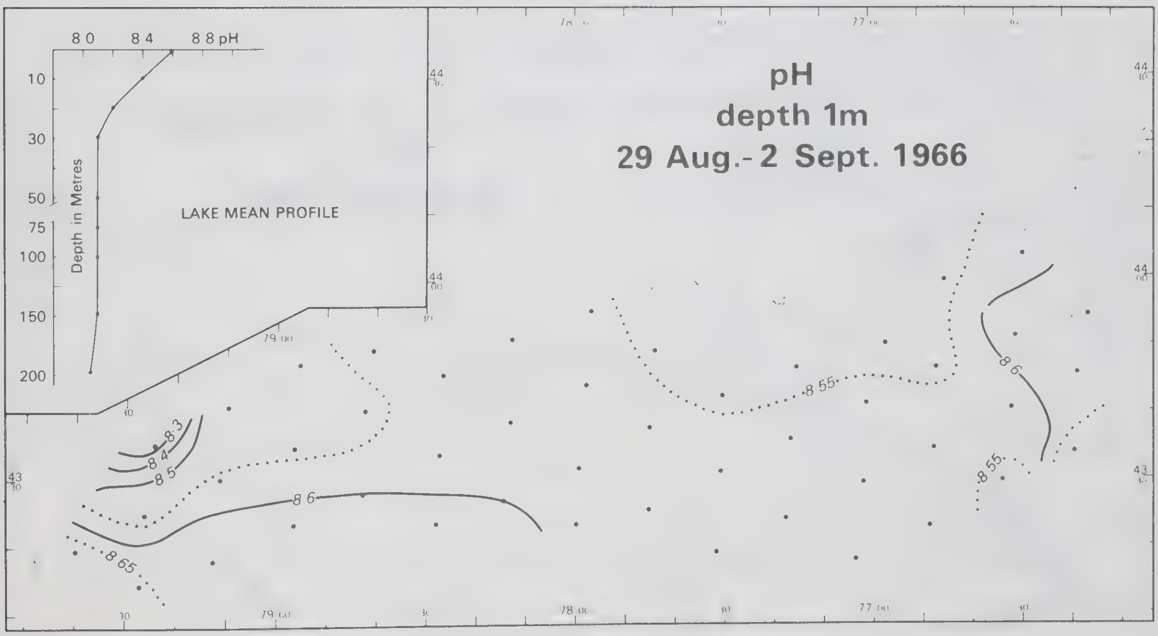

Figure F.40

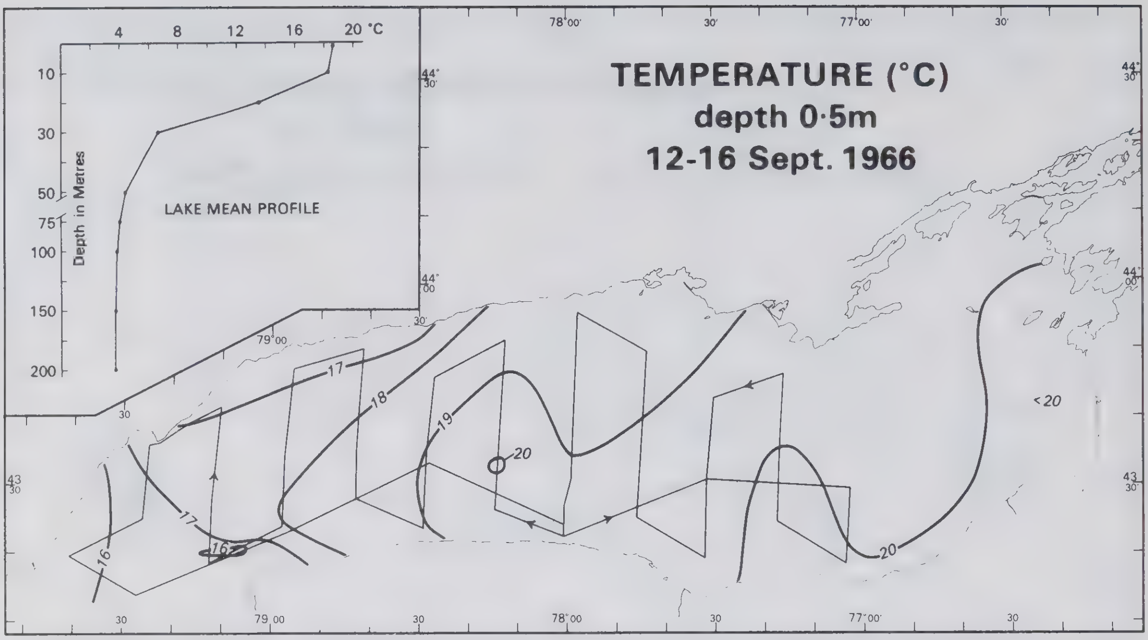

Figure F.41

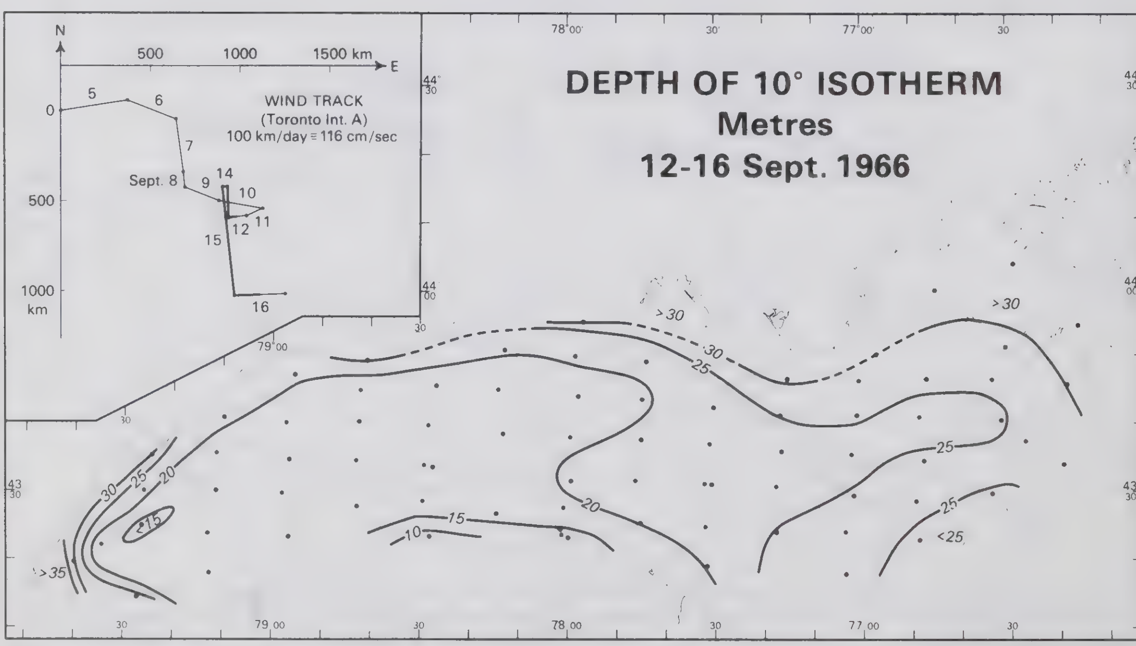

Figure F.42

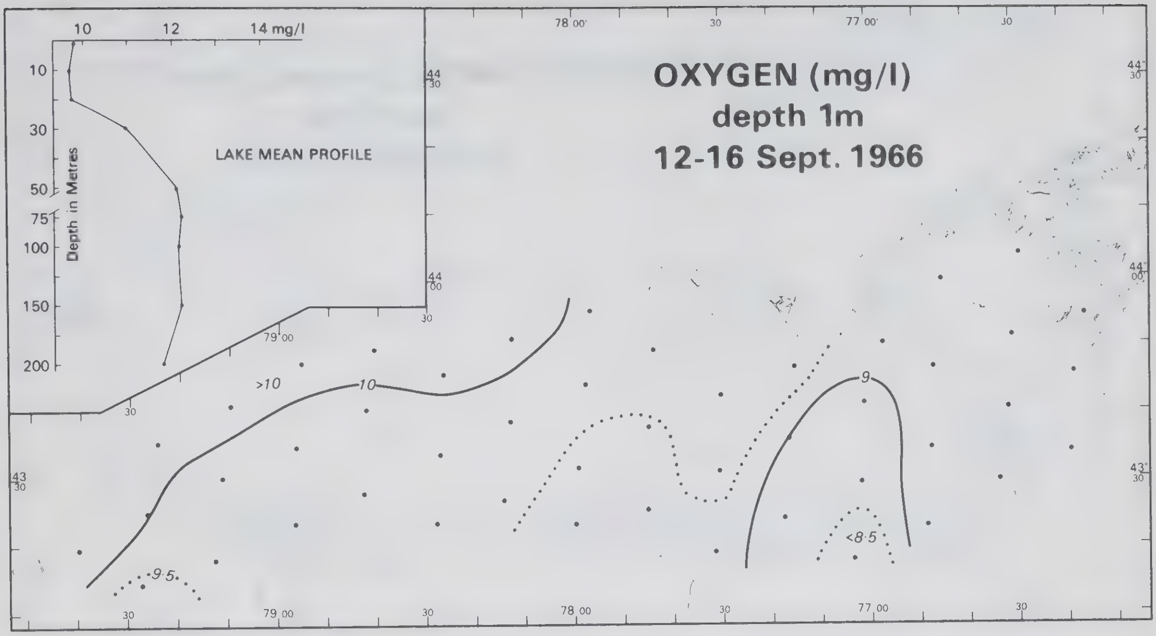

Figure F.43

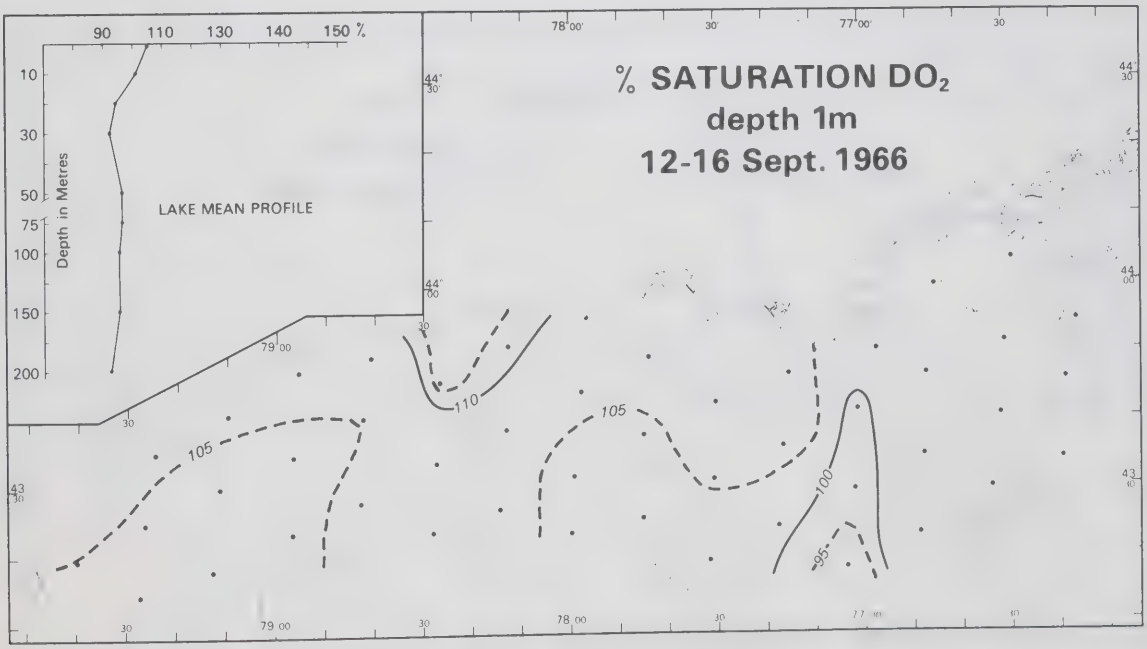

Figure F.44

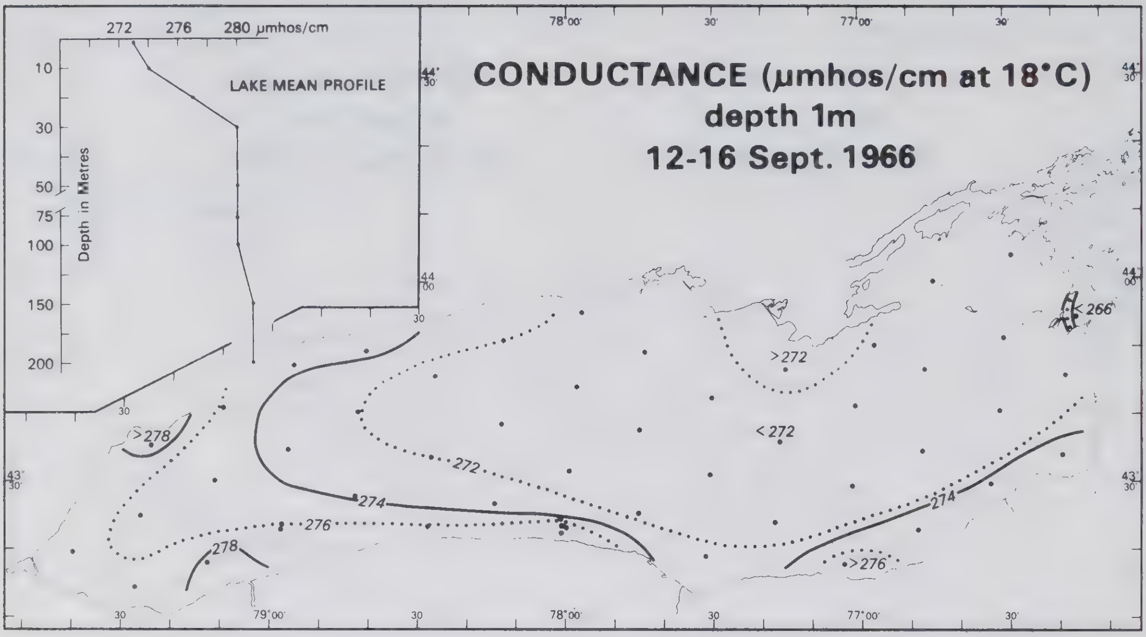

Figure F.45

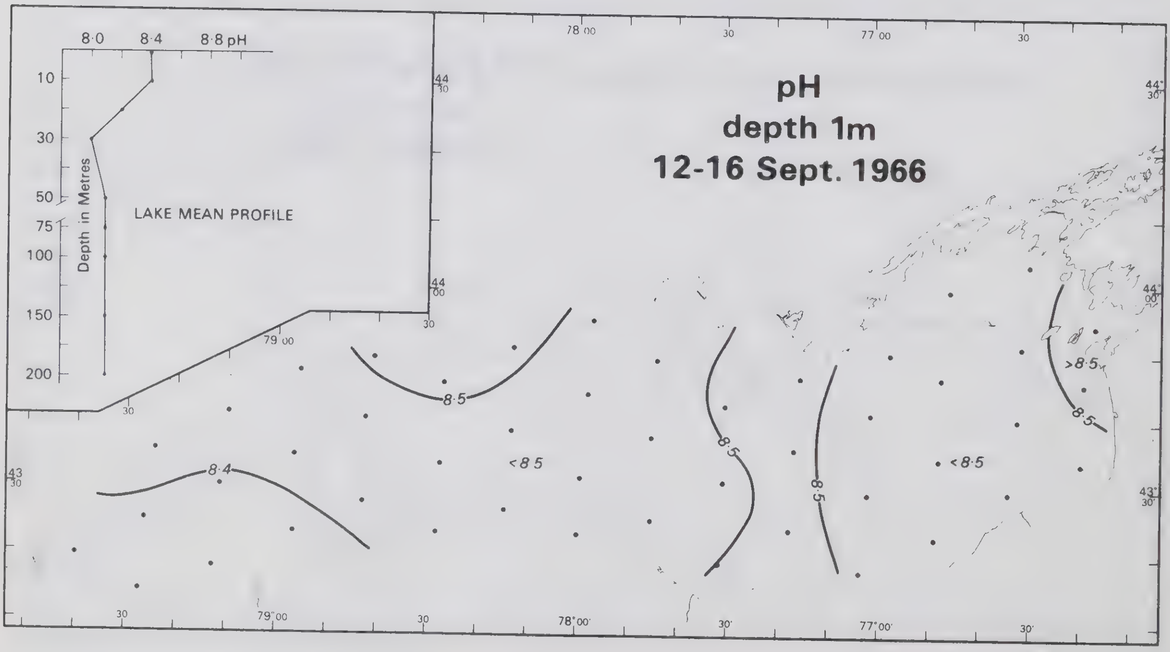

Figure F.46

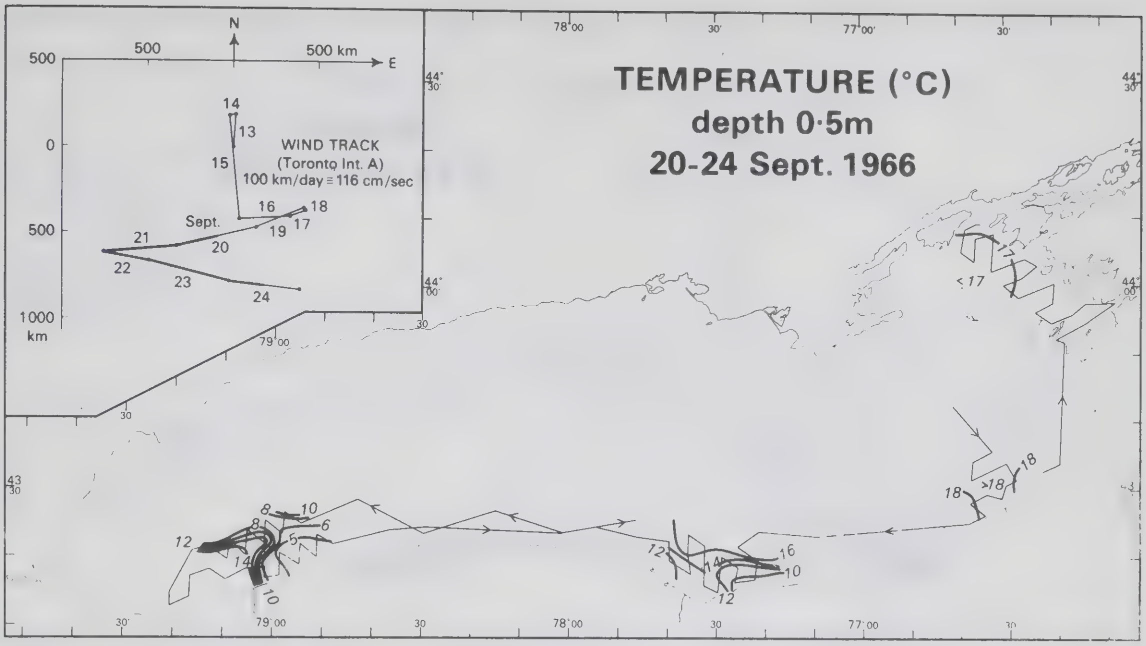

Figure F.47

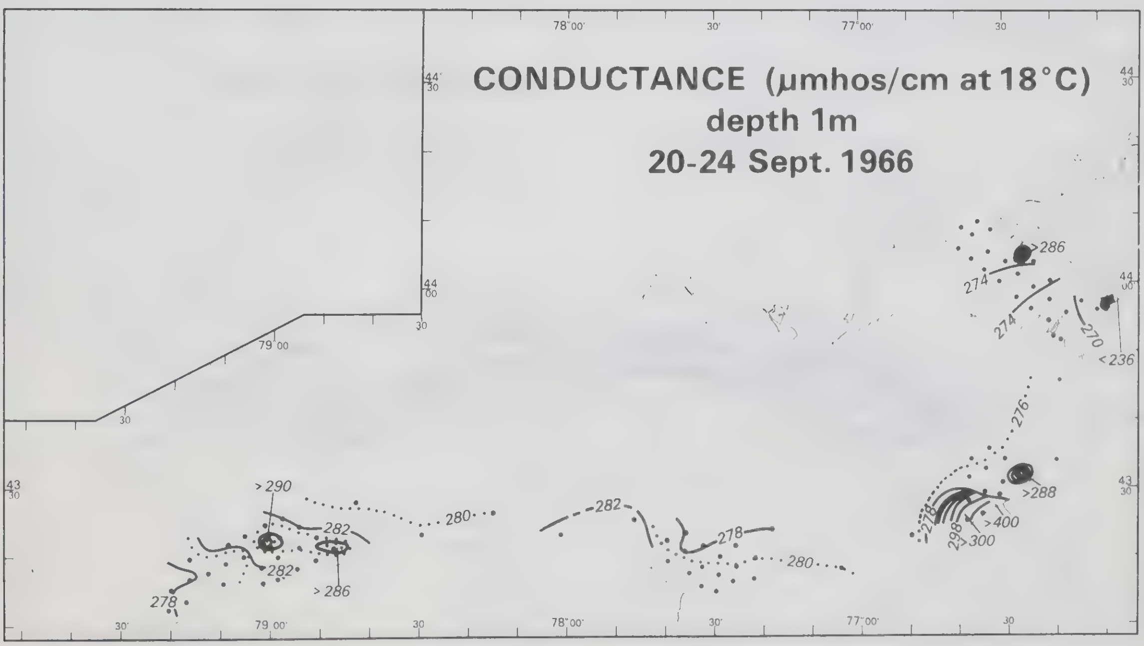

Figure F.48

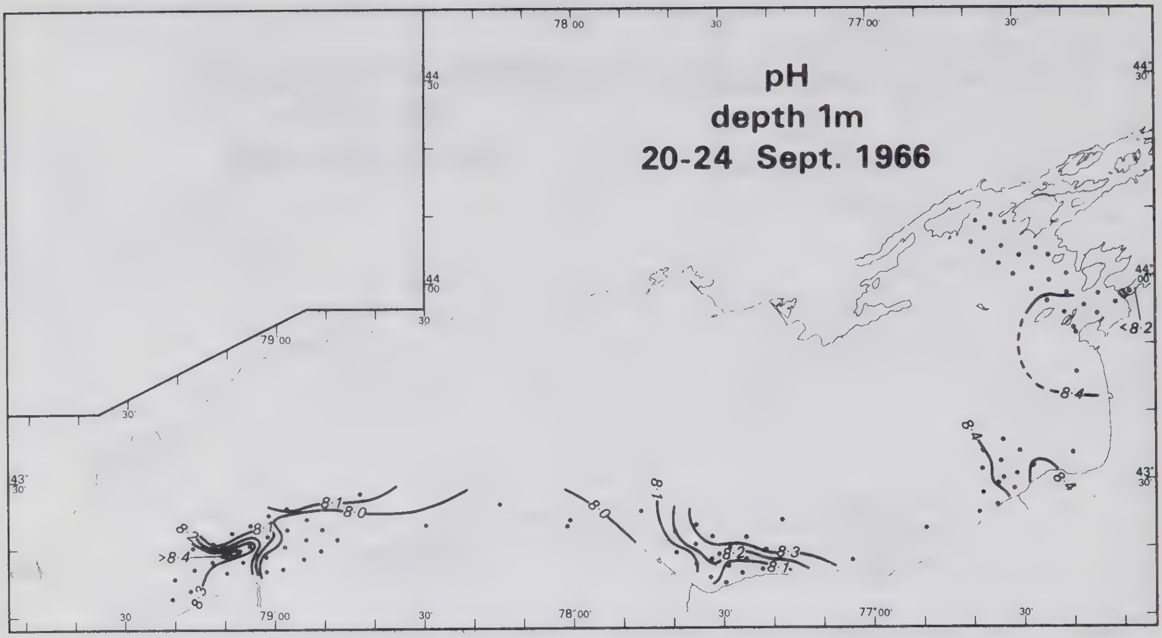

Figure F.49

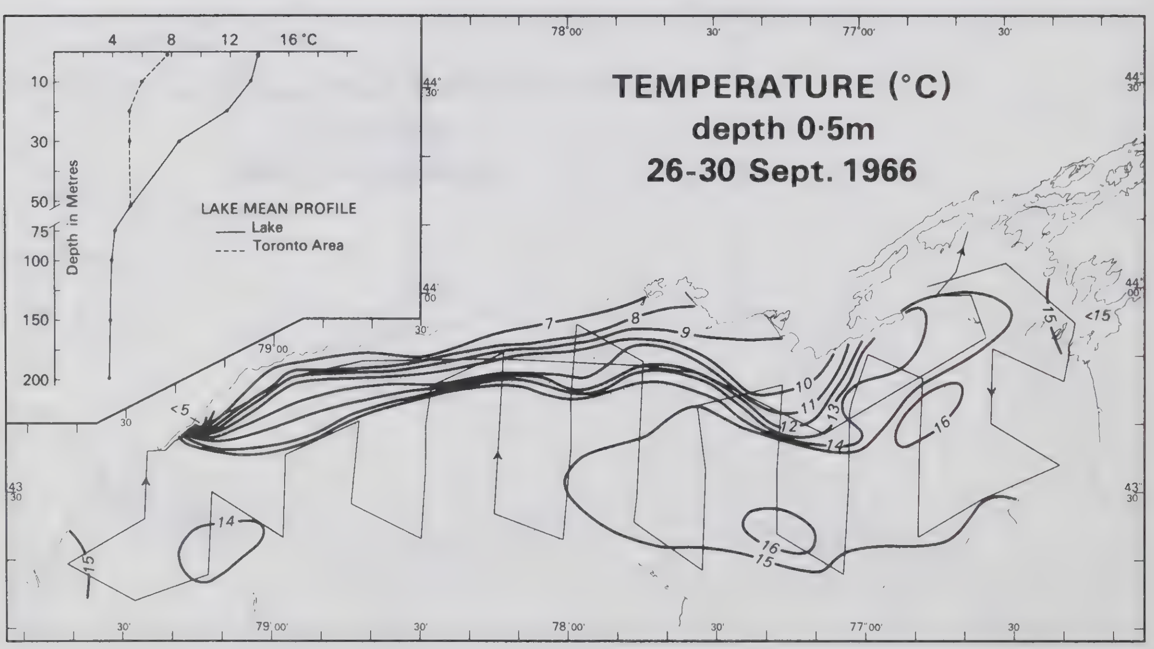

Figure F.50

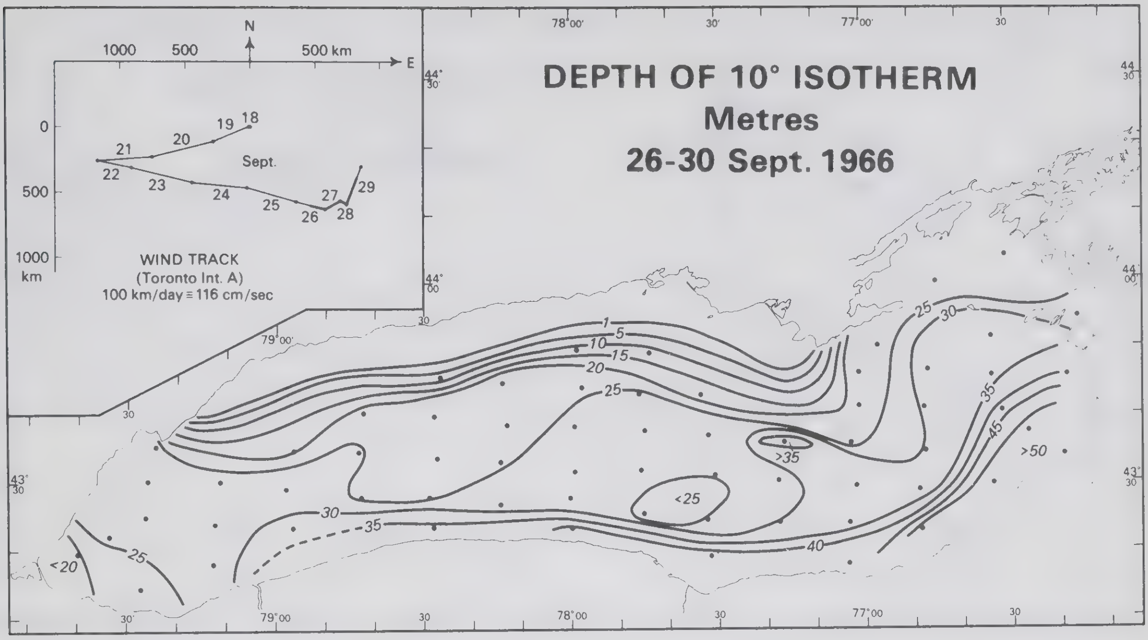

Figure F.51

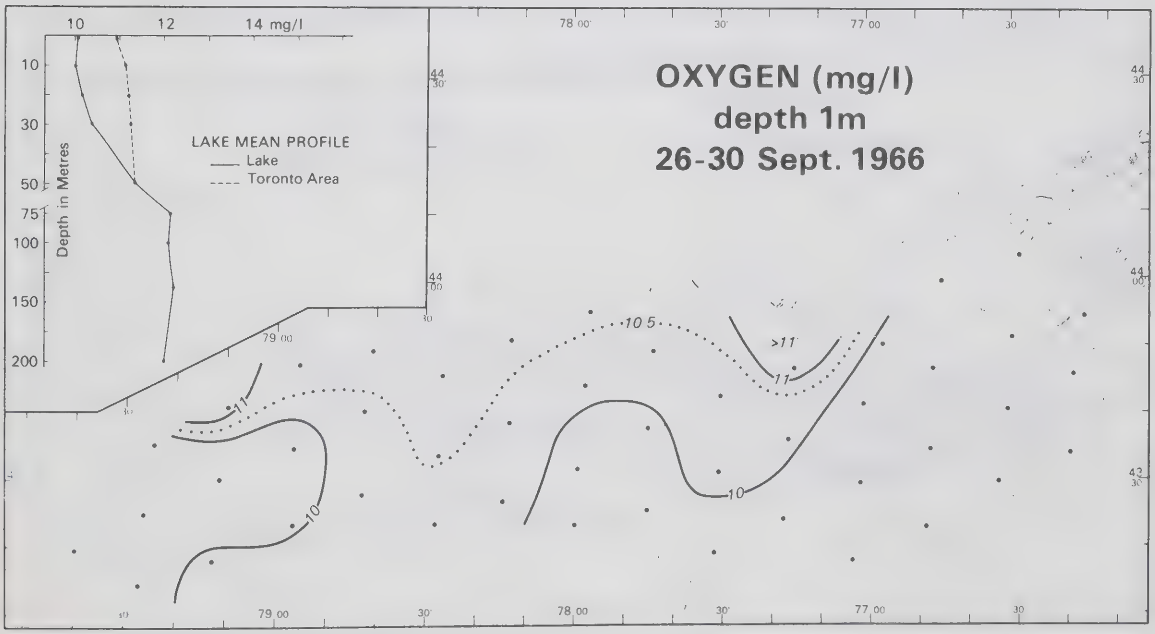

Figure F.52

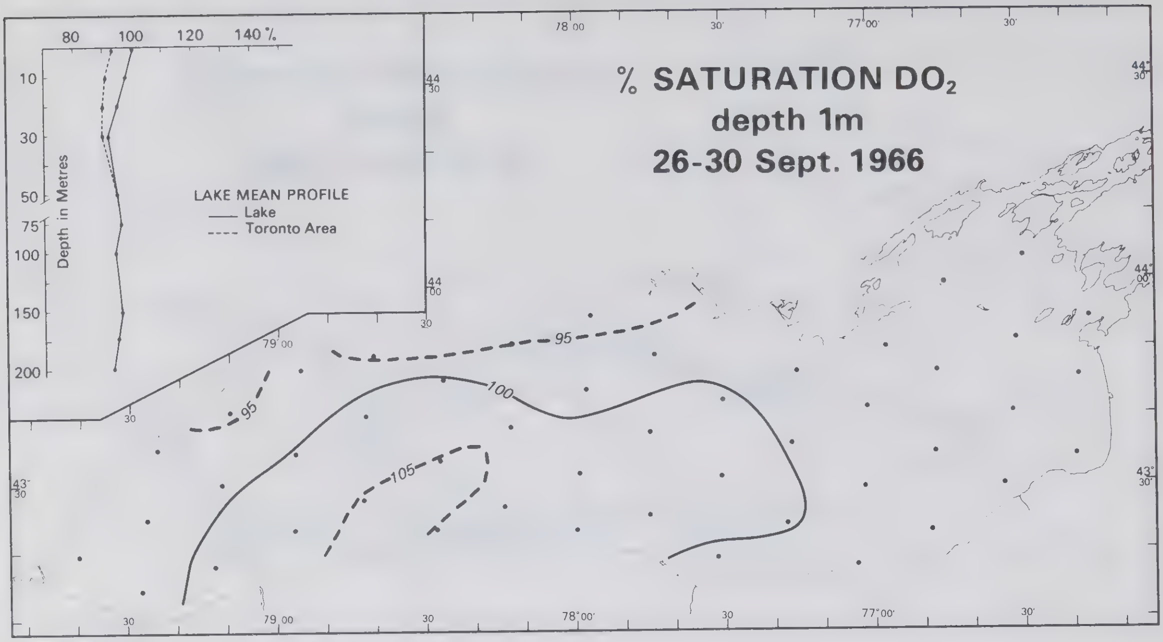

Figure F.53

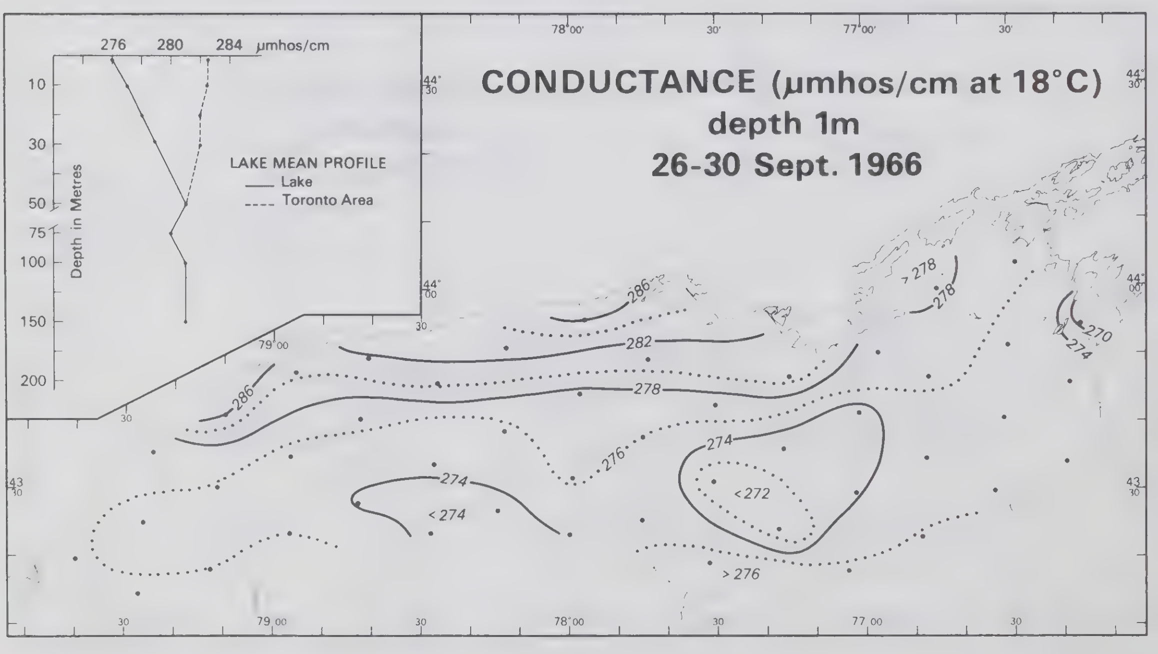

Figure F.54

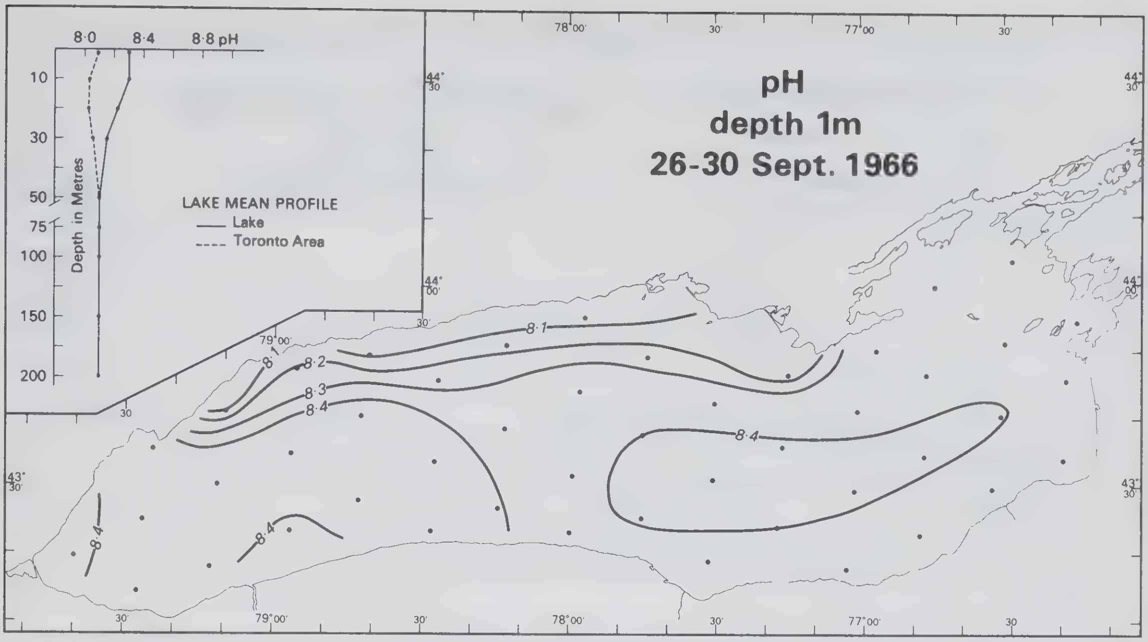

Figure F.55

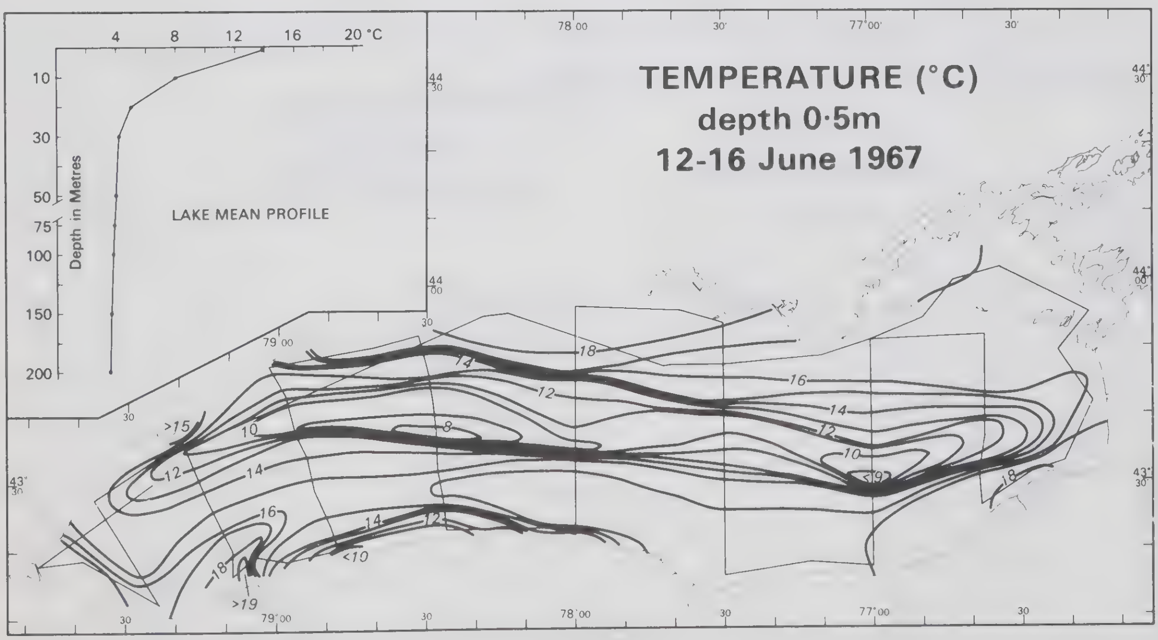

Figure F.56

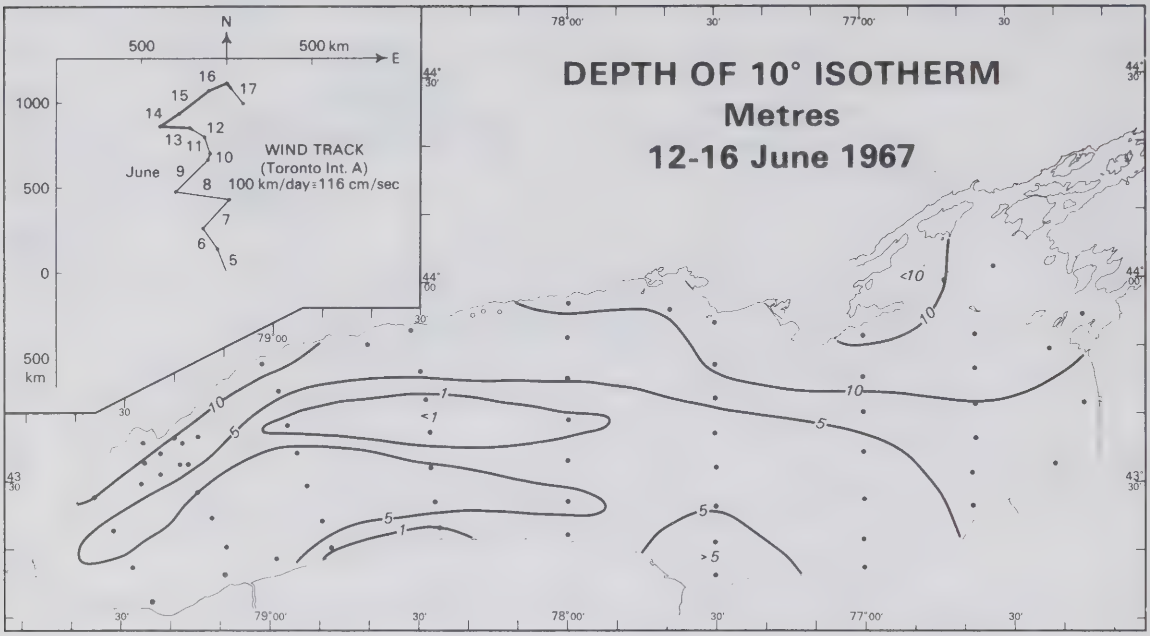

Figure F.57

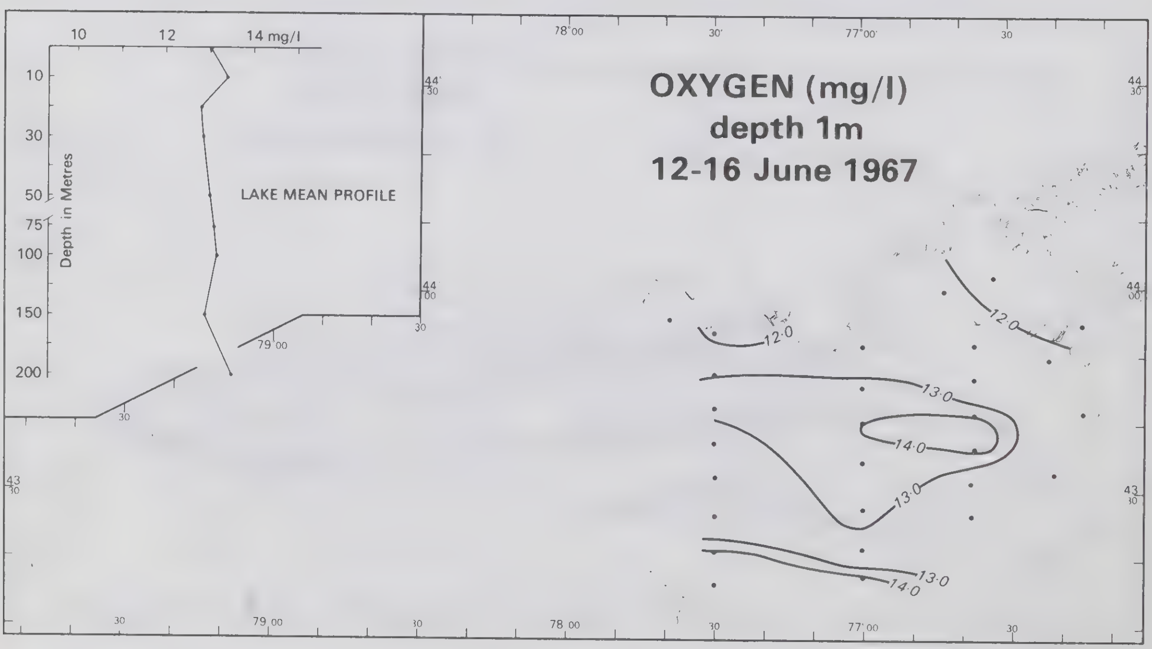

Figure F.58

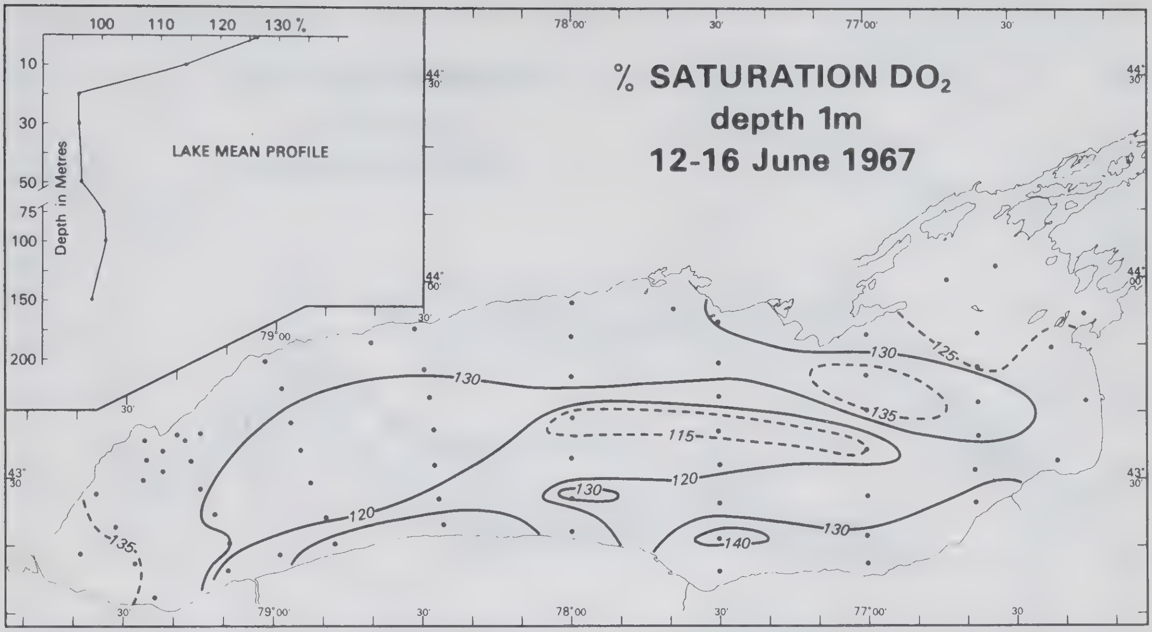

Figure F.59

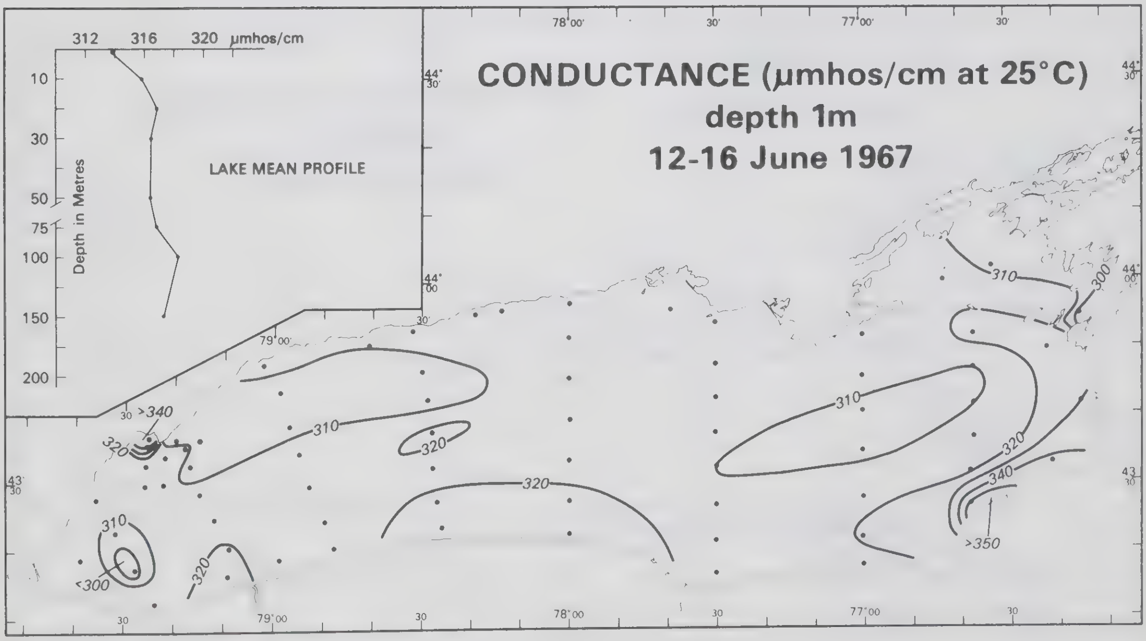

Figure F.60

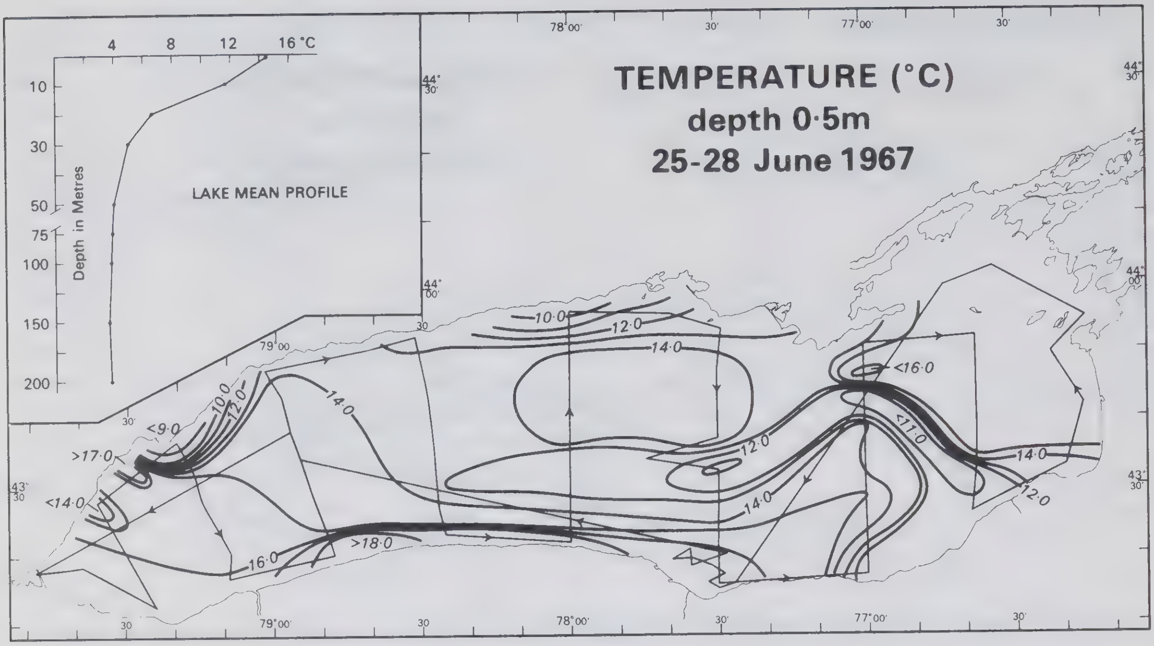

Figure F.61

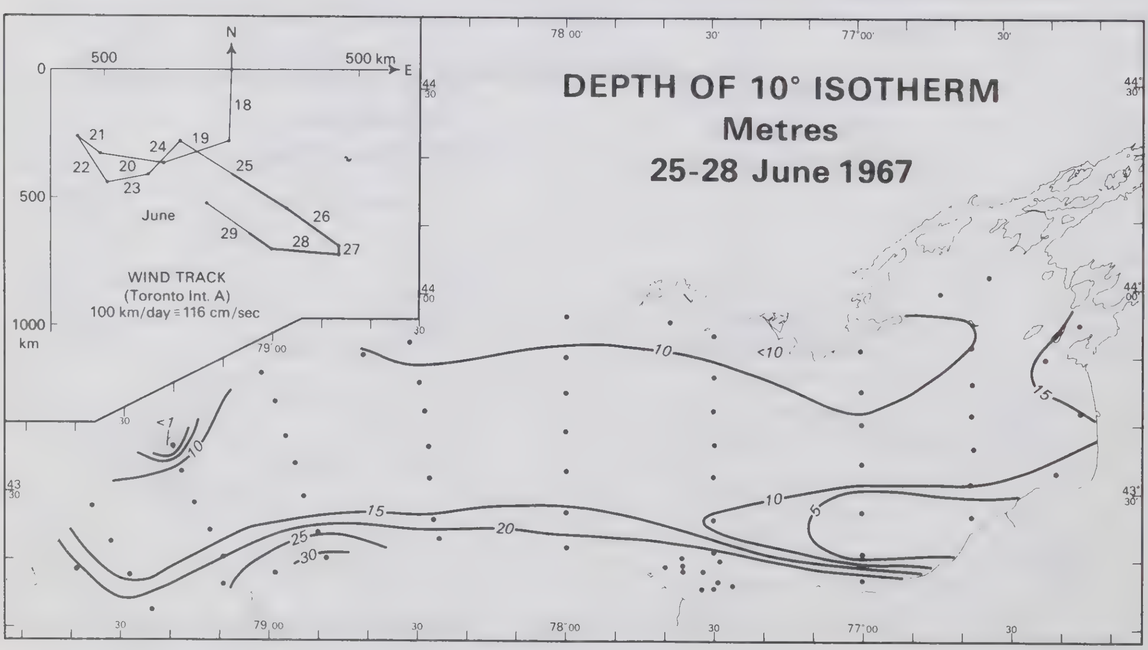

Figure F.62

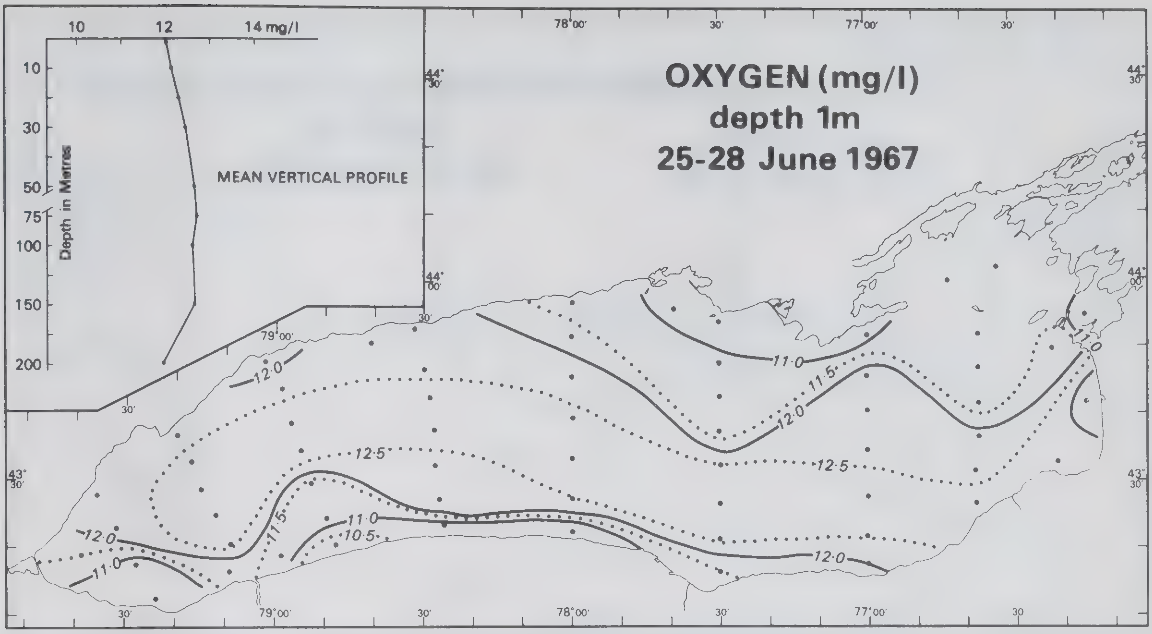

Figure F.63

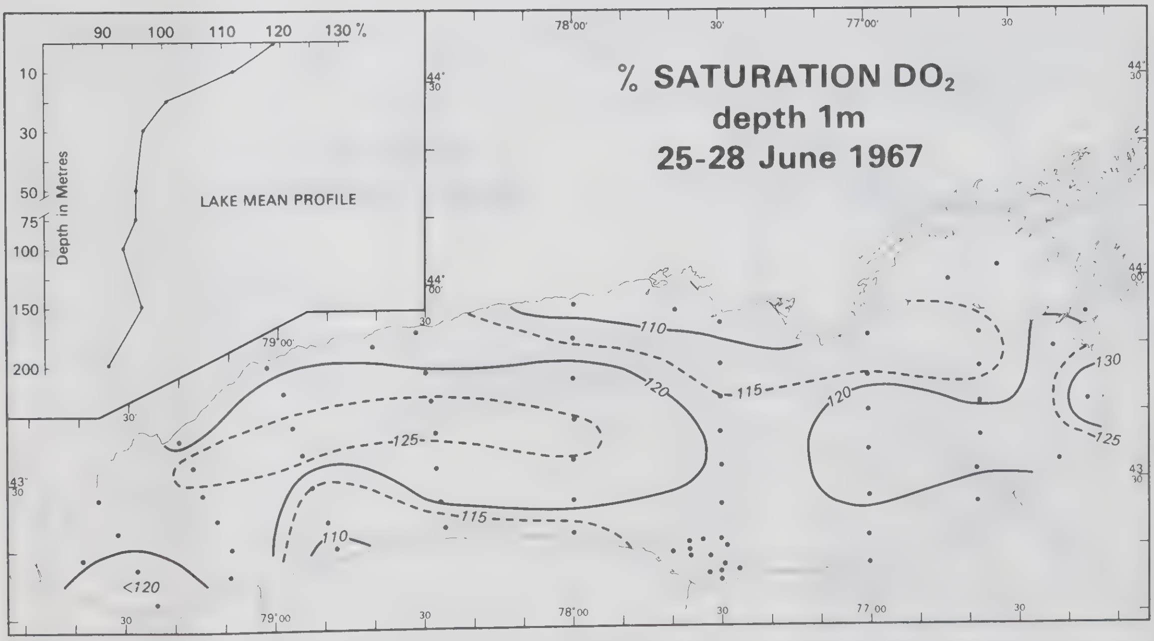

Figure F.64

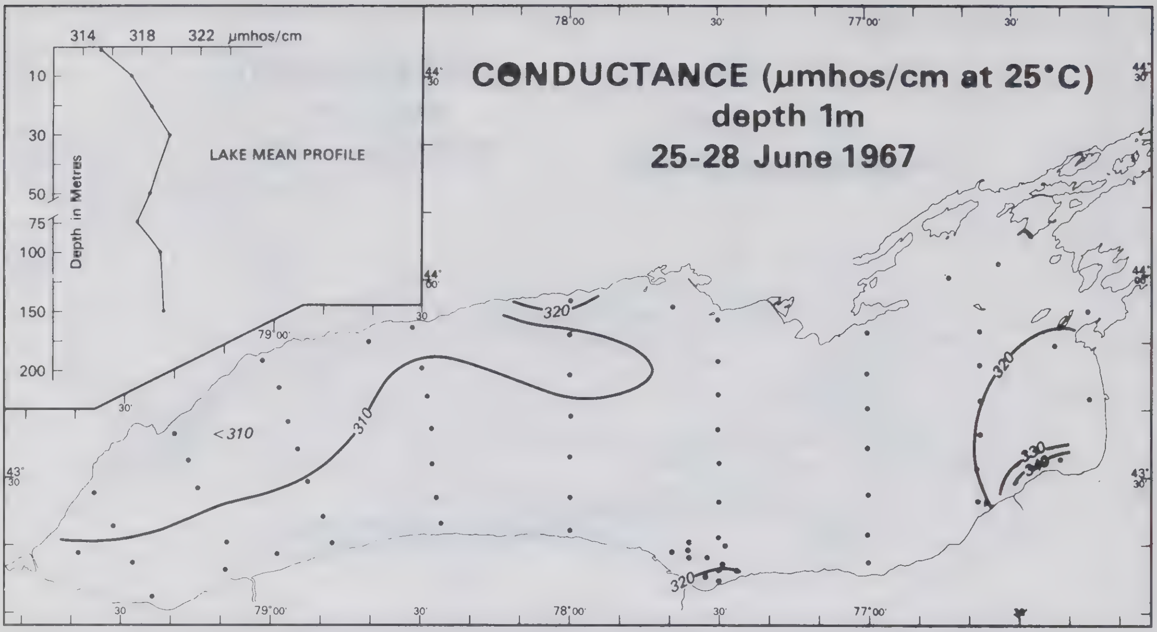

Figure F.65

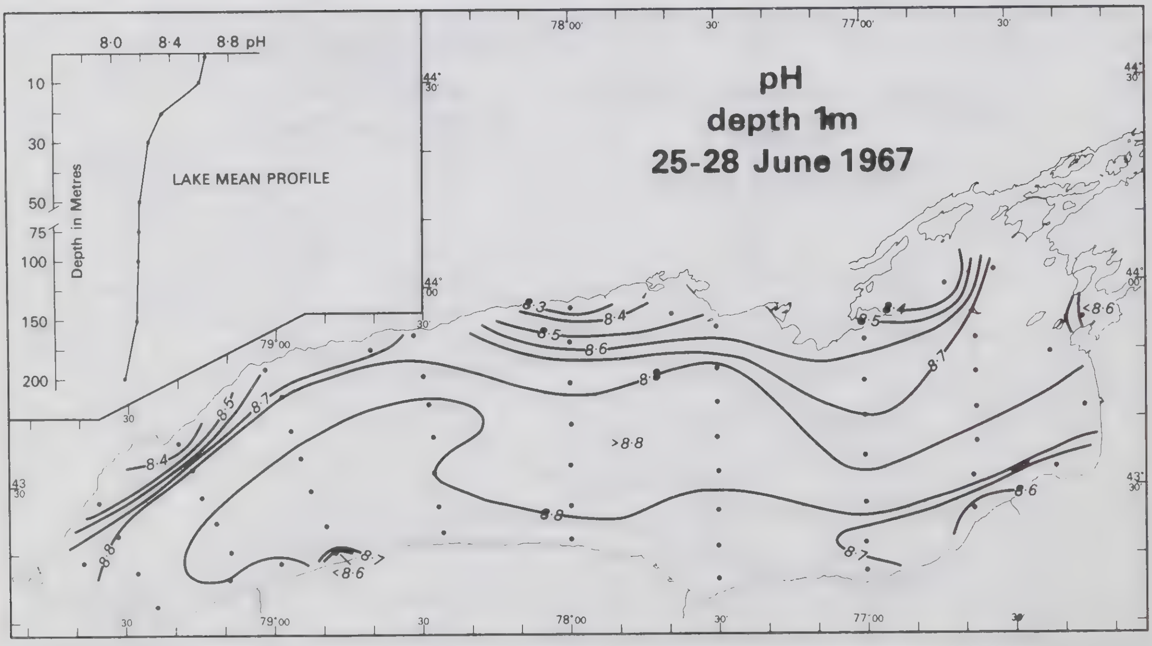

Figure F.66

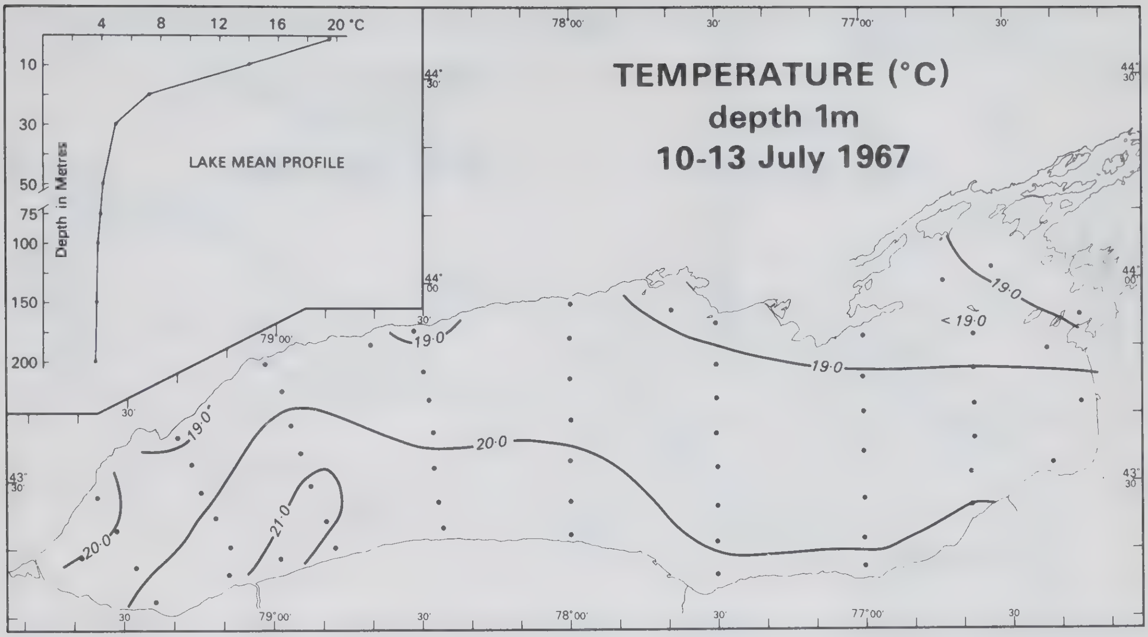

Figure F.67

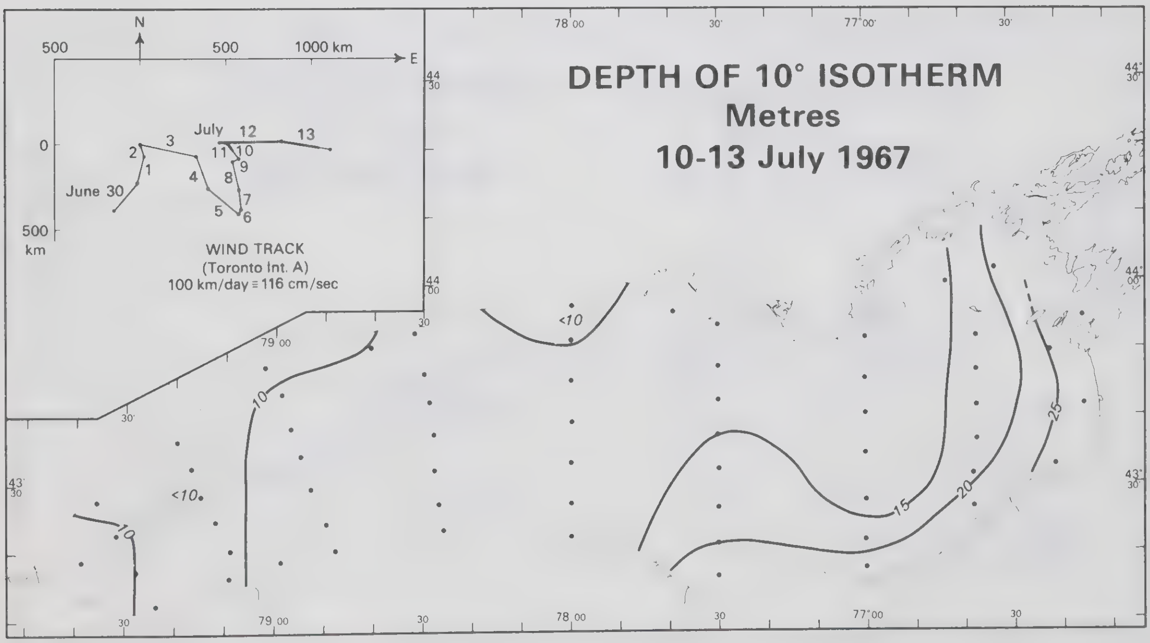

Figure F.68

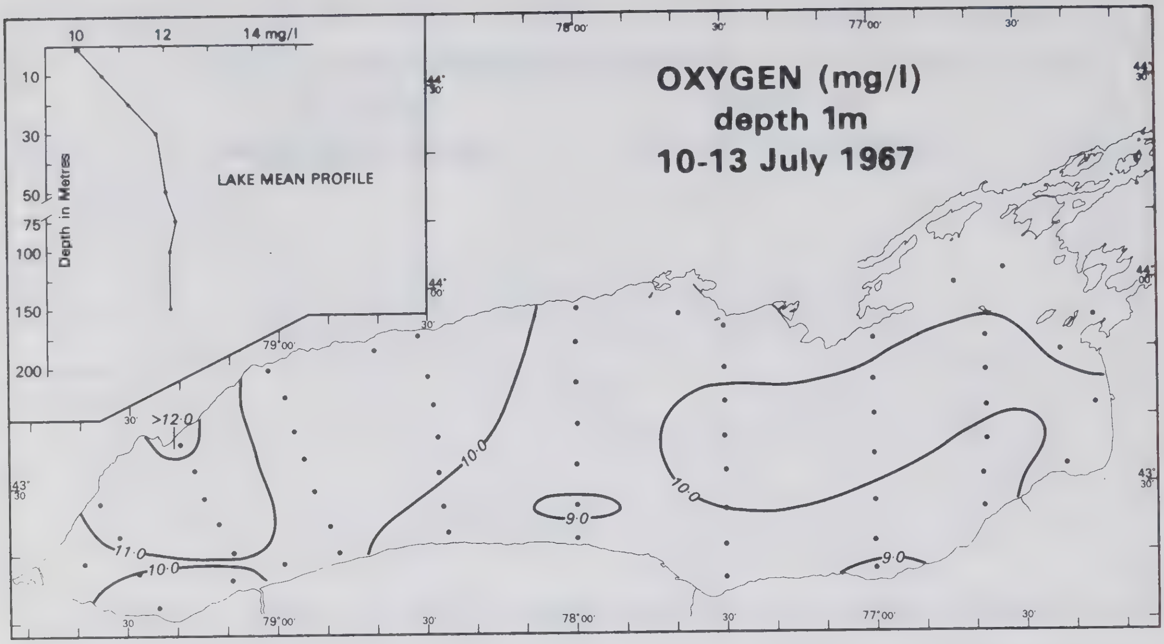

Figure F.69

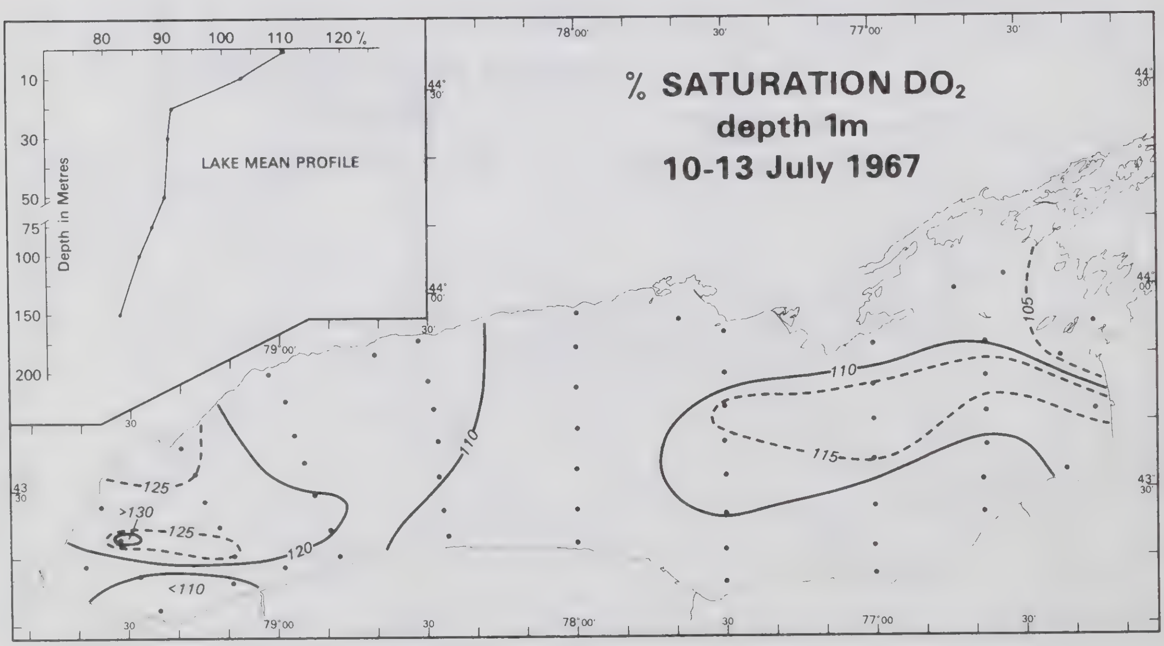

Figure F.70

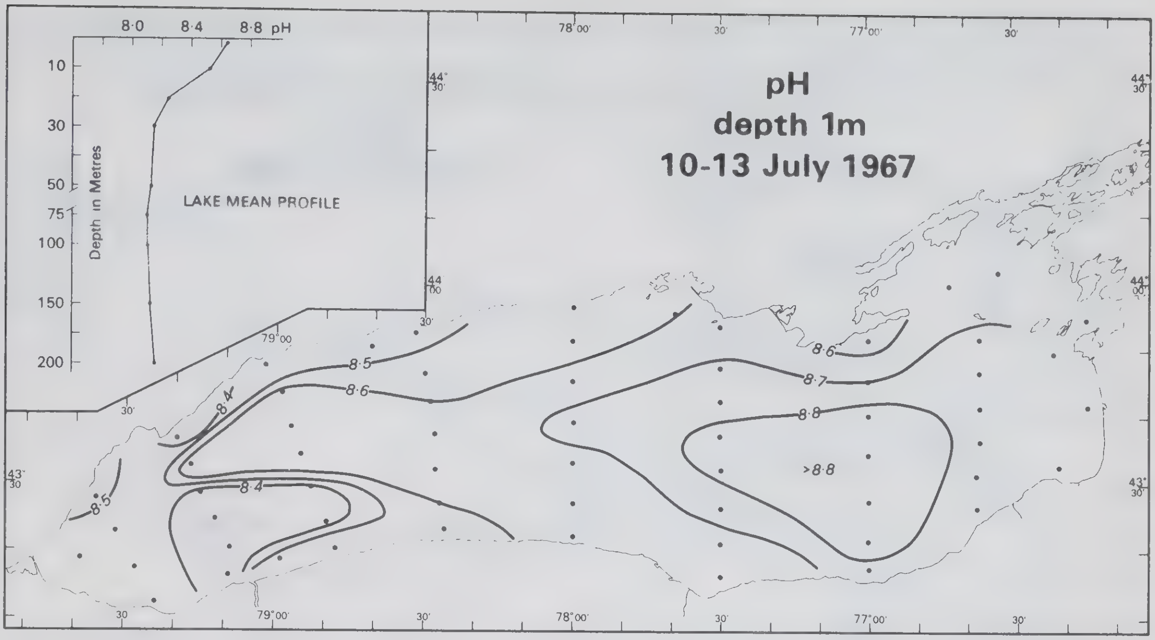

Figure F.71

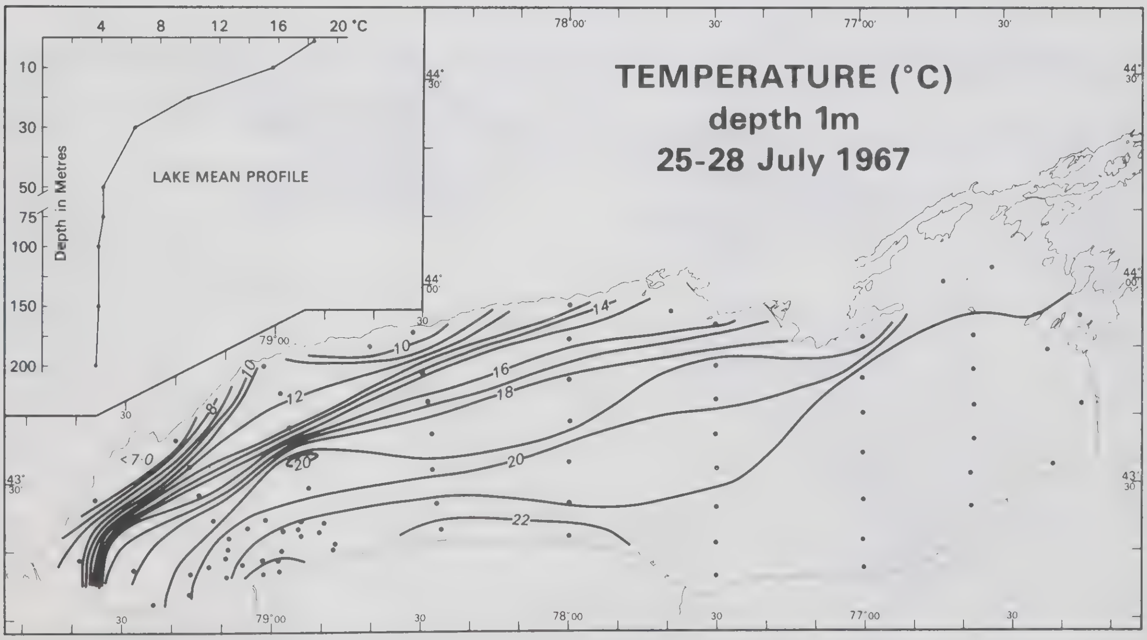

Figure F.72

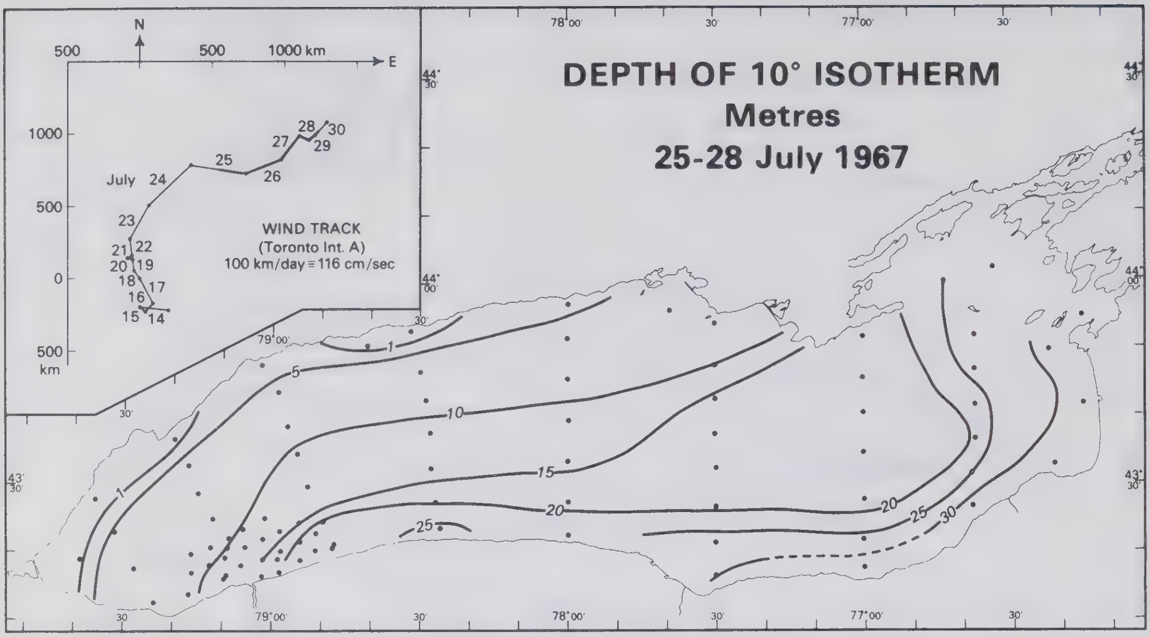

Figure F.73

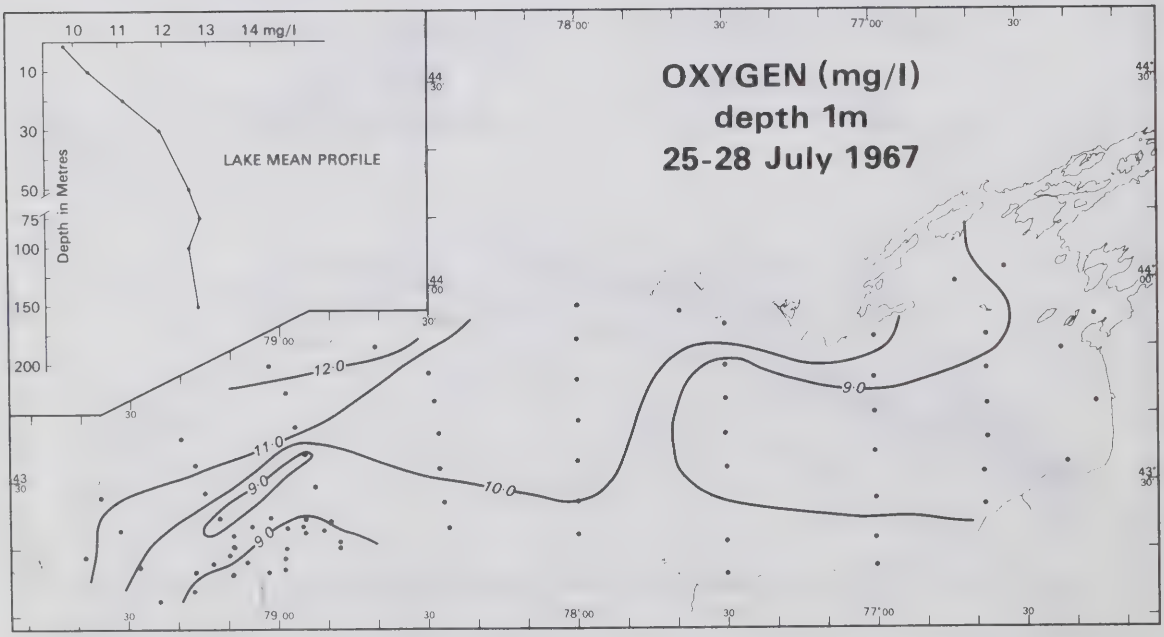

Figure F.74

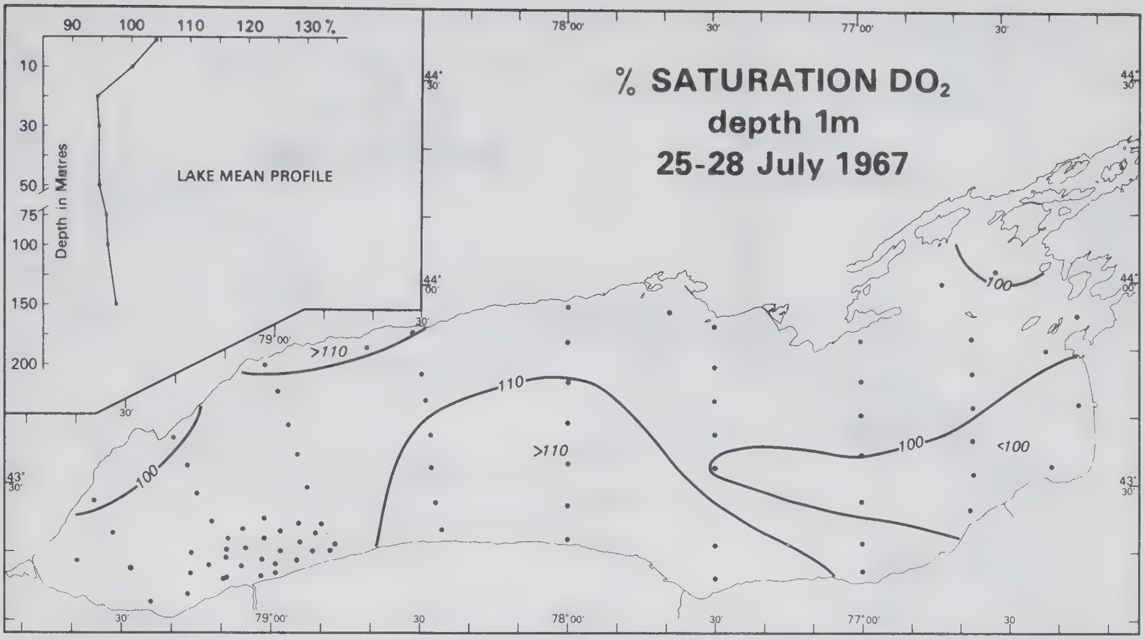

Figure F.75

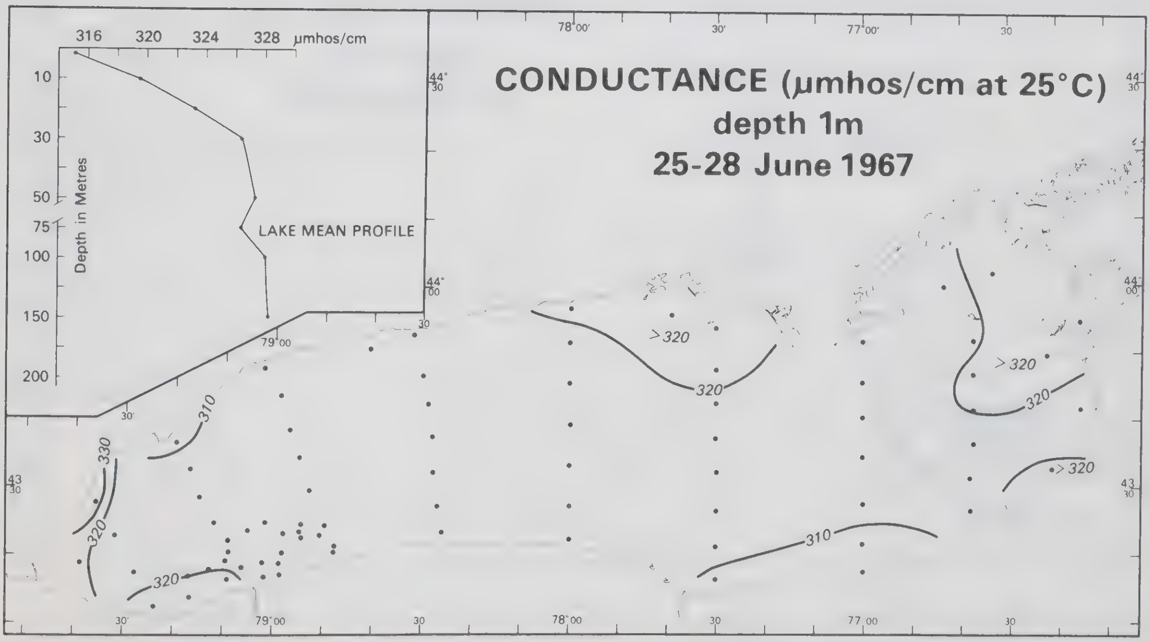

Figure F.76

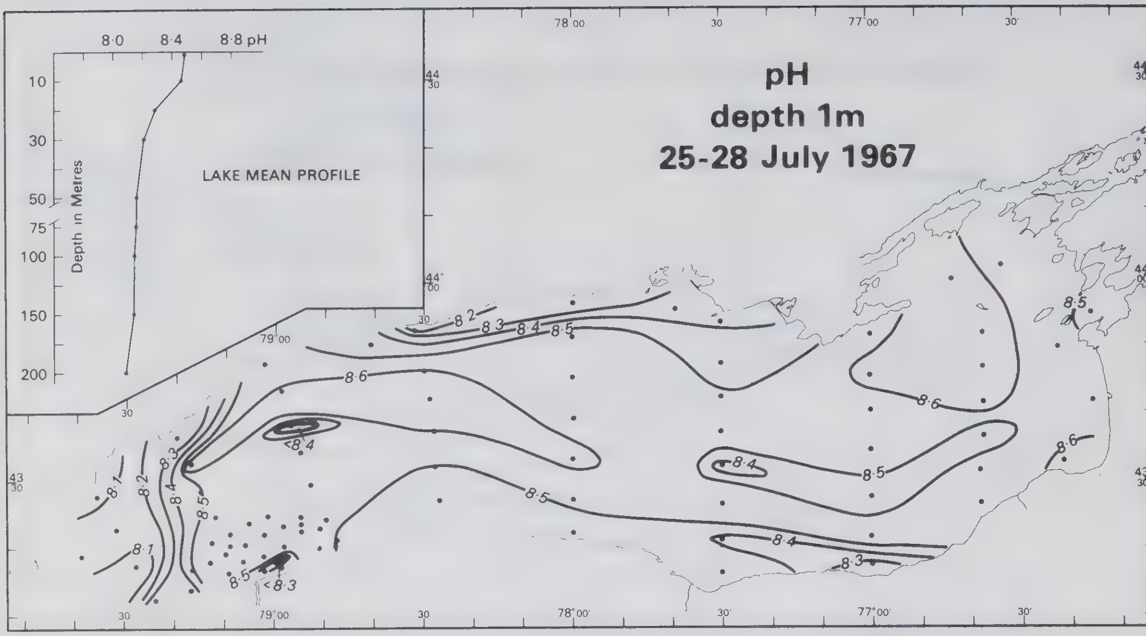

Figure F.77

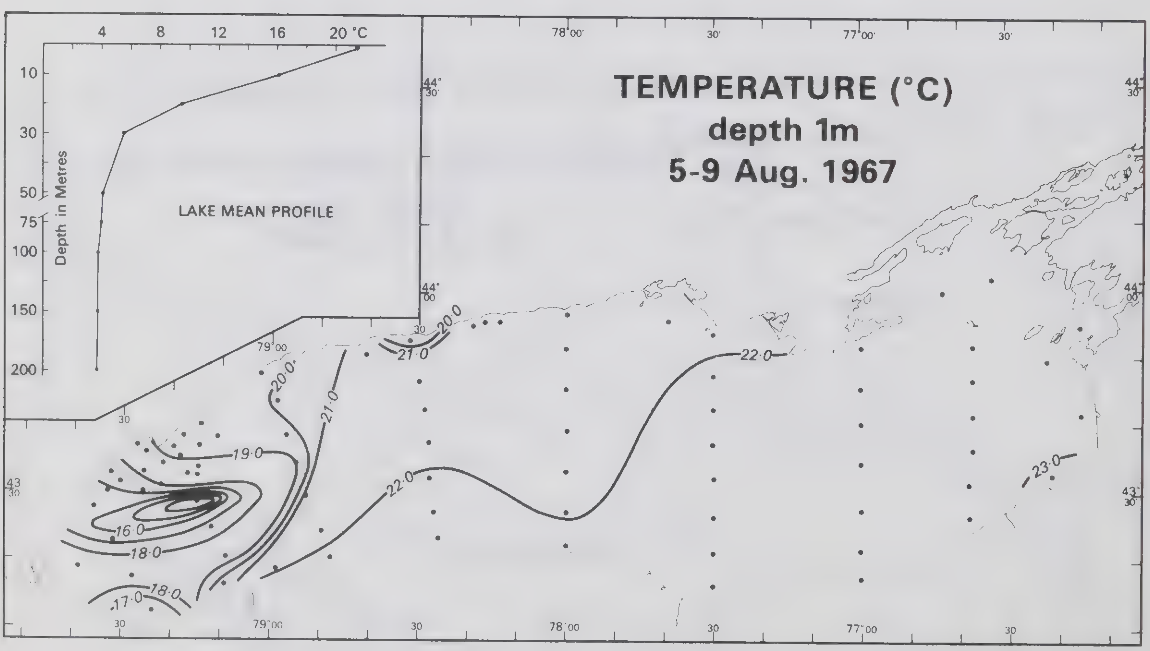

Figure F.78

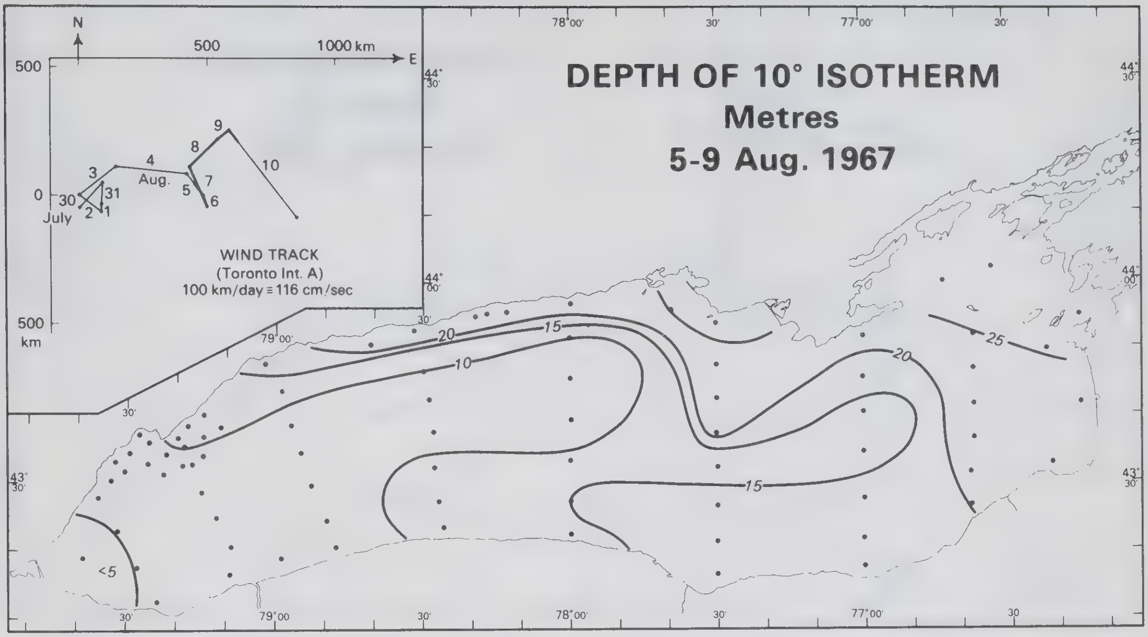

Figure F.79

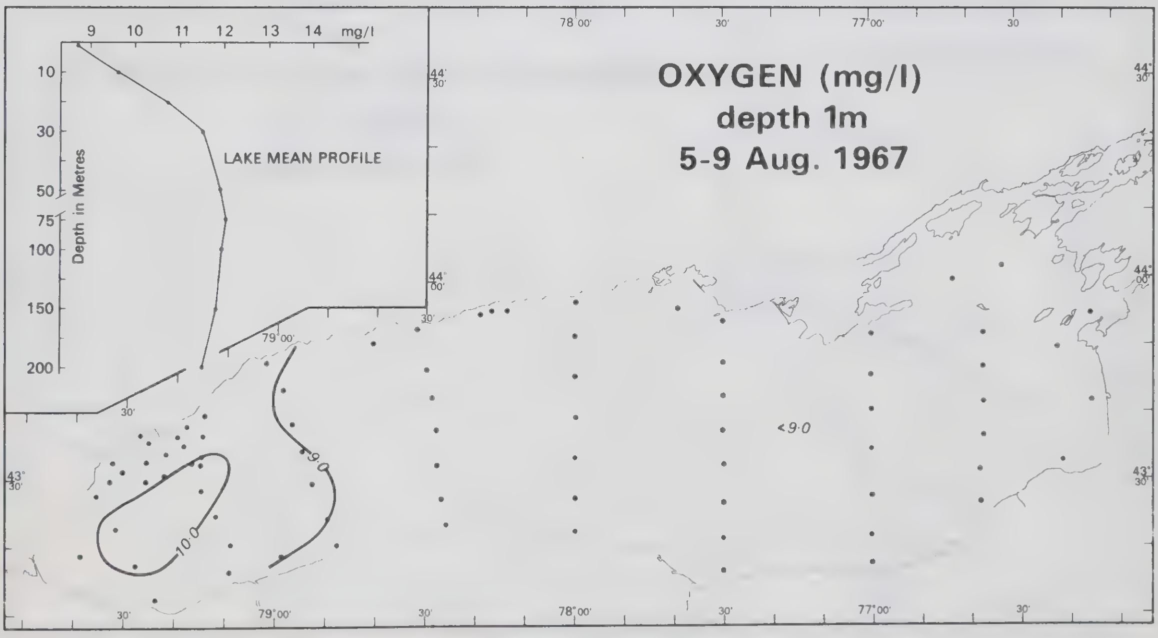

Figure F.80

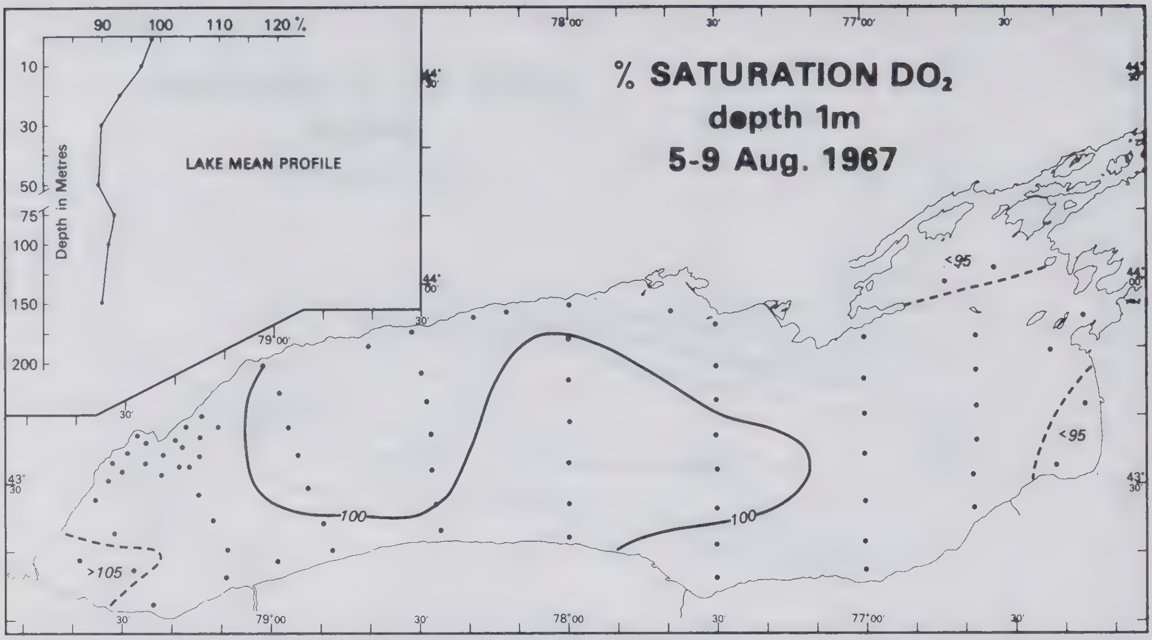

Figure F.81

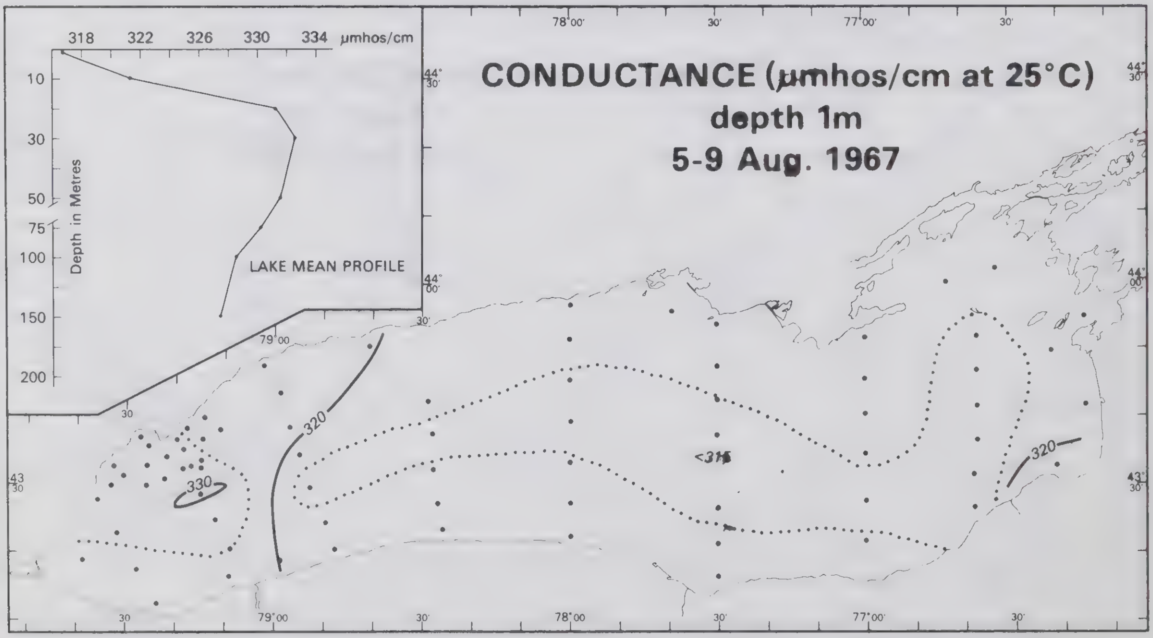

Figure F.82

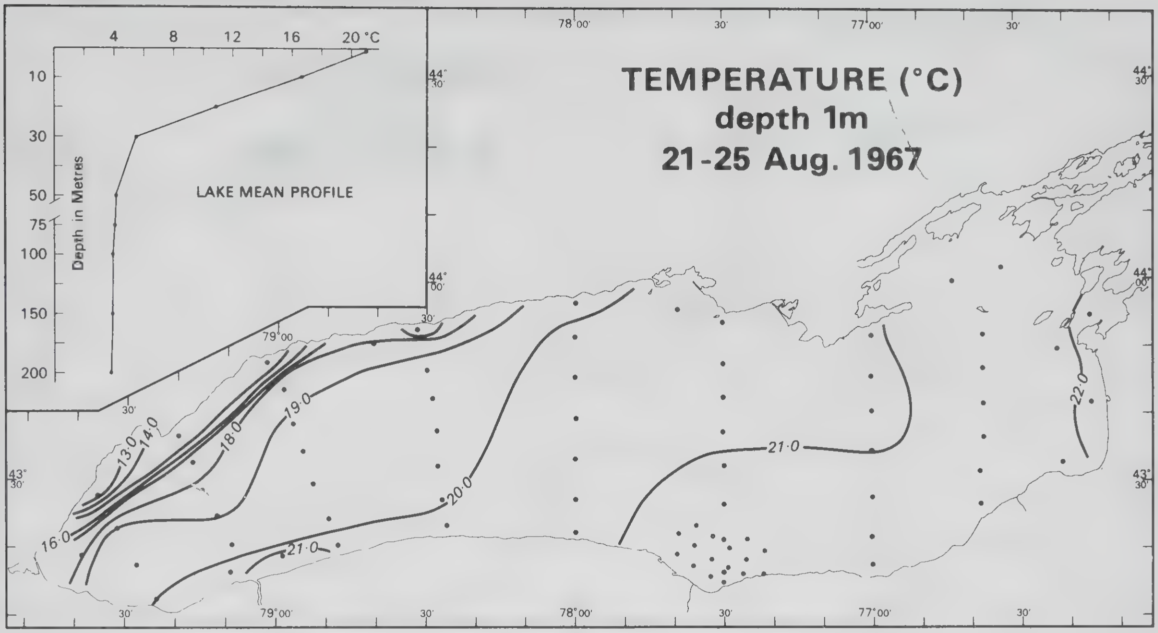

Figure F.83

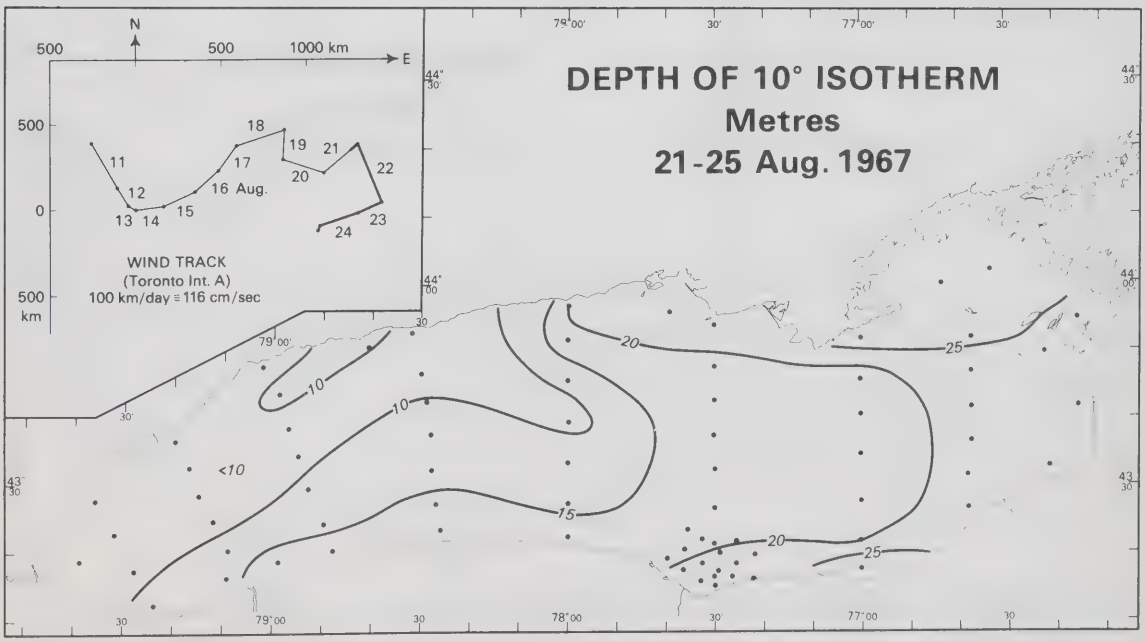

Figure F.84

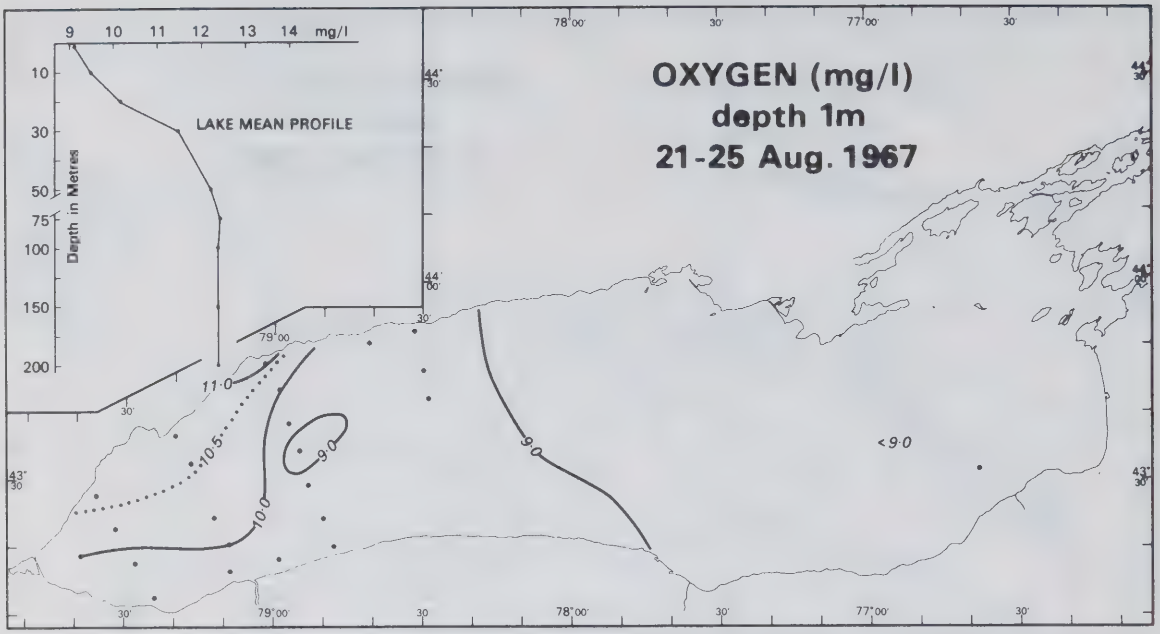

Figure F.85

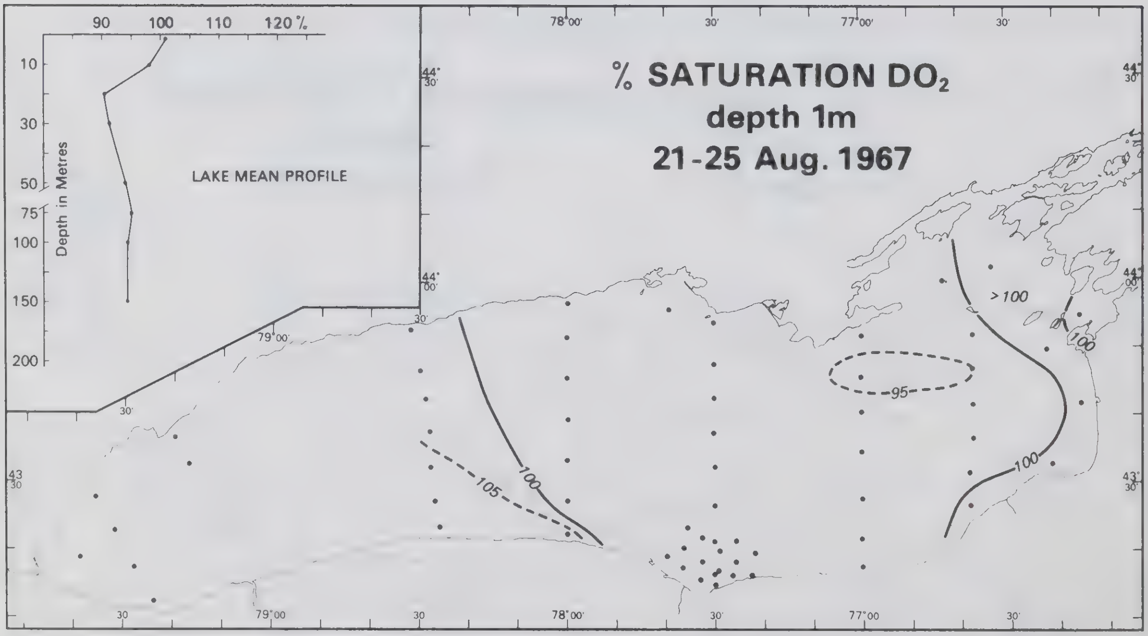

Figure F.86

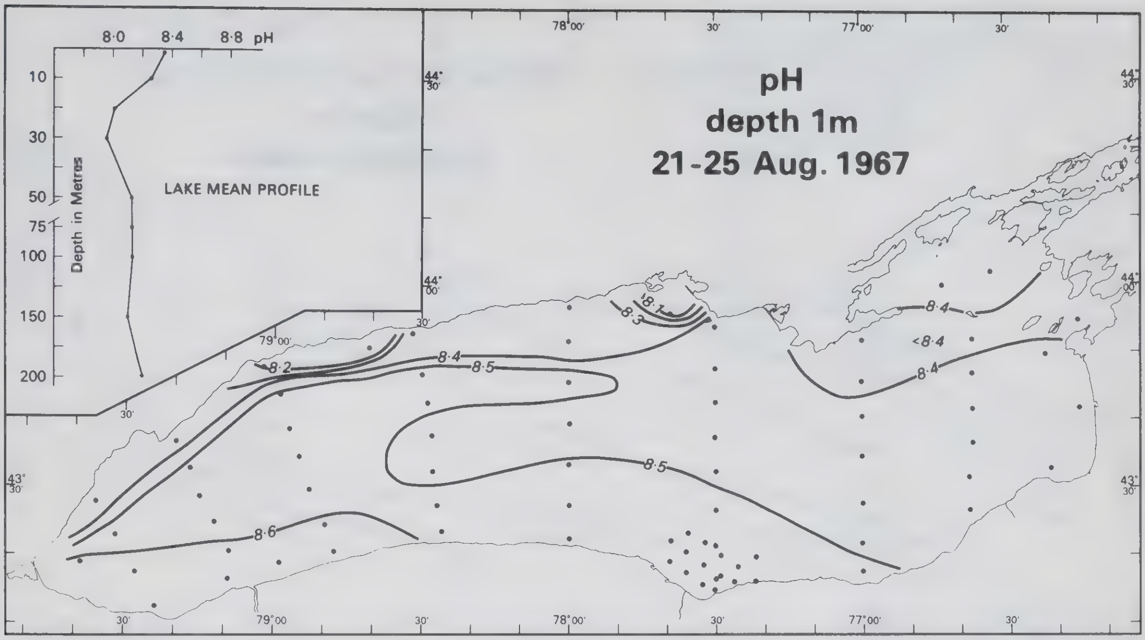

Figure F.87

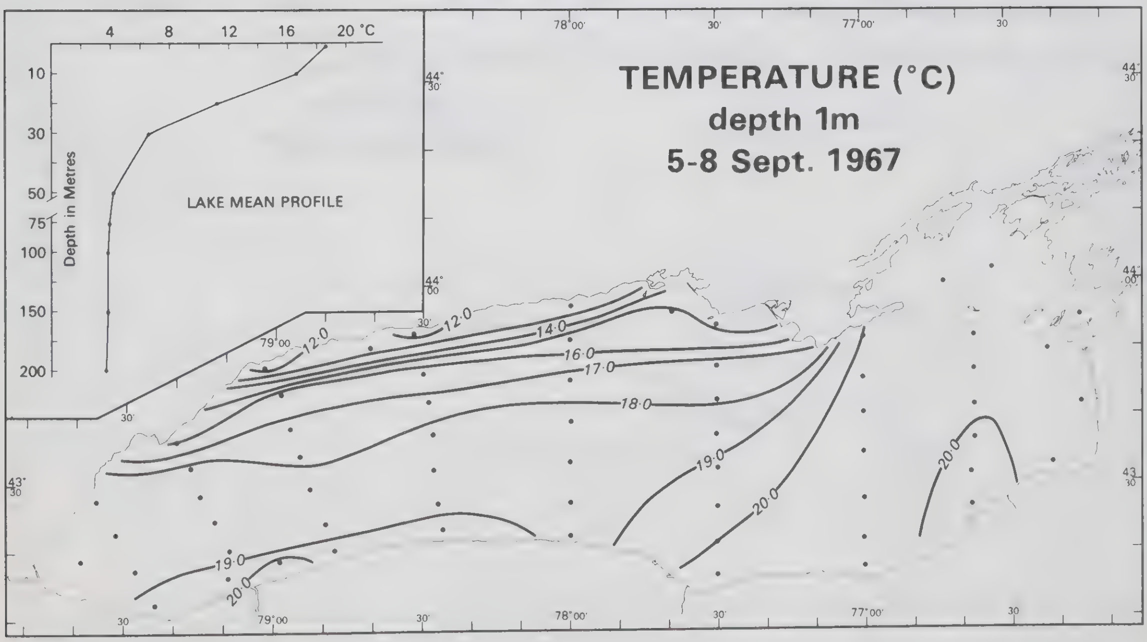

Figure F.88

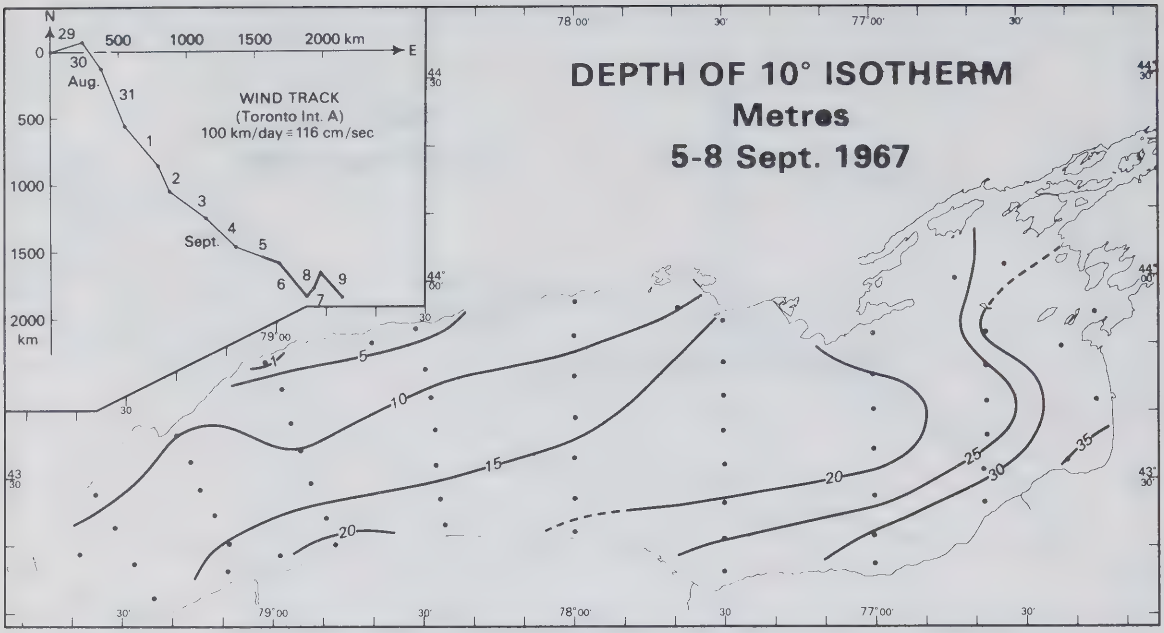

Figure F.89

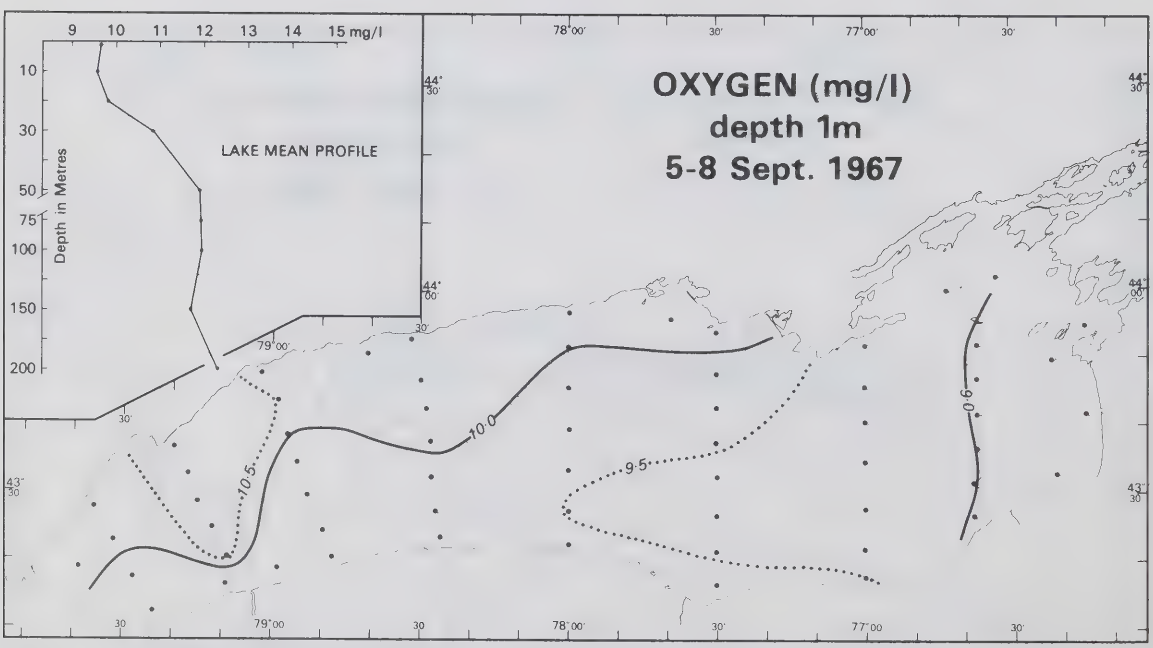

Figure F.90

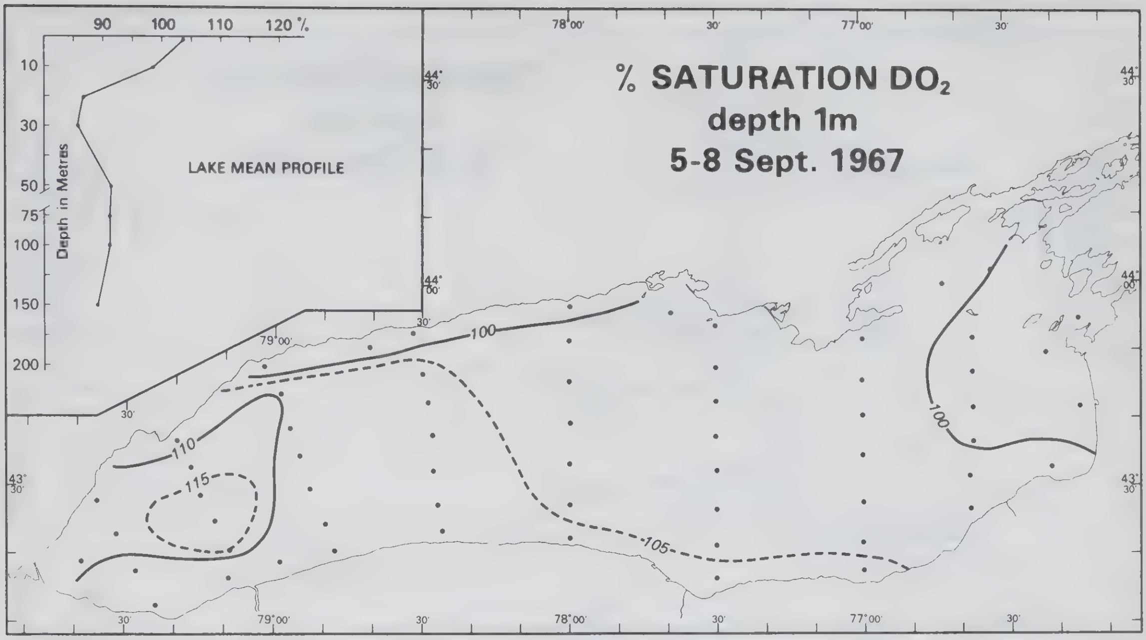

Figure F.91

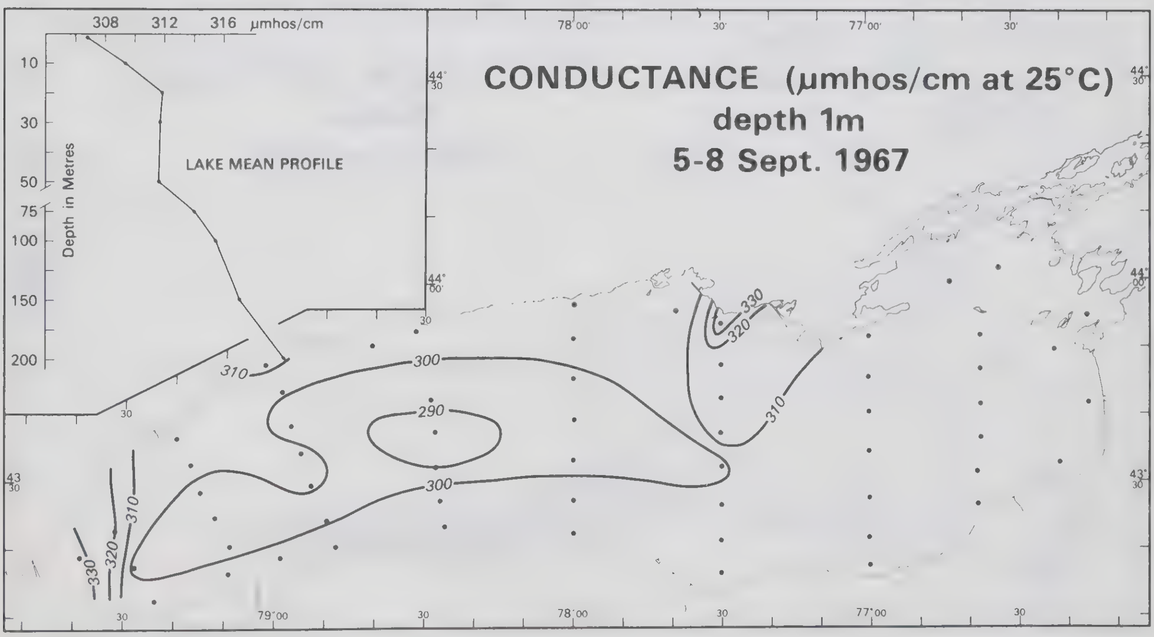

Figure F.92

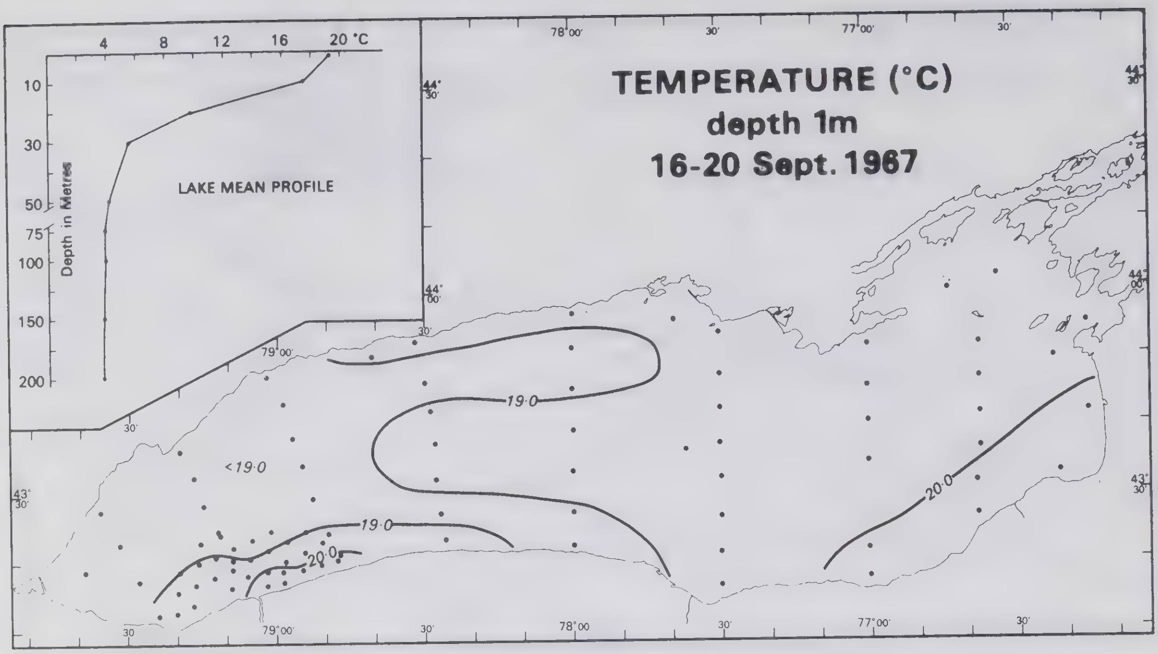

Figure F.93

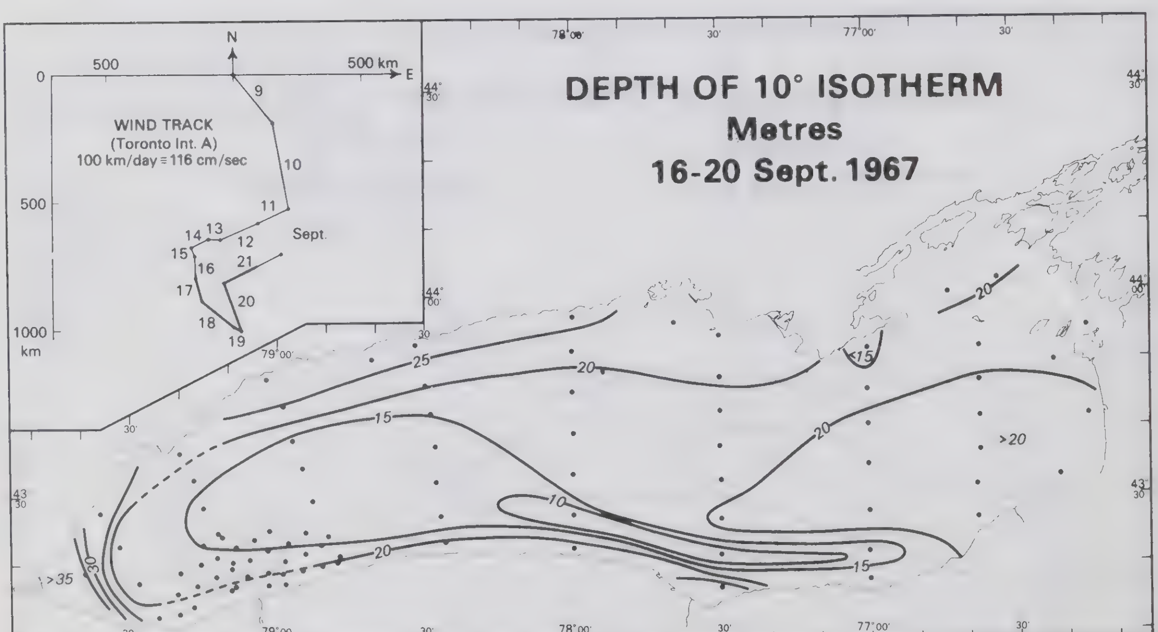

Figure F.94

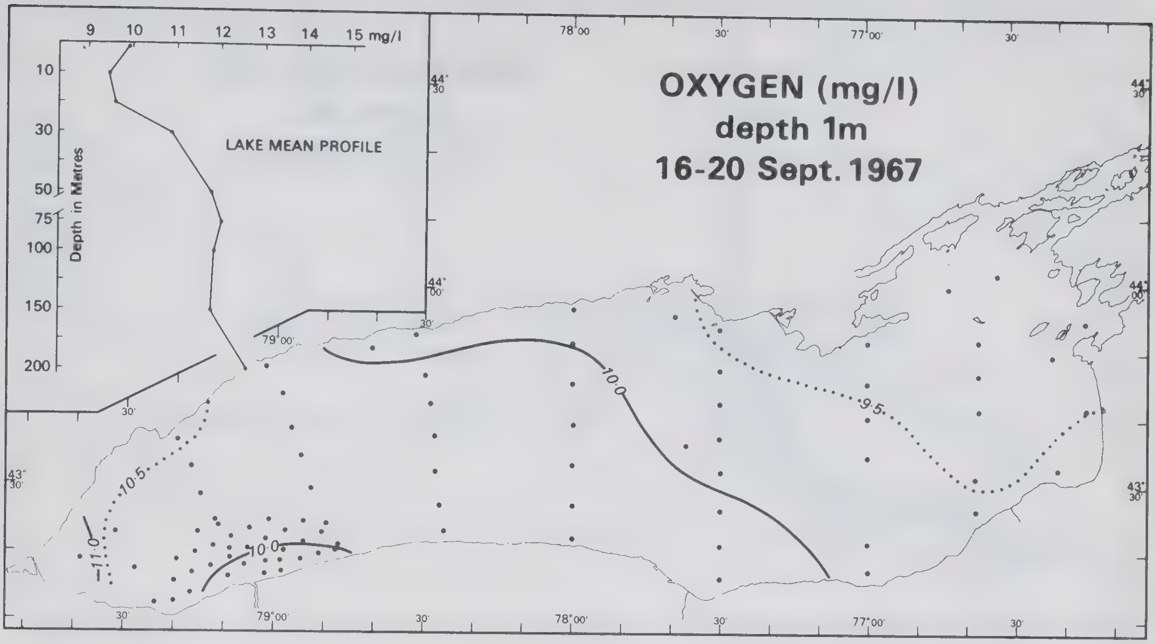

Figure F.95

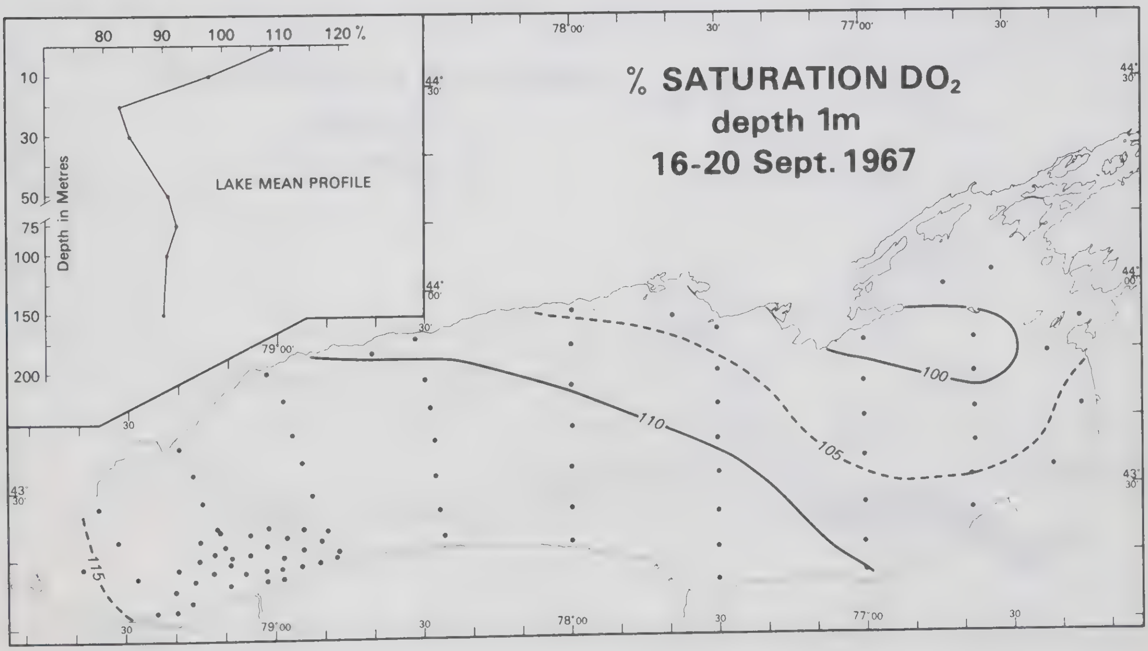

Figure F.96

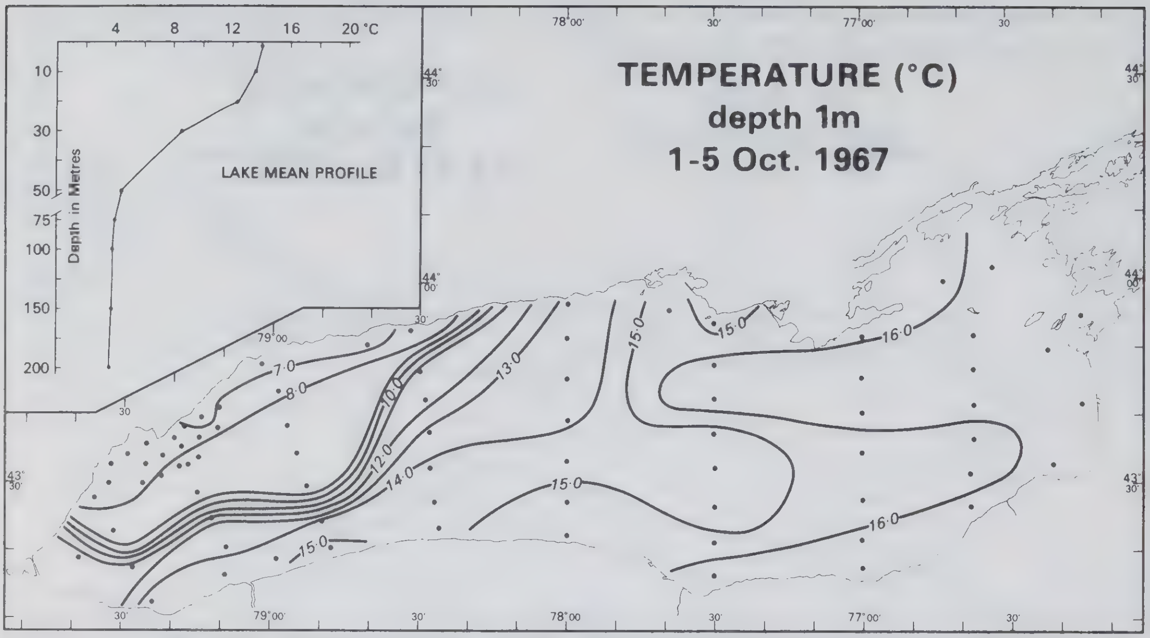

Figure F.97

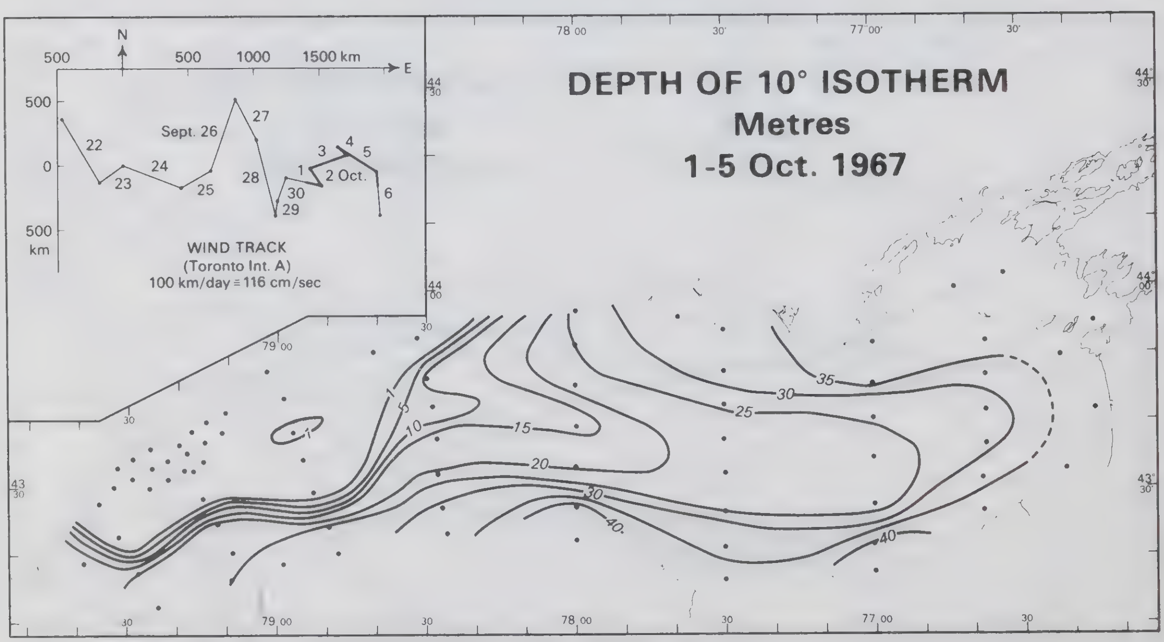

Figure F.98

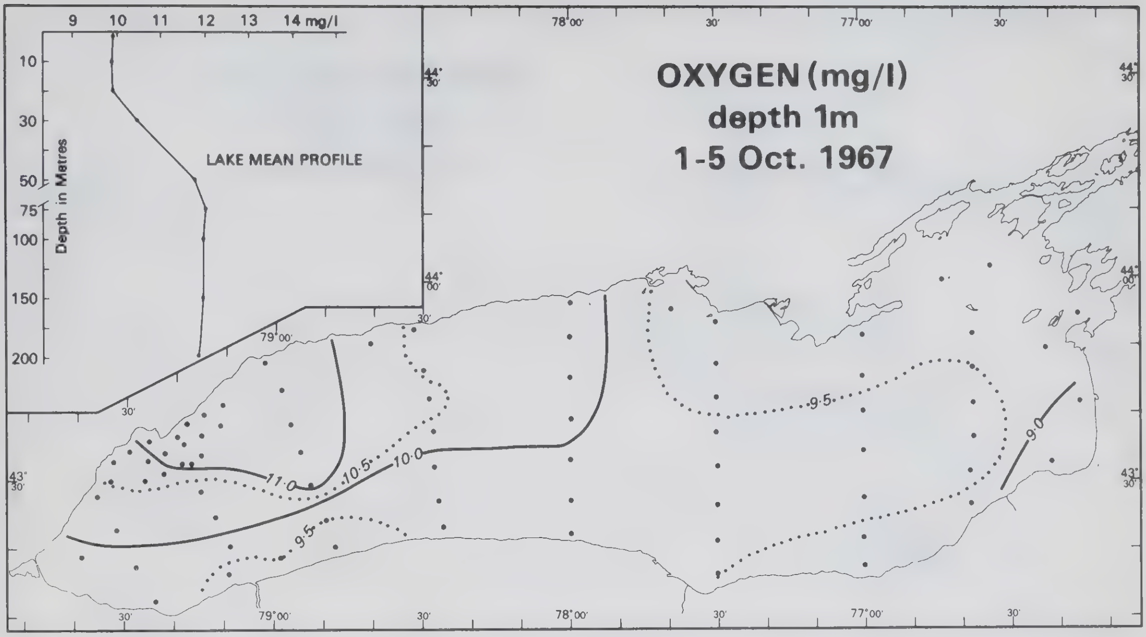

Figure F.99

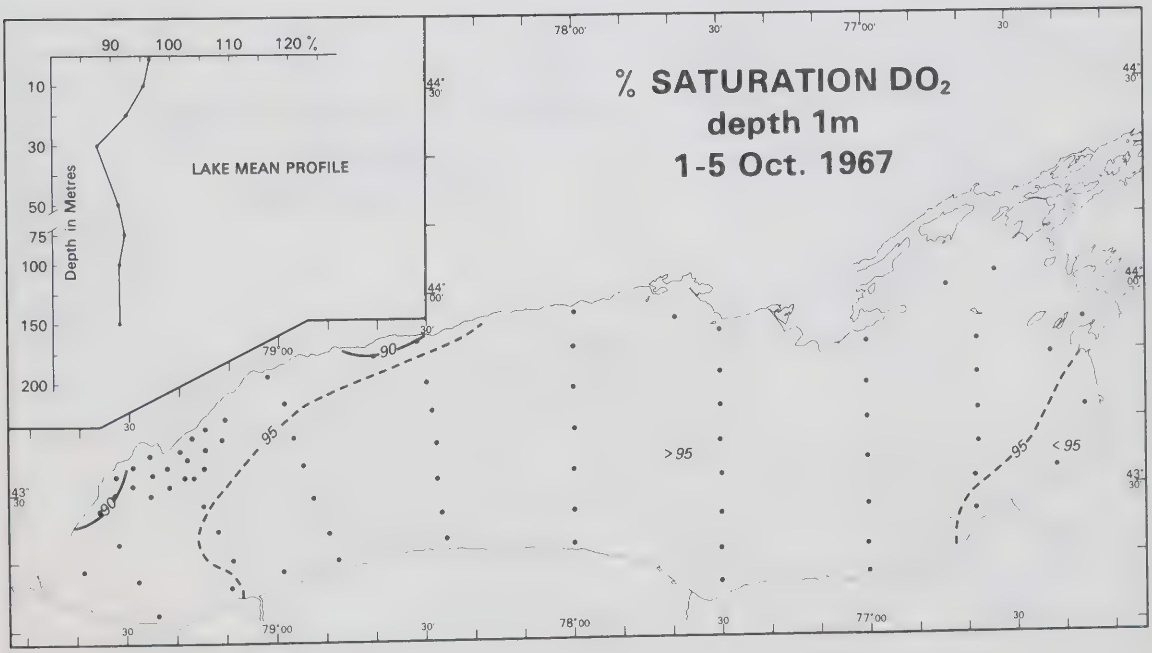

Figure F.100

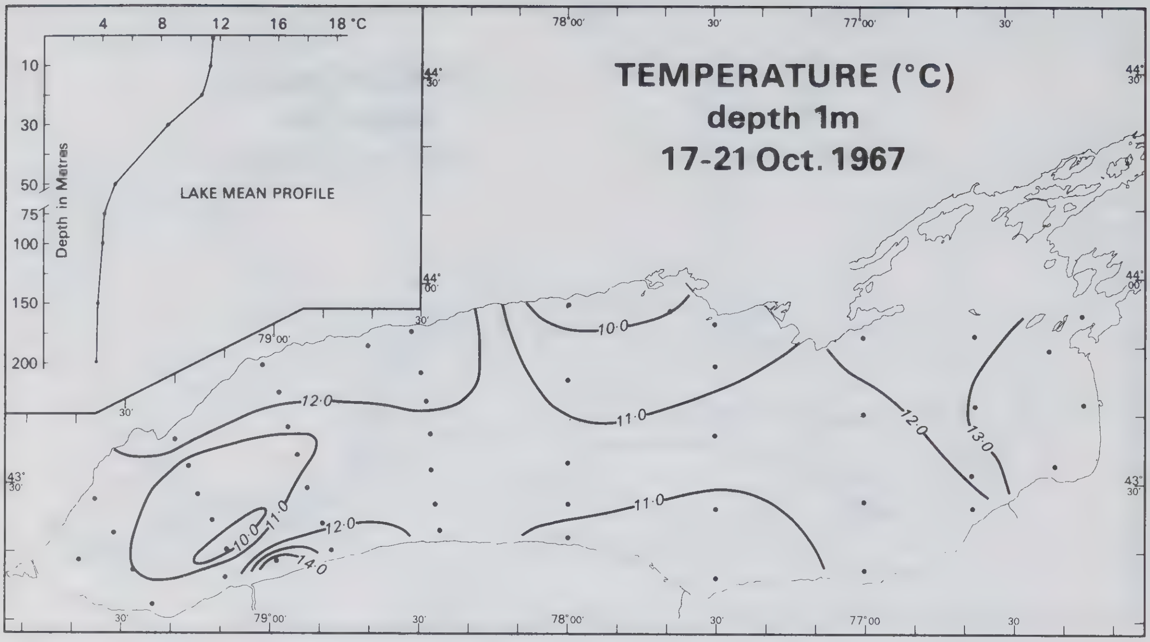

Figure F.101

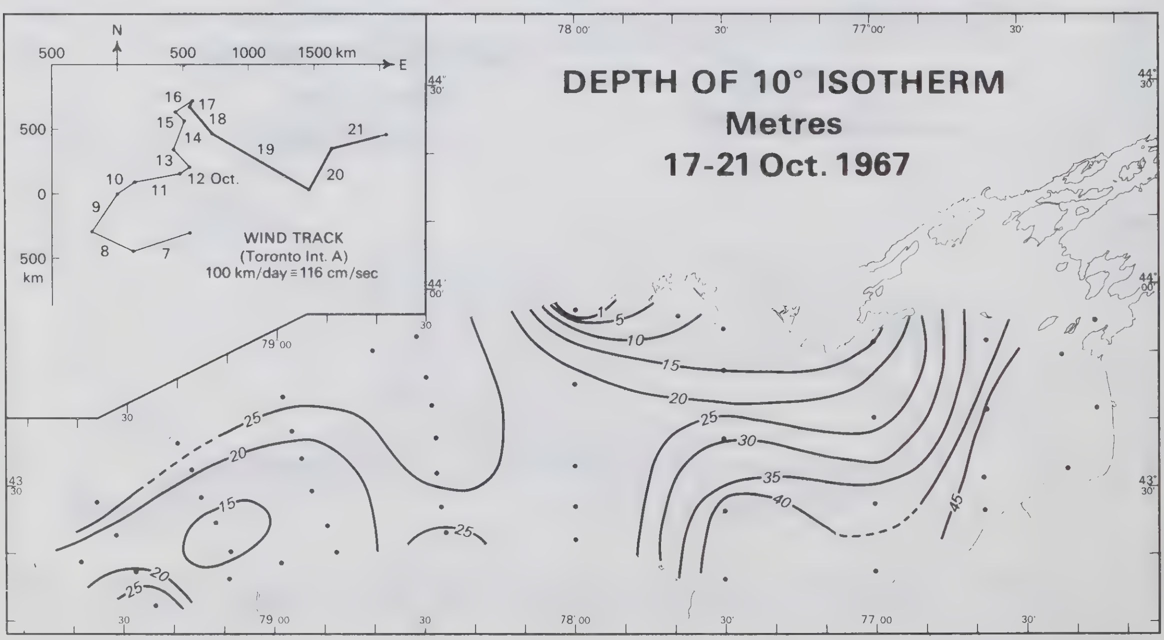

Figure F.102

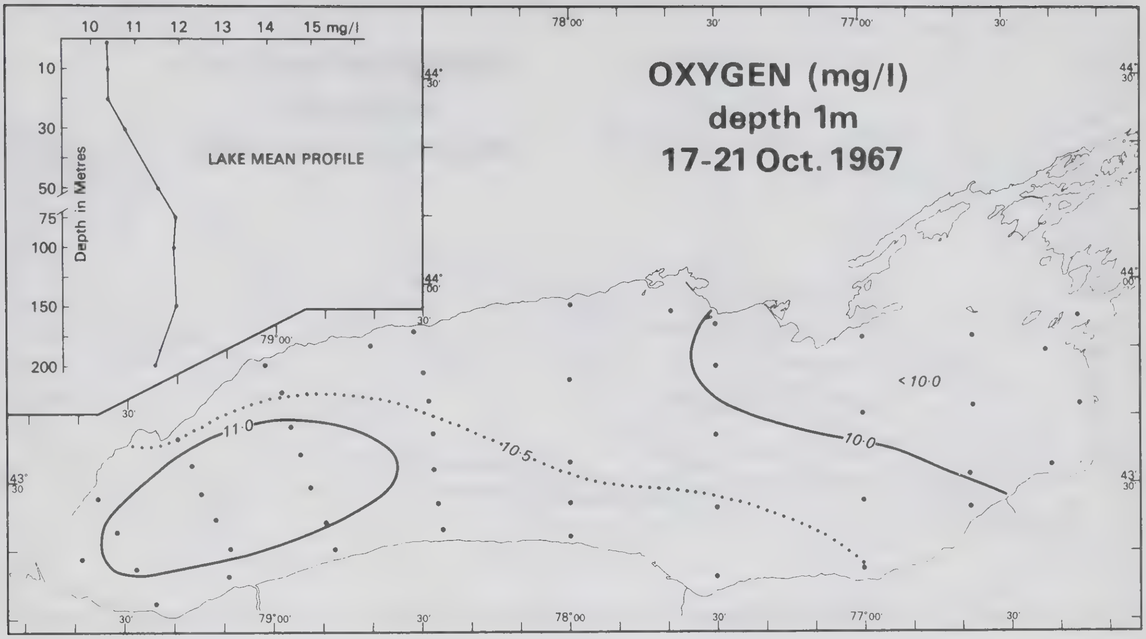

Figure F.103

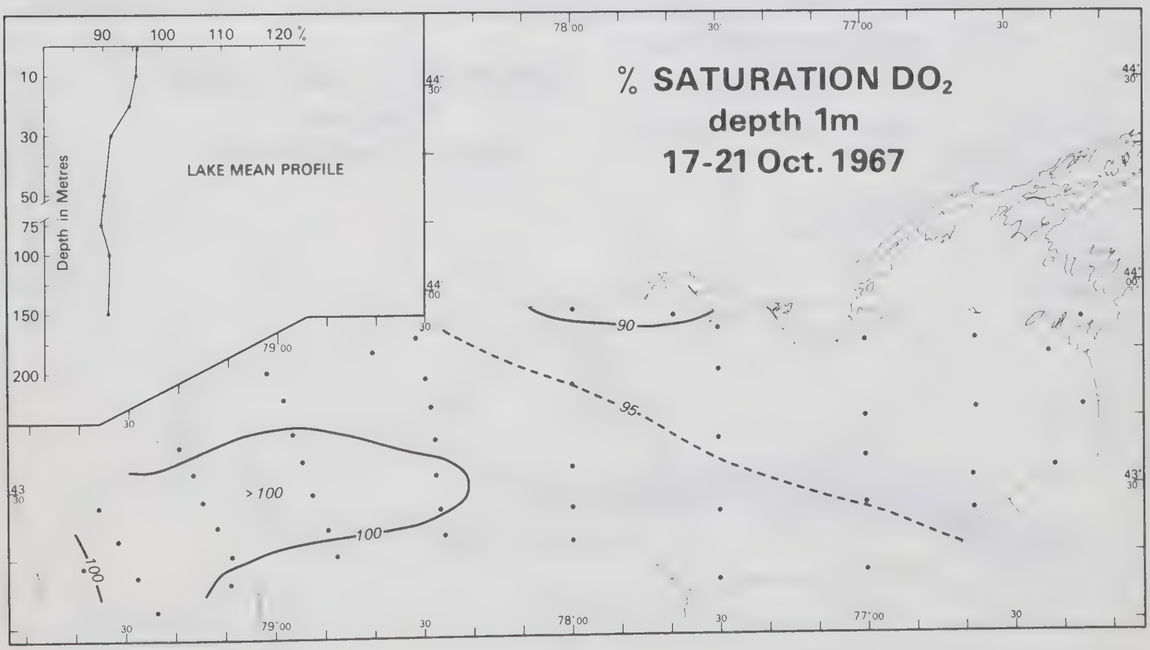

Figure F.104

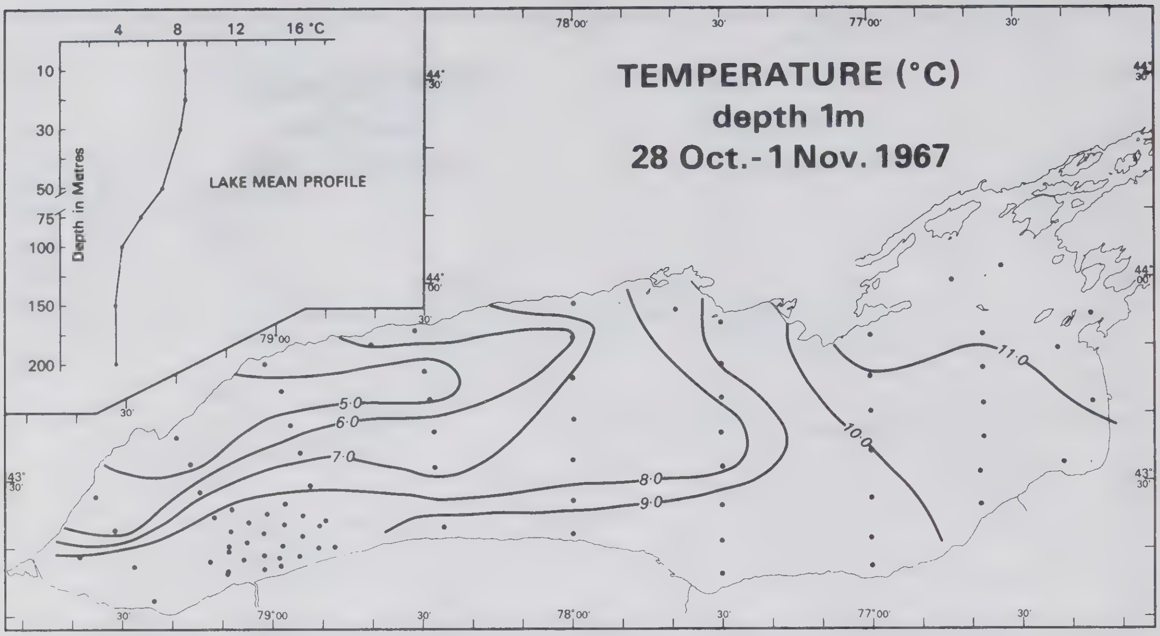

Figure F.105

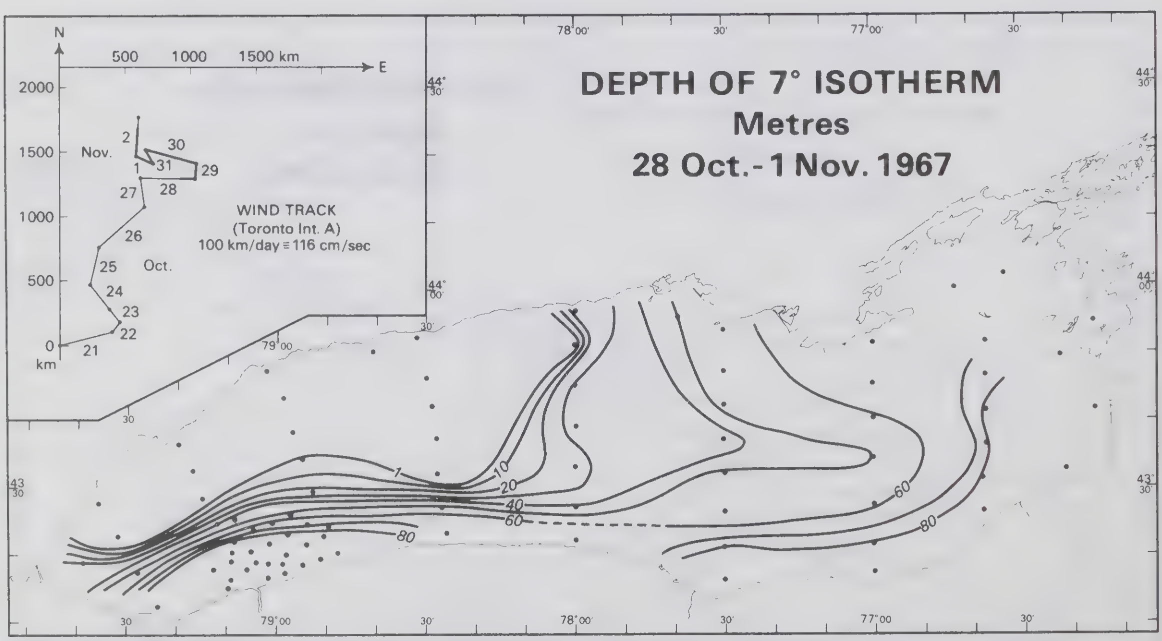

Figure F.106

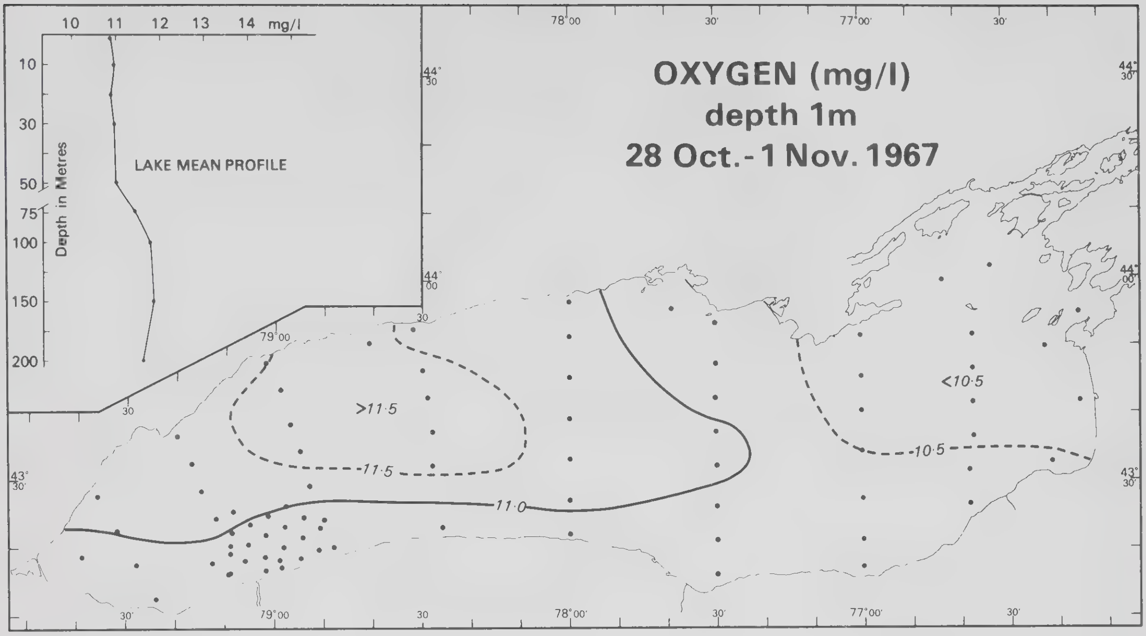

Figure F.107

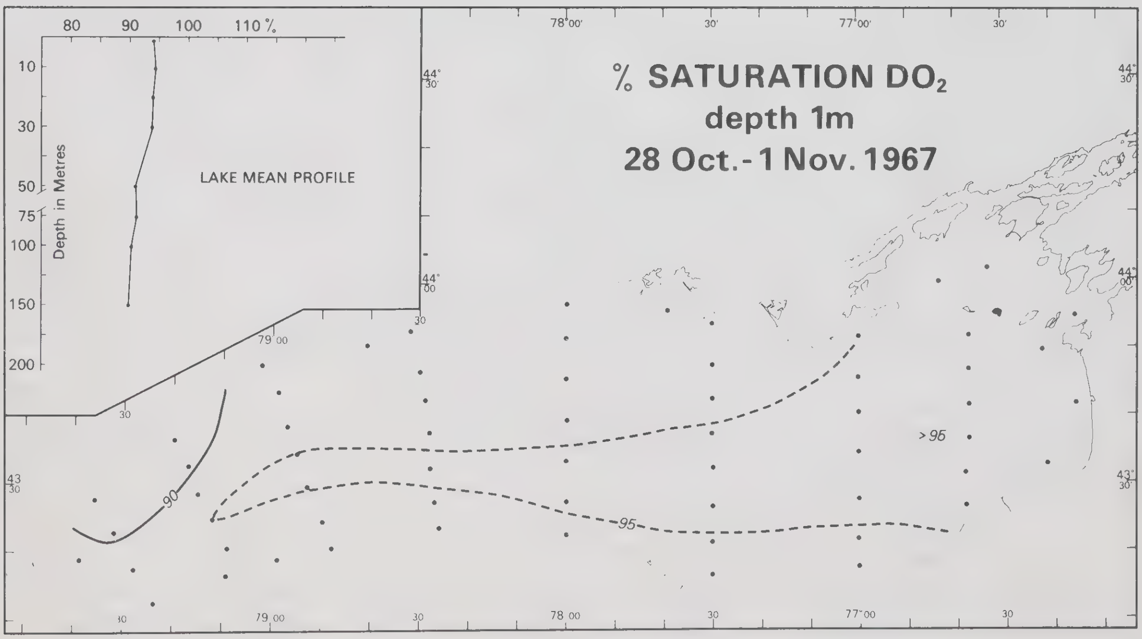

Figure F.108